

# Abstracts of the Eighth International Conference on Geochronology, Cosmochronology and Isotope Geology

ICOG 8  
*by the GOLDEN GATE*

*Berkeley California USA  
June 5 - 11, 1994*

U.S. GEOLOGICAL SURVEY CIRCULAR 1107

---

# AVAILABILITY OF BOOKS AND MAPS OF THE U.S. GEOLOGICAL SURVEY

---

Instructions on ordering publications of the U.S. Geological Survey, along with prices of the last offerings, are given in the current-year issues of the monthly catalog "New Publications of the U.S. Geological Survey." Prices of available U.S. Geological Survey publications released prior to the current year are listed in the most recent annual "Price and Availability List." Publications that are listed in various U.S. Geological Survey catalogs (see **back inside cover**) but not listed in the most recent annual "Price and Availability List" are no longer available.

Reports released through the NTIS may be obtained by writing to the National Technical Information Service, U.S. Department of Commerce, Springfield, VA 22161; please include NTIS report number with inquiry.

Order U.S. Geological Survey publications **by mail** or **over the counter** from the offices given below.

## BY MAIL

### Books

Professional Papers, Bulletins, Water-Supply Papers, Techniques of Water-Resources Investigations, Circulars, publications of general interest (such as leaflets, pamphlets, booklets), single copies of Earthquakes & Volcanoes, Preliminary Determination of Epicenters, and some miscellaneous reports, including some of the foregoing series that have gone out of print at the Superintendent of Documents, are obtainable by mail from

**U.S. Geological Survey, Map Distribution  
Box 25286, MS 306, Federal Center  
Denver, CO 80225**

Subscriptions to periodicals (Earthquakes & Volcanoes and Preliminary Determination of Epicenters) can be obtained **ONLY** from the

**Superintendent of Documents  
Government Printing Office  
Washington, DC 20402**

(Check or money order must be payable to Superintendent of Documents.)

### Maps

For maps, address mail orders to

**U.S. Geological Survey, Map Distribution  
Box 25286, Bldg. 810, Federal Center  
Denver, CO 80225**

Residents of Alaska may order maps from

**U.S. Geological Survey, Earth Science Information Center  
101 Twelfth Ave., Box 12  
Fairbanks, AK 99701**

## OVER THE COUNTER

### Books and Maps

Books and maps of the U.S. Geological Survey are available over the counter at the following U.S. Geological Survey offices, all of which are authorized agents of the Superintendent of Documents.

- **ANCHORAGE, Alaska**—4230 University Dr., Rm. 101
- **LAKEWOOD, Colorado**—Federal Center, Bldg. 810
- **MENLO PARK, California**—Bldg. 3, Rm. 3128, 345 Middlefield Rd.
- **RESTON, Virginia**—National Center, Rm. 1C402, 12201 Sunrise Valley Dr.
- **SALT LAKE CITY, Utah**—Federal Bldg., Rm. 8105, 125 South State St.
- **SPOKANE, Washington**—U.S. Post Office Bldg., Rm. 135, W. 904 Riverside Ave.
- **WASHINGTON, D.C.**—Main Interior Bldg., Rm. 2650, 18th and C Sts., NW.

### Maps Only

Maps may be purchased over the counter at the U.S. Geological Survey offices:

- **FAIRBANKS, Alaska**—New Federal Building, 101 Twelfth Ave.
- **ROLLA, Missouri**—1400 Independence Rd.
- **STENNIS SPACE CENTER, Mississippi**—Bldg. 3101

# Abstracts of the Eighth International Conference on Geochronology, Cosmochronology, and Isotope Geology

Edited by M.A. LANPHERE, G.B. DALRYMPLE, and  
B.D. TURRIN

U.S. GEOLOGICAL SURVEY CIRCULAR 1107

**U.S. DEPARTMENT OF THE INTERIOR**  
**BRUCE BABBITT, Secretary**

**U.S. GEOLOGICAL SURVEY**  
**Gordon P. Eaton, Director**

For sale by  
U.S. Geological Survey, Map Distribution  
Box 25286, MS 306, Federal Center  
Denver, CO 80225

Any use of trade, product, or firm names in this publication is for descriptive purposes only and does not imply endorsement by the U.S. Government.

## PREFACE

It all began in Canada in 1967 with *The International Conference on the Geochronology of Precambrian Stratified Rocks*. There followed, in 1969, *The Colloquium on the Geochronology of Phanerozoic Orogenic Belts* in Switzerland, at which time the name *The nth Conference on Geochronology, Cosmochronology and Isotope Geology (ICOG)* was adopted for future conferences. This now-quadrennial conference has become the most prestigious forum in the world devoted exclusively to the application of isotope research to solving problems in the physical and natural sciences.

The *ICOG* conferences arose because of a genuine need within the scientific community. The conferences have no formal organization behind them; there are no bylaws, no rules and regulations, no officers, and no permanent funding. They have been perpetuated by a vote of the *ICOG* conference attendees, who choose the venue and the Chair for the succeeding meeting. It then becomes the responsibility of the new Chair to set about organizing the next meeting from scratch, although the outgoing previous chairs provide valuable records and advice.

Since the first conference 27 years ago, the following *ICOGs* have been held:

1. Edmonton, Alberta, Canada, June 12-14, 1967
2. Bern/Zurich, Switzerland, August 23-September 4, 1969
3. Paris, France, August 26-31, 1974
4. Snowmass, Colorado, USA, August 20-25, 1978
5. Nikko, Japan, June 27-July 2, 1982
6. Cambridge, UK, June 30-July 4, 1986
7. Canberra, Australia, September 24-29, 1990

And now, June 5-11, 1994, at the University of California, Berkeley, *ICOG* returns to a North American venue for the first time in sixteen years. At this writing *ICOG-8 by the Golden Gate*, with 743 abstracts submitted, promises to be the largest of the *ICOG* conferences to date.

*ICOG-8*, of course, would not have been possible without the assistance and support of a great many people and other organizations and I would like to thank the Convening Institutions, the Co-Sponsors, and the Underwriters, listed on the following page, for their generous support. I would especially like to thank Pacific Gas and Electric Company for their substantial contribution to our Education Project and the Bank of America for their generous support of the Host Committee's program to bring scientists from developing countries. I am also deeply grateful to the Ann and Gordon Getty Foundation for providing matching funds for all of the moneys raised for *ICOG-8*.

Finally, it was the wish of the Organizing Committee to provide the delegates with a *referenceable* abstracts volume and on their behalf I wish to express gratitude to the U.S. Geological Survey for publishing this volume as a USGS Circular, and for providing each delegate with a copy.

Garniss H. Curtis  
Chair, *ICOG-8*  
June, 1994

### **ICOG-8 Convening Institutions**

**Institute of Human Origins  
University of California  
U.S. Geological Survey  
Lawrence Berkeley Laboratory  
Lawrence Livermore Laboratory  
Leland Stanford, Jr., University**

### **ICOG-8 Co-Sponsors**

**American Geophysical Union  
Association of Women Geoscientists  
California Division of Mines and Geology  
Canadian Geophysical Union  
European Geophysical Society  
Geochemical Society  
Geological Society of America  
International Association of Geochemistry and Cosmochemistry  
International Union of Geological Sciences  
Subcommission on Geochronology  
Meteoritical Society  
Nevada Bureau of Mines and Geology**

### **ICOG-8 Underwriters**

**Bank of America  
BHP Minerals International  
Charles Evans and Associates  
Chevron Corporation  
Finnegan Mat  
Ann and Gordon Getty Foundation  
Homestake Mining Company  
Interocean Oil and Gas Company  
John E. Kilkenny  
Mass Analyser Products, Ltd.  
Niles and Associates, Inc., Publishers of EndNote  
Pacific Gas and Electric Company  
Western Mining Corporation (USA)  
VMI, Inc.**

## **ICOG-8 Organizing Committee**

**Garniss H. Curtis, Chair**

**Walter Alvarez**

**Joseph Arth**

**Tim Becker**

**Scott G. Borg**

**Marc Caffee**

**Mark Conrad**

**Robert E. Criss**

**Brent Dalrymple**

**Al Deino**

**Donald J. DePaolo**

**Robert Fleck**

**Phillip B. Gans**

**Brian Hausback**

**Lynn Ingram**

**B. Mack Kennedy**

**Marvin Lanphere**

**Michael McWilliams**

**Michael Moore**

**Syd Niemeyer**

**Paul Renne**

**John H. Reynolds**

**Sharie Shute**

**Doris Sloan**

**Brian M. Smith**

**Carl Swisher**

**Brent Turrin**

**Robert C. Walter**

**Joseph Wooden**

## CONTENTS

Preface	iii
Abstracts	1
Author Index	374

## EXPLANATION

Abstracts are organized alphabetically by first author and were printed as received from the author-prepared copy. The Author index is comprehensive and includes all authors.

# Abstracts of the Eighth International Conference on Geochronology, Cosmochronology, and Isotope Geology

*Edited by M.A. Lanphere, G.B. Dalrymple, and B.D. Turrin*

## BORON ISOTOPIC COMPOSITION OF ICELANDIC GEOTHERMAL SYSTEMS: MAGMATIC DEGASSING OR WATER-ROCK INTERACTION ?

AGGARWAL, J.K., PALMER, M.R., RAGNARSDOTTIR K.V, Dept of Geology, University of Bristol, Bristol, UK. BS8 1RJ.

A variety of geothermal systems have been sampled across Iceland ranging from cold carbonate springs on Snaefellsnes, low temperature geothermal systems of the Southern Lowlands, the high temperature systems of Krafla, Bjarnaflag, Nesjavellir, and the saline systems of Svartsengi and Reykjanes. Boron isotope ratios of the fluids have been determined using a new and rapid technique based on that of Leeman et al (1991).

Samples collected from the Snaefellsnes Peninsular have also been analysed for carbon and sulphur isotopes. These elements show that the fluids contain signatures suggesting magmatic degassing. The variability in the boron isotope ratios reflects a primary magmatic signature with modification due to fractionation of boron into secondary mineral phases.

A detailed sampling strategy of both the Nesjavellir and Krafla systems, has allowed for a more complete evaluation of processes that fractionate boron isotopes, (Aggarwal et al 1992). Samples have been obtained from both of these systems over the last ten years and the boron isotope ratios have been examined in conjunction with known magmatic episodes.

At all of high temperature geothermal wells, the fluid phase was separated into a steam phase and a water phase. Examination of both of these phases showed that very little boron was partitioned into the steam phase. In these high temperature systems there is no evidence to suggest that boron is taken into secondary minerals. Therefore the  $\delta^{11}\text{B}$  of the water phase represents the boron isotope ratio of the fluid at depth.

Preliminary results indicate that the boron in the high temperature fluids are derived from both water-rock reactions and also from magmatic degassing. In the lower temperature systems the boron  $\delta^{11}\text{B}$  values are likely to be further modified by the incorporation of  $^{10}\text{B}$  into secondary phases such as carbonates, silica or clay minerals.

Aggarwal, J.K., Palmer, M.R., Ragnarsdottir, K.V., 1992, Boron Isotopic Composition of Icelandic Hydrothermal Systems. Water-Rock Interaction. Kharaka Y.F., Maest A.S., (ed), 893-895. Rotterdam: Balkema.

Leeman, W.P., Vocke, R.D., Beary, E.S., Paulsen, P.J., 1991, Precise Boron Isotopic Analysis of Aqueous Samples: Ion Exchange Extraction and Mass Spectrometry: *Geochim.Cosmochim. Acta*, 55, 3901-3907.

Oxygen stable isotope compositions of oceanic crust rocks exposed in the Hess Deep. Implications for the buffering of the seawater  $\delta^{18}\text{O}$  composition by seawater hydrothermal interaction in the oceanic crust.

P. Agrinier, M. Javoy (Lab. Géochimie Isotopes Stables, I.P.G.Paris, 2 place Jussieu, 75251 PARIS cedex 05, France)  
R. Hékinian and D. Bideau (IFREMER - Centre de Brest, BP 70, 29263 Plouzané, France)

A large variety of rocks, consisting of basalts, dolerites, gabbros and ultramafics, are exposed at Hess Deep, representing a section of the oceanic crust formed at the East Pacific Ridge. We have conducted an oxygen stable isotope study in order to assess the nature and intensity of interaction of seawater with the oceanic crust in this region. Fresh basalt and dolerite samples have magmatic MORB values ( $\delta^{18}\text{O} \approx 6.0$  and low  $\text{H}_2\text{O}^+$  (<0.3 wt.%). The metabasalts are enriched in  $^{18}\text{O}$  ( $\delta^{18}\text{O} \approx 7$ ) and have  $\text{H}_2\text{O}^+$  contents higher than 2 wt.%. The metadolerites are depleted in  $^{18}\text{O}$  ( $\delta^{18}\text{O} \approx 4.9$ ), with  $\text{H}_2\text{O}^+$  contents (> 1.3 wt.%).

Most gabbros have  $\delta^{18}\text{O}$  around 5.6, essentially identical to their initial magmatic values although their mineralogy shows that they have reacted with fluids. In gabbros, displaying little or no evidence of alteration of their plagioclases and pyroxenes,  $\Delta^{18}\text{O}_{\text{plag-px}}$  is small ( $\approx 0.3$ ) and consistent with magmatic values. The calcic plagioclases have magmatic  $\delta^{18}\text{O}$  ( $\approx 5.8$ ), while altered plagioclases have variable  $\delta^{18}\text{O}$  values (4 to 8). It appears also that the  $^{18}\text{O}$  modified gabbros are those in which plagioclase is transformed into albite or prehnite. The lack of calcic plagioclases depleted in  $^{18}\text{O}$  suggests that most of the gabbros did not react extensively under amphibolite facies with seawater-derived fluids ( $T \geq 400^\circ\text{C}$ ) or that they were subsequently altered in the greenschist facies.

The serpentized peridotites were depleted in  $^{18}\text{O}$  (3.3 to 4.9). In one sample, the  $\Delta^{18}\text{O}_{\text{serpentine-magnetite}}$  ( $\approx 5.7$ ) corresponds to a temperature of about  $325 \pm 50^\circ\text{C}$ . These values are compatible with serpentization temperature between 200 and  $350^\circ\text{C}$  and suggest that seawater-derived fluid may have been responsible for the serpentization process. Another sample has a  $\delta^{18}\text{O}$  value of 10 corresponding to a serpentization temperature less than  $50^\circ\text{C}$ .

The  $^{18}\text{O}$  mass balance between seawater and oceanic crust seems to have attained steady-state where enrichment in  $^{18}\text{O}$  of metabasalts is balanced by the depletion in  $^{18}\text{O}$  of metadolerites. The contribution of the gabbros is minor.

## U-Pb EVIDENCE FOR PROVENANCES OF HOLOCENE SAND DUNES, NORTHEASTERN COLORADO AND THE NEBRASKA SAND HILLS

ALEINIKOFF, John N., MUHS, Daniel R., and WALTER, Marianne, U.S. Geological Survey, Box 25046, DFC, MS 963, Denver, CO, 80225, USA

Eolian sand seas (dune fields  $>125 \text{ km}^2$ ) form in areas of abundant sand supply, strong winds, and suitable climatic and topographic conditions for long-term sand accumulation. Most sand seas occur in tropical or subtropical latitudes, but important exceptions are the large dune fields of the North American Great Plains. The Nebraska Sand Hills ( $>50,000 \text{ km}^2$ ) are comparable in size to many of the sand seas of the Sahara and central Asia. Knowledge of the sources of sediments in presently stabilized sand seas is important for understanding the conditions of reactivation due to possible future global climate change.

U-Pb analyses of single zircons from Holocene eolian sand dunes of northeastern Colorado have yielded ages (1.06-1.16, 1.38-1.5, 1.65-1.73, and 2.0 Ga) indicative of derivation from Middle Proterozoic crystalline rocks of the Colorado province. These data are supported by measurements of Pb isotopic compositions of multigrain and single microcline samples. All samples also contain a sanidine component, derived from Tertiary volcanic centers in the western U.S. These results support geomorphic, geochemical, and sedimentologic interpretations that the dunes formed by eolian processes that removed sand from fluvial deposits of the South Platte River.

In contrast, no major modern river system is upwind (north-northwest) of the Nebraska Sand Hills, and most workers have considered the Tertiary Ogallala Group, in primary or reworked form, to be the main source of sand. U-Pb ages from single zircons (1.03-1.18, 1.4, 1.6-1.68, and 2.5-2.75 Ga) and Pb isotopic compositions from multigrain fractions and single grains of microcline and sanidine indicate that these Holocene dunes have provenances in both the Colorado province and the Archean Wyoming province. Three possible sources are considered: (1) sediments of the North Platte River (which heads in north-central Colorado but flows north into Wyoming and then east along the southern margin of the Sand Hills), (2) the Miocene Ogallala Group, and (3) the Oligocene-Miocene Arikaree Group. The North Platte River sediments contain zircons that are Middle and Early Proterozoic and Archean, but lack zircons of the 1.4-Ga age group. Zircons from the Ogallala are solely derived from the Colorado province (no Archean grains found), in contrast to interpretations of Tertiary paleo-drainage patterns suggesting a source to the northwest in Wyoming, and thus the Ogallala could not be the sole source of the sand. Although the Arikaree has previously been ignored as a potential source, it contains zircons whose ages match the age distribution found in the Sand Hills. Thus, the source(s) of the Sand Hills sediments must be (1+2) or (3) or (1+2+3). We conclude that the Nebraska Sand Hills have multiple sources, including sources not previously recognized.

## PRESOLAR SiC: PRISTINE SAMPLES FROM OTHER STARS.

ALEXANDER, Conel M. O'D., McDonnell Center for Space Sciences, Washington University, St Louis, MO 63130, U.S.A.

Since its initial identification as the long sought for carrier of Ne-E(H) (almost pure  $^{22}\text{Ne}$ ), presolar SiC isolated from meteorites has become the focus of in-depth isotopic studies both of bulk samples and of individual grains. The results of this work have important implications for models of stellar, galactic and nebular evolution.

The noble gases released from bulk samples are highly enriched in isotopes produced by s-process nucleosynthesis [1] and the emerging consensus is that most of the SiC formed in the envelopes of C-rich red giant stars which are known to be enriched in s-process material [2]. In apparent confirmation of this, the C isotopic compositions of individual SiC grains show a very similar distribution to those of C-rich red giants. Although a few SiC grains from super novae and massive Wolf-Rayet stars may also be present. The relative abundances of grains from these sources are in broad agreement with dust production estimates based on astronomical observations.

Individual SiC grains provide a snapshot of a star's evolution at the time the grain formed. Most grains are enriched in refractory s-process elements and depleted in most other elements in accordance with the predicted volatility of their carbides [3]. However, Si and Ti isotopic compositions of individual grains do not conform to expectations of simple s-process nucleosynthesis [3,4]. Rather it appears that the s-process signatures are superimposed on a general trend produced by galactic chemical evolution [3]. Thus the SiC found in meteorites must have been produced by many stars that formed at different times and/or places in the galaxy.

The noble gases trapped in the SiC exhibit significant absolute abundance and isotopic variations with grain size [1]. Most of the  $^{21}\text{Ne}$  in SiC is thought to have been produced by cosmic ray spallation reactions while the grains resided in the interstellar medium (ISM) [1]. The abundances of  $^{21}\text{Ne}$  in different SiC size fractions have been used to obtain average cosmic ray exposure ages and these vary from 13Ma in the finest fractions to 133Ma in the coarser ones [5]. This variation with size has been alternately interpreted as due to partial degassing in the solar system [5] or reflecting the average residence times of SiC in the ISM [6]. The latter has been used to develop a model that appears able to account for the variations of all the noble gases with size [6].

The use of interstellar grains to infer conditions in the nebula is just beginning to be explored. SiC is only preserved in the fine grained meteorite rim/matrix [7,8] confirming the long held belief that this is the most primitive material to be found in meteorites. The abundances of interstellar grains in rim/matrix prior to the onset of metamorphism appear to have been more or less the same in all the most primitive meteorites [8]. This observation presents some problems for the 'standard' hot nebula evolution model used to explain variations in the bulk compositions of the different chondrite classes.

[1] Lewis R.S. et al. (1990) *Nature*, **348**, 293.

[2] Gallino R. et al. (1990) *Nature*, **348**, 298.

[3] Hoppe et al. (1994) *Ap. J.*, in press.

[4] Alexander C.M.O'D. (1993) *G.C.A.*, **57**, 2869.

[5] Lewis R.S. et al. (1994) *G.C.A.*, **58**, in press.

[6] Alexander C.M.O'D. (1994) *L.P.S.C.*, **XXV**, submitted.

[7] Alexander C.M.O'D. (1990) *Nature*, **348**, 715.

[8] Huss G. (1990) *Nature*, **347**, 159.

## MELT IMPREGNATION OF HESS DEEP PERIDOTITES; CONSTRAINTS FROM SPINEL PETROGENESIS

J. F. Allan, Ocean Drilling Program, 1000 Discovery Drive, Texas A&M Univ., College Station, TX 77845 and Leg 147 Shipboard Party

Melt-impregnated upper mantle peridotites, recovered by the JOIDES Resolution at Site 895, record melt-wallrock interaction processes during transport of MORB through the uppermost mantle beneath the adjacent East Pacific Rise. The recovered stratigraphy shows progressive sequences of harzburgite, dunite, troctolite, olivine gabbro and gabbro, troctolite, dunite, and harzburgite, with the troctolites representing basalt impregnation of peridotite on an intimate, sometimes intergranular scale. High precision microprobe analyses were obtained of Cr-spinel from these samples. Harzburgite Cr-spinels are unzoned and have low  $\text{TiO}_2$  ( $\leq 0.07\%$ ) and  $\text{Fe}^{3+}/(\text{Cr}+\text{Al}+\text{Fe}^{3+})$  ( $\text{Fe}^{3+\#}$ ;  $< 0.04$ ). Dunite Cr-spinels have higher  $\text{TiO}_2$  (0.44-0.48%) and  $\text{Fe}^{3+\#}$  (0.05-0.07), reflecting exchange during the metamorphic transformation of host harzburgite to dunite during melt intrusion. Large (to 1 cm), skeletal Cr-spinels within the troctolites represent rapid crystallization associated with melt/wallrock exchange. They are individually unzoned but vary in composition within an individual thin section ( $\text{TiO}_2$ , 0.7-1.5%;  $\text{Fe}^{3+\#}$ , 0.08-0.11; Cr#, 0.48-0.61; and Mg#, 0.47-0.60). Their composition and spinel-olivine geothermometry show that they equilibrated at 870-900°C with Ti-rich, evolved melts (Mg# of 0.43-0.53). Olivine gabbros contain sub-rounded Cr-spinel (to 800  $\mu\text{m}$ ) as intergranular grains and inclusions; these have higher  $\text{TiO}_2$  (to 2.7%) and low Mg# ( $\leq 0.58$ ). Inclusions within plagioclase are armored and unzoned, but others show profound zoning in ZnO (0.2-0.75%) and Mg# (to as low as 0.15) that reflects post-crystallization metamorphic exchange at temperatures of 600° C or less, perhaps with Zn-rich fluids. The troctolite and gabbro Cr-spinels show that pockets of highly evolved, Ti-rich melt (Mg#'s as low as 0.35) developed during impregnation of the Hess Deep peridotites, with melt impregnation occurring at the periphery of the EPR magmatic system in harzburgite wallrock having ambient temperatures of 900° C or less.

## STABLE ISOTOPES (O,H,S) DISTINGUISH SOURCES OF ACID DRAINAGE AT PENN MINE, CALIFORNIA

Alpers, C.N. and Hamlin, S.N., U.S. Geological Survey, Water Resources Division, Sacramento, CA, 95825, U.S.A. and Rye, R.O., U.S. Geological Survey, Geologic Division, Denver, CO, 80225, U.S.A.

Acid drainage with elevated concentrations of base metals and sulfate has contaminated surface and ground waters at the Penn Mine, Calaveras County, California. Contaminated surface and ground waters occur less than 100 m from Camanche Lake, a local water supply. The acid drainage results from oxidation of sulfide minerals in surface and subsurface environments: surface environments include waste rock and tailings piles, and the subsurface environment consists of unmined, mineralized rock in underground mine workings extending to more than 1 km depth. In this study, stable isotopes of O and H in water and O and S in dissolved sulfate are used to distinguish the surface and subsurface sources of acid mine drainage.

Sulfide minerals found on waste-rock piles are pyrite ( $\text{FeS}_2$ ), sphalerite ( $(\text{Zn,Fe,Cd})\text{S}$ ), chalcocite ( $\text{CuFeS}_2$ ), and bornite ( $\text{Cu}_5\text{FeS}_4$ ). Wall rocks consist of greenschist facies intermediate-to-felsic metavolcanic rocks of Jurassic age. Acid surface drainage (pH 2.3 to 3.0) is formed by sulfide oxidation in waste-rock and tailings piles. The subsurface is drained seasonally by seeps (pH 4.0 to 4.2) associated with a shaft connected to the underground mine workings. Surface and subsurface drainage mixes in unlined impoundments that recharge contaminated, acid water (pH 2.6 to 2.9) to a fractured metavolcanic-rock aquifer, which flows toward Camanche Lake.

The impoundment waters are the most enriched in  $^{18}\text{O}_{\text{H}_2\text{O}}$  and D, and contain the highest dissolved metal and sulfate concentrations. An evaporative trend with slope 4.4 is revealed on a plot of  $\delta^{18}\text{O}_{\text{H}_2\text{O}}$  vs.  $\delta\text{D}$  for ground water (pH 3.6 to 7.8) from the metavolcanic-rock aquifer plus surface water from the impoundments. The data span a range of 12‰ in  $\delta^{18}\text{O}_{\text{H}_2\text{O}}$  and 55‰ in  $\delta\text{D}$ . Seeps and samples from the underground workings and uncontaminated ground waters plot near the meteoric water line, indicating minimal evaporation. Good correlations between  $\delta^{18}\text{O}_{\text{H}_2\text{O}}$ ,  $\delta\text{D}$ , pH, and dissolved  $\text{SO}_4$ , Fe(II) and Cu in the aquifer provide strong evidence that evaporated water in the impoundments is the major source of contamination of the metavolcanic-rock aquifer.

The highest values of  $\delta^{34}\text{S}_{\text{SO}_4}$  and  $\delta^{18}\text{O}_{\text{SO}_4}$  correspond to water samples from the underground mine workings and the seasonal seep that drains the workings. Values of  $\delta^{34}\text{S}_{\text{SO}_4}$  show a bimodal distribution with two ranges: +1.0 to +2.6‰ and +4.1 to +4.8‰. Values of  $\delta^{18}\text{O}_{\text{SO}_4}$  range from -1.4 to +2.5‰. Possible explanations for variations in  $\delta^{34}\text{S}$  are: (1) preferential removal of  $^{32}\text{S}$  during sulfate reduction resulting in higher values of  $\delta^{34}\text{S}$  in the underground workings, and (2) heterogeneity in primary ores. Values of  $\delta^{18}\text{O}_{\text{SO}_4}$  do not correlate with  $\delta^{18}\text{O}_{\text{H}_2\text{O}}$  and probably reflect differences in microbial activity and sulfide oxidation mechanisms ( $\text{O}_2$  vs.  $\text{Fe}^{3+}$  as oxidant).

In summary, stable isotopes can provide a useful hydrogeochemical tool in mine drainage environments.

## ISOTOPIC ANALYSIS OF 47 LOW DENSITY GRAPHITE GRAINS FROM MURCHISON

AMARI S., ZINNER E., McDonnell Center for the Space Sciences and the Physics Department, Washington University, One Brookings Dr., St. Louis, MO 63130, and LEWIS R. S., Enrico Fermi Institute, University of Chicago, 5630 Ellis Ave., Chicago IL 60637

We have measured C-, N-, Si-, Mg- isotopic ratios of graphite grains in the low density graphite fraction KE3 (1.57-2.12 g/cm<sup>3</sup>, >3 μm, Amari *et al.*, 1993a).  $^{12}\text{C}/^{13}\text{C}$  and  $^{14}\text{N}/^{15}\text{N}$  ratios in 47 grains show that more of the grains are enriched in  $^{13}\text{C}$  and  $^{15}\text{N}$  than are in the higher density graphite fractions (Amari S. *et al.*, 1993b); seventeen grains have  $^{12}\text{C}/^{13}\text{C}$  lower than 60 (2σ) and 16 grains have  $^{14}\text{N}/^{15}\text{N}$  lower than 240 (2σ). Grains in this density range have relatively high trace element concentrations, which enable us to measure isotopic ratios of several elements.

Among 46 grains measured for Si, 14 have isotopic anomalies deviating from normal more than 2σ. Most of them have  $^{28}\text{Si}$  enrichments of up to 40% compared with normal Si, while 4 grains have either  $^{29}\text{Si}$  or  $^{29}\text{Si}$  and  $^{30}\text{Si}$  excesses. Twenty-six out of 40 grains have large  $^{18}\text{O}$  excesses of up to a factor of 100. In contrast,  $^{16}\text{O}/^{17}\text{O}$  ratios are normal within relatively large errors. There is a tendency that grains enriched in  $^{12}\text{C}$  and  $^{15}\text{N}$  have larger excesses in  $^{18}\text{O}$ . Twenty-seven out of 38 grains have  $^{26}\text{Mg}$  excesses with  $(^{26}\text{Al}/^{27}\text{Al})_0$  ratios ranging up to 0.15. Of the 7 grains in which we measured Ca and Ti, all have  $^{49}\text{Ti}$  excesses, ranging up to 1720±972‰ (2σ). Grain 662, the grain with the largest  $^{12}\text{C}/^{13}\text{C}$  ratio and largest  $^{18}\text{O}$  excess has, in addition to a  $^{49}\text{Ti}$  excess of 862±90‰, excesses of 175±72‰ and 429±132‰ (2σ) in  $^{42}\text{Ca}$  and  $^{43}\text{Ca}$ , respectively. The low density graphite grains show a similarity in their C, N, Si and Ti isotopic compositions to SiC grains of type X, for which a supernova origin has been invoked (Amari S. *et al.*, 1992). While Wolf-Rayet stars also can have  $^{18}\text{O}$  enrichments, it is doubtful that an  $^{18}\text{O}$  excess of more than a factor of 10 can be achieved (M. Arnould pers. commun.). On the other hand, the He-burning shell in pre-supernovae has an  $^{16}\text{O}/^{18}\text{O}$  ratio of about 5, which is comparable to the most extreme ratios observed in this study.

Amari S. *et al.* (1992) Interstellar SiC with unusual isotopic compositions: Grains from a supernova? *Ap. J.* **394**, L43

Amari S. *et al.* (1993a) Interstellar grains in meteorites I.

Isolation of SiC, graphite, and diamond; Size distributions of SiC and graphite. *G.C.A.*, in press.

Amari S. *et al.* (1993b) The isotopic compositions and stellar sources of meteoritic graphite grains. *Nature* **365**, 806-809.

SYSTEMATICS OF METAMORPHIC MONAZITE AND ITS BEARING ON THE PETROGENESIS OF THE KIGLUAIK GNEISS DOME, SEWARD PENINSULA, AK  
AMATO, Jeffrey M., Dept. Geological and Environmental Sciences, Stanford University, Stanford, CA, 94305-2115, USA; and J. E. Wright, Dept. Geology and Geophysics, Rice University, Houston, TX 77251, USA

Monazite U-Pb isotopic data from upper-amphibolite-facies orthogneiss, metapelite, and partial-melt pegmatites document a  $91 \pm 1$  Ma age for a high-temperature metamorphic event that overprints an earlier blueschist-facies metamorphism recorded in the mantling schists and gneisses of the granite cored Kigluaik gneiss dome on the Seward Peninsula, Alaska. Zircon U-Pb isotopic data from the compositionally diverse granitoid pluton in the core of the dome indicate an age of  $92 \pm 2$  Ma thus supporting a genetic relationship between Late Cretaceous magmatism and metamorphism.

Monazite dates from orthogneisses range from 96 to 91 Ma, whereas monazite dates from metapelite and pegmatite cluster between 90 and 91 Ma. We interpret the older dates in orthogneiss as reflecting Pb inheritance from their original igneous crystallization at  $555 \pm 25$  Ma as determined from U-Pb analyses of zircon. Monazite from the metapelite and pegmatite instead crystallized initially during Late Cretaceous metamorphism and thus do not record an earlier history. All monazite analyses vary systematically with grain size; 75-150  $\mu\text{m}$  grains are 1-2 m.y. older than 45-75  $\mu\text{m}$  grains.

Field relations together with Nd and Sr isotopic data indicate that the Kigluaik pluton contains a significant mantle derived component. The pluton consists of a ~0.5-1 km biotite granite cap overlying quartz diorite to granodiorite whose root is not exposed. Mafic pillows with crenulate margins indicate mixing of two coeval magmas along the mafic/felsic contact. Geochemical data indicate mixing of mafic magma with an older, crustal source. Combined Nd and Sr isotopic data from the mafic root, the granitic cap, and from a related diabase dike swarm lie on a trend from initial ratios (@ 91 Ma) of  $^{87}\text{Sr}/^{86}\text{Sr} = 0.706$  to  $0.709$  and  $\epsilon_{\text{Nd}} = -0.2$  to  $-8.0$ . Isotopic ratios from the country rocks (calculated for 91 Ma) are  $^{87}\text{Sr}/^{86}\text{Sr} > 0.720$  and  $\epsilon_{\text{Nd}} > -8.0$  and lie on the extension of the trend of the analyses from the pluton. Initial ratios from the pluton also correlate with silica content (positively for Sr, negatively for Nd) which would be expected if the magma were incorporating older crustal material. REE plots show mixing between a LREE-enriched source and a source with a flat REE distribution.

The geochronological and geochemical data indicate that the igneous rocks and coeval metamorphism resulted from the emplacement of mantle-derived magmas which provided the heat necessary for upper-amphibolite-facies metamorphism and partial melting during a Late Cretaceous extensional event that post-dated crustal thickening in northern Alaska. The Kigluaik gneiss dome may help understand magmatic processes at the deeper levels of extensional core complexes such as those in the Basin and Range province of the western United States.

CONSTRAINTS ON THE EVOLUTION OF GRENVILLIAN LITHOSPHERE FROM Nd-Sr-Pb CPX AND GARNET AND U-Pb ZIRCON STUDY OF PYROXENITIC AND MAFIC GRANULITIC XENOLITHS

AMELIN, Yuri, Dept. of Geology, Royal Ontario Museum, Toronto, ON M5S 2C6, Canada, CORRIVEAU, Louise, and MORIN, David, Centre géoscientifique de Québec, C.P. 7500, Sainte-Foy, QC, G1V 4C7, Canada

Clinopyroxene and garnet separates from 14 xenoliths of clinopyroxenites, websterites, garnet pyroxenites and mafic granulites, extracted from an  $1.088 \pm 46$  Ma (Sm-Nd internal isochron) ultrapotassic lamprophyre dyke in the Central Metasedimentary Belt, SW Grenville Province, Québec, were studied for Sm-Nd, U-Pb and Rb-Sr. All 6 analyzed Gnt-Cpx pairs yielded similar Sm-Nd ages from 1091 to 1074 Ma, indistinguishable from the age of the lamprophyre.  $^{206}\text{Pb}/^{204}\text{Pb}$ - $^{238}\text{U}/^{204}\text{Pb}$  and  $^{207}\text{Pb}/^{204}\text{Pb}$ - $^{206}\text{Pb}/^{204}\text{Pb}$  ages for the same mineral pairs are less precise but also cluster around 1.08 Ga, while the younger Rb-Sr ages between 630-840 Ma are indicative of post-crystallization resetting in garnets. Concordant U-Pb age of titanite from a clinopyroxenite xenolith  $1072 \pm 12$  Ma is consistent with Gnt-Cpx ages.

The variations of initial isotopic values in the Cpx from -3.3 to +5.7 for  $\epsilon_{\text{Nd}}(1.08 \text{ Ga})$  and from 16.77 to 17.79 for  $^{206}\text{Pb}/^{204}\text{Pb}(1.08 \text{ Ga})$  are consistent with the values determined in coeval potassic plutons of the Central Metasedimentary Belt (Corriveau & Amelin 1994), but the  $^{87}\text{Sr}/^{86}\text{Sr}(1.08 \text{ Ga})$  from 0.70398 to 0.70520 are distinctly higher, so the lithosphere region sampled by the studied xenolith suite is unlikely to represent the source of these potassic rocks.

Zircons from two websterites and one garnet-bearing granulite have U contents between 60-200 ppm and model Th/U ratios between 0.2 and 0.4. Six single grain ID U-Pb analyses are nearly concordant with  $^{207}\text{Pb}^*/^{206}\text{Pb}^*$  ages between 1112 and 1182 Ma and together define a slightly scattered array with upper and lower concordia intercepts of ca. 1300 and 1110 Ma, respectively. The upper intercept age coincides with a major episode of tholeiitic volcanism in the Central Metasedimentary Belt, and we thus interpret it as the protolith age of the studied xenoliths, which could represent cumulates of a tholeiitic basaltic magma formed in the upper mantle or lower crustal magma chamber. The lower intercepts (and two concordant points) reflect the beginning of mantle reactivation at 1127-1110 Ma marked by new zircon growth in sub-solidus conditions.

Two single grain zircon analyses from a two-pyroxene granulite sample have low U concentrations about 20 ppm and unusually high model Th/U ratios 9.4 and 22. These zircons are also nearly concordant but their  $^{207}\text{Pb}^*/^{206}\text{Pb}^*$  ages are significantly younger, 1100 and 1091 Ma. The unusual chemistry and absence of older components may indicate that the formation of these zircons was related to the episode of mantle metasomatism. The garnet-cpx ages therefore reflect either the closing of isotopic systems in garnets during mantle cooling or heating by the host magma with possible partial resetting of isotopic systems in both garnets and zircons.

**U-Pb ZIRCON DATING OF ULTRA HIGH-PRESSURE ECLOGITES WITH IMPLICATIONS FOR COLLISION OF THE NORTH AND SOUTH CHINA BLOCKS.**

**AMES, L.**, Dept. of Geological Sciences, University of California, Santa Barbara, CA, 93106; e-mail ames@magic.geol.ucsb.edu

The collision zone between the North and South China Blocks is marked by subduction-related metamorphic rocks composed of crustal protoliths ranging in metamorphic grade from ultrahigh-pressure eclogite to low-greenschist facies. The paragenesis of the ultra high-pressure structural blocks (coesite and diamond-bearing) indicates subduction to a depth of approximately 120 km as a result of continental collision. The ultrahigh-pressure belts are largely composed of amphibolite facies quartzofeldspathic gneiss, but also contain boudins of mafic eclogites.

The two belts of ultra high-pressure rocks (Dabie and Shandong) are offset from each other along the Tan-Lu fault by about 500 km, but the fault does not continue beyond the collision zone. The relationship between the timing of ultra high-pressure metamorphism in the two belts bears directly on the mechanism of collision of the micro continents and origin of the Tan-Lu fault. Comparison of preliminary U-Pb zircon ages from ultrahigh-pressure eclogites from the Dabie Mountains and Shandong Peninsula shows that the two areas have the same U-Pb concordia lower intercept ages, indicating that there may not be a significant difference in the timing of collision between the two areas. Although the timing of ultra high-pressure metamorphism in the Dabie belt is well constrained to be  $209 \pm 2$  Ma (U-Pb zircon), the preliminary ages from the Shandong area have large enough errors that an earlier collision cannot be ruled out.

Despite extreme metamorphic conditions, zircons in ultra high-pressure rocks show significant inheritance from their original crystallization and pervasive, fine-scaled zoning. Single zircons from paragneiss indicate a range of protolith ages from 670-800 Ma.

**AN ISOTOPE STUDY OF SOILS ON ALLUVIAL DEPOSITS IN THE MOJAVE DESERT: IMPLICATIONS FOR TIMING OF DEPOSITIONAL EVENTS AND PALEOCLIMATE CHANGE**

**Ronald Amundson, Yang Wang**, Department of ESPM, University of California, Berkeley, CA 94720.

Two soil chrono/climo-sequences in the Providence Mountain area in the Mojave desert, California were analyzed for their carbon (both  $^{13}\text{C}$  and  $^{14}\text{C}$ ) and oxygen isotope composition.  $^{14}\text{C}$  dates of soil carbonate were interpreted in the light of a diffusion/reaction model, which takes into account various processes and factors controlling the  $^{14}\text{C}$  content of soil carbonate. Model ages calculated from  $^{14}\text{C}$  dates of soil carbonate are in correct relative order as suggested by geomorphic evidence, and are also consistent with model ages from  $^{14}\text{C}$  dates of soil organic matter. Stable isotope paleoclimate reconstruction in terms of model ages are consistent with results from other studies.  $^{14}\text{C}$  model ages suggest that the older geomorphic surfaces we studied are of Pleistocene age and the younger surfaces formed during Holocene. Alluvial deposits on limestone terrain consistently had younger  $^{14}\text{C}$  ages than equivalent deposits on granitic terrain. Stable carbon isotopic composition of soil carbonate indicates a slight increase in C4 or CAM plants, or a decrease in plant density in local ecosystems in the Holocene. Both carbon and oxygen isotopic composition of soil carbonates suggest that the climate in the eastern Mojave desert has become warmer and drier since early Holocene.

**BULK SEDIMENT COSMOGENIC RADIONUCLIDE CONCENTRATIONS CONSTRAIN RELIEF PRODUCTION RATES IN EVOLVING ALPINE LANDSCAPES**

ANDERSON, Robert S., Department of Earth Sciences, University of California Santa Cruz, Santa Cruz, California, 95064, USA (rsand@bagnold.ucsc.edu)

The production of topographic relief in evolving mountain ranges is the key to a large scale feedback between geomorphic and tectonic processes. Relief is produced when the erosion rates at mountain crests are lower than those in the valley bottoms, and vice versa. As relief grows, the effective density of the range diminishes, generating flexural isostatic uplift. Comparison of relief generation from basins of significantly differing tectonic and climatic settings may allow us to test existing hypotheses about the geomorphic processes involved, and their relative rates.

I present a theoretical rationale for documentation of relief generation rates using cosmogenic radionuclide (CRN) concentrations of bulk basin sediments. I make use of the measurable probability distribution of elevations within the basin,  $D(z)$ , and the known elevational dependence of *in situ* CRN production rates,  $P(z)$ , in constructing an expression for the CRN concentration of basin sediments.

I assume steady state erosion at all points within the basin. This allows the calculation of the CRN concentration in surface rock at all points from which sediments are derived. For the default case of spatially uniform erosion rates, a measured CRN concentration of basin-derived sediments,  $C$ , yields a mean

erosion rate of  $\dot{\epsilon} = \frac{z^*(P^* - C\lambda)}{C}$ , where the basin's effective

production rate,  $P^* = P_{z_{max}} \int_{z_{min}}^{z_{max}} D(z) e^{-(z_{max}-z)/L} dz$ ,

$z^*$  is the length scale for decay of CRN production with depth below the rock surface (order 0.6m),  $L$  is the length scale for increase of CRN production with altitude (order 1.5km),  $z_{min}$  and  $z_{max}$  are the minimum and maximum elevations within the basin,  $P_{z_{max}}$  is the surface CRN production rate at  $z_{max}$ , and  $\lambda$  is the radionuclide decay constant. The probability density of elevation and the dependence of *in situ* production with altitude serve to weight the CRN flux from each elevational slice of topography, as represented by the integral. When the basin relief ( $R=z_{max}-z_{min}$ ) is much less than  $L$ , the expression for basin erosion rate reduces to that of Bierman and Steig (1992).

The slightly more complex expression arising when erosion rates depend on elevation can be solved numerically for a number of possible erosion functions,  $\dot{\epsilon}(z)$ . If the mean erosion rate is known, for instance from modern sediment and solute fluxes, we can use departures from CRN concentrations expected from elevationally uniform erosion case (the above equation) to infer the relief generation rate,  $\dot{R} = \dot{\epsilon}_{z_{max}} - \dot{\epsilon}_{z_{min}}$ .

Among other assumptions to be discussed, the analysis requires that there be no significant sediment storage within the basin, that steady state erosion be justified, and that fluvial transport times be short relative to weathering time scales.

Bierman, P. R. and Steig, E., 1992, Using cosmogenic isotopes to measure basin-scale rates of erosion. GSA Abstracts with Programs, v. 24, p. A122.

**WATER FLOWPATHS IN A SMALL CATCHMENT DURING STEADY, ARTIFICIAL RAIN AND A NATURAL STORM**

ANDERSON, Suzanne Prestrud, DIETRICH, W.E., TORRES, R., Dept. of Geol. and Geophys., U.C. Berkeley, Berkeley, CA 94720, MONTGOMERY, D.R., QRC, Univ. of Washington, Seattle, WA 98195, and LOAGUE, K., ESPM, U.C. Berkeley, Berkeley, CA 94720, USA

The subsurface routing and residence time of water in catchments are fundamental controls on runoff chemistry. In a small, steep catchment with a thin, highly conductive soil mantle in the Coast Range of Oregon, we have found surprisingly long residence times for water and substantial flow through the bedrock. Our study site is an 860 m<sup>2</sup> unchanneled valley, with 45° slopes, and an average 1m thick colluvial soil mantling flat-lying sandstone. We have used deuterium and bromide tracers in addition to intensive piezometric, tensiometric, and geochemical measurements to document hydrologic processes during artificial sprinkler experiments and natural rainstorms.

Deuterium spiked rain tracked in 34 lysimeters during a whole-catchment sprinkling experiment moved in a slow plug-like manner through the soil vadose zone. The spiked water travelled at approximately the rainfall rate during three days of steady 1.6 mm/hr rain, reaching a maximum depth of 0.45m. In contrast, bromide injected into saturated colluvium travelled at rates similar to the saturated hydraulic conductivity of 10<sup>-1</sup> cm/s. The bromide did not appear in all of the lysimeters down-gradient from the injection point because of flow into and out of the bedrock. In summary, flow through the vadose zone is controlled by the rainfall rate, while flow through the saturated colluvium and bedrock is controlled by the saturated hydraulic conductivity.

A two component mixing model for deuterium in the runoff shows that "old" water (water on the slope before the rain event) comprises 80-90% of the storm runoff in both our spiking experiment and a natural storm we analyzed. The slow flow of water through the vadose zone in these highly conductive soils leads to this non-intuitive result. The small proportion of "new" water comes from the shallow soil near the catchment exit.

The water storage capacity of the colluvium is roughly 0.25m. A mean annual rainfall of 2.5m implies that the average residence time for water in the soil is on the order of 1 month. Storage of water in the soil can increase its dissolved organic carbon content and therefore substantially increase its weathering potential. Runoff chemistry is expected to be strongly buffered to that of the deep soil water chemistry.

## ISOTOPIC CONSTRAINTS ON AGE AND SOURCES OF SOME MINOR RAPAKIVI COMPLEXES, CENTRAL SWEDEN.

ANDERSSON, U.B., Inst. of Earth Sciences, Uppsala University, Norbyvägen 18 B, S-752 36 Uppsala, Sweden  
NEYMARK, L.A., Inst. of Precambrian Geology and Geochronology, Russian Academy of Sciences, Makarova emb. 2, St. Petersburg 199034, Russia

The suite of Fennoscandian rapakivi intrusions consists of 7 major and >10 minor plutons, distributed from Russian Karelia in the east to central Sweden in the west. We present here new isotope data on four minor intrusive complexes intruding the Svecofennian rocks in central Sweden, which on petrographical and structural grounds have been included in the rapakivi suite. Bimodal magmatism is typical and mafic to intermediate rocks dominate three of these. The granites are even-grained and lack the typical rapakivi texture, but show the characteristics of dry, high-T A-type granites.

U/Pb zircon dating was performed on two of the complexes, Mårdsjö and Mullnåset. Three single air-abraded zircon grains of the Mårdsjö granite was measured, of which one was more discordant. The weighted average of the two almost concordant grains gives the most reliable age estimate,  $1524 \pm 3$  Ma. Three almost concordant abraded grains of the Mullnåset granite give an age of  $1526 \pm 3$  Ma. Age range for Fennoscandian rapakivi plutonics was until now 1645-1540 Ma. Our ages are thus about 15 Ma younger than the previously youngest intrusion, but clearly put these complexes in this general age frame.

Nd isotope data were collected for both mafic, intermediate and granitic rocks. They all have low initial (1.52 Ga)  $\epsilon_{Nd}$ -values, in the range -8.5 to -5.7, (av. -7.1), suggesting significant involvement of older crustal components. DM-ages range from 2.16 to 2.64. However, no rocks of such ages are known in the Svecofennian (2.03-1.86 Ga). Metasediments in the region have identical  $\epsilon_{Nd}$  (1.52) values (av. -7.1) as the rapakivis, but an upper crustal peraluminous source is geochemically unlikely. Furthermore,  $^{87}Sr/^{86}Sr$  (1.52) values for rapakivi granites are much lower (0.703) than for the sediments (0.714). A metasedimentary protolith can thus be rejected. Instead the presence of a lower crustal basement beneath central Sweden, that contain a major Archean component, is indicated. The average  $\epsilon_{Nd}^{1.52}$ -value of early Svecofennian metaigneous rocks is -2.7, and similarly for Archean rocks (NE part of the Fennoscandian shield), -18.5. A generation of the felsic rocks from a mixed source requires  $\approx 40\%$  Archean material.

Perhaps most conspicuously, the mafic-intermediate rapakivi rocks show overlapping  $\epsilon_{Nd}$ -values with the granites. Since it is petrologically untenable to derive large amounts of felsic magmas from the mantle, we advocate that the mafic and felsic rapakivi rocks have different sources. The following scenario for the formation of these complexes is suggested: mafic magmas generated from an enriched upper mantle intrude the lower crust. The lower crust is composed of a heterogeneous mixture of Archean and early Svecofennian calcalkaline metaigneous rocks. Lower crustal melts (rapakivi granite magmas) are generated by the heat from the mafic magmas from a 2:5 Archean:Svecofennian source ratio. The mafic magmas are further enriched by assimilation in the lower crust. The magmas coexist and hybridize (forming intermediate magmas) and intrude to higher levels together.

The present data strongly suggest that Archean basement rocks occur much further south than previously known ( $\approx 300$  km to the north). This necessitates a revision of the tectonic models for the evolution of the shield.

## EVOLUTION FROM TRANSITIONAL TO HIGHLY ALKALIC POTASSIUM-RICH MAGMATISM IN THE NORTHERN UDOKAN VOLCANIC FIELD WITHIN THE BAIKAL RIFT SYSTEM (RUSSIA).

ANDRÉ, L., Dept. of Geology, Musée Royal de l'Afrique centrale, 3080 Tervuren, Belgium, RASSKASOV, S., Inst. of the Earth Crust, 664033 Irkutsk, Russia, IVANOV, V., Vinogradov Inst. of Geochemistry, 664033 Irkutsk, LIEGEOIS, J-P, Dept. of Geology, Musée Royal de l'Afrique centrale, 3080 Tervuren, and BOVEN, A. Vrije Universiteit Brussel, Pleinlaan, 2 1040 Brussels, Belgium.

The Udokan volcanic field (UVF) occupies a large area at the Northeast of the Baikal Lake. The northern part of this rift-related succession is composed of a sequence of 4 volcanic packages overtopped by recent cinder cones. The basaltic stratigraphic sequence range from transitional basalts (TB) (packages 1 and 3) through alkali olivine basalts (AOB) (packages 2 and cinder cones) and basanites (BAS) (package 4) to olivine melaneophelinites (OMN) and olivine melaleucitites (OML) (cinder cones). A time span from 17 Ma to 2.7 Ma is inferred for their emplacement by whole-rock K-Ar measurements. Representative samples from the whole succession were studied for major and trace (V, Cr, Co, Ni, Nb, Sr, Y, Zr, Nb, Ba, REE, Hf, Ta, Th, U) elements and Sr-Nd-Pb isotopes. The Mg number decreases from the OML (71-67) and BAS (65-60) to AOB (59-54) and TB (62-49) showing that OML and BAS could represent rather primitive melts while AOB and TB correspond to differentiated magmas.

The initial TB and AOB magmas have features (e.g.  $10 < La/Th < 14$ ;  $13 < La/Ta < 30$ ;  $0.7040 < ^{87}Sr/^{86}Sr < 0.7051$ ;  $0.51227 < ^{143}Nd/^{144}Nd < 0.51255$ ;  $15.37 < ^{207}Pb/^{204}Pb < 15.39$ ;  $17.83 < ^{206}Pb/^{204}Pb < 17.95$ ) which are compatible with a rather significant contribution of some Rb-U-Th depleted lower crustal material in their source. In contrast, the following AOB and BAS have typical OIB geochemical features except higher K/Yb, Ba/La and Ce/Pb ratios in the range of those obtained for the basalts of the western branch of the African Rift System. The decrease with time of the crustal contribution is confirmed with the late eruption of the OML that show typical OIB signatures for all the parameters.

From these preliminary data, we infer that the evolution of transitional to highly alkalic potassium-rich magmatism at the eastern Baikal Rift System was controlled by a gradual increase in the proportion of enriched sub-continental lithospheric derived melts (leucitites) over lower/intermediate mantle-derived melts (TB-AOB) through time. This is coupled with a decrease of the crustal contamination rate.

HIGH COOLING RATES AND TECTONIC UNROOFING IN THE INTERNAL ZONE OF THE ALPINE BELT OF THE BETIC CORDILLERA, S SPAIN, DURING EARLY MIOCENE NAPPE EMPLACEMENT : ADDITIONAL CONSTRAINTS FROM FISSION TRACK ANALYSES

ANDRIESEN, P.A.M., M. RÖRHMANN, P. VAN DER BEEK AND C. SANDERS, Institute of Earth Sciences, Vrije Universiteit De Boelelaan 1085, 1081 HV Amsterdam, The Netherlands.

The Betic Cordillera in southern Spain belongs to the western termination of the Alpine Belt of Europe and Africa. The Internal Zone of the Betic Cordillera consists of three nappe complexes of variable metamorphic grade. The stratigraphic sequences of these nappes are roughly comparable and consist of pre-Permian-Triassic basement, Permian-Triassic pelitic sequence, and Triassic carbonate rocks. On top or between nappes Early Miocene marine transgressive formations are found and they are interpreted as tectonic seals after emplacement of the Mesozoic nappe complex of the Internal Zone.

Previous Sm-Nd and Rb-Sr analyses of the basement dated the emplacement of the Alpujarride nappe at  $22 \pm 2$  Ma, Aquitanian-Burdigalian. K-Ar and Ar-Ar dating of mica's of the (pre) Permian-Triassic mica schists and gneisses from this nappe complex yielded cooling ages between 18.8 and 20.3 Ma. All the geochronometers pointed to very high cooling rates of 200-300°C/Ma during nappe emplacement. However, the cooling trajectory could only be determined to temperatures down to some 350°C and no information is available on the low temperature side.

A fission track analysis program was performed to constrain the cooling to (near) surface temperatures. Samples of the Torrox-gneiss body, occurring within the Alpujarride nappe complex, gave F.T. ages of  $18.9 \pm 2.1$  Ma and between 20-15 Ma for one zircon and nine apatites concentrates, respectively. The zircon age, representing cooling to below 200°C, supports the previous conclusion of very high cooling rates during Early Miocene nappe emplacement. The apatite ages display a range, but a mean age of  $16.6 \pm 0.8$  Ma is calculated for 126 individual apatite grains from 7 apatite samples with mean spontaneous fission track lengths of between 14 and 14.7 µm. The mean apatite age of the Torrox-gneiss of  $16.6 \pm 0.8$  Ma is interpreted to represent the time of cooling to below 50°C. This conclusion seems to be in error with the paleontological dating of  $19 \pm 1$  Ma of the marine transgressive Vinuela formation, that seals of the Triassic carbonate rocks of the youngest stratigraphic unit of the Alpujarride nappe complex.

P-T-t determinations suggest that the Alpujarride basement rocks underwent medium to high temperature metamorphism of 575°C and 4-6 kbar, some  $22 \pm 2$  Ma ago. The assumption of an ambient high thermal gradient of 50°C/Ma would still imply tectonic unroofing of at least 10 km at the end of the orogenic development in the Betic Cordilleras. Similar amounts of tectonic unroofing are not uncommon for active margins or continent-continent collision zones.

Orogenic models explaining late Oligocene and early Miocene extension and compression regimes during the Alpine orogeny of the Betic Cordilleras in southern Spain, must take into account the constraints derived from the fission track analyses

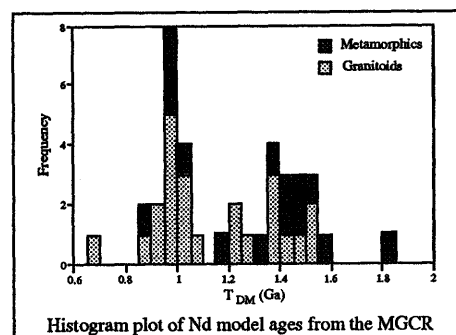
ND- AND SR-ISOTOPIC CONSTRAINTS ON THE EVOLUTION OF THE MID GERMAN CRYSTALLINE RISE, VARISCAN FOLD BELT

ANTHES, G. and REISCHMANN, T., Institut für Geowissenschaften, Johannes Gutenberg-Universität, 55099 Mainz, Germany

Granitoids and metamorphic rocks from the Mid German Crystalline Rise (MGCR), which represents a belt of igneous and metamorphic rocks within the east-west trending Saxothuringian zone of the Variscan fold belt of central Europe were investigated in order to evaluate crustal residence ages and characterize Sr and Nd isotopic signatures of distinct crustal segments.

The analysed metamorphic rocks comprising felsic gneisses and amphibolites yield  $\epsilon_{Nd}(T)$ -values ranging from -4.8 to +2.7 and  $^{87}Sr/^{86}Sr$  initial ratios from 0.7040 to 0.7523. The granodiorites, granites and some rare gabbros and diorites provide a large spread in  $\epsilon_{Nd}(T)$ -values from -5.9 to +4.3 and in the  $^{87}Sr/^{86}Sr$  initial ratios from 0.7039 to 0.7543 which is similar to the range observed in the metamorphic samples.

Calculated Nd model ages from the MGCR vary from 0.67 to 1.54 Ga for the granitoids and from 0.88 to 1.81 Ga for the metamorphic rocks indicating a slightly older provenance.



These data from the MGCR are in contrast to crustal residence ages of plutonic rocks from the Moldanubian zone such as granitoids of the Schwarzwald and Bohemian Massif and granites from the Harz mountains of the Rhenohercynian zone which show a very narrow variation between 1.4 and 1.7 Ga whereas the metamorphic rocks from these regions vary between 1.3 and 3.0 Ga (Liew & Hofmann, 1988). The lower model ages of the MGCR can be explained by a larger amount of juvenile Palaeozoic material added to this segment of the Saxothuringian zone in comparison to the other parts of the Variscan belt with incorporated more Archean and Proterozoic material.

The results of this isotope study indicate that the MGCR can be interpreted as a distinct terrane within the main structures of the central European Variscan fold belt.

Liew, T.C., and Hofmann, A.W., 1988, Precambrian crustal components, plutonic associations, plate environment of the Hercynian Fold Belt of central Europe: Indications from a Nd and Sr isotopic study: Contrib. Mineral. Petrol, v. 98, p. 129-138.

GEOCHRONOLOGY AND PALEOMAGNETISM OF  
THE QUATERNARY POTRILLO VOLCANIC FIELD,  
RIO GRANDE RIFT, NEW MEXICO

ANTHONY, E.Y., Geol, Univ TX, El Paso, 79968;  
MCINTOSH, W.C., Geochron Lab, NM Inst Min &  
Tech, 87801; POTHS, J., INC-6, LANL, NM, 87545;  
WILLIAMS, W.J.W., Geol, Univ TX, El Paso, 79968;  
WHITELAW, M., Geol, Univ TX, El Paso, 79968; and  
GEISSMAN, J., E&PS, Univ NM, 87131.

We report preliminary results on the chronology (using a combination of  $^3\text{He}$  surface exposure and  $^{40}\text{Ar}/^{39}\text{Ar}$  dating) and paleomagnetism of the Potrillo volcanic field. This field includes cones, flows and maars and is considered here as three geographic sections: western, central and eastern. Data indicate that the western part of the field has had the greatest longevity, resulting in more than 200 cones and flows with some cones clearly more degraded than others. Our study shows that the majority of the field erupted during the Bruhnes chron; we have, however, documented reverse polarities for several flows emanating from more eroded cones in the western part of the field. A flow from this area yields an  $^{40}\text{Ar}/^{39}\text{Ar}$  date of  $823 \pm 14$  ka (determined using furnace step-heating).

The presence of feldspar megacrysts in many flows allows us to investigate the suitability of pairing megacryst and host rock analyses for high precision  $^{40}\text{Ar}/^{39}\text{Ar}$  dating. One such pair gives dates of  $521 \pm 17$  ka from a feldspar megacryst and  $475 \pm 23$  ka for its basanitic host. Our research is also focussed on determining the oldest flows for which we can obtain reliable  $^3\text{He}$  surface exposure dates. The oldest surface we have dated thus far is from a flow near Malpais Maar, situated in the western part of the field. It yields an exposure date of  $274 \pm 15$  ka; we are currently obtaining an  $^{40}\text{Ar}/^{39}\text{Ar}$  date for this flow. Another flow in the vicinity yields an  $^{40}\text{Ar}/^{39}\text{Ar}$  date of  $249 \pm 12$  ka.

A number of surface exposure dates for the central part of this field support the youthful geomorphology observed. The Afton flows, through which Kilbourne Hole maar erupted, are  $101 \pm 7$ ,  $114 \pm 7$  and  $120 \pm 8$  ka for three samples from separate units. (Uncertainties on surface exposure dates represent fully propagated analytical errors; they do not reflect uncertainties in production rate.) Flows from within the Potrillo maar depression, located 10 km south of the Afton flows, yield dates of  $69 \pm 6$  and  $76 \pm 6$  ka. The youngest dates in the Potrillo field are from Aden Crater, a spatter ring complex northwest of the Afton flows. Samples from an interior spatter cone, lava lake and breach flows yield dates of  $20.9 \pm 4.3$ ,  $21.4 \pm 3.3$ ,  $23.3 \pm 4.1$ , and  $24.2 \pm 3.5$  ka. We are acquiring  $^{40}\text{Ar}/^{39}\text{Ar}$  dates for all of the features in this section of the field.

The eastern part of this field is an alignment of several cones. Surface exposure dates on two separate flows from Black Mountain, the southernmost cone, yield  $101 \pm 9$  and  $84 \pm 7$  ka. An  $^{40}\text{Ar}/^{39}\text{Ar}$  date on the first flow gives  $127 \pm 9$  ka. Also although we have not seen geomorphic evidence for polycyclicality at this cone, we have a second  $^{40}\text{Ar}/^{39}\text{Ar}$  date of  $184 \pm 10$  ka.

SR-ND ISOTOPIC AND GEOCHEMICAL  
CHARACTERISTICS OF THE TWO TYPES OF  
GRANITIC PLUTONS IN THE HIDA BELT,  
JAPAN

ARAKAWA, Y., Earth Sci., Faculty of Education,  
Saitama University, Urawa, Saitama, 338, Japan

Late Triassic to early Jurassic igneous activity occurred in the Hida belt, which is the northern-most geotectonic unit in the Inner Zone of Southwest Japan and is considered to have occupied a marginal part of the Sino-Korean craton before the Southwest Japan arc drifted away from the craton at 15 Ma. The igneous activity produced various sizes of calc-alkaline granitic plutons which show wide varieties of lithology, chemistry and internal structures of the pluton.

Based on the chemical compositions, and Sr and Nd isotope data, the plutons are grouped into two types (Type 1 and Type 2). The Type 1 is the pluton with a limited range of variations in initial Sr and Nd isotope ratios ( $\epsilon\text{Sr}=+1.4$  to  $+15.9$ ;  $\epsilon\text{Nd}=-0.8$  to  $+5.5$ ) irrespective of the variety of rock compositions, whereas the Type 2 pluton has wide variations of isotope ratios ( $\epsilon\text{Sr}=+17.8$  to  $+89.0$ ;  $\epsilon\text{Nd}=-10.3$  to  $+0.7$ ), forming a linear data array connecting a mafic rock and basement gneisses in the  $\epsilon\text{Nd}-\epsilon\text{Sr}$  diagram. These isotope data and element characteristics (including REE) of the rocks suggest that there were contrasting differences in magma source and dominant process of magma formation between Type 1 and Type 2 plutons. The rocks of the Type 1 pluton are interpreted to have been formed mostly by fractional crystallization from a parental mafic (to intermediate) magma with lesser amounts of crustal contributions, while those of the Type 2 pluton are explained by the mixing between a parental mafic magma and the middle Proterozoic crustal materials (or crust-derived felsic melt). Mafic rock units (gabbro and diorite) which correlate to the parental mafic magma yield the lowest Sr and highest Nd isotope ratios within the pluton, and they possibly represent isotope compositions of their source regions (subcontinental mantle). Two contrasting types of plutons, being attributed to the differences in the magma source and the main mechanism of magma production, reflect the across arc difference in the Mesozoic crust-mantle structure beneath the Hida belt.

## THE KAAPVAAL CRATON - A CHRONOLOGY OF 1.6 BILLION YEARS OF CRUSTAL GROWTH

ARMSTRONG, R.A., Department of Geological Sciences, University of Cape Town, Rondebosch 7700, South Africa.

The Kaapvaal Craton in southern Africa contains a near complete record of Archaean and Early Proterozoic Earth history. As one of the best-preserved and most intensely studied areas of the Earth's early continental crust and lithosphere, the Kaapvaal Craton has provided unique information which has contributed greatly to the formulation of fundamental global models concerned with the growth and evolution of continents over this time span. A number of these models have lacked the essential constraints on events and processes provided by precise modern geochronology and isotope geochemistry. In recent years, however, intensive U-Pb zircon geochronology in particular, together with integrated radiogenic and stable isotope, geophysical, structural, field and tectonic studies have shed new light on the development of the Kaapvaal Craton, including the recognition, definition and inter-relationships between Archaean sub-terrains, the timing and correlation of major intra- and inter-continental events, the evolution of granite-greenstone belts and the development of the thick, stable continental lithosphere. This paper reviews these developments and presents new U-Pb zircon data from the craton.

The earliest history of the craton is recorded in the Ancient Gneiss Complex (AGC) and the Barberton Greenstone Belt (BGB), where detailed U-Pb zircon geochronological studies have revealed a complex chronology starting some 3.65 Ga ago and continuing episodically for approximately 800 Ma. This core region (shield) of the craton comprises several well-defined tectono-stratigraphic terrains, each with its own history prior to amalgamation about 3.2 Ma ago. Xenocrystic zircons and Sm/Nd studies indicate the presence of substantially older, already evolved continental crust and the extent of recycling of this material in the growth of the shield region.

Extensive intra-crustal melting and emplacement of a granitic basement marked the consolidation of the crust into a stable continental platform by 3.1 Ga. The next 1.1 Ga is characterized by the craton-wide development of large mineralized volcano-sedimentary intracratonic basins (*viz.* the Dominion, Witwatersrand, Pongola, Ventersdorp and Transvaal sequences), features which have been modelled as being characteristic of the transition from the Archaean to the Proterozoic. New U-Pb zircon data show that they are Archaean features with previous dating underestimating the ages of these sequences by up to 500 Ma. Near-continuous chronostratigraphic records in some sequences show that these basins formed over extraordinarily long periods of time, of the order of several hundreds of millions of years.

Precise U-Pb zircon geochronology has provided important insights into the inter-relationship between tectonic processes which operated and controlled continental crustal development in the Archaean/Early Proterozoic in southern Africa.

## DATING OF HIGH PRESSURE METAMORPHISM WITH A NEW HIGH RESOLUTION ULTRA-VIOLET LASER ABLATION MICROPROBE $^{40}\text{Ar}/^{39}\text{Ar}$ TECHNIQUE: DORA MAIRA, WESTERN ALPS, ITALY.

ARNAUD, N.O., and KELLEY, S.P., Dpt. of Earth Sciences, Open University, Milton Keynes, UK

Ultra-high pressure eclogite/amphibolite grade metamorphism of the Dora Maira Massif in the western Alps is a well established and intensively studied event. However, the age of peak metamorphism and early cooling remains controversial.  $^{40}\text{Ar}/^{39}\text{Ar}$  step-heating and laser spot ages from high pressure phengites yield plateau ages as old as 110 Ma which has been interpreted as the time of early cooling after the high pressure event. Recent U/Pb and Sm/Nd results challenge this assertion, indicating a much younger age for the event, around 45 Ma and thus obviously a radically different tectonic evolution for the western Alps. In a new approach to the problem, samples from the undeformed Hercynian metagranite, Brossasco, were studied using an ultra-violet laser ablation microprobe technique for  $^{40}\text{Ar}/^{39}\text{Ar}$  dating. The new technique allowed selective in situ analysis, at a spatial resolution of 50  $\mu\text{m}$ , of quartz, phengite, biotite and K-feldspar. The results demonstrate the frequent occurrence of excess argon with high  $^{40}\text{Ar}/^{36}\text{Ar}$  ratios (1000-10000) and a strong relationship between apparent ages and metamorphic textures. The highest excess argon ratios are always associated with high closure temperature minerals or large diffusion domains within single mineral phases. The best interpretation of this relationship seems to that excess argon incorporated in all phases during the high pressure event, mixed with an atmospheric component during rapid cooling and retrogression, producing the wide range of  $^{40}\text{Ar}/^{36}\text{Ar}$  ratios. Step-heating of minerals which have experienced time integrated growth of this initial mixture will produce linear arrays on a  $^{36}\text{Ar}/^{40}\text{Ar}$  vs  $^{39}\text{Ar}/^{40}\text{Ar}$  correlation diagram, leading to geologically meaningless plateau ages, older than the real time of closure to argon diffusion. Though the results of in situ analysis and modelling do not rule out the existence of a Cretaceous high pressure metamorphism in the Dora Maira, they strongly suggest that ages in the range 60-110 Ma are best explained by the presence of excess argon incorporated around 45 Ma ago, reconciling argon geochronometers with other systems such as U/Pb or Sm/Nd. The common occurrence of excess argon in high-pressure phases from the Alps and other areas reflects crystallisation in the presence of deep crustal or mantle fluids followed by rapid exhumation and as such, Ar-Ar analysis of single separated phases, may be misleading.

## ABSOLUTE TIMING OF THRUST FAULTING - A THERMOCHRONOLOGICAL APPROACH

ARNE, D.C., Fission Track Research Laboratory,  
Dalhousie University, Halifax, Nova Scotia B3H 3J5,  
Canada.

The absolute timing of movement across thrust faults has important implications for both the tectonic and kinematic evolution of thrust belts. Absolute timing constraints provide a link between regional tectonics and structural development at a local scale, whereas kinematic models for fold and thrust belts generally assume a particular chronology for the formation of structures that is often untested. Apatite fission track thermochronology has the potential to provide absolute timing constraints at shallow erosional levels in fold and thrust belts if it is accepted that distinct breaks in cooling history across discrete structures are related to the denudation of actively thrusting plates. In practice, fold and thrust belts are often deeply eroded, such that low-temperature thermochronometers often only provide evidence for regional cooling.

An approach involving the integration of vitrinite reflectance data and apatite fission track thermochronology is proposed to assess this potential limitation. Both theoretical and empirical considerations suggest that fission tracks in apatite will be totally annealed at  $R_o$  values between 0.7 and 0.9%. Thus in sedimentary rocks containing vitrinite, it is possible to evaluate the degree of regional cooling to have affected a fold and thrust belt, and to predict whether fission tracks in apatite were likely to have been totally annealed prior to regional cooling. Contrasts in cooling history across specific structures can also be recognized using vitrinite reflectance data allowing those sites favorable for thermochronometric analysis to be identified. In general, a situation in which fission tracks in apatite from the hangingwall of a thrust fault have been totally annealed ( $R_o > 0.8\%$ ), whereas those in the footwall were only partially annealed ( $R_o < 0.8\%$ ) is favored for detailed apatite fission track thermochronology.

Across the Burnt Timber Thrust in southwest Alberta (Rocky Mountain Foothills, Canada),  $R_o$  values vary from  $\sim 0.6\%$  in the footwall to  $\sim 1.5\%$  in the hangingwall. Fission tracks in apatite in the hangingwall of this structure were totally annealed prior to the onset of track retention during the early Tertiary. By contrast, early Tertiary sedimentary rocks from the footwall of the Burnt Timber Thrust give Late Cretaceous apatite fission track ages, consistent with fission tracks in these samples having been only partially annealed following deposition. Apatite fission track data from the hangingwall of the Burnt Timber Thrust are therefore interpreted to indicate cooling during late-stage thrusting.

Apatite fission track ages from western Sichuan Province, China vary dramatically from 100 to 200 Ma in sedimentary rock samples from the western Sichuan Foreland Basin, at elevations of  $\sim 1$  km, to less than  $\sim 10$  Ma in the southwest Songpan-Garzê Fold Belt, at elevations between 1 and 4 km. The observed reduction in apatite fission track age occurs rapidly across the intervening southern Longmen Mountains Thrust-Nappe Belt in which southeast-verging thrust faults have brought Proterozoic basement complexes to relatively high structural levels. Thus Late Miocene cooling of the southwest Songpan-Garzê Fold Belt is attributed to denudation driven by the reactivation of inferred Late Triassic structures.

## THE COMPOSITION OF THE SOLAR NEBULA: NU- CLEOSYNTHESIS CONTRIBUTIONS TO THE BULK MATERIAL AND TO THE ISOTOPIC ANOMALIES

ARNOULD, M., Institut d'Astronomie et d'Astrophysique,  
Université Libre de Bruxelles, B-1050 Bruxelles,  
Belgium

There is now ample observational evidence that the solar system is made of material from compositionally different and imperfectly mixed reservoirs.

One of them, which comprises the bulk solar system material, is considered to be made of the well-homogenized ashes of many nucleosynthesis events. Its composition can be studied through models of the chemical evolution of the Galaxy. The main nucleosynthetic agents responsible for that evolution are very briefly reviewed.

The remaining, very minute, fraction of the solar system material exhibits anomalies (with respect to the bulk) in the isotopic composition of a variety of elements from carbon to neodymium (including the rare gases). It is carried in part by high-temperature inclusions of primitive meteorites that formed from solar reservoirs out of equilibrium with the rest of the solar nebula, and in part by various types of grains (diamond, graphite, SiC found in, mostly carbonaceous, chondrites) that are considered to be of circumstellar origin, and have survived the process of incorporation into the solar system.

The isotopic anomalies provide new clues to many important astrophysical issues, and raise in particular the question of their nucleosynthetic origin. In fact, they offer the exciting perspective of confronting abundance observations with nucleosynthesis models for a very limited number of events. This situation is in marked contrast with the one encountered when trying to understand the bulk solar system composition.

Some selected examples are given to illustrate the potential diversity of nucleosynthetic sources (Red Giant or massive mass losing stars, novae, supernovae) that might have produced the isotopically anomalous material. Some difficulties encountered by and uncertainties involved in the nucleosynthesis models that try to interpret the array of observed anomalies are stressed.

## ILLITE/SMECTITE, A VALUABLE K/AR CLOCK FOR THE SECONDARY HISTORY OF SEDIMENTARY BASINS

ARONSON, James L., Department of Geology, Case Western Reserve University, Cleveland, OH 44106, USA and ELLIOT, Crawford, Case Western Reserve University, Cleveland, OH 44106, USA.

The mineralogic continuum between very thin particles of the clay minerals smectite (non K-bearing) and illite (K-bearing) is called Illite/Smectite (I/S), the most common family of clay minerals. The degree of illitization of I/S is quantifiable by XRD from 0 - 100%. In mudstones, smectite exposed to diagenetic temperatures and fluids converts to I/S, whereas in sandstones neofomed illite grows as a common cement in the pore space.

I/S is an excellent clock by conventional K/Ar, e.g. equivalent to hornblende if not reheated after formation. Remarkable for sub-micron sized grains, its blocking temperature is at least 180° C.

The conversion of smectite to illite in mudstones accelerates at 80° - 100° C, the same temperature range over which hydrocarbons form. Observing the degree of transformation of smectite to illite and dating the mean time of transformation quantifies the thermal history of sedimentary basins. The least ambiguous dates are obtained on K-bentonites, which begin as pure smectite, without the detrial illite present in shales. We have related K/Ar dates of K-bentonites to the mean time of deep burial diagenesis in sedimentary basins; to the time of overthrusting and tectonic burial of sediments in proximal parts of foreland basins; and to the passage of hot brines in distal parts of foreland basins which have been flushed there during tectonic collapse of the proximal basin.

In the pore space of siliciclastic sandstones, neofomed whisker-like ribbons of I/S have grown in response to the passage of brines accompanying oil and gas migration. The I/S growth is inhibited in the oil and gas zones of these reservoir rocks. In ideal conditions, as for the Rotliegendes of the North Sea area, hydrocarbon emplacement can be dated.

Conventional K/Ar is the method of choice for I/S. At some increased size, thicker 100% illite (approaching sericite) may be large enough to date by  $^{40}\text{Ar}/^{39}\text{Ar}$ .

## PROPORTIONS OF JUVENILE AND RECYCLED CRUST IN A PALEOZOIC CONTINENTAL COLLISION ZONE, NORTHERN APPALACHIANS OF NEW ENGLAND, U. S. A.

ARTH, JOSEPH G., US Geological Survey, Menlo Park, CA 94025 USA; and AYUSO, Robert A., US Geological Survey, Reston, VA 22092 USA

Detailed petrologic, chemical, and isotopic-tracer studies of a suite of Acadian plutons in the northern Appalachians of Vermont provide insight into the proportions of magma that are added to the crust, or recycled from the deeper crust during a collision of cratons- in this case the North American and outboard terranes that collided during the Paleozoic. The plutons were intruded into metasediments of the Connecticut Valley- Gaspe synclinorium, and were chosen for genetic study because they form a complete suite of largely calc-alkaline character, and range from gabbro through diorite, tonalite, quartz monzodiorite, and granodiorite, to one- and two-mica granites; and they were emplaced in a part of the Appalachians that has been little affected by post-Acadian regional metamorphism.

Rb-Sr isochrons indicate that most of the plutons were emplaced from 380 to 370 million years ago. Their initial Sr ratios have a wide range from 0.7040 to 0.7125.

Oxygen isotopes also have a large range of delta values from +6 to +14. Nd initial ratios range from .51177 to .51213, and initial  $^{206}\text{Pb}/^{204}\text{Pb}$  from 18.13 to 18.46.

The isotopic and chemical features of the plutons and zones within plutons suggest subdivision into three groups, each having a different origin. Group 1 consists of gabbro, diorite, and granodiorite that are generally of magmatic-arc composition. The magma sources were dominated by either a mafic to ultra-mafic assemblage in the mantle or deepest crust, or an Acadian subduction zone. Group 2, representing the largest volume of magma, consists of quartz monzodiorite, granodiorite, and granite that probably originated by melting of lithologically-diverse assemblages of Grenville gneisses in the deep crust. The sources for Group 2 were mostly orthogneisses, but paragneisses were also involved. Group 3 consists of a small volume of two-mica granite that has the features of melts from country-rock metasediments.

Viewed collectively, the plutons preserve a record of melting in a significant vertical section extending from the mantle to the middle crust. About 20 percent of the magma was generated in mafic to ultramafic mantle and deepest crust. Nearly 80 percent was generated in Grenville-age gneisses, and much of this was orthogneiss. Less than 20 percent resulted from melting of metasediments. Thus the Acadian collisional orogeny in this area largely represented a recycling of older crustal rocks.

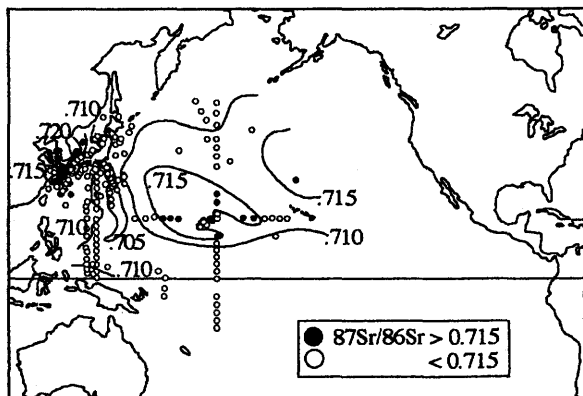
CONTINENTAL NATURE OF  $^{87}\text{Sr}/^{86}\text{Sr}$  RATIOS IN THE NORTH CENTRAL PACIFIC SEDIMENTS

Asahara, Y., Tanaka, T., Dept. of Earth and Planetary Sciences, Nagoya University, Nagoya, 464-01, Japan, Kamioka, H. and Nishimura, A., Geological Survey of Japan, Tsukuba, 305, Japan.

$^{87}\text{Sr}/^{86}\text{Sr}$  ratios were examined for 171 deep-sea and continental-shelf surface sediments from the Pacific Ocean to estimate the provenance of them. Carbonates in sediments, which would inherit an isotopic signal from seawater, were leached with 0.25 to 1.0N-HCl for 1 hour. Sr isotopic compositions in the residues were determined by thermal ionization mass spectrometry after chemical separation of Sr.

Major characteristics of spatial variation of Sr isotopes and their interpretations are summarized as follows; (1) Sediments in the Pacific Ocean have a lower average of  $^{87}\text{Sr}/^{86}\text{Sr}$  ratios (0.7110) and narrower range (0.703 to 0.723) than those in the Atlantic Ocean (0.7166, 0.704 to 0.743; Dasch, 1969).  $^{87}\text{Sr}/^{86}\text{Sr}$  ratios higher than 0.720 occur on the north side of 30 degree south latitude in the Atlantic, while, in the Pacific, ratios higher than 0.720 occur only in and around the Yellow Sea. Large old continental crusts supply materials of high  $^{87}\text{Sr}/^{86}\text{Sr}$  ratio to the Atlantic, while many volcanos in the circum-Pacific volcanic belt, including the Izu-Ogasawara, Mariana and Japan island arcs, and young continental crusts supply those of low ratios. (2)  $^{87}\text{Sr}/^{86}\text{Sr}$  ratios are high in the north central Pacific (0.711 to 0.719). The areas of higher ratios (>0.715) are limited on the abyssal plain. On the abyssal plain, the farther from the Izu-Ogasawara and Mariana island arcs to east, the higher  $^{87}\text{Sr}/^{86}\text{Sr}$  ratios are. This is due to relatively abundant supply of loess from the Asian continent ( $^{87}\text{Sr}/^{86}\text{Sr}$ =ca.0.720) to the north central Pacific Ocean by middle-latitude westerlies, which is more predominant input to the area compared with volcanogenic input from the Izu-Ogasawara and Mariana island arcs (ca.0.704) by ocean current.

A part of this work is Northwest Pacific Carbon Cycle (NOPACC) study consigned to Kansai Environmental Engineering Center (KEEC) by NEDO and a special program of MITI, studying on element cycles in the Oceans.



DATING ORDINARY CHONDRITE INCLUSIONS BY LASER  $^{40}\text{Ar}$ - $^{39}\text{Ar}$  AND LASER/RIMS I-Xe

ASH R.D., GILMOUR J.D., TURNER G. Dept. of Geology, University of Manchester, Manchester, M13 9PL, UK, BRIDGES J.C. and HUTCHISON R. Mineralogy Dept., Natural History Museum, London SW7 5BD, UK.

Ar-Ar dating using laser probe techniques has been widely used in the analysis of small terrestrial samples. However fewer applications to extraterrestrial samples have been reported despite there being many potentially interesting problems to which this technique could be applied. We have used an IR ( $\lambda=1060\text{nm}$ ) laser for the extraction of gas for Ar-Ar dating of clasts separated from ordinary chondrites. Clasts of this type have been described as xenoliths and may have an exotic origin, although an origin as reprocessed host material cannot be discounted. Although these samples are generally larger than chondrules the desire to characterise the samples in other ways led to the allocation of only 0.5-2 mg sized samples hence stepped heating analysis was impractical. The laser probe allows the extraction of multiple gas aliquots for the determination of  $^{40}\text{Ar}/^{39}\text{Ar}$  ratios and the subsequent construction of an isochron.

Barwell: The Ar-Ar age determined by laser extraction for a large H-group, re-equilibrated clast was identical (4.48Gyr) to that determined for whole rock sample by stepped heating (1). This supports the inference that the analysis of small samples by laser is applicable to meteoritic material

Parnallee: Large porphyritic clasts, one silica and K-rich, the other containing Mg-rich olivine, gave Ar-Ar ages of 3.45 ( $\pm 0.06$ ) and 3.57 ( $\pm 0.13$ )Gyr whereas whole rock stepped heating indicates a highly disturbed system with an integrated age of ca. 2.9Gyr.

Quenggouk: A large porphyritic clast gave an anomalously high Ar-Ar age of 4.63( $\pm 0.038$ )Gyr. The material in this inclusion includes mosaiced olivine with blebs of Fe-Ni metal and may have been shock produced. This can lead to anomalously old Ar-Ar ages as observed in shock melt veins in the ordinary chondrite Peace River (2) although the existence of a well defined isochron in Quenggouk would make this appear an unlikely explanation.

Julesburg: An age of 0.95Gyr was determined for a large olivine crystal poikilitically enclosing anorthite, but Julesburg shows evidence for shock hence this young age could be due to shock resetting of the Ar age. The inclusion from Isoulane gives an age indistinguishable from that of Julesburg.

Initial results from high sensitivity [3] I-Xe work on Parnallee inclusions suggest that some of the complexities observed in the whole rock Ar-Ar stepped heating analyses are attributable to a mixture of degassed material, apparently resulting from shock ca. 1Gyr ago, and material which has retained its full complement of gas during the shock event or did not experience a shock heating event.

- [1] Turner G. *et al.*, 1978, The early history of chondrite parent bodies inferred from  $^{40}\text{Ar}$ - $^{39}\text{Ar}$  ages: Proc. Lunar Planet. Sci. Conf., 9, 989-1025.
- [2] McConville P. *et al.*, 1988, Laser probe  $^{40}\text{Ar}$ - $^{39}\text{Ar}$  studies of the Peace River shocked L6 chondrite: Geochim. Cosmochim. Acta, 52, 2487-2499.
- [3] Gilmour J.D. *et al.*, 1994, RELAX: An ultrasensitive, resonance ionisation mass spectrometer for xenon: Rev.Sci. Inst. (in press).

**<sup>40</sup>Ar/<sup>39</sup>Ar SYSTEMATICS IN A DIAGENETIC- TO CONTACT METAMORPHIC-GRADE CLAY MINERAL SUITE, NORTHERN NORTH SEA**

**AWWILLER, D. N., BURGESS, R., AYLIFFE, L. K., and TURNER, G.,** Department of Geology, University of Manchester, Manchester M13 9PL, United Kingdom.

Clay mineral size-separates from a suite of diagenetic- to contact metamorphic-grade mudrocks (ca. 150-600 °C) have been studied in order to ascertain the extent to which illite and illite/smectite Ar systematics are dependant upon grain size and crystallinity (i.e. temperature of formation). All samples investigated are from late Cretaceous mudrocks, collected from a well drilled in the Møre Basin, located northeast of the Shetland Islands. Numerous late Cretaceous or Paleocene sills have intruded the sediments, and as a result the samples have experienced widely different maximum temperatures.

Samples were encapsulated prior to irradiation to contain recoil <sup>39</sup>Ar. It was found that the fraction of <sup>39</sup>Ar which recoils out of the clay mineral lattice decreases not only with increasing particle size, but also with increasing mineral crystallinity (i.e. formation temperature). For example, the lowest diagenetic grade, <0.1 µm clay fraction has lost ca. 50% of its <sup>39</sup>Ar by recoil, compared with the 1-2 µm size fraction from the same sample which has lost only 16% of its <sup>39</sup>Ar. The 1-2 µm size fraction from the highest-temperature sample has lost only 4% of its total <sup>39</sup>Ar from recoil, or 25% of the <sup>39</sup>Ar lost by the equivalent low-temperature size fraction.

Step-heating experiments reveal the presence or absence of contaminating detrital material in diagenetic-grade clay fractions which would be undetectable by conventional K/Ar and total-fusion <sup>40</sup>Ar/<sup>39</sup>Ar dating techniques. Low temperature steps (≤400 °C) release <sup>40</sup>Ar\* and <sup>39</sup>Ar which, when re-combined with recoil <sup>39</sup>Ar, appear to record reasonable diagenetic ages; this low-temperature Ar is interpreted to be released from fine-grained authigenic illite and illite/smectite. Subsequent higher-temperature steps (450-600 °C) release more elevated <sup>40</sup>Ar\*/<sup>39</sup>Ar, corresponding to much greater than depositional ages. These higher temperature-released ages are presumably from detrital illite or mica. Samples which have been heated to somewhat greater maximum temperature (ca. 300 °C) produce step-heated age spectra similar to those of the low-temperature samples, but with lower maximum ages, which suggests that the Ar systematics of the detrital component have been partially reset during the heating event.

The samples which have been heated to the greatest degree yield consistent <sup>40</sup>Ar/<sup>39</sup>Ar ages (64 ± 4 Ma) over 60-70% of their <sup>39</sup>Ar release range. The ages are in accordance with K/Ar ages reported for the adjacent sill complex, and their consistency over broad Ar-release temperatures suggests that they have not been reset since the time of sill intrusion.

**STABLE ISOTOPE EVIDENCE FOR THE ORIGIN OF DIAGENETIC CARBONATE MINERALS FROM THE LOWER JURASSIC INMAR FORMATION, SOUTHERN ISRAEL**

**AYALON, A.,** Geological Survey of Israel, 30 Malkhe Yisrael Street, Jerusalem 95501, Israel, and **LONGSTAFFE, FRED, J.,** Department of Geology, University of Western Ontario, London, Ontario Canada N6A 5B7

The oxygen and carbon isotope compositions of diagenetic minerals from the Lower Jurassic Inmar Formation, southern Israel are used to identify changes in pore-water composition during diagenesis. These changes can be related to major geologic events within southern Israel. Saline water has played an important role in the formation of diagenetic dolomite and ferroan dolomite/ankerite cements in these rocks on a basinwide scale during the Pliocene-Pleistocene.

Diagenetic carbonate phases include early siderite ( $\delta^{18}\text{O}_{\text{SMOW}} = +24.4$  to  $+26.5$  ‰;  $\delta^{13}\text{C}_{\text{PDB}} = -1.1$  to  $+0.8$  ‰) followed by dolomite and ankerite ( $\delta^{18}\text{O}_{\text{SMOW}} = +18.4$  to  $+26.3$  ‰;  $\delta^{13}\text{C}_{\text{PDB}} = -2.1$  to  $+1.3$  ‰). Calcite shows a much larger range ( $\delta^{18}\text{O}_{\text{SMOW}} = +21.3$  to  $+32.6$  ‰;  $\delta^{13}\text{C}_{\text{PDB}} = -4.2$  to  $+3.2$  ‰).

These results indicate that shallow burial, early in the diagenetic history included formation of siderite and early calcite cements. Further burial led to formation of dolomite and late calcite cements. Ankerite formation took place late in the diagenetic history.

A significant negative correlation obtained between burial depth and the  $\delta^{18}\text{O}$  composition of the dolomitic cements indicates that dolomite formation postdated the tectonic activity and uplift that formed the present relief of southern Israel, most likely following Pliocene migration of subsurface brines.

The  $\delta^{18}\text{O}$  composition of the dolomites in the northern Negev and Judea Mountains is in perfect accord with that of the present-day formation waters whereas formation waters in the central Negev have much lower salinity and  $\delta^{18}\text{O}$  values, indicating invasion of fresh water. Recharge of the Inmar Formation by low  $^{18}\text{O}$  meteoric water occurred in the Pleistocene, leaving no effect on the dolomite isotopic composition.

PALAEOTEMPERATURES FROM NOBLE GAS ABUNDANCES IN SPELEOTHEM FLUIDS

AYLIFFE, L.K., TURNER, G. and BURNARD, P.G.,  
Department of Geology, University of Manchester,  
Manchester M13 9PL, U.K.

Atmospheric noble gases have solubilities in aqueous solutions that display a strong temperature dependence. Ar, Kr and Xe are factors of 1.7, 1.8 and 2.4 less soluble at 30 °C than at 0 °C. Determination of the absolute abundances of noble gases dissolved in speleothem inclusion fluids should therefore provide information on cave formation temperatures.

With this aim in mind a series of modern speleothem samples from caves with a range of temperatures were investigated for noble gas and fluid contents. Calcite samples (100-500 mg) were crushed in-vacuo to release inclusion fluids and associated noble gases. Pressure changes observed with a baratron (absolute high precision pressure gauge) provided estimates of the water released from crushing. Determinations of the absolute noble gas abundances were obtained by mixing the gases liberated during the crush with that of a mixed noble gas spike (enriched in  $^{21}\text{Ne}$ ,  $^{38}\text{Ar}$ ,  $^{80}\text{Kr}$  and  $^{128}\text{Xe}$ ).

Speleothem samples analysed have Ne/Ar, Kr/Ar and Xe/Ar which generally lie between the values for air and air saturated water. This suggests that these two components are principally controlling the noble gases released during crushing. Noble gas concentrations measured for individual samples during successive crushes are moderately reproducible or show variations which correlate with variations in F-values. The implied concentrations of Ne, Ar, Kr and Xe are however, typically an order of magnitude greater than air saturated water concentrations.

There are two possible explanations which could account for the above observations (1) water measurements are biased towards lower values by adsorption onto mineral and/or vacuum system surfaces and/or (2) another noble gas component is present in addition to that of trapped air and air saturated water in speleothems. Such a component could be fractionated air absorbed onto mineral surfaces and/or fractionated air trapped in the mineral lattice during the growth of the speleothem.

It is clear from our data that meaningful estimates of speleothem formation temperatures using a simple two component noble gas mixing model are not plausible. Although the existence of at least one non-equilibrium noble gas phase in speleothems complicates the interpretation of our data, it should in theory be possible to disentangle up to four distinct noble gas reservoirs on the basis of a sample's Ne/Ar, Kr/Ar, Xe/Ar and  $\text{H}_2\text{O}/\text{Ar}$  ratios, possibly providing information on speleothem precipitation temperatures.

Pb/Pb DATING ON CARBONATE ROCKS FROM THE SÃO FRANCISCO CRATON, BRAZIL.

BABINSKI, M., Instituto de Geociências, Universidade de São Paulo, SP, 05508-900, Brazil, and VAN SCHMUS, W.R., Geology Department, University of Kansas, Lawrence, KS 66045, USA.

Pb/Pb dating was performed on Paleoproterozoic carbonate rocks from the Minas Supergroup, São Francisco Craton. Undeformed carbonates (Gandarela Fm.) yielded a depositional age of  $2,420 \pm 19$  Ma, whereas marbles from the Piracicaba Group indicated the age of the metamorphism of the Transamazonian Orogeny (ca. 2,100 Ma). These results are in agreement with regional geology and previous geochronological data (Rb/Sr and U/Pb).

Pb isotope studies were also carried out on Neoproterozoic limestones from the cover of the craton (Bambuí Group, São Francisco Basin), which is bordered by Neoproterozoic mobile belts of the ca. 600 Ma Brasiliano Orogeny. The Pb in these carbonates showed complex behavior. Limestones displaying original structures, as well as very weakly deformed ones, showed four distinct types of Pb, here called types I, II, III and IV. Type I Pb is present in samples with relatively low-Pb and high-U (U/Pb ratios  $> 1$ ) and represents in situ growth of radiogenic Pb; it is variably radiogenic. Type II is found in samples with relatively high-Pb and low-U; it is non-radiogenic Pb with isotopic compositions ( $\alpha = 18.8$ ;  $\beta = 15.75$ ) similar to those of average crustal Pb at ca. 600 Ma. Type III is also present in samples with high-Pb and low-U, but it is radiogenic crustal Pb and can be divided in Type IIIa ( $\alpha = 36.0$ ;  $\beta = 18.3$ ), IIIb ( $\alpha = 34.0$ ;  $\beta = 17.8$ ), etc., according to isotopic ratios. Type IV is intermediate in composition between Type III and Type I Pb.

Samples containing Type I Pb, the only one that is able to yield Pb/Pb isochron ages, showed values between  $686 \pm 69$  Ma and  $520 \pm 53$  Ma. These ages are concordant to the metamorphic peak and post-tectonic phases of the adjacent Brasiliano mobile belts. Because of that, we believe that the isotopic system was disturbed by the Brasiliano Orogeny. In some areas the carbonates incorporated large amounts of average crustal common Pb (Type II Pb) so that they do not show sufficient radiogenic enrichment to be useful for age measurements. In other areas radiogenic Pb from the basement (Type III Pb) was incorporated into the carbonate rocks, probably during a large scale fluid percolation. Regression of Pb isotope compositions of types II and III yielded a Stacey & Kramers third stage geochron of 500 - 550 Ma. Type IV Pb occurs in samples from the same outcrops where Type I and Type III were found, indicating that it is a mixture between those two types.

According to our results, the Pb/Pb method was successfully applied to Paleoproterozoic Minas Supergroup carbonates. However, this method did not give conclusive geochronological results when applied to Neoproterozoic Bambuí Group carbonate rocks, probably due to tectonic effects, which disturbed the U/Pb system. Despite this, the results obtained can provide good information about the Pb isotope geochemistry in such areas.

VARIED MANTLE SOURCES AND MULTI-LEVEL  
CRUSTAL CONTAMINATION OF ARC MAGMAS AT  
CRATER LAKE, OREGON

BACON, Charles R., GUNN, Susan H., LANPHERE,  
Marvin A., and WOODEN, Joseph L., U.S. Geological  
Survey, 345 Middlefield Road, Menlo Park, CA 94025-  
3591, U.S.A.

Quaternary volcanic rocks of the Crater Lake area in the southern Cascade arc are characterized by a range of isotopic compositions. High-alumina olivine tholeiites (HAOT) have  $^{87}\text{Sr}/^{86}\text{Sr}$  ratios of 0.70346 - 0.70364; basaltic andesite, 0.70349 - 0.70372; shoshonitic basaltic andesite, 0.70374 - 0.70388; and andesite, 0.70324 - 0.70383. Dacites of Mount Mazama have  $^{87}\text{Sr}/^{86}\text{Sr}$  ratios of 0.70348 - 0.70373. Most rhyodacites converge on 0.7037. However, rhyodacite of the caldera-forming, climactic eruption has  $^{87}\text{Sr}/^{86}\text{Sr} = 0.70354$  because of an admixed low- $^{87}\text{Sr}/^{86}\text{Sr}$  component. Andesitic to mafic-cumulate scoriae of the climactic eruption and enclaves in pre-climactic rhyodacites show nearly the entire  $^{87}\text{Sr}/^{86}\text{Sr}$  range of the data set, confirming previously suggested introduction of diverse parental magmas into the growing climactic chamber. Pb and Nd isotope ratios display less variation ( $^{206}\text{Pb}/^{204}\text{Pb} = 18.838 - 18.967$ ,  $^{207}\text{Pb}/^{204}\text{Pb} = 15.556 - 15.616$ ,  $^{208}\text{Pb}/^{204}\text{Pb} = 38.405 - 38.619$ ;  $\epsilon_{\text{Nd}} = +3.9 - +6.1$ ) and generally covary with  $^{87}\text{Sr}/^{86}\text{Sr}$  ratios. Radiogenic isotope data from Crater Lake plot with published data for other Cascade volcanoes on isotope ratio correlation diagrams.

The isotopic data for the Crater Lake area require sources of primitive magmas to consist of depleted mantle and a subduction component, introduced in variable quantity to the depleted mantle wedge. Variable degrees of melting of this heterogeneous mantle, possibly at different depths, produced the diversity of isotopic compositions and LILE abundances in primitive magmas. Trace element ratios do not indicate presence of an OIB component that has been reported in lavas of some other Cascade volcanoes.

Crustal contamination may have affected isotope ratios and LILE concentrations in evolved HAOT, where initial LILE concentrations were low. Contamination is more difficult to detect in the calc-alkaline lavas because of their higher LILE concentrations and the small isotopic contrast with likely contaminants. Crustal assimilation appears to be required for calc-alkaline rocks only by  $\delta^{18}\text{O}$  values, which range from lows of +5.6 to +6.0‰ in HAOT and primitive basaltic andesites to +7.0‰ in a dacite. Elevated  $\delta^{18}\text{O}$  values may be attributed to interaction with relatively  $^{18}\text{O}$ -rich,  $^{87}\text{Sr}$ -poor deep crustal rocks such as igneous rocks of the Klamath Mountains and associated lower crust. Partially melted granodiorite, whose  $^{18}\text{O}/^{16}\text{O}$  ratio had been lowered by exchange with meteoric hydrothermal fluids, occurs as blocks in the climactic ejecta. Assimilation of such upper crustal granodiorite lowered  $\delta^{18}\text{O}$  values of rhyodacites without significantly affecting their magmatic composition in other ways.

TEXTURAL AND STABLE ISOTOPE DEVELOPMENT OF  
MARBLE ASSEMBLAGES DURING THE BARROVIAN-  
STYLE M2 METAMORPHIC EVENT, NAXOS, GREECE.

BAKER, J. Department of Earth Sciences, University of  
Cambridge, Cambridge CB2 3EQ, UK. and MATTHEWS,  
A. Institute of Earth Sciences, Hebrew University of  
Jerusalem, 91904 Jerusalem, Israel.

The effects of fluid-rock interaction during metamorphic processes have been the focus of considerable attention over the past decade. The Miocene M2 metamorphic event on the island of Naxos in the Cycladic Archipelago provides a well known example in which fluid flow has been cited to be a primary cause of metamorphism. The purpose of this study is to examine this assumption through an analysis of the textural development and isotopic compositions of siliceous dolomite assemblages within high grade marbles. A detailed petrologic analysis of the siliceous dolomite assemblages shows that two distinct periods of mineral growth can be documented; the first associated with prograde M2 metamorphism and the second with high temperature retrograde M2 metamorphism occurring during the ductile extensional thinning of the complex. The textural and carbon and oxygen isotope characteristics of each generation have been determined, and the P-T- $\text{X}_{\text{CO}_2}$  conditions at which these two mineral generations were stable and the compositions of the fluids present during the metamorphism have been characterized.

The P-T- $\text{X}_{\text{CO}_2}$  variations, low variance, and stable isotope compositions of dolomites and calcites of the prograde siliceous dolomite assemblages are consistent with internally buffered fluid evolution. In contrast the retrograde tremolite-calcite-talc mineral assemblages are shown to have grown as the result of the infiltration of a water-rich fluid phase that transported silica,  $\text{Al}_2\text{O}_3$ ,  $\text{Na}_2\text{O}$ , and FeO into the host rocks. Carbon and oxygen isotope compositions of calcites of this second generation are in distinct isotopic disequilibrium with those of coexisting prograde dolomite ( $\Delta_{\text{dol-calc}}^{18}\text{O}$ ) varies from 5.5‰ to 17.2‰; this precludes an origin through simple decarbonation reactions and requires the infiltration of an isotopically light fluid phase. The calculated oxygen isotope compositions of the waters in equilibrium with the retrograde calcites are consistent with their formation from crystallizing melts. The above observations, together with the fact that occurrences of veins of this type are limited to marbles in the highest grade areas ( $T > 600^\circ\text{C}$ ) of the metamorphic complex, suggests that the fluids responsible for vein formation were generated during the crystallization of melts as the metamorphic complex cooled from peak metamorphic temperatures.

The existence of this second generation of retrograde minerals has significant implications for previous studies of fluid transport on Naxos, because many of the unusually low  $\delta^{18}\text{O}$  compositions of pelites at high grades may be ascribable to the effects of interaction with retrograde M2 fluids rather than with prograde fluids. This view is strengthened by our observation of metapelitic assemblages whose quartz  $\delta^{18}\text{O}$  values are lower by several permil than the quartz of coexisting prograde veins and adjacent whole-rock pelites. Although the minerals within these pelites show no obvious alteration or retrogression, the low quartz  $\delta^{18}\text{O}$  values suggest that they have been affected by high temperature retrograde infiltration.

Lowering of  $\delta^{18}\text{O}$  in minerals of pelitic rocks of high grade metamorphic terrains down to values characteristic of igneous granites has been noted in a number of studies. The results of this study have identified a mechanism which could contribute to such a lowering, i.e., infiltration of water-rich fluids that have exsolved from melts generated during prograde metamorphism as these melts crystallize during cooling and ductile extensional tectonism.

## LASER FLUORINATION OXYGEN ISOTOPE EVIDENCE FOR CRUSTAL CONTAMINATION OF FLOOD BASALTS FROM YEMEN.

BAKER, Joel A., MACPHERSON, C., MATTEY, D., MENZIES, M., and THIRLWALL, M., Department of Geology, Royal Holloway University of London, Egham, Surrey TW20 OEX, UK.

Laser fluorination (LF) oxygen isotope analysis of phenocryst phases from volcanic rocks has two principal advantages over conventional O isotope analysis: 1. small *ca.* 1 mg samples can be rapidly analysed allowing easy replicate analysis of different mineral phases in a rock; 2. analysis of fresh mineral phases such as clinopyroxene bypasses the nearly ubiquitous effect of alteration on the O isotope composition of whole rock samples.

O isotope analysis of clinopyroxene, olivine and plagioclase phenocrysts from *ca.* 35 samples of flood and intraplate basalts from western Yemen suggests the basalts were derived from a homogeneous source with respect to O isotopes. Clinopyroxene, olivine and plagioclase in equilibrium with crustally uncontaminated melts have restricted O isotope compositions of 5.6, 5.2 and 6.0‰ ( $\pm 0.2\%$ ). These values are identical to the range of  $\delta^{18}\text{O}$  reported for mantle olivine and clinopyroxene analysed by LF. Basalts with Sr-Nd-Pb isotopic ratios distinct from the Afar plume and Gulf of Aden/Red Sea MORB, in particular those with low  $\epsilon\text{Nd}$  and  $^{206}\text{Pb}/^{204}\text{Pb}$ , high  $\Delta^{207}\text{Pb}/^{204}\text{Pb}$  and lithospheric trace element signatures, display more O isotope variation (5.6-7.0‰ rel. to cpx), although this variation is small compared with the range commonly reported for conventional whole rock analysis. Clinopyroxene values upto 7.0‰ suggest the flood basalts assimilated continental crust *en route* to the surface. Moreover, the O isotope data supports evidence from correlations between indices of fractionation and radiogenic isotope data that AFC operated during magma storage and ascent.

One high MgO basalt with low  $\epsilon\text{Nd}$  and the most extreme  $\Delta^{207}\text{Pb}/^{204}\text{Pb}$  might be interpreted as being derived from enriched lithospheric mantle (LM). However, it displays marked O isotope heterogeneity within zoned clinopyroxene phenocrysts. Clinopyroxene populations can be separated on the basis of colour, with zonation from deep green cores through to greenish brown, brownish green and finally dark brown/black types. Different clinopyroxene populations display the following **correlated** range in isotopic composition from early to late crystallizing clinopyroxene that nearly encompasses the entire isotopic range found in the Yemen flood basalts:  $^{87}\text{Sr}/^{86}\text{Sr} = 0.7035\text{-}0.7048$ ;  $^{143}\text{Nd}/^{144}\text{Nd} = 0.51293\text{-}0.51273$ ;  $^{206}\text{Pb}/^{204}\text{Pb} = 18.65\text{-}17.97$ ;  $\delta^{18}\text{O} = 5.68\text{-}6.87\%$ . Furthermore, olivine which crystallized before the brown, but after the green clinopyroxene, has a  $\delta^{18}\text{O}$  of 6.3‰, which is not in equilibrium with either end-member pyroxene. The Sr-Nd-Pb-O isotopic variation is attributed to phenocryst crystallization from a magma undergoing rapid assimilation of Pan-African continental crust whilst still hot and mafic. Modelling of the isotopic variation suggests the magma contains at least 20% continental crust.

LF oxygen isotope analysis of mineral separates allows small differences in  $\delta^{18}\text{O}$  to be correlated with radiogenic isotope data, and allows rigorous identification of crustal contamination in suites of continental basalts. If the mantle is uniform with respect to O isotopes then this technique will prove a powerful test of the relative roles of enriched LM and crustal contamination in suites of continental flood basalts.

## INTERCALIBRATION OF STANDARDS USED FOR $^{40}\text{Ar}/^{39}\text{Ar}$ DATING.

Baksi, Ajoy K., Dept. of Geology & Geophysics, Louisiana State Univ., Baton Rouge, LA 70803, USA), Archibald, D.A. and Farrar, E., Dept. of Geological Sciences, Queen's Univ., Kingston, Ont., Canada K7L 3N6).

$^{40}\text{Ar}/^{39}\text{Ar}$  ages are reported by laboratories relative to a number of different standards. Intercomparison of such ages has proved problematical, and is perhaps most critical for geological time scale related studies. We report the results of two sets of experiments on a number of standards commonly used for argon dating work. The first study utilized SB-3 Bio, LP-6 Bio 40-60#, FCT-3 Bio and MMHb-1. The second used the same standards and also GA-1550 Bio, Bern 4M and Bern 4B. Numerous splits of each sample were arranged within aluminium capsules, and irradiated in position 5C of the McMaster University Reactor. Samples were individually fused at 1200°C and analyzed on a modified MS10 mass spectrometer.

Results were evaluated by plotting the J value versus height within each capsule, and yielded the best results with the following ages: SB-3 Bio = 162.9 Ma (primary standard), LP-6 Bio = 128.1 Ma, GA-1550 Bio = 97.9 Ma, FCT-3 Bio = 27.95 Ma, Bern 4M = 18.5 Ma and Bern 4B = 17.2 Ma. All these samples are homogeneous in replicate analysis in "age", K and Ca contents (based on manometric measurement of  $^{39}\text{Ar}$  and  $^{37}\text{Ar}$ , respectively). Individual splits of MMHb-1 yielded ages ranging from ~512 Ma to ~520 Ma, with an internal 1 $\sigma$  precision of about 1.0 m.y.; though K and Ca contents appear reproducible from split to split, MMHb-1 is inhomogeneous in age at the ~20 mg sub-sample level, and is unsuitable for use as an interlaboratory standard. Splits of Taylor Creek Rhyolite Sanidine, Penn State OR-1A, Nancy biotite mica-Fe and Engels' Amphibole were also evaluated against these standards; attempts to flux the feldspar standards with degassed zero age basalt at 1200°C were only partially successful.

A stepheating run on FCT-3 Bio yielded 100% gas on the plateau and an age of 27.9 Ma. LP-6 Bio shows a disturbed age spectrum, with step ages ranging between ~120 Ma and ~135 Ma; this appears to support a suggestion that LP-6 Bio 40-60# consists of two types of material ("blocky" and "flaky") with K-Ar ages of ~119 Ma and ~136 Ma. Our results suggest many of these standards are suitable for use as monitors in  $^{40}\text{Ar}/^{39}\text{Ar}$  dating work; SB-3 Bio, LP-6 Bio 40-60# and GA-1550 at the ~15-20 mg subsample level, and FCT-3 Bio, Bern 4M and Bern 4B at the ~30-35 mg subsample level.

## P-T-t PATHS OF AEGEAN METAMORPHIC CORE COMPLEXES: IOS, PAROS, AND SYROS

BALDWIN, S.L., Dept. of Geosciences, University of Arizona, Tucson, AZ 85721, USA, and LISTER, G.S., VIEPS, Dept. of Earth Sciences, Monash University, Melbourne 3168, Australia

In the Aegean, Miocene extension followed Eocene collision, and core complexes formed that resemble those in the Basin and Range Province. At least four metamorphic events have been recognized in the pre-Alpine gneissic basement ( $M_0$ ), Eocene high-P, low-T metamorphic rocks ( $M_1$ ), Miocene greenschists and amphibolites ( $M_2$ ), and contact metamorphic rocks ( $M_3$ ) associated with Aegean metamorphic core complexes. Thermochronologic and structural studies of shear zones and  $M_1$  rocks of Paros, Ios, and Syros provide insight into the evolution of this polymetamorphic terrane, and the role of plutonism during the evolution of these core complexes.

Undisturbed  $^{40}\text{Ar}/^{39}\text{Ar}$  age spectra for white micas from Syros date  $M_1$  at 50-54 Ma. However, the majority of white micas from Syros and Ios yielded disturbed age spectra which are interpreted to reflect variable partial outgassing and/or recrystallization of  $M_1$  white micas during subsequent  $M_2$  metamorphism. The degree of overprinting varies considerably, but age spectra patterns are similar to those previously documented on Naxos and Sifnos.

Biotite, muscovite, and K-feldspar from mylonitized granites on Paros indicate rapid cooling from 12-10 Ma. Results are concordant with previously reported K/Ar ages on S-type granites, indicating cooling of granites occurred pencontemporaneously with shearing events which produced the spectacular S-C mylonites.

Within the kilometer-scale Mylopotas ductile shear zone on Ios,  $^{40}\text{Ar}/^{39}\text{Ar}$  ages record  $M_{0-3}$  events. Boudins within the shear zone gave ages indicative of pre-Alpine basement, some mica schists record  $M_1$  ages while others apparently record both  $M_1$  and  $M_2$  events. Analyses on biotite, muscovite and K-feldspar from the S-C mylonites yielded Miocene ages with youngest apparent ages of 13 Ma. Preservation of  $M_{0-1}$  ages suggest that temperatures were not sufficiently high to cause complete resetting of the schists and granite boudins caught up in the shear zone. The mylonites do not reflect a depth-dependent transition but rather formed during a Miocene transient thermal pulse caused by the intrusion of granitoids. Modelling the effects of specific P-T-t histories on  $^{39}\text{Ar}$  diffusion profiles obtained from white mica, K-feldspar and biotite in the shear zone on Ios suggests that ambient temperatures in the "basement" unit were lower than 250-270°C prior to the Miocene thermal event (i.e. less than the temperatures required to form greenschist facies mylonites), and that cooling subsequent to the thermal pulse may have involved timescales as short as  $10^4 - 10^5$  yr. Rapid cooling continued after the Miocene thermal pulse as the core complexes were unroofed due to ongoing extension. The central granite gneiss terrane of Ios likely occupied a shallow crustal setting characterized by low ambient temperatures close to the foreland of the mountain belt that once defined the Aegean Alps. Subsequently the entire complex was stretched in a Miocene ductile shear zone resulting in recrystallization of some of the rocks to produce the S-C mylonites.

## A HIGH-RESOLUTION LASER EXTRACTION TECHNIQUE FOR STABLE ISOTOPE ANALYSIS OF CARBONATES: THE EFFECT OF LASER-SAMPLE INTERACTION ON THE COMPOSITION OF EVOLVED $\text{CO}_2$

BALL, J.D., Crowley, S.F., Marshall, J.D., Dept. of Earth Science, University of Liverpool, P.O.Box 147, Liverpool, L69 3BX, UK.

A laser extraction system is under development at Liverpool for the ultra-fine scale analysis of carbonates. Using a high-power Nd:YAG laser, areas of carbonate  $\sim 50 \mu\text{m}$  in diameter are thermally decomposed to yield  $\text{CO}_2$  gas.

It is widely accepted that during the conversion of carbonate to  $\text{CO}_2$  some isotopic fractionation occurs, and experiments performed to date confirm this. Hence, it is necessary to carry out a series of standardisation experiments, by analysing a range of isotopically homogenous materials using the laser extraction and traditional acid digestion methods, in order to establish a fractionation correction factor for the technique.

The standardisation experiments carried out at Liverpool indicate that, while it is possible to establish a correction factor for a given material to a precision on 0.1 per mil, the implied correction varies depending on mineralogy, chemistry and physical composition of the sample. Therefore, no overall correction factor can be given for the technique. Recent experiments have shown that the difference in fractionation factors can be significantly reduced if close attention is given to the conditions under which the laser interacts with the sample and the  $\text{CO}_2$  is extracted.

An overview of the extraction system will be presented, including details of the laser, optical train, vacuum system and mass-spectrometry. The procedure for extracting, purifying and analysing the evolved  $\text{CO}_2$  will also be discussed.

Data from a range of standardisation materials of varying properties will be used to demonstrate possible problems associated with the technique and to support the fractionation correction factors quoted.

## ISOTOPE STUDIES OF THE SYSTEMATICS OF SULPHATE REDUCTION IN TWO CONTRASTING AQUIFERS

BARKER, A.P., BOTTRELL, S.H., MONCASTER, S.J.,  
Department of Earth Sciences, University of Leeds, Leeds,  
LS2 9JT, UK, LLOYD, J.W., and TELLAM, J.H.,  
Hydrogeology Section, School of Earth Sciences, University  
of Birmingham, Edgbaston, Birmingham, B15 2TT, UK.

Groundwater quality is controlled by many factors such as water-rock interactions and biological activity. Bacterial sulphate reduction is a process that can result in the degradation of water quality, and an understanding of the mechanisms of this process would be of great benefit to water resource evaluation.

Data are presented on studies from two sites where sulphate reduction has occurred in groundwaters. One is in a Permo-Triassic sandstone aquifer where sulphate reduction is believed to be a recent phenomenon. Here time-series data show increase in  $\text{HCO}_3^-$  concentrations, decrease in  $\text{SO}_4^{2-}$  and progressive  $^{13}\text{C}$  depletion in  $\text{HCO}_3^-$  at certain depths. The difference in sulphur isotopic composition between  $\text{S}^{2-}$  and  $\text{SO}_4^{2-}$  ( $\Delta^{34}\text{SSO}_4^{2-}\text{-S}^{2-}$ ) is 18‰. The second site is in the deep confined section of the Lincolnshire Limestone, a gently dipping Mid Jurassic limestone aquifer confined by overlying clays. Here values of  $\Delta^{34}\text{SSO}_4^{2-}\text{-S}^{2-}$  of over 50‰ are observed but  $\text{HCO}_3^-$  is not  $^{13}\text{C}$  depleted.

The data are modelled in terms of the effects of both bacterial sulphate reduction and groundwater mixing. At the sandstone site sulphate reduction appears to be proceeding at an appreciable rate, whereas in the limestone net rates of reduction are small as rates of  $^{13}\text{C}$  depleted  $\text{HCO}_3^-$  production must be less than the rate of re-equilibration with  $\text{CaCO}_3$  in the limestone matrix. Groundwater mixing best accounts for the observed chemical and isotopic distributions. However these very slow rates of sulphur redox reactions may be important in establishing large  $\Delta^{34}\text{SSO}_4^{2-}\text{-S}^{2-}$  values here, by effectively catalysing isotope exchange reactions promoting an isotope distribution close to equilibrium.

Flow to wells in the Lincolnshire Limestone sites are dominated by fissure flow. Data on chemical and isotopic compositions of porewaters from a recently cored well will also be presented for comparison with fissure water compositions, as well as time-series data on the evolution of the new well since substantial perturbation of chemical and isotope compositions of groundwater were observed following drilling.

## AN ISOTOPIC INVESTIGATION OF MAGMA CHAMBER PROCESSES AT THE TRANSITION BETWEEN TWO CYCLES IN THE BJERKREIM-SOKNDAL LAYERED INTRUSION, S. NORWAY.

BARLING, J., WEIS, D. and DEMAIFFE D., Pétrol.  
Géodyn. Chimique, CP160/02, Université Libre de  
Bruxelles, Av. F.D. Roosevelt, 50, 1050 Brussels,  
Belgium.

The Bjerkreim-Sokndal massif is a layered intrusion in the late Proterozoic Rogaland Anorthosite Complex of S. Norway<sup>1</sup>. The upper part of the intrusion is composed of mangerite and quartz-mangerite, whilst the lower part consists dominantly of plag-opx cumulates (anorthosite-norite) and comprises five macrocyclic units (MCU), subdivided in zones, which have been interpreted<sup>2</sup> as reflecting repeated magma chamber replenishment events. The MCU III/IV boundary is marked by a strong compositional reversal of the main minerals (increases of An in plag, of En in opx and appearance of Fo75 olivine). Isotopic and mineralogical indicators of replenishment are displaced upward relative to the stratigraphically defined base of MCU IV. For this reason, Jensen et al.<sup>3</sup> propose that MCU IV started with a hybrid zone (IVa) before sufficient dense parental magma could pond on the floor of the chamber and crystallize as leucotroctolites (IVb).

Plagioclase separates from a sequence of samples across the MCU III/IV boundary have been analysed for Sr, Nd and Pb isotope ratios and Rb, Sr, Sm, Nd, U and Pb concentrations.  $^{87}\text{Sr}/^{86}\text{Sr}_i$  (940Ma) ranges from 0.7048 (base of zone IVb) to 0.7061 (IIIe) together with systematic changes in  $^{143}\text{Nd}/^{144}\text{Nd}_i$  (0.51155 ( $\epsilon_{\text{Nd}i}$  = +2.5) to 0.51143 ( $\epsilon_{\text{Nd}i}$  = +0.1)) and Pb isotopic ratios ( $^{206}\text{Pb}/^{204}\text{Pb}_i$  = 17.49 to 17.73;  $^{207}\text{Pb}/^{204}\text{Pb}_i$  = 15.52 to 15.54). The isotopic data are consistent with the influx of a batch of magma, whose isotopic composition is reflected by the plagioclases at the base of IVb into a magma chamber containing a resident magma whose isotopic composition is represented by plagioclases from zone IIIe. The positive  $\epsilon_{\text{Nd}i}$  value (+2.5) of plagioclase crystallized from the inferred replenishing magma indicates that this incoming melt came from a source either in the depleted upper mantle or recently derived therefrom. Whilst the higher  $^{87}\text{Sr}/^{86}\text{Sr}_i$  and  $^{206}\text{Pb}/^{204}\text{Pb}_i$  and lower  $^{143}\text{Nd}/^{144}\text{Nd}_i$  values of the resident magma suggest that it has been contaminated by continental crust.

These data enable us to divide the transition zone at MCU III/IV boundary into two parts. The lower part, reflecting a magma chamber replenishment event (IIIe to the base of IVb) approximates to simple binary mixing, whereas the upper part (IVb - IVd) shows evidence for more complex processes.

1. Michot, J., and Michot, P., 1969, New York State Museum Service Memoir 18, 399-410.
2. Duchesne, J.-C., 1972, J. Petrology. 13, 57 - 81 .
3. Jensen, J.C. et al., 1993, Lithos. 29, 311-325.

## STRUCTURAL CONTROLS ON VOLCANISM IN THE NORTHERN KENYA RIFT

BARREIRO, Barbara, NERC Isotope Geosciences Laboratory, Keyworth, NG12 5GG, United Kingdom, and DUNKLEY, Peter and SMITH, Martin, British Geological Survey, Keyworth, NG12 5GG, United Kingdom

Crustal thickness, topography, lithospheric heterogeneity, and magma plumbing systems all affect the chemistry of volcanic rocks in the Kenya Rift. The largest contrast is between volcanoes in the south, erupted through Archaean craton and its reworked margin, which exhibit many characteristics suggesting derivation from continental lithosphere, and those of the north, erupted through Proterozoic mobile belt. Volcanoes in the northern rift, between Lake Baringo and Lake Turkana (0°30'N to 2°30'N) show more subtle changes from south to north, due to structural controls.

The shield volcanoes immediately to the north of Lake Baringo (Korosi, Paka, and Silali) are composed of bimodal, weakly-undersaturated transitional basalts and trachytes. Magma was stored and fractionated in large magma chambers, which were drained to form calderas. Paka and Korosi show Nd isotope evidence for two distinct magma sources (Paka,  $\epsilon_{Nd}$  = 3 and 6, Korosi,  $\epsilon_{Nd}$  = 3 and 5), similar to Silali (MacDonald et al.); trachytes have higher  $^{87}Sr/^{86}Sr$  than basalts. Paka and Silali tend toward elevated  $^{207}Pb/^{204}Pb$  relative to  $^{206}Pb/^{204}Pb$  (15.53 at 18.4 to 15.65 at 19.4), although extra-caldera flank eruptions have lower  $^{207}Pb/^{204}Pb$ .

At 1°30'N, Emurangogolak is situated on a major ductile-brittle shear zone within the Proterozoic basement. Between this shear zone and Lake Turkana, volcanoes are characterised by uniform but distinct  $\epsilon_{Nd}$  (Emurangogolak = 3.8-4.4, Namarunu = 5.6-7, Barrier = 4.8-5.5) and low  $^{207}Pb/^{204}Pb$  (15.57-15.62) relative to  $^{206}Pb/^{204}Pb$  (19-19.7). Trachytes and phonolites have the same Nd and Pb isotopic compositions as the basalts, but elevated  $^{87}Sr/^{86}Sr$ , suggesting only small degrees of crustal input.

The trend towards 'plume' isotopic signatures going from south to north in the Gregory Rift correlates with absence of evidence for large-scale crustal magma chambers, a decrease in elevation of the rift floor, narrowing of the rift, and decrease in depth to crystalline basement.

## EVIDENCE FOR CLOSED-SYSTEM BEHAVIOR OF $^{232}Th$ - $^{208}Pb$ IN ALLANITE UNDER HYDROTHERMAL CONDITIONS: A STUDY OF ALTERED RHYOLITE AND GRANODIORITE FROM THE ATESINA - CIMA D'ASTA VOLCANO-PLUTONIC COMPLEX (N ITALY)

BARTH, Susanne\*, OBERLI, Felix, and MEIER, Martin, Institut für Kristallographie und Petrographie ETH, Sonneggstr. 5, CH-8092 Zürich, Switzerland

\* Now at: Centre de Recherches Péetrographiques et Géochimiques, C.R.P.G.-C.N.R.S., BP 20, F-54501 Vandœuvre-lès-Nancy Cédex, France

Magmatites from the Early Permian Atesina volcanic complex (AVC) and Cima d'Asta pluton (CAP) display variable degree of major/trace element mobility, open-system behavior of total-rock Rb-Sr, and shift in oxygen-isotope signatures induced by Triassic water-rock interaction. Total-rock REE and Sm-Nd isotopic signatures, however, are not affected by hydrothermal overprint. Oxygen isotopic evidence points to alteration temperatures of ~210° C and 160° C for AVC rhyolite and CAP granodiorite, respectively, assuming exchange with sea water (Barth et al., 1993).

Single allanite crystals whose outer parts have been removed by abrasion prior to isotope analysis yield  $^{232}Th$ - $^{208}Pb$  ages (95% c.l.) of  $276.2 \pm 3.2$  Ma and  $276.3 \pm 3.0$  Ma ( $n=2$ ;  $276.3 \pm 2.2$  Ma mean) and identical ages of  $274.0 \pm 2.9$  Ma to  $277.0 \pm 3.0$  Ma ( $n=4$ ;  $275.5 \pm 1.5$  Ma mean) for hydrothermally altered rhyolite and granodiorite, respectively. The allanite Th-Pb ages conform to published Rb-Sr total-rock isochron ages of CAP granitoids ( $275 \pm 9$  to  $274 \pm 2$  Ma;  $1\sigma$ ) as well as to published Rb-Sr and K-Ar biotite isochron ages of AVC rhyolites/rhyodacites. This indicates that the Th-Pb isotope system in allanite is virtually unaffected by hydrothermal overprint. In contrast, an allanite sample from the granodiorite showed considerably rejuvenated  $^{238}U$ - $^{206}Pb$  and  $^{235}U$ - $^{207}Pb$  ages (i.e.,  $264.3 \pm 1.2$  Ma and  $258 \pm 18$  Ma, respectively; ages not corrected for initial radioactive disequilibrium), pointing to differential loss of radiogenic  $^{206}Pb$  and  $^{207}Pb$  as compared to  $^{208}Pb$ , presumably by exchange with hydrothermal fluids. This observation suggests the existence of domains in allanites characterized by distinct Th/U and varying stability with respect to hydrothermal fluids, giving rise to preferential loss of U-derived Pb isotopes. This clearly underlines the superior stability of the Th-Pb system in allanite in comparison to its U-Pb systems and - in conjunction with the insensitivity of the Th-Pb ages to initial radioactive disequilibrium - makes the Th-Pb method the favorite choice for dating even hydrothermally altered magmatites.

Barth, S., Oberli, F., Meier, M., Blattner, P., Bargossi, G.M., and Di Battistini, G. (1993): *Geochim. Cosmochim. Acta*, v. 57, pp. 4285-4300.

THE GRANITE BELT ON THE EASTERN PART OF SOUTHERN BRAZIL AND URUGUAY

BASEI, M.A.S., Instituto de Geociências/Universidade de São Paulo, Caixa Postal 20899, 01498-970 São Paulo, SP, Brazil and HAWKESWORTH, C.J., The Open University, Department of Earth Sciences, Milton Keynes, MK7 6AA, U.K

The eastern part of Southern Brazil and Uruguay is composed mainly by granitic rocks generated during the Rio Doce Orogeny whose ages are in the 620-440 Ma interval. This Granite Belt (GB) that is younger than the Brasiliano-Pan African magmatism (700-620 Ma) observed in the adjacent Schist Belt (SB) is represented by granitoid rocks that can be roughly grouped in three major igneous suites: S.A.Imperatriz, S.P. Alcantara and Pedras Grandes.

Geochemical and mineralogical data show several differences between the GB magmatism and that observed in the SB where alkaline and peraluminous granites predominate when compared with the more expanded calc-alkaline to alkaline suites of the GB. On Harker diagrams both domains have a small silica range with the high concentrations related to the two mica granites (SB) and the best trends related to the S.P. Alcantara Suite. The GB granites also show a smaller spread, steeper slope and higher concentration of REE than the granites in the SB.

The isotope data emphasize the differences pointed out by the geochemical data and strongly suggest the involvement of two different source areas in the generation of these magmatisms. In both cases important crustal component is recognized with  $\epsilon_{Nd}$  ranging from -3.4 to -8.3 in the GB and from -10.1 to -20.4 in the SB. Model Nd ages are consistently different with values around 2.0 Ma in the GB and 1.6 Ma in the SB.

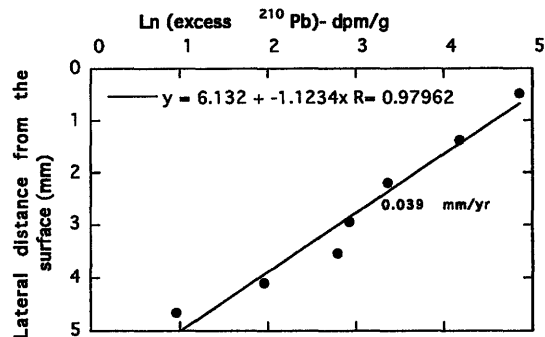
The NE-SW contact between the two belts can be discontinuously recognized for more than 1200 Km, always parallel to a strong negative gravimetric anomaly. It is characterized by a set of low to high temperature shear zones where protomylonites to mylonites predominate. This megastructure of lithospheric scale is interpreted as a Lower Paleozoic (535 Ma) suture zone developed during the collision between the Granite Belt and the marginal cratonic volcanosedimentary sequences represented by the Brusque, Porongos and Lavaleja Groups.

DATING OF SPELEOTHEMS USING EXCESS  $^{210}\text{Pb}$ : IMPLICATIONS TO THEIR USEFULNESS AS PROXY PALEOCLIMATIC RECORDERS

BASKARAN, M., Department of Marine Sciences, and ILIFFE, T. M., Department of Marine Biology, Texas A&M University, Galveston, TX 77553-1675, USA.

It has been shown recently that presently growing speleothems can be dated using excess  $^{210}\text{Pb}$  (Baskaran and Iliffe, 1993). Subsequent study showed promise that these speleothems can be used as a proxy to retrieve  $\delta^{13}\text{C}$  variations in atmospheric  $\text{CO}_2$  (Baskaran and Krishnamurthy, 1993). We have extended our study to many more speleothems, including stalagmites from caves in the San Saba and Travis Counties in Texas. This study provides information on the following aspects: (i) the uniformity on the growth rates at various segments of a speleothem (ii) the discontinuity of the growth rates, if any and (iii) the inventory of excess  $^{210}\text{Pb}$  and its relationship to the water drip rate.

The excess  $^{210}\text{Pb}$  ( $^{210}\text{Pb}_{\text{XS}}$ ) concentration in the uppermost layers of speleothems sampled varies between 51 and 200 dpm/g. The  $^{210}\text{Pb}_{\text{XS}}$  based growth rates vary typically between 0.01 and  $0.1 \text{ mm yr}^{-1}$ . A model discussing the growth rates of stalagmites and stalactites will be presented.



- Baskaran, M. and T. M. Iliffe. 1993. Age determination of recent cave deposits using excess  $^{210}\text{Pb}$ - a new technique. *Geophys. Res. Lett.* 20: 603-606.  
 Baskaran, M. and R. V. Krishnamurthy. 1993. Speleothems as proxy for the carbon isotope composition of atmospheric  $\text{CO}_2$ . *Geophys. Res. Lett.* 20: 2905-2908.

TEMPORAL ISOTOPIC VARIATIONS IN THE HAWAIIAN MANTLE PLUME, THE LANAI ANOMALY, THE MOLOKAI FRACTURE ZONE AND A SEAWATER-ALTERED LITHOSPHERIC COMPONENT IN HAWAIIAN VOLCANISM

BASU, ASISH R. and FAGGART, B.E., Dept. of Earth and Environmental Sciences, University of Rochester, Rochester, New York, 14627, USA.

Several recent studies have documented the temporal variations in major and trace elements and Nd, Sr, Pb and He-isotopic ratio variations in single Hawaiian volcanoes. In this study we examined Nd and Sr-isotopic variations on forty-five basaltic rocks (collected during the 1985 ALCYONE expedition) from both the Hawaiian Islands and the leeward islands to the northwest. These data demonstrate relatively limited isotopic variations over most of the 1900 km long and 27 million years of volcanism examined here. However, there is a short-lived but major shift in isotopic compositions towards enriched values that center about the island of Lanai. The Lanai rocks ( $\epsilon_{Nd} = 2.1-5.5$ ;  $^{87}Sr/^{86}Sr = 0.70388-0.70455$ ) are similar to those of Koolau, though with somewhat more radiogenic Sr. Lanai, Koolau and Kahoolawe all show extreme variation in Sr and Nd isotopic compositions relative to other Hawaiian tholeiites. These three volcanoes thus appear more closely related to one another and are of great importance in understanding Hawaiian volcanism. As the Molokai Fracture Zone crosses the Hawaiian trend near these volcanoes, we suggest that it has allowed a tremendous influx for about 3 Ma of a more-enriched lower mantle plume component to swamp the isotopic signatures of other source-components.

The Hawaiian Sr, Nd-isotopic data are distinguished by stages of volcanism; the progression reported by Chen and Frey for the Haleakala volcanics is generally supported over the entire Hawaiian chain. The tholeiitic shield to post-shield alkalic to post-erosional alkalic volcanism correlates with decreasing  $^{87}Sr/^{86}Sr$  and increasing  $\epsilon_{Nd}$ . However, in the Nd-Sr correlation plot as the MORB-field is approached, Sr-isotopic ratios are increasingly displaced to the right of the mantle array. This observation clearly suggests a seawater-altered ancient lithospheric component in Hawaiian volcanism.

NITROGEN AND CARBON ISOTOPIC COMPOSITION OF ORGANIC MATTER IN PRECAMBRIAN CHERTS.

BEAUMONT, V., JAVOY, M., Géochimie des Isotopes Stables, Université de Paris 7, Paris, 75251 cédex 05, France, and ROBERT, F., Minéralogie, Muséum National d'Histoire Naturelle, Paris, 75005, France.

Carbon isotopes in sedimentary organic matter (kerogen) have been shown to reflect the isotopic composition of living organisms (Galimov, 1980), i.e., the signature of carbon photosynthesis via enzymatic processes. In Precambrian environments, the difference between carbon isotopic compositions of kerogen in cherts and in bulk carbonates is featuring the reality of photosynthesis as early as 3.5 Ga (Schidlowski, 1988).

Nitrogen is included - during early diagenesis - in stable sites of kerogen heterocycles (Behar *et al.*, 1987). This situation limits isotopic exchanges. Then, nitrogen isotopic compositions of organisms are preserved in kerogen, featuring the metabolism and/or the redox conditions of environments. Few previous data exist on the nitrogen isotopic compositions of Precambrian kerogen, primarily because of experimental difficulties.

Both nitrogen and carbon isotopic compositions have been measured in HF-HCl residues from Precambrian cherts of ages ranging from 3.5 Ga to 2.0 Ga. Data are compared to those obtained from Phanerozoic samples.

As documented by previous workers,  $\delta^{13}C$  values of Precambrian organic matter are depleted in  $^{13}C$  relative to those from the Phanerozoic. Possible reasons are discussed by Schidlowski *et al.* (1983).  $\delta^{15}N$  values of Precambrian organic matter show a depletion in  $^{15}N$  for oldest samples (3.5 Ga), with  $\delta^{15}N$  values as low as -6‰ (exceptional in Phanerozoic environments). This depletion progressively disappears with decreasing age and as early as 2.0 Ga years ago,  $\delta^{15}N$  distribution is similar to the modern one. Three hypotheses can be made concerning the origin of this geochemical variation: (1) a late diagenesis effect (previous works has shown this hypothesis improbable, as an opposite effect with burial is usually observed); and/or (2) a source effect (depletion in  $^{15}N$  of the early atmosphere); and/or (3) a metabolic effect (if so, the nitrogen isotopic composition is a criteria for studying the evolution of metabolic processes linked to atmospheric oxygen level). The likelihood of each aspect will be developed and discussed.

Galimov, 1980, Kerogen, Ed Technip, 271-298.

Behar *et al.*, 1987, Org. Geochem 11, p.15.

Schidlowski, 1988, Nature 333, 313-318.

Schidlowski *et al.*, 1983, Earth's Earliest Biosphere.

Princeton University Press, 149-186.

## APPLICATIONS OF NITROGEN ISOTOPES IN STUDIES OF HIGH-TEMPERATURE FLUID-ROCK INTERACTIONS

**BEBOUT, G. E.**, Dept. Earth & Environ. Sci., Lehigh University, Bethlehem, PA 18015

Many igneous and metamorphic rocks contain appreciable amounts of N, primarily as structurally bound  $\text{NH}_4^+$ ; however, the N isotope system has not been extensively exploited as a tracer of high-T fluid-rock interactions and other mixing processes in the crust and mantle. Recent studies demonstrate that N isotope compositions of silicate mineral and whole-rock samples can be routinely measured with accuracy and precision approaching that of the other stable isotope systems (see Bebout and Fogel, 1992).

Several characteristics of the N isotope system make it suitable for tracer studies. First, significant observed variation in  $\delta^{15}\text{N}$  of igneous and metamorphic rocks is consistent with calculated N-isotope fractionations; the calculations predict significant N-isotope variation as a result of devolatilization, metasomatic alteration, and magma volatile release. Second, because N abundance in the crust is largely tied to its fixation by organic processes in sedimentary environments, the N isotope system may be particularly sensitive in tracing sediment-derived fluids. Third, because N is generally a trace element, N isotopes may exhibit differing sensitivity to fluid-rock interactions relative to other isotope systems and may thus provide unique information regarding metasomatism in igneous and metamorphic settings.

A study of the distribution of N isotopes in the Catalina Schist subduction complex, California, demonstrates significant N-isotope fractionation during devolatilization and metasomatic processes. The overall variation in  $\delta^{15}\text{N}$  in the Catalina Schist ( $\sim 5.5\%$ ) is easily resolved using combustion extraction techniques and conventional gas-source mass spectrometry; precision of the measurements ( $1\sigma$  for  $n \geq 3$ ) is typically near  $0.1\%$ . Study of devolatilization and large-scale fluid transfer in the Skiddaw Granite and Aureole (England; Bebout et al., 1993) reveals  $>10\%$  variation in  $\delta^{15}\text{N}$ . Large, systematic N isotope variations in these suites indicate great potential of the N system to yield information regarding sources of fluids and silicate melts, fluid-rock interactions, and crust-mantle exchange. Continuing improvements in techniques for routine extractions and mass spectrometry of N will make the N-isotope system yet more accessible in petrologic studies.

Bebout, G. E., and Fogel, M. L., 1992, *Geochim. Cosmochim. Acta*, 56, 2839-2849.

Bebout, G. E., Bradley, A. D., and Cooper, D. C., 1993, *Geol. Soc. Amer. Abstr. Progr.*, 25, 78.

**$^{40}\text{Ar}/^{39}\text{Ar}$  DATING OF YOUNG LOW-K THOLEIITES: EXAMPLES FROM NORTHEAST CALIFORNIA, U.S.A.**  
**BECKER, T.A.**, SHARP, W.D., RENNE, P.R., Institute of Human Origins Geochronology Center, 2453 Ridge Road, Berkeley, CA, 94709, U.S.A.,  
TURRIN, B.D., U.S. Geological Survey, MS 901, 345 Middlefield Road, Menlo Park, CA, 94025, U.S.A.,  
PAGE, W.D. Pacific Gas and Electric Co., Geosciences Dept., P.O. Box 770000, San Francisco, CA, 94177, and  
WAKABAYASHI, J., Consultant, 1329 Sheridan Lane, Hayward, CA, 94544, U.S.A.

Young low-K (Ca/K  $\sim 25$ -40) basalts pose challenges to K-Ar and  $^{40}\text{Ar}/^{39}\text{Ar}$  dating because of their low radiogenic Ar contents and resulting sensitivity to corrections for blanks, mass discrimination, nucleogenic Ar isotopes and trapped Ar of anomalous isotopic composition.

We have developed an automated resistance furnace, employing an infra-red pyrometer, that provides reproducible blanks of  $<10^{-16}$  mol for  $m/e = 40$  at  $1200^\circ\text{C}$ . Heating time and residence time in the extraction system for gas purification are adjusted for minimizing blank contribution and optimizing isotope intensity measurement. Full automation of the furnace, along with the extraction line and air pipette, allows unattended operation and makes frequent characterization of procedural blanks and spectrometer discrimination feasible.

Our M.A.P. 215-50C mass spectrometer is configured for a resolution of 450, making  $^{40}\text{Ar}/^{39}\text{Ar}$  ratios of 100 or more acceptable. This allows neutron fluences to be reduced, and in conjunction with thermal neutron shielding and detailed characterization of production ratios, minimizes the effects of nucleogenic Ar isotopes.

Incremental heating produces intermediate-temperature steps with enhanced radiogenic Ar contents and provides data for isochron analysis, revealing subtle anomalous trapped Ar ( $^{40}\text{Ar}/^{36}\text{Ar}$  in the range of 297-305) in many samples. Samples may yield *sensu stricto* plateaux, but have well-defined isochron ages that are significantly younger. Two samples, potentially from different flows, yield distinct plateau ages of  $493 \pm 22$  and  $423 \pm 7$  ka, but give indistinguishable isochron ages of  $409 \pm 18$  and  $415 \pm 3$  ka, with initial  $^{40}\text{Ar}/^{36}\text{Ar}$  of  $304.6 \pm 1.3$  and  $301.2 \pm 0.9$ , respectively. Another flow yielded well-defined plateau ages of  $1113 \pm 81$ ,  $921 \pm 51$ , and  $907 \pm 51$  ka from three closely-spaced samples, whereas isochron ages of  $889 \pm 136$ ,  $834 \pm 51$ , and  $879 \pm 40$ , and initial  $^{40}\text{Ar}/^{36}\text{Ar}$  of  $297.8 \pm 1.4$ ,  $297.8 \pm 1.0$  and  $296.3 \pm 0.9$ , respectively, were obtained.

Basalts with lower Ca/K ( $<15$ ) are much less sensitive to slight departures in the trapped Ar from atmospheric air ratio. One such flow yields a plateau age of  $68 \pm 18$  ka and an indistinguishable isochron age of  $50 \pm 16$  ka with initial  $^{40}\text{Ar}/^{36}\text{Ar}$  of  $296.8 \pm 1.0$ .

These results indicate that detailed  $^{40}\text{Ar}/^{39}\text{Ar}$  incremental heating analyses are needed for precise and accurate dating of Late Pleistocene low-K basalts.

DEPLETED  $^{238}\text{U}$  AND EXCESS  $^{234}\text{U}$  AND  $^{230}\text{Th}$ :  
ENHANCED DISEQUILIBRIUM OF U-SERIES ISOTOPES  
IN HYPERSALINE MEDITERRANEAN BRINES

BEETS, C. J. (Kay), WASSERBURG, G.J., and CHEN,  
J.H., Lunatic Asylum, Division of Geological and  
Planetary Sciences, California Institute of Technology,  
Pasadena, CA 91125, and DE LANGE, G.J., Institute of  
Earth Sciences, Department of Geochemistry, Budapestlaan  
4, 3584 CD Utrecht, The Netherlands

Anoxic hypersaline brines in the Bannock Basin, Eastern Mediterranean Sea, show extreme physico-chemical properties. High density (1.21) due to salinities of more than 10 times that of normal seawater make the configuration of the brine stable, separated from the overlying waters by a well-defined interface. The brine is further characterized by lack of oxygen, a high concentration of  $\text{H}_2\text{S}$  (~2.5 mM) and compositional layering. The upper brine (I) has a slightly lower salinity and contains more Ca and Sr and less Mg, S and  $\text{SO}_4$  than the lower brine (II); however, both Brine I and II are believed to result from redissolution of Messinian late-stage evaporitic salts which outcrop in the basin walls<sup>1</sup>.

We analyzed unfiltered 0.5-1 liter samples of overlying Mediterranean seawater and of the two brines for U- and Th-isotopic compositions and abundances by TIMS. Normal Mediterranean seawater has a  $^{238}\text{U}$  content of 3.56 ng/g (salinity of 38.68 psu) which is slightly higher than that of open ocean water (3.24 ng/g: North Pacific<sup>2</sup>), and  $\delta^{234}\text{U}$  of  $151.8 \pm 12.9 \text{‰}$  (vs.  $144 \pm 2$  for North Pacific seawater<sup>2</sup>). Both Brine I at a waterdepth equivalent to 3330 - 3470 dbar, and Brine II (3530 - 3784 dbar) show extreme depletion of  $^{238}\text{U}$ , with concentrations of 19 pg/g  $^{238}\text{U}$  and 17 pg/g, respectively, which are ~200 times lower than seawater. The  $\delta^{234}\text{U}$  in the brines, on the other hand, shows a large enrichment in  $^{234}\text{U}$  over seawater;  $\delta^{234}\text{U}$  of Brine I is 223‰ and that of Brine II is 266‰, indicating a  $^{234}\text{U}$  enrichment over normal seawater of 50% and 77%, respectively. The  $^{230}\text{Th}$  and  $^{232}\text{Th}$  contents of the brines are also highly enriched; with 0.15 fg/g  $^{230}\text{Th}$  and 3.98 pg/g  $^{232}\text{Th}$  in Brine I and 0.06 fg/g  $^{230}\text{Th}$  and 2.01 pg/g  $^{232}\text{Th}$  in Brine II vs. 0.004 fg/g  $^{230}\text{Th}$  and 0.12 pg/g  $^{232}\text{Th}$  for seawater. This results in ~5 times higher  $^{230}\text{Th}/^{232}\text{Th}$  ratio for the brines. In addition the  $^{232}\text{Th}/^{238}\text{U}$  ratios of the brines are also much higher than that of seawater: 0.21 for Brine I and 0.12 for Brine II vs.  $33.9 \times 10^{-6}$ . Scavenging on particles alone cannot account for the relative  $^{230}\text{Th}/^{232}\text{Th}$  and  $^{232}\text{Th}/^{238}\text{U}$  enrichments; an additional source besides seawater has to supply both  $^{230}\text{Th}$  and  $^{232}\text{Th}$ . Moreover, the Sr-isotope composition of the brines<sup>3</sup> also shows a strong deviation from that of seawater (0.70917): 0.70861 for Brine I and 0.70866 for Brine II, both values close to those reported for Messinian evaporites (0.70801-0.70886).

The excess of  $^{234}\text{U}$  is consistent with enrichment due to recoil of  $^{234}\text{U}$  in groundwaters with long residence times and high water-rock interaction, and suggests that outflow of hypersaline groundwater from the Messinian evaporites is a likely source for the brine. This would also provide the  $^{230}\text{Th}$  and  $^{232}\text{Th}$  to the brines, explaining the Th excesses, and would be consistent with the Sr-isotope values of the brines.

Division contribution 5372 (846)

1] De Lange et al., 1990. Mar. Chem. 31, 63.

2] Chen et al., 1986. EPSL 80, 241

3] De Lange et al., 1990. Mar Chem. 31, 89.

CADOMIAN CONTINENTAL GROWTH RECORDED IN  
METASEDIMENTS AND HERCYNIAN GRANITOIDS OF  
THE IBERIAN MASSIF, N. PORTUGAL.

BEETSMA, J.J. and ANDRIESEN, P.A.M., Dept. of  
Petrology & Isotope Geology, Free University, 1085 HV,  
Amsterdam, The Netherlands.

The Iberian Massif forms part of the European Hercynides, and is occupied by metasedimentary successions of Late Proterozoic to Paleozoic (LPP) age. The basal parts of the terrigenous sequence are affected by partial melting associated with the generation and intrusion of a variety of Hercynian granitoids, which include 350-310 Ma syntectonic (sub)alkaline granites and 320-280 Ma late/posttectonic calcalkaline granitoids.

The Nd isotopic evolution recorded in the Late Proterozoic ( $\epsilon_{\text{Nd}}[i]$  -5.3), Late Proterozoic/Cambrian (-1.8), Ordovician (-9.5) and Silurian (-9.0) metasediments is not compatible with derivation from a single crustal source. It signifies the addition of juvenile crustal material to the sedimentary mass during the Late Proterozoic/Cambrian, in an active tectonic setting related to the Cadomian/Pan-African orogenic period. The geochemical signatures including high Zr contents (220 vs. ~200 ppm) and depressed Th/Sc (0.55 vs. >0.65) and La/Cr (0.55 vs. >0.7) ratios are typical for terrigenous sediments deposited in active continental settings, relative to passive marginal/cratonic settings for the remaining LPP sedimentary units. The abundance of Cadomian/Pan-African juvenile components in the metasediments contrasts with the scarcity of Paleozoic (Caledonian) juvenile components, which are commonly present in the Central European Hercynides. This results in a bimodal distribution, rather than a continuous range, of Nd isotopic signatures of the LPP metasediments and its basement constituting the Iberian upper and middle crustal protoliths for Hercynian partial melts.

The Nd isotopic signature of the crustal-derived (sub)alkaline Hercynian granites shows a bimodal distribution with culminations at  $\epsilon_{\text{Nd}}[i]$  -3.0 to -5.5 and -7.0 to -10.0. These values are interpreted to represent two discrete protoliths and correspond to the Hercynian Nd isotopic signature of LPP metasediments containing and lacking juvenile components respectively. The calcalkaline Hercynian granitoids are characterized by a large but continuous range in trace element geochemistry and Nd-isotopic compositions ( $\epsilon_{\text{Nd}}[i]$  +0.1 to -7.2). The (isotope) geochemical variation is attributed to hybridization of mantle-derived gabbroic magmas with crustal-derived partial melts with similar (isotope) geochemical compositions as the (sub)alkaline Hercynian granites.

The presence of Cadomian/Pan-African juvenile components in Hercynian granitoids of the Iberian Massif shows that crustal recycling is an efficient and important process. The potential for Nd isotopic systematics to constrain the relative age of crustal protoliths for partial melts in a particular region thus depends on the rate of succession of earlier orogenic periods and the amounts of juvenile detrital components delivered to the sedimentary mass during these periods.

## HIGH DYNAMIC RANGE SIMS MEASUREMENTS USING THE ISOLAB-120

Belshaw, N. S., O'Nions, R. K., von Blanckenburg, F., and Gibb, A. (Dept. of Earth Sciences, Univ. of Cambridge, Downing St. Cambridge, CB2 3EQ, U.K)

Several isotope systems of importance in the Earth sciences require high dynamic range measurements which present a number of technical challenges. Examples of these are Beryllium and Thorium isotopes where in the case of Beryllium a dynamic range of  $\sim 10^{-7}$  to  $10^{-10}$  for  $^{10}\text{Be}/^{9}\text{Be}$  in natural materials is required. Be is ionised efficiently by ion beam sputtering, with a yield of  $\geq 0.1\%$ . Th on the other hand which requires a range of  $\sim 10^{-5}$  to  $10^{-7}$  for  $^{230}\text{Th}/^{232}\text{Th}$  can be measured by thermal ionisation but displays an improved ionisation efficiency of  $\sim 1\%$  by sputtering, a factor of 10 higher than for thermal ionisation. The high abundance sensitivity of the ISOLAB-120,  $< 10^{-11}$  for Be and  $< 10^{-8}$  for Th, combined with its SIMS capability makes it suitable for these measurements.

Techniques have been developed for the routine separation and measurement of Be and Th in a range of natural materials. While the  $^{10}\text{Be}$  concentration of even the most enriched natural samples is insufficient for in-situ measurement, the study of Th indicates areas where the high mass resolution and high transmission capabilities of the ISOLAB-120 may allow in-situ measurement of  $^{230}\text{Th}/^{232}\text{Th}$ .

The technique for high dynamic range measurements using the ISOLAB-120 will be detailed, along with developments for in-situ applications.

## THE MANTLE SOURCES OF BASALTS FROM CANARY ISLANDS WITH REFERENCE TO Pb-Sr-Nd ISOTOPIC SYSTEMATICS

BELYATSKY, B.V., VNIIOkeangeologia, Maklina 1, St.Petersburg 190121, Russia, OVCHINNIKOVA, G.V., and LEVSKY, L.K., Institute of Precambrian Geology and Geochronology RAN, Makarova 2, St.Petersburg 199034, Russia

Canary islands are usually divided into three groups according to the distance from the African continent. This position is determined by the differences in the structure of the crust of each island.

The basalts from ancient and young volcanic serieses from each group of islands as well as mantle xenoliths enclosed in these basalts have been investigated. On the  $^{207}\text{Pb}/^{204}\text{Pb}$ ,  $^{206}\text{Pb}/^{204}\text{Pb}$  and  $^{208}\text{Pb}/^{204}\text{Pb}$ ,  $^{206}\text{Pb}/^{204}\text{Pb}$  plots the isotopic ratios of Pb have trends with regular decreasing of  $^{206}\text{Pb}/^{204}\text{Pb}$  values from the most radiogenic for the island of La Palma (19.846) up to the least radiogenic values for basalts from the island of Lanzarote (19.506-19.064). The obtained data in the frame of contamination model prove that the mantle source for the investigated volcanic rocks originated as a result of mixing of the substances from the reservoirs HiMu, DM and EM in different proportions. The most valuable contribution of HiMu have the basalts from the western island of La Palma and on the eastern islands (Tenerife, Gran Canaria) the contribution of HiMu decreases with the increasing of the role of the depleted mantle enriched a little bit with EM. Basalts from the island Lanzarote which is situated more close to the continental boundary correspond to the source of depleted mantle contaminated with EM. The contribution of HiMu is very insignificant or doesn't occur at all.

Sr-Nd isotopic data of the investigated basalts haven't such distinct evidences. The range of isotopic data for all islands is the following:  $^{87}\text{Sr}/^{86}\text{Sr}$ : 0.703082-0.703410,  $^{143}\text{Nd}/^{144}\text{Nd}$ : 0.512802-0.513037. Data points are mainly in the field of MORB near the Hi Mu. Nd-Sr data of basalts from the island of Lanzarote unlike the Pb isotopic data do not fall into the field of enriched DM. The contradiction can be explained by the fact that the material of the end member of the enriched mantle under the island of Lanzarote can be melted out of the continental lithospheric mantle of the West-African shield during the desintegration of Pangaea. In case that contaminated lithosphere was rather young ( $\sim 200$  m.y.) and according to valuable difference in time of decay of  $^{238}\text{U}$  and  $^{147}\text{Sm}$  the  $^{143}\text{Nd}/^{144}\text{Nd}$  isotopic ratio in modern basalts mustn't be very different from MORB and  $^{206}\text{Pb}/^{204}\text{Pb}$  ratio must increase.

Comparison of isotopic data for Canary with the same data for NES and Ahaggar evidences the similar mantle source under these volcanoes. At the same time the nearest analogue of the basalts from Canary is volcanics from Azore islands connected with young hot spot.

EARLY ARCHEAN HIGHLY DEPLETED  
MANTLE: Nd AND U-Pb ZIRCON EVIDENCE  
FROM SOUTHWEST GREENLAND

BENNETT, Vickie C., Allen P. Nutman and  
Malcolm T. McCulloch, Research School of  
Earth Sciences, The Australian National  
University, Canberra, ACT 0200, Australia

The excellent exposures, good state of preservation and large areal extent of >3700 Ma rocks combined with the wide diversity of rock types makes southwest Greenland a key area for the study of early Archean geochemical processes. Extremely positive initial  $\epsilon_{Nd}$  values determined for a suite of well dated 3870 Ma to 3760 Ma metadiorites and tonalites from this area demonstrate the existence of a LREE depleted mantle reservoir with an  $\epsilon_{Nd}$  value of  $\approx +4$  at 3800 Ma. Although initial Nd values for all Precambrian rocks, in particular early Archean ones, must be carefully evaluated owing to the possibility of secondary Sm/Nd fractionation, evidence for the accuracy of determined initial isotopic compositions include: high U (1000 ppm) zircons in some areas show no Pb loss indicating minimal fluid and/or thermal disturbance; some gneisses are from an extensive (>200 km<sup>2</sup>) 3800 Ma terrane minimizing the possibility of exchange with, or contamination by younger rocks; highly positive values are not observed in nearby slightly younger (<3700 Ma) rocks which have almost identical post crystallization histories.

We have also determined the <sup>142</sup>Nd/<sup>144</sup>Nd isotopic compositions of three of the high  $\epsilon_{Nd}$  gneisses. The absence of measurable (>10ppm) complimentary <sup>142</sup>Nd isotopic anomalies in the high  $\epsilon_{Nd}$  samples constrains the timing of LREE fractionation of the mantle reservoir to be younger than  $\approx 4300$  Ma. Thus the Sm/Nd fractionation is not related to a primordial global differentiation event. Furthermore a 4300 Ma differentiation age requires the time averaged <sup>147</sup>Sm/<sup>144</sup>Nd of the mantle reservoir to be >0.26. It would be difficult to account for this degree of depletion for the *whole* upper mantle by extraction of continental crust. Rather we favor a model of isolation and depletion of *limited* portions of the upper mantle by extraction of felsic crust. The early Archean Nd database is currently not sufficient to determine whether the ultradepleted reservoir was a global phenomena, or restricted to the region of the North Atlantic Craton and thus related to the formation of the overlying continent.

Owing to the significance of initial  $\epsilon_{Nd}$  values for constraining models of early Earth differentiation, it is necessary to validate the Nd isotopic compositions. To this end we are continuing isotopic and geochemical studies of additional  $\geq 3800$  Ma gneisses and also of recently identified  $\geq 3800$  Ma large ultramafic enclaves whose relict mineral compositions (aluminous spinels, Fo 90 olivine) suggest they were derived from the upper mantle.

THE H CHONDRITE PARENT BODY(IES):  
INTERNAL STRUCTURE AND TEMPORAL  
CONTRIBUTION TO THE METEORITE FLUX

BENOIT, P.H. and SEARS, D.W.G., Dept. Chemistry  
and Biochemistry, University of Arkansas, Fayetteville,  
AR, 72701, USA.

The Antarctic meteorite collection has made many contributions to the study of parent body structure and evolution. Among these is the discovery of a group of unusual ordinary chondrites which is not found among the modern falls. These H chondrites, referred to here as "Group A", have high induced thermoluminescence (TL) peak temperatures, high metallographic cooling rates, significantly lower abundances of certain REE elements and have cosmic ray exposure (CRE) ages of about 8 Ma and were apparently fairly small during irradiation in space. Among the modern falls there are numerous H chondrites with CRE ages of about 8 Ma ("Group B"), but these meteorites have induced TL peak temperatures, metallographic cooling rates and REE element abundances indistinguishable from H chondrites with larger CRE ages ("Group C") from both the Antarctic and modern falls collections and were larger than Group A meteorites during irradiation (Benoit and Sears, 1992).

Our original study of the Group A Antarctic meteorites was based largely on H5 chondrites. We have since examined Antarctic H4 and H6 chondrites as well. We find that there are members of Group A among both the H4 and H6 chondrites. However, for the H4 chondrites the difference between Group A and the Group B and C meteorites is not as distinct as is the case for the H5 and H6 chondrites. The H6 members of Group A appear to be rare relative to Group B, compared to the proportions observed for the H5 chondrites in the Antarctic collection. Considering only the Group B and C meteorites, there is a tendency for H4 chondrites to have higher metallographic cooling rates and somewhat higher TL peak temperatures than H5 and H6 chondrites. No such tendency is observed among the Group A chondrites of types 4-6, but this must be viewed with caution due to the relative insensitivity of both metallographic determinations and induced TL response at the high cooling rates (about 100 K/My) observed.

The existence of the unusual Group A meteorites among the H chondrites, which have generally been considered fairly homogeneous, suggests that: (1) The meteorite flux has changed in composition over the relatively short time interval represented by the Antarctic meteorite collection (<800 ka), (2) the metallographic cooling rate data of the Group B and C chondrites can be explained by a simple stratified parent body model, with H6 having slower cooling rates than H4, but (3) the unusual group A meteorites do not fit this simple model. The group A meteorites may be derived from a totally different parent body or may have been created by extensive thermal processing during the 8 Ma event which generated large numbers of meteoroid bodies. If this latter situation is the case, the rarity of H6 members of Group A may be evidence of the survival of a stratified parent body up until the 8 Ma event.

Benoit, P.H., and Sears, D.W.G., 1993, Breakup and Structure of an H-chondrite Parent Body: The H-chondrite flux over the last million years: *Icarus*, v. 101, 188-200.

## CHRONOLOGY OF INTERIOR ALASKAN LOESS-PALEOSOL DEPOSITS BY THERMOLUMINESCENCE

BERGER, Glenn W., Dept. of Geology, Western Washington University, Bellingham, WA 98225, USA, and PÉWÉ, T. L., Dept. Geology, Arizona State University, Tempe, AZ 85287, USA.

The thick (25m+) and widespread loess deposits of interior Alaska have interbedded micro and macro fossils, organic beds and paleosols. They thus represent an important source of paleoclimatic and paleoecologic information. However, the chronology of deposition has only recently (1990) been quantified, in a broad sense, using fission-track dating of interbedded tephra beds. We applied thermoluminescence (TL) sediment dating methods to loess near Fairbanks thought to be younger than ~200 ka, to provide a chronology of key deposits for an age range usually inaccessible to other dating methods.

We have ~20 TL preliminary ages (from the fine-silt total-bleach and partial-bleach procedures) for loess and buried soils. More samples are being analyzed. As an age check, we dated loess just above and below the  $140 \pm 10$  ka Old Crow tephra (OCt) at the Birch Hill site, obtaining TL ages of  $128 \pm 22$  ka ( $1\sigma$ ) and  $144 \pm 22$  ka respectively. At the Sheep Creek Cut site loess 2 cm above the regionally important Sheep Creek tephra (SCt) gave an age of  $184 \pm 27$  ka, in agreement with TL ages of  $191 \pm 24$  ka and  $205 \pm 31$  ka for loess 2 cm above and 2 cm below (respectively) this ash at the Dawson Cut site. These results support the recent suggestion of Preece that this tephra is older than the OCt. However, at site Eva Creek II loess above and below an ash also correlated to SCt gave ages of  $117 \pm 19$  and  $150 \pm 28$  ka.

At two sites we confirm that the significant erosional unconformity at the top of the Gold Hill Loess corresponds to the time of the Eva Interglacial (Sangamon). At Dawson Cut we obtained loess TL ages of  $61 \pm 6$  ka above and  $177 \pm 30$  ka below the unconformity. At Sheep Creek Cut, loess just below this unconformity gives a TL age of  $115 \pm 19$  ka. We also obtain the first direct ages for two significant buried organic horizons at the Gold Hill 1 site. A  $76 \pm 10$  ka age for a thick organic silt at 11 m depth could represent paleosol development during isotope stage 5a warming. A thick, laterally extensive organic silt at 3 m depth here is dated directly at  $29 \pm 4$  ka. In other parts of interior and northwestern Alaska there are prominent or recognizable "buried soils" in stratigraphically similar positions to our upper "soil", with radiocarbon ages near 30 ka B.P. at one site (Egiguruk), thus suggesting that a regional, late Wisconsin paleoclimatic stratigraphic marker may exist.

At some localities there is evidence that post-depositional reworking or contamination (e.g., via translocation of fine silt through modern rootlet channels) have lowered TL ages. Future TL samples at certain sites would probably need to be excavated from at least 60 cm behind "fresh" section faces.

## STRUCTURE & CONSTITUTION OF INTERSTELLAR GRAPHITE SPHERULES.

Bernatowicz, T. and Amari, S., McDonnell Center for the Space Sciences, Washington University, St. Louis Mo. 63130 and Lewis, R. S., Enrico Fermi Institute, University of Chicago, Chicago, IL 60637.

Transmission electron microscopy of 500Å slices of presolar (Amari *et al.*, 1993) interstellar graphite spherules (1–2 µm diameter) by direct imaging, convergent beam diffraction and energy dispersive x-ray analysis shows a range of crystallinity and internal structure in the graphite as well as a variety of carbide inclusions 100s of Å in diameter (Bernatowicz *et al.*, 1991). Recent work (Bernatowicz *et al.*, 1994) has extended observations of these polymineralic assemblages to include many more grains of the graphite separate KFC1 (Amari *et al.*, 1994) from the Murchison meteorite. Typically there is an amorphous carbon core surrounded by a well graphitized shell with interspersed carbides ranging from nearly pure TiC to Mo, Zr carbides with only a few % Ti. The Mo & Zr are enriched relative to Ti over solar abundances by factors as high as several thousand, evidently effects due to both nucleogenic enrichments in AGB stars and chemical (condensation) enrichments in the stellar atmospheres. These grains are randomly dispersed throughout a large fraction, perhaps most, of the graphite spherules. Occasionally a nearly pure TiC crystal is found in the precise center of the graphite spherule, evidently a heterogeneous nucleation site, in which case the whole spherule is well crystallized graphite. These kinds of observations should provide evidence for stellar atmosphere condensation conditions. For instance (Lodders and Fegley, 1992 & 1993; Sharp and Wasserburg, 1993) Ti, Mo, Zr carbides are calculated to condense under equilibrium conditions ahead of graphite for reasonable s-process elemental enrichments. The random distribution of grains of different composition within single spherules is consistent with occlusion of these precondensed grains within later growing graphite spherules. Hopefully, more refined thermodynamic models, including e.g. solid solutions, combined with more extensive elemental, mineralogical, & isotopic data for these grains will determine chemical compositions & physical conditions of stellar atmospheres and the underlying stellar nucleosynthesis. Come and see the pictures.

Amari, S., Hoppe, P., Zinner E., and Lewis, R.S. 1993, The isotopic compositions and stellar sources of meteoritic graphite grains: *Nature* **365** 806-809.

Amari, S., Lewis R.S., and Anders, E. 1994, Interstellar grains in meteorites: I. Isolation of SiC, graphite, and diamond; size distributions of SiC and graphite: *Geochim. Cosmochim. Acta*, in press.

Bernatowicz T.J., Amari, S., Zinner, E.K., Lewis, R.S. 1991, Interstellar grains within interstellar grains: *Astrophys. J.* **373** L73-L76.

Bernatowicz, T. J., Amari, S., and Lewis, R.S. 1994, Refractory carbides in interstellar graphite: *Lunar Planet. Sci. Conf.* **25**, submitted.

Lodders K., and Fegley, B. Jr., 1992, Trace element condensation in circumstellar envelopes of carbon stars: *Meteoritics* **27** 250-251.

Lodders K., and Fegley, B. Jr., 1993, Chemistry in circumstellar envelopes of carbon stars: the influence of P, T, and elemental abundances: *Meteoritics* **28** 387.

Sharp, C.M. and Wasserburg, G.J. 1993, Molecular equilibria and condensation sequences in carbon rich gases: *Lunar Planet. Sci. Conf.* **24** 1281-1282.

EXCITATION FUNCTIONS OF 31 TO 500 MEV PROTON INDUCED REACTIONS ON C, Mg, Al, SiO<sub>2</sub>, AND Si  
BEVERDING, A.M, Englert, P.A.J., Gans, C. , Kim K., Chakravarty, N., Nuclear Science Facility, San Jose State University, San Jose, CA 95192-0163, Castaneda, C., Crocker Nuclear Laboratory, University of California, Davis, CA 95616, Young, J., Department of Physics, Chico State University, Chico, CA 95929, Sisterson, J., Koehler, A.M., Harvard Cyclotron Laboratory, Harvard University, Cambridge, MA, 02138, Jull, T., Donahue, D.J., NSF Arizona Accelerator Mass Spectrometer Facility, University of Arizona, Tucson, AZ, 85721, Vincent, J., TRIUMF, 4004 Westbrook Mall, Vancouver, B.C. V6T 2A3, and Reedy, R.C., Los Alamos National Laboratory, Group SST-9, Los Alamos, NM 87545.

Excitation functions for several cosmogenic nuclides were determined by experimental and theoretical methods. These data are essential for interpretation of solar-proton-produced radionuclides in extraterrestrial material. Targets of C, Mg, Al, SiO<sub>2</sub>, and Si, major components of planetary surfaces, were irradiated with protons over the energy range of 31 to 500 MeV. For the energies of 31 to 67.5 MeV, <sup>7</sup>Be, <sup>22</sup>Na, and <sup>24</sup>Na cross sections were determined by gamma ray spectroscopy. <sup>14</sup>C cross sections were measured by accelerator mass spectroscopy for SiO<sub>2</sub> and Si targets and agree well with Sisterson et al. (1993), work on <sup>10</sup>Be and <sup>26</sup>Al is in progress. Experimental values for the short-lived isotopes compare well with those measured previously, where available. The theoretical calculations were optimized by choosing input parameters for the ALICE-91 code to best fit the measured benchmark excitation functions up to the pion production threshold. In addition, further insight is gained in modeling cross sections, especially for neutrons since these have been seldom measured.

Sisterson et al., Proton Production Cross Sections for <sup>14</sup>C from Silicon and Oxygen: Implications for Cosmic-Ray Studies: Proceedings 6th International Conference in Accelerator Mass Spectroscopy, NIM B, in press.

#### ISOTOPIC RECORDS OF GONDWANA GLACIATION IN TALCHIR SEDIMENTS

Bhattacharya, S.K., Physical Research Laboratory, Ahmedabad 380 009, India, and Chakravarti, A., Indian Institute of Technology, Kharagpur, 721 302, India.

Talchir formation in eastern India represents early Permian glacial outwash deposits from the famous Gondwana glaciation and contains fine sandstone and siltstone in its upper part. Spherical nodules of a few cm size cemented by fresh-water carbonates have been found in siltstone horizon of Talchir sediments in West Bokaro, Bihar. These were analysed for oxygen and carbon isotopic composition to infer about the nature of the ice sheet and the environmental regime.

The oxygen isotopic composition of these calcrete nodules ranges from -20% to -27.9% (w.r.t. PDB) and would correspond to similar values in SMOW unit for the nodule forming water. These values are extremely depleted compared to the expected meteoric water composition at 50°S, the approximate palaeolatitude of this area during the Permian. Therefore, the glacial melt water used in these cements was derived not from local valley glaciers but from the edges of a continental ice sheet originating in higher latitudes (>80°S). The isotopic values of these cements are similar to those of the fresh-water early Permian cements in the continental tillites from Antarctic and South Africa and suggest that the glaciation was continental in nature and extended over a major part of the Gondwanaland.

The carbon isotopic composition of these nodules ranges from -2% to -11% (w.r.t. PDB) and indicate vegetational source for the carbon in HCO<sub>3</sub>. Since the deposition of these sediments took place in marginal areas like lakes supported by melt water, there may be organic production in summer. Decomposition of these organic carbon could have supplied <sup>13</sup>C depleted HCO<sub>3</sub> to diagenetically alter the original carbon isotope values of the sediments.

**ISOTOPIC STUDY OF THE KIMBERLITE DIKE OF MASONTOWN, PA, USA**

BIKERMAN, Michael, PRELLWITZ, H.S., Geology & Planetary Science Dept, University of Pittsburgh, Pittsburgh, PA 15260, USA, and SIMONETTI, A., BELL, K., Ottawa-Carleton Geoscience Center, Department of Earth Sciences, Carleton University, Ottawa, Canada

The Masontown (Fayette Co) PA dike intrudes upper Pa and lower Pm (?) sedimentary rocks with little contact metamorphism. The phlogopite-bearing kimberlite was considered on mineralogic grounds to be formed from mixing of two magmas (Hunter & Taylor, 1984). K-Ar analyses on coarse and fine phlogopite, and on olivine, were dates of:  $147.3 \pm 1.5$  Ma,  $353.2 \pm 2.2$  Ma and no detectable radiogenic argon, respectively. If the olivine result means no excess argon, then the two phlogopites may indicate different times of formation.

Rb-Sr and Sm-Nd analyses on Cr-rich and Cr-poor garnets, a calcite vein and a whole rock sample produced results which lie slightly above the field of South African Group 1 kimberlites, on an  $\epsilon_{Nd}$  vs  $\epsilon_{Sr}$  plot. The whole rock has the most radiogenic Sr isotopic ratio.

Sr and Nd isotopic analyses on whole rock and mineral samples are:

	$^{87}Sr/^{86}Sr_i$	$\epsilon_{Sr}$	$^{143}Nd/^{144}Nd_i$	$\epsilon_{Nd}$
calcite vein	0.70365	-9.7	0.51287	8.1
whole rock	0.70513	11.4	0.51280	6.8
Cr-rich garnet	0.70414	-2.7	0.51279	6.7
Cr-poor garnet	0.70437	0.5	0.51290	8.8

The garnets are not in Sr isotopic equilibrium with the whole rock or the vein calcite. A "scatterchron" Sm-Nd date of about 146 suggests that the garnets and fine phlogopites are roughly coeval.

This dike has had a complex history, perhaps involving mixing of mantle-derived magma with metasomatized Acadian "mantle" at about 146 Ma. The partially equilibrated mix was emplaced by gas-driven fluidization. The low initial Sr calcite vein may reflect the composition and source of some of the carrier gas.

Hunter, R.H., & Taylor, L.A., 1984, Magma mixing in the low velocity zone: *American Mineralogist*, 69, p. 4-40.

**CARBON ISOTOPE STRATIGRAPHY OF THE LIESBERG BEDS MEMBER (OXFORDIAN, SWISS JURA)**

BILL, Markus Institut de Géologie et Paléontologie, Université de Lausanne, BFSH 2, Lausanne, CH-1015, Switzerland, and BAUMGARTNER, P.O., same address, and HUNZIKER, J. C. and SHARP, Z. D. Institut de Minéralogie et Pétrographie, Université de Lausanne, BFSH 2, Lausanne, 1015-CH, Switzerland

The Liesberg Beds Member forms the transition between the lower to middle Oxfordian dark coloured marls (Renggeri Member and the Terrain à Chailles Member) and the middle Oxfordian reefal limestones (St-Ursanne Formation). Both litho- and biofacies are very diverse and evolve rapidly up-section. Isotopic studies of whole rocks are therefore excluded. In search for a convenient isotopic marker, we measured several fossil groups and chose crinoid stems of *Millericrinus* sp. and echinoid spines of *Paracidaris* sp., because of their abundance throughout the section and because of small variations of  $\delta^{13}C$  within one fossil and between fossils of the same stratigraphic level.

Values measured in echinoderms largely reflect earliest diagenetic conditions at the seawater-sediment interface. The porous stereome structure secreted as high Mg-calcite by echinoderms has a high reactive surface/volume ratio, which triggers the precipitation of very early syntaxial cements.

In the four studied sections reproducible carbon isotope shifts were observed both for *Millericrinus* sp. stems and *Paracidaris* sp. spines.

A negative shift of 1 - 1.5 ‰  $\delta^{13}C_{PDB}$  was observed near the base of the section, just above the transition from the Terrain à Chailles Member, where the first corals occur. In the middle and upper part of the three sections, characterised by a stepwise increase of corals and the macrofossils, a positive shift of about 2 ‰  $\delta^{13}C_{PDB}$  was observed.

Despite of the highly variable lithologic composition of the Liesberg Beds Member carbon isotopic shifts seem to be consistent and warrant an interpretation as an original signal, controlled by the isotopic composition of dissolved carbonic acid in sea water.

In a platform area, local factors may cause a particular isotopic signature in restricted water masses. For instance, the compaction and dewatering of the lower Oxfordian marls could have released pore waters rich in light organic carbon (as methane and CO<sub>2</sub>) explaining the negative shift at the base of the Liesberg Beds Member.

The following positive shift, however, seems to correspond to a general trend of opening up of the platform and connection to open marine waters. In that case, they could be interpreted as a result of important global organic carbon burial, that occurred possibly during periods of warm and humid climate.

OBSERVED  $^{87}\text{Sr}/^{86}\text{Sr}$  ISOTOPIC VARIATION IN PELAGIC MUDROCKS OF Pliocene AGE ARE THE RESULT OF ORBITALLY FORCED PERIODIC VARIATION IN CONTINENTAL RUNOFF

Blenkinsop, John; Patterson, R. Timothy; Reinhardt, Eduard; Department of Earth Sciences and Ottawa-Carleton Geoscience Centre, Carleton University, Ottawa, Canada, K1S 5B6; and William Cavazza, Department of Mineralogical Sciences, University of Bologna, 40126 Bologna, Italy

$^{87}\text{Sr}/^{86}\text{Sr}$  ratios measured in planktic foraminifera extracted from rhythmically deposited Early Pliocene (4.5-4.3 Ma) limestone-marl couplets of the Trubi Formation (Calabria, southern Italy) indicate that strontium isotopic analyses may record paleoclimatic and paleoceanographic information in addition to age estimates. Previous hypotheses have correlated deposition of the Trubi couplets with changes in monsoon intensity driven by 23,000 ka Milankovitch precession cycles.

Individual marl and limestone units yielded  $^{87}\text{Sr}/^{86}\text{Sr}$  ratios oscillating in harmony with lithology. While the results from the limestones correlate well with open ocean strontium regression curves, the marls are characterized by lower  $^{87}\text{Sr}/^{86}\text{Sr}$  ratios, probably the result of monsoon influenced increases in fluvial flow to the Mediterranean Sea. Based on present-day discharge rate, strontium concentration, and isotopic ratio of the major rivers discharging into the Mediterranean Sea, the observed 0.00003 shift in  $^{87}\text{Sr}/^{86}\text{Sr}$  ratio between the limestones and marls could be generated in about 10,000 years, consistent with the known depositional rate. Although tentative, our results suggest that in restricted basins strontium isotopic ratios may be a useful indicator of past marine environments.

A SILICATE WEATHERING MECHANISM FOR ELEVATING MARINE  $^{87}\text{Sr}/^{86}\text{Sr}$  FOLLOWING GLACIAL-INTERGLACIAL TRANSITIONS

BLUM, J.D., EREL, Y.<sup>†</sup>, and BROWN, K., Dept. of Earth Sciences, Dartmouth College, Hanover, NH, 03755, USA, <sup>†</sup>also Inst. of Earth Sciences, Hebrew Univ., Jerusalem, 91904, Israel.

The isotopic composition of Sr in stream waters and exchangeable Sr in soils was investigated in recently glaciated granitoid terranes in the Sierra Nevada (SN), California and the Wind River Range (WRR), Wyoming. In both cases a negative correlation was observed between the  $^{87}\text{Sr}/^{86}\text{Sr}$  ratio and the soil age, indicating that the  $^{87}\text{Sr}/^{86}\text{Sr}$  ratio released in the early stages of weathering following glaciation is significantly higher than in later stages.

In the SN, drainages that were glaciated ~10 kyr ago (exposing fresh surfaces) have average stream water  $^{87}\text{Sr}/^{86}\text{Sr}$  ratios 0.0004 to 0.0011 higher than drainages that were not glaciated in the past ~100 kyr. Based on  $^{87}\text{Sr}/^{86}\text{Sr}$  ratios and major cation concentrations of bedrock minerals and stream water we have argued that stream water  $^{87}\text{Sr}/^{86}\text{Sr}$  is controlled largely by plagioclase and biotite weathering and that biotite is weathering ~4 and ~6 times more rapidly than plagioclase in the recently glaciated and non-glaciated drainages, respectively (Blum et al., 1993).

In the WRR exchangeable Sr was analyzed in soils developed on six moraines varying in age from ~0.3 to ~350 kyr as well as in stream water from drainages glaciated ~20 and ~100 kyr ago. Because granitoids in the WRR are much older than the SN (2.5 versus 0.1 byr) the contrast in the  $^{87}\text{Sr}/^{86}\text{Sr}$  ratio of the bedrock minerals is greatly enhanced due to the much longer time for radioactive decay of  $^{87}\text{Rb}$  to  $^{87}\text{Sr}$ . Using the ~350 kyr old soils as a baseline,  $^{87}\text{Sr}/^{86}\text{Sr}$  in younger soils is elevated by 0.0029, 0.0053, 0.0127, 0.0240, and 0.0835 in the ~100 kyr, ~20 kyr, ~10 kyr, ~1 kyr and ~0.3 kyr old soils respectively. Similarly, stream water draining a ~10 kyr weathering surface has  $^{87}\text{Sr}/^{86}\text{Sr}$  elevated by 0.0015 relative to a ~100 kyr old weathering surface.

The shifts we observe in the  $^{87}\text{Sr}/^{86}\text{Sr}$  ratio released by silicate weathering provide a previously unrecognized mechanism for elevating global riverine  $^{87}\text{Sr}/^{86}\text{Sr}$  ratios following global glacial advances. This may help to explain the correlation between the marine  $^{87}\text{Sr}/^{86}\text{Sr}$  ratio and global climate cycles over the past 450 kyrs (with ~100 kyr periodicity) which requires increases in global riverine  $^{87}\text{Sr}/^{86}\text{Sr}$  by ~0.0040 and/or dramatic increases in global riverine Sr flux following glacial to interglacial transitions (Clemens et al., 1993).

Blum, J.D., Erel, Y. and Brown, K., 1993, *Geochim. Cosmochim. Acta*, 58, 5019-5025.  
Clemens, S.C., Farrell, J.W. and Gromet, L.P., 1993, *Nature* 363, 607-610.

GEOCHEMISTRY OF LOWER OCEANIC CRUST-  
DATA FROM SITE 735B

BLUSZTAJN, J., HART, S.R. and DICK, H., Woods  
Hole Oceanographic Inst., Woods Hole, MA 02543,  
USA

Due to a lack of suitable dredged samples our knowledge of the geochemistry of the oceanic crust is mostly restricted to the upper crust. Site 735B on the southwest Indian Ridge, which recovered a 500m section of Layer 3 gabbros, provides a unique opportunity to study the geochemistry of the lower oceanic crust. In order to get representative analyses of the whole core, we cut 1-2 meter long strip samples, 1-2 cm wide, from 22 sections, covering the whole range in lithologies and deformation styles. In addition, we analyzed carbonate, amphibole, diopside and felsic veins. Sr and oxygen isotopic compositions of carbonate veins indicate that sea water circulation at low temperature ( $<10^{\circ}\text{C}$ ) ceased within 5-7m.y. of crust formation. Higher temperature plagioclase, amphibole and diopside veins show small sea water  $^{87}\text{Sr}/^{86}\text{Sr}$  signatures ( $^{87}\text{Sr}/^{86}\text{Sr}$  up to 0.7036), but primary igneous  $^{143}\text{Nd}/^{144}\text{Nd}$  (0.51312). The strip samples show a slight sea water signature at shallow depths ( $^{87}\text{Sr}/^{86}\text{Sr}=0.7030$ ) which decreases down hole;  $^{143}\text{Nd}/^{144}\text{Nd}$  is virtually constant throughout the hole at 0.51312. The elevated  $^{87}\text{Sr}/^{86}\text{Sr}$ , and Cs, U enrichment in the shallowest part of hole 735B indicate that only this upper 70m of the core was significantly modified by low temperature interaction with sea water. Excluding these shallow samples, the average Rb, Cs and U content is 0.32ppm, 5.5ppb and 35.5ppb respectively. In conjunction with the lack of evidence for strong sea water alteration, this indicates that alkalis and U were not stripped from the gabbros by high temperature hydrothermal circulation. The putative hot smoker flux of Rb and Cs is thus still much too large to be supported by crustal inventories. The primary protolith has an isotopic composition of  $^{87}\text{Sr}/^{86}\text{Sr}=0.7029$ ,  $^{143}\text{Nd}/^{144}\text{Nd}=0.51312$  and  $^{206}\text{Pb}/^{204}\text{Pb} \approx 17.5$ . Preliminary analyses document very low Os content (from 0.4 to 3ppt) with only one troctolitic unit having a high Os content (400 ppt) and elevated  $^{187}\text{Os}/^{186}\text{Os} = 1.217$ . The gabbros are quite enriched in Pb (average 0.52 ppm) causing the average  $^{238}\text{U}/^{204}\text{Pb}$  ratio to be low (around 4.2). Without additional processes like dehydration removal of lead in subduction zones, the low  $\mu$  value does not support existing models for generating the HIMU mantle component by recycling and long-term storage of oceanic crust.

SINGLE CRYSTAL LASER  $^{40}\text{Ar}/^{39}\text{Ar}$  AGES OF  
QUARTZ PROTOCRYSTS IN THE 0.761 MA BISHOP  
TUFF RHYOLITE (LONG VALLEY, U.S.A.)

BOGAARD, P.V.D. and SCHIRNICK, C., Dept. of  
Volcanology and Petrology, Geomar Research Center,  
D-24148 Kiel, F.R.G.

The Bishop Tuff (BT) erupted  $0.761 \pm 0.001$  Ma BP (weighted mean; MSWD=1.2; N=20; all errors  $1\sigma$ ) according to laser  $^{40}\text{Ar}/^{39}\text{Ar}$  analyses of sanidine phenocrysts from fallout and flow deposits. Fresh obsidian glass spherules from highly welded late flows yield a mean apparent age of  $0.754 \pm 0.008$  Ma. The BT rhyolite contains 5-25% phenocrysts, chiefly quartz, sanidine and plagioclase (3:3:1; Hildreth, 1979), with the quartz crystals showing abundant potassium-rich rhyolite glass inclusions, bipyramidal outlines and frequent embayed and resorbed surfaces. We have studied the Ar isotope composition of meticulously cleaned, inclusion-rich quartz crystals picked from essential lapilli of early airfall deposits (Type A) and from bulk samples of late highly welded ignimbrite cooling units (Type B).

Individual Type A quartz crystals contain fresh glass inclusions which release up to  $3.7\text{E}-13$  ccSTP  $^{36}\text{Ar}$ ,  $6.7\text{E}-11$  ccSTP  $^{39}\text{Ar}$ , and  $1.9\text{E}-10$  ccSTP  $^{40}\text{Ar}$  upon laser fusion (typical system blanks are  $5.5\text{E}-14$ ,  $6.5\text{E}-14$ , and  $1.8\text{E}-12$  ccSTP for  $^{36}\text{Ar}$ ,  $^{39}\text{Ar}$ , and  $^{40}\text{Ar}$ ). They yield a mean apparent age of  $1.89 \pm 0.03$  Ma (MSWD=2.2; N=25), and a decent isochron with an age of  $1.93 \pm 0.06$  Ma (MSWD=2.3) and an initial  $^{40}\text{Ar}/^{36}\text{Ar}$  ratio of  $290 \pm 7$ , indicating that the high  $^{40}\text{Ar}$  contents are derived from in situ decay of  $^{40}\text{K}$  in the glass inclusions and not from excess  $^{40}\text{Ar}$  in the quartz. Quartz crystals lacking inclusions yield argon signals similar to blank values. Type B quartz crystals contain more devitrified "glass" inclusions, abundant cracks and release much smaller Ar volumes (i.e.  $^{39}\text{Ar} < 8\text{E}-12$  ccSTP). Yet still, the data define an isochron with an age of  $2.3 \pm 0.4$  Ma, and an initial  $^{40}\text{Ar}/^{36}\text{Ar}$  ratio of  $296 \pm 2$  (MSWD=1.4; N=7).

Our study indicates that the age of individual quartz crystals can be determined by means of the Ar isotope composition of their glass inclusions, and that the vast majority, if not all of the quartz crystals in the BT rhyolite are neither phenocrysts nor xenocrysts sensu stricto. Instead, we interpret these crystals to represent remnants (protocrysts) of a crustal magma body that intruded the Long Valley basement, crystallized quartz phenocrysts trapping melt inclusions, and cooled below the Ar blocking temperature of quartz at 1.9 Ma BP. Glass Mountain rhyolites of the same age probably represent the surface projection of that intrusion. 1.14 Million years later, that magma had acquired a more evolved composition and erupted to form the Bishop Tuff.

What about the magma in the meantime? Was it a melt at high temperature all along (Halliday et al. 1989), then why didn't the glass inclusions equilibrate isotopically? Was it a granite in-between (Sparks et al., 1990), then where are the remaining granite crystal assemblage and abundant granite xenoliths? We envisage a super-cooled, only partially crystallized and consolidated, glass-like state, permitting near-instantaneous transformation into a partial melt upon re-heating due to emplacement of mantle-derived basalt melts into the crust.

SM-ND AGE OF SUBOPHIOLITIC METAMORPHIC SOLES OF SEVANO-AKERA ZONE (LESSER CAUCASUS)

BOGDANOVSKI O.G., Vernadsky Inst. of Geochemistry, Moscow, 117975, Russia, JAGOUTZ E., Max-Planck Inst. fur Chemie, Mainz D-6500, Germany, ZAKARIADZE G.S., Vernadsky Inst. of Geochemistry, Moscow, 117975, Russia, KARPENKO S.F., Vernadsky Inst. of Geochemistry, Moscow, 117975, Russia, and SILANTJEV S.A., Vernadsky Inst. of Geochemistry, Moscow, 117975, Russia.

The ophiolitic zones of Lesser Caucasus reveal a prolonged period of tectonic accretion of paleoceanic allochthones:  $229 \pm 10$  Ma, Sm-Nd for tholeiitic sequence (Bogdanovski et al., 1992) and  $160 \pm 4$  Ma, U-Pb for boninitic sequence (Zakariadze et al., 1990). Several blocks of garnet amphibolites were considered earlier as the most ancient (Early Carboniferous) paleoceanic fragments of the accretionary melange of Lesser Caucasus (330 Ma, Rb-Sr, Meliksetian et al., 1984). Our recent studies of these garnet amphibolites have shown that: a) they were metamorphosed at  $T=600-800^\circ\text{C}$  and  $P=7-12$  kb; b) their protolith was a low-K and low-Ti differentiated tholeiitic series (basalts, andesites):  $(\text{La}/\text{Sm})_n = 0.27-0.92$ ,  $(\text{Yb})_n = 9-19$ ; and c) the age of metamorphism of these rocks (three-mineral Sm-Nd isochrone) is  $155 \pm 11$  Ma ( $\text{epsNd}(T) = 4.5 \pm 0.3$ ,  $\text{MSWD} = 0.175$ ). Studied amphibolites are interpreted as subophiolitic series of metamorphic rocks. The obtained age value of metamorphism corresponds well to the age of obduction ( $J_{2-3}$ ) of Mesozoic ophiolites along the Vardar-Ismir-Ankara-Erzincan-Lesser Caucasus belt of Eurasian margin.

Bogdanovski O.G., et al., 1992, - Dokl. Ac. Nauk USSR, v. 327, p. 566-569, (in Russian).  
Zakariadze G.S. et al., 1990, - Izv. Ac. Nauk USSR, Ser. Geol., 3, p. 17-30 (in Russian).  
Meliksetian B.M., et al., 1984, - Izv. Ac. Nauk ArmSSR, Nauki o Zemle, v. 37, p. 3-22 (in Russian).

ND ISOTOPES AND THE SOURCE OF SEDIMENTS IN THE MIOGEOCLINE OF THE CANADIAN CORDILLERA

BOGHOSSIAN, N.D., PATCHETT, P.J.,

Dept. of Geosciences, University of Arizona, Tucson, AZ 85721, U.S.A. and ROSS, G.M., Institute of Sedimentary and Petroleum Geology, Calgary, Alberta T2L 2A7, Canada

Nd isotopes in clastic sediments from the miogeoclinal sequence of Alberta constrain sediment sources and document continental input to crustal growth in the Cordillera. The samples range in age from ca. 750 to 70 Ma. The goal was (1) to develop a North American miogeoclinal reference for Nd isotopes and to provide a baseline for continental input to the terranes of the Canadian Cordillera; (2) to constrain the importance of proximal and distal North American basement sources for these sediments; (3) to constrain timing of arrival of juvenile terranes to the Canadian continental margin.

Initial  $\epsilon_{\text{Nd}}$  values for Upper Proterozoic to Upper Ordovician samples range -14 to -22 and can be explained by derivation of clastics from a mixture of proximal Archean and Proterozoic basement. A positive shift of 6  $\epsilon_{\text{Nd}}$  units occurs in Upper Devonian time, and this more positive signature persists until foreland basin formation in Upper Jurassic time.  $\epsilon_{\text{Nd}}$  values for this time slice of 370 to 150 Ma range from -6 to -9 and require involvement of a more juvenile source. After emplacement of terranes in the Cordillera beginning in Jurassic time, a foreland basin developed on top of the miogeocline. The foreland basin sediments show extreme heterogeneity, with  $\epsilon_{\text{Nd}}$  values as high as zero.

Two hypothesis can explain the shift in  $\epsilon_{\text{Nd}}$  in Upper Devonian time. The higher  $\epsilon_{\text{Nd}}$  signature could represent a mix of Cordilleran juvenile component plus Precambrian basement. The  $\epsilon_{\text{Nd}}$  shift is coeval with tectonic activity along the western margin of North America in Devonian-Mississippian time. However, in the southern Canadian Cordillera any western juvenile sources should have ceased to supply sediments to the miogeocline by mid-Mississippian time and thus cannot explain the persistence of the juvenile signature until Upper Jurassic.

The second hypothesis requires transport of sediments across the craton from Appalachian sources. The Appalachian belt (which includes Grenville age basement and sediments ultimately derived from this basement) provides the appropriate isotopic signature. It constituted the main mountain belt in North America during most of the Paleozoic and was a major source of detritus to the craton throughout that time. Pennsylvanian sediments of Appalachian origin with isotopic signature identical to our samples ( $\epsilon_{\text{Nd}} = -6$  to  $-10$ ) were documented as far into the interior of the craton as the central U.S.A. Our hypothesis would require the transport of Appalachian-derived sediments a distance around twice that documented by Gleason et al. (1994), maybe in a multi-step journey.

Gleason, J.D., Patchett, P.J., Dickinson, W.R., Ruiz, J., 1994, Nd isotopes link Ouachita turbidites to Appalachian sources: Geology, in Press.

PRE- AND POST CRYSTALLIZATION CONTAMINATION OF SILICIC PERALKALINE ROCKS BY SEAWATER-DERIVED COMPONENTS: SOCORRO ISLAND, MEXICO  
**BOHRSON, W.A.**, Dept. of Geological Sciences, UCSB, Santa Barbara, CA 93106, USA, and **REID, M.R.**, Dept of Earth and Space Sci., UCLA, Los Angeles, CA 90024, USA

$^{40}\text{Ar}/^{39}\text{Ar}$  GEOCHRONOLOGY OF ACCRETED TERRANES FROM SOUTH-WESTERN BAJA CALIFORNIA SUR, MEXICO.

**BONINI, Jennifer, A.**, and **BALDWIN, Suzanne, L.**, Department of Geosciences, University of Arizona, Tucson, Arizona 85721, U.S.A.

Peralkaline trachytes and rhyolites (63-70 wt%  $\text{SiO}_2$ ) dominate the last 540 ka of volcanism on Socorro Island, an ocean island situated in the Eastern Pacific on a mid-ocean ridge spreading center abandoned at ~3.5 Ma. The dominance and peralkaline nature of silicic rocks on Socorro provide the ideal opportunity to evaluate magma chamber processes and silicic magmagenesis in the absence of continental crust.

Silicic whole-rock  $^{87}\text{Sr}/^{86}\text{Sr}$  (0.7034 - 0.7086, Fig 1) are elevated compared to values for Socorro Island alkaline basalts (0.7031-0.7034, Fig 1) and approach that of modern seawater (0.7091). Low Sr concentrations ([Sr]) in silicic WR (<20 ppm) render them susceptible to contamination; whole-rock alkali-feldspar (WR-AF) pairs (n=20) show pronounced  $^{87}\text{Sr}/^{86}\text{Sr}$  disequilibrium (AF = 0.7031-0.7041, Fig 1).

Acid-leaching of silicic WR yield less radiogenic  $^{87}\text{Sr}/^{86}\text{Sr}$  ( $\Delta=0.004$ ) and lower [Sr] ( $\Delta=12$  ppm) with increasing acid strength, demonstrating that a dominant component of the Sr is secondary.

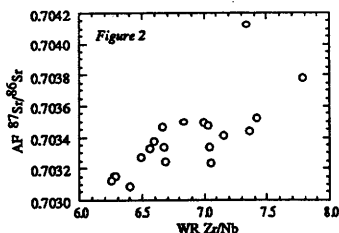
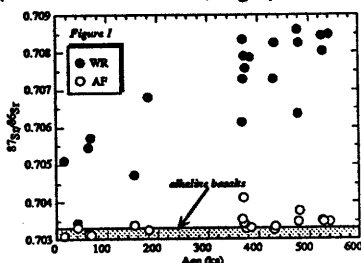
Leachates have

$^{87}\text{Sr}/^{86}\text{Sr}$  (0.7086) similar to summit hydrothermal fluids (0.7079-0.7086). The remarkable correlation between age and unleached WR  $^{87}\text{Sr}/^{86}\text{Sr}$  (Fig. 1) strongly suggests progressive, post-crystallization fluid-rock interaction where hydrothermal fluid/rock ratios increase from <1 in younger rocks to ~10 for older rocks.

Post-crystallization contamination had a minimal effect on AF phenocrysts; acid-leaching of AF produced only minor decreases in  $^{87}\text{Sr}/^{86}\text{Sr}$  ( $\Delta=0.0001$ ) due to higher [Sr] and lower permeability compared to WR. Leached AF  $^{87}\text{Sr}/^{86}\text{Sr}$  that are more radiogenic than alkali basalts and  $^{87}\text{Sr}/^{86}\text{Sr}$  disequilibria between WR-AF pairs that persist despite acid-leaching illustrate that not all of the Sr isotopic variation is secondary. AF  $^{87}\text{Sr}/^{86}\text{Sr}$  correlates with WR indices of fractionation (e.g., Zr/Nb, Fig 2), indicating that assimilation of a

component with radiogenic  $^{87}\text{Sr}/^{86}\text{Sr}$  occurred during feldspar growth and magmatic differentiation within a magma chamber. The identity of the assimilant is tied to negative Ce anomalies and unusually

high abundances of other REE in many silicic rocks. Concomitant enrichments in HFSE such as Zr, Hf, Nb are not evident; rather, abundances are consistent with fractional crystallization. These trace element characteristics, together with radiogenic Sr, strongly favor assimilation of hydrothermal deposits, particularly Fe-oxyhydroxides, present in the shallow ocean crust. Isotopic and trace element data for Socorro silicic rocks provide unequivocal evidence that crustal contamination affects ocean island magmas and should be considered in petrogenetic studies of ocean island volcanic suites.



A geochronologic study of Mesozoic oceanic rocks from Isla Magdalena and Isla Santa Margarita, Baja California Sur, Mexico provides constraints on the metamorphism and deformation of this disrupted terrane. These islands are comprised predominantly of ophiolitic and island-arc affinity rocks forming an upper-plate, and blueschist-facies subduction complex rocks forming a lower-plate. Between these units, within intervening fault zones, is a serpentinite-matrix melange containing exotic blocks.  $^{40}\text{Ar}/^{39}\text{Ar}$  results have been obtained for upper-plate metamorphic and igneous rocks, and for exotic blocks from the serpentinite matrix melange.

Results from hornblende separated from an amphibolite exotic block and muscovite from two greenschist facies exotic blocks indicate early-Cretaceous metamorphism. These data are consistent with previous work on exotic blocks from west-central Baja California that indicate mid-Jurassic through early-Cretaceous subduction related metamorphism.

$^{40}\text{Ar}/^{39}\text{Ar}$  analysis of hornblende from upper-plate amphibolite and garnet-amphibolite thrust sheets that overlie the ophiolitic rocks yielded complex age spectra suggesting late-Jurassic to early-Cretaceous metamorphism. A complex muscovite age spectrum from a sheared metavolcanic unit exposed at the contact between the upper plate and the serpentinite matrix melange suggests a minimum age of late-Jurassic shearing. Biotite from a lamprophyre dike that cross-cuts the upper-plate ophiolite yielded an undisturbed age spectrum indicating mid-Oligocene intrusion, which we interpret to mark the end of extension within the ophiolite unit. Step heat experiments on whole rock samples from undeformed rhyodacites yield ages that suggest a more prolonged period of arc-related magmatism than has been previously proposed.

IMPLICATIONS OF GROUNDWATER WEATHERED PROFILE INTERACTIONS TO THE MOBILIZATION OF RADIONUCLIDES

BONOTTO, D.M., Departamento de Petrologia e Metalogenia, Instituto de Geociências e Ciências Exatas, Rio Claro, São Paulo, 13506-900, Brasil.

This study reports the nature and extent of open-system interaction between groundwater and a weathered profile developed in the high grade thorium and rare earth elements ore body in Morro do Ferro, Poços de Caldas plateau. The radioelement mobility in the shallow oxidizing environment was considered on using chemical data in conjunction with U-234/U-238, Th-228/Th-232, Ra-226/Th-230 and Th-230/U-234 activity ratios for borehole spoil and groundwater samples.

Recharging groundwater from the studied borehole has low salinity values, with total dissolved solids content of 14.7 mg/l and total ionic strength of 0.00018. The ratio of the weight of dissolved radioelement per unit volume of solution to the weight of radioelement in solid phase per unit weight of solid phase showed that the radioelement solubility in the studied waters varied according to the following order: radium >> uranium > thorium.

U-234/U-238 activity ratios less than 1 were measured in solid phase and can justify the enhancement of U-234 in solution. Th-228/Th-232 activity ratio greater than 1 was found at about 18.75 m depth and is related to ingrowth of Th-228 from Ra-228 held in this site. Ra-226/Th-230 activity ratios greater than 1 and Th-230/U-234 activity ratios less than 1 were evaluated between 20 and 27 m depth, where a 2.1-m thick magnetite dike was intersected. These ratios could be justified by deposition of U and Ra associated with ferric oxyhydroxides and kaolinite. Typical adsorption coefficient values for these phases and mineral saturation indices evaluated from the available data confirm this possibility.

K/Ar AND Rb/Sr AGES OF CELADONITES FROM THE TROODOS OPHIOLITE, CYPRUS

BOOIJ, E. and STAUDIGEL, H., Instituut voor Aardwetenschappen, Vrije Universiteit, De Boelelaan 1085, 1081 HV Amsterdam, The Netherlands and GALLAHAN, W.E., College of Oceanic and Atmospheric Sciences, Oregon State University, Corvallis, USA.

Chemical interaction between oceanic crust and seawater begins immediately after the formation of new basaltic basement material at mid-ocean ridges. As long as the circulation provides fresh seawater and unstable (high temperature) volcanic phases are available for alteration, seawater reacts with these primary assemblages and new low temperature phases are formed. Little is known, however, about the duration of these secondary processes in the oceanic crust. We determined K/Ar and Rb/Sr geochronological data for celadonite, a predominant low temperature hydrothermal alteration mineral from the Troodos Ophiolite, Cyprus.

K/Ar data yield ages for the celadonites between  $54.8 \pm 0.6$  and  $90.9 \pm 1.0$  Ma, with the oldest in close agreement with the estimated 91 - 92 Ma crystallisation age of the Troodos igneous complex.

Rb/Sr model ages were calculated using  $^{87}\text{Sr}/^{86}\text{Sr}$  initial ratios of 0.7073 (90 Ma seawater) and 0.7037 (fresh basaltic glass), and assuming that the "true" Rb/Sr age is the mean of both model ages. These calculations yield ages varying between  $59.7 \pm 0.6$  and  $90.9 \pm 0.9$  Ma. Together the K/Ar and Rb/Sr data establish that the low temperature alteration of the Troodos ophiolite continued for at least 30 Ma.

When compared in a histogram (Figure 1), K/Ar and Rb/Sr data define a similar range of ages, whereby the mean of K/Ar ages is lower than the mean of the Rb/Sr ages. This observation may be interpreted in terms of the possibility that the celadonites were not completely Ar retentive during the alteration process.

Although there are some discrepancies between the K/Ar and Rb/Sr ages, these results clearly demonstrate that the low temperature geochemical exchange between seawater and the oceanic crust is a long lived process, continuing for at least 30 Ma.

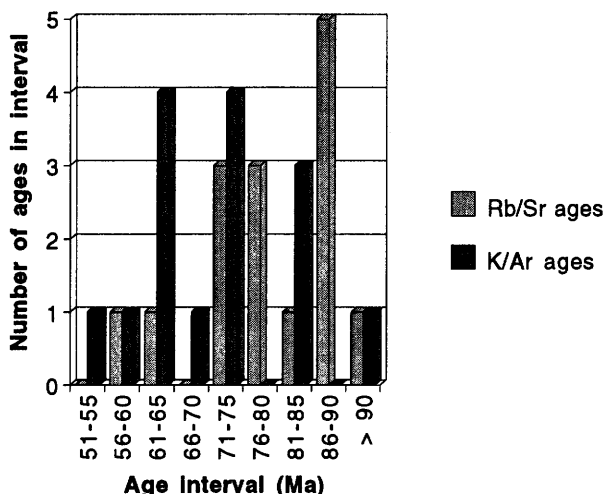


Figure 1: K/Ar and Rb/Sr age frequency distributions, using age intervals of 5 Ma. Note the shift of the K/Ar ages towards lower values.

PEDOGENIC CALCITE AS AN INDICATOR  
OF AN EARLY HOLOCENE DRY PERIOD IN  
THE SAN FRANCISCO BAY AREA

BORCHARDT, Glenn, Soil Tectonics,  
Berkeley, CA 94705, USA,  
and LIENKAEMPER, J.J., U.S.  
Geological Survey, Menlo Park,  
CA 94025, USA.

Rainfall at Union City, California during the early Holocene may have been half the current level. Bk (calcitic) horizons in paleosols in a well-dated alluvial fan indicate a relatively dry climatic period from 10 ka to 7 ka (calendar corrected  $^{14}\text{C}$  ages). The well-drained paleosols and their associated Bk horizons developed mostly in thin, clayey overbank units associated with <2 m deep channel fills containing gravel, sand, and cobble. The pedogenic calcite exists primarily as vertically oriented filaments and fine, hollow nodules formed at ped-face intersections. Under today's climate (MAP=645 mm, MAT=13.9°C) at this site modern soils and paleosols <7 ka do not develop Bk horizons. The calcitic paleosols lie buried at depths over 1.5 m on the thick central portion of the fan where the alluvial deposition rate is highest. As the late Holocene alluvial cover thins away from the fan axis, modern leaching has destroyed those portions of the Bk horizon within 1.5 m of the surface. The thickness of the paleo-Bk horizon thus decreases as a function of distance from the axis of the fan. No evidence for the Bk horizon was found >70 m from the axis. Thus, except at rapidly aggrading sites like this one, any Bk horizons formed elsewhere in the Bay Area during the dry period would have been subsequently destroyed.

Some of the early Holocene paleosols in the thick part of the fan yield evidence for the effective percolation depth of rainwater during the dry period. Remnants of paleosol P3, for example, had leaching depths no greater than 0.6 m for five widely spaced stations. This is about half the current depth of leaching.

TWO CONTRASTING INTRUSIVE SUITES IN THE SERIE  
DEI LAGHI (SOUTHERN ALPS): GEOCHEMICAL AND  
ISOTOPIC (Sr, Pb) INFERENCES ON THE GENETICAL  
ENVIRONMENTS

BORIANI, A., GIOBBI ORIGONI, E., Dip.to Scienze della Terra, University of Milano, Milano, Italy, 20100, and PINARELLI, Laura, Istituto di Geocronologia e Geochimica Isotopica, C.N.R., Pisa, Italy, 55100.

The Western Southalpine crust of Northern Italy and Southern Switzerland consists of high-grade (Ivrea Zone) and medium grade (Serie dei Laghi) metasediments and metabasites that underwent Hercynian metamorphism and which contain intrusive rocks of Ordovician and Permian age. This paper compares the geochemical and isotopic (Sr, Pb) characteristics of the Ordovician (OG) and Permian Granitoids (PG) of the Serie dei Laghi.

The OG, which range in composition from gabbro-diorite to leucogranite, have a calc-alkaline meta-aluminous character. They show moderate LILE and HFSE enrichments, with negative spikes of Nb, Sr, P, and Ti, and plot in the VAG (Volcanic Arc Granites) field in the Pearce's diagrams. The felsic lithologies yielded a whole rock Rb/Sr isochron at  $466 \pm 5$  Ma, with I.R. of 0.7087. The most mafic lithologies, instead, do not plot on the isochron, but arrange along a mixing line indicating mantle-crust interaction ( $(^{87}\text{Sr}/^{86}\text{Sr})_i = 0.704-0.709$ ). The initial Pb isotope ratios of the OG ( $(^{206}\text{Pb}/^{204}\text{Pb})_i = 17.49-18.00$ ;  $(^{207}\text{Pb}/^{204}\text{Pb})_i = 15.55-15.63$ ;  $(^{208}\text{Pb}/^{204}\text{Pb})_i = 37.66-38.12$ ) fall within typical values of the lower crust. Linear trends in the Pb-Pb diagrams are in agreement with the mantle-crust interaction hypothesis.

The PG range in composition from gabbro to leucogranite, and are calc-alkaline and weakly peraluminous. They are strongly enriched in LILE and moderately-to-strongly enriched in HFSE, showing deep negative spikes of Ba, Nb, Sr, P, and Ti. They plot as WPG (Within Plate Granites) in the Pearce's diagrams. The felsic plutons give two whole rock isochrons at  $276 \pm 6$  and  $277 \pm 8$  Ma, with the same I.R. of 0.710. The mafic dykes show Sr isotopic variations indicating mantle-crust interaction, as well ( $(^{87}\text{Sr}/^{86}\text{Sr})_i = 0.705-0.710$ ). The Pb isotope ratios of PG ( $(^{206}\text{Pb}/^{204}\text{Pb})_i = 17.88-18.53$ ;  $(^{207}\text{Pb}/^{204}\text{Pb})_i = 15.60-15.71$ ;  $(^{208}\text{Pb}/^{204}\text{Pb})_i = 38.08-38.71$ ) are distinctly higher than those of the OG, and are similar to those of the Ivrea Zone metasediments.

For both the OG and PG, the following model can be suggested: the most mafic samples were generated by interaction of a mantle-derived magma with crustal material, while the most differentiated samples represent derivatives from the hybrid magma mainly through crystal fractionation. Nevertheless, OG appear to be depleted in both LILE and HFSE, show less pronounced negative spikes of Sr, P, and Ti, have lower initial Sr and Pb isotope ratios than PG. It follows that the ultimate sources of the Ordovician and Permian magmatism were different both geochemically and isotopically, reflecting two different geodynamic environments: a convergent plate boundary in the Ordovician, a post-orogenic, extensional regime in the Permian.

**HOW INTENSE IS THE MONSOONAL  
SCAVENGING OF  $^{210}\text{Pb}$  IN THE WESTERN  
ARABIAN SEA?**

BOROLE, D.V. and NAIR R.R.,  
Geological Oceanography Division,  
National Institute of Oceanography,  
Dona Paula, Goa, 403004, India.

$^{210}\text{Pb}$  concentrations determined from serial, sediment trap samples from the northwest Arabian sea during December 1986 to October 1987 varied from  $11.25 \pm 0.43$  to  $107.66 \pm 3.40$  dpm/g and  $57.98 \pm 1.81$  to  $587.78 \pm 17.32$  dpm/g for the shallow and deep levels though the average flux increased from 0.21 to 0.58 dpm/cm<sup>2</sup>/y. The predicted  $^{210}\text{Pb}$  settling flux on the sediment particles differed by a factor of 3 to 4 when compared to those settled in the traps.

The  $^{210}\text{Pb}$  flux via the settling particles exhibited strong seasonal pattern in tune with the variations of mass sediment flux and productivity. During NE monsoon season homogeneous conditions prevailed for  $^{210}\text{Pb}$  flux as seen by high correlation with that of mass flux and  $C_{\text{org}}$  while heterogeneity, with poor correlation, underlined the rich, wet season. This is more conspicuous for the sediments from deeper trap than the shallower one.

The observed non-uniformity  $^{210}\text{Pb}$  and  $C_{\text{org}}$  flux in this area is in contrast to other world oceanic regions. Plausible causes for these departures have been detailed in terms of monsoon dominated effects such as i) simultaneous occurrence of intense aeolian input and productivity ('Prospero hypothesis'), ii) episodic variation of  $^{210}\text{Pb}$  input via atmospheric fall out as well as upwelling, and iii) bottom sediment re-suspensions as a result of bathymetric configuration (e.g., Owen ridge) in the vicinity of the sediment traps. The measured  $^{210}\text{Pb}_{\text{xs}}$  inventories (148 to 160 dpm/cm<sup>2</sup>) in the bottom sediments from locations southwest of the sediment traps (at KL-74 and KL-87) could support boundary scavenging making this area as a sink for  $^{210}\text{Pb}$ .

The results of this study attain greater relevance to the ongoing JGOFS programme.

**$^{230}\text{Th}/^{238}\text{U}$ -AXIAL DEPTH CORRELATION:  
EVIDENCE FOR RIDGE-HOTSPOT  
INTERACTION NEAR THE AZORES**  
BOURDON, B., ZINDLER, A., and  
LANGMUIR, C.H., Lamont-Doherty Earth  
Observatory, Palisades NY 10964, USA.

Geochemical modelling of hotspots and hotspot-influenced ridges is often complex because source effects obscure the melting signature. For example, several hotspots fall off the global  $\text{Fe}_{8.0}$ -depth correlation of Klein and Langmuir (1987) and emphasize the difficulty inherent in the geochemical parameterization of plume.

U-Th disequilibrium data should provide information about the melting process, independent of source composition, presuming that, at the inception of melting, the mantle source is in secular equilibrium. Thus, we have used  $^{230}\text{Th}$ - $^{238}\text{U}$  to investigate melting along plume-influenced segments of the MAR, north of the Azores triple junction ( $37^{\circ}30'$  to  $40^{\circ}30'\text{N}$ ). We analyzed 22 hand-picked fresh glasses, collected during the FAZAR cruise for U-Th disequilibrium as well as major and trace elements. Our new data shows that  $\text{Fe}_{8.0}$  is negatively correlated with  $\text{Ba}/\text{TiO}_2$ , perhaps indicating mantle heterogeneity. There is also a positive gradient in  $\text{Ba}/\text{TiO}_2$  towards the Azores platform, which can be taken as an index of enrichment due to the influence of the hotspot.

Thorium concentrations range from 0.14 ppm to 2.4 ppm and the Th/U ratios vary between 3.16 to 3.64.  $^{230}\text{Th}/^{232}\text{Th}$  ratios show remarkable homogeneity for samples from a single dredge. Additionally, samples with the highest Th concentrations (2.4 ppm) have the highest Th isotopes ratios. Taken together, these observations argue against assimilation of  $^{230}\text{Th}$ -rich sediment as an explanation the  $^{230}\text{Th}$ - $^{238}\text{U}$  systematics.  $^{230}\text{Th}$  excesses range from 20 and 35%, which is markedly larger than  $^{230}\text{Th}$  excesses reported for the EPR, and are positively correlated with axial depth. Additionally, in three of the ridge segments studied,  $^{230}\text{Th}$  excesses are more extreme in the center of the segments. The  $^{230}\text{Th}$  excesses reflect larger extents of melting in the garnet field, and suggest greater than normal depths (~30kbar) for the initiation of melting beneath the MAR near the Azores. These results demonstrate the potential for U-Th systematics to constrain the nature of mantle melting, independent of source chemical heterogeneity.

## SUPPORT FOR STEADY-STATE CRUSTAL GROWTH FROM THE 4.0 GA ACATA GNEISSES

BOWRING, S. A., HOUSH, T. B. \* ISACHSEN, C. E. and COLEMAN, D.S. Department of Earth, Atmospheric and Planetary Sciences, MIT, Cambridge, MA 02139 \*now at Dept. Geol. Sciences Univ. Texas, Austin, TX 78712

Central to Armstrong's steady-state model for crustal growth is early massive differentiation of the planet into crust, depleted mantle, and core. The lack of abundant pre-3.5 Ga crust, and detritus shed from it, is often cited as compelling evidence that large volumes never existed. However, as the geologic record may reflect an increasing probability of preservation with time, one cannot presume any relationship between the volume of crust preserved and the volume formed.

The growth of Archean cratons involves amalgamation of dominantly oceanic tectonic elements (island arcs, accretionary prisms, etc.) and juxtaposition of these with older sialic basement. Much of the evidence cited against a steady-state model involves reconnaissance geochemical and isotopic analysis, such as REE abundances and Nd isotopic compositions, of sedimentary and volcanic rocks of greenstone belts which assume that sedimentary rocks "average" exposed crust. If the juxtaposition of greenstone belt rocks with sialic basement is tectonic, the geochemistry and geochronology of the greenstone belts reveals little about the presence of older sialic crust, and may even obscure its presence.

Nd isotopic data from Archean to Recent rocks have been used to constrain the isotopic evolution of the mantle and to conclude that the crust and depleted mantle are complementary to one another, forming at the expense of "primitive" mantle. The retarded isotopic evolution of the mantle over earth history is generally attributed to progressive growth of the depleted mantle and crust with limited recycling of crust. This interpretation is not supported by the Nd isotopic database for early Archean rocks.

The 3.4 to > 4.0 Ga Acasta gneisses are a compositionally diverse suite of tonalitic and granitic orthogneisses, amphibolites, and ultramafic gneisses. Nd isotopic data show considerable variability: 3.9 to 4.0 Ga gneisses have a range in initial  $\epsilon_{Nd}$  of +4 to -4; the ca. 3.4 to 3.6 Ga gneisses have a range of initial  $\epsilon_{Nd}$  of +1 to -4. Tonalites and granites record a protracted history of evolution with the formation of LREE-enriched magma from sources characterized by both long term LREE depletion and enrichment. These features require the involvement of an older, enriched crustal component; abundant inherited zircon cores in most of the gneisses support this interpretation. An  $\epsilon_{Nd}$  of +4 at 4.0 Ga represents a minimum value for the depleted mantle and the coexistence of tonalites that have interacted with enriched crust ( $\epsilon_{Nd}=-4$ ) suggests that rapid recycling of older crustal material was buffering the isotopic evolution of the crust/mantle system at 4.0 Ga. The Nd isotopic evolution of Archean rocks in the context of the data from the Acasta gneisses is consistent with progressive homogenization of large volumes of enriched crust and a complementary depleted mantle. The lack of evolution of the depleted mantle during the Archean and the small volume of rocks greater than 3.5 Ga are testimony to vigorous reprocessing of early-formed crust, not progressive growth. Early formation of a core, depleted mantle and crust followed by nearly steady-state evolution is consistent with the recent suggestions that plumes sample a largely depleted reservoir.

## REGIONALITY OF $\delta^{34}S$ IN SEDIMENTS, GRANITES AND RELATED MINERALIZATION IN THE CALEDONIAN TERRANES OF NORTHERN BRITAIN.

Boyce, A.J.<sup>1</sup>, Lowry, D.<sup>2,3</sup>, Fallick, A.E.<sup>1</sup>, Stephens, W.E.<sup>3</sup> & Hall, A.J.<sup>4</sup>

<sup>1</sup> Isotope Geosciences Unit, S.U.R.R.C., East Kilbride, Glasgow, G75 0QU, Scotland

<sup>2</sup> Dept of Geology, Royal Holloway College, Univ. of London, Egham Hill, Surrey, TW20 0EX, England

<sup>3</sup> Dept of Geography & Geology, Univ. of St. Andrews, Fife, KY16 9ST, Scotland

<sup>4</sup> Dept of Geology & Applied Geology, Univ. of Glasgow, Glasgow, G12 8QQ, Scotland

Extensive sulphur isotopic analysis of sulphides in sediments, granites and related mineralization in the Lower Palaeozoic and older terranes of northern Britain show a remarkable, distinctive though complicated regionality, which can be related to the development of the area during opening and closure of Iapetus.

With the exception of the Northern Highlands Terrane, sulphides in the sediment-hosted veins of each segment appear to represent principally a homogenised value of local sedimentary sulphide. Sedimentary sulphide is strikingly enriched in  $\delta^{34}S$  in most of the Lakesman-Leinster and Dalradian Terranes ( $\leq +42\%$ ), a feature we believe relates to the palaeogeography of each terrane during Iapetus development. In contrast, the Southern Uplands Terrane is characterized by relative  $^{34}S$  depletion, with values of  $-17\%$  to  $-1\%$  (more typical of diagenetic sulphide).

Granite-related sulphide in each terrane, while being dominated by a lower crustal or magmatic sulphide source ( $0 \pm 4\%$ ), show small deviations from  $0\%$  towards the  $\delta^{34}S$  of the host or underlying sediments (ranging from  $-12\%$  to  $+12\%$ ). We suggest that this was a result of crustal contamination during granite genesis and/or development of related mineralization.

The Northern Highlands Terrane is distinctive because granite-related mineralization is dominated by a limited sulphur reservoir, and because oxidation is uniquely prevalent in this terrane. Rapidly increasing  $f_{O_2}$  is evidenced by a paragenesis in which sulphides are closely associated with sulphates and late Fe-oxide. Such an  $f_{O_2}$  increase is associated with sulphides displaying  $\delta^{34}S$  from  $-1\%$  ( $\approx \delta^{34}S$  of initial magmatic sulphur source) to  $-21\%$ , and sulphates with  $\delta^{34}S$  from  $+7\%$  to  $+12\%$ . The ultimate source of sulphur in these systems is thought to be the underlying North Atlantic Lewisian craton.

Comparisons with the better developed ores in the Appalachians of Eastern Canada, in terms of mineralization styles and associated  $\delta^{34}S$  characteristics, bear fruit regarding terrane correlation.

TRACE ELEMENT AND ISOTOPIC CONSTRAINTS FOR THE ORIGIN OF MESOZOIC GRANITOIDS IN THE SOUTHERN CANADIAN CORDILLERA

BRANDON, A.D., EAPS, MIT, Cambridge, MA, USA,  
LAMBERT, R.STJ. (Deceased), Geology, U. Alberta,  
Edmonton, Alberta, Canada.

Trace element and isotopic compositions of Mesozoic granitoids in southeast British Columbia constrain mechanisms for granitoid production in the Cordilleran interior in W. North America. These granitoids were emplaced in Middle Jurassic and mid-Cretaceous pulses into Paleozoic-Mesozoic accreted terranes, Paleozoic metasediments, and Proterozoic metasediments. Middle Jurassic rocks range from quartz diorite to tonalite to granite, with relative high Ba and low Rb and Nb abundances characteristic of granitoids found in Mesozoic arc complexes of western North America. Initial  $^{87}\text{Sr}$  range from 27 to +33,  $^{143}\text{Nd}$  from 0 to -7, and initial Pb isotopic ratios lie between the NHRL, lower and upper crust Pb compositions. These isotopic relations can be produced by addition of 5 to 25% Precambrian crust to basalt. These granitoids were part of an arc magmatic complex during subduction of ocean crust and as accretion of outboard terranes occurred west of the North American continent. In contrast, mid-Cretaceous batholiths are composed of high- $\text{K}_2\text{O}$ , weakly peraluminous hornblende-biotite granitoids and strongly peraluminous 2-mica granites. These granitoids have lower  $^{143}\text{Nd}$ , higher  $^{87}\text{Sr}$ , and more radiogenic Pb isotopic compositions than the Middle Jurassic granitoids and completely overlap isotopic compositions of southeast British Columbia Precambrian crust. Oxygen, Sr, Pb, and Nd isotopes, REE modelling, and phase equilibrium constraints are consistent with crustal anatexis of Precambrian basement gneisses and Proterozoic metapelites exposed in southeast British Columbia. The sequence of intrusion in one of the the mid-Cretaceous batholiths (White Creek) constrains the melting sequence, and can be modelled as a zone of anatexis migrating upwards through the crust, first melting basement gneisses followed by melting of overlying metapelites. Basaltic magmatic underplating cannot be a primary cause of anatexis as there is an absence of Early Cretaceous basalt in the southern Canadian Cordillera. Rather, crustal anatexis was likely a response to crustal thickening in association with terrane accretion and collision along the western margin of the North American continent.

The evidence from this study constrain the origins of the compositional distinctions between the predominantly tonalite/granodiorite belts along the Cordilleran margin and the mostly high- $\text{K}_2\text{O}$  granitoid belts in the interior to be the result of distinct processes rather than wholly from melting different crustal sources. In subduction zone tectonic settings where basalt magma is produced, this juvenile component is recorded in the isotopic compositions of the granitoids, and has played a key role in their petrogenesis. To generate granitoids in the interior regions without contemporaneous mantle input, an alternate tectono-thermal control is required to induce crustal anatexis. In southeast British Columbia, this control can be constrained to terrane accretion and collision resulting in crustal thickening.

PROVENANCE AND DISCORDANCE MECHANISM OF ZIRCONS IN THE AUSTRALIAN REGOLITH USING SHRIMP AND ELECTRON MICROPROBE MAPPING.

BRIMHALL, G. H. DONOVAN, John, and SINGH, Balbir, Dept. of Geology and Geophysics, Berkeley, California, 94720, USA.

SHRIMP study of zircons in the Jarrahdale bauxite deposit in the Darling Range of Western Australia shows that rounded concordant zircons dominating the gravel and duricrust portions of the profile are a mixed exotic suite derived ultimately from several younger orogenic belts surrounding the Yilgarn Craton. Euhedral zircons, often discordant and ubiquitous in all parts of the profile but most common in the saprolite, are indigenous, chemically-resistant minerals surviving weathering of the local granodiorite parent material. These results in combination with aluminum mass balance, require that the in situ residual concentration theory of cratonic bauxite formation be modified to incorporate long-distance, probably eolian, transport of a chemically-mature surficial detrital suite as an important part of regolith mineralization.

The genesis of a concordant abraded zircon suite requires further explanation. An important question is: How much of the selectivity occurs below ground in the weathering profile of the source region? Combined SHRIMP and electron microprobe mapping of euhedral zircons shows that the range of discordance is related to the presence and frequency of intracrystalline micro crack defects exposed in the SHRIMP craters. In areas free of micro cracks, zircons are concordant while micro-cracked areas are highly discordant.

Rather than "recent lead loss" explaining zircon discordance, intracrystalline electron microprobe mapping proves that it is controlled instead by introduction of excess uranium and accumulated along the micro crack networks. Uranium is introduced into permeable network in zircon along with other soil solution components (Al, Fe, Ti, Pb, Th and Y). Uranium comes from the advance of the incipient weathering front where sphene containing uranium-rich micro-inclusions such as brannerite is replaced pseudomorphically by porous anatase with release of Ca and Si. The other soil solution components deposited along with U arise from weathering of other minerals besides sphene including feldspars and other major, minor and trace minerals. The principal feature in common between U and the other mobilized elements is simply their migration through the same fracture network.

The internal micro structural architecture of zircon and the crack network emanating from metamict and presumably expanded zircon, ensures that uranium mobilized from sphene sites eventually will enter the permeable portions of cracked zircons by ground water circulation. It also provides a means of mixing soil solution components such that they are localized together in cracks though derived from distinct mineral sites.

Bedrock zircon metamictization and the micro-structural architecture of the granitic parent material offer insights as to the dual selectivity mechanisms of preservation of the exotic concordant rounded zircon suite and the destruction of imperfect indigenous euhedral crystals in the local weathering environment. The concordant zircon suite represents the most durable, structurally perfect and uncracked portion of a spectrum of co-genetic perfect to imperfect zircons. At depth within the Jarrahdale bauxite profile, we see the incipient stages of zircon weathering providing structural fragmentation and chemical alteration controlled by micro cracks. These effects increase upwards leaving severely damaged euhedral zircons in the pisolitic gravels.

**RELATIONSHIPS BETWEEN ISOTOPE GEOCHEMISTRY OF BASIC LAVAS, TIME, LOCATION AND MANTLE UPWELLING : BASALTS FROM THE FRENCH MASSIF CENTRAL (FMC)**

BRIOT, D., NERC Isotope Geology Laboratory, Keyworth, Nottingham NG125GG UK, and URA10 CNRS, Dpt Sci. Terre, Univ. B. Pascal, 5 rue Kessler 63038 Clermont-Ferrand Cedex, France

Classical isotopic intercorrelation diagrams show that depleted (DM), enriched (EM I and/or EM II) and HIMU-type mantle signatures must exist in the upper mantle beneath the Massif Central (France) to account for the Sr-Nd-Pb-isotope geochemistry of the FMC basalts and basanites. The main questions we address here are : (1) are these mantle components parts of the lithospheric mantle, the asthenospheric mantle or both; (2) or is there a mantle plume beneath western Europe. Such questions may be answered by looking carefully to how the mantle components have been sampled by the rift related-volcanism. Taking location and time constrains into account, we show that relationships exist between isotope and trace element features of the basalts and their chronological and tectonic setting.

Considering the complicated history of western Europe, particularly the possible effects of the Hercynian orogeny on the subcontinental mantle, we claim that all the components that are needed to account for the isotopic variations in the mafic magmas exist in the subcontinental lithospheric mantle beneath the FMC without any intervention of upwelling asthenospheric (rift-related) material or deep mantle plume substances.

In our proposed model, differences in the trace element geochemistry of volcanic districts which are located at the same place but have not the same age can be explained by differences in the mineralogical composition of the residual mantle for slightly different degrees of partial melting. The differences in these proportions and in the amount of melts produced reflect changes in the thermodynamical conditions and/or depth of melting and are to be related with isotopic heterogeneities in the subcontinental mantle. This would place important constrains on the geochemical structure of the subcontinental lithosphere beneath the french Massif Central.

**SEPARATION OF THE NATURAL AND BOMB-TESTING CONTRIBUTIONS TO OCEANIC RADIOCARBON**

**BROECKER, W.S.**, Lamont-Doherty Earth Observatory, Palisades, NY 10964, and Stewart Sutherland, Lamont-Doherty Earth Observatory, Palisades, NY, 10964, and Tsung-Hung Peng, Oak Ridge Natl. Lab., Envl. Sciences Div., Oak Ridge, TN 37830.

The distribution of radiocarbon in the ocean offers the most powerful constraints on general circulation models used to estimate the uptake of anthropogenic CO<sub>2</sub> by the sea. The utility of this tracer will be far greater if a separation between its natural and bomb-testing components can be made. We discuss a new attempt to do this which involves the use of tritium and dissolved silica data.

## CONSTRAINTS ON THE HISTORY OF THE SCANDINAVIAN ICE SHEET USING *IN SITU* COSMOGENIC NUCLIDES.

EDWARD J. BROOK, Graduate School of Oceanography, University of Rhode Island, Narragansett Bay Campus, Narragansett, RI, USA 02882, ATLE NESJE, Department of Geography, University of Bergen, N-5035, Bergen-Sandviken, Norway, GRANT M. RAISBECK and FRANÇOISE YIOU, CSNSM, Bâtiment 108, 91405, Campus Orsay, France .

The age and origin of *in situ* weathered bedrock surfaces and associated weathering boundaries on mountain summits in western Norway and other areas of Scandinavia have been controversial for over a century. The weathering boundaries are important because they appear to delineate the vertical limits of an ice sheet and may constrain vertical ice limits at the Late Weichselian maximum.

To further constrain ages of these features we made  $^{10}\text{Be}$ ,  $^{26}\text{Al}$ , and  $^3\text{He}$  measurements in a number of surface samples of quartz veins from four different bedrock weathering zones in an altitude transect at Skåla in western Norway.  $^{10}\text{Be}$  exposure ages calculated assuming no erosion are 8.8 kyr for a Younger Dryas surface at 1145 m, 12.7 kyr for bedrock at 1420 m, above the Younger Dryas limit but below a "trimline" at 1350 m, 20.1 kyr above that trimline, at 1500m, but below a trimline defined by the lower limit of the autochthonous weathered blockfield at the mountain summit (1740 m), which has an exposure age of 53.6 kyr. Assuming the oldest surface is at erosional steady state the erosion rate is 1.2 cm/kyr and corresponding ages for the three younger samples are 9.6, 18.6, and 36.3 kyr.

The data clearly show relative age differences between all four surfaces and that the blockfield surface is pre-Late Weichselian in age. Uncertainty in the true erosion rate precludes absolute determination of the location of the Late Weichselian vertical limit and therefore the exposure ages suggest three possible scenarios. 1) If erosion is negligible the Late Weichselian limit may be at the upper trimline. 2) If the erosion rate is  $\sim 1$  cm/kyr the Late Weichselian limit may be at the lower trimline. 3) The upper trimline may represent a thermal boundary in a Late Weichselian ice sheet where older topography was preserved between cold-based ice and the lower trimline may be the Late Weichselian limit. Both of the former two scenarios must explain the existence of two weathering boundaries above the younger Dryas limit.

$^3\text{He}$  concentrations were determined in two samples;  $^3\text{He}/^{10}\text{Be}$  ratios are  $0.2 \pm 0.04$  and  $1.1 \pm 0.6$ , indicating significant  $^3\text{He}$  loss (the production ratio is  $\sim 20-25$ ). In thin section the vein quartz is extremely fine-grained; rapid loss from small grains is the likely explanation for the low ratios.  $^{26}\text{Al}/^{10}\text{Be}$  ratios range from  $6.1 \pm 0.8$  to  $9.5 \pm 5.4$ , consistent within error with predicted production ratios ( $\sim 6$ ), indicating that these surfaces have not been subject to long-term burial since exposure.

## APPLICATIONS OF $^{10}\text{Be}$ AND $^{26}\text{Al}$ IN EXAMINATION OF THE DEVELOPMENT OF TROPICAL SOILS AND LANDFORMS

BROWN, Erik T., BOURLES, Didier L., RAISBECK, Grant M., and YIOU, Françoise, (all at Centre de Spectrométrie Nucléaire et de Spectrométrie de Masse, CNRS-IN2P3, Bâtiment 108, 91405 Campus Orsay, France) and COLIN, Fabrice, SANFO, Zakaria, and DESCARCEAUX, Sophie (all at ORSTOM and Lab. Géoscience de l'Environnement, UMGECO, Aix-Marseille III, 13397 Marseille Cedex 13, France)

We have investigated the development of iron crust lateritic systems in arid tropical environments and of rain forest soil profiles using  $^{10}\text{Be}$  and  $^{26}\text{Al}$  produced *in situ* in quartz veins and pebbles.

In the stable West African Craton in northern Burkina Faso a series of sequential and connected iron auriferous crust systems (including an active river drainage, and a series of lateritic surfaces which are presumed to represent relict drainages dating from as early as the Tertiary) were examined. They may have formed either through *in situ* chemical alteration or colluvial transport. The first scenario requires that the lateritic material has always been in its present position, while the other implies previous surface exposure of material currently emplaced at depths up to several meters. Systematic study of distributions of cosmogenic nuclides provides criteria for distinguishing between the proposed chemical and physical processes. In addition such results may be used to constrain the histories of erosion and burial, and potentially, of climatic conditions associated with formation of lateritic systems.

Results from outcropping quartz veins suggest that the mean erosion rate in this region is about 3 to 7 m per Myr. Depth-dependent distributions of  $^{10}\text{Be}$  and  $^{26}\text{Al}$  in quartz cobbles and pebbles incorporated in iron crusts were used to distinguish surfaces undergoing burial from those undergoing erosive loss. Results from sections of the lowland fan are consistent with mean accumulation rates of a few meters per Myr. Quartz cobbles, presently at depths of a few meters in a paleochannel filled with rapidly deposited fluvial-colluvial material, have  $^{10}\text{Be}$  distributions suggesting that formation of the lowland lateritic surface may have been initiated during an erosive episode, presumably associated with wetter climate, roughly 300 ky B.P.

A contrasting environment, the rain forest at Dimonika, Congo, has also been examined using  $^{10}\text{Be}$  and  $^{26}\text{Al}$ . Preliminary measurements indicate very low erosion rates ( $\sim 3$  m Myr $^{-1}$ ) at ridgecrests, consistent with the stability and great age of the regional surface formations. Samples from soil pits and road cuts provide the possibility of determining whether quartz cobbles found at discrete horizons in soil profiles "stonelines" are alluvial deposits or relicts of chemical weathering. In conjunction with estimates of collapse these data may also be used to study rates of penetration of weathering fronts.

## VISUALISING THE STRUCTURE OF CONTINENTAL LANDSCAPES: AN AFRICAN VIEW

**BROWN, Roderick.** Fission Track Research Group, Department of Geological Sciences, University College, Gower Street, London, WC1E 6BT, United Kingdom, FOSTER, David and GLEADOW, Andrew, Victorian Institute of Earth and Planetary Sciences, La Trobe University, Melbourne, 3083, Australia

Regional apatite fission track analysis (AFTA) studies within eastern and southern Africa (Kenya, Namibia and South Africa), and indeed other parts of the world, have all revealed a close temporal and spatial association between the tectonic and denudational histories of continents. In particular, two Late Mesozoic tectonic episodes, characterised by major intracontinental deformation involving rifting and basin inversion, have been identified in Africa: one during the Early Cretaceous (140-120 Ma) associated with opening of the South Atlantic and a second during the late Cretaceous-early Tertiary (80-60 Ma), associated with a major change in the spreading geometry within the Central and South Atlantic ocean basins. Both these episodes were accompanied by enhanced rates of crustal denudation and cooling.

A third episode of crustal cooling (at  $90 \pm 10$  Ma) has been documented along the eastern margin of southern Africa, and its effects extend well inland (westwards) into the Kaapvaal craton region. This episode is accompanied by a dramatic increase in the rate of sediment accumulation (from  $\sim 30 \text{ m.Ma}^{-1}$  to over  $300 \text{ m.Ma}^{-1}$ ) and basement subsidence within the offshore basins along the continental margin of Mozambique. The timing and magnitude of cooling of this event is difficult to reconcile with the view that geomorphic stability is a characteristic of cratonic regions.

More interesting though, is the remarkable similarity between the chronology of landscape change determined from AFTA within northern Namibia and eastern Kenya. Taken in conjunction with the recent interpretations of the regional tectonic history of West, Central and East Africa, this similarity suggests that reactivation of major, pre-existing crustal structures (such as regional shear zones and fault systems) played a significant role in determining the pattern of landscape development across the African continent.

Importantly, the chronology and style of landscape evolution revealed through fission track analysis challenges some of the fundamental concepts of previous models of long-term, continental landscape evolution put forward for Africa, and also widely applied to other continents. The new long-term landscape history for southern Africa revealed through AFTA also accords well with the record of clastic sedimentation within the offshore basins and is easier to reconcile with current models of rifted continental margin development.

## DATING OF GEOMORPHOLOGIC SURFACES IN THE ANTARCTIC DRY VALLEYS WITH IN SITU PRODUCED COSMOGENIC $^3\text{He}$ AND $^{21}\text{Ne}$

**BRUNO, L.A.**<sup>1</sup>; **BAUR, H.**<sup>1</sup>; **IVY, S.D.**<sup>2</sup>; **SCHLÜCHTER, C.**<sup>3</sup>; **SIGNER, P.**<sup>1</sup>; **WIELER, R.**<sup>1</sup>

<sup>1</sup>Isotopengeochemie, ETH Zürich, 8092 Zürich, Switzerland;

<sup>2</sup>Ingenieurgeologie und Institut für Teilchenphysik, ETH Hönggerberg, 8093 Zürich, Switzerland; <sup>3</sup>Geologisches Institut, Universität Bern, 3012 Bern, Switzerland

Abundances of cosmic-ray-produced nuclides have been determined in different rock types exposed in the Dry Valleys, North Victoria Land, Antarctica, to provide constraints on geomorphologic, glaciologic and climatologic histories. Emphasis was put on samples from erratic boulders within the Sirius Formation and on bedrocks from the Table Mountain (Schlüchter et al., 1994). For comparison, aliquots of quartz separates from Table Mountain were also analyzed for their concentrations of cosmogenic  $^{10}\text{Be}$  (Ivy et al., 1994).

The stable nuclides  $^3\text{He}$  and  $^{21}\text{Ne}$  were extracted from pyroxene- and quartz-separates from dolerites, granites as well as sandstones and measured in a mass spectrometer resolving  $^3\text{He}$ - from HD-ions. Noble gases were released either in a single melting step at  $1800^\circ\text{C}$  for 30 min. or by step-wise heating to separate cosmogenic and atmospheric Ne. In our first measurements it turned out that He is always partially lost from quartz. Thus, we analyzed only Ne in later quartz fractions. All samples showed clear contributions of cosmogenic  $^{21}\text{Ne}$  besides variable concentrations of atmospheric Ne.

Presently available data of the  $(^3\text{He}/^{21}\text{Ne})_{\text{cos}}$  ratios in the pyroxenes point to a value of  $4.5 \pm 0.2$ , whereby no corrections for possible variations of the chemical compositions of the minerals have been possible at present.

To calculate  $^3\text{He}$  and  $^{21}\text{Ne}$  exposure ages, we use the production rates and altitude/latitude adaptations proposed by Lal (1991). The  $^3\text{He}$  and  $^{21}\text{Ne}$  ages obtained from the pyroxenes are generally identical within a few %. Preliminary exposure ages from a doleritic erratic boulder within the Sirius Formation are 4.9 Ma and 4.8 Ma as deduced from  $^3\text{He}_{\text{cos}}$  and  $^{21}\text{Ne}_{\text{cos}}$ , respectively. An origin of the Sirius Formation in the Upper Pliocene/Lower Pleistocene is not corroborated by these ages.

### References:

S. Ivy et al. (1994), this volume.

D. Lal, *Earth Planet. Sci. Lett.* 104, 424-439 (1991).

C. Schlüchter et al. (1994), this volume.

SULFUR RICH ENVIRONMENTS IN THE INITIAL TRANSGRESSIVE PHASE AT LEG 144 GUYOTS (OCEAN DRILLING PROGRAM, WESTERN PACIFIC): SULFUR ISOTOPES AS INDICATOR FOR SULFATE REDUCTION.

BUCHARDT, B., and ISRAELSON, C. Institute of Geology, University of Copenhagen, Øster Voldgade 10, DK-1350 Copenhagen K, Denmark.

The Initial Transgressive Phase (ITP) at the Leg 144 Guyots is characterized by a typical association of sedimentary facies. From bottom to top: I) in situ weathered volcanic rocks (flow basalt and volcanoclastics), II) variegated clays, partly pyritic, III) grey clay, pyritic, homogeneous, with plant roots, IV) black clay, peaty, laminated or bioturbated, V) muddy grainstone, black to grey, bioturbated, with well preserved shell remains, VI) lagoonal limestone. Site 877 at the Wodejabato guyot represents the typical development of the ITP. At Sites 871, 873, 874 and 879, one or several of the ITP facies can be observed.

The black clay facies (facies IV) is highly carbonaceous (TOC up to 40%) and sulfurous (TS up to 25%). The organic matter is dominantly of terrestrial origin and contains plant fragments, spores, charcoal and disseminated plant material. The sulfur occurs as pyrite, markasite, organically bound sulfur and probably also as free elemental sulfur.

The variegated clays (facies II) typically consist of a red lower part and a blue to grey-blue upper part. The lower part is free of sulfur, while the upper part contains an increasing amount of sulfur developed as sub-millimeter euhedral grains of pyrite. Organic carbon is not observed in this facies.

The high content of sulfur in facies II to IV has been interpreted either as a result of hydrothermal activity or of bacterial sulfate reduction. In order to clarify this, sulfur isotope determinations have been performed on sediments from the ITP. Hydrothermal sulfides would either have a magmatic composition ( $\delta^{34}\text{S} \approx 0$  o/oo) or sea water composition ( $\delta^{34}\text{S} \approx +10$  to  $+20$  o/oo).  $\text{H}_2\text{S}$  produced by bacterial reduction of sea water sulfate would be strongly depleted in heavy sulfur ( $\delta^{34}\text{S} \approx -50$  to  $0$  o/oo).

The isotope composition of sulfur from facies II, III and IV varies from  $-50$  o/oo to  $0$  o/oo. These numbers clearly point to a bacterial origin. This implies the following model for sulfur enrichment in ITP-sediments: 1) Marine flooding of an organic-rich back-reef mangroval swamp represented by facies IV and V. 2) Intense bacterial reduction of marine sulfate within the black clay of facies IV. 3) Downwards diffusion of  $\text{H}_2\text{S}$  into the underlying clays, reduction of red iron oxides to blue-grey iron sulfides and growth of pyrite.

DIAMOND FORMATION AND ERUPTION AGES BY LASER  $^{40}\text{Ar}$ - $^{39}\text{Ar}$  DATING OF SYNGENETIC INCLUSIONS

BURGESS R., Dept. of Geology, University of Manchester, Manchester, M13 9PL, UK, KELLEY S.P., Dept Earth Sciences, Open University, Milton Keynes, MK6 7AA, UK, TURNER G. Dept. of Geology, University of Manchester, Manchester, M13 9PL, UK and HARRIS J.W., Dept of Geology, University of Glasgow, Glasgow, G12 8QQ, UK.

Laser dating of individual syngenetic clinopyroxene inclusions in diamonds can potentially give both the diamond crystallisation and host kimberlite, or lamproite, eruption ages. Inclusions within diamonds that pre-date eruption will lose  $^{40}\text{Ar}^*$  at the diamond/inclusion interface during mantle residence, this process will cease at eruption. Therefore, use of a laser to drill into diamonds in which inclusions are completely encapsulated, will initially release the interface gas, followed by Ar from within the inclusions. The latter can be used to calculate the eruption age and, when combined with the interface Ar, should give the age of diamond formation.

An UV laser ( $\lambda=266\text{nm}$ ) has been used to drill into diamonds which contain clinopyroxene inclusions, to release the interface  $^{40}\text{Ar}^*$ . Following this, the inclusion was melted with an IR laser ( $\lambda=1064\text{nm}$ ). Samples include two stones from the Argyle lamproite and one stone from the Finsch kimberlite. The Finsch diamond was cleaved prior to analysis, to expose the inclusion at the diamond surface, in order to directly compare the UV and IR extraction methods. The UV laser experiments on the Finsch sample gave apparent ages that decreased from  $>1\text{Ga}$  to  $121 \pm 33$  Ma, the latter age is identical with those obtained subsequently by IR laser ( $113 \pm 6$  Ma) and are also identical with the eruption age of the Finsch kimberlite ( $\approx 120$  Ma, [1]). The high age for the initial extraction using the UV laser probably resulted from release of some residual interface gas that was not released by cleaving. This is also reflected in the integrated age of  $205 \pm 30$  Ma indicating that the diamond is older than the kimberlite, however a formation age could not be obtained because some of the interface  $^{40}\text{Ar}^*$  was lost during cleaving.

The UV laser extracted about 50% of the total  $^{40}\text{Ar}^*$  from one of the Argyle samples (A1), together with negligible  $^{39}\text{Ar}$  above the blank level. IR laser extraction of A1 gave an apparent age of  $1091 \pm 42$  Ma which is the eruption age [2]. However, the integrated age of  $1521 \pm 80$  Ma is essentially identical to the crystallisation age obtained previously of  $1580 \pm 80$  Ma [3]. The second Argyle sample (A4) yielded negligible  $^{40}\text{Ar}^*$  using the UV laser, but gave two IR laser extractions with high apparent ages of  $\geq 2$  Ga. Besides indicating the possibility of an old crystallisation age, these high ages may also result from either incomplete melting of the inclusion (i.e.  $^{39}\text{Ar}$  not totally extracted), or the presence of excess  $^{40}\text{Ar}^*$  (e.g. in volatile-rich inclusions). Experiments are underway on a suite of garnet and clinopyroxene inclusions in diamonds from the Orapa kimberlite to further test the method.

[1] Smith C.B., Gurney, J.J., Harris J.W., Robinson D.N., Shee S.R. and Jagoutz E., 1989, Proc. 4th Int. Kimberlite Conf., v. 2, p. 853-863.

[2] Skinner E.M., Smith C.B., Bristow J.W., Scott-Smith B.H. and Dawson J.B., 1985, Trans. Geol. Soc. S. Africa, v. 88, p.335-340

[3] Richardson, S.H., 1986, Nature, v. 322, p. 623-626.

**LASER PROBE STUDY OF HE, AR AND CO<sub>2</sub> TRAPPED IN A DUNITE XENOLITH, REUNION ISLAND.**

BURNARD, P.G. and TURNER, G., Department of Geology, Manchester University, Manchester M13 9PL, and STUART, F.M., S.U.R.R.C., East Kilbride, Scotland

The 'Dupal' island of Réunion in the southern Indian Ocean is characterised by exceptionally consistent  $^{87}\text{Sr}/^{86}\text{Sr}$  (0.70397 - 0.70436),  $^{143}\text{Nd}/^{144}\text{Nd}$  (0.51282 - 0.51286) and  $^3\text{He}/^4\text{He}$  ( $12.9 \pm 0.05$ ) ratios. In contrast,  $^{40}\text{Ar}/^{36}\text{Ar}$  ratios vary widely (300 - 8000).

Specific fluid inclusion generations in a dunite xenolith were analysed using the Ar-CO<sub>2</sub>-He (ARCHE) analysis system in Manchester, England, in order to determine mantle CO<sub>2</sub>/He ratios and place limits on the  $^{36}\text{Ar}$  concentration of high  $^3\text{He}/^4\text{He}$  mantle volatiles. Laser decrepitation permitted particular inclusion generations to be targeted, vital to distinguish volatiles trapped in 'primary' inclusions from those associated with fractures or secondary melt features.

Normalised plots indicate a constant  $^4\text{He}/^{40}\text{Ar}$  of 1.92 for all inclusion generations. Fluid CO<sub>2</sub>/He ( $0.38 - 1.7 \times 10^5$ ) and CO<sub>2</sub>/ $^{40}\text{Ar}$  ( $0.38 - 7.3 \times 10^5$ ) compositions did not show any systematic variation with inclusion morphology.  $^{40}\text{Ar}/^{36}\text{Ar}$  ratios average higher in 'primary' inclusions (4600) than in planar or fracture associated inclusions (1900). Linear correlations between CO<sub>2</sub>/ $^{36}\text{Ar}$  and  $^{40}\text{Ar}/^{36}\text{Ar}$  are consistent with atmospheric contamination reducing  $^{40}\text{Ar}/^{36}\text{Ar}$  and CO<sub>2</sub>/ $^{36}\text{Ar}$  ratios in fracture associated inclusions.

The range in CO<sub>2</sub>/He observed in Réunion is similar to that of hotspots globally. These variations occur on a millimetre scale and are independent of He-Ar fractionation or inclusion generation. The CO<sub>2</sub>/He variations **cannot** be attributed to fractionation during fluid-melt partition as there is no concomitant He-Ar fractionation (Ar being less soluble in basaltic melts than both He and CO<sub>2</sub> [Lux, 1987]). It is possible the CO<sub>2</sub> - noble gas fractionation is related to solid C (i.e. CO<sub>3</sub><sup>2-</sup>) - CO<sub>2</sub> partitioning.

Sediment recycling to the mantle would increase C/ $^3\text{He}$  but reduce C/ $^4\text{He}$  over time. The similarity in CO<sub>2</sub>/ $^3\text{He}$  and CO<sub>2</sub>/ $^4\text{He}$  in Réunion and non-Dupal islands (Hawaii, Iceland) may indicate a separate, uncontaminated, high  $^3\text{He}/^4\text{He}$  mantle source exists (the PHEM) which dominates mantle volatiles.

Lux., G., 1987, The behaviour of noble gases in silicate liquids: solution, diffusion, bubbles and surface effects, with applications to natural samples, *Geochim. Cosmochim. Acta*, v51, 1549-1560.

**PRELIMINARY PETROLOGIC AND SEDIMENTOLOGIC COMPARISONS BETWEEN PALEOCENE CONGLOMERATES OF POINT REYES AND POINT LOBOS, CALIFORNIA, U.S.A.**

BURNHAM, Kathleen, and Anderson, Thomas B., Sonoma State University, Rohnert Park, Ca. 94928, U.S.A.

Preliminary studies reveal many similarities between the Point Reyes Conglomerate at Pt. Reyes and the lower conglomerate section of the Carmelo Formation at Pt. Lobos, which are on opposite sides of the San Gregorio Fault. Outcrop appearance, sedimentary sequence and structures, distinctive clasts, abundance of clast types, stratigraphic and structural relationships to bedrock, and interpreted facies of origin are virtually identical.

Both conglomerates rest nonconformably upon and in fault contact with granitic basement of the Salinian Block. Both are clast supported, poorly sorted, and occur in lensoidal beds up to several meters thick. Both include beds of conglomerate grading upward into sandstone, with sharp basal definition and scour channels. Matrices are angular and poorly sorted, and are very coarse in conglomerate beds and finer in sandstone beds. Flame structures, shale rip-up clasts, and fine laminae are locally abundant in the sandstone beds. The most abundant and largest (up to 2.5 m) clasts are granitic, and match the basement rock. Second in abundance and size are well-rounded distinctive purple K-spar porphyry clasts. All other clasts are smaller, and most are well-rounded, fine-grained, and very hard. Both conglomerates are interpreted as having formed in a submarine canyon. Previous workers have used paleontological evidence to establish a Paleocene age for both the Pt. Reyes Conglomerate (Galloway, 1977) and the Carmelo Formation (Bowen, 1965). Several of the fossil species and genera they identified occur in both units.

These results indicate the Point Reyes Conglomerate could be a part of the Carmelo Formation, separated by 180 km of lateral movement on the San Gregorio Fault since the Paleocene. However, K-Ar dates on feldspar concentrates of the purple porphyry clasts yielded disparate dates. Three clasts of the Pt. Reyes Conglomerate registered 82 Ma to 89.5 Ma, and one clast from the Carmelo Formation registered 102 Ma. Thus, superficially, the limited geochronologic comparisons do not support a simple correlation between the two units. Further study is planned.

Bowen, O.E., 1965, Stratigraphy, Structure and Oil Possibilities in Monterey and Salinas Quadrangles, California. in: Rennie, E. W., Jr., ed., Symposium of Papers, AAPG, Pacific Sect., 40th Ann. Mtg., Bakersfield, Calif., 1965, p. 48 - 67.

Galloway, A. J., 1977, Geology of the Point Reyes Peninsula, Marin County, California. Calif. Div. Mines and Geology Bull. 202, 72 p.

## TRACING THE WATER MASS EVOLUTION OF Sr, Nd AND Pb IN THE CENTRAL PACIFIC OCEAN

BURTON, K.W., O'NIONS, R.K., and MARTEL, D.J.

(Dept. of Earth Sciences, Univ. of Cambridge, Downing St., Cambridge, CB2 3EQ. U. K.; E-Mail kwb10@esc.cam.ac.uk) HEIN, J.R. (U.S. Geological Survey, Pacific Marine Geology, 345 Middlefield Road, Menlo Park, California, CA 94025, USA)

The residence time of Sr is much greater than the mixing time of the major oceans. Consequently, the Sr isotopic composition of seawater is spatially uniform on a global scale. However, there are significant variations in the Sr isotopic composition of seawater over time. This combination of spatial uniformity and temporal variation enables the use of this system for high-resolution dating. By comparison, the residence times of Nd and Pb are less than the mixing times of the oceans, and the Nd and Pb isotopic compositions of seawater are likely to reflect spatial variations in the sources of those elements. Thus, in principle, the combined use of Sr, Nd and Pb isotopes provides both temporal and spatial information on water mass evolution.

Hydrogenous Fe-Mn crusts are considered to grow directly from seawater, and potentially preserve a record of the chemistry of the seawater from which they grow. This study presents high-precision Sr, Nd and Pb isotopic data for a single Fe-Mn crust sampled from the South Karin ridge, at a water depth of 2390-2290 m, in the Central Pacific Ocean. Sr isotope compositions indicate that growth of the crust started some 20 Ma ago. Initial growth during the period 20 to 15 Ma appears to have been rapid, about 12 mm/Ma. Whereas, growth rates from 15 Ma to the present day were lower, between 3 and 6 mm/Ma. The Pb isotopic composition of the outermost 1 mm of crust gives a  $^{206}\text{Pb}/^{204}\text{Pb} = 18.624 \pm 0.012$ . Whereas, Nd for the same sample gives an  $\epsilon_{\text{Nd}}$  value of  $-3.12 \pm 0.11$ , in good agreement with present day seawater compositions at similar depths (Piepgras & Jacobsen, 1988). Both, Pb and Nd isotopes show significant variations during growth. Nd shows a systematic decrease in  $\epsilon_{\text{Nd}}$  to a value of  $-5.79 \pm 0.12$  at the base of the crust. While Pb shows an increase in  $^{206}\text{Pb}/^{204}\text{Pb}$  to a value of  $18.855 \pm 0.012$  over the same interval.

These results indicate that there have been significant changes in the sources of Nd and Pb at this locality and that the Nd isotopic composition of seawater supplying the crust some 20 Ma ago was significantly less radiogenic than the present day, whereas Pb was more radiogenic.

Piepgras, D.J. & Jacobsen, S.B., 1988, The isotopic composition of neodymium in the North Pacific: *Geochim. Cosmochim. Acta*, v. 52, p. 1373-1381.

## PEDIMENT FORMATION INTERVALS IN THE GRAND CANYON: A TEST CASE FOR THE USE OF COSMOGENIC NUCLIDES

CAFFEE, MARC W., L-237, Livermore, CA 94550; LUCCHITTA, IVO, USGS, 2255 N. Gemini Dr., Flagstaff, AZ 86001; FINKEL, ROBERT C., SOUTHON, JOHN R., LLNL, L-237, Livermore, CA 94550; DAVIS, SIDNEY, and DAVIS, MARIE, P. O. Box 724, Georgetown, CA 95634, USA.

The Quaternary history of the Colorado River in the eastern Grand Canyon is one of overall downcutting punctuated with periods of backfilling. These activities were probably controlled by climatic fluctuations in the Rocky Mountain source region. Washes tributary to the Colorado show similar downcutting and backfilling controlled by the grade established by the Colorado River. The processes involved on the tributaries are debris-flow emplacement and pedimentation. Continued downcutting of the Colorado river results in multiple terraces and pediments in which the lowest levels are the youngest and have the lowest number in our stratigraphic nomenclature. These surfaces are mantled by locally derived rocks, many of which contain quartz and chert.

An obvious way to determine the conditions under which these features are formed is to compare their ages with those of known climate fluctuations (e.g. glacial events), but there are few direct means of dating these debris flows. One promising method for obtaining quantitative data is to measure nuclides produced *in-situ* in surface rocks by cosmic-ray bombardment. The production rates of  $^{10}\text{Be}$  and  $^{26}\text{Al}$  are well known in quartz.

We have measured  $^{10}\text{Be}$  and  $^{26}\text{Al}$  from four stratigraphically distinct debris-flow levels in the Tanner Creek area and from one pediment in the Comanche Creek area. Samples were collected from several boulders at each level to test the reliability of the technique. Samples from the same surface should give concordant ages and samples from the lowest level (3) should be younger than those from higher levels (5 and 6). Measurements of  $^{26}\text{Al}$  in Comanche-3 and Tanner-3 indicate minimum exposure ages of  $1590 \pm 1000$  and  $< 2600$  yr., respectively. Measurements of  $^{26}\text{Al}$  and  $^{10}\text{Be}$  in cherts indicate minimum exposure ages of  $42 \pm 5$  Ka from Tanner-4 (1 sample), 75-94 Ka for Tanner-5 (3 samples), and 142-180 Ka for Tanner-6 (2 samples). We have analyzed  $^{10}\text{Be}$  and  $^{26}\text{Al}$  in nine samples from the Comanche-4 level and the apparent exposure ages are 70-100 Ka.

Our results thus far indicate that there is a good qualitative correlation between apparent exposure age and stratigraphic level for the pediments up through Tanner-6. We also see a reasonable qualitative correlation between apparent exposure age and our observations of carbonate development, although these ages appear young from the perspective of soil morphology. One possible explanation is that the surfaces have been deflated.

This work was performed under the auspices of the U.S. D.O.E. by LLNL under contract W-7405-Eng-48.

TRACING STABLE ISOTOPES IN THE GRAPE  
PLANT ENVIRONMENT TO UNDERSTAND THE  
COMPOSITIONS OF VINTAGE WINES

CALDWELL, E. A. and INGRAHAM N. L., Water  
Resources Center, Desert Research Institute,  
University of Nevada System, Las Vegas, Nevada  
89132.

Precipitation, vapor, ground water, soil water, grape leaf and berry water were collected in Napa Valley, California for stable isotopic analysis. In addition grape must and selected vintage wines from the region were analyzed for their oxygen isotopic compositions. The grape leaf water falls on a transpiration line of slope 2.3 with the composition of the soil and ground water, while the grape berry water falls on a transpiration line of 3.0. These waters are up to 18 per mil more enriched in oxygen-18 than the soil waters, showing the largest observed isotopic shift from their source. The different transpiration slopes observed are controlled by differing isotopic kinetic effects imparted by the different surface transmissivities of the berry and leaf.

In addition, the leaves and berries responded to a small rain shower of a more depleted isotopic composition, the leaf water being most responsive shifted 8 per mil in  $\delta^{18}\text{O}$  while the grape berries showed a delayed shift of only 3 per mil in  $\delta^{18}\text{O}$ . These systems behave differently due to their different surface area/volume ratios of water and may be modeled as a terminal flow system.

The compositions of the vapor fluctuate some but appear to be in isotopic equilibrium with the soil and ground water (as controlled by precipitation) without direct contact. And, a correlation is observed between the temporal variations in the compositions of the vapor, and grape leaves and berries as controlled by direct contact by kinetic equilibrium.

The isotopic differences between the grape waters, and the grape must and wines are more controlled by transpiration (as affected by atmospheric conditions) from the grape prior to harvest than they are by the isotopic compositions of annual rainfall. Nevertheless, climate information may be obtained by the analysis of wine as fermentation does not significantly alter the isotopic composition of the grape juice. The isotopic compositions of selected wines from Napa Valley, California show variations of more than 5 per mil in  $\delta^{18}\text{O}$  in wines produced in the last 30 years and indeed represent variations in environmental conditions.

EVALUATION OF C AND N INVENTORIES,  $\delta^{13}\text{C}$  AND  $\Delta^{14}\text{C}$  IN DEEP SOILS FROM MATURE AND  
REGROWING FOREST (CAPOEIRA), AND PASTURE  
OF EASTERN AMAZONIA.

CAMARGO P.B.DE\*, Martinelli L.A., Pessenda L.C.R.,  
Centro de Energia Nuclear na Agricultura, CP 96,  
Piracicaba, SP 13400-970, Brazil; TRUMBORE S. E.,  
Dept. of Geosciences, University of California, Irvine,  
CA 92717-3100; Davidson E.A., and Nepstad D.C., The  
Woods Hole Research Center, Woods Hole, MA 02543.

To better understand how tropical forest clearing, pasture management, and forest regrowth affect deep soil C cycling we investigate: C and N inventories to estimate below-ground C and C/N dynamics,  $\delta^{13}\text{C}$  analysis to calculate C inputs to pasture soils from C-4 grasses and  $\Delta^{14}\text{C}$  analyses of soil  $\text{CO}_2$  to estimate residence times of soil organic matter.

Much of the eastern Amazon Basin, including our study area in Paragominas, Para, is characterized by deep oxisols (more than 8m). This region experience a significant dry season, although most of its forests retain leaf canopies continuously. Deep rooting of trees in mature forests support evapotranspiration during the dry season and impact C and N inputs at depth.

Measurements of the 0-8 m soil layer show that C and N decrease from the surface (2.00 - 0.15%) to 3m (0.20 - 0.01%) respectively, then remain constant to the bottom. The C/N ratio varies between 10 to 20 and usually increases below 2m. There are no significant differences below 2m between the three ecosystems.

In the upper 10cm the bulk density increases from mature forest and "capoeira", to pasture (0.96, 1.07, 1.24g/cc) respectively. Below that, bulk density is roughly constant (1.3±0.5g/cc). Large bulk density at the surface in pastures is due to compaction because of loss of organic matter and physical disturbance.

The  $\delta^{13}\text{C}$  values in the upper 10cm are -27.3, -26.7, -24.4‰, for forest, "capoeira" and pasture. These results indicate that only 20% of the SOM from pasture has been added since the change of vegetation (1969). The influence of C-4 vegetation can be seen in pastures to a depth of 25cm, but not below. The values of  $\delta^{13}\text{C}$  increase with the depth (by 1 to 4‰) in the soil profile. No difference is observed at depth among mature, regrowing forest and pasture, probably because the deep pasture and "capoeira" profiles retain the characteristics of the primary forest before vegetation change. This increase could reflect fractionation due to decomposition or movement of organic matter down the profile.

The few  $\Delta^{14}\text{C}$  data that we have now, show higher positive values in the surface of forest and pasture (+149 and +130‰) and indicate that turnover of soil C in this layer is rapid (less than 30 years).  $\Delta^{14}\text{C}$  values decrease with depth quickly in the first meter to -700‰ and -630‰ in forest and pasture and remain between -750 and -800 at greater depth in both profiles.

Our observations, together with  $\text{CO}_2$  flux in the soil will be used to construct models with predict changes in C and C isotopes accompanying forest-pasture vegetation change.

\*Current address: Depart. of Geosciences  
UC Irvine, Irvine, CA 92717

## MAGMATIC UNDERPLATING IN THE SOUTHERN BASIN AND RANGE DURING CENOZOIC EXTENSION: A XENOLITH PERSPECTIVE

CAMERON, K.L., Earth Sciences, Univ. of California, Santa Cruz, CA 95064; McMILLAN, N.J., Geological Sciences, New Mexico State Univ., Las Cruces, NM 88003; SMITH, R.D., Earth and Space Sciences, SUNY, Stony Brook, NY 11794; McDOWELL, F.W., Geological Sciences, Univ. of Texas, Austin, TX 78713.

The xenolith localities of Kilbourne Hole (KH), New Mexico, USA, and La Olivina (LO), northern Mexico, occur in areas that experienced substantial mid- to late Cenozoic volcanism and both lie in areas affected by Basin and Range faulting (KH is in the southern Rio Grande rift). Mafic rocks are a major component of the granulite suite at each locality. In order to test the hypothesis that these xenoliths represent new crust formed by underplating during Cenozoic extension, we analyzed ~15 representative mafic granulites from each locality for Sr-Nd-Pb isotopes, and we compared their isotopic compositions to those of igneous rocks of known age exposed nearby.

At least four isotopically distinct pulses of magmatism occurred in the LO area during the past 40 Ma. With one exception, the isotopic compositions of the LO mafic granulites, closely match those of 32-31 Ma intermediate to silicic volcanic rocks ( $^{87}\text{Sr}/^{86}\text{Sr} \approx 0.705$ ;  $\epsilon_{\text{Nd}} \approx +1$  to  $-1$ ;  $^{206}\text{Pb}/^{204}\text{Pb} \approx 18.6$ ), and the xenoliths are isotopically distinct from all other age groups of exposed igneous rocks.

In contrast, few mafic granulites from KH have isotopic compositions in the range of Cenozoic volcanic rocks from the southern Rio Grande rift. About half have  $\epsilon_{\text{Nd}}$  values between  $-7$  and  $-11$ , and this group plots in the field of exposed early Proterozoic granites and gneisses on a Sm/Nd isochron diagram. The remaining xenoliths have  $\epsilon_{\text{Nd}}$  values ranging from  $+2$  to  $-10$ , and most of these plot near a 1.04 Ga reference Sm/Nd isochron defined by Grenville age granites and mafic lavas exposed in the region. The xenoliths have lower  $^{206}\text{Pb}/^{204}\text{Pb}$  (16.2 to 17.2) than all but a very few Cenozoic volcanic rocks (17.0 to 19.7).

Few if any of the KH or LO mafic granulites appear to represent lower crust formed by magmatic underplating associated with Cenozoic extension. The great majority of KH mafic granulites are most reasonably interpreted to be Precambrian basement. We can not rule out the possibility that the protoliths of some were Cenozoic gabbros that contained a much larger component of ancient crust than any of the rift-related volcanic rocks, but the data do not require or support that interpretation. The LO mafic granulites represent one specific magmatic event at 32-31 Ma that preceded Basin and Range faulting. The isotopic data indicate that the protoliths of both the KH and LO mafic xenoliths are related by differentiation processes to identifiable silicic rock types. This stands in contrast to underplating models where basaltic magmas pooled near the crust-mantle boundary and generated silicic melts principally by melting the overlying crust. The KH and LO studies demonstrate that information on the isotopic and trace-element compositions of exposed igneous rocks is most useful in interpreting the age and tectonic significance of deep crustal mafic xenoliths.

## CONSTRAINING ATMOSPHERIC INPUTS AND IN SITU WEATHERING IN SOILS DEVELOPED ALONG A CLIMATE GRADIENT USING STRONTIUM ISOTOPES

CAPO, R.C., Division of Geological & Planetary Sciences 170-25, California Institute of Technology, Pasadena, CA 91125, USA, CHADWICK, O. A., JPL-Caltech, MS183-501, Pasadena, CA 91109, and HENDRICKS, D. M., Soil and Water Sci., Univ. of Arizona, Tucson AZ 85721, USA

Soils developed on the Hawi Lava (~180 Ky) along the western slope of Kohala volcano were sampled along an elevational transect (77 to 1254 m). Detailed morphological, mineralogical, geochemical and isotopic analysis of soil, basalt parent material, and weathered basalt clasts have been undertaken to provide a better understanding of the influence of climate on mineral weathering rates and to study the relationship between *in situ* weathering processes and atmospheric inputs under widely varying climatic conditions. Pedogenic response to climatic variability was determined using a paleoenvironmental model based on present rainfall and past orographic effects. The time-weighted mean rainfall along the transect increases with elevation and ranges from 18 to 350 cm; the increasing amount of rainfall corresponds to an increasing intensity of weathering.

Strontium isotopes can be used to examine the relationship between the weathering of primary minerals and atmospheric addition. The Sr isotopic composition of the endmembers of the soil-atmosphere system along the Kohala transect are well-constrained. The  $^{87}\text{Sr}/^{86}\text{Sr}$  ratio of the parent material Hawi lava ranges from 0.7035-0.7036 [1, 2]. Atmospheric input consists primarily of rainfall, which would have an  $^{87}\text{Sr}/^{86}\text{Sr}$  ratio similar to seawater (0.7092), and dryfall. Dust over Hawaii is predominantly derived from Asia; eolian micas from Hawaiian soils have  $^{87}\text{Sr}/^{86}\text{Sr}$  ratios of 0.713 - 0.727 [3, 4]. Eolian input to the soil is recognized by increased amounts of quartz and mica in the <2mm soil fraction, generally in the upper soil horizons.

Preliminary results suggest considerable isotopic inheritance from atmospheric sources even where present dust and rainfall inputs are low. At Site B (18 cm rainfall),  $^{87}\text{Sr}/^{86}\text{Sr}$  ratios of bulk soil decrease from 0.70422 in the dust-rich A horizon (0-10 cm depth; 2.9 wt % qtz; 3.8 wt % mica) to 0.70405 in the Bw2 horizon (37-65 cm depth; 0.2% qtz; 0.2 % mica). These values are significantly higher than Hawi lava values, and suggest mixing of parent material with the more radiogenic atmospheric components. Along the climate transect, the  $^{87}\text{Sr}/^{86}\text{Sr}$  ratio of the exchangeable Sr of the dust-poor lower B horizon (leached with  $\text{NH}_4\text{Cl}$  [5]) is similar for Sites B, E and I (18-148 cm rainfall;  $^{87}\text{Sr}/^{86}\text{Sr} = 0.7040$ -0.7041) but increases to 0.7089 at Site L (300 cm rainfall). This most likely reflects the much greater intensity of weathering at Site L which has leached away parent material Sr and left Sr derived primarily from rainfall on the exchange complex.

References: [1] Lanphere, M. and Frey, F., (1987) *Contrib. Mineral. Petrol.* 95: 100; [2] Hofmann, A., Feigenson, M. and Raczek, I. (1987) *Contrib. Mineral. Petrol.* 95: 114; [3] Dymond, J., Biscaye, P. and Rex, R. (1974) *GSA Bull.* 85: 37; [4] Nakai, S., Halliday, A. and Rea, D. (1993) *EPSL* 119: 143; [5] Jackson, M. (1969) *Soil Chemical Analysis*, 2nd ed., Madison, 895 p.

## DYNAMICS OF MELTING AND MANTLE SOURCES FOR QUATERNARY CONTINENTAL ALKALINE MAGMAS IN THE NORTHERN CANADIAN CORDILLERA.

Carignan, J. and Ludden, J., Département de Géologie, Université de Montréal, Montréal, Québec, H3C 3J7, Canada and Francis, D., Department of Earth and Planetary Sciences, McGill University, Montréal, Québec, H3A 2A7, Canada.

Five Quaternary to recent volcanic centres in the Northern Canadian Cordillera comprising alkaline lavas ranging in composition from olivine nephelinite to Hy-normative basalt, have been analysed for their Sr, Nd and Pb isotopic compositions. Previous studies on these lavas indicate that the compositional spectrum is best explained by the melting of variable proportion of amphibole-rich veins hosted in a lherzolite lithospheric mantle. Samples covering the entire magmatic spectrum were selected to document the isotopic composition of endmembers and evaluate the hypothesis of a single heterogeneous reservoir as the source of alkaline magmas in the Northern Cordillera.

Three mantle components have been identified as potential source endmembers. These are: 1) an unradiogenic Sr, Nd and Pb component from which olivine nephelinite formed; 2) a radiogenic Pb - non radiogenic Sr component (HIMU-type) represented by Mt.Edziza lavas; 3) spinel lherzolite mantle characterized by high  $^{207}\text{Pb}/^{204}\text{Pb}$  (enriched mantle-II type), that is involved in the formation of basanites and alkali olivine basalts from some centres.

The distinct isotopic character of the Edziza centre relative to most of the alkaline magmas indicates that the Mt.Edziza reflects upwelling of sub-lithospheric Pacific mantle below central British Columbia. Incipient melts from amphibole-garnet-pyroxenite veins in the subcontinental lithospheric mantle were generated in response to the thermal upwelling and resulting in the small (<1Km<sup>3</sup>) nephelinite to AOB centres characteristic of the Northern Cordilleran Province. The nephelinite source is slightly more radiogenic than present day Pacific MORB and is best represented by the most depleted component of the Aleutian magmas perhaps indicating an enrichment of subcontinental lithosphere in northern Cordillera by melts of this composition during Cretaceous subduction. The AOB magmas of the Fort Selkirk volcanic complex appear to lie on a binary mixing trend between the nephelinite component and spinel lherzolite xenoliths from the region, whereas the Alligator lake complex lavas are highly radiogenic, display evidence for crustal contamination, but may nonetheless represent a highly radiogenic lithospheric mantle.

## PLUMBOTECTONICS OF THE LACHLAN FOLD BELT OF EASTERN AUSTRALIA: CRUST-MANTLE INTERACTION IN THE FORMATION OF PALAEOZOIC MINERALIZATION

CARR, G.R., DEAN, J.A., CSIRO Division of Exploration and Mining, North Ryde, NSW, 2113, Australia, SUPPEL, D.W., Geological Survey of New South Wales, St Leonards, NSW, 2065, Australia, and HEITHERSAY, P.S., Geopeko, Melbourne, VIC, 3004, Australia.

In contrast to most large Phanerozoic orogenic systems, the Lachlan Fold Belt (LFB; > 500 000 km<sup>2</sup>) has similar lithological assemblages and structural style throughout. This relative homogeneity is mirrored by the Pb isotope systematics of magmatic units and minerals formed from magmatic and metamorphic hydrothermal activity. A study of over 100 mineral deposits in the LFB ranging in age from Ordovician to Permian has indicated a three fold subdivision based on the sources of Pb: (1) deposits containing almost exclusively mantle derived Pb, (2) deposits containing Pb which has had a very long crustal residence time (~1 Ga) and, (3) deposits containing Pb of mixed mantle and crustal origin. The distribution through time of these source-types has implications for the tectonic development of the LFB.

In Ordovician sequences, both Besshi-style mineralization with crustal Pb isotope signatures and porphyry to epithermal Cu and Au mineralization with mantle signatures occur. This latter mineralization is associated with mafic igneous rocks, commonly shoshonitic in character, and the ores and corresponding unaltered host rocks have similar Pb isotopic compositions suggesting Pb is magmatic in origin. On each of the conventional Pb isotope diagrams, the data for these deposits plot on a very precise line which is not a typical arc-like mixing trend but represents mixing of Pb from two or more mantle reservoirs. It is postulated that the position of each deposit along this line is an indication of the timing of metallogenesis within the Ordovician magmatic cycle, and possibly also the degree of mixing of melts derived from a more primitive asthenosphere and a more enriched lithosphere, potentially fertile for Cu and Au.

Magmatic rocks and large scale magmatic hydrothermal mineralization of Silurian and Devonian age are dominated by crustal Pb, but evidence of hydrothermal mixing of crustal Pb, and mantle Pb mobilised from Ordovician mafic units, is common. There is very little evidence for direct mantle input of Pb. Similarly, large scale incorporation of mantle Pb in Carboniferous and Permian granites and associated mineralization probably represents recycled Ordovician Pb.

The homogeneous nature of the crustal and dominant Ordovician mantle source regions in the LFB allows the development of a plumbotectonic model which yields mineralization model ages with precision better than  $\pm 15$  Ma based on mixing isochrons between a crustal growth curve ( $\mu = 13.3$ ) and a mantle growth curve ( $\mu = 10$ ). The model also appears to be valid for older (Kanmantoo Fold Belt) and younger (New England Orogen) units of the Tasman Fold Belt System.

APPLICATION OF INVERSE  
NUMERICAL TECHNIQUES IN  
RADIOISOTOPE GEOCHRONOLOGY  
CARROLL, J., ABRAHAM, J. D., CISAR, D. J., RUST  
Geotech, Grand Junction, CO, 81502 USA, and  
LERCHE, I., Dept. Geological Sciences, University of  
South Carolina, Columbia, SC 29208, USA.

Many methods for determining sedimentation rates in lacustrine and marine environments use naturally occurring radioisotopes as geochronometers (e.g. Pb-210, C-14, Th-230, Ra-226). These methods work best when both adsorption to sediments and sedimentation rate are constant. Most often, neither process is constant, producing radioisotope activities which vary nonexponentially with depth in sediment cores. Without techniques to separate the effects of source from sedimentation variations, such profiles do not yield useful sediment ages.

We have developed a procedure to analyze these complex isotopic profiles. The procedure uses inverse numerical analysis techniques to produce a model of appropriate resolution and matching the degree of complexity of a given isotopic profile. We demonstrate the procedure using synthetic profiles of known source and sedimentation components, which represent isotopic behavior in a variety of sedimentary environments. This new procedure removes limitations on the application of radioisotopes as geochronometers in paleoceanography, as well as providing variable source and sedimentation rates with time.

COSMOGENIC  $^3\text{He}$  AND  $^{21}\text{Ne}$  FROM TIOGA AGE  
SURFACES, SIERRA NEVADA, CALIFORNIA  
CERLING, T. E., Department of Geology and Geophysics,  
University of Utah, Salt Lake City, Utah 84112 USA,  
POREDA, R. J., and KU, T., Department of Geological  
Sciences, University of Rochester, Rochester, NY, 14627 USA

Tioga age glacial surfaces in on the east side of the Sierra Nevada can be dated using cosmogenic  $^3\text{He}$  and  $^{21}\text{Ne}$ . At June Lake and at Devils Postpile in the Mammoth Lakes region volcanic rocks which were glacially scoured during the Tioga glaciation provide excellent surfaces for cosmogenic dating using  $^3\text{He}$  and  $^{21}\text{Ne}$ . In addition, the close proximity of glaciated Bishop Tuff and basalts allows comparison of  $^{21}\text{Ne}$  production rates in olivine and quartz, without the complication of  $^{18}\text{O}(\alpha, n)^{21}\text{Ne}$  production problems associated with glaciated Sierra Nevada granites. Cosmogenic dates on volcanic flows of the Big Pine field in Owens Valley, which are overlain by glacial outwash, provide additional constraints on the Tioga glaciation.

## TIMS U-SERIES STUDY OF THE GROWTH HISTORY OF FERROMANGANESE CRUSTS

CHABAUX, F., COHEN, A.S., O'NIONS, R.K. Dept. of Earth Sciences, Cambridge University, CB2 3EQ, UK, and HEIN, J., US Geological Survey, Menlo Park, CA)

Hydrogenous ferromanganese crusts grow from sea water, at rates which would be related to climatic variations<sup>1</sup>. In this case, the detailed determination of growth rates together with details of chemical and isotopic composition could provide important information on sea water composition through climatic cycles. However this record is only easily accessible if the growth processes are uniform over an useful portion of the crust.

In order to assess these questions we present TIMS measurements of <sup>234</sup>U and <sup>230</sup>Th excesses along different profiles of the outermost 2 mm rim of a single Mn crust, from Lomilick seamount in the Marshall Islands. Our results are as follows :

1-Within a single profile, the variations of <sup>234</sup>U- and <sup>230</sup>Th-excesses provide generally consistent growth rates or ages for Mn oxide layers. Small discrepancies between these two chronometers are nevertheless observed, which may indicate local disturbance of Mn layers since deposition, or alternatively contamination by detrital minerals incorporated into the Mn crust and partially dissolved during chemical treatment in the laboratory.

2-Comparison of two profiles, obtained only a few centimetres apart on the same crust, shows that one has an age of 400,000a older than the other. This indicates that growth stopped during this interval of time, or that local abrasion or dissolution of the Mn oxides occurred after deposition. Similar observations were made by von Blanckenburg *et al.* (*pers. comm.*) using <sup>10</sup>Be data from the same crust. In addition Sharma *et al.*<sup>2</sup> reported spatial variability on a scale of a few centimetres of U-Th series nuclides in surface layers of deep-sea ferromanganese encrustations. These results demonstrate significant variability in the growth process of Mn crust, which will make the observation of fine-scale growth histories difficult in many cases.

1-Eisenhauer *et al.* E.P.S.L., 109, 25-36, 1992

2-Sharma *et al.* E.P.S.L., 67, 319-326, 1984.

## ISOTOPIC TRACING OF SONG BIRD MIGRATORY PATTERNS AND PALEOENVIRONMENTS OF FOSSIL BIRDS

CHAMBERLAIN, C.P., BLUM, J.D., HOLMES, R.; POULSON S., Dartmouth College, Hanover, NH 03755; GRAVES, G., Dept. of Vertebrate Zoology, Smithsonian Institute, Washington, D.C. 20560; SHERRY, T., Dept. of Biology, Tulane Univ., New Orleans, LA.

We are exploring the isotopic variations in modern song birds as a possible tool for tracing migratory patterns as well as determining paleoenvironmental conditions of fossil birds. The motivation for this research is two-fold. First, song bird populations in North America are in decline, but the exact cause is unknown and requires a detailed understanding of the birds' migratory patterns. Unfortunately, at present there are no methods available to determine these migration routes with any certainty. Second, isotopic studies of modern birds are needed prior to using fossil birds to reconstruct paleoenvironmental conditions.

We determined the H, C and Sr isotopic values of feather and bone material of Black-Throated Blue Warblers (*Dendroica caerulescens*). Our studies show that isotope values of birds collected in their nesting grounds correlate with isotope variations in the hydrosphere and lithosphere. This correlation demonstrates that it is possible to use isotopes to determine both migration patterns of modern birds and paleoenvironmental conditions of fossil birds.

The  $\delta D$  and  $\delta^{13}C$  values of feathers from over 200 birds collected from nesting sites vary in a predictable and systematic fashion. The  $\delta D$  of feathers vary by over 30‰ from the southern range ( $\delta D=69\pm 10\text{‰}$ ) to the northern range ( $\delta D=101\pm 14\text{‰}$ ). The variations in  $\delta D$  values of feathers mimics the observed variations in  $\delta D$  of rain water with latitude.  $\delta^{13}C$  of feathers vary from a low of  $\delta^{13}C=22.0\pm 0.6\text{‰}$  in the southern breeding range to a high of  $\delta^{13}C=24.2\pm 0.7\text{‰}$  in the northern breeding range. Although the variations in  $\delta^{13}C$  are small they are extremely systematic with no overlap occurring between the  $\delta^{13}C$  of northern and southern birds. We determined the  $^{87}Sr/^{86}Sr$  values for bone for 9 birds from 7 localities. These values show a wide range between localities ( $^{87}Sr/^{86}Sr=0.71155$  to  $0.71852$ ) and a much narrower range within single localities reflecting unique  $^{87}Sr/^{86}Sr$  signatures dependent on soil protolith and atmospheric deposition within each nesting site.

**GEOCHRONOLOGIC EVIDENCE FOR EPISODIC STRUCTURAL AND MAGMATIC REACTIVATION OF A MAJOR CONTINENT-ISLAND ARC SUTURE OVER A 400 MYR PERIOD**

**CHAMBERLAIN, K. R., SCOATES, J.S., and FROST, C.D., Dept. of Geology and Geophysics, University of Wyoming, Laramie, WY 82071, USA**

The Cheyenne belt in southeastern Wyoming, a Proterozoic (ca 1.78 Ga) suture between the Archean Wyoming Province to the north and Proterozoic island arc rocks to the south, has been the site of multiple periods of magmatism and deformation, and may have responded to orogenies occurring 100's of km to the south. Recent discoveries and isotopic results that bear on the 400 myr tectonic activity of the Cheyenne belt include 1) recognition of thick-skinned basement deformation within the craton during collision, 2) evidence for transtension during late stages of suturing, and emplacement of the 1.76 Ga Horse Creek anorthosite complex, 3) widespread 1.66-1.60 Ga magmatism, metamorphism and uplift along the Cheyenne belt, and 4) direct age of crystallization of 1.43 Ga from anorthosites located within the pre-existing zone of transtension.

Thick-skinned deformation of the craton during collision is manifested by a minimum of 10 km vertical uplift across the mylonitic Laramie Peak shear zone 60 km north of the trace of the Cheyenne belt. U-Pb apatite dates from both sides of the Laramie Peak shear zone constrain movement to ca 1.78 Ga. Lack of a metamorphic gradient within the block between the shear zone and the Cheyenne belt suggests nearly vertical uplift without rotation. South of this block, the Horse Creek anorthosite complex was emplaced at 1.76 Ga, coincident with the timing of late, dextral strike-slip motion along the Cheyenne belt, and thus in an inferred transtensional tectonic setting. Isotopic data from the Horse Creek complex imply a stratified crustal section with a gently dipping suture between Proterozoic upper crust and a rifted Archean lower crust. Additional 1.76-1.74 Ga syn- to post-tectonic plutonism occurs in a broad, 200 km long, triangular-shaped region along the southern edge of the Cheyenne belt and may demarcate the extent of transtensionally weakened crust. U-Pb mineral dates, including zircon, monazite, sphene, and apatite, indicate later 1.66 to 1.60 Ga magmatism, metamorphism and uplift within this transtensional zone at a time that island arc collision was occurring along the Mazatzal orogeny at least 300 km to the south. Finally, this zone was the site for the generation and emplacement of a second anorthosite complex, the 1.43 Ga Laramie complex, suggesting renewed extension. The anorthosites within this younger complex have been directly dated by U-Pb baddeleyite and zircon analyses.

The 400 myr tectonic activity of the Cheyenne belt demonstrates the influence of pre-existing structures and zones of crustal weakness on later tectonic events. There may be strong structural controls on the generation of anorthosites, on deformation of the hinterland during orogeny, and on the locations of 'anorogenic' 1.4 Ga magmatism.

**PALEOMAGNETIC CONSTRAINTS ON EPISODES OF BASALTIC VOLCANISM**

**CHAMPION, D.E.,** Isotope Geology, U.S. Geological Survey, 345 Middlefield Rd., Menlo Park, CA 94025

Field-based paleomagnetic studies, when coupled with geologic mapping, petrology, and chronometric techniques such as  $^{14}\text{C}$ , K-Ar, or  $^{40}\text{Ar}/^{39}\text{Ar}$ , repeatedly demonstrate that basaltic volcanism is characterized by brief episodes of eruption and that the products of these eruptions may be large in volume and may also be compositionally zoned despite being erupted in short periods of time (<100 years). This type of volcanism occurs in the Cascade arc and adjacent Basin and Range province. Within the Shasta-Medicine Lake segment of the Cascades, paleomagnetic studies confirm the suggestion from field mapping that as few as 7 brief eruptions, each at least  $2\text{ km}^3$  in volume, produced basaltic lavas which cover about  $1500\text{ km}^2$ . This represents almost 25% of the entire Quaternary volcanic axis between Mt. Shasta and the Medicine Lake Highlands. One well-documented example is the Giant Crater lava field on the Medicine Lake volcano. Detailed field and petrologic studies (Donnelly-Nolan et al., 1991), demonstrate compositional variation from basaltic andesite to high-alumina basalt ( $\text{SiO}_2$  53→48%), in  $4.4\text{ km}^3$  of lava from at least 10 vents. Paleomagnetic data from 41 sites show no more than  $2^\circ$  of direction variation among the average directions of 6 mapped compositional variants. By analogy with modern geomagnetic records, all the Giant Crater eruptions, and approximately one half the chemical evolution, took at most a few decades. The basalt of Mammoth Crater, which covers about  $250\text{ km}^2$  on the N. flank of Medicine Lake volcano shows even more compositional variation ( $\text{SiO}_2$  55–48%). Paleomagnetic data from 27 sites again indicate all Mammoth Crater lavas share the same paleomagnetic direction (< $3^\circ$  of variation).

Studied alkalic basalts of the Basin and Range in southern Nevada also erupted in brief eruptions such that only single directions of remanent magnetization were recorded within individual cinder cones and lava fields. This is not surprising as historic observations at Paricutin in Mexico showed that cinder cones typically erupt in brief ( $\leq 9$  years) and sometimes compositionally varying ( $\text{SiO}_2$  55→60%) lavas. Lavas of the 3.7 Ma and 1.1 Ma cinder cone eruptions at Crater Flat record similar, but individually distinguishable reversed polarity directions, while also showing chemical and trace element variations. Four different cinder cone centers of the 1.1 Ma episode record the same reversed polarity direction indicating all erupted within 100 years. Alkalic basalt of the Lathrop Wells center shows minimal trace element variation, but does record two different but allied directions of magnetization. Petrologic arguments which insist that these very small chemical differences are inconsistent with monogenetic origin, and are necessary evidence of independence of magma evolution and eruption, are probably incorrect.

Donnelly-Nolan, J.M. et al., 1991, The Giant Crater Field: Geology and Geochemistry of a Compositionally Zoned, High-Alumina Basalt to Basaltic Andesite Eruption at Medicine Lake Volcano, California, *Jour. Geophys. Res.*, v. 96, p. 21843-21863.

## THE GEOCHEMISTRY AND CYCLE OF LITHIUM ISOTOPES IN THE MARINE ENVIRONMENT

CHAN, L. H., Dept. of Geology and Geophysics, Louisiana State University, Baton Rouge, Louisiana 70803, U.S.A.

Unlike other light isotopes, the geochemistry of Li isotopes has not been well known. An improved mass spectrometric technique permits measurement of Li isotopic ratios to a precision of 1 per mil (Chan, 1987). Using this method, the Li isotopic compositions of river water, seawater, fresh and variously altered oceanic basalts, submarine hot springs, marine sediments including hydrothermally altered and subduction zone sediments, pore waters, and island arc volcanics have been measured. This report presents an overview of the oceanic distribution of Li isotopes with respect to (1) the basic geochemistry of Li isotopes; (2) the isotopic constraints on the Li balance in the oceans; and (3) the tracer capability of Li in the study of oceanic processes.

Seawater has a  $\delta^6\text{Li}$  value of -32.3 per mil (relative to NBS standard L-SVEC). The  $\delta^6\text{Li}$  values of MORB range from -3.4 to -4.7 per mil. These distinct endmember values make Li isotope ratios a valuable tracer for seawater-basalt exchange. Hydrothermal solutions from various ridge crest systems show isotopic values ranging from -6 to -11 per mil, which can be understood in terms of a path-dependent dissolution-precipitation process in response to progressive changes in temperature and water/rock ratio. The similarity of the Li isotopic compositions in fluids from fast and slow spreading ridges argues against contribution of recycled Li from older, weathered crust to the large hydrothermal flux as calculated from the  $^3\text{He}/\text{heat}$  ratio. Fluids from sediment-covered spreading centers (e.g., Guaymas Basin) exhibit Li concentrations and  $\delta^6\text{Li}$  values similar to those of the mid-ocean ridge systems, implying an open flow-through system with rapid water recharge that largely obliterates contributions from the sediments.

Seafloor basalts weathered at low temperatures show Li enrichment and more negative  $\delta^6\text{Li}$  values as a result of addition of seawater Li. Metabasalts usually have lighter isotopic compositions as a result of retention of basalt-derived Li. The secondary minerals in these altered basalts show preferential incorporation of the lighter isotope with an apparent temperature dependency of the isotopic fractionation factor.

The Li isotopic ratios of marine sediments vary with source and composition. The hemipelagic sediments of Guaymas Basin have a  $\delta^6\text{Li}$  value of -10 per mil while the trench turbidite of Nankai Trough has -2 per mil. The strong depletion in Li associated with lighter  $\delta^6\text{Li}$  values in the greenschist facies sediments of Guaymas Basin demonstrates high mobility of sedimentary Li at elevated temperatures. In the decollement zone of the Nankai Trough, a maximum in  $\delta^6\text{Li}$  with corresponding low Li concentration in the pore water has been observed. The anomaly can be taken as an evidence of migration of low-Li fluid from deeper in the accretionary complex where mineral dehydration occurs. These results indicate the usefulness of Li isotope in the study of subduction zone processes.

The isotopic values of rivers range from -15 to -29 per mil. Thus seawater is enriched in  $^7\text{Li}$  relative to the inputs from riverine and hydrothermal sources and  $^6\text{Li}$  must be preferentially removed to maintain a steady state composition. Isotope balance considerations favor a hydrothermal flux that is comparable to the river flux unless more important  $^6\text{Li}$  sinks than the authigenic clays exist.

## CONSTRAINTS ON METAMORPHIC FLUID FLOW FROM STRONTIUM AND OXYGEN ISOTOPIC PROFILES ACROSS CARBONATE - SILICATE CONTACTS, LIZZIES BASIN, NEVADA.

CHAPMAN, H. J., BICKLE, M. J., Dept. of Earth Sciences, University of Cambridge, Cambridge CB2 3EQ, U.K. and WICKHAM, S. M., PETERS, M. T., Dept. Geophysical Sciences, University of Chicago, Chicago, Illinois 60637, U.S.A.

Strontium, oxygen and carbon isotope profiles were measured across two marble layers, and into adjacent calcsilicate gneiss and leucogranite, in the migmatitic amphibolite-facies gneiss complex at Lizzies Basin in the East Humboldt Range. Displacement of the isotopic tracers are used to assess the relative significance of advective and diffusive transport, porosity (and thus permeability) contrasts between lithologies, together with the fluid Sr and  $\text{H}_2\text{O}/\text{CO}_2$  ratio.

The Neoproterozoic and Palaeozoic metasediments from Lizzies Basin were metamorphosed to sillimanite grade during the Tertiary, overprinting earlier Mesozoic metamorphic events. Wickham and Peters (1992) have previously ascribed major oxygen isotope mobility in this sequence to infiltration of hydrous fluids accompanying Tertiary metamorphism. Both oxygen and strontium isotopic profiles indicate minimal advective transport across the marble bands. Modelling of oxygen-isotope diffusion distances indicates porosities in the calc-silicates were at least a factor of 10 more than porosities in the marbles. In contrast one of the strontium isotopic profiles (Fig 1) exhibits symmetrical diffusive broadening about the contacts consistent with nearly equal porosity between the calc-silicate and the marble. This discrepancy between the oxygen and strontium isotopic profiles may result from 1) a marked contrast in fluid Sr contents between marble and calc-silicate, 2) O and Sr diffusion responding differently in the several metamorphic events or 3) significant porosity variation within calc-silicates, (the Sr isotopic profile is spatially limited). Comparison of Sr and O isotopic diffusion distances indicates fluid Sr concentrations between ~50 - 500 ppm. Comparison of  $\delta^{18}\text{O}$ - $\delta^{13}\text{C}$  profiles indicates that fluids were water-rich ( $X_{\text{CO}_2} < 0.02$ ) and were probably derived from adjacent crystallising leucogranites.

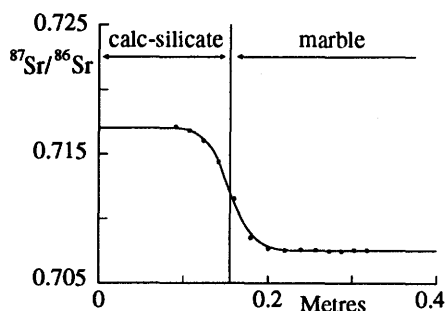


Figure 1. Sr-isotopic profile across upper contact of marble band. Line is least-squares fit assuming differing diffusivities in marble and calc-silicate and implies porosity contrast (calc-silicate to marble) of  $1.7 \pm 0.25$ .

Wickham, S. M. and Peters, M. T., 1992, Oxygen and carbon isotope profiles in metasediments from Lizzies Basins, East Humboldt Range, Nevada: *Contrib. Mineral. Petrol.*, v. 112, p. 46-65.

**BORON ISOTOPE VARIATIONS IN CHONDRULES:  
CONSEQUENCES ON CHONDRULE FORMATION AND  
BORON COSMOCHEMISTRY**

CHAUSSIDON M., CRPG-CNRS, BP 20, 54501  
Vandoeuvre-lès-Nancy, France and ROBERT F., Museum  
d'Histoire Naturelle-CNRS, 61 rue Buffon, 75005 Paris,  
France.

A boron isotope study of chondrules was undertaken in several chondrites (Semarkona LL3, Allende CV3, Hedjaz L3 and Estacado H6) to (1) evaluate the potential of B isotopes for constraining the mechanism of chondrule formation and to (2) document the possible B isotope heterogeneity of nebular precursors and of chondrites. Measurements were made with a IMS 3f ion microprobe at CRPG (Nancy) on  $\approx 25\mu\text{m}$  spots, following the procedures developed for mantle rocks<sup>[1,2]</sup> and with careful attention paid to problems of surface contamination.  $\delta^{11}\text{B}$  values are given versus NBS 951 ( $^{11}\text{B}/^{10}\text{B}=4.04558$ ) with an accuracy varying between  $\pm 5\%$  to  $\pm 10\%$  according to the B contents. Elemental ratios of B, Na, Mg, Al, K and Ca versus Si were determined simultaneously on the same spots by ion probe.

Large discrepancies exist between the only two existing B isotope studies of bulk chondrites which report 3  $\delta^{11}\text{B}$  measurements between  $-35\pm 4$  and  $-57\pm 4\%$  for the oldest one<sup>[3]</sup> and 6  $\delta^{11}\text{B}$  measurements between  $+1.8$  and  $-8.5\%$  for the most recent<sup>[4]</sup>, while they both report B concentrations in the same range, between 0.4 and 0.9 ppm. These differences are un-explained, but large isotopic heterogeneities may have existed in the solar nebula since calculations of the  $^{11}\text{B}/^{10}\text{B}$  ratios, produced during the synthesis of B via the inter-action between high energy cosmic rays and the interstellar matter, can theoretically vary between 2.5 and 4.1<sup>[5,6]</sup>.

The  $\delta^{11}\text{B}$  values found in this study are extremely variable between  $\approx +40\pm 10$  and  $-50\pm 10\%$  in chondrules from Semarkona, Hedjaz and Estacado, and more homogeneous at  $-25\pm 15\%$  in chondrules from Allende. Strong linear correlations are observed in several cases between the  $\delta^{11}\text{B}$  values and some major element ratios (e.g. Na/Si, Mg/Si, Ca/Al). In addition,  $\delta^{11}\text{B}$  variations in some barred chondrules follow mineralogical structures. These results imply that several processes concur to control the  $\delta^{11}\text{B}$  variations in chondrules, among which the most important are (1) isotopic fractionations occurring during heating (e.g. due to volatilization loss of B) and the cooling (e.g. due to disequilibrium partitioning of B between the different phases) of the chondrule and (2) B isotopic heterogeneity of the nebular precursors. The mean  $\delta^{11}\text{B}$  value of chondrules, similar to mean solar compositions in terms of their B/Si, Mg/Si, Al/Si, K/Si and Ca/Si ratios, is of  $-25\pm 10\%$ , significantly lower than the mean  $\delta^{11}\text{B}$  value of the Earth mantle (between  $\approx -7.5\%$  and  $0\%$ )<sup>[2]</sup>.

1. Chaussidon M. and Libourel G. (1993) *Geochim. Cosmochim. Acta*, 57, 5053-5062
2. Chaussidon M. and Jambon A. (1994) *Earth Planet. Sci. Lett.* (in press)
3. Shima M. (1963) *Geochim. Cosmochim. Acta*, 27, 911-913
4. Agyei E. K. and McMullen C. C. (1978) *Geol. Surv. Op. File Rep.* 78-701, 3-6.
5. Reeves H. (1974) *An. Rev. Astr. Astrophys.*, 12, 437-469.
6. Curtis D. et al. (1980) *Geochim. Cosmochim. Acta*, 44, 1945-1953.

**ORE DEPOSITS DATING THROUGH  $^{40}\text{Ar}/^{39}\text{Ar}$   
LASER SPOT ANALYSIS**

CHEILLETZ A., GIULIANI, G., CRPG-CNRS,  
BP 20, 54501 Vandoeuvre-lès-Nancy, France,  
and ORSTOM, TOA, UR 1H, 213 rue La Fayette,  
75480, Paris, France, FÉRAUD, G., and  
RUFFET, G., URA CNRS 1279, Université de  
Nice-Sophia Antipolis, Parc Valrose, 06034 Nice  
Cedex, France.

Three emerald deposits in Brazil and Colombia have been dated by using  $^{40}\text{Ar}/^{39}\text{Ar}$  techniques. Due to large amounts of excess argon in beryl-type minerals like emerald, particular laser procedure have been applied to obtain formation ages. Firstly, emerald occurring in K-metasomatic rocks developed at the contact of the Carnaúba leucogranite (Bahia state, Brazil) has been dated<sup>[1]</sup> combining step heating and laser spot fusion experiments on (1) individual phlogopite crystals from enclosing host-rock and (2), syngenetic solid inclusions precipitated along growing zones of the emerald host crystals. Reliable ages of  $1951 \pm 8$  ma and  $1944 \pm 8$ Ma have been measured in spite of a polyphased history during the Transamazonian (2 Ga) orogenesis. Secondly, two emerald deposits of the Eastern Cordillera of Colombia have been dated for the first time<sup>[2]</sup> by  $^{40}\text{Ar}/^{39}\text{Ar}$  induction and laser-probe methods on contemporaneous Cr-V-rich K-mica aggregates consisting of muscovite as a dominant phase associated with  $\pm$  kaolinite,  $\pm$  paragonite,  $\pm$  quartz,  $\pm$  albite,  $\pm$  pyrite and calcite. Contamination of the K-mica aggregates by wall-rock impurities is eliminated by in situ  $^{40}\text{Ar}/^{39}\text{Ar}$  analysis. Two distinct plateau and spot fusion ages of 35-38 Ma and 31.5-32.6 Ma were obtained for the Coscuez and Quipama mines respectively. Concordant conventional K-Ar ages show that in spite of the small size of the K-micas, they did not suffer significant  $^{39}\text{Ar}$  loss due to recoil during irradiation of the samples. Internal  $^{39}\text{Ar}$  recoil may explain the slight disturbances observed on the age spectra. These results allow the reconstitution and timing of hydrothermal circulations inducing emerald veins formation with regard to the Eastern Cordillera tectonic evolution.

1. Cheilletz A., Féraud G., Giuliani G. and Ruffet G., (1994), *Earth Planet. Sci. Lett.*, 120, 471-483.
2. Cheilletz A., Féraud G., Giuliani G. and Rodriguez C.T. (1994), *Economic Geology* (in press).

COMPARISON OF LATE CENOZOIC BASALTIC MAGMA GENERATION IN RYUKYU ARC, OKINAWA TROUGH AND ADJOINING AREA (NW. KYUSHU, JAPAN AND N. TAIWAN)

Chang-Hwa Chen, Inst. of Earth Sci., Academia Sinica, P.O.Box 1-55, Taipei, Taiwan, ROC, and Nakada Setsuya, Dept. of Earth and Planet. Sci., Kyushu Univ., Fukuoka 812 Japan

The Philippine Sea plate started to subduct under the Eurasia plate at about 7 Ma. This subduction produced the Ryukyu volcanic arc from SW. Kyushu to eastern offshore Taiwan. The Okinawa Trough is considered as a back arc basin behind the Ryukyu volcanic front. The basaltic samples were collected from the northwestern Kyushu (NWK), central Kyushu (Aso volcano)(CK), northern Ryukyu volcanic arc (RVA) and northern Taiwan volcanic zone (NTVZ). The data of central Okinawa Trough (COT) also was included to discuss the systematic variations (Ishizuka et al., 1990)

The NTVZ has been considered as a part of Ryukyu Arc, but the depth of the Benioff zone present more than 200 km under this belt. From the spider diagram of incompatible elements of basalts for NTVZ, it reveals two different patterns. The one shows no obvious Nb negative anomalies like as ocean island basalt (OIB) trend, the other shows a medium Nb negative anomalies a little like as island arc basalt (IAB) trend. The Nb/Zr vs. K/Zr and Nb/Zr vs. Ba/Zr diagrams also show that the magma source in NTVZ distribute between OIB and IAB. Comparison of the basalts from COT, CK, RVA and the adjoining area (NWK and NTVZ) reveals that the magma source beneath NTVZ is similar to that of NWK and CK. Otherwise, it exists a distinct difference with RVA. The trend of COT in above diagrams reveals the transition between NWK and RVA.

The Sr isotopic study of basaltic rocks indicates that the range in NTVZ are much narrower than that of RVA, which is 0.7039-0.7045 and 0.7041-0.7053, respectively. Whereas, the Sr isotopic values of NTVZ are shown the similar range with that in NWK basalts. The Nd isotopic compositions of NTVZ also show the same situation.

These relationship indicates that the mantle wedge was contaminated by the slab-derived materials in a subduction system, but this influence has gradually decrease with the depth of slabs. When this subducting slab did not reach under volcanic zone or go downward to more than 200 km beneath volcanic belt, the island arc behaviors in volcanic rocks might be obscured.

Ishizuka H., Kawanobe Y. and Sakai H. (1990) *Geochem. J.*, 24, 75-92.

ORIGIN OF MESOZOIC CONTINENTAL BASALTS FROM SOUTHEASTERN CHINA: EVIDENCE FROM ND ISOTOPE AND TRACE ELEMENT COMPOSITIONS

CHEN JIANGFENG, ZHOU TAIXI, CHENG ZHONGQI, Department of Earth and Space Sciences, University of Science and Technology of China, Hefei, 230026, China, and YU YUNWEN, Regional Geologic Survey Party of Zhejiang Province, Xiaoshan, Zhejiang, 311200, China

It is found recently that except for majority of intermediate and felsic volcanic rocks there are basalts in the Mesozoic volcanic sequences in southeastern China. They are 110-100 Ma in age. These basalts together with felsic volcanic rocks form bimodal volcanic rock suits in some volcanic basins. Initial Nd isotope ratios for these basalts range from +1.2 to -7.1 and are negatively correlated with initial Sr isotope ratios which might be affected by secondary alteration and with SiO<sub>2</sub> contents suggesting a mixing between mantle-derived parent magma and crustal materials. In addition, Nd initials are correlated with trace element parameters and the thickness of the basalt flows. Basalts from thick flows show positive epsilon Nd values with low La/Nb ratios of about 1 suggesting the dominance of the mantle-derived materials, while rocks from thin layers have more negative epsilon Nd values and high La/Nb ratios up to 3. This suggests a more significant crustal contamination for basalts from thin layers because of a large surface area. Extrapolation from known trace element and isotope relations indicates that the mantle source region for these basalts is similar to the ones of many oceanic island basalts and basalts from continental rifting areas, that is a slightly depleted mantle. The bimodal rock association also suggests an extension tectonic setting which is different from previously commonly accepted conclusion that Mesozoic volcanic rocks from southeastern China were formed in an active continental margin or arc like environment.

A SEARCH FOR  $^{107}\text{Ag}$  AND  $^{205}\text{Pb}$  IN METEORITES  
CHEN, J. H., and WASSERBURG, G. J. The Lunatic  
Asylum, Division of Geological & Planetary Sciences,  
California Institute of Technology, Pasadena, CA 91125, USA

The nuclear astrophysical processes and stellar sources responsible for short-lived nuclei in the early solar system have been the subject of considerable discussion. Of particular interest are  $^{107}\text{Pd}$  and  $^{205}\text{Pb}$  which were produced by an "s" process. We have reported the Pd-Ag data on metal, sulfide and phosphide phases in a wide variety of meteorites. There is a good correlation between  $^{107}\text{Ag}/^{109}\text{Ag}$  and  $^{108}\text{Pd}/^{109}\text{Ag}$  for metal samples from Gibeon (IVA). The sulfides lie near the origin but are disturbed. The slope of this correlation line corresponds to a  $^{107}\text{Ag}^*/^{108}\text{Pd}$  ratio of  $2.4 \times 10^{-5}$  and an initial  $^{107}\text{Ag}/^{109}\text{Ag}$  near normal silver. The  $^{107}\text{Ag}^*$  is inferred to be due to the *in situ* decay of  $^{107}\text{Pd}$  ( $t_{1/2} = 6.5 \times 10^6$  y). However, Pd-Ag data from Santa Clara (IVB) and several other IVB and "anomalous" groups irons do not lie on the isochron and require a more complex history, possibly reflecting different formation times. To date,  $^{107}\text{Ag}^*$  is present in meteorites from group II, III, IV irons, and in pallasites and mesosiderites. These results constitute strong evidence for the presence of live  $^{107}\text{Pd}$  in the early solar system and early planet formation.

Assuming  $(^{107}\text{Pd}/^{108}\text{Pd})_{\odot} = 2 \times 10^{-5}$  after dilution with the ambient ISM, Wasserburg *et al.* (1994) have estimated the isotopic abundances of s-process nuclei for an AGB star and predicted a value of  $(^{205}\text{Pb}/^{204}\text{Pb})_{\odot} = 6.5$  to  $11 \times 10^{-4}$  at the onset of solar system formation. We previously carried out Pb-Tl studies on two iron meteorites which have primordial Pb and thus have not suffered terrestrial Pb contamination. A hint of  $^{205}\text{Tl}^*$  ( $\sim 4\%$ ) was found for sulfide from an iron meteorite. It was evident that samples with higher  $(^{204}\text{Pb}/^{205}\text{Tl})/(^{204}\text{Pb}/^{205}\text{Tl})_{\odot}$  were needed to obtain unambiguous results. We have determined Pb and Tl abundances and Pb isotopic compositions in the metal and sulfide phases of seven iron meteorites: Canyon Diablo (CD), Bogou, Derrick Peak, Cape York, Trenton, Nantan, and Gibeon and two stones: Mezo-Madaras (MM) and Angra dos Reis (ADOR). The primordial  $^{204}\text{Pb}/^{205}\text{Tl}$  ratios in both metal and sulfide of iron meteorites and two stony meteorites range from 0.15 to 22. Assuming  $^{205}\text{Pb}/^{204}\text{Pb} = 5.4 \times 10^{-4}$  in the meteorite parent bodies, we have estimated the amounts of excess  $^{205}\text{Tl}$  to be from 0.1 to 12 ‰. In summary, we found a general enrichment of Pb relative to Tl in most iron meteorites, a chondrite and an achondrite, as compared to the  $(^{204}\text{Pb}/^{205}\text{Tl})_{\odot}$ . However, only a few samples may be suitable candidates for detecting  $^{205}\text{Tl}^*$  at  $> 4\%$  level. Thermodynamic condensation studies showed that Pb and Tl gas in equilibrium down to 500°K with Fe-Ni metal should have  $(^{204}\text{Pb}/^{205}\text{Tl})/(^{204}\text{Pb}/^{205}\text{Tl})_{\odot}$  enhanced by a factor of  $\sim 40$ . This suggests suitable candidates may be found for this work, but it is not evident that the fractionation found here in a chondrite and in iron meteorites can be simply related to a condensation model. Div. Contrib. 5365(839) NASA NAGW-3337.

ARGON IN THE CRYSTAL STRUCTURE OF MICA AND ITS MULTI-PULSE RELEASE *IN VACUO*: IMPLICATIONS FOR  $^{40}\text{Ar}/^{39}\text{Ar}$  GEOCHRONOLOGY

CHEN, Yanshao, Department of Geological Sciences, Queen's University, Kingston, Ontario K7L 3N6, Canada and Department of Physics, University of Toronto, 60 St. George St., Toronto, Ontario M5S 1A7, Canada, FARRAR, Edward and CLARK, Alan H., Department of Geological Sciences, Queen's University, Kingston, Ontario K7L 3N6, Canada.

An hypothesis for argon distribution in micas is presented to explain their *in vacuo* release patterns and age spectra. It is proposed that radiogenic and irradiation-derived argon is located in vacancies in interlayer and octahedral sites, corresponding to the cleavage plane and octahedral layer positions suggested by Melenevskiy *et al.* (1978). Upon heating in high vacuum, argon in the octahedral site is expelled at low temperatures ( $< 850^{\circ}\text{C}$ ), probably due to the destruction of the hydroxyl located on octahedral anion junction planes, especially those connected to vacant octahedra. However, argon located in the interlayer site vacancies is released above  $850^{\circ}\text{C}$ .

Argon release in biotite commonly shows a "two-pulse" pattern. The lower-temperature pulse ( $\sim 700^{\circ}\text{C}$ ) may be correlated with the dehydration of the vacant octahedral site but only broadly with the dehydrogenation related to the oxidation of the octahedrally-coordinated  $\text{Fe}^{+2}$ . The remaining argon is released at  $\sim 950^{\circ}\text{C}$  with complete dehydroxylation. In nearly entirely trioctahedral phlogopite, dehydroxylation begins above  $1000^{\circ}\text{C}$  and the absence of vacant octahedral sites results in only a single release pulse above  $1000^{\circ}\text{C}$ . Dehydroxylation of muscovite begins at  $\sim 700^{\circ}\text{C}$  and, because of the overlap in the release of argon from octahedral and interlayer vacancies, most muscovites yield one-pulse release patterns with maxima at  $\sim 900^{\circ}\text{C}$ , although some release argon in two closely-separated pulses, at  $\sim 800^{\circ}\text{C}$  and  $\sim 950^{\circ}\text{C}$ . The difference in temperature between the argon release pulse of phlogopite and the high-temperature pulses of biotite and muscovite suggests that the distortion in crystal structure caused by the dehydroxylation may speed up argon release from the interlayer site.

Octahedral and interlayer sites are distributed uniformly in the mica structure, and thus argon release from these sites at different temperatures offers a novel explanation for the "two-faced" spectra of both biotite (York and Lopez-Martinez, 1986) and muscovite. This model provides reasonable explanations for the diverse mica age spectra and permits the deduction of geologically meaningful information even from complex spectra. The presence of argon in two uniformly distributed sites also prompts caution in the interpretation of laser spot fusion results, owing to possible low temperature contributions from the areas adjacent to the spots.

Melenevskiy, V.N., Morozova, I.M. and Yurgina, Ye.K., 1978, The Migration of Radiogenic Argon and Biotite Dehydroxylation: *Geochem. Int.*, v. 15, p. 7-16.  
York, D. and Lopez-Martinez, M., 1986, The Two-faced Mica: *Geophys. Res. Lett.*, v. 13, p. 973-975.

**PRECISE ZIRCON GEOCHRONOLOGY ON ARCHEAN ROCKS SAMPLED BY THE WORLD'S DEEPEST CONTINENTAL BOREHOLE, SD-3 SUPERDEEP WELL, KOLA PENINSULA, RUSSIA**  
CHEN, Y. D., KROGH, T. E., Geochronology Lab, ROM, 100 Queen's Park, Toronto, Ont., Canada M5S 2C6; VETRIN, V. R. and MITROFANOV, F. P. Institute of Geology, Kola Science Center, Russian Academy of Sciences, 14 Fersman St., Apatity 184200, Russia

Low procedural blank/single zircon techniques have been used to date Archean rock samples (ranging in depth from 6.8 to 12 km) recovered by the world's deepest continental borehole, SD-3 Superdeep Well, drilled on Kola Peninsula. Zircon analyses of two tonalite samples (seven analyses for sample #42 and six for #48) from the Amphibolite-Tonalite-Plagiogranite Complex (ATPC, 11708-12066 m) define upper intercept ages of 2832  $\pm$  6/-5 Ma (#42) and 2835  $\pm$  6/-4 Ma (#48). Four analyses of three pegmatite samples (#40 from 11747-11750 m, #37 from 11570-11575 m, and #22533 from 6850 m) define an upper intercept age of 2740  $\pm$  10/-9 Ma. All tonalite and pegmatite zircon data point to a similar lower intercept of 1790  $\pm$  80 Ma as a result of thermal diffusion or new growth at this time. Four analyses from three fine-grained porphyritic granite dykes (#56 from 9665-9700 m, #54 from 9354-9370 m and #55 from 9088-9100 m) are concordant or less than 1 percent discordant and indicate emplacement during the thermal event at 1766  $\pm$  3 Ma. Eleven analyses from a biotite gneiss sample (#28 from 10837-10844 m) show a complex age pattern; ages obtained by projecting from 1766 Ma range from 2730 to 2836 Ma. New growth or resetting within this rock during the pegmatite growth is implied.

In addition to the age information, the following facts are observed: (1) analyses of the 1766 Ma granite dyke zircons are almost concordant with or without abrasion; (2) the air abrasion technique helps create more concordant data points on the primary discordia line but recent Pb loss is absent even in unabraded grains. This indicates that recent surface-related Pb loss from zircons at depth is insignificant, probably due to spontaneous annealing of radiation damage in these zircons. Investigation of this phenomenon as a function of ambient temperature is under way. A full understanding has strong implications for understanding zircon discordance mechanisms.

**SEA-LEVEL CHANGE OVER PAST SEVERAL MILLENNIUMS AROUND PENGHU ISLANDS IN THE TAIWAN STRAIT**

CHEN, Yue-Gau and LIU, Tsung-Kwei., Dept. of Geology, National Taiwan University, Taipei 107, Taiwan, ROC

Taiwan is an active mountain belt created by a collision between Luzon arc and Asian continent since 12 Ma (Teng, 1990). The region of Penghu Islands may be the only area around Taiwan, which has not yet been tectonically affected by the collision. Geologic and neotectonic evidence indicates that this region is stable for time intervals not only in a long-term (several million years) but also in a short-term (several thousand years). Therefore, it can provide important information for the local Holocene sea-level change. Due to the falling of the sea-level in the western Pacific since several thousand years ago (Kidson, 1982), the ancient shorefaces have emerged and become coastal plains in Penghu Islands. Abundant coarse-grained detrital bioclastics (i.e., shells and corals) occurring in these plains were collected to study the Holocene sea-level change. Among them, twelve carbonate samples were dated by the  $^{14}\text{C}$  method.

Our radiocarbon age data show that a progradational deposition model is applicable to Penghu region. In this model, bioclastics occurring near the shoreline angle are considered as deposits formed earlier at the highest waterstand period whereas bioclastics occurring around the outer edge should be younger products. Because in Penghu Islands most coastal plains are associated with vast reef flats, the surge energy would be hence greatly diminished and these plain surfaces should be regarded as integrated tracks of the paleo-HTL (high tide line). If the tidal range during past several thousand years can be assumed to be the same as that of the present-day, ground altitudes of the sampling localities may represent the paleo-HTL position. The paleo-HTL can be reasonably converted into its contemporaneous MTL (i.e., mean tide line) by subtracting a component of the modern tidal range. Consequently a sea-level change curve of the late Holocene in Penghu region can be constructed by a time-altitude plot.

This sea-level curve suggests that the highest sea-level in Penghu region took place from 4300 to 4500 yrBP (conventional  $^{14}\text{C}$  age) with a magnitude of about 2.3 meters above the modern sea-level. Subsequently, the sea-level fell gradually to the recent state without observable fluctuation by this approach.

Teng, L. S., 1990, Geotectonic evolution of late Cenozoic arc-continent collision in Taiwan: *Tectonophysics* 183, 57-76.

Kidson, C., 1982, Sea-level changes in the Holocene: *Quat. Sci. Rev.*, 1, 121-151.

## LEAD ISOTOPES AS INDICATOR TO CONSTRAIN THE MARINE SEDIMENTARY PROVINCE IN SOUTH CHINA SEA

CHEN YU-WEI, Guangzhou Branch, Institute of Geochemistry, Chinese Academy of Sciences, Wushan, Guangzhou 510640, P.R. China; and CHEN SHAO-MAO, South China Sea Institute of Oceanography, Chinese Academy of Sciences, Guangzhou 510301, P.R. China

Several significant features of Pb isotopic compositions of the marine sediments from South China Sea (SCS) can be observed as following:

1. Pb isotopic compositions of sediments vary spacially, reflecting the nature of the source materials. In the northern region of SCS, the sediments have lower  $^{206}\text{Pb}/^{204}\text{Pb}$  (18.6), but slightly higher  $^{207}\text{Pb}/^{204}\text{Pb}$  (15.7) and  $^{208}\text{Pb}/^{204}\text{Pb}$  (39.0) than those of recent marine sediments. Such Pb isotopic compositions are significantly different from those of sea-floor basalt in this region. The Pb isotopic compositions along the volcanic chain in the Central Nanhai Basin can be divided into two groups: (1) eastern group with Pb model ages of 100-125 Ma; and (2) western group with Pb model ages of 0-20 Ma.

2. The South region of SCS can be divided into six geographic domains, based on the  $^{207}\text{Pb}/^{204}\text{Pb}$  ratios of the sediments. Each domains are correlated with the surrounding continental materials.

3. The Pb isotopic compositions of carbonates in marine sediments vary not only spacially, but also with the depth of sea water. The  $^{206}\text{Pb}/^{207}\text{Pb}$  ratios increase with decreasing depth of sea water.

4. The  $(^{206}\text{Pb}/^{207}\text{Pb})_{\text{CO}_3} / (^{206}\text{Pb}/^{207}\text{Pb})_{\text{SiO}_3}$  of marine sediments can be used as an isotope indicators for investigating sedimentary environment, i.e., the ratios of carbonate reef, pelagic sediments, and inner shelf and relictic sediments are equal to 1, greater than 1 and less than 1, respectively.

## NEW GEOCHRONOLOGICAL CONSTRAINTS ON THE BIMODAL VOLCANISM IN THE NORTHERN MAIN ETHIOPIAN RIFT - SOUTHERN AFAR TRANSITION REGION

CHERNET T., HART W. K., Geology Dept., Miami University, Oxford, Ohio 45056. and ARONSON J. L., Department of Earth Sciences, Case Western Reserve University, Cleveland, Ohio 44106.

Thirty new K-Ar ages from the Northern Main Ethiopian Rift (NMER) - Southern Afar transition region are presented and their implications to the volcano tectonic evolution of this region are discussed in light of about one hundred fifty new major and trace element analyses. Our studies show that unlike other areas on the northwestern plateau, flood basalt volcanism in the study area initiated as early as 30Ma (Oligocene) and continued episodically until about 10Ma (Middle Miocene). At the culmination of the flood basalt volcanism initial subsidence of the NMER started around 10Ma.

Sedimentological and other lines of evidence suggest that most parts of the Afar Depression started forming earlier than the NMER (Upper Miocene). Episodic and occasionally localized flood basalt volcanism with subordinate silicic volcanism continued in the evolving Afar rift floor through the Middle Miocene and into Plio-Pleistocene. Post/syn subsidence volcanic activity in the NMER is on the contrary dominated by silicic volcanic products (Nazret Group) from centers which are now deeply covered by Quaternary volcanoclastic sediments. This Mio-Pliocene silicic volcanism is associated with subordinate fissural basaltic products more prominent in the NMER-Afar transition region than other parts of the MER. The presence of ignimbrites of Pliocene age on the northwestern and southeastern plateaus as well as in the NMER floor indicates that the NMER gradually attained its present form with the escarpments as high as 1.5km over the entire 10Ma time period. Mio-Pliocene silicic centers (5-6.5 Ma) along the southern Afar and the eastern NMER margin are proposed to have been formed in a protorift which ran parallel to the southern escarpment of the Afar on trend with the structures defining the Gulf of Aden. This was followed by the formation of the Addis Ababa rift embayment and the growth of silicic centers (3-4 Ma) of the Addis Ababa area at the point of intersection of the Gulf of Aden structure to the Yerer-Gugu transverse structure.

The evolution of the rift in the transition region is therefore characterized by a complex history of flood basalt volcanism, graben (protorift) formation, volcanoclastic and/or volcanogenic sediment deposition, dextral (transverse) crustal movements and isostatic adjustments. Since the initial subsidence of the rift started each stage of volcanic activity has been accompanied by major episodes of rift subsidence. It is probably the volcanism along the Wonji Fault Belt in the Quaternary that marked the beginning of an end to major tectonic movements along the escarpments and/or subsidence of the rift floor.

RADIOGENIC ISOTOPIC INVESTIGATIONS OF THE  
ESKAY CREEK VOLCANIC HOSTED MASSIVE  
SULPHIDE DEPOSIT, BRITISH COLUMBIA, CANADA

CHILDE, F. C., Mineral Deposit Research Unit,  
Department of Geological Sciences, University of  
British Columbia, Vancouver, B.C., V6T 1Z4, Canada.

The Eskay Creek deposit is a precious metal enriched massive sulphide deposit hosted within a sedimentary and bimodal volcanic sequence of the Jurassic Hazelton Group in the Iskut River area of northwestern British Columbia. Current mineable reserves for the deposit are 1.2 million tons grading 1.9 oz/t Au, 86 oz/t Ag, 5.6% Zn and 0.77% Cu (The Northern Miner, October 4, 1993).

Stratabound mineralization of the 21A, 21B and HW zones consists of bedded clastic sulphides and sulphosalts within an impure mudstone. The immediate footwall to stratabound mineralization and host to discordant mineralization is an intensely altered (quartz-sericite-chlorite) massive rhyolite and rhyolite breccia.

The Pumphouse, Pathfinder and 109 mineralized zones are discordant to stratigraphy and interpreted as feeder pipes to the overlying stratabound mineralization (Edmunds and Kuran, 1991). The discordant mineralization is characterized by quartz-sulphide veins within intensely altered wall rocks. Analyses of sulphide minerals from discordant and stratabound mineralization from this and previous studies (Godwin et al., 1991) show a considerable range of compositions ( $^{206}\text{Pb}/^{204}\text{Pb} = 18.779\text{--}18.899$ ;  $^{207}\text{Pb}/^{204}\text{Pb} = 15.565\text{--}15.677$ ;  $^{208}\text{Pb}/^{204}\text{Pb} = 38.264\text{--}38.598$ ) despite a very limited spatial distribution, suggesting mixing from two compositionally distinct reservoirs.

A U-Pb zircon date of  $173.6 \pm 5.6/-0.5$  Ma has been determined from an unaltered flow-banded rhyolite from the eastern limb of the Eskay Anticline, this date is consistent with paleontological data but is 5-10 Ma younger than intrusive rocks within the footwall. Trace element litho geochemistry indicates that this rhyolite is compositionally distinct from the altered rhyolite which hosts mineralization. However, field relationships suggest that the two rhyolites lie within the same stratigraphic interval (H. Marsden, pers. comm., 1993).

Work in progress includes U-Pb dating of rhyolite from the western limb of the Eskay Anticline, and of hydrothermal monazite from the 109 zone.

- Britton, J. M., Blackwell, J. D., 1990, #21 Zone Deposits, Eskay Creek, Northwestern British Columbia: Exploration in British Columbia 1989, B.C. Ministry of Energy, Mines & Petroleum Resources, p. 197-223.
- Edmunds, C., and Kuran, D., 1991, Tok-Kay and GNC 1991 Exploration Program Geological and Diamond Drilling Results: Internal Report for International Corona Corporation.
- Godwin, C. I., Pickering, A. D. R., Gabites, J. E., and Alldrick, D. J., 1991, Interpretation of Galena Lead Isotopes from the Stewart-Iskut Area (103O, P, 104A, B, G): in Geological Fieldwork 1990, Grant, B. and Newell, J. M., B.C. Ministry of Energy, Mines and Petroleum Resources, Paper 1991-1, p. 235-243.

CHLORINE-36 IN AUSTRALIAN RAINFALL AND  
PLAYAS AND THE RESIDENCE TIME OF CHLORIDE  
IN THE AUSTRALIAN LANDSCAPE

CHIVAS, A.R., KISS, E., KEYWOOD, M.D., Research School of Earth Sciences, The Australian National University, Canberra, ACT 0200, Australia;  
FIFIELD, L.K., ALLAN, G.L., Research School of Physical Sciences and Engineering, The Australian National University, Canberra ACT 0200, Australia, and DAVIE, R., BIRD, J.R., Australian Nuclear Science and Technology Organisation, Lucas Heights, NSW, Australia.

Bulk deposition for a series of 15 collectors sampled at seasonal (3-monthly) intervals over four years (September 1988-December 1992) has been analysed for  $^{36}\text{Cl}$ , and major and trace ions. Several collectors of varying construction were deployed at each site to monitor evaporation (ie. collection under paraffin oil), and to allow for analysis of  $\delta^{34}\text{S}$  and  $\delta^{11}\text{B}$ . Ten sites comprise the southeastern array that forms an arc from the eastern coast to central New South Wales to the south coast near Adelaide. The remaining 5 sites near Birdsville in central Australia sample the driest part of the continent. Minor constituents, particularly  $\text{PO}_4$ ,  $\text{NO}_3$ ,  $\text{NH}_4$ , and  $\text{SO}_4^{2-}$  are used to assess 'baseline' conditions, and reject collections with agricultural contamination (soil, fertilizer).

The east coast site (Kioloa, lat.  $35.5^\circ\text{S}$ ) shows a range of  $^{36}\text{Cl}/\text{Cl}$  ratios for individual collection periods from  $6 \times 10^{-15}$  to  $115 \times 10^{-15}$ , with an inverse relationship to total chloride content (13.5 to 1.2 mg/L); and a mean weighted fallout of 35 atoms  $^{36}\text{Cl}/\text{m}^2/\text{s}$ . Inland stations from the southeastern array ( $\sim 34^\circ\text{S}$ ) have a mean, but variable fallout of  $\sim 25$  atoms  $^{36}\text{Cl}/\text{m}^2/\text{s}$ , whereas those from central Australia ( $\sim 25^\circ\text{S}$ ) have a mean flux of  $\sim 13$  atoms  $^{36}\text{Cl}/\text{m}^2/\text{s}$ .

Modern salt lakes (playas) are abundant in the western two-thirds of the continent. Halite from these lakes has  $^{36}\text{Cl}/\text{Cl}$  ratios of  $28 \times 10^{-15}$  to  $150 \times 10^{-15}$ . The  $^{36}\text{Cl}/\text{Cl}$  values in lakes from the Lake Eyre Basin (coincident with the central rain-collector array) are low even though this is an area where bulk atmospheric deposition has  $^{36}\text{Cl}/\text{Cl}$  ratios of 150 to  $500 \times 10^{-15}$ . The majority of chloride in these salt lakes has a long residence time and ancient ultimate sources, ie. the constantly redissolving and reprecipitating salt-crust of Lake Eyre and discharge/leakage from the underlying Great Artesian Basin. By contrast, halite from modern salt lakes in Western Australia shows progressively higher  $^{36}\text{Cl}/\text{Cl}$  ratios away from coastlines that mimics (at lower ratios) the trend of modern atmospheric  $^{36}\text{Cl}$  fallout (Keywood et al., ICOG-8 abstract). This correspondence indicates that a principal source of surficial chloride in the western half of the continent is of meteoric origin with an integrated residence time in the landscape of  $\sim 1$  Ma.

DUPAL ISOTOPE SIGNATURE IN MANTLE DOMAINS OF EASTERN ASIA: IMPLICATIONS FOR DYNAMIC PROCESSES OF MANTLE CONVECTION AND LITHOSPHERE EROSION

CHUNG, Sun-Lin, Dept. of Geology, National Taiwan University, Taipei, Taiwan, ROC, and SUN, Shen-su, Australian Geological Survey Organisation, P.O. Box 378, Canberra ACT 2601, Australia

Cenozoic intraplate basalts are widespread in eastern China and adjacent areas. Numerous published data show that these rocks have incompatible element patterns and radiogenic isotope compositions similar to OIBs. Moreover, they exhibit overall higher  $^{208}\text{Pb}/^{204}\text{Pb}$  and  $^{207}\text{Pb}/^{204}\text{Pb}$  ratios than the Northern Hemisphere Reference Line (NHRL) indicative of the Dupal Pb isotope anomaly commonly observed in the southern hemisphere. Mixing of three mantle components, i.e., the depleted mantle (DMM) and two types of the enriched mantle (EM1 and EM2), can account for their geochemical signatures. It is generally agreed that the depleted mantle component corresponds to the asthenosphere whereas both the enriched mantle components are derived from the continental lithosphere (e.g., Tu et al., 1989). Because all these intraplate basalts show  $^{208}\text{Pb}/^{204}\text{Pb}$  ratios above and parallel to the NHRL, the depleted mantle source is further required to have Pb isotope characteristics resembling the Indian Ocean MORBs in the Dupal region. In this sense, Pb-Sr-Nd isotope systematics of the basalts suggest that there may be a Dupal convecting mantle domain underlying the entire eastern Asian continental margin. Isotope compositions of basalts from the South China Sea (Chung and Sun, 1992) and from the Sea of Japan (Cousens and Allan, 1992) strongly support such a suggestion. These marginal basin basalts show Dupal Pb isotope signature of MORBs from the Central and the Southeast Indian Ocean Ridges. A coherent Dupal isotope feature is also observed in MORB-type basalts from the Philippine Sea (Hickey-Vargas, 1991). It appears that the Indian Ocean geochemical province may have extended to eastern Asia, and have a boundary with the Pacific mantle convection delineated by trench systems extending from NE Japan through the Izu-Bonin to the Mariana. A northward transport of the Dupal isotope anomaly by entrainment of subduction zones has been proposed for the Philippine Sea (Hickey-Vargas, 1991). A larger scale and long lasting mantle process, such as convective influx of the asthenosphere with Indian Ocean geochemical characteristics, however, is necessary to explain the distribution of Dupal signature in the convecting mantle up to the Sea of Japan. On the other hand, paleomagnetic studies reveal that many Asian continental terranes were once parts of the disintegrated Gondwanaland. They drifted northward from the southern hemisphere and amalgamated during late Paleozoic-early Mesozoic time. Our preferred interpretation for the Dupal Pb signature of Cenozoic intraplate basalts in eastern Asia is that continental rifting and thermal erosion of the lithospheric mantle with Dupal properties have played a major role.

Chung, S.L., and Sun, S.-s., 1992, *Earth Planet. Sci. Lett.*, 109,133-145.

Cousens, B.L., and Allan, J.F., 1992, *Proc. ODP*,127/128, 805-817.

Hickey-Vargas, R., 1991, *Earth Planet. Sci. Lett.*,107,290-304.

Tu, K., Flower, M.F.J., Xie, G., Carlson, R.W., Wang, Q., and Zhang, M., 1989, *Abst. 28th IGC*, Washington, D.C.

AFC MODEL FOR SINGLE VOLCANO PLOSKIE SOPKY (KAMCHATKA)

CHURIKOVA Tatiana G., Institute of Volcanic Geology and Geochemistry, Peep av. 9, Petropavlovsk-Kamchatsky 683006 Russia, and KOSTITSYN Yu.A., Institute of Mineralogy, Geochemistry and Crystallic Chemistry of Rare Elements (IMGRE), Moscow 121357 Russia.

Ploskie Sopky is largest basaltic volcano of Kamchatka disposed within the Central-Kamchatka depression. Volcanic rocks from basalts to andesites with different alkaline (normal and subalkaline) are united in it. The volcano includes the rocks with different structures from aphyric to megaplagiophyric. It was found by radiocarbon method, that the volcano has passed through three stages of evolution, interrupted with long-term periods: 45-50 Ty – the origin of shield volcano, 30 Ty – the formation of strata volcano, 9-10 Ty – the development of superimposed zone, which embraces slag and slag-lava cones, arranged along the traverse north-eastern fault zone, and two contemporary calderas.

The Sr isotope compositions and concentrations of Rb and Sr were determined for 20 rock samples, collected from all three structural floors. They constitute the representative set, ranging from calc-alkaline basalts to subalkaline andesites, attributed to both aphyric and megaplagiophyric varieties. Furthermore, 5 plagioclase phenocrystals from megaplagiophyric rocks were analyzed. Both central and border parts of the crystals were analyzed separately.

Overall variations of  $^{87}\text{Sr}/^{86}\text{Sr}$  in the lavas are from 0.70340 to 0.70370. Basalts of shield and stratovolcano have almost constant  $^{87}\text{Sr}/^{86}\text{Sr}$  (0.70342±5) but wide range of Sr concentrations (320–574 ppm) that might reflect plagioclase fractionation from primary basaltic magma that is typical for island arc mantle.

The strata volcano and the superimposed zone rocks show a negative correlation of  $^{87}\text{Sr}/^{86}\text{Sr}$  (0.70340 – 0.70367) with Sr concentrations (421–282 ppm). These results are compatible with a model [1] of concurrent assimilation and fractional crystallization (AFC), when crystallals not fully removed from a liquid. The best fitting was achieved for mixture of 30% cumulate plagioclase with the melt. Initial melt in the model has  $[\text{Sr}]=350$  and  $^{87}\text{Sr}/^{86}\text{Sr}=0.7034$  – the average values for aphyric basalts from shield volcano and stratovolcano. The volcanic structure assumed to be developed over the metamorphic basement, so the model contaminant isotope composition (0.7070) taken out from data [2] on plagiogneisses and metamorphosed granites of Kolpakovskaya and Kamchatkaya series. The maximum quantity of the assimilated matter are 5-6%.

The assimilation process was of considerable importance in the late stage of volcano evolution, probably, due to within-crust intermediate magmatic chamber appearance, that is implied by two large calderas existence.

1. D.J.DePaolo. *Earth and Planetary Sci. Letters*. 1981. V.53. P.189-202.

2. V.I.Vinogradov, V.S.Grigoriev, V.M.Kastrykina. *Reports of Academi of Sciences*. 1991. P.58-64.

EARLY PROTEROZOIC DEVELOPMENT OF THE WESTERN PART OF THE EAST EUROPEAN CRATON  
**CLAESSON, S.**, Swedish Museum of Natural History, S-104 05 Stockholm, Sweden; **BIBIKOVA E.**, Vernadsky Institute of Geochemistry, 117 334 Moscow, Russia; **MANSFELD, J.**, Stockholm University, S-106 91 Stockholm, Sweden; **BOGDANOVA, S.**, Lund University, S-223 62 Lund, Sweden; **REINFRANK, R.**, Australian National University, Canberra ACT 2601, Australia

The Precambrian crust of the East European Craton between the Fennoscandian (Baltic) and Ukrainian Shields is covered by platform sediments, but is known from thousands of boreholes. Structurally, it is divided into a series of generally N-S trending belts of varying lithologies, characterized by alternating granulite and amphibolite facies metamorphism. Towards the southeast, it is delimited by the NE-trending Osnitsk-Mikashovich belt of igneous rocks, which has been interpreted to form the NW margin of the Ukrainian Shield (Bogdanova et al., 1993). Traditionally, most of this crust has been considered to be Archaean, but recent results (Bogdanova et al. 1993, Huhma et al. 1993, Sundblad et al. 1993) have shown that much of it is Proterozoic in age. In this contribution, we present new U-Pb zircon and reconnaissance Sm-Nd whole-rock data from the basement between the Fennoscandian and Ukrainian Shields.

A metasediment in the structurally oldest unit in eastern Lithuania has a bulk U-Pb zircon age of 2.3 Ga, similar to that of Svecofennian metasediments. An undeformed granitoid in northern Latvia has a U-Pb zircon age of  $1820 \pm 9$  Ma, suggesting that no orogenic event has affected that area after 1.8 Ga.

Single zircon crystals from a basement gneiss in NE Poland, previously considered to be  $>2$  Ga, have been analysed with the SHRIMP II ion microprobe and yielded ages between 1.4 and 2.0 Ga, interpreted to reflect the rock ages in the local crust.

A metadacite from western Belorussia has a U-Pb zircon age of  $1999 \pm 6$  Ma, while an orthogneiss has a U-Pb age of  $1903 \pm 2$  Ma. A U-Pb age of 1855 Ma for an enderbite is interpreted to give the age of granulite facies metamorphism. In the area north of the Ukrainian Shield, U-Pb data on zircons from a metapelitic granulite and a pegmatitic granite give ages of 2.1–2.0 Ga.

Various rocks from Lithuania and Belorussia analysed so far invariably yield  $\epsilon_{Nd}(1.9 \text{ Ga})$ -values between +3 and -2.

Together with recently published data, the results presented here show that most of the Precambrian basement between the Fennoscandian and Ukrainian Shields is Proterozoic, with no major Archaean component. Significant parts of the crust in the Baltic states and Belorussia are comparable to the Svecofennian crust in the Fennoscandian Shield, but the orogenic development seems to have started somewhat earlier in the SE. The granulite facies metamorphism appears to be c. 1.8 Ga old.

Bogdanova, S., Bibikova, E. and Gorbatshev, R., 1993, Paleoproterozoic U-Pb zircon ages from Belorussia: New geodynamic implications for the East European Craton. *Precambrian Research*, in press.

Huhma, H., Puura, V., Klein, V., and Mänttari, I., 1993, Nd-isotopic evidence for Paleoproterozoic crust in Estonia. *Geol. Surv. of Finl., Spec. Paper 12: 67-68.*

Sundblad, K., Mansfeld, J., Motuza, G., Ahl, M., and Claesson, S., 1993, Geology, geochemistry, and age of a Cu-Mo-bearing granite at Kabeliai, southern Lithuania. *Mineralogy and Petrology*, in press.

ISOTOPE ARRAYS AND PLUME SOURCES: THE NINETYEAST RIDGE & COMORO PLUMES  
**Class, C.** and Goldstein, S.L., Max-Planck-Institut für Chemie, D-55020 Mainz, Germany.

It is still a matter of debate whether isotope arrays of oceanic island basalts reflect heterogeneity within the rising mantle plumes, or mixing between plume and non-plume components. Recently Class et al.<sup>1</sup> argued that the isotopic evolution of the Ninetyeast Ridge hotspot track indicates a distinct composition for the plume, associated with one end of the isotope arrays formed at each point in time. Here we show that isotope arrays of the Ninetyeast Ridge and Comoro hotspots reflect mixing of plumes having singular compositions with lithospheric components.

For the Ninetyeast Ridge hotspot, trace element and isotope systematics indicate that the Heard Island isotope array reflects contamination of plume magmas with the Kerguelen Plateau lithosphere, on which the island is situated. Isotope ratios of lavas from the Kerguelen islands are consistent with this interpretation. New helium isotope data<sup>2</sup> confirm the deep mantle origin of the mixing endmember we previously identified as representing the plume<sup>1</sup>.

Grande Comore Island is a volcanic doublet. Karthala is a shield volcano consisting of alkali basalts. La Grille is smaller, covered by strombolian cones, and has erupted mainly basanites. The isotopic variation of Grande Comore indicates mixing of three components. One, almost exclusively in Karthala lavas, forms the high-Sr, high-Pb and low-Nd end of the array (K-endmember). The others are at the low-Sr end of the La Grille array (G-endmember) and at the intersection of the Karthala and La Grille arrays (X-endmember). The spatial relationships of these endmembers can be deduced from the following considerations. (1) Karthala has produced much more magma, and lavas are related by shallow level fractional crystallization in a magma chamber. La Grille eruptions are fissure controlled, with lavas reflecting variable low degrees of partial melting, precluding significant residence in a magma chamber. (2) Both G and K mix with X, but mixtures of all three components are not present, indicating they are not all part of the plume. (3) Few Karthala samples show mixing with G, therefore G is separated in space from K. Trace elements in G-rich lavas indicate a metasomatized source, probably of continental origin. (4) X and G are similar in composition, but X-rich samples show higher degrees of melting and have lower Tb/Yb ratios than G-rich samples. Therefore, X is located at a shallower level. It is added to Karthala magmas in the shallow magma chambers. Thus, K clearly represents the plume and G and X are in the lithosphere.

<sup>1</sup>C. Class et al. (1993) *Nature* 362, 715-721.

<sup>2</sup>D. Hilton et al. (1994) this abstract volume

ISOTOPIC CONTOURS OF AUTHIGENIC CLAYS IN SOILS: INSIGHTS INTO THE MINERAL-FLUID INTERACTIONS IN SOIL ENVIRONMENTS AND IMPLICATIONS OF ISOTOPIC DATING OF CONTINENTAL EROSIONAL DEBRIS

CLAUER, N., Centre de Geochimie de la Surface, C.N.R.S., 67084 Strasbourg, France, and CHAUDHURI, S., Kansas State University, Manhattan, Kansas 66502, U.S.A.

Authigenic clays in a given soil environment can be widely varied in their Sr and Ar isotopic compositions. The newly formed clays have been found to inherit from their feldspar and biotite precursors varied amounts of the radiogenic isotopes, causing very often the apparent isotopic dates to be excessively high in comparison to the age when the parent materials weathered to form the clay minerals. The variations in the content of radiogenic isotopes for the authigenic clays across a soil profile signify that the growth of individual clay particles occurs often under the influence of a small scale environment or microenvironment. The idea of a spatially limited restricted environment or a microenvironment for the growth of clay particles in soils also receives support from oxygen isotope evidence of clays in soils, as clays in soils have been found with significant variations in their oxygen isotope compositions which do not relate to the composition of local meteoric water.

Changes in the Rb-Sr systematics produced in crystalline rocks as a result of progressively increased alteration of feldspar and biotite may be described in terms of models depicting the displacement of the Sr isotopic and the Rb/Sr ratios along a curvilinear trend below the theoretical isochron line corresponding to the age of the rock. The model illustrations for the isotopic changes have supports from examples of several natural occurrences of weathered products. The models also show, by depicting that the soil clays are high in Sr isotopic ratios relative to ambient waters, why the Sr isotope ratios of runoffs are not significantly elevated due to the effects of weathering of feldspars and biotites.

$\delta^{18}\text{O}$  OF DEEP CONTINENTAL CRUST: COMPARISON OF GRANULITE XENOLITHS WITH THE MAFIC COMPLEX OF THE IVREA ZONE, ITALY

CLEMENS-KNOTT, Diane, Dept. Geol. Sci., California State University Fullerton, CA 92634 USA, TAYLOR, Hugh P., Jr., Geology 170-25, Pasadena, CA 91125 USA, and SINIGOI, Silvano, Inst. Min. Pet., Univ. Trieste, Italy.

The Ivrea Zone is arguably the best exposed cross section through deep continental crust on Earth. The Mafic Complex, a thick intrusive series emplaced into a granulite- and amphibolite-facies volcanosedimentary section, can be divided into the ultramafic-mafic Basal, Intermediate and Upper Zones (BZ, IZ, UZ), overlain by the Main Gabbro (MG), in turn overlain by normal and roof "Diorites" and charnockites. The Mafic Complex serves as a geochemical reference for *in situ* deep crust, because the values of  $\delta^{18}\text{O}$  and Mg number ( $\text{Mg}^\#$ ) are similar to those of nonmetasedimentary granulite xenoliths collected worldwide. Possible petrogeneses of granulite xenoliths are revealed by classifying Mafic Complex samples by  $\text{Mg}^\#$  and  $\text{SiO}_2$  according to the xenolith classification scheme of Kempton and Harmon (1992; groups M1, M2, M3, "intermediate", "silicic"). M1 rocks ( $\text{Mg}^\# > 0.7$ ) of the Mafic Complex are found only in the BZ and IZ ( $\delta^{18}\text{O} = 6.3$  to  $8.7$ ;  $n=16$ ), which are interpreted as being formed from initial intrusions of mantle-derived magma into relatively cool (subsolidus) crust. The M2 group contains samples from all units of the Mafic Complex except the charnockites. Most UZ, MG, and normal "Diorite" samples plot in the M3 field. These units are believed to have formed within a thermally-buffered magma chamber undergoing RTF and AFC processes. Subsequent modification of the UZ and normal "Diorite" cumulates resulted from the upward percolation and intercumulus crystallization of (1) charnockitic melt derived from a metapelitic septum at the UZ-IZ boundary, and (2) fractionated and contaminated magma concentrated in the late-stage, MG chamber. Five roof "Diorite" samples ( $\delta^{18}\text{O} = 8.9$  to  $10.6$ ) that contain melt derived from amphibolite-facies paragneiss overlap a high- $^{18}\text{O}$  subset of the "intermediate" xenolith class ( $\delta^{18}\text{O} = 8.9$  to  $12.5$ ). Absent from the Mafic Complex are "intermediate" rocks with  $\delta^{18}\text{O} < 8.4$ . Mafic Complex rocks of the "silicic" class are represented by 7 charnockites ( $\delta^{18}\text{O} = 9.6$  to  $11.2$ ) formed in part from melts of granulite-facies paragneiss. Thus, essentially all types of granulite xenoliths have counterparts in the Ivrea Zone. This correlation implies that many deep-crustal xenoliths could be generated during "Mafic Complex-type" events, and that generation of high- $^{18}\text{O}$  mafic xenoliths does not necessarily require metasomatic reequilibration with mantle-derived fluids.

Based on the observed covariation of  $\delta^{18}\text{O}$ ,  $\text{SiO}_2$  and ( $^{87}\text{Sr}/^{86}\text{Sr}$ )<sub>i</sub> there appear to be petrogenetic similarities between Ivrea Zone lithologies and approximately coeval, mid- to upper-crustal gabbroids and granitoids found in the neighboring Strona-Ceneri Zone and in the Massif Central of France. The Mafic Complex thus may be interpreted as a snapshot of magmatism in the lower European crust during Permian crustal growth events manifest at all crustal levels. The generation of high- $^{18}\text{O}$  lithologies in the Ivrea Zone very likely took place during synmagmatic extension of the deep continental crust, and did not require a high- $^{18}\text{O}$  mantle source.

Kempton, P.D., and Harmon, R.S., 1992, Oxygen Isotope Evidence for Large-Scale Hybridization of the Lower Crust During Magmatic Underplating: GCA, v. 56, p. 971-986.

ION PROBE PARAMETERS FOR VERY HIGH RESOLUTION WITHOUT LOSS OF SENSITIVITY  
CLEMENT, S.W.J. and COMPSTON, W. Australian National University, Canberra, A.C.T. 0200

The original SHRIMP ion probe at ANU uses a secondary mass-analyser corrected for aberrations to second order (Matsuda, 1974). A new generation of designs is now possible in which a large ratio of mass-dispersion / image magnification, combined with aberration correction to third order, permits the achievement of much higher mass resolution without loss of sensitivity (Matsuda, 1990).

The main features of this new family of designs are a 'reverse geometry' layout, i.e. the ions pass through the magnetic analyser before reaching the electrostatic analyser, and the addition of several more electrostatic quadrupole lenses. For an ion probe the same size as SHRIMP I or II, such a design will achieve mass resolution greater than 20000 with flat-topped peaks for the same sensitivity as SHRIMP II operating at resolution 5500.

An ion probe with this capability will open a new range of applications that are not presently practical because of hydrides and other isobars which cannot be separated on existing instruments without unacceptable loss of sensitivity. Examples are Ca isotope dimers such as  $^{44}\text{Ca}^{43}\text{Ca}$  on  $^{87}\text{Sr}$  ( $m/\Delta m$  16000) which discourage serious  $^{87}\text{Sr}/^{86}\text{Sr}$  studies in Ca rich minerals;  $^{206}\text{Pb}^1\text{H}$  on  $^{207}\text{Pb}$  ( $m/\Delta m$  29000) in hydrous minerals such as pitchblende, and separation of  $^{58}\text{Ni}$  and  $^{58}\text{Fe}$  ( $m/\Delta m$  29000) for studies of meteoritic isotope anomalies in the Fe-group of elements.

In addition, such an instrument could be operated with a very wide source slit for other applications such as stable isotope analysis, which do not demand high mass resolution but are especially susceptible to variable mass discrimination. Use of very wide slits and apertures will reduce beam truncation during the transfer of ions from the analysed spot into the mass analyser, leaving the sputtering process itself as the main remaining source for variable discrimination.

The prototype for such an instrument, named SHRIMP 7000, is now under development at the ANU.

Matsuda, H., 1974, Double Focussing Mass Spectrometers of Second Order: *Int. J. Mass Spect. Ion Phys.*, 14, 219-233  
Matsuda, H., 1990, *Nucl. Inst. and Meth. in Phys. Res.*, A298, 199-204.

Rb-Sr DATING OF WHITE MICA - NEW POTENTIAL IN METAMORPHIC GEOCHRONOLOGY.

Cliff, R.A., Department of Earth Sciences, University of Leeds, LEEDS, LS2 9JT, UK

Despite being one of the oldest methods in geochronology and having a  $T_c \geq 500^\circ\text{C}$ , Rb-Sr dating of white micas has been little used in recent studies of young metamorphic belts. At least in part this stems from unsatisfactory experiences in earlier studies in the Alps. These showed that the relatively low Rb/Sr ratios of most metamorphic white micas yielded rather poor precision with the mass spectrometric techniques then available and, moreover, demonstrated major problems in defining initial isotopic compositions in many samples.

Modern techniques result in analytical errors significantly less than 1Ma for white micas in the 10-50 Ma age range and because of the relatively high Sr concentration in many white micas it is possible to analyse sub-milligram samples. Using a 21Ma white mica previously dated with 100mg samples, reproducibility better than 1Ma has been demonstrated on 0.1mg samples.

The initial ratio problems were accentuated by concentration on the analysis of micas from basement gneisses. Recent results from the Tauern Window in the Austrian Alps show that, despite lower Rb/Sr ratios, better results can be obtained from metasediments and in favourable cases from intensely deformed/recrystallised basement rocks. In the Central Tauern, Inger & Cliff (1993) find white mica ages are reproducible to 1 Ma in once-metamorphosed metasediments over a 6 km area. Reddy *et al.* (in press) find a factor of 5 less scatter in white mica ages from intensely mylonitised gneisses than in other gneisses from the Sonnblickkern.

The petrological study of Dempster (1992) shows preservation of major element growth zoning in white micas, confirming the potential to preserve aspects of prograde history. If white mica and a low Rb/Sr phase could be extracted from known microstructural settings then this prograde history could be dated. Techniques have been developed to extract microsamples from sub-millimetre domains under the petrological microscope using 100 $\mu\text{m}$  thick sections. Sr concentrations in typical phengitic white micas are sufficiently high for such samples to be analysed isotopically. Results of such analyses on 30Ma metasediments and gneisses from the Tauern Window will be presented.

Dempster, T.J., 1992

Zoning and recrystallisation of phengitic micas: implications for metamorphic equilibration. *Contributions to Mineralogy and Petrology* 109, 526-537.

Inger, S. & Cliff, R.A. 1993

More precise dating of tectonometamorphic evolution in the Eastern Alps; Rb-Sr white mica and U-Pb sphene and allanite ages from the Tauern Window. *Terra Nova* 5 Abstracts Suppl.1, 388.

Reddy, S.M., Cliff, R.A. & East, R. in press

The thermal history of the Sonnblick Dome, SE Tauern Window, Austria: Implications for heterogeneous uplift within the Pennine basement. *Geologische Rundschau*

**ISOTOPIC ANALYSIS OF BOTH  $\delta^{18}\text{O}$  AND  $\delta^{17}\text{O}$  IN ATMOSPHERIC NITROUS OXIDE. NEW INSIGHTS FROM AN OBSERVED MASS INDEPENDENT ANOMALY**

CLIFF, S.S., and THIEMENS, M.H., Dept. of Chemistry, University of California, San Diego, La Jolla, CA 92093-0356, U.S.A.

Nitrous oxide is an important trace species in the earth's atmosphere due to its role in stratospheric ozone depletion, and its contribution to global greenhouse warming. The global  $\text{N}_2\text{O}$  budget remains poorly defined due to a lack of source identification, presumably anthropogenic. Resolution of all significant sources is critical because of its role in the atmosphere coupled with a long (150 year) atmospheric lifetime. A system has been developed for the collection and analysis of air  $\text{N}_2\text{O}$  which allows measurement of three oxygen isotopes. The use of stable isotope ratio measurements is established as a method for obtaining budgetary and transformation mechanism information. Stable isotope ratio ( $^{18}\text{O}/^{16}\text{O}$ ,  $^{17}\text{O}/^{16}\text{O}$ ) measurements of tropospheric  $\text{N}_2\text{O}$  have been performed in order to better constrain its budget. Tropospheric  $\text{N}_2\text{O}$  shows a clear mass independent isotopic signature ranging from 0 to +1.3‰. The  $\delta^{18}\text{O}$  in air  $\text{N}_2\text{O}$  ranges from ca. 38 to 43‰ (SMOW), showing isotopic variability between collections.

Stratospheric  $\text{N}_2\text{O}$  samples have been collected and analyzed from the southern hemisphere. From the data a correlation between mass independent magnitude and an index of altitude is observed. It has been shown that reaction with electronically excited atomic oxygen produces a small (ca. 6‰) strictly mass dependent fractionation. Nitrous oxide photolysis produces no observable fractionation (<0.1‰). Based upon the laboratory experiments and field observations, a stratospheric source or sink of  $\text{N}_2\text{O}$  exists that has yet to be identified. The observation of a yet undefined stratospheric  $\text{N}_2\text{O}$  process could not have been detected from single isotope ratio or concentration measurements. It is the mass independent character which provides this specific insight.

**SHORT TERM VARIATIONS IN THORIUM AND URANIUM-SERIES ISOTOPES IN MAUNA LOA**

COHEN, A. S., O'NIONS, R. K., (Dept of Earth Sciences, University of Cambridge, Downing Street, CB2 3EQ, UK), KURZ, M. D. (WHOI, Woods Hole, MA 02543, USA)

During the shield-building phase of Hawaiian volcanoes, the major element composition of erupted lavas is relatively uniform (having allowed for olivine fractionation). However, significant variations do exist in the isotopic compositions and trace element ratios of material from different volcanoes. More recently, it has been shown that short term (1-10 ka) variations in He, Pb, Sr and Th isotope compositions and in Th/U ratios are present within a suite of tholeiitic lavas collected from a single shield volcano, Mauna Loa (Kurz and Kammer 1991; Cohen et al. 1993). A minimum of two distinct sources is required to explain these observations. The crucial question is whether the range in composition of erupted lavas results from melt/matrix interaction during extraction and transport, from the mixing of more than two distinct sources, or from both.

Precise determination of disequilibrium within the  $^{226}\text{Ra}$ - $^{230}\text{Th}$ - $^{238}\text{U}$  decay series forms a useful approach to this problem. ( $^{230}\text{Th}/^{238}\text{U}$ ) ratios (measured by TIMS) in samples of young lavas from both Kilauea and Mauna Loa are frequently close to unity, and Th/U ratios have a mean value of 2.96 ( $\pm 0.03$ ). Interpretation of these results using a dynamic melting model constrains the rate of melting, which must be at least an order of magnitude greater than for MORB. In contrast, the Th/U ratios of samples from Mauna Loa which are older than 8 ka are around 10% larger than the Th/U ratios of samples less than 2 ka in age (ages determined by  $^{14}\text{C}$  dating). The ( $^{230}\text{Th}/^{238}\text{U}$ ) ratios of those samples which are either older than 28 ka, or younger than 2 ka, are also close to unity. However,  $^{230}\text{Th}$  and  $^{238}\text{U}$  are not close to secular equilibrium in some samples in the age range 2-28 ka, as these are found to possess small  $^{230}\text{Th}$  excesses of up to 10%. This observation indicates that there has been a transient departure from radioactive equilibrium in the erupted liquids. Furthermore, the data presently available show that the change in Th isotope composition occurred at constant Th/U ratio, and that this change preceeded the 10% decrease in Th/U ratio which took place between 8 ka and 2 ka ago. It is very difficult to produce these transient disequilibria by mixing multiple sources. It is also unlikely that there has been any appreciable disturbance to the U series nuclides in the lavas after their eruption, because the measured ( $^{234}\text{U}/^{238}\text{U}$ ) ratios in all the samples are very close to unity. A more plausible explanation of these observations is that they reflect the consequences of the interaction of melt and matrix during melt extraction and transport.

Kurz M.D. and Kammer D.P., *EPSL* 103 (1991), 257-269.  
Cohen A.S., O'Nions R.K., Kurz M.D., *EOS* 74 (1993), 629.

CHLORINE STABLE ISOTOPES AS A TRACER OF WATERS EXPELLED FROM MUD-ROCKS

COLEMAN, Max. L., BP Exploration, Sunbury-on-Thames, TW16 7LN UK & Postgraduate Research Inst. for Sedimentology, Reading Univ., RG6 2AB, UK and EGGENKAMP, Hans, G.M., Geochemistry Dept., Utrecht Univ., 3508 TA Utrecht, The Netherlands. and CURTIS, Chas, D., Geology Dept., Manchester Univ., Manchester M13 9PL, UK

Formation waters produced from Forties Field (U.K.C.S.) appear to be a range of mixtures consisting of a typical North Sea saline formation water and a much more dilute brine from a mudrock source.

Samples are uncontaminated, cover the full geographical extent of the field and were taken over a five year period. Analyses of  $\delta^{37}\text{Cl}$ ,  $\delta^2\text{H}$ ,  $\delta$ ,  $^{87}\text{Sr}$ , Na, K, Mg, Ca, Sr, Ba, Cl, Br and  $\text{SO}_4$  were made. There are linear correlations of all chemical components (except Ba and  $\text{SO}_4$ ) which is the same for between-well and within-well variations. These data imply that all produced waters are the result of mixing on a field-wide scale of two NaCl brines, the end member compositions are less than 26,000 ppm Cl and about 60,000 ppm Cl.  $\delta^2\text{H}$ ,  $\delta^{18}\text{O}$  give a line of negative slope, unlike most other formation water plots, thereby confirming that the waters are mixtures rather than products of evolution by water-rock interaction. The stable isotope values prove that there is no sea-water contamination in the samples.  $\delta^{37}\text{Cl}$  plots linearly against Cl concentration, which is surprising and implies a complex batch mixing process; diffusion cannot explain the data distribution. There is vertical zonation of salinity of oil zone waters, which increase in salinity from the top of the reservoir down to the oil water contact. This pattern extends over the whole oilfield. Thus, there is a range of fossil formation waters trapped by oil emplacement, forming mixtures with a water which approximates to the aquifer beneath the oil-water contact.

$\delta^{37}\text{Cl}$  values also show that the more saline brine resulted from dissolution of evaporite salts and that the more dilute one contains salts affected by a physical process (diffusion or ion filtration). The most likely origin for such a water is a shale, probably the source rock for the oil, since the over-lying seal to the reservoir would not have given the observed spatial distribution of compositions. The hypothesis which best explains all these observations is that less saline brine (warmer and thus lower-density fluid than the pre-existing saline formation water) "migrated" from the shale associated with oil migration. However, preliminary  $\delta^{37}\text{Cl}$  data from shales confound this idea. We hope they are anomalous.

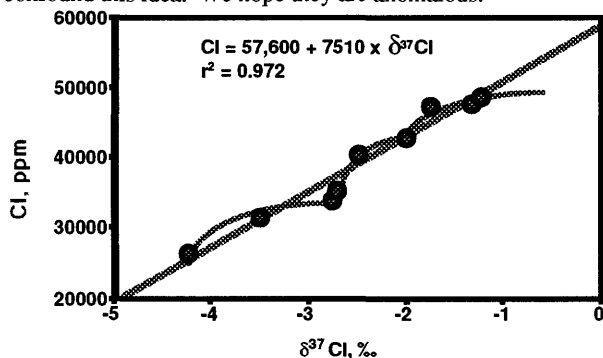


Fig.1. (Pseudo?) linear correlation of  $\delta^{37}\text{Cl}$  and Cl concentration, implying a complex mixing process

Nd AND Pb ISOTOPES OF ALLEGHANIAN GRANITES FROM THE GOOCHLAND TERRANE, SOUTHERN APPALACHIANS: EVIDENCE FOR A JUVENILE SOURCE COMPONENT.

COLER, David G., SAMSON, Scott, Dept. of Earth Sciences, Syracuse University, Syracuse, NY 13244-1070 and SPEER J. A., Dept. of MEAS, North Carolina State University, Raleigh, NC, 27695-8208

The Goochland terrane of Virginia and North Carolina has been considered to be the easternmost piece of Grenville crust in the Southern Appalachians. This terrane and its southern extension, the Raleigh Belt, were intruded by numerous granitic magmas during the Alleghanian Orogeny (327-265 Ma). The resulting plutons are dominantly metaluminous biotite- granites with major element compositions of  $\text{SiO}_2$  (69.0-76.6%),  $\text{Al}_2\text{O}_3$  (14.3-16.1%),  $\text{CaO}$  (0.62-1.8%),  $\text{Na}_2\text{O}$  (3.3-4.6%),  $\text{K}_2\text{O}$  (3.8-5.3%), although some volumetrically minor peraluminous bodies also occur. These compositions are most similar to plutons intruded in a continental collisional to post-collisional tectonic regime.

Detailed Nd isotopic studies of these plutons were undertaken because they serve as excellent probes of the lower crust in the Goochland terrane. The plutons analyzed include the Rolesville Batholith, the Wise, Wilton, Louisburg and the Archer's Lodge plutons and yield initial  $\epsilon_{\text{Nd}}$  values between +3.0 and -1.9, with associated  $T_{\text{DM}}$  ages between 600-950Ma. These values clearly indicate the bulk of the source material is juvenile and could not contain a large percentage of recycled Grenville crust. The Wyatt pluton, however, has  $\epsilon_{\text{Nd}}$  values of -2.6 and -4.4 and therefore could include a larger component of recycled Grenville crust. Overall, however, the Goochland terrane cannot be entirely composed of Grenville crust, or the plutons were formed from a different crustal source located below the Goochland terrane.

The least radiogenic leaches of K-feldspars from the Wise, the Archer's lodge and the Rolesville batholith yield uniform initial common lead ratios of  $^{206}\text{Pb}/^{204}\text{Pb} = 18.36-18.44$ ,  $^{207}\text{Pb}/^{204}\text{Pb} = 15.53-15.58$  and  $^{208}\text{Pb}/^{204}\text{Pb} = 38.02-38.09$ . These data are similar to those reported from other Alleghanian granites, but are slightly less radiogenic. This agrees with the higher  $\epsilon_{\text{Nd}}$  of the Goochland terrane granites compared to most other Alleghanian granites in the southern Appalachians. Melting of crust like that in the Carolina terrane, a late Proterozoic-Cambrian volcanic terrane that lies to the west of the Goochland terrane, could produce the range in Nd isotopic composition observed in the Alleghanian granites. Thus we infer that crust like that of the Carolina terrane must structurally underlie the Goochland terrane. The generally high  $^{143}\text{Nd}/^{144}\text{Nd}$  ratios of the Alleghanian granites in the Goochland terrane indicate that the contribution of Grenville, or older, crust must be quite limited.

U-Pb AGE CONSTRAINTS ON EARLY PROTEROZOIC GOLD DEPOSITS, PINE CREEK INLIER, NORTHERN AUSTRALIA, BY HYDROTHERMAL ZIRCON, XENOTIME AND MONAZITE. COMPSTON, David M., and MATTHAI, S. K., Research School of Earth Sciences, Australian National University, Canberra, A.C.T., 0200, Australia.

Recent ion-microprobe U-Pb age determinations on hydrothermal minerals extracted from a gold-bearing quartz vein from the Goodall mine in the Early Proterozoic Pine Creek Inlier, northern Australia, identify two occurrences of hydrothermal activity in the area.

At the Goodall deposit, gold mineralisation occurs in a wide halo of potassic alteration (K-spar+biot+and+cord+qtz) which hosts quartz stockworks and bedding-concordant veins, formed at 550 - 620°C and 200 MPa. In general, gold deposits in the region are concentrated within the inner contact aureole of the 1820 - 1835 Ma Cullen Batholith (Stuart-Smith et al, 1993), which is considered to be a potential source of the mineralising fluids. The Goodall deposit is hosted by greywackes and metasilstones (with local carbonaceous intercalations) of the Burrell Creek and Mount Bonnie Formations which have a maximum  $^{207}\text{Pb}/^{206}\text{Pb}$  age of  $1885 \pm 2$  Ma, obtained from the underlying Gerowie Tuff (Needham et al, 1988). Mineralised veins elsewhere in the region contain pronounced Zr anomalies (to 2000 ppm), suggesting the precipitation of zircon during vein formation.

Zircon, xenotime and monazite were extracted from a mineralised quartz-sulphide vein (20 - 40 ppm Au) and isotopically analysed by ion-microprobe. The  $^{207}\text{Pb}/^{206}\text{Pb}$  age distribution of the analysed zircons results from the presence of several distinct populations, the ages of which suggest that the majority of zircons are mechanically incorporated into the vein from the host environment. Minor populations, with  $^{207}\text{Pb}/^{206}\text{Pb}$  ages of ca 2.50, 1.95 and 1.90 Ga, probably represent minor detrital populations within the sediment. The largest group has a mean age  $1863 \pm 7$  Ma, which is interpreted as the maximum depositional age. About 30% of the analyses have a younger mean  $^{207}\text{Pb}/^{206}\text{Pb}$  age of  $1817 \pm 16$  Ma, within error of the age of the Cullen Batholith. Although there are no chemical distinctions between these populations, the younger analyses were mostly of grain rims.

This age of vein formation is supported by preliminary  $^{207}\text{Pb}/^{206}\text{Pb}$  ages of xenotime and monazite, which, although with excess scatter, have a mean age of  $1810 \pm 10$  Ma.

In addition, a small number of analyses are much younger, with a slightly discordant mean  $^{206}\text{Pb}/^{238}\text{U}$  age of  $536 \pm 38$  Ma. This unexpected result does not represent sample contamination. The age and higher U contents of these grains suggests that they represent new zircon growth. Some of the older zircons appear to have lost some Pb at this time, as their isotopic composition lies on a discordia trajectory between 2.5 Ga and 0.5 Ga. The geological significance of these data is not yet fully understood, but, at the least, they are recording the occurrence of previously unknown fluid activity in the basement of a Cambrian basin.

Needham, R. S., Stuart-Smith, P. G. and Page, R. W., 1988, Tectonic evolution of the Pine Creek Inlier, Northern Territory: *Precambrian Res.*, v40/41, p. 543-564

Stuart-Smith, P. G., Needham, R. S., Page, R. W., and Wyborn, L. A. I, 1993, *Geology and Mineral Deposits of the Cullen Mineral Field, Northern Territory, Northern Territory: AGSO Bulletin 229*, pp 145

TIME POINTS WITHIN THE VENDIAN BY ION PROBE COMPSTON, W. Australian National University, Canberra. A.C.T. 0200 and JENKINS, R.J.F. Dept Geology, University of Adelaide, South Australia, 5001

Few Vendian and Cambrian ages are based on volcanogenic sediments within sections where key fossils indicate useful biostratigraphic constraints. We report two new U-Pb zircon ion-probe ages for tuffs associated with occurrences of the 'Ediacara assemblage' at Mistaken Point on the Avalon Peninsula, SE Newfoundland, and at Mogilev-Podolsky in the Ukraine. We also describe a new assessment procedure for ion probe  $^{206}\text{Pb}/^{238}\text{U}$  ages based on mixture-modelling, both for age variation within the SL13 standard zircon, as well as for multiple detrital age populations.

Ages for euhedral zircons from the Mistaken Point tuff can be resolved into three age groups in about equal proportions:  $607 \pm 4$  Ma ( $2\sigma$ ),  $591 \pm 5$  Ma and  $571 \pm 4$  Ma. The last is the most plausible for the tuff eruption and is close to a much-cited isotope dilution age by G. Dunning. It allows ca. 15 Ma for the accumulation of the 4.2 km thick pile of the Conception Group, and implies a rate of sedimentation of ca. 290 m / Ma. If the same (maximal) rate persisted in the Avalonian Orogen, the age of the upper exposed part of the Signal Hill Group would be 544-540 Ma. The two older groups are consistent with known ages in volcanogenic complexes that underlie the Conception Group. The Mistaken Point soft-bodied megafossil assemblage represents a biota not known elsewhere. However, elements with a wider distribution, *Charnia masoni* and *Charniodiscus concentricus* first appear in the fossil record near the top of the Mistaken Point Formation, so that the 571 Ma age applies closely to this important first occurrence.

Four age groups are found in the Ukrainian tuff: a minor detrital / xenocryst group at 560 Ma, the biggest group (46%) at  $541 \pm 4$  Ma inferred to represent the likely eruption age of the tuff, the zircons of which include a large proportion of finely acicular crystals, and a further large (35%) group  $530 \pm 4.0$  Ma and a small group at 512 Ma, together suggested to reflect Pb loss after deposition. The 530 Ma age is indistinguishable from present estimates of the base of the Cambrian. Interpretation of the 541 Ma age as the tuff deposition requires explanation of the 530 and 512 Ma groups undergoing Pb leaching, possibly through circulation of ground-waters during terminal Proterozoic and Cambrian exposure of the still presently unconsolidated sediments.

A tuff high in the Slawatyce Fmn on the East European Platform, SE Poland, has given a SHRIMP U-Pb zircon age  $551 \pm 4$  Ma. Elsewhere the Slawatyce Fmn grades upwards into a shale-siltstone-sandstone sequence transitional from the Neoproterozoic (*Vendotaenia* and *Sabellites* Zones) into the Early Cambrian. The Slawatyce Fmn itself is believed equivalent to the Volhyn Series which underlies the early Valdaian or Redkino Horizon through a large area of the adjacent Moscow Syncline. The 551 Ma age therefore relates to the close of the Early Vendian.

Regardless of which interpretation is used for the Ukrainian zircon age groups, the age difference between 571 Ma from the Avalonian Orogen and either 530 Ma or 541 Ma for the Vendian of the Ukraine, the fossil record of soft-bodied late Precambrian 'metazoans' spans a time interval of at least 30 Ma, or virtually the same duration as the whole of the Cambrian itself.

## THE USE OF DEUTERIUM-ENRICHED WATER AS A TRACER FOR HYDROLOGIC TESTS.

CONRAD, M.E., KARASAKI, K., and FREIFELD, B., Earth Sciences Division, Lawrence Berkeley Laboratory, Berkeley, CA 94720.

D<sub>2</sub>O is a relatively inexpensive, non-polluting tracer that may present an alternative to other tracers in environmentally-sensitive areas. To test the viability of water artificially enriched in deuterium as a tracer for hydrologic tests, D<sub>2</sub>O was used in a tracer test at the Raymond Field Site (a site dedicated to the characterization of ground-water flow in fractured rock). Along with deuterium, four other "conservative" tracers (fluorescein, bromide, fluoride and micro-spheres) were also used.

The Raymond Field Site is located in the Sierra Nevada foothills of California, approximately 100 km north of the city of Fresno. It consists of a series of nine 90m-deep boreholes drilled into an equigranular, non-foliated granodiorite. The boreholes are arranged in V-shaped pattern at increasing distances of 7.5, 15, 30, and 60m from the central hole. Hydrologic and geophysical tests have demonstrated that most of the flow between the wells is confined to two fracture zones.

For a radial convergent tracer test, the upper of the two fracture zones was isolated using pneumatic packers. Before the tracer test, water was pumped from the packed interval in the central well at a constant rate of 11 liters/min for several days in order to establish a steady flow field. Solutions containing the tracers were injected into the packed interval in one of the boreholes at 30m from the central well.

Increased  $\delta D$  values were measured in samples collected from the central (pumping) well 10 hours after injection. The arrival times for fluorescein and bromide were identical to that of deuterium. No micro-spheres were detected and the fluoride concentration was too low to give meaningful results. Breakthrough curves for fluorescein, bromide and deuterium have the same form, but level off at C/Co values of 0.0006, 0.0004 and 0.00035, respectively. Fluorescein has been reported elsewhere to react with certain minerals causing it to fluoresce more, resulting in an apparent increase in mass. The difference between deuterium and bromide is small, but significant (corresponding to a difference in  $\delta D$  of about 3‰). The reasons for this difference are not clear at this time.

## MANTLE METASOMATISM VERSUS CRUSTAL CONTAMINATION IN THE GENESIS OF K-RICH MAGMAS: Sr & Nd ISOTOPES OF PRIMITIVE ULTRAPOTASSIC AND POTASSIC ROCKS FROM THE ITALIAN PENINSULA

S. CONTICELLI, Dip. Sci. Terra, Firenze, Italy, L. CIVETTA and M. D'ANTONIO, Dip. Geofisica & Vulcanologia, Napoli, Italy, A. PECCERILLO, Ist. Sci. Terra, Messina, Italy.

The Tyrrhenian border of the Italian peninsula has been the site of an intense magmatism from Pliocene to recent times. Although Calc-Alkaline, Potassic and Ultrapotassic volcanisms overlap in space and time, a decreasing of alkaline character with time and southward is observed. Alkaline ultrapotassic and potassic volcanic rocks are characterized by a variable enrichment in K and incompatible elements, but with consistently uniform high LILE/HFSE values, similar to those of calc-alkaline volcanic rocks.

Initial  $^{87}\text{Sr}/^{86}\text{Sr}$  and  $^{143}\text{Nd}/^{144}\text{Nd}$  values for ultrapotassic and potassic rocks range from 0.70506 to 0.71649 and from 0.51272 to 0.51202 respectively. The general  $\epsilon_{\text{Sr}}$  vs.  $\epsilon_{\text{Nd}}$  array along with correlations among initial isotopic values and incompatible trace elements abundance, clearly indicate that a crustal component has played an important role in the genesis of these magmas. The further question as to where this crustal component has been acquired by magmas. Volcanological and petrological data indicates crustal contamination to be a leading process along with fractional crystallization and magma mixing during magmatic evolution (e.g. *Francalanci et al., 1989; Civetta et al. 1991; Conticelli et al., 1991; D'Antonio & Di Girolamo, 1994*).

Taking into account only selected samples believed to represent "primary" magmas in equilibrium with mineralogy of their mantle source a clearer picture is displayed. A large variation of  $\epsilon_{\text{Sr}}$  vs.  $\epsilon_{\text{Nd}}$  is still observed, with a general array running from  $\epsilon_{\text{Sr}} = -20$ ,  $\epsilon_{\text{Nd}} = +5$  to  $\epsilon_{\text{Sr}} = +180$ ,  $\epsilon_{\text{Nd}} = -12$ . A bifurcation of this array is observed in the samples plotting in the lower right quadrant. In this light samples from the Northernmost part of the peninsula point to an upper crustal end-member, whereas samples from the Central sector of the peninsula point to  $\epsilon_{\text{Sr}}$  and  $\epsilon_{\text{Nd}}$  values similar to those of Miocene carbonatic sediments. Major and incompatible trace elements have consistently a behaviour similar to that of isotopes.

In this light we may envisage that the source of magmas contain at least two different geochemical crustal components mixed with a double mantle component as well. One crustal component might be generated by melting of silicatic upper crustal rocks or sediments from an ancient subducted slab. The second one might be represented mostly by CO<sub>2</sub> rich fluid released more recently by carbonate sedimentary rocks incipiently subducted.

Consistently with the increase of alkaline degree Northward, an increase of the amount of the upper crustal components in the inferred mantle source is observed. This may be due to the occurrence of a lower degree of partial melting in a heterogeneous mantle. Metasomatism in the mantle may have resulted in the formation of intense veins pattern cutting the mantle country rock. This physical heterogeneity and diverse degree of partial melting of the peridotitic country rocks may have generated the trends of mixing observed.

*Civetta L, Carluccio E, Innocenti F, Sbrana A & Taddeucci G (1991). Europ.J.Mineral., 2:415-428.*

*Conticelli S, Francalanci L & Santo AP (1991). J. Volcan. Geoth.Res., 46: 187-212.*

*Francalanci L, Manetti P & Peccerillo A (1989). Bull Volcanol., 51: 355-378*

*D'Antonio A & Di Girolamo P (1994). Acta Vocanol. In the press.*

## ON PLATEAUS

COPELAND, Peter, Dept. of Geosciences, Univ. of Houston, Houston, Texas 77204-5503, U.S.A. (copeland@uh.edu), and SPELL, Terry, Res. School of Earth Sciences, Australian National University, Canberra, ACT 0200, Australia (t1s150@cscgpo.anu.edu.au)

The concept of the  $^{40}\text{Ar}/^{39}\text{Ar}$  age plateau has been a common approach in reporting the results of  $^{40}\text{Ar}/^{39}\text{Ar}$  analysis. We believe, however, that the use of "plateau analysis" has disadvantages which promote either over- or underinterpretation of data. The first problem with  $^{40}\text{Ar}/^{39}\text{Ar}$  age plateaus is that any definition of a plateau is always subjective. There are many definitions of "plateaus" in the literature but it is not clear if one is better than any other. All of these *have been made up* in order to describe the age spectrum with a single number. What makes this worse is that even if a single plateau definition could be shown to be superior, the manner in which the sample is heated can have a significant effect on the value that is calculated for the plateau or even whether or not a plateau is defined. Thus, although experience can be a guide in the choice of heating schedule, this choice still introduces another element of subjectivity. A third choice that must be made is how to calculate the single number and associated uncertainty which represents the steps on the plateau; most workers chose either to weight by the amount of gas present or by the precision in the age of each step. To illustrate the variability introduced by these obstacles we have run five splits of a K-feldspar from a granite from Tibet with different heating schedules and applied five published plateau definitions to the results. This sample exhibits increasing ages (from ~20 Ma) in the initial ~25% gas release followed by steps with ages which vary around 30 Ma for the remainder of gas released. Of the 25 possibilities, only 8 defined plateaus. Weighting by gas fraction, the 8 calculated plateaus are  $29.26 \pm 0.22$  (2X),  $29.43 \pm 0.29$  (3X),  $29.06 \pm 0.28$ ,  $29.15 \pm 0.22$ , and  $29.28 \pm 0.22$ . Weighting by the uncertainty in the age the values are  $29.25 \pm 0.12$  (2X),  $29.42 \pm 0.08$  (3X),  $29.52 \pm 0.17$ ,  $29.27 \pm 0.08$ , and  $29.26 \pm 0.12$ . These data show that for this sample the choice of heating schedule *and* plateau definition effect the calculated plateau age at the 0.1 Ma level. Unfortunately, some workers attach geologic significance to a single plateau age at this (or an even smaller) level of precision. Since there are at least 3 subjective choices that go into this formulation, we feel such overinterpretation is not warranted. On the other hand, it is entirely reasonable to say that the bulk of the gas in this sample corresponds to an age of "about 29.4 Ma" (this can also be said of the 16 other examples which failed to define "plateaus"). To put a finer point on it is not reasonable, particularly since this age corresponds to a temperature which is not known nearly as well as might be suggested by any one calculated "plateau" age. Moreover, to assign a single number to this sample is to ignore important information. The structure of this age spectrum is a reflection of a complicated cooling history that can be unraveled through the multi-diffusion-domain model. These results indicate that this sample cooled from ~350 to 200°C from 30 to 29 Ma, followed by an interval of slower cooling, reaching ~190°C at 20 Ma. While the cooling history of volcanic rocks is much simpler, the concerns about the subjectivity of plateau analysis still hold. In order to justifiably claim precision of better than ~1%, the uncertainties in all relevant factors should be propagated. These factors include the age and  $^{40}\text{Ar}^*/^{39}\text{Ar}_K$  of the flux monitor (which are commonly not included), the values of the correction factors for interfering reactions, the value of the initial  $^{40}\text{Ar}/^{36}\text{Ar}$ , and the discrimination of the mass spectrometer. All of these become more important as the age of the sample decreases. It seems unreasonable that the precision of any plateau age should be less than the uncertainty in the most important of these factors (which in most cases will either be the uncertainty in  $J$  or in the  $(^{39}\text{Ar}/^{37}\text{Ar})_{\text{C}_k}$ ).

## U-Pb GEOCHRONOLOGY FOR MAGMATISM AND METAMORPHISM IN THE ENGLISH RIVER SUBPROVINCE, SUPERIOR PROVINCE

CORFU, F., Dept. of Geology, Royal Ontario Museum, 100 Queen's Park, Toronto, Ont., M5S 2C6, Can., STOTT, G.M. and BREAKS, F.W., Ontario Geological Survey, Willet Green Miller Centre, 933 Ramsey Lake Road, Sudbury, Ont., P3E 6B5, Can.

The English River Subprovince (ERS) is an Archean metasedimentary belt in the northwestern Superior Province that underwent plutonism, low-pressure / high-temperature metamorphism and anatexis in the period 2700 - 2670 Ma. Thick turbiditic sequences were deposited just prior to and during the terminal stages of the compressional orogeny that quickly followed the episodic assembly of the volcanic-plutonic Uchi Subprovince (US) to the north, mainly between 2710 and 2700 Ma. The ERS was subsequently intruded by a suite of dioritic, tonalitic and granodioritic plutons at 2698-2696 Ma. These are essentially coeval with late-tectonic plutons intrusive into the adjacent US. Several high-grade metamorphic events caused widespread anatexis in the ERS and in adjacent domains of the Winnipeg River Subprovince to the south at 2692-2690 Ma, 2680-2678 Ma and 2670 Ma. The earliest metamorphism accompanied and followed regional deformation. The youngest events occurred under more static conditions and appear to have been of more local significance. In general, the multi-stage metamorphic and magmatic evolution caused repeated growth of zircon and monazite leading to the common occurrence of multiple age populations and complex U-Pb relations within individual units. The relative moderate pressures (0.4-0.6 GPa) reported for the metamorphic assemblages of the ERS, the rapid sequence of events, and the heterogeneous distribution of metamorphic and anatectic assemblages suggest that metamorphism was not primarily the consequence of tectonic thickening by thrusting but that it was caused by magmatic underplating mechanisms. The pattern of early calc-alkalic magmatism followed by complex, multistage metamorphism and the gradual increase in the abundance of S-type granitoid rocks observed in the ERS is akin to that observed in the other metasedimentary belts of the Superior Province and in recent low-pressure / high-temperature metamorphic belts.

SOURCES OF PROTEROZOIC K-RICH ALKALINE AND SHOSHONITIC MAGMATISM IN THE SW GRENVILLE PROVINCE, QUÉBEC: Nd-Sr-Pb ISOTOPIC STUDY

CORRIVEAU, Louise, Centre géoscientifique de Québec, C.P. 7500, Sainte-Foy, QC, G1V 4C7, Canada, and AMELIN, Yuri, Dept. of Geology, Royal Ontario Museum, Toronto, ON M5S 2C6, Canada.

The 1089-1076 Ma potassic (*K*) and shoshonitic (*S*) plutonic suites in the Central Metasedimentary Belt (CMB) of the SW Grenville Province, Québec, are close geochemical analogs of modern subduction-related K-rich alkaline magmas. A small but distinguishable difference in initial Nd and Sr isotopic ratios exists between individual plutons and between *K* and *S* rock series. This difference is not a result of contamination of magmas by older continental crust but rather could have originated from slightly different degrees of enrichment of mantle sources of *K* and *S* magma series.

Initial Pb and Nd ratios are consistent between whole rocks and feldspars, but Rb-Sr systems of whole rocks and feldspars and all isotopic systems in apatites were modified to variable degrees by post-crystallization alteration.

Unaltered rocks of both *K* and *S* series show a range of isotopic variations from +1.2 to +3.3 for  $\epsilon_{Nd}(1.08 \text{ Ga})$ , and from 0.7031 to 0.7038 for  $^{87}\text{Sr}/^{86}\text{Sr}$  (1.08 Ga). The range of initial Pb ratios, obtained for both acid-leached feldspars and U decay corrected whole rocks, is 16.65 to 16.90 for  $^{206}\text{Pb}/^{204}\text{Pb}$ , 15.36 to 15.41 for  $^{207}\text{Pb}/^{204}\text{Pb}$  and 36.25 to 36.50 for  $^{208}\text{Pb}/^{204}\text{Pb}$ . This range is more restricted than that observed in most of the modern potassic rock series (Nelson 1992) and demonstrate that there was no significant involvement of Archean or Paleoproterozoic enriched components in sources of the CMB potassic magmatism, in contrast to contemporary potassic rocks of Australia and W.Greenland.

Based on the two-stage modelling using the Pb, Nd and Sr isotopic data, we can infer the following scenario of evolution of mantle sources of the CMB potassic magmas:

1) Enriched component (upper continental crust?) was separated from depleted mantle with  $\mu=8.0$  at ca. 1.45 Ga. This component was characterized by  $\mu=18\pm 3$ ,  $\text{Th}/\text{U}=3.56\pm 0.13$  and  $^{87}\text{Rb}/^{86}\text{Sr}=0.40\pm 0.05$ , 2) Sediments derived from this crustal source were transported into the mantle during orogeny at ca. 1.2 Ga, with lowering of U/Pb and Rb/Sr ratios during sediment formation and subduction, 3) Potassic magmas were generated by partial melting of this metasomatized mantle at ca. 1.08 Ga.

THERMAL AND TECTONIC EVOLUTION OF THE DENT BLANCHE NAPPE (SWISS AND ITALIAN ALPS)

COSCA, Michael A., Sharp, Zachary D., and Hunziker, Johannes C., Institut de Minéralogie, Université de Lausanne, 1015 Lausanne, Switzerland

The Dent Blanche nappe, which contains the Matterhorn, is located high in the Swiss and Italian Alps. It comprises two Austroalpine units, the Valpelline and Arolla series, which are in thrust contact with the underlying Combin zone. The Valpelline series comprises high grade metasedimentary and metavolcanic rocks, and on the basis of similarities in lithology and isotopic cooling ages appears to correspond to Austroalpine units of the Ivrea zone. Rocks of the Arolla series are similar to the high grade rocks of the external Sesia zone, comprised predominantly of orthogneisses and gabbros, and overlain in places by a Mesozoic cover (e.g., Mont Dolin and the Roisan zone). Published Rb/Sr and K/Ar dates indicate that these Austroalpine units escaped pervasive Alpine metamorphic overprinting, thus offering the potential of accurately reconstructing its pre-Alpine thermotectonic evolution as well as providing insights into the early geological history of the Ivrea and Sesia zones.

Marbles containing the primary assemblage *calcite-muscovite-quartz - phlogopite - tremolite - graphite* with secondary *phengite-talc-chlorite* have been studied from the contact between the Arolla and Valpelline units. Metamorphic temperatures determined by stable isotope thermometry yield the following results: calcite-graphite  $\sim 700^\circ\text{C}$ ; calcite-muscovite-phlogopite  $\sim 590^\circ\text{C}$ ; calcite-quartz-phengite  $\sim 400^\circ\text{C}$ . Large muscovites and phlogopites separated from the marble yield  $^{40}\text{Ar}/^{39}\text{Ar}$  plateau and total fusion dates between 170 and 190 Ma. Smaller phengites occurring as rims on muscovites and phlogopites, and as discrete neocrystallized grains, have saddle-shaped age spectra consistent with excess argon. Argon isochron calculations clearly indicate trapped argon reservoirs of atmospheric and non-atmospheric composition in the phengites. Isochron ages calculated with steps containing trapped atmospheric argon vary between 112 and 136 Ma. Collectively we interpret these data as recording two tectonometamorphic stages: middle Jurassic cooling following high temperature metamorphism and a later, lower temperature, deformation episode during the early Cretaceous. The early Cretaceous episode dates the juxtaposition of the Valpelline and Arolla units and marks the early stages of Eoalpine high pressure metamorphism. A phengite  $^{40}\text{Ar}/^{39}\text{Ar}$  plateau date of  $40.8 \pm 0.3 \text{ Ma}$  from near the base of the Arolla series dates the emplacement of the Dent Blanche nappe to its current structural position. Combined with published dates, we propose a new tectonic model for the evolution of the Dent Blanche nappe.

DEPLETED AND ENRICHED COMPONENTS IN THE UPPER MANTLE OF THE NE PACIFIC: EVIDENCE FROM THE NORTHERN JUAN DE FUCA RIDGE

COUSENS, B.L., Dept. Earth Sciences, Carleton University, Ottawa, K1S5B6, Canada; ALLAN, J.F., ODP, College Station, TX., 77845, USA; LEYBOURNE, M.I., Dept. of Geology, University of Ottawa, Ottawa, Canada, K1N6N5; CHASE, R.L., Geological Sciences, UBC, Vancouver, B.C., V6T2B4, Canada; VAN WAGONER, N.A., Dept. of Geology, Acadia University, Wolfville, N.S., B0P1X0, Canada.

Young basalts dredged from ocean ridges, near-ridge seamounts, and intraplate volcanoes of the NE Pacific are extremely heterogeneous in trace element content and character, yet are fairly homogeneous in isotopic composition. There is also no simple relationship between tectonic setting and geochemistry: "hotspot" basalts are isotopically MORB-like, while at some the spreading centres E-MORB's predominate. West Valley, at the northern end of the Juan de Fuca Ridge, may be a microcosm of the NE Pacific, within which is found a variety of basaltic rocks encompassing the geochemical spectrum of the NE Pacific.

West Valley is a young immature spreading centre of 3200 m depth, dominated by extension over volcanism, which is volcanically active only within its southern half (50 km). Eruptions form small, isolated cones that emit small-volume lava flows. Basalts recovered from this area are tholeiites, ranging in Mg# from 0.69 to 0.55, K<sub>2</sub>O from 0.02 to 0.76%, La/Sm<sub>ch-n</sub> from 0.29 to 1.85, <sup>87</sup>Sr/<sup>86</sup>Sr from 0.70235 to 0.70260, and <sup>206</sup>Pb/<sup>204</sup>Pb from 18.2 to 19.2. Together, the lavas form near-linear arrays on trace element ratio vs. concentration, ratio vs. ratio, ratio-isotope ratio, and isotope-isotope plots, suggesting that they are mixtures of a depleted and an enriched component. Further evidence for magma mixing comes from large phenocrysts in West Valley floor basalts which are complexly zoned and contain spinel and melt inclusions (R. Neilson, pers. comm.) that are not in equilibrium with host glasses.

The incompatible-element-enriched basalts (from a single cone and lava flow) can be modeled as melts of amphibole-spinel peridotite (5% modal amph), as has been shown for alkaline basalts from the Tuzo Wilson Volcanic Field at the Explorer Ridge-Queen Charlotte-Cascadia RFT triple junction. Amphibole in the source may also control the composition of intraplate alkaline rocks from the Pratt-Welker and other seamount chains in the NE Pacific. The most incompatible-element-depleted basalts, from the near-ridge Heck Seamount Chain, West Valley rift walls, and one young flow on West Ridge, could be second-stage melts of mantle that produced MORB at older segments of the Juan de Fuca Ridge. Basalts from the floor of West Valley are mixtures of varying proportions of these two end members.

NE Pacific basalts from all tectonic environments form mixing arrays between DM and HIMU mantle components. Our work suggests that the HIMU-like component in the NE Pacific may be amphibole. If the amphibole formed ~ 1 Ga ago from depleted mantle, it would "age" isotopically to the ratios now observed in the enriched basalts from West Valley. Alternatively (and perhaps more likely), amphibole may have formed more recently from metasomatic fluids derived from a less depleted source.

FISSION-TRACK INVESTIGATIONS ON SPHENE FROM THE KTB DEEP DRILLING PROJECT (GERMANY): POST-PERMIAN COOLING HISTORY AND *IN SITU* ANNEALING

COYLE, David A., and WAGNER, Günther A.  
Max-Planck Institut für Kernphysik, 69117 Heidelberg, Germany.

The German *Kontinentale Tiefbohrung* (KTB) will reach a total depth of 10 kilometres in 1994, with a maximum bottom-hole temperature likely to be in excess of 300°C. Thus it is expected to completely cross the predicted partial annealing zone for fission tracks in sphene, the upper temperature limit of which has been estimated to be ca. 240°C [1].

The lengths of confined fission tracks indicate that at a depth of 7000 metres and a temperature of ca. 200°C, the top of the sphene partial annealing zone may now have been reached. At this depth the mean confined track length is less than 10 micrometres, compared to a mean length of ca. 13.5 micrometres in rapidly cooled sphene from the sub-volcanic Mt. Dromedary standard (Australia).

The apparent sphene ages do not decrease linearly with depth, but exhibit structure at ca. 2.5 km depth which may represent an uplifted partial annealing zone. In addition, there is evidence that more than a kilometre of section has been duplicated as a result of post-Cretaceous thrusting along the Franconian Line where it intersects the KTB below 6800 metres.

As drilling is still continuing in the depth range of the partial annealing zone for sphene, the latest data from these depths will be presented.

- [1] T.M. Harrison, R.L. Armstrong, C.W. Naeser and J.E. Harakal. Geochronology and thermal history of the Coast plutonic complex, near Prince Rupert, British Columbia. *Can. J. Earth Sci.*, 16, pp 400-410.

## THE DISCOVERY OF ARGON: 100 YEARS AGO

CRAIG, H., Isotope Laboratory, Scripps Institution of Oceanography, University of California San Diego, La Jolla CA 92093, USA

The year 1994 marks the 100th anniversary of the discovery of Argon by Sir William Ramsay and Lord Rayleigh. This remarkable research led to the modern understanding of the Periodic Table of the elements and the further discovery by Ramsay of terrestrial helium, and of neon, krypton, and xenon, thus contributing an entirely new group of elements to science.

The discovery of the Noble Gases probably aroused more interest than any other scientific discovery (possibly excepting Fire), and as is generally the case, it was marked by extensive and bitter criticism and disbelief, now largely forgotten. The names of many distinguished scientists are involved in these discussions, including van't Hoff, Dewar, Crookes, Cavendish, and of course Morris Travers who carried out much of the experimental work in Ramsay's laboratories. Rayleigh and Ramsay stand alone from their contemporaries in physics and chemistry as two men of genius who recognized from the beginning the significance of the problem and who were able both to carry out the experimental research and correctly understand and extend the results. The well-known story of Ramsay's request to Lord Rayleigh for permission (!) to work on the problem of the atomic weight of atmospheric nitrogen, and Rayleigh's generous invitation to collaborate, are relics of a bygone gentility in science marking happier and more leisurely days, but the entire story of this research and its reception by scientists provides a metaphor for the process of scientific discovery that is as relevant today as it has been for a century.

## NOBLE GASES IN THE MANTLE AND ATMOSPHERE

CRAIG, H., Isotope Laboratory, Scripps Institution of Oceanography, UCSD, La Jolla CA 92037, USA

This paper summarizes recent work in the Isotope Laboratory ([1]; Craig, Farley, & Wiens, submitted), plus literature data, with the aim of constructing a unifying model for rare-gas isotope systematics in the Earth's mantle and atmosphere. Our own work is based on studies of He, Ne, and Ar isotopes in olivine phenocrysts in Ocean Island Basalts (OIB) and in MORB olivines and glasses. We proceed audaciously in the style of George Danton [2], without, it is to be hoped, reaching his final conclusion. The following results are *axiomatique*.

We show that all Ar-36, Kr and Xe (minus radiogenic and fission isotopes), and ~ 1/2 the Ne and Ar-40 in OIB phenocrysts and glasses are uncorrelated with He-3, and are, in fact, derived from air contamination. Further, the Ar-36 is trapped in fluid inclusions in the phenocrysts [1], and was therefore derived from Air/Seawater (ASW) injection into a magma during crystallization. Thus the "Air-like 40/36 ratio" Ar component in OIBs is Air, rather than the "Lower Mantle component" conjured by the *Ecole Parisienne*. Ar 40/36 ratios in OIBs are => 8000 in Juan Fernandez "High-He-3" basalts [1]. He-4/Ar-40\* (the Ar mantle component) ratios are 1.1 in JFZ basalts, and 2.0 in Reunion and Grande Comore, showing the presence of different K/U domains in the lower mantle.

Neon in the mantle was long ago shown to be of the "solar" persuasion in MORB and OIBs, with added radiogenic Ne-21 and ASW components [3]. We now show that (1) no planetary Ne or Ar components exist in the mantle, (2) Solar Ne has a 20/22 Ne ratio of 12.3 in both upper and lower mantle basalts, and (3) Atmospheric Ne, Ar-36, and Kr are mixtures of solar and planetary gases, in which the solar component is due to outgassing and the planetary component was derived from impact degassing after the primary accretion. (Xe has been lost from the atmosphere to an unknown sink, as generally assumed). Further (4), this is true of both Ne-22 and Ne-21 in OIBs (except that atmospheric Ne contains a slight degassing addition of Ne-21 from the upper mantle). Ne-21 is not a radiogenic component in the lower mantle, but simply represents the original solar neon composition.

"Low-He-3" OIB phenocrysts show a different Ne and Ar isotopic pattern: they crystallized in magmas that had first been flushed with ASW (to the air 20/22 ratio), followed by degassing loss from the magmas prior to eruption, resulting in Ar, Kr, and Xe depletion due to their lower solubilities in silicate melts. These observations provide a method for reconstructing the details of air injection and degassing in sub-oceanic magma chambers on a fine scale, and for deconstructing the observed isotope ratios.

Ocean-basalt magmas thus possess two unique rare-gas isotope tracers for studies of mantle provenance and of ASW injection and magma degassing: He-3, derived from the lower mantle (in OIBs) or from MORB, and Ar-36, derived from air, probably by release from seawater trapped in lithospheric basalts during their sojourn at seafloor spreading centers.

1. Farley, K.A. & Craig, H., 1994, *Geochim. Cosmochim. Acta* (in press).
2. Danton, G.: "De l'audace, et encore de l'audace, et toujours de l'audace!", *Le Moniteur*, 4 September, 1792.
3. Craig, H. & Lupton, J., 1976, *Earth Planet. Sci. Lett.* 31, 369.

## OSMIUM ISOTOPE SYSTEMATICS OF MODERN ARC MANTLE LITHOSPHERE.

CREASER, R. A., Dept. of Geology, University of Alberta, Edmonton, Alberta, T6G2E3, Canada, and BRANDON, A. D., Dept. Earth Atmospheric and Planetary Sciences, Massachusetts Institute of Technology, Cambridge, MA, 02139-4307, USA.

The subduction of oceanic crust is a fundamental process which influences the geochemistry of the mantle and arc magmas. Element transport from subducted oceanic crust to the overlying mantle wedge is well-established, but significant amounts of material are also returned to the deeper mantle. The Os isotopic system presents an interesting geochemical case as a result of the vastly different geochemical behavior of Os relative to other isotopic tracers (Sr, Nd, Pb). Because both sediments and basalts of oceanic crust have very high Re/Os ratios relative to the mantle, their Os isotopic compositions evolve very rapidly, and subducted oceanic crust will have highly radiogenic Os isotopic compositions. The fate of this radiogenic Os is at present poorly constrained. This Os, if removed from the oceanic crust in subduction zones, could lead to radiogenic Os isotopic compositions in the overlying mantle wedge and / or in arc magmas. If the Os is not removed from the subducted oceanic crust then radiogenic Os could be returned to the deep mantle. Recent studies of Os isotopic compositions from some ocean island basalts have invoked a recycled crustal component to account for radiogenic Os isotopic compositions observed, suggesting return of crustal Os to the deep mantle via subduction of oceanic crust.

In order to investigate the geochemical behavior of Os in subduction zones, we have analyzed spinel peridotite xenoliths from the Japan arc (Ichinomegata) and the Cascade arc (Simcoe) for Os isotopic composition. These peridotite xenoliths have also been analyzed for sulfur isotopic composition, and show S isotopic evidence for interaction with and metasomatism by subduction-derived fluids / melts. Spinel peridotites (Type I) from Ichinomegata, Japan, show values of  $^{187}\text{Os} / ^{188}\text{Os}$  from 0.1240 to 0.1267 ( $\gamma_{\text{Os}}$  -3 to -1). A single peridotite sample from the Cascade arc shows a similar Os isotopic composition with  $^{187}\text{Os} / ^{188}\text{Os}$  of 0.1247 ( $\gamma_{\text{Os}}$  -2.5). These Os isotopic compositions are less radiogenic than an average mantle value of 0.1278 and are similar to the average Os isotopic composition for modern depleted mantle determined from abyssal peridotites.

These unradiogenic Os isotopic compositions determined from arc peridotite xenoliths place constraints on the geochemical behavior of Os, and possibly other platinum group elements, during subduction of oceanic crust. The preliminary data obtained here suggests little or no transport of radiogenic Os present in the oceanic crust to the overlying mantle wedge during subduction. It is therefore likely that radiogenic Os is returned to the deep mantle, and subducted oceanic crust is a viable source of radiogenic Os observed in some ocean island basalts.

## ISOTOPIC CHARACTERIZATION OF GROUNDWATER RESOURCES IN THE SACRAMENTO VALLEY, CALIFORNIA: A NEW TYPE OF GROUNDWATER MINING

CRISS, Robert E., Geology Department, University of California, Davis, CA 95616 USA; DAVISSON, M. Lee, Lawrence Livermore National Lab L-237, Livermore, CA 94550 USA; CAMPBELL, Karla R., Geology Department, University of California, Davis, CA 95616 USA.

The coupled use of  $\delta^{18}\text{O}$  and  $\delta\text{D}$  values of water and of the apparent  $^{14}\text{C}$  ages of dissolved bicarbonate provide a powerful means of characterizing and imaging different bodies of groundwater, and of quantifying their sources, apparent ages, migration paths, and the effects of pumping and degradation. An important conclusion derived from these data is that a heretofore undefined type of groundwater "mining" is widespread in the Sacramento Valley, whereby the recharge of young surface waters is induced by pumping of ancient pristine groundwaters. In intensively irrigated areas, as much as 90% of the total recharge is dominated by agricultural return water characterized by elevated  $\delta^{18}\text{O}$  and  $\delta\text{D}$  values on evaporation trajectories, very young  $^{14}\text{C}$  ages of  $< 1$  ka, and commonly elevated contents of nitrate and possibly other anthropogenic constituents that pose a threat to water quality. This type of groundwater degradation occurs in many municipalities surrounded by agricultural activity in the Central Valley, and commonly causes 2 to 4x increases of  $\text{NO}_3$  concentrations over time periods of 20 years or less, and in cases has resulted in non-potable water and production shutdown. This type of groundwater mining is not necessarily associated with a permanent decline in the water table, in contrast to the traditional concept of groundwater mining. Both processes are occurring in the City of Sacramento where pumping has induced the infiltration of Sacramento and American River water over length scales of 3 km, and also resulted in the development of two ~30m deep cones of depressions in the water table. Even though the city of Sacramento pumps 6 times less groundwater per  $\text{km}^2$  than intensely irrigated areas to the west, the heavily urbanized areas of Sacramento are not as conducive to the natural or artificial recharge to the groundwater as the flood-irrigated agricultural lands, so the water table has declined more than it has further west.

OLIGO-MIOCENE EXTENSION DURING ARC-CONTINENT CONVERGENCE CREATING THE SEPIK-RAMU AND AITAPE BASINS IN NORTHERN PAPUA NEW GUINEA.

Crowhurst, P.V., Hill, K.C., & Foster, D.A.,  
Victorian Institute of Earth and Planetary Sciences,  
School of Earth Sciences, La Trobe University,  
Melbourne, Victoria, Australia 3083

Papua New Guinea was the northern 'passive' margin of the Australian craton in the Mesozoic, but now comprises the northwest margin of the Indo-Australian Plate and is tectonically active due to ongoing convergence with the Pacific Plate. Convergence since at least the Eocene has resulted in collision with an island arc, creating a typical 'Rocky Mountain type' structure across Papua New Guinea. The structure can be divided into three major zones; the Fly Platform in the southwest is a flat-lying foreland adjacent to the mountainous Papuan Fold and Thrust Belt. This is bound to the northeast by a distal sediment, igneous, metamorphic and ophiolitic province, the New Guinea Mobile Belt. The Mobile Belt is of interest because it is an active collision zone from which a working model for the evolution of convergent boundaries can be generated. Such a model can then be applied to and tested against ancient collisional zones. The information obtained in recent studies indicates the northern New Guinea collision zone is very complicated which implies that models describing older terrains may be oversimplified.

Thermochronological techniques are now being used to help unravel the complicated tectonic history of northern Papua New Guinea. Fission track and  $^{40}\text{Ar}/^{39}\text{Ar}$  thermochronological analysis of the igneous and high-grade metamorphic basement around the Sepik-Ramu basins reveals regional Pliocene cooling from temperatures of  $>100^\circ\text{C}$ , consistent with the deformation in the Fold Belt to the south and due to Late Miocene-Pliocene arc-continent collision.

An Early Miocene collision has been previously proposed, primarily based upon cooling ages from metamorphic basement rocks. However the data suggests very rapid cooling of these rocks from temperatures of  $>500^\circ\text{C}$  and  $\sim 10\text{-}15\text{km}$  of erosion, which is clearly inconsistent with Early Miocene starved graben and carbonate deposition. We suggest that increased subduction beneath New Guinea in the Late Oligocene caused extension above the slab as well as the Maramuni volcanic arc. Early Miocene extension may have been manifested locally as low angle detachment faults which exposed mid-crustal rocks in metamorphic core complexes, with negligible erosional denudation. Extension caused rapid Miocene subsidence of the whole PNG margin, enabling deposition of thick limestone and creating the Sepik and Ramu basins.

Thus, Northern Papua New Guinea comprised a broad 'passive' margin in the Miocene, the site of local deep extensional graben and carbonate deposition until the Bewani-Torricelli Mountains were upthrust in the Pliocene to form the current boundaries of the Sepik, Ramu and Aitape basins.

CLOSING IN ON ARGON CLOSURE TEMPERATURES?: AN EXTENDED "IONIC POROSITY" MODEL FOR THERMOCHRONOMETRIC MINERALS, WITH APPLICATION TO AMPHIBOLES

DAHL, Peter S., Department of Geology, Kent State University, Kent OH 44242, USA

Refined estimates of argon closure temperatures ( $T_c$ ) for compositionally diverse, thermochronometric minerals like amphiboles and micas are important in establishing precise cooling histories of orogenic terranes. This paper presents an extended "ionic porosity" approach for quantifying compositional effects on  $T_c$  within a given mineral family, then applies the model to calcic/subcalcic amphiboles. The model rests on the demonstration that ionic porosity ( $Z$ ; defined as the percentage of unit cell volume not occupied by ions) uniquely links mineral composition ( $X$ ) to the volume-diffusion parameters  $E$  and  $D_0$  for both O and Ar in the Dodson (1973) equation for  $T_c$ . As applied to amphiboles, the model is buttressed by observed  $T_c$ - $Z$ - $X$  trends that are fully consistent with predictions from basic crystal-chemistry. Values of  $Z_{24^\circ\text{C}}$  calculated from published compositional and unit cell data for 25 synthetic clinopyroxene amphiboles exhibit a continuous range from 36.5% to 39.7% (end-member edenite to ferro-actinolite, respectively). Corresponding model  $T_c$  values for Ar range from  $562^\circ\text{C}$  to  $443^\circ\text{C}$  ( $80\mu\text{m}$  grain radius;  $10^\circ\text{C}/\text{Ma}$  cooling rate; infinite sphere). Natural hornblendes amenable to  $^{40}\text{Ar}/^{39}\text{Ar}$  dating yield a somewhat narrower, yet still significant, range of model  $T_c$  (i.e.,  $\sim 480\text{-}550^\circ\text{C}$ ).

Three compositional effects on Ar retentivity modeled from the synthetic-amphibole  $Z$ - $X$  data are readily attributable to Mg#, A-site occupancy, and Al-Tschermak's substitution. Specifically, the model generates  $T_c$  values some  $60\pm 10^\circ\text{C}$  higher for Mg end-member calcic/subcalcic amphiboles than for their Fe analogues, and values some  $40\pm 15^\circ\text{C}$  higher for amphiboles with full A-sites relative to those with empty A-sites. A  $\sim 35^\circ\text{C}$  increase in model  $T_c$  may accompany the increase in Al-Tschermak's substitution in the progression from end-member tremolite to end-member tschermakite. Parallel extension of the model to micas is in progress.

The model results for argon in amphiboles (and micas) have important implications for interpretation of thermochronologic data. *First*, a 35 Ma  $^{40}\text{Ar}/^{39}\text{Ar}$  age discordance among compositionally diverse hornblendes in a terrane cooled at  $1^\circ\text{C}/\text{Ma}$  may arise from a 1% absolute variance in  $Z$  within the sample suite. Such variance in  $Z$  is well within the 2% absolute range demonstrated among natural hornblendic amphiboles. Thus, ionic porosity effects constitute a potential alternative to strictly tectonic explanations for age discordance. At  $10^\circ\text{C}/\text{Ma}$ , the model age discordance is only 3-4 Ma, such that the inherent compositional effects become lost within the  $\sim \pm 3$  Ma uncertainty common in  $^{40}\text{Ar}/^{39}\text{Ar}$  ages. *Second*, previous field-based and experimental efforts to isolate Mg/Fe effects on Ar retentivity in hornblende have led to varying conclusions. This ambiguity may largely reflect the simultaneous influence of yet other compositional effects (such as those isolated above by empirical means), and/or variable tectonic and micro-textural factors both within and among cooling terranes.

**<sup>40</sup>Ar/<sup>39</sup>Ar LASER SYSTEM DATING OF PHENGITE FROM DABIE MOUNTAIN, CHINA**

Dai Tongmo Xie Jinlong and Pu Zepin(All at Guangzhou Branch, Institute of Geochemistry, Chinese Academy of Science. Guangzhou, Box 1131 code 510640 P.R.China)

A laser fusion system in combination with a low volume high vacuum inlet system and VG 1200 mass spectrometer with an electron multiplier has been established in our Lab. The laser fusion system consists of a He Ne laser and a YAG continuous laser (-10 $\mu$ m diameter laser spot sizes at single mode mode--10 watt and <1000  $\mu$ m diameter laser spot sizes at multiple mode--70 watt ).

Measurement of <sup>40</sup>Ar/<sup>39</sup>Ar age spectra on single white mica crystals is a new test of obtaining detailed geochronological information. The three samples of phengites with different sizes were picked from eclogites on the deferent zone located on the southern part of Dabie mountain, Anhui province, China. The mineral grain were checked optically with a petrographic microscope for crystal class, and every sample were measured by bulk step heating and single grain step heating in order to obtain three pairs of date for comparing each other.

Two samples of phengite (D1, D2) yields two plateau age of 661.4 $\pm$  3.4 Ma and 212.2 $\pm$  2.0 Ma, respectively. But a third sample of phengite (D3) appears a saddle-shape spectrum and an elevated initial <sup>40</sup>Ar/<sup>39</sup>Ar ratio of 810, suggestive of excess argon. Our results indicate that there were multiple times of the tectonic evolution in the Dabie mountain. The data reveals that the time of previous origin was no later then 661Ma ago, and the last once was finished in the time of Indo-China movement.

**<sup>40</sup>Ar/<sup>39</sup>Ar DATING ON A MICROSCOPIC SCALE WITH A CONTINUOUS LASER SYTEM: AN ENLIGHTENING APPROACH TO GEOCHRONOLOGY**

DALRYMPLE, G. BRENT, Branch of Isotope Geology, U.S. Geological Survey, Menlo Park, CA 94025

Since its introduction more than four decades ago, K-Ar dating has undergone two significant advances in methodology. The first occurred in the mid-1960s with the development by Merrihue and Turner (1966) of the <sup>40</sup>Ar/<sup>39</sup>Ar technique , which allowed K-Ar dating to be applied to open systems. The other was the extension by York and others (1981) of the <sup>40</sup>Ar/<sup>39</sup>Ar method to single crystals, which was made possible by the availability of ultra-clean, ultra-sensitive, and very precise rare gas mass spectrometers, and by the application of a continuous laser for fusing and heating very small samples. The addition of very low blank furnaces have significantly extended the applications of these very sensitive <sup>40</sup>Ar/<sup>39</sup>Ar dating systems.

Today, the <sup>40</sup>Ar/<sup>39</sup>Ar method using lasers and ultra-low blank furnaces is being used to solve problems in geochronology that were intractable only a decade ago. Using these systems, it is now possible to routinely date single crystals of less than a milligram in mass, obtain detailed age spectra on samples weighing as little as 0.05 mg, differentiate between indigenous crystals and xenocrysts, determine impact ages on both terrestrial and lunar samples using very small fragments of melt rocks, precisely date samples as young as 0.1 Ma, extract thermal history information from disturbed samples, and obtain detailed "age contours" showing the distribution of radiogenic Ar within a single crystal.

These new methods have numerous applications in geochronology, thermochronology, tectonics, stratigraphy, impact dynamics, and studies of sedimentary provenance.

Merrihue, C., and Turner, G., 1966, Potassium-argon dating by activation with fast neutrons: Jour. Geophys. Res., v. 71, p. 2852-2857.

York, D., Hall, C.M., Yanase, Y., Hanes, J.A., and Kenyon, W.J., 1981, <sup>40</sup>Ar/<sup>39</sup>Ar dating of terrestrial minerals with a continuous laser: Geophys. Res. Lett., v. 8, p. 1136-1138.

PROTEROZOIC CRUSTAL HISTORY OF WESTERN IRELAND AND ROCKALL: PRECAMBRIAN TECTONIC RECONSTRUCTIONS IN THE NORTH ATLANTIC REGION

DALY, J.S., FITZGERALD, R.C., MENUGE, J.F., Department of Geology, University College Dublin, Belfield, Dublin 4, Ireland, BREWER, T.S., University of Nottingham, England, HEAMAN, L.M., Royal Ontario Museum, Toronto, Canada and MORTON, A.C., British Geological Survey, Keyworth, England.

Because of their geographic position, Precambrian rocks in Britain, Ireland and on the adjacent continental shelf and Atlantic plateaux are important in tectonic reconstructions for the north Atlantic region over a long time period. Until recently our understanding of such regions has, of necessity, often been based on poor quality geochronology, Nd model ages or geological inferences alone. Moreover large volumes of submarine continental crust in the north Atlantic region are either inaccessible, or limited by the small sample sizes available from drill or grab sampling.

Some previous studies of recently discovered Proterozoic continental crust in Britain, Ireland and the submarine Rockall Plateau have over-emphasised Sm-Nd  $t_{DM}$  ages of c. 1.9 Ga throughout the region.

Single grain and small fraction U-Pb abraded zircon geochronology were essential in order to establish a well-constrained chronology for the Annagh Gneiss Complex of N Mayo, Ireland, where the pitfalls of bulk fraction zircon dating can be amply demonstrated. Here juvenile Palaeoproterozoic crust is represented by c. 1.75 Ga calc-alkaline orthogneisses. Late Mesoproterozoic granitoids with A-type geochemistry and Palaeoproterozoic  $t_{DM}$  ages, emplaced at c 1.26 Ga, were followed by thermal disturbance and deformation during both the Grenville and Caledonian orogenies. A small volume of juvenile c. 1.25 Ga crust is present as a tectonic sliver, incorporated along a Grenville high strain zone.

Single grain and small-fraction U-Pb zircon data from the southern Rockall region indicate close comparison with the Irish Proterozoic but with a very different crustal history.

The new age data provide the basis for testing current tectonic models for the North Atlantic Precambrian. Pre-Grenville refits have a beguiling simplicity in spite of the complex Grenville and Caledonian history of the region.

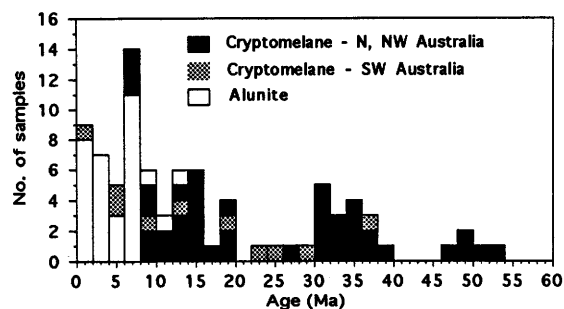
K-Ar DATING OF WEATHERING-RELATED CRYPTOMELANE AND ALUNITE FROM WESTERN AND NORTHERN AUSTRALIA

DAMMER, D., CHIVAS, A. R. and McDOUGALL, I., Research School of Earth Sciences, The Australian National University, Canberra, ACT 0200, Australia

K-Ar dating of K-bearing weathering products developed on very old bedrock (Archean and Proterozoic in this case) is commonly invalidated by the presence of small amounts of fine-grained micaceous minerals inherited from bedrock. The larger the differences in their K-Ar ages the smaller the proportion of mica that causes measured ages to be quite unrelated to the age of weathering. To quantify the effect of inherited K-silicates on K-Ar age, the weathering phase was selectively dissolved and radiogenic Ar and K in the silicate residue were determined. Using material balance equations, estimates of the age of the weathering mineral were obtained.

In this study more than 90 samples of weathering-related cryptomelane ((K,Ba)MnO<sub>16</sub>·xH<sub>2</sub>O) and alunite (K,Na)Al<sub>3</sub>(SO<sub>4</sub>)<sub>2</sub>(OH)<sub>6</sub> were dated using the approach described above. The samples of cryptomelane come from the Groote Eylandt Mn deposit (Northern Territory), the Eastern Pilbara Province (Woodie Woodie, Mt. Sydney) and the Peak Hill Province (Horseshoe). In addition there are small occurrences of locally concentrated Mn oxides scattered over the Kimberley, Pilbara and Yilgarn Cratons. Alunite comes from the southern Yilgarn and Pilbara Blocks.

This study is unique in that it compares the results of extensive dating of two minerals formed during weathering from the same general area. Results from cryptomelane, corrected for silicate residue, form three distinct age groups (see figure): 6-20 Ma (Middle to Late Miocene), 30-40 Ma (Oligocene) and 46-54 Ma (Early to Middle Eocene). The results obtained suggest that there were three major periods of intense chemical weathering in N and NW Australia corresponding to more humid climatic conditions. All corrected ages of alunite fall into the range of 0-14 Ma recording the youngest weathering event. It is probable that each new weathering event caused complete recrystallisation and resetting of the K-Ar clock in the case of alunite. Measured ages are interpreted as marking the time of cessation of intense weathering, and beginning of drier climatic conditions. This is compatible with essentially zero K-Ar ages measured on alunite being formed at present under humid climatic conditions in the very south of western Australia.



In further work, <sup>40</sup>Ar/<sup>39</sup>Ar laser microprobe dating will be used to date banded void fillings and thin veinlets of cryptomelane free of silicate residue. This will enable us to estimate the rate of growth, as well as further refine the timing of periods of intense chemical weathering.

**SCHEELITE Sm-Nd AND FLUID INCLUSION Rb-Sr DATING OF SHEAR ZONE - HOSTED GOLD DEPOSITS, AFRICA.**

DARBYSHIRE, D.P.F., NERC Isotope Geosciences Laboratory, Keyworth, Nottingham NG12 5GG, UK and SHEPHERD, T.J., British Geological Survey, Keyworth, Nottingham NG12 5GG, UK.

Information concerning the timing of mineralization for many world class ore deposits is scant, or even unknown, preventing objective appraisal of their genesis. Direct determination of the age is hampered by the lack of ore minerals that can be dated by conventional radiometric methods. An additional problem is the effect of prolonged mineral-fluid interaction at moderate to low temperatures subsequent to mineral deposition and the likelihood of open system behaviour. However two techniques have been developed which allow constraints to be placed on the age and evolution of hydrothermal fluids.

Scheelites from the auriferous lode deposits of the Midlands Greenstone belt, Zimbabwe have been dated by an application of the Sm-Nd mineral technique. Two phases of scheelite deposition and gold mineralisation have been established which correlate with Late Archaean and Early Proterozoic magmatic events in the region.

An alternative approach to the dating of shear zone-hosted gold deposits involves the use of fluid inclusion Rb-Sr geochronology which we have successfully applied to Palaeozoic mineral deposits. A suite of gold-bearing, vein quartz samples from the Ashanti Mine, Ghana, have yielded an age of c. 1850 Ma, thus providing the first direct geochronological evidence for the age of auriferous mineralization. This permits the Ashanti deposit to be placed in a regional setting and suggests that the mineralization is an end-Eburnian event (2400 - 1800 Ma), possibly linked to the emplacement of late orogenic granites. The data also reveal evidence of multiple reactivation of the shear zone as suggested by complementary fluid inclusion and mineralogical observations.

**SPATIAL AND TEMPORAL VARIATIONS IN THE GEOCHEMISTRY OF THE ETHIOPIAN "FLOOD" BASALTS PROVINCE**

DAVIES, Gareth R., Vrije Universiteit, De Boelelaan 1085, 1081 HV Amsterdam, The Netherlands, NORRY, M.J., Leicester University, LE1 7RH, UK and Jones P.W., Leeds University, LS2 9JT, UK.

Tertiary magmatism in Ethiopia originally covered an area of 750,000 km<sup>2</sup> and produced a volume in excess of 350,000 km<sup>3</sup>. In order to constrain the geodynamic setting of the Ethiopian "flood basalt province", K-Ar ages, major and trace element and Sr-Nd-Pb isotope data have been determined from >15 volcanic successions from the north, central, south-west, south-central and east of Ethiopia.

At least four distinct stages of volcanism occurred during the Eocene-Miocene: i) Initial magmatism between 49-45 Ma appears confined to SW Ethiopia (although pre-1980 K-Ar ages of ~ 50 Ma have also been reported from NW Ethiopia); ii) Volcanic activity between 45 and ~32 Ma, although of more regional extent, was mainly limited to the S and SW. In the SW 3000m of volcanics were produced prior to 30 Ma. The third and fourth volcanic stage ~30-20 Ma and ~20-15 Ma are the main periods of magmatism in N, C and E Ethiopia. Significant crustal extension is not apparent prior to the final magmatic event. Development of the Main Ethiopian Rift began between 18-14 Ma. Regional uplift appears to post-date the earliest magmatism.

Basalts from the province as a whole record large variations in both trace element and isotope ratios (<sup>206</sup>Pb/<sup>204</sup>Pb = 17.9 to 20.8). Within a single volcanic succession, trace element ratios can be correlated with variations in Sr and Pb isotopes. However, successions of the same age, even within 100 km of each other, have distinct isotope ratios (<sup>206</sup>Pb/<sup>204</sup>Pb; SW, 20.8-20.4; SC, 18.0). In the SW and SC successive volcanic episodes have distinct trace element and isotope compositions (e.g. SC; <sup>206</sup>Pb/<sup>204</sup>Pb ~18, 18.7, 19.7).

At high levels in the lava pile in the N, NW and E, correlations between fractionation indexes, Sr, Pb and K, Rb and Ba/Nb establish that crustal contamination was extensive. Significant volumes of rhyolites are associated with these basalts. In contrast, basal flows in N and SC are characterised by unradiogenic <sup>206</sup>Pb/<sup>204</sup>Pb and high <sup>207</sup>Pb/<sup>204</sup>Pb, marked Ba enrichment and positive Eu anomalies. The lack of K and Rb enrichment argues against an origin due to crustal interaction. The trace element characteristics, particularly the positive Eu anomalies, are not characteristic of oceanic volcanism implying a contribution from the subcontinental lithosphere. The Eu anomaly argues for a source that has at some stage suffered shallow melting while retaining residual plagioclase. In contrast, basal lavas in other regions are characterised by a HIMU-like isotope signature.

Early basalts (50-32 Ma) record a signature from the subcontinental lithosphere whereas later flows (30-15 Ma) have a large crustal signature implying that isotherms have been raised over the ~30 Ma of igneous activity. The temporal variations in the magmatism and extremely heterogeneous mantle sources imply that Ethiopian volcanism was not related to a single large scale thermal event (plume). Equally, volcanism is not caused by lithospheric extension which does not occur until after the bulk of the volcanics have been formed. The extreme isotopic heterogeneity demonstrates a marked local control over volcanism but does not explain the nature of the thermal anomaly that caused the mantle melting.

## EVAPORATION OF ROCKS AND MINERALS IN THE LABORATORY AND IN NATURE

DAVIS, Andrew M.<sup>1</sup>, WANG, Jianhua<sup>2</sup>, and CLAYTON, Robert N.<sup>1,2,3</sup>; <sup>1</sup>Enrico Fermi Institute, <sup>2</sup>Department of the Geophysical Sciences, <sup>3</sup>Department of Chemistry, University of Chicago, Chicago, IL 60637.

In recent years, high temperature evaporation has come to be recognized as an important mechanism for isotopic mass fractionation as well as chemical fractionation. We present three examples of natural chemical and isotopic fractionation effects that have been reproduced in evaporation experiments.

Wüstite-magnetite spherules collected from deep-sea sediments are believed to have been Fe-Ni particles that were oxidized during atmospheric entry. We have shown that these particles contain mass-fractionated Fe and Ni; each spherule has uniform isotopic composition, but among 10 spherules, heavy isotope enrichments of 8.6–19.2 ‰/amu (avg. 14.5 ‰/amu) for Fe and 6.8–49.0 ‰/amu (avg. 22.9 ‰/amu) for Ni were found. O isotopic analyses of several aggregates of many spherules give isotopic composition enriched by 12–16‰/amu compared to fusion crust from iron meteorites. We evaporated synthetic wüstite in a vacuum furnace at a variety of temperatures above the melting point for a variety of durations. Analysis of the evaporation kinetics indicates that the evaporation reaction is  $\text{FeO}(\ell) = \text{Fe}(\text{g}) + \frac{1}{2} \text{O}_2(\text{g})$ . Residues are enriched in the heavy isotopes of Fe and O. Isotopic compositions for both elements follow the Rayleigh fractionation law. The gas/solid fractionation factor for Fe is identical to that expected for the inverse square root of the masses for  $\text{Fe}(\text{g})$ ; the value for O is somewhat lower than that expected from  $\text{O}_2(\text{g})$ , indicating some kinetic hindrance to O evaporation. Natural magnetite-wüstite spherules have experienced substantial mass loss during atmospheric heating.

A number of refractory inclusions from carbonaceous chondrites are enriched in the heavy isotopes of O, Mg and Si. We have shown that these mass-fractionation effects are consistent with Rayleigh fractionation during high temperature evaporation and that, for  $\text{Mg}_2\text{SiO}_4$ , the residue must be molten to allow isotopic equilibration in the residue during fractionation, as required by the Rayleigh law.

A group of hibonite-rich inclusions (HAL-type inclusions) in carbonaceous chondrites contain mass-fractionated O, Ca and Ti and REE patterns with large negative Ce anomalies. We recently conducted evaporation experiments on a melt whose starting composition consisted of chondritic proportions of  $\text{MgO}$ ,  $\text{Al}_2\text{O}_3$ ,  $\text{SiO}_2$ ,  $\text{CaO}$ ,  $\text{TiO}_2$  and  $\text{FeO}$ , doped with 100 ppm each of the REE. The residues showed chemical fractionations of major elements similar to those found previously: Fe was the most volatile element; Mg and Si had similar volatilities and Al, Ca and Ti did not evaporate under the conditions of our experiment. Most of the REE did not evaporate either, but Ce was much more volatile than the other REE. A 2440× depletion in Ce was found in the most extreme residue (95% mass loss). Enrichments in the heavy isotopes of O, Mg and Si were similar to those found in the liquid  $\text{Mg}_2\text{SiO}_4$  evaporation experiments. The results of our experiments on chondritic composition samples support earlier conjectures that the HAL-type inclusions are evaporation residues.

## COMBINED USE OF <sup>14</sup>C AND STABLE ISOTOPES TO MAP AND MODEL GROUNDWATER SYSTEMS

DAVISSON, M. L. and VELSKO, C.A., Lawrence Livermore Lab L-237, Livermore CA 94550, USA, CRISS, R. E., and CAMPBELL, K.R., Geology Department, University of California, Davis, CA 95616, MACFARLANE, P.A., Kansas Geological Survey, Lawrence, KS. 66047

AMS techniques make available abundant and detailed <sup>14</sup>C measurements that, when coupled with stable isotope data, can define spatial images, apparent ages, and fluxes in hydrologic systems at different scales. A new extraction technique routinely utilizes 35 ml water samples that require only simple field sampling methods, making <sup>14</sup>C analyses for hydrologic samples straight forward and convenient. Such easy access of these data make possible generation of detailed quantitative models of groundwater systems or validation of previously derived groundwater models. For example, groundwater beneath the City of Sacramento, California (100 km<sup>2</sup>) has two large groundwater cones of depression (~30m below sea level) that are reflected by <sup>18</sup>O variations. Progressive groundwater depletion causes ancient (to 16 ka) groundwater beneath the city to be replaced by recharged modern American and Sacramento River waters ( $\delta^{18}\text{O} = -11.0$ , and <sup>14</sup>C = >100% modern carbon) into the aquifer at a rate of ~5% of the annual groundwater consumption. Lateral groundwater flow rates adjacent to the rivers calculated from the  $\delta^{18}\text{O}$  isopleths are 30-60m/yr, where vertical flow rates calculated from downward migration of bomb-pulse <sup>14</sup>C is about one order of magnitude lower. These same rates are observed in other parts of the southern Sacramento Valley, where groundwater cycling from intensive agricultural irrigation is calculated to be six times greater than the natural groundwater flow rates and have led to degradation of the water quality.

As another example, large scale (450 km x-section) <sup>14</sup>C and stable isotope characterization of groundwater systems in the Great Plains regions differentiates groundwater of young local-flow systems from older intermediate-scale flow systems. Local flow systems dominate areas of hill and valley-type topography, where apparent ages vary between 2-15ka and the  $\delta^{18}\text{O}$  values (-8.5 to -11.5‰) reflect local recharge. Intermediate-scale flow systems vary between 10 to >40ka and have  $\delta^{18}\text{O}$  values (-11.5 to -14.0‰) that reflect recharge from higher elevations just east of the Front Range of Colorado. These data are used to validate and calibrate a previously derived finite difference model.

Funding for this work was performed under the auspices of the U.S. DOE by LLNL under contract No. W-7405-Eng-48.

GROUND-WATER RECHARGE FROM RIVER WATER IN NORTHWEST HUNGARY

DEAK, J., Research Center for Water Research Institute, Budapest, Hungary H-1095,  
REVESZ, K., U.S. Geological Survey, Reston VA. 22092,  
DESEO, E., Research Center for Water Research Institute, Budapest, Hungary, H-1095,  
BOHLKE, J.K., U.S. Geological Survey, Reston VA. 22092.

The largest potential drinking water reservoir in Hungary is located in a 100 to 500-meter-thick Pleistocene gravel aquifer (deposited by the Danube River) underlying the Szigetkoz area of northwest Hungary. Recharge conditions and potential contamination of this aquifer were investigated by use of environmental isotopes.

Oxygen(O) and hydrogen(H) isotope ratios of Danube river water are significantly different from those of local infiltrated ground water, because the Danube water is recharging from the high Alps. The so-called "altitude effect" makes the Danube water isotopically more negative than the locally infiltrated ground water. O and H isotope ratios in the gravel aquifer are approximately equal to river values, indicating that river water is the dominant source of recharge to the entire aquifer. Infiltration of locally recharged precipitation water is negligible.

High tritium concentrations (>40 Tritium Units) in the ground water correspond to the mid-1960's atmospheric tritium-deposition peak in the Danube. This tritium peak can be found at flow-path distances of 5 to 15 kilometers from the river, indicating that horizontal ground-water-flow velocities are about 150 to 450 meters per year.

Tritium concentrations in the deepest parts of this aquifer are higher than the detection limit (1 Tritium Unit), indicating that recharge flushes out the entire aquifer in < 100 years.

<sup>14</sup>C data show that ground water beneath the Pleistocene gravel aquifer is much older (20,000 to 30,000 years), and it was recharged not by Danube water, but 30 to 50 kilometers west of Szigetkoz.

<sup>14</sup>C AND <sup>40</sup>AR/<sup>39</sup>AR DATING OF THE CAMPANIAN IGNIMBRITE, PHLEGREAN FIELDS, ITALY

DEINO, A.L., and CURTIS, G.H., Geochronology Center, Institute of Human Origins, Berkeley, CA 94709, USA; SOUTHON, J., Center for Accelerator Mass Spectrometry, Lawrence Livermore National Laboratory, P.O. Box 808, L-397, Livermore, CA 94551-9900, USA; TERRASI, F., and CAMPAJOLA, L., Dipartimento di Scienze Fisiche, Universita' di Napoli "Federico II", Pad. 20 Mostra d'Oltremare, 80125 Napoli, Italy; and ORSI, G., Dipartimento di Geofisica e Vulcanologia, Universita di Napoli "Federico II", Largo S. Marcellino, 10, 80138, Napoli, Italy.

We have carried out a series of geochronologic measurements of the Campanian Ignimbrite, a widespread and prominent ash-flow tuff in the Phlegrean Fields and outlying area in the Naples region of Italy. Precise ages for this eruption have some important volcanological and stratigraphic implications, but we will focus here on intercalibration with the <sup>14</sup>C time scale.

We have previously reported on single-crystal laser-fusion <sup>40</sup>Ar/<sup>39</sup>Ar dating of three samples of the ignimbrite with an average isochron age of 36.8 ± 0.5 ka (Deino *et al.*, 1992). We have reproduced this age within error redating one of the original samples, but using a conventional resistance furnace and the incremental release <sup>40</sup>Ar/<sup>39</sup>Ar dating technique, obtaining an isochron age of 37.4 ± 0.5 ka. The overall mean age obtained by the <sup>40</sup>Ar/<sup>39</sup>Ar method for this eruption is 37.1 ± 0.4 ka.

New radiocarbon measurements were carried out on charcoal from a carbonized branch exposed within the ignimbrite on the wall of an active quarry. The sample was split and analyzed at both the Naples AMS facility and the Center for AMS at LLNL. The samples at both laboratories received routine acid-base-acid treatment, while the samples at LLNL also received a subsequent bleaching/oxidation treatment, followed by additional base washes. The final steps of oxidation to CO<sub>2</sub>, reduction to graphite, and AMS measurement were similar in both labs. Coal blanks were measured following the same pretreatment.

The mean background-corrected radiocarbon age obtained at the Naples AMS and LLNL facilities were 32.3 ± 0.6 ka and 34.60 ± 0.15 ka, respectively, calculated using a half-life of 5568 years. Recalculating to the true 5730-year half life yields 33.2 ± 0.6 ka and 35.60 ± 0.15 ka. As these results are discrepant further studies are underway that will hopefully resolve this conundrum.

The radiocarbon age determined for the ignimbrite thus ranges between 1,500 ± 400 years to 3,900 ± 700 years younger than the <sup>40</sup>Ar/<sup>39</sup>Ar age, or 4-11%. This range encompasses the shift of ~2,300 ± 300 ka toward young radiocarbon ages for this interval predicted by Mazaud *et al.* (1991) based on geomagnetic field variations.

Deino, A.L., *et al.*, 1992, <sup>40</sup>Ar/<sup>39</sup>Ar dating of the Campanian Ignimbrite, Campanian Region, Italy: 29th Abstracts, International Geological Congress, Japan, 3:2654

Mazaud, A., *et al.*, 1991, Geomagnetic field control of <sup>14</sup>C production over the last 80 ky: Implications for the radiocarbon time-scale: Geophys. Res. Let. 18:10:1885-1888.

## EARLY PALAEOZOIC BIOTITE Rb-Sr DATES IN WESTERN AUSTRALIA

DE LAETER, J.R., Curtin University of Technology, GPO Box U1987, Perth, Western Australia, 6001, Australia and LIBBY, W.G., Geological Survey of Western Australia, 100 Plain Street, East Perth, Western Australia, 6004, Australia.

Biotite from granite and gneiss from the Yilgarn Craton in Western Australia, dated by the Rb-Sr technique, indicates that much of the margin has been tectonically active during post-Archaean time, whereas most biotite dates in the main body of the Craton are Archaean in age.

A belt at the western margin of the Yilgarn Craton gives ages of 430-500 Ma, which merges into a transition zone to the east some 15-40 km wide, which separates the young dates from the eastern chronological plateau where biotite dates range from 2300-2600 Ma, and in general are slightly younger than regional Rb-Sr whole rock dates which average about 2550 Ma. The 430-500 Ma dates probably represent resetting during uplift in the Early Palaeozoic.

At the northwestern corner of the Yilgarn Craton biotite dating gives three distinctive dates : 750-800 Ma in the Capricorn Orogen to the North, 1650 Ma in the west and 2400-2600 Ma in the east. The 1650 Ma dates probably represent tectonic loading which resulted from the collision of the Yilgarn and Pilbara Cratons, the dates being set by cooling associated with subsequent erosional rebound.

Biotite dating has also been carried out along a number of traverses to the south of the Yilgarn Craton. Dates of 450-500 Ma at the margin of the Craton suggest early Palaeozoic uplift and sets an upper limit for emplacement of the Albany-Fraser Province.

## HYDROGEN ISOTOPIC COMPOSITION IN THE EARLY SOLAR SYSTEM : IN SITU ANALYSIS OF METEORITES BY ION MICROPROBE.

DELOULE Etienne, CRPG-CNRS, BP 20, 54501 Vandoeuvre les Nancy cedex, France, and ROBERT François, Museum d'Histoire Naturelle, Lab. de Minéralogie, 61 rue Buffon, 75005 Paris, France.

The D/H ratios of 3 meteorites (Renazzo CR, Abee E3 and Semarkona LL3) have been measured with the CRPG Nancy ion-microprobe. These meteorites are well known for their large deuterium enrichments found in the organic macro-molecules [1,2]. The observed in situ variations of the D/H ratio cover the range of  $7.10^{-5}$  to  $8.10^{-4}$ , i.e. -600 to +5000‰. Other secondary ions (C, Mg, Si, K, ...) were measured together with H and D to characterize the hydrogen carriers. The internal correlations observed between the D/H ratio and the hydrogen carriers pointed out that, contrary to previous interpretations, the organic macromolecules are not the only carriers of the deuterium-rich hydrogen but are in close association with deuterium-rich phyllosilicates. These correlations also show that solar-type hydrogen ( $\delta D \leq -700\text{‰}$ ) is present in organic macro-molecules of E3 meteorites.

The high D/H ratios measured in water bearing minerals ( $\geq 7.10^{-4}$  in Semarkona and  $\geq 3.10^{-4}$  in Renazzo) could not have been reached thermally within a dense solar nebula. Ion or radical chemistry is certainly necessary to provide this heavy hydrogen, which therefore must have originated in the interstellar medium or in the outer part of the nebula. Until now, only organic macro-molecules have been identified in the interstellar medium [3]. These new data suggest that 1) interstellar water should also be enriched in deuterium (its D/H ratio has not been yet measured spectroscopically) 2) water condensed in a interstellar environment has been preserved during the formation of solar system solids.

[1] Robertt & Epstein, 1982, *Geochim. Cosmochim. Acta* 46, 81.

[2] Yang & Epstein, 1983, *Geochim. Cosmochim. Acta*, 47, 2199.

[3] Erhenfreund et al., 1991, *Astron. Astrophys.* 252, 712.

A SINGLE KIMBERLITIC EVENT ON THE KUNDELUNGU PLATEAU (SHABA, ZAIRE): A SR, ND AND PB ISOTOPIC STUDY OF THE KIMBERLITES AND THEIR MEGACRYST SUITE.

DEMAÏFFE, D., WEIS, D. Pétrol. Géodyn. Chimique, CP160/02, Université Libre de Bruxelles, Av. F.D. Roosevelt, 50, 1050 Brussels and KAMPATA, M., MOREAU, J., Lab. Minéralogie, Univ. de Louvain, 1348 Louvain-La-Neuve, Belgium.

Twenty four diamond-poor kimberlite pipes of probably late Cretaceous (70 Ma) age are known on the Kundelungu Plateau over an area of 4,500 km<sup>2</sup>. They intruded a 1.8 Ga gneissic basement. Ten pipes have been studied in detail, most of them are made of unbrecciated fresh kimberlites which contains two generations of olivine (Fo<sub>85-91</sub>), monticellite, ilmenite, spinels, perovskite and calcite. Phlogopite is absent. Typical megacryst suite (Cr-diopside, pyrope, olivine, ilmenite, orthopyroxene) occurs as well as both crustal (felsic gneiss) and mantle (lherzolite, eclogite) xenoliths.

The kimberlites are geochemically very similar. They have high MgO (28-34 %), Ni (950-3,000 ppm) and Cr (1,400-1,750 ppm) contents, low K<sub>2</sub>O (0.05-0.6 %) and appear very enriched in LREE (La<sub>N</sub>:3-400) but depleted in HREE (Yb<sub>N</sub><3) when compared to other 'group 1' kimberlites. Chondrite-normalized spidergrams show enrichment (200 to 3,000) for most LILE (except K). Two altered samples show extreme enrichment of all REE (La<sub>N</sub>:3-9,000; Yb<sub>N</sub>:70-200) except Ce resulting in an apparent negative Ce anomaly.

Initial (at 70 Ma) Sr and Nd isotopic compositions fall within a narrow range of values, between 0.70393 and 0.70487 for <sup>87</sup>Sr/<sup>86</sup>Sr and 0.51266 and 0.51277 (ε<sub>Nd</sub>: +2.1 to +4) which is comparable to the values of diamond-rich kimberlites from Mbuji Mayi (2d kimberlite province in Zaire). These typical 'group 1' kimberlite values indicate a time-integrated slightly LREE-depleted mantle source-region comparable to an OIB-type source. Initial Pb isotopic data are: <sup>206</sup>Pb/<sup>204</sup>Pb: 18.51-20.35, <sup>207</sup>Pb/<sup>204</sup>Pb: 15.64-15.75.

Crustal contamination is not detected in the Sr and Nd isotopic systems (except in one altered kimberlites with ε<sub>Nd</sub> = -1) but is visible in Pb ratios. The (<sup>207</sup>Pb/<sup>204</sup>Pb)<sub>i</sub> ratios are significantly higher than MORBs and OIBs suggesting crustal contamination.

The megacrysts (Cr-poor cpx, opx, pyrope) and the mantle xenoliths (one lherzolite, one eclogite) have ε<sub>Nd</sub> values (+1.1 to +2.6) comparable to but slightly less positive than their host kimberlites. Cpx have low Sr isotopic ratios (close to 0.7040) while opx and garnet have higher Sr isotopic ratios, up to 0.710. Initial Pb ratios of cpx are in the kimberlite range but the opx and lherzolite show much more scatter, suggesting crustal disturbance.

Mineralogical, geochemical and isotopic homogeneity of the fresh kimberlites implies an homogeneous mantle-source region and very uniform magmatic processes (degrees of melting and/or fractional crystallization) from one pipe to the other. This in turn suggests that the whole kimberlite province may have been formed by a single magmatic event.

STABLE CARBON AND OXYGEN ISOTOPES IN AN ALKALINE BASALTIC SUITE: PRIMARY COMPOSITIONS AND LOW TEMPERATURE RE-EQUILIBRATION PROCESSES

DEMÉNY, A., Laboratory for Geochemical Research, Hung. Acad. Sci., Budapest, Budaörsi út 45, 1112, Hungary, HARANGI, Sz., Dept. of Petrology and Geochemistry, Eötvös Loránd University, Budapest, Múzeum krt. 4/A, 1088, Hungary

The Mecsek alkaline basaltic suite formed in a continental rifting process during the lower Cretaceous and comprises mainly pyroxene-olivine basanites and alkaline basalts with subordinate amounts of tephrites, trachites, phonolites. The fluid-rich nature of these magmatic rocks is indicated by the presence of amphiboles and micas. The basaltic rocks contain calcite amygdales that are divided to two main types: recrystallized limestone xenoliths enclosed by lava rocks at magma-sediment contacts and calcite amygdales with fibrous texture often containing analcime. The latter type occurs in dyke rocks.

Oxygen isotopic compositions of mineral separates show positive shifts from primary magmatic values presumably depending on the degree of low temperature isotope exchange: pyroxenes (6.0 to 6.5 ‰), amphiboles (4.7 to 7.1 ‰), biotites (7.1 to 7.4 ‰), feldspars (7.6 to 15.0 ‰), analcimes (17.5 to 19.0 ‰). Calcite amygdales with carbon isotopic compositions (-8.4 to -6.3 ‰) characteristic for mantle-derived carbonates gave δ<sup>18</sup>O values ranging from 12.3 to 16.5 ‰. Those amygdales that show low temperature recrystallization gave higher δ<sup>18</sup>O values (15.1 to 16.5 ‰) than those without signs of recrystallization (12.3 to 13.4 ‰). Calcites amygdales formed at magma-sediment contacts have δ<sup>13</sup>C values (-1.0 to 0.6 ‰) characteristic for sedimentary carbonates.

The most controversial data were obtained on analcimes. The C and O isotope compositions and textural characteristics of calcites coexisting with analcimes suggest high temperature formation conditions, thus the δ<sup>18</sup>O values of analcimes (17.5 to 19.0 ‰) indicate the sensitivity of this mineral toward retrograde isotope exchanges.

SPATIAL AND TEMPORAL EVOLUTION OF MANTLE SOURCES DURING CONTINENTAL RIFTING: THE VOLCANISM OF AFAR.

DENIEL, C., CNRS, Université Blaise Pascal, Clermont-Ferrand, 63038, France, PIK, R. and COULON, C., CNRS, Université Aix Marseille III, Marseille, France, and VIDAL, Ph., CNRS, Université Blaise Pascal, Clermont-Ferrand, France.

Afar is a very favorable area for studying the interactions between lithosphere and asthenosphere during the opening of a continental rift by progressive stretching and thinning of continental crust and lithosphere, leading to oceanization. Magmatism occurred almost continuously over the past 25 m.y. and 50 m.y. in the Republic of Djibouti and in Ethiopia respectively. Only basaltic rocks, mainly of transitional type, are considered in this study. Large chemical and isotopic variations among the volcanic series are interpreted in terms of mantle source heterogeneity. In Djibouti, a clear evolution through time of the mantle sources is observed in relation to rifting (Vidal et al., 1991; Deniel et al., 1994). Three sources were involved in the genesis of these lavas: (1) an old subcontinental lithospheric component ( $^{87}\text{Sr}/^{86}\text{Sr}=0.706$ ,  $^{206}\text{Pb}/^{204}\text{Pb}\approx 17.9$ ), mainly observed in the oldest lavas (25 to 10 Ma), (2) an HIMU (high U/Pb ratio)-type reservoir, and (3) a depleted mantle. As rifting goes on, there is an increasing contribution of an HIMU-type mantle source. It is attributed to the influence of a mantle diapir (Afar plume). The geochemical characteristics of 9 to 1 Ma old lavas, erupted after the strong increase of spreading rate in Afar, reflect this evolution of mantle sources. The influence of the mantle plume is most prominent in the northern youngest lavas (<1 Ma), particularly Manda, characterized by the strongest HIMU signature ( $^{87}\text{Sr}/^{86}\text{Sr}=0.7035$ ,  $^{206}\text{Pb}/^{204}\text{Pb}\approx 19.2$ ). The contribution of the depleted mantle component originating from the asthenosphere is best recognized in the young (<4 Ma) lavas, particularly Tadjoura and Asal lavas (3 to 1 Ma). Preliminary results on Quaternary lavas from Ethiopia indicate that they have rather homogeneous Nd isotopic ratios, similar to those of <4 Ma Djibouti lavas. Although some lavas exhibit Sr and Pb isotopic compositions similar to those of Manda and Inakir lavas, two groups of lavas plot below the Sr-Pb trend defined by Djibouti lavas. Manda Hararo lavas with less radiogenic Sr and Pb isotopic compositions than Asal lavas and Tana lavas with lower Sr isotopic ratios than Inakir lavas, although with similar Pb isotope ratios. All these data will be discussed in terms of spatial and temporal evolution of mantle sources in relation to rifting and mantle plume dynamics.

Deniel, C., Vidal, Ph., Coulon, C., Vellutini, P.J., and Pigué P., in press, Temporal evolution of mantle sources during continental rifting: the volcanism of Djibouti (Afar): J. Geophys. Res.

Vidal, Ph., Deniel, C., Vellutini, P.J., Pigué, P., Coulon, C., Vincent, J., and Audin, J., 1991, Changes of mantle sources in the course of a rift evolution: the Afar case. Geophys. Res. Lett., 18, p. 1913-1916.

NUMERICAL SIMULATIONS OF COSMOGENIC NUCLIDE PRODUCTION IN ROCKS FOR VARIOUS EXPOSURE GEOMETRIES

DEP, Linus, ELMORE, D., Department of Physics, Purdue University, West Lafayette, IN 47907, U.S.A., FABRYKA-MARTIN, MASARIK, J., and REEDY, R.C. Los Alamos National Laboratory, Los Alamos, NM 87545, U.S.A.

*In-situ* produced cosmogenic nuclides in terrestrial rocks provides a means of determining exposure ages and erosion histories of landforms. To obtain useful quantitative information requires a good understanding of nuclide production systematics. The build-up of nuclides is sensitive to physical and chemical processes such as weathering, uplifting, and covering by snow and soil. Often more than one of these effects are present making experimental study of nuclide production difficult, requiring theoretical methods to understand production fundamentals.

A model based on a low-energy neutron Monte Carlo transport code, MCNP, has shown a great promise in predicting the systematics of nuclide production by neutron capture. Incorporating a high energy nucleon-meson Monte Carlo transport code, LAHET, the model can include systematics of high-energy spallogenic nuclide production.

We will present the MCNP-based model predictions for the depth dependence of thermal neutron fluxes in a concrete block covered with a water layer and compare them with experimental measurements. We will present predicted depth profiles of cosmogenic neutron-capture produced  $^{36}\text{Cl}$  for rocks covered with snow and soil using the MCNP-based model. We will also present the predictions of production dependence on rock size for both spallogenic and neutron capture products using a model based on both LAHET and MCNP.

## FILTERING OF MANTLE ISOTOPIC HETEROGENEITY BY MAGMA GENERATION PROCESSES

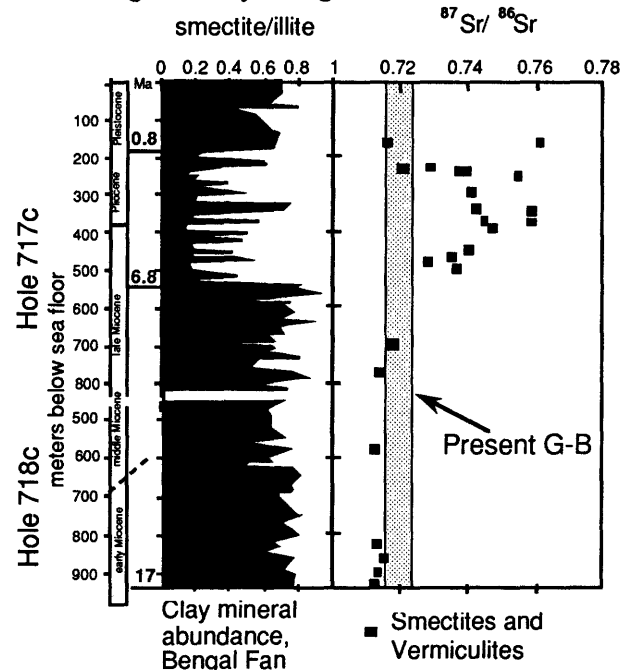
DEPAOLO, D.J., Berkeley Center for Isotope Geochemistry, Department of Geology and Geophysics, University of California, Berkeley, CA 94720

The geochemistry of basaltic lavas is useful as a means of characterizing mantle convection. The "sourcing" of heterogeneities puts qualitative constraints on large scale convection, and the lengthscale spectrum of heterogeneity can yield quantitative constraints on flow properties. Stacks of lavas yield a time series of geochemical properties that need to be converted to a spatial pattern in the mantle source. Improving the ability to do this mapping is necessary to fully utilize the data on lavas for understanding the interior of the earth. Recent development of models that describe the magma generation and transport in the mantle, coupled with analysis of the effects of residence in magma chambers or melt collection zones, allow construction of analytical expressions that relate, for instance, isotopic ratio-versus-time data from lava sequences, to isotope ratio-versus-depth in the mantle source material. A simple analysis for a steady-state melt zone continuously resupplied with heterogeneous material at its lower boundary suggests that diffusive effects through the melt zone will attenuate heterogeneities of wavelength 3m for incompatible elements and 30m for compatible elements. At 10cm/yr upwelling rate these correspond to periods of 30 and 300 years in the lava sequence. Another way of stating this is that variability in lavas on ca. 100 year time scales represents a highly attenuated version of the heterogeneity in the mantle source at 10m wavelength. Magma storage at the top of the melt zone or in shallower chambers has a further, and larger, attenuating effect on the expression of mantle heterogeneity in the lavas. For magma residence times of 1000 to 100,000 years, mantle heterogeneity wavelengths of 300m to 30km are effectively attenuated. Phase shifts of elements with different compatibilities are also expected, and their observed magnitude places limits on the melting parameters. The definition of homogeneous versus heterogeneous magma sources needs to be reevaluated in these terms, as do inferred mixing relations between source components.

## INTERPRETING MARINE TRACER RECORDS: A NEOGENE RECORD OF CHANGING RIVER $^{87}\text{Sr}/^{86}\text{Sr}$ FROM THE HIMALAYAN REGION

DERRY L.A., Cornell U., Dept. of Geol. Sci., Ithaca, NY 14853-1504, USA (derry@geology.cornell.edu) and FRANCE-LANORD, C., CRPG-CNRS, BP20 54501 Vandoeuvre, France.

The ability to interpret variations in marine tracer records such as  $^{87}\text{Sr}/^{86}\text{Sr}$  and Ge/Si is limited by our ability to quantify the tradeoff between changing river compositions and/or fluxes. Here we present data from secondary minerals derived from chemical weathering in the Ganges-Brahmaputra watershed.  $\delta^{18}\text{O}$  -  $\delta\text{D}$  measurements show that these minerals have been equilibrated in the G-B floodplain. Sr-bearing phases include smectites and vermiculites. Recrystallization during formation of these minerals implies extensive exchange of interlayer cations and thus isotopic reequilibration. Thus these minerals can constrain the  $^{87}\text{Sr}/^{86}\text{Sr}$  of ambient waters.  $^{87}\text{Sr}/^{86}\text{Sr}$  of smectites and vermiculites are near modern G-B river values prior to 7 Ma and after 0.8 Ma. From 7 to 0.8 Ma, smectite/illite ratios are much higher, and smectites are much more radiogenic. We infer that during this period of intense chemical weathering,  $^{87}\text{Sr}/^{86}\text{Sr}$  in G-B river water was significantly greater than at present. An increase in river water  $^{87}\text{Sr}/^{86}\text{Sr}$  is also suggested by measurements from coeval Siwalik carbonates (Quade, 1993). Shifts in late Miocene-Pliocene seawater  $^{87}\text{Sr}/^{86}\text{Sr}$  and Ge/Si may be related to changes in the composition of the dissolved load of the G-B system, driven by both climate-related weathering intensity changes and tectonics.



## ORIGIN AND RATE OF FLUID CIRCULATION IN CONVERGENT MARGINS

DIA, A.N., Laboratoire de Géochimie, Géosciences Rennes, Université Rennes 1, Campus Beaulieu, 35042 Rennes cédex - France, AQUILINA, L., BRGM, 45060 Orléans cédex 2 - France, CASTREC, M. and BOULEGUE, J., Laboratoire de Géochimie et Métallurgie, Tour 26 -16, E5, 4 place Jussieu - 75252 Paris - France.

Fluid circulation in subduction zones has been studied in two areas: Barbados and Peru.

Pore fluids have been recovered from an active diapiric field located in the accretionary complex of Barbados (13°5N). The chemical analyses show that Cl and other major element-depleted fluids are rapidly expelled through the diapiric structures. The structures characterized by the strongest thermal and chemical anomalies correspond also to the highest expulsion rates: up to 1m/yr for the central zone of the "Atalante" diatreme. The  $^{87}\text{Sr}/^{86}\text{Sr}$  ratios of the fluids suggest that the fluids cannot firstly originate from the South American basin of Orinocco, and secondly result from a seawater/sediments interaction.

A comparable study has been undertaken on samples collected off Peru (5-7°S). These fluids show Cl, Ba and  $^{87}\text{Sr}$  enrichments as compared to common bottom seawater. These enrichments can be related to a mixing between meteoric waters circulating within the metamorphic basement and sedimentary brines from the upper part of the margin. Reactions between seawater and continental-derived material can be suggested to explain such high  $^{87}\text{Sr}/^{86}\text{Sr}$  ratios in the fluids. The Sr isotopic compositions of large authigenic barite deposits only located close to the fluid venting imply a continental origin for the fluids responsible for the barite deposit. The fluids responsible for the deposition of the barite can be proposed as good candidates. The occurrence of such barite deposits implies an increase of the fluid temperature in the past without any evidence today. This paroxysmal event has to be probably related to important tectonic events, even earthquakes.

This study shows that if faults are always efficient conduits for focusing fluid flow and fluid expulsion in subduction zones, the origin and the nature of fluids inferred using geochemical and isotopic analyses is not unique, and the expulsion sometimes violent.

## THE SILICON ISOTOPE VARIATIONS IN GEOCHEMICAL CIRCULATION

DING, T., JIANG, S., WAN, D. and LI, Y.,  
Institute of Mineral Deposits, CAGS,  
Beijing 100037, P.R. China.

The silicon isotope compositions of over 1,000 terrestrial samples have been determined, and a general picture of Si isotope variation in geochemical circulation has been configured in recent years.

In magmatic processes, thermodynamic Si isotope fractionation is significant, causing remarkable difference between Si isotope composition of mafic rocks and that of acidic rocks. The former has a mean  $\delta^{30}\text{Si}$  value of  $-0.6$ , and the latter has a mean  $\delta^{30}\text{Si}$  value of  $-0.1$ .

In the weathering processes, the clay mineral products have normally lower  $\delta^{30}\text{Si}$  value ( $-0.1$  to  $-1.9$ ) than that of the original rocks, and the silicon dissolved in solution has higher  $\delta^{30}\text{Si}$  value.

In the biochemical processes; the Si isotope fractionation trends are very complex: the diatom, sponges and bamboo intend to have lower  $\delta^{30}\text{Si}$  values than those of dissolved Si in the water, but the equisetum intend to have higher  $\delta^{30}\text{Si}$  values than those of dissolved Si in the water.

The Si isotope compositions are quite variable in the ocean water. The deep water near the middle ocean ridge and in the ocean trough has  $\delta^{30}\text{Si}$  values similar to those of submarine volcanic rocks. However, the nearshore sea water has higher  $\delta^{30}\text{Si}$  value for the input of river water silicon having higher  $\delta^{30}\text{Si}$  value. Accordingly, the radiolaria of shallow water has higher  $\delta^{30}\text{Si}$  values (0.2 to 0.8) than those of deep sea radiolaria ( $-0.3$  to  $-0.6$ ). The  $\delta^{30}\text{Si}$  values of siliceous carbonate (0.1 to 2.8) and stromatolite (2.4 to 3.4) are even higher.

In the hydrothermal processes, the silica precipitates have always lower  $\delta^{30}\text{Si}$  values than those of Si remaining in the solution, as a result of kinetic isotope fractionation. For example, the silica sinter has  $\delta^{30}\text{Si}$  values from 0.2 to  $-3.4$ , the siliceous rocks from black smoker in the Mariana Trench have  $\delta^{30}\text{Si}$  value from  $-0.4$  to  $-3.1$ , and the quartz in BIF have  $\delta^{30}\text{Si}$  value of  $-0.8$  to  $-2.2$ .

As to the metamorphic processes, no large scale Si isotope fractionation has been found yet. We can only see the small scale Si isotope fractionation among coexisting silicate minerals.

MODELING AND MEASUREMENTS OF  
RADIOGENIC NUCLIDES IN URANIUM MINERALS:  
IMPLICATIONS FOR SPENT FUEL STABILITY

DIXON, P.R., FABRYKA-MARTIN, J., CURTIS,  
D.B., ROKOP, D.J., Chemical Science and  
Technology Division, Los Alamos National  
Laboratory, Los Alamos, NM 87545; CRAMER, J.,  
AECL Research, Pinawa, Manitoba R0E 1L0;  
CORNETT, J., Environmental Research Branch, Chalk  
River Laboratories, Chalk River, Ontario, K0J 1J0;  
KILIUS, L., Isotracer Laboratory, University of  
Toronto, Toronto, Ontario, M5S 1A7; SHARMA, P.,  
PRIME Lab, Physics Laboratory, Purdue University,  
West Lafayette, IN 47907

Among the most persistent radioactive constituents of spent fuel are long-lived  $^{239}\text{Pu}$ ,  $^{99}\text{Tc}$ , and  $^{129}\text{I}$ . The extent to which these nuclides will be retained by a waste repository will be in large part a function of their retention by the waste form and retardation by the natural geologic environment along any flow path. Uranium minerals offer a means to evaluate the geochemical transport and retention properties of these nuclides in natural materials analogous to spent fuel under a variety of geochemical conditions.

Measured abundances of natural occurrences of these nuclides in uraninite and other U-bearing mineral phases are compared to abundances predicted using the Monte Carlo neutron transport code MCNP to evaluate the degree of retention of these radionuclides by the host minerals. Measurements of neutron-capture product  $^{36}\text{Cl}$  are used to assess the validity of the code predictions and to constrain production rate estimates where modeling uncertainties are excessively large.

Release rates are shown to be immeasurably slow at the Cigar Lake uranium deposit (Canada), which is a reducing environment isolated by a clay barrier from the surrounding aquifer. In contrast, large deficiencies of  $^{129}\text{I}$ , and small ones of  $^{99}\text{Tc}$ , are observed in ore samples from the shallow Koongarra deposit (Australia), which is subject to relatively fast-moving, oxidizing groundwaters. No deficiencies of  $^{239}\text{Pu}$  are observed in any of the samples studied to-date.

PLUMBOTECTONICS OF THE ABSAROKA-GALLATIN  
VOLCANIC PROVINCE, WY AND MT

DOE, B.R., U.S. Geological Survey, 923 National  
Center, Reston, VA 22092

Thirteen new analyses of Pb isotopes in igneous whole rocks and ore minerals from the Absaroka-Gallatin volcanic province (AG) of Wyoming and Montana help fill out the Pb isotope picture of AG and the Yellowstone Plateau volcanic field (YP). The Quaternary bimodal YP field overlaps with the western part of the Tertiary andesite-series AG. Values of  $^{206}\text{Pb}/^{204}\text{Pb}$  ( $\alpha$ ),  $^{207}\text{Pb}/^{204}\text{Pb}$  ( $\beta$ ), and  $^{208}\text{Pb}/^{204}\text{Pb}$  ( $\gamma$ ) for the new data range from 15.66 to 18.11, 15.24 to 15.50, and 36.43 to 37.95, respectively. These isotopic ranges lie within those previously reported for the region although some samples are at the isotopic extremes. The new data, however, have no clear representative for the previously reported data from the Independence volcanic center (IVC) in the northeastern AG involving a 3,800 Ma source.

Most new data lie close to a 2,800 Ma regression noted previously that encompasses both the YP rhyolite and the Archean igneous rocks of the Beartooth Mtns. on an  $\alpha\beta$  plot. The new data are only slightly higher in  $\beta$  than YP basalts but significantly higher than most rocks of the IVC. In spite of the similarity among the YP rhyolites, AG andesite-series, and Beartooth Mtns. surface Archean rocks in  $\alpha\beta$  plots, surface Archean rocks tend to have much higher values of  $\gamma$  than the Cenozoic igneous rocks. This difference precludes major involvement of shallow Archean in any Cenozoic igneous melts, as previously noted for rhyolites.

Unlike the values of  $\beta$ , values of  $\gamma$  in the AG andesite series tend to be lower than YP rhyolites and more similar to those of YP basalts, the AG IVC, and other mafic igneous centers to the northwest. Therefore, these three series could not have solely generated the rhyolites. Two main trends are apparent on  $\alpha\beta$  and  $\alpha\gamma$  plots for the andesite series and basalts -- one from a previously proposed Archean mix of mantle Pb with subducted sediment Pb of high initial  $\beta$  (lithospheric mantle(?)) toward a Plumbotectonic II modern mantle; the other from the lithospheric mantle(?) that evolved until the Cenozoic with reduced  $^{238}\text{U}/^{204}\text{Pb}$  (~3-6) and  $^{232}\text{Th}/^{204}\text{Pb}$  (~19-30), compared to "normal" values (9.7 and 37, respectively). The trend towards a Plumbotectonic II mantle also trends toward regional Phanerozoic sediment Pb isotopes, but the Pb concentration balance obviates sediment involvement.

LASER  $^{40}\text{Ar}/^{39}\text{Ar}$  DATING OF BENTONITES AND SHALE FROM WALES

DONG, H., HALL, C.M., PEACOR, D.R. and HALLIDAY, A.N., Dept. of Geological Sciences, U. of Michigan, Ann Arbor MI, 48109-1063, USA

Three bentonites and one shale were studied using the laser probe  $^{40}\text{Ar}/^{39}\text{Ar}$  method. This was a preliminary test prior to the use of vacuum encapsulation experiments to directly determine the extent of  $^{39}\text{Ar}$  loss due to recoil from these clay-dominated rocks. The sub-millimeter clumps of clay were irradiated in a vacuum and thermal contact with the reactor's cooling water was optimized to reduce Ar loss due to self-heating.

An epizone-grade Cambrian bentonite ( $\Delta 2\theta=0.21$ ) from S. Wales yields plateau ages averaging to  $421\pm 1$  Ma ( $2\sigma$ ) and an average integrated age of  $410\pm 2$  Ma. The integrated age is consistent with an Rb-Sr whole-rock age of  $409\pm 11$  Ma for epizone-grade Paleozoic mudrock suites from Snowdonia (Evans, 1989) and probably represents the blocking age of late Silurian to early Devonian Acadian regional metamorphism. The 421 Ma plateau age is consistent with Sm-Nd ages of  $420\pm 20$  Ma for epizone-grade Ordovician slates (Ohr et al., 1994) and possibly records the peak of metamorphism. Neither diagenetic ( $\Delta 2\theta=0.52$ ) nor low-anchizone ( $\Delta 2\theta=0.38$ ) Ordovician bentonite (Roberts & Merriman 1990) gives meaningful ages, presumably due to  $^{39}\text{Ar}$  recoil loss from imperfection-rich smectite, I/S and illite.

Since the previous clay samples released Ar at extremely low temperatures, subsequent runs were performed on samples which had not been baked prior to analysis. Three size fractions ( $<5\mu\text{m}$ ,  $<1\mu\text{m}$  and  $<0.2\mu\text{m}$ ) of one diagenetic grade Ordovician shale (depositional age 449-461 Ma) yielded integrated ages of  $481\pm 3$ ,  $465\pm 2$  and  $466\pm 3$  Ma respectively. This agrees well with Sm-Nd ages of  $500\pm 26$ ,  $468\pm 25$  and  $463\pm 26$  Ma on identical size fractions from a slightly older shale (464-470 Ma). The Ar age for the  $<0.2\mu\text{m}$  fraction is identical to the Sm-Nd result on the same size fraction from the same shale (Ohr et al. 1994).

The excellent match between the  $^{40}\text{Ar}/^{39}\text{Ar}$  and Sm-Nd ages suggests that there has been little net loss of  $^{39}\text{Ar}$  due to recoil, although later experiments using vacuum encapsulation will measure this directly. It is also encouraging that the ages from both the  $<0.2\mu\text{m}$  and  $<1\mu\text{m}$  fractions, which are rich in authigenic clay, correspond well with the known depositional age of the shale. However, most of the clay age spectra have a characteristic "hump" shape with large apparent age swings both above and below the integrated age, suggesting that there is significant  $^{39}\text{Ar}$  redistribution due to recoil. Both TEM observations and vacuum encapsulation experiments are underway to clarify these features.

Evans, J.A. 1989, A note on Rb-Sr whole-rock ages from cleaved mudrocks in the Welsh Basin, *J. Geol. Soc. Lond.* 146, 901-904.

Ohr, M., Halliday, A.N. and Peacor, D.R., 1994, Mobility and fractionation of rare-earth elements in argillaceous sediments ..., *Geochim. Cosmochim. Acta.* in press.

Roberts, B and Merriman, R.J., 1990, Cambrian and Ordovician metabentonites ..., *Geol. Mag.* 127, 31-43.

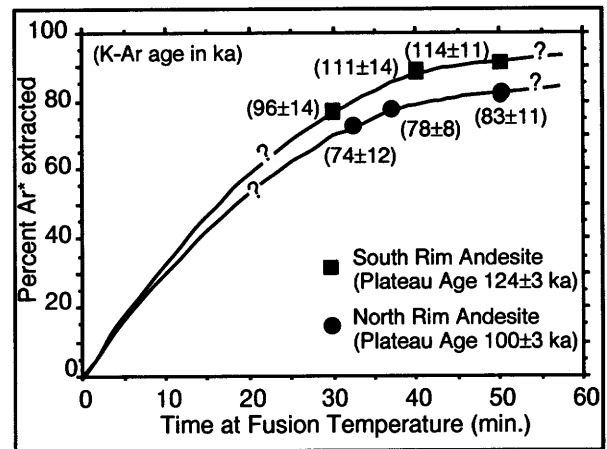
INCOMPLETE EXTRACTION OF RADIOGENIC ARGON FROM HIGH-SILICA ANDESITES: IMPLICATIONS FOR K-Ar DATING

DONNELLY-NOLAN, J.M., TURRIN, B.D. (1), GRAY, L.B., and CONRAD, J.E., U.S. Geological Survey, 345 Middlefield Rd., Menlo Park, CA, 94025, USA.

(1) also affiliated with Institute of Human Origins, Geochronology Center, 2453 Ridge Rd., Berkeley, CA, 94709, USA.

K-Ar and  $^{40}\text{Ar}/^{39}\text{Ar}$  dating of rocks from Medicine Lake volcano, California, indicate that incomplete quantitative extraction of radiogenic  $^{40}\text{Ar}$  ( $^{40}\text{Ar}^*$ ) can occur in high-silica (59-63%  $\text{SiO}_2$ ) andesites (HSA), resulting in K-Ar ages that are too young. Provided that the system is undisturbed, incremental  $^{40}\text{Ar}/^{39}\text{Ar}$  heating analysis obviates this problem because absolute concentrations of potassium and argon are not required to calculate an apparent age.

$^{40}\text{Ar}/^{39}\text{Ar}$  analysis from two Medicine Lake volcano HSA units (north and south rim andesites) yield undisturbed plateau ages ( $\geq 95\%$  of the total  $^{39}\text{Ar}$ ) of  $100\pm 3$  ka and  $124\pm 3$  ka, respectively. These ages are significantly older (as much as 25%) than the corresponding K-Ar ages of  $74\pm 12$  ka and  $96\pm 12$  ka. The original K-Ar dated samples were heated to fusion temperatures ( $\sim 1300$  to  $1400^\circ\text{C}$ ) for 30 min. Replicate extractions of these samples using longer fusion times show a regular increase in percent extracted  $^{40}\text{Ar}^*$  (see Figure). Even with fusion times of 50 min, apparently 10 to 20% of the  $^{40}\text{Ar}^*$  was still not extracted from the samples based on comparison with the  $^{40}\text{Ar}/^{39}\text{Ar}$  plateau ages.



This phenomenon, well documented for sanidine K-Ar ages (McDougall et al. 1980; McDowell 1983), was first observed for K-Ar ages on HSA in the Clear Lake volcanic field (Donnelly-Nolan et al., 1981). As in this case, increased extraction time demonstrated a consistent increase in age. This suggests that K-Ar ages of other HSA should be considered suspect.

McDougall, I., Brown, F.H., Cerling, T.E., and Hillhouse, J.W., 1992, *Geophys. Res. Lett.*, v. 19, p. 2349-2352.

McDowell, F.W., 1983, *Chem. Geol., Isotope Geosci.*, v. 1, p. 119-126.

Donnelly-Nolan, J.M., Hearn Jr., C., Curtis, G.H., and Drake, R.E., 1981, *U.S. Geol. Surv. Prof. Paper* 1141, p. 47-60.

**GEOCHEMICAL MORPHOLOGY OF THE NORTH MID-ATLANTIC RIDGE: NEW DATA (10°-24°N) PUT IN THE PERSPECTIVE OF THE 10°-70°N SECTION**

DOSSO, Laure, URA 1278, Ifremer, B.P. 70, 29280 - Plouzané, France, BOUGAULT, Henri, Ifremer, B.P. 70, 29280 - Plouzané, France, JORON, Jean-Louis, Laboratoire P.Süe, C.E.N.S., B.P. 2, 91191 - Gif/Yvette, France.

The new data presented here from the 10-24°N MAR ridge segment

- show that the 10° - 24°N segment is the most depleted from the 10° - 70°N section of the N-MAR .
- show the existence of a geochemical gradient from the 14°N anomaly to 17°10'N: decreasing Sr and Pb isotopic ratios, increasing Nd isotopic ratios while K/Nb ratio stays constant with latitude.
- show the existence of a very depleted mantle source (lowest Sr isotopic ratios found so far in the North Atlantic), located at about 17°N.
- show the existence of a geochemical «deep» located at about 17°10'N, with no relation to a structural feature. The 15°20'N fracture zone does not form a geochemical boundary.
- show a constant K/Nb ratio from 12 to 17°N for basaltic glasses with widely different XREE patterns and Sr, Nd, Pb isotopic ratios (very depleted to enriched). This emphasizes the strong coherence of behaviour between the three elements K-Nb and Ta during the petrogenetic processes involved in the generation of these mid-ocean ridge basalts.
- lead us to favour the existence of local individual mantle sources at the scale of a ridge segment over interpretations in terms of binary mixing between mantle sources of types described in far away places all over the globe.
- and allow to talk about different «chemical memories» as recorded by different geochemical tools whether they are trace element ratios or isotopic ratios.

The compilation of data from 10 to 70°N shows a generally good correlation between trace element and isotopic ratios. However only the Sr isotopic ratios reveal the Azores superstructure whereas both Sr isotopic ratios and trace element ratios (La/Sm-Nb/Zr) trace the second order structures (Azores Triple Junction and 45°N) superimposed on the superstructure.

The N-MAR section between 17°10'N and 33°N (Hayes F.Z.) and the South East Indian ridge section between 25°N and 33°N display comparable depleted trace element ratios (La/Sm and Nb/Zr) typical of N-MORBs but variable Sr isotopic ratios ranging from 0.7022 to .7030. This suggests that the mantle domains involved suffered fractionation events of comparable extent but at different times.

**LAKE ONTARIO AND LAKE ERIE SEDIMENT INTERSTITIAL WATER - AUTOCHTHONOUS OR ALLOCHTHONOUS**

DRIMMIE, R.J., FRAPE, S.K., and THOMAS, R.L.  
Department of Earth Sciences, University of Waterloo,  
Waterloo ON, N2L 3G1 Canada.

Land based groundwater geochemical surveys in Ontario and New York State have found highly saline fluids in the shallow environment. These fluids are believed to have their origin in the deep sedimentary rock environment. Recent investigations have shown a direct link between groundwater input and possible pollution sources to the Great Lakes. Over sixty cores up to eighteen meters long have been collected from Lake Ontario courtesy of the Canada Center for Inland Waters.

Interstitial pore water from every meter in a number of cores has been analyzed for major ions, oxygen-18, deuterium and chlorine 37/35. Ostracod and pelecypoda were separated and analyzed for oxygen isotope content. The results show progressive increases in Na and Cl with depth at all sites. The general increase towards depth indicates ion movement from a higher concentration under the sediments. The isotope signature indicates mixing of at least four different sources, one of which appears to be a relict glacial melt water. Comparison of shell and interstitial water oxygen isotope values indicate zones where groundwater has moved into the sediment. Chlorine isotope content helps delineate the bedrock source.

## NOBLE GASES IN GRANULITES FROM THE NILGIRI HILLS, SOUTHERN INDIA

DUNAI, T.J.<sup>1,2</sup> and HILTON, D.R.<sup>2</sup>; 1) Isotope Geochemistry, NO-C0 61.5, ETH Zürich, 8092-Zürich, Switzerland, 2) Earth Sciences, Isotope Geology, Free University, 1081 HV Amsterdam, The Netherlands.

Mantle-derived noble gases contained in primary carbonic fluid inclusions were reported recently for a 2.5 Ga granulite sample from the Nilgiri Hills, Southern India (Dunai and Touret, 1993). Because this finding has important implications for regional granulite formation, our aim in the present work was to validate this finding utilising an extensive suite of lower crustal rocks from the area. We report new He, Ne and Ar isotopic and elemental results for enderbites, charnockites and meta-sediments from the Nilgiri Hills and for a meta-gabbro from the adjacent Bahvani Shear Zone. The samples come from localities scattered over an area of 650 km<sup>2</sup>.

We analyzed coarse-grained (1-3mm) garnet separates as the primary carbonic fluid inclusions were present only in the garnets or in quartz inclusions in the garnets (Srikantappa et al. 1992). The garnets had inclusion free rims but the cores were distinctive and contained abundant mineral- and primary fluid-inclusions. Only garnets from a meta-gabbro from the Bahvani Shear Zone contained abundant secondary fluid inclusions.

The analysis of the noble gases liberated by crushing of the garnet separates confirm the findings of Dunai and Touret (1993). The fluid inclusions of most garnets contained helium with <sup>3</sup>He/<sup>4</sup>He ratios between 0.8 and 1.7 times the atmospheric ratio ( $R_a$ ). Only in garnets from localities in the immediate vicinity of the Moyar Shear Zone and from within the Bahvani Shear Zone we did find more radiogenic <sup>3</sup>He/<sup>4</sup>He ratios, with values of 0.2 and 0.6 $R_a$  respectively. The highest <sup>3</sup>He/<sup>4</sup>He values (>0.8  $R_a$ ) were preserved in meta-intrusives as well as meta-sediments: thus, the carrier of the high <sup>3</sup>He/<sup>4</sup>He signature - mantle-derived carbonic fluids - were probably ubiquitous in the lower crustal segment now exposed in the Nilgiri Hills.

The presence of nucleogenic Ne in the fluid inclusions of some garnets (<sup>21</sup>Ne/<sup>22</sup>Ne up to 0.16±0.02) indicates that a substantial proportion of the <sup>4</sup>He in the fluid inclusions has grow-in by radiogenic decay. Therefore, the original <sup>3</sup>He/<sup>4</sup>He ratio of helium trapped in the garnets was considerably higher than today thereby substantiating the presence of a mantle-derived carbonic fluid.

Dunai, T.J. and Touret, J.L.R., 1993, A noble gas study of a granulite sample from the Nilgiri Hills, southern India: implications for granulite formation: *Earth Planet. Sci. Lett.*, v. 119, p. 271-281.

Srikantappa C., Raith, M. and Touret, J.L.R., 1992, Synmetamorphic high-density carbonic fluid inclusions in the lower crust: evidence from the Nilgiri granulites, southern India: *Jour. Petrol.*, v. 33, p. 733-760.

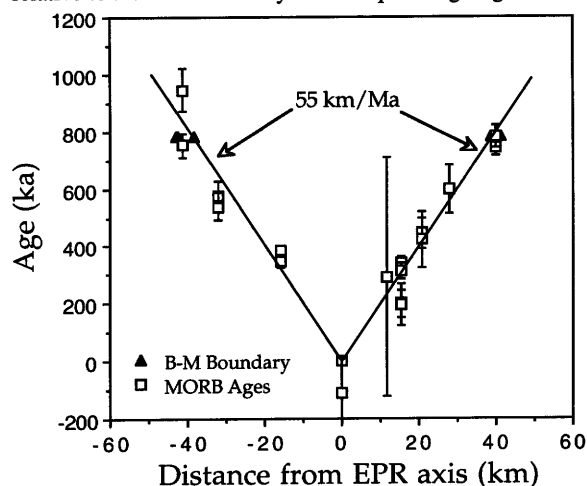
## RADIOMETRIC DATING OF YOUNG MORBs: INITIAL RESULTS USING A <sup>40</sup>Ar-<sup>39</sup>Ar INCREMENTAL HEATING PROCEDURE

R A DUNCAN and L G HOGAN (COAS, Oregon State University, Corvallis, OR 97331; rduncan@oce.orst.edu)

Determination of reliable crystallization ages by K-Ar methods for young (<1 Ma), fresh basalts from the seafloor has been frustrated by several issues. The small amounts of radiogenic <sup>40</sup>Ar developed over these timescales in such low-K rocks are difficult to resolve from predominantly atmospheric <sup>40</sup>Ar. An additional concern is that mantle-derived <sup>40</sup>Ar may not be totally outgassed when magmas quench at seafloor hydrostatic pressures, and the initial composition of Ar may not be atmospheric. However, developing quantitative chronologic methods is essential for determining the sequence and rates of volcanic and tectonic events associated with seafloor spreading.

We report initial results of an exploratory program of dating MORBs using <sup>40</sup>Ar-<sup>39</sup>Ar incremental heating experiments. Our new analytical system employs a high-sensitivity mass spectrometer (model MAP 215-50) with low-blank, all-metal gas extraction line. Samples (100-200 mg mini-cores and ground rocks) are dropped into a Mo-lined, Ta crucible and heated in a double vacuum resistance furnace in which T is thermocouple-controlled.

Samples from detailed transects across "zero-age" pillow blocks, from glassy margins to holocrystalline interiors, show that excess <sup>40</sup>Ar is confined to the outermost few cm, in agreement with previous studies. We have developed a successful strategy for partially separating sample <sup>40</sup>Ar(atm) from <sup>40</sup>Ar(rad), following Hall and York (1978). Pre-heating samples to 400°C removes surficial <sup>40</sup>Ar(atm). Subsequent heating at 600°-1000°C produces favorable proportions of <sup>40</sup>Ar(rad), especially at T~800°C. Ar extracted at higher temperatures is largely atmospheric. We have calibrated our procedure using "zero-age" samples, Quaternary standards, and a suite of stratigraphically-controlled basalts from Iceland which we have dated previously using conventional K-Ar methods. A geologically-controlled suite of MORB samples from the East Pacific Rise near the Clipperton Fracture Zone has been dated using our procedure. These come from three dredge transects run perpendicular to the EPR, each out to the Brunhes-Matuyama magnetic polarity boundary. In general, measured ages fall very close to those extrapolated from dredge location relative to the B-M boundary and the spreading ridge.



**Fission track evidence on the Pliocene-Quaternary uplift of the margin of the Pannonian basin (Hungary)**

DUNKL, I., Lab. for Geochemical Research,  
Hungarian Acad. Sci., Budapest, H-1112,  
Hungary

The deposition of the sediment filling of the Pannonian basin started in Middle Miocene (~ 17 Ma). The deepest water and the highest sedimentation rate formed around 7-5 Ma. During the last 5 Ma the evolution of the Pannonian realm has changed. The margins and some zones show significant emergence related to the newly formed compressional tectonics. The evidences of the uplift are (I): folding, erosion and overthrust on Late Miocene sediments, (II): remnants of Miocene sediment on raised basement highs, above the top level of the sediment filling of the basin -at the altitude of 7-800 m, (III): basalt flows of Pliocene age preserved as monadnock above the surrounding relief.

The apatite fission track analysis is the most sensitive method to detect and evaluate the size of this young uplift. Basement rocks of Paleozoic and Mesozoic age, Paleogene and Neogene volcanic tuff layers and synrift clastic sediments were chosen for fission track thermochronology.

The apparent fission track ages and the shortening of almost all the tracks prove the young termination of the burial. The different zones of the margins of the basin have been exhumed during 5-2 Ma. The thickness of the eroded sequences in some zones exceeded 1000 m.

**A Major Element, Trace Element, and Isotopic Study of the Large-volume, Chemically-zoned Eruption of Baitoushan, 1010 AD**

C E Dunlap and J B Gill (Earth Sciences  
Department, University of California, Santa  
Cruz, CA 95064; cdunlap@cats.ucsc.edu)

Baitoushan volcano (located in the Changbai mountains on the China/N. Korea border) erupted more than 150 km<sup>3</sup> of bulk rock (50 km<sup>3</sup> dense rock equivalent) in 1010 ±10 AD. The eruption is compositionally zoned from comendite in pumiceous airfall and proximal lag deposits to a mixture of comendite and trachyte in pyroclastic flow units.

Trachyte compositions range from 61 to 69 wt. % SiO<sub>2</sub>, comendites range from 72 to 73 wt. %. In Harker diagrams (eg. K<sub>2</sub>O vs. SiO<sub>2</sub> and Al<sub>2</sub>O<sub>3</sub> vs. TiO<sub>2</sub>) the rocks form two distinct groups: one related by crystal fractionation, the other by magma mixing. Trace element concentrations vary by factors of less than 3, in the case of Rb, to over 100, in the case of Sr. Compatible vs. incompatible element diagrams separate the deposits into groups identical to those identified using major elements.

Trachytes contain phenocrysts of sanidine, hedenbergite, fayalite and apatite. Comendites contain Na-sanidine, ferroaugite, apatite and chevkinite. Least squares modeling of differentiation from trachyte to comendite suggests that >70 relative wt. % of the fractionating assemblage is sanidine. This is consistent with the sense of the fractionation trends identified in both major and trace element plots. Rocks apparently related by mixing exhibit black and grey banding and intermingling in outcrop. Further evaluation of the nature, causes, and timescale of chemical zonation will be presented using elemental and Nd, Pb, Sr, and U-Th isotopic data.

#### **$^{40}\text{Ar}/^{39}\text{Ar}$ DATING OF DEFORMATION: COMPETING CLOSURE MECHANISMS**

Dunlap, W. J., UCLA, Earth and Space Sciences,  
Los Angeles, California, 90024 USA

Resolving the timing of lower greenschist facies deformational events by  $^{40}\text{Ar}/^{39}\text{Ar}$  geochronology has been aided by 1) kinetic studies of argon diffusion in K-feldspar and 2) the identification of dominant mechanisms of closure in synkinematic and relict white micas (i.e. neocrystallization, cooling through closure temperature, cessation of intracrystalline glide, etc). By combining the thermal history information from multi-diffusion-domain modeling of K-feldspars with isotopic, geochemical and microstructural data from synkinematic and relict white micas it is possible, in special cases, to date specific deformational events (as opposed to cooling).

Depending on the mechanism by which argon is quantitatively retained, white micas from rocks deformed at  $\sim 150\text{--}350\text{ }^\circ\text{C}$  will yield various types of tectonic information. For example, fine grained white micas are expected to close to diffusion in this temperature range, depending strongly on grain size. For grains with infinite cylinder geometry, activation energy of  $42\text{ Kcal/mol}$ , frequency factor of  $3 \times 10^{-4}\text{ cm}^2/\text{sec}$ , and  $dT/dt = 5\text{ }^\circ\text{C/Ma}$ , closure temperatures of  $326\text{ }^\circ\text{C}$ ,  $293\text{ }^\circ\text{C}$  and  $251\text{ }^\circ\text{C}$  can be calculated for grain radii of  $150\text{ }\mu\text{m}$ ,  $50\text{ }\mu\text{m}$  and  $10\text{ }\mu\text{m}$ , respectively. Alternatively, synkinematic white micas may preserve ages of neocrystallization if the grains grow below their closure temperature. In addition, white micas consisting of intergrowths of more than one phase may yield disturbed age spectra if the intergrowths have different closure temperatures, or if re-equilibration has resulted in argon loss below the closure temperature of the host.

*In vacuo* room-temperature deformation experiments on biotite standard Fe-Mica yields  $^{40}\text{Ar}/^{39}\text{Ar}$  ages identical to the age of the standard.  $^{40}\text{Ar}/^{39}\text{Ar}$  ratios are unaffected by the deformation suggesting that both isotopes are similarly sited and that argon loss is facilitated by cleavage-perpendicular cracking and likely dislocation glide along K interlayers. Distortion of the lattice by dislocation glide may change the diffusivity of argon and promote outgassing in the sheared portions of grains.

The cooling history of exhumed midcrustal rocks can be constrained to  $\pm 25\text{ }^\circ\text{C}$  by multi-diffusion-domain modeling of K-feldspar, which provides a continuous cooling curve from  $\sim 150\text{--}350\text{ }^\circ\text{C}$ . When combined with age data from white micas from deformed rocks, the temperature history during deformation and/or neocrystallization of the white mica can be constrained, and the mechanism of white mica closure can be assessed. If, for example, an apparently synkinematic white mica gives the same age as the associated K-feldspar when it closed through about  $200\text{--}300\text{ }^\circ\text{C}$  then it is possible that the age of the white mica approximates the time that neocrystallization and ductile deformation ceased. Thermal modeling of white mica and K-feldspar from shear zones in central Australia indicates that the synkinematic white mica neocrystallized while the K-feldspar closed through  $\sim 240\text{ }^\circ\text{C}$ . This is below calculated closure temperatures for the white micas,  $261\text{--}281\text{ }^\circ\text{C}$ . Relict white micas may have lost argon during dislocation glide, but further work is needed to confirm this. In addition, the results of thermal modeling of the K-feldspar are not unexpected in that relatively rapid cooling immediately postdates the neocrystallization age of white micas from shear zones which have accommodated significant uplift.

#### **GEOCHEMICAL AND ISOTOPIC CHARACTERISTICS OF AN EARLY PROTEROZOIC ACCRETED MAGMATIC ARC (NARSAJUAQ TERRANE), NORTHERN QUEBEC, CANADA**

DUNPHY, J.M., and LUDDEN, J.N., Géosonde Research  
Group, Département de Géologie, Université de Montréal,  
C.P. 6128, Succursale A, Montréal, Québec, H3C 3J7,  
Canada

The Narsajuaq terrane is a major component of the Ungava (Trans-Hudson) orogen of northern Quebec. It is a well exposed mid-crustal block interpreted to be the plutonic root of a magmatic arc which is preserved in oblique cross-section within the Ungava orogen. The Ungava orogen represents an arc - collision belt of Early Proterozoic age recording more than  $200\text{ Ma}$  of divergent and convergent tectonic activity. The Narsajuaq terrane comprises a suite of granulite grade plutons and supracrustal rocks which were accreted to the Archean Superior Province basement during Early Proterozoic time.

The predominately calc-alkaline plutonic complex of the arc is comprised of an older suite ( $1898\text{--}1861\text{ Ma}$ ) consisting primarily of well layered (cm- to m-scale) tonalite and quartz diorite, intruded and interlayered with granitic veins, and a younger suite ( $1850\text{--}1826\text{ Ma}$ ) of plutons ranging in composition from pyroxenite to granite which form km-size bodies intrusive into the older suite. Collision related granites (I-type) of even younger age (ca.  $1803\text{ Ma}$ ) occur as km-size sheets within the other two magmatic suites. The overall composition and volume of the granitoid rocks of the Narsajuaq plutonic complex is analogous to that exposed in the massive Mesozoic batholiths located along the western margin of North and South America.

Although geochemically variable, the plutonic complex is characterized by high concentrations of Ba, Th and U and other LILE's, pronounced negative Nb and Ti anomalies and fractionated REE's ( $(\text{La}/\text{Yb})_N$  up to 73). The major and trace element chemistry of the Narsajuaq plutonic complex is similar to that previously reported for other volcanic arc granites.  $\epsilon_{\text{Nd}(0)}$  and  $^{87}\text{Sr}/^{86}\text{Sr}_{(t)}$  values for the complex range from juvenile ( $+4.0$ ,  $0.7020$ , respectively) to very enriched ( $-18.4$ ,  $0.7062$ , respectively) but show no consistent trends with age of emplacement, although a strong negative correlation exists between initial  $\epsilon_{\text{Nd}}$  and  $T_{\text{DM}}$  ages. The most isotopically enriched granites require the involvement of anomalously radiogenic crust which is present in the region as very old crust (documented by inherited zircons up to  $3.1\text{ Ga}$ ).

The geochemical and isotopic data for the Narsajuaq magmatic arc indicate a complex petrogenesis involving variable contamination of juvenile mantle-derived magmas by crustal sources (both continental crust and sediments derived from it). The magmas of the Narsajuaq terrane represent a significant addition of crustal material to the North American continent during the Early Proterozoic.

ISOTOPIC RECORD OF BALTIC GLACIATION IN  
CURIOUS CALCITE PRECIPITATE FROM A CAVE IN  
DEVONIAN MASSIF, CENTRAL POLAND

DURAKIEWICZ, T., Mass Spectrometry Laboratory,  
Institute of Physics, Maria Curie-Skłodowska University,  
Lublin, 20 - 041 Poland.

Speleothems are commonly used for paleoclimate reconstruction. The unique "calcite groats", found during the geologic exploration of the Chelosiowa cave in the Holy Cross Mts., preserved a record of climatic event that occurred during the Baltic glaciation period. The entrance of the cave is located in the quarry of Jaworzna, close to the city of Kielce. The geologic column of the site consists of Devonian limestones. Beginning from the South-Polish glaciation time the cave was cut off from the surface due to filling of the adjacent valley. The present-day entrance was exposed by open excavation of the bedrock (a deep quarry) in the sixties of this century.

The "calcite groats" samples were examined by petrographic and isotopic methods. The two basic morphological forms were recognized: (1) aggradational (pin- and fan-shaped, grainy concretions) and (2) degradational (isometric grains, skeletal forms, pins).  $^{14}\text{C}$  dating revealed the model age of 25 ky. The realistic estimation yields younger age, coinciding with the Baltic glaciation period. C and O stable isotope measurements were performed on 64 samples of the "calcite groats". The values of  $\delta^{13}\text{C}$  range from -9.89‰ to -3.67‰, whereas of  $\delta^{18}\text{O}$  from -20.98‰ to -10.85‰ (relative to PDB). In general, the "calcite groats" are enriched in  $^{13}\text{C}$  as compared to the speleothems, and differ significantly from other calcites (bedrock, veins, speleothems) because of their extremely negative  $\delta^{18}\text{O}$ , locally exceeding -20‰. There is a significant negative correlation ( $r = -0.86$ ,  $n = 64$ ) between the  $\delta^{13}\text{C}$  and  $\delta^{18}\text{O}$  in the "calcite groats". The regression line is:  $\delta^{18}\text{O} = -1.438\delta^{13}\text{C} - 25.41$ .

The following model of "calcite groats" origin is proposed. Isotopically light water ( $\text{d}18\text{O} = -15\text{‰}$  SMOW) infiltrated through the cave bedrock, dissolving limestone and calcites, and was finally stored in shallow pools. The pools were partially covered by ice sheet, what caused isotope fractionation, driving off the heavier oxygen isotope from the remaining water. In a closed system, the carbon dioxide reached the saturation level. The partial pressure of  $\text{CO}_2$  in cave atmosphere was increasing. This specific isolated environment of the cave may have been "frozen" for thousands of years. "Calcite groats" formed when the cave became suddenly open to the atmosphere. The probable reasons for such an event could be the gravitational collapse or thawing. With the decompression, the  $\text{CO}_2$  was rapidly expelled from the water. Calcite concretions started to crystallize very fast, what caused several fractionation mechanisms, discussed in details elsewhere [1].

[1] Durakiewicz, T., Hatas, S., Migaszewski, Z. M., and Urban, J., 1993, Origin of the "calcite groats" from Chelosiowa cave near Kielce (Holy Cross Mts.), Poland, inferred from petrographic and isotopic investigations: submitted to Quat. Res.

THE NATURE OF THE ARCHAEOAN CRUST IN NIGERIA  
A NEW DISCOVERY

Ekwueme, B.N., Dept. of Geology, University of Calabar,  
Nigeria and Kroner, A., Institut für Geowissenschaften,  
Universität Mainz, Germany.

The Nigerian basement complex is situated within a Pan-African mobile zone extending between the West African craton in the west and the Gabon-Congo craton in the southeast. Previous geochronological studies indicate the dominance of Pan-African ( $600 \pm 150$  Ma) ages in the region though ages ranging up to 2700 Ma had been reported. The area is therefore, characterized by mixed ages which reflect the imprints of at least four tectonothermal events; Liberian ( $2700 \pm 20$  Ma), Eburnian ( $2000 \pm 200$  Ma), Kibaran ( $1100 \pm 200$  Ma) and Pan-African ( $600 \pm 150$  Ma).

Recent geochronological studies have, in addition shown that the Nigerian basement contains relicts of the oldest rocks in the West African shield. Zircons extracted from migmatitic orthogneisses in the Kaduna area of northern Nigeria yielded Zircon  $^{207}\text{Pb}/^{206}\text{Pb}$  ages of  $3460 \pm 9$  Ma,  $3437 \pm 7$  Ma and  $3416 \pm 8$  Ma respectively which indicate that early Archaean crust is exposed in the Nigerian basement complex. These ages reflect the time of emplacement of the gneiss pre-cursors which were granitic and granodioritic plutons. The Kaduna gneisses are the oldest rocks known so far from the West African Shield, and rocks with similar zircon ages were recently reported from the Sao Francisco craton of Brazil, suggesting a possible link between these two terrains in early Archaean time.

**RAPID REDOX SHIFTS IN GOLD-DEPOSITING  
HYDROTHERMAL SYSTEMS; THE SHRIMP  
SULFUR ISOTOPIC EVIDENCE FOR BOILING**

**ELDRIDGE, C.S.**, Geol. Dept. and R.S.E.S.,  
Australian National University, Canberra,  
A.C.T., 0200, Australia; **AOKI, M.**, Geol. Surv.  
Japan, Higashi 1-1-3, Tsukuba Science City,  
Ibaraki, 305, Japan; **AREHART, G.B.**,  
Geosciences/CMT-205, Argonne Natl. Lab,  
Argonne, IL 60439, **DANTI, K.**, Western Mining  
Corporation, Olympic Dam Operations, P.O. Box  
150, Roxby Downs, S.A., 5725, Australia;  
**HEDENQUIST, J.W.**, Geol. Surv. Japan,  
Higashi 1-1-3, Tsukuba Science City, Ibaraki,  
305, Japan; **McKIBBEN, M.A.**, Dept. of Earth  
Sci., Univ. of California, Riverside, CA 92521

**SHRIMP** microanalytical sulfur isotopic  
determinations on pyrite crystals from several  
gold-bearing precincts have a common theme of low  
 $\delta^{34}\text{S}$  values in high-grade gold regions. These data  
derive from gold-bearing rocks as diverse as those  
from the altered tuffs of the Valles Caldera in the Rio  
Grande Rift, to the sediment-hosted disseminated  
gold deposit of the Carlin Trend at Post/Betze in  
central Nevada, to the giant copper-gold-uranium  
orebody at Olympic Dam in South Australia. The  
 $\delta^{34}\text{S}$  values found in some pyrite from these deposits  
can be 20 to 40‰ isotopically lighter than the typical  
pyrite found elsewhere in the system. In many cases  
such isotopically light pyrite is also internally zoned  
by tens of per mil over distances of tens to hundreds  
of microns. It is easiest to explain such isotopic  
heterogeneity and shifts to low  $\delta^{34}\text{S}$  values in terms  
of rapid oxidation, or boiling, of the hydrothermal  
fluid. Such a process might preferentially oxidize  
 $^{34}\text{S}$ , leaving more  $^{32}\text{S}$ -rich  $\text{H}_2\text{S}$  to precipitate  
successive pyrite generations. Moreover, it would  
provide an effective mechanism to destabilize  
gold-bisulfide complexes and deposit native metal.

Sulfur isotopic variability of a similar magnitude  
(10‰) has been discovered in single hydrothermal  
alunite crystals and crystal aggregates from the  
Philippines and Japan, suggesting that the oxidized  
caps of hydrothermal systems may well record the  
same process.

Clearly, the sulfur isotopic microanalytical data  
offer a new perspective on the workings of  
hydrothermal systems and may help predict zones of  
elevated gold concentration. It seems likely that these  
sorts of isotopic anomalies would remain undetected  
in conventional isotopic studies of the same material.

**SLAB DEHYDRATION BENEATH THE  
MARIANA ARC: CONSTRAINTS FROM  
U-TH ISOTOPE SYSTEMATICS**

**ELLIOTT, Tim**, LDEO (see below) and Faculty  
for Earth Sciences, Vrije Universiteit, Laboratory  
of Isotope Geology, De Boelelaan 1085, 1081 HV  
Amsterdam, Netherlands, **ZINDLER, Alan**,  
Lamont-Doherty Earth Observatory, Palisades,  
NY, 10964, USA, and **PLANK, Terry**, Dept. of  
Geological Sci., Cornell University, Ithaca, NY  
14853, USA.

U-Th systematics, together with other geochemical  
tracers, have been measured on an extensive suite of  
recent lavas from the Mariana arc, West Pacific. A  
very wide range of disequilibrium is observed with  
( $^{238}\text{U}/^{230}\text{Th}$ ) activity ratios varying from 0.98-1.52.  
Notably, the lavas that show the greatest U excesses  
also have the most "depleted" trace element  
characteristics (i.e., low La/Sm and Ba/Zr). All  
lavas show low Nb/U (3 to 5), compared to the mean  
of 47 for OIBs and MORBs. However, there is no  
correlation of Nb/U with inferred U excess, and  
more than one process must be invoked to explain  
combined Nb/U and U/Th systematics.

These results are consistent with addition of U to  
the arc-magma source mantle by dehydration of the  
down-going altered ocean crust near to the zone of  
melting. This aqueous fluid enriches U over Th and  
results in isotopic disequilibrium in the mantle  
source. Because Pb isotopic compositions and Ce/Pb  
ratios correlate well with U-Th disequilibrium in the  
Marianas lavas, the fluid is probably rich in Pb as  
well.

Two end-member scenarios are proposed to  
explain the anomalously low Nb/U. The first, which  
would have to occur long before the above  
dehydration event to permit re-equilibration of the U-  
Th system, would involve enrichment of the mantle  
overlying the down-going slab by a fluid or melt  
derived from the subducting sediment column. U  
would be strongly enriched over Nb during this  
process, but, due to either primary sediment  
chemistry or partitioning during fluid or melt  
separation, the U/Th ratio of the affected mantle  
would not be dramatically altered. In the second  
scenario, the Nb/U fractionation would occur in the  
mantle wedge, due to preferential retention of Nb in  
the residual source mantle during melting, or during  
subsequent mantle-melt interaction. Further results  
for trace elements and isotope ratios, including those  
in the sediments being subducted at the Mariana  
trench, will be presented at the meeting and used to  
evaluate the viability of these two scenarios.

## DEPTH PROFILES OF COSMOGENIC RADIONUCLIDES IN SURFACE ROCKS

ELMORE, David, DEP, L., SHARMA, P., Department of Physics, Purdue University, West Lafayette, IN 47907, LIPSCHUTZ, M.E., VOGT, S., Department of Chemistry, Purdue University, West Lafayette, IN 47907 USA, and PHILLIPS, F.M., ZREDA, M. Department of Geosciences, New Mexico Tech, Socorro, NM 87801 USA

The build-up of cosmogenic nuclides in rocks is a new and important method for determining exposure ages and erosion rates of landforms. Measurements of multiple samples, multiple nuclides in each sample, and depth profiles help to separate the effects of exposure and erosion and to determine the exposure history. The depth distribution of cosmogenic nuclides within a rock depends on the composition (in particular, water content) of the rock, the energy distribution of the cosmic rays, the erosion rate, and the geometry of the rock. The production of nuclides produced by high energy neutron spallation decreases approximately exponentially with depth. The production of nuclides by low energy neutron capture increases to a maximum and subsequently decreases exponentially with increase in depth.

For many geologically interesting problems, such as dating sequences of glacial moraines, samples are collected from small rocks and large boulders of various geometry. Especially for neutron activation products such as  $^{36}\text{Cl}$ , the production rate on the surface and at depth depends on the rock size and geometry. To determine surface effects and to test our model, we are measuring depth profiles of  $^{10}\text{Be}$ ,  $^{26}\text{Al}$ , and  $^{36}\text{Cl}$  in rocks having simple exposure histories.

We will first present the latest rates for production of  $^{36}\text{Cl}$  from K, Ca, and Cl. Then we will present  $^{36}\text{Cl}$ ,  $^{10}\text{Be}$ , and  $^{26}\text{Al}$  depth profiles in a silicious dolomite boulder from Meteor Crater, AZ, in a granodiorite moraine boulder from Bishop Creek, CA, and the  $^{36}\text{Cl}$  depth profile in a glacially polished basalt column at Devils Postpile National Monument, CA. We will compare the results with predictions of a nuclide production model based on Monte Carlo neutron-proton transport codes.

$^{40}\text{Ar}/^{39}\text{Ar}$  CALIBRATION OF THE MID-CRETACEOUS TIME SCALE: ODP RESULTS FROM THE W. PACIFIC ERBA, E., Dipartimento di Scienze della Terra, Università di Milano, I-20133 Milano, Italy; PRINGLE, M.S., and WIJBRANS, J.R., Faculty of Earth Sciences, Vrije Universiteit, 1081 HV Amsterdam, Netherlands; DUNCAN, R.A., COAS, Oregon State University, Corvallis, OR 97331, USA; and the ODP Leg 143&144 Scientific Staffs.

Drilling in the western Pacific during ODP Legs 130, 143, and 144 recovered samples suitable for integrated studies of critical mid-Cretaceous sections near the beginning of the long Cretaceous Normal Polarity Superchron (K-N), one of the most poorly calibrated portions of the Geologic Time Scale.

All of the basalts at Site 807 on the Ontong Java Plateau (ODP Leg 130) are normally magnetized; their weighted age is  $121.2 \pm 1.2$  Ma. Based on Early Aptian upper *C. litterarius* nannofossil zone assemblages found within the basalt sequence, these basalts must have been erupted shortly after the beginning of the K-N Superchron. Polarity Chron M0 occurs entirely within the lower part of the *C. litterarius* zone, above the first occurrence of *R. irregularis*. We estimate that the basalts at Site 807 are between 0.30 and 0.55 m.y. younger than the top of Chron M0, based on Milankovich-driven cyclostratigraphy (Herbert, *EPSL*, 1992) and tephra- and biostratigraphy from DSDP Site 463 (Erba, *Paleoceanol.*, in press). Thus, the age of the top of Chron M0, i.e., the beginning of the K-N Superchron, is within analytical precision of the  $121.2 \pm 1.2$  Ma age of the basalts at Site 807. As Chron M0 is only 0.3 to 0.4 m.y. long, and as both the first occurrence of *R. irregularis* and the base of Chron M0 occur very near the Barremian / Aptian boundary, 121.2 Ma is a good minimum estimate for the age of that boundary, too.

The volcanic basement at MIT Guyot (ODP Site 878) may be divided into an upper, normally-magnetized section and a lower, reversely-magnetized section of subaerial alkalic basalts. The weighted age of the four basalts on either side of the reversal is  $122.9 \pm 0.6$  Ma. The oldest dated sediments, platform carbonates located approximately 25 m above volcanic basement, are attributable to the lower portion of the *C. litterarius* nannofossil zone. If the lowermost shallow-water carbonates were deposited quickly (faster than about 75 m/m.y.), and if there was no significant hiatus between the eruption of the basalts and the deposition of the first sediments, then the magnetic reversal seen in the basalts could be the top of polarity Chron M0. However, assuming slower sedimentation rates, the possibility of a reversal in the lower limestone unit, and a minimum hiatus of 1 m.y. between the limestones and basalts, the reversal seen in the basalts is more likely the top of polarity Chron M1. The 122.9 Ma age of the basalts would then provide a precise age for the top of Chron M1, constrain the maximum age of the beginning of the K-N Superchron, and suggest a significantly younger Barremian / Aptian boundary than the 124.5 Ma of Harland et al. (1990).

The age of the oldest lavas at Resolution Guyot (ODP Site 866) is  $127.6 \pm 2.1$  Ma. A complete mid-Cretaceous magnetostratigraphy down to at least polarity Chron M5 or M7 has been documented in the sediment section; the majority of the basalts are also reversed. If these basalts represent true volcanic basement, then the Hauterivian benthic foraminifer and Sr isotopic age of the basal limestone suggest that the 131.8 Ma age for the Hauterivian / Barremian boundary of Harland et al. (1990) should be revised significantly downward.

(Sites 807 and 878 ages relative to TCR 85G003 sanidine at 27.92 Ma; Site 866 ages relative to FCT-3 biotite at 27.7 Ma)

## THE SEAWATER OSMIUM ISOTOPE RECORD AND THE MARINE CARBON CYCLE IN THE NEOGENE OCEAN.

Esser, Bradley K., L-396, Lawrence Livermore Nat'l Lab., Livermore, CA, 94550, and Ravizza, Gregory E., Dept. of Geology and Geophysics, Woods Hole Oceanographic Inst., Woods Hole, MA 02543.

Temporal changes in the Os isotopic composition of Neogene seawater are recorded in North Pacific pelagic clay (Pegram et al., 1992) and in East Pacific Rise metalliferous carbonate (Ravizza, 1993). These seawater Os isotope records, which are similar, exhibit a pattern of change which differs in detail from the seawater Sr isotope record. From 28 to 15 Ma, seawater  $^{87}\text{Sr}/^{86}\text{Sr}$  increased rapidly while  $^{187}\text{Os}/^{186}\text{Os}$  remained relatively constant. Sometime between 15 and 17 Ma, seawater  $^{187}\text{Os}/^{186}\text{Os}$  began to increase rapidly to the modern-day ratio of 8.5 (Ravizza and Turekian, 1992), while the rate of  $^{87}\text{Sr}/^{86}\text{Sr}$  rise diminished. For both Sr and Os, continental crust is more radiogenic than the oceanic lithosphere. Their decoupling suggests that an increase in terrigenous silicate weathering cannot be solely responsible for secular change in seawater Os. We suggest that accelerated weathering of old organic-rich sediment accounts for the rapid increase in seawater  $^{187}\text{Os}/^{186}\text{Os}$  over the past 15 Ma.

Relative to average continental crust (Esser and Turekian, 1993), organic-rich sediments have high Os concentrations and high Re/Os ratios (Ravizza and Turekian, 1989). Because of the decay of  $^{187}\text{Re}$  to  $^{187}\text{Os}$ , old organic-rich sediments also have high  $^{187}\text{Os}/^{186}\text{Os}$  ratios and represent an important crustal reservoir for excess  $^{187}\text{Os}^*$ . During weathering of organic-rich sediments, liberation of soluble  $^{187}\text{Os}^*$  should be coupled to organic C oxidation. Bulk carbonate  $\delta^{13}\text{C}$  profiles from the South Atlantic display a negative shift of 2‰ over the past 15 Ma, which Shackleton (1987) interpreted as indicative of net oxidation of the global organic C reservoir. Whether net oxidation occurred by enhanced weathering or by diminished burial of organic C cannot be distinguished with the  $\delta^{13}\text{C}$  data alone. Although diminished organic matter burial or enhanced weathering of young marine organic matter will decrease seawater  $\delta^{13}\text{C}$ , they will have no effect on seawater  $^{187}\text{Os}/^{186}\text{Os}$ . Enhanced weathering of old organic-rich sediment is compatible with both the observed increase in seawater  $^{187}\text{Os}/^{186}\text{Os}$  and decrease in bulk carbonate  $\delta^{13}\text{C}$ .

Both the  $\delta^{13}\text{C}$  shift to more negative values and the  $^{187}\text{Os}/^{186}\text{Os}$  shift to more radiogenic values commence at ~15 Ma. We suggest that the correlation is not coincidental and reflects an increase in the weathering rate of old organic matter. If the Shackleton model is used, in which riverine organic  $\delta^{13}\text{C}$  is assumed to have remained constant, the excess  $^{187}\text{Os}^*$  influx integrated over the past 15 Ma is ~13% greater than the pre-15 Ma steady-state flux. An alternative interpretation is that the  $\delta^{13}\text{C}$  shift was driven by a change in riverine organic  $\delta^{13}\text{C}$ ; in this model, the size of the global organic C reservoir does not change. Lighter riverine organic  $\delta^{13}\text{C}$  values may have resulted from an increase in the mean age of riverine organic C over the past 15 Ma—Cretaceous marine organic C is lighter than modern marine organic C (Dean et al., 1986). An increase in the mean age of riverine organic matter would also result in an increase in riverine  $^{187}\text{Os}/^{186}\text{Os}$ . In both models, increased weathering of old organic C is more consistent with the Os data than a change in organic C burial.

## $^{40}\text{Ar}/^{39}\text{Ar}$ DATING OF ANORTHOCLASE, MOUNT EREBUS, ANTARCTICA: PROBLEMS OF EXCESS ARGON IN MELT INCLUSIONS

ESSER, R.P., HEIZLER, Matthew, T., KYLE, P.R. and McINTOSH, W., at: N.M. Bureau of Mines and Dept. of Geoscience, New Mexico Tech, Socorro, NM, 87801, USA.

Mt. Erebus is a 3794 m high active phonolite volcano on Ross Island, Antarctica. Anorthoclase phonolite lava flows are exposed around the flanks and infill a major caldera. The summit cone is mainly composed of anorthoclase phonolite bombs erupted over the last 20 years. Mechanical disintegration of the bombs has left a lag of anorthoclase crystals up to 10 cm in length. In the bombs and lavas anorthoclase is abundant (~30-40%) and is often riddled with melt (glass) inclusions trapped during rapid growth. The high  $\text{K}_2\text{O}$  content (3-4%), abundance and large size potentially makes the anorthoclase ideal for  $^{40}\text{Ar}/^{39}\text{Ar}$  dating.

Conventional K/Ar ages of anorthoclase, glass and whole rock samples from Erebus ranged from 0.94 to 0.15 Ma. Historically erupted anorthoclase have an age of 0.44 Ma, indicating excess  $^{40}\text{Ar}$  is a significant problem.

$^{40}\text{Ar}/^{39}\text{Ar}$  age spectrum analyses on pure and impure (1 to 5% glass contaminated) anorthoclase were obtained on summit (1984 eruption) samples. A clear correlation between apparent age and degree of glass contamination is observed for duplicate analyses of summit phenocrysts. Nearly pure anorthoclase gave total gas ages of 68 and 41 ka whereas glass contamination of about 1% yielded total gas ages of 184 and 165 ka and 5% contamination produced total gas ages of 283 and 276 ka. Isochrons for each of the summit samples yield no apparent linear correlation and therefore suggest a heterogeneous trapped  $^{40}\text{Ar}/^{36}\text{Ar}$  composition.

Mt. Erebus glass typically contains ~1600 ppm Cl. The measurement of  $^{38}\text{Ar}$  formed from a nuclear reaction on  $^{37}\text{Cl}$  provides a measure for sample Cl during age analysis. As the anorthoclase is presumed Cl-free, the glass content is directly proportional to the Cl signal. Unfortunately, there is not a straight-forward relationship between Cl and excess  $^{40}\text{Ar}$  for the summit samples, thus it may not be possible to quantitatively correct for excess argon.

Geologically older samples from the flanks were also analyzed in duplicate (non-contaminated versus glass contaminated). Unlike the historic samples, the flank samples yield nearly identical apparent ages for both pure (isochron age =  $88 \pm 2$  ka) and glass contaminated (isochron age =  $84 \pm 9$  ka) anorthoclase. The glass causes a significant drop in radiogenic yield as well as a large increase in chlorine. However, there appears to be minimal excess argon associated with the glass for these samples. Therefore we believe that the apparent ages from the flank samples are geologically relevant.

Additional, older samples were also analyzed. Although minor amounts of glass were found to be present within these samples, the apparent ages were all less than 100 ka. Because glass enriched duplicates were not analyzed for these samples the presence of excess argon is difficult to assess. These ages, however, do represent a maximum age that are substantially younger than previously determined conventional K/Ar ages. Therefore, we conclude that while excess argon resides in the glass, the presence of glass itself does not confirm the existence of excess argon. However analysis of nearly clean versus glass contaminated samples does provide a technique whereby non-anorthoclase excess argon may be verified.

DATING THE SMECTITE ILLITE TRANSITION USING K-Ar AND Rb-Sr WHOLE-ROCK TECHNIQUES.

J.A. Evans NERC Isotope Geosciences Laboratory, Keyworth, NOTTM NG12 5GG, UK.

The different behaviour of the Rb-Sr and K-Ar systems at low temperatures makes it possible to show that mudrock Rb-Sr whole-rock ages from Palaeozoic mudrocks date the smectite-illite transition.

Rb-Sr whole-rock regressions and K-Ar data from the < 2m illite fraction of samples of Ordovician and Silurian mudrocks are presented. K-Ar ages from the < 2m fractions generate a normal distribution with a mean and quadratically combined  $2\sigma$  error giving a Devonian age of  $399 \pm 4$  Ma. This dates the passage down-temperature of the illite through  $260 \pm 30$  ° C during Acadian metamorphism. Rb-Sr whole-rock ages from the same rocks do not show the same consistency of ages, giving  $431 \pm 10$ ,  $414 \pm 6$  and  $403 \pm 15$  Ma. The Rb-Sr whole-rock isochron ages are interpreted as dating the time of passage of the rock through the smectite-illite transition because the radiometric ages correspond well to the estimated time of this reaction calculated from sediment thicknesses. Other explanations of the ages, such as the possibility that they were generated by mixing, or that they date sediment provenance ages, peak metamorphism, or cleavage, are rejected on geological grounds.

The discrepancy between the K-Ar ages and Rb-Sr whole-rock ages is caused by the different behaviour of the two systems at low temperatures. K-Ar records thermal events, whereas the Rb-Sr whole-rock system is trolled by mineral stability and is dependent on water for moving and rehomogenising  $^{87}\text{Sr}/^{86}\text{Sr}$  over sufficient distance to create a common isotope composition in mudrocks at a specific time. This occurred in the mudrocks of this study during the smectite-illite reaction which is a major, prograde, dehydration reaction.

DISTRIBUTION OF CHLORINE-36 IN THE UNSATURATED ZONE AT YUCCA MOUNTAIN: AN INDICATOR OF FAST TRANSPORT PATHS

FABRYKA-MARTIN, J., Group CST-10, Los Alamos National Laboratory, Los Alamos, NM 87545; BODVARSSON, G.S., Earth Sciences Division, Berkeley National Laboratory, Berkeley, CA 94720; WIGHTMAN, S., MURPHY, W., WICKHAM, M., Hydro Geo Chem, Inc., 1430 North 6th Ave., Tucson, AZ 85705; CAFFEE, M., NIMZ, G., SOUTHON, J., Center for Accelerator Mass Spectrometry, Livermore National Laboratory, Livermore, CA 93550; SHARMA, P., PRIME Lab, Dept. of Physics, Purdue University, West Lafayette, IN 47907

The  $^{36}\text{Cl}/\text{Cl}$  ratios for Cl extracted from soil and rocks are being used to provide information on characteristics of water movement through the unsaturated zone at Yucca Mountain. Deep penetration of the bomb-pulse signal in alluvium provides evidence for the variable effectiveness of alluvium and associated vegetation in attenuating infiltration, possibly as a result of different runoff characteristics of the watersheds. Fast transport of water via fractures through the Tiva Canyon welded unit is indicated by detection of elevated levels of  $^{36}\text{Cl}$  in the underlying Paintbrush nonwelded unit.  $^{36}\text{Cl}$  data for one deep borehole indicates average residence times of  $5$  to  $7 \times 10^5$  yr in the deeper Topopah Spring welded units, and  $1$  to  $3 \times 10^5$  yr in the underlying Calico Hills nonwelded unit.

The apparently younger ages observed in the deeper unit suggests that moisture in this unit may not derive predominantly from vertically-downward matrix flow, but rather that a faster transport path may be involved such as lateral transport down-dip from the direction of the Solitario Canyon Fault Zone. Numerical modeling studies are underway to evaluate possible moisture migration pathways that are consistent with the observed  $^{36}\text{Cl}$  distributions.

C AND O ISOTOPE RECORDS OF THE ADRIATIC SEDIMENTS: INFLUENCE OF ALLOCHTHONOUS INPUT AND TEMPERATURE

FAGANELI, J., Marine Biological Station, Piran, 66330, Slovenia and DOLENEC, T. and PEZDI, J., Jozef Stefan Institute, Ljubljana, 66000, Slovenia

The C and O stable isotope composition of bulk carbonates and C isotope composition of sedimentary organic matter in the Adriatic Sea were used as an indicator of their origin and condition of deposition. The areal distribution of surficial carbonates depleted in  $^{13}\text{C}$  was restricted to the NW and W parts of the Adriatic strongly influenced by the river Po and other Italian river inflows and to SE part of the Adriatic affected by local riverine inputs. These are isotopically lighter carrying  $^{13}\text{C}$  depleted organic matter. This areal distribution is a consequence of the general water circulation system and sedimentological properties of the Adriatic Sea. The vertical profiles of  $\delta^{13}\text{C}$  values of organic C in short cores from the northern and central Adriatic matched the organic C content, indicating this distribution as a function of allochthonous organic C input. Lower  $\delta^{13}\text{C}$  value and high organic C content observed in the central Adriatic in the horizon from ca 15000 years B.P. during the last postglacial period was therefore a consequence of a larger terrestrial contribution in the past by increased riverine flow. The area of higher  $^{13}\text{C}$  and  $^{18}\text{O}$  contents in carbonates appears along the NE Adriatic coast due to the sediment enriched in dolomite. The carbonates with the highest  $^{13}\text{C}$  and  $^{18}\text{O}$  contents are located in the deepest basins of the Adriatic - Jabuka and south Adriatic Pits, due to the ingression of colder and isotopically heavier water from the eastern Mediterranean. These areas are also characterized by higher  $^{13}\text{C}$  content in sedimentary organic matter indicating the provenance from the autochthonous biological production.

PRESOLAR OXIDE GRAINS IN METEORITES. EVIDENCE FROM OXYGEN AND MAGNESIUM ISOTOPES.

FAHEY, A. J. and HUSS, G. R., Lunatic Asylum, Division of Geology and Planetary Sciences, California Institute of Technology, Pasadena, CA 91125

Carbon rich phases were the first materials of interstellar origin to be separated from meteorites and identified as having formed outside the solar system. Several oxide grains have recently been found in the ordinary chondrites Bishunpur and Tieschitz and in the carbonaceous chondrites Orgueil and Murchison that clearly are of extra-solar-system origin. Most of the grains are corundum ( $\text{Al}_2\text{O}_3$ ) (e.g. Huss *et al.*, 1994, Nittler *et al.*, 1994).

We have measured the oxygen isotopic ratios in ~100 oxide grains from Orgueil and Bishunpur, 57 of which were corundum, and 2 of these 57 were found to be presolar. The oxygen isotopic composition of Orgueil corundum B is:  $^{16}\text{O}/^{17}\text{O} = 1028 \pm 11$ , and  $^{16}\text{O}/^{18}\text{O} = 502 \pm 10$  (Hutcheon *et al.*, 1994), and of Bishunpur corundum B39 is  $^{16}\text{O}/^{17}\text{O} = 385 \pm 9$ , and  $^{16}\text{O}/^{18}\text{O} = 854 \pm 25$  (Huss *et al.*, 1994) ( $(^{16}\text{O}/^{17}\text{O})_{\odot} = 2610$ , and  $(^{16}\text{O}/^{18}\text{O})_{\odot} = 499$ ). The oxygen isotopic compositions of these corundum grains set them apart from oxygen bearing phases that formed in the solar system. The measured ratios in these grains is similar to those observed in red giant or AGB stellar atmospheres (Smith and Lambert, 1990). Stellar evolution calculations show that the oxygen isotopic compositions of the grains to be dominated by the first dredge-up event in such stars. Nittler *et al.* (1994) have observed isotopic compositions similar to the corundum grains that we have measured, but have also found two ( $\text{Al}_2\text{O}_3$ ) grains from Tieschitz with more extreme  $^{16}\text{O}/^{18}\text{O}$  values (~7000 and ~20000). The authors suggested Wolf-Rayet stars as a possible source for these two grains.

The Mg isotopic composition Orgueil corundum B has been measured and shows  $(^{26}\text{Mg}/^{27}\text{Mg})_0 = 8.9 \pm 0.1 \times 10^{-4}$ . This is ~18 times higher than the canonical solar system value of  $\sim 5 \times 10^{-5}$ . Similar ratios have been observed in other corundum grains with values as high as  $8 \times 10^{-3}$  (Nittler *et al.*, 1994). This is also consistent with formation of these grains in red giant or AGB stars that have experienced the first dredge-up event.

The isotopic compositions of Orgueil corundum B and Bishunpur B39 do not uniquely identify a stellar source for their formation since even the envelope of a Type II supernova is a possible source. Rather, they distinctly show the products of H-burning and point to the first dredge-up event to produce their isotopic signatures. Division Contribution 5367(841)

Huss, Fahey, Gallino and Wasserburg, 1994, Presolar  $\text{Al}_2\text{O}_3$  with a Large Excess of  $^{17}\text{O}$  and Depleted  $^{18}\text{O}$ , LPSC 25, submitted.

Nittler, Alexander, Gao, Walker, and Zimmer, 1994, Interstellar Corundum and Spinel from the Tieschitz Ordinary Chondrite, LPSC 25, submitted.

Hutcheon, Huss, Fahey, and Wasserburg, 1994, Extreme  $^{26}\text{Mg}$  and  $^{17}\text{O}$  enrichments in an Orgueil corundum: Identification of an interstellar oxide grain, *Ap. J. Let.*, submitted.

Smith and Lambert, 1990, The Chemical Composition of Red Giants III. Further CNO Isotopic and s-process Abundances in Thermally Pulsed Asymptotic Giant Branch Stars, *Ap. J.*, 72, 387

## ND-SR ISOTOPIC CHARACTERISTICS OF HERCYNIAN POST-RIFTING GRANITES AND XENOLITHS IN HAINAN ISLAND, S. CHINA: IMPLICATIONS FOR GENESIS OF THEM

FANG, Zhong, ZHANG, G-D., TAO, X-C., LI, H-M., and YANG, J-D., Department of Earth Sciences, Nanjing University, Nanjing 210008, P. R. China.

The great granitic batholites, Hercynian (320~270Ma) porphyroblastic granite-monzonites of ca. 7000Km<sup>2</sup>, are main part of granitoid rocks in Hainan Island, South China. They intruded into Pre-Cambrian gneiss of Baoban Group, and either intruded into or transferred from Carboniferous (340~330Ma) lower metamorphic flysch with volcanics of Shilu Group. Authors have studied and Confirmed the Upper Palaeozoic rifting on Hainan Isl. There are similar REE patterns both of pre-granitic basement rocks and the granitoids. The latter is belonged to crustal source type, that is based on  $\epsilon(\text{Nd}(t)) - 17.2 \sim -5.2$ ,  $\epsilon(\text{Sr}(t)) + 23 \sim +141$ , and  $\delta^{18}\text{O} + 6.02 \sim +12.97$ , an average value of the  $\delta^{18}\text{O} + 10.66$ , etc..  $T_{\text{DM}}^{\text{Nd}}$  ages of the granitoids are from 1351~1797Ma, which are compatible with an U-Pb concordant age (1352Ma) of clastic zircons from Shilu Group, and a Sm-Nd whole rock isochron age (1702Ma) of meta-basalts from Baoban Group. The Nd and Sr isotopic characteristics of the granitoids suggest the primitive origin rocks of them could be Proterozoic metamorphic rocks. It is very interested in that the rhyolites, a member of bimodal volcanic rocks in Shilu Group, keep their own  $\epsilon(\text{Nd}(t)) - 6.73 \sim -6.48$ ,  $T_{\text{DM}}^{\text{Nd}}$  ages 1562~1610Ma, those are like the corresponding values of the granite near by. Their ages and petrographical facies are different, but it was possible that they were developed from an origin.

A lot of xenoliths in the granitoids are belonged to restite ones. Their  $\epsilon(\text{Nd}(t)) - 12.9 \sim -10.2$ ,  $\epsilon(\text{Sr}(T)) - 86 \sim +6$ , and especially high ratios of Sm/Nd 0.38~0.52. The elemental and isotopic features of the xenoliths show a drastic Nd-Sr fractionation between melt and the restites. There are some variations on chemical components between the xenoliths and the pregranitic meta basalts, which could be identified source rocks of the former, their SiO<sub>2</sub>, K<sub>2</sub>O and Rb are higher, and MgO, CaO, Sr, Ni are lower than those in the meta-basalts indicate some assimilation and contamination from Hercynian granitic melt.

## VARIABLE U-Pb TIME DOMAINS IN A DEVONIAN LIMESTONE

FAROUHAR, Ronald M., SMITH, Patrick E., Dept. of Physics, University of Toronto, Toronto, Ontario, Canada, M5S 1A7 and HANCOCK, Ron G. V., Slowpoke Reactor Facility, University of Toronto, Toronto, Ontario, Canada, M5S 1A5.

Significant variations in U and Pb concentrations are present on length scales of a few meters in limestones from the mid-Devonian Lucas Formation in the Michigan basin, southwestern Ontario. Pb is correlated with the elements Fe, Al and Sc, which are predominantly associated with non-carbonate (clay) minerals in the samples. Isotope analyses of carbonate and associated non-carbonate fractions in the samples suggest that the rocks have experienced exchange reactions during an Acadian diagenetic event, where significant amounts of radiogenic Pb were sequestered by clays at 333 ± 5 Ma (1σ).

Total-rock subsamples of the limestone in an area slightly enriched in organic carbon show wide variations in U/Pb over distances of a few mm. Combined, these give isochron ages of 380.2 ± 4.4 Ma for <sup>206</sup>Pb/<sup>238</sup>U and 368 ± 15 Ma for <sup>207</sup>Pb/<sup>235</sup>U. The results agree with the stratigraphic age, and demonstrate that the use of total-rock samples from this site can effectively compensate for the radioelement redistributions. However, less radiogenic data for other stratigraphically equivalent sites are not entirely concordant with the above results. We believe this is related to partial or total resetting of the U-Pb isotopic systems in these samples during diagenetic events. Apparent ages determined by selective leaching for samples from sites characterized by high Pb are 332 ± 6 (<sup>206</sup>Pb/<sup>238</sup>U) and 320 ± 39 (<sup>207</sup>Pb/<sup>235</sup>U), identical to the internal isochron ages for the samples.

An extensive sequential leaching of another sample reveals that redistributions of U and Pb have taken place in smaller U-Pb domains which appear to result from 240 and 45 Ma secondary events. The apparent secondary ages can be correlated with (1) regional fission-track, K-Ar and Rb-Sr cooling/diagenetic ages in strata of the North American mid-continent; and (2) local U-Pb ages of secondary calcite spar.

**DETECTION OF I-129 IN ENVIRONMENTAL SAMPLES ASSOCIATED WITH THE NUCLEAR FACILITY AT WEST VALLEY, NY**

**FEHN, U., RAO, U., MORAN, J.E., and TENG, R.T.D.,** Department of Earth and Environmental Sciences, University of Rochester, Rochester, NY, 14627 and Nuclear Structure Research Laboratory, University of Rochester, Rochester, NY, 14627

West Valley is a former civilian reprocessing plant located in Western New York State. Although reprocessing activities stopped in 1975, significant amounts of radioactive materials are still present there. For a preliminary study of the level of radioactive materials currently released from this site we collected water samples and plant material from the watershed near West Valley. We report here initial results for  $^{129}\text{I}/\text{I}$  ratios determined using the AMS system at Rochester.

For background determination of  $^{129}\text{I}/\text{I}$  ratios in this region, samples were collected in two of the Finger Lakes. The ratios, around  $10^{-8}$ , are somewhat higher than typically found for anthropogenic I, probably reflecting a higher atmospheric ratio prevalent in New York State.

The measurements around West Valley show a striking pattern of  $^{129}\text{I}$  release from this site. The highest values were found in samples taken downstream from the site in Buttermilk Creek with  $^{129}\text{I}/\text{I}$  ratios in excess of  $10^{-6}$ . These values are more than two orders of magnitude higher than those found upstream from the site in the same creek. The signal is also clearly visible in Cattaraugus Creek, and can be followed at least into Lake Erie. Ratios found in the water and in the plant material were generally in good agreement. The results suggest continued release of radionuclides from buried waste in West Valley entering the surface waters. At the same time they demonstrate the sensitivity of the  $^{129}\text{I}$  system for the detection of the release of radionuclides from buried nuclear waste.

**APATITE FISSION TRACK (AFT) AND ORGANIC MATURITY (OM) PALEOTHERMOMETRY OF THE EASTERN MARGIN OF THE GULF OF SUEZ**

**FEINSTEIN, S.,** Dept. of Geology, Ben Gurion University of the Negev, Beer Sheva 84105, Israel, Kohn, B.P., Victorian Institute of Earth and Planetary Sciences, School of Earth Sciences, La Trobe University, Bundoora, Victoria 3083, Australia, Steckler, M.S., Lamont-Doherty Earth Observatory of Columbia University, Palisades, New York 10964, and Eyal, M., Dept. of Geology, Ben Gurion University of the Negev, Beer Sheva 84105, Israel.

Time-space relationships between vertical movements and thermal history of the lithosphere relative to rift-related extension provide essential constraints for the relative role of different possible rifting-subsidence-uplift mechanisms. Large rift-flank uplifts, such as observed along the Gulf of Suez (>4 km in southern Sinai mountains), result from tectonic effects of lithospheric thinning and heating, and/or the isostatic response to unloading associated with extension. Erosion of the rift flank can greatly augment the depth of exhumation of rocks for either mechanism.

Miocene strata at ~2-2.5 km in deep boreholes within the eastern Gulf of Suez graben yield a relatively wide AFT age range between 31 to 269 Ma and mean track-length (TL) of ~10.5-11.5 mm. AFT ages exceed the stratigraphic age of the syn-rift host rocks indicating that rift-related thermal effects were not sufficient to totally reset AFT clocks. However, the range of measured AFT data is similar to that previously recorded in the Precambrian crystalline basement flanking the Gulf of Suez which is believed to be the provenance for the rift-fill.

In the southeastern part of the Gulf of Suez AFT ages are younger than those recorded to the north and appear to become younger with depth, possibly reflecting a partial thermal overprint related to burial in the present rift setting. However, the TL data do not show such a clear relationship. In addition, both present day bottom-hole temperatures and paleotemperatures indicated by the level of OM in the Miocene sediments appear too low to account for the level of AFT shortening recorded, particularly for the relatively short time involved. Thus, the AFT data do not record any major rift-related thermal effects, but rather, they mainly retain a pre-rift provenance signature which reflects the order and depth of erosion at the uplifted flanks.

The level of heat flow at the surface indicated by AFT and OM paleothermometry, and by BHT data in the Gulf of Suez appear too moderate to account for the vertical movements observed at the flanks. Hence, we conclude that either the full effects of the rift-related thermal anomaly have yet to reach the near surface environment, or that the isostatic response to denudation is the primary source for the flank uplift.

## THE D/H RATIOS OF TREE-RINGS IN 12 TREES FROM WORLD WIDE LOCATIONS AND THE IMPLICATIONS FOR CLIMATE CHANGE OF THE PAST 100-200 YEARS

FENG, Xiahong and EPSTEIN, Samuel,  
Division of Geological and Planetary Sciences,  
170-25, Caltech, Pasadena, CA 91125

It has been shown that the  $\delta D$  values of nonexchangeable hydrogen in cellulose of tree-rings are systematically correlated with the source water used by trees in photosynthesis. A highly significant correlation between  $\delta D$  of tree-rings and mean annual temperature has also been reported for trees of widely distributed geographic locations where the  $\delta D$  values vary by more than 100 permil. However, the  $\delta D$ -temperature relationship has not been well established for a time series of any location. In this case, we must deal with much smaller variations and smaller signal to noise ratios.

Detailed studies on the relationship between the  $\delta D$  values of tree-rings and climatic parameters, such as temperature and precipitation, have been carried out for three locations. These locations vary from a flat area with simple topography, such as Manitoba, Canada, to locations in Southern California where the climatic regime is rather complicated due to the variable topography. The results show 1. that correlations between  $\delta D$  of tree-rings and temperature are much more significant in a flat area in comparison to a mountainous area, 2. that in Manitoba, the  $\delta D$  values of tree-rings can be correlated to a temperature record of a meteorologic station 270 miles away, indicating that one single tree may be used as a proxy temperature indicator for a large area, 3. that correlations between the  $\delta D$  of tree-rings and temperature are particularly good for data sets that are smoothed using moving average.

Twelve  $\delta D$  records show that from the 1850's to approximately the 1920's, the  $\delta D$  values continuously increased in all trees. In a few cases where the time series go further back in time, the warming seems to have started as early as 1820, 1800 or even 1780. The rate of warming shown by a given tree roughly correlates with the mean  $\delta D$  value of that tree, meaning that a greater rate of warming occurs at colder locations. The trees of Alaska and Siberia are two exceptions. After about the 1920's, the trends become variable among the trees. Some series show continuous warming, some show little warming, and some show significant fluctuations. This time period also seems to be characterized by increased temporal fluctuations shown in the individual  $\delta D$  time series. Overall, the warming trends are much more pronounced and consistent in the 19th century than in the 20th century when the climate forcing by anthropogenic  $CO_2$  is stronger. In addition, the warming seems to have started as early as in the 1820's and continued until 1920's in most of the locations. The question remains, therefore, whether the forcing mechanism is natural (recovery from Little Ice Age), anthropogenically induced, or a combination of the two. The observations also raise a question as to whether the increased spatial and temporal variations in the  $\delta D$  climatic records are related to the anthropogenic activities.

## 40AR/39AR PLATEAU AGES ON PHENGITES AFFECTED BY EXCESS ARGON

FERAUD, G., RUFFET G., DE JONG K., URA CNRS 1279,  
Université de Nice, 06108 NICE Cedex 2, France,  
BALLEVRE M., Laboratoire de Tectonique, UPR CNRS  
4661, Université de Rennes I, 35042 Rennes Cedex, France,  
AMOURIC M., CRMC2 CNRS, Université Marseille,  
13288 Marseille Cedex 9, France.

$40Ar/39Ar$  phengite ages are commonly used for reconstruction of Pressure/Temperature/time paths of regional metamorphism. It is therefore necessary to know if the  $40Ar/39Ar$  plateau age criterion used to test the validity of the measured ages is reliable in all cases for phengites or if insignificant plateau ages may exist as for biotites affected by excess argon. Two distinct cases showing  $40Ar/39Ar$  plateau ages obtained on single grains and bulk samples of phengites affected by excess argon are presented.

(1) Fresh phengites from two restrictive areas of the Sesia Zone (Western Alps, Italy) display either plateau ages ranging from 104 to 180 Ma, geologically insignificant (Mucrone area), or well defined plateau ages ranging from  $69.3 \pm 0.7$  to  $76.9 \pm 0.6$  Ma on rocks sampled on a 50m wide outcrop (Marine area). These last ages which may be geologically significant, show discordant but reproducible plateau ages with a maximum difference of 10%, which may be only explained by the existence of undetectable excess argon.

(2) Partially recrystallized phengites separated from a 5 km<sup>2</sup> part of a gneiss body of the Mulhacen Complex (Betic Zone, SE Spain), display plateau ages ranging from  $15.8 \pm 0.4$  Ma to  $90.1 \pm 1.0$  Ma. These phengites are characterized by a high atmospheric Ar contamination, an easy detachment over the basal plane, and different populations of recrystallized micas as observed by HRTEM. These characteristics may make these micas susceptible for the uptake of variable quantities of excess argon from metamorphic fluids during a Miocene thermal event.

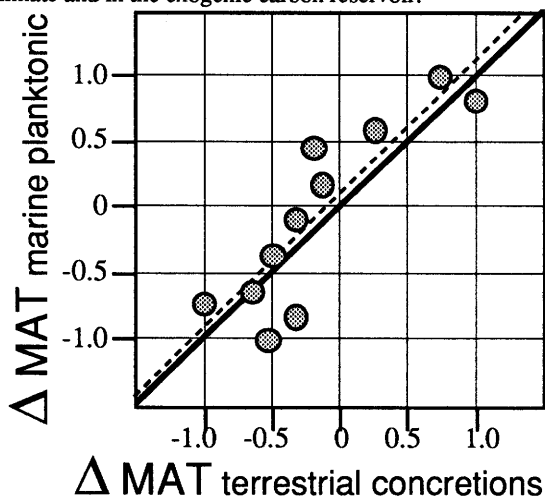
**A TERRESTRIAL ISOTOPIC RECORD OF LOWER CRETACEOUS CLIMATIC CHANGE FROM SOUTHEASTERN AUSTRALIA**

Kurt M. Ferguson, and Robert T. Gregory; Dept. of Geol. Sci., Southern Methodist Univ., Dallas, Texas 75275; Andrew Constantine, Dept. Earth Sci., Monash Univ., Clayton, Victoria 3168, Australia.

Organic carbon isotopic data from insoluble residues, and oxygen isotope data from carbonate cements, in concretions taken from fluvial sediments at twelve sites in the Otway and Strzelecki Ranges of southeastern Australia, coupled with palynological dating, provide a record of high latitude continental climatic change from the early Aptian to the late Albian. Average calcite oxygen isotopic values (SMOW) increase from a minimum of +4.3 in the middle Aptian (~120 Ma) to a maximum of +17.7 in the late Albian (~100 Ma). Meteoric water  $\delta^{18}\text{O}$  values inferred from the calcite data range from -24.8 to -11.3. Using the modern correlation between mean surface temperature and the mean isotopic composition of precipitation indicates that surface temperatures increased by  $\approx 10^\circ\text{C}$  from 120 to 100 Ma, with a mean surface temperature of  $\approx 0^\circ\text{C} \pm 5^\circ$  over that time interval. The surface temperature record derived from the concretion oxygen isotope data correlates well with an increase of  $\approx 3^\circ\text{C}$  in temperature over the same time interval derived from the oxygen isotope composition of marine foraminifera. Comparison of the deviations from the mean of the maximum and minimum values, normalized to  $\pm 1$ , of the temperature records is shown below.

Carbon isotopic values from the insoluble organic carbon residues of the concretions define a trend from a low value of -25.5‰ at  $\approx 120$  Ma to a maximum value of -25 in the late Albian at  $\approx 100$  Ma. The shape of this trend and the stratigraphic position of the maximum carbon isotopic value mimic the carbon isotopic trend defined by pelagic marine limestones. The correlation of the terrestrial and marine carbon isotopic records suggest that the concretions are recording changes in the global carbon reservoir.

Comparison of the terrestrial concretion carbon and oxygen isotope data with the corresponding marine data suggests that the concretions provide an accurate record of global changes in climate and in the exogenic carbon reservoir.



**BORON ISOTOPIC COMPOSITION OF FUMAROLIC FLUIDS, VULCANO CRATER, AEOLIAN ISLANDS, ITALY.**

FERRARA, G. Ist. Geocronologia, CNR, 56127 Pisa, Italy  
 LEEMAN, W., P. Keith-Wiess Geological Laboratory, Rice University, Houston, TX 77251, USA;  
 PENNISI, M. and TONARINI, S., Ist. Geocronologia, CNR, 56127 Pisa, Italy.

New boron isotopic data are presented bearing on the origin of fluids from Vulcano crater. Changes in composition and temperature of fumarolic emissions in this century, and correlations of these data with seismicity indicate that periodic reconfigurations of the hydrothermal system occasionally occur involving the development and/or the sealing of permeability connecting different reservoirs. An increase of steam output since 1987 reflects an increased input of water into the system. Evidence for contributions from a degassing magma body at depth remains inconclusive.

Boron isotopic measurements were undertaken to characterize the sources of boron in the fumarolic fluids.  $\delta^{11}\text{B}$  data are presented as permil deviation of  $^{11}\text{B}/^{10}\text{B}$  relative to NBS SRM 951. Typical values are +40 for seawater,  $\pm 5\text{‰}$  for volcanic rocks, from 0 to -20‰ for sediments.  $\delta^{11}\text{B}$  values in condensates from a single fumarole (F5) have generally increased with time (-4 to +3‰) since 1978; this trend is interrupted by significant decreased (up to 3‰) in 1985, 1989, and early 1993. The reversal in 1985 was associated with intense seismic activity and increased  $\text{CO}_2$  content of the fluid, which suggests an increased magmatic contribution.

These trends suggest mixing between fluids having at least two distinct compositions: (1) a high  $\delta^{11}\text{B}$  fluid like seawater (possibly modified by extensive interaction with igneous rock), and (2) a low  $\delta^{11}\text{B}$  component linked to direct magmatic fluid or fresh-water/rock interaction processes.

Analyses of 1993 fluids from higher temperature fumaroles (F0, FA, F5AT) show only minor differences in  $\delta^{11}\text{B}$  (<1‰) from the F5 fluids. Significantly lower  $\delta^{11}\text{B}$  values (-8 to -10‰) were measured in sublimates (sassolite) collected in quartz tubes from the same fumaroles. The difference between sublimates and aqueous fluids suggests that isotopic fractionation may be significant between these phases.

Sr, Nd, O AND S ISOTOPIC SIGNATURES AND THE MANTLE SOURCE FOR ULTRAPOTASSIC SYENITIC MAGMAS IN NORTHEASTERN BRAZIL

FERREIRA, V.P.; SIAL, A.N., Stable Isotope Lab., Dept. of Geology, UFPE, C.P. 7852, Recife, PE, 50732-970, Brazil; LONG, L.E., Univ. Texas, Dept. of Geological Sciences, Austin, TX, 78713, USA; PIN, C., Univ. Blaise Pascal, 5, rue Kessler, 63038, Clermont-Ferrand, Cedex, France

Elongate plutons consisting of alkali-feldspar syenitic rocks containing alkalic pyroxenite as enclaves and syn-plutonic dikes, form a unique Late Proterozoic plutonic ultrapotassic province, along the southern boundary of the Cachoeirinha-Salgueiro foldbelt, northeastern Brazil. Coexisting syenite and pyroxenite have same mineral phases (aegirine-augite, microcline, apatite and sphene) at different modal amounts. Field and textural relationships indicate that they were mostly in liquid state when came into contact with each other. Angular to sub-rounded mica pyroxenite xenoliths, up to 10 cm-long, are found in some of the plutons. They consist of pale-green pyroxenite containing major diopside-salite, that forms "mosaics" in which phlogopite, and occasionally calcite and feldspar, are interstitial, replacing pyroxene along its grain boundaries, a textural relationship which suggests metasomatic replacement.

Syenite and pyroxenite have high pyroxene-corrected  $\delta^{18}\text{O}$ , with limited variation (+8.1 to + 8.5‰<sub>SMOW</sub> in syenite and +7.6 to +7.7‰ in pyroxenite),  $\delta^{34}\text{S}$  (+ 12.3‰ in syenite and +11.2‰<sub>CDT</sub> in pyroxenite), and initial  $^{87}\text{Sr}/^{86}\text{Sr}$  ratio (0.7098, syenite and pyroxenite lying on the same Rb-Sr isochron), and low  $\epsilon\text{Nd}$  (-15.3 to - 17.2 in syenite and -16.1 in pyroxenite). Whole-rock  $\delta^{18}\text{O}$  for mica pyroxenite xenoliths varies from +7.5 to +9.4‰<sub>SMOW</sub>. Syenite and pyroxenite have similar LREE-enriched chondrite-normalized patterns and are large-ion lithophile element-enriched. Xenoliths show significant incompatible element concentrations when compared to normal mantle compositions, particularly Ba, La, K, Ce, Nd, Sm, Sr and Y.

Geochemical and isotopic signatures for the ultrapotassic syenite magma suggest that it derived from an enriched mantle source. Such mantle enrichment likely resulted from hybridization by addition of crustal material via subduction, producing mica pyroxenite masses, at around 2.1 Ga, as estimated from Nd crust-formation model ages. Reactivation of extensive, deep shear zones seem to have triggered melting of these mica pyroxenites producing ultrapotassic magma. Shear zones were the pathway for emplacement of this magma, during the late stage of the Brasiliano (= Pan-African) orogeny, around 580 Ma, as indicated by the Rb-Sr isochron age for the syenites.

STABLE ISOTOPE ANALYSES OF LATE-GLACIAL TO HOLOCENE LACUSTRINE SEDIMENTS FROM DIFFERENT LAKES IN THE JURA (SWITZERLAND-FRANCE)

FILIPPI, M. L., Inst. de Minéralogie et Pétrographie, Université de Lausanne, BFSH2 Lausanne, 1015-CH, Switzerland, and HUNZIKER, J. C., same address.

Stable isotope analyses were made of whole-rock lacustrine chalks and shell materials from three lakes in Switzerland and in France for the purpose of obtaining paleoclimatic information.

Detrital carbonate components can mask or obliterate the isotopic record of a lake, particularly a large lake (e.g., Lake Lemán, SW Switzerland) where carbonates outcrop in the hydrological catchment area. In addition, tests must be made for the presence and quantity of aragonite in the composite samples (e.g., Lake Ilay, France). In the present study, X-Ray analyses was used to identify and quantify such components. In favourable cases, it may be possible to separate authigenic calcite from detritic phases.

The temperature of bottom waters of the lakes is relatively constant. A comparison was therefore made between the oxygen isotope composition of bulk carbonates and benthic mollusks in order to distinguish between temperature and isotopic composition of the environmental water.

From the lack or presence of covariance between  $\delta^{18}\text{O}$  and  $\delta^{13}\text{C}$  values, it was possible to distinguish between open- and closed-system behaviour of the lakes.

Coupled X-Ray and isotopic analyses were made of a core 12 m long from the peri-Jura Lake Loclat (Neuchâtel, Switzerland, Rolli *et al.*, in press). The bottom part of the core is rendered useless for paleoclimatological work because of the presence of a large detrital component which is reflected by abnormally high values of  $\delta^{18}\text{O}$  and  $\delta^{13}\text{C}$ . In the upper part of the core, there is a well-delineated lowering of about 2 ‰ in  $\delta^{18}\text{O}$  of bulk authigenic carbonates that corresponds to the Younger Dryas biozone. Two other smaller shifts in  $\delta^{18}\text{O}$  are related to the "Gerzensee" (Allerød-Younger Dryas) and "Aegelsee" (Bølling-Allerød) oscillations. There is a rather abrupt decrease in  $\delta^{13}\text{C}$  values from -2.5 to -8.0 ‰ after the Boreal. This large change is interpreted to reflect a major change in bio-productivity and conforms with sedimentological data.

The covariation observed between  $\delta^{18}\text{O}$  and  $\delta^{13}\text{C}$  ( $R=0.83$ ) over the interval 380 cm to 0 cm is interpreted to reflect precipitation of carbonates from a closed lake that experienced no fundamental change in basin hydrology over this period. Absence of a similar trend before the Younger Atlantic suggests an open lake system complicated by climatic changes.

Rolli, M. *et al.*, (in press), Late-glacial climatic oscillations recorded in lake sediments of Loclat (Neuchâtel, Switzerland): sedimentology, palinology, mineralogy, geochemistry and isotopic evidences. Preliminary data: II Quaternario

## $^{10}\text{Be}$ and $^{36}\text{Cl}$ in the GISP2 Ice Core

R Finkel<sup>1</sup>, K Nishiizumi<sup>2</sup>, M Caffee<sup>1</sup>, C Kohl,<sup>3</sup> and J Southon<sup>1</sup>

<sup>1</sup>LLNL, PO Box 808 L-237, Livermore CA 94550

<sup>2</sup>Space Sciences Laboratory, UC Berkeley, 94702

<sup>3</sup>UCSD, La Jolla, CA 92093

Cosmogenic radionuclide concentrations in ice cores can be used to study the history of solar activity, of the geomagnetic field and of climate. With these objectives in mind, we are currently measuring a continuous profile of  $^{10}\text{Be}$  and  $^{36}\text{Cl}$  in the 3.05 km-long GISP2 ice core, from the ice cap summit in central Greenland. The time resolution of our sampling varies from annual in the upper part of the core to centennial in the lower part. The annual samples show variations correlated with the 11-year Schwabe solar activity cycle. The  $^{10}\text{Be}$  and  $^{36}\text{Cl}$  concentrations also show significant climate-related variations. These variations are correlated with the climate swings (Oldest Dryas - Bølling-Allerød and Younger Dryas - Preboreal) which occurred at the end of the last glacial period. Using the high resolution depth-age relation determined by annual layer counting on the GISP2 core[1], we have calculated radionuclide fluxes on a sample by sample basis in order to examine the role of changing annual layer thickness in determining the changes in radionuclide concentration. We have also revisited the variability in the  $^{10}\text{Be}/^{36}\text{Cl}$  ratio in ice cores [2, 3]. We find that the ratios observed in these samples are significantly less variable than has been observed in cores from other sites in Greenland.

References: [1] Alley, R.B., *et al.* *Nature* **362**, 527-529 (1993); [2] Elmore, D., *et al.*, *Nucl. Inst. Meth.* **B29**, 207-210 (1987). [3] Suter, M., *et al.*, *Nucl. Instr. Meth.* **B29**, 211-215 (1987).

This work was performed under the auspices of the U.S. Department of Energy by the Lawrence Livermore National Laboratory under contract W-7405-Eng-48 and supported by the NSF Division of Polar Programs.

## THERMOCHRONOLOGIC CONSTRAINTS ON POST-PALEOZOIC TECTONIC EVOLUTION OF THE CENTRAL TRANSANTARCTIC MOUNTAINS, ANTARCTICA.

FITZGERALD, P.G., Dept. of Geosciences, University of Arizona, Tucson, AZ 85721, USA

The development of topography is one of the most visible and obvious effects of the forces that drive plate tectonic processes throughout geologic time. Determining the age of the development of topography is important as it has fundamental implications for regional geological history, as well as a myriad of subsidiary processes, one of the most obvious being the effect that topography has on the world climatic systems. The ~4500 km long Transantarctic Mountains (TAM) bisect Antarctica dividing it into two distinctly different geologic terrains, and acting as a buttress against which the East Antarctic Ice Sheet rests. The roots of the mountains are a late Proterozoic-early Paleozoic orogenic belt (Ross Orogen), but the present day range is a rift shoulder stemming from uplift episodes begun in the Cretaceous.

Apatite fission track thermochronology on samples collected from the central TAM records a complex thermo-tectonic history for this region over the past 350 Ma. This part of the central TAM can be divided into a number of semi-independent fault blocks on the basis of topography and sub-glacial morphology. Apatite ages in the Miller Range vary from ~250 to ~350 Ma and record an uplifted fossil apatite partial annealing zone formed subsequent to cooling of Ross Orogen granitic intrusives, peneplanation of those granites to form the Kukri Penplain, and deposition of Devonian through Triassic Beacon Supergroup sediments. A period of Cretaceous uplift (~1.5-2 km), beginning at about 115 Ma, is recorded in data from Moody Nunatak on the inland side of the Queen Elizabeth Range. Uplift at this time may be related to the formation of a broad, southward plunging syncline in the Kukri Penplain. Timing of the formation of this syncline is problematical and it may only be an apparent syncline formed by differential and variable block uplift associated with uplift of the mountains. Along the Beardmore Glacier, samples record rapid cooling indicative of uplift initiated in the early Cenozoic (~50 Ma). The amount of uplift ~70 km inland of the coast in the Queen Alexandra Range since the early Cenozoic is ~7 km, with the likelihood of ~3 km more at the coast. Eastward facing topographic escarpments in the Queen Alexandra Range mark the likely position of steeply dipping normal faults, which offset apatite ages. Ages on the east side of the Beardmore Glacier mouth are generally younger (average 27 Ma) than on the west side (average 33 Ma) interpreted to reflect a greater amount of denudation. Assumptions made regarding the use of an assumed paleogeothermal gradient and paleo-land surface elevation are tested with available geologic evidence. Fission track data do not constrain whether there has been significant surface uplift of the TAM since the Pliocene as suggested by other evidence. The results build upon the available fission track database along the TAM and emphasize the subtle variability of uplift along the TAM due to episodic uplift involving differential block movements, both of which are important constraints on models proposed for the uplift of the TAM.

CHRONOLOGY OF MULTIPLE INTRUSION IN THE  
TUOLUMNE INTRUSIVE SUITE, YOSEMITE  
NATIONAL PARK, SIERRA NEVADA, CALIFORNIA

**FLECK, Robert J.** and **KISTLER, Ronald W.**, Branch  
of Isotope Geology, U.S. Geological Survey Mailstop 937,  
345 Middlefield Road, Menlo Park, CA 94025, U.S.A.

The Tuolumne Intrusive Suite is a zoned intrusive complex within the Sierra Nevada batholith. The zonation is lithologic, mineralogic, chemical, and isotopic, forming an irregular,  $\approx 1500 \text{ km}^2$ , plutonic complex elongate parallel to the regional structure. From the margin to the center of the suite, lithologically and mineralogically distinct zones are mapped as the Sentinel Granodiorite, granodiorite of Yosemite Creek, granodiorite of Kuna Crest, Half Dome Granodiorite, Cathedral Peak Granodiorite, and Johnson Granite Porphyry. Published age data are consistent with emplacement of the entire intrusive suite during a geologically brief interval at about  $87 \pm 4 \text{ Ma}$ .  $^{40}\text{Ar}/^{39}\text{Ar}$  and Rb-Sr mineral ages reported here, however, decrease from about 89 Ma at the margin of the intrusive complex to less than 81 Ma near the center, requiring either a prolonged, variable-rate, inward-progressing cooling or a much more complicated, multiple-intrusion history. Geobarometry indicating emplacement of the intrusive suite at  $\approx 7 \text{ km}$  does not permit holding temperatures in a single intrusion above  $300^\circ\text{C}$  for an 8-m.y. period, even with a 10-km plutonic radius. Mirolitic cavities in the youngest unit of the intrusive suite, the Johnson Granite Porphyry (80.5 Ma, K-Ar on biotite), suggest a shallow emplacement and raise further questions on the efficacy of an extended, lateral cooling rather than more rapid, vertical heat-loss to the surface.

Patterns of mineral-age discordance indicate that most of the Tuolumne Intrusive Suite formed during three major intrusive pulses with maxima at about 89 Ma, 86 Ma, and 84 Ma with the Johnson Granite Porphyry emplaced at 81 Ma. Coeval intrusive units defined by the distribution of mineral ages are consistent with chemical, isotopic, and geophysical data, but not all correlate with previously-mapped lithologic contacts. Based on zircon U-Pb and hornblende  $^{40}\text{Ar}/^{39}\text{Ar}$  ages, the 89-Ma group includes the outer three units and the outer part of the Half Dome Granodiorite. The inner part of the Half Dome Granodiorite and the outer part of the Cathedral Peak Granodiorite were emplaced sequentially at about 86 Ma with little or no disturbance of hornblende isotopic systems in the older units.  $^{40}\text{Ar}/^{39}\text{Ar}$ , K-Ar, and Rb-Sr ages of biotite within 1-2 km of the 86-Ma group, however, are reset. U-Pb ages on sphene and  $^{40}\text{Ar}/^{39}\text{Ar}$  age spectra of hornblende from the younger, inner part of the Cathedral Peak Granodiorite indicate that it was emplaced at about 84 Ma. Biotite ages of the 86-Ma group reflect similar patterns of discordance due to thermal effects of this 84-Ma body. Interpretation of an 80.5-Ma biotite K-Ar age as the time of emplacement of the Johnson Granite Porphyry is consistent with its shallow intrusion and with similar ages for Rb-Sr and K-Ar on biotite and microcline in adjacent rocks of the inner part of the Cathedral Peak Granodiorite that it intrudes. Minerals interpreted to be partially reset by younger phases of the suite commonly yield discordant  $^{40}\text{Ar}/^{39}\text{Ar}$  age spectra.

Isotope Geochemistry of Antarctic Flood Basalts (Ferrar Group): establishing the effects of alteration and upper crustal contamination and constraining the source signature.

**FLEMING, T.H.**, **FOLAND, K.A.**, **ELLIOT, D.H.** and **HEIMANN, A.** Byrd Polar Research Center and Department of Geological Sciences, Ohio State University, Columbus, OH, 43210, USA.

Jurassic tholeiites of the Ferrar Group, with volume of more than  $5 \times 10^5 \text{ km}^3$ , crop out in a linear belt extending over 3000 km along the Transantarctic Mountains. They are represented by flood basalts, sills and a large layered basic intrusion and are characterized by enriched crustal-type trace-element ratios and radiogenic isotopic compositions ( $^{87}\text{Sr}/^{86}\text{Sr} = 0.709$  to  $0.713$ ,  $\epsilon\text{Nd} = -4.0$  to  $-5.9$ ). Considerable uncertainty and debate has revolved around the age, the significance of variations in Sr and O isotopic compositions, and the meaning of the apparent elevated initial  $^{87}\text{Sr}/^{86}\text{Sr}$  ratios. Our recent work on the basalts has demonstrated: the formation of most of the province in a restricted interval ( $< 1 \text{ m.y.}$ ) at 177 Ma from  $^{40}\text{Ar}/^{39}\text{Ar}$  measurements on plagioclase; alteration in the mid-Cretaceous is based on several lines of evidence, including direct  $^{40}\text{Ar}/^{39}\text{Ar}$  and Rb/Sr dating of secondary minerals; and, the production of  $\delta^{18}\text{O}$  variations by low temperature alteration at the surface. New Sr and Nd isotopic study of both rocks and separated minerals from north Victoria Land and the central Transantarctic Mountains further clarify: the effects of alteration; the role of upper crustal assimilation; and, constrain the apparent isotopic composition of primitive magmas. We demonstrate that some of the previously observed variations in calculated initial  $^{87}\text{Sr}/^{86}\text{Sr}$  ratios reflect alteration but that  $^{143}\text{Nd}/^{144}\text{Nd}$  ratios are not similarly affected. Many calculated initial  $^{87}\text{Sr}/^{86}\text{Sr}$  ratios are simply incorrect due to post-formation changes in Rb/Sr; this has masked petrogenetic relationships. Good correlations exist between initial  $^{87}\text{Sr}/^{86}\text{Sr}$ ,  $\epsilon\text{Nd}$ , and major and trace element chemistry. Isotopic-chemical relationships are consistent with upper crustal evolution by an assimilation-fractional crystallization process involving a crustal end member similar to  $\approx 500 \text{ Ma}$  basement granitoids of the Ross Orogen. This mode of evolution appears remarkably uniform over much of the province. The composition of the most primitive end member, representing the least contaminated magma, is  $^{87}\text{Sr}/^{86}\text{Sr} = 0.7087$ ,  $\epsilon\text{Nd} = -4.0$ ,  $\text{Mg}\# = 70$ , and  $\text{Zr} = 50 \text{ ppm}$ . The earlier (e.g., lower crustal and upper mantle) petrogenetic history of the primitive magma remains uncertain. Their isotopic and geochemical characteristics could potentially be attributed to several processes. Coincidence of the outcrop belt and chemical and isotopic similarities to the Ross Orogen granite suite suggests that the enriched isotopic characteristics of these rocks are either inherited by earlier assimilation or maybe derived from an enriched source that was impacted by material from the Ross Orogeny.

## PHYSICAL CONTROLS ON THE COMPOSITION GRANITIC MAGMAS: THE ROLE OF OROGENIC STRAIN HISTORIES AND THE STATE OF THE LITHOSPHERE.

FODEN, J.D., *Dept. of Geology and Geophysics, University of Adelaide, Box 498 GPO Adelaide, South Australia, Australia, 5001.*

Orogenic belts often experience early syn-tectonic intrusion of granites of I- to S-type composition and may have undergone rapid transition from previous extensional sedimentary basins with active mafic magmatism. They may also abruptly end their active deformation with a phase of rapid uplift and the post-tectonic appearance of bimodal magmatism in which the granites (or their volcanic equivalents) have A-type characteristics.

These granites are related to influx of heat carried by mafic magmas and their chemistry reflects the degree of interaction between crust and mantle-derived melts. The proportion of crustal contribution is maximal during maximum crustal thickening, but is minor in pre- and post-deformational regimes.

Simple calculations based on the conductive cooling of initial sill-like mafic intrusions were a basis for the modelling, as a function of time, of the following parameters: residual melt composition, crystallisation and fractionation, wall-rock heating and melting, assimilation, density, viscosity, Stokes Law buoyancy, Nd-Sr isotopic composition and zircon inheritance. Results imply that the cooling history of mafic intrusions falls into two classes:

1. Those which heat significant volumes of their roof rocks to temperatures > crustal minimum melting temperatures (700 degrees).
2. Those for which the crustal minimum melting isotherm always falls within the margins of the intrusion. These distinctions are strongly depth dependant and are fairly independent of geothermal gradient.

Type 1 magma chambers arise when mafic magmas stall at the density step at the Moho. These will evolve to produce I-S type granite melts with SiO<sub>2</sub> contents > 67% with masses equivalent to > 70% of the initial mafic body in between 0.3 and 1.5 Ma ( $\pm 0.5$  Ma). They will have Pb-, Sr- and Nd isotopic compositions which are strongly influenced by the crust and contain significant proportions of inherited zircons.

Type 2 magma chambers arise when the crust is undergoing extension, and mafic magmas experience only lithostatic loads and travel via dilatant fractures to levels approaching their levels of neutral buoyancy. Intrusions experience only slight crustal contamination and may develop to highly fractionated melts (A-type granite, rhyolite, dacite, latite or trachyte). They experience rapid decline in melt mass reaching 70% silica with between 20 and 40% of their original mafic parent mass and have few inherited zircons.

This model fits well with recent descriptions of A-type granites developed during advancing Tertiary crustal extension prior to the development of the Red Sea. It is also interesting to note that the Australian Palaeo- to Mesoproterozoic is characterised by extensive intracratonic A-type granite magmatism evolution from mid- to high level crustal mafic intrusions and by a pervasively thinned lithospheric structure. By contrast the Palaeozoic of eastern Australia is dominated by I-S type granites suggesting more crustal interaction and thicker, cooler lithosphere.

## INTERPRETATION OF <sup>40</sup>Ar/<sup>39</sup>Ar AGES AND INCREMENTAL-HEATING DATA IN THE CONTEXT OF Ar VOLUME DIFFUSION

FOLAND, K.A., *Department of Geological Sciences, Ohio State University, Columbus, OH, 43210, USA.*

Transport of Ar in minerals by volume diffusion processes is generally viewed as important to Ar losses in nature and also during laboratory experimentation. Volume diffusion transport leads to the concept of a closure temperature and, as well, to straightforward modeling. However, there are several reasons and factors that make <sup>40</sup>Ar/<sup>39</sup>Ar incremental-heating relationships much more complicated than described by elementary theory. These include: (1) the mechanical degradation of mineral grains and reactions that during laboratory heating; (2) the heterogeneities on various scales in the physical and chemical characteristics of almost all natural samples; (3) sample reaction and the formation of grains below the characteristic blocking temperature in nature; (4) the occurrence of Ar in inclusions and other microstructural features; (5) the effects of neutron irradiation especially <sup>39</sup>Ar recoil and redistribution; and, (6) trapping of Ar in defects and such features as embedded inclusions, sealed micropores, or healed cracks. These factors are important not only for the hydrous minerals (micas, amphibole) but also anhydrous ones (feldspars). They affect both the ages and the kinetics of Ar release. Further, they combine to make the classic "Ar loss" incremental-heating spectrum basically a concept that is virtually never applicable to natural samples. Such spectra appear to result from the temperature dependence of laboratory degassing as a consequence of phase instability or particle size. As a result, spectra are commonly convolutions of gas released from heterogeneous samples. The physical processes operating during laboratory heating as well as in nature must be realistically taken into account in the interpretation and modeling of incremental-heating age and kinetics data.

SR-ND-PB ISOTOPE AND TRACE ELEMENT  
CONSTRAINTS ON ASSOCIATED HFSE VARIABLY  
DEPLETED SHOSHONITIC VOLCANISM IN THE  
HALMAHERA ARC, INDONESIA

FORDE E.J., THIRLWALL M.F., and VROON P.Z.,  
Dept. of Geology, Royal Holloway, University of London,  
Egham, Surrey, U.K. and HALL R., Dept of Geological  
Sciences, University College, London, U.K

The Halmahera arc is an intraoceanic calc-alkaline arc with a wide range in K<sub>2</sub>O contents, ranging from medium-K to shoshonitic values. Volcanism dates from the early Neogene in the south of the arc to the Quaternary in the north, where it is still currently active, due to the ongoing subduction of the Molucca Sea plate.

A relationship between K content and depth to the Benioff zone is not seen; instead shoshonitic volcanism is restricted to the south-western area of the island of Bacan at the arc front, where lavas have been dated at 6.7Ma- 0.9Ma. They are characterised by large enrichments in LILE and LREE, particularly Th, Pb, Sr, Ba, La, Ce and Nd. Sr-Nd-Pb isotopic systematics have been used to divide the shoshonites into three groups, and to constrain the sources contributing to their geochemical characteristics.

Group I has low <sup>87</sup>Sr/<sup>86</sup>Sr (0.7031- 0.7036), in comparison with the rest of the arc (0.7038 - 0.7044), despite similar <sup>143</sup>Nd/<sup>144</sup>Nd (0.5129). They also show the greatest enrichments in LILE and LREE (eg Sr 1700-2600ppm, La 50-80ppm). Group II, however, has relatively radiogenic <sup>87</sup>Sr/<sup>86</sup>Sr (0.7050- 0.7055) and <sup>206</sup>Pb/<sup>204</sup>Pb (18.7- 18.8) and lower <sup>143</sup>Nd/<sup>144</sup>Nd (0.5127). LILE and LREE enrichments are also lower than Group I (eg Sr 850-1400ppm, La 35-45ppm). Various different sources and/or magmatic processes are therefore considered to account for the isotopic variation of the shoshonites themselves, and relative to the rest of the arc.

Isotopic variation between Group I and II can only be explained by mixing with a large proportion (up to 50%) of a crustal component, due to the high Sr-Nd-Pb concentrations in the most depleted end-member. However, this crustal component is not recognised elsewhere in the medium to high K volcanics. The isotopic and trace element variation between the shoshonites relative to the rest of the arc must be due to the involvement of different sources. Elevated Ba/La (20-40) for the major part of the arc suggests a dominant influence from fluids derived from the subducted slab, whereas reduced Ba/La (10-20) and extreme La/Nb values (10-22) favour a more LREE-enriched source for the shoshonites, within the mantle wedge.

Finally Group III shoshonites have intermediate <sup>87</sup>Sr/<sup>86</sup>Sr (0.7041), <sup>206</sup>Pb/<sup>204</sup>Pb (18.6) and high <sup>143</sup>Nd/<sup>144</sup>Nd (0.5129), comparable with Group I. These volcanics however show relative enrichment in HFSE, (eg Nb=10-18ppm). This suggests a controlling influence on the HFSE concentrations by a suitable mineral phase, such as phlogopite in an enriched source in the mantle wedge. Residual phlogopite in the mantle wedge thus produces Group I and II, whilst melting of phlogopite within the source produces the high Nb shoshonites of Group III.

THERMOCHRONOLOGIC CONSTRAINTS ON THE  
DEVELOPMENT OF METAMORPHIC CORE  
COMPLEXES IN THE LOWER COLORADO RIVER  
AREA

FOSTER, D. A., VIEPS, School of Earth Sciences, La  
Trobe University, Bundoora, Victoria 3083, Australia,  
HOWARD, K.A. USGS, Menlo Park, CA 94025, JOHN,  
B.E., Department of Geology and Geophysics, University  
of Wyoming, Laramie, WY 82071.

The recent literature abounds with models for the development and exhumation of metamorphic core complexes. Thermal histories of footwall and hanging wall rocks determined by <sup>40</sup>Ar/<sup>39</sup>Ar and fission-track thermochronology provide valuable constraints on the nature of extension and evolution of metamorphic core complexes. In addition to dating the timing of extension in core complexes, thermochronologic data reveal information about rates of cooling, exhumation, and fault displacement, as well as the geometry of faults and paleogeothermal gradients.

Major extension in the lower Colorado River area, California and Arizona, occurred between ~24 and ~14 Ma, based upon geologic and thermochronologic data. Biotite and K-feldspar K-Ar and <sup>40</sup>Ar/<sup>39</sup>Ar apparent ages, and zircon and apatite fission-track apparent ages from the Chemehuevi, Sacramento, Whipple, Buckskin, and Harcuvar Mountains metamorphic core complexes consistently young in the displacement direction (southwest to northeast) of exposed detachment faults. An abrupt change in the age/distance gradients at 24-20 Ma for biotite and high temperature K-feldspar data marks the onset of rapid extension, while linear trends with slopes of ~3-8 km/m.y. for low temperature K-feldspar and fission-track data in these complexes estimate displacement rates on detachment faults.

Gradients of age vs. slip direction across tilted upper plate fault blocks reveal information about the temperature variation with depth at the onset of extension, when the amount of tilting is known from paleohorizontal indicators. These trends can be used to estimate pre- to syn-extensional geothermal gradients when more than one mineral curve yields the characteristic "break-in-slope", indicating the depth at which pre-extensional ages were zero. In the Mohave Mountains (tilted ~90°) the paleodistance between intercepts of biotite and K-feldspar (low temperature steps) apparent age trends with the time of tilting (a difference of ~100°C) is ~4 km, suggesting a syn-extensional gradient of ~25°C/km. Similarly, apatite and zircon fission-track data from the Tortilla Mountains (southeast of the lower Colorado River area) give a gradient of ~18°C/km, and apatite and K-feldspar ages from the Piute Mountains reveal a paleogradient of 25°-40°C/km.

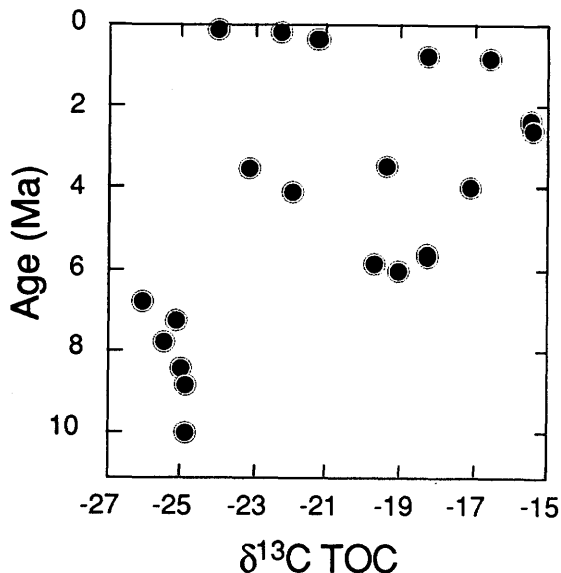
The dip at which brittle detachment faults operate in the upper crust is still highly controversial. In the Chemehuevi Mountains the thermochronologic data reveal a trend of increasing temperature in the slip direction from ~200° to 350°-400°C over an exposed distance of 23 km, at the onset of extension. Assuming the geothermal gradients listed above, the relatively gradual increase in temperature with original depth, suggests only gentle southwest tilting of the footwall and constrains the Chemehuevi detachment fault to have had an original dip of ~15°-30°.

**A NEOGENE RECORD OF  $\delta^{13}\text{C}$  OF TERRIGENOUS ORGANIC CARBON BURIED IN THE BENGAL FAN: IMPACT ON CARBON CYCLING**

FRANCE-LANORD, C., CRPG-CNRS, BP20 54501 Vandoeuvre - France (cfl@crpg.cnrs-nancy.fr) and DERRY L.A., Cornell U., Dept. of Geological Sciences, Ithaca, NY 14853-1504 - USA.

Sediments deposited in the Bengal fan and recovered by ODP Leg 116 contain an 18 Ma record of erosion from the Himalaya. Estimates of organic carbon burial rates suggest that the Bengal Fan has been a sink for 10-15% of global OC burial during the Neogene. Previous studies including gas chromatography and pyrolysis imply that the organic carbon is dominated by terrigenous sources (Poynter & Eglinton, 1990, ODP Sc. Res. 116). Thus the isotopic composition of organic carbon in the Bengal Fan should reflect the POC load of the Ganges-Brahmaputra rivers. We report  $\delta^{13}\text{C}$  analysis of total organic carbon (TOC) buried in the Bengal fan, in order to obtain a time series of the river inputs. TOC ranges from 0.5 - 2.0 wt. %.  $\delta^{13}\text{C}$  values are near -25‰ between 18 and 7 Ma. Values shift dramatically to -19‰ by 6 Ma, reaching a maximum of -15‰ at 2.4 Ma.  $\delta^{13}\text{C}$  in Pleistocene samples returns gradually to depleted values.

The >10‰ positive shift beginning at 7 Ma mirrors similar magnitude changes in the  $\delta^{13}\text{C}$  of paleosol carbonates from the Siwaliks (Quade et al., 1989). This change reflects the radiation of C4 plants. Our data show that the export of terrigenous carbon from India was dominated by C4 material during the Pliocene. Mass balance calculations suggest that the isotopic change in river OC can account for a +0.5‰ shift in the late Mio. marine carbonate  $\delta^{13}\text{C}$  record.



**OXYGEN ISOTOPIC COMPOSITION OF ORDINARY CHONDRITES - A MINERALOGICAL CONTROL?**

FRANGLI, I.A., PILLINGER, C.T., Planetary Sciences Unit, Dept. of Earth Sciences, Open University, Milton Keynes, MK7 6AA, UK, BRIDGES, J.C. and HUTCHISON R., Dept. of Mineralogy, Natural History Museum, London, SW7 5BD, UK.

The oxygen isotopic variation of ordinary chondrites is limited to only 2-3‰ in both  $\delta^{17}\text{O}$  and  $\delta^{18}\text{O}$ , with the H, L and LL groups occupying distinct fields in the oxygen three isotope plot (1). However, Clayton and co-workers have also shown that the range in  $\delta^{17}\text{O}$  and  $\delta^{18}\text{O}$  of chondrules from unequilibrated ordinary chondrites (UOCs) is the same for all three groups and define a mixing line of slope approximately 0.75, with no clear variation with host meteorite type or chondrule composition (eg. 1,2). However, one parameter which was found to influence oxygen isotopic composition of UOC chondrules was their size, the smallest chondrules falling at the lighter end of the mixing line, the largest towards the heavier end. The explanation favoured by Clayton and co-workers is that larger chondrules are more processed and have undergone a higher degree of exchange with a relatively heavy gas phase.

Recently we reported the highest ever  $\delta^{17}\text{O}$  and  $\delta^{18}\text{O}$  values in cristobalite-rich material separated from chondrules in UOC Parnallee (LL3.6) using a laser micro-analysis technique (3). These chondrules define a mixing line (dependent on the proportion of cristobalite) which is an extension of the mixing line defined by chondrules from all UOCs, but with a  $\delta^{18}\text{O}$  5‰ heavier than any other chondrules. A cristobalite-bearing sample from the L5 ALH76003 ordinary chondrite has an enrichment approximately half that seen in the Parnallee chondrules (4). Clues to the origin of this enrichment may come from density fractions of the Mezö-Madaras L3 meteorite which have oxygen isotopic compositions which also fall close to the same mixing line, with the densest fractions (olivines and pyroxenes) at the isotopically lighter end and the least dense fractions (feldspar with glass) towards the heavier end (5). The relative positions of the various mineralogical components of chondrules in UOCs along this mixing line starting at the isotopically light end are olivine, pyroxene, feldspar (with glass) and finally cristobalite.

There are a number of processes which could have produced mineralogical ordering of oxygen isotopic compositions. Perhaps one of the most intriguing is that the order of increasing  $\delta^{17}\text{O}$  and  $\delta^{18}\text{O}$  is essentially that of increasing diffusion co-efficients of oxygen in the various mineral phases. This would support the view that the oxygen isotopic composition of these phases was controlled by some exchange process between isotopically light solids and an isotopically heavier gas reservoir (1,6).

We are currently separating additional phases from Parnallee and other UOCs to determine how common or variable these effects are in UOCs in order to explore further mineralogical controls responsible for this isotopic variation.

- (1) Clayton, R.N. *et al.* 1991, *GC.A.* 55, 2317-2337.
- (2) Gooding, J.L. *et al.* 1983, 65, 209 - 224.
- (3) Bridges, J.C. *et al.* 1993, *Meteoritics* 28, 329 - 330.
- (4) Olsen, E.J., *et al.* 1991, *Lett.* 56, 82-88.
- (5) Mayeda, T.K., Clayton, R.N. and Sodonis, A. 1989, *Meteoritics* 24, 301.
- (6) Clayton, R.N. 1993, *Ann. Rev. Earth Planet. Sci.* 21, 115 - 149.

## THE STABLE CHLORINE ISOTOPIC SIGNATURE OF GROUNDWATERS IN CRYSTALLINE SHIELD ENVIRONMENTS

FRAPE, S.K., BRYANT, G., Dept. of Earth Sciences, University of Waterloo, Waterloo, Ontario, N2L 3G1, Canada, and BLOMQVIST, R., Geological Survey of Finland, Betonimiehenkuja 4, SF-02150 Espoo, Finland.

The evolution and origin of groundwaters in crystalline shield environments has been an issue for a number of years. Recent studies have expanded the use of stable chlorine isotopes to evaluate the evolution of saline waters and brines in the Canadian and Fennoscandian Shields.

Groundwaters in ancient Shield environments are composed of Ca or Na and Cl; often with dissolved loads in excess of 100 g l<sup>-1</sup>. The origin of salinities in excess of sea water salinity has been attributed to a variety of processes; but the effects of water/rock interaction are generally assumed to overprint any original fluid signatures.

The <sup>37</sup>/<sub>35</sub> Cl signatures for each Shield are quite different. Canadian Shield brines are almost all isotopically negative with values ranging from -1.5 to SMOC. Fennoscandian Shields brines are all positive, with values ranging from SMOC to + 2.0. Most field sites have distinctive isotopic signatures and generally more mafic, volcanogenically open systems tend to have more positive isotopic signatures.

As the major anion, chlorine has a limited number of possible sources. The seawater stable chlorine isotopic signature is assumed to be constant through time, although this is not proven. Therefore changes in chlorine isotopic ratios within shield rocks can be attributed to various processes such as boiling - volatilization rock-water exchange and mixing of very different waters through time. The data available from our studies suggests that all of these processes play a role in modifying the isotopic signatures observed.

## RB-SR DATING OF HYDROTHERMAL ILLITES - POTENTIALS, LIMITATIONS AND POSSIBLE CONSTRAINTS ON THE GENESIS OF A MINERALIZING FLUID; AN EXAMPLE FROM THE KASSANDRA MINING AREA (GREECE)

FREL, R., Group for Isotope Geology, Mineralogical-Petrographical Institute, University of Berne, Berne, 3012, Switzerland

The Kassandra mining district in Northern Greece consists of porphyry copper mineralizations, proximal copper skarns and distal high-temperature carbonate hosted Pb-Zn-Ag-Au replacement ores. Polymetallic mineralization is temporally related to the emplacement of granodioritic to quartz dioritic porphyries (24-25 Ma; Gilg and Frei (1993)), Tompouloglou, 1981). Andesite porphyry dikes, which crosscuts the Pb-Zn-Ag-Au ores and associated alterations, represent the last magmatic phase in the area (19.1±0.6 Ma, Gilg and Frei (1993)). The Pb-Zn (Ag, Au) mineralization forms complex, structurally controlled replacement bodies in marbles and meta-pegmatites/ meta-aplites at a distance of 2-3 km from the porphyry copper system. Rb-Sr analyses were performed on different illite size fractions of two samples from the altered contact zone. Considerable amounts of adsorbed Sr (up to 92 wt.% of the total Sr) was removed by an ammonium acetate treatment. The <sup>87</sup>Sr/<sup>86</sup>Sr ratios of the leachates from both samples are similar and vary between 0.7081 and 0.7090. These values are indistinguishable from the <sup>87</sup>Sr/<sup>86</sup>Sr ratios of hydrothermal carbonates, a galena-hosted fluid inclusion leachate from the mineralization and porphyry copper-type vein fluids (0.7079 - 0.7089). <sup>87</sup>Sr/<sup>86</sup>Sr versus <sup>87</sup>Rb/<sup>86</sup>Sr plots of ammonium acetate-treated clay size fractions from each sample show a linear data array. However, data from coarse fractions (>2µm) exhibit an enhanced scatter due to significant amounts of feldspars, which have apparently not been completely homogenized by the illitization process. The Rb/Sr age (21.6 ± 1.2 Ma) of the ammonium acetate-treated <2 µm fraction of one sample is significantly lower than the K/Ar isochron age of the same sample (24.3 ± 1.0 Ma, Gilg and Frei (1993)), which is interpreted as the formation age of the clay. Consequently it is assumed, that in this case the Rb/Sr system has been partly open and disturbed by retrograde alteration after formation of the illites. The second sample, which was taken in the vicinity of the crosscutting andesite porphyry, yields a Rb/Sr isochron age of 20.4 ± 0.4 Ma, well in accordance with the corresponding K/Ar age (19.7 ± 0.6 Ma). Thus both systems in clay fractions <2 µm can be reset by reheating events. Initial <sup>87</sup>Sr/<sup>86</sup>Sr values in the range of 0.7072-0.7096 point to a contribution of both, Sr from the marbles (0.7071 - 0.7076) and from the meta-aplites (0.7103), to the mineralizing fluid.

Gilg, H.A., and Frei, R., 1993, Chronology of magmatism and mineralization in the Kassandra mining area (Greece): The potentials and limitations of dating hydrothermal illites, *Geochim. Cosmochim. Acta*, in press.

Tompouloglou, C., 1981, Les minéralisations tertiaires, type cuivre porphyrique, du massif Serbo-Macédonien (Macédoine grèce) dans leurs contexte magmatique, Ph.D. thesis, Ecole National Supérieure des Mines de Paris.

JUVENILE CRUST IN THE SOUTHERN COAST BELT OF BRITISH COLUMBIA: EVIDENCE FROM A REGIONAL Nd-Sr ISOTOPIC STUDY OF THE SOUTHERN COAST PLUTONIC COMPLEX BATHOLITH

Friedman, R.M., and Cui, Y., Department of Geological Sciences, University of British Columbia, 6339 Stores Road, Vancouver B.C., V6T 1Z4, Canada.

New Nd and Sr isotopic data are reported for 26 Coast Plutonic Complex plutons and 2 volcanic flows from the southern Coast Belt, which collectively range from Early Jurassic to Miocene in age. These data are integrated with previously published Nd and Sr data from the area. Initial Nd ( $\epsilon_{Nd}(T)$ ) and Sr ( $^{87}Sr/^{86}Sr(i)$ ) isotopic ratios vary from +9.8 to -3.5 and 0.7029-0.7048, respectively, consistent with formation of southern Coast Belt igneous rocks within a juvenile magmatic arc, with minimal incorporation of old or isotopically evolved crustal material. There are no significant systematic isotopic trends on the basis of geographic position or age. The probable main sources for these igneous rocks are mantle and juvenile terrane material.

Several Middle Jurassic through Late Cretaceous igneous rocks from the southeastern part of the study area contain zircon with Precambrian inherited components, which is viewed as inconsistent with the regional juvenile Nd-Sr isotopic signature in the area. Restoration of 80-140 km of dextral strike-slip motion along the Fraser-Straight Creek fault system aligns these rocks with Precambrian rocks of the Cascade Metamorphic Core to the east. Two end-member scenarios which could account for the old inheritance and relatively primitive Nd-Sr isotopes in these rocks are: 1) incorporation of small volumes (<5%) of old material, such that old zircons were imparted, without causing a significant shift in Nd-Sr values, or 2) the assimilation of sedimentary rocks with a relatively primitive Nd-Sr signature, that contain old detrital zircons.

Exclusively juvenile Nd-Sr isotopic ratios for igneous rocks of the southern Coast Belt contrast with those of the northern Coast Belt, which in some cases contain significant proportions of evolved material. Igneous rocks from the southernmost Coast Plutonic Complex are viewed as juvenile material on the threshold of the more evolved Cascade Metamorphic Core crustal block to the east.

TWO MECHANISMS OF GRANITE FORMATION, LARAMIE ANORTHOSITE COMPLEX, WYOMING

FROST, C.D., SCOATES, J.S., CHAMBERLAIN, K.R., and EDWARDS, B.R., Dept. Geology and Geophysics, University of Wyoming, Laramie, WY 82071, USA.

Nd, Sr and Pb isotopic compositions provide evidence of multiple origins for the 1.43 Ga granites and monzonites of the Laramie Anorthosite Complex (LAC) and Sherman batholith. These K-rich rocks may incorporate residual liquids to anorthosite or may be solely products of crustal melting induced by intrusion of high temperature anorthositic magmas. The LAC was intruded across the boundary between the Archean Wyoming Province and the Proterozoic Colorado Province, so crustal sources vary both in age and rock type. We have isotopically analyzed over 160 samples from the LAC, Sherman and country rocks in order to characterize the various magmas and their potential source materials.

The Sherman batholith extends south from the LAC for more than 60 km into the Colorado Province. It contains both hydrous and water-undersaturated granites, aplites, granodiorites, and small volumes of monzodiorite. The contemporaneity of these different rock types is confirmed by commingling monzodiorite and both granite and aplite. Initial  $^{87}Sr/^{86}Sr$  ratios for the batholith range from contemporary depleted mantle values to values in excess of 0.725, but initial  $\epsilon_{Nd}$  is a uniform  $0 \pm 1$ . Feldspar Pb isotope ratios are similarly uniform and plot slightly above model mantle values, ruling out substantial involvement of Archean crust. The isotopic data constrain the Sherman batholith to be largely the product of melting of Proterozoic volcanic, pelitic and gneissic crust, although the monzodiorites may be related to anorthositic magmas.

Granitic rocks also occur in three predominantly monzonitic satellite plutons to the LAC: Red Mountain, Sybille, and Maloin. The Red Mountain and Sybille plutons are in direct contact with Archean crust, and partially digested xenoliths in Sybille provide clear evidence for the involvement of Archean assimilants. Each has a characteristic initial  $\epsilon_{Nd}$  that records varying amounts of Archean assimilant in the parental magma. Extensive differentiation of this parental magma accompanied by further assimilation of up to 30% Archean granitic and pelitic crust yields the monzonite to granite suite composing these plutons.

The major element chemistry of the granitic endmembers of the Red Mountain, Sybille and Maloin plutons are indistinguishable from that of the Sherman batholith granites. However, their origins are almost completely independent, demonstrating that multiple petrogenetic processes can produce granites that are geochemically similar.

**CORAL-BASED ISOTOPIC RECORDS OF THE AUSTRALIAN MONSOON, INDONESIAN THROUGHFLOW, AND SYNCHRONIZED MASS SPAWNING**

**GAGAN, M.K., CHIVAS, A.R.,** Research School of Earth Sciences, The Australian National University, Canberra, ACT 0200; **ISDALE, P.J.,** Australian Institute of Marine Science, Townsville, Qld 4810.

Pandora Reef provides nearshore Great Barrier Reef corals which accurately record river runoff as a proxy for the timing and magnitude of the Australian monsoon, as well as the far western Pacific precursors to the east Pacific El Niño. A high-resolution coral  $\delta^{18}\text{O}$  and  $\delta^{13}\text{C}$  time-series (1978-84), having near-weekly sample intervals, was produced using the consistent arrival-time ( $\pm 2$  weeks) of the mid-winter minimum sea-surface temperature, recorded by the  $\delta^{18}\text{O}$ . The dependable chronology and high-resolution sampling demonstrate that the arrival-time of monsoonal floods is precisely preserved ( $\pm 1$  week) within the skeleton of *Porites*. Weekly sampling resolves a subtle warm-to-cool sea-surface temperature anomaly which preceded, by more than one year, the much larger warm-to-cool anomaly associated with the 1982-83 El Niño in the east Pacific.

The strength of the anomalously warm, southward-flowing Leeuwin Current, Western Australia is thought to closely reflect the strength of the Indonesian throughflow. Initial observations of a near-weekly coral  $\delta^{18}\text{O}$  record (1978-1993) for Ningaloo Reef, Western Australia suggest that Indo-Pacific tradewind velocity may periodically be important in driving the throughflow, particularly during El Niño-La Niña transitions. For example, prior to El Niño events when the tradewinds relax (or reverse), the Leeuwin Current response is much weaker than would be expected if it were driven by thermal forcing from the western Pacific alone. The opposite response (stronger than expected Leeuwin Current) occurs prior to La Niña events, when the tradewinds are enhanced. By studying Ningaloo Reef corals, as well as corals in the western Pacific, it should be possible to obtain multi-century records of the interannual variability of the Indonesian throughflow and define the balance between thermal- and wind-forcing (Southern Oscillation controlled) effects.

It is essential to identify new chronometers, having much greater precision than coral density bands, to fully utilise the high-resolution information being extracted from corals. The annual synchronized mass-spawning event may provide a way around the chronology stumbling block. Every year, a few days after the full moon in October-November (Great Barrier Reef) or March-April (Western Australia), most corals synchronously release their gametes. The early work at Pandora Reef showed a pronounced  $^{13}\text{C}$  enrichment in the coral  $\delta^{13}\text{C}$  values that corresponds closely to the October-November spawning event in the Great Barrier Reef. A similar signal appears in the new Ningaloo Reef  $\delta^{13}\text{C}$  record that corresponds closely to the March-April spawning event in Western Australia. We believe this signal reflects the rapid build-up of gamete tissue which would form a significant sink for  $^{12}\text{C}$  resulting in  $^{13}\text{C}$ -enrichment of the skeleton up to the spawning date. A new mass-spawning chronometer would be particularly useful because its timing is reliable and, at present, it offers the only known means for constructing precise chronologies that are independent of temperature.

**GENETIC ALGORITHMS : A POWERFUL NEW METHOD FOR MODELLING FISSION TRACK DATA AND THERMAL HISTORIES.**

**GALLAGHER, KERRY** School of Geological Sciences, Kingston University, Kingston, KT1 2EE, England & Fission Track Research Group, University College London, England.

Recent advances in our understanding of fission track annealing have led to empirical predictive models such that, given various assumptions, it is possible to predict the expected fission track parameters (age, track length distribution) for a given thermal history. In practice, however, it is the fission track parameters that are measured, and the thermal history is unknown. In sedimentary basins, the thermal history is intimately linked to the burial history and a reasonable reconstruction of both is often possible when a suite of downhole samples is used. However, in situations where only surface samples are analysed, the thermal history and cooling/exhumation rates must often be constrained from the fission track data alone.

In principle, analytical inversion methods could be used to determine the thermal history directly from the data, but the mathematical formulations are non-linear, may be unstable and a rigorous resolution analysis of the solution is difficult. Alternatively, more robust optimisation methods can be used and genetic algorithms represent one such approach which has the advantages of being rapid, easy to invoke and the ability to test many different thermal histories at the same time. Unlike the more conventional random Monte Carlo methods, genetic algorithms actually learn the form of the better data-fitting thermal histories and the progressive sampling is automatically geared to finding the more optimal thermal histories. Genetic algorithms therefore provide an extremely efficient method to assess the information on the thermal history contained in the measured fission track data.

An overview of the methodology will be given, using both synthetic and real data examples. The fact that many ( $> 1000$ ) thermal histories can be tested rapidly allows the spread in good data fitting solutions to be examined directly to assess the characteristics required to fit the observed data. The methodology may be applied to any type of thermochronological data, although fission track data is particularly useful because of the information on cooling rates contained in the length distribution.

## THORIUM-230 DATING OF GLACIAL-INTERGLACIAL CYCLES BY TIMS: RESULTS TO DATE

GALLUP, C. D., EDWARDS, R. L., and JOHNSON, R. G., Minnesota Isotope Laboratory, Department of Geology and Geophysics, University of Minnesota, Minneapolis, MN 55455

The main application of thermal ionization mass spectrometric (TIMS) techniques for measuring  $^{234}\text{U}$  (1) and  $^{230}\text{Th}$  (2), has been the dating of carbonates. The chronometer's great advantage is its potential range of 3 to 500,000 years. Thus, it is uniquely suited to examine chronologies on glacial-interglacial time scales. One exciting problem has been the extent to which glacial-interglacial cycles have followed changes in earth's orbital geometry, an issue that could not have been addressed with earlier measurement capabilities. Ironically, the high-resolution data have led to renewed controversy about the relationship between orbital and climate changes (3). The TIMS dated Devils Hole calcite vein appears to indicate that the oxygen isotope shift associated with the penultimate deglaciation preceded a rise in northern hemisphere summer solar insolation (3). Thus, the record is inconsistent with direct orbital forcing of climate change. Another TIMS dated chronology that bears on this issue is sea-level as recorded in corals. As of yet, no corals recording the penultimate deglaciation have been dated; however, many last interglacial corals have. The age of the oldest last interglacial coral places constraints on the timing of the penultimate deglaciation. However, on the basis of  $^{234}\text{U}/^{238}\text{U}$  ratios, there is clear evidence for diagenetic alteration of most corals older than about  $10^5$  years. We have found that diagenesis in Barbados corals shows systematic trends. We generated a model that reproduces this correlation between  $^{234}\text{U}/^{238}\text{U}$  ratios and  $^{230}\text{Th}$  ages and provides a criterion for distinguishing between accurate and inaccurate ages. By applying this criterion to both Barbadian and Bahamian coral data we find that the oldest date for the last interglacial (that is accurate to within 2 ka) is 130.4 ka (4). This postdates most of the rise in  $65^\circ\text{N}$  summer insolation and is consistent with orbital forcing. The Devils Hole record may also be consistent with orbital forcing if a non-linear growth rate is considered (the date for the penultimate deglaciation is based on linear interpolation between two  $^{230}\text{Th}$  ages).

When we generalize our analysis to include other sea level events (see 5), we find that data from Barbados and the Bahamas constrain the timing of 5 high sea-level events during the last 200 ka. The timing of these high sea levels also supports orbital forcing of climate change, as each one occurs at or after a major peak in northern hemisphere summer insolation (5). Furthermore, a several ka lag between insolation and sea level drop appears to be a general characteristic of transitions from interglacial to glacial states (5).

- (1) Chen, J.H., R.L. Edwards, and G.J. Wasserburg, 1986, *Earth Plan. Sci. Lett.* **80**, 241-251.
- (2) Edwards, R.L., J.H. Chen, and G.J. Wasserburg, 1987a, *Earth Plan. Sci. Lett.* **81**, 175-192.
- (3) I. J. Winograd *et al.*, 1992, *Science* **258**, 255 ; K. R. Ludwig *et al.*, 1992, *Science* **258**, 284.
- (4) Chen, J.H., H.A. Curran, B. White, and G.J. Wasserburg, 1991, *Geol. Soc. Amer. Bull.* **103**, 82-97.
- (5) Gallup, C.D., Edwards, R.L., and Johnson, R. G., 1994, *Science*, in press.

## U-Th-Pb SYSTEMATICS IN MOLYBDENITE FROM THE EASTERN CANADIAN SHIELD: IMPLICATIONS FOR METAL SOURCES AND TIMING OF MINERALIZATIONS.

Gariépy, C., GEOTOP/Département des Sciences de la Terre, Université du Québec à Montréal, Montréal H3C 3P8, Québec, Canada and Carignan, J., Département de Géologie, Université de Montréal, Montréal, Québec, H3C 3J7, Canada.

U-Th-Pb isotope data were obtained on molybdenite ( $\text{MoS}_2$ ) of various ages and environments (skarns, pegmatites, granites) in the Eastern Canadian Shield (Late Archean Wabigoon and Abitibi greenstone belts and Late Proterozoic Grenville Province) in order to document the geochemical behavior of the U-Pb system and its dating potential. A number of leaching experiments have been done on single  $\text{MoS}_2$  crystals using acids like  $\text{CH}_3\text{COOH}$ , HF, HBr, HCl and  $\text{HNO}_3$  in order to remove preferentially radiogenic Pb located in cationic sites damaged by the radioactive decay. This was done to generate secondary Pb-isochrons. Bulk  $\text{MoS}_2$  crystals generally yield radiogenic Pb isotopic compositions ( $^{206}\text{Pb}/^{204}\text{Pb}=20-35$  for Proterozoic samples and  $^{206}\text{Pb}/^{204}\text{Pb}=40-127$  in Archean ones). Leachates and residues from 8  $\text{MoS}_2$  occurrences out of 12 define linear arrays in the Pb diagrams corresponding to ages in good agreement with those of their host rocks. The Th/U ratios of  $\text{MoS}_2$  calculated from the linear arrays in the  $^{208}\text{Pb}$ - $^{206}\text{Pb}$  diagram are always low (0.7-1.7). This either reflects an input of meteoric water sources or a solid-liquid partition coefficient for Th in  $\text{MoS}_2$  lower than that of U. K-feldspars from these 8 deposits regress well with  $\text{MoS}_2$  data in Pb-diagrams and are systematically more radiogenic than U-poor sulfides from other base metal deposits in respective areas. This suggests that Pb, and possibly other metals, came from rocks having a residence time in the crust long enough to produce Pb more radiogenic than the residual mantle. Three deposits have yielded significantly younger ages than their host rocks, but the reset ages correspond exactly to well dated post-depositional thermal events (Early Proterozoic) in the respective areas. The resetting induced calculated loss of 30-40% of uranium parent isotopes. U-content measured by isotope dilution in selected samples indicates also an actual deficit of U (45-95%). For example, a  $\text{MoS}_2$  crystal with a  $^{206}\text{Pb}/^{204}\text{Pb}=127$ , has yielded a  $^{238}\text{U}/^{204}\text{Pb}$  of 0.15.  $^{207}\text{Pb}/^{206}\text{Pb}$  ages obtained preclude any continuous U diffusion so that recent changes in redox conditions must be responsible for U-losses.  $^{230}\text{Th}/^{234}\text{U}$  activity ratios of 1.7-2.9 measured in  $\text{MoS}_2$  crystals indicate an excess of  $^{230}\text{Th}$ , which also suggests a recent departure of U. Work is in progress to better constrain chemical fluxes in  $\text{MoS}_2$ .

A P-T-t PATH FOR SOME HIGH-PRESSURE ULTRAMAFIC/MAFIC ROCK ASSOCIATIONS AND THEIR FELSIC COUNTRY-ROCKS BASED ON SHRIMP-DATING OF MAGMATIC AND METAMORPHIC ZIRCON DOMAINS. EXAMPLE: CENTRAL SWISS ALPS

GEBAUER, D., Department of Earth Sciences, ETH Zürich, CH-8092 Zürich, Switzerland

Numerous boudinaged garnet-peridotite bodies occur in gneisses of the Alpine Adula-Cima Lunga nappe system. Geothermobarometric data (e.g. Evans and Trommsdorff, 1978 or Heinrich, 1986) demonstrate a significant P-T increase to the S suggesting low, i.e. subduction related geothermal gradients. SHRIMP-ages are reported for various rock types from the two classical areas of Cima di Gagnone (CdG, ~ 20 kbar, 750 °C) and Alpe Arami (AA, ~ 25 kbar, 850 °C). All U-Pb data were obtained within distinct zircon domains that - based on their cathodoluminescence patterns - indicate either magmatic or various types of metamorphic origins. At AA zircons from two garnet-peridotites record pre-Alpine ages (1.72 Ga, ~ 650 Ma and 456 Ma) that probably reflect inter-granular HP-melting and formation of trapped mantle liquids during orogenic processes. Although the peridotites have suffered extreme Alpine P-T conditions, zircon domains that registered this episode, could not be found in one sample. The other one, however, contains metamorphic zircon domains that average  $36.3 \pm 1.2$  Ma. Zircons extracted from various types of garnet-pyroxenites that occur as layers and boudins within the garnet-peridotites have formed magmatically under still HP-conditions 35 Ma ago. The same was found for magmatic zircons of an eclogite that probably also formed magmatically under HP-conditions. The zircons of the pyroxenites, one eclogite and one peridotite contain variably small amounts of inherited cores of Phanerozoic, Proterozoic and probably also Archean ages. Between these old cores and the Alpine metamorphic, respectively magmatic zircon domains metamorphically recrystallized areas in the range of ~ 40 Ma to 45 Ma can occur. The latter formed most likely during prograde metamorphism in the course of deep subduction of the peridotite.

A country-rock gneiss at AA was found to be a Hercynian granite (297 Ma) proving tectonic intermingling of the mafic/ultramafic rocks with the felsic country-rocks. Similarly, at CdG tectonic introduction of mafic/ultramafics occurred much later than formation of the sedimentary protolith of the present country-rocks as the youngest detrital zircon is of Caledonian age and no Hercynian detrital zircons were found so far. Thus, there is now good evidence that the peridotites were emplaced tectonically into typical Hercynian basement rocks found all over the European Hercynides. The probable peak of Alpine metamorphism in the metagranitic and metasedimentary country rocks at AA and CdG occurred at  $33.0 \pm 0.6$  Ma as detected in metamorphic domains within detrital zircons at CdG and magmatic zircons from a deformed leucosome inside the Hercynian orthogneiss at AA. This 33 Ma event is also registered in U-poor, metamorphic domains rimming only 2 Ma older domains of zircon from the garnet-pyroxenites, one eclogite and one peridotite at AA. The youngest event, post-dating the last of the four deformation phases (e.g. Möckel, 1969), was the emplacement of numerous pegmatite dikes ( $26.5 \pm 0.8$  Ma). This event was probably coeval with both reheating during intrusion of intracrustal granites and introduction of large amounts of fluids. Some metamorphic zircon domains within mainly the felsic country-rocks record this event.

The data obtained so far indicate that subduction of continental lithosphere, post-dating subduction of Mesozoic oceanic crust, was active at ~ 40 Ma to 45 Ma. The solidus of the peridotitic sources above 1000 °C was passed at ~ 35 Ma, possibly during isothermal uplift of this heterogeneous and polymetamorphic mantle material. Tectonic intermingling of the cooling peridotite and its enclosed partial melting products with the felsic country-rocks must have occurred during rapid uplift between 35 Ma and 33 Ma. Both the age signatures in the 33 Ma old metamorphic zircon domains of the felsic and ultramafic/mafic rocks as well as the structural data on these rocks (e.g. Möckel, 1969) are in line with this conclusion. There are at present no constraints on the further cooling path as ~26 Ma ago considerable magmatic and fluid activity must have existed under still amphibolite-facies conditions. This Upper Oligocene event is probably responsible for complete or at least partial rejuvenation of numerous mineral ages (Rb-Sr, K-Ar, U-Pb monazite and Sm-Nd). Geodynamically, the corner flow or orogenic wedge model - in combination with uplift caused by buoyancy, extensional faulting and erosion - seems to fit the observed age pattern best as it accommodates both subduction and uplift processes within a single P-T-t loop at plate tectonic speeds.

DETRITAL ZIRCON GEOCHRONOLOGY OF CAMBRIAN TO TRIASSIC STRATA OF THE CORDILLERAN MIOGEOCLINE, WESTERN NORTH AMERICA

GEHRELS, G.E., DICKINSON, W.R., Dept. of Geosciences, Univ. of Arizona, Tucson AZ 85721, ROSS, G.M., Geological Survey of Canada, Calgary, STEWART, J.H., HOWELL, D.G., U.S. Geological Survey, Menlo Park

Shelf-facies siliciclastics have been sampled from Cambrian, Ordovician, Devonian, Penn-Permian, and Triassic units of the miogeocline along transects in northwestern Sonora, central Nevada, southern British Columbia, northern British Columbia, and east-central Alaska. 586 abraded single zircon grains have been analyzed from these units by isotope dilution and TIMS. Of these, 499 grains yield high-precision, concordant to slightly discordant ages. The zircon ages, combined with stratigraphic relations and the known distribution of basement provinces, suggest the following provenances.

Grains from Cambrian, Devonian, and Penn-Permian units consistently record derivation from cratonal rocks that were exposed over a broad area inboard of each sample site. The only exception to this is a Cambrian quartzite in Sonora which was sourced almost entirely from nearby(?) Grenville-age plutons. Triassic strata in B.C. and Alaska show the same craton-derived provenance, whereas the Chinle Formation in Nevada records derivation almost entirely from Cambrian plutons exposed in Ancestral Rocky Mountain uplifts, and the Barranca Group of Sonora was sourced mainly in Permian and Triassic arc rocks developed along the Cordilleran margin. Ordovician quartzites record a very different provenance, with detritus in all units coming primarily from the Peace River Arch area of northwestern Canada. Longshore currents apparently transported detritus southward along the margin at least as far as Sonora.

Except during Ordovician time, the detrital zircon ages can be divided into a northern versus southern Cordilleran provenance with a boundary between central Nevada and southern British Columbia. The northern provenance region is characterized by 1.84-2.0 Ga and 2.0-2.4 Ga grains which are not present to the south. The southern provenance region has grains that are 1.65-1.76 Ga, 1.4-1.45 Ga, and, at least locally in Triassic time, 525 Ga, which are not seen to the north. This latitudinal zonation provides a powerful tool for determining the paleolatitudinal position of displaced terranes outboard of the Cordilleran miogeocline.

## LATE MESOZOIC GRANITES OF THE SIBERIAN NORTHEAST

Gelman, M. L., Northeastern Interdisciplinary Research Institute, Far Eastern Division, Russian Academy of Sciences, Portovaya 16, Magadan 685000, Russia

Late Mesozoic plutonic complexes of the Siberian Northeast represent the most extensive belt of Phanerozoic granites known on Earth. Their emplacement occurred over 70 m.y. from the Middle Jurassic to the Late Cretaceous. This magmatic event is separated by 300 m.y. from earlier granitic magmatism. General trends in composition are controlled in part by the nature and age of the basement, specifically whether this basement is Precambrian continental crust or Phanerozoic accreted terranes. Along the Paleo-Pacific boundary the ancient continent has been rimmed by the Taygonos island arc system and then during the mid-Cretaceous by the Okhotsk-Chukchi volcanic belt (OCVB). The "inner zone" of the OCVB lies proximal to the Paleo-Pacific and its "outer zone" closer to the continent. Younger accreted, ophiolitic terranes lie SE of the OCVB. The plutons are referred to as types 1a and 1b where they intrude the OCVB and its basement, and types 2 and 3 where they intrude epicratonic or inboard rocks.

1a pluton emplacement is controlled by major faults and rifts at high angles to the belt. The representative rock types are tonalite to granodiorite and also trondhjemite. The inner zone of the OCVB contains layered anorthitic gabbroid similar to those plutons in neighboring outboard ophiolitic province. Gabbroic intrusion is generally separated from granitic magmatism by regional metamorphism, but emplacement overlaps in age in many places. Granitic plutons range from epizonal where emplaced into volcanic rocks and mesozonal in metamorphic culminations. K/Ar ages range from 120 to 84 Ma,  $^{40}\text{Ar}/^{39}\text{Ar}$  ages from 102 to 96 Ma, and a Rb/Sr isochron date is 108 Ma.  $\text{Sri} = 0.7036$ .

In the flanks of the OCVB, quartz monzonite to granodiorite and quartz syenites (type 1b) predominate. Gabbroic intrusions are associated with silicic rocks and are less common than in the inner zone. Granites are associated with voluminous mid-Cretaceous ignimbrites. Rb/Sr isochron ages are 119, 94, 77 and 70 Ma. Sri ranges from 0.7029 to 0.7085. Granites of the 1a and 1b types show features of the M- and I-type granites. In the largest batholiths, 1a- and 1b-types are found together. Batholith zonations are similar to those in the Sierra Nevada, Baja, and Idaho Batholiths.

Type-2 granites range from rare gabbrodiorite and monzonite to leucogranite. Within the craton, these rocks form the cores of granite-metamorphic domes as well as numerous high-level stocks, laccoliths, and minor intrusions. K/Ar and Rb/Sr ages are 140 to 135 Ma and 95 to 90 Ma. Sri is  $>0.7010$ . These are A-type and similar to plutons in the Boulder-San Juan belt.

2-mica adamellite with cordierite, garnet, and ilmenite constitute type 3 plutons. Voluminous epizonal and epimesozonal batholiths are intruded along deep-seated faults. Rb/Sr isochron ages are between 154 and 146 Ma. Younger subalkalic biotite granite has a Rb/Sr age of 89 Ma and Sri from 0.7045 to 0.7086. These more unusual granites are S-type and have no North American analogues in the Mesozoic.

## ISOTOPE SIGNATURES OF VARISCAN GRANITOIDS AND THEIR POTENTIAL PROGENITORS IN THE HERCYNIAN FOLD BELT OF WESTERN CENTRAL EUROPE

Heinz Gerstenberger, GeoForschungsZentrum Potsdam, D-14473 Potsdam, Germany

The isotope signatures (initial values) of the Variscan granitoids in Western Central Europe are in many cases readily distinguished from those of pre-Variscan ortho-gneisses and other low and medium-grade metamorphics. Initial Sr isotope ratios of the granitoids of Variscan age occupy the field between bulk earth/-depleted mantle and an extended ortho-gneissic Sr isotope evolution line (0.714 - 0.718 between 350 and 250 Ma). This line results from a diagram of initial Sr isotope ratios vs. Rb-Sr-ages of orthogneiss samples. The best fit line in this diagram representing the Sr isotope evolution in the gneisses with time correspond to  $^{87}\text{Rb}/^{86}\text{Sr} = 3.3$ . The highest frequency of data points of initial Sr isotope ratios of the granitoids is between 0.706 and 0.711 with a trend of higher values for younger granites.

The granites of the Saxothuringian zone of the Hercynian Fold Belt are the oldest among the Variscan granitoids, these exhibit lower initial Sr isotope ratios and tend to have higher  $\epsilon_{\text{Nd}}(\text{T})$  values than the Moldanubian and Rhenohercynian granitoids. This is in full agreement with the I-type character of the Saxothuringian granitoids (Liew & Hofmann, 1988).

Data demonstrates the broad coincidence of isotope signatures of granulites occurring in the Hercynian Fold Belt and the Variscan granitoids. This might be well the result of an initial mantle diapirism triggered the Variscan orogenesis and producing a magma chamber in the lower crust. Progressive melting of lower crustal material enhanced the proportion of the crustal component in the ascending magma. Thus the magma contained at the beginning a higher portion of a lower crustal component and got an increasingly upper crustal signature as the melting of lower crustal material proceeded. However the formation of the Variscan granitoids from mixed upper mantle and upper crustal source rocks cannot be completely excluded.

Liew, T.C. & Hofmann, A.W. (1988) Contrib. Mineral. Petrol., 98, 129-138

## MODELS OF CHEMICAL EXCHANGE IN REACTIVE FLUID-ROCK SYSTEMS; GEOCHRONOLOGIC APPLICATIONS IN METAMORPHIC ROCKS

GETTY, S.R., Berkeley Center for Isotope Geochemistry, Dept. of Geology and Geophysics, University of California, Berkeley, CA, 94720, USA, and DEPAOLO, D.J., same address.

Models for chemical exchange in reactive fluid-rock systems are used to relate spatial patterns of isotopic ratios (Sr, Nd, O...) to bulk ionic diffusivities ( $D\phi/K$ ;  $\phi$ =porosity,  $K$ =solid:fluid partition coeff.), rates of mineral reaction ( $R$ ), wavelength(s) of isotopic variation ( $L_n$ ), durations of metamorphic conditions ( $\Delta t$ ), and rates of radioactive decay ( $\lambda$ ). The objective for geochronology is to combine solutions to the chemical transport equations with field, petrologic, and isotopic measurements to understand the isotopic evolution of whole rock samples or growing porphyroblasts. The model demonstrates that many of the tacit assumptions of geochronology are difficult to defend.

The exchange model is one-dimensional and emphasizes diffusive transport through pore fluids rather than advective flow. Isotopic communication between fluid and rock occurs by solution-precipitation. For a profile of initial isotopic variations, two dimensionless parameters dictate the pattern of isotope redistribution, a Damköhler number ( $DeK$ ) relating reaction rate and wavelength(s) of isotopic variation to pore fluid diffusive transport, and a diffusion-decay parameter ( $Dd$ ) relating diffusive transport to radioactive decay. The radioactive decay constant  $\lambda$  describes the in situ increase of the daughter isotope with parent/daughter ratio, whereas the parameter  $\alpha(L)$  describes the rate of decrease of the amplitude of isotopic variation along the profile due to exchange between adjacent rock layers:

$$\alpha(L) = \frac{R}{1+DeK}, \quad DeK = \frac{R \rho_s(1-\phi) L_n^2 K}{4\pi^2 \rho_{fl} D\phi}$$

These parameters allow one to estimate the effects of chemical exchange between layers on their isotopic evolution, leading to new rules for sampling and data interpretation for whole rock and mineral isochrons, and studies of porphyroblast chronology.

In fossil fluid-rock systems, vein minerals in tensile fractures may proxy for fluid isotopic compositions. The model shows that measurements of isotopic profiles across interlayered rock units and differences between fluid and host rock ratios, coupled with time-scales derived from porphyroblast studies, can be inverted for effective bulk ionic diffusivities and reaction rates.

## STUDIES OF EXTRATERRESTRIAL XENON SAMPLES USING RELAX

J D GILMOUR and G TURNER

Geology Department, Manchester University, Manchester, M13 9PL, Unnited Kingdom

RELAX<sup>1</sup> (Refrigerator Enhanced Laser Analyser for Xenon) is an ultrasensitive time-of-flight mass spectrometer designed to analyse xenon components. It combines a species selective resonance ionization ion source with a cryogenic sample concentrator. Sensitivites in excess of 1cps/500 atoms have been achieved. When combined with the 'multicollection' inherent in the time-of-flight technique this corresponds to an increase in sensitivity by a factor of more than 100 over conventional, single collector mass spectrometers.

The ultrasensitivity of RELAX allows higher resolution stepped heating experiments to be conducted than previously possible. A series of analyses of acid residues from the Murchison meteorite<sup>2</sup> in a filament microfurnace shows evidence for separation of two sub-components of Xe-HL: one with a different ratio of light to heavy isotopes from that of the other. This was most marked in samples from which a preliminary purification step had removed the majority of Cδ (the microdiamond component believed to carry Xe-HL).

A continuous wave laser microprobe has been developed and used to perform in-situ stepped heating experiments on irradiated chondrules from the Bjurböle L4 and Parnallee LL3.6 meteorites. Six Bjurböle chondrules exhibit good separation of <sup>128</sup>Xe\* (produced during the irradiation from <sup>127</sup>I) between components correlated and uncorrelated with <sup>129</sup>Xe, suggesting that the host phases are well separated. Initial <sup>129</sup>I/<sup>127</sup>I and <sup>129</sup>Xe/<sup>132</sup>Xe values are consistent with that of Caffee et al<sup>3</sup>. However, in these experiments <sup>131</sup>Xe\* correlates with <sup>128</sup>Xe\* suggesting that its parent isotope (probably tellurium) and iodine are predominantly in the same phase, possibly sulfide.

The two Parnallee samples were a 'macrochondrule'<sup>4</sup> and a cristobalite bearing chondrule of unusual oxygen isotope signature<sup>5</sup>, termed here 'chondrule 1'. In chondrule 1 the correlated and uncorrelated <sup>128</sup>Xe\* components were less well separated than in Bjurböle, possibly due to more intimate mixing of the host phases. However, an age of 4.6±0.4 million years after the mean Bjurböle age is indicated. Although <sup>128</sup>Xe\* is present, the macrochondrule shows no evidence of <sup>129</sup>Xe excess, suggesting a resetting event after the decay of <sup>129</sup>I but presumably before its incorporation into the meteorite.

1. Gilmour J.D., Lyon I.C., Johnston W.A. and Turner G. 1994, (accepted for publication) Rev. Sci. Inst.
2. Gilmour, J.D., Johnston W.A., Lyon I.C., Arden J. and Turner G. (1993) Meteoritics 28, 353.
3. Caffee M W, Hohenberg C M, Swindle T D and Hudson B (1982) J. Geophys. Res. 87, A303.
4. Dodd R.T. (1969) Min. Mag. 37, 231-237
5. Bridges J C, Franchi I A, Hutchison R and Pillinger C T (1993) Meteoritics 28, 329.

## TOWARDS AN APATITE FISSION TRACK MORPHOTECTONIC IMAGE OF THE SNOWY MOUNTAINS, SE AUSTRALIA.

GLEADOW, A.J.W., Kohn, B.P., Victorian Institute of Earth and Planetary Sciences, School of Earth Sciences, La Trobe University, Bundoora, Victoria, 3083, Australia, and Cox, S.J.D., Victorian Institute of Earth and Planetary Sciences, Dept. of Earth Sciences, Monash University, Clayton, Victoria, 3168, Australia.

The Snowy Mts of SE Australia, centred around the highest peak on the Australian continent (Mt. Kosciusko - 2228 m), largely consist of Paleozoic granitic rocks of the Lachlan fold belt. A striking feature of the region is the contrast between the stepped fault block morphology of the uplifted Kosciusko massif and the old, gently dipping, erosion surface of the Monaro Tableland to the east. The mountain blocks rise up to ~1 km above the Tableland surface. Remnants of the erosion surface are also preserved at higher elevations in the Kosciusko uplift.

In this geomorphic setting, vertical and areal variations of apatite fission track (FT) parameters in basement rocks potentially provide unique thermochronological markers. Such markers can be used for reconstructing the neotectonic "disruption" of the old erosion surface. In the area of the Kosciusko massif five separate vertical profiles, covering ~1700 m of relief yield apatite FT ages ranging from ~90-290 Ma. Such an age range has only previously been revealed in the vicinity of the SE Australian margin where it is exposed laterally over some 150 km inland from the present coast.

A positive correlation between age and elevation describes a regional master reference profile which preserves a pre-uplift partial FT annealing zone. The slope and form of the profile in the Snowy Mountains suggests a pre-uplift geothermal gradient of ~25-30°C/km. An inflection point in the age-elevation profile on the western side of the massif indicates the area of greatest uplift, and records the position of the pre-uplift ~110°C isotherm. The inflection point at  $90 \pm 10$  Ma approximates the onset of the Kosciusko massif uplift and establishes a firm temporal link between Snowy Mt. tectonism and the formation of the SE Australian passive margin during Cretaceous rifting.

The relatively simple relationship between elevation and age may be used as the basis of an interpolation using a map algebra. Starting with a gridded digital elevation model, we have divided the massif and Monaro Tableland into a set of blocks on the basis of mapped and inferred faults. The age-elevation profile determined for each block is then applied to predict the local apatite FT age. The result is a complete image of FT age at the surface, tied to the set of control points. The age mismatch across each fault may in turn be used to infer vertical offset based on the master reference profile. The resulting image may be visualised in a variety of ways, including shaded relief maps and pseudo perspective views with various overlays of faults and two dimensional profiles showing relative offset of blocks. The use of a GIS in combination with apatite FT data provides a new and invaluable means of visualising and modelling tectonism in the SE Australian Highlands.

## Nd-Sr ISOTOPIC STUDY OF THE PALEOZOIC OUACHITA SEQUENCE: IMPLICATIONS FOR SEDIMENTATION WITHIN COLLISIONAL BELTS

GLEASON, J.D., PATCHETT, P.J., DICKINSON, W.R., and RUIZ, J., Department of Geosciences, University of Arizona, Tucson, Arizona, 85721, USA

We have completed a Nd-Sr isotopic provenance study of sediments from the Ordovician through Pennsylvanian Ouachita sequence of Arkansas-Oklahoma and west Texas. Correlated Nd-Sr relations are typical of evolved upper crust throughout the sequence but Nd isotopes distinguish three distinct groups: 1) lower to middle Ordovician strata with  $\epsilon_{Nd}(t) = -13$  to  $-16$  ( $T_{dm} = 1.8$  to  $2.1$  Ga); 2) upper Ordovician through Pennsylvanian with  $\epsilon_{Nd}(t) = -6$  to  $-10$  ( $T_{dm} = 1.4$  to  $1.7$  Ga); 3) Mississippian tuffs with  $\epsilon_{Nd}(t) = -2$  ( $T_{dm} = 1.1$  Ga). These data document a rapid late Ordovician shift in sedimentary sources within the off-shelf passive-margin sequence of deep-marine cherts and shales of the Ouachita sequence. The lower to middle Ordovician strata are interpreted to have a dominantly older provenance of mixed Archean and Proterozoic cratonic sources. Early Silurian turbidites ( $\epsilon_{Nd} = -7$  to  $-8$ ) may represent the arrival of distal fan facies of an Appalachian Taconic clastic wedge. Middle Ordovician turbidites of the Sevier basin (Tellico Formation) in eastern Tennessee, representing sediment shed from the Taconic highlands, have the same Nd isotopic signature ( $\epsilon_{Nd} = -7$  to  $-8$ ), lending support to the hypothesis.

Pennsylvanian non-marine sandstones and shales from the Arkoma basin, Illinois basin, and Black Warrior basin, in addition to 14 samples representing the thick (>10-12 km) Ouachita Pennsylvanian turbidite flysch sequence, have  $\epsilon_{Nd} = -8$  to  $-10$ . Of nine Pennsylvanian sandstone-shale pairs in our data set, all exhibit differences in initial  $\epsilon_{Nd}$  of <1, and four have differences of <0.5 with uniform  $^{147}\text{Sm}/^{144}\text{Nd}$  ratios (0.10-0.12). The remarkable isotopic homogeneity of sediments delivered to the Ouachita-Appalachian region over this period implies extremely effective mixing and dispersal processes on a large (continent-wide) scale, consistent with a collisional belt provenance.

Ouachita Mississippian silicic ash-flow tuffs have Nd isotopic compositions ( $\epsilon_{Nd} = -2$ ) consistent with a continental-margin arc source, and can be modelled as mixing of depleted mantle and an older (Precambrian) crustal component. Though arc material represented by the tuffs could be a significant component (up to 30%) of a small proportion of Mississippian turbidites ( $\epsilon_{Nd} = -6$  to  $-10$ ), this material is not a significant component of Pennsylvanian sediments analyzed. We suggest that the Appalachian collisional orogen of Pennsylvanian age produced a large, continent-scale sedimentary dispersal system which effectively overwhelmed all other available sources within the Appalachian-Ouachita region of North America, flooding the surface of the continent and its margins with sediment of a single homogenized isotopic signature.

MIXED-AGE MOLLUSK ASSEMBLAGES IN HOLOCENE MARINE DEPOSITS: ANALYSIS BY AMINO ACID RACEMIZATION

GOODFRIEND, GLENN A., Geophysical Laboratory, Carnegie Institution of Washington, 5251 Broad Branch Rd., NW, Washington, DC 20015

Amino acid racemization analysis (D/L aspartic acid and D-alloisoleucine/L-isoleucine ratios) of individual shells is used to examine the age distribution of shells in several Holocene marine deposits: a relict salt marsh along the coast of Georgia, sediments of the Nile Delta, and cheniers (beach ridges) in the northern Gulf of California. Racemization rates were determined by calibration against radiocarbon dates. Racemization analyses require only very small samples (5-40 mg of shell) and are much less time consuming than radiocarbon analyses, thus making it practical to carry out very detailed chronostratigraphic studies.

On St. Catherines Island, Georgia, relict salt marsh muds presently exposed in the intertidal zone contain an assemblage of both shallow marine and salt marsh bivalve species in life position. Aspartic acid racemization analysis of individual shells shows that different species date to different periods. The muds were populated by several salt marsh and tidal channel species several hundred years ago. In the last few decades, the muds were briefly recolonized by two other marine species as well as one species that had previously lived there.

Aspartic acid racemization analysis of two species of bivalves in a 5-m core from the Nile Delta shows that mixed-age assemblages are present at many levels. The time of sedimentation at each level was determined by the age of the youngest shells at that level.

Several generations of late Holocene cheniers along the Baja California coast in the northern Gulf of California record variations in the discharge of the Colorado River. Amino acid epimerization analysis of individual shells shows that each chenier consists of shells of a wide variety of ages. The time of deposition of the cheniers was determined by the age of the youngest shells.

UNDERSTANDING LATERITISATION PROCESSES THROUGH COMPOSITIONAL, U DECAY SERIES ISOTOPES AND Sr-87/Sr-86 STUDIES.

GOPALAN, K., PANTULU, G.V., National Geophysical Research Institute, Hyderabad 500 007, India, RADHAKRISHNA, B.P., Geological Society of India, Bangalore 560 019, India, and RENGARAJAN, R., SARIN, M.M., and SOMAYAJULU, B.L.K., Physical Research Laboratory, Navrangpura, Ahmedabad 380 009, India

Three vertical profiles of laterites each comprising of three to five samples have been analysed for thirty elements (major and trace) including eleven REE by ICPMS and AAS, U-234, 238, Th-230, 232, Ra-226 and Pb-210 by radiochemistry and alpha spectrometry and Sr-87/Sr-86 using mass spectrometric techniques. Two of the profiles were collected from coastal town Mangalore (annual rainfall=250 cm) and one from inland Bangalore City (annual rainfall=75 cm) both in the State of Karnataka, Southern India. All measured parameters in the laterites at various stages of evolution are compared with those of the basal archaean rocks.

Al, Fe, U and Th are enriched during lateritisation by a factor of about 5 to an order of magnitude whereas Mg, Ca, Mn and Cu are depleted by the same factors. The LREE get depleted more than the HREE and the positive Eu anomaly in the basal rock is lost. The whole rock Sr-87/Sr-86=0.70172-0.751138 increase to 0.72353-0.75182 indicating the retention of resistant K and Rb rich minerals during lateritisation.

The daughter/parent activity ratio ranges are as follows:

U-234/U-238=1.0-1.1; Th-230/U-234=0.2-1.1; Ra-226/Th-230=0.8-4.5; and Pb-210/Ra-226=0.8-1.1

The U-U disequilibrium is not very significant whereas the Pb-Ra one can be attributed to gaseous radon loss. However, the gross disequilibrium in the Th-230/U-234 and Ra-226/Th-230 which have about 400,000 and about 10,000 year equilibrium time scales respectively, suggest that lateritisation is ongoing in the Karnataka.

**$^{87}\text{Sr}/^{86}\text{Sr}$  INITIAL RATIOS IN RIPHEAN, VENDIAN AND CAMBRIAN CARBONATES OF SIBERIA: EVALUATION OF CATAGENETIC IMPACT**

GOROKHOV, I.M., Inst. of Precambrian Geol. & Geochronol., RAS, St. Petersburg, 199034 Russia, SEMIKHATOV, M.A., Geological Inst., RAS, Moscow, 109017 Russia, BASKAKOV, A.V., KUTYAVIN, E.P., MELNIKOV, N.N., and TURCHENKO, T.L., Inst. of Precambrian Geol. & Geochronol., RAS, St. Petersburg, 199034, Russia.

Secular variations in the Sr isotopic composition in carbonate sediments are a powerful tool for decoding relative roles of the continental and mantle influx into paleoceans. However, post-sedimentary transformation and neof ormation of the carbonate minerals hamper interpretation of the  $^{87}\text{Sr}/^{86}\text{Sr}$  ratios in pre-Cenozoic whole-rock samples. The latter are often found to contain more than one generation (phase) of the carbonate minerals, each having its own  $^{87}\text{Sr}/^{86}\text{Sr}$  and Rb/Sr ratios.

Chemical treatment of the carbonate samples was used for discriminating between uncogenetic mineral phases. The technique included leaching with 1N ammonium acetate, the dissolving of a residue in acetic acid, and study of these readily soluble carbonate (RSC) and less soluble carbonate (LSC) for the Rb and Sr contents and the  $^{87}\text{Sr}/^{86}\text{Sr}$  ratio.

Fifty one samples of Lower-Upper Riphean, Vendian and Lower Cambrian limestones and dolostones from the Olenek, Turukhansk and Ura uplifts, Siberia were studied. The leaching leads to RSC extraction from the whole rock sample (usually, <10% of the total weight). This RSC phase appears to be a secondary calcite. Sr concentration in that tends to be in dolostones higher than, and in limestones similar to the concentration in the LSC. The RSC is characterized by increased (up to tenfold) Rb content and a much higher  $^{87}\text{Sr}/^{86}\text{Sr}$  ratio in comparison with the LSC. The LSC is considered as consisting of "primary" (early diagenetic) carbonate minerals. The transformation of the Rb-Sr systems in the whole rock sample scale was associated with an enrichment of limestones and dolostones in Rb, Fe and Mn that can be regarded as an indicator of a freshwater catagenesis. The primary and secondary carbonate minerals (the LSC and RSC) have also different  $^{87}\text{Sr}/^{86}\text{Sr}$  initial ratios.

Thus, whole rock samples of limestones and dolostones, contrary to the routine practice, should not be used for determination of the Sr isotope composition in paleoceans because such determinations potentially may be in error due to presence of uncogenetic carbonate phases. The magnitude of this error depends on the differences in both the Sr content and the  $^{87}\text{Sr}/^{86}\text{Sr}$  values in the primary and secondary phases. The leaching technique provides the better understanding of the postsedimentary processes affecting carbonate rocks and their Rb-Sr systems and opens a possibility to separate uncogenetic mineral phases. This technique proves to be more effective for limestones than for dolostones.

The obtained values of the  $^{87}\text{Sr}/^{86}\text{Sr}$  initial ratios in primary phases of the studied carbonate rocks are used for chemostratigraphic purposes and for evaluating the presently accepted pathway of the  $^{87}\text{Sr}/^{86}\text{Sr}$  variation in the sea water through the Late Proterozoic time.

This work was supported by the Russian Foundation of Basic Research (Grant 93-05-9404).

**PRECISION DATING OF GLACIAL EVENTS BASED ON AMS MEASUREMENTS OF COSMOGENIC  $^{10}\text{Be}$  PRODUCED IN BOULDERS**

GOSSE, J.C.<sup>1)</sup>, KLEIN, J.<sup>2)</sup>, EVENSON, E.B.<sup>1)</sup>, LAWN, B.R.<sup>2)</sup>, and MIDDLETON, R.<sup>2)</sup>

<sup>1)</sup>Dept. of Earth and Environmental Science, Lehigh Univ., Bethlehem, PA 18015-3188

<sup>2)</sup>Dept. of Physics, Univ. of Pennsylvania, Philadelphia, PA 19104-6396.

Cosmogenic nuclides (especially  $^{10}\text{Be}$ ,  $^{26}\text{Al}$ ,  $^{14}\text{C}$ ,  $^{36}\text{Cl}$ , and the stable nuclides  $^3\text{He}$  and  $^{22}\text{Ne}$ ) are produced in rocks at the Earth's surface by secondary particles produced by cosmic rays. Geologists are rapidly recognizing the potential of cosmogenic nuclides to solve Quaternary chronological problems. We provide a formal field test of the technique to date glacial events using boulders deposited on the crests of moraines.

We have dated more than 60 samples from Pinedale, Wyoming, the Wisconsin (marine  $\delta^{18}\text{O}$  stage 6) type locality for Rocky Mountain glaciation. Based on samples from the terminal moraines around Fremont Lake, Soda Lake, and Mud Lake, the last glacial maximum commenced  $21 \pm 1.5$  ka, lasted 5.3 ka, and ended  $15.7 \pm 1.1$  ka. ago. Eleven measurements on five nested recessional moraines around Mud Lake have an average age of  $15.5 \pm 0.6$  ka (internal error includes non-instantaneous time of deposition and variations in transport of boulders to moraine). We dated a moraine high in the Wind River Mts. in Titcomb basin, ~ 1 km from the head wall of the cirque and ~35 km from Fremont lake, to  $10.9 \pm 0.5$  ka (10.6 ka including anomalous sample), thus establishing the retreat rate for 5.1 ka of 6.9 m/a.

Extensive dating of the inner Titcomb Lake moraine (10 samples) allows us to estimate the precision of the technique. Nine samples cluster with a single sample-standard deviation of 3.6% (370 a); one sample is anomalously young (by ~2 ka). Dates from the recessional moraines around Mud Lake suggest a similar precision. Estimates of boulder surface erosion were possible from samples collected from moraines deposited during the Bull Lake (Illinoian, marine  $\delta^{18}\text{O}$  stage 6) glaciation. Our best estimate for erosion is 1.3 mm/ka; an absolute maximum is 3.1 mm/ka. The effect of this erosion was to reduce the apparent age of glaciation by 2% (ages quoted have not been corrected for the effect of erosion). Production rates were calibrated using glacially striated bedrock surfaces with associated  $^{14}\text{C}$  dates of 11,000 a (calendar years)<sup>[1]</sup>. Quoted uncertainties include both analytic errors and estimates of systematic uncertainties due to erosion, calibration, and changes in production rate.

The dates we have determined for the Pinedale maximum are in general agreement w/ dates determined by other methods—although there is a suggestion that ages for the past 20 ka may be ~1 ka too young.

1. Nishiizumi, K., et al., Cosmic ray production rates of  $^{10}\text{Be}$  and  $^{26}\text{Al}$  in quartz from glacially polished rocks. *J. Geophys. Res.*, 1989, **94**(B12): p. 17,907-17915.

SINGLE ZIRCON AGES FROM THE PRE-CAMBRIAN BASEMENT OF THE SOUTHERN ARAVALLI MOUNTAINS (RAJASTHAN, INDIA)

Goswami, J.N., Wiedenbeck, M., Physical Research Laboratory, Navrangpura, Ahmedabad 380009, India, and Roy, A.B., Department of Geology, M.L. Sukhadia University, Udaipur 313001, India.

We are conducting a detailed survey of zircon ages from the Precambrian basement of the Aravalli Mountains of northwestern India. Here we report our  $^{207}\text{Pb}/^{206}\text{Pb}$  age results obtained using a Cameca ims 4f ion probe (technique described by Wiedenbeck and Goswami; companion abstract, this volume).

The Mewar Gneiss is a heterogeneous assemblage of orthogneisses and paragneisses containing inliers of metasedimentary rocks and amphibolites. This assemblage experienced multiple deformation and metamorphic events followed by the emplacement of voluminous granites and basaltic dikes. Based on previously available Sm-Nd whole rock data (Gopalan *et al.*, 1990) this activity spanned from 3.3 to 2.4 Ga. Subsequently, this entire assemblage served as the basement on which both the Aravalli and Delhi Supergroups were deposited.

Zircons from a sample of orthogneiss collected near the village of Jhamarkotra yielded a minimum age of  $3281 \pm 3$  Ma ( $1\sigma$ ), which we interpret as the time of emplacement of the igneous protolith. A unique, 30  $\mu\text{m}$  wide overgrowth on a zircon from this population gave an age of  $2536 \pm 20$  Ma, which we tentatively attribute to a period of *in situ* growth. Zircons from a second sample, a leucocratic gneiss collected from Vali River 15 Km to the SE, gave a minimum age of 2.5 Ga, thereby attesting to the presence of multiple age components within the basement gneisses.

We have now conducted age measurements on five granitic bodies from this same region: the Ahar River Granite (minimum age 2.56 Ga), the Gingla Granite (2.4 to 2.5 Ga), the Berach Granite (2.44 Ga), the Untala Granite (2.50 Ga) and an unnamed foliated granite from near Jhamarkotra (2.53 Ga). These data point to the gross stabilization of the Aravalli Craton during the earliest Proterozoic.

Gopalan, K., Macdougall, J.D., Roy, A.B. and Murali, A.V. (1990) Sm-Nd evidence for 3.3 Ga old rocks in Rajasthan, northwestern India: *Precamb. Res.*, v. 48, 287-297.

COSMIC-RAY-PRODUCED NEON IN TERRESTRIAL QUARTZ

GRAF, Th., KIM, J.S., MARTI, K., and NIEDERMANN, S., Dept. of Chemistry, University of California, San Diego, La Jolla, California 92093-0317, U.S.A.

We have developed new techniques for studies of  $\leq 10^6$  atoms of cosmic-ray-produced noble gases in terrestrial rocks, which are expected to provide important geomorphological and glaciological information such as surface exposure ages, erosion rates, and extent of glacial cover. In the case of  $^{21}\text{Ne}$ , the cosmic-ray-produced component represents one of several components. A component resolution based on three-isotope correlations and stepwise heating is essential. Our new techniques permit accurate corrections for all interfering ions, including corrections for doubly charged species. The assumption that charge state ratios are constant is not satisfactory. The spallation ratio  $(^{22}\text{Ne}/^{21}\text{Ne})_c$  from Si was calibrated using a quartz separate from an Allan Hills sandstone and yields a value of  $1.243 \pm 0.022$ . This ratio is expected to be essentially constant for terrestrial quartz samples and is useful in component resolutions. The stepwise release of Ne at increasing temperatures showed that cosmic-ray-produced Ne is released from quartz at rather low temperatures (Niedermann *et al.*, 1993).

At present the cosmic-ray production rates of stable  $^{21}\text{Ne}$  are not very well known. We determined the production rate ratio  $P_{21}/P_{26}$  of  $^{21}\text{Ne}$  and  $^{26}\text{Al}$ . The  $^{26}\text{Al}$  concentrations in our samples were measured by Nishiizumi *et al.* (1989). The quartz was separated from Sierra Nevada rocks which were exposed to cosmic rays since the Tioga period of the last ice age. Ne in these rocks represents mixtures of several components: trapped Ne, nucleogenic  $^{21}\text{Ne}$  and  $^{22}\text{Ne}$  produced by  $(\alpha, n)$  reactions in oxygen and fluorine, respectively, and cosmic-ray-produced Ne. The trapped component was substantially reduced by crushing, grain size, and density separations, permitting the isolation of cosmic-ray spallation and  $(\alpha, n)$  components.

Two  $P_{21}/P_{26}$  determinations are consistent within error limits, and the value  $0.65 \pm 0.11$  agrees with ratios observed in extraterrestrial matter. The observed production rate ratio is substantially larger than theoretical estimates for Si targets, reflecting poorly known neutron excitation functions. The above  $P_{21}/P_{26}$  value, coupled to the observed  $^{26}\text{Al}$  production rate, corresponds to a  $^{21}\text{Ne}$  production rate  $P_{21} = 21$  atoms  $\text{g}^{-1} \text{a}^{-1}$  in quartz or to  $P_{21} = 45$  atoms  $(\text{g Si})^{-1} \text{a}^{-1}$  (at sea level and high latitudes).

Niedermann, S., Graf, Th., and Marti, K., 1993, *EPSL*, 118, 65.

Nishiizumi, K., Winterer, E.L., Kohl, C.P., Klein, J., Middleton, R., Lal, D., and Arnold, J.R., 1989, *J. Geophys. Res.*, 94, B12, p. 17907.

## ISOTOPIC AND CHEMICAL VARIATIONS IN HISTORICAL LAVAS FROM MOUNT ETNA

GRAHAM, DAVID, College of Oceanic & Atmospheric Sciences, Oregon State University, Corvallis, OR 97331, GIACOBBE, ATTILIO and SPERA, FRANK, University of California, Santa Barbara, CA 93106, U.S.A.

We have conducted a detailed survey of the major, trace element and isotope chemistry (Sr-Nd-Pb and He) of a suite of 32 historical and 17 prehistoric lavas spanning the ~200,000 year subaerial history of Mt. Etna. Historical lavas are alkalic, while prehistoric lavas include both alkalic and tholeiitic types. Major element variations primarily reflect the multiple saturation with olivine, plagioclase, clinopyroxene and oxides. Analyses of minerals and glasses suggest that some crystal sorting has occurred, usually by addition of plagioclase and/or subtraction of olivine+clinopyroxene. Thermochemical modelling indicates a polybaric history dominated by low pressure (1-3 kbar) crystallization, but higher pressure (5-8 kbar) crystallization also occurred in some cases. Incompatible element ratios and isotope compositions, such as Rb/Nb- $^{87}\text{Sr}/^{86}\text{Sr}$ , Rb/La- $^{87}\text{Sr}/^{86}\text{Sr}$  and Zr/Nb- $^{208}\text{Pb}/^{206}\text{Pb}$ , show strong positive correlations for both prehistoric and historical lavas.

Within the resolution allowed by our sampling, from 1329 A.D. until the 20<sup>th</sup> century there was a continuous increase in  $^{87}\text{Sr}/^{86}\text{Sr}$ , from 0.70335 to 0.70343. The 1669 eruption, by far the largest in historical time, showed a small  $^{87}\text{Sr}/^{86}\text{Sr}$  increase and a relatively large decrease in  $^{206}\text{Pb}/^{204}\text{Pb}$ . Since 1971 the  $^{87}\text{Sr}/^{86}\text{Sr}$  ratio has increased dramatically, to 0.70359 in 1989. This increase since 1971 was accompanied by enrichment in K and Rb, a corresponding decrease in  $^{206}\text{Pb}/^{204}\text{Pb}$  from 19.95 to 19.87, and increased  $^{226}\text{Ra}$  disequilibrium [1].  $^{143}\text{Nd}/^{144}\text{Nd}$  and  $^3\text{He}/^4\text{He}$  ratios are within analytical uncertainty for all historical lavas studied, with average values of 0.51288 and  $6.6 \pm 0.4 R_A$ , respectively. Single stage  $\kappa_{\text{Pb}}$  values deduced from the  $^{208}\text{Pb}$ - $^{206}\text{Pb}$  systematics are ~3.8, greater than the present day  $\kappa_{\text{Th}}$  of ~3.3 [2]. Basalts which are isotopically similar in all respects to these Mt. Etna lavas also occur at some ocean island localities, such as in the Canary Islands.

The rapidity of the isotopic changes since 1971 suggests that magma mixing plays an important role. A simple mixing model of a constant volume magma reservoir, using the known effusion rates of historical eruptions and the observed isotopic changes, indicates that the magma body beneath Mt. Etna is small, presently ~0.3 km<sup>3</sup>. During the period 1329-1900 this model suggests a larger body of ~1 to 4 km<sup>3</sup>. Our observations indicate that the volcanic plumbing of Mt. Etna has changed during historical times, consistent with inferences from previous work [3-6]. The different magmas originate either by changes in the melting dynamics of a mantle source which is isotopically heterogeneous on a small scale (km?), or by varying degrees of interaction with the lithosphere or crust [7].

1. Condomines et al. [1987] Nature 325, 607
2. Condomines et al. [1982] Geochim. Cosmochim. Acta 46, 1397
3. Guest and Duncan [1981] Nature 290, 584
4. Cristofolini et al. [1984] Neues Jahrb. Min. Abh. 149, 267
5. Tanguy and Clochiatti [1984] Bull. Volc. 47, 879
6. Armienti et al. [1989] J. Volc. Geother. Res. 39, 315
7. Clochiatti et al. [1988] J. Volc. Geother. Res. 34, 241

## ESTIMATING CATCHMENT-WIDE DENUDATION RATES FROM COSMOGENIC ISOTOPE CONCENTRATIONS IN ALLUVIAL SEDIMENT: FORT SAGE MOUNTAINS, CALIFORNIA

GRANGER, D.E., and KIRCHNER, J.W., Dept. of Geology and Geophysics, University of California, Berkeley, CA, 94720, USA.

Cosmogenic isotope concentrations in alluvial sediment can be used to infer catchment-averaged denudation rates, despite individual mineral grains' complex cosmic ray exposure histories. We have mathematically modelled how bedrock erosion, soil mixing, and sediment transport affect *in-situ* cosmogenic isotope accumulation in mobile sediment. Our analysis shows that cosmogenic isotope concentrations yield reliable estimates of catchment denudation rates under the conditions that (1) the sediment grains' cosmic ray exposure times during both exhumation and transport are much less than the isotope's radioactive meanlife, (2) the stream sediment is well-mixed, and is derived from the entire catchment, and (3) the sampled mineral is distributed throughout the catchment. Variations in erosion rate, soil depth, sediment storage, and isotope production rate can potentially confound interpretations of cosmogenic isotope concentrations. We have quantified the sensitivity of inferred denudation rates to these factors -- thereby delineating a practical range of field conditions over which cosmogenic isotope concentrations in alluvial sediment may be interpreted in terms of catchment denudation rates.

We have inferred denudation rates from  $^{26}\text{Al}$  and  $^{10}\text{Be}$  concentrations in quartz sand from streams draining two adjacent catchments in the Fort Sage Mountains, California. Material eroded from these catchments has been deposited as alluvial fans overlying Lake Lahontan shorelines dated at 12.5 ka<sup>1</sup>. We have measured the volumes of these fans to estimate the catchments' erosion rates since lake retreat. Preliminary data from these mass balances indicate erosion rates of  $3.5 \pm 0.9 \text{ cm}\cdot\text{ka}^{-1}$  and  $8.0 \pm 2.0 \text{ cm}\cdot\text{ka}^{-1}$  for the two catchments. These estimates agree with denudation rates of  $4.8 \pm 1.2 \text{ cm}\cdot\text{ka}^{-1}$  and  $9.9 \pm 2.5 \text{ cm}\cdot\text{ka}^{-1}$ , respectively, inferred for the two catchments from cosmogenic isotope concentrations.

This study shows that denudation rates inferred from cosmogenic isotopes in stream sediment can be independently verified over timescales comparable to cosmic ray exposure times. Further verification over a range of field conditions should permit long-term, catchment-scale denudation rates to be confidently estimated from cosmogenic isotope concentrations. These can be contrasted with modern sediment fluxes, which may reflect short-term rates of sediment mobilization rather than long-term denudation rates.

<sup>1</sup>Benson, L.V., and Thompson, R.S., 1987, Lake Level Variation in the Lahontan Basin for the Past 50,000 Years: Quaternary Research, v.28, p. 69-85.

NEW RADIOMETRIC ARGON AGES FOR  
VOLCANIC ROCKS FROM THE NORTHERN LINE  
ISLANDS, CENTRAL PACIFIC OCEAN

GRAY, L. B. and DAVIS, A. S., both of Branch of  
Pacific Marine Geology, U.S. Geological Survey,  
MS 939, 345 Middlefield Rd., Menlo Park, CA, 94025,  
USA.

The Line Island chain is a major bathymetric feature in the central Pacific Ocean consisting of many seamounts, atolls, and linear ridges that extend from Horizon Guyot in the northwest to the Tuamotu Islands in the southeast. The Line Islands chain has been proposed to be a major hot spot trace, analogous to the Hawaiian-Emperor chain. However, available radiometric ages indicate a complex history not compatible with the age progression that would be associated with a simple hot spot trace.

We report 23 new ages for 10 volcanic edifices along the Line Islands trend between 5°N and 20°N latitude. Age data were produced using primarily  $^{40}\text{Ar}/^{39}\text{Ar}$  laser fusion analyses of mineral separates, but also include  $^{40}\text{Ar}/^{39}\text{Ar}$  laser incremental heating,  $^{40}\text{Ar}/^{39}\text{Ar}$  induction incremental heating, and conventional K-Ar analyses of mineral separates and whole rock samples. Volcanic rocks analyzed range from alkalic basalt and hawaiite to mugearite and benmoreite. Mineral separates are mostly feldspars, including plagioclase and sanidine, and some kaersutite amphibole. If the evolutionary stages developed for Hawaiian volcanoes were applicable to these edifices, then the samples would be classified as being from the post-shield and/or rejuvenated stage.

These data establish two parallel trends of differing ages within the northern Line Islands chain. Karin Ridge forms the easternmost, older trend, with three dredge sites located on the ridge yielding ages between 93 and 82 Ma, and a sample dredged from an unnamed seamount southeast of Karin Ridge along the same trend at 10°N latitude yielding an age of 83.7 Ma. Ages of 82.1 to 81.4 Ma for plagioclase from Horizon Guyot indicate that this large edifice, trending nearly perpendicular to Karin Ridge, was volcanically active at the same time.

The younger, western trend is parallel to Karin Ridge and extends from Johnston Island at 17°N to Kingman Reef at 6°N latitude. Samples from seven locations yielded ages ranging from 72 to 67 Ma. An additional dredge site on a seamount to the northwest of Johnston Island, near Hess Rise, yielded an age of 73.4 Ma, although this seamount is apparently part of the Mid-Pacific Mountains.

In agreement with previous studies, these new ages do not show an age progression, but rather indicate two episodes of widespread, synchronous volcanism in the northern Line Islands chain, occurring about ten million years apart.

STABLE ISOTOPE STUDIES OF THE ARCHEAN  
PILBARA BLOCK: IMPLICATIONS FOR THE  
ARCHEAN HYDROSPHERE.

GREGORY, Robert T., Department of Geological  
Sciences & Stable Isotope Laboratory, S.M.U., Dallas,  
TX 75275, U.S.A.

The Pilbara block, Western Australia provides an opportunity to examine a well-preserved, essentially undeformed ~3.5 Ga greenstone-granite succession. The isotopic compositions of the rocks reflect the conditions of hydrothermal alteration that is ultimately tied to exogenic cycles which are coupled to climate. Over 140 samples from whole-rocks, vesicles, and veins have been analyzed for either oxygen, carbon or hydrogen isotopic composition. The range in greenstone silicate fraction,  $6 < \delta^{18}\text{O} < 12$ , is the same as that of the carbonate fraction,  $7.5 < \delta^{18}\text{O} < 13.5$ . The similarity of the ranges in the  $\delta^{18}\text{O}$  values of coexisting carbonate and silicate fractions of greenstones (70 pairs) is consistent with an approach to isotopic equilibrium with greenstone carbonate-greenstone silicate  $\Delta^{18}\text{O} \approx +2$ . Over 50 chert analyses give an average  $\delta^{18}\text{O} = 13.8$  and chert-greenstone silicate  $\Delta^{18}\text{O} \approx +3$ , which would correspond to an approach to isotopic equilibrium at ~300 °C. The isotopic compositions of these cherts, therefore, have no simple direct paleoclimatic significance. The lowest  $\delta^{18}\text{O}$  values for mafic rocks are found within the hornfelsic contact aureoles ( $3.4 < \delta^{18}\text{O} < 7.2$ ). Hydrogen isotope ratios on pillow basalt whole-rocks are given by  $-33 < \delta\text{D} < -84$ . The  $\delta^{13}\text{C}$  values of secondary carbonate (average modal calcite > 10%) from the North Pole dome greenstones show limited variability,  $-3.7 < \delta^{13}\text{C} < 1.6$  (mean  $\delta^{13}\text{C} = -0.8 \pm 1.2$ ). The spread in  $\delta^{13}\text{C}$  values for carbonates in these Archean greenstones is virtually the same as carbonates formed during the seafloor weathering of modern basalts suggesting no significant difference between modern and Archean dissolved seawater carbonate  $\delta^{13}\text{C}$  values. The similarity of the alteration assemblages, the inferred temperatures of alteration, and the ranges of  $\delta^{18}\text{O}$  and  $\delta\text{D}$  values of ~3.5 Ga Archean greenstones to modern greenstones, all suggest that the isotopic composition of seawater was not significantly different even back to the earliest preserved sections of the Archean. Finally, the most  $^{18}\text{O}$ -depleted feldspar and the most D-depleted hydrothermally altered rocks associated with the intrusion of granitic magmas suggest that meteoric fluids at 3.5 Ga were close to the isotopic composition of modern meteoric fluids near the 15 °C cutoff surface temperature necessary to produce isotopically-depleted meteoric fluids.

## HOTSPOT HELIUM IN GEOTHERMAL WATERS FROM ETHIOPIA AND DJIBUTI (EAST-AFRICAN RIFT SYSTEM)

E.Griesshaber \*, S. Weise \*\* and G.Darling #

\* MPI für Chemie, 6500 Mainz, FR Germany,

\*\* Institut für Hydrologie, GSF München, FRG,

# British Geological Survey, Wallingford, U.K.

$^3\text{He}/^4\text{He}$  compositions are presented for groundwater samples from the Ethiopian segment of the East-African Rift and from its northern extension, the adjacent Afar region (Djibuti). Helium isotope data are compared to those obtained previously from the Gregory Rift, south of Ethiopia. The distribution pattern of mantle-derived volatiles along the entire East-African-Rift (-from south Kenya to Djibuti-) is discussed and their sources are identified.

Helium isotope ratios (R) for samples from the Ethiopian part of the Rift range from 6.3 to 16.0 times the atmospheric ratio ( $R_a=1.4 \times 10^{-6}$ ) and thus show together with a MOR component a considerable hot spot helium component. These mantle helium concentrations are comparable to those observed in groundwaters and volcanic rocks from the Afar plume region in Djibuti. Here R/ $R_a$  values range from 9 to 13 times the atmospheric composition, with mantle-derived helium concentrations being higher than at spreading ocean ridges. Helium isotope compositions from Ethiopia and Djibuti are entirely different from those observed in groundwaters at the southerly extending Gregory Rift in Kenya, where R/ $R_a$  values scatter between 0.5 and 6. At the northernmost part of the Gregory Rift, close to Ethiopia mantle helium contents are slightly higher, with R/ $R_a$ -values varying between 6.5 and 8.0.

The distribution pattern of primordial helium along the East-African-Rift clearly shows an increase in mantle helium contents from south to north, culminating at present at the central rift zone in Ethiopia and at the Afar region in Djibuti. Thus, the obtained helium isotope compositions clearly demonstrate that, in contrast to other major rift zones, volatiles in groundwaters that issue at the East-African-Rift derive from three distinct sources regions: a crustal, a MOR and a hotspot source. Whereas crustal helium is a dominant component in groundwaters in the southern part of the East-African-Rift along its northern segment it is almost negligible, where MOR and hotspot sources are the prominent components. The transition zone between a MOR and a hotspot source can be located between Lake Turkana in Kenya and the southern edge of the Lakes District in Ethiopia. The observed geochemical observations are in good agreement with seismotectonic and magmatic models along the East-African-Rift.

1. Darling G., Griesshaber E., Andrews J, Armannsson H and O'Nions K. (1993): Composition and sources of outgassing from the Kenya Rift Valley. Submitted to Geochim. Cosmochim. Acta 1992, reviewed 1993.

2. Griesshaber E. (1990): Helium and carbon isotope systematics in groundwaters from W.Germany and E.Africa. Ph.-D. Thesis submitted to the University of Cambridge in 1990.

## STABLE ISOTOPE EVIDENCE FOR CRUSTAL CONTAMINATION DURING THE FORMATION OF DIFFERENT TYPES OF LAYERED BASIC INTRUSIONS

GRINENKO, L.N., Dept. of Geology, Moscow State

University, Moscow, 119899, Russia, and KROUSE,

H.R., Dept. of Physics and Astronomy, The University of Calgary, Calgary, AB, T2N 1N4 CANADA

Sulphur and carbon isotopes and contents and oxygen isotope data for whole rock samples collected over cross-sections of intrusions were used to investigate the formation conditions of two types of layered mafic-ultramafic intrusions: I - normal stratigraphic sequence (Norilsk and Pechenga regions, Russia) and II - rhythm-layered (Karelia, Preebaikal, Russia; Rhum, Scotland; Fox River, Canada).

Type I intrusions have high sulphur contents ranging from 0.2 to 3% and  $\delta^{34}\text{S}$  values from 0 to +12 ‰. The graphite carbon content is low (0.006%) with  $\delta^{13}\text{C}$  values from -34 to -28 ‰. The  $\delta^{18}\text{O}$  values are near +8 ‰. Type II intrusions have low sulphur contents (less than 0.2%, usually ~100 ppm). Most  $\delta^{34}\text{S}$  values are  $0 \pm 1.5$  ‰, but some intrusions have anomalous values, e.g., -7.5 ‰, Rhum, and +8.5 ‰, Fox River. The carbon content is higher than for Type I and the  $\delta^{13}\text{C}$  values range from -25 to -16 ‰. The  $\delta^{18}\text{O}$  values are close to the mantle value (~ +6 ‰) or lower. The vertical distributions of sulphur isotopes and contents are different in the two type of intrusions.

Not only do the data identify specific crustal sources of magmatic contamination, but they also provide information about its incorporation and peculiarities of the ore body formation. Crustal contamination for Type I intrusions took place in intermediate magma chambers and for Type II during emplacement. The former were formed by a single magmatic pulse, the latter during several magmatic pulses.

STABLE ISOTOPE ABUNDANCES IN PLANTS  
GROWING IN THE ARAL SEA REGION

GRINENKO, V.A., MINEEV, S.D., V.I. Vernadsky  
Institute of Geochemistry and Analytical Chemistry,  
Russian Academy of Science, Moscow 117975, Russia and  
KROUSE, H.R., Dept. of Physics and Astronomy, The  
University of Calgary, Calgary, AB, T2N 1N4  
CANADA

Little is known about sulphur metabolism during plant development on highly saline soils. Data were obtained for contents and  $\delta^{34}\text{S}$ -values of sulphate and organic -S, and  $\delta^{13}\text{C}$  and  $\delta\text{D}$  values for 5 species of plants at 4 locations in the Aral Sea area. The  $\delta^{34}\text{S}$  values and concentrations were also measured for soil sulphate.

*Tamarix*, *Halocnemum strobilaceum*, and *Salicornia stricta* had  $\delta^{13}\text{C}$  values ranging from -30.0 to -23.3 ‰ consistent with  $\text{C}_3$  photosynthesis. *Haloxylon aphyllum* sampled at three of the locations, had higher and more uniform  $\delta^{13}\text{C}$  values (-13.0 to -12.8 ‰) consistent with  $\text{C}_4$  photosynthesis. In contrast, *Atriplex tatar*, growing in soil with less than 5000 mg/kg sulphate had a  $\delta^{13}\text{C}$  value of -23.3 ‰ whereas that for a specimen at another location with much higher soil sulphate concentration, was -12.8 ‰.

The soluble sulphate concentrations in soil, ranged from 300 to 12,000 mg/kg and the  $\delta^{34}\text{S}$  values from -7 to +15 ‰ dependent upon location. For many plants, the total sulphur  $\delta^{34}\text{S}$  values were close to those of soluble sulphate in the soil and the differences between  $\delta^{34}\text{S}$  values of plant sulphate and organic-S were small. However, there were also anomalies where adjacent different species differed in  $\delta^{34}\text{S}$  value by as much as 25 ‰. Also, in some plants, the organic-S had  $\delta^{34}\text{S}$  values which were 10 ‰ lower than those of sulphate. The data suggest that even if sulphate is the dominant form of sulphur in soil, sulphide and perhaps intermediate oxidation states of sulphur may be metabolized by these plants.

ARGON LOSS FROM F-OH PHLOGOPITE

GROVE, M., and HARRISON, T. Mark, Department of  
Earth & Space Sciences, UCLA, Los Angeles, CA 90024  
marty@argon.ess.ucla.edu

Replacement of  $\text{OH}^-$  by  $\text{F}^-$  and/or  $\text{Cl}^-$  has a significant effect upon the thermal stability and other physical properties of trioctahedral micas. Previous studies have exploited the high temperature stability of phlogopite (>900°C for OH-Phl; >1300°C for the F-Phl) to measure diffusion coefficients over a wider temperature range than that possible with biotites containing appreciable iron and octahedral aluminum. Overlooked, however, has been the opportunity to measure Ar diffusivities as a function of hydroxyl content. Ionic porosity model considerations predict lower argon diffusivities for halogen-rich trioctahedral micas. This expectation is based upon observations that lattice dimensions within the interlayer region of trioctahedral mica decrease, and interlayer bond energies increase, when proton-potassium repulsion is reduced by replacement of hydroxyls by F (or Cl). In addition, the potential for argon loss to be enhanced by structural failure driven by dehydroxylation processes is mitigated by uptake of halogens in the hydroxyl sites of mica.

Previous radiogenic  $^{40}\text{Ar}$  diffusion experiments performed with F-rich phlogopite (68% F-Phl) yielded argon diffusivities 1.5 orders of magnitude lower than those obtained from halogen-poor (5-20% F), intermediate Fe-Mg-Al biotite at 700°C. Hydrothermal annealing experiments (650-850°C; 500 bars  $\text{P}_{\text{H}_2\text{O}}$ ) carried out in the present study using comparatively F-poor phlogopite (35% F-Phl), yield  $^{40}\text{Ar}$  diffusivities about one half an order of magnitude lower than those determined for intermediate biotite. Relative short run durations needed to achieve 20-30% loss coupled with the low confining pressures permitted by the broad stability field cause only minimal recrystallization (<< 1%) and grain comminution of run products. Diffusion coefficients calculated by assuming infinite cylinder geometry and using diffusive length scales equivalent to grain dimensions yield Arrhenius parameters of  $E_a = 50.1$  kcal/mol and  $D_0 = 0.12$   $\text{cm}^2/\text{s}$  (based upon available results from four experiments from 750°C to 850°C). Very short duration (~ hour) experiments to 850°C yield low degrees (<2-5%) of fractional loss. Additional hydrothermal experiments are in progress to examine other compositions along the F-OH phlogopite join.

## Sr ISOTOPE GEOCHEMISTRY OF MARINE SEDIMENTS FROM SOUTH CHINA SEA

GUI XUN-TANG, YU JIN-SHENG, LI XIAN-HUA, Guangzhou Branch, Institute of Geochemistry, Chinese Academy of Science, Wushan, Guangzhou, 510640, P. R. China, and CHEN SHAO-MAO, South China Sea Institute of Oceanology, Chinese Academy of Science, Guangzhou, 510301, P. R. China.

The range of our investigation is limited in the Nansha area of 3-12°N and 105-118°E. The Sr isotope compositions of silicate-facies of surface sediments from 36 stations were analyzed. The main lithological characters are pelagic clay, arenaceous clay, pelagic mud, metargillitic mud, arenaceous mud, as well as mid-fine grain sand and sand.

The geographic isogram of  $^{87}\text{Sr}/^{86}\text{Sr}$  ratios of silicate-facies surface sediments in the Nansha area is clearly constructed.

The major axis of isogram is NE-SW direction. The closed circle of 0.710 of  $^{87}\text{Sr}/^{86}\text{Sr}$  ratios, as a center of isogram is constructed in the area between 7-10°N and 112-117°E. The increase tendency of  $^{87}\text{Sr}/^{86}\text{Sr}$  ratio ( $>0.710$ ) is in the SW direction of isogram, which can be divided into 0.714; 0.718; 0.719 and 0.720 four isolines. The decrease tendency of  $^{87}\text{Sr}/^{86}\text{Sr}$  ratios ( $<0.710$ ) is in the NE direction of isogram. The distribution feature of  $^{87}\text{Sr}/^{86}\text{Sr}$  isogram have proved that the source materials of surface sediments in west and south parts are different from that of northeast part. The former is controlled by the continental clastic constituents from Sunda Shelf and the washings from delta of Mekong River and the latter is controlled by the mantle derived volcanic materials from surrounding tectonic environment.

The dynamic ocean current picture in the research area is quite similar to the above isogram of  $^{87}\text{Sr}/^{86}\text{Sr}$  ratios, and perhaps it also has some correlation between them.

## IMPLICATIONS OF Sr, Nd, O, AND COMMON-Pb ISOTOPIC VARIATIONS FOR THE ORIGIN AND EMPLACEMENT OF THE LAGUNA JUAREZ PLUTON, BAJA CALIFORNIA, MEXICO

GUNN, S. H., Branch of Isotope Geology, U.S. Geological Survey, MS 937, 345 Middlefield Road, Menlo Park, CA 94025, USA.

Isotopic evidence indicates the normally-zoned, 700 Km<sup>2</sup>, 90 Ma Laguna Juarez pluton of Baja California, Mexico is a composite body formed by the nested emplacement of sequential batches of magma. From margin to core, the pluton ranges from tonalite to monzogranite, and is characterized by four nearly concentric mineralogic zones: hornblende, biotite, medium-grained muscovite-biotite, and fine-grained muscovite-biotite.

Isotopic ratios display a systematic trend from margin to core: O isotopic ratios increase, initial Sr ratios become more radiogenic while Nd ratios become less radiogenic. Initial  $^{87}\text{Sr}/^{86}\text{Sr}$  ranges from 0.7043 to 0.7074,  $\delta^{18}\text{O}$  from +7.3 to +12.1 and  $\epsilon_{\text{Nd}}(90 \text{ Ma})$  from +1.8 to -4.9. Common Pb-isotopic ratios of a feldspar separate from each of the four mineralogic zones demonstrates the core has been derived from a Pb reservoir different from the three outer zones.

A low-magnesium, high-alumina basalt (HAB) is hypothesized to be the parental magma by extrapolating trends from the major-element variation diagrams back to a basaltic composition. HAB's are common subduction zone magmas, and represent a feasible composition for modeling purposes. AFC processes can model all samples using isotopic data from W.P. Leeman on a Cascadian HAB and the averaged composition of two host metasediments, a quartzite and a sillimanite schist, for the end members.

The results suggest wet, high-alumina magmas, differentiates of hydrous, primary melts from the mantle wedge, migrated to mid-crustal levels where they ponded and established a wall rock interaction zone (WRIZ). The accumulation of these magmas in the mid-crust provided the heat necessary to melt the wall rock, while simultaneously, exsolution of aqueous fluids from the basalts forced their crystallization and differentiation. Initially, wall-rock melts mixed with relatively undifferentiated basalt and rose through the overlying crust, establishing a pathway for succeeding magmas. Episodically, batches of magma, each more fractionated and containing greater quantities of assimilated, rose and nested within the previous batch creating the pattern of normal zonation.

Relative to samples from the outer mineralogic zones, core samples are characterized by discrete geochemical signatures on trace-element and Sr, Nd, O, and common Pb isotopic diagrams. Although all samples can be modeled by AFC processes using a crustal end member represented by a composite of the analyzed host-rocks, the distinctive chemical and isotopic character of the core may indicate the involvement of a different crustal component. The core may have incorporated melt from an exotic block of crust situated in the WRIZ or possibly from a crustal source located along the path of emplacement or near the final level of emplacement.

## RAPID EMPLACEMENT OF YOUNG OCEANIC LITHOSPHERE

HACKER, B. R., Geological & Environmental Sciences, Stanford University, Stanford CA 94305

Emplacement of oceanic lithosphere onto continents results from a rare phenomenon that has long sparked interest and yet remained poorly understood. Speculations on the age of most ophiolites at the time of emplacement range from 5 to 20 m.y. Consequently, potential tectonic mechanisms for ophiolite emplacement have faced few rigid temporal constraints. The Oman ophiolite is the best exposed and most studied mid-ocean-ridge-like piece of oceanic lithosphere and is of considerable importance for understanding ophiolites worldwide. Our  $^{40}\text{Ar}/^{39}\text{Ar}$  study reveals that sudden cooling deep beneath the Oman ophiolite began within 2 m.y. of igneous crystallization, and therefore, the emplacement process must have initiated very near the ridge crest.

Eleven U/Pb zircon ages from the mafic, crustal intrusive sequence are in the range 95.4–93.5 ± 0.5 Ma (±2σ), although two are slightly older (96.9 and 97.3 Ma) [Tilton et al., 1981]. Amphibolite-facies metamorphic rocks from the thrust zone 17 km below the top of the ophiolite yield  $^{40}\text{Ar}/^{39}\text{Ar}$  hornblende ages of 94.9–92.6 ± 0.6 Ma (±2σ) and muscovite ages of 93.4–91.9 ± 0.6 Ma (±2σ). Combined with biotite K/Ar ages of Gnos and Peters [1993], these data indicate cooling rates of ~100 K/Ma for the first 2 m.y. after igneous crystallization and ~30 K/Ma for the next 4 m.y. This dramatic cooling 17 km below the sea bottom must be related to emplacement, which in turn must have already been underway for some time for cold material to reach such depths so soon after igneous crystallization.

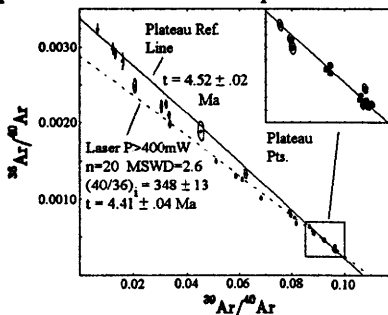
These results are compatible with thermomechanical modeling which indicates that the heat necessary to sustain metamorphism beneath the Oman ophiolite likely dissipated within 5 m.y. [Hacker, 1990, 1991], and with buoyancy calculations [Sacks, 1983; Cloos, 1993], which indicate that oceanic lithosphere younger than 5–10 m.y. is less dense than underlying asthenosphere.

## LASER $^{40}\text{Ar}/^{39}\text{Ar}$ DATING OF TEPHRA IN MARINE SEDIMENTS: CALIBRATING THE GPTS

HALL, Chris M., Dept. of Geol. Sci., U. of Michigan, Ann Arbor, MI 48109-1063, USA, and FARRELL, John W., Dept. of Oceanography, U. of British Columbia, Vancouver, BC V6T 1Z4, Canada.

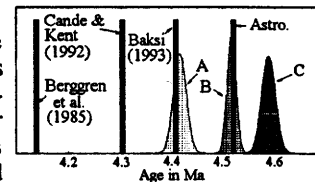
Tephra from ODP site 758 have been examined for the purposes of radiometric dating of marine sediments. Site 758 has both well documented magnetic stratigraphy and several distinct ash layers which erupted from the Indonesian Arc [1]. Ash D dates the Brunhes-Matuyama boundary at 781 ± 16ka (all errors 2σ) as reported in [2], in excellent agreement with modern astronomical and radiometric estimates [3,4]. Ash I, which erupted during the Nunivak event, yielded enough biotite for 5 laser step-heating analyses. Each age spectrum showed high apparent ages at low T, levelling to a plateau at high T. An Ar isochron diagram reveals the presence of at least 3 components of Ar.

We interpret the diagram as: A) atmospheric Ar mixed with initial  $^{40}\text{Ar}/^{36}\text{Ar} \approx 348$  based on a ragged "isochron" through medium to high T points; or B) atmospheric Ar mixed with small amounts of excess  $^{40}\text{Ar}$  and/or small  $^{39}\text{Ar}$  loss due to



recoil (this assumes an atmospheric ratio initial Ar correction for the plateau points, giving the "plateau reference line"); or C) internal redistribution of  $^{39}\text{Ar}$  due to recoil (integrated age 4.59 ± 0.04 Ma).

The second figure shows our three models compared with age estimates based on linear interpolation between ages assigned to the onset and termination of the Nunivak



event from various recent time scales. Our preferred interpretation is the relatively conservative "B" model, agreeing exactly with astronomically derived ages of the Nunivak event in [5,6], although "A" matches [7] and cannot be ruled out. We feel that "C" is the least likely because of the freshness of the biotite, the survival of glass shards in the tephra and the lack of chlorite in XRD. In any case, all models are significantly higher than ones based upon either [8] or [9]. We feel that this is strong evidence for revising the GPTS and it further confirms the accuracy of astronomically derived time scales.

- [1] Farrell & Janecek, *Proc. ODP Sci. Res.* 1991 121 297-355.
- [2] Hall & Farrell, 1993 *EOS* 74 110.
- [3] Shackleton et al. 1990 *Trans R. Soc. Ed.* 81 251-261.
- [4] Baksi 1992 *Science* 256 356-357.
- [5] Hilgen 1991 *Earth Planet. Sci. Lett.* 107 349-368.
- [6] Shackleton et al. 1994 *ODP Leg 138 Sci. Res. in press.*
- [7] Baksi 1993 *Geophys. Res. Lett.* 20 1607-1610.
- [8] Cande & Kent 1992 *J. Geophys. Res.* 97 13917-13951.
- [9] Berggren et al. 1985 *Geol. Soc. Lond. Mem.* 10 211-260.

**MODIFICATION OF THE LITHOSPHERE DURING CONTINENTAL RIFTING: GEOCHEMICAL AND ISOTOPIC EVIDENCE FROM THE SOUTHEASTERN COLORADO PLATEAU TRANSITION ZONE, NEW MEXICO**

HALLETT, R.B., and KYLE, P.R., both at: Dept. of Geoscience, New Mexico Tech, Socorro, NM, 87801, USA, MUKASA, S.B., Dept. of Geological Sciences, University of Michigan, Ann Arbor, MI, 48109, USA.

The elemental and isotopic signatures of both asthenospheric and lithospheric portions of the mantle (acknowledged to be source reservoirs during continental extension-related magmatism) are well documented for the Rio Grande rift and adjacent provinces. We have analyzed Pliocene-age alkaline basalts from the Rio Puerco Valley (RPV), located just east of Mount Taylor volcano in west-central New Mexico, in the transition zone between the southeastern Colorado Plateau and Rio Grande rift tectonic provinces. This setting offers an unique opportunity to monitor the evolution of mantle source regions associated with continental rifting.

Over 40 volcanic necks occur in the RPV as small volume plugs, flows, and dikes. RPV basalts are low SiO<sub>2</sub> (42-49 wt. %), *ne*-normative, high in Ni, Cr, and Mg#, and have REE and spider-diagram trends similar to OIB. Nd and Sr isotopic data define a homogeneous group;  $\epsilon_{Nd} = +3.5$  to  $+4.8$ ;  $^{87}Sr/^{86}Sr = 0.70361 - 0.70407$ , also within the compositional range of OIB. Pb isotopes are fairly radiogenic ( $^{206}Pb/^{204}Pb = 18.84 - 19.26$ ;  $^{207}Pb/^{204}Pb = 15.56 - 15.61$ ;  $^{208}Pb/^{204}Pb = 38.64 - 39.00$ ), plot above the NHRL and overlap both OIB and MORB fields. There is no geochemical or isotopic evidence for crustal assimilation.

Alkaline basalts from highly extended portions of the southern Rio Grande rift and Basin and Range provinces, believed to have originated in the asthenosphere, typically have low  $^{87}Sr/^{86}Sr$  ( $\leq 0.7035$ ) and high  $\epsilon_{Nd}$  ( $\geq +5$ ), close to MORB or a depleted (asthenospheric) mantle end member. Less extended portions of the northern Rio Grande rift (e.g. Taos Plateau and Cerros del Rio in New Mexico; Yampa province and Elkhead Mts in NW Colorado) tend towards enriched (lithospheric) mantle sources (e.g.  $^{87}Sr/^{86}Sr \geq 0.7035$ ,  $\epsilon_{Nd} \leq +2$ ). By comparison,  $^{87}Sr/^{86}Sr$  and  $\epsilon_{Nd}$  values for RPV basalts lie between depleted and enriched mantles, indicating a source contribution from both reservoirs. Pb isotopes further suggest the enriched component is an old (1.8 Ga ?), radiogenic (with respect to Pb only) subcontinental lithosphere. When placed in a tectonomagmatic evolutionary framework for the Rio Grande rift we believe the RPV basalts represent a lithospheric source that has been modified by the asthenosphere by the following processes: (a) asthenospheric upwelling brought on by continental rifting and resulting in thermal, mechanical, and chemical transformation of the lithosphere, (b) clockwise rotation of the Colorado Plateau since the late Miocene, and (c) preexisting Laramide structure facilitating the transport of alkaline magmas by channeling melts along crustal weaknesses.

**INDUCTIVELY-COUPLED PLASMA MAGNETIC SECTOR MULTI-COLLECTOR MASS SPECTROMETRY**

A. N. Halliday, J. N. Christensen, C.M. Hall, C. E. Jones, D.-C. Lee, D. Teagle (All at: Dept. Geol. Sci. Univ. of Michigan, Ann Arbor, MI 48109)  
A. J. Walder (FI Elemental, Winsford, Cheshire, U.K.)  
P. A. Freedman (Fisons Instruments, VG Isotech, Middlewich, Cheshire, U.K.)

Inductively-coupled plasma (ICP) sources offer considerable advantages over thermal sources because of the high ionization efficiency, facilitating relatively high sensitivity measurements for elements such as Hf. The mass discrimination (bias) is larger than for thermal ionization (typically about a percent per a.m.u. for Pb), and favors the heavier ions, decreasing with increasing mass. However, unlike for TIMS, this discrimination is largely independent of chemical or physical properties of the element or duration of the analysis. This can be demonstrated at high precision with a double focusing multi-collector magnetic sector mass spectrometer with an ICP source (ICPMS). For example, the reproducibility of Pb isotopic data using TI to correct for mass bias is superior to that achieved by TIMS. An additional feature of such an instrument is that it offers the possibility of accurately measuring parent/daughter ratios by direct comparison with standards of known composition, critical in the development of laser probe techniques. A new wide flight tube and modified magnet capable of measuring U and Pb simultaneously have been incorporated into an ICPMS. Measurements on accurately prepared standard solutions show that for elements with high first ionisation potential (e.g. Sm, Nd, U, Th, Pb) the element ratios are affected by the adjustment of RF power to the plasma. However, at constant and high RF power (1.5 kW) and using the wide flight tube, U/Pb ratios can be accurately determined by running a similar standard and comparing relative ion beam intensities with those of the unknown. Correction is possible despite mass bias effects over this large mass range and differences in the ionisation efficiency of U and Pb. Isobaric interferences from molecular species are usually minor and simple because complex molecules are unstable in an ICP source. Use of a dry plasma, as with laser ablation or a desolvating nebulizer, minimizes hydride and oxide formation.

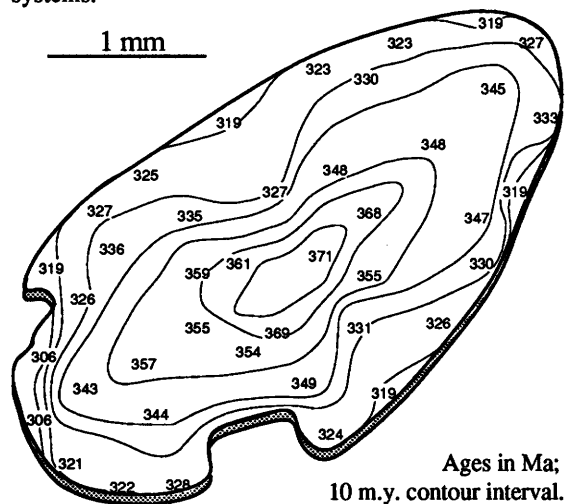
**THE DYNAMIC RANGE OF ARGON RETENTION IN SINGLE CRYSTALS, EXAMPLES FOR MUSCOVITE ACROSS THE ACADIAN METAMORPHIC FIELD GRADIENT IN WESTERN NEW ENGLAND**

HAMES, W.E., Department of Earth, Atmospheric, and Planetary Sciences, M.I.T., Cambridge, MA, 02139, USA.

This study tests the practical limits of closure theory for laser  $^{40}\text{Ar}/^{39}\text{Ar}$  muscovite age measurements by evaluating their relationship to peak metamorphism and unroofing along the Acadian metamorphic field gradient (MFG) of western New England. Peak metamorphic conditions vary by 500-700° C at 5-10 kb from west to east on the MFG. The unroofing path is characterized by isothermal decompression, rapid cooling, and water-saturated melting of granitic rocks. Geochronologic data published in several sources provide the following regional constraints: ca. 385 Ma U/Pb and Nd/Sm crystallization ages for garnet and accessory minerals in schists; ca. 375 Ma U/Pb crystallization ages for accessory minerals in post-kinematic granite dikes; 390—360 Ma hornblende  $^{40}\text{Ar}/^{39}\text{Ar}$  plateau; and, 365—340 Ma muscovite and biotite  $^{40}\text{Ar}/^{39}\text{Ar}$  plateau.

New data indicate the integrated closure of  $^{40}\text{Ar}$  in muscovite, determined by laser fusion of entire crystals, occurred over 380-360 Ma in rocks of lower metamorphic grade; the range in intercrystalline  $^{40}\text{Ar}/^{39}\text{Ar}$  ages was generally minimized at higher metamorphic grades by recrystallization and more rapid unroofing paths. However, large muscovite crystals from the highest-grade rocks (as that shown below) record retention of radiogenic argon during most of their metamorphic and unroofing history. Laser spot fusion age measurements (with size and placement indicated by the apparent ages) for this muscovite phenocryst from a granite dike indicate initial retention of  $^{40}\text{Ar}$  at  $371 \pm 4$  Ma (very near to the timing of crystallization), and loss of  $^{40}\text{Ar}$  by volume diffusion over the ensuing 50 m.y.

The new data are compatible with volume diffusion models (Dodson, 1973; Dodson, 1986) and geophysical models for metamorphic paths (e.g., England and Thompson, 1984). These data demonstrate that relatively complete metamorphic histories can be evaluated with  $^{40}\text{Ar}/^{39}\text{Ar}$  dating of muscovite crystals selected on the basis of size and paragenesis from a single exposure, and that the dynamic range of argon retention in muscovite can be extended to the range of U/Pb and Nd/Sm systems.



**AN EMPIRICAL STUDY OF FACTORS CONTROLLING  $^{40}\text{Ar}$  RETENTION IN MUSCOVITE FROM THE GASSETTS SCHIST, VERMONT APPALACHIANS**

HAMES, W.E., Department of Earth, Atmospheric, and Planetary Sciences, MIT, Cambridge, MA, 02139, USA.

Variations in the size, major element composition, deformation characteristics, and relative crystallization history of minerals are evident in most metamorphic rocks. Microanalytical techniques permit age determinations to be made in the direct context of these variations, and thus empirical studies can readily test their influence on  $^{40}\text{Ar}$  retention during metamorphism and cooling.

An exposure along the western flank of the Chester-Athens domes in Vermont (the locality for classic studies of the "Gassetts schist") contains feldspathic gneiss with high K-Fe muscovite and aluminous schist with high K-Na muscovite, and thus provides a setting to test the influence of several parameters on  $^{40}\text{Ar}$  retention in white micas. Penetrative metamorphic fabrics were developed in these lithologies during the Acadian (Devonian) event, a single schistosity is dominant within the exposure, and porphyroblasts are pre- to synkinematic with respect to this schistosity. Regional geochronologic and petrologic constraints indicate peak Acadian metamorphic temperatures (ca. 600° at a pressure of 8 kb) were reached at about 385 Ma.

Early formed muscovite crystals from both the schist and gneiss (selected for their comparable size and lack of internal cleavage or deformation features) yield maximum laser spot fusion  $^{40}\text{Ar}/^{39}\text{Ar}$  ages of  $380 \pm 4$  and  $386 \pm 4$  Ma in their cores. These crystals exhibit similar, radial patterns of age discordance that suggest loss of  $^{40}\text{Ar}$  via cylindrical volume diffusion over ca. 50 m.y. The population distribution of argon ages among single muscovite crystals does not vary appreciably for the schist and gneiss (based on 50 single crystal age determinations for each of two samples). These relationships indicate that retention of  $^{40}\text{Ar}$  in muscovite is strongly a function of physical grain size (consistent with previous laser studies), however, K-Na substitutions have relatively minor effects on mica retention characteristics. The data also indicate that argon retention can initiate in the cores of millimeter-diameter crystals at relatively high temperatures.

Large early-formed muscovite crystals with obvious internal cleavage boundaries and mineral intergrowths yield ages that do not vary systematically with crystal size and are no older than about 360 Ma. In these crystals the effective path length for volume diffusion has been reduced from the physical crystal size to a distance controlled by the spacing of defects.

*In situ* laser analyses of neoblastic, millimeter-diameter muscovite which defines the dominant schistosity indicate that the cores of these crystals initiated retention of  $^{40}\text{Ar}$  at ca. 360 Ma, and experienced volume diffusion loss of  $^{40}\text{Ar}$  over a shorter interval of 20 m.y. Regional geochronologic and structural data indicates these crystals grew after the peak conditions of Acadian metamorphism.

Bulk sample methods for determining muscovite  $^{40}\text{Ar}/^{39}\text{Ar}$  age in these lithologies would homogenize the observed age discordance; the resulting age would not reflect the integrated closure of a specific mica, but rather the mass balance of different mica sizes and structural types represented in the mineral separate. However, rather than emphasizing the problematic and complex nature of age discordance, microanalytical  $^{40}\text{Ar}/^{39}\text{Ar}$  studies offer the potential to develop new standards for determining age discordance and representative estimates of closure age.

**DETAILED EMPLACEMENT CHRONOLOGY OF BASIC MAGMAS OF THE MID-PROTEROZOIC NAIN PLUTONIC SUITE, LABRADOR: INSIGHTS FROM U-Pb SYSTEMATICS IN ZIRCON AND BADDELEYITE**

**HAMILTON, Mike A., EMSLIE, Ron F., and RODDICK, J. Chris, Continental Geoscience Division, Geological Survey of Canada, Ottawa, Ontario, Canada.**

The Elsonian Nain Plutonic Suite (NPS) consists of a composite array of predominantly granitoid intrusions and large plutons of massif anorthosite, emplaced anorogenically over 19,000 km<sup>2</sup>. Associated with the largely accumulated anorthositic rocks are smaller, but numerous bodies of troctolite and gabbro. Ferrodiorite also occurs, probably as late-stage differentiates from anorthosite crystallization. We report U-Pb data on zircon and baddeleyite which permits examination of the duration and high-resolution emplacement chronology of basic magmatism in the NPS. All cases yield concordant or only weakly discordant (<0.5%) U-Pb results, which help strengthen models involving genetic ties between anorthositic and ferrodioritic magmatism, in contrast to models favouring association of the latter with granitoid rocks.

Zircons in NPS leucotroctolites and anorthosites (TR-AN) are typically clear to pale pink-brown euhedral prismatic grains exhibiting few fractures or inclusions, no overgrowths, and low U (~30 ppm) contents. Rare, individual acicular euhedra may reach up to 30 cm in length. Preliminary U-Pb data from AN in the eastern and southern flanks of the complex indicate that the majority of magma batches crystallized over at least 17 Ma from 1322±1 Ma (leuconorite, Makhavinekh) to 1305±2 Ma (anorthosite, Koliktalik I.). Massive anorthosite of the Paul Island intrusion yields an age of 1319±1 Ma. Anorthosite and leuconorite of Kikkertavak Island and Tabor Island, and leucotroctolite cumulates from the Jonathan intrusion have identical ages of 1311±2 Ma. The entire magmatic interval for AN is doubled by inclusion of an Ukaume intrusion leuconorite (1331±2 Ma) and leucotroctolite from southernmost Sango Bay (1294±1 Ma).

Fe-Ti oxide-rich, silica-poor differentiates such as ferrodiorites may contain appreciable amounts of both zircon (8-200 ppm U) and euhedral baddeleyite (~70 ppm U). The duration of ferrodioritic (FD) magmatism (~24 Ma) appears to mirror that described above. FD rocks at the margin of the mostly troctolitic Barth Island intrusion yield a concordant age of 1322±2 Ma. Isolated diorites exposed in the Jonathan intrusion crystallized simultaneously, within error (1312±3 Ma) of adjacent troctolites. Immediately west, Tigalak intrusion ferrodiorites were intruded at 1306±3 Ma, while some sheet-like intrusions were emplaced in the southern quadrant of the NPS (Cabot Lake) as late as 1298±2 Ma. In some instances, large and often corroded or embayed zircons have the appearance of being xenocrystic, potentially from NPS monzonitic to granitic magmas, some of which are known to have crystallized earlier. By example, zircons from the Satorsuakullik ferrodiorite dyke exhibit such morphology and yield a 1315±2 Ma age, in contrast to a 1301±2 Ma age from magmatic baddeleyite in the same sample. Diorite from the Ukaume intrusion has an age of 1333±2 Ma, and extends the known duration of FD magmatism to 35 Ma.

The coincidence of ages between TR-AN and FD magmatism supports contemporaneous development of FD magmas from less evolved precursors, as is suggested by mineral compositional trends and tracer isotopic (Nd, Sr) compositions linking the two groups petrogenetically.

**STABLE ISOTOPE COMPOSITION OF CONCRETION IN LOESS AS TRACERS OF THE PAST CLIMATE CHANGE**

**HAN, Jiamao and JIANG, Wenying, Institute of Geology, Chinese Academy of Sciences, P. O. Box 634, Beijing 100029, China**

About 700 carbon and oxygen isotopic measurements were carried out on the samples from concretions of paleosols (S1 - S14) in Lishi Loess Formation. It shows that there are clear differences in both carbon and oxygen isotope composition between different kinds of paleosols. Usually the more developed the paleosols, the less negative the  $\delta^{18}\text{O}$  value and the more negative the  $\delta^{13}\text{C}$  value will be.  $\delta^{18}\text{O}$  values vary within a range of about 1.3‰,  $\delta^{13}\text{C}$ , however, within a relative large range of 5.3‰.

The isotopic record of the continental deposits is also a very useful tool in reconstruction of past environment. Based on our knowledge to the isotopic composition of modern carbonate in soil, an attempt was carried out using the isotope results semi-quantitatively to estimate the environmental information from the time of each paleosol formation.

## HIGHLY CORRELATED Pb - He - Sr ISOTOPES IN MID-ATLANTIC RIDGE BASALTS FROM 33°S

B B HANAN San Diego State University, San Diego, CA  
D W GRAHAM Oregon State University, Corvallis, OR  
P J MICHAEL University of Tulsa, Tulsa, OK 74104

We report Pb, He, and Sr isotopic analyses of MORB glasses from four southern MAR ridge segments from 31° to 34°S. The 33°S ridge segment (32.52°-33.47°S) is the central of three segments that are separated by left lateral offsets and bounded by the Cox and Meteor fracture zones. The remaining segment is located just north of the Cox fracture zone. Maxima in ridge axis elevation, K/Ti,  $^{206}\text{Pb}/^{204}\text{Pb}$  and  $^{87}\text{Sr}/^{86}\text{Sr}$ , minima in  $\text{Na}_2\text{O}$  and  $^3\text{He}/^4\text{He}$ , and a pronounced "bulls-eye" Bouguer gravity low occur simultaneously near 33°S.

Previously we have shown that the asthenosphere from 2°S to 47°S has been polluted by the off-ridge hotspots of Circe, St. Helena, and Tristan da Cunha, Gough, and Discovery (TGD). Variations in isotopic and incompatible element ratios along the ridge coincide with anomalous elevations of "zero age" crust [1-3]. Basalts from the spike-like geochemical anomalies define distinct binary-mixing vectors in Pb/Pb isotopic space between the off-ridge hotspots and the LILE-depleted asthenosphere. Basalts that would be considered "normal" MORBs by their  $(\text{La}/\text{Sm})_N < 0.63$ , from ridge-segments between these anomalous segments, are also contaminated with respect to Pb isotopes. There is a broad maximum in  $^{206}\text{Pb}/^{204}\text{Pb}$  and minimum in  $^3\text{He}/^4\text{He}$  opposite the  $^{206}\text{Pb}$ -rich St. Helena plume, while  $^{208}\text{Pb}/^{204}\text{Pb}$  is maximum opposite the  $^{208}\text{Pb}$ -rich TGD hotspots. We interpret this discrepancy between  $(\text{La}/\text{Sm})_N$  and radiogenic Pb and He to result from broad pollution of the asthenosphere by dispersion of these plumes during the time when they were intraplate, prior to being over-ridden by the migrating MAR.

The 33°S geochemical anomaly has a short wavelength, high-amplitude spike-like profile superimposed on the broad, long wavelength trend. The anomalous enrichment shown by Pb and He isotopes, relative to the regional trend, is restricted to segment 4 (<100 km along strike length), where  $^{206}\text{Pb}/^{204}\text{Pb}$  increases to 19.3,  $^{87}\text{Sr}/^{86}\text{Sr}$  to 0.7029 and  $^3\text{He}/^4\text{He}$  decreases to 6.3  $R_A$ . The  $^{206}\text{Pb}/^{204}\text{Pb}$  (18.0-19.3) and  $^3\text{He}/^4\text{He}$  (8.0-6.3  $R_A$ ) variations encompass much of the global range for MORB erupted away from the influence of known hotspots;  $^{87}\text{Sr}/^{86}\text{Sr}$  ranges 0.7025-0.7029. The  $^{206}\text{Pb}/^{204}\text{Pb}$ ,  $^{87}\text{Sr}/^{86}\text{Sr}$ , and  $^4\text{He}/^3\text{He}$  ratios are highly correlated, show good correlation with K/Ti, poor negative correlation with  $\text{Na}_2\text{O}$ , and lack correlation with  $\text{Fe}_2\text{O}_3$  or Mg#. All of the other ridge segments have distinct isotope signatures, suggesting that their magma sources are isolated from each another. Although the 33°S anomaly is similar to other MAR anomalies caused by hotspot-ridge interaction, the correlations in Pb, Sr, and He isotopic space are not consistent with binary mixing between the MORB asthenosphere beneath the 33°S segment and the off-axis TGD hotspots. Instead, an enriched source with  $^{206}\text{Pb}/^{204}\text{Pb}$  greater than 19.3 is required. The combined Pb, Sr, and He isotope signature of the 33°S anomaly is distinct relative to the South Atlantic hotspots, and may reflect the drawing up by the migrating ridge system of a relatively small scale passive mantle domain, apparently unrelated to the South Atlantic hotspots at this time.

1. Schilling et al. (1985) Nature 313, 187
2. Hanan et al. (1986) Nature 322, 137
3. Graham et al. (1992) EPSL 110, 133

## COOLING AND UPLIFT IN A TERTIARY PLUME AREA: FISSION TRACK EVIDENCE FROM THE KANGERLUSSUAQ AREA, EAST GREENLAND.

HANSEN, K. Geological Institute, University of Copenhagen, Øster Voldgade 10, DK-1350 København K, Denmark.

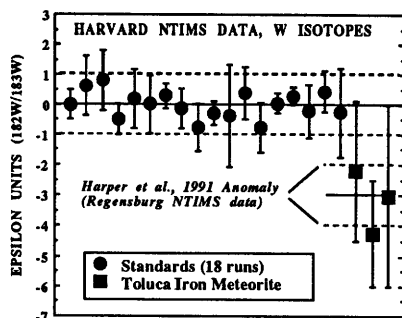
In the early Tertiary, the Icelandic plume was located under the east coast of Greenland. Rifting across the plume was accompanied by extensive magmatic activity including flood basalts. The morphological features show that central uplift occurred and that the continental rims were uplifted subsequent to the rifting.

New fission track (FT) investigations have been undertaken to yield information on cooling and uplift history in the region. Earlier FT investigations were performed for intrusive rocks confirming that Tertiary doming occurred in the area. Further information about the Tertiary cooling and uplift history can be obtained from sedimentary, metamorphic and pre-Tertiary intrusive rocks using the FT method. Mean track lengths range between c. 10.5  $\mu\text{m}$  and c. 14.0  $\mu\text{m}$  (the highest means were obtained for Tertiary intrusive rocks) while mean ages and single grain ages range from Permian to Tertiary. The present investigation shows the presence of several cooling paths in the area. Intrusive rocks in the center of the dome first cooled to the temperature of the surroundings and then followed the cooling paths of their surroundings determined by exhumation and uplift. The temperature histories of the surroundings show a variable amount of Tertiary overprint. Their surviving pre-Tertiary tracks record the early cooling/erosion history. FT analysis has shown late fast cooling to occur along the east coast of Greenland between 66° and 73° and thus no relaxation along rift shoulders occurred as would be expected.

**$^{182}\text{Hf}$ - $^{182}\text{W}$ : A NEW EXTINCT RADIONUCLIDE CHRONOMETER OF ACCRETION & CORE FORMATION**  
**HARPER, C.L. Jr., and JACOBSEN, S.B.,** Dept. of Earth & Planetary Sciences, Harvard Univ., 20 Oxford Street, Cambridge, MA, 02138, USA.

The  $^{182}\text{Hf}$ - $^{182}\text{W}$  chronometer is likely to become a powerful tool in studies of the accretion and very early differentiation histories of planets. Careful investigation of the  $^{182}\text{Hf}$ - $^{182}\text{W}$  system is also important in astrophysics because a determination of the initial abundance of  $^{182}\text{Hf}$  will provide a key constraint on models of the molecular cloud environment within which the sun formed. The 9 Ma half-life of  $^{182}\text{Hf}$  provides an excellent timescale for studies of both star-forming and planet-building processes. Several geochemical aspects also make the  $^{182}\text{Hf}$ - $^{182}\text{W}$  systematics particularly well suited for dating planetary accretion-related (as opposed to nebular) processes, especially core formation.

**$^{182}\text{W}$  Measurements:** W isotopic measurements using  $\text{WO}_3^-$  beams were developed by Heumann and co-workers in Regensburg, and the first high precision measurements of meteoritic W made there were reported by Harper *et al.* (1991). Relative to a  $^{183}\text{W}/^{184}\text{W}$  normalization, an apparent shift of about  $-3.0 \pm 0.9$  epsilon-units in  $^{182}\text{W}/^{184}\text{W}$  was observed in Toluca (iron meteorite) W relative to a standard. Radiogenic growth of  $^{182}\text{W}$  in the silicate portion of the Earth (high-Hf/W) after core formation would explain the anomaly, (with iron meteorites representing initial  $^{182}\text{W}/^{183}\text{W}$ ). To confirm the effect we developed a high precision multicollector technique utilizing a 7-cup configuration with comonitoring of  $^{18}\text{O}/^{16}\text{O}$  fractionation and  $\text{ReO}_3^-$  interference. Reproducibility for  $^{182}\text{W}/^{183}\text{W}$  measurements (normalized to  $^{184}\text{W}/^{183}\text{W}$ ) is shown indicating an  $\sim \pm 1\epsilon$ -unit precision for standards. Three new preliminary measurements appear to confirm the previously-reported  $-3 \pm 1 \epsilon$ -unit anomaly.



**MAGMATIC PROCESSES AND ENVIRONMENTS AS REVEALED FROM NOBLE GAS ISOTOPES - A CASE STUDY FOR UNZEN VOLCANO, JAPAN**  
**HANYU, T. and KANEOKA, I.,** Earthquake Research Institute, Univ. of Tokyo, Bunkyo-ku, Tokyo, 113, Japan.

Noble gas study of coexisting minerals in volcanic rocks might provide a new approach for the magmatic processes and environments. It is commonly assumed that minerals, except for xenocrysts, observed in a volcanic rock are formed under an equilibrium state and the occurrence of an unequilibrium state among some kinds of minerals in a volcanic rock has not always been emphasized. Isotope studies for each kind of minerals would give us more information concerning the magmatic processes and environments where minerals crystallized. Among them, noble gas analyses would be quite effective, because noble gases are chemically inert and include both radiogenic and stable isotopes, which make them to be sensitive for small changes of magmatic environments.

As a case study, we have performed noble gas analyses of volcanic rocks of Unzen Volcano, Japan. In November, 1990, it started to erupt and dacitic lava domes are still growing. It also poured out dacitic lava flows in 1792. Rocks in both cases contain large phenocrysts (up to about 10mm in size) of plagioclase, hornblende and biotite. Phenocrysts of different kinds of minerals were prepared for noble gas analyses by handpicking. Phenocrysts of plagioclase and hornblende were sorted out further according to their size. Noble gases were extracted from samples by using an induction heater at 700°C and 1600°C, respectively and measured on a quadrupole mass spectrometer.

The most remarkable result is that plagioclase samples show systematically higher  $^{40}\text{Ar}/^{36}\text{Ar}$  ratios (310-360) than hornblende and biotite samples (296-310) in the 1600°C fraction. In the 700°C fraction, most samples show  $^{40}\text{Ar}/^{36}\text{Ar}$  ratios similar to the air value (296), representing the high air contamination in this fraction. On the other hand, the gases extracted at 1600°C can be interpreted to represent magmatic ones.  $^{40}\text{Ar}/^{36}\text{Ar}$  ratios of hornblende and biotite samples are a little higher than the air value and obviously distinct from those of plagioclase samples. It indicates that the magmatic environment where plagioclase crystallized was different from that where hornblende and biotite did, implying the crystallization at a different place and/or at a different time in the magma. It is also notable that plagioclase and hornblende of larger grain sizes show higher  $^{40}\text{Ar}/^{36}\text{Ar}$  ratios than those of smaller grain sizes, respectively, which might be directly related to the crystallization process of minerals.

The variation of  $^{40}\text{Ar}/^{36}\text{Ar}$  ratios among different kinds of minerals and among samples of different grain sizes in the same kind of minerals might have been caused by mixing of original magmatic Ar and atmospheric Ar. The carrier of atmospheric Ar is considered to be groundwater. We infer that the  $^{40}\text{Ar}/^{36}\text{Ar}$  ratio of the magma chamber was originally high (350-400) and it gradually decreased as contamination of groundwater into the magma proceeded. Thus, it becomes possible to infer the time when each kind of minerals crystallized and we will get information of magmatic history.

**PRODUCTION OF COSMOGENIC NUCLIDES BY BOMBARDMENT OF THICK TARGETS WITH 60,90, AND 120 MEV ALPHA PARTICLES II. MEASUREMENT  $^{26}\text{Al}$  AND  $^{10}\text{Be}$  BY AMS.**

**L.L. Harris<sup>1</sup>, R.L. Paul<sup>1</sup>, P.A.J. Englert<sup>1</sup>, E.B. Norman<sup>2</sup>, K.T. Lesko<sup>2</sup>, R.M. Larimer<sup>2</sup>, I. Goldman<sup>2</sup>, C. Jackson<sup>2</sup>, B. Napier<sup>2</sup>, B. Sur<sup>2</sup>, M.A. Caffee<sup>3</sup>, R.C. Finkel<sup>3</sup>, J.R. Southon<sup>3</sup>.** 1) San Jose State University, Nuclear Science Facility, San Jose, CA 951922) Lawrence. Berkeley Laboratory, 1 Cyclotron Rd. Berkeley, CA 94720. 3) NCD/CAMS Lawrence Livermore National Laboratory, PO Box 808, Livermore, CA 94550.

We determined the average thick-target cross sections for the production of the long-lived cosmogenic nuclides  $^{26}\text{Al}$  and  $^{10}\text{Be}$  by alpha particle bombardment of cosmochemically important targets [1]. These cross-sections are needed to interpret measurements of cosmic ray induced nuclear reactions in terrestrial and extraterrestrial material [2]. Understanding the production parameters of cosmogenic nuclide levels in extraterrestrial matter (meteorites, cosmic dust, and planetary surfaces) provides a means of studying the history of both the irradiated matter and the cosmic radiation itself [3].

Pure targets of C, Mg, Al, Si,  $\text{SiO}_2$ , Fe, Ni, Bi, and Ge and  $\text{Bi}_4\text{Ge}_3\text{O}_{12}$  were bombarded with 60, 90, and 120 MeV alpha particles at the Berkeley 88 inch cyclotron. For all of these alpha energies the single-foil technique was used [4], where each target was individually wrapped or sandwiched between two high purity gold foils which are used as beam monitors. Following the separation chemistry [5]  $^{26}\text{Al}$  and  $^{10}\text{Be}$  were measured using accelerator mass spectrometry and the experimental cross sections were calculated [6]. The experimental cross sections were compared with earlier published data where found and agree to satisfaction.

**REFERENCES.** [1] Arnold, J.R. et al; *J. of Geophys. Res* 66, (1961) 3519-31.[2] Mahoney, W.A. et al; *Astrophysics J.*, 278, (1984) 784. [3] Reedy, R.C. et al; 20th Lun. and Plan. Sci. Conf. LA-UR-89-87 Hus. Tx, 1989. [4] O. Chamberlain. *Phys. Rev. Let.* 15 (1969) 485. [5] Theis, S. and Englert, P. et al, *J. of Radioanal. and Nucl. Chem.* 100 (1989). [6] Dittrich, B. et al; *Nucl. Instr. and Meth. in Phy. Res.* B52 (1990)588-94.

**OXYGEN ISOTOPE GEOCHEMISTRY OF MESOZOIC RHYOLITES AND GRANITES OF NW NAMIBIA**

HARRIS, Chris, Department of Geological Sciences, University of Cape Town, Rondebosch 7700, South Africa

The oxygen isotope ratios of unaltered phenocrysts from rhyolites are particularly useful in constraining the nature of the source from which the rhyolites were derived. The Etendeka/Paraná "flood" rhyolites which erupted just prior to the rifting of Africa and South America, can be divided into a high- $\delta^{18}\text{O}$  type ( $\delta^{18}\text{O} \sim 10\text{‰}$ ) and a low- $\delta^{18}\text{O}$  type ( $\delta^{18}\text{O} \sim 7\text{‰}$ ). In Namibia, the high- $\delta^{18}\text{O}$  rhyolite type occurs in the south and the low- $\delta^{18}\text{O}$  type occurs in the northern part of the province. The high- $\delta^{18}\text{O}$  rhyolite type appears to be the more abundant throughout the Etendeka/Parana province. Analyses of fresh mineral phases from the major Mesozoic complexes of NW Namibia show that the  $\delta^{18}\text{O}$  values of the original magmas are to some extent related to the nature of the crust through which they were intruded. Granites from the Spitzkoppe and Klein Spitzkoppe complexes and rhyolites from the Erongo complex, which are situated in the middle of the Central Zone of the Pan-African Damara orogenic belt, have the highest magmatic  $\delta^{18}\text{O}$  values of 11 and 12‰ respectively, whereas granitic rocks from the Brandberg and Messum complexes, to the north of the Central Zone, have lower  $\delta^{18}\text{O}$  values. Although they are not petrogenetically related, it seems probable that the granitic rocks from the Central Zone complexes and the southern rhyolites share a common origin; that is they formed by partial melting of Damara S-type granite restite. If the source(s) of the northern rhyolites and the Brandberg and Messum granites is within the crust, then that source must be dominantly Archaean lower crust of the Congo Craton. Alternatively, these rocks might have originated by partial melting and subsequent crustal contamination of underplated Mesozoic basalt.

The eruption of large volumes of crustally-derived magmas during the breakup of southern Africa and South America contrasts with the situation during the rifting of southern Africa and Antarctica where large volumes of rhyolite produced by partial melting of underplated basalt were produced. This contrast may be related to differences in the size and/or position of the underlying mantle plumes relative to initial rifting in the two areas.

## PROGRADE THERMOCHRONOMETRY USING SIMS ANALYSIS OF MONAZITE

HARRISON, T.M., McKEEGAN, K.D., AKERS, W., Dept. of Earth and Space Sciences & IGPP, UCLA, Los Angeles, CA, 90024, U.S.A., RYERSON, F.J., Lawrence Livermore Nat. Lab., Livermore, CA, 94550, U.S.A.

It is now well known that although monazite can retain Pb\* at sustained temperatures of >700°C, it is unstable during low grade metamorphism in pelites. Detrital monazite dissolves under diagenetic conditions and does not reappear until upper amphibolite facies. During this period, the components of monazite appear to be held in LREE/Th oxides, apatite, and allanite. This unusual behavior suggests the use of monazite as a thermochronological record for prograde metamorphism. Three related developments are required to exploit this approach; isotopic microanalysis of monazite, knowledge of the stability and reaction kinetics of LREE oxides in pelitic assemblages, and a Pb diffusion law for monazite.

Measurements of the U-Th-Pb systems in monazite using the UCLA CAMECA ims 1270 ion microprobe suggest three properties that make it analytically less demanding than zircon; 1) the concentrations of U and Th (and thus Pb\*) are typically  $10^2$ - $10^4$  times higher, 2) the mass resolution required to separate Pb isotopes from their principal interferences (mostly LREE(PO<sub>2</sub>)<sup>+</sup>) is ~4000 compared to ~7000 to resolve HfSi<sup>+</sup> in zircon, and 3) the yield of Pb ions from monazite is ~2x higher than that from zircon. Tests on a standard monazite indicate a sensitivity of 40 cps/ppm Pb/nA O<sub>2</sub><sup>-</sup>. Spot analyses of Tioga monazite yield (<sup>207</sup>Pb/<sup>206</sup>Pb)\*=0.0536±0.0008 (±2 σ<sub>min</sub>) which agrees with the Roden et al. (1990) TIMS determination of (<sup>207</sup>Pb/<sup>206</sup>Pb)\*=0.05442±0.00008. We are investigating several relationships for determining inter-element ratios: <sup>208</sup>Pb<sup>+</sup>/P<sup>+</sup> vs. ThO<sub>2</sub><sup>+</sup>/P<sup>+</sup>, <sup>208</sup>Pb<sup>+</sup>/<sup>232</sup>Th<sup>+</sup> vs. ThO<sup>+</sup>/Th<sup>+</sup>, and direct comparison of <sup>208</sup>Pb<sup>+</sup>/<sup>232</sup>Th<sup>+</sup> between sample and standard. The energy distributions of Pb<sup>+</sup>, U<sup>+</sup>, Th<sup>+</sup>, ThO<sup>+</sup>, and ThO<sub>2</sub><sup>+</sup> ions are markedly different, with Pb<sup>+</sup> behaving in a fashion more similar to molecular ions.

Ion imaging of monazites known to contain inherited Pb\* show clear core-rim relationships similar to the well-known zircon inheritance. Spot analyses (~15 μm) of the rim of a monazite grain from the Sweetwater Wash pluton, SE California, yield <sup>208</sup>Pb/<sup>232</sup>Th ages of 71±3 Ma, in accord with the known crystallization age of the pluton. The core yields a <sup>207</sup>Pb/<sup>206</sup>Pb age of 1,546±9 Ma which agrees with estimates of early crustal growth in the SE Mohave.

Our hydrothermal experiments preclude rhabdophane from being the immediate precursor to neofomed monazite in lower amphibolite facies, but rather suggest that equilibria involving the reaction apatite + LREE oxides = monazite + calcic phase are responsible for its appearance. We estimate the monazite isograd in pelites to be 450°-500°C at mid-crustal pressures.

Preliminary diffusion measurements using a La-monazite synthesized in a Pb-bearing flux heated in a reservoir of Pb-free La-monazite powder yield  $D_{Pb} = 4 \times 10^{-18} \text{cm}^2/\text{s}$  at 1000°C.

Roden, M.K., Parrish, R.R., and Miller, D.S., 1990, The absolute age of the Eifelian Ash bed: J. Geol., 98, 282-285.

## EMINENT DOMAINS: K-FELDSPAR THERMOCHRONOMETRY

HARRISON, T.M., LOVERA, O.M., GROVE, M., Dept. of Earth and Space Sciences & IGPP, UCLA, Los Angeles, CA, 90024, U.S.A., HEIZLER, M.T., New Mexico Bureau of Mines, Socorro, NM, 87801, U.S.A. and FITZGERALD, J.F., Research School of Earth Sciences, Australian National University, Canberra, A.C.T., 2601, Australia.

The observation of correlated inflections between K-feldspar age spectra and Arrhenius plots is compelling evidence that this phase behaves in a broadly similar fashion during laboratory heating as it did during slow cooling in nature. To assess the degree to which this approximation holds, we have employed three kinds of probes to image K-feldspar samples; electrons, X-rays, and Ar isotopes. In general, we find lengthscales for Ar diffusion ranging from ~½ to 100 μm, a low density of extended defects, and no significant changes to cell dimensions, Or content, or Si/Al ordering upon heating to 1100°C or from irradiation doses corresponding to J~0.01. Madagascar orthoclase reveals only small deviations from a single Arrhenius relationship relative to most perthites restricting intrinsic mechanisms to less than ~15% of the total observed variation in log(r/r<sub>0</sub>). Experiments to assess the effect of laboratory heating on K-feldspar microstructures show excellent reproducibility of D/r<sup>2</sup> and reveal no significant changes in diffusion properties up to 80% argon loss. Relative differences in domain size determined from sizing experiments indicate that domains have effective sizes between ~½ and 100 μm. Numerical analysis indicates that the effect of non-uniform <sup>40</sup>K distributions is small. For example, modeling perthite-like modulations as a cosine distribution results in an initial drop in D/r<sup>2</sup> of only a factor of ~3.

*In vacuo* crushing experiments of K-feldspars typical of those used for thermochronometry indicate that only ~0.1% of the <sup>39</sup>Ar can be accessed by crushing. Anomalous age spectra of samples crushed below the largest domain size indicate subtle differences in the siting of <sup>40</sup>Ar\* relative to <sup>39</sup>Ar. Identification of <sup>40</sup>Ar<sub>E</sub>/Cl component via isothermal step replicates (MRCLEAN) permits correction of excess <sup>40</sup>Ar from most K-feldspar age spectra. Ion imaging identifies ~100 nm sized inclusions as containing the Cl-correlated excess Ar.

The existence of discrete argon retentivities in basement K-feldspars is a fact that any K-Ar geochronologist can verify. We find that assuming these retentivities are due to a distribution of diffusion domain sizes reconciles otherwise problematic aspects of age spectra and Arrhenius results and permits recovery of high resolution thermal histories. The results of the experiments described above indicate that most of the contrast in argon retentivity in K-feldspars is diffusion domain size related. Although continually testing the underlying assumptions of the multi-diffusion domain model, we have yet to encounter evidence seriously challenging the basic approach.

## LASER EXTRACTION AND ANALYSIS OF EXTRATERRESTRIAL He AND Ne ISOTOPES

HARROP, Paul J., Department of Geology, University of Manchester, Manchester, M13 9PL, United Kingdom, STUART, F.M., S.U.R.R.C., East Kilbride, Glasgow, G75 0QU, United Kingdom, and TURNER, G., Department of Geology, University of Manchester, Manchester, M13 9PL, United Kingdom.

Ultra-sensitive noble gas mass spectrometry (MAP 215) combined with laser gas extraction with extremely low He and Ne blanks, has been used to analyse He and Ne in minute extraterrestrial samples (< 1µg), e.g. micrometeorites, rich in noble gases. The laser technique has a number of advantages including high spatial resolution of 10's µm, increased sensitivity by reducing extraction line volumes, low blank levels by localised heating of the sample surface and a rapid throughput of samples by reducing the time spent removing active gases.

A pulsed Nd-glass laser has been used to extract noble gases, either by vaporising pits in the surface of mineral grains or by melting/step heating individual grains.

Initial tests were performed on troilite from the Grant meteorite and individual glass spherules from a lunar clod (15426.41). The Grant troilite was tested as a possible calibration standard for laser extraction of extraterrestrial helium because it has a known helium abundance ( $5 \times 10^{-6} \text{ cm}^3 \text{STPg}^{-1} \text{ } ^3\text{He}$ ) and a very well characterised and consistent  $^3\text{He}/^4\text{He}$  of  $0.2635 \pm 0.0034$  (Schultz & Kruse, 1983).

Helium and neon was analysed from 12 individual basaltic glass spherules (100-150µm) from lunar clod 15426.41. In two cases step-heating experiments were performed by initially defocusing the laser beam from the sample surface and gradually bringing the beam into focus until the sample was totally degassed, the remaining 10 grains were fused individually as single laser extractions. Total helium released from individual spherules varied from  $< 1 \times 10^{-14}$  to  $3 \times 10^{-10} \text{ cm}^3 \text{STP } ^4\text{He}$  ( $< 3 \times 10^{-9}$  to  $1 \times 10^{-4} \text{ cm}^3 \text{STPg}^{-1} \text{ } ^4\text{He}$ ).  $^3\text{He}/^4\text{He}$  values of single spherules varied from  $(4-200) \times 10^{-4}$ . The observed  $^3\text{He}/^4\text{He}$  is the result of radiogenic  $^4\text{He}$  production since formation of the volcanic spherules and later addition of cosmogenic helium during near-surface exposure. If the spherules have existed as a coherent clod from soon after formation, and having a similar chemical composition, they would be expected to have similar  $^3\text{He}/^4\text{He}$  values and helium abundances. The variations observed in the individual spherules can be explained by differential amounts of devitrification causing partial loss of radiogenic  $^4\text{He}$  prior to near-surface exposure, thus affecting the resulting  $^3\text{He}/^4\text{He}$  value observed.

Preliminary analyses of cosmic dust particles (50-400µm) collected from the Antarctic ice sheet revealed that the majority of 50-100µm particles have  $^3\text{He}/^4\text{He}$  between  $(2-4) \times 10^{-4}$ , i.e. between SW- and solar energetic particle-derived helium. Only 2 larger cosmic dust particles (100-400µm) had detectable helium ( $> 2.5 \times 10^{-16} \text{ cm}^3 \text{STP } ^3\text{He}$ ), both showing significantly higher  $^3\text{He}/^4\text{He}$  values indicating the presence of cosmic ray spallation helium.

Schultz, L. and Kruse, H., 1983. Helium, Neon, and Argon in Meteorites: A Data Compilation. Max-Planck-Institut für Chemie, Mainz. 88pp.

## Sr ISOTOPIC CHARACTER OF ACCRETED TERRANES IN THE NORTHERN CANADIAN CORDILLERA:

### IMPLICATIONS FOR BASEMENT ARCHITECTURE

HART, Craig J.R., Canada/Yukon Geoscience Office, Yukon Territorial Government, Box 2703 (F-3), Whitehorse, Yukon, Y1A 2C6, Canada.

Stikinia, Cache Creek Terrane and Nisling Terrane are dissimilar crustal blocks that accreted to the western edge of ancestral North America in Early Jurassic time. Stikinia, north of 59°N latitude, is composed of Triassic arc volcanics and Late Triassic to Jurassic forearc (Whitehorse Trough) clastics. Cache Creek Terrane is an oceanic terrane composed of Mississippian to Triassic basalt, ultramafite, carbonate, chert and clastics. Nisling Terrane, part of the composite Yukon-Tanana Terrane, comprises metasedimentary schist, marble, orthogneiss and amphibolite of Cambrian and older age. These terranes (and their components) have characteristic Sr isotopic signatures.

Cache Creek basalts yield expected primitive Sr initial ratios (SIR;  $0.7039 \pm 5$ ) while the carbonates give higher values ( $0.7081 \pm 5$ ) reflecting Upper Paleozoic sea water composition. Clastic sediments give mixed signatures reflecting variable percentages of detrital carbonate and continentally derived material. Stikinian Triassic arc volcanics give low initial ratios ( $0.7040 \pm 5$ ), and arc-derived sedimentary rocks yield similar, but locally anomalous values (0.706).

Nisling Terrane metasedimentary schists have high present day SIR ( $0.725 \pm 10$ ) and  $^{87}\text{Rb}/^{86}\text{Sr}$  ratios (0.5-5). Although modified by Mesozoic and Cenozoic thermal events, most data plot within Rb/Sr boundary isochrons of 800 to 1600 Ma (with an SIR of ca. 0.706) supporting an ancient provenance for these rocks. Marble gives present day values of 0.711. Felsic orthogneiss yields high modern values (ca.  $0.7085 \pm 25$ ), but give geologically reasonable initial ratios ( $0.7058 \pm 15$ ) when corrected for 380 Ma of elapsed time. Similarly, amphibolite yields geologically reasonable initial ratios of  $0.7046 \pm 10$  assuming a 550 Ma age.

Primitive values from the Triassic Stikinian arc preclude suggestions that this arc was built upon Nisling Terrane basement. Locally evolved signatures in Stikinian sediments indicate a local and minor component of continental detritus, probably from Nisling Terrane, in Late Triassic time. Nisling Terrane comprises isotopically evolved crust of Middle Proterozoic age (or is composed of detritus of that age), Early Paleozoic amphibolite and Silurian-Devonian orthogneiss.

SIR of Late Triassic to Early Eocene plutons that intrude these terranes occupy a large range (0.735-0.707) that spatially defines a region of low Sr initial ratios bounded west, north and east by higher values marked by the  $>0.706$  line. A sharp SIR gradient coincident with the Nisling-Stikinia contact argues for a structural juxtaposition. Lower SIR values in more southerly (60°N) Nisling Terrane granites result from decreasing amounts of continental contamination and suggests that Nisling Terrane here is thin, without basement and possibly allochthonous. The disposition of rocks that yield continental values outboard (west) of accreted (and exotic) terranes is enigmatic.

## THE GEOCHEMISTRY OF MCMURDO GROUP VOLCANIC ROCKS, ANTARCTICA

HART, S. R., BLUSZTAJN, J. S., Dept. of Geology and Geophysics, Woods Hole Oceanographic Institution, Woods Hole, MA 02543, and KYLE, P. R., Dept. of Geoscience, New Mexico Tech, Socorro, NM 87801,

Young Cenozoic volcanic rocks from Marie Byrd Land (Futa and LeMasurier, 1983) and Scott and Balleny Islands (Hart, 1988) are unusual in showing  $^{87}\text{Sr}/^{86}\text{Sr}$  ratios lower than most oceanic island basalts, with some values approaching those typical of mid-ocean ridge basalt (MORB). To assess the geographic extent of this low  $^{87}/^{86}$  Sr province, and to decide whether a MORB-type mantle is involved, we have analyzed a reconnaissance sampling of basalts from the Hallett volcanic province, Northern Victoria Land, for Sr, Nd and Pb isotopic ratios. A number of Hallett Province basalts show  $^{87}/^{86}$  Sr ratios less than 0.7030, comparable to the low values reported earlier for Marie Byrd Land and Scott/Balleny islands. However, the Pb isotope data for all of these areas is quite radiogenic, with  $^{206}/^{204}$  Pb generally greater than 19.5 and ranging up to 20.4. This is in marked contrast with MORB, which rarely show  $^{206}/^{204}$  Pb ratios higher than 19.0. It is clear that many of the young Cenozoic volcanics from Antarctica are showing a strong involvement of the HIMU mantle component.

In addition to the prevalent HIMU signature of these volcanic provinces, there is also a radiogenic  $^{87}/^{86}$  Sr component evident, especially in the Hallett Province, with  $^{87}/^{86}$  Sr values as high as 0.7049. This suggests possible involvement of the EM2 endmember. However, many of the Antarctic basalts are erupted through continental crust, and contamination with crust typically produces an EM2-like isotopic signature. In the Hallett Province basalts, it is clear that the low  $^{87}/^{86}$  Sr (HIMU-type) samples all come from oceanic or continent-edge localities and the samples with a high  $^{87}/^{86}$  Sr (EM2-type) signature occur farther inland. Sr isotope data from the Mt. Melbourne area (Worner *et al.*, 1989) show values ranging from 0.7029 to 0.7039, so this area may be bridging the transition from "oceanic" to "continental" type isotopic signatures.

The boundary marked by the isotopic data is consistent with the general location of the West Antarctic rift shoulder of Behrendt and Cooper (1991), or locally the Terror Rift of Cooper and Davey (1985). Basalts on the seaward side of this rift edge are uniformly low in  $^{87}/^{86}$  Sr, whereas higher values are encountered in basalts on the inland side of the rift edge. We hypothesize that volcanics which erupt through significant continental crust become variably contaminated with radiogenic Sr, whereas those erupted through extensionally-thinned continental crust, or oceanic crust, are not significantly contaminated. In addition, the HIMU component appears to be present to some degree in virtually all of the Antarctic Cenozoic volcanic rocks thus far analyzed; the lateral extent of this HIMU volcanic belt is enormous (>4000 km). Verification of the isotopic "lineage" of this belt and illumination of the underlying causes and processes remains as a significant challenge for the future.

## MEASURED AND CALCULATED DEPTH PROFILES OF $^{26}\text{Al}$ IN QUARTZ MINERALS OF THE LITHOSPHERE

J. HARTMANN, B. HEISINGER,  
G. KORSCHINEK, E. NOLTE, E. STRACK,  
Faculty of Physics, Technical University of Munich,  
D-85747 Garching, Germany  
S. NEUMAIER, CERN, CH-1211 GENEVE 23,  
Switzerland,  
C. PETIT-JEAN, PSI, CH-5234 Villigen,  
Switzerland

The natural long-lived radioisotope  $^{26}\text{Al}$  ( $T_{1/2} = 716,000\text{y}$ ) is produced in quartz minerals by cosmic ray induced spallation reactions on Si and by cosmic muon capture reactions  $\text{Si}(\mu^-, \nu_\mu, xn)$ . Depth profiles of cosmogenic  $^{26}\text{Al}$  in quartz minerals of the lithosphere were calculated and measured. For the calculation, the branching of the reaction  $\text{Si}(\mu^-, \nu_\mu, xn)^{26}\text{Al}$  was measured by irradiating a quartz sample with slow negative muons at PSI in Villigen (CH) and by determining the produced  $^{26}\text{Al}$  with accelerator mass spectrometry (ams). For the measurement of the depth profile,  $^{26}\text{Al}$  concentrations of quartz samples from pre-drill cores of the continental deep-drill core in Northern Bavaria (Germany) from depths between 10 and 260 m were determined with ams. The comparison between measured and calculated depth profile allows to set limits for the erosion rate. The agreement between measured and calculated depth profile is excellent for vanishing erosion rate.

Other combinations of radioisotopes and minerals, such as  $^{53}\text{Mn}$  (3.7 million years) in pyrites, are discussed.

## THERMOCHRONOLOGIC VIEW ON THE EVOLUTION OF ACCRETIONARY COMPLEXES

HASEBE, N., TAGAMI, T. and NISHIMURA, S.

Department of Geology and Mineralogy, Faculty of Science, Kyoto University, Kyoto 606, Japan

Fission-track thermochronology was applied to Shimanto accretionary complex, Southwest Japan, to place thermotectonic constraints on the evolution of an accretionary complex from a viewpoint of material transport within the wedge. Sandstone samples were collected from coherent turbiditic sequences and blocks in melange matrix. Age spectra for individual samples were correlated to their depositional ages to judge the degree of thermal affection during accretionary processes (Hasebe et al., 1993).

Apatite ages show a good agreement around 10 Ma, in spite of their variation in depositional ages and rock facies. In consideration of their depositional ages consistently older than ~10 Ma, this demonstrates that the Shimanto accretionary complex was heated higher than ~125°C (apatite total annealing temperature) and subsequently cooled regionally below ~100°C (apatite closure temperature) at ~10 Ma. Zircon ages and track length distributions indicate that the materials with higher maximum temperatures are cropped out at the rear of the prism with some local variation, showing no difference in thermal parameter values for both coherent and melange facies. Hence melanges and surrounding coherent rocks are considered to have followed the similar time-temperature paths through their histories after accretion. Therefore the melange formation should generally be explained by the processes without long vertical transport of melange forming materials.

On the basis of the thermal history characteristics mentioned above, material transportation paths within accretionary prisms are proposed in consideration of following two aspects: First, the thermal structure of the wedge is parallel to the surface at shallow levels. Second, accreted materials move toward the rear of the wedge during successive accretion when the position of trench is fixed. The history of the accreted material is divided into two phases; the burial and uplift. The position of phase boundary in a wedge would be controlled by some accretionary tectonics; the formation of imbricated structure at the frontal part of the prism would contribute to the material burial, and underplating at depth that would disturb further burial could force the material uplift. When the accreted materials arrive at the boundary, the maximum temperature is recorded, and begin to uplift. Earlier accreted materials reach the boundary earlier, resulting in the exposure of the deeper buried materials at the rear of the wedge because they stayed longer in the uplift phase. The configuration of melange and coherent units would be attained during the local internal deformation caused by burial and uplift processes.

Hasebe, N., Tagami, T. and Nishimura, S., 1993, Evolution of the Shimanto accretionary complex; a fission-track thermochronologic study: *Geol. Soc. Am. Spe. Pap.*, v. 273, p. 121-136

## COMPLEX U-PB SYSTEMATICS OF PALEOPROTEROZOIC MONAZITE FROM THE GRAND CANYON, ARIZONA, USA

HAWKINS, David P., and BOWRING, Samuel A., Dept. of EAPS Massachusetts Institute of Technology, Cambridge, MA

Complex U-Pb monazite data are often explained by the presence of variable amounts of excess  $^{206}\text{Pb}$ , inheritance, and/or high temperature Pb loss. We present data from more than 65 clear, inclusion-free single monazite grains, or fragments of single grains, that suggest these monazites contain domains characterized by contrasting age and/or discordance. The monazites were separated from seven samples of ca. 1.7 Ga muscovite granites, pegmatites and biotite schists that have undergone a period of slow cooling from ca. 1.7 to ca. 1.6 Ga.

Within individual rock samples U-Pb and Pb-Pb ages of single monazite grains vary considerably and range from 40% reversely discordant to 10% normally discordant. Reverse discordance cannot be explained by excess  $^{206}\text{Pb}$  alone. The U-Pb ages of essentially concordant grains vary by as much as 20 Ma in a single sample. Backscattered electron imaging reveals no evidence for inheritance.

No relationship is observed between degree of discordance (and age) and: 1) grain size (long dimension ranging from 200 to 30  $\mu\text{m}$ ); 2) grain shape (prismatic, equant, and platy); and 3) U concentration (250 ppm to >350,000 ppm). Several single grains were broken into a number of fragments, some estimated to weigh as little as 100 nanograms. Within one grain, two fragments are nearly concordant with Pb-Pb ages of  $1676 \pm 1$  and  $1682 \pm 1$  Ga. Two other grains exhibit little U-Pb age variation between fragments, but show a large variation in the degree and sign of discordance. In one of these grains, the center part is 1% reversely discordant whereas part of the tip is 40% reversely discordant. The relationship between Th/U ratio and calculated excess  $^{206}\text{Pb}$  suggests that the reverse discordance in the tip resulted from loss of U relative to Th and Pb. In another grain, five fragments yield similar ages but range from being 1% reversely discordant (tip) to 1% normally discordant (center) with no correlation between position within the grain and either age or degree/sign of discordance.

In the absence of physical evidence for inheritance, the range of single grain ages remains problematic. However, the discordance behavior can be explained if single monazite grains comprise complex mixtures of domains which have exhibited open system behavior with respect to U, Th, and Pb, including excess  $^{206}\text{Pb}$ , during cooling. Concordant analyses of single grains may represent fortuitous mixtures of these domains. There is no evidence for preservation of simple diffusion gradients within single grains.

#### 2.45 Ga GLOBAL MAFIC MAGMATISM: EARTH'S OLDEST SUPERPLUME?

HEAMAN, L.M., Dept. of Geology, Royal Ontario Museum, 100 Queen's Park, Toronto, Ontario, Canada. M5S 2C6.

Radiometric dating, including new high precision U-Pb baddeleyite/zircon ages, of Paleoproterozoic flood basalts, dyke swarms, and layered mafic intrusions worldwide indicates that a substantial volume of mafic magma was produced on Earth in the interval 2.48 to 2.42 Ga with vestiges preserved in virtually all major Archean cratons. In North America, this event is well documented in the Superior (2.45 Ga Huronian flood basalts, 2.45 Ga Hearst-Matachewan dyke swarm, 2.47 Ga Mistassini dyke swarm, 2.48 Ga gabbro plutons) and Hearne (2.45 Ga Kaminak dyke swarm) cratons. Although poorly dated, other candidates exist in the Wyoming craton (e.g. leopard dykes) and together all this magmatism could be related to a common mantle plume system - the Matachewan plume. Elsewhere, temporally equivalent magmatic activity has been identified in the Lewisian craton, Scotland (2.42 Ga Scourie dyke swarm), the Karelian craton, Finland and Russia (2.44 - 2.45 Ga layered mafic intrusions, flood basalts and dyke swarms), the Yilgarn craton, Australia (c. 2.42 Ga Widgiemooltha dyke swarm and Jimberlana intrusion), Rhodesian craton (c. 2.46 Ga Great Dyke), Vestfold craton, Antarctica (c. 2.42 Ga Napier dyke swarm), and Dharwar craton, India (c. 2.42 Ga Bangalore dyke swarm).

The potential volume, magnitude and extent of this magmatism eclipses many of the better known Mesozoic flood basalt provinces and represents the earliest recognized superplume event on Earth. Although the style of the 2.45 Ga magmatism, such as the development of giant radiating dyke swarms and coeval flood basalts, has been subsequently repeated many times throughout the Proterozoic and Mesozoic, it is clearly distinct from the dominant style of mafic magmatism in the Archean (i.e. greenstone belts). This dramatic difference in style likely reflects a fundamental change in the mechanism of heat transfer in the mantle and possibly signals the initiation of a new mantle convection mode in Earth evolution. Where preserved, the stratigraphic record accompanying the 2.45 Ga magmatism clearly demonstrates the concomitant development of rift basins (Huronian/Snowy Pass basin in North America and the Sumi-Sariola basin in Karelia) that may herald the breakup of a pre-2.5 Ga supercontinent.

#### URANIUM-SERIES DATING OF CLOSED-SYSTEM PEAT FROM LONG TERRESTRIAL RECORDS.

HEIJNIS, H., Environmental Radiochemistry Laboratory, Australian Nuclear Science and Technology Organisation, PMB 1, 2234 NSW, Australia.

The successful dating of peat was reported in 1992 (Heijnis & van der Plicht, 1992 and Heijnis, 1992). In principle, this method can be used to date peat to ~ 350 ka. The application of the U/Th disequilibrium method provides us with the probability of constructing a new independent chronology for the Late Pleistocene Palaeoclimate record. The problems with regard to detrital Thorium and suspected open system behaviour were solved. Since 1992 much of the attention has been focused on the dating of the terrestrial equivalents of sub-stages of stage 5 of the deep-sea record. Long Terrestrial Records from Europe and Australia were sampled, analysed and dated. Individual isolated peat layers in Europe with an unknown or correlated on basis of the palaeoecological information were also sampled, analysed and dated. Equivalent of all three sub stages 5e, 5c and 5a were found in Europe as well as in the Long Records from Australia.

Heijnis, H., and van der Plicht, J., 1992,

Uranium/Thorium dating of Late Pleistocene peat deposits in NW Europe, Uranium/Thorium isotope systematics and open-system behaviour of peat layers: *Chemical Geology (Isotope Geoscience Section)*, 94 p. 161-171.

Heijnis, H., 1992, Uranium/Thorium dating of Late Pleistocene peat deposits in NW. Europe. Published PhD thesis, University of Groningen, The Netherlands. pp. 149.

<sup>40</sup>Ar/<sup>39</sup>Ar RESULTS OF INCOMPLETELY DEGASSED SANIDINE: AGE OF LATHROP WELLS VOLCANISM  
HEIZLER, Matthew T., McINTOSH, William C., New Mexico Bureau of Mines and Mineral Resources, Socorro, NM 87801, USA, PERRY, Frank, V., and CROWE, Bruce, M., Los Alamos National Laboratory, Los Alamos, NM 87545, USA.

Ash flow tuff xenoliths were collected from several of the basaltic flows and cone at Lathrop Wells volcano in southwest Nevada, as part of an on-going volcanic hazard study for the DOE's Yucca Mountain Project. Xenoliths ranged in size from ~1 to 30 cm in diameter. Pristine to variably partially melted sanidines were separated from 4 individual xenoliths from the QL-2 flow and cinder cone. A glassy matrix was separated from a nearly completely melted xenolith from the QL-1 flow and a pristine sanidine was recovered from a large xenolith occurring in a conduit. Also, a 1 cm xenolith from the Little Cone cinder cone north of Lathrop Wells provided a pristine sanidine separate.

To help characterize the sanidines prior to furnace step-heating, 5 single crystals from each xenolith were step-heated with a CO<sub>2</sub> laser.

An <sup>40</sup>Ar/<sup>39</sup>Ar age spectrum from the Little Cone xenolith shows a flat portion for the first 15% of argon released and yields an isochron age of 904 ± 11 ka. This is in excellent agreement with the 0.9-1 Ma whole rock basalt argon ages reported for the Little Cone flow.

Pristine sanidines from the xenolith from the conduit just south of the main cone yields an age spectrum with a flat portion for the first 40% of gas released and gives an isochron age of 77 ± 2 ka.

Three xenolith sanidines (samples A, G, and O) were analyzed from the QL-2 flow and reveal at least 95% argon loss. The age spectra have the same general form and are relatively flat over the first 40 to 60% of argon released, but in detail they can be interpreted as having significantly different ages. Isochron ages of 106 ± 3, 78 ± 2 ka, and 60 ± 5 are obtained for xenoliths A, G and O, respectively.

Single crystal laser analyses for cone xenoliths show that two samples have experienced very minor argon loss, one (sample J) is 90% degassed and one glassy sample is significantly contaminated with air. Sample J sanidine yields an age of 166 ± 4 ka for the first 15% of gas released during step-heating. The cone is geologically younger than QL-2 and thus the ~160 ka age may be problematic. Perhaps this xenolith was degassed during an older eruptive episodic and recycled, but not significantly heated, during cone formation.

An additional possibility for all of the xenoliths is that, due to the partial melting, and thus disruption of the diffusion domain distribution of these crystals, argon is lost from both non-retentive (young) and retentive (old) sites simultaneously in the laboratory. This could account for the variability of ages from QL-2 as well as the apparent 166 ka age for the cone. This hypothesis is being experimentally tested by partially melting Fish Canyon Tuff sanidines in a muffle furnace.

Since several factors could cause xenolith apparent ages to be anomalously old, the youngest age for any set of xenoliths may be the best age estimate for a given unit. Despite some complications, these data indicate that dating xenoliths will yield useful age constraints on Lathrop Wells volcanism and may provide a useful calibration for production rates of cosmogenic nuclide systems over the time interval ca. 50 to 100 ka.

Pb ISOTOPE SYSTEMATICS OF A LARGE HIGH GRADE QUARTZ VEIN, PIKWITONEI GRANULITE DOMAIN, MANITOBA, CANADA

HEMMING, S. R., Dept. of Earth & Space Sciences, SUNY Stony Brook, NY, 11794, USA, MEZGER, K., Max-Planck-Institut für Chemie, Postfach 3060, D55020 Mainz, Germany, McLENNAN, S. M., and HANSON, G. N., Dept. of Earth & Space Sciences, SUNY Stony Brook, NY, 11794, USA.

A Pb-Pb age of 2977±54 Ma and a  $\mu_i$  of 8.5 for a large quartz vein in the Pikwitonei granulite domain of the western Superior Province in Manitoba records one of the oldest metamorphic events known in this area. The Pb isotope data reported here are based on 5 to 500 mg samples of quartz from a hand specimen collected from an island in Natawahunan Lake that is composed almost entirely of a large quartz vein. Pods (~1 m) containing garnet-orthopyroxene-biotite gneiss also occur on this island. Large biotite inclusions (up to several mm) are common in the quartz vein. Dark red rutile inclusions (~50 to 500  $\mu$ m) occur, but are less common. Crushed quartz fragments were picked to avoid visible inclusions. The Pb concentrations in these samples range from 0.179 to 0.548 ppm and measured U concentrations range from 0.0197 to 0.087 ppm. <sup>206</sup>Pb/<sup>204</sup>Pb ranges from 16 to 40. Using K-feldspar from a metapelitic rock for the initial Pb isotopic composition (14.08, 15.03, 33.82), calculated <sup>238</sup>U/<sup>204</sup>Pb ranges from 6 to 44, and calculated <sup>232</sup>Th/<sup>238</sup>U ranges from 0.58 to 2.9. This variability in U-Th-Pb ratios may be the result of very small mineral inclusions within the quartz, that have different distribution coefficients for these elements.

Other evidence for the metamorphic event recorded by the quartz vein comes from a xenocrystic garnet within a nearby graphic granite (2984±2 Ma). In addition, the Pb isotope systematics of the quartz vein, notably the high  $\mu_i$ , implies the presence of even older crust in the region. Other evidence for older crustal history in the area is found in the Pb isotopic composition of K-feldspar from a nearby granulite grade metapelitic rock (see composition above), and in the Sm-Nd isotope systematics of some rocks from the area ( $T_{CHUR}$  as high as 3.6 Ga). There is considerable evidence for metamorphism as high as granulite facies recorded by U-Pb garnet and zircon ages between 2.7 and 2.6 Ga in the Pikwitonei granulite domain. Thus, the U-Pb system of this quartz vein appears to preserve the age of an old metamorphic event that has not been reset by a second high grade metamorphic event. The island that this quartz vein forms is about 100 m on a side. Accordingly, these data provide evidence that whatever contains the U-Pb system within large quartz veins may be armored and thus undisturbed through upper amphibolite to granulite grade metamorphism.

TRACE ELEMENT AND ISOTOPE GEOCHEMISTRY OF FRIDAY AND DOMINGO SEAMOUNTS, JUAN FERNANDEZ HOTSPOT

HEMOND Christophe, Geologisk Institut, Øster Volgade 10, 1350 Copenhagen K, Denmark, DEVEY C.W. and STOFFERS P. Geologisch-Paläontologisches Institut, Olshausenstr. 40, 24118 Kiel, Germany)

The Juan Fernandez hotspot trace lies on the Nazca plate in the south-east Pacific. Westward from the two islands of the archipelago (Robinson Crusoe and Alexander Selkirk), two young seamounts (Friday and Domingo) have been dredged using the German research vessel "Sonne". Quite fresh samples containing glass were recovered.

All samples are alkali basalts with a relatively narrow range of MgO (4-7%); most of them are basanitic in composition and some trachy-phonolites were also recovered. All basaltic samples are highly enriched in incompatible trace elements for both seamounts, with Friday being slightly more enriched (e.g. C1 norm. La/Sm  $\approx$  2.6-3.0) than Domingo (e.g. La/Sm  $\approx$  2.2). Ratios of incompatible immobile elements like Nb/Zr confirm this observation (Nb/Zr  $\approx$  0.21 and 0.18 in Friday and Domingo respectively). A ratio involving mobile and immobile incompatible elements like Ba/Zr shows a negative trend when plotted versus Ba concentration although Ba should be more incompatible than Zr during partial melting. REE patterns show that if Friday samples are more enriched in incompatible elements, they also have lower HREE concentrations than Domingo samples. The low SiO<sub>2</sub> samples from Friday have lower Ba and Nb contents but much higher Ba/Zr ratio while Nb/Zr remains constant and La/Yb decreases. This cannot be explained by fractionation of the mineral phases present in the samples (plagioclase+olivine) and the constancy of the Ba/Rb ratio excludes phlogopite fractionation. We also tried to calculate degrees of melting using source compositions in the spinel and garnet stability zones. This leads to unrealistic degrees of melting for alkali basalts. These observations together with the very steep trend defined by our data in SiO<sub>2</sub> vs MgO lead to the conclusion that the melts may have been produced in presence of a very undersaturated component probably nephelinitic in composition as seen in the Society and Austral plumes (Hémond et al., in press, Chem. Geol.). This component appears to be depleted in most incompatible elements, but particularly HFSE, producing negative mixing trends in Ba/Zr vs Ba in which low SiO<sub>2</sub> samples have lower Ba/Zr ratios than higher SiO<sub>2</sub> samples.

Pb isotope data on samples from both seamounts (e.g. <sup>206</sup>Pb/<sup>204</sup>Pb  $\approx$  19.10 - 19.15) as well as Sr and Nd isotopes are homogenous and included in the range of literature data from the islands. They are very similar to our data from Moua Pihaa seamount, an active seamount of the Society plume. This emphasizes the homogeneity of the source region in the mantle beneath the Juan Fernandez chain; it underlines also that similar magmatic processes can have taken place in various plumes in the Pacific.

<sup>40</sup>Ar/<sup>39</sup>Ar CHRONOLOGY OF LACCOLITH-CALDERA DEVELOPMENT, THE SOLITARIO, TRANS-PECOS TEXAS  
HENRY, Christopher D<sup>1</sup>, Bureau of economic Geology, University of Texas, Austin, TX, 78731, and KUNK, Michael J., U.S. Geological Survey, MS 981 Reston, VA 22092

<sup>1</sup>now at Nevada Bureau of Mines and Geology, University of Nevada, Reno, NV 89557-0088

The Solitario is a mid-Tertiary laccolith-caldera complex in southern Trans-Pecos Texas. The 16 km diameter laccolith is among the worlds largest. The laccolith apparently intruded at a depth of ~4 km into folded Paleozoic rocks that are unconformably overlain by ~1 km of Cretaceous rocks. Detailed geologic mapping reveals that the Solitario was formed by a complex sequence of laccolith, sill, and dike injection; doming during intrusion of the main laccolith; ash-flow eruption; caldera collapse; and intracaldera volcanism and sedimentation. <sup>40</sup>Ar/<sup>39</sup>Ar ages of various igneous units were determined by incremental heating of aliquots of alkali feldspar phenocrysts. The ages are consistent with all field relationships and indicate that Solitario evolution occurred in three distinct pulses over an interval of ~ 1 million years.

Small volumes of magma intruded as abundant rhyolitic to trachytic sills and small laccoliths during the first pulse, at 36.0  $\pm$  0.1 Ma. Emplacement of the main laccolith, doming, ash-flow eruption, and caldera collapse occurred at 35.4  $\pm$  0.1 Ma during the most voluminous pulse. Although the main laccolith is not exposed, dated rocks include a dike emplaced along radial fractures generated by doming, an ash-flow vent, and caldera-fill tuff. A complex sequence of debris-flow and debris-avalanche deposits, megabreccia, trachyte lava, and small-volume ash-flow tuff subsequently filled the 6 x 2-km caldera that developed over the laccolithic dome. The final magmatic pulse at 35.0  $\pm$  0.1 Ma consisted of several small laccoliths or stocks and numerous dikes in caldera fill and along the ring fracture. Solitario rocks appear to be part of a broadly cogenetic metaluminous suite.

A series of peralkaline rhyolite lava domes was emplaced around the northern periphery of the Solitario at 35.4  $\pm$  0.1 Ma, contemporaneous with laccolith emplacement and the main pulse. We interpret the temporal and sparse geochemical and Pb isotopic data to indicate the peralkaline rocks are crustal melts related to the magmatic-thermal flux represented by the main pulse of Solitario magmatism.

The size, duration, and episodic behavior of Solitario magmatism are more typical of large caldera systems than of most laccoliths. Although age data are sparse, current models of laccolith emplacement and evolution suggest a continuum of magmatic activity from initial sill emplacement through growth of the main laccolith. In contrast to existing models, our <sup>40</sup>Ar/<sup>39</sup>Ar results suggest that repeated injections of magma, separated by intervals of little or no magmatic activity, are required.

## THE THERMOCHRONOLOGICAL POTENTIAL OF AGE/GRAIN-SIZE RELATIONS

HESS, J.C. and LIPPOLT, H.J., Laboratorium für Geochronologie der Universität, 69120 Heidelberg, Germany.

The temperature of chemical mineral closure in a cooling geochronological system as well as diffusional loss out of minerals in the course of thermal overprinting strongly depend on the diffusion properties of the mineral and on the diffusion length. Accordingly, relationships between isotopic age and diffusion parameters on the one hand and between age and diffusion length on the other hand have to be expected. The dependences of isotopic ages on the diffusion properties had been subject of investigations frequently. Although of great thermochronological potential relations between age and diffusion length (or physical grain-size) have been investigated only occasionally.

To ascertain age/grain-size effects and to establish their thermochronological possibilities we performed  $^{40}\text{Ar}/^{39}\text{Ar}$  age measurements on carefully separated mica concentrates from granites from three regions with different geological histories.

On biotites from the 2.5 Ma old Eldzhurtinskiy granite (Caucasus) distinct age/grain-size dependences could be detected. They enable us to calculate cooling and uplift rates and a geothermal gradient at the time of biotite closure, which are in good accordance with independently obtained geophysical results.

Age/grain-size effects could also be found on biotite and muscovite of the 30 Ma old Bergell granitoids (southern Alps). Together with literature data the newly obtained mica results allow a detailed reconstruction of the temporal and spatial cooling of the Bergell pluton from intrusion time down to surface temperatures.

The Variscan Mittagfluh granite (western Alps) was thermally overprinted by Alpine metamorphism which partially rejuvenated the biotites of the rock. The portions of radiogenic Ar loss strongly depend on the size of the biotites and can be used to estimate time, duration and peak temperature of the metamorphic event.

All the examples prove the existence of age/grain-size effects and clearly demonstrate their applicability and usefulness in thermochronology.

## TIMESCALE OF MAGMA PRODUCTION AND CRYSTAL GROWTH IN SILICIC MAGMA CHAMBERS, KENYA RIFT VALLEY

HEUMANN, Amd., DAVIES, G. R., and STAUDIGEL, H. Faculteit der Aardwetenschappen, Vrije Universiteit, De Boelelaan 1085, 1081 HV Amsterdam, The Netherlands.

Magma chamber processes are of fundamental importance in understanding the genesis of highly fractionated silicic magmas. Quantifying the kinetics and the timing of magma production and fractionation rates helps to explain the rate at which silicic magma systems form and evolve.

The rhyolite suites under study contain highly fractionated magmas with high Rb/Sr ratios (100-700). These high Rb/Sr ratios result in rapid changes in  $^{87}\text{Sr}/^{86}\text{Sr}$  ratios potentially allowing resolution of events on time scales as low as 1000 years. Strontium contents are low (<1 ppm) for these rocks and can only be explained by fractional crystallization involving substantial volumes of cumulate feldspar.

At the low crystallization temperatures (700-750°C) of silicic magma systems the diffusion of strontium in feldspars is slow ( $10^{-17}$  cm<sup>2</sup>/s). Mineral analyses of core/rim distributions of strontium in alkali feldspar may therefore provide information on the time and rate of crystal growth in slowly cooling magma chambers. Mineral growth rates in silicic magma chambers are still unknown under typical magmatic cooling rates in the upper continental crust.

In this study, we present analytical data from fresh obsidian glasses and minerals from the most recent eruptions of the bimodal Naivasha volcanic complex in the Kenya Rift Valley. Our samples comprise peralkaline rhyolites (comendites) from silicic domes within the Naivasha complex which form seven different chemostratigraphic groups with distinct trace element and isotope systematics. The generation of the high viscosity melts forming the domes can be attributed to spatially separated, but genetically related small-volume ( $\approx 0.1$  km<sup>3</sup>) magma chambers at the roof of which highly evolved differentiates accumulated. A young eruption age of the domes is confirmed by a  $^{14}\text{C}$  radiometric age determination (< 15,000 y) of lake sediments.

The investigated comendites are from two of the seven chemostratigraphic groups. Relative high concentrations of halogens ( $\approx 1.2$  %) in the comendites are coupled with extreme enrichment of certain incompatible elements (e.g. Nb $\approx$ 500 ppm and Zr $\approx$ 2000 ppm) for the different groups. The rocks show Rb/Sr ratios ranging from 240 to 508 and have strontium contents between 1 and 2 ppm. Present day strontium isotope ratios range from 0.70691 to 0.71189. The  $\epsilon_{\text{Nd}}$  values prove that the rhyolites are not simply melts of old continental crust, but have the signature of young mantle-derived material. In general, such melts have strontium contents of  $\gg 100$  ppm in contrast to the low contents of the rhyolites. This requires a marked chemical differentiation in a relative short period of time.

Preliminary Sr data on obsidian glasses suggest an isochron at 70,000 years which implies that the magma chamber system has been in existence for  $\approx 60,000$  years. Based on this age, production rates can be estimated. Microdrilling of alkali feldspars is in progress to investigate core/rim relationships of strontium isotope systematics and to estimate mineral growth rates.

## ESTIMATION OF NEUTRON FLUENCE FROM THE ISOTOPIC COMPOSITIONS OF SAMARIUM AND GADOLINIUM IN METEORITES AND URANINITES

HIDAKA, H. and EBIHARA, M., Dept. of Chemistry, Tokyo Metropolitan University, Hachioji, Tokyo 192-03, Japan., TAKAHASHI, K., Institute of Physical and Chemical Research (RIKEN), Saitama 351-01, Japan., HOLLIGER, P., CEA, Centre d'Etudes Nucleaires de Cadarache, 13108-Saint-Paul-les-Durance, France, and HONDA, M., Dept. of Chemistry, Nihon University, Setagaya, Tokyo 156, Japan.

Isotopic deviations of Sm and Gd in geological and cosmological samples are useful for the estimation of neutron dose the samples acquired, because  $^{149}\text{Sm}$ ,  $^{155}\text{Gd}$  and  $^{157}\text{Gd}$  have fairly large values of cross sections for thermal neutron capture reactions. Some meteorites were reported to show the depletion of  $^{149}\text{Sm}$ ,  $^{155}\text{Gd}$  and  $^{157}\text{Gd}$  isotopic abundances due to the capture reactions of cosmic ray-induced neutrons. Similar effect on isotopic variations has been observed in terrestrial uranium ore samples. In order to extend our understanding of the effect on isotopic compositions due to neutron capture reactions, we have started to measure Sm and Gd isotopic compositions of meteoritic samples (Norton County, Allende, Bruderheim and St. Severin) and terrestrial uraninites (sampled at Oklo (outside fission reactor zone, Gabon, 2.0Ga old), Labrador (Canada, 1.8Ga), Morogoro (Tanzania, 0.80Ga), Shinkolobwe (Zaire, 0.78Ga) and Madagascar (0.55Ga)).

Thermal ionization mass spectrometry (TIMS) potentially offers precise isotopic measurements for Sm and Gd with reproducibilities of less than 0.01%, which must be sufficient enough to investigate the irradiation effect due to cosmic ray-induced neutrons for meteorites having long cosmic ray exposure ages such as Norton County. The effect yielded from spontaneous fission of uranium can also be investigated for terrestrial uraninites with old formation ages. After acid digestion of each sample, Sm and Gd were sequentially separated on a cation exchange column with  $\alpha$ -hydroxy isobutyric acid (0.15M and 0.20M, pH=4.5). Significant isotopic variations of  $^{155}\text{Gd}/^{160}\text{Gd}$  (-0.9‰ for Norton County, and -5.0‰ for Oklo) and  $^{157}\text{Gd}/^{160}\text{Gd}$  (-1.5‰ for Norton County, and -3.3‰ for Oklo) could be observed in some samples. The isotopic decrements of  $^{155}\text{Gd}/^{160}\text{Gd}$  and  $^{157}\text{Gd}/^{160}\text{Gd}$  seem to quantitatively correspond to the increments of  $^{156}\text{Gd}/^{160}\text{Gd}$  and  $^{158}\text{Gd}/^{160}\text{Gd}$ , respectively, suggesting that these isotopic variations resulted from neutron capture reactions of  $^{155}\text{Gd}(n,\gamma)^{156}\text{Gd}$  and  $^{157}\text{Gd}(n,\gamma)^{158}\text{Gd}$ . Moreover, geologically old uraninites sampled at Oklo and Labrador showed a slight positive anomaly in  $^{152}\text{Gd}/^{160}\text{Gd}$ , possibly derived from the neutron capture reaction on  $^{151}\text{Eu}$ , namely  $^{151}\text{Eu}(n,\gamma\beta^-)^{152}\text{Gd}$ .

Besides the analyses of natural samples, we also analyzed REE reagents irradiated in a reactor. On the basis of on the preliminary results obtained, it is inferred that the isotopic systematics on Sm and Gd can be utilized for the estimation of neutron fluence of  $10^{15} \sim 10^{16} \text{ n/cm}^2$  in nature.

## ISOTOPIC STUDY OF SEARCH FOR FISSION PRODUCTS IN OKLO NATURAL FISSION REACTORS

HIDAKA, H., Dept. of Chemistry, Tokyo Metropolitan University, Hachioji, Tokyo 192-03, Japan, and HOLLIGER, P., CEA, Centre d'Etudes Nucleaires de Cadarache, 13108-Saint-Paul-les-Durance, France

Isotopic measurements of Oklo natural fission reactor samples play an important role as an ideal natural analogue for nuclear waste disposal. This study has implications for clarification of the behaviour of (fissiogenic) radioactive nuclides in geosphere through stable isotopic measurements of Oklo samples by mass spectrometric techniques.

The samples used in this study are from one of drilling cores SF84 of Oklo reactor zone 10: This zone has been kept in geochemically good conditions with little weathering and alteration, because it locates underground. Isotopic compositions of Rb, Sr, Zr, Mo, Ru, Pd, Ag, Te, Ba, REEs and U for whole rock samples have been determined by thermal ionization mass spectrometry (TIMS) and inductively coupled plasma mass spectrometry (ICP-MS). The behaviour of long-lived radioactive nuclides such as  $^{90}\text{Sr}$ ,  $^{99}\text{Tc}$ ,  $^{107}\text{Pd}$ ,  $^{126}\text{Sn}$ ,  $^{135}\text{Cs}$  and  $^{137}\text{Cs}$  can be deduced from the present stable isotope abundances of  $^{90}\text{Zr}$ ,  $^{99}\text{Ru}$ ,  $^{107}\text{Ag}$ ,  $^{126}\text{Te}$ ,  $^{135}\text{Ba}$  and  $^{137}\text{Ba}$ , respectively. Moreover, *in-situ* isotopic analyses were performed with secondary ion mass spectrometry (SIMS) on uranium oxide grains and some inclusions in reactor core samples for the purpose of detection of fissiogenic nuclides on  $\mu\text{m}$  scale.

The combination of isotopic results from whole rock analyses and *in-situ* observation provides a comprehensive information on the geochemical characters of radionuclides: (1) Fissiogenic Ru, Pd and Te have been well preserved in uraninite whole rock, but some part of them have microscopically localized and formed metallic inclusions in uraninite grains. (2) In general, fissiogenic REEs have been well retained in uraninite. But fissiogenic light REEs such as Ce are relatively mobile to heavier REEs. Apatite minerals in reactor core samples contains larger amount of fissiogenic Ce than uraninite matrices. (3) The existence of fissiogenic Rb, Sr, Cs and Ba were confirmed from the significant isotopic deviations, although retentivities of them are very low and do not exceed 5% to the best retention.

## HELIUM ISOTOPE VARIATIONS IN HEARD ISLAND LAVAS: IMPLICATIONS FOR MANTLE SOURCES.

HILTON, D.R.<sup>1,2</sup>; 1) Earth Sciences, Vrije Universiteit, 1081 HV Amsterdam, The Netherlands; 2) FR Geochemie, Freie Universität Berlin, 14195-Berlin, Germany; BARLING, J. Universite Libre de Bruxelles, Belgium; WHELLER, G.E. Mineral Resources Dept., Fiji.

We report  $^3\text{He}/^4\text{He}$  analyses of olivine and/or clinopyroxene phenocrysts from a suite of 16 lavas from Heard Island in the Indian Ocean. These lavas display the greatest range in radiogenic isotope compositions yet encountered for a single oceanic island (Barling & Goldstein, 1990; Barling et al., 1994). Eleven samples come from the Big Ben Series which are characterised by high  $^{87}\text{Sr}/^{86}\text{Sr}$  and low  $^{206}\text{Pb}/^{204}\text{Pb}$  and  $^{143}\text{Nd}/^{144}\text{Nd}$ : these samples have been interpreted to contain the greatest proportion of an "enriched Heard" component ultimately derived from continental crust. Five samples come from the Laurens Peninsula Series and have lower  $^{87}\text{Sr}/^{86}\text{Sr}$  but higher  $^{206}\text{Pb}/^{204}\text{Pb}$  and  $^{143}\text{Nd}/^{144}\text{Nd}$  ratios: the origin of this "depleted Heard" endmember is considered to be either the Heard-Kerguelen mantle plume component (Barling & Goldstein, 1990; Class et al., 1993) or lithospheric mantle (Barling et al., 1994). In all cases, helium was released from the phenocrysts by crushing.

The Big Ben lavas are characterised by a wide range in  $^3\text{He}/^4\text{He}$  ratios which appears related to helium concentrations ([He]). Six olivine samples with the highest [He] (43-217 nccSTP/g) have MORB-like  $^3\text{He}/^4\text{He}$  values ( $\sim 8R_A$  where  $R_A = \text{air } ^3\text{He}/^4\text{He}$ ) whereas only 1 of the remaining 5 lower [He] olivines (13-28 nccSTP/g) plots within error of MORB. The other 4 olivines have more radiogenic  $^3\text{He}/^4\text{He}$  ratios of 3.9-7.5 $R_A$ . For co-existing clinopyroxenes, 4 high [He] samples (17-52 nccSTP/g) plot close to MORB whereas the lower concentration group ([He]= 1-20 nccSTP/g) range from 0.4-4.7 $R_A$ . The results are consistent with a MORB-like  $^3\text{He}/^4\text{He}$  signature for the Big Ben Series with both low-[He] olivine and clinopyroxene phenocrysts being variably susceptible to contamination by radiogenic helium (cf. Hilton et al., 1993). No correlation is observed between  $^3\text{He}/^4\text{He}$  and  $^{87}\text{Sr}/^{86}\text{Sr}$  indicating that the radiogenic helium addition is a shallow-level phenomena. The results have a strong bearing on the nature of mantle sources for the Heard Island lavas and for the origin of low- $^3\text{He}$  hotspots.

The same patterns of  $^3\text{He}/^4\text{He}$  vs. [He] are seen for the Laurens Peninsula samples: 4 olivine samples of varying concentration (26-82 nccSTP/g) have a narrow range in  $^3\text{He}/^4\text{He}$  - 17.8-18.3 $R_A$ . Both co-existing and a single clinopyroxene have lower [He] (8-9 nccSTP/g) and slightly lower  $^3\text{He}/^4\text{He}$  - 16.2-17.8 $R_A$ . Again, no correlation between  $^3\text{He}/^4\text{He}$  and other (radio)isotope tracers is evident. The overlap between olivine and clinopyroxene samples indicates that radiogenic-He contamination of these samples is minimal. The high  $^3\text{He}/^4\text{He}$  of the Laurens Peninsula thus supports the view that the low  $^{87}\text{Sr}/^{86}\text{Sr}$ , high  $^{206}\text{Pb}/^{204}\text{Pb}$  endmember is representative of the Heard-Kerguelen plume.

Barling, J. & Goldstein, S.L. *Nature* **348** pp 59-62 (1990).

Barling, J., Goldstein, S.L. & Nichols, I. J. *Petrol. in press* (1994).

Hilton, D.R., Hammerschmidt, K., Teufel, S. & Friedrichsen, H. *EPSL* **120**, pp265-281 (1993)

Class, C., Goldstein, S.L., Galer, S.J.G. & Weis, D. *Nature* **362** pp 715-721 (1993).

## STATIC MASS SPECTROMETRY OF NANOMOLE CARBON WITH A QUADRUPOLE-TYPE MASS SPECTROMETER

HIYAGON, H., SUGIURA, N. and MIYAZAKI, A., Department of Earth and Planetary Physics, University of Tokyo, Bunkyo-ku, Tokyo 113, Japan.

We are constructing a vacuum system equipped with a quadrupole-type mass spectrometer (MSQ400, ULVAC Co., Japan) for analyzing isotopic composition of nano-mole carbon in a static mode.

We analyze carbon isotopes as carbon-dioxide and measure mass 42, 44, 45 and 46. Peaks are electrically scanned and 10 sets of data are obtained in 160 seconds. Carbondioxide tends to decompose partly into CO and partly into C to form possibly metal-carbide during the analysis due to interaction between gas and hot filament. In order to minimize this effect, we replace first a tungsten filament with a yttria( $\text{Y}_2\text{O}_3$ )-coated iridium filament which has lower work function. This lengthens the "half life" of  $\text{CO}_2$  in the mass spectrometer by a factor of about 5. Secondly, we lower the emission current from 1.0 mA to 0.1 mA. In this condition, the "half life" of  $\text{CO}_2$  becomes longer than 120 sec. The ion source we are using is an "open-type" (Prosser et al., 1990). However, the observed "half life" of  $\text{CO}_2$  is much longer than that for other "open sources" ( $\sim 35$  sec, Carr et al., 1986) and only a factor of three shorter than that for the "closed source" ( $\sim 450$  sec, Prosser et al., 1990). We found more than 80% of the gas existed as  $\text{CO}_2$  even at the end of the analysis.

At present, the  $^{13}\text{C}/^{12}\text{C}$  ratios observed for repeated analyses of a standard gas (about 1 nano-mole  $\text{CO}_2$ ) are reproducible within  $\pm 0.5\%$ . However, there seems to be some pressure dependence in the discrimination factor for  $^{12}\text{C}$  and  $^{13}\text{C}$ . The lower limit of the sample size for carbon isotope analysis with this system is about 0.1 nano-mole.

Prosser, S. J. et al., 1990: *Chem. Geol.*, v.83, p.71-88.

Carr, R.H. et al., 1986: *J. Phys. E. Sci. Instrum.*, v.19, p.133-149.

## MASS INDEPENDENT FRACTIONATION IN TROPOSPHERIC CARBON MONOXIDE

HODDER, P.S., Department of Chemistry, 0356, University of California - San Diego, La Jolla, CA 90293-0356, BRENNINKMEIJER\*, C.A.M., National Institute of Water and Atmospheric Research, Lower Hutt, New Zealand, and THIEMENS, M.H., Department of Chemistry, 0356, University of California - San Diego, La Jolla, CA, 90293-0356. \* Present address: Max Planck Institute for Chemistry, Airchemistry Department, Mainz, Germany.

The measurement of multi-isotope, mass independent kinetic isotopic fractionation effects has previously been applied with notable success in the field of atmospheric chemistry as a sensitive technique to better understand the global budget of several atmospheric species. Multi-isotope measurements have provided constraints on sources and global budgets of certain atmospheric species (e.g., ozone and methane) to a considerable degree, and also have helped understand the nature of the kinetics of the production mechanisms. The use of multi-isotope ( $\delta^{17}\text{O}$ ,  $\delta^{18}\text{O}$ ) ratio measurements of atmospheric nitrous oxide have elucidated the possible importance of new stratospheric reactions. In the case of nitrous oxide, this technique provides a resolution that could not be obtained from concentration or combined  $\delta^{15}\text{N}$  and  $\delta^{18}\text{O}$  measurements.

Carbon Monoxide (CO) is a trace gas in the atmosphere (~ppbv) with as much as 2/3 of its source signal influenced by anthropogenic activities. In addition, CO plays a key role in the budgets of important atmospheric species (ozone, OH, methane, NMHC's), necessitating a better understanding of the otherwise poorly constrained CO cycle. Considerable effort has been expended on measuring the kinetic isotope effects of  $^{13}\text{C}$  and  $^{18}\text{O}$  to characterize the different source strengths and to model the observed trends in the highly variable concentrations of atmospheric CO.

Recently, a mass independent fractionation of large magnitude has been measured in the stable isotope ratios ( $^{18}\text{O}/^{16}\text{O}$ ,  $^{17}\text{O}/^{16}\text{O}$ ) of tropospheric CO from the southern hemisphere. Based upon our present physical-chemical knowledge of mass independent fractionations, we are able to eliminate several sources as being responsible for this effect. This discovery may help better constrain the major source strengths, as well as different production pathways and circulation of CO.

## U-Pb AND $^{40}\text{Ar}/^{39}\text{Ar}$ THERMOCHRONOLOGY OF VERY SLOWLY COOLED SAMPLES

HODGES, K.V., BOWRING, S.A., and HAMES, W.E., Dept. Earth, Atm., and Planetary Sciences, MIT, Cambridge, MA, 02139, USA

Reconstructing the cooling history of very slowly cooled terrains from geochronologic data from is not straightforward. At cooling rates of  $\leq 1$  K/m.y., the integrated closure temperatures of mineral-isotopic systems are strongly dependent on cooling rate. Moreover, slow cooling can lead to the development and maintenance of large age gradients in minerals that are commonly overlooked in the course of conventional analysis of multigrain samples. Recent  $^{40}\text{Ar}/^{39}\text{Ar}$  and U-Pb studies of samples from the Proterozoic orogenic belt of the southwestern United States provide examples of complexities caused by slow cooling.

The Crazy Basin plutonic complex of central Arizona yields U-Pb zircon ages ranging from 1690 to 1710 Ma. Incremental heating of single  $\sim 700$   $\mu\text{m}$  crystals of muscovite and biotite from a Crazy Basin monzogranite using a defocused Ar-ion laser resulted in simple, relatively flat  $^{40}\text{Ar}/^{39}\text{Ar}$  release spectra indicating closure ages of  $1412 \pm 5$  and  $1410 \pm 10$  Ma, respectively. However, analysis of the same samples by laser microprobe revealed large age gradients. Within one carefully mapped {001} cleavage fragment from a 740  $\mu\text{m}$ -diameter muscovite crystal, total fusion ages ranged from  $1650 \pm 10$  Ma in the core to  $1270 \pm 10$  at the rim in broadly concentric fashion. An adjacent cleavage fragment from the same crystal, though mapped in less detail, yielded an identical concentric age pattern. Five cleavage fragments from a smaller (550  $\mu\text{m}$ ) crystal yielded statistically indistinguishable core ages between 1560 and 1530 Ma. Rim ages were much younger but more variable (1440 to 1350 Ma), due at least in part to steep near-rim age gradients. An {001} cleavage fragment from a 1 mm biotite crystal also exhibited a concentric age zoning pattern from  $1420 \pm 10$  Ma in the core to  $1150 \pm 10$  Ma at the rim. The lack of evidence for such large and reproducible age gradients in the incremental heating data suggest caution in the interpretation of simple release spectra from very slowly cooled samples.

U-Pb titanite data from the  $\sim 1690$  Ma Horse Mountain granite from the same area provide additional evidence for very slow cooling. Cores of abraded  $\sim 300$   $\mu\text{m}$  titanites cluster along concordia from  $> 1660$  to 1650 Ma. Rim fragments and multigrain separates of smaller ( $\sim 100$   $\mu\text{m}$ ) titanites give substantially younger  $^{206}\text{Pb}/^{238}\text{U}$  ages ranging from  $1459 \pm 6$  to  $1339 \pm 5$  Ma.

**PB ISOTOPE SYSTEMATICS OF GOLD  
MINERALIZATIONS AT ASHANTI (OBUASI,  
GHANA)**

**HOEHNDORF, A., OBERTHUER, T.,  
SCHMIDT MUMM, A., VETTER, U., Federal  
Institute for Geosciences and Natural  
Resources, Hannover, Germany.**

The Ashanti gold mine at Obuasi (Ghana) is the largest gold producer in West Africa having produced in excess of 700 t of gold historically. The mine workings are hosted in Palaeoproterozoic metasediments of the Birimian Supergroup.

Gold mineralization is found in two major types of primary ores, namely (i) sulfide mineralization in the wall rocks with auriferous arsenopyrite as the dominant ore mineral, and (ii) quartz veins containing free gold associated with Pb, Sb sulfides. Both ore types are controlled by the same structural patterns and occur together or alternate with each other in the major ore zones.

To get age information for the mineralization, Pb isotopic investigations were carried out on concentrates of gold-bearing arsenopyrites from sulfide ores in the host rocks, Pb sulfides (galena and bournonite) occurring in quartz veins, and native gold from quartz veins.

For the arsenopyrites a Pb/Pb isochron age of  $2224 \pm 40$  Ma (2s) was obtained which may correspond to the age of the Birimian sedimentation. Geological and mineralogical evidence, however, implies an epigenetic nature of the arsenopyrite formation.

Model ages around 2.1 Ga, calculated (using the Stacey-Kramers model) for Pb sulfides and Pb minerals intergrown with native gold from quartz veins, are assumed to mark the age of the epigenetic gold mineralization.

**STABLE WATER ISOTOPES IN THE AT-  
MOSPHERIC GENERAL CIRCULATION  
MODEL ECHAM**

G. Hoffmann (Max-Planck-Institut für Meteorologie, D-20146 Hamburg, Germany)

M.Heimann (Max-Planck-Institut für Meteorologie, D-20146 Hamburg, Germany)

We have established a water tracer model in the atmospheric general circulation model (AGCM) ECHAM. Water tracers like the stable water isotopes  $^1\text{H}_2\ ^{18}\text{O}$  and  $^1\text{H}^2\text{H}\ ^{16}\text{O}$  pervade the whole hydrological cycle, i.e. evaporation from oceans, atmospheric transport, condensation inside clouds, precipitation as rain or snow and finally seepage into groundwater and rivers. We calculate the atmospheric transport of both water tracers and "normal" water  $^1\text{H}_2\ ^{16}\text{O}$  by a semilagrangian advection scheme. During any phase transition water isotopes undergo a fractionation relative to normal water. We have incorporated both kinetic and equilibrium fractionation according to the well-known experimental results. The ECHAM is a spectral model which is run for our tracer studies in T42 resolution (spectral truncation at wave number 42 and a physical grid of about  $2.5^\circ \times 2.5^\circ$ ). We present here the results of a five year simulation under both today's climate conditions and the boundary conditions of the last glacial maximum (LGM). In a first step we compare the simulated isotopic composition of precipitation, soil moisture, snow etc. with observations (I.A.E.A. precipitation data,..) in order to assess the quality of the hydrological cycle of the ECHAM model. Afterwards regarding our LGM experiment we focus on the question if the linear relation between temperature and  $\delta^{18}\text{O}$  is insensitive against climate change, which is the basic assumption reconstructing paleotemperatures from the isotopic composition of ice cores and paleowaters.

## CARBON ISOTOPE CHARACTERISTICS OF CO<sub>2</sub> AND CH<sub>4</sub> IN GEOTHERMAL AND MINERAL WATER SPRINGS FROM THE CENTRAL ANDES.

HOKE, Leonore, Dept. of Earth Sciences, University of Oxford, Oxford, OX1 3PR. SPIRO, Baruch and CHENERY, Carolyn, NERC Isotope Geosciences Laboratory, Keyworth, NG125GG, U.K.

We report results of carbon stable isotope analyses on methane and carbon dioxide extracted from 12 gas and water samples collected from geothermal and mineral water springs across the Central Andes of northern Chile and Bolivia. The Central Andes provide an unique tectonic setting for the study of terrestrial degassing processes in an active plate boundary zone. This zone is characterised by an active volcanic arc and unusually thick continental crust (~70km) which extends beneath the arc and the high plateau region of the Altiplano to the east of the arc. Furthermore, helium isotope evidence suggests active mantle degassing in a wide zone beneath the thick continental crust in the Central Andes (Hoke et al, 1994).

The results show a wide range of  $\delta^{13}\text{C}_{\text{CO}_2}$  (-14.9 to -0.6‰) and a surprisingly narrow range of  $\delta^{13}\text{C}_{\text{CH}_4}$  (-20.9 to -13.4‰). The difference  $\Delta\delta^{13}\text{C}_{\text{CO}_2\text{-CH}_4}$  for individual samples varies between -1.7 and +13.4‰. The  $\delta^{13}\text{C}_{\text{CO}_2}$  results show wide and overlapping ranges in the samples collected from the volcanic arc, the Altiplano and the Eastern Cordillera, though they tend to show the widest range and most negative values in the Eastern Cordillera (-15.0 to -4.8‰). The  $\delta^{13}\text{C}_{\text{CO}_2}$  results of the geothermal samples from the volcanic arc gave -8.0‰ (Surire) and -0.6‰ (Abra de Nappa), whereas  $\delta^{13}\text{C}_{\text{CO}_2}$  measured in gases collected from CO<sub>2</sub> bubbling mineral water springs from the Altiplano range from -6.1 to -10.1‰.

The relationships between <sup>3</sup>He/<sup>4</sup>He,  $\delta^{13}\text{C}_{\text{CO}_2}$  and  $\delta^{13}\text{C}_{\text{CH}_4}$  will be discussed and compared with other geothermal areas. Geothermal geothermometry based on  $\Delta\delta^{13}\text{C}_{\text{CH}_4\text{-CO}_2}$  fractionation will be discussed. It suggests very high equilibrium temperatures in excess of 530°C for some geothermal systems analysed.

It is concluded that the formation of methane is neither bacteriogenic, nor by thermal decomposition of organic matter, but rather abiogenic by high temperature reaction of H<sub>2</sub> and CO<sub>2</sub>. The  $\delta^{13}\text{C}_{\text{CH}_4}$  results are similar to those reported from hydrothermal fluids emitted from the East Pacific Rise (Welhan, 1988), suggesting a mantle derived carbon component in the methane. The wide, 15‰ range in the  $\delta^{13}\text{C}_{\text{CO}_2}$  is interpreted to reflect contributions from different CO<sub>2</sub> sources that include crustal organic and inorganic carbon as well as mantle carbon.

Hoke, L., Hilton, D.R., Lamb, S.H., Hammerschmidt, K., Friedrichsen, H., 1994, <sup>3</sup>He evidence for a wide zone of active mantle melting beneath the Central Andes: (E.P.S.L., in press).

Welhan, J.A., 1988, Origins of methane in hydrothermal systems. In: Origins of Methane in the Earth (ed. M. Schoell): Chem. Geology 71, 183-198.

## <sup>18</sup>O/<sup>16</sup>O DATA ON CONTRASTING CRUSTAL-SCALE AQUEOUS FLUID REGIMES BEFORE AND DURING EOCENE EXTENSION IN THE SOUTHERN OMINECA CRYSTALLINE BELT, BRITISH COLUMBIA

HOLK, Gregory J. and TAYLOR, Hugh P., Jr., Geology, 170-25NM, Caltech, Pasadena, CA 91125 USA

The southern Omineca belt contains 3 fault-bounded zones: 1) Precambrian gneiss basement, 2) mid-crustal amphibolite-facies metamorphic rocks and leucogranites, and 3) an upper zone of brittlely deformed rocks. Deep-seated E-W convergent shear zones separate zones 1 and 2, and zone 3 is bounded by giant N-trending detachment faults. This large area was chosen for stable isotope study because: (a) it has great structural relief; (b) its structures are well mapped and dated; and (c) its high-latitude location insures that meteoric waters were very low in  $\delta^{18}\text{O}$  and  $\delta\text{D}$ . In the early Tertiary, two major episodes of water-rock interaction are recognized: (I) a pre-extensional metamorphic-hydrothermal event mainly affecting the mid-crustal layer; and (II) a synextensional meteoric-hydrothermal event affecting detachment faults (e.g. Columbia River fault).

Episode I is best documented in the hanging wall of the Monashee Decollement (MD) in the Thor-Odin core complex, where it resulted in large-scale anatexis. Concordant leucogranitic segregations in migmatites ( $\delta^{18}\text{O}_{\text{Q}} = +12.2 \pm 0.5$  and  $\delta^{18}\text{O}_{\text{F}} = +10.9 \pm 0.5$ ) and pelites ( $\delta^{18}\text{O}_{\text{Q}} = +12.1 \pm 0.9$  and  $\delta^{18}\text{O}_{\text{F}} = +11.0 \pm 0.9$ ) are remarkably uniform in <sup>18</sup>O, suggesting equilibration with metamorphic fluids ( $\delta^{18}\text{O} = +11.0$ ) at  $T \approx 650^\circ\text{C}$ . Similar  $\delta^{18}\text{O}$  values from an overlying, coeval Ladybird-Series pluton (LSP) ( $\delta^{18}\text{O}_{\text{Q}} = +12.2 \pm 0.4$  and  $\delta^{18}\text{O}_{\text{F}} = +10.4 \pm 0.3$ ) indicate it formed during the same anatexis event. Paleozoic marbles (>95% calcite) show a 12‰ downward shift in <sup>18</sup>O, but are unchanged in <sup>13</sup>C, further evidence for exchange with H<sub>2</sub>O-rich metamorphic fluids. Below the LSP, calcite from calc-silicates is uniform in <sup>18</sup>O ( $\delta^{18}\text{O} = +15.4 \pm 0.2$ ), but variable in <sup>13</sup>C ( $\delta^{13}\text{C} = -7.6$  to  $-3.5$ ). However, calc-silicate calcite from above and within the LSP is not uniform in <sup>18</sup>O or <sup>13</sup>C ( $\delta^{18}\text{O} = +9.6$  to  $+20.3$ ,  $\delta^{13}\text{C} = -6.4$  to  $+0.3$ ), suggesting contrasting styles of water-rock interaction fixed by position relative to the LSP. Data from another Ladybird granite pluton ( $\delta^{18}\text{O}_{\text{Q}} = +11.2 \pm 0.5$ ) and associated hybrid gneiss ( $\delta^{18}\text{O}_{\text{Q}} = +11.4 \pm 0.9$ ) in the Valhalla metamorphic core complex farther south are also compatible with deep-seated fluid-driven anatexis.

Episode II occurred during Eocene detachment faulting associated with rapid unroofing of the metamorphic core complexes. Disequilibrium quartz-feldspar  $\delta^{18}\text{O}$  values ( $\Delta_{\text{Q-F}} = 1.5$  to  $16.0$ , with  $\delta^{18}\text{O}_{\text{F}}$  low as  $-5.0$ ) are diagnostic of this event. On a  $\delta_{\text{F}} - \delta_{\text{Q}}$  plot, values typically define a steep array, suggesting that water-rock interaction was intense and short-lived ( $\approx 10^5$ yr) during extensional faulting at  $T \approx 300\text{-}350^\circ\text{C}$ . A systematic  $\delta^{18}\text{O}_{\text{F}}$  decrease occurs in both upper and lower plates as detachment faults are approached, suggesting that fluid-flow was channelized by faults and occurred when faults were active. The tectonic juxtaposition of a hot lower plate ( $T > 500^\circ\text{C}$ ) against a cold upper plate ( $T < 300^\circ\text{C}$ ) was the likely driving force for circulation of meteoric water to great depth.  $\delta - \delta$  arrays are less steep at detachment faults associated with late-stage Coryell alkalic intrusions, indicating that more heat was advected toward the surface where these plutons are present than along more distant faults. Remarkably, these effects are also seen along the MD, implying that meteoric H<sub>2</sub>O locally migrated deep into the lower plate.

LITHOSPHERIC MAGMA SOURCES DURING TERTIARY CONTINENTAL BREAK-UP IN EAST GREENLAND: ELEMENTAL AND SR-ND ISOTOPIC GEOCHEMISTRY OF BASALTIC DYKES FROM THE KANGERLUSSUAQ AREA

HOLM, P.M., Geological Institute, University of Copenhagen, Øster Voldgade 10, DK-1350 Copenhagen, Denmark, and N.-O. PRÆGEL, University Library, Nørre Alle 37, DK-2200 Copenhagen, Denmark.

Early Tertiary basaltic dykes intruded in the Kangerlussuaq area during continental rifting in East Greenland both as a coastal swarm parallel to the continent/ocean transition and along the Kangerlussuaq fjord stretching c. 70 km inland. The area was uplifted c. 6 km in a domal structure during the Oligocene and its probable cover of flood basalts was eroded away. Elemental and isotope geochemistry of 65 picrites, tholeiitic basalts, basaltic andesites, transitional basalts, alkali basalts and basanites is presented. These rocks may represent the magmas generated over the central part of the proto-Icelandic mantle plume. In all sub-areas, both alkaline and sub-alkaline compositions are present. The liquid lines of descent of the dyke magmas are rather similar: ol+chr, ol+cpx and late in the basaltic interval ol+cpx+plg. The dykes cover the same range of elemental and isotopic compositions as the related CFBs but also extend to highly alkaline and extreme isotopic compositions not seen among the lavas.  $^{87}\text{Sr}/^{86}\text{Sr}_{50\text{Ma}}$  range from 0.7030 to 0.7202 and  $^{143}\text{Nd}/^{144}\text{Nd}$  span 0.5118-0.5131. The geochemistry of the majority of dykes can largely be explained as mixing between an Icelandic type components (MORB and plume) and a highly LILE and LREE enriched component with  $^{87}\text{Sr}/^{86}\text{Sr} = \text{c. } 0.7055$  and  $^{143}\text{Nd}/^{144}\text{Nd} = 0.5125$ ,  $\text{Ce}/\text{Y}_N = \text{c. } 25$ ,  $\text{Ti}/\text{Y} = \text{c. } 600$ . This component is not seen in Icelandic lavas and is suggested to be derived from the lithospheric mantle. The group of dykes trending towards very high  $^{87}\text{Sr}/^{86}\text{Sr}$  and low  $^{143}\text{Nd}/^{144}\text{Nd}$  comprises a wide range of rock types only excepting the most alkaline but including all basaltic andesites. Although more than one component is involved, the overall elemental character is relatively well-defined:  $\text{Ce}/\text{Y}_N = 2-4$ ,  $\text{Zr}/\text{Nb} = 5-10$ ,  $\text{Ti}/\text{Y} = 300-400$  and  $\text{K}/\text{Ti}$  lower than in the proposed lithospheric mantle component. There is no suggestion that this component may be derived from the lower crust. It is seen especially in late dykes and is also the dominant component in an early central intrusion in the area and may be related to the ending of an extensional tectonic regime in the fjord area. Upper crustal contamination seems to be of relatively unimportant in most dykes magmas. Modelling the evolution of the sources for the magmas is facilitated by the strong isotopic contrast between asthenosphere and Archean lithosphere.

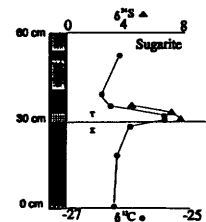
Early basaltic magmas derived mainly from MORB and Icelandic plume material interacted with the subcontinental mantle increasingly with distance to the coastal rift. Later magmas more frequently paused and interacted with the lower crust which at that time had an enhanced geotherm.

STABLE ISOTOPE (C,S,N) DISTRIBUTIONS IN COALS SPANNING THE CRETACEOUS/TERTIARY BOUNDARY IN THE RATON BASIN, COLORADO AND NEW MEXICO

Charles W. Holmes and Bruce F. Bohor, U.S. Geological Survey, Box 25046, MS 972, Denver Federal Center, Denver, CO. 80225

The distribution of the stable isotopes of carbon, sulfur, and nitrogen was measured in coal beds and their associated carbonaceous shales and the K/T boundary claystones at five sites in the Raton basin.  $\delta^{13}\text{C}$ , measured on 35 carbonate-free samples, ranged from -24.9 to -27.2‰.  $\delta^{34}\text{S}$ ‰, measured on 15 sulfide and sulfate-free samples, ranged from 4.6 to 8.0‰.  $\delta^{15}\text{N}$ ‰, measured on 15 coal samples, ranged from 1.9‰ to 2.7‰.

The Sugarite site is particularly well suited for this study because the K/T boundary claystone is completely enclosed in coal. Thus, the influences of pre- and post-impact lithologic variations are minimized.



Previous studies of the Sugarite site documented the presence of the palynologically defined K/T boundary within the coal bed at the level of a thin, iridium-bearing claystone-shale unit (Nichols and others, 1985). This unit contains 22-25% carbonaceous material; the coal below it has a low ash (~7%) and the coal above it is high in ash content (~15%).

The  $\delta^{13}\text{C}$  value is -2‰ heavier in the boundary claystone unit than the surrounding coal and the  $\delta^{34}\text{S}$  value also increases by 3.5‰ (Figure). In contrast, the  $\delta^{15}\text{N}$  value decreases through the boundary interval. By comparison, the  $\delta^{13}\text{C}$  and  $\delta^{34}\text{S}$  across tonsteins within a Cretaceous coal shows no change.

It has been suggested that the event that caused the mass extinctions at the K/T boundary was an asteroid impact near Chicxulub on Mexico's Yucatan peninsula. O'Keefe and Ahrens (1989) modeled the results of a large bolide impacting a carbonate/evaporite sequence and pointed out that the increased flux of  $\text{CO}_2$  into the atmosphere would be significant, on the order of a 2-10 fold increase. In addition, a large volume of anhydrite would be vaporized, releasing  $>10^{16}$  moles of  $\text{SO}_2$  into the atmosphere. The impact-generated carbon and sulfur from vaporized marine target rocks would be isotopically heavier than their pre-impact equivalents in the Late Cretaceous paleoatmosphere. Our analyses verify the presence of heavier S and C isotopes in the boundary ejecta unit at Sugarite, thus appearing to validate the impact model of O'Keefe and Ahrens (1989). Nichols, D.J., Fleming, R.F., Upchurch, G.R., Tschudy, R.H., and Pillmore, C.L., 1985, SEPM Midyear Meet., v. 2, p. 68. O'Keefe, J.D., and Ahrens, T.J., 1989, Nature, v. 338, p. 247-249.

**CORRELATION BETWEEN MANTLE NEON, OXYGEN AND RADIOGENIC ISOTOPES IN OCEAN ISLAND BASALTS FROM THE PITCAIRN SEAMOUNTS, SOUTHEAST POLYNESIA**

HONDA, M., WOODHEAD, J.D., McDOUGALL, I., Research School of Earth Sciences, Australian National University, Canberra, ACT 0200, Australia, and DEVEY, C.W., Geologische Institut der Universität Kiel, 40-60 Olshausenstrasse, 2300 Kiel, Germany.

Fresh basaltic glasses recently have been dredged from sites of youthful volcanism on the Pitcairn Seamounts, Polynesia. Radiogenic isotope results (Sr, Nd and Pb) suggest that the mantle source for the Pitcairn samples is strongly influenced by an enriched mantle component of so-called EM-1 type. The oxygen isotope compositions of the Pitcairn samples appear to require the presence of subducted crustal material for the EM-1 component (Woodhead et al., 1993).

In order to further understand the characteristics of the EM-1 component we have measured all five noble gas elemental and isotopic abundances in eleven fresh basaltic glasses from the Pitcairn Seamounts, whose radiogenic and oxygen isotope results were previously obtained by Woodhead et al. (1993). The  $^3\text{He}/^4\text{He}$  ratios observed in the Pitcairn samples range from  $13.5 \times 10^{-6}$  (9.8 R/R<sub>A</sub>) to  $2.3 \times 10^{-6}$  (1.6 R/R<sub>A</sub>). Neon isotopic ratios measured on the Pitcairn samples are enriched in  $^{20}\text{Ne}$  and  $^{21}\text{Ne}$  by as much as 19% with respect to atmospheric ratios. The neon isotopic results do not show any obvious correlation when they are plotted in  $^{20}\text{Ne}/^{22}\text{Ne}$ - $^{21}\text{Ne}/^{22}\text{Ne}$  space, suggesting that mantle neon in the source for the Pitcairn samples is extremely heterogeneous on a small scale.

In general, mantle neon appears to comprise a mixture of a primordial solar component together with variable (time-integrated) amounts of nucleogenic neon. Further, based on the calculated nucleogenic  $^{21}\text{Ne}$  ( $^{21}\text{Ne}^*$ ) / solar  $^{20}\text{Ne}$  ( $^{20}\text{Ne}_S$ ) ratios, generally it is possible to predict  $^3\text{He}/^4\text{He}$  ratios in the mantle source (e.g., Honda et al., 1993). For the Pitcairn samples there are weak correlations between calculated  $^{21}\text{Ne}^*/^{20}\text{Ne}_S$  ratios and  $^{206}\text{Pb}/^{204}\text{Pb}$ ,  $^{143}\text{Nd}/^{144}\text{Nd}$  (positively), and  $^{87}\text{Sr}/^{86}\text{Sr}$ ,  $\delta^{18}\text{O}$  (negatively). At least two end members are required to account for the correlations, one of which is a MORB component. In contrast, there are no apparent correlations between  $^3\text{He}/^4\text{He}$  ratios actually observed in the samples and isotopic compositions of radiogenic elements and oxygen, suggesting that helium in the samples has been influenced by secondary processes such as loss of helium from the magmas and interactions with seawater.

These observations from the Pitcairn samples suggest that the EM-1 component is enriched in a primordial-solar noble gas composition relative to the MORB component.

Honda, M., McDougall, I., Patterson, D.B., Doulgeris, A., and Clague, D.A., 1993, *Geochim. Cosmochim. Acta*, v. 57, p. 859-874.

Woodhead, J.D., Greenwood, P., Harmon, R.S., and Stoffers, P., 1993, *Nature*, v. 362, p. 809-813.

**THORIUM ISOTOPES AND SR-ND-PB TRENDS IN VOLCANICS AND SEDIMENTS ALONG THE SUNDA-BANDA ARC (INDONESIA)**

HOOGWERFF, J.A., VAN BERGEN, M.J., VROON, P.Z., Faculty of Earth Sciences, Utrecht University, P.O. Box 80021, 3508TA Utrecht, the Netherlands, and HERTOGEN, J., Div. of Physicochemical Geology, University of Leuven, Celestijnenlaan 200C, B-3001 Leuven, Belgium.

The oceanic and continental domains of the Indian-Australian plate exert a different influence on magma genesis in the Sunda-Banda Arc which can be evaluated with currently available isotope data on volcanics and sediments. Along-arc correlations between Sr, Nd, Pb isotopes in the volcanics reflect variations in the tectonically controlled supply of continental material to the trench. Strongest isotopic deviations from mantle values are not restricted to the Banda Arc but are found in the eastern part of the Sunda Arc and SW Banda Arc, near a volcanically inactive sector close to the location of earliest collision between the Australian passive margin and the arc. An important finding is that changes in Pb isotopic compositions of the volcanics along the East Sunda-Banda Arc correspond to similar changes in the sediments entering the trench. In addition, trace-element characteristics of the volcanics closely resemble those of detrital sediments derived from the Australian continent. All these observations are compelling evidence for source contamination by recent sediment subduction.

New and compiled ( $^{230}\text{Th}/^{232}\text{Th}$ ) ratios of recent lavas in the Sunda-Banda arc are all  $< 1$ . The values are low compared to those in other island arcs, are close to the ratio in the terrigenous fraction of the sediments near the collision zone, and argue against a contribution from altered oceanic crust. The ( $^{230}\text{Th}/^{232}\text{Th}$ ) ratios do not exhibit a clear along-arc trend as do Sr, Pb, Nd and He isotopes, and correlations between Th and the other isotope tracers are generally poor. In a transect across the collision zone, however, lowest ( $^{230}\text{Th}/^{232}\text{Th}$ ) ratios were found at the volcanic front in combination with lowest  $^3\text{He}/^4\text{He}$ , relatively high  $^{143}\text{Nd}/^{144}\text{Nd}$ , and strong enrichment of  $^{238}\text{U}$  and  $^{226}\text{Ra}$  over  $^{232}\text{Th}$ . The cases of U enrichment (and high  $^{143}\text{Nd}/^{144}\text{Nd}$ ) are restricted to low-K centres at the front in the collision zone.

It is concluded that the along-arc changes in the nature and amount of subducted source components are a dominant control in generating the isotope characteristics of the volcanics. The influence of terrigenous sediments and continental crust is widespread around the domain of the Australian margin. Mantle sources in this region were contaminated largely by bulk addition of continental material, although signatures of low-K frontal volcanoes locally favour the role of fluids as a more selective transfer medium.

Selected refs: Whitford et al. (1977) *Geology* 5:571-575; Whitford and Jezek (1982) *Geol.Soc.Am.Bull.* 93: 504-513; Varne and Foden (1986) *In: Wezel, The origin of arcs, Elsevier:* 159-189; Ben Othman et al. (1989) *EPSL* 94:1-21; Hilton and Craig (1989) *Nature* 342: 906-908; Rubin et al. (1989) *JVGR* 38: 215-226; Gill and Williams (1990) *GCA* 54:1427-1442; Stolz et al. (1990) *CMP* 105: 585-601; Vroon (1992) *Geol.Ultrai. (Utrecht)* 90:205pp.; Hilton et al. (1992) *GCA* 56: 851-859; Edwards et al. (1993) *Nature* 362: 530-533; Van Bergen et al. (1993) *Tectonophys.* 223: 97-116; Vroon et al. (1993) *JGR* 98:22349-22366; Condomines and Sigmarsson (1993) *GCA* 57: 4491-4497.

**SALT EFFECTS ON STABLE ISOTOPE PARTITIONING BETWEEN BRINES, AND VAPOR AND MINERALS AT ELEVATED TEMPERATURES**

**HORITA, J., COLE, D. R., and WESOLOWSKI, D. J.,**  
Chemical and Analytical Sciences Division, Oak Ridge  
National Laboratory, Oak Ridge, TN 37831-6110, U.S.A.

A series of hydrothermal experiments have been conducted at elevated temperatures, in order to determine the effect of dissolved salts in water on equilibrium oxygen and hydrogen isotope partitioning between brines and other coexisting phases (vapor and minerals). The equilibrium fractionation factors of oxygen and hydrogen isotopes between pure water and vapor, and the effect of dissolved salts have been precisely determined from 25 to 350°C. In all of the single salt solutions (0-6 molal NaCl at 50 to 350°C, 0-5 molal CaCl<sub>2</sub> at 50-200°C, and KCl, MgCl<sub>2</sub>, Na<sub>2</sub>SO<sub>4</sub>, and MgSO<sub>4</sub> at 50-100°C), values of  $10^3 \ln \alpha_{1,v}(D)$  for the salt solutions are appreciably smaller (up to 20‰) than those between pure water and vapor in the order pure water > Na<sub>2</sub>SO<sub>4</sub> > KCl ≈ NaCl > MgSO<sub>4</sub> > MgCl<sub>2</sub> ≥ CaCl<sub>2</sub>. Except for KCl solutions at 50°C, values of  $10^3 \ln \alpha_{1,v}(^{18}O)$  for the salt solutions were larger (up to 4‰) than, or very close to, those of pure water in the order MgSO<sub>4</sub> ≈ MgCl<sub>2</sub> > CaCl<sub>2</sub> > Na<sub>2</sub>SO<sub>4</sub> > NaCl ≈ pure water ≥ KCl. The observed oxygen and hydrogen isotope salt effects in the single salt solutions are all linear with molality of the salt solutions, and were regressed to simple equations as a function of temperature and molality. The isotope salt effects in several mixed salt solutions of the system Na-K-Mg-Ca-Cl-SO<sub>4</sub>, including those resembling natural brines, were found to be exactly additive of the effects of single salts separately between 50 and 100°C. Thus, the simple empirical equation generated in this study can be used to predict the isotope salt effect in complex natural brines.

In order to determine salt effects on isotope partitioning between brines and minerals, experiments of partial isotope exchange were carried out on calcite-water at 300°C and 1 kbar for a duration of 126 days. Calculated equilibrium oxygen isotope fractionation factors,  $10^3 \ln \alpha_{\text{calcite-water}}$  were  $5.9 \pm 0.3\text{‰}$  for pure water, and  $5.6 \pm 0.2$ ,  $5.0 \pm 0.15$ , and  $4.9 \pm 0.2\text{‰}$  for 1, 3, and 5 molal NaCl solutions, respectively. The observed oxygen isotope salt effects (-0.3 to -1.0‰) from the calcite-water experiments are consistent with those obtained from the above liquid-vapor equilibration method at 300°C (-0.2 to -0.6‰ for 1 and 5 molal NaCl solutions).

Our study demonstrates that salt effects on stable isotope partitioning between brines and other phases (vapor and minerals) indeed persist up to at least 350°C, but that the complex temperature and molality dependence reported in the literature is almost certainly an experimental artifact. The isotope salt effects observed in this study must be taken into account for isotopic studies involving brines, both experimental and natural.

This study was supported by the Geoscience Program of the Office of Basic Energy Sciences and the Geothermal Technology Program of the Office of Energy Efficiency and Renewable Energy, U. S. Department of Energy, under contract number DE-AC05-84OR21400 with Martin Marietta Energy Systems, Inc.

**RAPID EXTENSION RECORDED BY COOLING-AGE PATTERNS AND BRITTLE DEFORMATION, NAXOS METAMORPHIC CORE COMPLEX, GREECE**

**HOWARD, K.A.,** U.S. Geological Survey, Menlo Park, CA 94025, USA, and **JOHN, B.E.,** Dept. of Geology and Geophysics, University of Wyoming, Laramie, WY 82071, USA

The island of Naxos in the Aegean Sea records an unusually complete sequence of Miocene structures developed as a result of continental extension. The structures formed during rise and cooling from ductile, upper amphibolite-facies and anatectic conditions to near-surface conditions beneath the Naxos extensional fault system. Top-to-the-north ductile shear fabrics, which initially developed during amphibolite-facies prograde metamorphism in the footwall, were overprinted by a succession of north-directed lower temperature brittle structures as the footwall was tectonically unloaded and unroofed: pseudotachylite, cataclasis and brittle faulting, alteration, tectonic denudation, erosion of the footwall, and continued slip. Intrusion of a granodiorite pluton at ~12.5 Ma coincided with a lull in development of extensional microstructures, possibly when shear strain abandoned one level and transferred to a higher level in the crust.

Geographic patterns of cooling ages in the footwall, derived from published geochronologic studies, provide a basis for interpreting the unroofing history of the domal footwall (at different mineral closure temperatures for hornblende, muscovite, and biotite) as the footwall moved from under the north-slipping hanging wall. Analysis of the published K-Ar and <sup>40</sup>Ar/<sup>39</sup>Ar ages lead us to estimate the fault slip rate as the footwall was tectonically denuded and cooled. Contoured values of mineral age decrease northward in the slip direction in two stages. The southern stage (17-50 Ma) corresponds to areas of low metamorphic grade where pre-extension argon was partly retained.

The northern stage (10-16 Ma) records cooling of high-grade rocks during the period of rapid extension. Northward-younging is seen for each mineral, at rates that depend little on the criteria used for selecting data. Ages for biotite, muscovite, and amphibole each decrease northward at rates between 0.13 and 0.22 m.y./km, to about 10 Ma. Assuming that these rates represent cooling during extension, they can be used to interpret the slip rate at which footwall rocks moved >20 km relative to their hanging wall along the base of the north-dipping Naxos extensional fault system. Extensional slip calculated this way accelerated from 16 to 14 Ma (from amphibole ages), and reached a rate averaging 5-8 mm/yr (5-8 km/m.y.) from 14 to 10 Ma (from muscovite and biotite ages). Maximum rates reported from the Basin and Range province, derived from lower closure-temperature minerals, are comparable at 7-9 mm/yr.

## SOIL-WATER OXYGEN ISOTOPE PROFILES ALONG A CLIMATE TRANSECT

HSIEH, Jean C.C., Div. of Geol. and Plan. Sci., Caltech, Pasadena, CA, 91125, USA, KELLY, Eugene F., Dept. of Agronomy, Colo. State Univ., Ft. Collins, CO, 80523, USA, CHADWICK, Oliver A., JPL-Caltech, Pasadena, CA, 91109, USA, and SAVIN, Samuel M., Dept. of Geol. Sci., Case Western Reserve Univ., Cleveland, OH 44106, USA.

Understanding soil-water oxygen isotope profiles in relation to rain water and evaporation is critical to interpreting the isotopic composition of pedogenic minerals. Theoretical models of variations in the isotopic compositions of soil-water as a function of depth, such as Barnes and Allison (1983), predict that there should be a maximum value near the surface with nearly no change below. These models are based on initial filling of pore space with water of a uniform isotopic composition. Subsequent evaporation near the surface results in  $^{18}\text{O}$  enrichment. However, under natural conditions, substantial amounts of antecedent moisture create greater complexities.

We have measured the  $\delta^{18}\text{O}$  values of precipitation and soil-water along an elevational transect in Hawaii. As elevation increases from 77 to 1250 m, mean annual temperature ranges from 23 to 17°C and median annual precipitation ranges from 20 to 300 cm with corresponding rain water  $\delta^{18}\text{O}$  values ranging from -4.41‰ (SMOW) to -11.43‰. With increasing elevation, evaporative demand decreases and the amount of vegetative cover increases. Our measurements of the isotopic composition of soil water are used to determine the relative proportion of water lost through evaporative vs. transpirative processes. Although evaporation is highest at low rainfall and high temperature, our data indicate that even in areas of high rainfall and low temperature, significant evaporation occurs.

Most techniques for extracting soil water remove water from pores, water adsorbed on mineral surfaces, and water fixed in mineral structures which have isotopically distinct compositions. For isotopic analyses of soil water, we have determined that it is important to measure the  $\delta^{18}\text{O}$  value of pore water which we have operationally defined as *liquid water* (Hsieh et al., 1993).

Barnes, C.J. and Allison, G.B, 1983, The Distribution of Deuterium and Oxygen-18 in Dry Soils:I. Theory: J. Hydrology, v. 60, p. 141-156.

Hsieh, J.C.C., Savin, S.M., Kelly, E.F., and Chadwick, O.A., 1993, A New Method for Oxygen Isotope Analysis of Soil Water, GSA Abstracts, v 25(6), p.315.

## 3.3GA SM-ND AGE AND THE CRUSTAL EVOLUTION OF XINJIANG OF NORTHWESTERN CHINA

HU Aiqin, Institute of Geochemistry, Chinese Academy of sciences, Wu shan, Guang Zhou, Guang Dong Prov., 510640, P.R.China

The northern part of Xinjiang, as a major region of study, is belonged to the paleoplate of Tarim, Junggar and Siberia respectively.

Recently,  $3263 \pm 129\text{Ma}$  of Sm-Nd isochron age with  $\epsilon_{\text{Nd}}(t) = +3.2 \pm 0.7$  for 10 amphibolites, 3050Ma of the average TDM for 8 acid rocks have been obtained, which indicated the existence of Early-Middle Archaean continental basement in the Tarim Block firstly. The events of crustal growth were happened during the precambrian period (3.3-3.0Ga, 2.2Ga, 1.8Ga and 0.7Ga) mainly, but some continental crust, may be, was formed during the phanerozoic period in the northern Xinjiang.

Based on the different characteristics of Nd-Sr isotopic evolution and statistical age of TDM, the north Xinjiang continent can be divided into four continental blocks, those are: the Tarim Block is of Archaean basement; the Tianshan-Early-Middle Proterozoic; the Junggar-Upper Proterozoic and Phanerozoic; Artai-Middle Proterozoic. There were different geological tectonic histories in the four blocks, especially, during the phanerozoic it was very obvious that the Tarim block was in the relative stable tectonic environment, but in the north continent to the Tianshan there was occurred extensive and vast orogeny.

PRECISE MEASUREMENT OF RUTHENIUM ISOTOPES  
BY THERMAL IONIZATION MASS SPECTROMETRY  
HUANG, M., and MASUDA A. Dept. of  
Chemistry, The University of Electro-  
Communications, Chofu-shi, Tokyo 182,  
Japan

Ruthenium is a very interesting element whose seven stable isotopes are related to p, s and r nuclear processes. A basic study to search for isotopic abundance anomalies in Ru by TIMS is tried in this work.

Pothes et al. employed a V-shaped filament with silica gel technique to measure the isotopic compositions of Ru in the Alledé and Leoville carbonaceous chondrite. The potential interferences on masses 100 and 104 were found, although the sensitivity was improved considerably. To get accurate result without any additional interferences, no modifier is used in our work. 10  $\mu$ g of Ru (Aldrich) is loaded on Re filament to create a strong ion beam. And the zone-refined Re filament is carefully outgassed at 5A over 3 hours beforehand in order to reduce isobaric interferences by Mo emitted from the filament.

After corrections for interfering impurity ions, the results are normalized using  $^{102}\text{Ru}/^{99}\text{Ru}=2.47404$  for direct comparison of the data with those of Pothes et al.. The deviations about  $+0.5\epsilon$  and  $+10\epsilon$  on masses 100 and 104 are found, respectively. The interfering species are most probably to be  $^{40}\text{Ca}^{28}\text{Si}^{16}\text{O}_2$  and  $^{88}\text{Sr}^{16}\text{O}$  due to the silica gel technique used in their work, although they carefully tried to eliminate the interferences.

It is interesting to find that there appears to be about  $-10\epsilon$  deviation in mass 98 as compared with the result of Pothes et al.. However, further research work is necessary to make it sure.

Pothes, H., Schmitt-Strecker, S., and Bege-  
mann, F., 1987, *Geochim. Cosmochim.*  
*Acta*, v. 51, p. 1143.

IMPLICATION FOR THE EVOLUTION OF THE  
LITHOSPHERE IN SOUTHERN AFRICA FROM ISOTOPE  
SYSTEMATICS IN GRANULITE XENOLITHS

HUANG, Y.-M., VAN CALSTEREN, P. AND  
HAWKESWORTH, C. J., Department of Earth Sciences,  
Open University, Milton Keynes MK7 6AA, U.K.

The nature and evolution of the lower crust around the margins of Archaean cratons is not well constrained. New data are presented on granulite facies xenoliths from kimberlite pipes in N. Lesotho and the Markt area, Namaqualand, southern Africa, close to the margins of the Kaapvaal Craton. Granulites from both areas have similar major element compositions with  $\text{SiO}_2$  between 46-51%. Sr and Nd isotope ratios are 0.70479-0.70723 and 0.51251-0.51149 respectively in the Markt granulite xenoliths, which have, on average, higher Sr and lower Nd isotope ratios than those in the N. Lesotho granulites<sup>1</sup>. Whole rock Sm-Nd isotope data from the Markt granulites scatter on an errochron, corresponding to  $1.18\pm 0.2$  Ga, within error of the age of  $1.24\pm 0.17$  Ga for the N. Lesotho granulites. Selected mineral (cpx, gt, plag)-whole rock isochrons from Markt yield ages of  $851\pm 56$  and  $604\pm 36$  Ma, and one from Lesotho gives an age of  $595\pm 10$  Ma.

Measured  $^{206}\text{Pb}/^{204}\text{Pb}$  ratios from the N. Lesotho granulites range from 16.25 to 17.58, and  $^{207}\text{Pb}/^{204}\text{Pb}$  from 15.19 to 15.58. All but two of the granulites from N. Lesotho fall on an array which yields an age of  $1.49\pm 0.36$  Ga. This age is indistinguishable within error from their Sm-Nd whole rock age. In contrast, the Markt granulites have  $^{206}\text{Pb}/^{204}\text{Pb}$  ratios in the range 15.17 to 17.67, with relative low  $^{207}\text{Pb}/^{204}\text{Pb}$  ratios between 14.87 to 15.10. These data fall on a trend corresponding an age of  $3.19\pm 0.04$  Ga, which is much older than either the Pb-Pb age for the N. Lesotho samples and their own Sm-Nd age. Mineral-whole rock Pb-Pb isochrons from two Markt granulites with low whole rock Pb isotope ratios give ages of  $2.93\pm 0.07$  and  $2.91\pm 0.08$  Ga, respectively.

Thus, both Sm-Nd and Pb-Pb whole rock ages indicate that the N. Lesotho granulite xenoliths were mostly derived from a Proterozoic lower crust. However, taken at face value, Pb isotope data for the granulite xenoliths from Markt indicate Archaean ages. Correlations between major and trace element data indicate that the granulite xenoliths from Markt are genetically related and preclude simple mixing models for the Pb-Pb trend. Contamination from kimberlites is also unlikely because there is no correlation between Pb contents and isotope compositions. There are two explanations for the Pb and Nd isotope systems, one is that the Pb-Pb trend from the Markt granulites was been inherited from an Archaean lithospheric mantle source and the Sm-Nd whole rock age represents the time of the lower crust generation. Alternatively, ages of 2.9 Ga yielded by the mineral-whole rock isochrons from two U-depleted samples represent early metamorphic ages, and the Markt granulites are inferred to have been derived from the mantle in the Archaean, probably at 3.2 Ga as indicated by the whole rock Pb-Pb age. In this explanation, the Nd whole rock age may reflect re-equilibration in an Archaean lower crust during the generation of Proterozoic crust, which in turn implies that Sm and Nd have higher diffusion rates than U and Pb, consistent with the conclusions of recent geochronological studies<sup>2,3</sup>.

1 Rogers and Hawkesworth, 1982, *Nature* 299, pp. 409-413.

2 Burton et al., 1993, *Terra Nova* 5, pp. 382.

3 Mezger et al., 1992, *Earth Planet. Sci. Lett.* 113, pp. 397-409.

HUHMA, Hannu, Geological Survey of Finland, 02150 Espoo, Finland

The continental crust in the Svecofennian Domain of the Fennoscandian Shield was mostly formed between 1.91 and 1.86 Ga. The U-Pb zircon ages on gabbros and synorogenic granitoids are generally 1.87-1.89 Ga. Some felsic volcanics are slightly older at ca. 1.91 Ga. The initial  $\epsilon$ -values for mafic rocks range from 0 to +3, and the felsic rocks have a range from -1 to +3. Most detrital zircons from the Svecofennian metasediments analysed by SIMS are 1.9-2.05 Ga old (Huhma et al., 1991\*). Due to mixtures between Archaean and Proterozoic crystals apparent conventional multi-grain U-Pb zircon ages of these samples are about 2.2-2.3 Ga, which are also close to the Nd-model ages  $T_{DM}$ . As the ion micro-probe results are quite similar in eight samples throughout the Svecofennian domain, it is likely that all metasediments (including palaeosomes in migmatites) with an average zircon age of 2.2-2.3 Ga represent analogous mixtures of Archaean and Proterozoic components. There are quite a few such zircon data from various parts of the Shield (including samples from southern Sweden, Estonia, southern and central Finland, "upper Kalevian" in eastern Finland, and even the Lapland granulite belt). All this calls for large 1.9-2.05 Ga crustal blocks in erosion position at about 1.9 Ga ago, and an effective mixing and transport processes that filled the Svecofennian basins after the formation of the 1.97 Ga Jormua and Outokumpu ophiolites. The site of this ca. 2 Ga felsic crust remains unknown.

Excluding detrital materials, the oldest zircon ages from the Svecofennian domain have been measured from gneissose tonalites near the palaeosuture in Central Finland (ca. 1.93 Ga). These rocks have been sometimes described as domes and considered as possible candidates for reworked older (Archaean) crust. The Sm-Nd data on several samples, however, provide  $\epsilon_{Nd}(1.93)$  values of about +3, which clearly show that these rocks represent new Proterozoic crust. Geochemical data on some of these rocks suggest that they probably originated through melting of a low-K island arc tholeiite source leaving gabbroic to amphibolitic residue. In the Pyhäsalmi area also a 1.92 Ga felsic volcanic rock adjacent to the gneissic tonalites provides a positive  $\epsilon$  of +3.4. These Sm-Nd data together with analyses on slightly younger (1.88-1.89 Ga) granitoids suggest that juvenile rocks with positive  $\epsilon_{Nd} \approx +3$  occur mainly in a "belt" adjacent to the Archaean craton. The Pb isotopes from the Svecofennian galenas show an analogous pattern: The  $\mu$ -values get higher further away from the Archaean crust.

There are thus several felsic rocks which yield initial isotopic signatures similar to the convective upper mantle. In fact initial  $\epsilon$ -values for many mafic rocks (eg. Haveri and Jormua) are less positive, suggesting involvement of older LREE enriched lithosphere in their genesis.

\*Huhma, H., Claesson, S., Kinny, P.D. and Williams, I.S., 1991. The growth of Early Proterozoic crust: New evidence from Svecofennian detrital zircons. *Terra Nova*, 3, 175-179.

HULSTON, J. R., Nuclear Sciences Group, Institute of Geological & Nuclear Sciences, PO Box 31-312, Lower Hutt, New Zealand; KAPLAN, I. R. and JEFFEREY A., Global Geochemistry Corporation, 6919 Eton Avenue, Canoga Park, CA 91303, USA; HILTON, D. R., Isotope Laboratory, Scripps Institution of Oceanography, University of California, San Diego, La Jolla, CA 92093, USA (Present address: Laboratorium Isotopen-geologisch Onderzoek, Vrije Universiteit Amsterdam, De Boelelaan 1085, 1081 HV, Amsterdam).

The chemical and isotopic compositions of the gases from Maui, Kapuni and Kupe South hydrocarbon fields of the Taranaki Basin of New Zealand display distinct differences. The Maui gas contains almost 10% ethane and higher hydrocarbons, with small quantities of CO<sub>2</sub> and N<sub>2</sub>. The iso/n-butane ratio indicates a mature gas, and the methane is isotopically rather heavy compared to deep sedimentary gas from areas such as the Permian Basin of West Texas. The Kapuni gas is wetter than the Maui gas, and is much richer in CO<sub>2</sub>, which appears to be derived from decomposition of organic matter, based on the light carbon isotope value ( $\delta^{13}C$  -14.5‰). The Kupe S gas is also wet but contains virtually no CO<sub>2</sub>. The Kapuni and Kupe S gases are both less mature than the Maui gas as shown by the higher iso/n-butane ratio and the lighter methane  $\delta^{13}C$  value (-42.6‰). The two groups of gases when plotted on the genetic characterization diagram of Schoell fall within the regime of gas associated with condensate.

The most striking difference between the two groups of gases is the helium content and its isotopic ratio. The Maui gas is over an order of magnitude higher in helium concentration (up to 190 ppm) and its  $^3He/^4He$  ratio ( $3.8R_A$  where  $R_A =$  the air  $^3He/^4He$  ratio of  $1.4 \times 10^{-6}$ ) is approximately half that of upper mantle helium issuing from volcanic vents of the Taupo volcanic zone. In contrast, the Kapuni and Kupe S natural gases have little or no mantle input ( $0.08-0.19R_A$ ) and low helium concentrations (12-19ppm). This indicates that up to half of the helium in the Maui gas field could be of upper mantle origin and is most likely related to the subduction system that generates the volcanic arc to the east.

The isotopic ratios of helium and carbon in methane and carbon dioxide are found to vary consistently and significantly from NE to SW across the Maui field. With the exception of carbon dioxide content, the differences between Kapuni and Kupe S are less significant than those across the Maui field.

Two major processes can be envisioned to account for the hydrocarbon-rich,  $^3He$  rich gas in the Maui field: (1) Mixing of a hydrocarbon-rich gas with a  $^3He$  rich gas of deep origin. (2) Intrusion of  $^3He$  bearing magmas into shallower than normal petroleum source sediments.

The evaluation of these processes needs to consider that release of  $^3He$  enriched helium from magmatic intrusions usually involves generation of considerable quantities of volatiles, either from the magma itself or by heating of crustal rocks.

## IMPLICATIONS OF MANTLE HELIUM IN TARANAKI BASIN, NEW ZEALAND, NATURAL GAS WELLS

HULSTON, J. R., Nuclear Sciences Group, Institute of Geological & Nuclear Sciences, PO Box 31-312, Lower Hutt, New Zealand; KAPLAN, I. R. and JEFFEREY A., Global Geochemistry Corporation, 6919 Eton Avenue, Canoga Park, CA 91303, USA; HILTON, D. R., Isotope Laboratory, Scripps Institution of Oceanography, University of California, San Diego, La Jolla, CA 92093, USA (Present address: Laboratorium Isotopen-geologisch Onderzoek, Vrije Universiteit Amsterdam, De Boelelaan 1085, 1081 HV, Amsterdam).

The chemical and isotopic compositions of the gases from Maui, Kapuni and Kupe South hydrocarbon fields of the Taranaki Basin of New Zealand display distinct differences. The Maui gas contains almost 10% ethane and higher hydrocarbons, with small quantities of CO<sub>2</sub> and N<sub>2</sub>. The iso/n-butane ratio indicates a mature gas, and the methane is isotopically rather heavy compared to deep sedimentary gas from areas such as the Permian Basin of West Texas. The Kapuni gas is wetter than the Maui gas, and is much richer in CO<sub>2</sub>, which appears to be derived from decomposition of organic matter, based on the light carbon isotope value ( $\delta^{13}\text{C}$  -14.5‰). The Kupe S gas is also wet but contains virtually no CO<sub>2</sub>. The Kapuni and Kupe S gases are both less mature than the Maui gas as shown by the higher iso/n-butane ratio and the lighter methane  $\delta^{13}\text{C}$  value (-42.6‰). The two groups of gases when plotted on the genetic characterization diagram of Schoell fall within the regime of gas associated with condensate.

The most striking difference between the two groups of gases is the helium content and its isotopic ratio. The Maui gas is over an order of magnitude higher in helium concentration and its <sup>3</sup>He/<sup>4</sup>He ratio is approximately half that of upper mantle helium issuing from volcanic vents of the Taupo volcanic zone. It is over two orders of magnitude higher than in Kapuni and Kupe S natural gases which have no apparent mantle input. This indicates that up to half of the helium in the Maui gas field could be of upper mantle origin and is most likely related to the subduction system that generates the volcanic arc to the east.

The isotopic ratios of helium and carbon in methane and carbon dioxide are found to vary consistently and significantly from NE to SW across the Maui field. With the exception of carbon dioxide content, the differences between Kapuni and Kupe S are less significant than those across the Maui field.

Two major processes can be envisioned to account for the hydrocarbon-rich, <sup>3</sup>He rich gas in the Maui field: (1) Mixing of a hydrocarbon-rich gas with a <sup>3</sup>He rich gas of deep origin. (2) Intrusion of <sup>3</sup>He bearing magmas into shallower than normal petroleum source sediments.

The process of release of <sup>3</sup>He enriched helium from magmatic intrusions appears to involve generation of considerable quantities of volatiles, either from the magma itself or by heating of crustal rocks. Mixing of such a gas with a shallower hydrocarbon gas should result in considerably higher quantities of carbon dioxide, nitrogen or hydrogen than is observed. The only sizable quantities of diluting components in the Maui gas are hydrocarbons.

## THIRTY-TWO YEARS OF GEOCHRONOLOGICAL WORK IN THE CENTRAL AND WESTERN ALPS: A REVIEW ON SEVEN MAPS

HUNZIKER, J.C., Inst. de Minéralogie, UNIL BFSH2, Lausanne, 1015-CH, Switzerland, and DESMONS, J., C.N.R.S. C.R.P.G., 15 r. N.D. des Pauvres, B.P. 20, Vandoeuvre-lès-Nancy Cedex, 54501, France, and HURFORD, A. J., Dept. of Geological Sciences, University College, London, WC1E6BT, UK.

This paper represents a review of the last 32 years of geochronological work in the Central and Western Alps. Some of these data, distributed in over 240 papers, are poorly accessible, thus starting to fade away from the view of Alpine geologists. The data have been represented on 7 maps, 3 of which, at a scale of 1:800'000, cover the area from the Alpine/Apennine boundary near Genova, through to the western Silivretta. Map I contains Rb-Sr data, map II summarizes the K-Ar and Ar-Ar mineral data. Map III shows U-Pb and whole rock data, and therefore represents our knowledge of the pre-Alpine history. The ages on maps I and II are represented by a colour code, the symbol on the maps represents the mineral concerned. A number, printed near the symbol leads to the references, which are given both in numerical and alphabetical order. 4 maps of the Central Alps are at a scale of 1:635 000, Maps IV and V give the fission track data for apatite and zircon respectively. On maps VI and VII, the K-Ar and Rb-Sr data are given respectively at the same scale for direct comparison. All ages are calculated using the IUGS recommended constants.

The present compilation of joint geochronological research in the Central and Western Alps reveals surprising inhomogeneities both in regional and temporal distribution. The Western Alps contain practically no Rb-Sr and U-Pb data. A majority of the data deals with the Alpine metamorphism and with the cooling after the Alpine orogeny. From pre-Variscan times, only little can be said with certainty, no pre-Variscan mica ages having been found so far. In the Austroalpine/Southalpine units, mica ages between 240 and 140 Ma mark the slow uplift and cooling of these zones, from lower to upper crustal conditions.

The Eoalpine orogeny has been subdivided into an early eclogitic stage (140-85 Ma) and a later blueschist and cooling stage (85-60 Ma). The coincidence of two or more different chronometers facilitates the interpretation of the Eoalpine age data.

The Tertiary has been subdivided into 2 phases, the  $\pm 30$  Ma calcalkaline magmatism subdividing the Cenozoic era into the Mesoalpine and Neoalpine.

The 45-30 Ma period marks the Mesoalpine metamorphic phase, found dominantly outside the area. therefore The term Lepontine phase (as used by the Bern group) for this age range implies a more local distribution and is thus inappropriate.

Ages between 30 and 0 Ma mark the Neoalpine event, subdivided (arbitrarily at 15 Ma - a more or less quiet period) into early and

Late Neoalpine.

The Alpine movements of major tectonic lines, such as the Insubric line, the Simplon line and the Aosta-Ranzola line, have been dated both during their ductile as well as their brittle movements, by means of mineral ages. Thus periods of polyphase Alpine movements, ranging from as early as Jurassic and lasting throughout the whole Tertiary have been identified.

REGIONAL THERMO-TECTONIC HISTORIES OF THE RHINE GRABEN AND ADJACENT HERCYNIAN BASEMENT: A KEY TO ASSESSING THE ALPINE INFLUENCE IN NORTH-WEST EUROPE?

HURFORD, Anthony J., CARTER, Andrew, Research School of Geological Sciences, Birkbeck College and University College London, London WC1E 6BT, U.K. and BRIX, M., Institut für Geologie, Ruhr-Universität Bochum, D-4630 Bochum-1, Germany.

Published and unpublished apatite fission data for UK crystalline and sediment samples have identified a regional late Cretaceous to early Tertiary cooling event which, in part, is associated with important basin inversions in the North and Irish Sea hydrocarbon fields. Plausible mechanisms considered for this major cooling event relate to either rifting of the north-east Atlantic and/or the synchronous Laramide phase of deformation in the Alpine domain. The extent and magnitude of Alpine thermo-tectonic effects in north-west Europe is poorly defined. Although the Massif Central, Rhenish Shield and Bohemian Massif were most probably exhumed at around  $k/T$  boundary times, the precise amounts and mechanisms are subject to much debate. The formation of the European Cenozoic Rift System coincident with Alpine deformation, and with identical principal stress directions suggests, it should provide a sensitive record of the effect and extent of Alpine deformation in the European plate. In a major study, 150 samples from the Rhenish Massif and Rhine Graben have provided new apatite fission track data as part of a wider study throughout north-west Europe from the Alps to the Atlantic margins. Interpretation of initial results from the Rhine Area confirm the Upper Cretaceous timing of initial rifting, and associated flank uplift and high heat-flow. Results from outcrop and borehole samples in sediments in the rift itself provide clear evidence that the present-day high heat-flow is a very recent phenomenon. Discussion will be offered of the significance of the Rhine data to our wider understanding of the thermal and tectonic histories of north-west Europe.

INTERSTELLAR DIAMONDS IN METEORITES

HUSS, G. R., Lunatic Asylum, Division of Geological and Planetary Sciences, California Institute of Technology, Pasadena, CA 91125

Nanometer-sized diamonds were the first objects isolated from meteorites that could be shown with reasonable certainty to have originated outside of the solar system. They have been found in the least metamorphosed members of all classes of chondritic meteorites. The extra-solar-system origin of the diamonds is shown by the isotopic compositions of several trace elements (e.g., noble gases, H, N, Ba), which differ from bulk solar system values in ways not accounted for by known solar-system processes. Their presence within chondrites, which date from the formation of the solar system, indicates that the diamonds pre-date the solar system.

Interstellar diamonds are very small,  $\sim 2$  nm ( $20\text{\AA}$ ) in diameter, and each contains only a few thousand carbon atoms. Diamonds are the most abundant interstellar grains with abundances in unmetamorphosed 'matrix' material of 0.1–0.3% (vs. 10–14 ppm SiC, 2–10 ppm graphite, 5–10 ppb  $\text{Al}_2\text{O}_3$ ). Trace elements in diamonds exhibit large isotopic anomalies. For example, Xe-HL is enriched 2x in the lightest and heaviest isotopes relative to solar-system Xe. Nitrogen is highly enriched in  $^{14}\text{N}$  ( $\delta^{15}\text{N} \approx -345\text{‰}$ ). Ba has excesses of r-process isotopes. In combination, these isotopic signatures point toward supernovae as the nucleosynthetic source. Interestingly, the isotopic composition of the carbon ( $\delta^{13}\text{C} = -32$  to  $-38\text{‰}$ ) falls within the range of terrestrial carbon.

The process by which diamonds form is not understood, but three basic mechanisms are under consideration. 1) Diamonds may condense directly in stellar outflows. H-rich stellar ejecta is similar in composition to the gases used to produce diamond films by chemical vapor deposition (CVD). 2) Diamonds may be formed from graphite through shock pressure during grain-grain collisions in interstellar space. 3) Diamonds may be produced from graphite or organic material either through annealing of particles by ultra-violet irradiation or through restructuring induced by collisions with energetic particles. Of these ideas, direct condensation of diamond seems to have the fewest problems.

Because diamonds contain so few atoms, isotopic compositions can be measured only on bulk samples and it is not known how many sources contributed to the measured compositions. Measurements of individual SiC and graphite grains, which apparently provide 'snapshots' of conditions in the stellar atmosphere where they formed, show that these grains come from many stars. Thus, it is likely that the more-abundant diamonds also come from more than one star. If so, then the isotopic characteristics of diamonds do not represent a distinct source, which helps explain why such a source has not been identified.

The abundance of diamonds indicates that either diamond production is much more efficient than production of other presolar grains or that the diamonds are less subject to destruction in interstellar space. Division Contribution 5366 (840) Supported by NASA NAGW-3040, NAGW-3297.

Anders E. and Zinner E. (1993) Interstellar Grains in Primitive Meteorites: Diamond, Silicon Carbide, and Graphite: *Meteoritics*, v. 28, p. 490–514.

Huss, G. R. and Lewis, R. S. (1994) Noble Gases in Presolar Diamonds I: Three Distinct Components and Their Implications for Diamond Origins: *Meteoritics*, in press.

## CARBON AND NITROGEN ISOTOPIC COMPOSITION OF MOISSANITE IN YAKUTIAN KIMBERLITES

I.D. Hutcheon, Lunatic Asylum, Caltech, Pasadena, CA 91125 and Lawrence Livermore Laboratory, Livermore, 94551; E.A. Mathez, R.A. Fogel, American Museum of Natural History, New York, NY 10024; V.K. Marshintsev, National Centre for Research, 677892 Yakutsk, Russia

Trace quantities of moissanite (a-SiC) occur in mineral concentrates of diamond-bearing kimberlites and lamproites but little information about the chemical and isotopic composition, stability in upper mantle rocks and origin of SiC is available. We present new data on C and N isotope abundances, minor element chemistry and inclusion mineralogy of moissanite from the Mir and Aikhal kimberlite pipes, Yakutia. Moissanite was recovered from ~700-800 kg of kimberlite drill core and occurs as elongate (0.5-1 mm), gemmy crystals varying in color from a characteristic blue-green to pale green to nearly colorless to blue-black [1]. Iron (<940 ppm) is present in nearly all crystals; Al (<920 ppm), Ca (<100 ppm), V (<270 ppm), Cr (<330 ppm) and Mn (<200 ppm) were also detected. No correlation between color and chemistry is apparent. Moissanite contains a variety of mineral inclusions. The most common is metallic Si (up to 100  $\mu\text{m}$  in size). Several, compositionally distinct Fe- and Fe-Ti-Zr-silicides were observed, typically at Si metal-SiC contacts. The Ti-rich silicides contain high levels of LREE (up to 16% Ce) and Th (up to 4%). Two O-bearing phases occur in SiC: sinoite ( $\text{Si}_2\text{N}_2\text{O}$ , previously found only in enstatite chondrites) and a rare earth silicate containing ~75% LREE-oxides. This unusual inclusion mineralogy is unknown in synthetic SiC and is further evidence the Mir and Aikhal moissanites are natural.

Ion probe analyses of 23 individual SiC crystals reveal a tight distribution of C isotope compositions:  $-32\text{‰} < \delta^{13}\text{C} < -26\text{‰}$ ; individual SiC are homogeneous in  $\delta^{13}\text{C}$  within  $\pm 1.5\text{‰}$ . One micro-diamond recovered from the Mir SiC fraction has  $\delta^{13}\text{C} = -30.7 \pm 2.1\text{‰}$ , while the mean of all SiC analyses is  $\delta^{13}\text{C} = -28.3 \pm 3.4\text{‰}$ . In contrast, most "large" diamonds from Mir and Aikhal have  $\delta^{13}\text{C}$  in the normal mantle range of -8 to -3‰ [2]. Moissanite in the Fuxian kimberlite is similarly enriched in  $^{12}\text{C}$  relative to diamond [3]. Two moissanites contain, respectively, 53 and 140 ppm N with  $\delta^{15}\text{N}$  of  $9.7 \pm 4.0\text{‰}$  and  $5.6 \pm 2.2\text{‰}$ . The difference in C isotope composition between moissanite and diamond within kimberlites is not plausibly attributed to fractionation of a homogeneous mantle C reservoir and appears to require isotopically heterogeneous mantle C sources. Based on the C and N isotope abundances and the requirement of an  $f(\text{O}_2)$  more than  $10^6$  times lower than the IW buffer, we suggest moissanite formed by metamorphism of reduced, carbonaceous sediments during subduction.

Refs.: [1] Marshintsev, V.K. (1990) *Mineral Mag.* **12**, #3, 17-26 (in Russian); [2] Galimov, E.M. (1991) *SS*, 1697-1708; [3] Leung, I.S., et al. (1990) *Nature* **346**, 352-354.

## DATING HIGH PRESSURE METAMORPHISM IN THE WESTERN ALPS; REFINING ISOTOPIC AND TECTONIC INTERPRETATIONS

INGER, Simon, Department of Earth Sciences, University of Leeds, Leeds, LS2 9JT, UK, and CLIFF, Bob, Department of Earth Sciences, University of Leeds, Leeds, LS2 9JT, UK.

The Western Alps record a collision orogeny in which basement rocks of both continents, and oceanic units, preserve eclogite facies assemblages. Understanding the timing of their polymetamorphic histories is crucial to geodynamic reconstructions of the belt, which have long assumed "Early Cretaceous" eclogite metamorphism in all such units. These models may need revision in light of increasing isotopic indications of high pressure conditions persisting into the Tertiary in some units. As with all metamorphic geochronology, meaningful age determinations rely upon adequate understanding of the relationships between mineral formation, thermal history and chemical equilibrium, which are not always clear in eclogite assemblages.

Polymetamorphic marbles in the Eclogitic Micaschist Complex of the Sesia Zone basement have well-preserved eclogite facies assemblages which post-date amphibolite-granulite facies relics. High-alumina titanite yields U-Pb ages from 140 to 107Ma, while phengite Rb-Sr ages range from 58-61Ma. A cover sequence believed to have experienced *only* the high pressure event gives a U-Pb titanite age of 66Ma, indistinguishable from the Rb-Sr ages on coexisting phengites and Sm-Nd garnet ages from eclogites in the underlying ophiolitic Piémont Unit. Titanites in polymetamorphic samples may therefore contain inherited lead, whereas those in the monometamorphic marble crystallised at the eclogitic stage.

The lower portion of the Sesia Zone - the Gneiss Minuti Series - has been pervasively metamorphosed under greenschist facies conditions at 38-39Ma, and may have suffered a common earlier history with the upper unit despite the absence of convincing eclogitic relics. Titanite from a calc-silicate rock within this unit yields a U-Pb age of 249Ma, the age of the Variscan magmatism and metamorphism which generated the protoliths of these units. By contrast with those in the EMC, these titanites have therefore survived greenschist-facies, and possibly eclogite-facies, overprinting without lead exchange or new crystal growth.

Underlying the Sesia Zone, the Piémont Unit contains metasedimentary and metabasic rocks of oceanic affinity whose lowermost subdivision records eclogite conditions. Greenschist-facies regional metamorphism in the eclogitic and non-eclogitic sections is dated at 38-39Ma by white mica Rb-Sr analyses. These fabrics are reworked by a top-to-SE-directed greenschist shear fabric which may be dated by 34Ma Rb-Sr ages from micas throughout the zone. This fabric defines a regionally significant shear zone which may backthrust more external units into the high grade nappe pile, or may have been responsible for the extensional unroofing of the eclogitic Piémont units. In either case, constraining differences in thermal (and baric) histories across such structures by structurally-focussed isotopic studies offers the best means to distinguish between geodynamic models.

**STRONTIUM, OXYGEN, AND CARBON ISOTOPIC RECORDS OF PALEOSALINITY AND PALEO-STREAMFLOW IN ESTUARINE SEDIMENTS**

INGRAM, B.L., Dept. of Geology and Geophysics, University of California, Berkeley CA, 94720

Strontium, oxygen, and carbon isotopic compositions of molluscan and foraminiferal carbonate from estuarine sediments cored beneath San Francisco Bay are used to derive a record of salinity and average freshwater inflow to the estuary for the past several thousand years. The large difference in the  $^{87}\text{Sr}/^{86}\text{Sr}$  ratio between seawater (0.7092) and the freshwater sources to the estuary (0.7065) produces a correlation between  $^{87}\text{Sr}/^{86}\text{Sr}$  and salinity in bay waters that can be detected with high-precision measurements. Similarly, the oxygen and carbon isotopic composition varies between  $\delta^{18}\text{O}$  and  $\delta^{13}\text{C}$  values of about -12‰ and 14‰ for river water, and 0‰ and 1‰ in seawater. Paleosalinity is inferred from the  $^{87}\text{Sr}/^{86}\text{Sr}$ ,  $^{18}\text{O}/^{16}\text{O}$ , and  $^{13}\text{C}/^{12}\text{C}$  ratios measured in calcite from fossil bivalves (*Macoma balthica* and *Mytilus edulis*) and foraminifera (*Ammonia becarrii* and *Elphidiella hannai*) preserved in the sediment. Because salinity in San Francisco Bay is primarily controlled by the freshwater inflow from the Sacramento and San Joaquin rivers, the paleosalinity record can be converted to a paleo-discharge record using a transfer function derived from historic data.

The Sr isotopic data indicate there were extended periods (several hundred years long) when salinity was significantly lower than the modern, pre-diversion salinity, indicating higher freshwater inflow, particularly prior to 2500 years ago. There were also periods of high salinity, indicating low freshwater inflow, between 2500 years and the present. Modern freshwater inflow appears exceptionally low, less than one-half of the 4300-year average. High resolution  $\delta^{18}\text{O}$  indicates cyclical variations in salinity in San Francisco Bay with periodicities of 500, 200, 90, and 55 years, similar to those seen in the  $\Delta^{14}\text{C}$  production rate, implying a common forcing mechanism linked to fluctuating solar activity. The data generally agree with other proxy climate records in California, such as lake level records from eastern California and Nevada, tree-ring records, and treeline fluctuations.

**OXYGEN AND CARBON ISOTOPIC RECORDS OF PALEOSALINITY IN SAN FRANCISCO BAY**

INGRAM, B.L., Dept. of Geology and Geophysics, University of California, Berkeley CA, 94720, INGLE, J. C., Dept. of Environmental and Geological Sciences, Stanford University, Stanford, CA 94305, and CONRAD, M. E., Earth Science Division, Lawrence Berkeley Lab, Berkeley, CA, 94720.

Oxygen and carbon isotopic compositions of molluscan shells separated from San Francisco Bay estuarine sediments are used to derive a high-resolution record of salinity variations over the past 5000 years. The large difference in the  $\delta^{18}\text{O}$  value of seawater (-0‰) and the freshwater inflow (-11‰) produces a simple mixing relation between  $\delta^{18}\text{O}$  and salinity in bay waters that is recorded in fossil carbonate shells. Similarly, the  $\delta^{13}\text{C}$  varies between about -14‰ for river water, and 1‰ for seawater.

The  $\delta^{18}\text{O}$  of river water entering the Bay through the Delta over a three-year period (1991-1993) varied by about 1-2‰ between wet and dry years, with average values during wet years of about -12‰. Because salinity in San Francisco Bay is primarily controlled by the freshwater inflow from the Sacramento and San Joaquin rivers, the paleosalinity record can be converted to a paleo-discharge record using a transfer function derived from historic data.

The  $\delta^{18}\text{O}$  of the mussel (*Mytilus*) shells vary between -1‰ and -4‰ (averaging -2.6‰), corresponding to salinities of between 22‰ and 28‰ (averaging 25.5‰). Because modern salinity at this location is 28‰, we infer that the modern average river inflow into the Bay is significantly lower than that over the past 5000 years. The  $\delta^{13}\text{C}$  correlates with the  $\delta^{18}\text{O}$  variations downcore, indicating salinity (not temperature) is the primary control.

The  $\delta^{18}\text{O}$  data indicates cyclical variations in salinity and freshwater inflow in San Francisco Bay with periodicities of 500, 200, 90, and 55 years, similar to those seen in the  $\Delta^{14}\text{C}$  production rate. The data generally agree with other proxy climate records in California, such as lake level records from eastern California and Nevada, tree-ring records, and treeline fluctuations.

ZIRCON AGE DISTRIBUTIONS IN GRANITES,  
GREYWACKES, AND GNEISSES FROM THE  
SOUTHWEST PACIFIC GONDWANA REGION.

IRELAND, T.R., Research School of Earth Sciences,  
Australian National University, Canberra ACT 0200  
Australia, BRADSHAW, J. D., MUIR, R., WEAVER, S.,  
Department of Geology, University of Canterbury,  
Christchurch, New Zealand, and ADAMS, C., Institute of  
Geological and Nuclear Sciences, Lower Hutt, New Zealand

The southwest Pacific region consists of New Zealand, eastern Australia, and western Antarctica which were once contiguous on the margin of Gondwana prior to continental fragmentation and dispersal in the Cretaceous. Ion probe zircon dating offers a powerful method for the rapid characterization of terranes and sedimentary provenances in this region and allows correlations to be made across submerged areas. The ages yield direct chronological information on the source rocks and the zircon age profile can be used as a fingerprint for a given unit. In addition, U and Th concentrations can be used to place constraints on protoliths.

New Zealand has been broadly divided into two provinces on the basis of regional geology of the South Island. The western province consists of sediments, gneisses and granites of continental (Gondwana) affinity, while the eastern province consists predominantly of Permo-Triassic arc margin rocks that were accreted onto New Zealand.

In the western province, two major phases of granite plutonism are recognized in the Carbo-Devonian and Cretaceous. S-type granites have incorporated large components of Ordovician-Devonian Greenland Group greywacke. Metamorphic core complexes in the western province reveal Cretaceous gneisses that represent metamorphosed granite and greywacke protoliths. The Greenland Group greywackes have a characteristic zircon age profile consisting of a dominant peak at 500-650 Ma, a smaller peak at 1000-1200 Ma, a poorly defined peak at 1500-1600 Ma and a scattering of ages out to 3500 Ma. This is the same age profile as has been determined for zircons from Lachlan Fold Belt Ordovician sediments in southeastern Australia. This signature has also been traced into North Victoria Land and Marie Byrd Land, Antarctica, as well as Campbell Island to the south of New Zealand and indicates that these areas once formed a single contiguous sedimentary horizon.

The eastern province of New Zealand is dominated by the Torlesse terrane composed mainly of quartzofeldspathic greywackes and schists. Torlesse greywacke in the South Island is characterized by a major peak of Permian age, and a small but significant contribution of zircons with the western province greywacke signature. The Torlesse signature has been found on outlying Chatham Island and indicates an extensive horizon of this greywacke as well.

The sources of the greywackes still remain a matter of conjecture although the age profiles will allow better constraints to be placed on prospective source areas. The Torlesse terrane remains enigmatic in that it apparently contains western province material, but it is separated from the western province greywacke by intervening volcanogenic terranes which show no evidence of any western province contribution. The identification and further documentation of the Permian granites in the Torlesse will also be an important key to the source area.

DIVERSE ORIGINS OF FLUID IN MAGMATIC  
INCLUSIONS AT ASCENSION I., BINGHAM, BUTTE and  
ST. AUSTELL, INDICATED BY LASER MICROPROBE  
ANALYSIS OF Cl, K, Br, I, Ar, Kr and Xe.

IRWIN, J. J., Scripps Institution of Oceanography  
UCSD, La Jolla, California, 92093, ROEDDER, E.,  
Department of Earth and Planetary Science,  
Harvard University, Cambridge, Massachusetts,  
02138, U.S.A.

Saline fluid inclusions (FI) trapped at close to the temperature of solidification of a granitic melt occur at Bingham (Utah), Ascension Island (mid Atlantic Ocean) and St. Austell, (Cornwall). Slightly lower temperature FI occur at Butte (Montana). Argon, Kr and Xe were extracted from FI by laser microprobe decrepitation of minute portions of samples after neutron irradiation and measured in a low blank, high sensitivity mass spectrometer. Results enable measurement of abundances of Ca, Cl, K, Br, Se, Ba + Te, I and U simultaneously with  $^{36}\text{Ar}$ ,  $^{40}\text{Ar}$ ,  $^{84}\text{Kr}$  and  $^{129}\text{Xe}$  in FI within less than  $10^{-5}$  cc of quartz.

In all samples, the absolute and relative abundance of halogens and gases varies on a scale of less than a millimeter, reflecting different generations of FI. In most FI,  $^{40}\text{Ar}/^{36}\text{Ar}$  is greater than atmospheric,  $>3,000$  in some FI at Bingham. Average K/Cl values are consistent with high temperature fluid-rock equilibria. Overall, I/Cl and Br/Cl indicate a restricted range, with I/Cl in Ascension and Bingham FI between  $\sim 1$  and  $8 \times 10^{-5}$  and Br/Cl between 1 and  $3 \times 10^{-3}$ , similar to the composition of the Earth's mantle as indicated by halogens in basalts and diamonds. Slightly higher I/Cl and lower Br/Cl in FI from St. Austell and possibly Butte may indicate a crustal source of salinity.

Concentrations of  $^{36}\text{Ar}$  and  $^{84}\text{Kr}$  in FI at Butte are similar to fresh waters equilibrated with the atmosphere (ASW), with some Ar and Kr added from magmas. In contrast, many FI from Bingham, Ascension and St. Austell indicate  $\text{Cl}/^{36}\text{Ar} > 10^8$ , and  $^{84}\text{Kr}$  and  $^{36}\text{Ar}$  concentrations an order or magnitude less than fresh ASW, reflecting an unmodified magmatic origin

Systematic variations in  $^{40}\text{Ar}_g/\text{Cl}$ , I/Cl and Br/Cl between FI in different quartz veins at Bingham indicate trapping of fluids derived from an evolving magma system. The importance of multiple-component, elemental and isotopic analysis in defining fluid types is illustrated by these samples, where some FI groups have similar halogen abundances and different noble gas isotope ratios and vice-versa.

**STRONTIUM ISOTOPE VARIATIONS AS AN INDICATOR OF SEDIMENT REWORKING: THE UPPER OLIGOCENE - NEOGENE INTERVAL FROM ODP SITES 871 AND 872**

ISRAELSON, C., Institute of Geology, University of Copenhagen, Øster Voldgade 10, DK-1350 Copenhagen K, Denmark, PEARSON, P. N., Dept. of Earth Sciences, University of Cambridge, Downing Street, Cambridge, CB2 3EQ, U.K., and BUCHARDT, B., Institute of Geology, University of Copenhagen, Øster Voldgade 10, DK-1350 Copenhagen K, Denmark

Sr isotopes together with biostratigraphy are used to evaluate the subsidence and sedimentation history of the Limalok (ODP Site 871) and Lo-En (ODP Site 872) guyots in the western Pacific. Samples consist of remarkable well preserved planktonic foraminifera.

It is found that the Sr isotope data from pelagic sediments deposited after the drowning of the guyots not only reflect the variations in seawater isotopic composition during the Neogene but also the amount of sediment reworking. Limalok subsided and started to accumulate pelagic sediments about 20 ma BP and Lo-En about 27 ma BP.

The sediment accumulation was not continuous and sediments were considerably reworked at several intervals. Reworking may be recognised by: 1) a disparity between the biostratigraphic age and the "Sr age"; 2) an inconsistency between a bulk sediment sample and a single species sample and 3) by unexpected variation and reversals in the measured Sr curve.

In general, sediment reworking occurred during the initial pelagic sedimentation immediately after carbonate platform drowning. On Lo-En, another interval of moderate sediment reworking between 13 and 15 ma BP has been identified.

Reworking could be caused by ocean current which lead to migration of large carbonate sand dunes on top of the guyots.

**MODEL FOR NEW VOLCANISM IN CENTRAL JAPAN**

ITAYA, T and OKADA, T., Hiruzen Research Institute, Okayama University of Science, Okayama 700, Japan

In central Japan, the arc volcanism has been controlled by the two overlapping subducted slabs of the Pacific and Philippine Sea plates at least since 7 million years ago. The evolution from E-W to N-S trending volcanism in the Ryohaku-Hida mountains was due to the change of direction of movement of the Philippine Sea plate from northward to west-northwestward 4 million years ago and the resulting disappearance from the area of the subducted slab of the Philippine Sea plate which had previously obstructed the ascent of the magma derived from the underlying subducted slab of the Pacific plate (Shimizu and Itaya, 1993). This suggests that the further western region may have important implications with respect to the recent geotectonic evolution of central Japan and the potential in new volcanism.

The Kinki region including Osaka plain 200km SW of the Ryohaku-Hida mountains has many hot water springs which have high  $^3\text{He}/^4\text{He}$  ratios similar to the active geothermal gases (Wakita et al., 1987) though no active volcanism has been identified so far in the region. Deep bore holes sunk recently in the Osaka plain for the exploitation of underground water reservoirs allow sampling of deep waters unaffected by surficial processes. Okada et al. (in contr.) presented  $^4\text{He}$ ,  $^{20}\text{Ne}$ ,  $^{36}\text{Ar}$ ,  $^{84}\text{Kr}$  and  $^{132}\text{Xe}$  abundance patterns and He and Ar isotope ratios of the deep bore hole water samples to study the behavior of noble gases in underground waters. The elemental abundance patterns of representative noble gases show a progressive enrichment of the heavier noble gases (e.g.,  $^{84}\text{Kr}$ ,  $^{132}\text{Xe}$ ) compared with the composition of atmospheric air and that helium was found to be strongly enriched in deep bore hole water samples. Bore holes in sedimentary rocks that overly the pre-Tertiary basement contain He enriched in radiogenic  $^4\text{He}$  (e.g.,  $^3\text{He}/^4\text{He} = 0.5 \times 10^{-6}$ ). In contrast,  $^3\text{He}/^4\text{He}$  values in the bore holes reaching the Ryoke granitic basement were higher than the atmospheric value ( $1.4 \times 10^{-6}$ ), suggesting a release of mantle He through the basement. The highest recorded value (e.g.,  $8.2 \times 10^{-6}$ ) is in the range of arc volcanism.

These facts suggest a presence of shallow magma body beneath the Kinki district, which was derived from the mantle wedge on the 400km of Wadati-Benioff zone of the subducted slab of the Pacific plate because of recent disappearance of the subducted slab of the Philippine Sea plate underneath the Kinki region.

Shimizu, S. and Itaya, T., 1993, Plio-Pleistocene arc magmatism controlled by two overlapping subducted plates, central Japan, *Tectonophysics*, v.225, p.139-154.

Wakita, H., Sano, Y. and Mizoue, M., 1987, High  $^3\text{He}$  emanation and seismic swarms observed in a nonvolcanic forearc region. *J. Geophys. Res.*, v.92(B12), p.12539-12546.

**A LONG PALEOMONSOON RECORD FROM NORGAI PLAIN, EASTERN TIBET**

**ITO, E., KELTS, K., HAN, Y.,** Dept. Geology and Geophysics, Univ. of Minnesota, Minneapolis, MN 55455, USA; **WANG, Sumin., SHI, Yafeng,** Nanjing Inst. of Geography and Limnology, Academia Sinica, PRC.

The Qinghai-Tibetan Plateau is a key-climatic region controlling Asian monsoon and possibly as a trigger to global climate change. Clearly, long continuous Quaternary records are valuable for reconstructing timing, magnitude, and rate of change of the paleoenvironments associated with monsoon.

We recovered a long (120+ meters) core spanning at least 400,000 years from the Norgai Plain in 1992, and selected 150 mollusk and rare authigenic carbonate samples from zones representing maximum variability between marsh-like to carbonate lacustrine muds. Norgai Plain is a large, flat, marshy, intermontane basin at 3500 m elevation along the eastern margin of the Tibetan Plateau where it currently receives monsoon moisture annually. Throughout the Quaternary the plain has been a lake basin with alternating warm-interval marsh facies and cold-interval green-gray, calcareous shallow lacustrine muds.

Preliminary results of stable isotope analysis of mollusk fragment samples revealed a  $\delta^{18}\text{O}$  variation of -5.5 to -9.5 ‰ (PDB) which is roughly covariant with  $\delta^{13}\text{C}$  with a range of -5.0 to -10.5 ‰. There are four positive isotope excursions which correlate with marsh facies, consistent with stronger monsoonal periods. The timing of these excursions is under study, but appears to be between 100 to 150 kyrs which would place marsh facies equivalent to interglacials. Because the Norgai record of paleohydrology represents a SE Asian monsoon signature, it may not necessarily correlate with loess stratigraphy which tracks ice sheet dynamics.

**$^{10}\text{Be}$  AND  $^{26}\text{Al}$  EXPOSURE DATING OF THE SIRIUS FORMATION, TABLE MOUNTAIN, ANTARCTICA**

**IVY, S. D.,** Ingenieurgeologie and Institut für Teilchenphysik, ETH Hönggerberg, CH-8093 Zürich, Switzerland, **SCHLÜCHTER, C.,** Geologisches Institut, Universität Bern, CH-3012 Bern, Switzerland, **KUBIK, P.W.,** Institut für Teilchenphysik, ETH Hönggerberg, CH-8093 Zürich, Switzerland, **BRUNO, L.,** Isotopengeochemie, ETH Zürich, CH-8092 Zürich, Switzerland, and **BEER, J.,** EAWAG, CH-8600 Dübendorf, Switzerland.

We are measuring the concentrations of  $^{10}\text{Be}$  and  $^{26}\text{Al}$  in a suite of samples from the Sirius Formation and associated bedrock surfaces from Table Mountain, Antarctica (Schlüchter et al., 1994). Exposure dating of the Sirius using these isotopes has been thwarted by the rareness of quartz-bearing lithologies, although  $^3\text{He}$  and  $^{21}\text{Ne}$  have been successfully measured in clinopyroxenes from Sirius dolerite boulders (Bruno et al., 1994).

So far, we have measured  $^{10}\text{Be}$  on quartz from sandstones and quartzites from Beacon Supergroup surfaces, and quartzite and granite boulders possibly associated with the Sirius drift. Exposure dates were calculated using the production rates and scaling factors of Lal (1991). Our preliminary exposure ages in the million-year-plus range for the granite clasts, which had not been previously recognized as belonging to the Sirius, are intriguing. Saturation  $^{10}\text{Be}$  values obtained on the quartzites of the Beacon surface (outside Sirius Formation and topographically higher) indicate that this landscape was carved at least 5 Ma ago. These speculations are being checked with our ongoing  $^{26}\text{Al}$  measurements.

Interpretations about the age of the Sirius drift must be constrained by comparison of  $^{10}\text{Be}$  and  $^{26}\text{Al}$  to elucidate erosion rates, as well as by combination with the noble gas results (Bruno et al., 1994). The full set of isotopes ( $^{10}\text{Be}$ ,  $^{26}\text{Al}$ , and  $^{21}\text{Ne}$  in quartz and  $^{10}\text{Be}$ ,  $^3\text{He}$ , and  $^{21}\text{Ne}$  in clinopyroxene, whose closed system behavior for  $^{10}\text{Be}$  is still being checked) are necessary to draw real conclusions about the exposure ages of these rocks.

Bruno et al., 1994, Dating of geomorphologic surfaces in the Antarctic Dry Valleys with in situ produced cosmogenic  $^3\text{He}$  and  $^{21}\text{Ne}$  (abstract this volume).

Lal, D., 1991, Cosmic ray labeling of erosion surfaces: in situ nuclide production rates and erosion models: Earth and Planetary Science Letters, v. 104, p. 424-439.

Schlüchter et al., 1994, Ancient surfaces in the Transantarctic Mountains and the age of the Sirius Formation (abstract this volume).

## ONE-TO-ONE CORRELATION OF FISSION TRACKS BETWEEN SPHENE AND MICA DETECTORS

IWANO, Hideki and DANHARA, Tohru,  
Kyoto Fission-Track Co., Kyoto 615, Japan.

One-to-one correlation of induced fission-tracks is a useful technique to investigate the difference in track registration efficiencies among minerals. This technique was successfully applied to zircon and apatite (Iwano *et al.*, 1992, 1993), and different track counting efficiencies (zircon/mica=0.75, apatite/mica=0.90) were found. It was also found that the presence of unetchable track ranges plays an important role in the track counting efficiencies of minerals. We report here further experimental results concerning sphene.

The Fish Canyon Tuff and the Mount Dromedary Complex sphenes were used for the experiment. Each sample was pre-annealed to erase spontaneous tracks and pre-etched to reveal background defects. The sphenes were attached with mica detectors and irradiated with thermal neutrons. Sphene grains with "scratched surface" were selected in this study. Induced tracks in the sphene and mica were traced on transparent sheets on a high-resolution video monitor. Tracks in sphene and mica were spatially correlated one-to-one by superimposing the reversed images of the mica tracks onto the corresponding images of sphene tracks. Preliminary one-to-one correlation data are as follows.

Sample	Sphene tracks	Mica tracks	Ratio (sphene/mica)
Fish Canyon	463	512(49)*	0.90
Mt. Dromedary	261	306(45)*	0.85

\*Numbers in parentheses are the numbers of uncorrelated tracks

The results revealed that the track counting efficiencies in the sphenes were about 0.85-0.90 times that in the mica and that uncorrelated tracks in the mica were remarkably short.

Analogous to the situation found in zircon and apatite, the lower counting efficiency in sphene can be attributed to a higher registration threshold required to produce an etchable track in sphene. Detailed track counting efficiency and unetchable track ranges in sphene will be discussed.

## SPATIAL DISTRIBUTION OF K-AR AGES OF MICA IN THE KAMUIKOTAN METAMORPHIC BELT AND THE GROWTH OF THE MESOZOIC-PALEOGENE ACCRETIONARY COMPLEX, HOKKAIDO, NORTHERN JAPAN

IWASAKI, I., WATANABE, T., YAMAZAKI, M.,  
Dept. of Geol. & Mineral., Hokkaido Univ., Sapporo,  
Japan, and ITAYA, T., Hiruzen Res. Inst., Okayama  
Univ. of Sci., Okayama, Japan.

Recent K-Ar age studies on mica in the central and southern parts of the Kamuikotan belt reveal that the Kamuikotan rocks span an age range of 100My from 145Ma to 45Ma and the Kamuikotan belt is divided into several units comprised of rocks with an age-cluster, i.e., 50-65Ma, 60-75Ma, 80-85Ma, 90-110Ma, 120-145Ma. Some of the rocks have a similar Ar-Ar age plateau (Takigami, unpublished data). P/T gradients of the metamorphic rock units become low with descending age-clusters, i.e., glaucophane schist facies to intermediate pressure type or lower pressure type as indicated by pumpellyite-biotite assemblage known in the Tanzawa low-pressure terrain. The metamorphic rock-units with a similar age-cluster are often bounded by strongly sheared serpentinite and form nappe-sheet structures. Some of serpentinite bodies form serpentinite melange including metamorphic rocks with diverse ages and P/T gradients.

Structural studies combined with the K-Ar age study enable us to explain that the Kamuikotan rocks continue to the accretionary complex of the Upper Cretaceous-Paleogene called the Idon'nappu belt, which is situated to the east of the Kamuikotan belt. The youngest uplift process of the Idon'nappu belt occurred at 35-40Ma which corresponds to the stage of bending of the western margin of the Paleo Kurile arc-trench system due to initiation of westward migration.

These dating studies mentioned above indicate that the accretionary complex along the NE margin of the Asian continent had successively grown with NNW-directional movement of the Pacific Plate and ceased immediately after the direction of movement of the Pacific Plate changed to WNW.

**<sup>40</sup>Ar-<sup>39</sup>Ar DATING OF FLOWS AND DYKE SWARMS IN THE DECCAN PLATEAU, INDIA**

IWATA, N. and KANEOKA, I., Earthquake Research Institute, University of Tokyo, Bunkyo-ku, Tokyo, 113, Japan

In the Deccan Plateau, mafic dyke swarms distribute in the Narmada river region, northern part of the Plateau and in the west coast areas. The northern swarms show E-W trend, but dykes with N-S trend are observed in the west coast regions (Deshmukh and Shegal, 1988). Such difference would reflect the orientation of tectonic stress fields when they were made. Hence, the age results of both dyke swarms might give a significant constraint on the change of the stress field related to the Deccan volcanism.

<sup>40</sup>Ar-<sup>39</sup>Ar dating results of the swarms and flows in the Deccan Plateau indicate that dykes with E-W trend might be overlap or older than the main Deccan volcanism which has been suggested by previous workers (e.g. Venkatesan et al., 1993). Flows, intrusives and dykes in the west coast areas yield disturbed age spectra in many cases. Major part of <sup>40</sup>Ar-<sup>39</sup>Ar total ages in this region show overlap or younger ages of the main Deccan volcanism, but some samples show obviously old total age, as old as 77 Ma, for example.

Based on our results and ages reported by previous workers, it is inferred a tendency seems to exist that ages of flows and/or dykes in the northeastern part of the Plateau might be a little older than these of the west coast areas. Since the age values of flows and dykes in the west coast areas are scattered in many cases, however, this point should be further examined under careful consideration.

Investigation to clarify the relationship between radiometric age and compositional, stratigraphical, regional features of the Deccan Volcanic Province are further required to reveal the origin of the Deccan volcanism.

Deshmukh, S.S. and Sehgal, M.N., 1988, Mafic dyke swarms in Deccan Volcanic Province of Madhya Pradesh and Maharashtra: Mem. Geol. Soc. India, 10, 323-340

Venkatesan, T.R., Pande, K. and Gopalan, K., 1993, Did Deccan volcanism pre-date the Cretaceous/Tertiary transition?: Earth Planet. Sci. Lett., 119, 181-189

**GEOGRAPHIC TRENDS IN STABLE ISOTOPE COMPOSITIONS OF CONTEMPORARY HUMAN HAIR SAMPLES FROM SOUTH AMERICA**

IYER, S.S., KROUSE, H.R., STOPFORTH, S. and WIESER, M., Department of Physics and Astronomy, The University of Calgary, Calgary, AB, T2N 1N4 CANADA

Stable isotope compositions ( $\delta D$ ,  $\delta^{13}C$ ,  $\delta^{15}N$  and  $\delta^{34}S$ ) of contemporary hair samples from different localities in Argentina, Bolivia, Brazil, Chile, and Paraguay were measured. The geographical distribution of the sampled populations ranged from 12°S (Salvador, Brazil) to 53°S (Punta Arena, Chile). Sampling (all ages and both sexes) included the El Chaco Indian tribe of Paraguay, as well as residents of the most populated industrial city of the Southern hemisphere (São Paulo, Brazil). A clear latitudinal trend in  $\delta^{13}C$  values was found (more negative with higher southern latitude, consistent with proportionately greater  $C_3$  photosynthesis), except for the El Chaco Indians. The latter had more negative  $\delta^{13}C$  values than urban dwellers at the same latitude, reflecting more reliance on  $C_3$  plants in their diets. A geographical trend in  $\delta D$  values of the hair samples was found for all groups, including the El Chaco Indians. It parallels that observed for modern precipitation. The  $\delta^{15}N$  and  $\delta^{34}S$  values did not show consistent trends. For the latter, localized lithospheric sources of soil sulphur should be a significant factor.

## MODELING THE DIFFERENTIATION OF THE EARTH USING COUPLED ISOTOPIC SYSTEMS.

JACOBSEN, S.B., & HARPER, C.L., Jr., Department of Earth and Planetary Sciences, Harvard University, 20 Oxford Street, Cambridge, MA 02138.

The coupled  $^{146,147}\text{Sm}$ - $^{142,143}\text{Nd}$  systematics are a powerful tool for investigating the history of the Earth. The bulk Earth evolution of  $^{143}\text{Nd}/^{144}\text{Nd}$  ( $\sim 116$   $\epsilon$ -units over the history the Earth) is relatively well determined while  $^{142}\text{Nd}/^{144}\text{Nd}$  increased only by about 2.8  $\epsilon$ -units, however, its evolution in the Earth is not well understood. The coupled U-Th-Pb and I-Pu-Xe chronometers, have large uncertainties in their bulk Earth evolution parameters, and in both cases pre-accretionary elemental fractionations tend to obscure the signature of post-accretionary processes. The coupled Sm-Nd systematics are particularly attractive as a tool for tracing the differentiation of the silicate portion of the Earth.

We have developed a multi-reservoir transport model to take advantage of such coupled isotopic systems. The rate of crustal growth and recycling may be inferred from  $^{143}\text{Nd}/^{144}\text{Nd}$  evolution in the depleted mantle over Earth history using such a model if detailed knowledge of the  $f^{\text{Sm}/\text{Nd}}$  evolution of the depleted mantle is available. The constraints from the  $^{143}\text{Nd}$  evolution may be used to calculate the average  $^{142}\text{Nd}/^{144}\text{Nd}$  evolution of depleted mantle. Such a continuous model would not allow the survival of  $^{142}\text{Nd}/^{144}\text{Nd} > +10$  ppm (w.r.t. bulk Earth) at any time in the depleted mantle, unless recycling of crust to this reservoir was insignificant during the first 0.5 Ga of Earth history. In that case enrichments of up to 30-40 ppm in  $^{142}\text{Nd}/^{144}\text{Nd}$  are possible in the early depleted mantle.

$^{142}\text{Nd}/^{144}\text{Nd}$  heterogeneity in the Earth is generated only as a result of early (i.e.  $> 4.3$  Ga) differentiation (plausibly protocrust formation). Subsequent to this time a progressive 'erasure' of the initial heterogeneity by geodynamic remixing of the complementary reservoirs may take place. For the post- $^{146}\text{Sm}$ -decay the mass transport coefficients may be obtained directly from the  $\epsilon_{^{142}\text{Nd}}$  evolution without any estimate of the Sm/Nd fractionation in the source region. After  $\sim 4.3$  Ga, therefore, the evolution of  $^{142}\text{Nd}/^{144}\text{Nd}$  in the Earth's depleted mantle reservoir becomes a tracer for geodynamic mixing and can be employed to quantify the 'global' geodynamic history of the crust-mantle system throughout geological time. Coupled chronometers, where one of the radioactive parents have a half-life much shorter than the age of the Earth (i.e. Sm-Nd, U-Th-Pb) are potentially useful tracers of geodynamic mixing.

## ISOTOPIC SYSTEMATICS OF METAMORPHIC ROCKS.

E. Jagoutz, Max Planck Institut für Chemie D55122 Mainz Saarstraße 23 Germany

Garnet and clinopyroxene form a common mineral association in metamorphic rocks. Sm/Nd is partitioned between these two minerals in a way, that this isotopic system should give ideal possibilities for the age measurements. Only in a few cases geologically meaningful ages were obtained, in the majority of cases the ages are clearly off and the data disappear in a lab-datafile. In most cases the garnet-clinopyroxene age appears younger. Other authors discuss this effect as a late closure of garnets in a slowly cooling system.

In young terrains as the Alps the garnet may even contain less-radiogenic Nd than the clinopyroxene. This is in contradiction with the higher Sm/Nd ratio in garnet compared to clinopyroxene. The negative-slope-isochrons ("futurechrons") clearly demonstrate that garnet and clinopyroxene were not equilibrated. When studying such cases, we found that garnet replaced another mineral such as plagioclase or amphibole. The garnet inherited the Nd-isotopic composition of the precursor mineral, but had changed the Sm/Nd ratio. Since most of the precursor minerals had low Sm/Nd ratio, the inherited Nd in garnet is unradiogenic compared to the clinopyroxene, which results in younger ages or even "futurechrons".

Evidence for this is found even in some highly metamorphed diamond-bearing eclogites. It seems that garnet is growing on the prograde path and the system is frozen after dehydration. The kinetics of metamorphic processes are commonly attributed to temperature and might effectively depend on dehydration, which is the dominant prograde reaction.

In some cases texture and composition of garnet and clinopyroxene give clear evidence for the replacement, while often only the isotopic relicts clearly demonstrate that garnet and clinopyroxene never equilibrated and other evidence of equilibrium is enigmatic.

STABLE ISOTOPE COMPOSITION OF BIOGENIC  
CARBONATE AND ORGANIC CARBON  
IN HACKBERRY ENDOCARPS:  
POTENTIAL AS A TERRESTRIAL PALEOCLIMATE  
INDICATOR

JAHREN, A. H., and AMUNDSON, R. G., Both at: Soil Science Group, University of California, Berkeley, CA, 94720, USA; M. Gabel, Department of Biology, Black Hills State University, Spearfish, SD, 57799, USA; and, L. Tieszen, Department of Biology, Augustana College, Sioux Falls, SD, 57197, USA.

Fossil endocarps of the Hackberry (*Celtis* sp.) are common in Cenozoic sediments of North America. Both the modern and fossil endocarps have been reported to be composed of up to 84.3 wt.% calcium carbonate, initially in the form of aragonite. This opens the possibility that a stable substrate exists for isotopic analysis and paleoclimate reconstruction using the Hackberry endocarp. Selective dissolution experiments followed by SEM revealed that modern endocarps have mineral frameworks of opal, which contains an "occluded" organic C fraction. The location and distribution of the occluded organic C is evaluated using fluorescence microscopy.

Stable C isotope analyses of organic matter in whole modern Hackberry seeds, cellulose from whole seeds, mesocarp, endosperm, whole endocarp, and opal-occluded endocarp C are presented; also presented are  $\delta^{13}\text{C}$  values of endocarp carbonate. Our objectives are the following: (1) determine the isotopic fractionation factor between the carbonate and the organic portions, and (2) to determine whether occluded C fractions, which may be most resistant to diagenesis (and therefore most likely to be preserved in fossil endocarps), reflect the isotopic composition of the whole Hackberry plant.

The sensitivity of the  $\delta^{13}\text{C}$  values of the various organic fractions, the  $\delta^{13}\text{C}$  values of the carbonate, and the  $\delta^{18}\text{O}$  values of the carbonate to climate is evaluated by measuring isotopic ratios in modern endocarps from a large portion of central North America. Measured C isotope ratios are interpreted in light of environmental effects on photosynthesis; measured  $\delta^{18}\text{O}$  values of the carbonate are interpreted in relation to the  $\delta^{18}\text{O}$  values of precipitation, and associated values of temperature and relative humidity.

Preliminary morphological and mineralogical observations of Quaternary and Tertiary fossil endocarps are presented, and the preservation of the various endocarp components in the geologic record is considered.

Carbon and Helium fluxes from Mid Ocean Ridges.

M. Javoy, (Lab. Géochimie Isotopes Stables, I.P.G. Paris, 2 Place Jussieu, 75251 PARIS cedex 05, France).

- Mantle helium fluxes have been estimated to be between 800 and 1100 moles  $^3\text{He}$ /year ( $\sim 8 \cdot 10^7$  to  $11 \cdot 10^7$  moles/year of total helium). This rather robust estimate (1) corresponds to a mean ocean turn-over time T of  $\sim 1000$  years and varies as  $1/T$ , discounting the possibility of transient buoyant flows during eruptions.

Corresponding carbon fluxes are then derived from the assumption that C/ $^3\text{He}$  ratios in MORB glasses are constant, the pseudo-canonical value being generally taken at  $2 \cdot 10^9$ . This assumption is far from true, the C/ $^3\text{He}$  ratio varying by more than one order of magnitude (from 0.5 to  $6 \cdot 10^9$  at least), correlated to carbon content and vesicularity.

This situation derives directly from the fact that helium is more soluble than carbon and that C/He ratios decrease in outgassing melts, whether under global equilibrium conditions during slow ascent from the source region or during distillation on the way from shallow magma chambers ( $\sim 1-3$  km depth below sea floor) to the ocean bottom. (2)

The above range ( $0.5$  to  $6 \cdot 10^9$ ) of C/He then corresponds to outgassed systems, with the lowest ratios corresponding to gases still dissolved in glass or to hydrothermal fluids, and the highest ratios to abundant vesicles. Modelling C/He ratio evolution according to the information obtained from carbon isotopes by Pineau & Javoy (2), we calculate that the average original C/ $^3\text{He}$  is more likely between  $8$  to  $12 \cdot 10^9$ , corresponding to an oceanic mantle carbon flux of  $6.5$  to  $1.3 \cdot 10^{13}$  moles/year. The aerial flux, corresponding essentially to subduction zone volcanoes and major aerial hydrothermal fields is probably similar in size.

1) H. Craig, W.B. Clarke and M.A. Beg, E.P.S.L. 26, 125, 1975.

2) F. Pineau and M. Javoy, E.P.S.L. 1994.

ISOTOPE AND FLUID INCLUSION STUDIES AS AN EXPLORATION GUIDE FOR GREENSTONE GOLD DEPOSITS AT LINGQIU NORTH HILL DISTRICT, SHANXI PROVINCE, NORTHERN CHINA

Zhiyu Jiang<sup>1)</sup>, Research Institute of Geology for Mineral Resources, CNNC, Guilin, 541004, China

Junming Chen and Youlu Guo, Research Institute of Geology of Shanxi Province, Taiyuan, China

The greenstone sequence comprising the Jinganku Formation in the Lingqiu North Hill district was regarded as a prospective area for gold mineralisation.

A recently published Sm-Nd age of  $2599.2 \pm 49$  Ma (Wang Rujing, 1989) is regarded as the age of the host sequences. Ore-bearing whole rocks and an apatite intimately intergrown with native gold yield a Rb-Sr isochron age of  $2214.5 \pm 61$  Ma and are believed to date the deformation and metamorphism related to the main phase of gold mineralisation in this area. A K-Ar age of 1780.5 Ma shows the next magmatic-tectonic episode with local limited gold mobilisation and enrichment associated with the metamorphosed basic dykes.

The calculated isotopic compositions indicate that the initial mineralising fluid was metamorphic in origin ( $\delta^{18}\text{O} = 6.3 \sim 10.7\%$ ,  $\delta\text{D} = -29.7 \sim -24.4$ ). The re-crystallisation of the rocks resulted in a marked increase in  $\delta\text{D}$  (from  $-29.7$  to  $+7.6\%$ ). The relationship between this variation of  $\delta\text{D}$  in the residual fluid and the gold contents in the rocks indicates that gold was derived from the older rock units to the younger rock units during the metamorphic process. The spatial distribution of temperatures calculated from the values of  $\delta^{18}\text{O}$  for coexisting mineral pairs supports this concept. An obvious decrease in  $\delta\text{D}$  from  $-24.4$  to  $-219.8\%$  which occurs in the major quartz veins is attributed to fluid boiling. Fluid inclusion studies indicate lower homogenisation temperatures for fluid boiling in the quartz veins (range  $334^\circ\text{C}$  to  $398^\circ\text{C}$ ). This pressure decrease and consequent boiling also resulted in an increase in the salinity of the fluid up to 48.2 wt% NaCl equivalent and concentration of gold in the veins.

The homogenisation temperatures for secondary fluid inclusions range from  $156^\circ\text{C}$  to  $213^\circ\text{C}$ , which represent the temperature of the second stage of stratabound mineralisation in laminated quartz veins formed during retrograde metamorphism. The O and H isotopic compositions of the second fluid may represent a mix of metamorphic water with meteoric water.

A positive correlation between the  $\delta^{34}\text{S}$  values and gold contents in pyrite points to a derivation of sulfur for the mineralisation in the Mesozoic structures from the underlying rocks.  $\delta^{34}\text{S}$  values of sulphides from all kinds of mineralisation are restricted to a narrow range and are near  $0\%$ , which can be explained by the homogenising effect of metamorphism for the greenstone terrane.

The lead isotopic data from native lead, whole rock and pyrite samples lie on an anomalous line and illustrates that the lead and the gold mineralisation in this area have experienced a multistage evolution.

Eight ore bodies have been determined by this isotope study and companion petrological, geochemical and structural studies.

<sup>1)</sup> Present address: Department of Geology, The University of Newcastle, NSW, 2308, Australia

BORON AND SILICON ISOTOPE SYSTEMATICS OF SEDEX-TYPE ORE DEPOSITS

JIANG, S.-Y., and PALMER, M.R., Dept. of Geology, University of Bristol, Bristol, BS8 1RJ, U.K., and Ding, T.-P., Institute of Mineral Deposits, Beijing, 100037, P.R.China

We have conducted a study of the boron and silicon isotopic systematics of some giant submarine hydrothermal exhalative ore deposits, such as, the Sullivan stratabound Pb-Zn-Ag deposit (Canada), the Qinling stratabound Pb-Zn deposits (China) and the BIF-type Gongchangling iron deposit (China), in an effort to determine the B- and Si-sources and the implications for ore genesis.

B isotope analyses of tourmaline from the deposits indicate that B in the hydrothermal fluids is leached from the underlying clastic sediments. Differences in the  $\delta^{11}\text{B}$  values in individual deposits may reflect seawater ingress into the submarine hydrothermal system which of significances for generation of the ores and may have exploration potential.

Siliceous rocks with negative  $\delta^{30}\text{Si}$  values are related to submarine hydrothermal processes. The Si isotope compositions of tourmalinites from the Sullivan deposit support the genetic model whereby tourmalinites from the feeder zone formed by replacement of clastic sediments which inherited their  $\delta^{30}\text{Si}$  values (0 to 0.1 ‰), and the stratiform tourmalinites and garnet-rich tourmalinites within or near the massive sulphide orebody formed by hydrothermal exhalative processes with negative  $\delta^{30}\text{Si}$  values (-0.3 to -0.5 ‰). It is possible to use Si isotopes to distinguish between Si derived from alteration of clastic sediments and that derived from hydrothermal fluids, despite post-depositional alteration and metamorphism of the deposit.

## MODELS FOR THE EVOLUTION OF ISOTOPE RATIOS IN REACTIVE GROUNDWATER SYSTEMS.

JOHNSON, Thomas M., and DEPAOLO, Donald J.,  
Dept. of Geology and Geophysics, U.C. Berkeley,  
Berkeley, CA 94720, and Earth Sci. Div.,  
Lawrence Berkeley Laboratory, Berkeley, CA 94720.

Isotopic measurements are valuable tools in hydrologic investigations, especially when water-rock interaction is to be investigated or in systems where physically-based predictions of water flow are highly uncertain. Usually, isotopic data take the form of spatial patterns formed by arrays of wells or other sampling points, and/or temporal patterns from samples taken in time series. These patterns result from the interplay of transport effects (advection, dispersion, mixing) and reaction effects (dissolution, precipitation, exchange, sorption). The interpretation of the patterns amounts to an inverse problem where the values of the parameters that control the system are to be extracted from the output of the system.

We have developed a modeling approach that relates the evolution of isotope ratios in the water as a function of time and position to the critical transport and reaction parameters. The model applies to any isotope ratio in any system that can be treated as a porous continuum. In an advective system where reaction with the rock or soil is important, one dimensionless parameter, a Damköhler number, most strongly defines the system. For the isotopic ratio problems discussed here, it can be expressed:

$$N_D = \frac{\ell M \bar{R}_d c_s}{v c_f}$$

where  $\ell$  is the characteristic length scale for the system,  $M$  is the solid-to-fluid mass ratio,  $\bar{R}_d$  is the reaction rate,  $c_s$  and  $c_f$  are the concentration of the element of interest in the solid and fluid, respectively, and  $v$  is the advection velocity.

The value of this parameter ranges widely among the chemical elements considered in isotopic studies, and a range of behavior, from conservative to reaction dominated, is to be expected in natural systems. When reaction effects are important, the key to extracting information from isotopic data is to characterize spatial variation in both the fluid and the rock or soil matrix. The relationship between the two carries information on advective velocity, reaction rates, and dispersion. We present field data and numerical modeling from several studies in which this approach was applied.

## DIFFERENTIATING THE TECTONIC AND EROSION COMPONENTS OF DENUDATION USING FISSION TRACK ANALYSIS: A CASE STUDY FROM S.E. SPAIN

JOHNSON, KIT Research School of Geological Sciences,  
Fission Track Research Group, Birkbeck & University  
Colleges London, WC1E 6BT, England.

The erosive (i.e. surface processes) and tectonic (i.e. structural processes) components of any denudational history are generally difficult to differentiate because they possess a complex interdependence. That we should want to do so is largely because an appreciation of the means by which rocks are brought to the earth's surface helps constrain our understanding of the driving mechanisms that are responsible for denudation. In particular it will help clarify the hitherto poorly understood role played by extension in convergent orogens.

It will be argued that it is possible to recognise the thermochronological consequences or 'signature' of both erosive and tectonic denudation and that such signatures may act as diagnostic tests for specific denudational regimes. In addition they can be used to constrain both the relative importance and timing of each component.

The Betic Cordillera in southern Spain is the westernmost portion of the European Alpine mountain belt. Evidence exists for initiation of northerly directed compressive deformation in the late Eocene and the Oligocene which continued throughout the Lower and Middle Miocene. Fission track analysis (FTA) reveals that broadly east - west extension within the Internal Zone probably commenced during the late Oligocene and that by the early Miocene mid-crustal rocks of the Alpujarride Complex had been tectonically exhumed and brought into contact with essentially unmetamorphosed rocks belonging to the Malaguide Complex in the eastern Betics. Continued extension resulted in the emergence of lower crustal rocks of the Nevado-Filabride Complex beginning in the (Langhian?) Serravallian and ending abruptly in the early Tortonian (~9 Ma). It was not until the cessation of extension, caused by a change in relative plate motions, that important erosive denudation commenced.

Quantitative modelling of both tectonic and erosive denudation suggest that cooling and relative foot-wall uplift rates of ~200°C.Ma<sup>-1</sup> and ~4mm.yr<sup>-1</sup> respectively were experienced during the former and that subsequently, foot-wall erosive denudational rates of 0.6mm.yr<sup>-1</sup> were experienced in the Sierra Nevada during the upper Miocene.

## ISOTOPIC ( $\delta^{18}\text{O}$ and $\delta^{17}\text{O}$ ) STUDIES OF TROPOSPHERIC OZONE

JOHNSTON, J. C. and THIEMENS, M. H., Dept. of Chemistry, University of California, San Diego, La Jolla, CA, 92093, USA

Although only 10% of atmospheric ozone is located in the troposphere, this relatively small amount plays a crucial role in maintaining the chemical composition and oxidation capacity of the atmosphere. Additionally, tropospheric  $\text{O}_3$  is an important greenhouse gas because of its strong infrared absorption at  $9.6\mu\text{m}$ . Measurements indicate that background tropospheric  $\text{O}_3$  concentrations are increasing at  $\sim 1\%/yr$  over northern midlatitudes. Thus, there is considerable interest in a better definition of the tropospheric  $\text{O}_3$  budget and transformation mechanisms. The budget is complex, with significant involvement of both photochemical and transport processes on differential spatial and temporal scales.

The isotopic characterization of tropospheric ozone will provide important information regarding the seasonal variations in photochemical and surface destruction mechanisms. Models incorporating photochemical and transport processes are in need of direct observations to validate their predictions; isotopic measurements of tropospheric  $\text{O}_3$  may provide an important new source of direct information. The isotopic data may also be helpful in defining the relative importance of various vertical and horizontal transport mechanisms, both within the troposphere and between the stratosphere and the troposphere.

The interpretation of isotope measurements of tropospheric ozone requires knowledge of the fractionation factors associated with  $\text{O}_3$  formation and destruction; fortunately, many of these values have been determined. For example,  $\text{O}_3$  formation and decomposition processes both produce distinctive mass independent isotopic fractionations.

Stratospheric  $\text{O}_3$  is known to possess a large (400‰) mass independent isotopic composition. These enrichments have proved difficult to interpret, due in part to the limited amount of chemical and meteorological data available to correlate with the isotopic measurements. In the troposphere, measurements of chemical and meteorological parameters are routine, thus it may be possible to interpret and model relations between these parameters and a given  $\text{O}_3$  isotopic enrichment.

Cryogenic techniques are used to collect and isolate  $\text{O}_3$  from ground level air. The sample is then converted to  $\text{O}_2$  and the  $\delta^{18}\text{O}$  and  $\delta^{17}\text{O}$  values measured on a Finnigan MAT 251. We will report results from ground level collections in La Jolla, CA.

## THE MAKE-UP AND MELTING OF A SUBDUCTION-ACCRETION COMPLEX: GENERATION OF S- AND I-TYPE GRANITOIDS

JONES, Catrin & TARNEY, J., Dept. Geology, U. Leicester, UK and BARREIRO, B., NERC Isotope Geoscience Laboratory, Keyworth, Nottingham, UK

It has been argued that subduction-accretion processes have made a major contribution to continental development during the Phanerozoic<sup>1</sup>. Where super-continent land-masses are rimmed by active margins, major river systems discharge their upper crustal sedimentary load onto the shallow-dipping down-going plate, which is then tectonically intermixed with other oceanic components (ocean islands, arcs, plateaus, carbonate banks, abyssal oozes, etc.) and re-accreted onto the continental margin. The resulting schistose or gneissose complex is thus a variable mixture of "crustal" metasediment and "mantle" amphibolite components that have been dragged down to deep crustal levels in the subduction complex, and have then suffered varying extents of metasomatism, migmatitisation and stages of melt generation during decompression through uplift and exhumation.

Using the well-exposed Rhodope Massif (Mesozoic) in N. Greece, where lithological packages with different proportions of mantle-derived (MORB, OIB, plateau) and crust-derived (sedimentary) components, usually separated by tectonically weak and buoyant marbles, we document the isotopic and trace element characteristics of different components of a subduction-accretion complex.

Migmatitic granitoids within totally metasedimentary segments are muscovite- or biotite-bearing, with essentially S-type chemical and isotopic characteristics: high K/Na and Rb/Ba ratios, low K/Rb ratios, low Sr abundances, moderate Y and HREE depletion,  $87\text{Sr}/86\text{Sr}$  ratios ranging 0.708 – 0.716 and  $\epsilon\text{Nd}$  -7 to -2.

However, where there is a small to significant amount of tectonically-intercalated amphibolite, the granitoids are all hornblende-bearing with clear I-type characteristics: low K/Na and Rb/Ba ratios, high K/Rb ratios, high Sr abundances, strong Y and HREE depletion,  $87\text{Sr}/86\text{Sr}$  ratios ranging 0.705 – 0.709 and  $\epsilon\text{Nd}$  -5 to 0. This implies that the chemical and isotopic influence on melt products (particularly LILE and Sr relative to Nd systematics) of the amphibolites is disproportionate to their volume. This has important implications for the genesis of magmas with mixed I- and S-type characteristics.

Coarse grained migmatitic gneisses in central Rhodope, despite having all the visual characteristics of Archaean high grade grey gneiss terrains, have peak-metamorphic (U-Pb monazite) ages of ca. 55Ma, signifying that such characteristics can be produced through Cenozoic subduction-accretion processes.

North to south increasing Nd crustal residence ages of gneisses from Rhodope to the Cyclades suggest that subduction-accretion has been an important mechanism of crustal growth throughout the Hellenides.

<sup>1</sup>Sengör *et al.*, 1993. Evolution of the Alaid tectonic collage and Palaeozoic crustal growth in Eurasia. *Nature* 364, 299-307.

STRONTIUM ISOTOPE STUDIES OF CHLORIDE  
CONTAMINATED GROUNDWATER FROM DENMARK  
JØRGENSEN, N.O. & HOLM, P.M., Geological Institute,  
University of Copenhagen, DK-1350 Copenhagen,  
Denmark.

The occurrence of chloride-contaminated groundwater is a well-known phenomenon in Denmark and is a serious problem in water resources management. Previous isotopic investigations of Danish aquifers have shown that isotopic hydrochemical criteria provide a strong tool to characterize groundwater qualities that are affected by naturally occurring sources such as water-rock interaction, intrusion of seawater and other sources of saline groundwater. The aim of the present case study is to demonstrate the applicability of strontium isotopes as natural tracers in a chloride-contaminated near-coastal aquifer in eastern Jutland, Denmark.

The study area includes a confined aquifer at Staurup Waterworks south of Århus. The aquifer consists of c. 70 m fluvio-glacial gravels, sands and silts covered by 10-20 m of boulder clays and resting on a pre-Quaternary basement of Oligocene marine mica clay. Two boreholes were drilled in the fall of 1993 and depth specific groundwater sampling was undertaken in order to investigate a chloride contamination of the aquifer. Water samples from the upper part of the aquifer show relatively low Cl contents in the range of 30-50 mg/l. However, the Cl contents increased significantly with depth to a maximum of 850 mg/l in the lower part of the aquifer. Selected freeze-dried groundwater samples, and seawater from the nearby Århus Bay, were analysed for their Sr isotopic composition using standard ion-exchange techniques and a VG Sector 54-30 mass spectrometer.

The  $^{87}\text{Sr}/^{86}\text{Sr}$  ratios and the Sr concentrations obtained from the groundwater samples show a well-defined mixing hyperbola with  $^{87}\text{Sr}/^{86}\text{Sr}$  ratios varying from 0.7088 in the low-Cl samples to 0.7084 in the high-Cl samples. The  $^{87}\text{Sr}/^{86}\text{Sr}$  ratio at 0.7092 for the seawater from Århus Bay falls significantly outside the mixing hyperbola for the groundwater samples and, therefore, excludes the possibility of any seawater infiltration. The remarkably low  $^{87}\text{Sr}/^{86}\text{Sr}$  ratios at c. 0.7084 of the high-Cl groundwater samples indicate that the chloride-contaminated groundwater is most likely heavily influenced by saline formation waters forced into the Quaternary aquifer from the underlying Oligocene marine mica clay.

#### NEW U-Pb DATA FOR SINGLE SHOCKED ZIRCONS FROM THE K/T BOUNDARY, SASKATCHEWAN: FURTHER PROOF FOR A CHICXULUB SOURCE

KAMO, S.L., KROGH, T.E., Geochronology  
Laboratory, Royal Ontario Museum, 100 Queen's  
Park, Toronto, Ontario, M5S 2C6;  
HILDEBRAND, A.R., Geophysics Division,  
Geological Survey of Canada, 1 Observatory  
Crescent, Ottawa, Ontario, K1A 0Y3.

Recent U-Pb dating of single shocked zircons from impact-related sites has proven extremely useful in "fingerprinting" the target source for K/T boundary ejecta and for correlating distal ejecta from widely-spaced localities<sup>1,2</sup>. Characterization of the target site using this method can uniquely link ejecta to its source because zircon, which is extremely refractory, represents a residual fragment of the target itself that records both its primary crystallization age and the time of impact.

New U-Pb data for five single shocked zircons from the K/T boundary near Rock Creek, south-central Saskatchewan, define a colinear array with an upper intercept age of  $548 \pm 6$  Ma and a lower intercept age of  $59.0 \pm 10.0$  Ma. These data points are 7, 19, 30, 59, and 98% discordant with a 52% probability of fit. A sixth grain has a younger upper intercept age of  $363 \pm 26$  Ma (20% discordant), assuming lead loss occurred at 65.5 Ma. This age is within error of that for a single unshocked zircon reported previously<sup>1</sup> from the K/T boundary in the Raton Basin, Colorado, and represents a minor target component in the fireball layer that has so far not been observed at the Chicxulub crater. The data points show a correlation between the intensity of shock metamorphism and the amount of discordance. These results from the Rock Creek site, located  $\approx 3500$  km from the Chicxulub crater, are remarkably consistent with zircon ages found at other K/T boundary sites in Colorado, Haiti, and the Chicxulub crater breccia, all of which give a predominant U-Pb primary zircon age of ca. 545 Ma (e.g. the primary source age for K/T Colorado zircons is  $545 \pm 5$  Ma).

While arguments for a terrestrial origin for the Chicxulub breccia and Caribbean tektite units have recently been proposed, U-Pb data and shock-related textural features of zircon unequivocally support a meteorite impact origin. Zircons with primary ages of ca. 545 Ma that display polycrystalline shock metamorphic textures<sup>3</sup> (that have never been reported in explosive volcanic rocks) that are isotopically reset to ca. 65 Ma, found in sites from across North America at the K/T boundary, cannot have been derived from a volcanic eruption (which would yield 65 Ma zircons) and are best explained by derivation from a single large bolide impact.

1. Krogh, T.E., Kamo, S.L., Sharpston, V., Marin, L., & Hildebrand, Nat. 366, 731-733, 1993.
2. Krogh, T.E., Kamo, S.L., & Bohor, B., Earth & Planet. Sci. Lett. 119, 425-429, 1993.
3. Bohor, B., Betterton, W., & Krogh, Earth & Planet. Sci. Lett. 119, 419-424, 1993.

## HOW HETEROGENEOUS ARE NOBLE GAS SIGNATURES IN THE EARTH'S MANTLE ?

KANEOKA, I., Earthquake Research Institute, University of Tokyo, Bunkyo-ku, Tokyo 113, Japan

Noble gas state in the Earth's interior has been inferred from many kinds of materials such as pillow glasses, olivine phenocrysts, ultramafic nodules, etc. Each material reflects both the primary signatures and secondary ones, the latter of which should be properly eliminated to infer the former ones. Based on such procedures, MORB sources are inferred to be characterized by relatively uniform  $^3\text{He}/^4\text{He}$  ratios (8+1R<sub>A</sub>) and systematically high  $^{40}\text{Ar}/^{36}\text{Ar}$  ratios (more than 5,000) together with the frequent occurrence of excess  $^{129}\text{Xe}$ . Plume samples show more variable signatures including higher or lower  $^3\text{He}/^4\text{He}$  ratios and systematically lower  $^{40}\text{Ar}/^{36}\text{Ar}$  ratios than those of MORB, but there are still controversies about the characteristic values for them. The occurrence of excess  $^{129}\text{Xe}$  has not been confirmed in the plume sources.

Although relatively low  $^{40}\text{Ar}/^{36}\text{Ar}$  ratios for plume samples are often attributed to the secondary atmospheric contamination, stepwise degassing experiments and the correlation between the high  $^3\text{He}/^4\text{He}$  ratios and low  $^{40}\text{Ar}/^{36}\text{Ar}$  ratios in the higher temperature fractions of mantle materials suggest that the occurrence of relatively low  $^{40}\text{Ar}/^{36}\text{Ar}$  ratios in the Earth's mantle are real. Even  $^{40}\text{Ar}/^{36}\text{Ar}$  ratios of less than the atmospheric value has been observed together with the occurrence of excess  $^{129}\text{Xe}$  in olivine megacrysts contained in South African kimberlites. Such information implies that noble gas signatures of the Earth's mantle might be rather heterogeneous for heavier noble gases at least in the lithosphere. Apparent variation of noble gas signatures for plume materials can be ascribed to the mixing of different sources. Among them, recycled materials would play an important role. Uniform noble gas systematics of MORB might reflect that of the source and/or the secondary processes to homogenize it. Detailed examination of the occurrence of excess  $^{129}\text{Xe}$  would reveal the degree of heterogeneity of noble gas systematics in the mantle by correlating it with the other isotopes.

## DETERMINING THE EFFECTIVE NEUTRON FLUX FOR $^{40}\text{Ar}$ - $^{39}\text{Ar}$ DATING OF FINE GRAINED CLAY MINERALS

KAPUSTA, Y., STEINITZ, G., KOTLARSKY, P., Geological Survey, Jerusalem, Israel.

The neutron fluence and its variation as utilized in  $^{40}\text{Ar}$ - $^{39}\text{Ar}$  dating is determined by using a mineral-monitor which is irradiated in a nuclear reactor together with the sample. It is assumed that the efficiency of the  $^{39}\text{K}(n,p)^{39}\text{Ar}$  reaction in the monitor and the sample is the same. Using standard monitors (LP-6, HD-B1, MMhb-1 etc.) for  $^{40}\text{Ar}$ - $^{39}\text{Ar}$  dating of clay minerals yields ages significantly too high. The conventional explanation assumes a  $^{39}\text{Ar}$  deficit within the mineral, due to its "recoil" from the fine grains, as the cause for the phenomenon.

Two different aliquats (0.028, 0.351 gr) of the same clay fraction ( $<0.2\mu$ ) irradiated together contained different amounts of  $^{39}\text{Ar}$  ( $1.3 \cdot 10^{-7}$ ,  $1.96 \cdot 10^{-7}$  cc/gr). The dependence of the  $^{39}\text{Ar}$  concentration on the mass of the sample indicates a varying neutron flux in the sample. In the irradiated samples no loss of  $^{40}\text{Ar}_{\text{rad}}$  was observed nor could implanted  $^{39}\text{Ar}$  be detected in the aluminum foil used for packing the samples.

The measured  $^{39}\text{Ar}$  content in different clay fractions irradiated together shows a linear correlation between the calculated  $^{39}\text{Ar}$  deficit (using their K-Ar age) and their  $\text{H}_2\text{O}$  content (determined by DTA). This implies that the water in the clay minerals moderates and/or absorbs the neutrons and thus is the source of the  $^{39}\text{Ar}$  deficit relative to the monitors which are devoid of water.

It is suggested to use clay fractions with calibrated K-Ar ages and known water contents as additional neutron flux monitors for  $^{40}\text{Ar}$ - $^{39}\text{Ar}$  dating of fine clay minerals. A first test using this approach yielded  $^{40}\text{Ar}$ - $^{39}\text{Ar}$  ages of  $\text{H}_2\text{O}$  bearing clay fractions close to their K-Ar ages. The deviations may be due to difference in size and geometry between the clay monitors and the samples. The results open the possibility of extending the approach to step-wise heating experiments.

PALEOPROTEROZOIC CARBON ISOTOPE RECORDS  
FROM THE FENNOSCANDIAN SHIELD: IMPLICATIONS  
FOR THE GLOBAL CARBON CYCLE

KARHU, J.A., Geological Survey of Finland, FIN-02150  
Espoo, Finland.

$\delta^{13}\text{C}$  and  $\delta^{18}\text{O}$  values of calcite and dolomite have been determined for 229 sedimentary carbonate samples from Paleoproterozoic supracrustal belts of the Fennoscandian Shield (Karhu, 1993). Generally only those sedimentary carbonates estimated to contain more than about 80% carbonate were chosen for analysis, and in addition, a few carbonate samples were rejected, if the measured  $\delta^{18}\text{O}$  values remained below 13‰ (SMOW).

The distribution of  $\delta^{13}\text{C}$  values of total carbonate is clearly bimodal, showing a pronounced maximum at about 2‰ and another less distinct maximum at about 10‰. Relying on formations for which the time of deposition could be estimated from radiometric age data, a carbon isotope evolution curve was constructed for the time period from 2.5 to 1.9 Ga. The most conspicuous and stratigraphically useful feature of the curve is the interval from about 2.2 to 2.1 Ga, which is represented by highly  $^{13}\text{C}$ -enriched sedimentary carbonates with  $\delta^{13}\text{C}$  values in the range  $10 \pm 3\%$ . These are followed between 2.11 and 2.06 Ga by a sharp, almost 10‰ drop in the  $\delta^{13}\text{C}$  values of carbonates, while from that time until 1.9 Ga, the  $\delta^{13}\text{C}$  values remain in the range  $0 \pm 3\%$ . The  $\delta^{13}\text{C}$  evolution pattern is also roughly compatible with the  $\delta^{13}\text{C}$  results from other well dated Paleoproterozoic carbonate formations, and it appears that these  $^{13}\text{C}$ -enriched carbonates represent a global perturbation in the carbon cycle.

Carbon isotope compositions for organic carbon in black shales associated with the  $^{13}\text{C}$  enriched carbonates show large variation. Most of the  $\delta^{13}\text{C}$  values fall in the range  $-19 \pm 3\%$ , suggesting a comparative  $^{13}\text{C}$ -enrichment in the coexisting organic matter, but some samples show more negative  $\delta^{13}\text{C}$  values, down to as low as -43‰, possibly resulting from local predominance of processes producing extremely light kerogens through methylotrophic pathways.

It is suggested that the positive carbon isotope shift recorded in the Paleoproterozoic sedimentary carbonates was related to an increased relative rate of burial of organic matter on a global basis. The shift was possibly enhanced by local burial of isotopically unusually light organic matter. As high burial rates of organic carbon are probably followed by a large flux of free oxygen, the positive carbon isotope shift may be fundamentally connected with the significant rise in atmospheric oxygen levels at about 2.0 Ga.

Karhu, J.A., 1993, Paleoproterozoic evolution of the carbon isotope ratios of sedimentary carbonates in the Fennoscandian Shield. Geol. Surv. Finland, Bull. 371, 87p.

$^{39}\text{Ar}$ - $^{40}\text{Ar}$  DATA ON EXCESSIVE  $^{40}\text{Ar}$  IN NEPHELINE  
FROM THE KOVDOR MASSIF, KOLA PENINSULA  
KARPENKO, Michael I. and IVANENKO, V. V.,  
Institute of Ore Deposit Geology, Petrography,  
Mineralogy and Geochemistry, Russian Academy  
of Sciences, 109017 Moscow, Russia

At the Gornoozero intrusion, the age of nepheline in the earliest nepheline-pyroxene rocks is 630 Ma, while the age of the main intrusive phase is 450 Ma and for the nephelinites is 400 Ma. The Kovdor intrusion has been examined in the most detail. Here the nepheline ages for five rock groups, distinguished on the basis of their structural position and composition, range from 600 Ma (nepheline from the oldest pegmatoid, ijolite dikes cutting through core olivinites) to 400 Ma (418 Ma nepheline and 370 Ma from mica in nepheline-syenite dikes in the Malyi Kovdor Intrusion). Such discrepancies within a intrusion raise doubts as to whether the values reflect breaks in the time of formation of the alkali rock or whether there are other causes.

Two samples of nepheline with maximal K-Ar ages of 700 Ma have been examined by stepwise heating and by laser  $^{40}\text{Ar}$ - $^{39}\text{Ar}$  methods.

It is evident that these samples contain 30% excess  $^{40}\text{Ar}$  in gaseous form. When the samples are ground, the inclusions containing the excess argon are destroyed. Then, the calculated age is 500 Ma, which approximates the crystallisation age, but may exceed it if the excess  $^{40}\text{Ar}$  is present not only in gaseous form but also as single atoms trapped in the lattice.

HIGH-RESOLUTION MEASUREMENT OF  
STRONTIUM/CALCIUM RATIOS IN MARINE  
BIVALVES USING PIXE

KASHGARIAN, Michaele, Graham BENCH, Center for Accelerator Mass Spectrometry, Lawrence Livermore National Laboratory, PO Box 808, L-397, Livermore, CA 94551, and Chris WIEDMAN, Dept. of Marine Geology and Geophysics, Woods Hole Oceanographic Institution, Woods Hole, MA 02543

We have calibrated a Sr/Ca paleothermometer in two bivalve mollusk species using the high resolution non-destructive method Proton Induced X-ray Emission (PIXE) to measure Sr concentration in thin sections of shell material. Using a spot size of 10-30  $\mu\text{m}$  we have been able to obtain continuous high resolution measurements of Sr concentration across annual growth bands of  $\geq 1$  mm and we have measured Sr/Ca ratios in shell carbonate to better than 1% precision.

Sr/Ca variability in scleractinian corals and mollusks has been shown to correlate with seasonal temperature changes (e.g. Beck et al., 1992, and Schifano and Censi, 1986). We have found greater than 10% variability of Sr/Ca in growth bands from individual specimens of *Mercenaria mercenaria* and *Arctica islandica*. Specimens were collected from Long Island Sound and Vineyard Sound off the US East Coast from areas with long term continuous temperature records in order to correlate the Sr/Ca in the shells with seasonal temperature variability. We have also correlated our Sr/Ca with  $\delta^{18}\text{O}$  measurements in one specimen of *Arctica islandica*.

Beck, J.W., et al., 1992, Sea Surface Temperature from Coral Skeletal Strontium/Calcium Ratios, *Science*, v.257, pp. 644-647.

Schifano, G., and P. Censi, 1986, Oxygen and Carbon Isotope Composition, Magnesium and Strontium Contents of Calcite from a Subtidal *Patella coerulea* Shell, *Chemical Geology*, v. 58, pp. 325-331.

URANIUM ISOTOPE DISTRIBUTIONS WITHIN  
MERCENARIA SHELLS: GEOCHRONOMETRIC  
POSSIBILITIES

KAUFMAN, Aaron, Dept. of Env. Sciences, Weizmann Inst. of Science, 76100 Rehovot, Israel, GHALEB, Bassam, GEOTOP, Univ. du Quebec a Montreal, C.P. 8888, Montreal, H3C 3P8, Que., Canada, and WEHMILLER, John, F., Dept. Geology, Univ. of Delaware, Newark, DL, 19716, U.S.A.

Uranium concentrations and  $^{234}\text{U}/^{238}\text{U}$  ratios were measured as a function of depth within the shell for 3 live and 10 fossil specimens of the marine bivalve, *Mercenaria*, from the U.S. mid-Atlantic coastal plain. The samples were prepared by grinding the shell into 5-6 portions, each of which represents a layer parallel to the shell surface. As expected, the live specimens had much lower whole-shell uranium concentrations (mean of 40 ppb) than did the fossils (mean of 300 ppb). However, the concentration gradients were much steeper than expected, especially for the live-collected specimens where the exterior typically had about 200 times the concentration of the interior; in the fossils this proportion was typically about 12.

Apparently, the uranium uptake process starts very shortly after shell formation and though the fossil continues to take up much more uranium, there are two lines of evidence which suggest that this lasts for only a relatively short period, especially in the shell interiors: 1) the  $^{234}\text{U}/^{238}\text{U}$  ratios of 9 of the 10 fossil shell interiors were such as to indicate that the uranium uptake ended before the shells left the marine environment which probably occurred less than 10 ka after deposition, though most of the shells probably formed 80-100 ka ago. While some of the specimens undoubtedly took up continental uranium, hence after emergence, this was restricted to their exterior layers. 2) Assuming that the process by which the uranium enters the shell is diffusion-controlled, one can estimate the relative amounts of time over which the diffusion occurred in the fossil vs. the live specimens by comparing their concentration gradients. This suggests that the diffusion typically occurred over a period of the order of less than 1 ka.

One consequence of the present findings is that though the apparent  $^{230}\text{Th}$  ages of whole mollusk shells are usually unusable because of complicated patterns of post-mortem uranium uptake, those of their interior layers may generally be too low by only a small amount.

## EVOLUTION OF FORMATION WATERS IN THE ILLINOIS AND APPALACHIAN BASINS AS INDICATED BY CHLORINE STABLE ISOTOPE COMPOSITIONS

Ronald S. Kaufmann, RUST Environment & Infrastructure, 1515 N. Federal Highway Boca Raton, FL, 33432, Siegel, Donald I., Department of Geology, Syracuse University, Syracuse, NY 13244-1070, Prinos, Scott, and Dickey, Neil, Department of Geology, Northern Illinois University, DeKalb, IL, 60115.

Chlorine stable isotope composition was determined for waters from Paleozoic formations in the Illinois and Appalachian Basins to identify similarities in the origin of these waters and diagenetic processes.

Br-Cl relationships in both basins suggest the presence of Ca-Cl saline formation waters that have evolved from residual evaporated ocean water with the initial Illinois Basin formation waters below halite saturation and Appalachian waters evolving from a water that has precipitated some halite. Plots of Na and Ca for both basins show a ternary mixing pattern, evidence of mixing among meteoric, Ca-Cl, and Na-Cl waters derived from dissolution of halites.

The chlorine isotope ratios of the Illinois Basin range from -0.2 to +0.89 per mil, (precision 0.1 per mil) with respect to SMOC and correlate with most major ion distributions and ratios of ions. In the Appalachian Basin, the range is from -0.11 to +0.98 per mil and correlated relationships for the chlorine isotope ratio among major ion is limited to Na, Cl and Br, and the ratio of Na/Cl. These correlated variations may be explained by diagenetic diffusion. Data from both basins suggest that if the formation waters were initially Silurian ocean water, than the isotope composition of the chlorine from the Silurian ocean is about +0.9 per mil as compared to modern oceans.

## GEOCHEMICAL ESTIMATION OF THE HALF-LIFE FOR THE DOUBLE BETA DECAY OF $^{96}\text{Zr}$

KAWASHIMA, Atsumichi, Dept. of Chemistry, Univ. of Tokyo, Tokyo, Japan (Present Address: Div. of Geological & Planetary Sci., California Institute of Technology, CA91125, U.S.A.), TAKAHASHI, Kazuya, Earth Sci. Lab., Inst. of Physical and Chemical Research, Saitama, Japan, and MASUDA, Akimasa, Dept. of Chemistry, Univ. of Tokyo, Japan

The precise determination of the decay constants of double beta decay has put a constraint on the mass of the neutrino. Their half-lives are estimated to be of the order of  $10^{18}$ - $10^{21}$  yr. Accordingly, it is difficult to directly detect the radioactivity accompanying double beta decays using counting methods. An alternative approach is the detection of the decay product accumulated in very old natural minerals. In the present work, we have attempted to estimate the half-life of double beta decay of  $^{96}\text{Zr}$  from the amount of radiogenic  $^{96}\text{Mo}$  found in the Zr mineral.

Natural zircon usually contains a few ppm of Mo. Mo, however, is believed to be present as a mineral inclusion (perhaps molybdenite) and the proportion of Mo substituting for Zr ions in the crystal lattice is anticipated to be low. Thus it is expected that radiogenic  $^{96}\text{Mo}$  is not present in molybdenite inclusions but can be detectable in intrinsic portions of zircon. In order to reduce the Mo background and to find out the isotopic effect on Mo due to double beta decay of  $^{96}\text{Zr}$ , molybdenite inclusions must be removed with aqua regia. Zircon is not eroded by this treatment, and the Mo produced by the decay of Zr is considered to be maintained in the pure zircon crystal grains.

After Mo was separated from Zr matrix, HCl solution of ascorbic acid and  $\text{NH}_4\text{I}$  was added to the sample in order to reduce the oxidation state of Mo from +6 to +3 and depress the volatility of the Mo during the TIMS measurement. A Re single filament technique was used for TIMS. Small amounts of a mixed powder of Re and Pt (Re:Pt=1:2) were added to enhance the ionization efficiency of Mo. (Pt was mixed because of its relative high work function, and Re powder was added to increase the surface area of the ionizing filament.)

The isotopic composition of Mo in zircon showed the anomalies of  $^{95}\text{Mo}$ ,  $^{97}\text{Mo}$ ,  $^{98}\text{Mo}$  and  $^{100}\text{Mo}$  caused by the spontaneous fission (SF) of  $^{238}\text{U}$ , and  $^{96}\text{Mo}$  caused by the double beta decay of  $^{96}\text{Zr}$ . The content of Mo in the zircon was calculated from the content of U, the half-life of the SF of  $^{238}\text{U}$  and the yield of Mo on the SF of  $^{238}\text{U}$ . Therefore, the half-life of  $^{96}\text{Zr}$  was calculated with the anomaly of  $^{96}\text{Mo}$  and the age of the zircon ( $1.7 \times 10^9$  yr), and the half-life was estimated as  $3.9 \times 10^{19}$  yr. The obtained half-life of  $^{96}\text{Zr}$  is consistent with those of other double beta decay nuclides,  $^{82}\text{Se}$  and  $^{130}\text{Te}$  in the view of the decay energy.

Kawashima, A., Takahashi, K. and Masuda, A., Physical Review C, 47, R2452-2456 (1993)

## A UV LASER ABLATION MICROPROBE TECHNIQUE FOR ARGON ISOTOPE ANALYSIS.

KELLEY, S.P., Dept of Earth Sciences, Open University, UK, ARNAUD N.O., Univ Blaise Pascal & CNRS, Clermont Ferrand, France, CARROLL, M.R. and DRAPER, D.S., Univ Bristol, UK.

A new ultra-violet laser ablation technique for noble gas extraction yields both true high spatial resolution analyses and the ability to analyse not only "opaque" minerals available to infra-red and visible laser techniques but all important silicate minerals. Sample ablation using a quadrupled Nd-YAG laser ( $\lambda=266\text{nm}$ ), is a slower extraction process than visible and infra-red lasers though the power density during 10ns pulses focused to a  $10\mu\text{m}$  laser spot is extremely high ( $\sim 3 \times 10^{10} \text{ W cm}^{-2}$ ) and the light is typically absorbed in the top few microns of the sample. An advantage of this effect is that the average rate at which energy is dumped into the sample during analysis is typically 0.01-0.1W (1-10mJ/pulse at 10Hz), over two orders of magnitude smaller than typical powers delivered by CW visible and IR lasers. Such low average powers yield insignificant sample heating during analysis. This opens the doors to new sample extraction procedures, including beam raster which can achieve a much higher spatial resolution than current techniques.

Early experiments on natural rocks have demonstrated high spatial resolution in clear minerals such as K-feldspar and plagioclase. It has even proved possible to achieve high spatial resolution at biotite/quartz boundaries (typically the most difficult). As a result, the UVLAMP technique has been used to measure diffusive profiles in biotites in dyke wall rocks, heated during emplacement. Natural argon diffusion profiles less than  $50\mu\text{m}$  deep have been measured which were combined with laboratory diffusion parameters for biotite to constrain thermal histories.

In another application, controlled laboratory heating of gem quality k-feldspar and basalt composition glasses yielded argon concentration gradients up to  $50\mu\text{m}$  deep, which have been imaged with a resolution of as little as  $2.5\mu\text{m}$  by the UVLAMP using a beam raster technique. Such experiments measure not only diffusion parameters but also the solubility of argon.

## THE PERFORMANCE CHARACTERISTICS OF THE WA SHRIMP II ION MICROPROBE

Kennedy A.K. and de Laeter J. R., Curtin University of Technology, GPO Box U1987, Perth, 6001 Australia; Internet: ikennedy@info.curtin.edu.au

The Sensitive High-Resolution Ion Microprobe (SHRIMP) at the ANU has produced numerous major advances in isotope geochronology and geochemistry. As part of the testing of the new SHRIMP II ion microprobe at the Western Australia Center for Isotope Science we have measured the following performance characteristics at a mass-resolution of 5000 (1% definition): (1) Mass discrimination for  $^{208}\text{Pb}/^{206}\text{Pb}$  is respectively  $< 0.5\%$ ,  $< 0.3\%$  and  $< 0.1\%$ , in K-feldspar with 4% Pb, SRM 610 glass with 426 ppm Pb, and zircon with 20 ppm Pb. For  $^{34}\text{S}/^{32}\text{S}$  in galena mass discrimination is 3%; (2) Ion transmission was measured using an Aluminium target. Approximately 11% of the total number of secondary ions emitted were recorded as  $\text{Al}^+$  ions on the faraday cup; (3) The abundance sensitivity at 1 mass unit offset was  $5 \times 10^{-9}$  at  $^{30}\text{Si}^+$  and  $3 \times 10^{-8}$  at  $^{254}\text{UO}^+$ ; (4) A 1 sigma precision based on counting statistics of 0.3% for  $^{206}\text{Pb}/^{238}\text{U}$  in a 570 Ma standard zircon, which contains 20 ppm Pb and 220 ppm U, and 0.7% for  $^{208}\text{Pb}/^{206}\text{Pb}$  in SRM 610 glass were achieved with total count times of 70 sec for each Pb isotope and 35 sec for  $^{238}\text{U}$ ; (5) A 1 sigma reproducibility of 1.0% for  $^{206}\text{Pb}/^{238}\text{U}$  for 15 analyses of the standard zircon and 0.5% for  $^{208}\text{Pb}/^{206}\text{Pb}$  for 6 analyses of SRM 610 glass; (6) A sensitivity of  $> 20 \text{ cps/ppm Pb/nA}$  of  $\text{O}_2^-$  is achieved during U/Pb analysis of zircon at the above mass resolution.

As a test of day-to-day operation, we have analysed zircons from separates that give ages between 100 and 200 Ma by conventional mass spectrometry. These zircons are from the plutonic rocks of the Sierra Nevada Batholith (SNB) and have been classified as internally concordant (I), thermally disturbed (D), or possibly containing an inherited component (IC), Average  $^{206}\text{Pb}/^{238}\text{U}$  ages and the range of ages from SHRIMP analyses and conventional analyses are listed below along with the type of zircon. Apart from a bimodal age distribution in the Coso-1 zircons, with 3 grains giving an age  $> 180 \text{ Ma}$ , there was no evidence of inheritance. This is consistent with very little recycling of ancient material during growth of the SNB.

Sample	Type	Conv.	IP av.	Range	n
SQ61	I	101	107 (5)	99-118	18
MA9	D	156	151 (6)	142-162	11
W32	I	103	107 (8)	105-112	6
Coso-1	I	156	162 (10)	154-184	17
MA17	D	201	202 (10)	190-227	11
MA7	IC	156	153 (7)	139-159	7

1 standard deviation for the the zircon sample population are given in brackets.

Additional performance characteristics of the SHRIMP II and zircon data from other SNB granites will be shown.

NEOPROTEROZOIC POST GLACIAL CARBONATE  
ROCKS: IMPLICATIONS FOR THE PRECAMBRIAN  
CARBON CYCLE.

Martin J. Kennedy Department of Geology and  
Geophysics, University of Adelaide, S.A. 5001, Australia,  
and Malcolm W. Wallace, School of Earth Sciences,  
University of Melbourne, Parkville, Vic. 3052, Australia

Thin (<15m) enigmatic dolostone units cap Neoproterozoic glacial sequences throughout the world and are particularly well represented in Australia's numerous Proterozoic Basins. The finely laminated and micro-crystalline nature of the Australian "cap dolomites" constitute deeper water (largely below storm wave base) post glacial transgressive deposits and are commonly overlain by deep water stromatolites representing the highly condensed downlap surface below prograding mudstones of the overlying highstand sediments. Stratigraphic profiles of stable isotopic values measured through these units in key Neoproterozoic sections across the Australian Craton indicate a consistently low values of  $\delta C^{13}$  (-2 to -5 PDB) with progressive depletion of up to -3%per/mil upsection. Texturally well preserved dolomite fibrous (marine) cements retain up to -1%per/mil depletion of  $\delta C^{13}$  relative to surrounding matrix material and overlying internal sediments. The retention of this trend within discreet sections, and lack of homogenisation of  $\delta C^{13}$  values within textural components suggest primary preservation of  $\delta C^{13}$  values. The persistence of this trend in basins across Australia indicates a broad scale control of  $\delta C^{13}$ , suggestive of secular variation of sea water during the post glacial period.

The coincidence of major deglaciation, transgression and widespread carbonate deposition in marine environments implies a causal link between these processes. The continent-wide and perhaps global nature of these post-glacial cap dolostones indicates that immense volumes of carbonate were precipitated during this period. Such hypothesised large-scale carbonate precipitation must have caused (or have been the product of profound changes in the carbon cycle and global climate at this time, which is likely reflected by the depletion of  $\delta C^{13}$ . In sharp contrast there are no equivalent carbonate horizons capping Phanerozoic glacial successions. This may be related to the transition from abiogenic to biogenic skeletal carbonate precipitation across the Precambrian-Cambrian boundary. The supersaturation of Ca and Mg needed to directly precipitate carbonate from Proterozoic sea water may now be taken up by biogenic precipitation in Phanerozoic oceans. Greater flux of bicarbonate to the oceanic reservoir may have been possible during the Proterozoic and modified the silicate weathering cycle by absorbing and releasing correspondingly greater amounts of atmospheric  $CO_2$ .

$^{40}Ar$ - $^{39}Ar$  DATING OF ARCHAEOAN GOLD  
MINERALISATION IN THE KALGOORLIE GOLDFIELD,  
WESTERN AUSTRALIA: EVIDENCE FOR MULTIPLE  
MINERALISATION EPISODES.

KENT, A.J.R. and McDUGALL, I., Research School of  
Earth Sciences, The Australian National University,  
Canberra, Australia, 0200.

Mineralisation in the Kalgoorlie goldfield, in the Archaean Yilgarn Craton of Western Australia, has been responsible for over 1300t of gold, making this region one of the most productive gold-mining districts in the world.

Mineralisation is hosted within a ca. 2700 Ma volcano-sedimentary sequence and occurs in two predominant structural settings: (i) along a complex series of anastomosing shear zones (Golden Mile style) and (ii) in stockwork zones adjacent to late dextral faults (Mt Charlotte style). Both styles of mineralisation exhibit many of the features typical of Archaean gold deposits, although field relations indicate that the shear-hosted Golden Mile style mineralisation occurred prior to formation of the Mt Charlotte stockwork systems.

Muscovite is a common hydrothermal mineral paragenetically associated with gold deposition in both settings.  $^{40}Ar$ - $^{39}Ar$  geochronology of hydrothermal muscovite has been used to investigate the timing of each style of mineralisation. Two samples of muscovite from Golden Mile style shear lodes have  $^{40}Ar$ - $^{39}Ar$  plateau ages of  $2627 \pm 12$  and  $2628 \pm 12$  Ma (all errors are  $2\sigma$ ). Three samples of hydrothermal muscovite associated with Mt Charlotte style stockwork veins have identical  $^{40}Ar$ - $^{39}Ar$  plateau ages (within  $2\sigma$  errors) and these have a weighted mean of  $2602 \pm 7$  Ma.

It is considered that the  $^{40}Ar$ - $^{39}Ar$  ages from hydrothermal muscovites represent the timing of the Golden Mile and Mt Charlotte styles of gold mineralisation. Mineralisation occurred after greenschist facies metamorphism of the host sequence, and ambient temperatures in host rocks were probably much lower than the closure temperature of argon in white mica (ca. 300°C) at this time. Further, fluid inclusion measurements indicate that gold mineralising systems cooled rapidly below this closure temperature during progressive mineralisation, precluding the possibility of argon loss during slow cooling. There is also little evidence of subsequent thermal activity which may have produced argon loss in hydrothermal muscovites, although it is possible that muscovite associated with Golden Mile style shears may have lost argon during subsequent formation of Mt Charlotte style stockworks.

Muscovite  $^{40}Ar$ - $^{39}Ar$  ages indicate that shear-hosted gold mineralisation at the Golden Mile occurred at, or before, ca. 2630 Ma, prior to stockwork mineralisation at Mt Charlotte at ca. 2600 Ma. This is consistent with the field relations between the two styles of mineralisation. Recent theories suggest that Archaean Gold deposits in the Yilgarn Craton formed broadly contemporaneously in response to large-scale crustal fluid circulation. Such theories must now also contain the caveat that discrete, and unrelated, mineralisation episodes may also produce significant gold deposits with features similar to other 'typical' Archaean gold deposits.

**METASOMATISM IN ISLAND ARC MANTLE CAUSED BY VARIABLY FRACTIONATED SLAB-DERIVED FLUIDS AND MELTS: CONSTRAINTS FROM ULTRAMAFIC XENOLITHS IN VOLCANIC ARCS**

**KEPEZHINSKAS, P.K.**, DEFANT, M.J., AUSTIN, P., all at the Dept. of Geology, University of South Florida, Tampa, Florida 33620, USA, DRUMMOND, M.S, Dept. of Geology, University of Alabama at Birmingham, Alabama, USA, and MAURY, R.C., Universite Bretagne Occidentale, Brest, France.

A common feature of the Kamchatka arc volcanoes is the presence of ultramafic xenoliths hosted within recent eruptions. Xenoliths are variably deformed under high P,T-conditions, consistent with their derivation from the mantle wedge below the volcanic arc. These xenoliths exhibit pervasive metasomatic features believed to record multi-stage reactions between fluids and melts and a sub-arc mantle.

Ultramafic xenoliths from 4 frontal-arc and 1 rear-arc volcanoes can be grouped as 1) Cr-rich harzburgites, dunites, and lherzolites believed to represent a sub-arc lithospheric mantle prior to metasomatism and 2) Cr-poor pyroxenites, wehrlites, and websterites which are thought to be formed during a melt-mantle interaction.

Cr-rich xenolith suites exhibit across-arc variations. The frontal arc xenoliths are harzburgites and dunites containing Cr-rich spinels and Na-/Al-depleted diopsides. The rear-arc xenoliths are lherzolites and Cpx-poor harzburgites with less Cr-rich spinels and more Na- and Al-rich clinopyroxenes. Ion-probe results indicate that rear-arc mantle diopsides are both LREE-enriched and depleted, while frontal-arc mantle clinopyroxenes are mainly LREE-depleted. Frontal-arc, Cr-poor xenoliths contain LREE-enriched, high-Sr, low-Y felsic glass veins with pyrope-almandine garnet, Al-rich spinel, and Na-rich plagioclase. Rear-arc, Cr-poor xenoliths include phlogopite and a LREE-enriched hornblende and clinopyroxene.

The across-arc mantle heterogeneity in Kamchatka is consistent with greater degrees of melting below the arc volcanic front. The rear-arc tends to be less affected by flux-induced melting but carry metasomatic signatures introduced by slab-derived melts and fluids. This suggests that the slab undergoes a major stage of melting and/or devolatilization at relatively shallow depths (45-55 km), but still is capable of generating siliceous melts and hydrous fluids at greater depths (65-85 km) below the rear-arc. Surprisingly, fluids introduced from the slab below the Kamchatka arc front are CO<sub>2</sub>-rich and contain detectable amounts of CH<sub>4</sub>, F, and Cl based on fluid inclusion study. Rear-arc fluids are water-rich as suggested by amphibole and phlogopite present in Bakening low-Cr xenoliths. Three types of metasomatism are recognized in the Kamchatka arc mantle: 1) related to siliceous, slab-derived melt-mantle interaction; 2) related to mafic melt-mantle interaction; 3) related to the introduction of slab-derived, CO<sub>2</sub>/H<sub>2</sub>O fluid into the sub-arc mantle.

**LITHOSPHERIC CONTRIBUTIONS IN THE GENERATION OF ISLAND ARC MAGMAS: GEOCHEMICAL VARIATIONS IN ALONG STRIKE VOLCANOES FROM NORTHERN HONSHU, JAPAN**

**KERSTING, A.B.**, Earth Science Dept. & Institute of Geophysics & Planetary Physics, Lawrence Livermore National Laboratory, Livermore CA 94550 email: Kersting@llnl.gov, ARCULUS, R.J. (Dept. of Geology and Geophysics, Univ. of New England, Armidale, NSW 2351, and GUST, D.A., Dept. of Geology, Queensland Univ. of Tech. QLD 4001

The genesis of island arc volcanoes results from a complex interaction of many different sources-subducted oceanic crust, sediments, fluids, overlying mantle, and arc lithosphere. Quantifying the extent and mechanisms by which these reservoirs contribute to island arc magmas has been controversial and difficult. The approach taken in this study is to identify lithospheric influences in a transect of along-strike island arc volcanoes that crosscut different tectonic terranes.

In northern Honshu, Japan, the Tanakura Tectonic Line (TTL), a left-lateral transform fault reactivated during the opening of the Japan Sea, crosscuts the recent volcanic front. The TTL is a boundary between a package of terranes accreted in the Mesozoic (to the North) to the Sino-Korean craton (to the south).

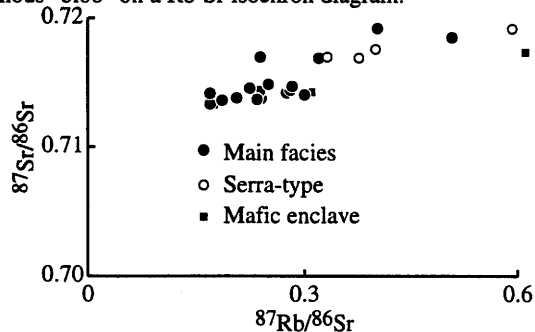
Preliminary results of a combined radiogenic isotope (Pb, Sr, & Nd), major and trace element investigation of a transect of Quaternary volcanoes in northern Honshu, Japan will be presented. Initial measurements of the Pb isotopic ratios of the Northern Honshu volcanic front lavas lie well above the MORB field in conventional <sup>207/204</sup>Pb and <sup>208/204</sup>Pb versus <sup>206/204</sup>Pb ratio diagrams. We interpret this to reflect crustal contamination in the generation of these magmas. In addition, elevated <sup>87</sup>Sr/<sup>86</sup>Sr has also been interpreted to reflect crustal involvement in some of the volcanic centers.

SÃO RAFAEL BATHOLITH, RIO GRANDE DO NORTE, BRAZIL: AN UNREGENERATE PLUTON

KETCHAM, D. H., LONG, L. E., Dept. of Geological Sci., Univ. Texas, Austin, Texas 78712, USA, and SIAL, A. N., Dept. of Geology, Fed. Univ. Pernambuco, Recife, PE 50732-970, Brazil

During the Brasiliano (Pan-African) orogeny from 700 to 550 Ma, the geologic province of Borborema in northeast Brazil was intruded by more than 80 granitoid bodies, one of them the primary epidote-bearing São Rafael Batholith located in the Seridó foldbelt. This unfoliated quartz monzonite pluton is thought to be of very late Brasiliano age, perhaps between 600 and 550 Ma based on field relations.

Twenty-four samples were analyzed isotopically, including 4 from a subtly different sub-facies of the pluton ("Serra-type"), and 2 mafic enclaves. In general, the rocks have high Sr ( $655 \pm 175$  ppm) and low Rb ( $61 \pm 9$  ppm), with consequent low enrichment in radiogenic Sr. Three biotite-apatite-whole rock isochrons provide cooling ages of  $0.49 \pm 0.01$  Ga. Data of 18 main-facies whole rocks plot as an amorphous "blob" on a Rb-Sr isochron diagram.



Inhomogeneous initial Sr ratios preclude the determination of a Rb-Sr age of crystallization. Somewhat more systematic data from the Serra-type samples suggest an age of  $\approx 0.6$  Ga. Sr ratios of main-facies rocks, projected back to 0.6 Ga, are high ( $0.713 \pm 0.001$ ), pointing to an ancient radiogenic crustal source.

Six whole-rock samples provide a Sm-Nd isochron apparent age of  $\approx 1.1$  Ga, which is inconsistent with field evidence for late Brasiliano emplacement. Anomalous Sm-Nd data indicate that initial Nd ratios also were inhomogeneous, just as Sr initial ratios were. Strongly negative values of  $\epsilon\text{Nd}_{0.6\text{Ga}}$  (-18 to -21) imply a source relatively enriched in Nd. Extrapolations of Nd evolution trajectories to intersection with the depleted mantle curve are consistent with *minimum* crust-formation ages of  $2.7 \pm 0.3$  Ga. Poorly understood Precambrian basement in northeastern Brazil has been complexly re-worked, and there is some evidence for presence of relict Archean crust.

The only "normal" isotope data from São Rafael are sharply delimited whole-rock  $\delta^{18}\text{O}_{\text{SMOW}} = +7.8$  to  $+8.1\%$  (Sial et al., in prep), and consistent mineral cooling ages of  $\approx 0.49$  Ga. Formed at about 0.6 Ga apparently by partial melting of Archean crust, the São Rafael magma mixed sufficiently to attain a distinctively uniform physical appearance and chemical-mineralogical composition, but it failed to homogenize isotopically. São Rafael is an "unregenerate" pluton, consisting neither of simply remobilized source rock nor of completely re-equilibrated material.

Sial, A. N., Ferreira, V. P., and Long, L. E., in preparation, High  $\delta^{18}\text{O}$ , High Al-Hornblende, Epidote-bearing Granitoids in Northeast Brazil.

CHLORINE-36 IN RAINFALL FROM AUSTRALIA

KEYWOOD, M.D., and CHIVAS, A.R., Research School of Earth Sciences, The Australian National University, Canberra 0200, Australia; FIFIELD, L.K., ALLAN, G.L. and CRESSWELL, R., Research School of Physical Sciences and Engineering, The Australian National University, Canberra 0200, Australia.

The  $^{36}\text{Cl}$  contents of bulk depositional precipitation was determined from remote sites in Central and Western Australia. Sampling transects included a west-east array trending inland from the coast of Western Australia (latitude  $27^{\circ}\text{S}$ ) and a north-south array through the Northern Territory and South Australia (longitude  $133^{\circ}\text{E}$ ). Precipitation was collected at three monthly intervals in coincidence with the seasons, for a period of two years.

$^{36}\text{Cl}/\text{Cl}$  ratios along the west-east array increase with increasing distance from the coast. This reflects a decreasing influence of marine Cl, (which contains negligible  $^{36}\text{Cl}$ ) at inland sites. Temporal variation of  $^{36}\text{Cl}$  fluxes across the west-east array reflect the dependence of  $^{36}\text{Cl}$  fallout on rainfall amount. This dependence explains the high fallout observed at coastal localities and suggests the importance of wet deposition for the removal of  $^{36}\text{Cl}$  from the atmosphere.

The extensive range of latitudes covered by the north-south sampling array allows an assessment of the predicted fallout rates of  $^{36}\text{Cl}$  to the Earth's surface. Cosmic ray fluxes to the Earth's surface are dependent on the Earth's magnetic field (Lal and Peters, 1967). A discontinuity in the tropopause at latitude  $35\text{-}40^{\circ}$  allows maximum transfer of air from the stratosphere to the troposphere at  $40^{\circ}$ . Thus a latitude dependence in the fallout rate is expected. The fallout rate along the west-east array of 15 atoms  $^{36}\text{Cl}/\text{m}^2/\text{s}$ , averaged over six seasons, is similar to the predicted flux of Andrews and Fonte (1991) at this latitude. However preliminary results from the north-south array show fallout rates that differ from predicted values, suggesting that mixing of air masses in the troposphere may be another factor in determining the fallout rates of  $^{36}\text{Cl}$  to the Earth's surface.

Andrews, J.N. and Fontes, J-Ch., 1991. Importance of in situ production of chlorine-36, argon-36 and carbon-14 in hydrology and geochemistry. *Isotope Techniques in Water Resources Development*, pp 245-269, IAEA, Vienna, 1992.

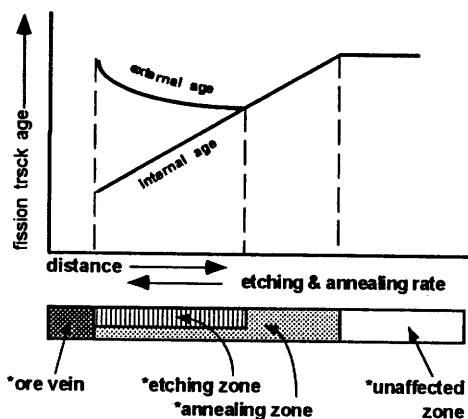
Lal, D. and Peters, B., 1967. Cosmic Ray Produced Radioactivity on the Earth. In K Sitte, ed. *Handbuch der Physik*, 46/2, Springer Verlag, Berlin, 551-612.

## Natural etching and annealing of fission tracks in zircons during hydrothermal alteration.

Nghiem Vu KHAI (University of Mining and Geology, Dongngac Tuliem, Hanoi, Vietnam) and WADATSUMI Kiyoshi (Osaka City University, Sigimoto Sumiyoshi, Osaka, Japan).

The fission track ages obtained from the internal ( $4\pi$ ) and external ( $2\pi$ ) surfaces of the zircon samples, collected in an orderly manner from near contact zone of a hydrothermal ore vein outward into the host rocks show two contrasting tendencies. The internal ages decrease toward the ore vein and, on the contrary, the external ages reveal an increasing for a limited distance. Consequently, the  $2\pi$  ages are consistently older than  $4\pi$  ones.

The decrease in  $4\pi$  ages is probably due to natural annealing of spontaneous tracks in zircon crystals during a high temperature ore forming stage. Considering the external tracks as an open system in term of physico-chemical interaction with surrounding environment, the behavior of  $2\pi$  ages can be explained as a result of the combined effect by both natural etching and annealing. It means that the external tracks underwent natural etching, during pre-ore hydrothermal alteration, before annealing process took place, so that the etched tracks could not be annealed effectively. Closer to ore fluids channel both natural annealing and etching rates are higher and they decrease with distance from the vein. The  $4\pi$ - and  $2\pi$  ages merge when the etching effect disappears.



This model demonstrates a real difference between  $4\pi$  and  $2\pi$  ages obtained for the samples and indicates that careful consideration is needed before interpreting their thermochronological meaning.

## OXYGEN AND SULFUR ISOTOPE STUDIES OF PRECAMBRIAN ANOROGENIC GRANITIC ROCKS IN THE MIDCONTINENT OF NORTH AMERICA

KIM, Sun-Joon, Dept. of Earth and Atmospheric Sciences, Purdue University, West Lafayette, IN 47907, U.S.A. (Now at Dept. of Mining and Mineral Engineering, Hanyang University, Seoul, Korea), and SHIEH, Yuch-Ning, Dept. of Earth and Atmospheric Sciences, Purdue University, West Lafayette, IN 47907, U.S.A.

Oxygen and sulfur isotope compositions have been determined for the granitic and related rocks from the Wolf River Batholith, Wisconsin; the Illinois Deep Holes; the Wet Mountains plutons, Colorado; and subsurface samples from Illinois, Iowa, S. Dakota, Nebraska, Missouri, Kansas, and Oklahoma. Hydrothermal alteration resulting in a decrease of  $\Delta_{Q-F}$  values was observed locally throughout the Wolf River Batholith. Feldspars of different colors (pink, gray, and red) were separated whenever feasible and analyzed. Most red feldspars ( $An_{10-30}$ ) show the highest and constant  $\delta^{18}O$  values (9.3-10.0 permil) suggesting near complete isotope exchange with hydrothermal fluid. Based on  $\delta^{18}O$  values and alteration temperatures estimated from fluid inclusions (260-350°C),  $\delta^{18}O$  of the fluid is calculated to be  $5.0 \pm 1.4$ . Sedimentary formation water is most likely the source of the fluid. Sulfur content and isotope composition of granitic rocks of the Wolf River Batholith range from 30 to 117 ppm and from 1.1 to 6.5 permil respectively and are considered to be magmatic. The positive correlation observed between oxygen and sulfur isotope data of granitic rocks may be due to assimilation of the Penokean plutonic rocks by a primary magma of deep-crustal origin, or to mixing at depth of a primary magma with another magma having higher  $\delta^{18}O$  and  $\delta^{34}S$ . Oxygen isotope fractionations among quartz, feldspar and biotite indicate two different isotope exchange processes at two different stages: 1) the continuous retrograde isotopic exchange shortly after emplacement, and 2) the hydrothermal alteration at a much later time.

When data from the present study are combined with data from previous studies on similar Precambrian anorogenic granitic rocks in the midcontinent of North America, a regular increase of  $\delta^{18}O_Q$  from NE to SW is observed: Wolf River Batholith, WI (mean  $\delta^{18}O_Q = 7.9$ ); Illinois Deep Holes (8.2); St. Francois Mts., MO (9.5); and Wet Mts., CO (9.8). The  $\delta^{18}O_Q$  values of subsurface samples range from 7.3-10.5. Thus, all the granites may have formed by partial melting of a low- $^{18}O$  source material in the lower crust, with an increasing contribution of high- $^{18}O$  material such as metasedimentary and/or metavolcanic rocks toward the southwest.

**MIDDLE AND LATE TRIASSIC TIME SCALE  
CALIBRATION OF THE MURIHIKU  
SUPERGROUP, SOUTHLAND, NEW ZEALAND**

KIMBROUGH, D.L., Department of Geological Sciences, San Diego State University, San Diego CA 92182, MATTINSON, J.M., Department of Geological Sciences, University of California, Santa Barbara CA 93106, RENNE, P.R., Institute of Human Origins, 2453 Ridge Road, Berkeley CA 94709, and CAMPBELL, J.D., Geology Department, Otago University, Dunedin, New Zealand.

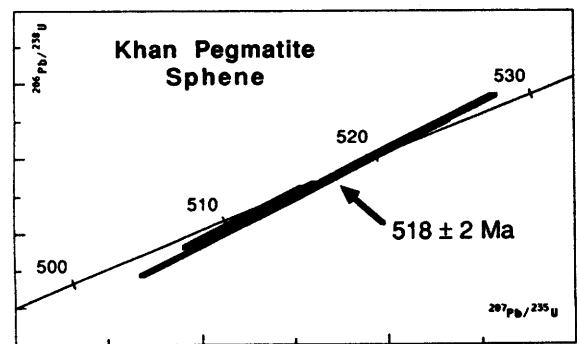
The New Zealand Triassic is divided into seven local stages based on subdivision of the Murihiku Supergroup and is representative of the time-span Scythian to the end of the Triassic. Faunal assemblages include hydrozoans, ammonoids, nautiloids, conodonts and halobiid bivalves and provide a firm basis for interregional correlation of these strata with North American and other sequences. Zircon U/Pb and biotite  $^{40}\text{Ar}/^{39}\text{Ar}$  dates from three crystal-vitric tuffs in the Middle and Upper Triassic portion of the Murihiku Supergroup constrain local and international biostratigraphic time scales. The stratigraphically lowest sample occurs in upper Etalian strata, close to the Etalian-Kaihikuan Stage boundary which in turn is tightly correlated to the Anisian-Landian international boundary. Two individual grains of biotite from this tuff yielded indistinguishable laser step-heating  $^{40}\text{Ar}/^{39}\text{Ar}$  plateau ages of  $242.3 \pm 0.8$  and  $243.4 \pm 0.8$  Ma. The weighted mean of the two plateaus is  $242.8 \pm 0.6$  Ma. Zircon  $^{206}\text{Pb}/^{238}\text{U}$  dates from the same sample range from  $236.8 \pm 2$  to  $243.1 \pm 2$  Ma. The later result is from a nearly concordant fine-grained fraction leached in HF prior to dissolution and is in good agreement with the more precise argon plateau age estimate. Zircon U/Pb dates from from Otamitan and Otapirian tuff beds higher in the section provide maximum ( $226 \pm 2$  Ma) and minimum ( $214 \pm 2$  Ma) ages, respectively, for the occurrence of *Monotis* in the New Zealand stratigraphic record. These two ages are based on  $^{207}\text{Pb}/^{206}\text{Pb}$  dates from zircon exhibiting slight amounts of relatively recent lead loss but no inherited components. Ammonite-bearing Triassic strata continue upsection for approximately 1500 meters above the  $214 \pm 2$  Ma Otapirian tuff bed.

**518 Ma SPHENE (TITANITE) FROM THE KHAN  
PEGMATITE, NAMIBIA, SOUTHWEST AFRICA:  
A POTENTIAL ION-MICROPROBE STANDARD**

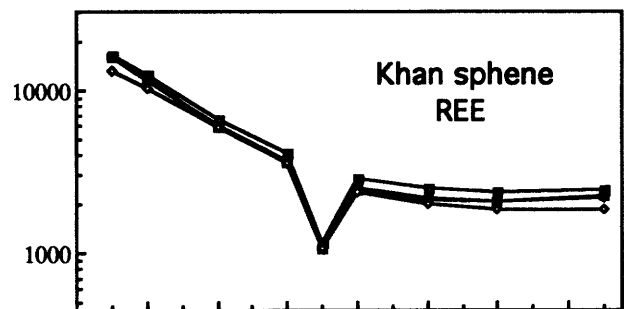
KINNY, P.D., Department of Applied Physics, Curtin University of Technology, Perth, WA, McNAUGHTON, N.J., Dept. of Geology, University of Western Australia, Perth, WA, FANNING, C.M. and MAAS, R., Research School of Earth Sciences, ANU, Canberra, ACT, Australia.

Large, euhedral crystals of black sphene (titanite) occur in copper-mineralized pegmatite at the Khan mine, Namibia. A 12 mm crystal has been investigated as a potential standard for U-Pb isotopic and trace-element studies by microprobe. Sphene can be a useful mineral for dating, particularly when associated with mineralization.

Six conventional U-Pb analyses of splits from two crushed fragments yielded concordant results with a  $^{207}\text{Pb}/^{206}\text{Pb}$  age of  $518 \pm 2$  Ma (95% conf.). U contents were in the range 682 to 712 ppm, and  $^{206}\text{Pb}/^{204}\text{Pb}$  ratios were ca. 2000. The 518 Ma age is in agreement with a sphene - K-feldspar isochron of  $521 \pm 27$  Ma (MSWD 0.15) derived from the same material.



REE abundances determined by isotope dilution on four chips agree to within 10% for each analyzed element. The pattern dips smoothly from La  $1 \times 10^4$  chondrites to Gd-Lu  $2 \times 10^3$  chondrites, with a negative Eu anomaly, as shown.



A series of ion-probe  $25\mu\text{m}$  spot traverses across transverse and longitudinal sections through the sphene has so far failed to detect significant heterogeneity in U-Pb isotopic composition or in trace-element abundances. The ion-probe U-Pb analytical routine is the same as for perovskite, using the  $\text{CaTi}_2\text{O}_4$  peak at mass 200 as a reference for concentrations, and  $^{206}\text{Pb}/^{206}\text{U}$  vs  $\text{UO}_2/\text{UO}$  covariation to calibrate the measured Pb/U ratios. Pb sensitivity on the Western Australia Isotope Science Centre SHRIMP II is comparable to that derived from zircons.

The method has been applied successfully to date sphenes associated with mineralization in the Olympic Dam deposit of South Australia, and elsewhere.

NEON DEGASSING OF THE SUBCONTINENTAL MANTLE UNDER THE EIFEL REGION, GERMANY

KIPFER, R.<sup>1</sup>, AESCHBACH-HERTIG, W.<sup>1</sup>, BAUR H.<sup>2</sup>, IMBODEN, D. M.<sup>1</sup>, HOFER, M.<sup>1</sup>, HOHMANN, R.<sup>1</sup> and WIELER, R.<sup>2</sup>

<sup>1</sup>Environmental Physics, Swiss Federal Institute of Technology, ETH/EAWAG, 8600 Dübendorf, Switzerland

<sup>2</sup>Isotope Geology, Swiss Federal Institute of Technology, ETH, 8092 Zürich, Switzerland

Phreatomagmatic eruptions formed the typical maar lakes of the Eifel region (Germany). The magmatic activity started 200'000 years ago in the western part and then moved towards east ending 11'000 BP with the formation of Laacher See, the youngest maar.

Recent degassing of fluids from the subcontinental mantle is common in this area as indicated by numerous mineral springs and CO<sub>2</sub> wells.

We analysed the light noble gases in several CO<sub>2</sub> wells and natural gas discharges. All samples contain isotopically light helium from a mantle source and radiogenic helium in different proportions. All <sup>3</sup>He/<sup>4</sup>He ratios are lower than the those found in fluid inclusions of xenoliths related to the magmatic cycle [Dunai and Baur, 1993]. Some well gases even contain non atmospheric isotopically light neon. <sup>20</sup>Ne/<sup>22</sup>Ne ratios as high as 11.2 and <sup>21</sup>Ne/<sup>22</sup>Ne ratios up to 0.048 have been measured. The neon results group the CO<sub>2</sub> gases in two different sets, representing the eastern and the western part of the Eifel, respectively. Assuming a common mantle origin for the noble gases in the Eifel, one can correct the neon data for radiogenic production using the difference between the measured <sup>3</sup>He/<sup>4</sup>He ratio and the initial mantle ratio conserved in xenolithic fluid inclusions. The corrected neon data define a mixing line between atmospheric neon and a mantle neon component which differs from MORB since it contains less nucleogenic neon.

Our divers sampled a CO<sub>2</sub> gas plume entering Laacher See at a depth of 31 m. The neon in this high pressure fluid contains up to 4 % of mantle neon with a mantle <sup>20</sup>Ne/<sup>3</sup>He ratio of about 1.4. Combining the elemental ratio with the known <sup>3</sup>He flux into the lake (6500 atoms/cm<sup>2</sup>/s, Kipfer et al., 1992) we estimate a recent mantle <sup>20</sup>Ne flux of about 9000 atoms/cm<sup>2</sup>/s.

Dunai, T. J. and Baur, H., 1993, Noble gas and Sr-, Nd-Systematics of the European Subcontinental Mantle: supplement to European Journal of Mineralogy, v. 5, p. 134

Kipfer, R., Aeschbach-Hertig, W., Baur, H., Hofer, M. and Imboden, D. M., 1993, Helium and CO<sub>2</sub> Fluxes from the Earth Mantle in Laacher See, Germany: supplement to Annales Geophysicae, v. 11, part II, p.236

FLUID MIGRATION AND THERMAL HISTORY OF THE MORCLES/DOLDENHORN NAPPE (HELVETIC ALPS):  $\delta^{18}\text{O}$  AND  $\delta^{13}\text{C}$  ANALYSES OF QUARTZ-CALCITE VEINS AND MYLONITES

KIRSCHNER, D.L. Institut de Minéralogie, Université de Lausanne BPSH-2, CH-1015 Lausanne, Switzerland, SHARP, Z. D., and MASSON, H. (same address) (e-mail: dkirschn@imp.unil.ch)

The western Helvetic Alps is a classic fold/thrust belt in the external zone of the Alpine orogen. Stable isotope analyses of mylonites and veins are used to constrain the sources and pathways of fluids and the thermal history of the lowest nappe in this belt (the Morcles and structurally-equivalent Doldenhorn nappe exposed 50 km along strike to the east).

One hundred mylonite samples were analyzed from five traverses at the basement-nappe thrust contact.  $\delta^{18}\text{O}$  values decrease by ~7‰ depletion toward the basement-Doldenhorn contact, while the  $\delta^{13}\text{C}$  values do not vary systematically in proximity to the contact. The strong oxygen isotope shift localized in a 5 meter zone about this contact is similar to  $\delta^{18}\text{O}$  shifts documented for the overlying Diablerets<sup>1</sup> and Glarus<sup>2</sup> thrusts, and are consistent with water-dominated fluids having entered the thrusts either from more deeply buried Mesozoic sediments or underlying basement massifs. Conversely, the  $\delta^{18}\text{O}$  values at the basement-Morcles nappe contact do not vary systematically, while the  $\delta^{13}\text{C}$  values are lowered by up to 8‰ in a 5 m wide zone at the contact. Fluids entering the base of the Morcles nappe must have been from an isotopically distinct (water-poor?) reservoir relative to the fluids entering the Doldenhorn, Diableret, and Glarus thrusts.

Additional analyses have been made of eleven syntectonic, fibrous quartz-calcite veins from Morcles nappe in order to constrain its thermal history during deformation. The temperature in the hinterland core of the Morcles fold nappe was 300°C during NW-extension (overthrusting?), it then increased to 350°C and subsequently dropped back down to 300°C during late orogen-parallel, NE-extension of the nappe. Farther to the foreland, analyses of crosscutting veins show that temperature during NW-extension was 330°C and decreased to 300°C during NE-extension. In the most foreland area sampled (Les Plans) the average temperature was 260°C. The  $\delta^{18}\text{O}$  and  $\delta^{13}\text{C}$  values of the calcite in all the veins analyzed are the same as those of their surrounding host marl and limestone, indicating that these isotopic systems were rock-buffered throughout most of the Morcles nappe.

<sup>1</sup>Crespo-Blanc et al. (in preparation)

<sup>2</sup>Burkhard et al. (1992). *Contrib. Min. Petrol.* 112, 293-311.

INTERPRETATION OF U/Pb AGES OF ZIRCONS FROM MESOZOIC PLUTONS IN THE SALINIAN BLOCK, CALIFORNIA

KISTLER, R. W., WOODEN, J. L., U. S. Geological Survey, Menlo Park, CA, U. S. A.

Mesozoic plutons exposed in the Salinian block to the west of the San Andreas fault in California commonly yield zircon fractions that have almost concordant to concordant  $^{206}\text{Pb}/^{238}\text{U}$ - $^{207}\text{Pb}/^{235}\text{U}$  ages (James, 1992; Mattinson, 1978). For most plutons dated, however, different zircon fractions yield different dates that form trends parallel to or on concordia on U/Pb plots. Complex explanations that rely on minor inheritance of Proterozoic zircons from source rocks of the plutons coupled with subsequent lead loss from newly formed zircons have been developed to interpret the U/Pb data. Interpreted and measured zircon ages in most cases are greater than ages from coexisting minerals dated by K-Ar or fission-track techniques and those ages have been interpreted to reflect cooling at the end of a prolonged high temperature post emplacement history of the plutons.

We have dated four fractions of zircons and two of sphene separated from a biotite, hornblende tonalite dredged at a depth of about 210 feet in the Pacific Ocean from the southern end of the Cordell Bank about 15 km northwest of the Farallon Islands. All six mineral fractions yield concordant U/Pb ages, but they span the interval from about 91 to 99 Ma. SHRIMP analysis of seven spots on zircons from the concordant 94 Ma 80-100 micron fraction yield concordant U/Pb ages that range from about 95 to 127 Ma.

There is a positive correlation of age with U concentrations that range from 346 to 420 ppm in the four zircon fractions dated by conventional techniques. The SHRIMP data show a surprising range of U concentrations from 146 ppm to 7836 ppm that do not correlate with age. There is obvious inheritance in the zircons, and it is impossible to select a meaningful age from the spectrum of concordant ages.

$^{206}\text{Pb}/^{204}\text{Pb}$  vs  $^{238}\text{U}/^{204}\text{Pb}$  and  $^{207}\text{Pb}/^{204}\text{Pb}$  vs  $^{235}\text{U}/^{204}\text{Pb}$  isochron plots of the conventional zircon and sphene U/Pb data yield ages of 93.9 Ma and 94.3 Ma, respectively. The  $^{206}\text{Pb}/^{204}\text{Pb}$  and  $^{207}\text{Pb}/^{204}\text{Pb}$  intercepts on these diagrams indicate a small radiogenic lead inheritance in the minerals and that the feldspar lead isotopic composition should not be used as the common lead correction in the age calculations. The zircon and sphene isochron age is the same, within experimental error, as the Rb-Sr whole-rock-mineral isochron and  $^{40}\text{Ar}/^{39}\text{Ar}$  biotite and hornblende incremental heating plateau ages.

A similar treatment of U/Pb zircon, sphene and apatite ages determined for tonalites at Bodega Head (Mattinson, 1978) and Montara (James, 1992) in the Salinian block brings them into agreement with Rb/Sr whole-rock-mineral isochron and  $^{40}\text{Ar}/^{39}\text{Ar}$  biotite and hornblende incremental heating plateau ages.

James, E. W., 1992, Cretaceous metamorphism and plutonism in the Santa Cruz Mountains, Salinian block, California, and correlation with the southernmost Sierra Nevada: *Geol. Soc. America Bulletin*, v. 104, p. 1326-1339.

Mattinson, J. M., 1978, Age, origin, and thermal histories of some plutonic rocks from the Salinian block of California: *Contrib. to Mineralogy and Petrology*, v. 67, p. 233-245.

Comparison of FT, K-Ar and Ar-Ar age using JAS-G1 obsidian glass: Calibration of each method and laboratory

Naoko KITADA\*<sup>1</sup>, Kiyoshi WADATSUMI\*<sup>1</sup>, Gulio BIGAZZI\*<sup>2</sup>, Alan DEINO\*<sup>3</sup>, Marinella LAURENZI\*<sup>2</sup>, Bart KOWALLIS\*<sup>4</sup>, Keisuke NAGAO\*<sup>5</sup>, Harue MASUDA\*<sup>1</sup> (\*<sup>1</sup>; Osaka City Univ. \*<sup>2</sup>; Istituto di Geochronologia e Geochimica Isotopica \*<sup>3</sup>; Geochronology Center of the Institute of Human Origin \*<sup>4</sup>; Brigham Young Univ. \*<sup>5</sup>; Earth's Interior Inst.)

The glass age determinations using FT, K-Ar and Ar-Ar were carried out for the purpose of get independent ages and comparison each other. The glass sample is used JAS-G1 obsidian that produced as a chilled margin of rhyolitic intrusive rock at Nagano prefecture in Japan.

On account of high K-content and obtain spontaneous fission-tracks enough to counting easily, JAS-G1 is appropriate sample in this experiment. At the dating of fission-track age, both ambient and plateau age were determined. Plateau method was used in order to take away of fading effect that observed in spontaneous fission.

At the result of this experiment, plateau ages indicate little bit old age rather than ambient one, and seemed to cancel of fading effect. In fact, plateau ages show as nearly same age as K-Ar and Ar-Ar age. On the point of comparison of K-Ar and Ar-Ar age, these do not necessarily coincide in  $1\sigma$ -error each other. The reason of this result is indicate following problem:

- 1) partial alteration may occur.
- 2) sample is not homogeneous about K-content.
- 3) at the comparison of each laboratory, calibration of each mass may have to use same standard sample.

## CARBON ISOTOPE THERMOMETRY IN THE ADIRONDACKS

KITCHEN, Nami E. and VALLEY, John W.,  
Dept. of Geology and Geophysics, Univ. of  
Wisconsin, Madison, WI 53706, USA

The fractionation of carbon isotopes between calcite and graphite provides a temperature sensitive thermometer for high grade marbles. We have conducted a study of calcite-graphite fractionations ( $\Delta_{cc-gr}$ ) in amphibolite and granulite grade rocks of the Adirondack Mtns., NY, to evaluate the accuracy of the thermometer. Detailed thermometry in the amphibolite grade NW Adirondacks shows small systematic changes in  $\Delta_{cc-gr}$  northwestwards from 3.7 to 4.3 to 3.9 over a 30 km distance, reflecting transitions from amphibolite facies towards granulite facies to the SE and NW. These fractionations correspond to temperatures of 685, 640, and 670°C respectively, based on the empirical calibration of Dunn and Valley (1992). Calcite-graphite pairs from the granulite grade Central Adirondacks give consistently smaller fractionations. 22 analyses from between the 725 and 775°C isotherms (petrologic thermometry, Bohlen et al, 1985) yield  $\Delta_{cc-gr} = 3.67$  to  $2.95$ , 690° to 750°C (average = 715°C). This suggests that the empirical calibration may be ~0.4‰ too low, in agreement with Chacko et al (1991), or that the calcite-graphite system has been reset from peak metamorphic conditions.

7 graphite flakes from 4 different localities with an average size of 0.4 x 1.8 mm were delaminated perpendicular to the c-axis in order to measure  $\delta^{13}C$  variations across individual flakes, and thereby test for zonation. In every case the cores of the flakes were heavier than the rims, by 0.1 to 0.6‰ ( $\pm 0.05$ ) across less than 0.25mm. Core  $\delta^{13}C$  values yield  $\Delta_{cc-gr}$  values as low as 2.6 and 2.7 (785 to 775°C), while the rims of the same samples give  $\Delta_{cc-gr} = 3.0$  to 3.2 (745 to 725°C). Although  $\Delta_{cc-gr}(\text{bulk})$  does not correlate with distance to the Marcy Anorthosite Massif (for 18 bulk analyses within 4 km of the contact, the average  $\Delta_{cc-gr} = 3.33$ , 725°C), the highest  $\Delta_{cc-gr}(\text{core})$  temperatures are from within 0.5 km of the anorthosite contact and may preserve early contact metamorphic temperatures. Late-stage overgrowths of graphite were not apparent in any of the samples, therefore diffusive exchange of C may be responsible for the zonation.

Values of  $\Delta_{cc-gr}(\text{core})$  correlate very well with petrologic temperature data in the Adirondacks. Thus, despite minor zoning in graphite, the calcite-graphite system provides a sensitive and reliable thermometer.

## NITROGEN ISOTOPE STUDY OF PRIMITIVE CHONDRITES BY A LASER PROBE METHOD

KIYOTA, K. and SUGIURA, N., Dept. of  
Earth and Planetary Physics, Univ. of Tokyo,  
Tokyo, 113, Japan.

In search for presolar grains, we have measured isotope ratios of nitrogen and noble gases in UOCs by a stepwise combustion method. Some types of isotopically anomalous nitrogen components which are probably due to unknown presolar grains have been found. Though some chemical and physical treatment have been performed, the carriers are not concentrated and they are not identified yet. UOCs are heterogeneous in mm scale, and in some UOCs, whole rock samples contain various amounts of anomalous nitrogen, according to the results of the stepwise combustion method. Therefore, to investigate where the carriers of anomalous nitrogen are, we measured nitrogen and rare gases by a laser probe method.

A sample was cut from a chunk of UOC by a diamond saw and a face was polished. After washing with water and acetone in an ultrasonic bath, it was heated in a vacuum system at 500C for an hour to remove terrestrial contaminations. The polished face was heated by a focused CW Nd-YAG laser and the extracted gases were measured with a static QMS. A diameter of a pit by the laser is about 0.1mm.

Mezo Madaras (LL3.4/3.7) was used for the preliminary experiments. Previously, we found by a stepwise combustion of bulk samples this UOC contains both light ( $\delta^{15}N < -70$  permil) and heavy ( $\delta^{15}N > 230$  permil) nitrogen components heterogeneously.

The abundance and isotopic composition of nitrogen from some laser pits are about 0.1ng and 50 permil.  $^{40}Ar/^{36}Ar$  ranges from 20 to 300. The sensitivity of N measurement of our laser extraction system is better than that reported by Franchi et al. (1986). Thus we will be able to analyze smaller regions in meteorites which will help us find where presolar grains are located.

Franchi, I. A., et al., 1986, The laser microprobe:

A technique for extracting carbon, nitrogen, and oxygen from solid samples for isotopic measurements: *Journal Geophys. Research*, v.91, No.B4, p.D514-D524.

## NICKEL-59 ACTIVITIES OF GRANT AND OTHER METEORITES MEASURED BY ACCELERATOR MASS SPECTROMETRY

KLEIN, J., MIDDLETON, R., Dept. of Physics, Univ. Pennsylvania, Philadelphia, PA, 19104, HERZOG G.F., and XUE, S., Dept. of Chemistry, Rutgers Univ., New Brunswick, NJ 08903.

The radioactive nuclide  $^{59}\text{Ni}$  is made in meteorites when  $^{58}\text{Ni}$ , the major stable isotope of nickel (~68%), captures thermal neutrons produced during cosmic ray bombardment. The nuclide holds much promise as a monitor of the thermal neutron fluxes in meteorites for several reasons: (1) the target element of the bombardment, nickel, occurs in convenient concentrations in many classes of meteorites; (2) the cross section  $\sigma_{\text{th}}$  for the reaction  $^{58}\text{Ni}(n,\gamma)^{59}\text{Ni}$ , 4.6 b, is appreciable; (3) the long half-life (76 ky) means that measurements need not be restricted to recent falls or very young finds. After a ~20-year lull, experimental interest in  $^{59}\text{Ni}$  has revived with the realization that accelerator mass spectrometry (AMS) makes the measurements easier. We report  $^{59}\text{Ni}$  activities measured by AMS in several meteorites as a first step toward the systematic investigation of its production rate.

After magnetic separation and HF etching where necessary, metal-rich phases were dissolved in 7%  $\text{HNO}_3$  to which Be, Al, and Ca carriers had been added for other measurements. Nickel was isolated by a series of ion exchange and precipitation steps.  $^{59}\text{Co}/^{58}\text{Ni}$  ratios were typically less than 400 (atom/atom). AMS analyses on the FN tandem at the Univ. Pennsylvania were made relative to a  $^{59}\text{Ni}$  standard prepared by irradiating high-purity nickel metal in a reactor. Backgrounds, due primarily to  $^{59}\text{Co}$ , were less than 5% of the measured values.

Measured  $^{59}\text{Ni}$  activities (dpm/g Ni) were as follows: Admire,  $3.1 \pm 0.5$ ; Charlotte,  $0.58 \pm 0.17$ ; Estherville,  $4.1 \pm 0.5$  and  $3.4 \pm 0.3$ ; Watson,  $0.40 \pm 0.05$ ; Zhaodong,  $0.33 \pm 0.03$ ; activities in four samples of the Grant iron meteorite had values between 1 and 2. Agreement with previously published values is satisfactory for Estherville, Grant and Admire. In contrast to the  $^{26}\text{Al}$  and  $^{10}\text{Be}$  activities but as expected, the  $^{59}\text{Ni}$  activities in the Grant samples increase with increasing  $^4\text{He}/^{21}\text{Ne}$  ratio, and hence depth in the meteorite.

Nominal thermal neutron fluxes  $\phi$  ( $\text{n}/\text{cm}^2\text{-s}$ ) calculated from the relation  $^{59}\text{Ni} = \sigma_{\text{th}}\phi N$  where  $N$  is the  $^{58}\text{Ni}$  concentration range from 0.17 for Zhaodong, an L4 chondrite with an unremarkable  $^{22}\text{Ne}/^{21}\text{Ne}$  ratio, to 2.1 for the mesosiderite Estherville. The neutron fluences estimated for the Grant samples are  $\sim 2 \times 10^{16}$   $\text{n}/\text{cm}^2$ ; published values for samples of the lunar regolith are similar.

## EVIDENCE FOR THE REWORKING OF CADOMIAN CRUST IN VARISCAN GRANITOIDS OF CENTRAL EUROPE (SOUTH BOHEMIAN PLUTON, BOHEMIAN MASSIF, AUSTRIA): A ZIRCON Pb-Pb AND U-PB STUDY.

Klötzli, U.S., Dep. of Geology, Lab. for Geochronology, Univ. of Vienna, Franz Grillstr. 9, A-1030 Austria, and Parrish, R.R., Geol. Survey of Canada, 601 Booth Street, Ottawa, K1A 0E8, Canada.

The existence of metamorphic and plutonic rocks of Cadomian (pan-African) age either consolidated with or reworked into the European basement during the Variscan orogeny is well documented for the middle and eastern part of the Bohemian Massif (i.e. "Moldanubikum" of Bohemia, "Bruno-Vistulikum"). For the composite South Bohemian Pluton in Austria and the Czech Republic such evidence has been lacking.

A combined Pb-Pb evaporation and conventional U-Pb study of zircons from quartz monzonitic enclaves of the Weinsberg type granite and the Rastenberg type granodiorite gives the following age results: enclaves in Weinsberg type granite:  $355 \pm 8$  Ma (rim or long prism.) and  $529 \pm 22$  Ma (core or short prism.); Rastenberg type granodiorite:  $339 \pm 5$  Ma (rim, short prism. or tabular habit),  $623 \pm 22$  Ma (core or long prism.). Upper intercept ages for both batholiths are in the range of 2000 – 2540 Ma.

The Carboniferous ages are interpreted as the time of intrusion of the Variscan granitoids.

The Cambrian and pre-Cambrian ages demonstrate the presence of inherited zircons from protoliths of Cadomian age in the investigated granitoids. As up to 50% of the investigated zircons show Cadomian ages, it is postulated that the amount of reworked Cadomian basement is quite substantial.

All the zircons investigated show true magmatic morphologies. This and the limited scatter in age distribution suggest that the reworked Cadomian protoliths were either intrusive rocks or orthogenic metamorphic rocks.

Thus the zircon investigations in the South Bohemian Pluton clearly demonstrate the presence of reworked Cadomian basement within or at least below the present Moldanubian upper crustal rocks. It is not yet clear whether the Cadomian rocks belong to the overridden basement complex of the "Bruno-Vistulikum" microplate or whether they belong to the Moldanubian microplate probably having been incorporated there during earlier stages of the Variscan orogeny. Sr isotope systematics favor the latter model.

## THE COSMOGENIC RADIONUCLIDES $^7\text{Be}$ , $^{10}\text{Be}$ , AND $^{36}\text{Cl}$ IN PRECIPITATION

KNIES D. L., ELMORE D., SHARMA P., Department of Physics, Purdue University, West Lafayette, IN 47901 USA, VOGT S., LIPSCHUTZ M.E., Department of Chemistry, Purdue University, West Lafayette, IN 47901 USA, and PETTY G., MONAGHAN M., Department of Earth and Atmospheric Sciences, Purdue University, West Lafayette, IN 47901 USA

Two-thirds of the  $^7\text{Be}$  ( $t_{1/2} = 53$  d),  $^{10}\text{Be}$  ( $t_{1/2} = 1.5$  My), and  $^{36}\text{Cl}$  ( $t_{1/2} = 0.3$  My) is produced in the stratosphere and one-third in the troposphere. The residence time of these radionuclides in the stratosphere is a few years and in the troposphere is a few weeks. Since  $^7\text{Be}$ 's half-life is short compared to its residence time in the stratosphere and similar to its residence time in the troposphere,  $^7\text{Be}/^{10}\text{Be}$  and  $^7\text{Be}/^{36}\text{Cl}$  concentration ratios should not equal their production ratios, but should have distinct tropospheric and stratospheric values. For this reason, these isotopes can be used to study processes involving mixing of air from the troposphere and air from the stratosphere.

We built a wet-only rain collector and located it 10 km west of West Lafayette, Indiana. The collector is equipped with an automatic roof and an automatic sample changer that can hold up to seven 8-liter bottles. During the period April 18, 1992 to August 31, 1993, 350 samples were collected with ~3 mm resolution. Three 125 ml aliquots were taken from every sample for cation (ICP-AES) and anion (IC) analyses and two 500 ml aliquots were taken from selected samples for future  $^2\text{H}$ ,  $^3\text{H}$ , and  $\delta^{18}\text{O}$  measurements on selected samples.

The  $^7\text{Be}/^{36}\text{Cl}$  and  $^{10}\text{Be}/^{36}\text{Cl}$  ratios varied by a factor of 60. The mean  $^{10}\text{Be}/^{36}\text{Cl}$  ratio was 8.9.  $^7\text{Be}$ ,  $^{10}\text{Be}$ , and  $^{36}\text{Cl}$  concentrations covaried through a single event. Typically they decreased from high values at the beginning of an event to lower values at the end. Mean concentrations were  $1.4 \times 10^7$  atoms/L  $^7\text{Be}$ ,  $1.8 \times 10^7$  atoms/L  $^{10}\text{Be}$ , and  $0.2 \times 10^7$  atoms/L  $^{36}\text{Cl}$ . A strong washout effect is evident in the  $^7\text{Be}$ ,  $^{10}\text{Be}$ , and  $^{36}\text{Cl}$  data, with up to an order of magnitude decrease from the first to the second sample.

We are investigating relationships between the radionuclide concentrations and event type, air masses history, and season. Using back trajectories and standard atmospheric data bases, we will determine the source regions of the isotopes and their residence times in the lower atmosphere. Furthermore, we will investigate whether the different isotopes are scavenged by similar mechanisms as they move through the atmosphere. This knowledge is critical to understanding the large anomalies observed in the  $^{10}\text{Be}/^{36}\text{Cl}$  ratio ice core data, where the measured  $^{10}\text{Be}/^{36}\text{Cl}$  ratio is lower than predicted by theory and varies with time in a way that cannot be explained by production rate variations alone.

$^{36}\text{Cl}$  has a high thermal neutron cross section for production from  $^{35}\text{Cl}$  and is usually present in reactors, reprocessing facilities, and low- and high-level nuclear waste.  $^{36}\text{Cl}$  can be released in gaseous, liquid, and solid phases and eventually reaches groundwaters where it is a highly mobile anion. Thus,  $^{36}\text{Cl}$  is a good tracer for studying radioactivity releases into the environment. Our studies of  $^{36}\text{Cl}$  in rain provide a monitor for atmospheric releases and a baseline for natural  $^{36}\text{Cl}$  concentrations.

## THERMOTECTONIC HISTORY OF THE CAJON PASS DEEP DRILLHOLE, SOUTHERN CALIFORNIA: AN APATITE FISSION TRACK STUDY

KOHN, B.P., Victorian Institute of Earth and Planetary Sciences, School of Earth Sciences, La Trobe University, Bundoora, Victoria, 3083, Australia, Saltus, R.W., USGS, Federal Center, Denver, CO 80225, USA, and Gleadow, A.J.W., Victorian Institute of Earth and Planetary Sciences, School of Earth Sciences, La Trobe University, Bundoora, Victoria, 3083, Australia.

The 3.5 km Cajon Pass deep drillhole (CPDDH) was drilled to provide information on the absolute stress state of the San Andreas fault (SAF). High heat flow could imply frictionally generated heat and therefore high absolute stress ("strong fault"). Low heat flow would imply a weak fault. High heat flow was measured at the surface, but it fell off rapidly with depth, an effect attributable to the recent sedimentation and erosion history, thus supporting a relatively low average shear stress for the SAF.

Apatite fission track (FT) analysis offers the potential to assess the thermo-tectonic history of the predominantly crystalline rocks in the CPDDH. Apatite FT data in 23 samples of surface and CPDDH core sediment and basement down to total depth reveal (1) a complicated sawtooth pattern of FT age versus depth relationships, with characteristic FT age and lengths providing distinctive thermochronological markers repeated down the section, an example of two such markers is indicated by the following data:

FT Age (Ma)	Mean track length	Present temp	Depth (m)
$46.8 \pm 2.3$	$9.85 \pm 0.24 \mu\text{m}$	58°C	1140
$51.5 \pm 2.6$	$9.47 \pm 0.19 \mu\text{m}$	90°C	2018
$9.8 \pm 1.1$	$8.77 \pm 0.31 \mu\text{m}$	76°C	1656
$10.2 \pm 1.0$	$9.08 \pm 0.28 \mu\text{m}$	111°C	2605

(2) occasional fission tracks preserved at bottom hole temperatures of 142°C, and (3) bimodal track length distributions associated with younger FT ages.

The distinctive markers preserved in the upper ~2.0 km of the section yield relatively young FT ages and short mean track lengths which are clearly not in equilibrium with present downhole temperatures. This indicates that parts of the upper CPDDH section have been considerably hotter in the recent past and cooled by ~32-35°C, which is equivalent to ~0.9-1 km of vertical displacement under the present day geothermal gradient. This cooling interpretation is also supported by previous zeolite mineralization studies. We attribute the observed sawtooth pattern to a complicated tectonic history whereby imbricate thrusting stacked slices of the pre-thrust partial annealing zone within the present CPDDH section. The repetition of markers through the section (over present day temperatures ranging from 58°-116°C) and the presence of fission tracks at present bottom hole temperatures imply a very brief heating time of <1Ma. The bimodal track length distributions indicate some reheating of the section (possibly due to burial) prior to thrusting.

The apatite FT data independently confirm and quantify the tectonic scenario previously postulated to account for the anomalous heat flow of the Cajon Pass area; in addition they indicate that Pleistocene imbricate thrusting (at too fine an interval to be preserved in the present day geotherm) was a fundamental mechanism in the uplift/erosion history of the CPDDH site.

OXYGEN ISOTOPE CONSTRAINTS ON METAMORPHIC FLUID FLOW, TOWNSHEND DAM, VERMONT, USA.

KOHN, Matthew J and VALLEY, John W., both at Dept. of Geol. and Geophys; Univ. of Wisconsin; Madison, WI 53706 USA

Fluid-rock interaction during amphibolite-facies metamorphism has been investigated for rocks exposed in a single 400 meter long, lithologically heterogeneous outcrop near Townshend, Vermont, USA. Oxygen isotopic compositions have been measured in profiles across coarse-grained garnets from 13 samples, and from hornblende and garnet separates from 33 fine-grained samples. This outcrop was previously studied by Chamberlain and Conrad (1991, 1993), who observed large oxygen isotope gradients (3‰) from core to rim in garnets from one sample, and inferred large amounts of pervasive fluid flow. None of the garnets that we have analyzed show strong isotopic zonation, and the mineral separate data imply both large gradients in peak metamorphic fluid isotopic compositions and a strong correlation of isotopic composition with rock type. Although devolatilization reactions in these rocks must have produced metamorphic fluids, the data preclude syn-metamorphic cross-foliation time-integrated fluid fluxes greater than 200 cm<sup>3</sup>/cm<sup>2</sup>.

The isotopic trends have significant implications regarding the physical transport of fluids in the crust during regional metamorphism. The data can all be interpreted in terms of closed system behavior (i.e., no lateral communication between adjacent rocks), channeled fluid flow (i.e., extremely limited advective communication between rocks), or diffusive transport of oxygen in an interconnected grain-boundary fluid (i.e., limited communication without cross-strike advection). This implies that any significant flow at this locality was dominantly either layer parallel or channeled out of the system in cracks or veins, and that pervasive cross-strike fluid flow was unimportant. If fast-transport channels were active, then the maximum fluid flux (~200 cm<sup>3</sup>/cm<sup>2</sup>) and the amount of fluid generated during garnet growth restrict the spacing of fluid conduits to have been less than ~300 meters. Veins of the appropriate size and spacing are present in the outcrop. The isotopic data do not support the models of Ferry (1992), Stern et al. (1992), and Chamberlain and Conrad (1993), who proposed that large volumes of metamorphic fluids (time-integrated fluid fluxes of 1x10<sup>4</sup> - 1x10<sup>6</sup> cm<sup>3</sup>/cm<sup>2</sup>) flowed pervasively across strike during metamorphism.

ISOTOPE GEOCHEMISTRY OF WEST PACIFIC CRETACEOUS SEAMOUNTS AND GUYOTS

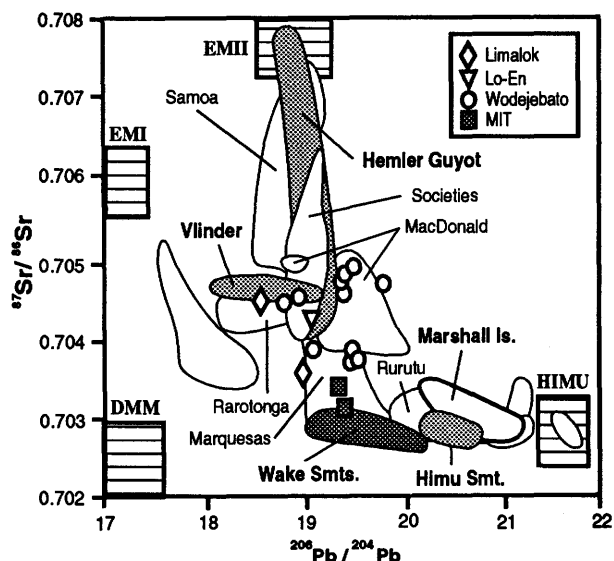
Koppers, Anthony A.P., Staudigel, H., Pringle, M.S., and Davies, G.R., Laboratory of Isotope Geology, Vrije Universiteit, Amsterdam, 1081 HV, The Netherlands.

The mantle underneath the South Pacific is both isotopically and thermally anomalous (SOPITA). Within the last 20 Ma, eight currently-active SOPITA hot spots formed a large number of seamounts on anomalously hot oceanic lithosphere. Their volcanogenic products display an extreme isotopic diversity that covers the entire range between the EMII and HIMU mantle components, including a small admixture of EMI.

The studied West Pacific Cretaceous volcanic edifices of Limalok, Lo-En, Wodejebato (Marshall Sm's), Vlinder, HIMU, Hemler (Magellan Sm's), MIT, and Takuyo Daisan are situated on the Jurassic aged oceanic crust. <sup>40</sup>Ar/<sup>39</sup>Ar-ages (Pringle *et al.*, this volume) were used to reconstruct their locations of formation, demonstrating that the West Pacific Sm's originated from the SOPITA region. The Marshall and Magellan Sm's originated close to the Rarotonga, Rurutu and MacDonald hot spots, whereas MIT formed near Society, and Takuyo Daisan in between Marquesas and Samoa.

Sr-Nd-Pb isotope data (see Diagram) from Cpx-Plag-Hbl, and leached bulk rocks of Cretaceous TUNES6 and ODP LEG-144 samples, display isotope compositions comparable to SOPITA volcanics: (1) intermediate EMII/HIMU signatures of Limalok, Lo-En and Wodejebato are similar to that of MacDonald, (2) individual samples from Limalok and Wodejebato, and the Vlinder data are indicative of minor EMI admixture (cf. Rarotonga), and (3) MIT slightly extends the isotopic field of the Wake Sm's towards EMII and has isotopic correlations comparable to the more HIMU-like Society volcanics.

In conclusion, the overall spatial and isotopic ranges for Cretaceous Sm's and SOPITA hot spots are comparable. Within these ranges individual correlations are persistent, suggesting that the isotopically and thermally anomalous mantle source in the South Pacific has been active since the Cretaceous. Such a long-lived correlation supports the need for a coherent genetic explanation of both features. Recycling of either sediments, oceanic crust, or lithospheric mantle may fuel the SOPITA mantle source with extreme radiogenic signatures, as well as with high abundances U, Th, K, etc. anomalously heating-up the mantle plume over periods >100 m.y. by radioactive decay.



## MAGMATIC CARBON DIOXIDE IN LOWER SILESIAN COAL BASIN, NW POLAND

KOTARBA, Maciej, Dept. of Fossil Fuels, University of Mining and Metallurgy, Cracow, 30-059, Poland

The Lower Silesian Coal Basin (LSCB) is situated within the Intra-Sudetic depression, in the Sudetes Mts. (SW Poland). The Sudetic Tectogen is cut by numerous deep fractures which may reach the upper mantle (e.g., Intra-Sudetic Deep-seated Fault). In LSCB numerous examples of the Variscan magmatism were found. Tertiary, multiphase basaltic magmatism has not been observed within the Upper Carboniferous coal-bearing strata of the LSCB but occurred in its vicinity. Beneath the Paleozoic complex of LSCB active magma chambers probably exist up to now.

Carbon dioxide accumulated in the coal seams of the LSCB reveal variability of both the content and isotopic composition.  $\delta^{13}\text{C}$ -values vary from -26.6 to +16.8 ‰ and CDMI\* from 0.12 to 99.96 % (Kotarba, 1988, 1990).

Stable isotope studies allowed distinction between magmatic, thermogenic and bacterial  $\text{CO}_2$ . The  $\delta^{13}\text{C}$  values of the endogenic (magmatic and/or upper mantle origin)  $\text{CO}_2$  are close to the mean values for elemental carbon in the upper mantle and vary from -8 to -5 ‰ (about -7 ‰ on average). Carbon dioxide occurring in some faults zones of the LSCB reveals CDMI values from 88.2 to 99.96 % and  $\delta^{13}\text{C}$ -values from -10.5 and -5.7 ‰. These data indicate endogenic origin of carbon dioxide. Somewhat wider interval of  $\delta^{13}\text{C}$ -values of  $\text{CO}_2$  than for typical endogenic one can be connected with mixing of thermogenic and/or bacterial carbon dioxides, and/or isotope fractionation during  $\text{CO}_2$ -migration through the microporous structure of coals. Carbon dioxide has migrated from the upper mantle and/or from the intermediate magma chambers along the Intra-Sudetic Deep-seated Fault and was re-distributed through the network of smaller dislocations. This migration continues even recently as is shown by the high content of carbon dioxide in coal seams in spite of conditions favourable for the releasing of gases during coal exploitation.

Kotarba, M., 1988, Geochemical criteria for the origin of natural gases accumulated in the Upper Carboniferous coal-bearing formations in Walbrzych Coal Basin, Stanislaw Staszic Academy of Mining and Metallurgy Scientific Bulletin, 1199, 119 p. (in Polish with English abstract.)

Kotarba, M., 1990, Isotopic geochemistry and habitat of the natural gases from the Upper Carboniferous Zacler coal-bearing formation in Nowa Ruda coal district (Lower Silesia, Poland), Durand, B., and Behar, F., eds., Advances in Organic Geochemistry, 1989, v.1, p.549-560.

\* Carbon dioxide-methane index,  $\text{CDMI} = [\text{CO}_2 / (\text{CH}_4 + \text{CO}_2)] 100 (\%)$

## USE OF HELIUM AND TRITIUM ANALYSIS FOR CHARACTERIZING FLUID MOVEMENTS IN A CONFINED AQUIFER

Kotzer, T.G., AECL Research, Chalk River, Ontario, and Noack, M. and Cornett, R.J., AECL Research, Chalk River Ontario, KOJ 1JO, CANADA.

Helium isotopic compositions and tritium concentrations have been measured on groundwaters collected from multi-level wells drilled along a hydrologically-characterized, sand aquifer at Chalk River Laboratories, Ontario, Canada to determine the migration path, residence times ( $^3\text{H}/^3\text{He}$  ages) and flow velocities for waters in the aquifer. Currently, the aquifer is recharged by meteoric waters which have elevated tritium concentrations (~800 TU) due to the close proximity of the recharge site to a waste management area. Helium isotopic analyses on groundwaters taken at depths of approximately 5 to 20 m indicate the waters have  $^4\text{He}$  concentrations similar to that expected for a groundwater which equilibrated with atmosphere at approximately  $10^\circ\text{C}$  whereas measured  $^3\text{He}$  concentrations exceed solubility equilibrium by a factor of 10 suggesting a substantial tritogenic  $^3\text{He}$  component. The measured  $^3\text{He}$  and  $^3\text{H}$  concentrations yield  $^3\text{H}/^3\text{He}$  ages of approximately <5 years and suggest flow velocities of <1 m/day which are comparable to a flow velocity of 0.63 m/day calculated from independent tracer studies. The helium isotopic and tritium data on these groundwater samples indicate minimal diffusive loss of helium from the groundwaters which are taken from a relatively shallow, confined aquifer.

## U- Th- Pb SYSTEMATICS, EARTH ACCRETION AND CRUST - MANTLE EVOLUTION

KRAMERS, J.D., Min.-Pet. Inst., Univ. of Berne, 3012, Switzerland, and TOLSTIKHIN, I.N., Dept. of Earth Sciences, University of Cambridge, CB2 3EQ, England.

A combination of two transport balance models, for accretion and subsequent evolution of the Earth, is presented. The homogeneous accretion model is based on the scenario of Azbel et al (1993) which satisfies siderophile element constraints. It is extended by a protocrust. Assuming 60-90 % impact volatilization Pb loss, Pb partitioning into metal ( $K_D$  c. 6) forming the core, and U, Th enrichment in the upper mantle-protocrust system, U/Pb and Th/Pb ratios and U, Th concentrations of the upper Earth are reproduced. Formation of a protocrust during accretion is essential for this.

After accretion the upper mantle, lower and upper crust are together considered as a closed system. Their estimated combined bulk present day Pb isotope composition yields an accretion time of 150 - 220 Ma (dependent on the chondritic U/Pb ratio), in agreement with constraints from the most realistic version of the Pu-U-I-Xe model using the same scenario (Azbel and Tolstikhin, 1993). No two-stage or continuously open Pb evolution model involving an unknown low  $\mu$  reservoir is required to solve the classical Pb paradox.

In addition to constraints imposed by present day Pb isotope ratios of crust and mantle reservoirs including HIMU, modelling of the crust-upper mantle system after accretion has to satisfy Pb isotope data from the crust and mantle in the geologic past. Archean provinces show extreme heterogeneity in  $^{207}\text{Pb}/^{204}\text{Pb}$  at similar  $^{206}\text{Pb}/^{204}\text{Pb}$ , which is not seen in younger crust. This "banana" aspect of terrestrial Pb history can be modelled postulating: (1) The syn-accretion protocrust was largely recycled into the upper mantle giving a minimum in crust mass at 4 Ga ago. (2) Crust formation dominated over recycling prior to about 3 - 2.5 Ga ago, and a near steady state total continental crust mass prevailed after that (the recycling fluxes used also yield the observed age distribution and the mean crustal age of 2 Ga). (3) The nature of crust forming and intracrustal processes changed at 3 - 2.5 Ga: Early intracrustal melting (large amounts of melt, bulk  $s/l$   $K_D$  for U, Th around 0.2) created high  $\mu$  upper crust; later i-c. melting (suspension, filter pressing, bulk  $s/l$  U, Th  $K_D$  closer to 1) differentiated  $\mu$  values much less. In early crust production processes a bulk Pb  $K_D$  of c. 0.04 is postulated (amphibole control) which is much reduced in later processes (eclogite formation). HIMU mantle can thus be produced since the Proterozoic. The interdependence of the set of assumptions is critically examined.

Azbel, Y., Tolstikhin, I.N., Kramers, J.D., Pechernikova, G.V. and Vityazev, A.V., 1993, Core growth and siderophile element depletion of the mantle during homogeneous Earth accretion. *Geochim. Cosmochim. Acta*, 57, 2889-2898

Azbel, I.Y. and Tolstikhin, I.N., 1993, Accretion and early degassing of the Earth: Constraints from Pu-U-I-Xe isotopic systematics. *Meteoritics*, 28, 609-621.

## CHEMICAL AND ISOTOPIC EVOLUTION OF CRYOGENIC CARBONATES: A LABORATORY STUDY.

KRISHNAMURTHY, R.V and MACHAVARAM, M both at Institute for Water Sciences and Dept. of Geology, Western Michigan University, Kalamazoo, Michigan 49008, USA

Calcium carbonate is one of the most important minerals that forms on the earth's surface at ordinary temperature and pressure conditions. The basic over all chemical process that drives the precipitation of calcium carbonate can be written as:  $\text{CaCO}_3 + \text{H}_2\text{O} + \text{CO}_2 \rightleftharpoons \text{Ca}^{++} + 2\text{HCO}_3^-$ . The  $\text{CO}_2$  is derived from the soil zones where it is generated by plant respiration and decay and the  $\text{H}_2\text{O}$  is derived from local precipitation. The carbonate rich waters, upon exposure to a region of low partial pressures of  $\text{CO}_2$ , precipitate  $\text{CaCO}_3$  through degassing of  $\text{CO}_2$ . Precipitation is also possible through evaporation of water, as might be expected in arid regions.

Yet another mechanism that is known but has received less attention is the precipitation of  $\text{CaCO}_3$  via freezing of carbonate rich waters. This is a significant process in many parts of the world which experience long seasons of sub-zero temperatures. In order to understand the chemical and isotopic behavior of carbon of solutions undergoing this process we carried out experiments using a natural ground water sample. The experiment involved freezing and thawing of the solution in succession. The  $\text{CO}_2$  that evolved during each of the thawing stage was collected and its carbon isotope ratio determined. The results for the evolution of  $\text{CO}_2$  is shown below (Fig.). The chemical and isotopic evolution of freezing carbonate rich waters would help us determine if the isotopic distributions are governed by: 1) Equilibrium fractionation process 2) Kinetic fractionation process 3) A Rayleigh type distillation process.

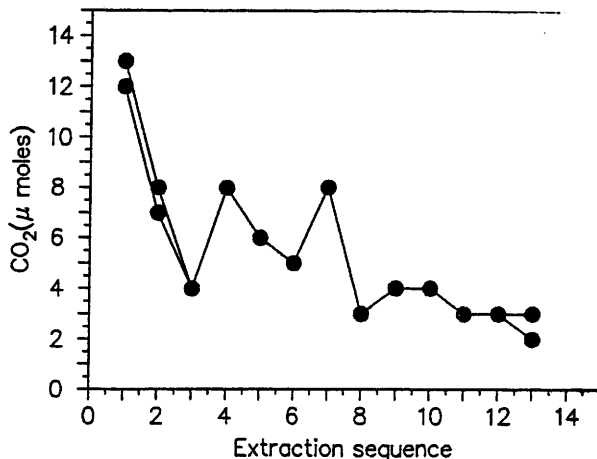


Fig. 1.  $\text{CO}_2$  Released During Successive Freeze-Thaw Cycles of a Carbonate-Rich Water. Results are for a Duplicate Run.

## IDENTIFICATION OF CONCORDANT ZIRCONS USING ETCH TECHNIQUES

**KROGH, T.E.**, Geochronology Laboratory, Royal Ontario Museum, Toronto, Ontario, Canada.

Discordance due to recent Pb loss must be eliminated to gain maximum precision in single-age populations and to allow primary and secondary ages to be defined in two-stage populations. In the latter, grains with the least secondary loss are needed to define the primary age. Analyses of microgram quantities of selected high quality abraded grains (that are invariably low in U) can achieve both objectives but in many cases equally perfect grains are variably discordant. A simple etch technique allows large numbers of grains to be screened for U level. Instead of a fission track approach we use the grains as the detector of radiation damage. Disturbed U-Pb systems are avoided because we analyse only the highest quality material after abrasion, as documented below. Grains remaining from a previous abrasion study (Krogh 1982), in which 4% discordant multigrain fractions were obtained from a 20% discordant population, were used. A repeat bulk fraction is 17% discordant (650 ppm U) and two abraded single grains are 1.0 and 3.4% discordant (230 and 175 ppm U). Two grains selected after 2.5 hr at 110°C in NaOH (room T saturated) are 1.8 and -2.0% discordant (112, 41 ppm U); the latter with a large error due to small Pb content. Four grains selected after a 3.5 hr, 220°C etch give data that are analytically concordant and identical to those previously published and are 0.4, 0.3, 0.3 and -0.2% discordant (152, 20, 58, 154 ppm U). Most grains turned white during etching and are excluded.

A two-stage circa 1.0-1.8 Ga discordia (Krogh 1973) defined by 80-90% discordant points (>800 ppm U) was used to try to isolate primary age components. Three selected high quality grains after abrasion are 59, 44, and 32% discordant toward 1745 Ma (453, 269, 129 ppm U). A clear multigrain fraction picked from turbid grains produced after a few minutes in room temperature Hf is 6% discordant (198 ppm U). Two clear fractions selected after a 2 hr 220°C Hf etch are 2.0 and 0.3% discordant (100, 80 ppm U). A third two-stage high angle discordia gave 8 abraded single grain results on a 1430-1740 Ma line bounded by 7/6 ages of 1560 and 1632 Ma. Progressively up the line U varies from 211, 218, 191, 156, and 88 ppm with the latter two selected by maximum lustre. The highest two grains were selected after 23 hr in a 220°C NaOH etch to maximize leaching but are still on the line.

Etching is especially important in Archean samples where the percentage of concordant material is extremely low, and where 1000's of two-stage variably discordant grains are present.

**Krogh, T.E. 1982.** *Geochimica et Cosmochimica Acta* **46**, pp.637-649.

**Krogh, T.E. and Davis, G.L. 1973.** *Carnegie Institute Washington Yearbook* **72**, pp.601-610.

## <sup>40</sup>AR/<sup>39</sup>AR CONSTRAINTS ON REGIONAL THERMAL RESETTING OF ALKALI FELDSPARS FROM THE NEWARK BASIN AND ADJACENT READING PRONG BASEMENT

**Krol, M.A. & Zeitler, P.K.**, Department of Earth & Environmental Sciences, Lehigh University, Williams Hall 31, Bethlehem, PA, 18015, USA.

Alkali feldspar from the Triassic-Jurassic Newark Basin and surrounding Precambrian Reading Prong basement gneisses were studied using <sup>40</sup>Ar/<sup>39</sup>Ar thermochronology in order to evaluate the thermal evolution of the basin. Utilizing duplicate isothermal heating in the early portion of the step heating experiments enables us to see through the effects of excess argon typical in these early steps. Application of this technique provides additional information on the age and thermal history these samples have experienced. The use of alkali feldspar multidomain theory allows us to evaluate the cooling history of these rocks within the temperature range of 150°-300°C and now possibly to lower temperatures.

Detrital alkali feldspar from the 225 Ma Stockton Fm. yielded minimum ages younger than the stratigraphic age. Ages of 155-180 Ma are associated with closure temperatures between 115°-170°C and record cooling following a Mesozoic thermal event. The stratigraphically youngest Boonton Fm. (198 Ma) yielded ages consistently older than the depositional age, suggesting either post-Alleghenian slow cooling or partial resetting due to Mesozoic heating. Ages ranged from 225 Ma to over 550 Ma with corresponding closure temperatures of 110° to 240°C. Small domains from samples of Precambrian Reading Prong gneisses with closure temperatures of 110° to 250°C record minimum ages between 131-260 Ma. These minimum ages may record cooling following a Mesozoic thermal event or may be consequence of erosional unroofing. In addition, a low temperature alkali feldspar extracted from a calcite vein within the Cambro-Ordovician Beekmantown carbonate associated with the early Paleozoic Friedensville zinc deposit. Small domains are associated with closure temperatures of 135°-180°C; corresponding to ages of 155-180 Ma. These ages indicate cooling following the Mesozoic thermal pulse providing a minimum temperature and time of this event.

The alkali feldspar data provide minimum estimates on the time and temperature of a Mesozoic thermal event. This thermal event probably occurred prior to the initiation of sea-floor spreading (~175 Ma) and was most likely the result of elevated heat flow due to lithospheric thinning and localized hydrothermal fluid circulation. Additional work is in progress in which we are evaluating the lateral and stratigraphic extent of this thermal event within the rift basin.

## PRECISE DATING OF GRANITOIDS BY SINGLE ZIRCON GEOCHRONOLOGY: A NIGHTMARE!

KRÖNER, A. and JAECKEL, P., Institut für Geo-wissenschaften, Universität Mainz, 55099 Mainz, Germany.

The dating of granitoid rocks used to be relatively simple matter when Rb-Sr whole-rock and U-Pb multigrain analyses were used and when errors were in the order of several tens of millions of years. Single zircon analysis has changed this belief by documenting the presence of variable amounts of inherited xenocrysts in virtually every granitoid rock, thus making it difficult to obtain the precise age of magmatic emplacement. We have used single zircon evaporation and the vapor digestion technique in the analysis of Archaean granitoids from southern Africa and late Proterozoic to early Palaeozoic granitoids from the eastern margin of the Bohemian Massif in east-central Europe to document extraordinarily complex zircon populations. Both I-type and S-type granitoids have older zircon xenocrysts, revealing precursor reservoirs which are more complex than commonly thought. Zircon morphology sometimes helps to distinguish between magmatic and xenocrystic zircons, but we also found perfectly euhedral and homogeneous varieties which were inherited. Mixture of such grains with magmatic zircons in multigrain analysis tends to produce ages which are invariably too high.

TTG-granitoids from the Barberton and Swaziland granite-greenstone terrain in southern Africa have ages between ~3.55 and 3.2 Ga and contain zircon xenocrysts as old as 3.7 Ga. These rocks are derived from a ~3.6-3.7 Ga old isotopically very homogeneous reservoir, as documented by Sm/Nd analyses.

Voluminous granitoids from the Lusatian terrane in eastern Saxony, Germany, have magmatic zircon ages between ~540 and 570 Ma and contain xenocrysts varying in age between 706 and 2020 Ma. These rocks are derived from melting of older continental crust as also revealed by  $\epsilon\text{Nd}(t)$  values of -4 to -19. One sample has more than 95 % xenocrysts.

I- and S-type granitoids from the eastern margin of the Bohemian Massif in eastern Czech Republic have magmatic emplacement ages between 503 and 515 Ma and contain a voluminous and variable xenocryst population with ages between 1100 and 2070 Ma. These granitoids probably formed along an active continental margin during Caledonian ocean closure and microcontinent accretion.

In all these cases conventional multigrain analysis would not have enabled the precise emplacement ages to be established. In summary, precise dating of granitoids frequently is a nightmare and requires careful study of zircon morphology and time-consuming single grain or grain-domain analysis.

## ISOTOPIC TRACING OF ANTHROPOGENIC SULPHATE & WATER/ROCK INTERACTIONS IN CONTAMINATED GROUND WATER

KROUSE, H. R., Department of Physics & Astronomy, VAN DONKELAAR, C and HUTCHEON, I, Department of Geology & Geophysics, University of Calgary, Calgary, Alberta, T2N 1N4 Canada

The environment surrounding sour ( $\text{H}_2\text{S}$ ) gas processing plants can be impacted by industrial sulphur loading. Objectives of this study were: 1) to assess whether  $\delta^{34}\text{S}$  was a conservative tracer of anthropogenic sulphate; 2) to use  $\delta^{34}\text{S}$  to trace anthropogenic sulphate in ground water surrounding a sour gas plant, 3) to understand how the ground water chemistry of the system had been altered by industrial sulphate loading.

The presence of sulphate reducing bacteria (SRB's) in ground water was a concern because they cause enrichment of sulphate  $\delta^{34}\text{S}_{\text{sulphate}}$  due to preferential  $^{32}\text{S}^{16}\text{O}_4^{2-}$  reduction and would affect the use of  $\delta^{34}\text{S}$  as a tracer. Bacteria were not active enough to shift significantly the  $\delta^{34}\text{S}$  of the ground water sulphate, nor did  $\delta^{34}\text{S}$  values of incubated ground water samples become enriched with  $\delta^{34}\text{S}$  over seven months. Further,  $\delta^{18}\text{O}$  enrichment in sulphate was not found. Finally, ground water at the site was oxygenated (dissolved oxygen 1.1 mg/l). Under aerobic conditions, bacteria that use oxygen in water dominate over those that use oxygen from dissolved sulphate.

Sulphate from gas processing enters ground water through runoff from the processing facility, precipitation and leaching from the sulphur storage area. At this site anthropogenic sulphate has a  $\delta^{34}\text{S}$  of +16‰ (CDT), while naturally occurring sulphate is depleted to about -10‰. As the  $\text{SO}_4$  concentration in ground water increases,  $\delta^{34}\text{S}$  approaches that of the anthropogenic source.

Water/rock interactions are dominated by the acid that originates from the gas plant and the minerals present in the soils. Shallow ground water at this site moves through a heterogeneous glacial deposit that contains clasts of limestone, dolomite and shale and some water samples are shifted away from the global meteoric water line. The enrichment in  $\delta^{18}\text{O}$  that this shift represents is indicative of evaporation due to the aridity of this region and calcite dissolution, resulting from acidic conditions created by sulphate release. As  $\text{SO}_4$  concentration rises, and Ca increases due to calcite dissolution, waters approach saturation with gypsum.

When the difference between natural and industrial  $\delta^{34}\text{S}$  is large and sulphate reducing bacteria are remittent,  $\delta^{34}\text{S}$  is an effective tracer of anthropogenic sulphate in ground water. The chemical and isotopic composition of ground waters shows strong indications that the addition of sulphate to the water causes acidic ground water conditions that are rapidly buffered by dissolution of calcite or other carbonate minerals.

## THE ISOTOPIC CHARACTER OF THE BUSHVELD COMPLEX MAGMAS.

KRUGER, F.Johan., Bernard Price Institute (Geophysics), University of the Witwatersrand, WITS 2050, South Africa.

O, Sr, Os, Nd and Pb isotopic data indicate that the magmas of the Bushveld Complex contained variable proportions of crustal material *prior* to intrusion into the magma chamber.

*Oxygen isotopic data* indicates that there was a significant crustal content in the magmas higher in the succession and especially in the magma injected into the Main Zone. A strong positive correlation of very radiogenic  $^{87}\text{Sr}/^{86}\text{Sr}$  initial ratios with the  $\delta^{18}\text{O}$  values also supports this model.

Magmas with both high and low *Sr concentrations and Sr isotopic ratios* were injected into the magma chamber.  $^{87}\text{Sr}/^{86}\text{Sr}$  ratios suggests that the first magma was less radiogenic (c. 0.7044) and that subsequent additions were more radiogenic (0.7085-0.7090). In the Lower Zone to Main Zone interval, at least three magma types can be identified which were derived from the subcontinental upper mantle and a continuum of "crustal" sources. A fourth mafic magma is needed to account for the Upper Zone.

*Os isotopic data* on the UG1, UG2 and Merensky reefs indicate a substantial crustal component in the magmas from which these rocks are derived. Nevertheless, the mantle remains the main source of PGE.

*Nd isotopic data and REE profiles* indicate a slightly enriched source for the Bushveld magmas. Bushveld rocks have LREE enriched profiles, but low absolute REE concentrations, and the Nd isotopic data also indicate a slightly enriched source. This is in contrast to the Sr and Os isotopic data which indicate a highly enriched but "unsupported" source. This is envisaged to be due to the compatible nature of Sr and Os during crustal melting so that the concentrations of these two elements are strongly enriched, whereas the incompatible REE were depleted in the residue after melting. Therefore the REE concentrations in the crustal residue were comparable to those of the mantle magmas and hence the crustal signature is subdued.

*Pb isotopic data* is positively correlated with the Sr isotopic data, and the large discontinuity at the Merensky level to more radiogenic (crustal) values also argues for a strong crustal imprint in the Main Zone consistent with the other isotopic data.

The available data indicates that there was minimal assimilation of roof rocks by the magmas in the chamber, except by the Lower Zone magma which was hot and undersaturated in silica. The lack of *in situ* assimilation indicates that the Bushveld magmas were stratified and that magma addition occurred mainly at the base of the chamber as fountains which caused minimal disturbance of the interface between the layered mafic magmas and the overlying "granophyric" magmas or rocks. The process of magma addition thus continuously elevated the residual magmas in the chamber.

## $^{26}\text{Al}$ AND $^{10}\text{Be}$ IN THE OCEAN

KU, Teh-Lung, WANG, Lei and LUO, Shangde, Dept. of Earth Sciences, University of Southern California, Los Angeles, CA 90089-0740, USA  
SOUTHON, John, Lawrence Livermore National Laboratory, Livermore, CA 94550, USA  
KUSAKABE, Masashi., Japan Marine Science and Technology Center, Yokosuka, 237 Japan

The long-lived cosmogenic  $^{26}\text{Al}$  (half-life 0.7 Ma) and  $^{10}\text{Be}$  (1.5 Ma) enter the ocean chiefly via wet/dry fallout. Their ratios in marine sediments can be used as powerful time and process tracers for problems such as marine geochronology and productivity changes in the past. A pre-requisite to the usage is the better understanding of the comparative oceanic geochemistry of these isotopes.

In this presentation, we report the first water-column profile (upper 1 km) of  $^{26}\text{Al}/^{27}\text{Al}$  in the sea. The  $^{26}\text{Al}/^{10}\text{Be}$  ratio in the surface Pacific near  $12^\circ\text{S}$  and  $135^\circ\text{W}$  is estimated to be approximately  $3 \times 10^{-4}$ . This is about an order of magnitude lower than the atmospheric production ratio and the ratio measured in rain water. The low surface ocean ratio may reflect the relatively intense particulate removal of Al relative to Be. The source of  $^{26}\text{Al}$  in the ocean, similar to that of  $^{10}\text{Be}$ , comes mainly from production in the atmosphere rather than from production in surface rocks on the continents.

We have also measured the authigenic  $^{26}\text{Al}/^{27}\text{Al}$  and  $^{10}\text{Be}/^9\text{Be}$  ratios in deep-sea sediments using a NaOH-leach technique. The authigenic  $^{10}\text{Be}/^9\text{Be}$  ratios extracted from surface sediments are close to  $^{10}\text{Be}/^9\text{Be}$  measured in the overlying sea water, indicating that isotopic equilibrium for Be exists between deep water and authigenic sediment phases. The ratio of  $\sim 4 \times 10^{-14}$  for  $^{26}\text{Al}/^{27}\text{Al}$  extracted from a Pacific sediment is similar to that found in the authigenic phillipsites. The results further indicate that (1) depositing deep-sea sediments incorporate  $^{26}\text{Al}$  and  $^{10}\text{Be}$  in a ratio close to their atmospheric production ratio, and (2) the authigenic  $^{27}\text{Al}$  and  $^9\text{Be}$  constitute, respectively,  $\sim 15\%$  and  $\sim 40\%$  of the total  $^{27}\text{Al}$  and  $^9\text{Be}$  in the sediments studied.

Our results point to the good feasibility of using  $^{26}\text{Al}/^{10}\text{Be}$  as an age-dating tool and as a proxy for paleoproductivity.

ISOTOPIC STUDIES ON GROUNDWATERS IN  
SOUTHWESTERN MAHANADI DELTA, ORISSA  
STATE, INDIA.

**KULKARNI, K.M.**, Isotope Division,  
Bhabha Atomic Research Centre,  
Bombay, MS, 400085, India, **RAO,**  
**S.M.**, Isotope Division, Bhabha  
Atomic Research Centre, Bombay,  
MS, 400085, India, and **NAVADA,**  
**S.V.**, Isotope Division, Bhabha  
Atomic Research Centre, Bombay,  
MS, 400085, India.

As part of a drinking water supply project isotope geochemical investigation was launched in Delang - Puri sector of Orissa. These studies were aimed at determining the origin of salinity and evaluating groundwater recharge conditions in the coastal, alluvial, multi-aquifer system.

In this system fresh, brackish and saline groundwaters occur in rather complicated fashion. The conditions change from phreatic to artesian flowing type with increasing depth. The groundwater flow is towards south, i.e., towards the sea.

The environmental stable isotopes of hydrogen, oxygen, carbon, sulphur and radioisotopes of hydrogen and carbon as well as minor and trace ions were studied. The findings based on isotope geochemical, sedimentological and paleontological studies indicate that a) shallow groundwaters are relatively young and are recharged through floodplains and outcrops of basement rocks, b) the groundwater salinity in aquifers occurring in the intermediate zone (depth 50-100 m) is largely due to Flandrian transgression during the Holocene, c) deep fresh and young groundwater forms a well developed aquifer which receives recharge through basement rocks. This could form main source of groundwater for exploitation, d) the deep saline groundwaters are marine waters entrapped due to eustatic level rise during the late pleistocene interglacial stage.

The stratification of saline groundwaters is also observed.

The study is expected to help in a better choice of well sites.

PROGRESS ON THE PREPARATION OF THE PROPOSED  
 $^{40}\text{Ar}/^{39}\text{Ar}$  STANDARD MMhb-2, PLANS FOR ITS  
CALIBRATION, AND INTERLABORATORY  
CALIBRATION OF ARGON FACILITIES.

**KUNK, M.J.**, U.S. Geological Survey, MS 981, Reston, VA  
22092, **DALRYMPLE, G.B.**, U.S. Geological Survey, MS  
937, Menlo Park, CA 94025, and **SNEE, L.W.** U.S.  
Geological Survey, MS 963, Denver, CO 80225

Intralaboratory precision of 0.1-0.25% for ages measured by modern  $^{40}\text{Ar}/^{39}\text{Ar}$  techniques is commonplace. However, comparison of high-precision ages between laboratories is made difficult because no high-precision interlaboratory standard is available and because no systematic interlaboratory calibration program has been designed. Because the supply of MMhb-1 (Alexander et al., 1978; Samson and Alexander, 1987) has been depleted, we are currently in the process of calibrating the conventional K-Ar age of MMhb-2, a new preparation of the international  $^{40}\text{Ar}/^{39}\text{Ar}$  hornblende standard from the McClure Mountain Syenite. More than 3 kg of high-purity hornblende, MMhb-2, has been prepared and split into 336 vials, each weighing about 10 g. Calibration of the potassium concentration of MMhb-2 by isotope dilution is in progress at the National Institute of Standards and Technology (NIST). The precision and accuracy of the K concentration measurements are expected to be 0.1% and 0.25% or better, respectively.

Calibration of the  $^{40}\text{Ar}_r$  concentration of MMhb-2 will be done jointly by NIST and the USGS. NIST will calibrate a pipette system that will deliver aliquots of high-purity  $^{38}\text{Ar}$  with precision and accuracy of 0.1% and 0.25% or better, respectively, of the molar quantity of argon delivered. NIST will also calibrate three pipette systems containing artificial mixtures of  $^{40}\text{Ar}$  and  $^{36}\text{Ar}$  with ratios of 1:1, 30:1, and 300:1. The isotopic composition of the artificial mixtures will be known to a similar level of precision and accuracy as the  $^{38}\text{Ar}$  molar quantity. The artificial  $^{40}\text{Ar}/^{36}\text{Ar}$  mixtures will be used to measure the mass discrimination of the spectrometers to be used, prior to using the  $^{38}\text{Ar}$  pipette in measuring the  $^{40}\text{Ar}_r$  concentration of MMhb-2 in USGS laboratories. In the process of making these measurements, the isotopic composition of atmospheric argon will be re-measured.

Upon completion of calibration, MMhb-2 will be certified by NIST for potassium and argon concentrations, and NIST will issue a Standard Reference Material Certificate for it. Distribution of the MMhb-2 standard will be through the NIST Standard Reference Material Program.

The NIST-calibrated  $^{38}\text{Ar}$  and  $^{40}\text{Ar}/^{36}\text{Ar}$  pipette systems will be constructed of all metal components and are designed to be transportable. These pipette systems, together with MMhb-2 and the re-measured atmospheric  $^{40}\text{Ar}/^{36}\text{Ar}$ , could form the basis for a systematic interlaboratory calibration program that would dramatically improve  $^{40}\text{Ar}/^{39}\text{Ar}$  interlaboratory precision.

Alexander, E.C., Jr., Mickelson, G.M., and Lanphere, M.A., 1978, Mmhb-1: a new  $^{40}\text{Ar}/^{39}\text{Ar}$  dating standard, in Zartman, R.E., ed., Short papers of the fourth international conference, geochronology, cosmochronology, isotope geology 1978: U.S. Geological Survey Open-File Report 78-701, p.6-8.  
Samson, S.D. and Alexander, C.A., 1987, Calibration of the interlaboratory  $^{40}\text{Ar}/^{39}\text{Ar}$  dating standard, MMhb-1: Chemical Geology (Isotope Geoscience Section) v. 66, p. 27-34.

**SURFACE CHRONOLOGY FROM COSMOGENIC  
NUCLIDES: THE ANTARCTIC GLACIAL RECORD**

KURZ, M. D., ACKERT, Robert, Dept. of Marine Chemistry and Geochemistry, Woods Hole Oceanographic Institution, Woods Hole, Massachusetts 02543, USA., and BROOK, Edward J., Graduate School of Oceanography, University of Rhode Island, Narragansett, Rhode Island 02882, USA.

Glacial deposits in the Dry Valleys region of Southern Victoria Land, contain an important record of advance and retreat of the great Antarctic ice sheets. The unique climate and extremely slow erosion rates result in remarkable preservation of the moraine surfaces and make them ideal for surface exposure dating. We have measured surface exposure ages in different moraines and bedrock surfaces, using in situ produced cosmogenic  $^3\text{He}$ ,  $^{10}\text{Be}$ , and  $^{26}\text{Al}$  in olivine, quartz and clinopyroxene. The results demonstrate that the technique can be utilized for surfaces as young as several thousand years and as old as millions of years. We have evidence of surfaces greater than 5 million years in age from the Sirius formation on Mount Fleming. However, these ages must be viewed as minimum ages because of helium leakage from quartz, and the restrictive half lives of  $^{10}\text{Be}$  and  $^{26}\text{Al}$ . These limitations are being overcome by the use of  $^{21}\text{Ne}$  on these samples. Ages from pleistocene moraines are particularly important, as they can be used to directly constrain ice sheet reconstructions. This is demonstrated by new results from Mt. Morning, a Cenozoic volcano on the southern side of McMurdo Sound, where interbedded glacial drift and lava flows record past ice levels in the Ross Sea. By combining surface exposure dating with field mapping and stratigraphy we have found evidence of three different glaciations on the North-east flank of Mt. Morning. Absolute chronology provided by  $^3\text{He}$  dates indicates that the deposits are marine isotope stage 6 (160 Ka), stage 4 (80 Ka) and stage 2 (< 28 Ka). The youngest drift (stage 2) overlies a well preserved lava flow (dated at 28 Ka), and a well preserved stage 4 moraine. The upper limit of the stage 6 deposit is the highest (approximately 456 meters), which is consistent with sea level records. The upper limit of the stage 2 deposit is at lower elevation than stage 6, but at a higher elevation than the stage 4 moraine, suggesting that the Ross Sea ice levels at this time were intermediate. As expected from this stratigraphy, exposure ages from the stage 4 moraines are scattered, because the surfaces have been partially reworked by the younger glaciation. These results demonstrate that surface exposure dating, combined with glacial stratigraphy, can be used to constrain past ice geometry, and hence to correlate the terrestrial glacial record with marine and ice core climate records.

**Sr, Nd AND Pb ISOTOPIC VARIATIONS IN THE  
MARIE BYRD PLUME, WEST ANTARCTICA**

KYLE, P.R.<sup>1</sup>, PANKHURST, R.<sup>2</sup>, MUKASA, S.<sup>3</sup>,  
PANTER, K.<sup>1</sup>, SMELLIE, J.<sup>2</sup>, MCINTOSH, W.<sup>1</sup>  
<sup>1</sup> Geoscience, N.M. Tech, Socorro, N.M. 87801  
<sup>2</sup> British Antarctic Survey, Cambridge, U.K.  
<sup>3</sup> Geol. Sci, Univ Michigan, Ann Arbor, MI 48109

Alkalic volcanism in Marie Byrd Land (MBL), West Antarctica is dominated by 18 major and many minor volcanic centers ranging in age from 35Ma to presently active. The formation ages for the major volcanoes young progressively outwards in a radial circular pattern with a diameter of 600 km. The four youngest volcanoes Mt. Takahe (7-40ka), Mt. Waesche (<0.5Ma), Mt. Siple (<2Ma) and Mt. Berlin (active) are located 90° apart around the outer edge of the volcanic province. Ranges of volcanoes show well-defined linear younging trends. The elevation of a prevolcanic erosion surface, although poorly exposed, also shows an ill-defined radial pattern. We interpret the radial patterns of age and elevations as a single large stationary mantle plume beneath the stationary Antarctic plate.

Basaltic samples from Mts. Aldez (19Ma), Takahe and 5 centers in the Executive Committee Range (ECR) (13 to <0.5Ma), show a small spread in  $^{87}\text{Sr}/^{86}\text{Sr}_i$  (0.7027 - 0.7038, n= 34) and  $^{143}\text{Nd}/^{144}\text{Nd}_i$  (0.51277 - 0.51292, n=25). There is no evidence of crustal contamination except in highly evolved comenditic and trachytic rocks. Seven samples from 3 different volcanoes show significant variations in Pb isotopes:  $^{206}\text{Pb}/^{204}\text{Pb}$  (19.52 - 20.47),  $^{207}\text{Pb}/^{204}\text{Pb}$  (15.65 - 15.72),  $^{208}\text{Pb}/^{204}\text{Pb}$  (39.10 - 39.94). The data define a distinct linear array above the NHRL on a  $^{207}\text{Pb}/^{204}\text{Pb}$  vs  $^{206}\text{Pb}/^{204}\text{Pb}$  plot.

The overall low  $^{87}\text{Sr}/^{86}\text{Sr}_i$ , distinct  $^{87}\text{Sr}/^{86}\text{Sr}_i$  vs  $^{143}\text{Nd}/^{144}\text{Nd}_i$  field and radiogenic Pb isotopes clearly demonstrate a mantle source dominated by a HIMU component. Mt. Takahe has higher  $^{87}\text{Sr}/^{86}\text{Sr}_i$  (0.7033 - 0.7038) and lower  $^{143}\text{Nd}/^{144}\text{Nd}_i$  (0.51277 - 0.51279) than other MBL volcanoes and is interpreted as mixing of plume-derived HIMU-rich mantle with lithospheric mantle as the plume head flowed horizontally along the base of the lithosphere. Similar processes could also account for some of the Sr and Nd isotopic variations at Mt Sidley (5Ma) in the ECR.

The strong HIMU isotopic signature of the MBL volcanics is also found in the Late Cenozoic alkali volcanics in the western Ross Sea and the Balleny Islands. This suggests the presence of a large and distinct mantle reservoir under Antarctica and the Southern Oceans extending for over 3200 km.

SEEING THROUGH THE EFFECTS OF HYDROTHERMAL ALTERATION USING Nd ISOTOPES: AN EXAMPLE FROM THE ABU KHURUQ COMPLEX, EGYPT

LANDOLL, J.D., and FOLAND, K.A., Dept. of Geological Sciences, Ohio State University, Columbus, OH 43210, USA, and HENDERSON, C.M.B., Dept. of Geology, The University, Manchester, England, M13 9PL.

The Abu Khuruq complex is a multi-intrusion, alkaline ring complex located in the Eastern Desert of Egypt. This 89 Ma complex consists of a gabbroic body which was intruded by rings of nepheline-, alkali-, and quartz syenite. This association of both quartz and critically undersaturated syenites is interesting in that it is not explicable by closed-system fractionation. The complex experienced sub-solidus hydrothermal alteration by circulating meteoric waters that modified the syenites isotopically and apparently, in part, chemically. Both O and Sr isotopes were so greatly affected that they cannot be used to address petrogenetic questions, in particular the role of crustal materials. The present study focuses on Nd isotopes in an effort to: examine the degree to which Nd may also have been modified hydrothermally; and, attempt to address the petrogenesis of Abu Khuruq by avoiding the alteration that affected other isotope systems. Small, but significant variations are observed in calculated initial  $^{143}\text{Nd}/^{144}\text{Nd}$  ratios. The variations occur not only between rocks of different units, but also among rocks of the same unit, particularly the quartz syenites. Initial  $^{143}\text{Nd}/^{144}\text{Nd}$  ratios range from: 0.512721 to 0.512748 for the gabbros; 0.512739 to 0.512750 for alkali syenites and trachytes; 0.512717 to 0.512755 for the nepheline syenites; and 0.512706 to 0.512732 for the quartz syenites. During hydrothermal modification, Nd appears to have been immobile as indicated, in part, by: a lack of correlation of  $^{143}\text{Nd}/^{144}\text{Nd}$  ratios with apparent degree of alteration as judged from petrographic and isotopic indicators; correlations of  $^{143}\text{Nd}/^{144}\text{Nd}$  with major element variations; and, a limited range in initial  $^{143}\text{Nd}/^{144}\text{Nd}$  ratios that would otherwise require uniform alteration of all rocks. The isotope ratios appear to represent primary magmatic signatures and thus can be used to address the petrogenesis of Abu Khuruq. The parental melt for the complex had  $^{143}\text{Nd}/^{144}\text{Nd}$  of 0.512750 ( $\epsilon_{\text{Nd}} = +4.4$ ) and an  $^{87}\text{Sr}/^{86}\text{Sr}$  of 0.7030, indicating derivation from a depleted mantle source. The variations in initial  $^{143}\text{Nd}/^{144}\text{Nd}$  ratios indicate that the parental magmas of the complex experienced input of crustal material, apparently by AFC processes. Furthermore, the quartz syenites are clearly more affected whereas the nepheline syenites experienced little or no contamination. This indicates an important link between the contamination and rock composition and provides the explanation for the association of over- and undersaturated syenites. The results further demonstrate that Nd isotope ratios can provide important petrogenetic information for hydrothermally altered rocks even when other isotopes are severely affected.

A COMPARISON OF CONVENTIONAL K-AR AND  $^{40}\text{Ar}/^{39}\text{Ar}$  DATING OF YOUNG MAFIC VOLCANIC ROCKS

LANPHERE, MARVIN A., Branch of Isotope Geology, U.S. Geological Survey, Menlo Park, CA 94025

Conventional K-Ar dating has been the typical method for measuring ages of mafic volcanic rocks younger than 1 Ma. The  $^{40}\text{Ar}/^{39}\text{Ar}$  technique was difficult to apply to these rocks because fairly large samples were required. However, the availability of ultra-clean, ultra-sensitive rare gas mass spectrometers and low-blank resistance-heated furnaces have significantly extended the application of the  $^{40}\text{Ar}/^{39}\text{Ar}$  technique to young volcanic rocks.

Measurements to compare these two methods were made on andesite and basalt from Crater Lake, OR (CL) and Mount Adams, WA (MA) and on basalt from the Snake River Plains, ID (SRP).

Conventional argon measurements were made by isotope dilution on samples of approximately 25 g;  $\text{K}_2\text{O}$  was determined by flame photometry.  $^{40}\text{Ar}/^{39}\text{Ar}$  incremental-heating experiments were made on samples of approximately 100 mg. Representative results on eight lava flows from these areas are as follows:

	Age (ka)	
	Conventional K-Ar	$^{40}\text{Ar}/^{39}\text{Ar}$ plateau
CL:	106 ± 7	117 ± 3
	306 ± 7	303 ± 3
	565 ± 14	567 ± 6
SRP:	626 ± 67	596 ± 18
	619 ± 22	619 ± 9
	33 ± 14	51 ± 3
MA:	106 ± 25	107 ± 3
	251 ± 6	241 ± 12

Ages determined by the two techniques agree in most cases within analytical uncertainties (1  $\sigma$ ).

Conventional ages are the mean of two or more Ar measurements and four  $\text{K}_2\text{O}$  determinations. The  $^{40}\text{Ar}/^{39}\text{Ar}$  plateaus contained between 49 and 98 percent of the  $^{39}\text{Ar}$  released.

The results indicate that high-quality ages can be measured on young, mafic volcanic rocks using either the conventional or  $^{40}\text{Ar}/^{39}\text{Ar}$  techniques. The precision of an  $^{40}\text{Ar}/^{39}\text{Ar}$  plateau age generally is better, but comparable precision probably can be obtained by pooling 4-6 conventional K-Ar measurements.

## HIGH RESOLUTION Ar/Ar CHRONOLOGY OF PREDAZZO MAGMATIC COMPLEX (SOUTHERN ALPS, ITALY)

LAURENZI, M.A., Istituto di Geocronologia e Geochimica Isotopica, CNR, 56127 Pisa, Italy, VISONA' D, Dip. Scienze della Terra, 35100 Padova, Italy, ZANTEDESCHI C., C.S. Geodinamica Alpina, CNR, 35100 Padova, Italy.

Predazzo magmatic complex comprises a volcanic sequence intruded by composite plutonic bodies at very shallow crustal level. These bodies, which display an annular shape, have been grouped into four families, corresponding to the supposed intrusive sequence (Lucchini, 1967): 1) monzonites, by far the more widespread lithotype, monzodiorites and diorites (and subordinate gabbros and cumulitic pyroxenites); 2) leucomonzonites; 3) syenites; and 4) biotite bearing and tourmaline bearing granites. A new detailed field work has shown a more complicate situation and this sequence is not strictly true in the entire area.

A tentative to discriminate small differences in age among different pulse of the multiple intrusion is the aim of this research. Previous radiometric investigations gave an age of 242 Ma for granites (Rb/Sr isochron on *wr* and related minerals, after Borsi and Ferrara, 1967, recalculated with the new decay constant). Amphiboles and biotites were taken into consideration for this purpose; all samples were irradiated together in nearby position to minimise source of errors which are of the order of 5 per mil.

Biotite ages, obtained on few lithotypes, are restricted into a narrow interval of time (232-235 Ma). Amphiboles data, which cover the majority of the area, are slightly more widespread. Some of their age spectra are not ideal, but a massive presence of massive parentless  $^{40}\text{Ar}$  can be excluded. The observed discrepancies are likely due to the presence of biotite exsolution in amphiboles, as shown by variation in the Ca/K ratios of different temperature interval.

Older ages (237 and 236 Ma) are obtained for a leucomonzonite and a monzodiorite in different sectors of the intrusion; another group of data, referred to more than one rock type, is restricted to an interval between 232 and 230 Ma. The more basic members of the magmatic body, among the first to be intruded in the classical reconstruction of this area, show slightly lower ages. Since their intrusion as dike cannot be excluded at this stage of research, radiometric data seem to fulfill this hypothesis.

Obtained ages display an emplacement of the composite pluton spanning over an interval of time of about 7-8 Ma.

Borsi S. and Ferrara G; 1967, Determinazione dell'età delle rocce intrusive di Predazzo con i metodi del Rb/Sr e K/Ar: *Miner. Petrogr. Acta*, 13, 45-66.

Lucchini, 1967, Studio petrografico degli affioramenti sienitici del M.te Mulat (Predazzo, Italia settentrionale): *Miner. Petrogr. Acta*, 13, 195-215.

## THE CONTINENTAL SHELF RECORD OF UPWELLING, SEA LEVEL AND ICE VOLUME FROM THE S.E. ATLANTIC

LAVELLE, M., ARMSTRONG, R.A., HARRIS, C., DE WIT, M.J., Department of Geological Sciences, University of Cape Town, Rondebosch 7700, South Africa, and GIRAUDEAU, J., South African Museum, P.O.Box 61, Cape Town 8000, South Africa.

The cold water Benguela System, off the west coast of southern Africa, forms one of the world's major eastern boundary currents. Strong offshore winds, related to the South Atlantic anticyclone, drive intense upwelling on the inner and middle shelf.

Six sediment cores, up to 6 m long, have been sited using high-resolution seismic data in water depths ranging from 96 m to 175 m in the southern Benguela System. Palaeoceanographic reconstructions are based on the analysis of K-Ar, strontium and oxygen isotope data, as well as the development of benthic and planktonic foraminiferal transfer functions. Data on bottom temperature, salinity, dissolved oxygen and organic matter, as well as surface temperature and salinity have been used to examine regional palaeoceanographic changes, as the South Atlantic responded to glacial fluctuations in the Quaternary.

Strontium isotope, K-Ar and biostratigraphic dating of the basal carbonate and glauconitic sands indicates an age of 24Ma. Oxygen isotope data obtained from bulk carbonate samples reveals a sea-bottom isotopic signature 2-3‰ lighter than the present day. This carbonate unit has since been correlated around the entire sub-continent, and is believed to be a marker for the Late Oligocene - Early Miocene global warming event.

A major erosional unconformity separates the basal Tertiary units from the overlying Quaternary deposits. Coccolith and oxygen isotope data reveal deposition of the lowest sequence taking place during the transition from isotope stage 10 to 9 (~340Ka). Extensive storm erosion during low sea levels has resulted in the preservation of transgressive and interglacial deposits only. Glacial sequences are marked by distinct erosional surfaces and reworked shell horizons.

Sea level variations have been investigated utilising 3 independent techniques: (1) from an estimate of ice volume from our sea bottom calculations of  $\delta^{18}\text{O}_{(\text{seawater})}$ ; (2) from our benthic foraminiferal transfer function; (3) from measurements of coastal onlap delineated by high resolution seismics. Sea level estimates obtained for the last 5 glacial cycles are all remarkably similar; sea level having dropped to between -120 m and -150 m during each regression. Sea level recovery during interglacial periods is estimated to be similar to modern mean sea level.

Sea bottom temperatures during oxygen isotope stages 9 and 7 (340Ka to 186Ka) were similar to modern Benguela values. Stages 5 and 3 (128Ka to 24Ka) however, show the Benguela System as being significantly warmer (by up to 2°C) than previous or modern day values. Variable upwelling intensity, perhaps linked to the magnitude of the glacial cycle, is considered to be the driving mechanism of palaeoceanographic change in the Benguela System.

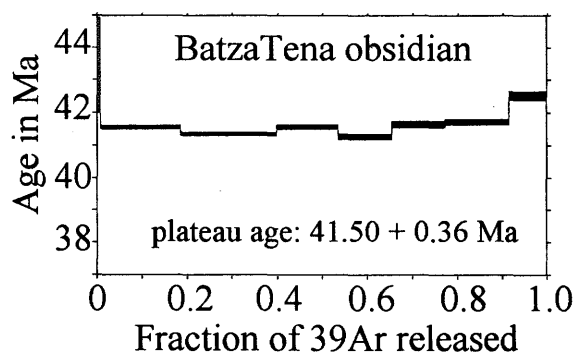
**$^{40}\text{Ar}/^{39}\text{Ar}$  DATING OF EOCENE OBSIDIAN FROM THE BATZATENA ARCHEOLOGICAL SITE, WEST-CENTRAL ALASKA**

LAYER, Paul W., Geophysical Institute, University of Alaska, Fairbanks, Alaska 99775, USA.

The BatzaTena (Indian River) obsidian site in west-central Alaska is thought to be the source for many obsidian artifacts found in northern Alaska. This site was first described by Patton and Miller (1970) who speculated that the deposit was mid-Tertiary in age based on stratigraphic relationships. The BatzaTena obsidian occurs as subround pelletal fragments up to 10 cm long and are thought to have formed as residual inclusions ('marekanites' or 'Apache tears') in hydrated perlitic volcanic glass. Several fresh obsidian fragments were analyzed by  $^{40}\text{Ar}/^{39}\text{Ar}$  step heating. The samples show no evidence of alteration and age spectra from the samples are flat with an average plateau age of 41 Ma. This age is consistent with stratigraphic controls and probably reflects the eruptive age of the obsidian.

If 41 Ma obsidian is unique to this site, then these results may be used along with Instrumental Neutron Activation Analysis, X-Ray fluorescence, microprobe and hydration measurements (compiled by John Cook at the Bureau of Land Management) to provide a distinctive 'finger-print' to identify artifacts derived from BatzaTena. Laser  $^{40}\text{Ar}/^{39}\text{Ar}$  dating techniques would allow small (<1 mm) fragments from actual artifacts to be dated without destroying the entire sample.

There are few accounts of reliable  $^{40}\text{Ar}/^{39}\text{Ar}$  ages obtained from terrestrial glass samples older than ~10 Ma. The BatzaTena study indicates that reliable ages may be obtainable from old obsidian elsewhere.



Patton, W.W. Jr. and Miller, T.P., 1970, A possible bedrock source for obsidian found in archeological sites in northwestern Alaska: *Science*, v. 21, p. 760-761.

**779 Ma MAFIC MAGMATISM IN THE NORTHWESTERN CANADIAN SHIELD AND NORTHERN CORDILLERA: A NEW REGIONAL TIME-MARKER**

LeCHEMINANT, A.N., Geological Survey of Canada, 601 Booth St., Ottawa, Ont. K1A 0E8, Canada, and HEAMAN, L.M., Department of Geology, Royal Ontario Museum, Toronto, Ont. M5S 2C6, Canada.

Precise dating of Neoproterozoic diabase dykes and gabbro sheets and sills emplaced during formation of the western rift margin of North America can determine the timing, duration and sequence of rifting and can establish time-markers to test plate reconstruction models. U-Pb baddeleyite ages have been obtained for two gabbros that are representative of a parallel set of NE-striking sheets within crystalline rocks of the Great Bear magmatic zone in the northwestern Canadian Shield. Baddeleyite ages have also been obtained for a gabbro sill emplaced within the Tsezotene Formation in the Mackenzie Mountains and for a N-striking diabase dyke that cuts the Tuchodi Formation in the Muskwa Range, northeastern British Columbia. Results indicate that intrusion of all four mafic rocks was synchronous and occurred at  $779 \pm 2$  Ma. This age establishes a new time-marker extending more than 1000 km from the western edge of the Slave Province into the northern Canadian Cordillera.

Hansen et al. (1993) suggest that the Neoproterozoic rift margin of western North America consists of alternating highly extended and less extended segments. The dated 779 Ma diabase and gabbros are within or adjacent to the proposed extended segment in the northern Cordillera. We interpret the 779 Ma mafic magmatism as a response to large-scale crustal extension along this northern segment of the rift margin. In basement uplifts in Montana and Wyoming, WNW-striking diabase dykes yield  $^{40}\text{Ar}/^{39}\text{Ar}$  hornblende ages of 760-770 Ma (Harlan, 1993), suggesting near-synchronous extension and rifting took place on the western edge of the Wyoming Province. The 0.76-0.78 Ga mafic magmatism along the developing western margin of North America occurred about 40-60 million years before the abrupt onset of the voluminous 0.72 Ga Franklin igneous events in the northwestern Canadian Shield and the Amundsen Basin. These discrete episodes of mafic magmatism establish precise markers to constrain the timing and sequence of break-up of the Neoproterozoic supercontinent Rodinia.

Hansen, V.L., Goadge, J.W., Keep, M., and Oliver, D.H., 1993, Asymmetric rift interpretation of the western North American margin: *Geology*, v. 21, p.1067-1070.

Harlan, S.S., 1993, New paleomagnetic results from middle and late Proterozoic intrusive rocks of the central and southern Rocky Mountains: *G.S.A., Abstracts with Programs*, v.25, p.48

SIMILARITIES AND DIFFERENCES IN ISOTOPIC AND CHEMICAL COMPOSITIONS BETWEEN CONTINENTAL AND OCEANIC BASALTS IN THE CAMEROON LINE

LEE, Der-Chuen, HALLIDAY, A. N. and HALL, C. M., Dept. of Geological Sciences, Univ. of Michigan, Ann Arbor, MI 48109, and FITTON, J. G., Dept of Geology and Geophysics, Univ. of Edinburgh, Edinburgh, EH9 3JW, UK.

Basaltic lavas away from the major continental volcanic centers of the Cameroon line have been dated by  $^{40}\text{Ar}/^{39}\text{Ar}$  step-heating and their Sr-Nd-Pb isotopic compositions determined. New  $^{40}\text{Ar}/^{39}\text{Ar}$  ages reveal that the basaltic volcanism of the Cameroon line extends back to *ca* 42 Ma, greatly extending the previous range of *ca* 30 Ma. The majority of basic lavas display little evidence of crustal contamination, plotting within the field of the Cameroon line ocean island basalts ( $(^{87}\text{Sr}/^{86}\text{Sr})_i = 0.7030\text{--}0.7035$ ,  $(^{143}\text{Nd}/^{144}\text{Nd})_i = 0.51285\text{--}0.51296$  and  $(^{206}\text{Pb}/^{204}\text{Pb})_i = 19.2\text{--}20.1$ ). However, some samples from near the Bambouto and Oku areas are apparently affected by contamination with continental crust, showing more radiogenic Sr and less radiogenic Nd and Pb isotopic compositions, comparable to the crustal xenoliths from Bambouto area. Basic lavas from around Mt. Cameroon display temporal trace element and isotopic variations, analogous to those observed in the Cameroon line ocean island basalts. Samples >1 Ma show trace element and isotopic compositions similar to the oceanic basalts, while samples < 1 Ma display lower Ba/Nb and enriched Nd and Pb isotopic compositions, similar to HIMU. In contrast to the oceanic basalts, no PREMA, like that of Pagalu, and no "St. Helena type" HIMU, like that of recent Principe volcanism, is observed in the continental sector. The HIMU isotopic signatures in the continental sector appear to be more radiogenic in Sr and less radiogenic in Nd, and may have been caused by an enrichment event beneath the continental lithosphere focused near the continent / ocean boundary during the Mesozoic. Isotopic variations in the continental sector are explicable through mixing between this modified HIMU and a second component that appears to be a mixture of "St. Helena type" HIMU and PREMA as found in the oceanic sector in their more distinct identities. Continental basalts are chemically similar to oceanic basalts with the exception that K/Nb is higher in the continental sector. This may be caused by amphibole in the source.

RAPID UPLIFT AND ROTATION OF MYLONITIC ROCKS, NORTHERN SNAKE RANGE, NEVADA: INSIGHTS FROM K-FELDSPAR  $^{40}\text{Ar}/^{39}\text{Ar}$  AND APATITE FISSION TRACK THERMOCHRONOLOGY

LEE, J., Geology Dept., Central Washington University, Ellensburg, WA 98926, USA, MILLER, E.L., Dept. of Geology, Stanford University, Stanford, CA 94305, USA, GANS, P.B., Dept. of Geological Sciences, University of California, Santa Barbara, CA 93106, USA and BROWN, R.W., Dept. of Geological Sciences, University College, London WC1E 6BT, United Kingdom

Metamorphic core complex detachment faults have been the subject of much study over the last 15 years, yet the origin and movement history of these faults and the mechanisms by which they translate mid-crustal rocks to the surface are still topics under debate. Questions remain as to whether these faults initiated and moved at low angles or whether they initiated at high angles and rotated to a shallow dip during slip.

To address this problem, we established the degree of footwall rotation by characterizing the thermal history of lower plate mylonitic rocks. The thermal histories of mylonitic rocks from the footwall of the northern Snake Range decollement (NSRD), east-central Nevada, USA were calculated using multiple diffusion domain analyses of potassium feldspar Arrhenius data and  $^{40}\text{Ar}/^{39}\text{Ar}$  age spectra, and apatite fission track studies to characterize the cooling (uplift) history of these mylonitic rocks. These data, along with published data on the structural and kinematic history of ductile extension, constrain the origin and movement history of detachment faults. The calculated thermal histories indicate three episodes of rapid cooling (10–55°C/Ma) related to extensional denudation as lower plate rocks cooled from ~350°C to ~90°C: 1) Middle Eocene (48–41 Ma), 2) Late Oligocene (30–26 Ma) and 3) Early Miocene (20–16 Ma). The first episode of rapid cooling may be related to the earliest period of normal faulting in east-central Nevada, initiation of slip along the NSRD and onset of ductile extension in the footwall. The second episode signals a pulse of slip along the NSRD, and the third episode marks the cessation of lower plate mylonitic deformation and the onset of the major pulse of uplift and rotation of lower plate rocks from beneath the NSRD and/or younger east-dipping normal faults. The thermal history data provide evidence for a temperature difference across the range within the same structural horizon (70–170°C); the northwestern flank of the range dropped below 300°C by 46 Ma and reached 115°C by 20 Ma, whereas in the eastern parts of the range, lower plate rocks were at temperatures above 300°C until 19 Ma and ductile extension was still ongoing. If isotherms were subhorizontal, these relations suggest either an eastward dip of lower plate units prior to the onset of Tertiary mylonitic deformation or that layering dipped eastward as a result of top-to-the-east shear within an east-dipping shear zone. Either case results in differential cooling (uplift) of lower plate rocks from beneath the NSRD. Simple palinspastic restorations of lower plate ductile extension based upon finite strain data, along with the calculated thermal histories, show that moderate to steeply dipping units were rotated to shallow dips during ductile shear and brittle slip from beneath the detachment fault and/or younger east-dipping normal faults. These reconstructions show that detachment faults initiate at moderate to steep angles and rotate to a shallow angle during slip. Such a history is compatible with a rotating shear zone-detachment fault model or rolling hinge/isostatic rebound model.

MULTIPATH DIFFUSION AND THE INFLUENCE OF MICROSTRUCTURES ON CLOSURE TEMPERATURES AND COOLING AGES

LEE, James K. W., Research School of Earth Sciences, Australian National University, Canberra, A.C.T. 0200, Australia; e-mail: jkl152@huxley.anu.edu.au

Traditionally, the interpretation of geochronological data has involved, directly or indirectly, the application of solid-state or volume diffusion (VD) theory, which describes the migration of atoms or ions through a homogeneous crystal structure. Crystals in geological materials are far from perfect, however, and commonly contain extended defects (e.g. dislocations, exsolution lamellae, micropores, microfractures, fission tracks) which may act as pathways for much more rapid transport. Although it is known that the diffusion of a solute species along such high-diffusivity pathways (here termed "short-circuit" [SC] diffusion) can enhance the bulk diffusivity of a mineral, the influence of microstructures on the diffusional behaviour of geochronologically important chemical species (e.g. Ar, Pb) has been largely ignored.

The importance of microstructures in the interpretation of geochronological data may be seen in examples from two of the most commonly used isotopic dating methods.  $^{40}\text{Ar}/^{39}\text{Ar}$ : Isothermal step-heating of Fe-hornblendes in vacuo at temperatures below those at which structural decomposition takes place yields Ar release patterns which do not reflect a VD mechanism but are consistent with enhanced SC transport resulting from defects created during the oxidation of Fe (Lee 1993). U/Pb: SHRIMP analyses of metamictization-induced and hydrothermally altered fractures in zircons from a granitic pluton yield U/Pb ages significantly less than the granite age, suggesting substantial Pb loss. Thus, metamictization-induced fractures can enhance Pb mobility by providing a network of pathways for fast transport (Lee and Williams 1993).

The simultaneous transport of a solute species through both the crystal lattice (via VD) and high-diffusivity pathways (via SC) is termed *multipath* (MP) diffusion (Aifantis 1979, Lee and Aldama 1992). Using MP theory, the effective diffusion dimension,  $a$ , for many minerals appears to remain on the order of the grain radius, and the model adequately explains increases in the diffusion coefficient,  $D$ , with  $a$  as observed in the hydrothermal bomb data of previously published Ar diffusion studies on hydrous minerals. In addition, Arrhenius diagrams reflecting a MP mechanism will have "kinked" curves, indicating a continuous change in the relative importance of the different diffusion mechanisms with temperature.

The most general and important consequence of MP diffusion is that the overall bulk diffusion coefficient of a mineral can be enhanced significantly above its volume diffusion coefficient. As a result, integrated ages and effective closure temperatures ( $T_c$ ) can be much lower than those predicted assuming only a VD mechanism. Under certain conditions, it is even possible that minerals normally characterized by low "VD"  $T_c$ 's (e.g. Ar in biotite) can have older integrated ages than minerals normally associated with higher "VD"  $T_c$ 's (e.g. Ar in hornblende) – an enigmatic phenomenon reported in some previous studies. Thus, it may be essential to carefully characterize mineral samples to be dated, since microstructurally dependent transport mechanisms may ultimately control the migration and intra-grain spatial distribution of geochronologically important isotopic species.

Aifantis EC (1979) *Acta Metall* 27: 683-691.

Lee JKW (1993) *Chem Geol (Isot Geosci Sect)* 106: 133-170.

Lee JKW and Aldama AA (1992) *Comput Geosci* 18: 531-555.

Lee JKW and Williams IS (1993) *EOS* 74: 650-651.

Cs PRODUCTION RATIO IN FALLOUT

LEE, Typhoon, CHEN, Hsin-Wei, Inst. Earth Sci., Academia Sinica, and Geology Dept. Nat'l Taiwan Univ., Taipei, Taiwan, R.O.C, KU, Teh-Lung, Dept. Geol. Sci., Univ. South. Calif., Los Angeles, CA. U.S.A.

Fallout Cs-137 and Cs-135 are present in soil and sediment with typical abundances of 0.1 to 1 ppb of natural Cs. Their ratio is potentially a powerful tool to quantitatively estimate modern sedimentation and erosion rates. Lee et al (*Geochim. Cosmochim. Acta (letter)*, 57, 3493, 1993) has recently developed mass spectrometric techniques to measure all three Cs isotopes in coastal sediments. A pre-requisite of applying this tool is the knowledge of the production ratio of Cs-137/Cs-135 in the nuclear fallout when they were initially deposited. We have measured Cs isotopic compositions of rain water samples collected in the 60's and in coastal sediments with well-established chronology from Santa Monica Basin (Table). Since weapon yields are dominated by tests around 1962, we consider the fallout Cs in both sediments to be essentially 30 years old. The rain samples have much higher 135/133 ratio. The two rain samples from southern California collected in 1963 and 1965 gave 137/135 ratios consistent with the sediment results within respective uncertainties. We thus believe that the Cs-137/Cs-135 ratio was dominated by fallout Cs having an initial of about 0.70-0.75. This is surprisingly low since the reactor fission yield seems to be about 1.

Table Cs Isotopes in Dated Samples

Sample	135/133*	137/135	Note
<b>Santa Monica Basin Sediment</b>			
1-2 cm	13.9±1.4	0.35±6	1964-1980#
2-3 cm	11.7±0.7	0.35±6	1946-1964#
4-5 cm	<0.4	----	1903-1927#
<b>Rain Water</b>			
1992	<6	----	Taipei
1965	107±15x10 <sup>2</sup>	0.41±9	La Jolla
1963	105± 7x10 <sup>2</sup>	0.37±4	Los Angeles

\* x10<sup>-10</sup>, # Pb-210 chronology

INCISION RATES DETERMINED BY COSMOGENIC DATING OF BEDROCK STRATHS ALONG THE INDUS RIVER IN NORTHERN PAKISTAN

LELAND, J. E., Department of Earth and Space Sciences, University of California, Los Angeles, CA 90024, BURBANK, D. W., Department of Geological Sciences, University of Southern California, Los Angeles, CA 90089, REID, M. R., Department of Earth and Space Sciences, University of California, Los Angeles, CA 90024, FINKEL, R. C., and CAFFEE, M. W., Lawrence Livermore National Laboratory, 7000 East Ave., Livermore, CA 94550, USA.

Abandoned river-cut bedrock terraces ranging between 10 and 400 m above the modern Indus River were sampled to use cosmogenic nuclides such as  $^{10}\text{Be}$  and  $^{26}\text{Al}$  to date the abandonment of these straths and determine local incision rates. Rapid incision and changes in gradient of the Indus River in northern Pakistan have occurred throughout the last 100 ka, especially within the Middle Indus Gorge, a west-flowing portion of the river located between the Skardu basin and the Gilgit-Indus River confluence bisected by a NNW trending axis of modern rapid uplift inferred from thermochronological studies (e.g., Zeitler, 1985). We report  $^{10}\text{Be}$  exposure ages for four different straths located many kilometers apart within the Middle Indus Gorge.

Sampled terraces generally showed excellent preservation of original fluvial features such as fluting and fluvial polish comparable to those found at the modern river bank implying very low erosion rates, especially along the very arid stretches of the river. Because much of the sample area sits in the rain shadow of the Himalaya and is at elevations below 2500 m, significant shielding by persistent deep snow cover in the past is unlikely. Regions showing evidence of prior glaciation such as the presence of moraines were avoided. Also, surfaces previously covered by landslide were avoided by sampling only on the lee side of or between large bedrock knobs or 100's of meters away from existing landslide deposits. It is assumed that exposure during strath cutting is negligible compared to the total exposure history after abandonment.

Preliminary  $^{10}\text{Be}$  dates on nine leached quartz samples from four different strath terraces ranging from 65 to 185 m above the Indus in the Middle Indus Gorge show the following features. Pairs or triplets of samples from single straths show consistent ages within 1- $\sigma$  deviations. Preliminary strath exposure ages range from 12 ka to 80 ka. Bedrock incision rates vary by a factor of 3, from 2 mm/a upriver near the mouth of the Skardu basin to 6 mm/a downriver within the axis of inferred rapid uplift. We await  $^{26}\text{Al}$  data to corroborate these findings; however, if accurate, our data suggest a differential uplift rate of 3-4 mm/a over the last 30 ka between the lower (rising faster) and upper portions of the Middle Indus Gorge.

Zeitler, P. K., 1985, Cooling history of the NW Himalaya, Pakistan: *Tectonics*, v. 4, p. 127-151.

SOLID HOSTED TRACERS FOR USE AS STANDARDS IN ISOTOPE DILUTION ANALYSIS OF ARGON (AND NOBLE GASES)

LEMPERT, G.D., Soreq Nuclear Research Center, Yavne, Israel, KAPUSTA, Y., STEINITZ, G., KOTLARSKY, P., Geological Survey, Jerusalem, Israel and BUKSHPAN, S., Soreq Nuclear Research Center, Yavne, Israel.

A solid spike (SSP) is defined as a solid material selectively enriched with one or more isotopes of the noble gases, to be used as a tracer in: 1) precise mass-spectrometric isotope dilution (ID) analyses of noble gases utilizing mono-isotope SSP; 2) improved mass discrimination control in the analyzer, between and within sample measurement, utilizing a double isotope SSP. SSP is produced using neutron nuclear reactions and/or ion implantation technology, enabling SSP production with predetermined concentrations of the tracer isotope. The rationale in using SSP in ID is identical to the classical one, avoiding the disadvantages of the pipette system, while providing significant advantages: a) flexibility is allowed with respect to an optimal spike quantity; b) simpler and automated analytical setups can be made; c) periodic calibration is not required.

In an initial experiment<sup>[1]</sup> a  $^{39}\text{Ar}$  SSP was prepared by neutron irradiation of a biotite standard (HD-B1). The relative error in the determination of the  $^{40}\text{Ar}$  content was <2%. In a second experiment<sup>[2]</sup> SSP was prepared by implanting argon ions, at 45KeV, into copper foil. Implanted Ar isotopes are retained in the Cu foil to a temperature of 150°C and completely released at 800°C. Thus ion implantation technology can be used for serial production of different SSP for mass-spectrometric analysis of Ar and other noble gases.

[1] Kapusta, J., Kotlarsky, P. and Steinitz, G., 1992. *Isr. Geol. Surv. Rep. GSI/20/92*, 14p.

[2] Kapusta, Y., Lempert, G.D., Bukshpan, S., Kotlarsky, P., and Steinitz, G., 1993. *Isr. Geol. Surv. Rep. GSI/15/93*, 15p.

ISOTOPE STUDY OF THE PONGOM-NAVOLOK  
HYPERSTHENE DIORITES PLUTON, BALTIC  
SHIELD, NORTH KARELIA

LEVCHENKOV, O.A., OVCHINNIKOVA, G.V.,  
ZINGER, T.F., KOTOV, A.B., LOKHOV, K.I.,  
YAKOVLEVA, S.Z., MATUKOV, D.I.,  
SINELNIKOVA, I.M., GOROKHOVSKY, B.M.  
Institute of Precambrian Geology and  
Geochronology, Russian Academy of  
Sciences, Makarova emb., 2, St.-  
Petersburg, 199034, Russian Federation

The hypersthene diorites of the Pongom-  
navolok pluton underwent granulite and  
amphibolite facies metamorphism and  
multiphase deformation. Isotopic  
composition of  $O_2$  corresponds to I-type  
granite ( $\delta^{18}O = 5.9-7.4\%$ ). The variation of  
 $\delta^{18}O$  is independent of the degree and  
character of hypersthene diorites  
transformation. The fluid composition of  
the hypersthene diorites is similar to  
granulite-facies metamorphism rock; H/C =  
10-15; N/C less 0.15 while H/C is about 30 in  
samples from amphibolite facies shear  
zones.

Three type zircons in pluton rocks have  
been established. The first type zircon of  
2725+/- 23 Ma age is magmatic. The second  
type zircon is considered to be the result  
of the transformation of magmatic zircon  
under the condition of granulite-facies  
metamorphism. The latest zircon of 2.4 Ga  
age occurs in hypersthene diorites samples  
from amphibolite facies shear zones. This  
zircon is rich U and has Th/U ratio less than  
in two other types of zircons.

The Pb-Pb isochron of whole rock samples  
yields the age of 2690+/- 80 Ma. Within the  
framework of plumbotectonic model the data  
of acid leaching residues favour the low-  
crust source of primary magma. The results  
of acid leaching also indicate that the  
intense metamorphic event with the gain of  
crust lead in plutons rocks took place about  
2.4 Ga.

THE NEW INTERPRETATIONS OF SOME  
INCORRECT RADIOCARBON AND  
PALYNOLOGICAL DATING OF THE  
ARCHAEOLOGICAL SITES.

LEVKOVSKAYA G.M.  
RUSSIA

Some radiocarbon dates sometimes do not  
agree with the pollen or archaeological dating.  
Sometimes different parts of one archaeological  
site are characterized with different types of  
pollen diagrams,

As a result of the vertical and horizontal  
man's impact on the surface, sometimes it's  
difficult to distinguish the following pollen  
dating obtained from the level with  
archaeological findings (Levkovskaya, 1983,  
1987, Table 2, p. 33):

1. the dating of the "floor" of  
archaeological layer (the level of inhabiting).
2. of the "cellar" (different pits).
3. of the "archaeological mainland" (the  
naturally sterile surface, where the  
archaeological site was springing up).
4. of the "roof" (the sterile sediments  
directly over archaeological layer).

According to the theory of the "floor" of  
buried stone age sites, archaeological layers  
could give (in some cases) the mixture of 3  
different but correct radiocarbon dates (the  
dating of the "floor", "roof" and "archaeological  
mainland").

The author's stratigraphical and  
planygraphical pollen materials on Gubsky cave  
with Neanderthal bones (Caucasus), on Upper  
Palaeolithic loess sites from Kostenki area  
(Russian plain), on Mezolithic, Neolithic, Early  
Bronze age pitbog sites with about 70  
radiocarbon dating from Latvia (Levkovskaya,  
1987) and others illustrate the conclusions,  
mentioned above.

THE BEHAVIOUR OF BORON AND ITS' ISOTOPES IN  
THE YELLOWSTONE HYDROTHERMAL SYSTEM

LEWIS, Anita J. and PALMER, Martin R.,  
Department of Geology, University of Bristol, Wills  
Memorial Building, Queen's Road, Bristol, BS8 1RJ, UK.

Boron concentrations have been measured in 35 hydrothermal waters in and around Yellowstone National Park including hot springs and pools, snow melt and stream water. Eighteen samples were collected in the fall (1991), 15 of which were re-collected in the spring (1993). Boron isotopic values have been measured on a representative sample of these waters.

The boron concentrations range from 0 to 2.54 mM/kg and broadly correlate with chloride concentrations except for two samples (with the highest boron concentrations) which do not appear to belong to the same geothermal regime. The range of boron concentrations is considered to be due to various degrees of dilution of original hydrothermal waters and meteoric waters. Preliminary results indicate that there is no seasonal variation in boron concentration.

Boron isotopic values range from -9.3‰ to +4.4‰. The lower values are reported from extra-caldera waters and are consequently considered to represent input from fluids which have leached boron from a sedimentary source. Boron isotopic values reported from intra-caldera fluids range from -6.1‰ to -3.6‰ reflecting the value of the volcanogenic rocks with which they have reacted.

Palmer, M. R. and Sturchio, N. C., 1990, The boron isotope systematics of the Yellowstone National Park (Wyoming) hydrothermal system: A reconnaissance. *Geochim. Cosmochim. Acta*, v. 54, p. 2811 - 2815.

PRISTINE PRESOLAR GRAPHITE SPHERULES.

Lewis, Roy S., Enrico Fermi Institute, University of Chicago, Chicago, IL 60637.

Graphite grains are the most fragile identified presolar material that survives in relatively pristine condition in primitive meteorites (Anders and Zinner, 1993). It (along with SiC) carries Ne-E, nearly pure  $^{22}\text{Ne}$ , although in only  $\sim 1/3$  of the grains. The presolar nature of the carrier was recognized by Black (1972, but largely ignored as being based on *neon*), the first such recognition, many years before its identification as graphite by Zinner *et al.* (1990). The grains are close to spherical, with most of the mass found in grains 1–4  $\mu\text{m}$  in diameter, but many grains are at least as small as 0.3  $\mu\text{m}$ , a few as large as 15  $\mu\text{m}$ . The grains typically have an amorphous core surrounded by a better crystallized outer layer, display a range of surface morphologies, and are commonly found to contain grains of various refractory Ti, Zr, & Mo carbides, presumably trapped within the growing graphite grains in carbon rich stellar atmospheres. All elements measured to date have isotopic compositions distinct from solar system values. *E.g.*, noble gases have Ne-E and s-process enrichments. Density separates of these grains yield distinct fractions in terms of noble gas abundances, release temperatures, and isotopic abundances of  $^{80,86}\text{Kr}$  – isotopes reflective of the nucleogenic conditions due to temperature and neutron density sensitive branch points in the s-process chain. The carbon itself is wildly anomalous, with individual grains scattering within the range  $^{12}/^{13}\text{C} = 6 - 3000$  (solar=89). Nitrogen ranges from solar to  $^{14}/^{15}\text{N}$  down by a factor of 3, oxygen from solar to  $^{16}/^{18}\text{O}$  down by a factor of 100. A clustering of some of the grains near the solar values for N & O may indicate that dilution with normal solar material is a common problem with these elements. Silicon has both enrichments and depletions at  $^{29,30}\text{Si}$  of up to 50%. Large quantities of  $^{26}\text{Mg}$  excesses are found, indicating  $^{26}/^{27}\text{Al}$  ratios as high as 0.1, far above the canonical primitive solar value of 5E-5. Additional elements are being measured (Amari *et al.*, 1994). These reactive elements are measured on single grains, and the experimental difficulties have rapidly become formidable as low abundance trace elements are examined in these tiny grains. While some rough correlations are evident, *e.g.* in the oxygen and nitrogen isotopic compositions, each grain appears to be distinct, requiring the treatment of each as a unique sample from some particular stellar environment, necessitating the measurement of multiple elements on each grain to disentangle the record. Isotopic abundances seem roughly consistent with an origin of these grains in a range of stellar environments, AGB stars, Wolf-Rayette stars, novae, and possibly (pre-)supernovae, but the view resembles that given not so much by a window as a kaleidoscope.

Amari, S., Hoppe, P., Zinner E., and Lewis, R.S. 1993, The isotopic compositions and stellar sources of meteoritic graphite grains: *Nature* 365 806-809.

Amari, S., Zinner, E., and Lewis, R.S. 1994, Isotopic analysis of low density graphite grains from Murchison, ICOG 8 abstr.

Anders, E. and Zinner, E. 1993, Interstellar grains in primitive meteorites: diamond, silicon carbide, and graphite: *Meteoritics* 28 490-514.

Black, D.C. 1972, On the origins of trapped helium, neon, and argon isotopic variations in meteorites. II. Carbonaceous meteorites: *Geochim. Cosmochim. Acta* 36, 377-394.

Zinner, E., Wopenka B., Amari S., and Anders E. 1990, Interstellar graphite and other carbonaceous grains from the Murchison meteorite: structure, composition, and isotopes of C, N, and Ne: *Lunar Planet. Sci.* 21 1379-1380.

FLUID INCLUSION Rb-Sr ISOCHRON AGE DATING OF XIHUASHAN AND DANGPING TUNGSTEN QUARTZ VEINS DEPOSITS, JIANGXI PROVINCE, CHINA

LI, Huaqing, LIU, Jiangji, Yichang, Institute of Geology and Mineral Resources, Chinese Academy of Geological Sciences, Yichang, Hubei Province, China; and LU, Huan-Zhang, Sciences de la terre, Université du Québec à Chicoutimi, Chicoutimi, Québec G7H 2B1, Canada.

China has the major tungsten ore reserves and production in the world which occur mainly in the southern part of China, especially in the Jiangxi, Hunan, Guangxi and Guangdong provinces. The tungsten mineralization is hosted and associated with granites of Yanshanian age (70-195 m.a.). The major type of tungsten ore deposits is in wolframite-quartz veins and the well known are Xihuashan, Dajishan, Dangping, Piaotang and Shanhu mines. The fluid inclusions in these quartz vein are aqueous and H<sub>2</sub>O-CO<sub>2</sub> inclusions with homogenization temperatures ranging from 250 to 400°C and salinities ranging from 1 to 10 wt.%

This study presents preliminary results of Rb-Sr isochron age dating of fluid inclusions of these tungsten mines in order to understand metallogenetic timing. Samples for fluid inclusion analyses were carefully selected based on the affinity between quartz host related to tungsten mineralization. Other samples including granite, and mineral are chosen to compare with the results from fluid inclusion dating. The Xihuashan tungsten mine is a big quartz vein occurred in the two phases Yanshanian granites. Two isochron ages have been obtained for this granite: 156 ± 4 m.a., (<sup>87</sup>Sr/<sup>86</sup>Sr)<sub>i</sub> = 0.7186 ± 0.0008 and 142.2 ± 3 m.a., (<sup>87</sup>Sr/<sup>86</sup>Sr)<sub>i</sub> = 0.70.7338 ± 48. The age of fluid inclusions in quartz is 139.8 ± 4.5 m.a., (<sup>87</sup>Sr/<sup>86</sup>Sr)<sub>i</sub> = 0.7437 ± 0.41. The age of wolframite dated by Sm-Nd isochron method: 139.2 ± 3 m.a., (<sup>143</sup>Nd/<sup>144</sup>Nd)<sub>i</sub> = 0.511970 which is concordance with the age dated by fluid inclusions in quartz. The results indicates that tungsten mineralization is about 16 m.a. later than the formation of the granite. The Rb-Sr isochron age for Dangping mine are : 150 ± 2 m.a., (<sup>87</sup>Sr/<sup>86</sup>Sr)<sub>i</sub> = 0.7160 ± 0.0015 and t = 140.8 ± 3 m.a., (<sup>87</sup>Sr/<sup>86</sup>Sr)<sub>i</sub> = 0.7653 ± 4 m.a. for the granites; t = 130.3 ± 6.3 m.a., (<sup>87</sup>Sr/<sup>86</sup>Sr)<sub>i</sub> = 0.7485 ± 14 for the fluid inclusions. The Sm-Nd isochron dating for fluorite in Dangping quartz vein is 137.4 ± 3 m.a., (<sup>143</sup>Nd/<sup>144</sup>Nd)<sub>i</sub> = 0.511930 ± 5 which resemble the age obtained from the fluid inclusions. These show that the tungsten mineralization is about 10 m.a. later than the formation of the Dangping granites. Combining with other fluid inclusion age data on Dajishan, Piaotang and Shanhu mines, we conclude that the tungsten mineralization age in south China are the same as the Yanshanian age but with 10 or 20 m.a. later than that of the granite hosts.

THE EFFECT OF PHOSPHORUS ON CHEMICAL AND PHYSICAL PROPERTIES OF BASALTS: AN EXPERIMENTAL AND ION PROBE STUDY

LIBOUREL, G., Univ. Nancy I, Lab de Petrologie, BP239, 54506 Vandoeuvre and CRPG-CNRS, BP20, 54501 Vandoeuvre, France), TOPLIS, M. J., CARROLL, M. R., both at: Dept. of Geology, University of Bristol, BS8 1RJ, UK, and DINGWELL, D. B., Bayerisches Geoinstitut, Universität Bayreuth, 95440, Bayreuth, Germany.

Despite the abundant evidence for enrichment of phosphorus during the differentiation of natural basalts, the role of phosphorus on the chemical and physical properties of basaltic melts is poorly understood. The situation is especially acute in the case of iron-rich melts, where extreme P-enrichments are observed.

To evaluate the effects of phosphorus on differentiation of evolved basaltic magmas, a series of one-atmosphere experiments on a ferro-basaltic composition were carried out, isothermally, over a range of P<sub>2</sub>O<sub>5</sub> contents and at oxygen fugacities from 2 log units below to 2 log units above the FMQ buffer curve. The results confirm the high solubility of phosphorus in basaltic magmas and show that, at fixed temperature, the progressive addition of phosphorus causes: (1) the disappearance of olivine at reducing conditions, (2) the disappearance of magnetite at oxidising conditions, (3) the stabilisation of pigeonite throughout the studied range of fO<sub>2</sub>, (4) an increase in the modal plagioclase/pyroxene ratio, and (5) concomitant changes in the composition of the coexisting liquids.

In order to complement and clarify the role of phosphorus on the chemical and physical properties of basic magmas, the same starting ferro-basaltic composition was also used to determine the effect of phosphorus on the ferric-ferrous ratio, viscosity and density of the melt, over a large range of temperature and at two different oxygen fugacities. The results suggest that addition of P<sub>2</sub>O<sub>5</sub> causes (1) a reduction of ferric iron, (2) an initial decrease and subsequent strong increase in viscosity, and (3) a decrease of density. The magnitude of the reduction of ferric iron is greater than that of all the quoted oxide components in the calculation scheme of Kilinc et al. (1983). The overall increase in viscosity at 1200°C is estimated to be of the order of 15% relative per wt% P<sub>2</sub>O<sub>5</sub>, which is of the same order of magnitude as SiO<sub>2</sub>. A partial molar volume of 64.5 cm<sup>3</sup>/mol has been determined for P<sub>2</sub>O<sub>5</sub> in this ferrobalt at 1300°C.

Together with new phosphorus partition coefficients (D crystal-liquid) measured with an ion probe on the same ferro-basaltic composition, we will show that these results provide insights into the role of phosphorus on differentiation of both lunar and terrestrial basalts, as well as providing information regarding the solubility behaviour of phosphorus in silicate melts.

Kilinc A. et al. (1983) Contrib. Mineral. Petrol., 83, 136-140.

## THE IMPORTANCE OF CATHODOLUMINESCENCE STUDY FOR ZIRCON U-PB DATING OF S-TYPE GRANITOIDS: AN EXAMPLE FROM THE SILVRETTA NAPPE, SWITZERLAND

**LIEBETRAU, V., POLLER, U.**, Institut. of Mineralogy & Petrography, Fribourg, 1700, Switzerland, **SERGEEV, S.A., STEIGER R.H.**, Lab. for Isotope Geochemistry ETH, Zürich, 8092, Switzerland, **FREI, R.**, Lab. for Isotope Geology, Inst. of Min. & Petr., Bern, 3012, Switzerland

The complex zircon U-Pb data for S-type granitoids in the Austroalpine Silvretta nappe called for a detailed study of the internal morphology of the zircons. A cathodoluminescence (CL) investigation was initiated which revealed the internal zircon structures and greatly aided in the interpretation of the data set.

The following three clear zircon morphologies were found to be present in the population of each rock sample: 1. prismatic type, 2. bipyramidal type and 3. flattened species. For one granitoid type (Mönchalp gneiss) the analyses of three different typological populations within the same size fraction suggest a discordia line with a lower intercept around 460 Ma. Bipyramidal single grains considered as last magmatic result in discordant data points which differ in age because of an optically invisible inherited component. But their combination with other grain size fractions leads to a discordia with an apparent lower intercept of 510 Ma. Upper intercept ages of both discordias indicate an inherited 2.3 Ga old Pb component. In contrast to this, the single-grain data of an other orthogneiss (Urezzas) give concordant points around 450 Ma. The data points close to the concordia from both rocks align to a new 450 - 800 Ma discordia line possibly indicating an additional inherited Pb component.

CL imaging by scanning electron microscope show that among (magmatic) zoned grains of the same typology and size there exist some which bear inherited cores of which at least three types may be distinguished: 1. a conglomerate of several small cores, 2. broken (detrital) well structured cores and 3. weakly structured resorbed cores. Grains bearing one of the first two core types, often exhibit a zone of metamorphic growth between core and rim.

In light of the internal zircon structures the different discordia ages can be reinterpreted, in correlation with the S-type characteristics of the rocks and the metamorphic and magmatic evolution of the Silvretta nappe (Maggetti & Flisch 1993). Special sample preparation combining CL studies with high resolution zircon fragment analysis may eventually allow systematic dating of the mentioned zircon phases.

Maggetti, M., & Flisch, M., 1993, Evolution of the Silvretta Nappe, in: v. Raumer, J.F., & Neubauer, F., Pre-Mesozoic Geology in the Alps, Springer Berlin, pp. 469-484

## A ROBUST METHOD FOR ESTIMATING SURFACE EXPOSURE AGES AND LONG-TERM EROSION RATES IN BEDROCK USING IN SITU-PRODUCED COSMOGENIC RADIONUCLIDES

**LIFTON, Nathaniel A.**, Dept. of Geosciences, University of Arizona, Tucson, Arizona, 85721, USA, and **JULL, A.J. Timothy**, NSF-Arizona Facility for Radioisotope Analysis, University of Arizona, Tucson, Arizona, 85721, USA.

Numerous ambiguities, limitations and uncertainties in geomorphic research have resulted from a historical inability to reliably and quantitatively estimate (1) the exposure age of a geomorphic surface, and (2) spatial variability of long-term erosion rates. Radioactive and stable nuclides produced in situ by cosmic ray bombardment of rock materials exposed at the earth's surface may enable us to estimate surface exposure ages and long-term average erosion rates directly. Recent development of techniques for measuring and interpreting concentrations of these nuclides may ultimately help to resolve many long-standing geomorphic debates. Cosmogenic radionuclide pairs such as  $^{10}\text{Be}$  and  $^{26}\text{Al}$  have been used most frequently to solve the governing equations for both surface exposure ages and erosion rates. However, the applicability of these techniques has been limited to some extent by the number of assumptions which had to be made to interpret the measured concentrations — particularly those pertaining to steady-state or non-steady-state erosion conditions.

We are developing a robust method for interpreting the depth distribution of cosmogenic radionuclides in bedrock which avoids the need for many of these assumptions. Monte Carlo methods are used to explore the range of erosion rate and exposure age conditions on a grid which would produce theoretical depth distributions of the radionuclide consistent with the measured depth profile. The  $\chi^2$  statistic is used to test the goodness of fit between the measured and theoretical profiles at each grid point. Scenarios were modeled to simulate potential bedrock environments, with no inherited cosmogenic nuclide component arising from prior exposure. Results suggest that a single erosion rate/exposure age pair may be found from the grid which would best fit the measured data. Thus, it should be possible, in theory, to find the most probable approximation for the exposure history of a bedrock surface *using a single radionuclide*.

We plan to corroborate the model results with new cosmogenic  $^{14}\text{C}$  data from bedrock depth profiles collected from pristine shoreline features of well-known age and unambiguous exposure history associated with Pleistocene Lake Bonneville, Utah. These features include wave-cut bedrock benches at the Bonneville and Provo level shorelines, scoured basalt surfaces associated with the Bonneville Flood, and the Tabernacle Hill basalt flow, which was erupted into a Provo-level lake. Although unanswered questions and potential problems remain, this method appears to hold great promise for unraveling spatial variation in both erosion rates and exposure ages of a wide range of geomorphic surfaces.

**CHRONOLOGY AND SR ISOTOPIC STUDY OF THE TRANS USA WET EVENT IN GREAT BASIN**

**LIN, JO C.**, BROECKER, W. S., and RUBENSTONE, J. L., Lamont-Doherty Earth Observatory, Palisades, NY, 10964, USA, DORN, R. I., Department of Geography, Arizona State University, Tempe, AZ, 85287-0104, USA, PHILLIPS, F., Department of Geosciences, New Mexico Institute of Mining and Technology, Socorro, NM, 87801, USA, HAJDAS, I., ETH-Zürich, Institut für Teilchenphysik, CH-8093 Zürich, Switzerland, and SMITH, G. I., U. S. Geological Survey, Menlo Park, CA, 94025-3591, USA.

Closed basin lakes in the Great Basin of the western United States underwent a major pluvial event just prior to the Bölling warm period in Europe, i.e. 13,000 to 14,000 years BP. Pollen records indicate that the Southeast United States also experienced unusually high precipitation at the same time. Better dating of the pluvial history of the Lahontan Basin and Searles Lake in Great Basin can help constrain the timing and duration of this trans USA wet event and its relationship to contemporaneous high frequency climate events in the North Atlantic Ocean.

Lacustrine carbonates collected from the last high shorelines in these two basins are dated by the radiocarbon and uranium-series methods. In addition, radiocarbon ages from organic materials preserved beneath desert varnish on cobbles from the same shorelines give minimum ages for the high lake levels. Sr isotopic ratios on ancient carbonates and modern river waters in the drainage basin are measured to monitor any change in the source of water during the wettest period.

The radiocarbon ages of lacustrine carbonates range from 12,200 to 13,200 ka.  $^{230}\text{Th}$ - $^{234}\text{U}$  isochron results yield an age of about 16,300 ka, equivalent to  $^{14}\text{C}$  age of 13,800 ka. Radiocarbon ages of the organic material from the rock varnish range from 12,700 to 13,600 ka.

Rivers originating from the Sierra Nevada today have much lower  $^{87}\text{Sr}/^{86}\text{Sr}$  than rivers draining from central Nevada into the Lahontan Basin. Sr isotope ratios in carbonates decrease through this pluvial event suggesting relatively greater flux from the western rivers at this time.

**DISTRIBUTION OF RADIOACTIVE NUCLIDES OF THE SEDIMENT CORES FROM SOME LAKES OF CHINA**

LIN R.-F., CHENG Z.-Y., WEI K.-Q., Guangzhou Branch, Institute of Geochemistry, Chinese Academy of Sciences, Wushan, Guangzhou 510640, China

The samples of five sediment cores were collected from Dianchi, Dongting, Bosten, Taihu and Kunming lake, respectively.

According to the  $^{210}\text{Pb}$  Constant Initial Concentration model (CIC), the sedimentation rates and the average fluxes of sediment were determined to be 0.41, 0.71, 0.43, 0.05 and 0.31 cm/yr for Dianchi, Dongting, Kunming, Taihu and Bosten, respectively. The average values of the sedimentation flux were 285, 497, 300, 79.5 and 136 mg/cm<sup>2</sup>/yr. Using the  $^{210}\text{Pb}$  Constant Flux model (CF), a sedimentation rate and sediment flux can be obtained for different durations for each lake. There was a sedimentation rate from 0.16 cm/yr before 100 yrs to 0.53cm/yr at present and a flux from 120 mg/cm<sup>2</sup>/yr before 100yrs to 300 mg/cm<sup>2</sup>/yr in 1960s for Dianchi lake and a rate from 0.40 cm/yr before 40 yrs to 0.85 cm/yr at present, and a flux from 450 mg/cm<sup>2</sup>/yr to 800 mg/cm<sup>2</sup>/yr for Dongting lake. These results reflect an increase in the processes such as deforestation, industry development, human activities, etc. since 1950s-1960s. The pollution of metal elements at different levels was found in these lakes since 1950s.

The sedimentation rates and sediment fluxes based on  $^{228}\text{Th}$  data for recent 10 yrs were calculated.

The  $^{239,240}\text{Pu}$  contents in sediment samples from Dianchi, Dongting and Bosten lake were determined. The maximum contents of  $^{239,240}\text{Pu}$  occur at the sediment layer of 1963±2 dated with  $^{210}\text{Pb}$  method. It fits very well with the peak period of atmosphere nuclear test during early 1960s. The depth obtained at  $^{239,240}\text{Pu}$  peak can be used to derive the sedimentation rate and sediment flux for recent forty years. The results are in agreement with those based on  $^{210}\text{Pb}$  data.

According to  $^3\text{H}$  data in pore water, the infiltration rate of lake water to sediment were estimated to be 2.7 cm/yr and 2.3 cm/yr for Bosten and Taihu lake, respectively. The turn over time of lake water is 7 years and 1 year for Bosten and Taihu lake, respectively.

ZIRCON AGES IN YOUNG FELSIC VOLCANICS AND UNDERLYING BASEMENT IN NORTHERN NEW ZEALAND: IMPLICATIONS FOR RHYOLITE GENESIS.

LINDSAY, J.M., Department of Geology, University of Auckland, Auckland, New Zealand, WILLIAMS, I.S., IRELAND, T.R., Research School of Earth Sciences, Australian National University, Canberra ACT 0200 Australia, SMITH, I.E.M., and BLACK, P.M., Department of Geology, University of Auckland, Auckland, New Zealand

Late Cenozoic volcanic associations in the Taupo and Coromandel Volcanic Zones (TVZ and CVZ) contain a large proportion of felsic rocks. The TVZ in particular is unusual because of the large proportion of rhyolite relative to more mafic magmas (rhyolite:(andesite + dacite):basalt = 80:20:<1)). Models of rhyolite genesis in the TVZ generally involve either crustal anatexis or AFC processes (in particular basalt fractionation). The huge volume of erupted rhyolite, the relative scarcity of compositionally intermediate rocks, and the lack of geophysical evidence for complimentary cumulates pose a major problem for models invoking fractionation of a parent mafic magma. The alternative of crustal anatexis can be tested by searching for inherited relics of the crustal source. We analysed zircons from five North Island rhyolite samples in an attempt to find inherited grains, with the aim of constraining petrogenetic models. We also analysed zircons from basement rocks to determine age profiles for comparison with the inheritance in the rhyolites.

Zircons from rhyolite samples were initially examined under cathodoluminescence to detect the presence of structural cores. Zircons showing promising structure were then analysed using the Sensitive High Resolution Ion MicroProbe (SHRIMP 2). Because of the young magmatic age (generally < 3 Ma) any grains older than 10 Ma could be rapidly identified by  $^{206}\text{Pb}/^{207}\text{Pb} \gg 1$ . Out of 5000 imaged grains, of which 300 were analysed, only two old cores were identified. These were both from one TVZ rhyolite, with ages of 660 Ma and 2600 Ma. No inherited cores were found in the Coromandel samples.

The exposed geological basement in northern New Zealand contains two distinct greywacke assemblages (Torlesse and Waipapa). The zircon ages in the Torlesse sample are dominated by two peaks at 175-190 Ma and 230-275 Ma. These peaks can be resolved into six distinct components. Other age peaks are apparent at ca 350 Ma and 490-600 Ma, and two Precambrian grains at 1650 and 3000 Ma were present.

One Waipapa sample gives a single broad peak around 213 Ma that can be resolved into 5 components between 202 Ma and 255 Ma. Another Waipapa greywacke is dominated by peaks at 155-186 Ma, 211 Ma and 244-266 Ma, with minor age peaks at 350 Ma and 450-700 Ma, and a few grains at 900-1050 Ma. There is no correlation between the inherited ages in the TVZ rhyolite and the age peaks in the greywackes.

The lack of significant inherited zircon in the rhyolites places constraints on the amount of greywacke assimilation involved in the formation of TVZ rhyolite. If greywacke was involved, then assimilation proceeded to a degree where essentially all zircon was dissolved. This is highly unlikely in such felsic magmas, particularly as zircon can survive even when out of equilibrium. The rarity of inherited zircon and discrepancy between its age and that of zircon in the exposed greywackes indicates that greywacke assimilation, even during eruption, has been minimal. We suggest instead, generation of the TVZ rhyolites by partial melting of a zircon-poor (intermediate-mafic) lower crust.

ISOTOPE GEOCHEMISTRY AND METALLOGENIC REGULARITY OF THE HAIGOU GOLD DEPOSIT IN JILIN PROVINCE

Yuqing Liu, Institute of Mineral Deposits, CAGS, Baiwanzhuang Road 26, Beijing 100037, CHINA

The Haigou gold deposit is located at the E end of the Huadian gold ore zone in Jilin Province, lying along the suture belt between the old Mongolian oceanic plate and the North China paleoplate. The gold deposit consists of >40 Au-bearing sulphide quartz veins which are distributed northeastward, 1600 m in total length, 250 m in width and >400 m downwards. Wall rocks include monzonitic granite, diorite porphyrite and metamorphic rocks of the middle Proterozoic Seluohu group, the Au abundance of which varies over the range 2.42-30ppb. Wall rocks on both sides of the Au-bearing quartz vein have undergone such alterations as silicification, sericitization and carbonatization.

The isotope geochemical characteristics of the gold deposit are given (S, C, O, D and Pb). Sulfur in both ore veins and wall rocks is rich in  $^{32}\text{S}$ , and average  $\delta^{34}\text{S}$  value of sulfide are -7.9‰ and -4.1‰ respectively, exhibiting an obvious temporal-spatial variation.  $\delta^{34}\text{S}$  of ore fluids is -8.8‰. It is considered that sulfur might have been derived from volcano-sedimentary-metamorphic rocks.  $\delta\text{D}$  and  $\delta^{18}\text{O}$  values of Mesozoic meteoric water in this area are -149‰ and -20‰ respectively. During the ore-forming process, oxygen isotope composition of water and rocks varied considerably, and  $\delta^{18}\text{O}$  value of the fluids tended to increase and drift. At the principal ore-forming stage,  $\delta\text{D}$  values of the fluids were -126- -100‰,  $\delta^{18}\text{O}$  values 2-6‰, and  $\delta^{13}\text{C}_{\text{CO}_2}$  values -7.8- -13.2‰. Ore fluids were mainly derived from magmatic source-hot meteoric water, Carbon came from deep carbon and organic carbon of strata. Lead in ores and wall rocks is old lead from two-stage evolution, with  $t_1$  being 2398Ma. Model ages of lead in single samples are 1000-1200Ma, with  $\mu$  values nearly 9.73. K / Ar Closed age of ores is 143Ma, whereas Rb / Sr isochron age of rock body (wall rock) is 181Ma.

The data show that the greenschist-facies metamorphic rock of the middle Proterozoic Seluohu group served as the source bed of Au, monzonitic granite was formed by remelting of the source bed, and meteoric water was the initial source of the ore fluids. It is thus inferred that during the early stage of the Yanshanian orogeny, due to the continuous expansion of the Mongolian oceanic plate and its subduction towards the base of the North China plate, strata in this area were intensely folded together with deep faulting and magmatic-hydrothermal activity, and this led to the formation of the remelting magmatic source-hot meteoric water type Au deposit. The rock-forming and ore-forming process might be divided into three epochs consisting of six stages, and the native gold-sulphides-quartz assemblage marks the principal ore-forming stage of gold during which the  $T$  was the range 250-350°C, ore fluids varied from acid to weakly acid, and the metallogenic environment was of the reduction type.

MID-PALEOZOIC AGE OF PROVENANCE OF TRIASSIC (DOCKUM GROUP) SANDSTONE, TEXAS PANHANDLE, USA

LONG, Leon E., Dept. of Geological Sciences, Univ. of Texas, Austin, Texas 78712, USA, and LEHMAN, Thomas, Dept. of Geosciences, Texas Tech Univ., Lubbock, Texas 79409, USA

Redbeds of the Upper Triassic (Carnian to Norian) Dockum Group are widely exposed around the Southern High Plains of the Texas Panhandle and adjacent eastern New Mexico. The Trujillo Sandstone and Cooper Canyon Formation in the upper Dockum contain abundant rock fragments and detrital mica flakes derived from metamorphic source(s). Paleocurrent data for these fluvial deposits indicate that streams flowed a direction opposite to that of modern streams, coming from a source lying to the south or southeast. Candidates for sedimentary provenance are 1.2-1.3 Ga basement such as that in the Llano Uplift of central Texas, or metamorphic rocks in the subsurface of west Texas and northern Mexico belonging to the Interior Zone of the Ouachita orogenic belt. Ouachita rocks were exposed by uplift during late Triassic opening of the Gulf of Mexico.

Muscovite is highly resistant to weathering, and to loss or exchange of Sr during mild thermal episodes. Fifteen detrital muscovite samples weighing 1 to 15 mg were separated from Dockum sandstones collected around the entire perimeter of outcrop, encompassing a vast tract that is 460 km (285 miles) wide in a direction away from the source region. Rb-Sr isotope data plot as a linear array corresponding to  $t = 369 \pm 8$  Ma ( $2\sigma$ ) and initial  $^{87}\text{Sr}/^{86}\text{Sr} = 0.7095 \pm 0.0018$  ( $2\sigma$ ). If the array defines a mixing line, then mica from diversely aged sources would have had to be mixed in correlated proportions in each sample, which is possible but unlikely. Nevertheless a high MSWD (44.6) indicates a large geologic contribution to scatter of data, as expected for detritus from a source whose age is not perfectly single-valued.

The indicated provenance is thus the Ouachita Interior Zone; Rb-Sr data for five muscovites from the Llano Uplift plot on a much steeper regression line. The new results and scant previous data suggest that metamorphic rocks of late middle Devonian age are present in the Ouachita orogenic belt. Metamorphism antedated the late Paleozoic collision that created the Ouachita Mountain foldbelt.

Rb/Sr ratios (8.9 to 35.9) in nine muscovite samples from near the base of the stratigraphic section are much higher than Rb/Sr (2.8 to 8.1) of six samples from higher in the section. Regression of data grouped stratigraphically provides identical ages within error:  $372 \pm 36$  Ma (lower) vs.  $371 \pm 7$  Ma (upper). Apparent initial ratios,  $0.707 \pm 0.016$  (lower) vs.  $0.709 \pm 0.001$  (upper), also overlap but with large uncertainties. Somewhat elevated initial ratios are consistent with metamorphism of a protolith that was Rb-rich or ancient, or both.

Suites collected from two geographically restricted areas hint of a fine structure of data. Four highly radiogenic muscovite samples collected from low in the Dockum section in the southernmost High Plains provide  $t = 330 \pm 8$  Ma,  $R_i = 0.732 \pm 0.006$ . Four less radiogenic muscovites from high in the Dockum section in the northernmost exposure provide  $t = 384 \pm 7$  Ma,  $R_i = 0.706 \pm 0.002$ . Possibly at different times the Triassic streams delivered detritus from sources of different age and initial ratio to different depocenters.

Model ages of two rather unradiogenic biotite samples are  $\approx 210$  Ma, possibly registering Triassic volcanism.

1.1 Ga OLD ZIRCONS IN W-ARGENTINA: IMPLICATIONS FOR A SEDIMENTARY PROVENANCE IN THE DEVONIAN OF WESTERN GONDWANA

LOSKE, W.P., Institut für Allgemeine und Angewandte Geologie, Ludwig-Maximilians-Universität, 80333 München, Luisenstr. 37, Germany

The validity of conventional U-Pb dating of detrital zircons is still in discussion due to the general difficulty to select homogeneous and cogenetic zircon populations. Precise visual selection and accompanying cathodoluminescence analysis (CL) can help to elucidate the diversity of detrital zircons extracted from sedimentary rocks.

The Argentine Precordillera, north of the city of Mendoza, delineates a Palaeozoic Orogen as a part of the western margin of Gondwana. Devonian sedimentary rocks consist mainly of turbiditic graywackes and mudstones.

The following morphological zircon populations were recognized in the Devonian sandstones:

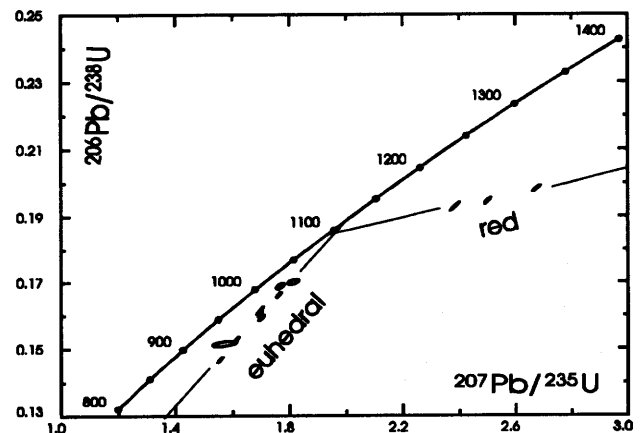
- (1) euhedral, magmatic
- (2) well rounded red coloured with transport marks
- (3) subhedral colourless, rich in inclusions

CL analysis of the euhedral, magmatic zircons (1) testify a polyphase, but homogeneous, apparently cogenetic population. Conventional U-Pb analysis yielded a slightly discordant isotope pattern (ca. 20 %) for this population, and a calculated regression line intersects with the Concordia at ca. 1.1 Ga. The lower intercept is indicative for recent Pb-loss processes (fig. 1).

Different styles of luminescence (oscillatory and sandglass-like) from the well rounded red population (2) give hints for a presumably not cogenetic crystallization. The isotopic U-Pb ratios of this zircon population point to an uncertain, but significantly higher crystallization age (fig. 1).

The subhedral population (3) often shows typical core-rim patterns. Diffuse scatter of the U-Pb ratios supports the CL information of a non-cogenetic zircon population (not in fig.1).

Comparison of the well constrained crystallization interval of 1.1 Ga with potential South American granitoid source areas of the same geological history at the western margin of Gondwana supposedly include the Rondonia Belt, the Arequipa Massif and most likely the Sierra Pie de Palo as provenance areas of the detritus.



## STABLE ISOTOPE AND CHEMICAL VARIATIONS IN DIAMOND FACIES MANTLE: EVIDENCE FOR FLUID INTERACTIONS ASSOCIATED WITH DIAMOND FORMATION

LOWRY, D., MATTEY, D.P., MACPHERSON, C. G., Department of Geology, Royal Holloway, University of London, Egham Hill, Egham, Surrey TW20 0EX, UK and HARRIS, J.W., Department of Geology, University of Glasgow, Glasgow, UK.

New high-precision oxygen isotope data have been obtained for a large suite of mantle peridotites and eclogites by laser fluorination (LF) analysis. LF data for garnet (and spinel) facies peridotites reveal much uniformity in terms of mineral  $\delta^{18}\text{O}$  values (notably  $\delta^{18}\text{O}_{\text{Olivine}}$  which averages  $5.2 \pm 0.1$ ,  $n=70$ ) and inter-mineral fractionations. Garnet  $\delta^{18}\text{O}$  values in non-diamondiferous peridotites are 5.2-5.7‰ ( $n=19$ ) but lower  $\delta^{18}\text{O}_{\text{garnet}}$  values in diamondiferous peridotites (4.9-5.3‰,  $n=9$ ) indicate that subtle disequilibrium effects may be associated with the presence of diamond.

Eclogites possess whole rock  $\delta^{18}\text{O}$  values ranging from 2.4-7.6‰ and  $\Delta^{18}\text{O}_{\text{garnet-cpx}}$  values measured by laser-fluorination are consistently positive, averaging 0.35‰. All diamondiferous samples have  $\delta^{18}\text{O} > 4.7$ ‰ with  $\Delta^{18}\text{O}_{\text{garnet-cpx}}$  values that are smaller than non-diamondiferous eclogites. All samples with fractionations  $< 0.25$ ‰ (mostly diamondiferous) yield unrealistic isotopic temperatures ( $> 1400^\circ\text{C}$ ) and again may represent disequilibrium assemblages.

Syngenetic inclusions in diamond have remained isolated from diffusive exchange since encapsulation and record initial conditions of diamond growth. Oxygen isotope compositions have been obtained by LF for peridotitic (P) and eclogitic (E) inclusion suites from the Finsch Mine, RSA. P-type purple 'G10' garnet inclusions have restricted  $\delta^{18}\text{O}$  values falling between 4.6‰ to 5.6‰ ( $n=13$ ) whereas E-type orange garnet inclusions have higher and more variable  $\delta^{18}\text{O}$  values (5.7‰ to 8.0‰,  $n=11$ ). Olivine inclusions in peridotitic diamonds have  $\delta^{18}\text{O}$  of 4.9‰ to 5.4‰ ( $n=7$ ).

Most encapsulated 'G10' garnets would not be in oxygen isotopic equilibrium with typical garnet peridotite and the data suggest a relationships between the magnitude of oxygen isotope disequilibrium of the P-type garnet  $\delta^{18}\text{O}$  inclusions and inclusion chemistry. The change in  $\delta^{18}\text{O}_{\text{garnet}}$  from equilibrium value of 5.6‰ to lower, presumably disequilibrium,  $\delta^{18}\text{O}$  values is related to both REE enrichment and Ca content. The enrichment in Ca in the garnets is also related to enrichment of  $^{13}\text{C}$  in the host diamonds with diamonds bearing diopside inclusions having heaviest  $\delta^{13}\text{C}$  and low  $\delta^{18}\text{O}_{\text{diopside}}$  (4.1‰). These changes may be consistent with interaction of garnet peridotite with Ca-deficient and REE-rich carbonate fluid with the main period of diamond growth associated with carbonation reactions.

REE profiles for Finsch E-type garnet inclusions are similar to MORB and  $\delta^{18}\text{O}$ - $\delta^{13}\text{C}$  systematics of E-diamonds have affinities with carbonated (i.e. shallow) oceanic crust. Ca enrichment and Fe and Mn depletion in both garnet and clinopyroxene is related to decreasing inclusion  $\delta^{18}\text{O}$  (+8.0‰ to +4.7‰) and increasing host diamond  $\delta^{13}\text{C}$  (-8.4‰ to -3.0‰). The jadeite component in E-type clinopyroxenes decreases as host diamond  $\delta^{13}\text{C}$  increases.

Tendencies toward  $^{18}\text{O}$  depletion,  $^{13}\text{C}$  enrichment and Ca enrichment during the major period of diamond growth in garnet and pyroxene inclusions of both peridotitic and eclogitic affinity at Finsch suggests a common process was involved, perhaps carbonation and exchange reactions between host rock and a carbonate-rich fluid. However it is less likely that the apparent disequilibrium observed in diamondiferous peridotites and eclogites is related to the diamond formation event, and may record a later fluid interaction, perhaps associated with movement and accumulation of protokimberlite melts.

## FLUID INCLUSION Rb-Sr ISOCHRON AGE DATING OF LINGLONG GOLD DEPOSIT, SHANDONG, CHINA

LU, HUAN-ZHANG, Science de la terre, Université du Québec à Chicoutimi, Québec, G7H 2B1, Canada and LI, Huaqing and LIU, Jiangji, Yichang Institute of Mineral resources, Chinese Academy of Geological Science, Yichang, Hubei prov. China.

The Linglong quartz vein gold deposit located in Shandong province, is one of the largest gold mine in China. The deposit is hosted by the Linglong gneissic biotite granite. Four mineralization stages have been recognized: 1. milky quartz-pyrite, 2. gold-quartz-pyrite, 3. gold-polymetallic sulfides-quartz and 4. carbonate stage. The ore minerals are native gold and electrum associated with pyrite and chalcopyrite. Associated alteration are mainly silicification, K-feldspathization, sericitization and chloritization. These alternations are superimposed on the mineral assemblages of the granitic rocks.

Four types of fluid inclusions: H<sub>2</sub>O-rich (with 3-17 wt. % equivalent NaCl), CO<sub>2</sub>-rich, CO<sub>2</sub>-H<sub>2</sub>O, and CO<sub>2</sub>-CH<sub>4</sub> have been found. The homogenization temperatures of fluid inclusions in the main gold mineralization stages (2 and 3) range from 200 to 380 °C. The present study is to date the gold mineralization age in fluid inclusion by using the Rb-Sr isochron dating method. All samples are from the second mineralization stage of No. 55 vein, but located in different levels. Following microthermometry the quartz sample was heated until 200 °C to decrepitate the secondary fluid inclusions. Then the Rb and Sr content were analyzed by mass spectrometer.

This study presents preliminary results of Rb-Sr isochron age dating of fluid inclusions in order to understand the metallogenetic timing. Samples for fluid inclusion analysis were carefully selected based on the affinity between hosted mineral quartz related to gold mineralization. Other samples including granites are chosen to compare with the results from fluid inclusion determination. Two isochron ages have been obtained for these granites: 156 m.a. and 154 m.a. The age of fluid inclusions in quartz is  $126.5 \pm 5.7$  m.a.,  $(^{87}\text{Sr}/^{86}\text{Sr})_i = 0.7111 \pm 2$ . Based on these data we conclude that the Linglong granite formed from 156 m.a. to 154 m.a. and the gold mineralization is about 30 years later than the formation of the granite.

## A BETTER APPROACH TO $^{230}\text{Th}/\text{U}$ ISOCHRONS

Ludwig, K.R., U.S. Geological Survey, Box 25046, Denver, CO 80225, U.S.A., and Titterton, D.M., Dept. of Statistics, University of Glasgow, Glasgow G12 8QW, United Kingdom.

Most materials of interest for  $^{230}\text{Th}/\text{U}$  dating contain significant amounts of initial  $^{230}\text{Th}$ ,  $^{234}\text{U}$ , and  $^{238}\text{U}$ , as evidenced by a measurable content of  $^{232}\text{Th}$ . To correct for the initial isotopes, linear trends are commonly fitted to the data on two X-Y isotope-ratio plots, such as  $^{230}\text{Th}/^{232}\text{Th}$ - $^{238}\text{U}/^{232}\text{Th}$  and  $^{234}\text{U}/^{232}\text{Th}$ - $^{238}\text{U}/^{232}\text{Th}$ . However, existing treatments of  $^{230}\text{Th}/\text{U}$  isochron ages are inadequate, because they (1) ignore (usually) the analytical errors and (always) the analytical-error correlations of the input data, (2) do not take into account the fact that the data in the two isotope-ratio plots are not independent, and (3) ignore the correlation between the errors of the isochron slopes (or intercepts) when calculating the isochron age.

Expanding on the earlier work of one of us (D.M.T.), we have developed a Maximum-Likelihood Estimate (MLE) approach to determine the single linear trend that fits both pairs of ratios at once, with appropriate weighting for both analytical errors and error correlations, and that properly determines the errors, error-correlations, and goodness-of-fit of all derived isochron parameters. Equations for determining the appropriate input-error correlations for both alpha spectrometric and mass spectrometric data are also given, as well as the correct propagation of the errors and error correlations of the isochron parameters (that is, the  $^{232}\text{Th}$ -free isotope ratios) in the  $^{230}\text{Th}/^{238}\text{U}$  age equation.

Our method is equivalent to determining the best-fit line to the  $^{230}\text{Th}/\text{U}$  data in three dimensions, with X-Y-Z equal to either  $^{230}\text{Th}/^{238}\text{U}$ - $^{234}\text{U}/^{238}\text{U}$ - $^{232}\text{Th}/^{238}\text{U}$  or  $^{238}\text{U}/^{232}\text{Th}$ - $^{234}\text{U}/^{232}\text{Th}$ - $^{230}\text{Th}/^{232}\text{Th}$ . A single goodness-of-fit parameter (the familiar MSWD) permits quantitative evaluation of the validity of the assumptions of the single isochron. Arguments about the "best" choice of axes for  $^{230}\text{Th}/\text{U}$  isochrons are shown to be irrelevant (except for visualization purposes) because, if a correct method of line-fitting is used, any set of three axes that yields linear isochrons must (because they use the same data) yield essentially the same  $^{230}\text{Th}/\text{U}$  age and errors.

This MLE method does not address the situation wherein significant scatter arising from non-analytical error exists. However, unless such scatter is gross, its presence cannot be evaluated until a realistic statistical evaluation (such as this procedure) has been done. Therefore, even if causes other than analytical error are responsible for data-scatter about an isochron, this procedure (or one similar) should be performed as a first step. Robust methods (which generally weight points according to their observed scatter rather than their analytical errors) are promising, but inefficient for the typically small  $^{230}\text{Th}/\text{U}$ -isochron data-sets.

The  $^{230}\text{Th}/\text{U}$  isochron approach discussed here is implemented in current versions of *Isoplot*, as well as *UIISO* (a small, stand-alone program that can be invoked by other programs).

## GLOBAL ATMOSPHERIC $\text{CO}_2$ UPTAKE BY THE OCEAN: SEASONAL AND GEOGRAPHICAL CONSTRAINTS

LUO, Shangde and KU, Teh-Lung, Dept. of Earth Sciences, Univ. of Southern California, Los Angeles, CA 90089-0740, USA

An analysis has been done on the oceanic  $\text{CO}_2$  partial pressure ( $p\text{CO}_2$ ) data observed in global oceans during the late 1980s to investigate the seasonal and regional variability of  $p\text{CO}_2$  in the surface ocean. Two important findings in this study have made it possible to evaluate the global  $\text{CO}_2$  uptake by the ocean from the observed  $p\text{CO}_2$  difference ( $\Delta p\text{CO}_2$ ) between the surface ocean and the atmosphere. First, the aqueous  $\text{CO}_2$  concentration [ $\text{CO}_2(\text{aq})$ ], expressed as  $p\text{CO}_2$  at  $20^\circ\text{C}$  ( $p\text{CO}_{2,20}$ ), at a specific location in the ocean decreases exponentially with increasing temperature from winter to summer. This can be explained by the seasonally-variable, vertical convective mixing between the surface and deep waters and/or biological productivity in the surface ocean. Second, the temperature coefficient of  $\text{CO}_2(\text{aq})$   $\beta_d$ , defined as the relative change in  $\text{CO}_2(\text{aq})$  per  $^\circ\text{C}$ , can be related to the y-intercept in a  $p\text{CO}_{2,20}$  vs.  $^\circ\text{C}$  plot by the relationship:

$$y\text{-intercept} = 195.6 + 1.50 \times 10^4 \beta_d - 4.67 \times 10^4 \beta_d^2$$

The data also show that there is a good correlation between winter  $p\text{CO}_{2,20}$  and the temperature in surface waters. On the basis of our analysis, we have deduced global  $p\text{CO}_2$  distributions in the surface ocean for different seasons of the year and calculated the season-dependent, global air-sea  $\text{CO}_2$  fluxes (in  $\text{GtC}/\text{y}$ , i.e.,  $10^{15}$  grams of carbon per year) during 1984-89 as follows: 1.8 (spring), 0.5 (summer), 1.7 (fall), and 3.5 (winter). They give an annual uptake rate of 1.9  $\text{GtC}/\text{y}$ . This uptake rate is in balance with the emission rate of fossil-fuel  $\text{CO}_2$  and its accumulation rate in the atmosphere during the same period. It appears that the terrestrial ecosystems act neither as a net sink nor as a net source of anthropogenic  $\text{CO}_2$ .

## ISOTOPIC COMPOSITIONS OF WARM SPRING AND NATURAL GASES FROM THE SOUTH ISLAND, NEW ZEALAND

LYON, Graeme L., and GIGGENBACH, Werner F.,  
Nuclear Sciences Group, Institute of Geological &  
Nuclear Sciences, PO Box 31312, Lower Hutt, New  
Zealand

Analyses of seep gases from prospective petroleum areas and from warm and cold springs in the South Island are presented and compared with data from elsewhere.

Several warm spring gases from fault zones are CO<sub>2</sub>-rich or N<sub>2</sub>-rich and have methane that appears to have been microbially oxidised giving isotopically heavier methane. Hanmer Springs CH<sub>4</sub> has a thermogenic composition that resembles that of gases from greywacke in the axial ranges of the North Island.

Isotopic analyses of gases from the sedimentary basins show that CH<sub>4</sub> from southern Marlborough is derived from mature sources, that from Wharf Stream is the most mature of the South Island hydrocarbon-rich gases. Three gases from the Murchison Basin show a trend in isotopic values indicating increasing maturity from W to E. Gases from Kotuku (Grey Valley) appear to be derived from thermogenesis at low maturity levels with variable additions of a microbial component. Gas from the Hindley Burn (Western Southland) is probably derived from a coal source as it is similar to that of the gas collected from a well drilled into the late Cretaceous, sub-bituminous Ohai coal deposit. Gases from three sites, Marlborough, the Murchison Basin and Kotuku, have high (>5%) ethane contents and high N<sub>2</sub>/Ar ratios confirming formation from mature sources.

An unusual H<sub>2</sub>-rich gas from Fiordland contains CH<sub>4</sub> that is similar in carbon isotopic composition to gases from greywacke but with very depleted hydrogen isotopic composition probably due to abiogenic reduction. In contrast, gas from an alluvial delta in Lake Te Anau shows that microbial reduction of CO<sub>2</sub> is occurring as buried vegetation decomposes producing CH<sub>4</sub> that is isotopically light in both carbon and hydrogen.

Ratios of <sup>3</sup>He/<sup>4</sup>He for most gases are generally above crustal values (>0.1 R<sub>A</sub>) implying addition mantle fluids. High values of >2.5 R<sub>A</sub> are observed in high CH<sub>4</sub> gases discharged in the Murchison and Grey Valley basins, in Fiordland (H<sub>2</sub>-rich) and East Otago (CO<sub>2</sub>-rich).

## ISOTOPIC CHARACTERISTICS OF ULTRADEEP ULTRAMAFIC XENOLITHS FROM KIMBERLITES

MACDOUGALL, J.D., Scripps Inst.  
Oceanography, La Jolla CA 92093, USA, and  
HAGGERTY, S.E., Dept. of Geology, U.  
Massachusetts at Amherst, Amherst, MA  
01003, USA.

Ultramafic xenoliths containing garnet with exsolved pyroxene are believed to originate at depths > 300 km, possibly within the seismologically identified transition zone (1). If unaltered during subsequent residence at shallower depths, their isotopic compositions would be of obvious importance for understanding mantle chemical structure and evolution. We have analyzed pure mineral phases from three such xenoliths from Jagersfontein, South Africa. Sr and Nd isotopic compositions of garnets vary widely between xenoliths. Most fall within the known fields of lamproites and some Group II kimberlites, but are substantially different from their Group I kimberlite host. Analyses of leach solutions from pre-analysis cleaning of mineral separates suggest the presence of surface-sited "contaminants" which are also unrelated to the kimberlite host or analyzed phases. Three garnet separates analyzed show a good correlation between Sm/Nd and Nd isotopic composition but this relationship is probably without time significance. The single clinopyroxene separate analyzed to date exhibits strong isotopic disequilibrium with coexisting garnet, which could be interpreted in terms of the time of cpx exsolution (i.e. time of transfer to moderate mantle depths) at approximately 670 Ma, with an initial Nd isotopic ratio corresponding to  $\epsilon_{Nd} = +4$  relative to CHUR. If correct, this would require that the (transition zone?) source of material in this xenolith was "depleted", at least in terms of its Sm/Nd ratio, before ~ 700 Ma. Alternatively, if continued isotopic exchange occurred, the time of cpx exsolution could be much earlier.

1. Haggerty, S.E. and Sautter, V. (1990) Ultradeep (greater than 300 kilometers), ultramafic upper mantle xenoliths: Science 248, 993-996.

## CHLORINE ISOTOPIC COMPOSITION OF OCEANIC ROCKS AND CARBONACEOUS CHONDRITES

MAGENHEIM, A.J., Scripps Inst. Ocean., UCSD, LaJolla, CA 92093, USA, Spivack, A.J., Dept. of Earth Sciences, University of North Carolina at Wilmington, Wilmington, NC, 28403, USA, and Michael, P. University of Tulsa, Tulsa, OK USA

We have developed a method for the precise low level determination of the stable Cl isotope ratios ( $^{37}\text{Cl}/^{35}\text{Cl}$ ) of silicates. Cl is extracted by pyrohydrolysis, purified by ion exchange chromatography, and isotopic abundances are determined by thermal ionization mass spectrometry of the cesium chloride ion. Isotopic compositions are reported as per mil deviations relative to sea water. Based on replicate extractions and analyses the external reproducibility is 0.2 per mil.

Chloramphibole rich whole rocks dredged and drilled from the seafloor are enriched with  $\delta^{37}\text{Cl}$  ranging between 0.5 and 3.4. per mil. Oxygen isotope and fluid inclusion thermobarometry suggest that these rocks formed between 450-500°C by reaction with Cl rich brines (up to 50 wt. %). In principle, the observed isotopic enrichment may be associated with phase separation and/or water/rock interaction. Brine and vapor pairs from supercritical phase separation experiments were analyzed for Cl isotope composition. Under the experimental conditions (301-397 bars, 419-450 °C) isotopic differences between brine and vapor pairs are less than 0.2 per mil. Therefore, it appears that isotopic fractionation occurs during incorporation of Cl into solid phases.

Fresh MORB and Marianas Trough basalt  $\delta^{37}\text{Cl}$  values are between 1.0 and 4.9 per mil. This large of a range in Cl isotope ratios in fresh glasses is unexpected and supports the notion that Cl abundances are effected by assimilation of seawater or altered oceanic crust (amphibole) during eruption on a local scale. In addition, the MORB and chloramphibole data suggest that Cl isotopes may be a useful tracer of water released from amphiboles following subduction.

The carbonaceous chondrites, Orgueil (Cl) and Murchison (CM), have  $\delta^{37}\text{Cl}$  of 2.9 and 3.5 respectively. Preferential volatilization of the light isotope from Murchison is consistent with the more evolved nature of CM meteorites relative to Cls. Assuming the isotopic composition of Orgueil as a constraint for the whole Earth and that the  $\delta^{37}\text{Cl}$  of the hydrosphere is 0.0, an enriched  $\delta^{37}\text{Cl}$  reservoir in the mantle is inferred. By mass balance, we calculate that if 60% of the Earth's Cl is in the mantle, its average  $\delta^{37}\text{Cl}$  is 4.8. This values is consistent with the MORB  $\delta^{37}\text{Cl}$  values which appear to be the least effected by assimilation.

## He AND Ar ISOTOPES IN HOT FLUIDS AND ROCKS OF VULCANO (AEOLIAN ISLANDS, ITALY): CONSTRAINTS ON MAGMA COMPOSITION

MAGRO G. and FERRARA G., Istituto di Geocronologia e Geochimica Isotopica, CNR, 56127 Pisa, Italy

The fluids of medium-high temperature (up to 650°C) fumaroles, issuing from La Fossa crater of Vulcano island are the result of a variable mixing between a deep magmatic component and a shallow one. The evolution in time of this mixing has been studied during a long period of observations (1979 up to now) either for the composition of the reactive and the inert gases. In a first time a two-component mixing was assumed between a deep magmatic fraction which does not seem to change and a shallow fraction carrying atmospheric components (ASW and/or seawater), as evidenced not only by Ar isotopes (Magro and Pennisi, 1991), but also by the bulk chemical and isotopic ( $\delta\text{D}$ ) composition (Chiodini et al., 1992).

Actually, on the light of the important changes occurred in the  $^3\text{He}/^4\text{He}$  and  $^{40}\text{Ar}/^{36}\text{Ar}$  ratios, a better definition of the deep component has been obtained. The increase of the  $^3\text{He}/^4\text{He}$  ratio (from 4.3 to 6 R/Ra), with the synchronous decrease of  $^{40}\text{Ar}/^{36}\text{Ar}$  (from 2000 to 300) points out that the deep component has changed in time the mixing between crust and mantle derived fluids. The crustal fraction, evidenced by  $^{40}\text{Ar}/^{36}\text{Ar}$  high values, decreased towards a mantle-enriched fraction, marked by a high  $^3\text{He}/^4\text{He}$  ratio and a relatively low  $^{40}\text{Ar}/^{36}\text{Ar}$  without an appreciable atmospheric contamination. Low  $^{40}\text{Ar}/^{36}\text{Ar}$  ratios (close to 320) have been found also in minerals (olivine) separated from lavas of Vulcano. The relatively low  $^{40}\text{Ar}/^{36}\text{Ar}$  and the high  $^3\text{He}/^4\text{He}$  suggests that the magma which had generated rocks with relatively low  $^{87}\text{Sr}/^{86}\text{Sr}$  ratios (0.70425-0.70520; Ellam et al., 1988; Del Moro, personal communication), is influenced by fluid-rock interactions with the surrounding basement rocks; this implies that low  $^{40}\text{Ar}/^{36}\text{Ar}$  ratios are representative of the magma originated in such a geological setting, where crust-mantle interactions occur.

We recommend the importance of determining both  $^3\text{He}/^4\text{He}$  and  $^{40}\text{Ar}/^{36}\text{Ar}$  in the hot fluids and in the volcanics rocks, and we emphasize the long-term observations as tools to discriminate between the events occurring in an active volcanic system.

Chiodini, G., Cioni, R. and Marini, L., 1993, Reactions governing the chemistry of crater fumaroles from Vulcano island, Italy, and implications for volcanic surveillance: *Appl. Geochem.*, v. 8, p. 357-371.

Ellam, R.M., Menzies, M.A., Hawkesworth, C.J., Leeman, W.P., Rosi, M. and Serri, G., 1988, The transition from calc-alkaline to potassic orogenic magmatism in the Aeolian Islands, Southern Italy: *Bull. Volcanol.*, v. 50, p. 386-398.

Magro, G. and Pennisi M., 1991, Noble gases and nitrogen: mixing and temporal evolution in the fumarolic fluids of Vulcano, Italy: *J. Volc. Geotherm. Res.*, v. 47, p. 237-247.

**Nd-Sr ISOTOPIC CORRELATIONS OF FINE-GRAINED CLASTIC SEDIMENTS IN WESTERN PACIFIC MARGINAL BASINS: A POTENTIALLY POWERFUL TOOL FOR STRATIGRAPHIC CORRELATION**

Mahoney, J. Brian, Department of Geological Sciences, University of British Columbia, Vancouver, B.C. V6T 1Z4

The Nd and Sr isotopic signatures of fine-grained sedimentary strata may provide a new tool applicable to stratigraphic correlation and basin evolution studies. The isotopic signature of a basinal sequence is a function of the weighted average isotopic composition of all the crustal domains providing sediment to a depositional basin. Thorough mixing of fine-grained sediments homogenizes the isotopic signal, thus providing a signature that may be unique to an individual basin. The basinal isotopic composition will vary within limits, reflecting changes in the sediment flux derived from isotopically distinct crustal domains within the source region(s). These temporally controlled compositional fluctuations impart a corresponding isotopic variation that may be used as a stratigraphic marker to correlate strata throughout a depositional basin. The isotopic signature of well-dated strata may be compared with sections with poor age constraints to provide stratigraphic control. In addition, fluctuations in the isotopic signature ultimately result from geologic events and paleoclimatic variations in the source region(s), and may therefore be useful in reconstructing basin evolution.

Isotopic analyses of Plio-Pleistocene sediments from western Pacific marginal basins (Sea of Japan, Philippine Sea, Sulu Sea) are presented as a test case for Nd-Sr isotopic correlation and basin discrimination. Results indicate that the isotopic signature of these basinal sequences fluctuates within narrow, predictable limits, and that the signature is sensitive to changes in sediment flux from isotopically heterogeneous source regions. Deviations from predicted isotopic values suggest extrabasinal sediment influx; values from the Shikoku Basin (Philippine Sea) are significantly lower than expected ( $\epsilon_{Nd}(-7) - (-9)$  vs. expected  $\epsilon_{Nd}(-2)$  to  $(+2)$ ). These values are interpreted to represent eolian sediment influx into the basin from eastern Eurasia, coincident with climatic change in Late Pliocene-Early Pleistocene time.

These results indicate that the isotopic signature of fine-grained clastic sediments may be an extremely useful tool in discriminating ancient, structurally disrupted basinal sequences, and placing constraints on basin history.

**OS ISOTOPES AND RECYCLED OCEANIC CRUST**

MARCANTONIO, F., ZINDLER, A., ELLIOTT, T., Lamont-Doherty Earth Observatory, Palisades, NY, 10964, USA, and STAUDIGEL, H., Vrije Universiteit, Laboratory of Isotope Geology, De Boelelaan 1085, 1081 HV Amsterdam, The Netherlands

The isotopic and trace element signatures of HIMU ocean island basalts (OIBs) have provided evidence for the role of subducted oceanic crust in their genesis [1]. Os isotope analysis of OIBs has the potential to further constrain crustal recycling hypotheses. Recent Os isotopic measurements of HIMU-endmember OIBs [2,3] reveal large and intriguing variations in  $^{187}\text{Os}/^{186}\text{Os}$  ratios that range from 1.12 to 1.72. Before attributing these variations to heterogeneous mantle source regions containing recycled crust, other possibilities, including contamination with radiogenic Os within the volcanic pile, or interaction between magma and lithospheric cumulates, must be ruled out [3].

In order to better distinguish between these possibilities, we have investigated Os isotope systematics at the island of La Palma, in the Canarian archipelago. We analyzed samples both from the older (4.0-2.9 Ma), altered, uplifted seamount section of the island, and the younger (1.6 Ma to Recent) subaerial lavas. Initial  $^{187}\text{Os}/^{186}\text{Os}$  ratios for the older altered samples are extremely heterogeneous and range from 1.21 to 3.36, while the younger subaerial samples are less heterogeneous in  $^{187}\text{Os}/^{186}\text{Os}$  and range from 1.13 to 1.59. Our results imply that significant contamination of the subaerial basalts with radiogenic Os from altered submarine basalts may occur. However, mixing calculations suggest that only the Os-poor subaerial magmas (with concentrations less than 30 ppt) are susceptible to observable isotopic modification by this process.

Os isotopic signatures for uncontaminated La Palma samples range from 1.13 to 1.25. Pb isotope ratios for the same samples show no correlation with Os isotope ratios. When potentially contaminated low-Os OIBs are screened from the literature data set [2,3], HIMU and transitional-to-HIMU OIBs have the highest (up to 1.25) and most variable Os isotopic signatures. However, simple mixing between recycled oceanic crust and ambient peridotitic mantle is not demonstrated by the Pb-Os isotope systematics. These systematics may, however, provide information about the specific chemical characteristics of the recycled material sampled at individual ocean islands.

- [1] Hofmann and White, 1982, *Earth Planet. Sci. Lett.*, 57, 421-436. [2] Hauri and Hart, 1993, *Earth Planet. Sci. Lett.*, 114 353-371. [3] Reisberg et al., 1993, *Earth Planet. Sci. Lett.*, in press.

## PHOSPHORUS CYCLING AND PHOSPHORUS SOURCES IN LAKE KINNERET; TRACING BY OXYGEN ISOTOPES IN PHOSPHATE

MARKEL Doron, KOLODNY Yehoshua, LUZ Boaz, The Institute of Earth Sciences, The Hebrew University of Jerusalem, Jerusalem, Israel, and NISHRI Aminadav, Israel Oceanographic Limnological Research, Kinneret Limnological Laboratory, Tabgha, Israel.

The isotopic composition of oxygen in phosphate ( $\delta^{18}\text{O}_p$ ) in sediments and suspended matter of Lake Kinneret (the Sea of Galilee, L.K.) serves as a tracer of the phosphorus sources and sinks.  $\delta^{18}\text{O}_p$ , and the distribution of phosphate concentrations in different fractions of the sediments were measured at a number of stations in the lake and in its catchment basin.

Sequential extracts of phosphate show that the major fraction of phosphorus in L.K. sediments is linked to calcium, either as apatite or as a surface complex on calcite crystals. A minor fraction is adsorbed on clays and iron hydroxides. No iron-phosphate or aluminum-phosphate minerals were detected. Approximately 70% of the particulate inorganic phosphate entering L.K. is from a basaltic source ( $\delta^{18}\text{O}_p \approx 6\text{‰}$ ). This includes the detrital sand fraction (probably fluor-apatite,) most of which sinks to the bottom immediately upon entering the lake, and is thus mechanically removed from the cycle. Only 40% of the phosphate in the silt and clay fractions is derived from a basaltic source; the rest is of sedimentary and anthropogenic origin ( $\delta^{18}\text{O}_p \approx 18$  to  $25\text{‰}$ ).

Isotopic mass balance shows that authigenic apatite is precipitated in L.K., mostly at the Jordan inlet delta, due to high pH and intermediate dissolved phosphate concentration. This apatite, possibly hydroxy-apatite, reaches the deep part of the lake and dissolves at relatively low pH ( $\sim 7.5$ ) mainly during the stratification period (April - November).

A phosphate surface complex on calcite crystals,  $\text{Ca}_3(\text{HCO}_3)_3(\text{PO}_4)$  (CCP), or  $\text{CaHPO}_4$  (DCP), is precipitated in the L.K. catchment basin and contributes one quarter of the particulate phosphate entering the lake from the Jordan. A large part of this complex is removed at the Jordan inlet delta at relatively high pH, but it is re-precipitated on calcite surfaces in the deep part of the lake.

The phosphorus which is released from dissolution of authigenic apatite in the deep part of the lake and from the dissolution of the phosphate surface complex are both internal sources of bio-available inorganic phosphate.

## PALEOHYDROLOGY FROM STRONTIUM ISOTOPES AT YUCCA MOUNTAIN, NEVADA

MARSHALL, B.D., PETERMAN, Z.E., and STUCKLESS, J.S., U. S. Geological Survey, Federal Center MS 963, Denver, CO 80225 USA.

Yucca Mountain, located in southwest Nevada, is being studied as the site for a potential nuclear waste repository. The host rock for the potential geologic repository, the Topopah Spring Tuff, is in the unsaturated zone. The elevation of the water table is fairly uniform beneath the site, but the depth to the water table ranges from approximately 480 to 780 m, due to topography, and the potential repository horizon is 180-410 m above the water table.

Calcite and other secondary minerals are being examined for their paleohydrologic implications. Core samples from holes drilled through the Tertiary volcanic section show that calcite occurs in both the unsaturated and saturated zones as fracture coatings and infillings. The calcite ages could range from the period of volcanism (11-14 Ma) to the present-day, but at least some samples are Quaternary.<sup>1</sup>

In the saturated zone, calcite  $^{87}\text{Sr}/^{86}\text{Sr}$  ranges from 0.7087 to 0.7098, similar to values observed in the volcanic rocks. However, both the rocks and secondary minerals may have been influenced by lower carbonate aquifer water that may have saturated the volcanic section early in its history. In the unsaturated zone,  $^{87}\text{Sr}/^{86}\text{Sr}$  in fracture calcite ranges from 0.7114 to 0.7127, similar to pedogenic calcite exposed at or near the surface. Six samples from 48 to 90 m above the water table have  $^{87}\text{Sr}/^{86}\text{Sr}$  significantly lower (0.7104 to 0.7112) than that of the pedogenic calcite, but similar to present-day groundwater in the region. There is a weak correlation between depth and  $^{87}\text{Sr}/^{86}\text{Sr}$  in the samples from the unsaturated zone, similar to the trend of  $^{87}\text{Sr}/^{86}\text{Sr}$  in the host volcanic rocks. This may indicate an additional influence of volcanic rock strontium on the infiltrating fluids from which the calcite precipitated.

Locally, the basal vitrophyre of the Topopah Spring Tuff is relatively impermeable and water is perched above it. This perched water sampled from 90 m above the water table has  $^{87}\text{Sr}/^{86}\text{Sr} = 0.7124$ , similar to average pedogenic carbonate, indicating its derivation as infiltration from the surface. Tuff samples from a nearby drill hole at the same stratigraphic horizon show extensive alteration; their strontium compositions are consistent with a fluid composition of 0.7124. The intense alteration of the volcanic section here, accompanied by a large increase in strontium concentration, indicates high water/rock ratios were attained locally.

Based on strontium isotope data, three tentative and preliminary conclusions may be drawn: 1) the water table beneath Yucca Mountain may have been up to about 90 m higher in the past; 2) perched water derived its strontium from pedogenic sources; and 3) perched water may be responsible for localized alteration of the volcanic rocks.

<sup>1</sup> Szabo B.J. and Kyser T.K. (1990) Ages and stable-isotope compositions of secondary calcite and opal in drill cores from Tertiary volcanic rocks of the Yucca Mountain area, Nevada. *Geol. Soc. Am. Bull.*, **102**, 1714-1719.

## LIMITS OF HIGH PRECISION TIMS ANALYSIS IN PALAEO-OCEANOGRAPHY

MARTEL, D. J., HENDERSON, G. M., BURTON, K. W. and O'NIONS, R. K. (Dept. of Earth Sciences, Univ. of Cambridge, Downing St., Cambridge, CB2 3EQ. U. K.; E-Mail DJM14@ESC.CAM.AC.UK)

Modern palaeo-oceanographic research sets some particularly challenging aims for high precision TIMS isotope ratio measurements. These challenges are set by the scope to use isotopic tracers of varying residence times to constrain palaeo-oceanographic response to climatic and tectonic forcing. When studying systems with residence times that are long in comparison with the events being studied (for example Sr), the magnitudes of the isotopic shifts may be small, and approach the limits to which they can be measured. In such circumstances the factors which may affect the measurements must be fully and carefully evaluated to ensure that any measured isotopic shift is not incorrectly ascribed.

Modern multiple collector mass spectrometers readily produce extremely precise (~5ppm) single analyses of Sr and Nd using either static or multi-dynamic procedures. However the accuracy of the measurement (long-term reproducibility) is the main criterion of interest.

Many factors affect the accuracy of analyses, some such as amplifier gain calibration, DVM linearity, and tau-correction may be measured accurately without using ion beams. Other factors such as uniformity of bucket efficiency, and fractionation behaviour may only be measured using ion beams, and are limited in accuracy due to beam instability during calibration, or the need to make many high precision isotope ratio analyses of a standard.

In this contribution particular attention is given to limitations that arise from fractionation behaviour. High precision Sr standard analyses were made over a period of several months using triple filaments at  $^{88}\text{Sr}$  beam currents of  $\sim 3 \times 10^{-11}$  amps. Observed  $^{87}\text{Sr}/^{86}\text{Sr}$  ratios were best reconciled with  $^{86}\text{Sr}/^{88}\text{Sr}$  by fitting an empirical fractionation correction, giving an external reproducibility of <10ppm. Conventional calculation assuming fixed (either exponential or power law) fractionation behaviour on the same data set degrades the reproducibility by a further 6 to 30 ppm depending on which law is used. Indications are that running conditions may affect fractionation behaviour.

By careful control of analytical procedures, and machine calibration it is possible to achieve reproducibility of the order of 10ppm using the current generation of mass spectrometers. Details are given of the procedures used for  $^{87}\text{Sr}/^{86}\text{Sr}$  and progress with high precision  $^{143}\text{Nd}/^{144}\text{Nd}$  ratio measurements.

## SIMULATION OF COSMOGENIC-NUCLIDE PRODUCTION IN TERRESTRIAL ROCKS

MASARIK, J. and REEDY, R. C., Astrophysics and Radiation Measurement Group, Los Alamos National Lab., Los Alamos, NM 87545, USA.

Some secondary particles produced by the interactions of galactic cosmic rays (GCR) in the Earth's atmosphere react with nuclei in the surface. Detectable amounts of stable or radioactive isotopes not present or rare in the target material can be produced in these interactions. For the interpretation of measured cosmogenic nuclides in terms of the target's exposure history (e.g., age or erosion rate), good modeling of their production rates is necessary.

We used a purely physical model that has been well tested with extraterrestrial materials [Masarik and Reedy, 1994] for the calculation of cosmogenic-nuclide production rates in the Earth's surface. The nucleon spectra as a function of depth in the Earth were calculated by Monte Carlo simulations using the LAHET Code System for interactions of cosmic-ray particles with the Earth's atmosphere and surface and the subsequent production and transport of secondary particles. An isotropic GCR particle flux irradiated a sphere with the Earth's radius and having an average continental-crustal composition with a 2% water content. This irradiation applies to geomagnetic latitudes  $>60^\circ$  where there is no cosmic-ray cutoff. The model atmosphere has a thickness of 1030 g/cm<sup>2</sup> (sea level) and observed composition and densities. Having calculated nucleon fluxes, the production rate of nuclides were calculated by integrating over energy the product of these fluxes and cross sections for the nuclear reactions producing each nuclide that had been tested using extraterrestrial materials. Running 650,000 primary GCR protons, we calculated surface particle fluxes with errors of ~30%. We are doing more calculations to get better statistics and to study attenuation lengths and different atmospheric thicknesses.

Our calculated surface production rates for high geomagnetic latitudes and sea level agree with those reported in natural samples. In quartz, our preliminary calculated production rates (atoms/year/g-SiO<sub>2</sub>) were  $^3\text{He} \approx 124$ ,  $^{10}\text{Be} \approx 6$ ,  $^{14}\text{C} \approx 19$ ,  $^{21}\text{Ne} \approx 19$ , and  $^{26}\text{Al} \approx 36$ . In CaO, the calculated  $^{36}\text{Cl}$  production rate was 47 atoms/yr/g-CaO. In olivine with Mg being 81% of the Mg+Fe atoms, rates per gram of olivine were  $^3\text{He} \approx 105$  and  $^{21}\text{Ne} \approx 40$ . These production rates were calculated with only neutron and proton fluxes; muon contributions were not calculated. For surface  $^{26}\text{Al}$ , only ~6% of the calculated production was by protons. Better statistics are needed to get good depth profiles, but our preliminary calculations show the production-rate-versus-depth profiles relatively flat to a depth of ~20 g/cm<sup>2</sup> and then decreasing roughly exponentially with attenuation lengths that, within large errors, are consistent with reported ones.

Masarik J. and Reedy R.C. (1994) *Geochim. Cosmochim. Acta* (submitted).

MAGMATIC PROCESSES AT A CONTINENTAL COLLISION ZONE: THE EAST CARPATHIAN ARC, ROMANIA.

MASON P.R.D. and DOWNES H., Dept Geology, Birkbeck College, University of London, Malet St, London, WC1E 7HX, UK, THIRLWALL M.F., Dept Geology, Royal Holloway, University of London, Egham, TW20 OEX, UK, SEGHEDI I., and SZAKACS A., Institute Geology and Geophysics, Str Caransebes, Bucharest, Romania

The East Carpathians represent the final episode of subduction-related magmatism in Eastern Europe, at the south-eastern end of a Mio-Pliocene arc stretching from Hungary and Slovakia into Romania. South-westwards subduction beneath the Pannonian microplate produced mainly andesitic to dacitic stratovolcanism. Activity became progressively younger south-eastwards along the arc, terminating at 1-2Ma with contemporaneous high-K arc lavas and back-arc alkali basalts.

Most volcanic centres are calc-alkaline to high-K calc-alkaline. Lavas are LILE- and LREE-enriched by slab fluid/melt metasomatism ( $Ce/Yb=4-7$ ) and exhibit a large range of silica contents (51-70%) and Mg#s (0.25-0.64). The wide range in trace element abundance and  $Eu/Eu^*$  (0.7-1.0) can be related to fractional crystallisation processes.  $\epsilon_{Sr}$  (-6.2 to +7.5) and  $\epsilon_{Nd}$  (+5.0 to -3.9) isotope ratios vary widely. Mixing is suggested between different primitive magmas and crustal end members in different parts of the arc. Some suites show systematic  $SiO_2$ - $^{87}Sr/^{86}Sr$  relationships consistent with varying degrees of crustal assimilation. Pb isotopes are strongly enriched ( $\Delta^{207}Pb=9.7-19.3$ ,  $\Delta^{208}Pb=35.7-112.3$ ) and can be, in part, linked to crustal assimilation as indicated by Nd isotopic correlations. However the least contaminated rocks still have Pb displaced well above the NHRL. Laser fluorination oxygen isotope analysis will further constrain the roles of crustal assimilation and source enrichment.

The youngest activity (1-3Ma) consists of small volume, high-K (2-4%  $K_2O$ ) volcanic centres and intrusions of shoshonitic affinity. Trace elements in these magmas were strongly enriched due to smaller degrees of partial melting related to the waning of magmatism. Shoshonitic rocks are strongly LREE-enriched ( $Ce/Yb=18-34$ ). Mineral disequilibrium assemblages indicate the existence of quartz+biotite- and Mg-olivine-rich end members. Mixing may have occurred between an evolved calc-alkaline magma and a contemporaneous alkali basalt magma.

An older (8-9Ma) group of low-K dacites (~1% $K_2O$ ) with primitive Sr-Nd isotopic compositions ( $\epsilon_{Nd}=+5.0$  to +2.5) are distinctive in the north of the region. Small positive Eu anomalies ( $Eu/Eu^*\sim 1.08$ ) and the lack of negative strontium anomalies, are common indicating derivation without extensive plagioclase fractionation. LREE enrichment is similar to the main arc trend ( $Ce/Yb=4-6$ ).

EVOLUTION OF CERIU AND NEODYMIUM ISOTOPIC RATIOS CONSISTENT WITH MASUDA-MATSUI'S MODEL

A. Masuda,  
Department of Chemistry,  
University of Electro-communications,  
Chofu, Tokyo-182, Japan

Thirty years ago, Masuda and Matsui [1] succeeded in mathematically dealing with the chondrite-normalized REE patterns. This treatment led them to a conclusion that the bulk partition coefficients (k) of REE between the co-existing equilibrated solid and liquid (molten) silicate phases is a linear function of difference in atomic number between REE. According to their analysis, the k values were estimated to be 0.119, 0.155, 0.227 and 0.299 for La, Ce, Nd and Sm, respectively. (Another set of k values, i.e., 0.191, 0.249, 0.364 and 0.480 has been proposed afterwards, but this does not affect the present discussion, because the relative magnitudes are given to be identical to each other of both sets.) The corresponding La/Ce and Sm/Nd abundance ratios for the earliest-stage solid phase separated from CHUR are evaluated to be 0.297 and 0.424. The calculation indicates that a set of the numerical values of  $\epsilon_{Ce} = -1.4$  and  $\epsilon_{Nd} = +10.6$  for T (separation time) = 2.2 Ga is consistent with Masuda-Matsui's model. The observed values for N-type MORB [2,3] are in pretty good agreement with the results mathematically inferred based on the above model. This agreement endorses empirically the validity of the important assumptions adopted in proposal of the model under consideration, for the evolution of the earth [1]. But other questions can be raised.

1. Masuda, A., and Matsui, Y., 1966, *Geochim. Cosmochim. Acta*, **30**, 239-250.
2. Makishima, A., and Masuda, A., 1994 (under submission to a journal)
3. Tanaka, T., Shimizu, H., Kawata, Y., and Masuda, A., 1987, *Nature*, **327**, 113-117.

EXPERIMENTAL STUDY OF  $^{18}\text{O}/^{16}\text{O}$  PARTITIONING BETWEEN CRYSTALLINE ALBITE, ALBITIC GLASS, AND  $\text{CO}_2$  GAS: IMPLICATIONS FOR MELTING AND DIFFERENTIATION.

MATTHEWS, A. Institute of Earth Sciences, Hebrew University of Jerusalem, 91904 Jerusalem, Israel, PALIN, J.M., EPSTEIN, S., and STOLPER, E.M., Division of Geological and Planetary Sciences, California Institute of Technology, Pasadena, CA 91125, U.S.A.

Oxygen isotope partitioning between gaseous  $\text{CO}_2$  (1 bar) and crystalline albite and albitic glass has been measured at  $750^\circ - 950^\circ\text{C}$ . Convergence of oxygen isotopic values of  $\text{CO}_2$  to equilibrium and avoidance of surface-correlated fractionation effects is achieved in long runs (>200 days) using relatively coarse grain sizes. Equilibrium  $\text{CO}_2$ -crystalline albite oxygen isotope fractionation factors are:  $4.74 \pm 0.22$  at  $750^\circ\text{C}$ ,  $3.77 \pm 0.23$  at  $850^\circ\text{C}$ , and  $3.36 \pm 0.21$  at  $950^\circ\text{C}$ . These values compare well with estimates made by combining the experimental calcite-albite data of Clayton et al. (1989) with  $\text{CO}_2$ -calcite fractionation factors. Our results thus provide independent support for the high pressure calcite-mineral fractionation factors of Clayton et al. (1989).

$\text{CO}_2$ -albite exchange experiments of relatively short duration give disequilibrium fractionation factors. Oxygen diffusion coefficients calculated from these experiments, however, are comparable with previous determinations of oxygen diffusion in feldspars under nominally anhydrous conditions. Diffusion coefficients calculated for albitic glass are slightly higher than those measured for silica glass by Stolper and Epstein (1991) and support the hypothesis that isotopic exchange is controlled by diffusion of molecular carbon dioxide in these glasses.

Equilibrium oxygen isotope fractionation factors determined for  $\text{CO}_2$ -albitic glass are identical within experimental uncertainty to those determined for  $\text{CO}_2$ -crystalline albite. Additional measurements of oxygen partitioning between  $\text{CO}_2$  and silica glass confirm the results of Stolper and Epstein (1991). A comparison of the silica glass-albitic glass fractionation from our work with the quartz-albite fractionation from Clayton et al. (1989) suggests that the silica glass-albitic glass fractionations are distinctly larger than the equivalent fractionations for the crystalline phases. Given that crystalline albite and albitic glass have essentially identical reduced partition function ratios, a clear implication is that the isotopic properties of silica glass differ significantly from those of crystalline quartz; i.e., silica glass is isotopically enriched with respect to crystalline quartz by 0.5 to 0.9‰ at  $650^\circ$  to  $950^\circ\text{C}$ .

An analysis of consequences of the experimental data for melting and differentiation processes in silicic magmas suggests that for given constant crystal compositions, crystal-liquid fractionation factors will also change systematically with melt composition with the magnitude quartz-melt fractionations decreasing and feldspar-melt fractionations increasing with increasing silica in the melt. An example calculation of the melting of a model quartz-feldspar-biotite gneiss at  $700^\circ\text{C}$  indicates that the initial minimum melt will be 0.8‰ heavier than the parent rock. Thus, although these changes are not likely to be much larger than 1‰ at magmatic temperatures, they are likely to be important in efforts to interpret and quantitatively model the evolution of oxygen isotopes during processes of melting and differentiation.

Clayton R. N., Goldsmith J. R. and Mayeda T. K. (1989) Oxygen isotope fractionation in quartz, albite, anorthite, and calcite. *Geochim. Acta* 53, 725-733.

Stolper E. and Epstein S. (1991) An experimental study of oxygen isotope partitioning between silica glass and  $\text{CO}_2$  vapor. In *Stable Isotope Geochemistry: A Tribute to Samuel Epstein. Special Publication No. 3, The Geochemical Society* (ed. H. P. Taylor jr., J. R. O'Neil, and I. R. Kaplan), pp. 35-51.

BASIC AND ULTRABASIC XENOLITHS FROM KERGUELEN: RECORD OF A DUPAL PLUME ACTIVITY  
MATTIELLI, N., WEIS, D., Pétrol. Géodyn. Chimique, CP160-02, Univ. Libre de Bruxelles, 50, Av. F.D. Roosevelt, 1050 Brussels, Belgium and SHIMIZU, N., WHOI, MA 02543, USA, GREGOIRE, M. and GIRET, A., Univ. J. Monnet, St. Etienne, France.

In order to understand the geochemical evolution of Kerguelen plume and its interactions with the upper mantle, we have studied ultrabasic and basic xenoliths from Kerguelen Archipelago.

Our samples come from pipes and dykes in the Upper Miocene Series of the Southeast Province.

The xenoliths are distributed in 2 categories: Type 1 - spinel-2 pyroxenes bearing ultrabasic and basic series (all terms from lherzolite to gabbro) with a predominant granoblastic texture and numerous relics of cumulate magmatic texture - and Type 2 - harzburgites and dunites with protogranular - porphyroclastic textures.

Trace element abundance patterns in cpx of Type 1 are characterized by low overall abundance levels (~1 times chondrite). Those of Type 2 show LREE enriched and/or LREE enriched convex down geometry  $(\text{La}/\text{Sm})_N=10$ .

Sr, Nd and Pb compositions and concentrations have been measured on whole rocks of 10 xenoliths (sp/sa±gt bearing metagabbros; ilm/gt/rut bearing metagabbro; websterite; harzburgites and dunite) and on separated leached cpx and/or pl and/or gt from 2 harzburgites and 2 sp/sa±gt bearing metagabbros. Xenoliths as a whole, cover the entire range of isotopic variations in plutonic and basaltic series of Kerguelen islands. Hence they carry a Dupal anomaly signature. Type 1 xenoliths isotopic signatures are very homogeneous ( $^{87}\text{Sr}/^{86}\text{Sr}$  from 0.70422 to 0.70447,  $\epsilon_{\text{Nd}}$  from 4.8 to 2.6,  $^{206}\text{Pb}/^{204}\text{Pb}$  from 18.102 to 18.184,  $^{207}\text{Pb}/^{204}\text{Pb}$  from 15.501 to 15.570,  $^{208}\text{Pb}/^{204}\text{Pb}$  from 38.136 to 38.592), similar to tholeiitic-transitional basalts, suggesting a common origin for those basalts and all xenoliths of this type. A preliminary Sm-Nd isochron on cpx and whole rocks suggests an age of  $161 \pm 73$  Myr, i.e. contemporaneous with the Kerguelen Plateau formation. We speculate that Type 1 xenoliths are cumulates from basaltic magmas formed by underplating<sup>1</sup> beneath the plateau during its formation. Type 2 peridotites display the most Dupal signature ( $^{87}\text{Sr}/^{86}\text{Sr}$  from 0.70506 to 0.70577,  $^{206}\text{Pb}/^{204}\text{Pb}$  from 18.390 to 18.456,  $^{207}\text{Pb}/^{204}\text{Pb}$  from 15.546 to 15.593,  $^{208}\text{Pb}/^{204}\text{Pb}$  from 38.846 to 39.024, and  $\epsilon_{\text{Nd}}$  3.9 to -0.1) comparable to the young (8 Myr) highly alkaline series signature. These isotopic ratios indicate that the Type 2 peridotites can correspond to residual products of the highly alkaline series. They have suffered a stronger enrichment (explaining their LREE enriched signature) through interaction with an alkaline magma and/or with a  $\text{CO}_2$  enriched magma<sup>2</sup>.

(1) Grégoire et al. (1993), in press in Nature.

(2) Schiano et al. (1993), submitted to EPSL.

REVERSE DISCORDANCE IN THE U-Pb SYSTEM IN ZIRCONS: THE ROLE OF SMALL-SCALE ZONING AND DIFFUSION AS REVEALED BY STEP-WISE DISSOLUTION EXPERIMENTS

MATTINSON, James M., PARKINSON, David L., McCLELLAND, William C., and GRAUBARD, Cinda M., Department of Geological Sciences, University of California Santa Barbara, California 93106 USA

Reverse discordance (here used in its original sense to mean 206/238 age > 207/206 age) is a relatively rare but well-documented phenomenon in zircons. Most previous explanations of reverse discordance have invoked introduction of radiogenic Pb from outside sources, preferential loss of U, or breakdown of zircon into badellyite and silica phases, with sequestering of radiogenic Pb in the silica phase.

Specially designed step-wise dissolution experiments reveal that some zircons contain zones that are highly insoluble and contain little or no U, but do contain significant amounts of essentially pure radiogenic Pb. The highly radiogenic nature of the Pb, together with its isotopic systematics, clearly reveal that the Pb is derived from within the zircon grains themselves, rather than from outside sources. The association of the "excess" Pb with the least soluble parts of the zircon argues against a silica host phase, which would be highly soluble in HF.

We suggest that magmatic zoning on a fine (i.e., sub-micron to few micron) scale in zircons is an important key to understanding reverse discordance. We propose that the zoning results from the interplay between episodic zircon crystallization and the relative diffusion rates for Zr and U. Episodic crystallization can be understood as follows: initiation of crystallization, either of seed crystals or of a layer of zircon on an existing zircon crystal, requires a finite level of supersaturation as a driving force. Zircon growth then proceeds fairly rapidly until Zr drops to the exact saturation level in the magma immediately surrounding the growing zircon crystal. This produces a hiatus in crystallization until the local Zr level is restored to the supersaturation level required for renewal of crystallization, either by diffusion, or by continued crystallization of major minerals that exclude Zr, thus driving its concentration back up in the residual magma.

During each cycle of crystallization, strong zoning of trace elements such as U will be produced if their diffusion rates in the magma are lower than that of Zr. In particular, under highly oxidizing conditions, U may be in a higher valence state, leading to higher field strengths, a higher degree of complexing, and hence, much slower rates of diffusion.

Small-scale strong zoning of U in zircon grains sets up a situation where, after radiogenic ingrowth, Pb need only diffuse sub-micron distances to be redistributed from high-U zones to adjacent low-U zones. This will produce "internal reverse discordance": the zircon as a whole might be slightly normally discordant or even concordant, but the low-U zones within it are reversely discordant.

"External reverse concordance" can be produced if fluids moving through the rock during metamorphism, hydrothermal activity, or even near-surface weathering cause dissolution and removal of the highest-U zircon zones, together with their U and remaining Pb. This leaves the residual zircon enriched in the low-U, relatively insoluble zircon zones that contain parentless radiogenic Pb, thus producing an overall reverse discordance for the bulk zircon sample.

SULPHUR DYNAMIC STUDIES IN FOREST ECOSYSTEMS USING STABLE ISOTOPES

MAYER, B., and KROUSE, H. R., Department of Physics and Astronomy, The University of Calgary, Calgary, Alberta, T2N 1N4, Canada

The sulphur cycle in terrestrial ecosystems has previously been studied mainly by input/output balances of whole watersheds or sub-compartments therein. These studies limit conclusions about sulphur dynamics since the obtained sulphur fluxes represent only the net-effect of various transformation processes. Stable sulphur isotopes have been used to further delineate sulphur sources, especially where  $\delta^{34}\text{S}$ -values of lithogenic (pyrite, evaporites) or anthropogenic ( $\text{SO}_2$ ) sulphur differs from those of unpolluted atmospheric deposition.

An isotope tracer technique with sulphate was tested as a new approach for understanding sulphur cycling in soil. It was used in a lysimeter experiment with five aerated German forest soils, where 15 soil cores of each soil type were irrigated with  $^{34}\text{S}$ - and  $^{18}\text{O}$ -enriched sulphate derived from Silurian gypsum. Since isotope fractionation during sulphur transformations under aerated conditions is rather small, it was shown by concentration and isotope measurements in seepage water sulfate and different forms of soil sulphur, that the applied sulphate was retained primarily as inorganic sulphate, secondarily as organic sulphur, and very little sulphate was exported in the seepage water. It was concluded that the mean residence time of sulphur in the pedosphere is of the order of many years to a few decades, much longer than previously suggested. Since these results are in excellent agreement with those of radioactive  $^{35}\text{S}$ -tracer studies, stable sulphur isotopes prove to be a valuable tracer for long term studies under aerated conditions.

The technique is currently being tested under field conditions in a Norway spruce forest near Munich (Germany), where isotopically enriched sulphate was applied to the forest floor. Preliminary concentration and isotope data for seepage water sulphate and soil sulphur have been obtained.

## AQUIFERS IMMUNE TO POLLUTION

MAZOR, E., Dept. of Environmental Sciences and Energy Research, Weizmann Institute of Sciences, Rehovot 76100, Israel

An aquifer is a body of permeable rock that contains water in all its voids and can sustain economical wells. This definition leaves room for active aquifers (with recharge, through-flow and discharge) and passive aquifers (trapped, with no recharge, through-flow and discharge). The most common example of an active aquifer is the phreatic aquifer, whereas examples of passive aquifers are traps of oil, gas and brines. Passive artesian fresh water aquifers can be passive when they are deeply buried, sealed above and beneath by impermeable rocks, e.g. in rift valleys or in subsidence basins. The observed artesian pressure is induced in these cases by compaction. The pressure in a new well, drilled into a passive pressurized aquifer, is expected to drop rapidly and not recover after shut down.

Geological criteria can support the passive aquifer case, but the properties of the stored groundwater itself are needed as augmenting evidence: (a) high water ages, indicated by no measurable C-14 (i.e. no recharge in the last 25,000 years), low {observed Cl-36/initial Cl-36} ratios, indicating water ages in the range of  $10^6$  years or greater, and in-situ He-4 concentrations, indicating ages in the range of  $10^4$  to  $10^8$  years; (b) paleo-recharge, indicated by deuterium and O-18 concentrations that differ from the present values; (c) hydraulic isolation, indicated by dissolved ion concentrations and relative abundances that typify a given artesian aquifer, and differ from the composition of overlying and underlying aquifers.

Passive pressurized aquifers containing potable water should be saved (a) for times of need - extreme droughts, or large scale pollution events, and (b) for future generations. Artesian aquifers that have already been exploited and ceased flowing, may be artificially recharged and used as safe water storage reservoirs.

Artesian aquifers that have been depressurized by exploitation, may be considered as potential sites for waste injection, for the following reasons: (a) they have been hydraulically well isolated by nature, for time periods equaling the age of the water, (b) no uncontrollable hydrofracturing is anticipated as a result of the waste injection, as long as the pressure is kept below the initial pre-exploitation pressure.

Examples of passive pressurized aquifers will be presented.

## RHENIUM-OSMIUM ISOTOPE ANALYSIS OF BASE METAL SULFIDES FROM LARAMIDE PORPHYRY DEPOSITS, SOUTHWESTERN NORTH AMERICA

MCCANDLESS, Tom E., RUIZ, Joaquin, and CHESLEY, John T., Department of Geosciences, University of Arizona, Tucson, Arizona, USA 85721

Base metal porphyry deposits represent major accumulations of chalcophile elements within the earth's upper crust. These deposits are related to subduction of oceanic crust beneath continental lithosphere, and the metals may originate from the mantle, lower crust, or intruded country rocks. Base metal porphyry deposits in southwestern North America have Re-Os mineralization ages that correspond to two Precambrian crustal domains which differ in age and lithology, suggesting that crust influences mineralization (McCandless and Ruiz, 1993); but the amount of crustal involvement in the formation of these deposits is still uncertain. The Re-Os isotope system is ideally suited to evaluate the crustal contribution to base metal porphyry mineralization, because both Re and Os are chalcophile elements, and the  $^{187}\text{Os}/^{188}\text{Os}$  ratio of the crust ( $>3.6$ ) is very different from that of the mantle ( $\sim 0.1$ ). Base metal sulfides from major porphyry deposits in southwestern North America have been analyzed for Re and Os isotopes using fusion/distillation and NTIMS methods. Preliminary results suggest that a very radiogenic (i.e. crustal) component of Os is recorded in the mineralization. Additional analyses will determine if these radiogenic signatures are unique to the Precambrian crustal domains in which they occur.

McCandless, T.E. and Ruiz, J., 1993, Rhenium-Osmium Evidence for Regional Mineralization in Southwestern North America: *Science*, v.261, p.1242-1246.

**RESOLVING HIGH PRECISION U/Pb AGES FROM TERTIARY PLUTONS WITH COMPLEX ZIRCON SYSTEMATICS: EXAMPLES FROM SE ALASKA**

McClelland, William C. and Mattinson, James M.,  
Department of Geological Sciences, University of California, Santa Barbara, CA 93106, USA

Complex zircon systematics due to the combined effects of inherited components and Pb-loss are relatively common in Mesozoic and Tertiary plutonic complexes. Interpreting slightly to strongly discordant conventional zircon data from such samples is difficult since the assumption of either simple Pb-loss or a singular inherited or entrained xenocrystic component necessary for conventional concordia analysis is invalid. In addition, commonly employed air abrasion techniques cannot decipher the effects of both inheritance and Pb-loss. In contrast, step-wise dissolution techniques entailing analysis of sequential partial digestion steps have proven instrumental in resolving useful age information from populations exhibiting complex discordance patterns.

Utility of the partial dissolution technique is exemplified by comparison of conventional and step-wise analyses on relatively low-U (200-500 ppm) zircon populations from two Tertiary plutons in the Coast Mountains batholith, SE Alaska. Conventional analyses on abraded and unabraded fractions of differing size and magnetic properties yield moderately discordant to concordant results defining arrays that clearly indicate the presence of inherited components (Fig. 1). Age interpretations for these samples are limited by the non-linear variation in U/Pb and Pb/Pb ages and uncertainty in the magnitude of Pb-loss suspected from independent evidence (A:  $56.5 \pm 1.1$  Ma assuming no Pb-loss; B:  $62 \pm 3$  Ma as reasonable estimate). Partial dissolution experiments tailored to relatively low-U, young zircons produced successive leach steps that define a trajectory of decreasing  $^{207}\text{Pb}/^{206}\text{Pb}$  ages and, with exception of sample B residue, increasing U/Pb ages (Fig. 1). In both cases, the residues are concordant allowing for a Th correction uncertainty of -1 Ma in the  $^{207}\text{Pb}/^{206}\text{Pb}$  age. Sequential leach steps are inferred to have preferentially removed outer high-U zones susceptible to Pb-loss as well as internal inherited or xenocrystic components. The resilient residues are interpreted to have been comprised of pristine magmatic zircon relatively free of these effects and thereby providing the best estimate of crystallization age for the samples (A:  $57.8 \pm 0.3$  Ma; B =  $62.6 \pm 0.3$  Ma).

We suggest that the step-wise dissolution technique allows resolution of complex zircon systematics and high precision age determinations that are unobtainable with conventional thermal ionization or ion microprobe techniques. Although absolute age estimates for young samples are plagued by decay constant and Th correction uncertainties, this technique will allow resolution of relative emplacement and deformational chronologies for plutonic and metaplutonic complexes.

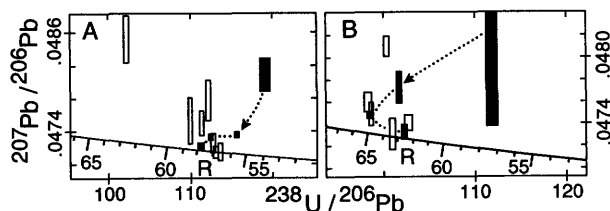


Figure 1. Terra-Wasserburg diagrams showing conventional analyses (open), partial dissolution steps (solid), and trajectory (dotted line) from initial steps to residues (R).

**OXYGEN ISOTOPE MICROANALYSES OF SILICIC ROCKS IN LONG VALLEY CALDERA: UNCOVERING TRENDS IN THE PALEOHYDROTHERMAL SYSTEMS**

McConnell, V.S.<sup>1</sup>, Valley, J.W.<sup>2</sup>, Spicuzza, M.J.<sup>2</sup>, and Eichelberger, J.C.<sup>1</sup>, <sup>1</sup>Geophysical Inst., Univ. of Alaska, Fairbanks, AK, 99775-0800, USA, and <sup>2</sup>Dept. of Geology and Geophysics, Univ. of Wisconsin, Madison, WI, 53706, USA.

Microanalysis of oxygen isotope compositions in samples from the Long Valley Exploratory Well (LVEW) centered on the resurgent dome of 760 ka Long Valley Caldera and LV13-26 Well located 4 km to the SE provide a basis for understanding the complex hydrothermal history in the central caldera. Previous work on LVEW whole rock samples indicated depleted  $\delta^{18}\text{O}$  values as low as  $-0.3\text{‰}$  for intracaldera volcanic rocks, but whole rock data do not sufficiently constrain water/rock interactions or degree of isotopic equilibrium. In this study,  $\text{CO}_2$  laser probe microanalyses of 0.5-2.0 mg samples from the wells reveal considerable isotopic heterogeneity between pumice, sanidine, matrix, and quartz phases in the intracaldera Bishop Tuff and  $\delta^{18}\text{O}$  values as low as  $-6.5\text{‰}$ . Overall trends become evident when values are plotted relative to depth and location in the caldera.

Oxygen isotopes in pumice and sanidine phenocrysts from the Bishop Tuff most readily exchange with hydrothermal fluids and display subparallel trends as  $\delta^{18}\text{O}$  decreases with depth in LVEW: 5.3 to  $-2.0\text{‰}$  and 6.9 to  $-6.5\text{‰}$ , respectively. Pumice ( $-0.1\text{‰}$ ) approaches equilibrium with hydrothermal quartz ( $-0.7\text{‰}$ ) where co-measurement was possible. Matrix samples of the Bishop Tuff in LVEW are also depleted in  $\delta^{18}\text{O}$  ( $3.5$  to  $-3.7\text{‰}$ ) but the trend with depth is obscure. Quartz phenocrysts remain relatively unaffected reflecting magmatic values ( $6.7$  to  $8.2\text{‰}$ ).  $\delta^{18}\text{O}$  is also depleted in the Bishop Tuff samples from LV13-26 Well but the trend with depth is reversed, pumice ( $-1.1$  to  $8.2\text{‰}$ ) and sanidine approach magmatic values by the bottom of the well. Basement metavolcanic and metasedimentary rocks display  $\delta^{18}\text{O}$  depletion ( $-6.3$  to  $14.8\text{‰}$ ) relative to Mt. Morrison Roof Pendant metamorphic rocks ( $8.8$  to  $19.5\text{‰}$ ). Sill-like Early Rhyolite hypabyssal intrusions identified in the Bishop Tuff in LVEW are depleted in  $\delta^{18}\text{O}$  ( $-1.3$  to  $3.1\text{‰}$ ) but the values do not vary with depth. These intrusions are thought to be partially responsible for resurgence. Hydrothermal vein quartz ( $2.7\text{‰}$ ) measured in an intrusion ( $-1.2\text{‰}$ ) at 784 m depth in LVEW was apparently deposited in a cooler hydrothermal domain assuming all hydrothermal fluids had similar  $\delta^{18}\text{O}$  values to the present day system ( $-14.0\text{‰}$ ).

The trends in isotope data can be explained by a centrally located magma body beneath the resurgent dome heating hydrothermal fluids to  $>250^\circ\text{C}$  at the base of the Bishop Tuff at 1800 m depth. Intrusions into the Bishop Tuff with lower local hydrothermal temperatures and isolated isotopic exchange may be related to this magma body or later post-caldera-collapse volcanic activity. Localized channel fluid flow and/or structural control on flow off the resurgent dome is a likely explanation for the pattern seen in LV13-26 Well.

## TIMING AND SOURCE OF LODE GOLD IN THE FAIRBANKS DISTRICT, INTERIOR ALASKA

McCOY, D., LAYER, P.W., NEWBERRY, R.J., Dept. of Geol. and Geophys., Univ of Ak., Fbks., 99775  
BAKKE, A., Fairbanks Gold Mining, Inc., Fbks., Ak. 99709  
MASTERMAN, S., Ryan Lode Mines, Fbks., Ak. 99709  
GOLDFARB, R., USGS, Denver, Co. 80225

The Fairbanks Mining District has produced over 7 million ounces of placer gold. Recently two large bulk-mineable vein/stockwork lode deposits have been discovered. The Ryan lode mine contains approximately 1 million ounces of gold grading .08 ounces per ton. It is hosted in greenschist facies schist and in a small granitic porphyritic intrusion. The ore is localized in brittle shear zones. Arsenopyrite is the main accessory mineral. The Fort Knox deposit contains approximately 4 million ounces of gold grading .028 ounces per ton. The deposit consists of stockwork veins and brittle shear zones hosted wholly in a multi-phase granitic porphyritic intrusive. Bismuthinite and tellurobismuthite are the main accessory minerals.

The Ryan lode and Fort Knox yield similar ages. Magmatic ages (U/Pb for zircon,  $Ar^{40}/Ar^{39}$  for hornblende and biotite) are  $91 \pm 1$  Ma whereas hydrothermal micas give  $Ar^{40}/Ar^{39}$  dates of  $89 \pm 1$  Ma with minor resetting from an early Tertiary heating event.

Fluid inclusions (all secondary) indicate trapping temperatures and pressures of  $310 \pm 15^\circ\text{C}$  and  $.5-.75$  kbar for the Ryan lode and  $310 \pm 15^\circ\text{C}$  and 1-1.5 kbar for Fort Knox. Aplite geobarometry gives pressure estimates of 1-1.5 kbar for intrusive rocks.  $CO_2$  contents are variable and average approximately 13 mole % for the Ryan lode and 22 mole % for Fort Knox; methane is a minor contaminant. Salinities are 1-3 wt. % for the Ryan and 3-6 wt. % for Fort Knox. The variable  $CO_2$  content is indicative of minor  $H_2O-CO_2$  immiscibility.

The dating, together with fluid inclusion and aplite geobarometry, indicate that the heat source for the deposits were intrusives emplaced at moderate to shallow depths. The similarity of fluid compositions and dates from both deposits indicate a common fluid genesis.

Fluid compositions and temperatures are similar to 1) secondary inclusions found in some porphyry molybdenum and porphyry tungsten deposits (implied magmatic origin) and 2) primary and secondary inclusions associated with gold districts identified as having a metamorphic fluid source. The high geothermal gradient, porphyry style veining, low methane content, low chlorine content of magmatic biotites, and reduced nature of the plutons presently point to a porphyry-type model with a probable magmatic source for both fluids and gold. This indicates that the fluids commonly found in schist-hosted mesothermal vein districts (low salinity, high  $CO_2$ , moderate temperatures) may have either magmatic or metamorphic sources.

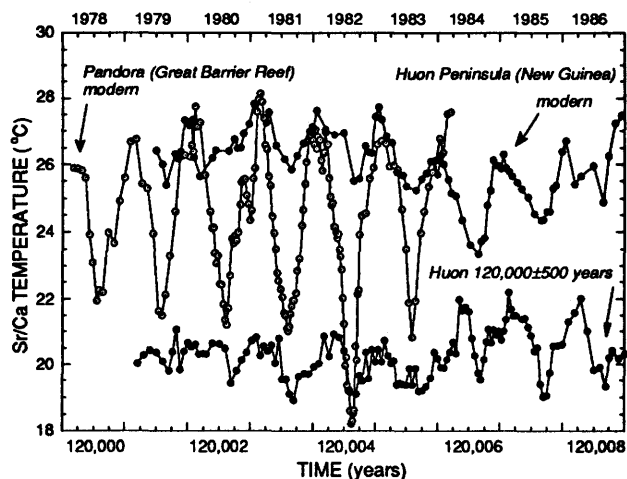
## HIGH FIDELITY Sr/Ca RECORD OF SEA SURFACE TEMPERATURES: 1982-83 EL NIÑO AND MIS-5e

McCULLOCH M.T., and MORTIMER G.  
Research School of Earth Sciences, The Australian National University, Canberra, ACT, 0200.

Both long and short-term changes in our climate are intimately associated with changes in ocean temperature. For example, the movement of warm water from the central western Pacific to the eastern Pacific, known as the El-Niño and the related Southern Oscillation (ENSO) occurs on average every 4 to 6 years. The El-Niño is now known to be directly responsible for the droughts that occur periodically throughout Australia and for the catastrophic floods in western South America.

Using high precision measurements of Sr/Ca ratios combined with high resolution sampling of *Porites* corals we have undertaken a detailed study of corals from the Great Barrier Reef (GBR) and the Huon Peninsula of New Guinea for the period 1979 to 1986. This period is of particular interest as it encompasses the 1982-83 El Niño, the strongest event that has occurred in this century. The results are shown in the figure below. It can be seen that a very marked decrease in the sea surface temperature occurs in the GBR in the winter of 1982, reflecting the influx of unusually cold water into this region. In New Guinea, a different behaviour is observed with the temperature decreasing steadily from mid-1983 to 1984, nearly two years after the 1982-83 El Niño. It is not until the beginning of 1987 that temperatures again reach similar levels to the 1982-83 period. This probably reflects the progressive buildup of the warm pool in the western Pacific.

In order to extend this approach further back in time an exceptionally well preserved *Porites* from Reef 6 in the Huon Peninsula with a U-Th age of  $120,000 \pm 500$  years has been analysed for Sr/Ca. This coral, which occurs ~70m below the main interglacial Reef 7, has a surprisingly low mean temperature of  $\sim 20$  to  $22^\circ\text{C}$  during this period (marine isotope stage 5e). This may provide confirmation of the findings of the Greenland ice core project for climate instability during the last interglacial, and implies that this is a global phenomenon.



## HOLOCENE CLIMATE CHANGE ON THE EASTERN N. ATLANTIC SEABOARD; A SPELEOTHEM RECORD

McDERMOTT, F., Dept. of Geology, University College Dublin, Dublin 4, Ireland; SWABEY, S.E.J., and HAWKESWORTH, C.J., Dept. of Earth Sciences, The Open University, Walton Hall, Milton Keynes, MK7 6AA, U.K.; MATTEY, D.P., Department of Geology, Royal Holloway, University of London, Egham, TW20 OEX, U.K.

Recently published stable isotope profiles for the Greenland ice-cores have highlighted unexpectedly large and rapid climatic fluctuations during the last glacial, but they indicate relatively stable conditions during the Holocene. The extent to which these high-latitude ice core profiles record global, or even regional, climatic patterns is still debated, although the correlation (Bond et al., 1993) with the mid-latitude North Atlantic (~44-55°N) sea surface temperatures (SSTs), is strong evidence for ocean-atmosphere coupling on a sub-millennium timescale.

In order to investigate palaeoclimatic conditions on continents adjacent to the N. Atlantic ocean we have undertaken a stable isotope study of U-Th dated speleothems (cave carbonates) from the mid-latitude eastern N. Atlantic seaboard (west coast of Ireland, 52-55°N). Speleothems have considerable potential as quantitative palaeoclimatic indicators; first because their O isotope ratios can reflect the temperature of calcite deposition (and the  $\delta^{18}\text{O}$  of meteoric water) and second because they can be dated precisely using the U-Th technique.

Mass-spectrometric U-Th ages for the 12 speleothems studied range from  $76.51 \pm 0.98$  kyr to <400 years, and continuous dated profiles have been obtained for the Holocene period. Here the calcite  $\delta^{18}\text{O}$  varies from 26.10 to 28.61‰ (SMOW) and  $\delta^{13}\text{C}$  varies from 5.43 to -10.95‰ (PDB). Typically,  $\delta^{18}\text{O}$  ratios exhibit a pattern of slow smooth increases (cooling) with time (over time scales of ~3000 years), followed by rapid (decadal) returns to lower values (warming). Three such asymmetric cooling cycles, representing relatively small temperature fluctuations of ~1-3°C have been detected during the Holocene, the oldest and most severe of which coincides with the Younger Dryas (Y.D.) event.

Apart from the Y.D. event, when *N. pachyderma* (s.) abundances increased markedly in sediments from the N. Atlantic core V23-81, SSTs appear to have remained relatively stable during the Holocene. Thus, the relatively small (1-2°C) mid-Holocene temperature changes inferred from the speleothems do not appear to be accompanied by SST variations. However, the pattern and magnitude of the temperature fluctuations resemble closely those inferred from European continental pollen records.

Bond, G. et al., 1993. Correlations between climate records from North Atlantic sediments and Greenland ice: Nature, v. 365, 143-147.

## SOLAR NOBLE GASES IN THE EARTH - EVIDENCE FROM NEON AND HELIUM

McDOUGALL, J., HONDA, M., and PATTERSON, D.P., Research School of Earth Sciences, The Australian National University, Canberra, ACT 0200, Australia.

The abundances and isotopic compositions of noble gases trapped in mantle-derived samples provide useful constraints on the origin and evolution of the Earth's atmosphere, crust, mantle and core. Identification of the noble gas composition of the primordial Earth is of particular importance in relation as to how and when the Earth acquired its volatiles and how its atmosphere evolved.

Noble gas studies on mantle-derived samples from a wide range of environments indicate that neon isotopic ratios commonly differ significantly from atmospheric in a systematic way, and that a correlation is evident in many cases between neon and helium isotopic compositions. These results are most readily interpreted as indicating that there is a noble gas primordial component in the Earth that is solar in composition, providing a much firmer basis than previously for the idea since Craig and Lupton (1976) suggested it on the basis of measurement of neon isotopic ratios in some submarine basaltic glasses and volcanic gases.

Neon isotopic ratios observed in some mantle-derived samples are enriched in  $^{20}\text{Ne}$  and  $^{21}\text{Ne}$  relative to  $^{22}\text{Ne}$  compared with atmospheric neon. In particular, Sarda et al. (1988) demonstrated correlated enrichments of  $^{20}\text{Ne}$  and  $^{21}\text{Ne}$  in a suite of mid-ocean ridge basalt (MORB) glasses; similar relationships were found subsequently by other workers in samples from a range of environments. We interpret these results in terms of mixing between three neon isotopic components: solar, nucleogenic and atmospheric. In general, we find that the solar and nucleogenic neon components in mantle-derived samples are strongly correlated with measured  $^3\text{He}$  (primordial) and  $^4\text{He}$  (dominantly radiogenic) in the same suite of samples. Such correlations are evident in MORBs, in MORB-like basalts from back-arc basins, from intraplate plume-related oceanic island basalts, mantle xenoliths, from ancient diamonds, from  $\text{CO}_2$  well gases and from a fluid sample from Yellowstone. Indeed, the correlations are so strong as to provide much confidence in the hypothesis that the mantle contains a significant primordial component of solar composition.

In contrast to neon and helium, isotopic compositions of the heavier noble gases, argon, krypton and xenon, in mantle-derived samples are less readily interpreted in terms of the presence of a primordial solar component, in part owing to the common dominance of atmospheric-like noble gas components in the samples. In addition, the hypothesis of a primordial solar component in the Earth is not yet fully reconcilable with the observed noble gas composition of the Earth's atmosphere derived from degassing of the Earth.

Craig, H., and Lupton, J.E., 1976, Earth Planet. Sci. Lett., v. 31, p. 369-385.  
Sarda, P., Staudacher, T., and Allègre, C.J., 1988, Earth Planet. Sci. Lett., v. 91, p. 73-88.

## GEOCHRONOLOGY OF MIDDLE TO LATE TERTIARY VOLCANISM ACROSS SOUTH-CENTRAL SONORA

MCDOWELL, Fred W., Dept. Geol. Sci., Univ. Texas at Austin, Austin, Texas 78712 USA, and ROLDAN-QUINTANA, Jaime, Estación Regional del Noroeste, Inst. Geol. UNAM, Hermosillo, Sonora, 83000, Mexico

During middle and Late Tertiary, plate interactions along western North America underwent a gradual and complex transition from Farallon plate subduction to Pacific plate transcurent motion. Contemporaneous volcanism in northwestern Mexico should retain a record of this transition. A mapping and K-Ar dating survey across south-central Sonora between 28 and 29° north latitude identifies three regional components to that volcanic record.

In eastern Sonora thick (>500 m), dominantly felsic and pyroclastic deposits comprise the western portion of the Sierra Madre Occidental (SMO) volcanic province, an arc related to Farallon plate subduction. Ages are from 32 to 27 Ma, and locally as young as 24 Ma. Flows of basaltic andesite occur just above or intercalated with the youngest felsic units. Abrupt thinning of these sequences marks a distinct western boundary to the SMO province.

Much thinner (<100 m) volcanic exposures in central Sonora are associated with coarse clastic sediments deposited in linear fault-bounded basins. Basin formation and sedimentation were associated with Basin-and-Range extensional faulting. Mafic flows (27 to 20 Ma) occur at or near the base of the sedimentary sequences, viscous porphyritic domes and flows are found along some basin margins, and thin felsic lavas and distal ash flows (14-10 Ma) cap the thickest and coarsest portions of the sedimentary sections. Tilting of the youngest volcanic units indicate that faulting continued to <10 Ma.

In western Sonora, adjacent to the Gulf of California, Neogene (23-10 Ma) volcanic accumulations are thicker (up to 1000 m) and lack intercalated clastic sediments. Although they are similar in composition to sections within the SMO province, they are younger and pyroclastic units are less prominent. Alkaline mafic lavas (10-8.5 Ma) are commonly the youngest volcanic units present. This volcanism could have been related either to the last stages of plate convergence and/or to proto-Gulf of California extension.

Variations in the timing and intensity of volcanism indicate the operation of distinct tectonic controls in each region. These volcanic rocks are not components of a single homogeneous arc or an arc that underwent a continual westward migration of focus.

## APPLICATIONS OF CO<sub>2</sub> LASER HEATING IN <sup>40</sup>Ar/<sup>39</sup>Ar GEOCHRONOLOGY

McINTOSH, William C. and HEIZLER, Matthew T., New Mexico Geochronology Research Laboratory, New Mexico Bureau of Mines and Mineral Resources, New Mexico Institute of Mining and Technology, Socorro, NM 87801, USA.

A 10 Watt CO<sub>2</sub> laser in the New Mexico Geochronology Research Laboratory has proven useful for controlled <sup>40</sup>Ar/<sup>39</sup>Ar incremental heating analyses of optically transparent silicates such as sanidine and anorthoclase, and for heating of Ar-bearing inclusions in quartz and diamond.

Near visible wavelength lasers have been successfully used for more than fifteen years in ultrahigh vacuum (UHV) <sup>40</sup>Ar/<sup>39</sup>Ar extraction systems: yielding extremely low argon blanks, rapid heating and the capability of *in situ* analysis. Drawbacks of these lasers systems have included high cost and inability to achieve and maintain consistent temperatures in transparent mineral phases due to poor coupling with their crystal lattices.

The 10.6μ wavelength CO<sub>2</sub> laser light has been known to couple extremely well with clear silicates, but its use in <sup>40</sup>Ar/<sup>39</sup>Ar analysis has been hindered by the lack of an appropriate bakable window material and window-to-metal seals for introduction of the laser beam into the UHV extraction system. This difficulty has been overcome by the use of a commercially available (ISI Corp.) 3.5 cm diameter anti-reflective coated ZnSe window sealed by double metal gaskets separated by a void space which is continuously pumped with a mechanical roughing pump. A KBr cover slip is used to protect the ZnSe window from precipitation of vaporized sample material. This window and cover slip combination is repeatably bakable to temperatures in excess of 150 °C, and yields <sup>40</sup>Ar blanks less than 5 X 10<sup>-18</sup> moles/min.

The chief advantage of the CO<sub>2</sub> laser over shorter wavelength lasers is enhanced coupling with silicate materials. Power levels of 1-2 watts are generally sufficient to fuse and repeatedly refuse sand-sized individual crystals of K-feldspar. Additional advantages of the CO<sub>2</sub> laser include reduced cost (<\$4k), small size (50 cm long), and modest input power requirements (<8 amps @ 112 volts).

The enhanced coupling of the CO<sub>2</sub> laser with clear silicates provides several capabilities useful for <sup>40</sup>Ar/<sup>39</sup>Ar analysis; including, achievement of complete degassing of transparent K-feldspar samples, the ability to fully degas fluid inclusions at very low power levels, removal of low radiogenic gas fractions prior to fusion and identification of excess argon associated with low temperature heating steps. As an example, sanidines from a pyroclastic fall tuff which is constrained to be between 1.1 and 1.6 Ma, yields total fusion ages which range from 1.3 to 2.1 Ma. Two step heating (0.75 and 2.5 W) of single crystals reveal low-temperature gas fractions with radiogenic yields varying from 47-88% and model ages of 1.4 to 2.1 Ma. These steps yield an isochron age of 1.23 ± 0.01 Ma and a trapped <sup>40</sup>Ar/<sup>36</sup>Ar = 623 ± 32. The second steps are extremely consistent with radiogenic yields of ~99% and, give a mean age of 1.23 ± 0.01 Ma. Clearly, the step-heating capability provides a much more precise age determination and lends additional insight to the argon systematics of this sample.

## ACTIVE SEDIMENT DEGASSING AND CO<sub>2</sub> FLUX FROM THE SALTON TROUGH RIFT

McKIBBEN, M. A., and WILLIAMS, A. E.,  
Dept. Earth Sciences, Univ. of California,  
Riverside, CA 92521-0423.

The Salton Trough rift is one of the most extensively explored areas of active crustal decarbonation. 6 km of deltaic-lacustrine sediments, deposited onto active spreading centers, are locally undergoing metamorphism and decarbonation. Initially containing  $\approx 12$  wt % diagenetic and detrital carbonate ( $\approx 5$  wt % CO<sub>2</sub>) with  $\delta^{13}\text{C} \approx -3$  ‰ and  $\delta^{18}\text{O} \approx 22$  ‰, they are progressively transformed to carbonate-poor, epidote-rich hornfels at  $\approx 300^\circ\text{C}$ . With increasing depth and temperature the diminishing carbonate undergoes progressive isotopic depletion, reaching values of  $\delta^{13}\text{C} \approx -8$  ‰ and  $\delta^{18}\text{O} \approx 2$  ‰ at 2–3 km depth. Coexisting oxidized brines (260–310°C) contain CO<sub>2</sub> with  $\delta^{13}\text{C} \approx -6$  ‰. Surface mudpots ( $\leq 75^\circ\text{C}$ ) are aligned along faults above and peripheral to the system and presently degas CO<sub>2</sub> with  $\delta^{13}\text{C}$  identical to CO<sub>2</sub> in the deep brines. Only hydrothermal dissolution of calcite to aqueous CO<sub>2</sub> can explain the isotopic depletions.

A drilled volume of  $\approx 55$  km<sup>3</sup> of metamorphosed sedimentary rocks contains  $\approx 11$  km<sup>3</sup> (10<sup>13</sup> kg) of hot (230–330°C) brine with 1000–5000 ppm dissolved CO<sub>2</sub>: 10–50 Mt of CO<sub>2</sub> are stored in the hot brines. At least 50% of the original sedimentary carbonate has been lost upon metamorphism, corresponding to at least 3 Gt of CO<sub>2</sub>. This is 100 times the mass of CO<sub>2</sub> presently stored in the hot brines. The metamorphic <sup>13</sup>C depletions of the deep carbonates and brines also require that a large mass of isotopically heavy C ( $\delta^{13}\text{C} \geq -3$  ‰) has been lost from the rock volume.

High sediment permeability, active rift tectonics and mudpot activity leave no doubt that most of this CO<sub>2</sub> was lost to the atmosphere over the lifetime of the rock volume's metamorphism. The heating duration of the rock volume is  $\leq 10^5$  years, so the minimum time-averaged decarbonation rate is 30,000 t CO<sub>2</sub>/yr ( $\approx 10^9$  moles/yr). The average flux may be much higher if shorter heating duration and decarbonation of deeper unexplored sediments is included.

Comparison of this mass balance based time-averaged CO<sub>2</sub> flux with the independent present-day heat flow based flux is excellent: both yield  $\approx 10^9$  moles CO<sub>2</sub>/yr. When the other less explored areas of high heat flow and likely sediment metamorphism in the Salton Trough are considered, the total CO<sub>2</sub> flux from this rift probably exceeds 10<sup>10</sup> moles/yr.

On a global scale, rift sediment decarbonation may make a major contribution to the total non-anthropogenic CO<sub>2</sub> flux.

## ISOTOPIC CONSTRAINTS ON EVAPORATION AS A CONTROL OF GROUNDWATER COMPOSITION IN A SEMIARID ENVIRONMENT, SOUTH-CENTRAL WASHINGTON

MCKINLEY, J.P., Pacific Northwest Laboratory,  
Richland, Washington, 99352, U.S.A., and HOOVER, J.D., Westinghouse Hanford Co., Richland, Washington, 99352, U.S.A.

Understanding the natural compositional variability of groundwater is an important part of the characterization efforts associated with environmental restoration and remediation at the U.S. Department of Energy (DOE) Hanford Site, Washington. The range of analyte levels in groundwater can serve as the site-specific baseline for defining groundwater contamination and assessing risk-based cleanup levels.

At Hanford, the unconfined aquifer is composed of Pliocene fluvial-lacustrine sediments but extends locally into overlying Pleistocene sands and gravels. The climate is semiarid, with little direct aquifer recharge. Surface recharge originates primarily from meteoric and spring-fed runoff in upgradient highlands that expose the underlying Columbia River basalts. Other sources include leakage from the underlying confined aquifer and side-bank recharge from the Columbia and Yakima rivers downgradient.

Evaluations based on groundwater compositions and mass balance indicated that the compositional variability could be explained by either evaporation or water-rock interaction. An understanding of the extent to which each of these processes affects groundwater composition is necessary because the relative concentrations and spatial variability of dissolved ions resulting from water-rock interaction and evaporation are different.

Experimental studies demonstrated that water-rock interaction could account for most of the observed compositional variation. Evaporation also could control compositions, and elevated concentrations of alkalis, halogens, nitrate, and sulfate in some parts of the aquifer have been interpreted by others as evidence of evaporative effects on groundwater composition. Therefore, the extent of evaporation was evaluated using oxygen and hydrogen isotopic data coupled with solute mass balance modeling.

Groundwater Cl concentrations are generally less than 10 mg/L but range as high as 25 mg/L. Spring waters contain 1–15 mg/L Cl. Spring and groundwaters define overlapping groups below the meteoric water line, with spring waters ( $\delta^{18}\text{O} = -17$  to  $-14$ ) more positive than groundwaters ( $\delta^{18}\text{O} = -18$  to  $-14$ ; most are  $\delta^{18}\text{O} = -18$  to  $-16$ ). These groups together overlie the range in compositions for regional surface and meteoric waters. Groundwater Cl concentrations of 25 mg/L imply 40% evaporation of spring waters with 15 mg/L Cl. Evaporation of more than 15% of spring waters would in all cases, however, result in an isotopic composition outside the boundaries of groups defined by spring and groundwaters. Isotopic constraints indicated that groundwaters having the highest Cl concentrations could not have derived solely from evaporation of spring or other runoff waters, and that water-rock interaction is the dominant process in controlling the natural composition of groundwater at the Hanford Site.

PROTEROZOIC CRUSTAL EVOLUTION OF THE  
ADIRONDACK SECTOR OF THE GRENVILLE  
PROVINCE.

McLELLAND, J., Department of Geology, Colgate  
University, 13 Oak Drive, Hamilton, NY 13346-1398,  
USA and DALY, J.S., Department of Geology,  
University College Dublin, Belfield, Dublin 4, Ireland.

Much of the Canadian sector of the Grenville belt comprises reworked older material ranging from Archaean to Palaeoproterozoic in terms of crustal residence age. By contrast, Sm-Nd data reveal major juvenile crustal additions in the Adirondacks and Grenville inliers of the northern Appalachians in the Mesoproterozoic. For example, 1.31 - 1.36 Ga old orthogneisses from the Green Mountains have initial  $\epsilon_{Nd}$  values of +3 and  $t_{DM}$  ages in the range 1.45 - 1.48 Ga, while granitoids of less certain age from the Hudson Highlands have  $t_{DM}$  ages of 1.38 - 1.56 Ga. These data, combined with geochronology and petrology indicate a predominantly juvenile Mesoproterozoic origin for the entire region. Crust formation began about c. 1.36 Ga ago and U-Pb data suggest a possible progression in the age of onset of arc-magmatism from east (Green Mtns) to west (Adirondack Lowlands). This suggests crustal accretion in a (present) westward direction either onto the western side of an unknown ancient continent or an intraoceanic juvenile terrane. Eastward accretion onto the eastern margin of Laurentia is not easily envisaged. Metasediments from the Adirondack Highlands/Lowlands and the Hudson Highlands have  $t_{DM}$  ages of 1.44 - 2.08 Ga indicating that both juvenile (arc-derived?) and Palaeoproterozoic (continental) material was present in the source lands. Following sedimentation and arc magmatism, further (and final) crustal addition took place in the form of massif anorthosite magmatism at c. 1.15 Ga. Associated voluminous granitoids of the AMCG suite comprise reworked crust and are not newly added material. Crustal assembly and accretion to Laurentia was accomplished during the Grenville orogeny. Lack of further tectonic activity (witness the disposition of the overlying Phanerozoic sediments) suggests that the bulk of the present day lower crust has been present for the entire Phanerozoic.

RELATIVE CHRONOLOGY OF EVENTS AT AND NEAR  
THE CRETACEOUS-TERTIARY BOUNDARY

MCWILLIAMS, M., Geophysics Department, Stanford  
University, Stanford, CA 94305-2215

$^{40}\text{Ar}/^{39}\text{Ar}$  age determinations are inherently relative because they depend upon the absolute age assumed for the neutron fluence monitor. To reduce the experimental uncertainty introduced by the use of different monitor minerals, differing irradiation parameters and other inter-laboratory differences, samples from five K/T boundary sequences in North America were co-irradiated with whole rock and plagioclase samples from Deccan Trap flood basalts. By monitoring neutron fluence in detail and by interfingering unknowns from different localities in the same irradiation capsule, relative ages of some important K/T boundary sections have been measured with considerable precision.

Bentonite beds at 3 localities in western North America lie 5-80 cm above the K/T Ir anomaly and yield a mean age of  $64.71 \pm 0.09$  Ma from a combination of laser fusion, laser step heating and resistance furnace experiments (uncertainties 2 standard errors; ages relative to sanidine from Taylor Creek Rhyolite at 27.92 Ma). Laser total fusion ages from the Beloc tektites in Haiti yield a slightly older mean age of  $64.91 \pm 0.12$  Ma. The magnitude of the difference is just statistically significant and its sense is in the correct stratigraphic order, assuming that the tektites date the event which produced the Ir anomaly.

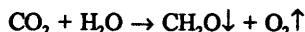
RF step heating of whole rock and plagioclase samples from the Igatpuri and Mahabaleshwar Formations of the Deccan sequence yield less well constrained ages, as might be predicted. The best results are constrained on the 67 to 63 Ma interval. Although the individual results are not as precise, it seems clear that Deccan volcanism began well before the K/T boundary as recorded by the Beloc tektites and associated Ir anomalies below the bentonites. This suggestion is consistent with the recent placement of the K/T boundary in Anjar intertrappean beds by Bhandari *et al.* (*LPI* 825:10).

Laser and RF step heating of whole rock and plagioclase samples from the Chicxulub C1 well at the K/T impact site on the Yucatan peninsula produced a range of apparent ages between 62 and 66 Ma. To date, none of the more than 20 follow-up experiments have reproduced either the age or quality of the 3 experiments published in 1992 by Swisher *et al.* (*Science* 257:954). The discrepancy cannot result from sample differences because some experiments used exactly identical sample splits.

**PRECAMBRIAN STABLE ISOTOPES EXCURSION:  
APPLICATION OF GLOBAL CYCLIC  
DEVELOPMENT MODEL**

**MELEZHNIK, V. A.**, Geological Survey of Norway, Post Box 3006-Lade, 7002 Trondheim, Norway, and **FALLICK, A. E.**, Scottish Universities Research & Reactor Centre, East Kilbride, Glasgow G75 0QU, Scotland, U.K.

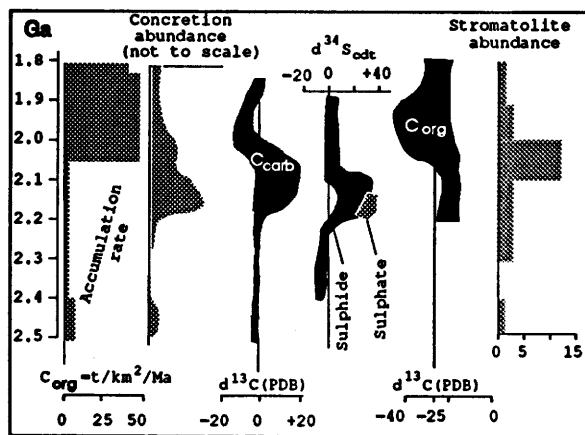
A secular trend of the production and accumulation of the freely available O<sub>2</sub> in the Precambrian still remains a matter of great discussion (eg. Des Marais et al., 1992 versus Schidlowski & Aharon, 1992; ). The main way for free-oxygen production is biological photosynthesis, in cases when the generated organic mass is subsequently buried



As a result there is an increase in the oxidizing power of the Earth's atmosphere-hydrosphere that causes a number of extensive alterations in the exogenic systems such as weathering, sedimentation, diagenesis. Therefore an investigation of mass balances within the carbon cycle, including isotope analyses of both C<sub>carb</sub> and C<sub>org</sub>; the growth of the crustal reservoir of reduced carbon; the diversity and abundance of biological oxygen producers; the grade of bacterial sulphate reduction; style of diagenetic transformations, all are parameters that should be studied to monitor the secular oxygen trend.

All these parameters listed above have been used in our investigation applied to the 2.5 to 1.8 Ga-old Precambrian sections of the Baltic Shield with high stratigraphic resolution dated at 2.5, 2.45, 2.4, 2.2, 2.11, 2.06, 2.0, 1.97, 1.8 Ga by a U-Pb (zircon) technique. Three main results in respect to the development of the secular oxygen trend can be made: (1) an irregular change all investigated parameters is observed; (2) almost all parameters are changed synchronously through time; 3-in the time interval from 2.5 to 1.8 Ga, at least one major cycle (Fig.), which reflects an episodic release of oxidising power, can be distinguished at 2.1±0.1 Ga ago.

The isotopic excursions, peculiarities of sedimentation and diagenesis can be understood within a framework of the irregular cyclic oxidation of the Precambrian hydrosphere-atmosphere-lithosphere terrestrial system.



**SPATIAL AND TEMPORAL PATTERNS IN THE STABLE ISOTOPE (O,H) COMPOSITIONS OF WATERS AT THE LAWRENCE BERKELEY LABORATORY, CA**

**MENCHACA, L. B.**, **SMITH, B. M.**, and **CONRAD, M.**, Lawrence Berkeley Laboratory, 1 Cyclotron Rd., Berkeley, California, 94720, USA.

With the advent of recent laws governing waste management and cleanup of contaminated sites in the United States, it has become increasingly important to understand the intricacies of surface and subsurface water movement. The new hydrogeologic challenges are especially imposing for DOE's National Laboratories and require the development of new, environmentally innocuous hydrogeologic tools, including tracers for water movement. At the Lawrence Berkeley Laboratory (LBL), we are developing and applying water tracer methods using the diverse stable isotopic signatures of local waters of different origins.

We have measured the O- and H-isotope compositions of groundwaters, surface waters and rain at LBL, a 130-acre site located on the western flank of the Berkeley Hills, ~8 km east of San Francisco Bay, California. Most groundwater samples show a restricted range of δ<sup>18</sup>O values (-6.0 to -7.0 ‰ vs V-SMOW) over periods of several months to one year. Exceptions are three local areas (-8.0 to -9.5 ‰) where facility water (-13.0 ‰) piped in from higher elevations is thought to have leaked from broken delivery pipes and a sanitary sewer. In addition, one well showed a higher δ<sup>18</sup>O of -4.9 ‰, perhaps due to local infiltration of cooling tower water. Local rain storms showed a much larger range in δ<sup>18</sup>O (-1.4 to -14.0 ‰), with a weighted mean value of -5.8 ± 1.0 ‰ for the rainy winter season of 1992-3. In general, tropical storms bring relatively <sup>18</sup>O-rich rains to the site, while storms that originate in the Gulf of Alaska bring rain with more negative δ<sup>18</sup>O values. It is possible to predict the stable isotopic signal of input rainfall in the region, based on satellite imagery of storm origin and storm track.

Repeated analysis of ground waters from ~45 monitoring wells before and throughout the rainy season provided a method to delineate permeable zones beneath the site. The O-isotope compositions of ground waters from 30 of the wells were constant to within 0.5 ‰ over the time of sampling, implying that the wells are properly constructed and that the rocks in these areas are relatively impermeable. Most of the wells with constant δ<sup>18</sup>O are uncontaminated. Fifteen of the wells showed changes in δ<sup>18</sup>O of 0.5 to 2.5 ‰, indicating influx of isotopically distinct water and suggesting relatively high local permeability. Most of these wells are located along inferred faults, and many have shown very low levels of contamination with chlorinated hydrocarbons and petroleum products.

The ability to characterize waters of differing origins and to identify permeable zones through repeated sampling and stable isotopic analysis will be particularly important in the characterization of contaminated sites with complex permeability structures and limited outcrop for direct study.

## EVOLUTION OF THE RED SEA VOLCANIC MARGIN - A MULTI-ISOTOPIC APPROACH

MENZIES, Martin A., YELLAND, A., BAKER, J., BLAKEY, S., CHAZOT, G., AL-KADASI, M., Department of Geology, Royal Holloway University of London, Egham, Surrey, England TW20 0EX & RUNDLE, C., NIG, Keyworth, U.K.

Traditionally rifting in the southern Red Sea-Gulf of Aden has been associated with early uplift of the Afro-Arabian dome *prior to* extension and magmatism related to the Afar plume. However selected geotraverses, perpendicular to the Red Sea margin, provide evidence for early magmatism followed by extension, uplift and exhumation. Although very little evidence exists for pre-volcanic uplift or extension geochemistry-chronostratigraphy indicates involvement of the Afar plume in magmatism for the last 30 m.y. **TIMING : Magmatism** - K-Ar & Ar-Ar data reveal that volcanism peaked in the Oligocene-Miocene with minor amounts of post-erosional volcanism. Magmatism may have begun in the Eocene with a possible northward migration during the Oligo-Miocene. **Extension** - Dating of the uppermost flows on domino fault blocks indicates a major episode of extension in the late Oligocene-early Miocene that post-dated much of the basalt-rhyolite volcanism. Little or no evidence exists in the pre-volcanic Jurassic-Tertiary stratigraphy for widespread pre-volcanic extension. **Exhumation** - Apatite fission track analysis of once deeply buried basement rocks indicates several distinct thermal domains on the rifted margin. While the rift shoulders have a complicated thermal history the area occupied by the Tertiary basalt-rhyolite province has experienced rapid exhumation in the Tertiary. Studies elsewhere indicate that reactivation of old & young basement lineaments may have played a fundamentally important role in the evolution of the rift margin. In Yemen rift development was dominated by Oligo-Miocene magmatism, late Oligocene extension & surface uplift followed by Miocene exhumation. **CRUST-MANTLE RESERVOIRS : Afar plume** - Sr-Nd-Pb isotopes in uncontaminated volcanic rocks in Yemen & its environs indicate that the Afar plume has a HIMU signature & that the plume has made a variable contribution to volcanism for some 30 m.y. In addition the spatial occurrence of this HIMU signature over several thousand kilometers may point to lateral movement of mantle material from the plume head, thus supporting deep seismic data. The presence of a broad asymmetric plume head in the Oligocene may account for the lack of early domal uplift & radial drainage patterns in western Yemen. **Pan-African lithosphere** : The temporal change from basalts to rhyolites-ignimbrites & the occurrence of granite-gabbro-syenite plutons/sheets indicates an important change in process. To help evaluate the role of shallow magma chambers, elemental & isotopic data have been linked with high precision O isotope data. In Yemen the majority of volcanic rocks have experienced high level contamination with continental crust. Detailed isotopic studies caution against the use of highly magnesian rocks as indicators of sub-crustal processes as even highly magnesian (>10%) volcanic rocks can be contaminated with crust in utilising. The precise contribution (if any) from the depleted lithospheric mantle is difficult to assess because of similarities in chemistry with sub-lithospheric components.

**CFF - XENON IN METEORITES AND ON THE EARTH**  
MESHNIK, Alexander P., SHUKOLYUKOV, Yuri A., Vernadsky Institute of Geochem. & Anal. Chemistry, 117975 Moscow, Russia, JESSBERGER, E. K., MPI für Kernphysik, Postfach 103980 Heidelberg, Germany

Since 1963 (Butler, 1963) xenon enriched in the isotopes  $^{132}\text{Xe}$ ,  $^{131}\text{Xe}$ ,  $^{134}\text{Xe}$ ,  $^{129}\text{Xe}$  has been observed in  $\text{CO}_2$  well gases, MORB glasses (Bennett, 1970), anorthosite (Jeffery, 1971) and in meteorites (Jessberger, 1992). The surprising similarity of xenon in these distinctly different objects was pointed out but no explanation had been suggested (Kirsten, 1981). We have found out that the difference between solar (AVCC)-Xe and terrestrial atmospheric Xe has the isotopic pattern similar to the *alien* Xe.

The *alien* Xe behaviour looks strange. The repeated Xe analysis in Greenland anorthosite (Azuma, 1993) did not confirm the undoubted Xe anomaly previously reported for the sample of the same locality (Jeffery, 1971). Some of  $^{129}\text{Xe}$  anomalies in MORB glasses turned out to be "gone with the wind" (Fisher, 1993).

Hints towards the origin of the strange Xe component came from our Xe measurements in rocks from the Oklo natural nuclear reactor. Follow-up experiments - analysis of Xe evolved in the ampoule during n-irradiation of pitchblends and Xe analyses of sandstone from the epicentre of a nuclear test - proved that the enrichment in middle isotopes of Xe results from the migration of  $\beta$ -radioactive Xe precursor produced during the fission of heavy nuclei.

The migration of Xe precursors have been occurred at a relatively high temperature and/or in external part of the samples, so this *alien*, Chemically Fractionated Fission Xe (CFF-Xe) could be or not be observed depending on the grain size of sample under study.

The existence of this CFF-Xe might be of great geochemical and cosmochemical importance.

- Azuma, S., Ozima, M. and Hiyagon, H., 1993, Anomalous neon and xenon in an Archaean anorthosite from West Greenland: *Earth and Plan. Sci. Lett.*, 114, p. 341-352.
- Bennett, G. A. & Manuel, O. K., 1970, Xenon in natural gases: *Geochim. Cosmochim. Acta*, 34, p. 593-610.
- Butler, W. A., Jeffery, P. M. and Reynolds, J., 1963, Isotopic variation in terrestrial xenon: *Journ. Geophys. Res.* 68, p. 3283-3291.
- Fisher, D. E., 1993, The  $^{129}\text{Xe}$  anomaly in MORB: gone with the wind? : *Meteoritics*, 28, No.3, p. 112.
- Jeffery, P. M., 1971, Isotopic Composition of Xenon from a Greenland Anorthosite: *Nature*, 223, p. 260-261.
- Jessberger, E. K., Jordan, J. L., Shukolyukov, Yu. A., Meshik, A. P., Dang Vu Minh, 1992, Widespread alien Xe and its formation: *LPSC XXIII*, p. 615-616.
- Kirsten, T., Jordan, J. and Jessberger, E. K., 1984, Two unexplained Xe-components in meteorites and on the Earth: are they linked?: *Terra cognita*, v.4, No.1, p.75.

**A COMBINED PB-ND-SR ISOTOPIC AND TRACE ELEMENT STUDY OF MID-OCEAN RIDGE BASALTS FROM EXPLORER RIDGE, NORTH-EAST PACIFIC**

MICHAEL, Peter J. (Dept. of Geosciences, University of Tulsa, Tulsa, OK, 74104; Chase, R. L. and Armstrong\* R. L. (Dept. of Geological Sciences, Univ. British Columbia, Vancouver, BC V6T2B4 (\*deceased)

Incompatible trace element and Pb, Nd and Sr isotopic data have been obtained for 15 basalts and glasses from the mid-ocean ridge north of Juan de Fuca Ridge (JdF). Of these, 9 are from Southern Explorer Ridge (SER); 4 from Northern Explorer Ridge (NER); and 2 from Explorer Deep (ED). One sample from Tuzo Wilson Seamounts (TWS) to the north was analyzed. In addition, 2 samples from Endeavor Seamount and West Ridge, at the northern end of JdF, were analyzed and found to be the most highly depleted samples of the study. The most enriched samples are E-MORB from SER and ED and a hawaiite from TWS.

There are good correlations between all isotopic systems and also between incompatible element enrichment (expressed as La/Sm or Nb/Zr) and isotopic ratios. Isotopic and trace element ratios are modeled as binary mixing of enriched and depleted end members. Hyperbolic arrays on isotope ratio diagrams of Pb vs. Sr, Pb vs. Nd, and Nb/Zr vs. Pb allow some characteristics of the mixing end members to be identified (see boldface type below). The enriched end member itself could be a mixture of DMM and HIMU. The depleted end member is nearly pure DMM. The sense of hyperbolic curvature suggests that the enriched end member has lower Nd/Zr and Sr/Zr ratios and higher Pb/Zr, Pb/Sr and Pb/Nd ratios than the depleted end member.

A two-stage model of mantle enrichment (possibly during plume activity) followed by MORB formation is proposed to explain the isotopic composition and Pb/Zr, Pb/Sr etc. ratios of end members.

The isotope-isotope and Nb/Zr-isotope arrays for the Explorer Ridge are distinctly different than published data for the East Pacific Rise. Our data substantiate the dearth of EM-I and EM-II components for the entire northeast Pacific, including perhaps in terrestrial volcanics.

	<u>Depleted component</u>	<u>Enriched component</u>
$^{87}\text{Sr}/^{86}\text{Sr}$	<b>0.70233</b>	0.70270
$^{143}\text{Nd}/^{144}\text{Nd}$	<b>0.51318</b>	0.51303
$^{206}\text{Pb}/^{204}\text{Pb}$	18.10	<b>19.20</b>
$^{207}\text{Pb}/^{204}\text{Pb}$	15.47	<b>15.56</b>
$^{208}\text{Pb}/^{204}\text{Pb}$	37.55	<b>38.45</b>

**ISOTOPIC SYSTEMATICS OF ROCK-FORMING MINERALS OF LAMPROPHYRES AND LAMPROITES OF CENTRAL EAST ANTARCTICA**

MIKHALSKY, E.V. and BELIATSKY, B.V., VNIIOkean-geologia, Maklina 1, St. Petersburg 190121, Russia

The central sector of Precambrian East Antarctic Shield (between 60 -80 E) has been known for a number of occurrences of alkaline rocks of different type and age. Two compositionally, spatially and temporally distinctive dyke rock types of lamproites (Rubin Massif, southern Prince Charles Mountains, PCM) and lamprophyres (Vestfold Hills, VH) were studied. Both rock types are high-K and high-Mg alkaline rocks strongly enriched in LILE, HFSE and REE.

VH lamprophyres represent a heterogeneous rock group ranging from alkaline to ultramafic varieties derived from somewhat different Grt-bearing source regions by varying degrees of partial melting. Phlogopite, clinopyroxene, feldspars, olivine are main rock-forming minerals. Rb-Sr isochron (phlogopite, clinopyroxene and WR) shows an age of last thermal reworking of a at c.800 Ma. Lamprophyres reveal a wide scatter of Sm-Nd data attributed to mantle source heterogeneity with E(0) ranging between -11 and -18 and T(DM) between 1500 and 1950 Ma. However, three rocks and a clinopyroxene define a reference line of  $1900 \pm 300$  Ma, which is likely to constrain the lower crystallization time limit. Clinopyroxene has  $^{87}\text{Sr}/^{86}\text{Sr}$  (1900) = 0.703, E(0) = -6 and T(DM) = 1820 while the host WR has T(DM) = 1890 Ma. Similarity between these model ages implies: i) Sm-Nd system of the rock has not been reequilibrated since c.1800-2000 Ma, and ii) the source region had isotopic characteristics akin of depleted mantle (E(1800) = +4 - +5).

PCM lamproites are composed of sanidine, phlogopite and K-richterite with microcline partly replacing sanidine. Rb-Sr isochron (phlogopite, microcline and WR) defines a  $460 \pm 23$  Ma reference line attributed to the latest thermal reworking roughly co-eval with low-grade metamorphism in the area. Sanidine shows extremely low  $^{87}\text{Rb}/^{86}\text{Sr}$  ratio, and its low  $^{87}\text{Sr}/^{86}\text{Sr} = 0.702$  is thought to reflect mantle source characteristics. Sanidine Sm-Nd data show extremely high  $^{143}\text{Nd}/^{144}\text{Nd} = 0.513357$  consistent with derivation from a depleted (E(1800) = +5 - +6) rather than previously enriched source. Model ages for sanidine and the host rock are 1500 and 1300 Ma respectively. The latter is co-eval with subduction-related igneous processes in the adjacent mobile belt and may reflect the age of lamproite dykes in PCM. The isotopic systematics of selected rock-forming minerals of two alkaline rocks reveal low  $^{87}\text{Sr}/^{86}\text{Sr}$  and high  $^{143}\text{Nd}/^{144}\text{Nd}$  ratios which are likely to reflect mantle source isotopic characteristics corresponding to those of depleted mantle. However, high LILE, HFSE and REE concentrations attributable of these rocks imply mantle sources to have been metasomatically enriched. To coincide the data presented the enrichment processes must not be supposed to predate the igneous processes for significant period of time being not only precursors to alkaline igneous activities but perhaps also triggering the partial melting of essentially depleted source regions.

TIMING OF DEFORMATION ON EXTENSIONAL SHEAR ZONES IN NORTH-WEST PALMER LAND, ANTARCTIC PENINSULA.

MILLAR, I.L., British Antarctic Survey, c/o NIGL, Keyworth, Nottingham NG12 5GG, Great Britain, and VAUGHAN, A.P.M., British Antarctic Survey, High Cross, Madingley Road, Cambridge CB3 0ET.

Extensional shear zones deform basement gneisses and a Mesozoic subduction-related plutonic and volcanic complex in the north-west Palmer Land region of the Antarctic Peninsula magmatic arc. New zircon ages from basement and arc-related rocks, together with mineral ages from shear zones are presented in order to constrain the timing of this extensional deformation.

Conventional zircon analyses of basement orthogneisses from several localities give consistent Late Triassic igneous emplacement ages. In particular, gneisses from Campbell Ridges, which were previously thought to be Palaeozoic in age, give an age of  $227 \pm 1$  Ma. The gneissic basement is cut by a suite of Early Jurassic foliated granitoids, typified by a syn-metamorphic granodiorite at Auriga Nunataks, which was emplaced into pre-Late Triassic basement paragneisses at  $205 \pm 3$  Ma.

Dextral transtensional ductile shear zones within the gneiss complex at Auriga Nunataks became active around the peak of upper amphibolite-granulite facies metamorphism (ca. 185 Ma). The extensional deformation may be related to the break-up of Gondwana, the high grade metamorphism resulting from high geothermal gradients during the initiation of break-up. An upper age limit for the timing of extensional shear deformation is given by a cross-cutting, unshaped gabbro, which is dated at  $132 \pm 4$  Ma.

Further shearing related deformation and amphibolite facies metamorphism occurred at around 150 Ma, with associated anatexis of the Campbell Ridges orthogneiss. Anatectic granite sheets from the gneisses have given an Rb-Sr whole-rock isochron age of  $153 \pm 10$  Ma.

At Creswick Peaks, Early Cretaceous arc-related magmatic rocks show evidence of syn-magmatic crustal extension within a major dextral shear zone. Textures ranging from sub-magmatic phenocryst alignment to ultramylonite are preserved in granodiorite. The age of emplacement of the magmatic rocks has been dated at  $141 \pm 2$  Ma, while hornblende separated from a ductile shear fabric has yielded conventional K-Ar ages of  $141 \pm 4$  Ma.

The extensional structures described above often show partial overprinting during a mid-Cretaceous episode of ductile thrusting, which is contemporaneous with, and may be related to, increased rates of Pacific sea-floor spreading at that time.

In conclusion, extensional shear zones were initiated in NW Palmer Land during the early stages of Gondwana break-up. Extensional deformation continued intermittently throughout the Jurassic. In Early Cretaceous times extensional shear zones developed during a major episode of magmatism and crustal growth.

ANCIENT CRUSTAL FLUIDS ASSOCIATED WITH HYDROTHERMAL PROCESSES, S W ENGLAND

MILLER, M. F., Glenny Associates, 9 Oak Piece, Welwyn, Herts. AL6 0XE, UK; SCRIVENER, R. C., British Geological Survey, St Just, 30 Pennsylvania Road, Exeter EX4 6BX, UK; BANKS D. A., Department of Earth Sciences, University of Leeds, Leeds LS2 9JT, UK; PILLINGER C. T., Planetary Sciences Unit, The Open University, Walton Hall, Milton Keynes, MK7 6AA, UK.

Recent U-Pb and  $^{40}\text{Ar}$ - $^{39}\text{Ar}$  studies (Chesley *et al.*, 1993) have confirmed that the Cornubian batholith, SW England, was emplaced diachronously over an interval extending from ca. 295 to ca. 275 Ma before present, with long-lived multiple intrusive episodes and no systematic trend in the age of pluton emplacement.

We present here the results of an investigation into the provenance of hydrothermal fluids associated with early pegmatitic quartz and lithophile mineralisation of the SW England granites. In particular, the chemical composition and isotopic characteristics of hydrothermal fluids associated with tourmaline-dominated and greisen mineralisation of the Dartmoor granite are compared with early-stage W±Sn oxide-associated fluids in the province.

Methods of investigation included the use of high-sensitivity techniques to characterise the stable isotopic composition of traces of palaeofluid carbon and nitrogen species, in conjunction with measurements of the associated electrolyte composition (including halogen ratios), as well as  $\delta\text{D}$  and  $\delta^{18}\text{O}$  values of the waters.

Together with geochemical and isotopic constraints from the characterisation of Palaeozoic metasediments of the region, the results of this integrated approach support the view that the early fluids were primarily of magmatic origin; there is little evidence for fluid interaction with the local metasedimentary rocks at a high level crustal. Very low levels of carbon and nitrogen in the Dartmoor-hosted fluids reflect the comparatively low 'S'-type character of the parent intrusive. The incorporation of sedimentary matter into granitic protoliths during anatexis, with subsequent transfer to an exsolved hydrous phase during pluton cooling, is believed to be the most probable route by which a significant proportion of the palaeofluid solutes entered the early hydrothermal systems. This has implications for the recycling of trace elements such as carbon and nitrogen from the sedimentary rocks.

There is little evidence for the involvement of meteoric water in early mineralising fluids hosted by either the Dartmoor or the adjacent Hemerdon Ball granite. This is not universally the case throughout the batholith, however.

Chesley J. T., Halliday A. N., Snee L. W., Mezger K., Shepherd T. J. and Scrivener R. C. (1993), Thermochronology of the Cornubian batholith: implications for pluton emplacement and protracted hydrothermal mineralization: *Geochim. et Cosmochim. Acta*, v. 57, pp. 1817-1835.

## Hf ISOTOPE CONSTRAINTS ON ANCIENT DEPLETION AND ENRICHMENT EVENTS IN THE MANTLE BENEATH THE SW USA

Milling, ME, Jr, Johnson, CM and Barovich, KM, Univ. Wisconsin, Madison, WI 53706, USA

Hf isotopes may constrain the depths of ancient mantle depletion and enrichment due to the large contrast in Lu/Hf  $K_D$  ratios for garnet (>24) and clinopyroxene (~1); such a contrast is not found in Sm/Nd  $K_D$  ratios.

New data from high- $\epsilon_{Nd}$  volcanic centers that are thought to have been derived from asthenospheric mantle (Cima, SE CA; Lunar Craters, cent NV) have anomalously low  $^{176}\text{Hf}/^{177}\text{Hf}$  ratios ( $\Delta\epsilon_{\text{Hf}} < -4$ ;  $\Delta\epsilon_{\text{Hf}}$  from Johnson & Beard, 1993, Nature) that are similar to those previously found in the southern Rio Grande rift and may reflect ancient depletion in the spinel peridotite stability field; these results suggest that large areas of the asthenospheric mantle beneath the SW USA may be sub-oceanic mantle that was overridden by the North American continent. The low Lu/Hf<sub>MEASURED</sub> ratios of these rocks, however, indicate derivation from the garnet stability field and indicate a major change in mantle mineralogy in the last few b.y. Moderate  $\Delta\epsilon_{\text{Hf}}$  values (~ -2) for high- $\epsilon_{Nd}$  (>+9) basalts associated with the Mendocino Triple Junction (Sonoma, N CA) suggest ancient depletion with a garnet component, and contrast with the high Lu/Hf<sub>MEASURED</sub> ratios that are best modeled by melting spinel peridotite.

New data for alkaline lavas from the Colorado Plateau show an extremely wide range of  $\Delta\epsilon_{\text{Hf}}$  (+6 to -6) at relatively constant  $\epsilon_{Nd}$  (~0); such a vertical  $\epsilon_{\text{Hf}}-\epsilon_{\text{Nd}}$  array at  $\epsilon_{\text{Nd}} \sim 0$  has not been found before, and may reflect mixing between ancient depleted spinel- and garnet-peridotite mantle (similar to the present-day MORB array), in addition to LREE metasomatism and isolation for 1-2 b.y. beneath the stable plateau.

Finally, new data from the highly extended Death Valley region indicate that low  $\epsilon_{Nd}$  lavas, possibly reflecting ancient enriched lithospheric mantle, have positive  $\Delta\epsilon_{\text{Hf}}$  values that are similar to those found in NW Colorado (Beard & Johnson, 1993, EPSL); these compositions may reflect ancient shallow metasomatism or contamination by pelagic sediments.

The diversity of Hf-Nd isotope and elemental variations for subcontinental basalts greatly exceeds that found in the oceans, and provides a unique view into the processes that shape the subcontinental mantle.

## PALEOTHEMOMETRY USING THE U/CA RATIO OF CORAL SKELETONS

MIN, G.R. and EDWARDS, R.L. Minnesota Isotope Laboratory, Dept. Geology and Geophysics, U. Minnesota, Minneapolis, MN 55455 USA; TAYLOR, F.W. Institute for Geophysics, University of Texas at Austin, Austin TX 78759 USA; RECY, J., Laboratoire de Geodynamique Sous-Marine, B.P. 48-06230, Villefranche S/Mer, France; GALLUP, C.D. and BECK, J.W. Minnesota Isotope Laboratory, Dept. Geology and Geophysics, U. Minnesota, Minneapolis, MN 55455 USA

Annual variations in the  $^{238}\text{U}/^{40}\text{Ca}$  ratio of *Porites lobata* coral skeletons have been discovered for both modern and fossil samples collected from Amedee Lighthouse, Noumea, New Caledonia (modern); Papeete, Tahiti (modern) and Espiritu Santo Island, Vanuatu (fossil). We sub-sampled coral on transects perpendicular to coral growth bands. The sub-sample size for U, Sr and Ca isotope analysis was about 3 mg, which represents an approximately monthly growth interval.  $^{238}\text{U}/^{40}\text{Ca}$  and  $^{88}\text{Sr}/^{40}\text{Ca}$  ratios were determined by isotope dilution thermal ionization mass spectrometry on aliquots of the same sub-sample. Errors for  $^{238}\text{U}/^{40}\text{Ca}$  were less than  $\pm 2\%$  ( $2\sigma$ ) on several nanograms of U. Errors for  $^{88}\text{Sr}/^{40}\text{Ca}$  were less than  $\pm 1\%$ . All samples have annual variations in  $^{238}\text{U}/^{40}\text{Ca}$ , which mimic and are in phase with variations in  $^{88}\text{Sr}/^{40}\text{Ca}$ . A plot of  $^{88}\text{Sr}/^{40}\text{Ca}$  vs.  $^{238}\text{U}/^{40}\text{Ca}$  for sub-samples of 4 corals from different localities shows a high correlation between  $^{88}\text{Sr}/^{40}\text{Ca}$  and  $^{238}\text{U}/^{40}\text{Ca}$ . This suggests that annual variations of  $^{238}\text{U}/^{40}\text{Ca}$  in coral skeletons are largely controlled by the sea surface temperature. Using our correlation for modern sub-samples and the known dependence of  $^{88}\text{Sr}/^{40}\text{Ca}$  on temperature, we calculated a temperature dependence for  $^{238}\text{U}/^{40}\text{Ca}$ :

$$T(^{\circ}\text{C}) = 43.703 - 17.477 \times 10^6 \times (^{238}\text{U}/^{40}\text{Ca})_{\text{(molar)}}$$

The fractional shift per  $^{\circ}\text{C}$  is about 7 times larger (5.3% per degree) for  $^{238}\text{U}/^{40}\text{Ca}$  than for  $^{88}\text{Sr}/^{40}\text{Ca}$  (0.7% per degree). Using our  $^{238}\text{U}/^{40}\text{Ca}$  vs. T and  $^{88}\text{Sr}/^{40}\text{Ca}$  vs. T correlations, we calculated temperatures for 8 and 10 Ky fossil corals from Vanuatu. Both thermometers give mean annual temperature that are well below the present mean annual temperature of  $26.5^{\circ}\text{C}$ . If these temperatures can be generalized in time and space, they suggest that tropical sea surface temperatures during deglaciation were 4 to  $6^{\circ}\text{C}$  lower than present. However,  $^{238}\text{U}/^{40}\text{Ca}$  and  $^{88}\text{Sr}/^{40}\text{Ca}$  do not correlate perfectly; the mean annual  $^{238}\text{U}/^{40}\text{Ca}$  temperatures for the fossil samples are about  $3^{\circ}\text{C}$  higher than the  $^{88}\text{Sr}/^{40}\text{Ca}$  temperatures and the seasonal amplitude is somewhat smaller. It is possible that  $^{238}\text{U}/^{40}\text{Ca}$  ratios may be sensitive to other paleoceanographic parameters, such as  $\text{PCO}_2$ , pH or alkalinity. Because annual cycles in  $^{238}\text{U}/^{40}\text{Ca}$  appear to be a general feature of primary coralline aragonite, the preservation of such features will be important in identifying unaltered corals for U-series dating studies. Furthermore,  $^{238}\text{U}/^{40}\text{Ca}$  thermometry may have advantages over  $^{88}\text{Sr}/^{40}\text{Ca}$  thermometry because the  $^{238}\text{U}/^{40}\text{Ca}$  ratio is more sensitive to temperature than the  $^{88}\text{Sr}/^{40}\text{Ca}$  ratio. Once high resolution calibration is completed, it is possible that less precise, higher throughput techniques (such as ICP-MS) may be used in routine measurement of  $^{238}\text{U}/^{40}\text{Ca}$ .

HIGH-TEMPERATURE WATER-ROCK INTERACTION: EXPERIMENTAL INVESTIGATION USING RADIO-ACTIVE TRACER METHOD

MIRONOV A.G., ZHATNUEV N.S.  
Buryat Geological Institute, Ulan-Ude, Russia

The radio-nuclides of gold (Au-195, Au-198), silver (Ag-110m+110) and hydrogen (tritium-bearing water) were used for the study of the high-temperature water-rock interaction. The use of the radio-active tracers method allowed to go into such problems the solution of which by traditional methods is difficult or impossible. The experiments in hydrothermal (T=200-500°C, P=200-1000 bar) and magmatic (T=825°C, P=2100-2300 bar) systems on the study of the water, gold and silver behaviour under water-rock interaction were carried out. The tritium was used a tracer in the water ( $^3\text{HHO}+\text{H}_2\text{O}$ ) with quantitative 10-15 MBc/g. Radio-isotopes of gold and silver were placed in basalt, andesite and rhyolite glasses melting beforehand with total concentration of gold 50 ppb, silver - 50-100 ppm. The mapping of the radio-isotopes distribution in glass samples was obtained by the beta radiography on the nuclear emulsion plate with the spatial resolution about 20 micron for tritium.

In process of the water-glass interaction (200-500°C) the hydration, re-crystallization and leaching zones were formed in the glass of different composition. Gold and silver were leached from hydration zone and were re-concentrated in re-crystallization zone. The high mobilization from rhyolite, andesite and basalt glasses is more typical for silver (60-95%), whereas the gold was leached from glasses only with increase of the oxygen fugacity in system. A conclusion was made that volcanic rocks may be a source of precious metals for the gold and silver deposits at hydrothermal alteration of host volcanic rocks depending on their composition, temperature, pressure and oxygen fugacity.

RB-SR SYSTEMATICS IN RECENT SEDIMENTS, AND ITS BEARING FOR GEOCHRONOLOGICAL INTERPRETATIONS

MISUZAKI, A.M.P., Petrobrás/Cenpes Cidade Universitária/ Quadra 7, Ilha do Fundão/ 21949-900 Rio de Janeiro, RJ, Brazil; CORDANI, U.G., Instituto de Geociências/ Universidade de São Paulo, C.P. 20899, 01498-970 São Paulo, SP, Brazil; KAWASHITA, K., Instituto de Geociências/Universidade de São Paulo; and THOMAZ-FILHO, Instituto de Geociências/Universidade de São Paulo.

In many known cases, when dealing with fine grained and argillaceous sedimentary rocks, the age values obtained from Rb-Sr whole-rock isochron calculation are of geological significance, despite of the fact that the initial condition of Sr isotopic homogenization cannot be envisaged, in such low temperature environments where deposition and diagenesis occur. To explain it, Cordani et al (1978), as well as Cordani et al (1985), proposed complete mechanical mixing, leading to material with fairly uniform  $^{87}\text{Sr}/^{86}\text{Sr}$  ratios in relation to the Rb/Sr ratios of the samples.

In this work, in order to investigate the chemical mobility of Rb and Sr during sedimentation and early diagenesis, more than 60 samples of fine grained recent sediments from selected coastal localities in Brazil were studied by several different techniques, including conventional chemical analyses, X-ray diffraction and fluorescence, scanning electronic microscopy, and isotope geochemistry through mass spectrometer. The samples were collected from the continental shelf at the Amazon river mouth (AM), the deltaic region of the Açu river (RN), the deltaic region of the Paraíba do Sul river and the Jacarepaguá coastal plain (RJ), as well as the continental slope in the Campos basin (RJ).

The results demonstrate clearly that, especially when smectites and illite predominate in the sediments, the initial conditions that may evolve to significant isochrones after the closure of the chemical systems to Rb and/or Sr mobility are indeed fulfilled. The Rb/Sr ratios of the rock systems are modified since the chemical weathering processes, but possibly the more radical changes occur when the sediments reach the coastal plains, and interact with sea water. In these conditions halmyrolysis occur, inducing most Sr to be dissolved into the sea water, producing relevant increases in the Rb/Sr ratio. At the same time, interaction and mixing with marine strontium, during halmyrolysis and early diagenetic processes, makes the  $^{87}\text{Sr}/^{86}\text{Sr}$  of the sediment to approach the marine value of about 0.709.

The above conditions, which confirm the existence of "horizontal" isochrons for fine grained recent sediments, seem to adequately justify the applicability of the Rb-Sr method to shales and related rocks.

Cordani, U.G., Kawashita, K., and Thomaz-Filho, A., 1978. AAPG Studies in Geology, v.6, p.93-117.  
Cordani, U.G., Thomaz-Filho, Brito-Neves, B.B. and Kawashita, K., 1985, Giornale di Geologia, v.47 (1-2), p.253-280.

**THERMAL VARIATIONS IN A PASSIVE MARGIN, FROM APATITE FISSION TRACK ANALYSIS IN THE WESTERN OTWAY BASIN, AUSTRALIA.**

MITCHELL, M.M., HILL, K.C., FOSTER, D.A., O'SULLIVAN, P.B. at VEIPS, School of Earth Sciences, La Trobe University, Bundoora, Victoria, 3083, Australia, DUDDY, I. R. at Geotrack International, Melbourne, Victoria, 3052, Australia.

The Otway Basin formed during rifting of Australia and Antarctica commencing in the Late Jurassic. A stable passive margin setting has been proposed for the basin since the mid-Cretaceous breakup. The Gambier Embayment, the western section of the Otway Basin, consists of fault-bound structural troughs and highs, including the Merino Uplift, which defines the eastern margin.

The apatite fission-track (AFT) thermochronology and vitrinite reflectance data for several wells in the Gambier Embayment indicate thermal variations in the Cretaceous and Tertiary. Data from the Penola-1 and Robertson-1 wells, within the Penola Trough at the northern margin of the basin, indicate different thermal histories. AFT ages of five samples from Penola-1 increase with depth from 143 to 279 Ma. Mean lengths (ML) for these samples decrease from 12-13  $\mu\text{m}$  to 10.2  $\mu\text{m}$  with depth. Single grain ages indicate detritus from multiple source regions, with pre-Mesozoic age grains dominating the lower section at the expense of contemporaneous volcanogenic material. Mesozoic(?) trachytic basement intersected at the base of Robertson-1 (presently at 97°C) has an AFT age of 104 $\pm$ 11 Ma and a ML of 10.4  $\mu\text{m}$ . A sample from the overlying Otway Group in Robertson-1 currently at 61°C, records an age (283 $\pm$ 20 Ma) older than the stratigraphic age (112-123 Ma). Intergration of vitrinite reflectance and AFT data suggests that Penola-1 experienced a recent decline in heat flow, while Robertson-1 underwent uplift and erosion prior to an increase in heat flow.

On the Beachport-Kalangadoo High elevated heat flow during burial in the Cretaceous occurs at Kalangadoo-1, and not at Geltwood Beach-1 and Beachport-1. Kalangadoo-1 penetrates Palaeozoic (?) metasediments which yield AFT ages from 94 to 20 Ma and a paucity of lengths <9  $\mu\text{m}$ , for samples at 77-98°C. Three samples from the Otway Group give ages from 166-111 Ma with ML decreasing with depth from 13.5 to ~12  $\mu\text{m}$ . AFT results from Geltwood Beach-1 and Beachport-1 are consistent with present temperatures, with samples retaining Mesozoic syndepositional single grain ages. Mocamboro-11 on the Merino Uplift, intersects Otway Group sediments near surface and metasedimentary basement at 1374 m. The basement gives an AFT age of 44 $\pm$ 6 Ma and a bimodal length distribution with ML of 8.9  $\mu\text{m}$ . The samples from the overlying Otway Group exhibit reduction in ML (11-10.2  $\mu\text{m}$ ) indicative of higher palaeotemperatures.

Variable thermal histories are also suggested for the Tertiary and are manifested as Miocene cooling at both Mocamboro-11 and Kalangadoo-1, and a Neogene increase in heat flow at Robertson-1. Variable amounts of denudation are suggested, the most significant in the vicinity of Mocamboro-11 and Robertson-1 on the basin margins with ~700 m and ~1000 m of apparent denudation, respectively. This uplift along the basin margins may have resulted from lithospheric flexure as the main depocenters of the basin loaded with sediment, or block faulting. In summary, the results show that the western section of the Otway Basin did not become thermally and tectonically stable following 'break-up'. Episodes of uplift, erosion, and fluctuations in geothermal gradient continued throughout the Late Cretaceous and Tertiary in the basin.

**DEGASSING HISTORY OF NITROGEN AND ARGON**

MIYAZAKI, A., HIYAGON, H., SUGIURA, N., Dept. of Earth and Planet. Phys., Graduate School of Sci., Univ. of Tokyo, Tokyo, 113 Japan.

Degassing process of nitrogen from the mantle is considered to be mostly controlled by physicochemical properties of nitrogen, such as gas/silicate melt and silicate/solid partition coefficients. Since there are very few data about these partition coefficients, we conducted an experiment to obtain them. We used  $^{15}\text{N}$ -labeled gas in synthesizing basaltic melt and melt/crystal pairs. From the obtained partition coefficients, we estimate the transport efficiencies of nitrogen and argon from the mantle to the atmosphere.

Then we constructed a simple 2-reservoir (atmosphere and mantle) and 2-stage (catastrophic and continuous) nitrogen and argon degassing model on the basis of the estimated transport efficiencies of nitrogen and argon and the  $\text{N}_2/^{40}\text{Ar}$  flux ratio of ~ 50 from the mantle estimated from MORB glass data. The present result indicates that nitrogen has a degassing history different from that for argon; either nitrogen may be degassed less efficiently at the catastrophic degassing event, or considerable amount of nitrogen once degassed may have been returned to the mantle. Assuming  $\text{N}_2/\text{Ar}$  transport efficiency ratio being ~ 0.1 estimated from the preliminary result of partition coefficients of nitrogen [1] and other published data [2,3], the amount of nitrogen in the mantle is calculated to be 1.5 times as much as that in the atmosphere.

1. Miyazaki, Hiyagon and Sugiura, 1993, 29th IGC abstract vol.3, 651.
2. Hiyagon and Ozima, 1986, G.C.A. 50, 2045-2057.
3. Yurimoto and Sueno, 1984, Geochem. J. 18, 85-94.

ISOTOPIC EVIDENCE OF ARCHEAN CRUST IN THE REINDEER ZONE OF THE TRANS-HUDSON OROGEN, NORTHERN SASKATCHEWAN

MOCK, Timothy D., and BICKFORD, M.E.  
Department of Earth Sciences,  
Syracuse University, Syracuse, NY 13244 USA

The Reindeer Zone of the Trans-Hudson orogen is a collage of volcanic arcs and related plutonic rocks that were assembled during the Early Proterozoic. Recent seismic reflection studies show that the Glennie Domain is a culmination between east-dipping reflectors beneath the Superior craton to the southeast and west-dipping reflectors to the west. Archean crust is exposed in small structural windows in the Iskwatikan and Hunter Bay region of the Glennie Domain and farther to the east in the Sahli Charnockite in the Hanson Lake Block. K-feldspar common Pb and Sm-Nd whole-rock data indicate extensive involvement of Archean crust in the generation of post-orogenic leucogranites but not in the formation of the "Hudsonian" plutons.

U-Pb zircon ages of plutonic rocks in the Reindeer Zone fall into three age ranges. (1) "Hudsonian" granodiorite and tonalite gneisses that have crystallization ages between 1880 and 1854 Ma. (2) Weakly deformed granites that were emplaced after peak metamorphism between 1833 and 1824 Ma. (3) Post-orogenic leucogranites and pegmatites that have zircon ages between approximately 1780 and 1770 Ma.

Pb K-feldspar analyses of the exposed Archean basement have  $(^{206}\text{Pb}/^{204}\text{Pb})_i = 14.615\text{-}14.769$  and  $(^{207}\text{Pb}/^{204}\text{Pb})_i = 15.167\text{-}15.378$ . Calculated  $(^{207}\text{Pb}/^{206}\text{Pb})$  ages for the "Hudsonian" plutons are between 2580 and 2350 Ma indicating that these rocks evolved in an environment with high  $^{238}\text{U}/^{204}\text{Pb}$  ( $\mu = 11$ ). The pegmatites that cut the Sahli Charnockite also formed in a high  $\mu$  environment but have lower  $^{207}\text{Pb}/^{206}\text{Pb}$  ages (2330-2250 Ma). "Hudsonian" K-feldspar  $^{207}\text{Pb}/^{206}\text{Pb}$  ages range from 1720-1650 Ma indicating that these plutonic rocks were derived from juvenile sources. Leucogranite and pegmatite K-feldspar data from the Glennie Domain and the Hanson Lake Block range from  $(^{206}\text{Pb}/^{204}\text{Pb})_i = 15.271\text{-}15.368$  and  $(^{207}\text{Pb}/^{204}\text{Pb})_i = 15.165\text{-}15.307$ . These rocks have  $^{232}\text{Th}/^{238}\text{U}$  ratios between 4.72-6.19 consistent with derivation from a high Th/U source such as the exposed Archean basement. In contrast, pegmatites from the volcanic La Ronge Domain have high  $(^{206}\text{Pb}/^{204}\text{Pb})_i = 15.634\text{-}16.344$  and  $(^{207}\text{Pb}/^{204}\text{Pb})_i = 15.228\text{-}15.307$ . This indicates that there was little or no involvement of Archean crust in the western part of the Reindeer Zone.

The "Hudsonian" plutons have  $\epsilon\text{Nd}_{(t)}$  values ranging from +3.0 to +4.5 and  $T_{\text{DM}}$  ages of approximately 1870 Ma, very similar to their crystallization ages. This indicates that little or no Archean crust was involved in the generation of the "Hudsonian" plutons. In contrast, the post-orogenic leucogranites have  $\epsilon\text{Nd}_{(t)}$  values of -13 to -14 and  $T_{\text{DM}}$  ages of 3400-3150 Ma. Both the Sm-Nd and K-feldspar common Pb data are consistent with an extensive region of buried Archean crust beneath the Glennie Domain and the Hanson Lake Block.

EROSION HISTORY OF THE CENTRAL SIERRA NEVADA USING COSMOGENIC  $^{10}\text{Be}$  AND  $^{26}\text{Al}$   
MONAGHAN, M.C., Department of Earth and Atmospheric Sciences, Purdue University, West Lafayette, Indiana, 47907-1397, USA.

The present physical geography of the central Sierra Nevada can be subdivided into regions of somewhat similar form. These are: i) deep valleys of large rivers that trend roughly orthogonal to the axis of the Sierra Nevada crest from the east to west or northeast to southwest; ii) broad, inclined, plateau-like interfluves between these deep valleys; iii) steeply-rising west- and south-west facing steps and step fronts found within some of these interfluve regions; iv) glaciated uplands; and v) weathered uplands that comprise west-dipping rough tables on mountain and ridge tops.

Through the study of in situ produced cosmogenic  $^{10}\text{Be}$  and  $^{26}\text{Al}$  we hope to constrain exposure ages and erosion rates of geomorphic surfaces found in these physiographic regions. We hope to determine whether or not our simple classification of physiography corresponds to a simple pattern of erosion rates and exposure ages. Two particular studies are presently underway. First, we are studying the weathered uplands of the Crystal Range in the Central Sierra Nevada that comprise west-dipping rough tables on mountain and ridge tops to determine whether or not these surfaces are remnants of pre-Wisconsin surfaces. Second, we are studying the steeply-rising west-facing steps and step-fronts in the Shaver Lake region of the Central Sierra Nevada in an effort to determine whether or not the exposure ages of these surfaces increase with distance from the Sierra Nevada/Great Valley boundary. The first study addresses an age-old geomorphic question - Do uplifted erosion surfaces survive as flat regions along mountain and ridge tops? The second study addresses Warhaftig's hypothesis that the steps and step-fronts developed through differential weathering rates.

ISOTOPIC EVIDENCE OF HOLOCENE AND PLEISTOCENE PALEOENVIRONMENTS IN THE CHIHUAHUAN DESERT, USA.

MONGER, H. Curtis, Dept. of Agronomy and Horticulture, New Mexico State University, Las Cruces, New Mexico, 88003, USA, and COLE, David R., Chemical and Analytical Sciences Division, Oak Ridge National Lab., Oak Ridge, Tennessee, 37831, USA.

As part of the USDA Desert Project, decades of effort have been invested in understanding the Quaternary soil stratigraphy in the Chihuahuan Desert of southern New Mexico (Gile et al., 1981). Because of the good chronologic control and because many calcic soils are buried beneath the zone of modern pedogenesis, the Desert Project is a good location for conducting stable isotope studies. For instance,  $\delta^{13}\text{C}$  values of pedogenic carbonates on alluvial fan soils decreased an average 6‰ just prior to a major erosion episode about 8 ka (Fig. 1). This isotope shift indicates the decline of  $\text{C}_4$  grasses and an increase in  $\text{C}_3$  desertscrub vegetation. Concurrent with the carbonate  $\delta^{13}\text{C}$  shift was a decrease in organic  $\delta^{13}\text{C}$  values from ~ -17 to -25‰ and a reduction in Gramineae pollen.

Although the vegetation change is apparent at about 8 ka,  $\delta^{18}\text{O}$  values remained relatively constant (Fig. 1), suggesting that a major temperature increase did not accompany the ecological change. This raises the possibility that increasing atmospheric  $\text{CO}_2$  during deglaciation contributed to the decline of the  $\text{C}_4$  grasses growing on the ecologically fragile alluvial fan soils. In contrast, the deep sandy soils of the basin floors do not contain the dramatic  $\delta^{13}\text{C}$  shift. These results support the usefulness of stable isotopes for recording the timing and nature of terrestrial environmental changes.

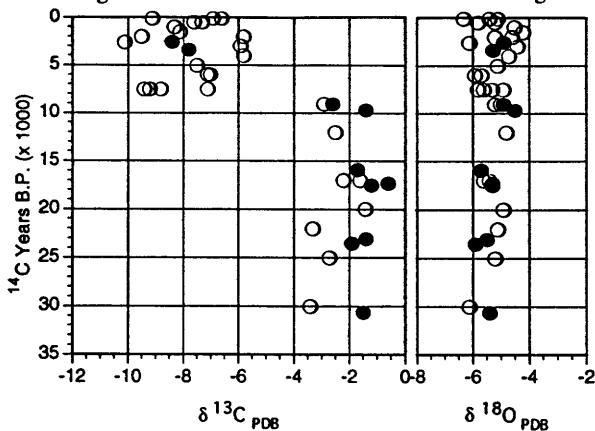


Figure 1.  $\delta^{13}\text{C}$  and  $\delta^{18}\text{O}$  values versus time for pedogenic carbonates from four alluvial fan soils. Solid circles indicate  $^{14}\text{C}$ -dated samples. Other samples are interpolated according to their stratigraphic position to dated samples.

Gile, L.H., Hawley, J.W., and Grossman, R.B., 1981, New Mexico Bureau of Mines and Mineral Resources Memoir 39, Socorro, 222p.

DRC sponsored by the Geoscience Research Program, Office of Basic Energy Sciences, USDOE Under Contract DE-AC05-84OR21400.

INTEGRATED STUDY OF THE MIOCENE TIME SCALE

MONTANARI A. (Osservatorio Geologico di Coldigioco, 62020 Frontale di Apiro, Italy), COCCIONI R. (Istituto di Geologia, 61029 Urbino, Italy) and ODIN G.S. (Dépt. Géologie Sédimentaire, Université P. & M. Curie, 75252 Paris, France)

Under the acronym of "Miocene Columbus Project" (MICOP) we have organized in 1991, an interdisciplinary working group focusing on high-resolution stratigraphic calibration of the Miocene Epoch.

The pelagic carbonate series of the Apennines (Italy) contains volcanoclastic layers which offer the rare opportunity to calibrate the biostratigraphic sequence with radiometric dates. Following petrographical and geochemical study, appropriate geochronometers have been selected. Radiometric ages are now available from 1- the Oligocene-Miocene boundary (Bosio) 40Ar-39Ar step heating on hornblende at 22.7 Ma; 2- the Gubbio section: 40Ar-39Ar laser fusion dates from plagioclase from 2 layers yielding  $21.2 \pm 0.5$  ( $2\sigma$ ) Ma and  $19.8 \pm 0.5$  Ma which bracket the magneto- and biostratigraphically calibrated Aquitanian-Burdigalian boundary (Montanari et al. 1991); 3- the Moria section: a biotite plateau age at 17.1, and 2 sanidine laser fusion ages at 16.2 and 15.5 Ma bracketting the Burdigalian-Langhian boundary; 4- other sections within the Apennines including an ash about 18 Ma old (upper Burdigalian, Santa Croce), a level about 15 Ma old (Langhian, L'Annunziata), and a biotite-rich level about 11.5 Ma old (base Tortonian, Monte dei Corvi); 5- Serravallian of Sicily: 40Ar-39Ar step heating on biotite at 13.9 Ma; 6- a series of biotite-rich layers delivering biotite and plagioclase consistent analytical ages between 7.34 and 8.25 Ma immediately below the Tortonian-Messinian boundary, (Faenza area) by Vai, et al. (1993) and supplemented in 2 laboratories; 7- Late Messinian: 40Ar-39Ar step heating on biotite at 5.5 Ma (Apiro, Italy).

More data are prepared from samples collected across the Burdigalian-Langhian boundary and in the Langhian to Messinian pelagic sequence exposed on coastal cliffs. A group of datings is also in way in 3 laboratories from Japanese volcanogenic layers located within the marine Serravallian and Mio-Pliocene sequence with some already available under published (Kasuya, 1990) or preliminary form.

Because of their qualities which include 1) applicability of bio-, magneto-, chemo-, and litho- stratigraphic tools, as well as geochronologic dating, allowing correlation with other sections in the world; 2) continuous and reasonably slow accumulation rate for accessible outcrops free of structural complexities; and 3) large quantity of diversified data from about 40 researchers presently involved in this project, we propose some of these sections as potential "Global Stratotype Sections and Points" for the 6 Stages of the Miocene Epoch.

The geochronological instrumental laboratories involved are Berkeley, Berne, Lausanne, Montpellier, Pisa, and Yamagata.

The results of this interdisciplinary study will be gathered in two volumes in preparation.

Kasuya, M., 1990. Quaternary Research, 33: 86-93.

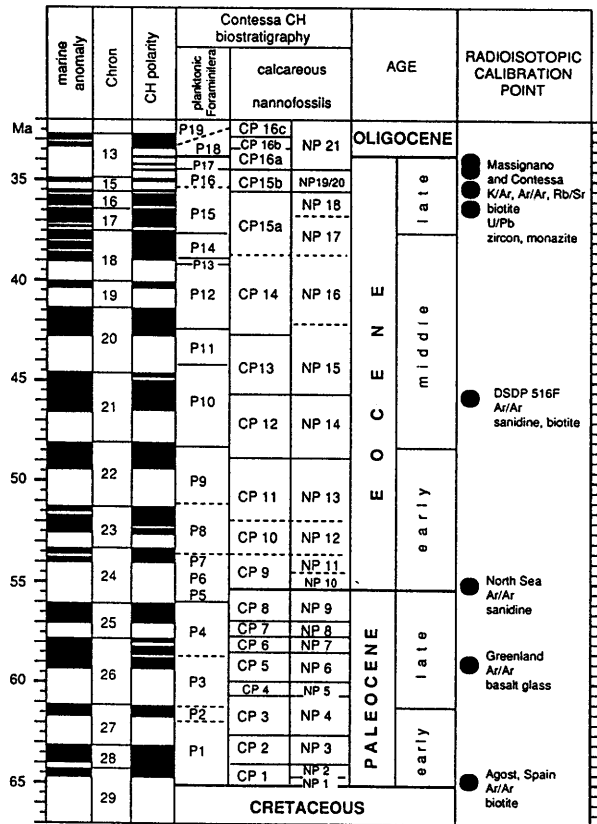
Montanari A., Deino A. et al., 1991, Newsl. Stratigr. 23: 151

Vai G.B. et al., 1993. C. R. Acad. Sci. Paris, 316: 1407-1411.

**RADIOISOTOPIC CALIBRATION OF THE PALEOCENE-EOCENE BIO-MAGNETOSTRATIGRAPHIC SEQUENCE AT GUBBIO (ITALY)**

MONTANARI, A. (Osservatorio Geologico di Coldigioco, 62020 Frontale di Apiro -MC- Italy), and SWISHER, C. III (Geochronology Center, Institute of Human Origins, 2453 Ridge Road, Berkeley, CA 94709)

Radioisotopic dates from several volcanic ashes contained in Paleocene and Eocene marine sediments in Italy, DSDP 516F (South Atlantic Ocean), a deep sea core from the North Sea, and on-land sections in Disko Island (Greenland), and Agost (Spain) are here utilized to calibrate, with unprecedented precision and accuracy, the age of bio-, and magnetostratigraphic boundaries in the continuous and complete pelagic sequence of the Contessa highway, near Gubbio (Italy -- see figure). Details on mineral separation and purification techniques, instrumentation, and computation of the numerical ages with their standard deviations, will be given orally, along with the illustration of the bio-magnetostratigraphic characteristics of the marine sequences containing the dated volcanic material.



**$^{129}\text{I}$  AS A HYDROLOGIC TRACER: DETERMINATION OF SOURCE AGES AND MIGRATION PATTERNS OF BRINES IN SEDIMENTARY BASINS.**

MORAN, J.E. and FEHN, U., Department of Earth and Environmental Sciences, University of Rochester, Rochester, NY 14627

$^{129}\text{I}/\text{I}$  ratios have been measured in brines from the Gulf Coast Basin, the Anadarko Basin in Oklahoma and Nevada oil fields. Results indicate that this isotope can be used to identify source formations of I and organic matter, and to track fluid migration from deeper parts of a sedimentary basin to present host formations.

Interpretation of  $^{129}\text{I}/\text{I}$  ratios measured in brines from sedimentary basins is based on estimation of the relative contributions of cosmogenic and fissiogenic  $^{129}\text{I}$ . Ratios measured in brines from the Louisiana Gulf Coast basin can be compared to the decay of cosmogenic  $^{129}\text{I}$  to get minimum source ages (when no fissiogenic contribution is included). These minimum ages are significantly older than present host formation ages, indicating migration of brine from older, deeper sources. Based on the measured ratios and conservative corrections for a fissiogenic contribution, brines sampled from Pleistocene and Pliocene reservoirs have migrated from Paleocene-Eocene sources several kilometres deeper. Some ratios measured in Texas Gulf Coast brines show evidence of a greater fissiogenic component which indicates that the brines have resided in formations with locally high U concentrations. Brines with extremely high I concentrations from a Pennsylvanian host formation in the Anadarko Basin point to the Woodford Shale as the probable source formation, based on comparison of potential fissiogenic contributions from underlying sandstones and shales. Ratios measured in brines from Nevada oil fields are higher than would be predicted for deep sources, and indicate mixing with shallower, younger formation waters.

DETERMINING THE CARBON ISOTOPE  
CHEMOSTRATIGRAPHY ACROSS THE  
PERMIAN/TRIASSIC BOUNDARY IN AUSTRALIA

MORANTE, R. School of Earth Sciences, Macquarie  
University, North Ryde, NSW, 2109, Australia.

A negative  $\delta^{13}\text{C}$  excursion at the palaeontologically determined Permian/Triassic boundary (P/Tr) in marine sediment has been well established. A similar  $\delta^{13}\text{C}$  excursion to more negative values occurs in organic carbon in pelitic whole rock samples from conventional or sidewall cores from seven Australian sedimentary basins. The  $\delta^{13}\text{C}$  excursion in marine and nonmarine sediment occurs within or near the base of the *Protospirifer microcorpus* palynology zone. This zone is therefore interpreted as straddling the P/Tr. The size of the  $\delta^{13}\text{C}$  excursion, interpreted environment of deposition at the boundary and degree of biostratigraphic control based upon palynology in each basin is summarised in the table below.

Basin	$\delta^{13}\text{C}$ ‰ excursion	Depositional environment	Palynological control
Bonaparte	-8	Marine	Good
Carnarvon	-4	Marine	Spot
Canning	-8.5	Marginal marine	Good
Bowen	-6	Fluvial	Good
Sydney	-6	Fluvial	Good
Perth	-5.5	Fluvial	Spot
Cooper	-6	Fluvial	Spot

The  $\delta^{13}\text{C}$  excursion in marine and nonmarine sediment alike is interpreted as reflecting a shift of up to -10‰ in the  $\delta^{13}\text{C}$  of atmospheric  $\text{CO}_2$  that masked expected variations in enclosed basins. The possible global extent of this  $\delta^{13}\text{C}$  excursion at the P/Tr may provide a correlation tool enabling calibration of biostratigraphy schemes world wide at the P/Tr across a range of sedimentary environments. The shape of the negative  $\delta^{13}\text{C}$  excursion varies from sharp to gradual. A sharp  $\delta^{13}\text{C}$  excursion indicates a lacuna, a condensed section, or a rapid change to more negative  $\delta^{13}\text{C}$  values in the Triassic. A gradual shift in  $\delta^{13}\text{C}$  indicates either a real, prolonged continuous  $\delta^{13}\text{C}$  excursion or a mixture of Permian and Triassic values. The  $\delta^{13}\text{C}$  excursion is explained by a flux of  $^{12}\text{C}$  enriched carbon as  $\text{CO}_2$  from the reduced to the oxidised global reservoir. Possible sources of  $^{12}\text{C}$  enrichment suggested include, a) oxidation of organic facies and clathrate methane and b) volcanic eruption of mantle carbon as carbon dioxide. Depleted  $\delta^{13}\text{C}$  values until at least the Middle to Late Triassic may reflect the loss of  $^{12}\text{C}$  fixers having high preservation potential at the Permian/Triassic extinction. A large transfer of carbon from the reduced to the oxidised global reservoir and release of methane may have produced greenhouse conditions that contributed to the Permian/Triassic extinction.

PB AND U ISOTOPE CHEMISTRY OF ACTINOLITE-TALC  
ASSOCIATIONS FROM HIGH-PRESSURE METABASIC  
ROCKS.

MOREE, Martijn, STAUDIGEL, H. and DAVIES, G.R.,  
Dept. of Petrology & Isotope Geology, Free University, De  
Boelelaan 1085, 1081 HV, Amsterdam, The Netherlands.

Chemical modification and open system geochemical behaviour in subduction zones plays an important role in producing the chemical components in the Earth's mantle and the sources of island arc magmas. Yet the fractionation of trace elements during metamorphic processes in this tectonic setting is very poorly understood, in particular for the U/Th/Pb systematics. We have begun to analyze the U and Pb abundances of metamorphic mineral phases from blueschist terranes in order to identify major mineral assemblages that control the distribution of U and Pb in accretion zones. Furthermore, we studied Pb isotopic compositions to determine the origin of any mobile Pb.

Our first data from a actinolite-talc association within the melange of Catalina Island, California yielded:

sample	WR	act	tlc
$^{208}\text{Pb}/^{204}\text{Pb}$	38.584	38.539	38.374
$^{207}\text{Pb}/^{204}\text{Pb}$	15.625	15.618	15.631
$^{206}\text{Pb}/^{204}\text{Pb}$	18.827	18.795	18.787
$\mu$	1.99	1.97	0.49
U (ppb)	70	60	20
Pb (ppb)	2180	2090	2820

A Pb mass balance shows that the rock consists of 90% actinolite and 10% talc, which is confirmed by thin section data. To balance the U, however, a U-rich third phase (e.g. zircon) is needed.

Due to the very low  $\mu$ -ratios, Pb isotopes do not display significant radiogenic ingrowth during the past  $10^8$  years, but they are reliable indicators for the fluid composition. Fluids released during low-grade metamorphism of the melange would be dominated by sediment derived Pb. The actinolite-talc associations which are commonly found as cap rock around metabasic rocks were apparently formed in equilibrium with fluids that are characterized by mantle-like Pb isotope compositions. We therefore conclude that the actinolite-talc association is an early metamorphic assemblage, reflecting fluid interaction during subduction rather than the emplacement of the melange.

**CARBON AND OXYGEN ISOTOPES OF TWO EARLY JURASSIC STRATIGRAPHIC SEQUENCES: POSSIBLE IMPLICATION FOR FORMATION OF RHYTHMIC MARL - LIMESTONE BEDDING (UMBRIA-MARCHE APPENNINES)**

MORETTINI, E. Institut de Geologie et Palaeontologie, Université de Lausanne BFSH-2, CH-1015 Lausanne, Switzerland, and BAUMGARTNER, P., HUNZIKER, J.C. (same address).

Differences in isotopic values of alternating marl-limestone bedding provide new means for understanding the mechanisms responsible for the formation of such rhythmic sequences. Preliminary carbon and oxygen stable isotope analyses have been made on two basinal stratigraphic successions, the Fiuminata<sup>1</sup> and the Colle d'Orlando sections, from the Umbria-Marche Appennines. The results of this isotope study are also combined with results from micropalaeontological, sedimentological, palaeomagnetic<sup>2</sup>, and calcium-carbonate analyses to constrain the  $\delta^{13}\text{C}$  curve through the early Jurassic (Pliensbachian-Early Aalenian).

Carbonate isotope analyses from 50 samples of marl and limestone in the Fiuminata section (Marne e Calcari a Posidonia unit) show a fluctuation in  $\delta^{13}\text{C}$  values related to the alternation of the two lithologies. The  $\delta^{13}\text{C}$  of the marls is on average 0.3‰ lighter than those of the limestones (the constantly observed difference between two alternating lithologies ranges between 0.2 and 0.9‰). It is not apparent in this preliminary data set whether oxygen values show any systematic fluctuations or variations in the sequence.

Differences in values could be due solely to diagenesis if originally isotopically similar marl and limestone lithologies would have followed different diagenetic paths. However, it is likely that observed isotopic differences reflect original isotopic fluctuations in the precipitated carbonate. These differences may depend on local or regional variations such as basin to basin fractionation and fluctuating vital effects. Or, alternatively, the observed oscillations document shifts in the global carbon reservoirs, linked to climatic cycles of Milankovitch-type.

<sup>1</sup> Morettini, E. *et al.* (in prog.)

<sup>2</sup> Channel, J.T. *et al.* (in prog.)

**GOLD-BEARING EPITHERMAL VEINS IN THE HOKUSATSU DISTRICT, SOUTHERN KYUSHU, JAPAN: CARBON AND OXYGEN ISOTOPIC EVIDENCE**

MORISHITA, Yuichi, Mineral Resources Department, Geological Survey of Japan, 1-1-3 Higashi, Tsukuba 305 Japan

The Hokusatsu gold district in southern Kyushu has produced more than 180 metric tons of gold. Production is continuing, with ore reserves of at least 200 tonnes of gold. The basement of the Hokusatsu gold district is the Cretaceous Shimanto Supergroup. Subaerial andesitic volcanism occurred in the late Miocene to early Pleistocene. Many of the epithermal gold deposits of the district, including the Hishikari deposit (1 Ma) and the Kushikino deposit (4 Ma), occur mainly in these andesitic volcanic rocks as fissure-filling veins consisting of gold- and silver-bearing quartz, calcite and adularia. Neutron activation analyses revealed that there are little gold concentrations in monomineralic vein samples of quartz or calcite in the area.

The  $\delta^{18}\text{O}$  distribution of vein quartz in the Kushikino mine area suggests that the hydrothermal fluid was supplied from below in the eastern part of the area, then flowed westward to the deposit, progressively mixing with a low-temperature meteoric ground water. Vein calcites from the Kushikino deposit show a  $\delta^{13}\text{C}$ - $\delta^{18}\text{O}$  trend which forms the basis for interpreting the  $\delta^{13}\text{C}$  and  $\delta^{18}\text{O}$  values of vein calcites from other deposits in the Hokusatsu gold district. Most isotopic compositions of vein calcites in the district lie on the Kushikino  $\delta^{13}\text{C}$ - $\delta^{18}\text{O}$  trend, suggesting that the hydrothermal fluids were isotopically similar to the Kushikino fluid.

The  $\delta^{13}\text{C}$  values of hydrothermal fluids in the Hokusatsu district during the mineralization stages were low ( $\sim -11\text{‰}$ ), compared with that of average crustal carbon ( $-7\text{‰}$ ). The relatively low and uniform  $\delta^{13}\text{C}$  value of the hydrothermal fluids in the district might have been regionally controlled by organic carbon in widely distributed sedimentary rocks of the Shimanto Supergroup basement. Although the quartz-calcite veins formed from ascending hydrothermal fluids, precipitation in some cases may have been caused by mixing with near-surface waters having relatively high  $\delta^{13}\text{C}$  values.

The  $\delta^{13}\text{C}$  values in the hydrothermal fluid responsible for the Hishikari deposit were also controlled by basement sedimentary rocks of the Shimanto Supergroup. Here it is inferred that the ascending ore-forming fluid mixed with near-surface water at the unconformity between the basement and the overlying volcanic rocks. As a result, relatively high  $\delta^{13}\text{C}$  values are present in vein calcites which occur above the unconformity.

A computer simulation analysis was carried out on the vein system in the Kushikino mine area in order to study the formation mechanism. The observed fracture (vein) system related to the Kushikino ore-forming hydrothermal system was proved to be formed by basement uplift as a consequence of intruding magma at depth. The localized sub-surface doming of magma is also thought to account for the positive Bouguer gravity anomaly over the area and which most likely provided the heat needed to drive the Kushikino hydrothermal system. According to the isotope data, incorporation of a large quantity of high  $\delta^{18}\text{O}$  thermal waters is not plausible, however, the potential magma intrusion might have discharged some magmatic fluids in the early stage of the evolving hydrothermal system.

Nd, Sr AND Pb ISOTOPIC CONSTRAINTS ON MECHANISMS OF CRUSTAL GROWTH IN THE YUKON-TANANA TERRANE IN YUKON TERRITORY, CANADA, AND EASTERN ALASKA, U.S.A.

MORTENSEN, J. K., Dept. of Geological Sciences, University of British Columbia, Vancouver, B.C., Canada, V6T 1Z4 (jmortens@geology.ubc.ca)

Yukon-Tanana Terrane (YTT) is a large, possibly composite, terrane whose constituent lithotectonic assemblages suggest a mainly continental affinity. Previous geological, geochemical, and U-Pb dating studies suggested that arc magmatism occurred across much of the YTT in latest Devonian to mid-Mississippian and in the central and southeastern parts of the terrane in Late Triassic to Early Jurassic time. These arc assemblages were built on a basement of Early Paleozoic and older passive margin sedimentary rocks. Broadly bimodal volcanic and plutonic rocks of mid-Permian age in western Yukon may be the product of either a more areally restricted intervening phase of arc magmatism or an anorogenic igneous event. Isotopic signatures of each of the Paleozoic to Early Mesozoic igneous suites indicate a marked component of contamination from continental crust. Metaluminous plutonic and related volcanic rocks of the Devonian-Mississippian arc assemblage have  $\epsilon_{Nd(T)}$  values of -10 to -13,  $Sr_i$  of 0.708-0.712, and feldspar Pb isotopic compositions that plot near the "shale curve" defined for evolution of Pb in strata of the miogeocline of western North America. Strongly peraluminous plutons, also of Devonian-Mississippian age, that were emplaced at deeper crustal levels within YTT have  $\epsilon_{Nd(T)}$  values of -13 to -16, and highly radiogenic  $Sr_i$  (0.716-0.730) and feldspar Pb compositions. This plutonic suite may be entirely crustally derived and not directly subduction-related. Both of the Devonian-Mississippian igneous suites contain a trace to strong inherited component of older zircon (average ages 1.7 - 3.1 Ga). Pb isotopic compositions for syngenetic sulfide deposits hosted by the Devonian-Mississippian volcanic arc rocks also fall on or near the "shale curve". The mid-Permian igneous suite has  $\epsilon_{Nd(T)}$  values of -5 to -15 and  $Sr_i$  of 0.706-0.711, and contains a relatively minor inherited zircon component. Compositions of Pb in feldspars and in sulfides from syngenetic base metal occurrences hosted by the mid-Permian volcanic rocks are slightly less radiogenic than the "shale curve". Available data do not permit distinction between a magmatic arc vs. anorogenic origin for this suite. Early Mesozoic plutonic rocks in YTT are compositionally less evolved than the older igneous suites, have more juvenile  $Sr_i$  values (0.704-0.706), and typically contain only a minor component of inherited zircon; however  $\epsilon_{Nd(T)}$  values of -1 to -7 indicate significant interaction with older continental crust.

Taken together, the isotopic and other data for the YTT indicate that the terrane is mainly a product of mid-Paleozoic to Early Mesozoic continental arc magmatism. The data are permissive of an origin for YTT as a distal portion of the western edge of North America.

THE CHEMICAL AND STABLE ISOTOPIC COMPOSITION OF MICROBIALLY-PRECIPITATED SIDERITE.

MORTIMER, R. J. G., \*COLEMAN, M.L., and RAE, J.E., Postgraduate Research Institute for Sedimentology, Reading University, Reading, Berkshire RG6 2AB, U.K.

\*also B.P. Exploration, Sunbury-on-Thames, U.K.

The composition of siderite is highly variable. The aim of the project is to show how well the chemical and isotopic composition of microbially-precipitated siderite reflects conditions of formation.

Many early diagenetic carbonate concretions previously described (e.g. Curtis *et al* 1986) were probably precipitated by microbially-mediated reactions. The use of stable isotopic data for such material is dependent on a knowledge of the effect of temperature upon fractionation processes. However, whilst equilibrium fractionation of oxygen isotopes between siderite and water has been measured down to 33°C (Carothers *et al* 1988), extrapolation to lower temperatures may not be wholly valid. Furthermore, inorganic measurements may not be applicable to microbiological systems.

The recent isolation of a specific iron-reducing microorganism, *Geobacter metallireducens*, has provided a unique opportunity to study microbial siderite precipitation. *Geobacter* can be cultured anaerobically in the laboratory using acetate as an organic substrate and amorphous FeOOH as an electron acceptor. The acetate is completely oxidised to CO<sub>2</sub>, with concurrent iron reduction and extracellular siderite precipitation.

Rhombohedral siderite crystals up to 25 microns in size have been precipitated over a range of temperatures (18-40°C). Chemical data produced from microprobe analysis to date show that the incorporation of trace elements such as Mn is dependent on the rate of growth rather than the temperature. This is compatible with results for inorganically precipitated ferroan calcites.

Preliminary stable isotopic data show that microbially precipitated siderite, the closest analogue to ancient concretions, has a different fractionation pattern from the established inorganic data. Further work is necessary to fully understand the systematics involved and calibrate the system.

Carothers, W.W., Adami, L.H., and Rosenbauer, R.J., 1988, Experimental Oxygen Isotope Fractionation Between Siderite-Water and Phosphoric Acid Liberated CO<sub>2</sub>-Siderite. *Geochim. Cosmochim. Acta*, v.52, p. 2445-2450.

Curtis, C.D., Coleman, M.L., and Love, L.G., 1986, Pore Water Evolution During Sediment Burial From Isotopic and Mineral Chemistry of Calcite, Dolomite and Siderite Concretions. *Geochim. Cosmochim. Acta*, v. 50, p. 2321-2334.

**PALEOPROTEROZOIC METAMORPHISM  
AT THE BASE OF THE NORTH AMERICAN  
CRATON REVEALED THROUGH U-PB  
ZIRCON DATING OF GRANULITE-FACIES  
XENOLITHS**

**MOSER, D.E.** and **HEAMAN, L.M.**, Jack  
Satterly Geochronology Laboratory, Royal  
Ontario Museum, Toronto, Ont., Canada M5S  
2C6

Granulite-facies xenoliths isolated from a Jurassic kimberlite pipe near Kirkland Lake, Ontario represent fragments of the lower crust that underlies Archean rocks of the southern Canadian Shield. Sixteen U-Pb analyses of single-grain and multi-grain zircon fractions from three xenoliths fall into two age groupings. The older group includes two metamorphic grains, from different xenoliths, that are concordant at  $2580 \pm 2$  Ma. Metamorphic conditions in the lower crust at 2580 Ma must therefore have been sufficient to cause growth of, or total Pb-loss from, zircon at this time. Most of the zircon grains define a second grouping of model ages that range between 2520 Ma and 2432 Ma, with the least discordant data clustering at  $2495 \pm 10$  Ma. These are interpreted to result from a second, previously unrecognized, crustal-scale metamorphic event that is related to re-setting of K-Ar mica ages in the upper crust, the deposition of the lower Huronian supergroup, and the opening of the Matachewan ocean along the southern margin of the Superior Province. Sm-Nd dating of garnet and clinopyroxene in textural equilibrium with metamorphic zircon is in progress to examine whether these minerals preserve either Archean protolith ages or ages which indicate Proterozoic growth and/or re-setting. The ca. 2.5 Ga lower-crustal metamorphic episode identified in this study is coeval with high heat-flow and re-melting of continental crust in other Archean Provinces of North America as well as in six other Archean cratons. Together, this implies significant transfer of thermal energy from the mantle to Archean continental nuclei in the Paleoproterozoic.

**K - AR AGES AND GEOCHEMISTRY OF THE  
MARIANA TROUGH BASALTS**

Mu, Z., LIU, C. & HUANG, B., Dept. of Geol.,  
Peking University, Beijing, 100871, P. R. China

The nine Mariana Trough basalts were collected by the China - Germany cooperation 'SONEE' (Voyage 59) in 7 - 8, 1990 from the places where located between  $14^{\circ}59.16' - 18^{\circ}12.76' N$  and  $144^{\circ}12.66' - 144^{\circ}50.17' E$ . The depth of sampling is from 3314 m - 4498 m. K - Ar age - dating, geochemical analyses on major and trace element, REE and isotope composition have been done. The majority of the basalts are enriched in LIL elements and volatiles and depleted in HES elements like the rocks found throughout MORB, but there is a little difference from N - MORB both in trace elements and in isotope compositions. The results are consistent with published papers. The age ranging is from 2.65 Ma to 10.1 Ma belong to upper Miocene to Pliocene, that means the formed age of the Mariana back arc basin should be older than 10 Ma. A calculated half spreading rate of the Mariana back arc basin should be bigger than 1 cm / yr. In addition to oceanic tholeiite, both altered Peridotite and old oceanic crust are found in the Mariana Trough firstly. The former are enriched in Mg, Cr and Ni, but depleted in Si, Al, Ca and REE. The later has an age of 90 Ma around belong to upper Cretaceous period.

Floyd, P. A., 1990, Oceanic Basalts, Blackie, Glasgow and London, P. 219 - 262.

Hawkins, J. W., Lonsdale, P. F., Macdougall, J. D. and Volpe, A. M., 1990, Petrology of the axial ridge of the Mariana Trough backarc spreading center: Earth and Planetary Science Letters, V. 100, P. 226 - 250.

Volpe, A. M., Macdougall, J. D., Lugmair, G. W. and Hawkins, J. W., 1990, Fine-scale isotopic variation in Mariana Trough basalts: evidence for heterogeneity and a recycled component in backarc basin mantle: Earth and Planetary Science Letters, V. 100, P. 251 - 264.

**<sup>40</sup>AR/<sup>39</sup>AR GEOCHRONOLOGY OF LATE CRETACEOUS VOLCANIC EVENTS IN THE CANADIAN ARCTIC ISLANDS: ARCTIC BIOTIC HETEROCHRONEITY REVISITED**

**MUECKE, Gunter K., REYNOLDS, Peter H.,** Dept. of Earth Sciences, Dalhousie University, Halifax, NS, B3H 3J5, Canada, and **MACRAE, R.A., NUNEZ-BETELU, L.** Koldo, Dept. of Geology and Geophysics, University of Calgary, Calgary, AB, T2N 1N4, Canada.

The Late Cretaceous depositional history of the northeastern Sverdrup Basin, Canadian Arctic islands, features episodic volcanism interspersed with an almost continuous succession of clastic sediments. Magmatism accompanied extensional phases of basin development in the Sverdrup Basin and the adjacent Canada Basin of the Arctic Ocean. Volcanic products include tholeiitic flood basalts, bimodal suites of alkali basalts associated with rhyolites and trachytes, as well as widespread ash horizons (bentonites). Sedimentary sequences include both marine and terrestrial organic-rich mudstones and shales that have yielded rich palynomorph assemblages for biostratigraphic age determination.

<sup>40</sup>Ar/<sup>39</sup>Ar plateau ages have been obtained for whole-rock basalt, rhyolite and trachyte samples, as well as single-grain and composite high-precision determinations on sanidines. Sample locations were chosen to provide unambiguous relations to palynologically studied sites. While argon spectra from the older volcanics (Late Albian) show some disturbances that may be attributed to alteration and later thermal events, all younger samples provide excellent concordant spectra.

Comparison of the absolute radiometric dates with biostratigraphic determinations yields discrepancies of between 2-5 Ma. For both the Cenomanian - Turonian and the Campanian - Maastrichtian boundaries radiometric dates appear to be older than biostratigraphic determinations. Previous investigators (Hickey et al., 1983) have noted age disparities, based on questionable paleomagnetic evidence, between Arctic and lower latitude biotas in this time span, and attribute it to biotic heterochroneity. We re-examine this hypothesis in the light of our new paleontological and radiometric data. Paleofloral provincialism of some of the Late Cretaceous age-diagnostic pollen genera may explain their earlier appearance at high latitudes. Other possible explanations for the discrepancy include an error in the currently accepted biostratigraphy, errors in the current time scale, or some combination of these.

Hickey, L.J., West, R.M., Dawson, M.R., and Choi, D.K., 1983, Arctic terrestrial biota: Paleomagnetic evidence of age disparity with mid-northern latitudes during the Late Cretaceous and Early Tertiary: *Science*, v.221, p.1153-1156.

**CALIBRATION OF TIME SCALE AND SEDIMENTARY CYCLES: HIGH RESOLUTION SINGLE-CRYSTAL U-PB AGE DETERMINATIONS ON MID-TRIASSIC TUFFS OF THE SOUTHERN ALPS**

**MUNDIL, R.<sup>1)</sup>, BRACK, P.<sup>2)</sup>, MEIER, M.<sup>1)</sup>, and OBERLI, F.<sup>1)</sup>**, 1) Isotope Geochemistry, 2) Department for Earth Sciences, ETH Zurich, CH-8092 Zurich, Switzerland

Carbonate platforms of the Dolomites (Southern Alps) display conspicuously regular cyclic stratal patterns ("Latemar Limestone"). The platform successions can be correlated in detail with pelagic sediments ("Buchenstein Beds") on the basis of large scale geometries and biostratigraphy (Brack & Rieber, 1993). The occurrence of multiple phenocryst-rich volcanoclastic layers in the pelagic successions offers a unique opportunity for a) time scale calibration and b) quantitative evaluation of cyclicity in the age-equivalent platform carbonates. High-frequency sea level fluctuations with Milankovitch characteristics have been suggested as primary control for these cycles (Goldhammer et al., 1987). This would imply a time span of 12 Ma for the lower part of the Ladinian alone. However, this is in conflict with current time scales, which suggest a duration of 4-7 Ma for the entire Ladinian stage.

For the present study, samples of volcanoclastic layers were collected from biostratigraphically well documented and correlated South Alpine sections. High resolution single zircon analytical techniques (Oberli et al., 1989) have been applied so far on zircon grains from a single layer in the Buchenstein Beds at Bagolino (Brescian Alps). Biostratigraphically, this horizon belongs to the Ladinian *Protrachyceras gredderi*-zone. Selected zircons were carefully examined using transmitted light microscopy in order to exclude potential core bearing crystals. Abrasion techniques were applied to minimize discordance by secondary lead loss. Four well abraded zircon grains reproduced <sup>206</sup>Pb/<sup>238</sup>U ages within a narrow time interval of 238.6-239.2 Ma yielding a mean age of 238.8 ± 0.4 Ma (95% confidence level ext.). Slightly younger apparent U-Pb-ages (223-235 Ma) were obtained on non- to moderately abraded zircons and demonstrate, that age values can be strongly affected by secondary lead loss. Moreover, presence of an inherited core component in one zircon grain is indicated by its older apparent age (246 Ma).

The age of 238.8 Ma for this Ladinian level is in contrast to most time scales. However, this age is compatible with an age of 239.5 Ma for the Anisian/Ladinian boundary suggested by Harland et al. (1989). Interestingly, the database for the latter time scale differs only slightly from data used for previous time scales. Furthermore, the result is in conflict with K-Ar- and Ar-Ar-ages of Hellmann & Lippolt (1981), who suggested a value of 232 Ma for the Anisian/Ladinian boundary based on data from slightly older volcanoclastic layers in the Southern Alps.

Considering the platform carbonate cycles and their biostratigraphic calibration, the present result may imply a periodicity that is significantly shorter than suggested previously.

Brack, P., and Rieber, H., 1993, *Eclogae geol. Helv.*, v. 86, p. 415-527.

Goldhammer, R.K., Dunn, P.A., and Hardie, L.A., 1987, *Am. J. Sci.*, v. 287, p. 853-892.

Hellmann, K.N., and Lippolt, H.J., 1981, *J. Geophys.*, v. 50, p. 73-88.

Oberli, F., Fischer, H., and Meier, M., 1989, *Abstr. 28th Int. Geol. Congress, Washington D.C.*, v. 2, p. 536-537.

HF-ZR INTERDIFFUSIVITY IN ZIRCON

NAGASAWA, Hiroshi, Dept. Chem. Gakushuin University, Toshima-ku, Tokyo, Japan.

Hf-Zr interdiffusivity in zircon has been determined on hafnon-zircon double-layered crystals using scattered electron image of scanning electron microscope.

The double-layered crystals were prepared by epitaxial overgrowth of zircon on synthetic hafnon (HfSiO<sub>4</sub>) seed crystal. After diffusion annealing diffusion profiles were determined by scattered electron image (SEI) contrast by calibrating with synthetic crystals of hafnon-zircon solid solution with known compositions.

Diffusion profiles are shown in Fig. 1 and the calculated diffusion coefficients are tabulated in Table 1. In a previous work only an upper limit value was obtained by the energy dispersive X-ray analysis which has a spatial resolution of a few μm (Suzuki et al, 1992). SEI with much better spatial resolution offered extremely low D values for zircon.

The observed low D values for Hf-Zr indicate that the isotopes of U and Th with the same ionic charge and similar ionic sizes have similarly low D values in zircon. This implies the daughter isotopes of U and Th would also have low D values in zircon, although the lower ionic charges may result somewhat higher D values.

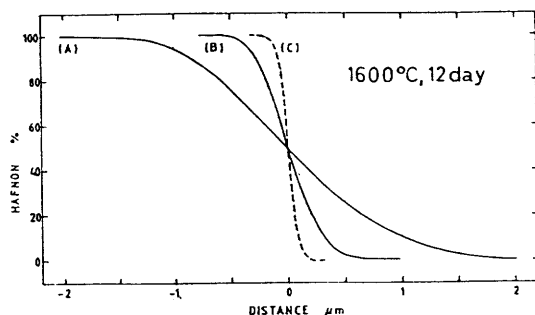


Figure 1. Diffusion profiles. (A) ⊥c (a or b), (B) //c, (C) ⊥c, before annealing.

Temperature (°C)	Axis	D, cm <sup>2</sup> ·sec <sup>-1</sup>
1600	⊥c	2 × 10 <sup>-15</sup>
	//c	~ 2 × 10 <sup>-16</sup>
	⊥c	~ 1 × 10 <sup>-15</sup> (1)
1550	⊥c	~ 2 × 10 <sup>-16</sup>

(1) Suzuki et al (1992) G.J. 26, 99.

PRODUCTION OF ACIDIC ROCKS BY PURE DIFFERENTIATION OF A DEPLETED MANTLE SOURCE: A COMBINED U-PB-ZIRCON, PB-PB-ND ISOTOPE STUDY ON THE MASIRAH OPHIOLITE / OMAN

NÄGLER, T.H.F., FREI, R., Min. -Pet. Inst., Lab. of Isotope Geology, Bern, 3012, Switzerland

Field- and sedimentary evidence within the Masirah ophiolite complex / Oman establish at least three different magmatic events:

- 1) generation of oceanic crust >150 Ma
- 2) production of alkali volcanites and
- 3) emplacement of acidic magmas, including real granites.

$E_{Nd}[150Ma]$  values of a variety of different rock types (i.e. troctolite, different gabbros, anorthosite, dolerite, pillow basalt, pegmatitic gabbro and granite) range from +7 to +9.7. The respective Nd-model age calculations indicate derivation from upper mantle somewhere between 160 Ma and 300 Ma. The poor resolution is inherent in the system, as young model ages are always strongly dependent on the used depleted mantle model and error magnification is large.

U-Pb zircon data of a trachyte from the alkali volcanic suite give a magmatic age of 123 ± 2 Ma, whereas two granites from the third stage yield 112 ± 10 Ma and 113 ± 11 Ma. Correspondingly corrected Pb-Pb data point to a uniform MORB-type source.

The tectonic setting of the acidic rocks and their initial Pb and Nd isotopic composition as well as the lack of correlation between Nd contents and isotopic composition exclude a significant admixture of continental material, although the sensitivity of the isotopic data towards such a contamination is large due to the extremely low Pb, U and REE concentrations (Pb: 0.008 ppm to 2.55; U: 0.002 ppm to 1.74; Nd: 0.16 ppm to 65 ppm.).

The absence of continental contribution is in sharp contrast to such contaminations in calc-alkaline plutonic suites within the Semail ophiolite (mainland of Oman; Briqueu et al., 1991).

At the present state of the investigation, the evolution of the ophiolite is assumed to have taken place as follows:

Partial melting of upper mantle material and generation oceanic crust occurred >150 Ma. Different parts of this crust have been remelted at about 123 (probably due to a hot spot activity with possible addition of new oceanic crust) and/or at c. 112 Ma without addition of material from the continental crust.

Moreover, the present study reveals the likelihood of granite genesis through pure remelting and subsequent differentiation of pre-existing oceanic crust.

Briqueu, L., Mével, C. & Boudier, F., 1991, Sr, Nd and Pb Isotopic Constraints in the Genesis of Calc-Alkaline Plutonic Suite in Oman Ophiolite Related to the Obduction Process, in: Peters, T. et al. (EDS). Ophiolite Genesis and Evolution of the Oceanic Lithosphere, Ministry of Petroleum and Minerals, Sultanate of Oman, p. 517-542

#### $^{40}\text{Ar}/^{39}\text{Ar}$ GEOCHRONOLOGY OF WHOLE-ROCK BASALTS.

NAUERT, J.L., and GANS, P.B., Dept. of Geology, UCSB, Santa Barbara, CA, 93117

Dating of mafic lavas is extremely important for a wide range of geologic problems (time scale, magnetic reversals, stratigraphic correlations, tectonics, etc.). The  $^{40}\text{Ar}/^{39}\text{Ar}$  method has been increasingly applied to the dating of mafic lavas, but results have been mixed. K-contents of mafic lavas range from <0.1% to >2.0%;  $^{40}\text{Ar}_{\text{atm}}$  ranges over several orders of magnitude, generally around  $10^{-14}$  mol/mg; and age spectra on both plagioclase separates and whole rock chips range from simple plateaus to hump-shaped, U-shaped, or S-shaped spectra. During step heating of whole rocks, maximum radiogenic yields are commonly obtained between 500° and 1000°, with a dip between 700° and 800°. We are attempting to better understand this range of behavior and the systematics of Ar in whole-rock basalts by looking at the effects of initial composition, grain size, and degree of alteration, as well as the effects of various sample preparation and analytical procedures.

Experiments were carried out on a variety of whole-rock basalts and basaltic andesites, ranging from 3 year old glassy sea-floor basalts to Miocene holocrystalline basalts, but focussing on holocrystalline groundmass concentrates. Not surprisingly, highest radiogenic yields are correlated with the highest K-contents and K/Ca ratios, but also depend critically on groundmass grain size, with coarse grained, holocrystalline samples from the interior parts of flows yielding substantially lower  $\%^{40}\text{Ar}_{\text{atm}}$ .

The size fraction of the whole rock separates may have a significant effect on the  $\%^{40}\text{Ar}_{\text{atm}}$  (e.g., a glassy basalt crushed to 90 $\mu$  showed a fivefold increase in  $^{40}\text{Ar}_{\text{atm}}$ /mg over a split crushed to ~60 $\mu$ , though the amount of  $^{40}\text{Ar}^*$ /mg remained unchanged).

HCl etching to remove calcite and HF etching to remove glass and alteration products may substantially improve K/Ca ratios and remove unwanted phases, but this benefit appears to be outweighed by a dramatic increase in  $\%^{40}\text{Ar}_{\text{atm}}$ , thereby lowering overall and maximum radiogenic yields (e.g., HCl etching resulted in a sevenfold increase in  $^{40}\text{Ar}_{\text{atm}}$ /mg).

Boiling to remove loosely-held atmospheric argon, followed by air drying or vacuum drying yielded no significant reduction of atmospheric argon.

Separation of the most magnetic one-third to one-half of whole rock splits tends to decrease the amount of  $^{40}\text{Ar}_{\text{atm}}$  by removing low-K phenocrysts, calcite, and alteration products, and increase  $^{40}\text{Ar}^*$  by concentrating the K-rich groundmass, with significant improvement in analytical results.

In addition to the sample preparation, correctly designed heating schedules can have a significant effect on the release of Ar. Cyclic heating schedules can greatly increase the radiogenic yield of the higher temperature (>800°) steps and help separate the atmospheric from the radiogenic Ar components.

Although our experiments to date are limited, we have found that the best analytical results for whole rock basalts are obtained from fresh, coarse grained holocrystalline samples, coarsely crushed, magnetically separated to concentrate the K-rich groundmass, and degassed using a cyclic heating schedule. Acid treatments generally do more harm than good. For example, when we follow these procedures on Miocene whole rock basalts from southern Nevada, we commonly get >95% radiogenic yields over much of the spectrum, and estimated uncertainties in plateau and isochron ages of <0.2%.

#### SHRIMP U - Pb ZIRCON DATING OF ARCHAEOAN GREENSTONE SEQUENCES FROM THE EASTERN GOLDFIELDS, WESTERN AUSTRALIA

NELSON, D.R., Geological Survey of Western Australia, East Perth, WA, 6004, and Curtin University of Technology, GPO Box U1987, Perth, WA, 6000, Australia, SWAGER C.P., WITT W.K., GRIFFIN T.J., WYCHE S. and SMITHIES H. Geological Survey of Western Australia, East Perth, WA, 6004, Australia.

Detailed mapping by the GSWA in the Eastern Goldfields Province of the Archaean Yilgarn Craton has delineated a series of fault-bounded tectonostratigraphic terranes. The westernmost Kalgoorlie Terrane consists of ultramafic and mafic flows and felsic volcanics with relatively simple and coherent regional stratigraphy. The eastern terranes have diverse and complex stratigraphic sequences comprised predominantly of laterally discontinuous basaltic and ultramafic units and proximal volcanoclastic units. High-precision U - Pb zircon dating using the recently-commissioned Perth SHRIMP indicates that felsic volcanoclastic rocks within the Kalgoorlie and eastern terranes were deposited contemporaneously at 2683  $\pm$  5 Ma. Similar emplacement ages of 2690 - 2680 Ma have been reported for early (pre-D2) granitoids (e.g. Hill et al. 1992). Geochemical and isotopic data indicate that the early granitoids and felsic volcanics were derived from similar sources and may have been cogenetic. Multiply-deformed monzogranite- to granodiorite gneisses are exposed at localities near the western, southern and eastern margins of the Eastern Goldfields Province greenstones. These gneisses typically preserve upper amphibolite facies mineral assemblages, are characterised by low zircon abundances, complex zircon age populations and contain zircons as old as c. 3300 Ma. Fragments of similar gneisses probably formed part of the basement to the greenstones and provided the source rocks from which the granites and felsic volcanics were derived.

The following evolutionary model of the formation of the Eastern Goldfields granite-greenstone terranes is consistent with the available field and geochronological constraints. At c. 2710 - 2690 Ma, asymmetric rifting, mainly by N - S-trending normal faulting, of pre-existing granitic and gneissic crust resulted in the development of a series of adjacent shallow basins, into which predominantly basaltic and ultramafic volcanics were deposited. At c. 2685 Ma, felsic volcanoclastic rocks were erupted from numerous volcanic centres and early (pre-D2) granitoids were emplaced mainly as thick sheets into the base of the greenstone sequences. This igneous activity may have been a consequence of heating of the base of the crust during crustal thinning. This was followed at c. 2675 - 2665 Ma by regional (D2) compression involving reactivation of early structures. Additional episodes of granitoid emplacement have been identified at c. 2665 - 2660 Ma and c. 2630 - 2600 Ma (Hill et al. 1992).

Tectonic models advocating the involvement of mantle plumes (e.g. Hill et al. 1992) cannot account for the compressional regime responsible for D2 structures and the volcanic rocks lack many of the diagnostic geochemical features found in the volcanic rocks of modern subduction zones. An active continental margin back-arc basin setting offers the closest modern analogous tectonic setting.

Hill R.I., Chappell B.W., and Campbell I.H., 1992, Late Archaean granites of the southeast Yilgarn Block, Western Australia: age, geochemistry, and origin: *Trans. R. Soc. Edinburgh: Earth Sciences*, v. 83, p. 211-226.

AGE AND ORIGIN OF THE LATE ARCHAEOAN DARLING RANGE BATHOLITH, SOUTH-WEST YILGARN CRATON, WESTERN AUSTRALIA

NEMCHIN, A.A. and PIDGEON, R.T., School of Applied Geology, Curtin University of Technology, Perth, 6001, Western Australia.

A major problem of Archaean geology is the origin and mode of emplacement of enormous masses of granitoids. Our aim in this study was to investigate the genesis of a typical Late Archaean granite batholith, the Darling Range Batholith, located in the south western part of the Yilgarn Craton of Western Australia. This batholith, which occurs over an area of more than 100 x 300 hundred kilometres, varies transitionally from porphyritic to even medium and coarse grained varieties with late stage leucocratic and pegmatite dykes. Granite samples from the central area of the batholith show relatively small chemical variations. Trends observed were decreasing TiO<sub>2</sub>, Al<sub>2</sub>O<sub>3</sub>, MgO, CaO, Sr, Zr and increasing Rb, La/Yb, Eu/Eu\* with increasing silica. Small variations in the chemical composition can be explained by crystallization of feldspars and to a lesser extent some accessory minerals.

Preliminary dating of the granites, using conventional U-Pb zircon and titanite analyses, gives the age of 2625±15 Ma. Epsilon Nd for 2.6 Ga calculated for 20 granite samples varies from 0 to -3.5, with the average -2. The average Depleted Mantle model age is 3.12 Ga, with a spread from 3.00 to 3.25 Ga. This spread as well as the chemical variations limit the possibility of mixing of chemically contrasting source components with different ages and we interpret the age of 3.12 Ga as close to the formation age of the granite source.

The low initial <sup>87</sup>Sr/<sup>86</sup>Sr (0.7009±35, 2 sigma of the mean) suggests low Rb/Sr ratios in the source rocks. This is estimated to be less than 0.2, based on ages of 2.6 Ga and 3.12 Ga for the granite and its source, and the value of mantle <sup>87</sup>Sr/<sup>86</sup>Sr at 3.12Ga. This level of Rb/Sr ratio is found in tonalitic rocks, whereas most sedimentary rocks are generally much higher. One present evidence the large mass of post tectonic granites of the South-West Yilgarn Craton appears to have formed at 2.6Ga by the melting of relatively homogeneous 3.12 Ga old tonalitic crust.

WHOLE-ROCK AND MINERAL U-Th-Pb SYSTEMATICS IN LOWER CRUSTAL XENOLITHS FROM THE BALTIC, ANABAR AND CANADIAN SHIELDS – EARLY ARCHAEOAN LITHOSPHERIC DIFFERENTIATION AND EVOLUTION.

NEYMARK, L.A., Inst. of Precamb. Geol. & Geochron., St. Petersburg, Russia, PACES, J.B. and ZARTMAN, R.E., U.S. Geol. Surv., Box 25046, DFC, Denver, CO, USA 80225

Access to the lowermost continental crust is limited to crustal xenoliths in basalts and kimberlites. Xenolith suites from Archaean cratons are noticeably under-represented in published studies. In this paper, we summarize new data for the Archaean lower crust represented by xenoliths from Paleozoic and Mesozoic kimberlites erupted through the Baltic (southern Kola Peninsula), Anabar (eastern Siberian), and Canadian (Superior province in northern Michigan) shields. Mafic granulites typically contain subequal proportions of Plg, Cpx, and Gt, but modes grade into both amphibolites and eclogites. Most granulites are mafic, and although some have major element contents similar to basaltic liquids, others clearly do not have magmatic compositions. Occasional Plg-Gt granulites have intermediate compositions. Peak temperatures and pressures are estimated from 700 to 1050°C and 8 -15 kbar.

Whole-rock and mineral separates were analyzed for Pb isotopes and U, Th, and Pb concentrations. Most whole rocks have low U contents (0.05-0.5 ppm) and K/U ratios from 1.6 to 23.6x10<sup>4</sup>. Despite the U depletion, observed Th/U ratios are not significantly elevated. Typically, xenoliths have low measured μ (<sup>238</sup>U/<sup>204</sup>Pb) values (0.5-8.5); however, μ values as high as 20 are observed. The total range of whole rock <sup>206</sup>Pb/<sup>204</sup>Pb is 14.7 to 23.3. All but one of the whole-rock Pb compositions from Michigan granulites plot above the Stacey-Kramers (S-K) <sup>206</sup>Pb/<sup>204</sup>Pb-<sup>207</sup>Pb/<sup>204</sup>Pb growth curve, in contrast to Baltic and Siberian xenoliths, which plot below the S-K curve.

Lead isotopic data from hand-picked, acid-leached mineral separates do not form well-defined linear arrays on Pb/Pb plots suggesting extended or complex cooling histories and variable blocking temperatures. Garnet-dominated Pb/Pb mineral ages group around 2.6-2.7, 1.8-2.1 and 0.9-1.5 Ga. Rutile U-Pb systematics date the host kimberlite ages. Some Siberian and Baltic garnets yield concordant U-Pb ages in the range of 1.4-2.6 Ga. Michigan garnets are discordant and reflect a thermal disturbance at about 1.1 Ga, also recorded by U-Pb ages for rims of metamorphic zircons. Lead compositions of many Plg separates from all three localities plot above the S-K growth curve -- suggesting an early history in a high-μ environment (μ = 16 from 3.7 to 2.7 Ga in one case). These data require that protoliths originated from ancient crustal differentiation events and imply substantial time between protolith formation and the granulite-forming event (granite melt extraction) that resulted in U depletion. In contrast, some mafic granulites display mantle-like Pb isotopic characteristics and may represent younger additions of basaltic magma into the lower crust. Collectively, Pb isotopes and supporting data imply that both basalt underplating and intra-crustal differentiation of older crust are important processes affecting the formation and evolution of the lower continental crust.

## MASS SPECTROSCOPY AND THE EARLY DAYS OF ISOTOPE GEOLOGY

Nier, A. O., School of Physics and Astronomy,  
University of Minnesota, Minneapolis, MN 55455,  
USA,

The application of mass spectroscopy to problems of geological interest owes its existence to the earlier application to basic problems in atomic and nuclear physics, and the simultaneous development of improved electronic, vacuum, and instrument techniques.

Prior to 1936 the isotopic composition of lead and uranium were uncertain. Determinations of geological age by the uranium-lead method relied on chemically determined atomic weights to ascertain the common lead content of the lead found in uranium minerals. The precise determination of lead isotope abundances [1] showed that common lead varied widely in spite of a near constant atomic weight, and led to the conclusion that the age of the solar system was approximately 4.5 by. [2]. Determination of the  $^{235}\text{U}/^{238}\text{U}$  abundance ratio [3] made possible the development of the  $^{207}\text{Pb}/^{206}\text{Pb}$  method for age determinations [4]. The discovery of  $^{40}\text{K}$  and the subsequent identification of  $^{40}\text{Ar}$  in potassium minerals led to the demonstration that the K/Ar method was feasible for age determinations [5].

Whereas early investigators had to construct their own instruments, following WW II commercial instruments became available, opening the field to many investigators and new applications, and mass spectrometers became routine tools for geological and planetary research.

[1] Nier, A.O. (1938) *J. Am. Chem. Soc.* **60**, 1571.  
[2] Patterson, C. (1956) *GCA* **10**, 230. [3] Nier, A.O. (1939) *Phys. Rev.* **55**, 150. [4] Nier, A.O. (1939) *Phys. Rev.* **55**, 153. [5] Aldrich, L.T. and Nier, A.O. *Phys. Rev.* **74**, 876.

## EVIDENCE FROM Nd ISOTOPIC SYSTEMATICS IN PERIDOTITES FOR THE TIMING OF MANTLE LITHOSPHERE FORMATION BENEATH NORTHERN MEXICO

Nimz, G.L., Isotope Geochemistry Section, Lawrence Livermore Laboratory, Livermore, CA, 94550 and Cameron, K.L., Department of Earth Sciences, University of California, Santa Cruz, CA 95064

Peridotite and orthopyroxenite xenoliths of the Cr-Diopside Group are found in ~2 Ma basanitic cinder at the La Olivina locality in northernmost Mexico. The samples form continuous arrays on chemical and isotopic co-variation diagrams, have similar coarse-granular textures, and have similar calculated mantle equilibration temperatures (~950-1050°C); all of which suggest that they existed in close proximity while within the upper mantle. Sr and Nd isotopic compositions of acid-washed diopsides ( $\epsilon_{\text{Nd}} = +1.9$  to  $+13.3$ ;  $^{87}\text{Sr}/^{86}\text{Sr} = 0.70220$  to  $0.70328$ ) indicate long-term Rb and Sm depletion similar to asthenospheric (MORB) mantle. However, Pb isotopic compositions are generally higher in  $^{207}\text{Pb}$  relative to  $^{206}\text{Pb}$  than is typical of MORB ( $^{206}\text{Pb}/^{204}\text{Pb} = \sim 18.53-19.40$ ;  $^{207}\text{Pb}/^{204}\text{Pb} = \sim 15.58-15.61$ ). The peridotites contain veins of pyroxenite that appear to have resulted from mid-Cenozoic magmatic activity in the La Olivina region. Chemical and isotopic evidence suggests that this mid-Cenozoic magmatism also produced chemical alteration in several of the peridotites. It is therefore believed that the peridotites were in-place and attached to the continent prior to the Cenozoic, and certainly before regional late-Cenozoic Basin-and-Range extension. This is in distinction to recent studies that suggest on the basis of basalt isotopic systematics that the region is underlain by recently emplaced asthenospheric mantle. Modeled chronological data from the peridotites can be related to known events in the geologic record of southwestern North America.

The peridotite suite as a whole is extremely depleted in both clinopyroxene and incompatible trace element concentrations ( $\text{Sm}/\text{Nd} = 0.5$  to  $0.8$ ;  $[\text{Nd}] = 1.19-2.69$  mg/g). Isotopic systematics require more than one depletion episode, but can be modeled as the result of just two melt extraction episodes. Calculations indicate that melt extraction during the second episode may have been about 10-15% of the existing mass. Chronologic modeling suggests that the second-stage melting event occurred no longer than ~280 Ma ago. Enrichment chronologies suggest the melting occurred prior to the mid-Cenozoic magmatism in the region, ~30 Ma. Nd isotopic similarities between the peridotites and late-Paleozoic arc-related basalts reported to the southeast of La Olivina suggest that the large-scale melting event may have produced these basalts. This arc may have been related to the Ouachita collisional tectonism in the region. The calculated magnitude of the melting implies that the La Olivina mantle was asthenospheric at the time. Increased buoyancy of the newly depleted asthenosphere coupled with a delamination of previously-existing lithosphere, suggested by other studies, may have led to the accretion of the La Olivina mantle to the crust by the end of the Ouachita orogeny. The La Olivina mantle at that time became lithospheric in character and the peridotites have apparently undergone little or no melting since.

## COSMOGENIC PRODUCTION OF $^{10}\text{Be}$ AND $^{26}\text{Al}$ ON THE SURFACE OF THE EARTH AND UNDERGROUND

NISHIZUMI, K., Space Sciences Lab, Univ. of Calif., Berkeley, CA 94720, U.S.A., Finkel, R.C., Caffee, M.W., Southon, J.R., Lawrence Livermore National Lab, Livermore, CA 94551, U.S.A., Kohl, C.P., Arnold, J.R., Dept. of Chemistry, Univ. of Calif., San Diego, La Jolla, CA 92093, U.S.A., Olinger, C.T., Poths, J., Los Alamos National Lab, Los Alamos, NM 87545, U.S.A., Klein, J., Dept. of Physics, Univ. of Penn., Philadelphia, PA 19104, U.S.A.

To apply in-situ produced cosmogenic nuclides to the study of the history of earth surface processes, production rates at the surface of the earth and the attenuation length of the production underground must be known. We have extended previous studies of production rates by using both geological and laboratory methods.

(1) Depth profiles of  $^{10}\text{Be}$  ( $t_{1/2}=1.5$  My) and  $^{26}\text{Al}$  (0.71 My) along with  $^{21}\text{Ne}$  in quartz extracted from the vertical face of a quarry in Bandelier Tuff near Los Alamos show a tight fit to a decreasing exponential with depth down to a depth of 500 g/cm<sup>2</sup>. The 1/e attenuation lengths are 159 g/cm<sup>2</sup> for  $^{10}\text{Be}$  and 166 g/cm<sup>2</sup> for  $^{26}\text{Al}$ .  $^{10}\text{Be}$  and  $^{26}\text{Al}$  produced by cosmic ray muon capture are observed below 500 g/cm<sup>2</sup>. The muon capture contribution are ~80 % of the total production of  $^{10}\text{Be}$  and  $^{26}\text{Al}$  in quartz at 965 g/cm<sup>2</sup>. The muon induced production ratio of  $^{26}\text{Al}/^{10}\text{Be}$  is  $5\pm 1$  in the sample. Surface erosion can yield samples with a high contribution of muon capture production.

(2) Until now geological studies involving cosmogenic nuclides have assumed that production occurs primarily by fast neutron reactions. The existence of muon-induced reactions was realized, but considered to be unimportant. Preliminary experiments indicate that  $^{10}\text{Be}$  and  $^{26}\text{Al}$  production by muon are different than expected. We collected quartz from deep mines (Kamioka and Homestake) at depths of up to several hundred meters below the surface. The production of  $^{10}\text{Be}$  and  $^{26}\text{Al}$  will be compared to the flux of high energy muons at the depth. For  $^{10}\text{Be}$  and  $^{26}\text{Al}$  studies, if the surface erosion rate is lower than 1 m/My ( $10^{-4}$  cm/y), neutron production dominates, but if the erosion rate is higher than 10 m/My, muon interactions become important. This problem has not been addressed in our earlier work. We will discuss the importance of the muon contribution for calculation of erosion rate.

(3) Over 500 kg of H<sub>2</sub>O and ~10 kg of Si targets were exposed to cosmic rays at high altitude (3246 m for H<sub>2</sub>O, 3246 m and 4298 m for Si) and sea level for a number of years. Be was extracted from H<sub>2</sub>O and Al was extracted from Si. The  $^7\text{Be}$  ( $t_{1/2}=53$  day) production rate is lower than previously reported values but the production rate ratio at 3246 m to sea level is in good agreement with the theoretical model. The production rate ratio of  $^{10}\text{Be}/^7\text{Be}$  from Oxygen is  $0.53\pm 0.03$  (preliminary result). The concentration of  $^7\text{Be}$ ,  $^{10}\text{Be}$ , and  $^{26}\text{Al}$  will be compared to the production rates obtained from measurements on geological samples and from theoretical calculation.

## U-Pb GEOCHRONOLOGY OF THE CORDILLERA REAL AND EL ORO PROVINCES, ECUADOR.

NOBLE, S.R., NERC Isotope Geosciences Laboratory, Keyworth, Nottingham, NG12 5GG, UK., ASPDEN, J., JEMIELITA, R., and LITHERLAND, M., British Geological Survey, Keyworth, Nottingham, NG12 5GG, UK.

The Cordillera Real (CR) and El Oro Provinces (EP) comprise part of the metamorphic "basement" of the northern Andes. The CR and EP consist mainly of metasedimentary rocks and migmatites cut by ca. 200 Ma S-type and later I-type dioritic and granitic batholiths. Major structures in the EP are currently oriented orthogonal to structures in the CR. Prior to this study key unresolved questions were: (1) the crystallization age of the S- and I-type granitoids in the CR and EP, given there is widespread and variable resetting of K-Ar and Rb-Sr systems; (2) the age of the Piedras metagabbros of the EP (published K-Ar ages range from 74 to 743 Ma); and (3) were the EP and CR originally part of the same terrane?

Concordant zircon and monazite ages of  $227.3 \pm 2.2$  Ma and  $227.5 \pm 1$  Ma for the Tres Lagunas batholith (CR) and the Marcabelli pluton (EP), respectively, show that S-type granitoids in the CR and in the EP are contemporaneous. Multi-grain fractions of strongly abraded rounded Tres Lagunas >10 % discordant zircons yield 454, 627 and 773 Ma  $^{207}\text{Pb}/^{206}\text{Pb}$  ages. Strongly abraded individual Marcabelli zircon cores are 0-10% discordant, giving  $546 \pm 3.3$  Ma,  $2220 \pm 2.1$  Ma, and  $2876 \pm 1.8$  Ma  $^{207}\text{Pb}/^{206}\text{Pb}$  ages. The ages of inherited zircons together with chemical, Sr-, and Nd- isotope evidence indicate significant contribution of older crust in 227 Ma granitoid genesis.

A  $221 \pm 18/-16$  Ma concordant zircon age is obtained from the Piedras intrusion. Hence, mafic intrusive activity is much earlier than anticipated, and accompanied granite emplacement. Latest I-type intrusive activity in the CR is constrained by a  $142.7 \pm 1$  Ma concordant zircon age for the Azafran batholith, revised from a 120 Ma Rb-Sr age.

The similarity of field and geochemical characteristics of EP and CR lithologies suggested they were parts of the same terrane before ca. 140 Ma. These data together with new U-Pb isotope data support the following conclusions. (1) S-type intrusions and host metasediments in the EP and CR were likely contiguous at 227 Ma and that the two regions were subsequently tectonically separated. (2) Components of the crustal protoliths of the S-type granitoids may be derived from the Amazonian and Guyana Shields together with younger more locally-derived material. This is supported by Nd  $T_{DM}$  ages of 1400-1600 Ma for metasediments from EP and CR suggesting sediment sources were mainly late Precambrian crust with some older components. Similar  $T_{DM}$  ages published for suspect terranes in Mexico suggests a connection with the EP and CR prior to the break-up of Gondwana. (3) K-Ar ages are often profoundly disturbed in the EP and CR, e.g. Piedras. Rb-Sr isochrons are also reset, typically being 20 Ma younger than U-Pb ages for the same intrusions.

## EXTENSIONAL TECTONIC EVOLUTION OF EASTERN TANZANIA FROM APATITE FISSION TRACK THERMOCHRONOLOGY

NOBLE, W.P., Foster, D.A. & Gleadow, A.J.W.  
Victorian Institute of Earth and Planetary Sciences,  
School of Earth Sciences, La Trobe University,  
Bundoora, Victoria, 3083, Australia.

The basement terrain of eastern Tanzania shows evidence of nascent rift development. Apatite fission track data elucidates the Mesozoic and Cenozoic structural evolution of the region, and has implications for processes involved in the initial stages of continental extension.

Apatite fission track thermochronology from 25 samples of basement rocks along an east-west transect, from Dar es Salaam to Dodoma, reveal a range in apatite fission track ages and mean confined track lengths from  $48 \pm 3$  to  $211 \pm 11$  Ma and  $11.6 \pm 0.7$  to  $14.1 \pm 0.2$   $\mu\text{m}$  respectively. The broad range reflects a protracted low temperature cooling history for the region with tectonism from early Permian to Recent times.

The youngest apatite fission track ages range from  $48 \pm 3$  to  $87 \pm 6$  Ma and occur in the vicinity of boundary faults between mountain blocks and Karoo to early Tertiary sedimentary basins. The relatively long mean confined track length of  $14.1 \pm 0.2$   $\mu\text{m}$  for one sample indicates that rapid cooling (from temperatures  $> 120^\circ\text{C}$  to  $< 60^\circ\text{C}$ ) occurred at 60 - 65 Ma. One sample with an age of  $48 \pm 3$  Ma and mean track length of  $13.8 \pm 0.2$   $\mu\text{m}$  suggests a later stage of final cooling, probably during Miocene times.

Samples collected away from the boundary faults show a range of ages from  $91 \pm 6$  to  $221 \pm 11$  Ma. The relatively long mean confined track length of  $13.7 \pm 0.2$   $\mu\text{m}$  for a sample with an apatite fission track age of  $103 \pm 5$  Ma indicates an episode of relatively rapid cooling during the Early Cretaceous.

Samples from similar elevations along parts of the east-west transect through the Uluguru and Ukuguru mountains display vastly different apatite fission track ages. The pattern of ages suggests that high angle block faulting was a fundamental mechanism in the Mesozoic and Cenozoic tectonic development of eastern Tanzania.

Apatite fission track age and mean confined track length information from the transect show periods of slow cooling punctuated by at least two periods of relatively rapid cooling from temperatures greater than  $120^\circ\text{C}$  to temperatures below  $60^\circ\text{C}$ . The results suggest cooling events at  $\sim 110$  Ma and  $\sim 65$  Ma, which were probably caused by denudation at rates  $> 30$  m/m.y. Normal faulting related to extension throughout Africa during Cretaceous time led to the development of sedimentary basins and adjacent horst blocks, and caused extensive regional denudation.

## ANNEALING CHARACTERISTICS OF SPONTANEOUS AND INDUCED FISSION TRACKS IN THE FISH CANYON TUFF ZIRCON

O'BRIEN, ALUN Research School of Geological Sciences,  
Fission Track Research Group, University College London,  
Gower Street, London, WC1E 6BT, England.

The aim of this study is to determine the annealing characteristics of fission tracks in zircon under laboratory conditions and experimental time periods, and to use this data to mathematically describe the annealing process. It may therefore be possible to determine and model temperatures needed to cause annealing over geological time periods.

The Fish Canyon zircon was chosen for its relatively low spontaneous track density and since it is already used as an age standard. A number of 1, 10 and 100 hour isochronal annealing experiments were carried out on both spontaneous and induced tracks. For the induced aliquot, zircons were heated to  $1000^\circ\text{C}$  for 1 hour to remove spontaneous tracks, and then irradiated with a fluence of  $1 \times 10^{15}$  ncm. The variation in track density with horizontal confined track length was measured at various temperatures between  $400^\circ\text{C}$  and  $750^\circ\text{C}$ . Both etching time and anisotropy increase for the spontaneous samples annealed above  $550^\circ\text{C}$  because of the loss of accumulated alpha damage. The etching time for the induced samples remains the same as that for the spontaneous samples annealed  $> 550^\circ\text{C}$ . A long term isothermal experiment was also carried out using both spontaneous and induced samples at  $350^\circ\text{C}$ . Significantly, no reduction in confined track length was observed after a 12 month period at this temperature.

## HISTORY OF EARTH'S DEGASSING

O'NIONS R.Keith and TOLSTIKHIN Igor Department of Earth Sciences, Cambridge University Cambridge CB2 3EQ, U.K

The Earth is an highly degassed body depleted in  $^{36}\text{Ar}$  and other noble gases by several orders of magnitude relative to the solar abundance. Attempts to reconstruct the timing and rates of gas loss from the Earth-atmosphere system have been made for more than 30 years (Ref.1).

The degassing of the Earth during accretion is constrained by Pu-U-I-Xe systematics. Degassing was much more efficient during the first 100-200 Ma, than subsequently, and it was more complete for Xe than for the lighter gases. More than 90% of the degassed Xe escaped from the atmosphere during this period. The combination of fractional degassing of melts (Ref.2) and rare gas escape from the atmosphere (Ref. 3) is able to explain the deficit of terrestrial Xe as a simple consequence of this early degassing history.

By the time Xe was quantitatively retained in the atmosphere, the abundances of Kr and the lighter gases in the Earth's interior were similar to or higher than the present-day atmospheric abundances. Subsequent transfer of these lighter rare gases into the atmosphere requires a high rate of post-accretion degassing and melt production. Considerations of Pu-U-Xe systematics suggest that relatively rapid post-accretion degassing was continued to ca 4.1 - 4.2 Ga.

It is shown that the small amount of  $^3\text{He}$  and other primordial rare gases in the present-day upper mantle may be residual (Ref. 4) or entrained from the low mantle (Ref. 5). In the latter case entrainment of only ~1% of the lower mantle mass per Ga is able to provide the  $^3\text{He}$  inventory in the upper mantle. In this case the residence time of He in this reservoir is estimated at ~ 1 Ga, which is very similar to earlier estimates for the highly incompatible lithophile elements, U, Th, Pb (Ref.6). However the amount of these lithophile elements that accompany the introduction of  $^3\text{He}$  into the upper mantle is too small to sustain their steady - state abundances. The continental lithosphere appears to be the major source of these lithophile elements.

- 1 Turekian K.K., 1959, The terrestrial economy of He and Ar: *Geochim. Cosmochim. Acta* v. 17, 37-43.
- 2 Tolstikhin I.N. and O'Nions R.K., 1993, The earth's missing Xe: a combination of early degassing and of Rare gas loss from the atmosphere: accepted by Nature.
- 3 Pepin R.O., 1991, On the origin and early evolution of terrestrial planet atmospheres and meteoritic volatiles: *Icarus* v. 92, 1-79.
- 4 Azbel I.Ya. and Tolstikhin I.N., 1990, Geodynamic, magmatism and degassing of the Earth: *Geochim. Cosmochim. Acta*, v. 54, 139-154.
- 5 O'Nions R.K. and Tolstikhin I.N., 1993, Behaviour and residence times of lithophile and rare gas tracers in the upper mantle: submitted to Earth. Planet. Sci. Lett.
- 6 Galer S.J.G. and O'Nions R.K., 1985, Residence time of thorium, uranium and lead in the mantle with implications for mantle convection: *Nature* v. 316, 378-782.

## APATITE FISSION TRACK STUDY OF A VERTICAL PROFILE THROUGH THE BOGONG HIGH PLAINS, VICTORIA, AUSTRALIA

O'SULLIVAN, A.J., O'SULLIVAN, P.B. and GLEADOW, A.J.W., VIEPS, School of Earth Sciences, La Trobe University, Bundoora, Victoria, 3083, Australia.

To help constrain the uplift and erosion history of the Bogong High Plains, in northeastern Victoria, the thermal history of a detailed vertical section in the Falls Creek area has been evaluated using apatite fission track data. Previous fission track studies of southeastern Australia have described a general decrease in apatite ages from ~250-350 Ma in the highland areas located up to 200 km inland, to ages as low as ~80 Ma towards the coast. It has been proposed that this age range was due to partial or complete resetting by a thermal pulse associated with the opening of the Tasman Rift to the east.

The Falls Creek area comprises the central part of the Wagga-Omeo Metamorphic Belt, a NNW trending zone of the Lachlan Fold Belt of southeastern Australia. The rocks in the region generally consist of Ordovician metasediments intruded by granitic rocks thought to have been emplaced during the Late Silurian to Early Devonian Bowring Orogeny. Further deformation was caused by the Middle Devonian Tabberabberan Orogeny. Subsequently, a long period of tectonic quiescence is thought to have occurred during the Late Paleozoic, resulting in peneplanation of the ancient land surface, which has since been uplifted and eroded. This uplift is considered to be the result of predominantly horst-like movements along steeply dipping normal faults on the eastern (seaward) side of the mountain range, and warping on the western flanks, with up to 800m of relative uplift along the eastern boundary faults.

For this pilot study, sixteen samples were collected along a 1280 m vertical profile. The results show a general decrease in apatite fission track age and mean confined track length with decreasing elevation, with the exception of two samples in the middle whose ages and lengths are greater than those immediately above and below, suggesting the presence of a previously unrecognised fault block. Samples from the top of the profile exhibited the greatest mean lengths (>13.3  $\mu\text{m}$ ), and ages of ~270-280 Ma, while samples near the base of the section have ages of ~230-240 Ma and mean track lengths of less than 12  $\mu\text{m}$ . Detailed modelling of these data suggests the samples experienced an initial episode of rapid cooling at some time between ~300 and 280 Ma, followed by a prolonged period of much slower cooling during the Late Palaeozoic and Mesozoic, before a final period of accelerated cooling beginning in the middle Cretaceous.

The two samples from within the proposed fault block in the middle of the vertical profile have apatite ages of ~373 and 319 Ma and track lengths between 13.2 and 12.7  $\mu\text{m}$ . Cross-cutting relationships suggest that the main episodes of faulting in the region were associated with Paleozoic deformation, but several faults show evidence of having been reactivated more recently, possibly as a result of uplift and erosion of the region during the Mesozoic or Cenozoic.

Based on these results, it is proposed that following peneplanation of the ancient land surface during the Late Paleozoic, the Falls Creek area started to cool in response to uplift and erosion during the Late Carboniferous to Early Permian. The subsequent episode of accelerated cooling beginning in the middle Cretaceous was probably related to uplift of the rifted margin in response to the opening of the Tasman Rift to the east and opening of the Gippsland Basin to the south.

CENOZOIC UPLIFT AND THERMAL HISTORY OF THE NORTH SLOPE FORELAND BASIN, NORTHERN ALASKA AND NORTHWESTERN CANADA

O'SULLIVAN, P.B., Victorian Institute of Earth and Planetary Sciences, School of Earth Sciences, La Trobe University, Bundoora, Victoria, 3083, Australia.

Results from apatite fission track analyses of Mississippian through Tertiary sedimentary rocks and Devonian granitic rocks from the Alaskan Cordillera of northern Alaska and northwestern Canada, have provided important information about the timing, amount, and rate of uplift experienced within the region. The analyses, together with regional geological observations indicate that several episodes of rapid cooling have occurred in the northern part of the Alaskan Cordillera throughout the Tertiary. Most of these episodes of rapid cooling were due primarily to uplift and erosion, but at least one case, during the Miocene, must have occurred in response to a major regional decrease in the mean annual surface temperature.

The northern part of the Alaskan Cordillera has long been interpreted as a component of a major Jurassic-Cretaceous convergent margin compressional orogen. The northern tectonic elements of this orogen include the North Slope foreland basin, and the Brooks Range fold and thrust belt. The geologic relationships across much of the foreland basin have been complicated by continued advancement of the fold and thrust belt to present time. However, due to poor geologic control, the timing of the deformational events responsible for uplift and erosion during the Tertiary have been constrained, for the most part, only in a relative sense.

Interpretations of apatite fission track analyses, suggest the region studied experienced rapid cooling due to uplift and erosion at various times during the Tertiary. This includes the Big Fish River area of the Mackenzie Delta region in Canada which experienced rapid uplift and erosion during the early Eocene at  $53 \pm 4$  Ma (all errors reported at  $\pm 2\sigma$ ). Sedimentary and granitic rocks exposed in the northeastern Brooks Range (NEBR) in northeastern Alaska, and along the Phillip Smith Mountains Front to the west of the NEBR, experienced four episodes of rapid uplift and erosion during the Tertiary. These occurred in the middle Paleocene at  $60 \pm 4$  Ma, in the middle Eocene at  $43 \pm 3$  Ma, in the early Oligocene at  $34 \pm 3$  Ma, and in the late Oligocene at  $25 \pm 3$  Ma. Fission track results from sedimentary rocks collected from both outcrop and subsurface localities along the northern foothills of the Brooks Range west of the Phillip Smith Mountains Front, and throughout the North Slope foreland basin, suggest the entire region experienced two episodes of rapid uplift and erosion, at  $60 \pm 4$  Ma and  $25 \pm 3$  Ma.

The interpreted fission track results also suggest that the region experienced a major decrease in the mean annual surface temperature of  $\sim 15^\circ\text{C}$  during the Early-to-middle Miocene at some time between  $\sim 20$ - $10$  Ma. This decrease in mean annual surface temperature has resulted in an equivalent amount of subsurface cooling at shallow depths (less than  $\sim 4$ - $5$  km), unrelated to either uplift and erosion or a decrease in heat flow.

Therefore, the results suggest that there were two major episodes of deformation which have affected the entire foreland basin in the Tertiary; during the Paleocene at  $60 \pm 4$  Ma, and during the late Oligocene at  $25 \pm 3$  Ma. Deformation and resulting uplift and erosion also occurred on the North Slope during the mid-Eocene to mid-Oligocene, at  $43 \pm 3$  Ma and  $34 \pm 3$  Ma, but deformation was localised and only affected the NEBR.

HIGH-RESOLUTION SINGLE-CRYSTAL U-PB DATING OF ORDOVICIAN ECLOGITES - TRACERS FOR THE EARLY EVOLUTION OF A CENTRAL SWISS ALPINE TERRANE

OBERLI, F. and MEIER, M., Isotope Geochemistry ETH, CH-8092 Zurich, and BIINO, G.G., Min. Petr. Inst., Univ., P erolles, CH-1700 Fribourg, Switzerland

Polymetamorphic mafic-ultramafic rock associations are the oldest igneous remnants in the pre-Variscan Helvetic basement of the central Swiss Alps. They can be divided into 1) a structurally older oceanic group consisting of lenses of meta E-N-MOR basalts, abyssal peridotites and minor metagabbros, and 2) a younger group of island arc (IA) - type intrusive metagabbros and ultramafic cumulates. Both groups together with their country rocks (accretionary wedge-type metasediments) were metamorphosed at eclogite facies ( $650$ - $750^\circ\text{C}$  |  $P > 1.8$  GPa), and later at granulite facies ( $600$ - $700^\circ\text{C}$  |  $P \sim 0.8$  GPa; Biino, 1994). Granites emplaced at  $\sim 440$  Ma postdate the granulite stage. Partial re-equilibration at amphibolite and greenschist grade occurred during Variscan and Alpine times, respectively. Based on ion-probe U-Pb data of zircons from an IA-type metagabbro, Gebauer et al. (1988) postulated a protolith age of  $\sim 870$  Ma and  $\sim 468$  Ma for the eclogite event. The resulting time interval is large compared to the mean life of modern oceans.

Zircons from four garnet bearing mafic rocks were analyzed by single-crystal U-Pb techniques to constrain origin and early metamorphic history and to correlate distinct basement segments. Complex evolution and prospect of multiple inheritance precluded application of analytically more precise but geologically less accurate multi-grain methods. Using microscopical criteria for rejection of inheritance (cores), abrasion and cathodoluminescence imaging, we arrive at the following results:

1) Two intrusive metagabbro stocks belonging to the younger group yield almost identical upper Concordia intercept ages of  $467 \pm 5/-4$  Ma (95% c.l. ext.) and  $471 \pm 7/-6$  Ma, respectively. U concentrations of 84-1087 ppm, euhedral magmatic morphology and multiple internal zoning suggest preservation of primary *magmatic* properties. The isotopic results are therefore interpreted to approximate the time of intrusion. Only rare, core-bearing zircons show pre-Ordovician inherited Pb components. Lower intercept ages of  $298 \pm 21$  Ma and  $272 \pm 11$  Ma and varying degree of discordance reflect Pb loss during the Variscan and, subordinately, Alpine orogenies.

2) Zircons from a fine-grained MORB eclogite display uniform low U contents of 28-37 ppm and apparent U-Pb ages of 334-474 Ma. Lack of magmatic zircon in undifferentiated MORB and absence of multiple internal zoning suggest an entirely *metamorphic* origin. Limited precision due to low radiogenic Pb contents (6-13 pg) precludes calculation of meaningful Concordia intercept ages. The highest U-Pb age,  $474 \pm 4$  Ma, defines a minimum age for subduction-related metamorphism.

In conclusion, our results are in support of a *Caledonian* evolutionary cycle of subduction, island arc magmatism, collision and uplift, occurring on an ordinary time scale of some 30 Ma.

Biino, G.G., 1994, Schweiz. Mineral. Petr. Mitt. (in press).  
Gebauer, D., Quadt, A., Compston, W., Williams, I.S., and Gr unfelder, M., 1988, Schweiz. Mineral. Petrogr. Mitt., v. 68, p. 485-490.

RECOIL REFINEMENTS: IMPLICATIONS FOR THE  
 $^{40}\text{Ar}/^{39}\text{Ar}$  DATING TECHNIQUE

Onstott, T.C., Dept. of Geological and Geophysical Sciences, Princeton University, Princeton, NJ 08544, and Miller, M., and Ewing, R.C., Dept. of Geology and Institute of Meteoritics, Univ. New Mexico, Albuquerque, NM 87131

Integration of the neutron energy distribution for a water-moderated reactor with the most recent cross-section data yields mean recoil energies of 180 keV for  $^{39}\text{K}$  (n,p)  $^{39}\text{Ar}$ , 970 keV for  $^{40}\text{Ca}$  (n,a)  $^{37}\text{Ar}$ , and 140 eV for  $^{37}\text{Cl}$  (n,g)  $^{38}\text{Cl}$  (b)  $^{38}\text{Ar}$ . Utilizing numerical simulations of collision cascades, we calculate a mean recoil range of 1620 Å for  $^{39}\text{K}$  (n,p)  $^{39}\text{Ar}$ , 3780 Å for  $^{40}\text{Ca}$  (n,a)  $^{37}\text{Ar}$ , and 11 Å for  $^{37}\text{Cl}$  (n,g)  $^{38}\text{Cl}$  (b)  $^{38}\text{Ar}$ . Integration of the recoil range distributions yield a mean depletion depth in a semi-infinite medium of 820 Å for  $^{39}\text{Ar}$ , 1950 Å for  $^{37}\text{Ar}$ , and 6 Å for  $^{38}\text{Ar}$ . The concentration gradients generated by recoil redistribution between thin slabs were then incorporated into standard diffusion equations. These calculations indicate that the argon release rates and  $^{40}\text{Ar}/^{39}\text{Ar}$  age spectrum derived from incremental heating of exsolved minerals are significantly affected by recoil redistribution.

If the exsolution lamellae are the effective diffusion dimension, the measured activation energy of diffusion will be greater than the true value and the age spectra will be discordant even if the feldspar has not experienced a complex or slow cooling history. Incremental step apparent ages will increase with the fraction of  $^{39}\text{Ar}$  released as the albite lamellae degas. The age spectra will exhibit decreasing apparent ages with increasing fraction  $^{39}\text{Ar}$  released as the potassium feldspar lamellae degas. The overall profile of the age spectrum will be depend upon the composition of the feldspar and the size of the lamellae.

Finally, the 11 Å mean recoil distance calculated for  $^{38}\text{Ar}$  indicates that it is not a proxy for anion-sited excess argon. Instead, published correlations of  $^{38}\text{Ar}$  with excess  $^{40}\text{Ar}$  probably reflect the degassing of fine-grained, Cl-rich inclusions.

EARLY IRRADIATION OF SILICON CARBIDE:  $^{21}\text{Ne}$   
PRODUCTION RATE AND RECOIL LOSS

Ott, U. and BEGEMANN, F., Max-Planck-Institut für Chemie (Otto-Hahn-Institut), Postfach 3060, D-55020 Mainz, F.R.Germany.

The isotope abundance anomalies carried by interstellar silicon carbide are highly important in their own right and with respect to the processes of nucleosynthesis in their parent stars (Ott, 1993; Anders and Zinner, 1993) - probably AGB stars for the majority of grains. However, a knowledge of their age is desirable in order to address additional areas of interest such as number of contributing AGB stars (Alexander, 1993) or a possible major contribution from a late AGB star. The latter may have contributed many of the extinct radionuclides the decay products of which have been identified elsewhere (Cameron, 1993; Wasserburg et al., 1993).

The approach that has been taken (Tang and Anders, 1988; Lewis et al., 1993) is based on observed excesses of  $^{21}\text{Ne}$  over the amount expected from mixing normal (Ne-A or solar) with Ne (Ne-E(H)) expected from the He shell of AGB stars. After correction for the recent spallogenic Ne produced during cosmic ray exposure of their meteorite host, this approach yields for the SiC grains nominal presolar cosmic ray exposure ages between a few and ~130 Ma, correlating with grain size and Ne-E(H) content (Lewis et al., 1993). There are, however, a number of uncertainties involved in this approach.

In order to address one of the problems - the extent to which cosmogenic  $^{21}\text{Ne}$  is lost from the grains due to recoil - we have irradiated size-separated terrestrial SiC in the range ~0.3 to ~5  $\mu\text{m}$  with 1.6 GeV protons to produce approx. 10(-12) ccSTP  $^{21}\text{Ne}/\text{mg}$  SiC. To avoid as much as possible recoil implantation into adjacent grains, the SiC grains (ca. 2-5 mg of each size fraction) were suspended and 'frozen in' in paraffin wax (1-2 grams) before irradiation. Results of the Ne analyses will be presented at the Conference. Also a different approach using cosmogenic Xe rather than Ne will be discussed.

Alexander, C.M.O'D, 1993, Presolar SiC in chondrites: How variable and how many sources? *Geochim. Cosmochim. Acta*, v. 57, p. 2869-2888.

Anders, E., and Zinner, E.K., 1993, Interstellar Grains in Primitive Meteorites: Diamond, Silicon Carbide, and Graphite, *Meteoritics*, v. 28, p. 490-514.

Cameron, A.G.W., 1993, Nucleosynthesis and Star Formation, in: *Protostars and Planets III* (E.H. Levy, J.I. Lunine and M.S. Matthews, eds.), p. 47-73.

Lewis, R.S., Amari, S., and Anders, E., 1993, Interstellar grains in meteorites. II. SiC and its noble gases, *Geochim. Cosmochim. Acta*, in press.

Ott, U., 1993, Interstellar grains in meteorites., *Nature*, v. 364, p. 25-33.

Tang, M., and Anders, E., 1988, Interstellar silicon carbide: How much older than the solar system? *Astrophys. J.*, v. 335, p. L31-L34.

Wasserburg G.J., Busso, M., Gallino, R., and Raiteri, C.M., 1993, Asymptotic Giant Branch Stars as a Source of Short-Lived Radioactive Nuclei in the Solar Nebula, *Astrophys. J.*, in press.

## THE OCEAN GEOCHEMISTRY OF OSMIUM AS INFERRED FROM MARINE SEDIMENTS.

OXBURGH, Rachel, MARCANTONIO, Franco and ZINDLER, Alan, Lamont-Doherty Earth Observatory, Palisades, NY 10964, USA.

Osmium isotopes in ocean systems have exciting potential as geochemical tracers. However the marine chemistry of osmium is not well constrained. Concentrations of osmium in sea water are too low to permit direct measurement, although this is anticipated in the near future. Currently, marine sediments provide the sole source of information on sea water composition.

In an attempt to establish the distribution of osmium in the modern oceans, we have analyzed surface sediments from a wide variety of locations as well as both shallow and deep dwelling corals. The surface oceans, as represented by analyses on planktonic foraminifera and surface dwelling corals appear to have a  $^{187}\text{Os}/^{186}\text{Os}$  ratios that are significantly lower than that of the deep ocean, as recorded by deep-sea corals and the authigenic phases of pelagic sediments. There are two important implications of this observation. First, for surface and deep isotopic signatures to be distinct, the residence time of osmium in the oceans cannot exceed the oceanic mixing time (1000 years). Second, a significant flux of osmium to the surface oceans with low  $^{187}\text{Os}/^{186}\text{Os}$  is required. We consider the most likely candidate to be the dissolution of ultra fine micrometeoritic material on contact with sea water.

## NOBLE GAS STATE IN THE MANTLE

OZIMA, M., Dept. of Earth & Space Sci., Fac. of Sci., Osaka Univ., Toyonaka-City, 560 Japan.

There are a variety of mantle degassing models based on noble gases. Because of different choices of noble gas data by the authors, however, their conclusions are often contradictory. To reduce such confusion, I examined all the published noble gas data available to me, and I present a mantle noble gas data base deduced from the recent high quality experiments.

Because of various elemental fractionation processes, it is difficult to conclude definitely the noble gas elemental abundances in the mantle from the noble gas analyses of mantle-derived materials. In contrast to the elemental abundances, however, isotopic fractionation in geological processes can generally be neglected, and we can infer the noble gas isotopic state in the mantle from the experimental results on mantle-derived materials. We conclude the following characteristics in the mantle noble gas isotopic state.

- (1) Apart from the addition of radiogenic isotopes, isotopic compositions of argon, krypton and xenon in the mantle (both degassed and less-degassed) are similar to those of the air noble gases within the experimental uncertainties of about 1 %.
- (2)  $^{20}\text{Ne}/^{22}\text{Ne}$  in the mantle (degassed and less-degassed) is distinctly higher (11 ~ 13) than that of atmospheric neon. The ratio resembles solar neon (either SEP or SW neon). There appears to be little difference in the isotopic ratio between the degassed and the less-degassed mantle.
- (3) Radiogenic isotopic ratios such as  $^3\text{He}/^4\text{He}$ ,  $^{21}\text{Ne}/^{22}\text{Ne}$ ,  $^{40}\text{Ar}/^{36}\text{Ar}$  which are in excess of the respective air ratios, are higher in the degassed mantle (except for  $^3\text{He}/^4\text{He}$ ) than in the less-degassed mantle.
- (4)  $^{40}\text{Ar}/^{36}\text{Ar}$  ratio in the less-degassed mantle is likely to be much higher (>3,000) than hitherto assumed (~500).
- (5) Xenon isotopic ratios containing radiogenic isotopes such as  $^{129}\text{Xe}/^{130}\text{Xe}$  and  $^{131}\text{-}^{136}\text{Xe}/^{130}\text{Xe}$  are significantly higher in the mantle than in the air. However, there appears to be little difference in these isotopic ratios between the degassed and the less-degassed mantle.
- (6) Because of possible air contamination, all the excess isotopic ratios observed in mantle-derived materials relative to the air noble gas isotopic ratios should be regarded as a minimum.
- (7) Present observational data do not support a significant contribution of subducted extra-terrestrial noble gases, either helium or neon, in the mantle noble gas inventory.

U-Pb ZIRCON AND Pb ISOTOPE STUDIES IN RELATION TO PROTEROZOIC SEDIMENT-HOSTED LEAD-ZINC-SILVER DEPOSITS IN NORTHERN AUSTRALIA

PAGE, R.W., Sun, Shen-su, Australian Geological Survey Organisation, Canberra, A.C.T., 2601, Australia, and Carr, G.R., CSIRO Division of Exploration and Mining, North Ryde, N.S.W., 2113, Australia.

Models for the tectonic and metallogenic evolution of major stratabound lead-zinc-silver mineral deposits are clearly enhanced by knowledge of both the sediments' age(s) and the coherence or otherwise of Pb isotope patterns associated with the primary sulfides. In the last few years, our motivation to better understand such economically important sequences in northern Australia has coincided with the huge growth and success of exploration for base metals and gold, especially in the Mount Isa Inlier and McArthur Basin.

The younger cover sequences in these terrains that host the Pb-Zn-Ag accumulations, also contain sparse felsic tuff beds. New SHRIMP U-Pb zircon work on these rocks effectively defines the times of deposition of the associated stratabound ores. For example, work on tuffs from the Mount Isa and Hilton orebodies provides a depositional age for this part of the Mount Isa Group at  $1653 \pm 7$  Ma. Preliminary data on high-grade rocks equivalent to those hosting the recently discovered Cannington Pb-Zn-Ag deposit, show that this succession has a maximum age of  $1677 \pm 9$  Ma, comparable to the depositional age of the Broken Hill ore host sequence at  $1690 \pm 5$  Ma.

Sequences similar to the Mount Isa Group are found in a number of basins and fault-bounded troughs containing the McNamara and McArthur Groups north of Mount Isa. Syngenetic or late diagenetic Pb-Zn-Ag deposition in these latter sequences has been dated, again by means of the SHRIMP U-Pb zircon work on concordant tuffs. These deposits are somewhat younger than the Mount Isa Group, ranging from  $1640 \pm 7$  Ma (HYC orebody), to  $1640 \pm 7$  Ma (Walford Creek deposit), to  $1595 \pm 6$  Ma (Century orebody). This points to a diachronous development of similar extensional tectonic and metallogenic environments over a period of 60-90 million years.

Comparison of these depositional ages with the abundant galena Pb isotope data for the respective deposits allows us to more finely tune the Pb evolutionary model and test the significance of these Proterozoic Pb model ages. Subtle variation in  $^{206}\text{Pb}/^{204}\text{Pb}$  (16.0 to 16.3) and the relative two-stage model ages for Pb from Broken Hill, Mount Isa, HYC, Lady Loretta, and Century broadly mimic the progressively younging stratigraphic ages of these deposits (1690 to 1595 Ma). This nexus between relative Pb model ages and actual depositional ages of the sediment-hosted Pb deposits of the Proterozoic of northern Australia allows refinement of part of the Pb isotope growth curve for this particular region, but we concede that a universally applicable single growth curve may not be achievable. The connection between stratigraphic ages and primary Pb isotope signatures in northern Australian Proterozoic terrains supports a syngenetic or diagenetic origin for mineralization in the deposits studied.

$^{40}\text{Ar}$ - $^{39}\text{Ar}$  DATING OF QUATERNARY BASALT, WESTERN MODOC PLATEAU, NORTHEASTERN CALIFORNIA: IMPLICATIONS TO TECTONICS

PAGE, W. D., Geosciences Department, F22A, Pacific Gas and Electric Company, P. O. Box 770000, San Francisco, CA 94177 and RENNE, P. R., Institute of Human Origins Geochronology Center, 2453 Ridge Road, Berkeley, CA 94709.

The Modoc Plateau has had low seismic activity, yet many faults have displaced the extensive Quaternary "Warner basalts" in this region. In order to help assess the seismic hazards and risks to PG&E's facilities in the region north and northwest of Mt. Lassen, we dated 15 samples from 10 flows by the  $^{40}\text{Ar}$ - $^{39}\text{Ar}$ , step-heating method. Dating of the rocks proved critical to understanding the tectonics and timing of faulting in the region. Discussion of the Ar-Ar results and tectonic implications for the area south of Mt. Lassen are presented in companion abstracts by Becker et al. and by Wakabayashi et al.

Basalts in the Modoc Plateau were mostly contained from spilling to the west and south by the Klamath Mountains and Sierra Nevada as they built up the plateau. The oldest dated basalt flows (~ 2.4 Ma) are small remnants that have been locally weathered to saprolite and are plastered on north flank of the Sierra Nevada. Geomorphic analysis suggests that the older flows may have locally spilled over the divide north of Mt. Lassen. The interconnected, north-striking McArthur, Hat Creek, and Almanor graben now separate the western Modoc Plateau from the mountains to the west and have been a major geomorphic feature for more than a million years.

The west-facing Hat Creek fault zone on the east side of the Hat Creek graben north of the Pit River (Soldier Creek fault) displaces the 1.2 Ma basalt on top of the scarp > 260 m, giving a long-term vertical separation rate of > 0.22 mm/yr. South of the Pit River the Hat Creek fault zone displaces the flow (1.0 Ma) on top of the scarp > 390 m (> 0.38 mm/yr). At the same locality the eastern two faults in the zone displaces the basalt flow west of Hogback Ridge (850 ka) > 85 m (> 0.10 mm/yr). These rates are less than the 1.3 mm/yr (post 15 ka) presented by Muffler et al. (1993 manuscript) for the Hat Creek fault in the near Lost Creek to the south. The Sam Wolfen Spring (800 ka), Rocky Ledge (?) (150 ka) and other flows younger than 1 Ma were deposited within the Hat Creek graben. Extensive diatomite lake beds in the graben underlie the Wolfen Spring flow and hence appear to have been deposited between about 1 Ma and 800 ka.

The Yellow Jacket (?) (840 ka) and the Tuft Creek flows (150 ka) are northwest of Indian Spring Mountain on the northeast side of the McArthur graben. The Mayfield fault displaces the Tuft Creek flow 12 m, down west (0.09 mm/yr). The entire west-facing Mayfield fault zone displaces it about 64 m (0.5 mm/yr). The Fall River Mills basalt (-- ka) and other younger flows partly fill the McArthur graben.

Northwest of Mt. Lassen the northeast-striking Battle Creek fault vertically displaces hypersthene andesite of Brokeoff Mountain flow (550 ka) about 43 m, down south (0.078 mm/yr). The scarp is overlain by the Black Butte basalt (~60 ka) that does not appear to be faulted.

The results of this study strongly indicate that Ar-Ar dating of basalts as young as late Quaternary can provide significant constraints to neotectonic processes.

PB, SR, ND ISOTOPE AND U-SERIES INVESTIGATION OF THE HOLOCENE INYO AND MONO HIGH SILICA RHYOLITE DOMES, E. CALIFORNIA.

ZENON PALACZ, JAMES GILL. Earth Science Board, University of California, Santa Cruz. CA95064.

The Mono and Inyo rhyolite domes are the most recent products of prolonged silicic volcanism in E. California. They form a series of northerly trending domes between the Long Valley Caldera and Mono Lake. The age of volcanism varies between 25ka and 0.5ka in the Mono domes, with the most recent eruption in the Inyo domes occurring 600 yrs BP.

Th-U disequilibria in the Inyo finely porphyritic magma type shows a progressive decrease in  $^{230}\text{Th}/^{232}\text{Th}$  and  $^{238}\text{U}/^{232}\text{Th}$  with increasing fractionation (Ba decreases from 1350 to 350ppm and Th increases from 13 to 23ppm). These data define a U-Th whole rock isochron of 55ka which is also shared by the high Ba Negit and Paoha island dacites and rhyolites within Mono Lake 30km to the north. Because  $(^{230}\text{Th})/(^{232}\text{Th})$  and  $1/\text{Th}$  are positively correlated, the isochron could be a two component mixing line between a high Ba magma with  $(^{230}\text{Th})/(^{238}\text{U})=1$  and  $(^{230}\text{Th})/(^{232}\text{Th})=1$ , and a more evolved low Ba low Zr magma with  $(^{230}\text{Th})/(^{238}\text{U})$  1.15,  $(^{230}\text{Th})/(^{232}\text{Th})$  0.91,  $^{143}\text{Nd}/^{144}\text{Nd}$  increases from 0.51258 to 0.51264, and  $^{206}\text{Pb}/^{204}\text{Pb}$  decreases from 19.16 to 19.13 with increasing fractionation and increasing  $(^{230}\text{Th})/(^{238}\text{U})$  while  $^{87}\text{Sr}/^{86}\text{Sr}$  remains constant at 0.7060. These data show that the change in Th isotopes is due to magma mixing and not time. The evolved low Ba magma may have fractionated zircon and lowered the  $(^{238}\text{U}/^{232}\text{Th})$  of the magma perhaps within the past 1-10ka, and mixed with the high Ba magma during eruption.

In marked contrast Mono rhyolite domes are all U enriched with  $(^{230}\text{Th})/(^{238}\text{U})$  0.94-0.87 and  $(^{230}\text{Th})/(^{232}\text{Th})$  0.86-0.89. The younger (<1ka) aphyric domes have the lowest Th isotope ratios while the older biotite bearing (~25ka) domes have the highest. The Th-U data are consistent with continual fractionation of an allanite bearing assemblage over 1-50ka. All the domes have similar Pb ratios ( $^{206}\text{Pb}/^{204}\text{Pb}$  19.13). Nd isotope ratios vary between 0.51260 and 0.51264,  $^{87}\text{Sr}/^{86}\text{Sr}$  between 0.706 and 0.7064. The older biotite domes have the highest Sr and Nd isotope ratios while the youngest aphyric domes have the lowest. The possible relationship between Th isotope ratio and eruption age may be significant, though magma mixing cannot be ruled out.

PETROGENETIC INTERPRETATIONS OF Sr, Nd, O AND Pb ISOTOPES FROM THE MOUNT SIDLEY VOLCANO, MARIE BYRD LAND, ANTARCTICA

PANTER, K. S.<sup>1</sup>, PANKHURST, R. J.<sup>2</sup>, KYLE, P.R.<sup>1</sup>, SMELLIE, J. L.<sup>3</sup>, MUKASA, S.<sup>4</sup> and McINTOSH, W.<sup>1</sup>  
<sup>1</sup> Geoscience, New Mexico Tech., Socorro, NM 87801, USA  
<sup>2</sup> Iso. Geosci. Lab., NERC-BGS, Keyworth, NG12 5GG, UK  
<sup>3</sup> BAS, High Cross, Madingley Rd, Cambridge CB30ET, UK  
<sup>4</sup> Geol. Sci., Univ. Michigan, Ann Arbor, MI 48109, USA.

Mt. Sidley (4281m) is a large (>200km<sup>3</sup>) alkaline stratovolcano within the Late Cenozoic Marie Byrd Land (MBL) volcanic province, Antarctica. Detailed mapping-stratigraphy and  $^{40}\text{Ar}/^{39}\text{Ar}$  geochronology reveals a complex, multicenter, polygenetic volcano constructed in successive stages over 1.5 m.y. (5.7 - 4.2 Ma). Rock compositions consist of strongly undersaturated sodic lavas, ranging from basanite to anorthoclase phonolite and trachyte with minor volumes of oversaturated trachyte.

Major changes in composition coincide with a southward migration of volcanic activity (~0.6 cm/yr). Four stages of eruptive activity are recognized and commenced with eruptions of phonolitic lavas (Stage I: 5.7 - 4.7 Ma) followed by deposition of trachytic lavas and tephras (Stage II: 4.6 - 4.5 Ma). A highly explosive eruption of trachytic magmas and sector collapse of the volcanoes southern flank, was followed by the deposition of intermediate composition lavas and tephras (Stage III: 4.4 - 4.3 Ma) approximately 9 km south of Stage I activity. The final stage (Stage IV: 4.2 Ma) produced xenolith-bearing parasitic cones of basanite.

Most samples display a narrow range in  $^{87}\text{Sr}/^{86}\text{Sr}_i$  (0.70283 - 0.70315),  $^{143}\text{Nd}/^{144}\text{Nd}_i$  (0.51280 - 0.51290) and  $\delta^{18}\text{O}$  (5.2 - 6.2‰), indicating their derivation from a primitive mantle source. Two basaltic samples have values of  $^{206}\text{Pb}/^{204}\text{Pb} = 19.5$ ,  $^{207}\text{Pb}/^{204}\text{Pb} = 15.7$  and  $^{208}\text{Pb}/^{204}\text{Pb} = 39.1$ , suggesting a significant HIMU mantle source component. Linear variation of  $^{143}\text{Nd}/^{144}\text{Nd}_i$  with  $^{87}\text{Sr}/^{86}\text{Sr}_i$  may be explained by interaction of a HIMU-rich source with an enriched mantle component (lithosphere or EMI). On the other hand, systematic variation of  $^{143}\text{Nd}/^{144}\text{Nd}_i$  with  $\text{SiO}_2$  and  $\text{Mg}\#$  ( $^{87}\text{Sr}/^{86}\text{Sr}_i$  and  $\delta^{18}\text{O}$  are relatively constant) may suggest evolution by AFC processes in a mafic lower crust. Four highly evolved trachyte samples show elevated  $^{87}\text{Sr}/^{86}\text{Sr}_i$  (0.70363 - 0.70422) and  $\delta^{18}\text{O}$  (7.6 - 8.4‰) indicating some assimilation of the upper crust by ascending melts.

A significant number (13 or 39) of samples analyzed for oxygen isotopes display relatively low  $\delta^{18}\text{O}$  values of -1.4 to 4.1‰. Low  $\delta^{18}\text{O}$  values are not associated with a specific rock composition or lithology, however, the extent of  $^{18}\text{O}$  depletion does correlate with measured loss on ignition (LOI contents up to 2.4 wt.%). Although the majority of these samples appear "fresh" in thin section, the  $^{18}\text{O}$  depletion is considered a result of low temperature exchange-hydration with extremely light ( $\delta^{18}\text{O} = -40$  to  $-30\%$ ) Antarctic meteoric water.

## HIGH ABUNDANCE SENSITIVITY MASS SPECTROMETER FOR U-Th STUDIES.

PAPANASTASSIOU, D.A., BERNIUS, M.T.<sup>1</sup>, CHEN, J.C., and WASSERBURG, G.J., The Lunatic Asylum, Div. Geol. & Planet. Sci. Caltech, Pasadena, CA 91125. <sup>1</sup>Dow Corning Co., Central Research Bldg. 1712, Midland, MI 48674

We report the abundance sensitivity (AS) and ion transmission characteristics of a modified Finnigan-MAT 262B-RP mass spectrometer (Table). This instrument is an outgrowth of our joint effort with Drs. Habfast and Laue of Finnigan-MAT. The instrument is compact, relatively low cost, and versatile, enabling dual use: a) high precision (10-20 ppm) with the 1st stage multiple collector; and b) high AS and transmission with the 2nd stage. The 2nd stage was configured to reduce the contribution to the beam of ions that have suffered collisions. The design includes a retarding potential (RP) lens; this serves the dual purpose: a) of stopping ions that have lost some energy due to collision or charge exchange and that would have formed the "low-mass" tail of the ion beam, and b) permitting the introduction of the decelerated ions through a second ion selective device, chosen to be a dynamic electric quadrupole, with AS of  $\sim 10^{-4}$ . The latter design was not pursued by F/MAT. An ion-optical study was carried out at Caltech, which indicated that it was necessary to have the ion beam optimized in angular dispersion for introduction into the RF-quadrupole. We have completed a new 2nd stage corresponding to the ion-optical design. It includes a static electric quadrupole doublet for beam shaping prior to the RP lens. The RP lens was designed to provide for gradual deceleration of the ions and increased ion transmission. The results of the unmodified and modified system (without the RF quadrupole) are shown in the Table. The abundance sensitivity of this system for a two mass unit difference, as is applicable for  $^{230}\text{Th}$ , is found to be better than  $5 \times 10^{-10}$ , obtained for 1.5 amu difference, for an accompanying transmission of 50%. Data have been obtained on U and Th gravimetric standards with  $^{236}\text{U}/^{238}\text{U} = 10^{-8}$  and  $^{230}\text{Th}/^{232}\text{U} = 10^{-7}$ . The mass spectrometric data agree with gravimetry within counting statistics. Measurements of  $^{230}\text{Th}/^{232}\text{Th}$  on young volcanics and on mineral separates are routinely obtained. We have checked the RF-quadrupole on the mass spectrometer. We have obtained up to 84% transmission through this RF quadrupole used in a static mode. However, the RF-quadrupole showed evidence for electric discharge at the 10 kV operating voltage. The system has been improved and is now under test. It is our expectation that the increased mass selectivity by the RF quadrupole will allow a wider energy range of ions through the RP lens and, therefore, higher transmission. We hope to reach an AS close to  $10^{-14}\text{amu}^{-1}$ , which is now available only with accelerator mass spectrometry. Division Contribution 5368 (842).

	Unmodified	Modified <sup>b</sup>
Abundance Sensitivity (U-Th region) <sup>a</sup>		
1 amu	$1 \times 10^{-8}$	$5 \times 10^{-9}$
1.5 amu	$4 \times 10^{-9}$	$5 \times 10^{-10}$
Transmission <sup>c</sup>	50%	50%

<sup>a</sup>For low mass side. <sup>b</sup>New ion-optical design. <sup>c</sup>Second stage.

## STABLE ISOTOPIC COMPOSITIONS OF OSTRACOD IN THE SOGWIPO FORMATION, KOREA

Park, B.K., Lee, K.S., Korea Basic Science Center, Taejeon, 305-333, Korea, and Lee, E.H., Dept. of Geology, Korea Univ. Seoul, 136-701, Korea.

The oxygen and carbon isotopic compositions of the ostracod species, *Normanicythere sp.*, in the Sogwipo Formation exposed at the southern part of Sogwipo city of Jeju Island have been measured. This work was intended to study the relationship between oxygen and carbon isotopic compositions of the ostracod and paleotemperature of the depositor of the formation and/or the global climate changes. The values  $\delta^{13}\text{C}_{\text{PDB}}$  varied from  $-6.77\text{‰}$  to  $-4.86\text{‰}$  with an average of  $-5.57\text{‰}$ , while the values of  $\delta^{18}\text{O}_{\text{PDB}}$  varied from  $-2.26\text{‰}$  to  $+0.45\text{‰}$  with an average of  $-0.76\text{‰}$ . The values of  $\delta^{18}\text{O}_{\text{PDB}}$  were decreased gradually from sample 1 to sample 19 except for sample 11 where the value was sharply increased. The minimum value of  $\delta^{18}\text{O}_{\text{PDB}}$  was at sample 11. The values of  $\delta^{13}\text{C}_{\text{PDB}}$  showed the similar trend of  $\delta^{18}\text{O}_{\text{PDB}}$  values. The variations of  $\delta^{18}\text{O}_{\text{PDB}}$  and  $\delta^{13}\text{C}_{\text{PDB}}$  values seemed to be dependent on the variations of sea water temperature during deposition of the Sogwipo Formation. Also it seemed that the Sogwipo Formation was deposited during glacial period with a short interglacial epoch.

## ISOTOPIC CHARACTER OF CAMBRO-ORDOVICIAN MAGMATISM IN SOUTH VICTORIA LAND ANTARCTICA, AND PRODUCTION OF SUB-CONTINENTAL MANTLE

PARKINSON, D.L., Geol. Dept. Univ. of Otago, P.O. Box 56, Dunedin, New Zealand, and Dept. of Geol. Sci. U.C. Santa Barbara, CA 93106, and Cox, S., Geol. Dept., Univ. of Otago, P.O. Box 56, Dunedin, New Zealand

The Dry Valley (DV) region of South Victoria Land (SVL) Antarctica is the site of voluminous granitoids that intrude the Late Proterozoic Koettlitz Group, a sequence of syn- to post-rift deposits. These intrusives range from foliation parallel orthogneisses to cross-cutting slightly deformed and undeformed plutons. Cox and Allibone (Ant Sci 3, 1991) and Allibone et al. (NZJGG, 1993), using mapping and geochemical data, divided these intrusives into three categories: DV1a (calc-alkaline, metaluminous hbl-bi granodiorites); DV1b (calc-alkaline, meta- to peraluminous bi granodiorites and granites); and DV2 (alkali-calcic granites).

Geochronologic and isotopic data from a variety of units support the division of SVL granitoids into the DV1a, DV1b, and DV2 suites. U-Pb zircon ages indicate a range from 530-520 Ma for DV1a suite; a large DV1b body yields U-Pb monazite ages of  $489 \pm 5$  Ma. Granites of the DV2 suite are probably correlative with Sil-Dev Admiralty intrusives of North Victoria Land (NVL, Borg et al., *AJS* 287, 1987).

Pb isotopic data from DV1a yields lower 207/204 values for equivalent 206/204 values than DV1b. DV2 samples plot more radiogenic in both 207/204 and 206/204 than either DV1a or DV1b.  $Sr_i$  and  $\epsilon_{Nd_i}$  from DV1a and DV1b indicate a crustal component in these arc related intrusives, plotting in the range 0.705-0.708 for  $Sr_i$  and -2 to -7 for  $\epsilon_{Nd_i}$ .

The DV1 event is correlated with the Ross Orogeny which has been identified from NVL through the Transantarctic Mountains. The DV1 intrusives correlate with the Granite Harbor Intrusives of Borg et al. (1987), and more specifically with the Gabbro Hills/Marsh Glacier intrusives in the Central Transantarctic Mountains described by Borg et al. (*JGR* 95, 1991). DV1a intrusives are interpreted to represent construction of a Cambrian arc, based on isotopic and geochemical data. The higher 207/204 values in DV1b indicate an increasing crustal component with time. We interpret this Cambro-Ordovician arc to have been built on transitional crust to the East Antarctic craton, and to have constructed a geochemically distinct sub-continental mantle.

The Jurassic flood basalts of the Ferrar Magmatic Province (FMP) are spatially coincident with DV1 and correlative Granite Harbor Intrusives. The FMP has uni-formly high, but variable,  $Sr_i$  (0.709 to 0.713), uniformly negative  $\epsilon_{Nd_i}$  (-3 to -6), and elevated 207/204 values with respect to the Northern Hemisphere Regression Line. Hergt et al. (*EPSL* 105, 1991) state that the source of the FMP and related flood basalts is the sub-continental mantle, and attribute the distinctive isotopic and trace element signature to incorporation of subducted sediment into this source region during a prior arc building event.

Calculated isotopic values for the DV1 suite for Jurassic time produces similar or overlapping fields in all three isotopic systems when compared with FMP data. This isotopic data is interpreted to indicate that the sub-continental mantle produced during the Cambro-Ordovician Ross Orogeny is the source for younger FMP magmas.

## U-Pb PROBLEMATICS OF VERY HIGH-U ACCESSORY MINERALS: EXAMPLES FROM THE HIMALAYA AND CORDILLERA AND IMPLICATIONS FOR U-Pb GEOCHRONOLOGY

PARRISH, R. R., Geological Survey of Canada, 601 Booth St., Ottawa, Ontario, Canada, K1A 0E8, and CARR, S. D., Ottawa-Carleton Geoscience Centre, Carleton University, Ottawa, Ontario, Canada, K1S 5B6

Orogenic belts rich in clastic sedimentary protoliths give rise to anatectic leucogranitic rocks during high grade regional metamorphism. Both the leucocratic rocks and the metasedimentary rocks will generally contain zircon, monazite, and sometimes xenotime as accessory minerals, and often these minerals will have very high uranium concentrations. Extensive studies in the Cordillera of British Columbia, Canada and the Pakistan and Nepal Himalaya indicate that the uranium concentration can exert an important control on Pb retentivity of these minerals, an effect not previously clearly documented. Dating of optically high quality igneous and metamorphic grains of these minerals indicates that when uranium concentrations exceed ca. 1000ppm in zircon or 4000ppm in monazite and xenotime, these minerals can act as substantially open systems during post-crystallization cooling over the temperature interval  $>400^{\circ}$ - $650^{\circ}$ C, despite their nominal Pb closure temperatures being regarded as in excess of  $650$ - $700^{\circ}$ C.

In the dating of more than 15 leucogranitic rocks from the Himalaya, minerals with these "very high" uranium concentrations inevitably yield a spread of U-Pb ages which vary between ca. 16 to 21-22 Ma, the actual crystallization age being 21-23 Ma. U-Pb age clearly correlates with U content in several cases. These samples did not cool below ca.  $400^{\circ}$ C until ca. 5-15 Ma ago. It is possible that many other published U-Pb dates of Himalayan leucogranites may be too young. Similarly, in detailed dating studies in the Cordillera, some U-Pb dates on very high-U minerals from deformed protoliths give ages which are younger than the rocks which crosscut them. We draw the conclusion that the notion that closure temperature is independent of U concentration is probably incorrect.

The dependence of Pb retentivity on U concentration is clearly evident in very young minerals where the effects of Pb loss caused by time-integrated radiation damage is insignificant, and where there was a period of relatively slow cooling of the rocks following metamorphism at upper amphibolite facies conditions. Cogenetic grains which lose some component of their radiogenic Pb immediately following crystallization will retain "concordant" U-Pb compositions, but will differ in age from neighboring grains depending upon their size and U concentration. Analysis of single grains reveals this natural effect, and causes significant ambiguity in the interpretation of the U-Pb systematics. It is possible that this effect is much more widespread than acknowledged, and it may account for small amounts of measured scatter in U-Pb ages in accessory minerals from rocks of older orogenic belts.

CRUST-MANTLE DIFFERENTIATION AND R.L. ARMSTRONG'S NO-CONTINENTAL-GROWTH MODEL

PATCHETT, P. Jonathan, Dept. Geosciences, University of Arizona, Tucson, AZ 85721, USA

From the time of its first proposal in 1968 (Armstrong, 1968), the hypothesis of no continent growth has been a key element of the debate on crust-mantle evolution. Initially, Armstrong viewed the continental crust as unchanged in mass since 2.5 Ga, but later advocated a steady state since 2.9 Ga and even as early as 3.5 Ga. The Armstrong hypothesis has been ignored by many, but accepted as truth by some. There have been quite a small number of attempts to evaluate and test the no-growth hypothesis, or build it into other models.

The main reason for the varied responses and the paucity of real evaluation of the no-growth hypothesis has been that the vast majority of geochemical and isotopic data for mantle and crustal rocks can be fit to either growth-dominated or no-growth models. This was of course repeatedly pointed out by Armstrong (1981a,b; 1991). As noted by Armstrong in his last paper of 1991, the response was often to proceed with growth-of-crust modeling and ignore the unsolved conundrum posed by the no-growth model.

Attempts to incorporate the Armstrong model into mantle evolution (e.g. DePaolo, 1983; Jacobsen, 1988) have shown how recycling of sediments into the mantle figures into such calculations. The same circularity remains, however, in all cases. Attempts have been made to limit the degree of continent destruction via recycling of sediments using geochemical and isotopic tests (e.g. Patchett et al., 1984; Stevenson and Patchett, 1990; see also Taylor, 1990). These tests have resulted in geochemical and geological plausibility arguments against a pure no-growth scenario, but have left the precise degree of continent-to-mantle recycling open. Modeling of crust-mantle evolution without significant recycling has certainly reached maximum sophistication (e.g. Allègre et al., 1983a,b).

A pure no-growth model involves recycling of a mass of continent equal to the present one over geologic time, as well as subduction into the deep mantle of most sediment on the ocean floor (Armstrong, 1981). It seems fair to say that present data and plausibility arguments weigh against the no-growth hypothesis in its end-member form. The extent of continent recycling into the mantle could still be very large, however. Thus the conundrum of growth vs. no-growth remains unsolved, and this problem will certainly outlive the late Dick Armstrong by many years.

- Allègre, C.J., Hart, S.R., and Minster, J.-F., 1983a, *Earth Planet. Sci. Lett.*, v. 66, p. 177-190.  
Allègre, C.J., Hart, S.R., and Minster, J.-F., 1983b, *Earth Planet. Sci. Lett.*, v. 66, p. 191-213.  
Armstrong, R.L., 1968, *Rev. Geophysics*, v. 6, p. 175-199.  
Armstrong, R.L., 1981a, *Geochim. Cosmochim. Acta*, v. 45, p. 1251.  
Armstrong, R.L., 1981b, *Phil. Trans. R. Soc. Lond.*, v. A301, p. 443-472.  
Armstrong, R.L., 1991, *Aust. J. Earth Sci.*, v. 38, p. 613-630.  
DePaolo, D.J., 1983, *Geophys. Res. Lett.*, v. 10, p. 705-708.  
Jacobsen, S.B., 1988, *Earth Planet. Sci. Lett.*, v. 90, p. 315-329.  
Stevenson, R.K., and Patchett, P.J., 1990, *Geochim. Cosmochim. Acta*, v. 54, p. 1683-1697.  
Taylor, S.R., 1990, *Nature*, v. 346, p. 608-609.

APPLICATION OF  $^{10}\text{Be}$  TO LOESS STRATIGRAPHY OF THE LOWER MISSISSIPPI VALLEY, U.S.A.

Pavich, M. J., U.S. Geological Survey, Reston, Virginia, Markewich, H.W., U.S. Geological Survey, Atlanta, Georgia, and Millard, H.T., U.S. Geological Survey, Denver, Colorado

Dating of continental glacial deposits beyond the range of  $^{14}\text{C}$  is needed. Correlations of continental and marine oxygen isotope stratigraphy must be tested prior to accepting "Milankovitch" orbital forcing as the driver of Quaternary glacial fluctuations. Richmond and Fullerton (1986) proposed correlation of late Quaternary glacial deposits to marine oxygen isotope "ages." This study tests the pre-Late Wisconsin and Illinoian age assignments made for Mississippi Valley paleosols developed in loess. Inventories of cosmogenic  $^{10}\text{Be}$  are used to test age assignments.

$^{10}\text{Be}$  concentrations range from  $10^6$  atom/g to  $10^9$  atom/g in soil samples measured by Accelerator Mass Spectrometry. Beryllium oxide targets are produced with a known concentration of  $^9\text{Be}$  and 10/9 ratios are determined by mass spectrometry. Analyses presented here were obtained from the Lawrence Livermore National Laboratory Center for Accelerator Mass Spectrometry.  $^{10}\text{Be}$  inventories (atom/cm<sup>2</sup>) can be calculated for soil horizons from (atom/g) X (g/cm<sup>3</sup>) X (cm of thickness), and inventories can be integrated for the entire soil profile. Assuming no inherited  $^{10}\text{Be}$  and no surface erosion, soil inventories divided by  $^{10}\text{Be}$  deposition flux (average =  $1.3 \times 10^6$  (atom/cm<sup>2</sup> yr for 100 cm/yr rainfall) approximate the exposure period for the soil.

Analyzed sites in Arkansas and Mississippi include loess exposures at Phillips Bayou on Crowley's Ridge, Arkansas and Yocona River, Mississippi. Each has multiple subsurface paleosols.

General observations for these sites are as follows. There is strong correlation of  $^{10}\text{Be}$  with the paleosols in all of the profiles.  $^{10}\text{Be}$  concentrations are highest in Bt horizons but not well correlated with percent clay. The depth distributions support evidence from other studies that  $^{10}\text{Be}$  is highly immobile in slightly acidic to neutral pH soils. The high values of  $^{10}\text{Be}$  in the basal parts of the loess sections at Phillips Bayou and Yocona River indicate that loess parent material commonly contains a concentration of about  $200 \times 10^6$  atom/g. This result is consistent with recent data from loess in China (Chengde and others, 1992) and supports the conclusion that loess is not derived directly from glacial "rock flour." This indicates that in the Mississippi Valley periglacial or post-glacial soil erosion contributed to the provenance of loess. Exposure duration calculations based on the assumption of a constant deposition flux of  $^{10}\text{Be}$  of  $1.3 \times 10^6$  (atom/cm<sup>2</sup>) yr, and corrected for the inherited component in loess, are very consistent with available  $^{14}\text{C}$  and thermoluminescence data for Late Wisconsinan (~20 ka) to Early Illinoian (~300 ka) deposits. The last interglacial soil, the Sangamon, was exposed to  $^{10}\text{Be}$  accumulation for at least 70,000 yr. This indicates that the continental interglacial climate at this latitude (35° N.) spanned all of oxygen isotope stage 5 and not just stage 5e.

CENTRAL EQUATORIAL PACIFIC HOLOCENE  
SEDIMENTATION RATES FROM RADIUM-226  
ACTIVITIES IN MARINE BARITE

PAYTAN, A., KASTNER, M., Scripps Institution of Oceanography, UCSD, La Jolla, CA 92093, USA, and MOORE, W. S., Department of Geological Sciences, University of South Carolina, Columbia, S.C. 29208. USA.

$^{226}\text{Ra}$  in marine barite from the Equatorial Pacific is enriched by at least an order of magnitude over  $^{230}\text{Th}$  activities (Borole & Somayajulu, 1977). If barite acts as a chemically closed system for Ra, the decay of unsupported  $^{226}\text{Ra}$  would allow dating of these barites and estimate of accumulation rates of the associated sediments.

The  $^{226}\text{Ra}/\text{Ba}$  ratios of marine barite separated from the upper 25cm of a box core from the central equatorial Pacific (0.6°N, 140°W) was determined by gamma counting. The Ra/Ba ratios of the bulk sediment were also measured and the data compared with their excess  $^{230}\text{Th}$  activities.

Preliminary results indicate that indeed barite in this core behaves as a closed system with respect to Ra, indicating that barite has not recrystallize nor exchanged with the pore water. The exponential decrease of the Ra/Ba ratio with depth in the upper 25cm of the core yields sedimentation rates of 3-4cm/1000y, a reasonable rate for the central equatorial Pacific. The Ra/Ba in barite separated from the upper 10cm of the core is rather uniform indicating bioturbation. This ratio is lower than the Ra/Ba ratio of particulate matter arriving at the sediment water interface in this area as measured in sediment traps (Moore & Dymond, 1991). This difference is consistent with the decay rate of Ra and the calculated "age" of the mixed-layer using the above sedimentation rate. Sedimentation rate calculated using excess  $^{230}\text{Th}$  activities of the bulk sediments in the same core yields approximately 0.3cm/1000yr, an order of magnitude lower than the  $^{226}\text{Ra}$  based rates. This may reflect higher fluxes of  $^{230}\text{Th}$  during the past 5-10 ky.

A second core with lower sedimentation rates is being analyzed for comparison.

Borole, D.V., and Somayajulu, B.L.K., 1977, Radium and Lead-210 in marine barite: *Marine Chemistry*, v.5, p.291-296

Moore, W.S., and Dymond, J., 1991, Fluxes of  $^{226}\text{Ra}$  and Barium in the Pacific ocean: the importance of boundary processes: *EPSL*, V.107, p.55-68.

GEOCHEMICAL VARIATIONS IN VANUATU ARC  
LAVAS: THE ROLE OF SEDIMENT SUBDUCTION  
AND VARIABLE MANTLE WEDGE COMPOSITION.

PEATE, David W., 170-25 Division of Geological and Planetary Sciences, California Institute of Technology Pasadena, CA 91125, USA, PEARCE, J. A., Dept. of Geological Sciences, University of Durham, Durham, DH1 3LE, UK, HAWKESWORTH, C. J., Dept. of Earth Sciences, Open University, Milton Keynes, MK7 6AA, UK, and COLLEY, H.C., Dept. of Geology, Oxford Brookes University, Oxford, OX3 0BP, UK.

Sr- and Pb-isotope and trace element compositions of Vanuatu arc lavas vary systematically along strike. The central islands (Efate to Vanua Lava) have high  $^{87}\text{Sr}/^{86}\text{Sr}$  (0.7037-0.7045) relative to the rest of the arc (0.7031-0.7036).  $\epsilon_{\text{Nd}}$ , in contrast, shows limited variation (+6 to +8) throughout the arc. Pb isotope compositions are controlled by mixing between three distinct components; attributed to 'Sediment', 'Pacific-MORB' mantle and 'Indian-MORB' mantle.

New major and trace element and isotopic analyses of sediments from the North Loyalty Basin (DSDP Site 286) should allow slab-derived elemental fluxes to be quantified for the Vanuatu arc. This arc differs from other arcs in that the subducted sediments are dominated by volcanoclastic material. The Pb isotope composition of the 'Sediment' component recognised in the arc lavas ( $^{206}\text{Pb}/^{204}\text{Pb} \sim 18.60$ ,  $^{207}\text{Pb}/^{204}\text{Pb} \sim 15.58$ ,  $^{208}\text{Pb}/^{204}\text{Pb} \sim 38.60$ ) is consistent with an average bulk composition for the sediment column at Site 286. This component is strongest in the central and southern islands (Tongoa, Efate, Tanna, Erromango) which are adjacent to the main sediment thickness (North Loyalty Basin) on the downgoing slab.

The presence of both 'Pacific-' and 'Indian-' MORB mantle in the Vanuatu arc lavas has implications for the location of the boundary between these two major mantle domains, and for the mantle dynamics within the Vanuatu arc-basin system. The 'Pacific-MORB' mantle component ( $^{206}\text{Pb}/^{204}\text{Pb} \sim 18.80$ ,  $^{207}\text{Pb}/^{204}\text{Pb} \sim 15.53$ ,  $^{208}\text{Pb}/^{204}\text{Pb} \sim 38.36$ ) is similar in composition to South Fiji Basin basement. It dominates the southern (Anatom, Futuna) and northern (Ureparapara, Vot Tande) islands and probably represents the unmodified mantle composition underlying most of the arc. The 'Indian-MORB' mantle component ( $^{206}\text{Pb}/^{204}\text{Pb} \sim 18.10$ ,  $^{207}\text{Pb}/^{204}\text{Pb} \sim 15.49$ ,  $^{208}\text{Pb}/^{204}\text{Pb} \sim 38.20$ ) is found in the central islands (Merelava, Vanua Lava, Aoba, Gaua, Ambrym), and also in the active North Fiji Basin back-arc spreading axis. The on-going collision and subduction of the D'Entrecasteaux Zone (since  $\sim 2$  Ma) has led to significant tectonic disruption of this central region of the arc, which may also have caused the recent influx of new, perhaps deeper, 'Indian-MORB' mantle material from the back-arc region.

## EPISODIC MAGMATISM IN THE PERMO-CARBONIFEROUS OSLO RIFT

PEDERSEN, L.E.<sup>a</sup>, HEAMAN, L.M.<sup>b</sup>, and HOLM, P.M.<sup>a</sup>,<sup>a</sup>Geological Institute, Øster Voldgade 10, DK-1350 Copenhagen, Denmark, <sup>b</sup>Geology Dept., Royal Ontario Museum, 100 Queen's Park, Toronto, Ontario, M5S 2C6 Canada.

The Permo-Carboniferous Oslo rift in southern Norway is an aborted continental rift in which both extrusives and intrusives are exposed today.

Precise U-Pb zircon and baddeleyite ages have been obtained for two intrusive complexes in the Vestfold Graben Segment. The Skrim-Mykle complex covers ca. 450 km<sup>2</sup> and the composition of the intrusions range from monzonite (larvikite) over syenite to peralkaline granite. The Siljan-Hvarnes complex outcrop over ca. 85 km<sup>2</sup> and comprises monzonitic and syenitic rocks.

Due to the steep slope of concordia for young ages, even small uncorrelated variations in the <sup>207</sup>Pb/<sup>235</sup>U and <sup>206</sup>Pb/<sup>238</sup>U ratios will have a large effect on the calculated <sup>207</sup>Pb/<sup>206</sup>Pb ages. Therefore, the ages discussed below are averages of 3-4 <sup>206</sup>Pb/<sup>238</sup>U ages for each sample, and must be considered minimum ages in the U-Pb system. All analyses are concordant within errors.

In the Skrim-Mykle complex 3 samples were analysed. Two are from the composite Skrim larvikite pluton and one is of the likewise composite Mykle peralkaline granite intrusion. The two Skrim larvikites yielded mean ages of 280.8 ± 0.7 Ma (2σ) and 281.2 ± 0.6 Ma, while the Mykle peralkaline granite is dated to 279.8 ± 0.7 Ma.

Further south, in the Siljan-Hvarnes complex, 4 samples were analysed; the Odberg larvikite, Siljan nordmarkite, and the Vierod and Ostvann syenites. The Odberg larvikite, which is also from field evidence inferred to be the earliest emplaced intrusion in this part of the area, yielded a mean <sup>206</sup>Pb/<sup>238</sup>U age of 278.5 ± 0.8 Ma. Two of the analyses of this sample are of baddeleyite. The Siljan nordmarkite yielded a mean age of 278.6 ± 0.6 Ma, while the Vierod and Ostvann syenites yielded 278.4 ± 0.9 and 277.3 ± 0.8 Ma, respectively.

On the basis of these ages, two periods of intense magmatic activity can be recognised at ca. 281-280 and 279-277 Ma. Each took place within less than 2 Ma, with the Skrim-Mykle complex being slightly older than the Siljan-Hvarnes complex. In addition, it is an interesting point, that not only larvikite but also peralkaline granite were emplaced in the Skrim-Mykle complex before activity began in the Siljan-Hvarnes complex.

## DEVELOPMENT OF PRECAMBRIAN CRUST IN THE SOUTHWESTERN PART OF THE BALTIC SHIELD

PEDERSEN, S. and KONNERUP-MADSEN, J., Institute of Geology, University of Copenhagen, Øster Voldgade 10, DK-1350, Copenhagen, Denmark.

Approximately 80 % of the Baltic Shield in Central South Norway consists of magmatic rocks emplaced 1500-900 Ma ago. The regional tectonic framework of the area was formed during the Sveconorwegian/Grenvillian Orogeny.

Detailed field work within key areas in conjunction with geochemical and Sr isotope analyses have provided new information on the magmatic crust-forming processes in the Baltic Shield.

Calc-alkaline rocks (s.s.) are rare and belong to the oldest period of magmatic activity with ages up to 1350 Ma.

Renewed magmatic activity between 1200 and 900 Ma reflects a largely continuous progressive evolution of crustal amalgamation.

The earliest magmatism (ca 1120 Ma) in this period includes acid intrusives and extrusives (high in silica, anorogenic in character, high FeO/MgO ratios, and Sr<sub>i</sub> = .706 +/- 2) and associated basic magmas (Sr<sub>i</sub> = .7028-.7024). Later, basic magmas intruded into the still warm crust in several pulses separated by periods of deformation.

The magmatic activity terminated with emplacement into a warm crust of K-rich magmas of alkaline affinity which form granodioritic-dioritic composite bodies and bimodal monzonitic-granitic complexes (age: 1025-900 Ma; Sr<sub>i</sub> = .7037-.7044), with associated rare mineral bearing pegmatites. Emplacement of individual bodies forming these complexes was separated by periods of deformation.

The magmatic activity collectively reflects an increasing cratonization of the SW Baltic Shield.

## PROVENANCE STUDIES OF AUSTRALIAN DUNE SANDS USING COUPLED RADIOGENIC AND STABLE ISOTOPIC TECHNIQUES

PELL, S.D., CHIVAS, A.R. and WILLIAMS, I.S., RSES, The Australian National University, Canberra, ACT 0200, Australia.

This study utilises both single-grain U/Pb (SHRIMP) analyses of zircon separated from dune sand, and the  $\delta^{18}\text{O}$  values of bulk quartz to investigate the provenance areas for sands presently located in the Australian Continental Dunefield (ACD).

Quartz-rich continental dunes of varying type and areal density cover an area of approximately  $3.1 \times 10^6 \text{ km}^2$  or 40% of the surface of Australia. The largest of the deserts making up the ACD is the Simpson Desert covering an area of  $1.3 \times 10^5 \text{ km}^2$  in the northeast corner of central Australia.

Three samples believed on the basis of preliminary characterization to be representative of the Simpson Desert as a whole have been selected for analysis of their U/Pb age distributions using the SHRIMP Ion Microprobe. It is intended to use the migration patterns of zircons to establish the scale and orientation of quartz sand dispersal in the same system.

There are distinct differences in the source regions for sand from the three areas. Samples from both the northwestern and northeastern corners of the desert show largely bimodal population distributions with peaks centred on 1125 and 1750 Ma, and 550 and 1750 Ma respectively. The third sample from the southeastern corner displays a greater spread of ages ranging between 100 and 3100 Ma. Comparing the age distribution of the samples with known ages of crustal material some preliminary comment can be made on sand source areas. The age range of the major population (1600-1900 Ma) from the northeastern and northwestern Simpson correspond well with that of the Arunta and Mt. Isa Blocks, while the minor population (1000-1300 Ma) may be related to the Musgrave Block. The 250-550 Ma population from both the southeast and northeast of the desert can be attributed to sediment derived from the northeastern Australian granitoids. The presence of this younger granitoid material is strong evidence for the fluvial transport of material from ultimate source regions 1000 km east of the dunefield and perpendicular to, or against the direction of aeolian transport.

The  $\delta^{18}\text{O}$  values of bulk quartz have been determined not only to investigate the source areas of sand, but also to examine the mixing trends between the different source areas. Preliminary  $\delta^{18}\text{O}$  results range between 10.2 and 12.6‰ (SMOW) and show significant variation with location. Such isotopic studies provide the means of carrying out provenance investigations on a much wider scale than is possible using zircon age dating, although on bulk samples and not individual grains.

Results obtained in the study point to there being numerous local sources of sand to the desert areas. The suggested mechanism for the transport of this material into the desert areas is via rivers and drainage channels. It is suggested that the effect of wind is only to shape dunes and not to transport sand significant distances.

## CHARISMA, A NEW MICROFOCUS SECONDARY NEUTRAL MASS SPECTROMETER EMPLOYING RESONANCE IONIZATION

PELLIN, Michael J.<sup>1</sup>, MA, Zhiliu<sup>1</sup>, THOMPSON, Rita N.<sup>1,2</sup>, DAVIS, Andrew M.<sup>3</sup>, LEWIS, Roy S.<sup>3</sup>, and CLAYTON, Robert N.<sup>2,3,4</sup>; <sup>1</sup>Materials Science and Chemistry Departments, Argonne National Laboratory, Argonne, IL 60439; <sup>2</sup>Department of the Geophysical Sciences, <sup>3</sup>Enrico Fermi Institute, <sup>4</sup>Department of Chemistry, University of Chicago, Chicago, IL 60637.

Despite the tremendously successful use of conventional secondary ion mass spectrometry in geochemistry and cosmochemistry, this technique suffers from two important limitations: (1) the presence of unresolvable isobaric interferences (between Zr and Mo or between many of the REE, for example) and (2) the low ionization efficiency of some elements, such as siderophiles. We have developed a new instrument, named CHARISMA (Chicago-Argonne Resonance Ionization Spectrometer for Micro-Analysis), that uses tuned lasers to resonantly ionize sputtered or laser-ablated neutral atoms, allowing elemental selectivity and useful yield (atoms detected/atoms removed from sample) in excess of 10%. A microscope employing reflected-light optics is built into the instrument, permitting samples to be viewed with sub- $\mu\text{m}$  resolution and allowing introduction of focussed light from a UV laser for laser ablation of samples a few  $\mu\text{m}$  across. Secondary neutrals can also be produced by sputtering using an ion gun with a 30° incident angle. Lasers tuned to resonant frequencies ionize neutral atoms immediately above the sample surface. The resulting ions are extracted normal to the surface and passed through a 4 m flight path reflectron-type time-of-flight mass spectrometer capable of a mass resolution ( $M/\Delta M$ ) of  $10^4$ . Testing of the recently-completed instrument has demonstrated sub- $\mu\text{m}$  imaging, laser ablation on few- $\mu\text{m}$  spots with photoionization by a second laser ( $M/\Delta M \geq 3000$ ) and laser photoionization of  $\text{Ar}^+$ -sputtered neutral Mo ( $M/\Delta M \geq 2500$ ). We anticipate significant increases in mass resolution as we gain familiarity with the tuning characteristics of the instrument. Planned future improvements to the instrument include installation of tunable solid-state lasers for resonance ionization.

Great strides have been made in understanding nucleosynthesis in the past few years through microbeam analysis of interstellar SiC and graphite grains isolated from primitive meteorites. Ti, Zr and Mo are important for understanding a variety of nucleosynthetic processes. SIMS analyses of large SiC grains have been done for Ti, but analyses of Zr and Mo have not been done because of mutual isobaric interferences. We plan to extend Ti isotopic measurements to smaller SiC grains as well as TiC-bearing graphite grains. We also hope to initiate Zr and Mo isotopic analysis of individual grains.

FIELD, GEOCHEMICAL AND GEOCHRONOLOGIC EVIDENCE FOR POLYCYCLIC VOLCANISM AT THE LATHROP WELLS VOLCANIC CENTER, SOUTHWESTERN NEVADA

PERRY, Frank V., CROWE, Bruce M., Los Alamos National Laboratory, Los Alamos, NM 87545, USA, WELLS, Stephen G., University of California, Riverside, CA 92521, USA, and McFADDEN, Leslie, D., University of New Mexico, Albuquerque, NM 87131, USA.

The Lathrop Wells volcano in southwestern Nevada is an isolated, small-volume ( $<0.15 \text{ km}^3$ ) basaltic eruptive center that has been studied in unprecedented detail as part of multidisciplinary volcanic hazard studies for the DOE's Yucca Mountain Project. Volcanoes of the Lathrop Wells type are generally interpreted to be monogenetic, representing the eruption of a single magma batch over a period of weeks to years. Erosional unconformities and soil horizon development, however, indicate that the Lathrop Wells center formed during four main eruptive episodes separated by significant ( $>10^4$  years) periods of inactivity (*polycyclic volcanism*). Multiple dating methods ( $^{40}\text{Ar}/^{39}\text{Ar}$ , U-Th disequilibrium, cosmogenic He, thermoluminescence) indicate that eruptive episodes occurred at  $>100 \text{ ka}$  to  $<4 \text{ ka}$  ago, but these methods do not yield consistent results in some cases.

All four eruptive episodes erupted compositionally similar, evolved hawaiite with Mg numbers that cluster tightly at a value of  $54 \pm 1$ . In detail, all of the eruptive episodes can be distinguished by small, but systematic, differences in incompatible-element concentrations and ratios (e.g., La/Sm, Th/K). The different incompatible-element ratios at the same Mg number for different eruptive units cannot be related to each other by simple fractionation of a single magma batch. We have modeled recharge of a more primitive magma into a fractionating magma as a mechanism for buffering the Mg number of a magma at a steady-state value, while allowing continued evolution of trace-element ratios. Recharge/fractionation of a single magma may account for differences in highly incompatible/incompatible-element ratios (e.g., La/Sm), but cannot account for differences in highly incompatible/highly incompatible element ratios (e.g., Th/K).

From differences in incompatible-element ratios, we conclude that a minimum of 6-8 magma batches were involved in the formation of the Lathrop Wells center, representing separate partial melts of a heterogeneous lithospheric mantle source. Systematic enrichment of La/Sm, Th/K and Th, and systematic depletion of Ti of the eruptive units with time may be related to changes in the mantle source or changes in the amount of partial melting through time.

The ascent and eruption of multiple magma batches over the last  $10^5$  years at a single persistent location may be related to a penetrating, northwest-trending zone of right-slip shear. The pattern of past eruptions suggests that the location of future eruptions is unlikely to change in the short term, which decreases the probability that magma will directly penetrate the proposed repository site at Yucca Mountain, located 18 km to the north, during the next  $10^4$  years.

ISOTOPIC AND TEXTURAL STUDIES OF MINERALS FROM THE CORDILLERA BLANCA BATHOLITH, PERU: IMPLICATIONS FOR CRYSTALLISATION PROCESSES IN LARGE GRANITOID INTRUSIONS

Nick PETFORD, School of Geological Sciences, University of Kingston, Surrey, KT1 2EE, UK, and Barbara BARREIRO, Isotope Geoscience Laboratory, Keyworth, Nottingham NG12 5GG, UK.

New isotopic data (Pb, Sr, Nd, O, D/H) are presented on mineral separates from five young (ca. 6 Ma) granitoid rocks from the Miocene Cordillera Blanca batholith, Peru. The samples, previously analysed for whole-rock  $^{87}\text{Sr}/^{86}\text{Sr}$  and  $^{143}\text{Nd}/^{144}\text{Nd}$  (0.7041-0.7057  $\epsilon\text{Nd}$  +0.16 to -2.46), show evidence at the grain scale for large degrees of mineral disequilibrium, inconsistent with simple (monotonic) cooling models for large intrusions. All of the variation in isotopic composition within a particular rock is bracketed by muscovite and sphene, which act effectively as compositional end members. Thus, the range in  $^{206}\text{Pb}/^{204}\text{Pb}$  between muscovite and sphene in one sample (17.84-22.33) is similar to that recorded for the entire Andean volcanic chain.

Muscovite textures, along with relatively low Ti contents ( $<0.18 \text{ wt}\%$ ) show them to be secondary in origin, consistent with their low  $^{206}\text{Pb}/^{204}\text{Pb}$  ratios and younger Rb-Sr and  $^{40}\text{Ar}/^{39}\text{Ar}$  ages. The development of secondary muscovite can be related to late-stage fluid influx from the country rocks along shear zones during the waning stages of batholith emplacement. More problematical are the consistently higher  $^{207}\text{Pb}/^{204}\text{Pb}$  ratios in K-feldspars from all rocks, and the high Nd contents (up to 94 ppm) of some biotite micas. However, detailed optical examination (TEM, CL) shows them to contain numerous tiny inclusions of accessory apatite and sphene. We consider these included phases to be the cause of much of the apparent isotopic disequilibrium within samples.

He, Ar AND Rb-Sr ISOTOPE SYSTEMATICS OF FLUID INCLUSIONS IN QUARTZ, VEIN MINERALS AND NATIVE GOLD FROM EPIGENETIC LATE ALPINE Au-VEINS IN NW ITALY

PETTKE<sup>1</sup>, Th.; DIAMOND<sup>1</sup>, L. W.; VILLA<sup>1</sup>, I. M.;  
TOLSTIKHIN<sup>2,3</sup>, I. N. AND KAMENSKY<sup>3</sup>, I. L.

(1) University, Inst. of Mineralogy, Erlachstr. 9a, Bern, CH-3012, Switzerland. (2) Dept. of Earth Sciences, University, Cambridge CB2 3EQ, U. K. (3) Geol. Inst., Kola Scientific Centre of Russian Acad. of Sci., Apatity, 184200, Russia

He, Ar and Rb-Sr systematics were investigated in Au-qtz veins (Brusson, Monte Rosa district) on qtz (He, Ar), carbonates (carb; He, Ar, Rb-Sr), native Au (He), bulk qtz inclusion fluids (Rb-Sr) and muscovites (Rb-Sr, <sup>40</sup>Ar/<sup>39</sup>Ar) respectively. The aim was to constrain modifications of the ore bearing fluid during its ascent, its age, and to estimate characteristics of its source.

<sup>3</sup>He/<sup>4</sup>He (always in \*10<sup>-6</sup>) of all qtz + carb range between 0.035 - 0.238. Meta-ophiolite hosted veinlets have 0.201 - 0.238, their Rb-Sr (qtz+cc+ms) yield the formation age of 30Ma (confirmed by <sup>40</sup>Ar/<sup>39</sup>Ar on ms) and the lowest Sr<sub>i</sub> = 0.708.

<sup>3</sup>He/<sup>4</sup>He of thick veins cutting various rock types all cluster between 0.084 - 0.134 (qtz) and 0.06 - 0.035 (carb) and show higher and variable Sr<sub>i</sub> (0.7095 - 0.729). He concentrations are higher for samples with a more radiogenic signature.

One freely grown Au-sample (300mg) was degassed in 5 steps. Most He came at ≈700°C (fluid inclusion decrepitation?): <sup>3</sup>He/<sup>4</sup>He = 0.34±9, [<sup>4</sup>He] = 5.7nl STP/g, significantly higher than all qtz <sup>3</sup>He/<sup>4</sup>He (0.084 - 0.107) from the same vein.

<sup>4</sup>He/<sup>40</sup>Ar\* varies, even within individual veins, from 1.3 (veinlets in meta-ophiolite, late qtz from thick veins in meta-granite) up to 23 (qtz from thick veins in metasediments and metagranite). <sup>40</sup>Ar/<sup>36</sup>Ar range between 1450 - 2290 for the 700°C step of qtz (most gas because of final fluid inclusion breakup), for associated dol between 1530 - 2350. Later cc is markedly lower (312 - 496).

The bulk He-Ar signature for qtz + carb is taken as the trapped signature, being aware of diffusive loss and radiogenic production affecting trapped gases. Given 30Ma, the low [U], [Th] and [K] in qtz + carb contribute less radiogenic <sup>4</sup>He, <sup>3</sup>He and <sup>40</sup>Ar than our analytical error. Further, the retentivity for in situ produced He is lower than for trapped He. If all <sup>4</sup>He\* produced from U/Th decay in 30Ma was retained in the gold we need a trapped <sup>3</sup>He/<sup>4</sup>He of ≈ 0.6.

In summary: (1) The Au-veins have qtz + carb with a radiogenic (crustal) He - Ar signature. <sup>3</sup>He/<sup>4</sup>He from thick veins cutting different rock types are indistinguishable, but the corresponding Sr<sub>i</sub> vary with host rock type and vein thickness.

(2) Higher <sup>3</sup>He/<sup>4</sup>He in qtz + carb from veinlets in meta-ophiolite are interpreted as a host-rock signature. (3) The elevated <sup>3</sup>He/<sup>4</sup>He found in native Au points to a <sup>3</sup>He input of a meteoric (or mantle?) component. (4) <sup>40</sup>Ar/<sup>36</sup>Ar for qtz of the free Au bearing vein are the lowest of all veins and support the idea of formation water, but not mantle, input with Au deposition.

The fluid signatures show important and variable modifications of He - Ar isotopic and Rb/Sr elemental ratios. The results allow to exclude the metagranites (wrong direction of Sr<sub>i</sub> evolution) and the meta-ophiolites (they increase <sup>3</sup>He/<sup>4</sup>He) as the fluid source for qtz + carb. The paragneisses remain as its most likely source rock.

He isotopic disequilibrium between native Au and qtz + carb questions the use of petrographically cogenetic vein minerals to estimate processes responsible for Au deposition. <sup>3</sup>He/<sup>4</sup>He of the native Au does not argue against a meta-ophiolitic source for Au, in contrast to qtz + carb.

THE MARINE OS-ISOTOPE RECORD OVER THE PAST 85 MA

PEUCKER-EHRENBRINK, B., MPI für Chemie, Geochemie, Postfach 3060, 55020 Mainz, Germany, RAVIZZA, G., WHOI, Woods Hole, MA 02543, USA, HOFMANN, A.W., MPI für Chemie, Geochemie, Postfach 3060, 55020 Mainz, Germany.

In order to extend the previously reported marine Os record back in time, we have measured the Os concentration and Os-isotopic compositions of 25 Pacific metalliferous sediments. Analyses of a few samples of Cretaceous and Jurassic age yield <sup>187</sup>Os/<sup>186</sup>Os values between 3.5 and 5.5. Re concentrations of several of these old samples have been measured. Resulting <sup>187</sup>Re/<sup>186</sup>Os values are lower (<55) than average crustal material (about 400) and age corrections to the measured Os-isotope ratios usually can be neglected (<0.1). Throughout the Cenozoic the observed isotopic variations are similar to existing data.

There is a pronounced <sup>187</sup>Os/<sup>186</sup>Os minimum at the K/T-boundary, probably reflecting the enormous input of cosmogenic input into the oceans by the K/T-impactor. Bulk- and leach-analysis of the K/T samples from DSDP site 596 yield nearly chondritic Os isotopic compositions (<sup>187</sup>Os/<sup>186</sup>Os about 1.25). Low <sup>187</sup>Os/<sup>186</sup>Os values persist for several million years after the impact at site 596 but analyses of sediment leachates from additional cores suggest that the Os isotopic composition of seawater recovered more rapidly, to a <sup>187</sup>Os/<sup>186</sup>Os of about 3.2 by 63 Ma ago. These data also indicate that some portion of the extraterrestrial Os in site 596 sediments is soluble during peroxide-leaching and therefore complicates our efforts to reconstruct the Os isotopic composition of seawater through time.

Data from the early and middle part of the Cenozoic show a continued gradual increase in <sup>187</sup>Os/<sup>186</sup>Os to about 6 at 15 Ma. The significant scatter in the data and the fact that bulk analyses generally show a smoother trend compared with leachates indicates that the peroxide-leach does not liberate exclusively hydrogenous osmium. Alternatively, this scatter could be interpreted as an indication that the Os isotopic composition of seawater is heterogeneous during this time period.

The period from 15 Ma to the present is characterized by good agreement of bulk- and leach-analysis and a gradual increase in the <sup>187</sup>Os/<sup>186</sup>Os from about 6 to approximately 8.5 in recent marine sediments. If the scatter in the data prior to 15 Ma is not due to analytical problems, and therefore reflects either short-term variations or regional differences in the isotopic composition of seawater, the change in slope of the seawater evolution curve at 15 Ma could coincide with a transition from a heterogeneous to a well-mixed ocean with respect to osmium.

**CHLORINE-36 CHRONOLOGY FOR THE LATE PLEISTOCENE LACUSTRINE HISTORY OF PANAMINT AND DEATH VALLEYS, CALIFORNIA**

**PHILLIPS, Fred M., and ZREDA, Marek G., Department of Geoscience, New Mexico Tech, Socorro NM 87801, SHARMA, P., and ELMORE, David, PRIME Laboratory, Physics Department, Purdue University, West Lafayette IN 47907-1396**

Panamint and Death Valleys were the last two lacustrine basins in the pluvial paleo-Owens River system. Both of them show clear evidence of occupation by large lakes, in the form of shoreline features and lacustrine/evaporite sediments in drill cores. However, the deeply eroded state of the high shorelines indicates that the lakes predated the last glacial maximum. In this study we have analyzed cosmogenic  $^{36}\text{Cl}$  in a variety of shoreline materials, including beach gravels, boulders from wave-cut shorelines, and tufas. In addition to these, we analyzed  $^{36}\text{Cl}$  in halite deposited out of the lake waters.

Of all these materials, the tufas appear to give the most reliable results. Tufas on the upper edge of the shoreline features in Panamint Valley gave exposure ages close to 90 ka, those near the bottom edge closer to 65 ka. These ages are in good agreement with U/Th age estimates by other investigators. The  $^{36}\text{Cl}$  measurements on the uppermost halite bed yield a deposition age of  $90 \pm 70$  ka. These ages indicate an effectively wetter climate in the area during the last interglaciation (isotope stage 5) and early Wisconsin than during the late Wisconsin maximum.

Other shoreline materials gave systematically older  $^{36}\text{Cl}$  exposure ages than the tufas. We attribute this to  $^{36}\text{Cl}$  accumulated during the alluvial history of the clasts prior to the lacustrine reworking. Caution should be used in interpreting cosmogenic nuclide exposure ages from any shoreline materials that were not precipitated from the lake waters.

**IN SITU-PRODUCED  $^{14}\text{C}$  IN LATE QUATERNARY LAVA FLOWS, WESTERN UNITED STATES**

**PHILLIPS, W. M., LIFTON, N. A., QUADE, J., JULL, A. J. T., Department of Geosciences, University of Arizona, Tucson, AZ 85721**

The buildup of in situ-produced radiocarbon ( $^{14}\text{C}_{is}$ ) is potentially useful for dating geomorphic surfaces exposed over the last 2000 to 20,000 years. We have developed methods to remove contaminant  $^{14}\text{C}$  and quantitatively extract  $^{14}\text{C}_{is}$  from basalts and quartzites (Lifton and others, 1993). These procedures do not require mineral separates and should work with any non-carbonate rock. We are testing our techniques on late Quaternary basalt flows from the western United States. These include the McCarty's, Bandera, and Twin Craters flows, El Malpais field, New Mexico; Blue Dragon flow, Craters of the Moon field, Idaho; and the Tabernacle Hill flow, Utah. In addition, we are applying  $^{14}\text{C}_{is}$  methods to the problem of dating the Lathrop Wells volcanic field, Nevada. Our samples are from pahoehoe flows with clear indication of original surfaces. Surface samples consist of the upper 2 to 4 cm of unshielded, horizontal pahoehoe slabs with less than 1 cm erosion and no evidence for shielding by soils, aeolian sediments, or nearby objects. Shielded samples greater than 2 m below flow surfaces were also taken from lava tubes and road cuts. The shielded samples test our ability to remove contaminant  $^{14}\text{C}$  and to detect subsurface  $^{14}\text{C}$  production mechanisms. Except for Lathrop Wells samples, the flows are dated by one or more conventional radiocarbon dates and range in age from about 17,800 to 2000 years old. Preliminary results indicate that shielded samples contain less than  $7 \times 10^4$   $^{14}\text{C}$  atoms  $\text{gm}^{-1}$ . This suggests removal of nearly all contaminant  $^{14}\text{C}$  and that subsurface production mechanisms are unimportant. A surface sample from the McCarty flow contains  $2.16 \times 10^5$   $^{14}\text{C}$  atoms  $\text{gm}^{-1}$ . The McCarty flow has two AMS dates on charcoal from rootlets at the base of the lava that give ages in calibrated years bp of 3332 - 3292 and 3271 - 3074 (1  $\sigma$ ). The apparent  $^{14}\text{C}_{is}$  production rate is  $37 \pm 10$   $^{14}\text{C}$  atoms  $\text{gm}^{-1}$   $\text{SiO}_2$  (normalized to rock surface, sea level, and latitude  $> 60^\circ$ ; rock density  $2.5 \pm 0.2$   $\text{g cm}^{-3}$ , absorption mean free path  $160 \pm 15$   $\text{g cm}^{-2}$ , geographic latitude  $35.08^\circ$ ). This is significantly greater than the 17,800 year integrated rate of  $19 \pm 3$  atoms  $\text{gm}^{-1}$  reported by Lifton and others (1993). Further work is needed to determine if this variation in production rate is real.

Lifton, N. A., Phillips, W. M., Jull, A. J. T., Quade, J., 1993, Integrated late Quaternary production rates for in situ-produced cosmogenic  $^{14}\text{C}$  from Lake Bonneville shoreline features using new extraction techniques: EOS, v. 74, no. 43, p. 649.

### <sup>231</sup>Pa/<sup>235</sup>U DISEQUILIBRIUM IN VOLCANIC ROCKS

PICKETT, David A., and MURRELL, Michael T., CST-8, MS J514, Los Alamos National Lab, Los Alamos, NM 87545. 110096@inccdp3.lanl.gov

<sup>231</sup>Pa is the only long-lived ( $t_{1/2}=32.8$  ka) intermediate nuclide in the <sup>235</sup>U decay chain. Radioactive disequilibrium in this parent-daughter pair in magmas, i.e., (<sup>231</sup>Pa/<sup>235</sup>U)  $\neq$  1, indicates recent fractionation between two highly incompatible elements, as in the <sup>230</sup>Th/<sup>238</sup>U and <sup>226</sup>Ra/<sup>230</sup>Th systems. We have measured (<sup>231</sup>Pa/<sup>235</sup>U) in young volcanic rocks by ID-TIMS in an attempt to better understand such disequilibria. Published data on MORB by Goldstein et al. (*EPSL* 115, 151) show large Pa enrichments, with (<sup>231</sup>Pa/<sup>235</sup>U) = 2.36-2.89, where (<sup>230</sup>Th/<sup>238</sup>U) = 1.13-1.25; these disequilibria have proven useful for age-dating (*Nature* 367, 157). We have recently reported (*Eos* 74, no. 16, 341) that Pa is markedly more incompatible than U in andesite, qualitatively consistent with Pa enrichment relative to U in melts.

We present data on 31 rocks of various tectonic settings and compositions (included are three analyses by R. Williams). With few exceptions, young volcanic rocks have (<sup>231</sup>Pa/<sup>235</sup>U) > 1, (<sup>231</sup>Pa/<sup>235</sup>U) > (<sup>230</sup>Th/<sup>238</sup>U) (i.e., Pa/U fractionation is greater than Th/U as in MORB), and show correlation between the two ratios. Compared to MORB, intraplate basalts have smaller, but still high, (<sup>231</sup>Pa/<sup>235</sup>U) ratios, indicative of fundamental differences in evolution. Ratios in Iceland tholeiites (1.9, 2.0) are much higher than in a Hawaii tholeiite (1.1), perhaps reflective of higher melting rates in the latter (see Beattie, *Nature* 363, 63). An Iceland basalt with other evidence for crustal contamination has appropriately lower (<sup>231</sup>Pa/<sup>235</sup>U) of 1.2. Among three Hawaii basalts ranging from tholeiite to basanite, there is a corresponding increase in (<sup>231</sup>Pa/<sup>235</sup>U) and (<sup>230</sup>Th/<sup>238</sup>U) (Sims et al., this volume) that is likely due to varying degrees of partial melting. Ratios of up to 2.0 in continental basalts argue against models invoking long (compared to 33 ka) crustal residence to explain their near-equilibrium (<sup>230</sup>Th/<sup>238</sup>U) values.

Among arcs, island arc lavas tend toward higher (<sup>231</sup>Pa/<sup>235</sup>U) than those on continental margins, but both suites show a rough correlation between (<sup>231</sup>Pa/<sup>235</sup>U) and (<sup>230</sup>Th/<sup>238</sup>U). This could be explained by U enrichment relative to both Th and Pa, consistent with a slab-derived fluid component. A Tonga andesite is the only non-carbonatite to show Pa depletion (0.93), perhaps due to this component. It is notable, however, that arcs typically still have (<sup>231</sup>Pa/<sup>235</sup>U) > 1 when (<sup>230</sup>Th/<sup>238</sup>U) < 1, either arguing against U enrichment or arguing for the dominance of the melt-related (?) Pa enrichment over the fluid-related U enrichment. Regardless of the process, the patterns suggest that the well-noted tendency of arc rocks for near-equilibrium (<sup>230</sup>Th/<sup>238</sup>U) (e.g., Condomines and Sigmarsson, *GCA* 57, 4491) is fortuitous and not due to a component in secular equilibrium.

The generally high (<sup>231</sup>Pa/<sup>235</sup>U) ratios noted in most samples, and especially in MORBs, are difficult to reconcile with current melt evolution models. Nevertheless, the (<sup>231</sup>Pa/<sup>235</sup>U) system promises to greatly enhance studies based on (<sup>230</sup>Th/<sup>238</sup>U) and (<sup>226</sup>Ra/<sup>230</sup>Th) disequilibria for two reasons: it is more sensitive to magmatic processes than the former and approaches equilibrium less rapidly than the latter.

### CALIBRATION OF ZIRCON STANDARDS FOR THE CURTIN SHRIMP II.

PIDGEON, R.T., FURFARO, D., KENNEDY, A.K. NEMCHIN, A.A., VAN BRONSWJK, W., Curtin University of Technology, Kent Street, Bentley, 6012, Western Australia and TODT, W.A., Max Planck Institute for Chemistry, Mainz, 55020, Germany.

A SHRIMP II has recently been installed at the Curtin University of Technology. A most important task in developing a capability to analyse zircons using this ion microprobe is the preparation of zircon standards. We are approaching this task in two ways. Firstly we are investigating large homogeneous zircon crystals as suitable standards and secondly we are investigating the suitability of zircon populations from certain rock types. The requirements for a standard are that it has a suitably high concentration of U and Pb and has concordant U-Pb systematics. Also there needs to be enough of the standard to allow three or more years ion microprobe analyses, assuming that a piece of the standard is included in every mount as is the present practice at the ANU. Our primary standard zircon CZ3 has been prepared from a Sri Lankan gem zircon weighing just under one gram. It has no observed zoning and XRD and Raman spectroscopy analyses confirm that the structure of this crystal is relatively undamaged by long term radiation. Conventional isotope dilution measurements on chips taken from various parts of the crystal show it to have a concordant age of 564Ma. SHRIMP measurements on the polished surfaces of a number of chips show these are homogeneous in Pb/U ratio and has a U concentration of 530-560ppm. In addition to CZ3 we are investigating a number of ca 2.6 Ga zircon populations which have crystallised or recrystallised under granulite facies conditions as potential standards.

NEOPROTEROZOIC ISLAND ARC ROCKS OF MARA ROSA, CENTRAL BRAZIL: PRELIMINARY U-Pb AND Sm-Nd DATA.

PIMENTEL, M.M., Instituto de Geociências, Universidade de Brasília, Brasília, 70910-900, Brazil, WHITEHOUSE, M.J., Dept. of Earth Sciences, University of Oxford, Oxford, OX1 3PR, U.K., MACHADO, N., Geotop, Université du Québec à Montréal, Montreal, H3C 3P8, Canada, FUCK, R.A., Instituto de Geociências, Universidade de Brasília, Brasília, 70910-900, Brazil, VIANA, M.G., Instituto de Geociências, Universidade de Brasília, Brasília, 70910-900, Brazil.

The Precambrian Mara Rosa sequence in northern Goiás, central Brazil, includes metavolcanic (mafic to felsic) and metasedimentary rocks which have geochemical characteristics compatible with an origin in an island arc system. The sequence occurs in several NNE belts, separated from each other by tonalitic/granodioritic orthogneisses. In this study we report preliminary zircon and titanite U-Pb geochronological data and whole-rock Sm-Nd results for the Mara Rosa rocks. The results are as follows: (i) calc-alkaline orthogneisses yielded a zircon age of  $856 \pm 13/-7$  Ma and  $\epsilon_{\text{Nb}}(\text{T})$  of +4.6, with  $T_{\text{DM}}$  model age of ca. 1.0 Ga; (ii) felsic metavolcanics from the Posse gold mine have a concordant zircon age of  $862 \pm 8$  Ma.  $\epsilon_{\text{Nd}}(\text{T})$  is positive (+3.7) and the  $T_{\text{DM}}$  model age is also ca. 1.0 Ga. Titanites from the same sample revealed a recrystallization age of  $632 \pm 4$  Ma which may represent a good estimate for the age of Au mineralization; (iii) a small syn-tectonic dioritic body emplaced into the Mara Rosa metavolcanics has a concordant zircon age of  $630 \pm 3$  Ma.  $\epsilon_{\text{Nd}}(\text{T})$  for this rock is +2.1 and  $T_{\text{DM}}$  model age is ca. 1.0 Ga; (iv) the Amador post-orogenic two-mica leucogranite (< ca. 630 Ma) has a slightly older  $T_{\text{DM}}$  model age (ca 1.2 Ga) and a negative  $\epsilon_{\text{Nd}}(600)$  of -2.1, compatible with a more "enriched", perhaps metasedimentary, source; (v) east of the Mara Rosa terrane, a sample of the Pau de Mel granite-gneiss, from the sialic basement of the Serra da Mesa supracrustals (pelite-psamite-carbonate association) yielded a zircon age of  $2175 \pm 12/-9$  Ma.

The data show that the Mara Rosa rocks were accreted to the continental crust during the Neoproterozoic and do not represent Archaean granite-greenstone associations, as previously thought. The older age of the Pau de Mel granitoid suggests that it is part of the continental foreland to which the island arc terrane was accreted.

The U-Pb and Sm-Nd isotopic/geochronological patterns obtained are very similar to those previously identified in similar metavolcanic-orthogneiss assemblages in western Goiás (Pimentel & Fuck 1992), demonstrating that the products of Neoproterozoic crustal accretion processes along island arc systems are exposed over very large areas in central Brazil. The data show that the Brasília fold belt includes an extensive area of juvenile crust and does not represent an ensialic orogenic belt.

Pimentel, M.M., and Fuck, R.A., Neoproterozoic crustal accretion in central Brazil: *Geology*, 20(4):375-379.

GEOCHEMICAL AND ISOTOPIC (Sr, Nd) MODELLING OF ORDOVICIAN INTRUSIVES FROM SERIE DEI LAGHI (S-ALPS)

PINARELLI, Laura, Istituto di Geocronologia e Geochimica Isotopica, C.N.R., Pisa, Italy, 55100, and PEZZOTTA, F., Dip.to Scienze della Terra, University of Milano, Milano, Italy, 20100.

Granitoid rocks belonging to an Ordovician magmatic cycle are present in many areas of the European Paleozoic basement. Calc-alkaline intrusive rocks attributed to this cycle (whole-rock isochron age of  $466 \pm 5$  Ma), occur in the central-western segment of the Alpine arc (Serie dei Laghi). Hercynian amphibolite facies regional metamorphism affected the Serie dei Laghi basement.

This paper deals with the petrogenesis of the Ordovician intrusives of the Serie dei Laghi using mineral chemistry, major and trace elements, REE and isotope geochemistry (Sr and Nd).

Four lithologies are present: Hornblende-bearing Metagranitoids (HM); Biotite+muscovite-bearing Metagranitoids (BM); (meta)Aplites and Microgranites (AM); Porphyritic Metaleucogranites (PM).

The mineral chemistry data evidence incomplete mineralogical modifications, indicating that the whole rock geochemistry of the studied samples was unaffected by the metamorphism.

As a whole, the intrusives studied range from gabbro-dioritic to granitic in composition. Major elements, as well as Co, Cr, Ni, Sc, and V, show mostly linear trends in the variation diagrams versus DI, LILE and HFSE, instead, do not show a regular distribution along the series. Indeed, most trace elements have bell shaped trends, the PM samples having opposite trends with respect to HM and BM. AM show largely scattered plots.

REE patterns show moderate LREE enrichment, and a progressive increase of the negative Eu anomaly and HREE fractionation from gabbro-diorite to granites. AM show highly variable cross-cutting REE patterns.

Initial Sr and Nd isotope ratios vary considerably along the series from the more mafic ( $(^{87}\text{Sr}/^{86}\text{Sr})_i = 0.70432$ ;  $\epsilon_{\text{Nd}} = -0.72$ ) to the more felsic ( $(^{87}\text{Sr}/^{86}\text{Sr})_i = 0.71232$ ;  $\epsilon_{\text{Nd}} = -6.64$ ) samples. These data indicate a mantle-derived parental magma, which evolved towards more crustal characteristics.

On the basis of trace element distribution and Sr and Nd isotopic covariation, a model of combined assimilation and fractional crystallization (AFC) is proposed for the mafic-intermediate part of the series (HM and BM). For the geochemical evolution of the more felsic samples (PM), an incomplete unmixing model between crystals (K-feldspar+plagioclase) and residual melt could be inferred.

SR- O -ISOTOPE SYSTEMATIC OF  
ALKALINE ROCKS OF RUSSIA  
POKROVSKY B.G. Geological  
Institute, Russian Academy of  
Science, Pyzhevsky per.,7,  
Moscow 109017, Russia

Rb-Sr systems and stable isotopes composition have been studied in the massifs of alkali-ultrabasic rocks, alkali-gabbro, nepheline sienites, ultrapotassic pseudoleucitic sienites, rare metal alkaline granites and alkaline extrusives of different regions of Russia. The isotope data indicate that alkaline rocks parental magmas were derived in the cases from depleted mantle source and then contaminated by crustal material in the magmatic chambers and conduits. Rocks of similar chemical composition (such as pseudoleucitic sienites for example) have different O- and Sr-isotope compositions and cannot be connected with any uniform mantle source.

Both high  $\delta^{18}\text{O}$  ( $\delta^{18}\text{O} > 7$ ), and low  $\delta^{18}\text{O}$  ( $\delta^{18}\text{O} < 5$ ) rocks were found. The former occurred in the sedimentary carbonate host, and the latter occurred in the precambrian metapelites. The form of dependence between Sr- and O-isotope ratios, and between isotope and elemental composition of alkaline rocks suggest that interaction of mantle magmas with high Sr brines is responsible for the isotope variations.

Examples of the strongest contamination are urtites-anchimonomineralic nepheline rocks of magmatic origin, widespread in the South Siberia. On their isotope composition:  $(\frac{87}{86}\text{Sr})_0 = 0.7058 \pm 0.7075$ ;  $\delta^{18}\text{O}_{\text{w.r.}} = 9.4 \pm 12.1$ ;  
 $\delta^{18}\text{O}_{\text{px}} = 9.0 \pm 11.5$  urtites are

close to nepheline-melilite scarns which form at the contact of gabbro with sedimentary carbonates. Material balance calculation indicate that up to 60-70% of Sr and 40-50% of O in the urtites were extracted from surrounding rocks.

## A STUDY ON CRUSTAL EVOLUTION AND TECTONIC SETTING APPLYING RB/SR, SM/ND AND TRACE ELEMENT ANALYSES (SILVRETTA, SWITZERLAND)

POLLER, U. & LIEBETRAU, V., Institut. of Min. & Petrography, Fribourg, 1700, Switzerland, NÄGLER, T., Lab. for Isotope Geology, Institut. of Min. & Petr., Bern, 3012, Switzerland, MAGGETTI, M. Institute of Min. & Petrography, Fribourg, 1700, Switzerland

The Silvretta crystalline complex, one of the upper austro-alpine nappes, is situated in the eastern part of Switzerland and the austrian regions Tirol and Vorarlberg. Beside amphibolites, gabbros, eclogites and paragneisses a large variety of orthogneisses exists. Generally they are divided into two groups: the Flüelagranitic Association and the so-called Older Orthogneisses including the Mönchalpogneiss.

The Mönchalpogneiss is classified as metagranodiorite to metagranite and the Flüelagranitic Association as former monzo- to syenogranites. Conforming to the common definition of granitoids an A-type characteristic can be excluded for all samples by trace element diagrams. The analyzed Silvretta gneisses show S-type characteristics in the diagrams of Hine et al. (1978) as well as in the more recent ones of Castro et al. (1991).

The original tectonic setting of the rocks was evaluated based on trace element-plots (e.g. Pearce et al. 1984). For most samples the within plate granites (WPG) and the ocean ridge granites (ORG) can be negated using Nb, Y and Si. Only a few orthogneisses of the Flüelagranitic Association plot inside the WPG field because of exceptional high yttrium contents. Plotting Rb against Y+Nb the Mönchalpogneisses clearly occupy the volcanic arc (VAG) field, whereas the Flüelagranitic Association plots in VAG and syn-collision fields. REE patterns from all analysed Silvretta gneiss types give a good conformity with VAG. The tectogenesis of the investigated orthogneisses will be discussed with special regards to the geochemically different influences of the sedimentogenesis and the last crystallisation.

Sm-Nd model ages from petrographically different, but chemically similar gneisses of both groups cluster in a narrow range around 1.7 Ga. However, samples from the xenolith bearing and geochemically exceptional type "Urezzas" show Nd model ages from 1.2 to 1.5 Ga. A xenolith sample again yielded  $\approx 1.7$  Ga. These results most probably reflect a mixture of 1.7 Ga old crust with variable amounts of younger crustal components. This model is supported by reinterpreted Rb-Sr whole rock data of granodioritic to gabbroic rocks and Nd model ages of metatonalites.

At the present state of investigations the origin of the Silvretta orthogneisses is interpreted as sediments that were remelted - possibly in an Volcanic Arc environment - and formed granitic rocks with a mean crustal residence age of 1.7 Ga. A subsequent addition of juvenile crust is only reflected in parts of the Flüelagranitic Association.

Castro, A. et al., 1991, H-type (hybrid) granitoids: a proposed revision of the granite-type classification and nomenclature, *Eart Sci. Rev.*, v. 31, p. 237-253

Hine, R. et al., 1978, Contrast between I- and S-type granitoids of the Kosciusko Batholith: *J. Soc. Austr.*, v. 25, p. 219-234

Pearce, J.A., Harris, N.B.W., Tindle, A.G., 1984, Trace element discrimination diagrams for the tectonic interpretation of granitic rocks: *J. of Petr.*, v. 5/4, p. 956-983

NEW METHODOLOGICAL APPROACH IN INVESTIGATION OF EVOLUTION OF PRECAMBRIAN OCEAN ISOTOPE COMPOSITION.

PONOMARCHUK, V.A., TRAVIN, A.V., KISELEVA, Valentina Yu., MOROZOVA, I.P., KUZMIN, D.S.; United Institute of Geology, Geophysics and Mineralogy, Siberian Branch, Russian Academy of Sciences. University Ave.3, Novosibirsk, 630090, Russia.

Absence of an exact time coordinate for particular carbonate sample seems to be one of the base problems to be solved for investigation of the isotope-geochemical time-chronicle of the Precambrian ocean. For decision of this problem the direct isochrone K-Ar dating of carbonate samples (dolomite, limestone) was devised.

For examination of this approach carbonate samples (stromatolites) from the Olenekskoe rise columns (North-East Siberian platform) were investigated.

Moreover, using conventional methods, the  $\delta^{13}\text{C}$ ,  $\delta^{18}\text{O}$ ,  $^{87}\text{Sr}/^{86}\text{Sr}$  isotope compositions on the same samples were determined. The Rb,Sr concentrations and the  $^{87}\text{Sr}/^{86}\text{Sr}$  ratio were determined on dissolvable and undissolvable components of stromatolites. Coincidence of the  $^{87}\text{Sr}/^{86}\text{Sr}$  ratio on dissolvable and undissolvable components was additional criterion for choice of samples suitable for reconstruction of the isotope-geochemical evolution of the Precambrian ocean. The ages measured are between 1100 Ma and 1400 Ma.

The  $\delta^{13}\text{C}$  and  $\delta^{18}\text{O}$  (for this age range) values are from -1.03 to 0.35‰ (PDP) and from -8.1 to -9.4‰ (PDP) respectively. The  $^{87}\text{Sr}/^{86}\text{Sr}$  ratio measured is equal to 0.70519±/-14(95%) for age 1118±/-28Ma(95%), 0.70554±/-23 for 1143±/-20 Ma, 0.70516±/-24 for 1151±/-20 Ma and so on.

Thus, using the direct isochrone K-Ar dating of the most "clean" carbonate samples, the reconstruction of "fine structure" of the Precambrian ocean isotope record appears to be real.

ESR DATING OF BURNED FLINT FROM THE HOMINID BEARING TABUN CAVE, ISRAEL - THE ISOCHRON METHOD

PORAT, N., Israel Geological Survey, Jerusalem 95501, Israel, SCHWARCZ, H.P., Geology Department, McMaster University, Hamilton, Ontario L8S 4M1, Canada, and RONEN A., The Zinman Institute of Archaeology, Haifa University, Haifa 31905, Israel.

Two dating methods have been used in recent years for constructing a time scale for human evolution, electron spin resonance (ESR) and thermoluminescence (TL). Both methods are based on similar physical principles and are applicable to a wide range of materials from archaeological sites over the time range from 1 to 2,000 ka. TL has been used to date burned flint, while ESR has been applied mainly to tooth enamel. Recent studies have demonstrated the feasibility of applying ESR dating to burned flint, and here is a further example of its applicability. Both ESR and TL signals are reset by heating to  $T > 400^\circ\text{C}$  and grow back with time due to natural radiation.

ESR and TL ages are calculated from the ratio  $D_E/d$ .  $D_E$ , the equivalent dose, is the amount of natural radiation the sample had absorbed since the last resetting event and is measured in the lab using artificial irradiation.  $d$ , the annual dose rate, is the natural radiation emitted by the sample and its environment per year. It can be measured directly or calculated from U, Th and K contents in the sample and sediment.

Tabun cave is situated at the foothills of Mt Carmel, Israel. Neanderthal hominids were found in Layer C and its archaeological sequence has been used extensively for Late Pleistocene correlations throughout the Levant. Burned flint from the site was dated by TL (Mercier et al., in press), and tooth enamel was dated by both ESR and U/Th methods (McDermott et al., 1993). However, the TL ages are almost twice as old as the ESR and U/Th ages, which are in a good agreement. Different external annual dose rates ( $d_{ex}$ ) used for TL and ESR age calculations can explain this discrepancy. Uncertainties in the  $d_{ex}$  could be caused by variations over time, but should be the same for samples buried in the same environment. Also, lab measurements of small sediment samples may not represent the true  $d_{ex}$ .

To overcome uncertainties in  $d_{ex}$  we used here the isochron approach. Different flint samples have different U contents, which would cause variations in the internal annual dose rate ( $d_{in}$ ) and as a consequence in the  $D_E$ . When  $D_E$  is plotted against  $d_{in}$ , coeval samples which were exposed to the same  $d_{ex}$  should fall on a line, whose slope is proportional to the age and its intercept is the  $d_{ex}$ .

Five burned flint samples from the top of level E in Tabun were analyzed. The Al signal was used to estimate the  $D_E$ , and  $d_{in}$  was calculated from U, Th and K contents in the samples. The 5 samples form an isochron, giving the age of  $177 \pm 34$  ka and a  $d_{ex}$  of  $400 \pm 130 \mu\text{Gy/a}$ . The age is close to ages obtained for level E using ESR on teeth (EU age of  $154 \pm 34$  and LU age of  $188 \pm 31$  ka) and U/Th on teeth ( $164 \pm 4$  ka), but differs substantially from the average TL age for burned flint from the same level ( $296 \pm 18$  ka).  $d_{ex}$  is similar to that used in the ESR age calculations ( $495 \mu\text{Gy/a}$ ), which was evaluated using sediments adhering to the teeth. Our  $d_{ex}$  differs from that used for the TL age calculations ( $710 \mu\text{Gy/a}$ ), which was measured directly in the field. We conclude that the age of the top of level E is in the range of 160-190 ka, and that the isochron method can be used when  $d_{ex}$  is not well constrained.

McDermott F., Grün R., Stringer C.B., and Hawkesworth C.J., 1993, Mass-spectrometric U-series dates for Israeli Neanderthal/early modern hominid sites: Nature 363, 252-255. Mercier N., et al., in press: Bar Yosef O., and Kra R., (eds), Late Quaternary Chronology and Paleoclimates, Peabody Museum, Harvard.

## Xe ISOTOPES IN A STEADY STATE UPPER MANTLE

PORCELLI, D. and WASSERBURG, G.J., The Lunatic Asylum, California Institute of Technology, Pasadena, CA 91125 USA

We present a model of steady-state transport of Xe through the upper mantle. The model is explored using the full mass transport equations for each isotope of Xe and is coupled with the steady state model for He [1]. Upper mantle Xe reflects the isotopic characteristics of external sources altered by internal production of radiogenic Xe, in contrast to the standard model [2] where upper mantle Xe is residual from atmosphere removal. The mantle is divided into two reservoirs; a lower mantle (P) that has evolved as an approximately closed system, and an upper mantle (D) of mass ( $M_D$ ). Xe fluxes into the upper mantle are by mass transfer from P at hotspots ( $M_{PD}$ ) (where a fraction  $r$  is degassed) and from the atmosphere by subduction. Xe leaves the upper mantle at mid ocean ridges and at hotspots. The silicate Earth initially had uniform U, Pu, I, and Xe concentrations and  $(Pu/U)_0 = 0.0068$ . We consider the generation of  $^{136}\text{Xe}$  excesses by both U and Pu in P and D. We assume that  $^{129}\text{I}$  was present in P (in unknown abundance) and is the source of the observed  $^{129}\text{Xe}$  excesses in D. The lower mantle Xe concentration ( $^{130}\text{C}_P$ ) and isotopic composition are unknown.

Radiogenic  $^{136}\text{Xe}$  in D is the sum of  $^{136}\text{Xe}$  generated in P that is dominated by decay of now extinct  $^{244}\text{Pu}$ , and  $^{136}\text{Xe}$  generated in D by the decay of U. For upper mantle Xe, the relative proportion of  $^{136}\text{Xe}^*$  derived from D to that derived from P is  $\delta_{SF} = \frac{^{136}\text{R}_D U_{CD} M_D / [^{136}\text{C}_P (1-r) M_{PD}]}{^{136}\text{R}_P}$ , with  $U_{CD} = U$  concentration in D,  $^{136}\text{R}_P = 1.4 \times 10^4$  atoms  $^{136}\text{Xe}^*/\text{gU}\cdot\text{yr}$ ,  $^{136}\text{C}_P = 3.3 \times 10^7$  atoms, and  $U_{CD} M_D / (1-r) M_{PD} = 6.3 \times 10^2$  from consideration of steady state He fluxes in D [1], so that  $\delta_{SF} = 0.27$ . Observed excesses of  $^{129}\text{Xe}$  and  $^{136}\text{Xe}$  (relative to atm) in mantle-derived materials are positively correlated [2]; we interpret the range to reflect different degrees of atmospheric contributions to a single D component, and a value of  $^{136/130}\text{Xe}_D = 2.45$  is used here (along with  $^{129/130}\text{Xe}_D = 7.35$ ). The Xe isotopic composition of D and P can be related by

$\delta_{SF} = \frac{^{136/130}\text{Xe}_D - ^{136/130}\text{Xe}_P}{^{136/130}\text{Xe}_P - ^{136/130}\text{Xe}_O}$   
Using  $^{136/130}\text{Xe}_O = 2.075$  [3],  $^{136/130}\text{Xe}_P = 2.37$ . For closed system evolution of P, this requires  $^{130}\text{C}_P = 1.2 \times 10^8$  atoms/g.

One consequence of the model is that because of the differences in isotopic composition between P and the atmosphere, the atmosphere has been formed largely from a source other than P material. From an Earth originally uniform in Xe isotopic composition and concentration (equal to values obtained for P)  $1.2 \times 10^{35}$  atoms  $^{130}\text{Xe}$  were contributed by D to the atmosphere. This is 32% of the present atmospheric  $^{130}\text{Xe}$  inventory. Simple mixing calculations indicate that the remaining Xe must have had  $^{136/130}\text{Xe} = 2.094$  and  $^{129/130}\text{Xe} = 6.094$ . These values are similar to proposed initial atmospheric values of  $2.075 \pm 0.006$  and  $6.061 \pm 0.045$  respectively, obtained from meteorite compositions [3], and suggest that the additional Xe was unradiogenic. Div. Contrib. 5364(838). 1. Kellogg & Wasserburg (1990) EPSL 99, 276. 2. Allègre et al. (1983) Nature 303, 762. 3. Pepin & Phinney (1976) Lunar Sci. VII, 682.

## $^3\text{He}$ SURFACE EXPOSURE AGES AT THE LATHROP WELLS, NV, VOLCANIC CENTER.

POTHS, J.; PERRY, F.; CROWE, B.M.; Los Alamos National Laboratory, Los Alamos, NM, 87545.

We have determined cosmogenic  $^3\text{He}$  surface exposure ages of samples from three eruptive units at the Lathrop Wells volcanic center. The units have been divided into four eruptive episodes from field relations, verified by trenching of contacts. Geochemical and petrology studies show that each episode is distinct and probably represents volcanic eruptions of short duration. Our goal is to determine the timing of these eruptive episodes.

Dates are given in the table below, and generally fall in stratigraphic order (QI1 the oldest, QI3 the youngest). Despite evidence for several meters of ash cover, surfaces from the QI1A flow yield reproducible dates within analytical uncertainty. Apparently the ash was stripped from these surfaces in a time that was short compared to the uncertainties ( $\leq 5\text{ka}$ ). A related (QI1B) and a stratigraphically younger flow (QI2) are identical to QI1A within uncertainty. The somewhat younger dates for QI1D and Qs1 may reflect thicker ash cover at their locations. Dates for bombs and scoria collected from the cone show scatter, probably reflecting difficulty in collecting a preserved surface. The oldest date provides a lower limit of 57ka for the age of the cone. We are investigating the discrepancy between the two samples from QI3. As a test of our method, we analyzed a sample shielded by  $> 5\text{m}$ . It contains  $\leq 7\%$  of the concentration of cosmogenic He at the surface.

Unit	Dates <sup>#</sup> (ka) $\pm 1\sigma$
QI1A	81 $\pm$ 7, 81 $\pm$ 6, 82 $\pm$ 5, 84 $\pm$ 7, 85 $\pm$ 5, 87 $\pm$ 6
QI1B	88 $\pm$ 8
QI1D	76 $\pm$ 7
Qs1	61 $\pm$ 8
QI2	82 $\pm$ 9, 88 $\pm$ 6, 82 $\pm$ 5
QI3	61 $\pm$ 6, 100 $\pm$ 9 ?same unit
Qs3 (cone)	30 $\pm$ 5, 35 $\pm$ 5, 36 $\pm$ 5, 43 $\pm$ 3, 57 $\pm$ 7

<sup>#</sup>Prod. rate =  $245 \text{ g}^{-1} \text{ a}^{-1}$  at 968m elevation

THE MODELLING OF XENON AND LEAD ISOTOPES  
MIGRATION IN ZIRCON AND PITCHBLENDE  
UNDER HYDROTHERMAL CONDITIONS

PRAVDIVTSEVA, Olga V., SHUKOLYUKOV, Yu. A.,  
Vernadsky Institute of Geochemistry and Analytical  
Chemistry, Russian Academy of Sciences,  
117975 Moscow, Russia.

$Xe_{5-8}-Xe_{n}$  isotope dating and classical U-Pb methods have been used for the comparative study of diffusion properties of Xe and Pb under laboratory hydrothermal conditions.

The first object was the metamict zircon from Uros Lake metasomatic rocks (Central Karelia). Even initial natural sample clearly showed discordant and too young U-Pb age ( $^{206}Pb/^{238}U$  - 2.1 Ga;  $^{206}Pb/^{238}U$  - 2.3 Ga) as compared to true age of this zircon - 2.5 Ga. Five  $Xe_{5-8}-Xe_{n}$  age spectra of initial and hydrothermally treated zircon were obtained. Two samples - initial one and treated under the extremely low conditions (1 kbar pressure of 2MNaCl solution vapour, temperature 300°C, 72 hours) showed  $Xe_{5-8}-Xe_{n}$  age to be 2.34+/-0.16 and 2.73+/-0.36 Ga close to the true age. Thus, under definite conditions U-Xe isotopic system turns out to be more robust than U-Pb one.

This conclusion was confirmed by the experiments with the pitchblende selected from Shlema-Alberoda U-deposit (Erzgebirge, Germany). Thirteen aliquots of different grain size were treated with HCl solutions of various concentrations. Independently from the grain size and the treatment condition all aliquots as well as initial sample have concordant  $Xe_{5-8}-Xe_{n}$  plateau ages. Even half dissolved sample did not lose radiogenic Xe. Nevertheless Xe release kinetics and fine structure of  $Xe_{5-8}-Xe_{n}$  age spectra depend on treatment conditions and grain size dramatically. This correlation helps to illuminate the diffusion mechanism and nature of high xenon retention.

The obtained results allow to conclude that the Xe migration is controlled by volume diffusion with a weak Xe trapping during the diffusion. The mechanism takes place usually at temperatures which are lower than a half of melting point value.

The  $Kr_{5-8}-Kr_{n}$  dating method (which is in progress now) would be a valuable adjunct to this study.

CRETACEOUS PACIFIC VOLCANISM: DISTRIBUTION  
IN SPACE, TIME, AND SOURCE COMPOSITION

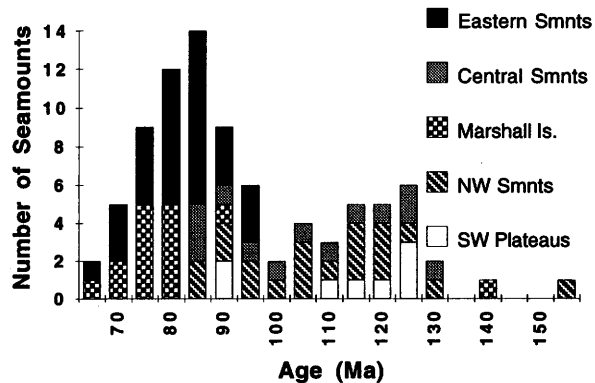
PRINGLE, M.S., KOPPERS, A.A.P., STAUDIGEL, H., and  
WIJBRANS, J.R., Faculty of Earth Sciences, Vrije  
Universiteit, 1081 HV Amsterdam, Netherlands;  
CHRISTIE, D.M., and DUNCAN, R.A., COAS, Oregon  
State University, Corvallis, OR 97331-5503, USA.

Radiometric ages for almost 90 distinct sites of Cretaceous Pacific Seamount volcanism (shown below) have a bimodal distribution, with peaks between 80-90 and 115-125 Ma. We compare the original positions of the melting anomalies that formed these seamounts with the modern South Pacific Isotopic and Thermal Anomaly (SOPITA), and speculate on the implications of these observations for mantle dynamics.

Cretaceous seamounts in the east-central Pacific formed between 100 and 64 Ma, with a peak near 85-80 Ma. The Musicians and South Hawaiian Seamounts had near-ocean ridge sources located to the north and east of the SOPITA. Sources for volcanism in the Line Islands define the northeastern extent of the Late Cretaceous SOPITA. Volcanism in the Marshall Islands had an age distribution similar to the east-central Pacific seamounts. However, all of the Marshall Islands and the older seamounts to the northwest originated in the central and western SOPITA. Also, the geochemical signatures of these western Pacific seamounts are similar to the extreme compositional range seen in the modern SOPITA (c.f., Koppers, et al., this session).

The plateau and flow and sill complexes of the western Pacific formed mainly 110-125 Ma, with sources to the south of, and geochemical signatures distinct from, volcanoes of the modern SOPITA. Either these flood basalts were not products of the Cretaceous SOPITA, or they were part of a more extensive and diverse precursor of the modern SOPITA.

Although the SOPITA region has been erupting lavas with unique geochemical signatures for at least 126 Ma, individual hot spot tracks cannot be traced for more than 20 m.y. In fact, hot spot tracks world-wide seem to be either less than 20 m.y. or greater than 65 m.y. long. As thermal plumes originate at thermal boundary layers, we suggest that mantle plumes responsible for shorter hot spot tracks originate at the shallower mantle thermal boundary layer, i.e. the 670 km transition zone, while mantle plumes responsible for the longer hot spot tracks originate at the deeper mantle thermal boundary layer, i.e. the core/mantle boundary. The Pacific SOPITA, consisting of individual hot spot tracks less than 20 m.y. long, would then be mainly the result of relatively shallow, upper mantle dynamics. Longer-lived hot spot tracks, such as the Hawaiian/Emperor and Louisville Ridges of the Pacific, would be the products of deeper mantle processes.



ISOTOPE COMPOSITIONS OF Sr, Pb, Nd, Os AND REE DISTRIBUTION IN OILS, BITUMENS AND BLACK SHALES AS INDICATORS OF MATTER SOURCES, MIGRATION WAYS AND GENESIS OF HYDROCARBON FLUIDS

PUSHKAREV, Y.D., Karpinsky Geol. Res. Inst. (VSEGEI), Sredny pr. 74, St.-Petersburg, 199026, Russia; GOTIH, R.P., PISOTSKY, B.I., (VNIIGEOSISTEM), Varshavskoye shosse 8, Moscow, 113105, Russia; ZURAVLEV, D.Z., (IGEM), Staromonetny per. 35, Moscow, 109017, Russia; ACHMEDOV, A.M., (VSEGEI), Sredny pr. 74, St.-Petersburg, 199026, Russia.

The problem of hydrocarbon fluids and oil generation is still widely being debated. In parallel with their low temperature generation in sedimentary basins high temperature generation of the deep-earth hydrocarbon fluids is assumed. However there are no evidences of available deep-earth organic fluid component. The results, obtained in this work, are the following.

1. Initial  $^{87}\text{Sr}/^{86}\text{Sr}$  values are often higher than average  $^{87}\text{Sr}/^{86}\text{Sr}$  for continental crust (0.720) and imply high temperature (>350°C) interaction with micas and potassium feldspars.

2. On the diagram of Sr-Pb isotope systematics of recent mafic volcanites the oil compositions occupies a specific space typical of lamproites and kimberlites. The similar place but in Nd-Sr isotope systematics of the same volcanites is occupied by bitumens compositions. That suggests the same contamination sources both for the oils and bitumens, and for the lamproites and kimberlites, i.e. crystalline rocks of the upper and lower crust.

3. High concentration of REE (up to 3000 ppm), their relative distribution and Nd isotope composition (from -20 up to +4.2  $\epsilon_{\text{Nd}}$ ) in some bitumens, unlike those in host rocks, indicate high temperature assimilation of these elements.

4. Os isotope composition in black shales of Onega Lake ( $^{187}\text{Os}/^{186}\text{Os}=1.06 \pm 0.04$ ) corresponds to a purely mantle component.

The data obtained show that there is a deep-earth component in the objects investigated that was assimilated by hydrocarbon fluids under temperatures too high to be interpreted in terms of the traditional biogenic hypothesis. It is left for further study to find out what role the deep-earth component played when major oil pools were being formed.

TERRESTRIAL MOLYBDENUM ISOTOPIC ABUNDANCE RATIOS

QI-LU<sup>1,2</sup> and A. Masuda<sup>1</sup>, <sup>1</sup>Dept. of Chem., University of Electro-communications, 1-5-1 Chofugaoka, Chofushi, 182 Tokyo, Japan  
<sup>2</sup>Dept. of Chem., Inner Mongolia University, Huhhot, China.

Potentially molybdenum is a very interesting element in cosmochemistry and geochemistry<sup>1,2</sup>. However, now the data on molybdenum isotopic abundance ratios regarded as reliable in terrestrial and meteoritic matters are sparse. We measured all of seven molybdenum stable isotopes of 12 molybdenites collected from different locations over the world<sup>3</sup>. A Faraday collector of thermal ionization mass spectrometer (VG Sector 54-30) was applied in peak jumping mode for the isotopic measurement. All the ratios have been normalized to  $^{94}\text{Mo}/^{98}\text{Mo} = 0.3802$ .

The normalized data provided no special evidence for large, mass-dependent isotopic anomalies of molybdenum isotopes, except for the depletion of  $^{97}\text{Mo}$  (-0.7  $\epsilon$ ) in Mulgine (Australia), the excess of  $^{95}\text{Mo}$  (+1.3  $\epsilon$ ) and the excess of  $^{100}\text{Mo}$  (+2.8  $\epsilon$ ) in China 110. Furthermore, some samples exhibit a hint of scatters in  $^{92}\text{Mo}$  and  $^{100}\text{Mo}$ .

Judging from the precision of isotopic measurement of our standard ( $\text{MoO}_3$ , 99.999%), it is unlikely that these discrepancies are due to the mass fractionation effect during the measurement. However, currently, our knowledge can not give a reasonable explanation for these discrepancies, since the terrestrial matter has experienced much chemical fractionation, and it is assumed that terrestrial matter is isotopically homogeneous.

<sup>1</sup>Hutcheon, I. D., Armstrong, J. T., and Wasserburg, G. J., 1987, *Geochim. Cosmochim. Acta*, 51, 3175-3192.

<sup>2</sup>Woodsley, S. E., and Howard, W. M., 1991, *Astrophys. J.*, 373, L5-L8.

<sup>3</sup>QI-LU and Masuda, A., 1994, *Int. J. Mass Spectrom. Ion Processes*, in press.

COMBINED U-Pb-Xe CHRONOLOGY, PRECISE DETERMINATION OF THE PRODUCT OF THE DECAY CONSTANT AND FRACTIONAL YIELD OF  $^{136}\text{Xe}$  FROM  $^{238}\text{U}$  SPONTANEOUS FISSION

R. Ragetli, Institut de Physique du Globe, F-75252 Paris and Isotopengeologie, ETHZ, CH-8092 Zurich, EH Hebeda, Ringstrasse 10, D-92331 Parsberg, R Wieler and P Signer, Isotopengeologie, ETHZ, CH-8092 Zurich.

Combined U-Pb and U-Xe analysis on aliquots of mineral separates offers a powerful approach for determining the time and nature of igneous and metamorphic processes. However, the application of the U-Xe technique requires the knowledge of the product of the decay constant ( $\lambda_{sf}$ ) and the fractional yield of  $^{136}\text{Xe}$  ( $^{136}\text{Y}_{sf}$ ) from the spontaneous fission of  $^{238}\text{U}$ . Recent estimates of this product obtained using U-minerals (Eikenberg et al., 1993) are in conflict with the value derived from earlier studies of zircon and monazite (Shukolyukov & Mirkina, 1963; Kapusta & Matukov, 1982).

In order to resolve this issue we have obtained precise U-Pb and U-Xe data from a carefully selected suite of zircons and monazites. All samples have precise and concordant U-Pb ages. Recoil losses of fissionogenic Xe were either corrected for numerically or were circumvented by abrading samples or by using very large minerals. Old crystal cores, that might have retained their fission Xe but not their radiogenic Pb, were not detected in any of the samples. For all these reasons the  $\lambda_{sf} \cdot ^{136}\text{Y}_{sf}$  value obtained of  $(6.82 \pm 0.36) \cdot 10^{-18}/\text{a}$  ( $1\sigma$  standard deviation) is considered to be correct, and is the best estimate thus far. The value obtained is similar to that determined from earlier studies of accessory minerals (Shukolyukov & Mirkina, 1963; Kapusta & Matukov, 1982) but some 20% higher than the value recently derived from carefully selected pitchblendes, uraninites and coffinites (Eikenberg et al., 1993). These results suggest that such U-minerals systematically lose around 20% of their fission Xe, possibly due to regeneration of the crystal lattice or change in oxidation state.

In addition, we will present U-Pb and U-Xe data for zircons and monazites from a diverse range of rock types, some having experienced varying degrees of metamorphism. Minerals from amphibolite facies gneisses from within the same geological unit show three different types U-Pb-Xe behaviour: 1) Zircons and monazites show minor lead loss and indicate an upper intercept age that is concordant with the U-Xe ages. 2) Zircons which have lost both fissionogenic and radiogenic daughters but where neither the U-Xe nor the U-Pb systems having been completely reset, neither of the systems give a meaningful age information. 3) Zircons which experienced 95-100% loss of radiogenic lead and yield a lower intercept age that is concordant with the U-Xe ages. Furthermore zircons from a granulite show minor lead loss and yield an upper intercept age younger than the corresponding U-Xe ages. These results illustrate the utility of combined U-Pb-Xe analysis in understanding the timing and nature of petrogenesis in complex geological terrains.

YuA Shukolyukov & SL Mirkina, 1963, *Geochemistry*, v 7, p 729-731

YaS Kapusta & DI Matukov, 1982, *Soviet Radiochemistry*, v 24, p 462-465

J Eikenberg et al., 1993, *GCA*, v 57, p 1053-1069

DETRITAL ZIRCON STUDIES OF NEOPROTEROZOIC QUARTZARENITES FROM NORTHWESTERN CANADA: ADDITIONAL SUPPORT FOR AN EXTENSIVE RIVER SYSTEM ORIGINATING FROM GRENVILLE OROGEN

RAINBIRD, R. H. and McNICOLL, V. J., Geological Survey of Canada, Ottawa, Ontario, K1A 0E8, Canada, and HEAMAN, L. M., Dept. of Geology, Royal Ontario Museum, Toronto, Ontario, M5S 2C6, Canada.

Provenance studies of quartzarenite from the Shaler Supergroup of Minto Inlier, Arctic Canada, suggested that during the Neoproterozoic a braided fluvial system with a reach of at least 3,000 km extended across Laurentia, a central block of the supercontinent Rodinia (Rainbird et al. 1992). Consistent northwest paleocurrents and a large proportion of detrital zircons with U/Pb ages of 1.2-1.0 Ga (characteristic of the Grenville Province within Laurentia) are consistent with provenance from the Grenville orogen, formed during the initial assembly of Rodinia. To test the validity of this hypothesis, detrital zircon geochronology was completed on samples of fluvial quartzarenite from the Nelson Head Formation (Rae Group - Shaler Supergroup) of Minto Inlier and from unit K7 (Katherine Group - Mackenzie Mountains Supergroup), a lithostratigraphically correlative unit located approximately 1,000 km to the southwest in the northern Canadian Cordillera.

U-Pb ages of 24 single concordant zircons from the two samples are Archean (2.6-2.8 Ga), Paleoproterozoic (1.9-2.0 Ga) and Mesoproterozoic (1.1-1.6 Ga). Mesoproterozoic zircons represent the majority of the analyses (18) and are distributed evenly between the two specimens. Eleven grains are between 1.08 to 1.2 Ga, reflecting significant contribution from a Grenville source.

These results firmly support the original hypothesis and we interpret the Nelson Head Formation and the Katherine Group as distal deposits of the same huge braided fluvial system that originated from the foreland of Grenville orogen.

Rainbird, R. H., Heaman, L. M. and Young, G. M., 1992, *Sampling Laurentia: detrital zircon geochronology offers evidence for an extensive Late Proterozoic river system originating from Grenville orogen: Geology*, v. 20, p. 351-354.

THE SHACHANG RAPAKIVI GRANITE COMPLEX,  
EASTERN CHINA: IMPLICATIONS FOR Sm-Nd,  
Th-U-Pb, AND Rb-Sr SYSTEMATICS OF THE  
ARCHEAN SINO-KOREAN CRATON

RÄMÖ, O. Tapani, Dept of Geology, P.O. Box 11, FIN-00014 University of Helsinki, Finland, HAAPALA, Ilmari, Dept of Geology, University of Helsinki, VAASJOKI, Matti, Geological Survey of Finland, FIN-02150 Espoo, Finland, YU, Jian Hua, Geological Institute of Beijing, Deshengmenwai, Beijing 100011, China, and FU, Hui Qin, Geological Institute of Beijing.

The Sino-Korean Craton, located in eastern China and adjacent regions around the Yellow Sea, registers over one b.y. of continental crustal evolution, commencing at least 3.7 Ga ago, with major tectonothermal events between 2.7 and 2.5 Ga (Liu et al., 1990). In the northwestern part of the Craton, just north of Beijing, a 1.7 Ga (U-Pb age) old anorogenic rapakivi granite-anorthosite suite transects Archean medium- to high-grade gneisses overlain by unmetamorphosed early Proterozoic and Phanerozoic supracrustal formations. This paper focuses on Nd, Pb, and Sr isotopes of one of the rapakivi intrusions (Shachang) and its metamorphic country rocks.

The Shachang intrusion is strongly enriched in LREE ( $^{147}\text{Sm}/^{144}\text{Nd}$  0.0758 to 0.1093) and has initial  $\epsilon_{\text{Nd}}(1.67 \text{ Ga})$  values averaging  $-5.9 \pm 0.3$  ( $1\sigma$ ,  $n=10$ ) and  $T_{\text{DM}}$  model ages averaging  $2.32 \pm 0.06$  ( $1\sigma$ ) Ga. Pb isotopic data on granites and feldspars define a  $^{207}\text{Pb}/^{206}\text{Pb}$  isochron with an age of  $1693 \pm 110$  Ma ( $2\sigma$ ) and a  $^{208}\text{Pb}/^{206}\text{Pb}$  errorchron with  $\kappa$  ( $^{232}\text{Th}/^{238}\text{U}$ ) of  $6.3 \pm 0.6$  ( $2\sigma$ ). S&K (Stacey and Kramers)  $\mu_2$  values of feldspars average at  $8.92 \pm 0.17$  ( $1\sigma$ ,  $n=10$ ). Sr isotopic data on the granites yield an errorchron corresponding to an age of  $1511 \pm 67$  Ma ( $2\sigma$ ) and initial  $^{87}\text{Sr}/^{86}\text{Sr}$  of  $0.7068 \pm 0.0017$  ( $2\sigma$ ).

The country rocks of the intrusion show a U-Pb age of 2.5 Ga and are strongly enriched in LREE ( $^{147}\text{Sm}/^{144}\text{Nd}$  0.0816 to 0.1315). They have positive initial  $\epsilon_{\text{Nd}}(2.5 \text{ Ga})$  values averaging  $+0.9 \pm 0.5$  ( $1\sigma$ ,  $n=5$ ) and  $T_{\text{DM}}$  model ages averaging  $2.63 \pm 0.06$  ( $1\sigma$ ) Ga. Whole rock and feldspar Pb isotopic ratios are very low (down to  $6/4=13.67$ ,  $7/4=14.55$ ,  $8/4=33.41$ ) and show S&K  $\mu_2$  values between 7.78 and 9.36 (average 8.86) and  $\kappa_2$  values between 3.75 and 7.08 (average 4.83). The country rocks are depleted in Rb and yield a Rb-Sr errorchron of  $2190 \pm 350$  Ma ( $2\sigma$ ) and initial  $^{87}\text{Sr}/^{86}\text{Sr}$  of  $0.7011 \pm 0.0037$  ( $2\sigma$ ).

The Shachang granites are felsic and homogeneous and probably crystallized from anatectic melts generated at deeper levels within the crust. Hence they presumably preserve a record of the isotopic composition of the lower crust. Comparison of the isotopic data on the granites and their exposed country rocks suggests that:

- (1) The lower crust in this area has a higher apparent Sm/Nd ( $\sim 0.22$ ) than its exposed upper parts ( $\sim 0.17$ ).
- (2) This part of the Sino-Korean Craton is characterized by low overall U/Pb and high overall Th/U. There is, however, not much difference between the upper and lower parts of the crust in terms of these ratios.
- (3) The initial Sr isotopic ratios of the granites and their country rocks are both low and not indicative of long-term upper crustal Rb-enrichment.

Liu, D.Y., Shen, Q.H., Zhang, Z.Q., Jahn, B.M., and Auvray, B., 1990, Archean crustal evolution in China: U-Pb geochronology of the Qianxi Complex: Precambrian Research, v. 48, p. 233-244.

U/Th DISEQUILIBRIA AND MAGMA MIXING AT SAN PEDRO VOLCANO, SOUTHERN VOLCANIC ZONE (SVZ), CHILE.

RAMOS F.C., REID, M.R., DAVIDSON, J.P., Dept. of Earth and Space Sciences, U.C.L.A., Los Angeles, Ca 90024-1567, USA.

San Pedro Volcano is a Holocene stratocone lying at 36°S latitude in the northern region of the Southern Volcanic Zone. This volcano has had an extensive volcanic history which includes the eruption of a composite flow of inferred Holocene age. This flow grades from basaltic andesite to dacite in composition and basaltic inclusions are contained within specific andesite and dacite portions of the flow. The variable compositions of this flow are postulated to be the result of magma mixing between dacite and basaltic andesite end-members (Singer, submitted).

Nd, Sr, and Pb isotopes ( $\sim 0.5128$ ,  $\sim 0.7041$ , and  $\sim 18.55$ ,  $\sim 15.58$ , and  $\sim 38.44$ ) in the composite flow show little variation and are therefore of limited utility in constraining magmatic mixing. ( $^{230}\text{Th}/^{232}\text{Th}$ ) isotopic values in this flow also have a limited range of between 0.80 and 0.84, but ( $^{238}\text{U}/^{232}\text{Th}$ ) values range extensively from 0.73 to 0.91. These samples range from Th- to U-enriched and ( $^{230}\text{Th}/^{232}\text{Th}$ ) and ( $^{238}\text{U}/^{232}\text{Th}$ ) are positively correlated. Basaltic inclusions found in host dacite and andesite define the end-members of the range, while host dacite and andesites fall between these end-members suggesting that magma mixing is generating the variations. If initial ( $^{230}\text{Th}/^{232}\text{Th}$ ) values were similar at the time of eruption, mixing occurred at approximately 25-30 ka. This is older than the inferred Holocene eruption age based on field relations to glacial features and suggests that mixing and evolution of these magmas may have occurred in less than 15 ka.

The basaltic inclusions ( $\text{SiO}_2=51-52\%$ ) analyzed suggest that U vs Th enrichment is magma dependent (individual magma characteristics) and not location dependent in the northern SVZ (as suggested by Sigmarsson et al., 1990). The U/Th isotopic data also indicate that the mixing array could be generated by mixing two basaltic end-members (as represented by the basaltic inclusions) with subsequent differentiation. This interpretation differs from Singer (submitted) which, based on major element considerations, suggests mixing between dacite and basaltic andesite.

Sigmarsson, O., Condomines, M., Morris, J.D., and Harmon, R.S., 1990, Uranium and  $^{10}\text{Be}$  Enrichments by fluids in Andean Arc Magmas, Nature, v.346, P.163-165.

EFFECT OF "BULK" ETCH RATE AS RECORDED  
IN ETCH PIT DIMENSIONS ON MEASURED  
FISSION TRACK LENGTH ANISOTROPY IN  
DURANGO APATITE

RAVENHURST, C.E., Dept. of Earth Sciences,  
Dalhousie University, Halifax, N.S., B3H 3J5, Canada  
and RODEN, M.K., Dept. of Earth and Environmental  
Sciences, Rensselaer Polytechnic Institute, Troy,  
N.Y., 12180 U.S.A.

Observed fission track (FT) lengths are a function of annealing and etching, both of which are dependent on crystallographic orientation. We used etch pits (the intersection of tracks with prismatic surfaces) to study etching effects. Etch pit aspect ratios are dependent on HNO<sub>3</sub> etchant strength and apatite chemistry. However, etchant strength does not effect the measured mean track length nor the crystallographic anisotropy of FT lengths, so long as etch pit width is held constant (Roden et al., 1991).

Oriented slabs of Durango apatite containing identically annealed induced tracks were etched with 5N HNO<sub>3</sub> for 20, 30, 40, 50, 60 and 70 seconds at 21°C. Prismatic section etch pits increase in width at about .016 μm/sec and in length at about .10 μm/sec. In each slab at least 200 confined track lengths were measured with respect to crystallographic orientation and then ellipse-fitted. FT lengths perpendicular to the c-axis increase at .018 μm/sec, similar to etch pit width, whereas those parallel increase at an order of magnitude less than the etching rate for etch pit length. Therefore, the etching effect on FT lengths is mainly "bulk" etching as determined from etch pit width.

Few measurable tracks oriented approximately parallel to the c-axis could be found in Durango apatite at a 20 second etching duration. Therefore the Laslett et al. (1987) annealing model is likely biased towards annealing of tracks oriented perpendicular to the c-axis, which anneal more readily than those parallel. In general, we suggest that etching conditions not be set at 5N HNO<sub>3</sub> for 20 sec @ 21°C, but instead that the etching time be adjusted for the dominant apatite composition in the sample so that etch pit widths of about 0.75 μm are produced (5N HNO<sub>3</sub> for 25 sec @ 21°C is suggested initially). These sample-dependent etching conditions will allow measurement of confined track lengths over all orientations, so that a more accurate mean length can be determined....

Roden, M.K., Ravenhurst, C.E. & Miller, D.S., 1991, Effect of etching on apatite fission-track annealing anisotropy (Abstract): AGU, Baltimore.

Laslett, G.M., Green, P.F., Duddy, I.R., and Gleadow, A.J.W., 1987, Thermal annealing of fission tracks in apatite 2. A quantitative analysis: Chemical Geol. (Isotope Geoscience Sect.), v.65, p.1-15.

OSMIUM IN PELAGIC SEDIMENTS FROM THE  
N-E ATLANTIC: ISOTOPIC COMPOSITION AND  
DISTRIBUTION.

RAVIZZA, G. WHOI, Woods Hole, Ma, 02543  
USA, COLODNER, D. C., L-DEO Palisades,  
NY 10964, USA and THOMSON, J. IOS Brook  
Road, Wormley, Surrey GU8 5UB, UK

In order to evaluate the potential influence of redox changes on diagenetic redistribution of Os in slowly accumulating pelagic clays, the Os concentration and isotopic composition of sediment samples from a well characterized turbidite-pelagic clay sequence have been investigated. In an otherwise homogeneous oxic brown clay sequence, a 10 cm reduction halo has formed due to organic matter degradation in a thin turbidite deposited immediately above this reduced horizon. Redistribution of Pt and Ir have accompanied this redox change with Pt, and to a lesser extent Ir, being depleted in the reduced horizon relative to the surrounding unaltered brown clay. In contrast, the Os concentration of the reduced horizon (116 ppt) is slightly elevated compared to surrounding sediment (≈ 100 ppt). These subtle concentration variations are suggestive of diagenetic PGE redistribution. In spite of these concentration variations, the Os isotopic composition of the bulk sediment is nearly homogeneous (<sup>187</sup>Os/<sup>186</sup>Os range: 8.21 to 8.54), except for the turbidite which is distinct (<sup>187</sup>Os/<sup>186</sup>Os = 7.02).

Model calculations using the <sup>230</sup>Th-based sediment accumulation rate (≈ 0.3 cm/Ka) and the cosmic Os flux ( 2-3 pg.cm<sup>2</sup> Ka<sup>-1</sup>) indicate that approximately 10% of the Os in this sediment is of cosmic origin. Assuming the silicates in the core carry an average crustal Os concentration (50 ppt), detrital Os accounts for an additional 50% of the sediment Os budget. The remaining 40% of the Os budget must therefore be attributed to a hydrogenous source. Leaching experiments intended to isolate a hydrogenous Os component liberate approximately 30% of the total Os in the sediment, which is in fairly good agreement with the above model calculation. This result and the accompanying calculation indicate that post-depositional redistribution of the hydrogenous Os component within the sediment pile can easily produce the observed 16% increase in the Os concentration of the reduced horizon. The deepest sample from the core, has a Th-based age of ≈ 550 Ka. The <sup>187</sup>Os/<sup>186</sup>Os ratio of leachable Os from this sample is 8.47, a more radiogenic value than in Pacific sediments of similar age. This discrepancy may be an additional indication of complexities associated with inferring the Os isotopic composition of seawater from pelagic clay data.

**APATITE FISSION TRACK THERMOCHRONOLOGY OF SELECTED WELLS FROM THE BOWEN/SURAT BASINS, EASTERN AUSTRALIA**

**RAZA, Asaf, GLEADOW, A.J.W., HILL, K.C., O'SULLIVAN, P.B., VIEPS, School of Earth Sciences, La Trobe University, Bundoora, Victoria, 3083, Australia., and KORSCH, R.J., AGSO, Canberra, ACT, 2601 Australia.**

As part of continuing research of the geologic evolution of the eastern margin of Australia, the thermo-tectonic history of the Bowen/Surat Basins in south-eastern Queensland, Australia, has been evaluated using apatite fission-track thermochronology and published vitrinite reflectance data. The Bowen Basin is a narrow, north-south basin containing up to 10 km of Permian and Triassic sediments. It was initiated as an extensional basin in the Early Permian and became a foreland basin in the Late Permian. Unconformably overlying these Permo-Triassic rocks are Jurassic and Cretaceous sedimentary rocks of the Surat Basin, which developed along the eastern margin of Australia in response to regional thermal subsidence. Interpretation of regional reflection seismic data suggests that up to 3 km of section was removed in the Middle to Late Triassic to create the unconformity separating the two basins.

Published vitrinite reflectance data from the Bowen/Surat basins suggest that rocks preserved had previously been exposed to higher temperatures, but give no indication of the time of cooling from these higher paleotemperatures. To constrain the thermochronologic history of the sedimentary rocks, 25 core samples from six wells were selected for apatite fission track analysis. The Cockatoo Creek-1, Burunga-1, Wandoan-1 and Cabawin-1 wells are situated west of the Burunga Leichhardt Fault, which is close to the eastern boundary of the Bowen Basin, and the Rockwood-1 and Cannan-1 wells on the up-thrown block east of the thrust.

The fission track results suggest that rocks within the basins were previously exposed to higher paleotemperatures, consistent with the vitrinite reflectance data, and that maximum paleotemperatures were achieved during the Jurassic to Early Cretaceous in response to Surat Basin deposition. Therefore the Middle to Late Triassic thermal history is not recorded by the fission track data. Subsequently, starting in the middle Cretaceous at ~105 Ma, a maximum of ~65°C of cooling has occurred. This cooling episode pre-dates continental rifting which commenced in the northern Tasman Sea in the Late Cretaceous (~85 Ma). Modelling of the data suggest that cooling from maximum paleotemperatures occurred in two stages, an episode of relatively rapid cooling between ~105-85 Ma which resulted in ~1.5 km of denudation, followed by slow protracted cooling to present-day conditions, possibly due to a further ~0.5 km of exhumation. Timing of cooling for host rocks from all wells is identical, regardless of their location with respect to the Burunga Leichhardt Fault suggesting that the thrust was not active in the middle Cretaceous.

This abrupt regional inversion and denudation is difficult to explain in terms of the known regional tectonics. It may be related to a middle Cretaceous (c. 105-95 Ma) deformational event, evidence for which is preserved in neighboring basins. It also coincides with similar middle Cretaceous regional inversion and denudation around the Bass Basin, ~2000 km to the south, thought to be related to plate realignment and extension propagating south of Tasmania. Perhaps the Bowen Basin inversion was related to the same plate realignment that caused regional isostatic rebound following rapid Jurassic to Cretaceous deposition.

**THE USE OF HETEROGENEOUS EXCESS ARGON AND ARGON LOSS TO CONSTRAIN THERMAL HISTORIES: LASER  $^{40}\text{Ar}/^{39}\text{Ar}$  DATING OF DEFORMED MICAS FROM THE SESIA ZONE, ITALIAN ALPS**

**REDDY, S.M., WHEELER, J., Dept. of Earth Sciences, University of Liverpool, Liverpool, UK. and KELLEY, S.P., Dept. of Earth Sciences, Open University, Milton Keynes, UK.**

A combination of detailed micro-textural analysis using scanning electron microscopy (SEM) and high-resolution laser  $^{40}\text{Ar}/^{39}\text{Ar}$  dating provides insights into the complex behaviour of argon in deformed metamorphic rocks that have previously been unobtainable. Two samples from the Eclogitic Micaschist Complex (EMC) and the Seconda Zona Diorite Kinzigitica (IIDK) of the Sesia Zone have been studied in detail to investigate the relationship between microstructure development and argon isotope systematics in metamorphic rocks that in the past have proved difficult to date.

Large phengites from the EMC sample record age profiles from Jurassic to end-Cretaceous which compare favourably with theoretically-derived volume diffusion profiles and suggest that the profiles probably developed at temperatures in excess of 400°C. The size of the profiles differ significantly between undeformed grain ends and those grain boundaries formed during boudinage of individual micas. Consequently we are able to use the asymmetry of these diffusion profiles to constrain the timing of deformation and infer the temperatures at which deformation was taking place.

Within the IIDK biotite gneiss sample, biotites record a range of  $^{40}\text{Ar}/^{39}\text{Ar}$  ages from Permian to end-Cretaceous with the youngest ages preserved in fine-grained biotite within pre-Alpine micro-shear zones. Rb-Sr data from biotites within equivalent structural units yield pre-Alpine ages suggesting that excess argon cannot account for the observed range of  $^{40}\text{Ar}/^{39}\text{Ar}$  ages. Comparing  $^{40}\text{Ar}/^{39}\text{Ar}$  ages with measured grain sizes shows a relationship that is best explained by partial resetting of biotites by an Alpine thermal event in which temperatures were less than 300°C. The sample lies only a few kilometres from metamorphic units that reached temperatures of around 600°C during the Alpine orogeny. These data therefore place important constraints on the Alpine tectonic evolution and the exhumation history of the Sesia Zone.

THE TRANSANTARCTIC MOUNTAINS AND  
THE BREAKUP OF GONDWANA:  
UNDERPLATING, UPLIFT, AND FLEXURAL  
SUPPRESSION

Redfield, T. E., Grimm, R. E., Dept. of Geology,  
Arizona State University, Tempe AZ  
85287, Fitzgerald, P. G., Dept. of Geosciences,  
University of Arizona, Tucson, AZ  
85721, and Stump, E., Dept. of Geology, Arizona  
State University, Tempe AZ 85287.

25 new apatite fission track (AFT) ages from a vertical transect in the Admiralty Mountains of northern Victoria Land (NVL), Antarctica indicate that an uplift/denudation event occurred at ~120 Ma, coincident with rifting between Australia and Antarctica (the last phase of Gondwana breakup). These and previously published AFT data from other areas in the Transantarctic Mountains (TAM) support our contentions that 1) growth of the entire TAM was episodic, with early Cretaceous, late Cretaceous, and early Cenozoic events, and 2) the TAM are broken longitudinally into discrete crustal blocks that act somewhat independently.

Coupled with regional geophysical data, the new AFT ages can be incorporated into a tectonic model describing the genesis of the TAM. Bouguer gravity data from the TAM show large mass deficiencies beneath the range. We attribute this anomaly to crustal roots, possibly emplaced by underplating and crustal thickening caused by Jurassic tholeiitic magmatism accompanying incipient Gondwana rifting, or alternatively by post-Ross subduction (suggested by volcanoclastic sediments in the Beacon Supergroup). The roots were flexurally suppressed until initial early Cretaceous rifting thinned the elastic lithosphere between Australia and Antarctica as well as along the present-day TAM range front, allowing a partial isostatic response. Late Cretaceous to early Cenozoic extension in the Ross Sea further thinned and fractured the lithosphere, allowing structural failure of discrete crustal blocks and initiating the main phase of uplift. Full isostatic adjustment has not occurred: the uncompensated portions of today's roots are restrained by regional flexure, warping the edge of the East Antarctic lithosphere and maintaining the TAM in a steady-state, largely aseismic equilibrium.

PRODUCTION OF COSMOGENIC NUCLIDES BY  
MUONS

REEDY, R. C., Los Alamos Nat'l Lab., Los Alamos, NM 87545 USA; NISHIZUMI, K., U. Calif., Berkeley, CA 94720 USA; KLEIN, J., DAVIS, R., and MIDDLETON, R., U. Penn., Philadelphia, PA 19104 USA; LAL, D., and ARNOLD, J.R., U. Calif., La Jolla, CA 92093 USA; KUBIK, P., PSI/ETH-Hönggerberg, CH-8093 Zürich, Switzerland; JULL, A.J.T., U. Arizona, Tucson, AZ 85721, USA; ENGLERT, P.A.J., San Jose State U., San Jose, CA 95192 USA; ELMORE, D., Purdue U., W. Lafayette, IN 47907 USA.

Cosmic-ray interactions in the Earth's atmosphere produce a cascade of particles. Some neutrons and muons reach the surface and produce nuclides. Long-lived radionuclides, such as 5730-year  $^{14}\text{C}$ , 0.3-Ma  $^{36}\text{Cl}$ , 0.7-Ma  $^{26}\text{Al}$ , 1.5-Ma  $^{10}\text{Be}$ , and 15.7-Ma  $^{129}\text{I}$ , and some noble-gas nuclides, such as  $^3\text{He}$  and  $^{21}\text{Ne}$ , made *in situ* in certain materials can be used to study their recent exposure histories, but their production rates are needed. Irradiations at the Los Alamos Meson Physics Facility (LAMPF) have simulated the *in-situ* production of radionuclides.

Below a few meters, muons become a major source of cosmogenic nuclides. Little work has been done on yields of long-lived radionuclides in muon-induced reactions. At the LAMPF Stopped Muon Channel,  $\text{SiO}_2$ ,  $\text{CaO}$ ,  $\text{KNO}_3$ ,  $\text{KCl}$ ,  $\text{CaCO}_3$ , and  $\text{Te}$  powders were mixed with nickel powder in plexiglas boxes and exposed to stopped negative muons ( $\mu^-$ ), and a  $\text{SiO}_2$  target was irradiated with  $\approx 70$  MeV  $\mu^-$  [Reedy *et al.*, 1988]. Low-Z materials such as paraffin, which produce few neutrons from muon reactions, were used to slow the muons and support the targets. The Ni was physically separated from stopped  $\mu^-$  targets after each irradiation. Radionuclides were measured by  $\gamma$ -ray spectroscopy in the Ni, in Fe, Ti, and Au foils used to study beam locations and neutron impurities, and in the targets (e.g.,  $^7\text{Be}$ ). Low-level gas counting was done for  $^{37}\text{Ar}$  and  $^{39}\text{Ar}$ . Accelerator mass spectrometry (AMS) was or will be used to measure  $^{10}\text{Be}$ ,  $^{14}\text{C}$ ,  $^{26}\text{Al}$ ,  $^{36}\text{Cl}$ , and  $^{129}\text{I}$ .

Radionuclides in the Ni showed that there were few neutrons in the targets and will be used to get the number of  $\mu^-$  stopping in each target. Measured were  $^7\text{Be}$ ,  $^{10}\text{Be}$ , and  $^{26}\text{Al}$  in all  $\text{SiO}_2$  targets;  $^7\text{Be}$  and  $^{10}\text{Be}$  in  $\text{CaCO}_3$ ;  $^{14}\text{C}$  and  $^{36}\text{Cl}$  in  $\text{KNO}_3$  and  $\text{CaO}$ ; and  $^{37}\text{Ar}$  and  $^{39}\text{Ar}$  in all K and Ca samples. The  $^{10}\text{Be}/^{26}\text{Al}$  ratio in  $\text{SiO}_2$  exposed to stopped  $\mu^-$  is  $7.0 \pm 0.4$ , similar to that in neutron-irradiated  $\text{SiO}_2$  (7.1) and natural surface quartz (6.0) and is  $3.2 \pm 0.9$  in the  $\text{SiO}_2$  irradiated by  $\approx 70$ -MeV  $\mu^-$ . The  $^{10}\text{Be}/^7\text{Be}$  ratios in  $\text{CaCO}_3$  ( $19 \pm 6$ ) and in  $\text{SiO}_2$  exposed to stopping ( $23 \pm 2$ ) and  $\approx 70$ -MeV  $\mu^-$  ( $3.2 \pm 0.9$ ) were much greater than for energetic neutrons and protons ( $< 1$ ). The relatively large amounts of  $^{10}\text{Be}$  and  $^7\text{Be}$  from  $\text{SiO}_2$  was unexpected as nuclide yields for stopped- $\mu^-$  reactions decrease rapidly for products farther from the target.

Reedy, R.C. *et al.* (1988) in *Progress at LAMPF 1987*, Los Alamos report LA-11339-PR, pp. 148-154.

SEPARATION OF CERIUM FROM OTHER RARE EARTH ELEMENTS WITH APPLICATION TO Sm-Nd AND La-Ce CHRONOMETRY AND TRACER STUDIES

REHKÄMPER, M., GÄRTNER, M., GALER, S.J.G., and GOLDSTEIN, S.L., Max-Planck-Institut für Chemie, Postfach 3060, 55020 Mainz, Germany.

The rare earth element (REE) pairs Sm-Nd and La-Ce include three radioactive decay systems that are widely used in geo- and cosmochemistry for dating and tracer purposes. In addition to the familiar  $^{147}\text{Sm}$ - $^{143}\text{Nd}$  isotope system,  $^{146}\text{Sm}$   $\alpha$ -decays to  $^{142}\text{Nd}$  with a half-life of  $1.03 \times 10^8$  a, allowing the study of processes that took place in the early history of the Earth (Goldstein and Galer, 1992) and the solar system. The  $^{138}\text{La}$ - $^{138}\text{Ce}$  decay scheme has been gaining increasing importance in geochemistry with the advent of high precision isotope analysis of Ce (Makishima and Nakamura, 1991).

Efficient chemical separation procedures are necessary prior to TIMS in order to remove isobarically interfering elements. Particularly important is the interference of  $^{142}\text{Ce}$  (11% of Ce) on  $^{142}\text{Nd}$  (27% of Nd). Mutual separation of the REE is commonly obtained by reversed-phase partition chromatography using HDEHP-coated Teflon powders. However, the separation factors for the elements Ce-Pr-Nd are generally inadequate for high precision  $^{142}\text{Nd}$  and Ce isotope studies.

Here we report a simple but highly efficient solvent extraction technique for the separation of Ce from the other REE. The procedure involves the oxidation of  $\text{Ce}^{3+}$  to  $\text{Ce}^{4+}$  using  $\text{NaBrO}_3$  and extraction of the tetravalent species into an organic solvent containing HDEHP while the remaining lanthanides are left in aqueous nitric acid. The solvent extraction technique can be used for (1) cleaning of Nd from Ce contamination and (2) the isolation of Ce from other REE prior to mass-spectrometric analysis.

The technique has been applied to the cleanup of Nd fractions obtained by HDEHP chemistry as part of a  $^{142}\text{Nd}$  isotope study of geological samples (Goldstein and Galer, 1992). The extraction procedure is quick, increases the Nd-Ce separation factor by up to several orders of magnitude and reduces the isobaric interference of  $^{142}\text{Ce}$  (as expressed by the  $^{142}\text{Ce}/^{142}\text{Nd}$  ratio) to  $<5$  ppm. We are currently investigating the potential of the extraction technique for a simple, one-step separation of Ce from the other REE for use in Ce isotope studies.

Goldstein, S.L. and Galer, S.J.G., 1992, Eos AGU Spring Meeting, p. 323.

Makishima, A., and Nakamura, E., 1991, Chem. Geol. (Isot. Geosci. Sect.), v. 94, p. 1-11.

CHEMICAL DYNAMICS OF MANTLE LITHOSPHERE FROM TH ISOTOPE SYSTEMATICS

REID, M.R. and RAMOS, F.C., Dept. Earth Space Sci., UCLA, Los Angeles, CA 90024. mary@argon.ess.ucla.edu

Basalts of the western USA sample tectonically distinct mantle reservoirs. Th isotope characteristics of these basalts, considered in conjunction with other isotope systematics, permit evaluation of U/Th fractionation associated with melting and metasomatism, and identification of the source of the basalts. Our work shows that the Th isotopic heterogeneity exhibited by basalts in the western USA is much greater than that exhibited by basalts erupted in the oceans. It is unlikely that this simply reflects greater participation of crust in the origin of continental basalts.

The eastern and western Great Basin (EWGB), as represented by eastern California and southwestern Utah respectively, are zones of Proterozoic continental crust thinned by Tertiary extension. Basalts erupted in these areas range from tholeiites to basanites, and their isotopic compositions typify the diversity of mantle reservoirs in the western USA. The range in ( $^{230}\text{Th}/^{232}\text{Th}$ ) is large in basalts of the EWGB (0.65-1.09) and includes the lowest value yet obtained in the western USA. No distinctions are evident between the Th isotope characteristics of silica-saturated and under-saturated basalts. Most samples lie close to the equiline but the range in ( $^{230}\text{Th}/^{232}\text{Th}$ ) is unlikely to be due solely to *in situ* decay: an unprecedented U/Th fractionation of  $>40\%$  would be required for some of the tholeiites. Similarly, this isotopic heterogeneity is also unlikely to be the result of crustal contamination: three case studies performed specifically to evaluate the effects of crustal assimilation yielded  $<12\%$  variation in ( $^{230}\text{Th}/^{232}\text{Th}$ ) over the compositional range of basalt to andesite.

Covariations of Th with other isotopic systems generally trend from depleted mantle compositions represented by lavas of the central Basin and Range and Mojave toward those of enriched mantle. In detail, the Th isotope composition of the enriched mantle endmember for the EWGB basalts is less than those of oceanic basalts with equivalent  $^{208}\text{Pb}^*/^{206}\text{Pb}^*$  compositions. Th seems to follow Nd more closely than Sr, supporting previous interpretations about heterogeneity in the nature of metasomatic phases.

Trace element characteristics of the enriched mantle reservoir in the EWGB are attributable to subduction-related processes. The paired Th-Pb isotopic compositions of the EWGB basalts are not those expected of relatively recent introduction of subducted components into the mantle indicating that Mesozoic to Tertiary plate convergence west of the Great Basin apparently did not modify the mantle under this region. Rather, the Th-Pb isotope systematics of the enriched mantle reservoir can be explained by evolution from an orogenic Pb reservoir that has been chemically isolated since the Proterozoic. Melting must have penetrated to  $<60$  km depths to explain the origin of tholeiites, placing the compositionally enriched mantle reservoirs at relatively shallow depths under the margins of the Great Basin. The depleted mantle reservoir may also be Proterozoic in origin but invasion of the lithosphere by depleted mantle like that under the central Basin and Range is more consistent with crustal extension and asthenospheric decompression in these areas.

## OS ISOTOPIC RESULTS FROM EASTERN PYRENEAN LHERZOLITE MASSIFS

REISBERG, L., CRPG/CNRS, B.P. 20, 54501 Vandoeuvre-les-Nancy Cedex, France, LORAND, J.-P., and PATTOU, L., Museum National D'histoire Naturelle, Laboratoire de Minéralogie, 61 rue Buffon, 75005 Paris, France.

Orogenic lherzolites present an opportunity to directly examine portions of the earth's mantle that have been tectonically emplaced in the crust. A recent study<sup>1</sup> of the Ronda Ultramafic Complex demonstrated that a strong correlation exists between Os isotopic composition and major element content in this massif. This contrasts with the results of Sr and Nd isotopic studies, which displayed no such correlations. These observations suggest that Os isotopes may provide information about the evolution of the major element content of mantle rocks that is not available from other isotopic systems.

To test whether similar correlations between Os isotopic ratio and major element composition are observed in other orogenic lherzolites, we have begun a Re-Os study of the Eastern Pyrenean ultramafic massifs.  $^{187}\text{Os}/^{186}\text{Os}$  ratios from six peridotites analyzed to date range from 0.98 to 1.10 and show some correlation with alumina content, but this relationship is considerably weaker than that observed in Ronda. This difference may result partly from the fact that the Pyrenean massifs comprise many small, distinct peridotite bodies while the Ronda massif is large and contiguous. Furthermore, unlike the Ronda massif, some of the Pyrenean lherzolite bodies have experienced modal metasomatism. The point which plots furthest from the  $^{187}\text{Os}/^{186}\text{Os}$  vs.  $\text{Al}_2\text{O}_3$  trend comes from the Cassou massif, where modal metasomatism was most developed. A somewhat stronger correlation exists between  $^{187}\text{Os}/^{186}\text{Os}$  and sulfur content, and includes the sample from Cassou.

In the coming months, we plan to determine the Re and Os compositions of numerous other peridotites, as well as pyroxenites and amphibolites, from the Eastern Pyrenean massifs. This study will be complemented by the analysis of platinum group element patterns from these rocks.

<sup>1</sup>Reisberg, L.C., Allègre, C.J., and Luck, J.-M., The Re-Os systematics of the Ronda Ultramafic Complex of southern Spain, *EPSL*, v. 105, p. 196-213.

## ISOTOPE MAPPING OF THE ARABIAN-NUBIAN SHIELD: IMPLICATIONS FOR LATE PROTEROZOIC CRUSTAL GROWTH.

REISCHMANN, T., Institut für Geowissenschaften, Johannes Gutenberg-Universität, Becherweg 21, D-55099 Mainz, Germany

The Arabian-Nubian Shield (ANS) is considered to have formed by accretion of arc terranes in the late Proterozoic and thus to document a major portion of continental crust formed at that time. In order to monitor the growth and evolution of this part of the continental crust, regional variation in Nd and Sr isotopes were used to map and to distinguish isotopic provinces. The samples for this study were taken from the central part of the ANS, namely from the Red Sea Hills, Sudan and from the western Arabian Shield.

The Nd isotopic variations observed in the selected areas of the central ANS of this study are  $\epsilon\text{Nd}_t$  between +5.4 and +8.0. These Nd data are considered to approximate late Proterozoic mantle values and to indicate a juvenile origin of this part of the ANS with no significant crustal contribution.

The  $^{87}\text{Sr}/^{86}\text{Sr}_i$  of these samples are generally low, most of them in the range of 0.702 - 0.703 and like the Nd data, the Sr data document the ensimatic origin of the central part of the ANS. This part is built up by juvenile continental crust that formed in the late Proterozoic.

A compilation of these new and previously published Nd and Sr isotopic data of the whole ANS is used to constrain the crustal growth rate in the late Proterozoic. The major part of that region is mantle-derived with  $\epsilon\text{Nd}_t$  of ca. +6.5 and  $\text{Sr}_i$  of ca. 0.703 and thus defines the area of juvenile crust of the shield probably formed by subduction related processes. Based on these data the arc accretion rate for the ANS can be calculated to be  $46 \text{ km}^3\text{km}^{-1}\text{Ma}^{-1}$  which is similar to recent rates.

Taking 300 Ma as the whole time span for crust formation of the ANS the crustal growth rate for this region can be calculated to be  $0.29 \text{ km}^3\text{a}^{-1}$ . This implies that about 30 % of the late Proterozoic crustal growth have to be assigned to the ANS, a number which is lower than those obtained in previous estimates and does not indicate disproportionate crustal growth in the ANS. Therefore, crustal growth during the late Proterozoic was probably the same as it is today.

ORBITAL TUNING OF  $^{40}\text{Ar}/^{39}\text{Ar}$  STANDARDS: THE CASE OF FISH CANYON SANIDINE

RENNE, P.R. (1), DEINO, A.L. (1), WALTER, R.C. (1), TURRIN, B.D. (2,1), SWISHER, C.C. (1), BECKER, T.A. (1), SHARP, W.D. (1), and CURTIS, G.H. (1): (1) IHO Geochronology Center, 2453 Ridge Rd., Berkeley, CA, 94709, USA; (2) U.S. Geological Survey, MS 901, 345 Middlefield Rd., Menlo Park, CA, 94025, USA.

The  $^{40}\text{Ar}/^{39}\text{Ar}$  dating method is well-established as one of the most precise and versatile methods in the geochronologic arsenal, but the accuracy of this method is limited by uncertainties as to the ages of neutron fluence monitors (dating standards). Conventional (K-Ar) age calibration of  $^{40}\text{Ar}/^{39}\text{Ar}$  standards has met with difficulties, and minerals yielding the most reproducible and correction-insensitive  $^{40}\text{Ar}/^{39}\text{Ar}$  isotopic data prove problematic for measurement of absolute isotopic abundances.

The astronomically-calibrated geomagnetic polarity time scale (APTS) developed by Shackleton *et al.*, (1990) and Hilgen (1991) offers a means to assess the ages of  $^{40}\text{Ar}/^{39}\text{Ar}$  dating standards that is independent of absolute isotopic abundance measurements. Seven published  $^{40}\text{Ar}/^{39}\text{Ar}$  dates for polarity transitions, nominally ranging from 0.78 to 3.40 Ma, are based on the Fish Canyon sanidine (FCs) standard and can be compared with APTS predictions. All were based originally on FCs at 27.84 Ma except the Brunhes/Matuyama datum, which is recalculated from Spell and McDougall (1992). Solving the  $^{40}\text{Ar}/^{39}\text{Ar}$  age equation for the age of FCs that produces coincidence with the APTS for each of these seven reversals yields mutually indistinguishable estimates ranging from 27.78 to 28.09 Ma, with an inverse variance weighted mean of  $27.95 \pm 0.09$  Ma. Normalized residuals are minimized at an FCs age of 27.92 Ma, indicating the robustness of the solution.

The APTS-optimized age for FCs corresponds to an age of  $522.1 \pm 1.6$  Ma for Mmhb-1, based on inter-calibration between the two standards.

Boundary or Event	APTS Age (Ma)	$^{40}\text{Ar}/^{39}\text{Ar}$ Age (Ma) $\pm$ s (FCs=27.84 Ma)	Calculated Age of FCs (Ma) $\pm$ s
Brunhes/Matuyama	0.78	$0.778 \pm 0.010$	$27.91 \pm 0.50$
Top Jaramillo	0.99	$0.992 \pm 0.039$	$27.78 \pm 1.53$
Cobb Mountain	1.19	$1.186 \pm 0.008$	$27.93 \pm 0.26$
Top Kaena	3.04	$3.042 \pm 0.039$	$27.82 \pm 0.50$
Bottom Kaena	3.11	$3.095 \pm 0.027$	$27.97 \pm 0.34$
Top Mammoth	3.22	$3.210 \pm 0.010$	$27.93 \pm 0.12$
Base Mammoth	3.33	$3.300 \pm 0.020$	$28.09 \pm 0.24$
Weighted Mean			$27.95 \pm 0.09$

Hilgen, F. J., 1991, Earth Plan. Sci. Lett., v. 107, p. 349-366.  
 Shackleton, N. J., Berger, A. and Peltier, W. R., 1990, Trans. Roy. Soc. Edinburgh, v. 81, p. 251-261.  
 Spell, T. L., and McDougall, I., 1992, Geophys. Res. Lett., v. 19, p. 1181-1184.

RATES CONSTRAINTS OF RIVER INCISION USING COSMOGENIC RADIONUCLIDES: EXAMPLES FROM FLUVIAL TERRACES ALONG THE FREMONT RIVER, UTAH

REPKA, James L., ANDERSON, Robert S., DICK, Greg S., (Earth Sciences Department, University of California, Santa Cruz CA 95064, USA; jlrpk@bagnold.ucsc.edu) FINKEL, Robert C., and SOUTHON, John R. (Center for Accelerator Mass Spectrometry, Lawrence Livermore National Laboratory, Livermore CA 94550, USA)

We are investigating the incision history of the Fremont River in south-central Utah by measuring concentrations of *in-situ* produced  $^{26}\text{Al}$  and  $^{10}\text{Be}$  in fluvial gravels found on the surfaces of strath terraces near Caineville, Utah. This in turn constrains the baselevel history of tributaries to the Fremont River, whose landscape evolution we are studying.

Downcutting of the Fremont River has created a series of distinct fluvial terraces. Strath surfaces cut into Ferron Sandstone and Blue Gate Shale members of the Mancos Shale are mantled by up to 3m of fluvial deposits that include boulders of basalt and cobbles of quartzite, sandstone, petrified wood and chalcedony. We are sampling siliceous cobbles, primarily quartzites, whose surfaces show no signs of post-deposition weathering.

Interpretation of cosmogenic radionuclide (CRN) results from these cobbles is, however, complicated by the potential for inherited CRN's from exposure during weathering from the source area and during hillslope and fluvial transport to the site of deposition. We believe the siliceous cobbles to be derived from the Shinarump Conglomerate member of the Chinle Formation in Capitol Reef National Park, within 20-30km of the sampling area. Such clasts weathering from this fluvial formation generally are already rounded and display a range of sizes similar to that found on the Fremont River terraces. This suggests a simple and limited exposure and pre-terrace depositional history. We present a numerical model used to generate a suite of synthetic cobble CRN concentration histories resulting from a range of hypothetical transport and burial paths. Measured CRN concentrations of cobbles obtained from a terrace surface and from several meters below the surface are contrasted in order to constrain the model parameters.

Preliminary results from two of the most extensive surfaces yield ages of 75-85ka for the lower terrace and 145-165ka for the highest terrace. These ages correlate well with isotope stages 4-5a and 6, respectively, corresponding to a relatively steady 0.6-0.8mm/yr long-term incision rate of the Fremont River.

THE TRANSFER OF TERRANES FROM SOUTH TO NORTH AMERICA BASED ON THE PROTEROZOIC AND PALEOZOIC EVOLUTION OF COLOMBIA AND SOUTHERN MEXICO

RESTREPO, P.; RUIZ, J., Department of Geosciences, University of Arizona, Tucson, Arizona 85721, COSCA, M., Institut de Minerlogie University of Lausanne, Lausanne, Switzerland.

The Precambrian and Paleozoic tectonic evolution of Colombia and southern Mexico is central to tectonic models related to the opening and closing of the proto-Atlantic and to the ultimate paleogeographic reconstructions of Pangea. Paleogeographic reconstructions based on paleomagnetic data suggest that parts of Colombia collided with southern Mexico at least twice during the Paleozoic. These models are supported by Ordovician trilobites of southern Mexico, which are very similar to those of Colombia and Argentina. Basement rocks in southern Mexico are Grenvillian in age based on U-Pb, Sm-Nd and Rb-Sr geochronology. Paleozoic tectonothermal events that affected parts of southern Mexico occurred at ca. 380Ma (Acadian Orogeny) and 270 Ma. There is no evidence for an early Paleozoic (Taconic) event (Yañez et al.1991). Because of the fossil evidence, as well as the fact that the Grenville age rocks occur to the east of the Paleozoic rocks, which is opposite to the geometry in North America, it is likely that Southern Mexico was part of South America prior to the final opening of the Atlantic. In Colombia, Proterozoic and Paleozoic rocks are found in the Santander, Garzon and Santa Marta Massifs and the Puqui Complex. The oldest rocks found in the Santander and Santa Marta massifs, based on  $^{40}\text{Ar}/^{39}\text{Ar}$  are Grenvillian in age (ca. 1000Ma) We have no evidence of older rocks in these areas. There are only two Paleozoic tectonothermal events recognized: a pre-380 Ma and ca. 200 Ma. The 200 Ma metamorphic rocks are related to the Jurassic arc of South America, which extends north into Colombia. The pre-Devonian age may represent the Taconic orogeny, which is absent in southern Mexico. The field paleontologic, and geochronological data of Colombia and southern Mexico suggest that the collision represented by the Taconic orogeny occurred south of what is presently southern Mexico. The collision represented by the Acadian orogeny must have occurred north of southern Mexico leaving most of Mexico behind in the final opening of the Atlantic. Thus during the Paleozoic, terranes that were part of south America were transferred to north America. These terranes are fingerprints of a geologic history but do not represent additions of continental crust during the Phanerozoic.

Yañez, P., Ruiz, J., Patchett, P.J., Ortega-Gutierrez, F., and Gehrels, G., 1991, The Acatlan Complex, Geological Society of America Bulletin v 103, p. 817-828.

EVALUATION OF ARGON STANDARDS WITH SPECIAL EMPHASIS ON TIME SCALE MEASUREMENTS.

REX,D.C. and GUISE,P.G., Dept of Earth Sciences, University of Leeds, Leeds, LS2 9JT, UK.

The urgent requirement for standards which have been analysed by K-Ar and other methods to calibrate Ar-Ar analyses is well known. The precision of the Ar-Ar method is as good as 0.1% but the accuracy depends on the K-Ar calibrated standards used to monitor the irradiation parameters.

The table below shows Leeds (for method, see LeMasurier & Rex 1989) and published K-Ar ages for various standards .

Standard	Published	Leeds
MMHb-1	514-525	**
Hb3gr	1064-1071	1064
HD-B1	24.0	24.4
LP-6	128.9	130.0
Bern 4M	18.6	18.5
BSP-1	2060	2073
133 Bio	1013	1033
Nancy Mg	318	314
RoM	--	424
Tinto	410	412
Fy12a	436	442
Fy12b	435	430

\*\* Evidence of inhomogeneity of MMHb-1 has been noted. We had insufficient material for K-Ar analysis, but report a %K content of  $1.552 \pm 0.002$  (2 sigma).

Aliquots of all the standards above were irradiated in the Ford Reactor at Ann Arbor. Using MMHb-1, Hb3gr and Fy12a as Roddick (1983) the flux gradient over the length of the silica tubes was 3% (full experimental details in Rex et al 1993). Recalculating the 'J' values using the K-Ar values from the table, changed the fit of the flux curve and increased the 'J' error from 1% to 1.5% ( 2 sigma ).

Roddick has shown that hand picking of standards produces 'J' curves with little scatter and therefore high precision. However, if this approach is to be used for time scale and interlaboratory comparison of unknown samples, then unpicked standards with agreed K-Ar ages must be included so that the J calibration can be adjusted to an absolute framework.

Le Masurier, W.E. & Rex,D.C. Evolution of linear volcanic ranges in Marie Byrd Land, West Antarctica. J.G.R., 94, (1989) No.B6 , 7223-7236.

Rex,D.C.,Guise,P.G. & Wartho J.-A. Disturbed  $^{40}\text{Ar}$ - $^{39}\text{Ar}$  spectra from hornblendes: Thermal loss or contamination? Chem . Geol .(Iso. Geo. Sec.), 103 (1993) 271-281.

Roddick,J.C. High precision intercalibration of  $^{40}\text{Ar}$ - $^{39}\text{Ar}$  standards. G.C.A. 47 (1983) 887-898.

ORIGIN OF LHERZOLITIC DIAMONDS SAMPLED BY  
SOUTHERN AFRICAN KIMBERLITES

RICHARDSON, Stephen H., Dept. of  
Geological Sciences, University of Cape  
Town, Rondebosch 7700, South Africa.

Diamonds with lherzolitic inclusions (olivine, orthopyroxene, garnet and clinopyroxene) constitute only a small fraction of inclusion-bearing diamonds worldwide. Nevertheless, there has been considerable interest in relating the conditions of origin of lherzolitic diamonds to those of harzburgitic diamonds (the dominant type of peridotitic diamond) or, alternatively, to those of eclogitic diamonds.

In the case of the 1180 Ma old Premier kimberlite, all three types are well represented. They vary in age from >3000 Ma (harzburgitic) to ~1180 Ma (eclogitic). In addition, they show a range in precursor isotope signature from strongly enriched (high Rb/Sr; harzburgitic) to strongly depleted (high Sm/Nd; eclogitic). Lherzolitic garnet and clinopyroxene inclusions yield an intermediate Sm-Nd isochron age of  $1930 \pm 40$  Ma with a mildly enriched isotope signature (Richardson et al., 1993). This age is ~100 Ma less than that of the adjacent Bushveld Complex which represents one of the largest mantle melting events beneath the Kaapvaal craton during the Proterozoic.

A similar age for lherzolitic diamonds from the Cretaceous Kimberley kimberlite cluster may be inferred by comparison of the above data with that for a 'websteritic' clinopyroxene inclusion from a Kimberley diamond (Smith et al., 1991). A temporal, spatial and compositional link between Bushveld style magmatism and lherzolitic diamond formation can be developed, by analogy with that between komatiitic magmatism and subsequent harzburgitic diamond formation in the Archean.

Richardson, S.H., Harris, J.W., and Gurney, J.J., 1993, Three generations of diamonds from old continental mantle: *Nature*, 366, 256-258.

Smith, C.B., Gurney, J.J., Harris, J.W., Otter, M.L., Kirkley, M.B., and Jagoutz, E., 1991, Nd and Sr isotope systematics of eclogite and websterite paragenesis inclusions from single diamonds, Finsch and Kimberley Pool, RSA: *Geochim. Cosmochim. Acta*, 55, 2579-2590.

ESR DATING OF TOOTH ENAMEL IN  
ARCHAEOLOGICAL SITES: INTERCOMPARISON  
WITH  $^{14}\text{C}$  DATES

RINK, W.J., Dept. of Geology, McMaster  
University, Hamilton, ON, Canada L8S 4M1, and  
SCHWARCZ, H.P., Dept. of Geology, McMaster  
University, Hamilton, ON, Canada L8S 4M1.

Electron spin resonance (ESR) dating of tooth enamel is based on the measurement of the growth of a radiation-sensitive ESR signal present in hydroxyapatite of mammalian tooth enamel. This material is a ubiquitous component of all archaeological sites. In contrast, other methods such as U-series dating of carbonates, TL dating of burned flints, or  $^{40}\text{Ar}/^{39}\text{Ar}$  dating of volcanics, all require samples which are relatively rare at Palaeolithic sites. The range of ESR dating is from about 10 ka to 2 Ma, which extends the dating range for most sites beyond the limits of  $^{14}\text{C}$  (c. 40 ka). We report here on attempts to make intercomparisons with  $^{14}\text{C}$  and other methods over their overlapping ranges, in order to confirm the validity of ESR dating. The site of Das Geissenklösterle (Germany) contains an archaeological sequence of Mousterian, proto-Aurignacian, Aurignacian, and Gravettian artifacts, whose enclosing sediments have been dated by  $^{14}\text{C}$ , and for which we will present comparative ESR data on teeth obtained from these deposits. The Spanish site of El Castillo contains a deep stratigraphic sequence including Acheulian, Mousterian and Aurignacian deposits. We have made comparative ESR dates on teeth from near the AMS/ $^{14}\text{C}$ -dated 39 ka boundary between Mousterian and Aurignacian; and for the Mousterian sequence whose age is constrained by a U-series isochron date for an intercalated flowstone.

## ISOTOPE SYSTEMATICS OF CONTAMINANT LEAD FLUXES IN THE SAN FRANCISCO BAY ESTUARY

RITSON, P.R., Earth Science, WIGS, University of California, Santa Cruz, California, 95064, USA, and FLEGAL, A.R., Earth Science, WIGS, University of California, Santa Cruz, California, 95064, USA.

Measurements of lead in the San Francisco Bay estuary were initiated after isotopic composition analyses of lead in the northeast Pacific indicated that relatively little of the lead discharged in the estuary was advected into adjacent coastal waters. This was corroborated by the heterogeneous distribution of dissolved lead concentrations ( $< 10$  to  $300$  pM) and its high partition coefficient ( $K_d \approx 10^5$ ) within the estuary, which both attest to the efficacy of biogeochemical scavenging processes in those waters. Conversely, the homogeneous distribution of lead isotopic compositions ( $^{207}\text{Pb}/^{206}\text{Pb} \approx 0.8446$ ) in the dissolved phase, suspended particulates and surficial sediments throughout the estuary attest to the extensive remobilization of lead from sediments deposited within the system. Those benthic lead fluxes were previously estimated to range from  $1.4 \times 10^5$  to  $2.2 \times 10^6$  kg  $\text{yr}^{-1}$ , which is 5 to 6-orders of magnitude greater than the fluvial input of dissolved lead to San Francisco Bay and comparable to the anthropogenic input of industrial lead to that embayment (Rivera-Duarte and Flegal, 1994). With the contrasting distributions of lead concentrations and isotopic compositions, those estimates corroborate Turekian's proposal that estuarine sediments are a trap for this particle reactive element even though it may be extensively remobilized by diagenic processes.

Rivera-Duarte, I., and A.R. Flegal. 1994. Benthic lead fluxes in San Francisco Bay. *Geochimica et Cosmochimica Acta* (in press).

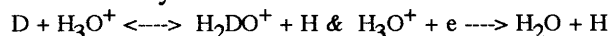
## DEUTERIUM-RICH WATER IN THE SOLAR SYSTEM.

ROBERT F., Muséum Histoire Naturelle, Lab. deMinéralogie. 61 rue Buffon.75005.Paris.France & DELOULE E. CRPG-CNRS, BP20, 54501 Vandoeuvre les Nancy Cedex France

The D/H ratio of the solar nebula  $\text{H}_2$  was close to  $20.10^{-6}$  (i.e.  $\delta\text{D} = -870$  ‰). Based on recent laboratory determinations on isotopic reaction rates (Lécluse & Robert), the classical exchange model  $\text{HD} + \text{H}_2\text{O} \leftrightarrow \text{HDO} + \text{H}_2$  has been re-investigated : D/H ratios in protosolar water, similar to those measured in meteoritic phyllosilicates or on Earth ( $\text{D}/\text{H} < 180.10^{-6}$  i.e.  $\delta\text{D} < +150$  ‰), can be reached during the life time of the nebula ( $10^6$  years).

However, the isotopic composition of the deuterium-rich water bearing minerals ( $\delta\text{D} +3500$ ‰ i.e.  $\text{D}/\text{H} = 700.10^{-6}$ ) discovered in the Semarkona meteorite (Deloule & Robert, 1994) is in clear disagreement with such a thermal model. These phyllosilicates are probably under form of deuterium-rich clusters where organic macromolecules are in close association with -OH bearing minerals.

An alternative interpretation for this deuterium enrichment in water, is to consider that an isotopic fractionation occurred via photo-chemical or ion-molecule reactions. It is possible to model such an environment by reactions such as :



Using the usual astrophysical approximations (Duley & Williams, 1984), reaction rate calculations show that, for a fractionational ionisation lying between  $10^{-5}$  and  $10^{-6}$ , the meteoritic phyllosilicate D/H ratio can be reached at temperatures between 120 and 80K. These results suggest that synthesis of water has been confined in the low pressure outer regions of the nebula (probably because of the high opacity in the mid plane of the nebula), where ions or radicals can be produced by UV molecular dissociation. The source of UV's in these regions is the interstellar radiation field.

According to the present isotopic results, it seems impossible to admit that the solar system water is a by-product of a condensation sequence in the solar nebula.

DELOULE E. & ROBERT F. See the present volume abstract.

DULEY W.W. & WILLIAMS D.A. *Interstellar chemistry*. Academic Press 1984.

LECLUSE C. & ROBERT F. *Geochim & Cosmochim. Acta* (in press)

### THREE REGIONALLY COHERENT LOWER CRUSTAL MAGMA SOURCES FOR MESOZOIC GRANITOIDS IN NEVADA AND EASTERN CALIFORNIA NORTH OF 37° N

ROBINSON, A. C., U. S. Geological Survey, Menlo Park, California, 94025

Strontium whole-rock isotopic analyses of 2137 Mesozoic granitoid samples from the western three quarters of Nevada and eastern California north of 37° N latitude form three coherent fields on a measured  $^{87}\text{Sr}/^{86}\text{Sr}$  versus  $^{87}\text{Rb}/^{86}\text{Sr}$  diagram. Although the granitoids are of diverse age, these fields relate functionally to inferred source isochrons of three regionally coherent lower crustal magma sources: (1) an Early Proterozoic (~1800 Ma) lower continental crust of basaltic composition, yielding granitoid magmas with initial  $^{87}\text{Sr}/^{86}\text{Sr}$  ( $\text{Sr}_i$ ) in the range 0.7048-0.7110; (2) a slightly alkalic basaltic (higher Rb/Sr) Late Proterozoic (~760 Ma) rift-generated lower crust, emplaced during incipient rifting beneath uplifted and attenuated continental crust along the locus of the rift, yielding  $\text{Sr}_i$  in the range 0.7050-0.7072; and (3) a Late Proterozoic (~760 Ma) rift-generated lower crust, of composition similar to (1) and emplaced as oceanic crust as the continental segments spread apart, yielding  $\text{Sr}_i$  in the range 0.7038-0.7052. Histograms of granitoid  $\text{Sr}_i$  are normally distributed for sources (2) and (3) and for source (1) over the range 0.7048-0.7080.

Forty-two published Nd whole-rock isotopic analyses of Mesozoic granitoid samples from the same region form three coherent fields on a measured  $^{143}\text{Nd}/^{144}\text{Nd}$  versus  $^{147}\text{Sm}/^{144}\text{Nd}$  diagram that are analogous to the Rb-Sr fields, and that relate to inferred source isochrons of comparable Early and Late Proterozoic ages. The granitoid  $\text{Nd}_i$  ranges are: source (1), 0.51180-0.51247; source (2), 0.51205-0.51245; and source (3), 0.51250-0.51278. This diagram illustrates that lower crustal sources (1) and (3) were derived from relatively depleted mantle, whereas lower crustal source (2) was derived from relatively undepleted mantle near CHUR in composition.

The  $\text{Sr}_i$  and  $\text{Nd}_i$  ranges for granitoids of source (2) lie within the granitoid  $\text{Sr}_i$  and  $\text{Nd}_i$  ranges of source (1), so that other criteria are needed to distinguish between granitoids of sources (1) and (2). The slightly alkalic composition of source (2) serves this need. Normally-distributed histograms of Rb and Sr concentration in granitoids from sources (1) and (3) are coincident, whereas normally-distributed histograms of Rb and Sr concentration in granitoids from source (2) are offset to higher concentrations. Consequently, the overlapping data fields for granitoids from sources (1) and (2) on the measured  $^{87}\text{Sr}/^{86}\text{Sr}$  versus  $^{87}\text{Rb}/^{86}\text{Sr}$  diagram tend to separate into discrete fields on the measured  $^{87}\text{Sr}/^{86}\text{Sr}$  versus Rb concentration diagram.

On the  $\epsilon\text{Nd}_i$  versus  $\text{Sr}_i$  diagram the three coherent lower crustal sources are manifested as discrete linear trends, the regressed slopes of which are proportional to the ratios of the parent/daughter Rb/Sr and Sm/Nd ratios in the sources. This is demonstrated graphically by plotting source  $^{147}\text{Sm}/^{144}\text{Nd}$  versus  $^{87}\text{Rb}/^{86}\text{Sr}$  obtained by solving intersections of granitoid isochrons with inferred source isochrons.

The geographic boundary between  $\text{Sr}_i < 0.7050$  and  $\text{Sr}_i > 0.7050$  conceptually locates the Late Proterozoic rifted continental margin. This boundary has two 90° ridge-transform-like bends, one north of Lovelock, Nevada and another a little south of Austin, Nevada. In eastern California, the boundary has been disrupted by at least 300 km of cumulative right-lateral offset along NNW-trending crustal shears of possible Early Jurassic age.

### KINETICS AND CHEMISTRY OF THE ZIRCON EVAPORATION TECHNIQUE

Roddick, J.C., Geological Survey of Canada, 601 Booth St., Ottawa, Ontario, K1A 0E8 Canada, and  
Chapman, H.J., Dept. Earth Sciences, University of Cambridge, Downing St., Cambridge CB2 3EQ, U.K.

The zircon evaporation technique is increasingly being used to determine  $^{207}\text{Pb}^*/^{206}\text{Pb}^*$  (radiogenic Pb) ages. The process is now understood to involve the breakdown of zircon to porous  $\text{ZrO}_2$  (baddeleyite), with the associated loss of mainly silica, along a reaction front which progresses into the interior of a grain (Ansdell and Kyser, 1993; Roddick and Chapman, 1991). To further understand the kinetics and chemistry of the process a series of experiments have been carried out. The rate at which the process takes place has been determined by heating a series of high quality non-metamict zircon grains at different temperatures and for a range of times. Polished sections of these grains show the progress of the reaction front as a function of temperature (1470°C to 1670°C) and time (10 min. to 6 hr.). Optical pyrometers used in the experiments were accurately calibrated by melting pure metals (Au, Ni, Pt) in folded Re filaments with the same geometry as used in heating zircon grains. The process is strongly temperature dependent and follows an Arrhenius relation with an activation energy of  $130 \pm 10$  ( $1\sigma$ ) kcal·mole<sup>-1</sup> and a reaction constant at infinite temperature of about  $4 \times 10^{12}$   $\mu\text{m}\cdot\text{sec}^{-1}$ . These parameters indicate that a 100  $\mu\text{m}$  diameter zircon grain is completely converted to  $\text{ZrO}_2$  in 6 hr. at 1600°C and 1 hr. at 1700°C.

The chemistry of the process has been determined by ICP-MS analyses of residual  $\text{ZrO}_2$  grains and ICP-MS laser ablation of companion deposits on filaments usually used for Pb isotopic analyses. Material vaporized and deposited consists mainly of a mixture of  $\text{SiO}_2$  (70%) from the zircon and Re (30%) from the filament used to heat the zircon. Other trace elements in zircon are also vaporized to varying degrees. Most Pb, Ce and about 50% of the U are quantitatively evaporated. Lesser amounts of Ba are transported. REEs (except Ce), Hf, Y and Th are retained in the residual  $\text{ZrO}_2$ . In evaporation dating U readily ionizes as  $\text{UO}_2^+$  at a lower temperature than  $\text{Pb}^+$  and is useful for focusing and optimizing the beam both during the deposition stage and prior to Pb isotopic analysis.

Ansdell, K.M. and Kyser, T.K., 1993, Textural and chemical changes undergone by zircon during the Pb-evaporation technique: *Am. Min.* 78, 36-41.

Roddick, J.C. and Chapman, H.J., 1991,  $^{207}\text{Pb}^*/^{206}\text{Pb}^*$  dating by zircon evaporation: Mechanisms of Pb loss: *EOS, Trans. Am. Geophys. Union* 72, 531.

EXCHANGE BETWEEN CO<sub>2</sub> AND Ag<sub>3</sub>PO<sub>4</sub> AT HIGH TEMPERATURES: A NEW METHOD FOR DETERMINING THE OXYGEN ISOTOPE COMPOSITION OF PHOSPHATIC MATERIALS

ROE, L.L., Dept. Geosci., Univ. of Arizona, Tucson, AZ 85718, O'NEIL, J.R. and REINHARD, E.A., Dept. Geol.Sci., Univ. of Michigan, Ann Arbor, MI 48109

Here we report for the first time that CO<sub>2</sub> exchanges readily with Ag<sub>3</sub>PO<sub>4</sub> at high temperatures and propose controlled equilibrium exchange as a method of determining the oxygen isotope composition of phosphates. The advantages of this method are: (1) it is the simplest, fastest, and least expensive method available for the analysis of phosphate oxygen; (2) it requires neither fluorination nor graphite reduction and (3) it can be done in glass tubes at temperatures low enough to reduce or eliminate the problem of exchange between the oxygen in the tube and the reagents.

In initial experiments done at the University of Arizona, fairly large (24-50 mg) samples of Ag<sub>3</sub>PO<sub>4</sub> precipitated from NBS-120C Florida phosphate rock were placed in 6mm SiO<sub>2</sub> tubes and evacuated to  $5 \times 10^{-4}$  torr. An aliquot of one of two different CO<sub>2</sub> reference gases was frozen into each tube, and the tube sealed. The  $\delta^{18}\text{O}$  values of the two reference gases were +7.6‰, and +34.0‰, and the  $\delta^{18}\text{O}$  of the NBS standard was +21.8‰. Thus, equilibrium exchange was approached from opposite directions. The samples were then heated at 875°C for 10 minutes, withdrawn rapidly from the furnace and quenched in a beaker of water. The CO<sub>2</sub> samples were expanded into the inlet system of the mass spectrometer without purification and ran very cleanly. The Ag<sub>3</sub>PO<sub>4</sub> retained its original color, giving support to the conclusion that no chemical reaction had occurred. In all cases the resultant isotopic composition of the CO<sub>2</sub> was different from its initial value, and had a  $\delta^{18}\text{O}$  value 1.95-3.25‰ higher than the Ag<sub>3</sub>PO<sub>4</sub> (corrected for mass balance). CO<sub>2</sub>-Ag<sub>3</sub>PO<sub>4</sub> exchange was confirmed in separate experiments run at the Institut de Minéralogie et Pétrologie in Lausanne, Switzerland, using a CO<sub>2</sub> reference gas with a  $\delta^{18}\text{O}$  value of 7.74‰ and 30-35 mg samples of a Ag<sub>3</sub>PO<sub>4</sub> standard made from KH<sub>2</sub>PO<sub>4</sub> at the Carnegie Institution and reputed to have a  $\delta^{18}\text{O}$  value of 11.9‰. These samples were heated at 875°C for 5 and 10 minutes, with no significant difference in the resultant  $\delta^{18}\text{O}$  value, indicating that isotopic exchange is complete within five minutes. The final  $\delta^{18}\text{O}$  value of the CO<sub>2</sub> in these experiments was 3.58‰ - 3.79‰ higher than the presumed value of the Ag<sub>3</sub>PO<sub>4</sub>.

We are now conducting experiments to determine the optimal conditions for the use of controlled CO<sub>2</sub>-Ag<sub>3</sub>PO<sub>4</sub> equilibrium exchange as a method for determining the oxygen isotope composition of phosphates and the fractionation factor over a wide range of temperatures. Initial results indicate that isotopic exchange does not require as high a temperature as did our earlier method of reacting graphite and Ag<sub>3</sub>PO<sub>4</sub> at 1250°C. It may therefore be possible to achieve oxygen isotope exchange between CO<sub>2</sub> and Ag<sub>3</sub>PO<sub>4</sub> at times and temperatures at which the glass tubes will not exchange their oxygen with the CO<sub>2</sub>. Alternatively, this exchange reaction could be done in metal tubes.

LARGE SCALE DOMING AND ASSOCIATED BASIN EVOLUTION IN SOUTH NORWAY: EVIDENCE FROM APATITE FISSION TRACK THERMOCHRONOLOGY

ROHRMAN, M., P.A. VAN DER BEEK and ANDRIESEN, P.A.M., Dept. of Geology, Free University, 1081 HV, Amsterdam, The Netherlands.

We present Apatite Fission Track (AFT) ages and confined track length distributions of Caledonian and Precambrian basement rocks in Southern Norway and offshore commercial boreholes. As no post-Permian rocks are present on the South Norwegian mainland, the post-Permian evolution has been badly constrained. This in contrast with the bordering North sea basin as a result of hydrocarbon exploration.

The combined results of AFT data from the mainland and reflection seismics and AFT data from the North sea basin constrains an unique combination of basin and margin evolution, which can be used to test rifting and erosion models.

AFT thermochronology on more than 50 samples of the Precambrian/Caledonian South Norwegian mainland, including transects and elevation profiles up to 2469 m above sea-level, show isochrons of AFT ages which closely follow the summit-heights and peneplanation surfaces.

The AFT ages show a bending of the isochrons, with the youngest ages of around 100 Ma and mean track lengths around 11.8  $\mu\text{m}$  with a broad (2 $\mu\text{m}$ ) standard deviation lying deep in the fjords at sea level. Ages and mean track lengths increase towards the peaks of the mountains and the West coast to about 160 Ma and 13.5  $\mu\text{m}$  respectively and narrow standard deviation (1.2  $\mu\text{m}$ ). No clear break-in-slopes are observed, this agrees with the low thermal gradient (20°C/km) for this area, which would require fast uplift of >3km to become visible. In the Southeast the ages increase to more than 200 Ma, defining a structural dome with a wavelength of 400 km and an amplitude of around 4 km. The AFT ages indicate that doming must have taken place less than 100 Ma ago.

AFT results from commercial wells offshore Norway show AFT ages of around 160 Ma for the 2 km thick Neogene sedimentary wedge. Mean track lengths are around 12.9 micron. They can be backstacked on the mainland and show a clear relation between basin evolution and hinterland erosion.

Modelling of AFT ages and confined track length distributions suggest two major episodes of exhumation and cooling; a Jurassic and Neogene event. We suggest a scenario in which Jurassic uplift coincides with active rifting in the North Sea and was followed by peneplanation during the Cretaceous and Paleocene. This is also shown in offshore carbonate and clay sedimentation during these times respectively. Furthermore the seismics and sedimentation patterns indicate sediment transport directions from the Shetlands in the Paleocene, arguing against uplift of the Norwegian margin around that time. Rapid Neogene domal uplift corresponds to the build-up of the Neogene sediment wedges in the Northern North Sea basin.

**BURIAL OF LIGHT SULFUR IN NEOPROTEROZOIC CONTINENTAL MARGIN STRATA, SOUTHERN CANADIAN CORDILLERA: IMPLICATIONS FOR UNDERSTANDING SEA WATER EVOLUTION**

**ROSS, GERALD M.**, Geological Survey of Canada, 3303 33rd St. N.W., Calgary, Alta. T2L 2A7; **BLOCH, John D.**, Sealu Modus, 2617 Cutler Ave NE., Albuquerque, New Mexico; 87106 and **KROUSE, H.R.**, Department of Physics, University of Calgary, Calgary, Alta. T2N 1N4

The Neoproterozoic was a fundamental time in Earth history during which the intertwining of tectonic, climactic and geochemical processes culminated in the first appearance of metazoan life forms. Available  $\delta^{13}\text{C}$  data from marine carbonates indicate dramatic variations in the record of organic carbon burial which affects the oxygen reservoir, a key control on evolution of metazoan respiration. A missing element from existing isotopic studies has been data from sedimentary rocks of deep water aspect, as well as a clear understanding of the role of sulfur in these changes. We present the results of the isotopic analysis of pyrite from deep water Neoproterozoic sedimentary rocks, thus providing a new perspective on evaluating paleoenvironmental changes in this time period.

The Neoproterozoic record in the southern Canadian Cordillera (SCC) is characterized by sedimentary rocks formed on the slope of a passive continental margin. Isotopic data (170 analyses) from the analysis of authigenic pyrite that is common in these rocks indicate a large component of  $^{32}\text{S}$ -enrichment with values up to  $\delta = -31$  permil. This degree of  $^{32}\text{S}$  enrichment is unknown from Neoproterozoic rocks but is a necessity to balance the isotopic composition of evaporitic sulfur. The isotopic compositions of the pyrites span a broad range of ca. 50 permil in each of two units examined, indicative of sulfide formation by bacterial sulfate reduction, perhaps in a euxinic marine basin, and influenced by diffusion-controlled sulfate availability. The most  $^{34}\text{S}$ -enriched values of the sulfides (+18 and +32) are inferred to approximate the isotopic composition of sea water preserved as a consequence of the rate of sulfate reduction exceeding the rate of sulfate diffusion (i.e. effectively a closed system).

A shift to  $^{34}\text{S}$ -enriched compositions (+32) of late Neoproterozoic sea water is known from evaporites (e.g. Claypool et al.) but the  $^{34}\text{S}$ -depleted sulfide reservoir has never been found, leading to an enigma in the mass balance of sulfur. We suggest that the SCC is an analogue of the process of  $^{32}\text{S}$  burial that may have occurred on a more widespread, but rarely preserved, scale in the Neoproterozoic and eventually led to enrichment of sea water sulfate in  $^{34}\text{S}$ . Our calculations, made with reference to a Rayleigh distillation model, imply bacterial reduction of 20-30% of the global sulfate reservoir in order to produce the observed shift. Sulfate reduction on this scale would dramatically affect the burial of organic carbon through anaerobic oxidation, hence releasing abundant  $^{12}\text{C}$  into sea water. This mechanism provides an alternative explanation for the dramatic  $^{12}\text{C}$  enrichment observed in Neoproterozoic marine carbonates, consistent with available stratigraphic correlations.

**OSMIUM ISOTOPIC COMPOSITION OF SULFIDES FROM BASALTIC GLASSES**

**ROY-BARMAN, M., WASSERBURG, G. J. and PAPANASTASSIOU, D. A.**, Div. Geol. Planet. Sci. (170-25), Caltech, Pasadena, CA, 91125 USA

Osmium isotopic composition is a potential tracer of old oceanic crust recycling and thus analysis of  $^{187}\text{Os}/^{186}\text{Os}$  in oceanic basalts should provide a lot of information on mantle processes. Direct measurement of  $^{187}\text{Os}/^{186}\text{Os}$  in MORBs is difficult due to the low osmium content of these rocks (1 - 200 ppt) and the possibility of contamination by sea-water [1]. Taking advantage of the highly chalcophile character of osmium (PGEs are scavenged from the magma by immiscible sulfide globules [2]), Martin et al. have demonstrated the possibility of analysing  $^{187}\text{Os}/^{186}\text{Os}$  on a single large sulfide globule from a MORB [3]. However, such large globules are rare and thus this simple procedure cannot be used for most MORBs. In order to analyse  $^{187}\text{Os}/^{186}\text{Os}$  on a large variety of MORBs, it is necessary to concentrate sulfides from a large amount of sample.

We have set up a procedure for extracting sulfides from up to several hundred grams of basaltic glass. This procedure is based on magnetic and heavy liquid separation. We obtain two sulfide fractions: a coarse grained fraction ( $>40\ \mu\text{m}$ ) which is an almost pure sulfide concentrate and a fine grained fraction ( $<40\ \mu\text{m}$ ) which contains sulfides diluted with olivine + chromite. We have tested this procedure with two osmium rich samples: a MORB from the FAMOUS area (ALV 526-1 also host of Martin's globule) and a lava from Loihi seamount (BENTH 4). Measurements are done by NTIMS. Results are listed below:

ALV 526-1	
fine fraction	$^{187}\text{Os}/^{186}\text{Os} = 1.1009 \pm 0.0014$
coarse fraction	$^{187}\text{Os}/^{186}\text{Os} = 1.0894 \pm 0.0017$
	[Os] sulfide = 445 ppb
BENTH 4	
fine fraction	$^{187}\text{Os}/^{186}\text{Os} = 1.0961 \pm 0.0014$
coarse fraction	$^{187}\text{Os}/^{186}\text{Os} = 1.0956 \pm 0.0018$
	[Os] sulfide = 890 ppb

These results are in good agreement with previously reported data [1,3-4]. Using the Ir concentration [2] as a proxy for Os concentration of sample 526-1, we estimate that osmium recovery is around 40% and that the enrichment factor of Os in the coarse and the fine fraction is 2800 and 6 respectively. This represents a substantial improvement in the analysis of osmium. It will permit the measurement on low concentration lavas with minimal sea-water contamination, very low blank contribution and possibly reduced effect of Re in situ decay. These preliminary results suggest that the sources of MORBs and Loihi are quiet similar in term of  $^{187}\text{Re}$ - $^{187}\text{Os}$  systematics. We are now using this procedure to obtain a series of MORB isotopic composition. Division contribution 5369 (843)

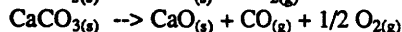
- [1] Roy-Barman et al., 1993, EOS, vol. 74, p 120
- [2] Peach et al., 1990, Geochim. Cosmochim. Acta, vol 54, p. 3379-3389
- [3] Martin et al., 1993, EOS, vol. 74, p 121
- [4] Pegram & Allegre, 1991, Earth Planet. Sci. Lett., vol. 111, p. 59-68

## ISOTOPIC CONTENT OF CO<sub>2</sub> EXTRACTED FROM CARBONATES DURING LASER PYROLYSIS

Romanek, C.S., Socki, R.A., and Gibson, E.K., Jr.,  
SN4 AND LESC, NASA, Johnson Space Center,  
Houston, TX 77058, USA.

Laser-assisted extraction of CO<sub>2</sub> was developed to provide a fast, high resolution, *in-situ* technique for the carbon and oxygen stable isotope analysis of carbonate minerals. This technique compliments established acid digestion procedures but eliminates the problems associated with the physical handling and reaction of micro-gram size samples. Like the acid digestion technique, the isotopic composition of the solid is determined from CO<sub>2(g)</sub> using a correction factor. However, correction factors used in laser-assisted analysis can vary for a given mineralogy. Variability is controlled not only by the flux of energy reaching the target, but also by the intrinsic (i.e., laser-solid coupling) and extrinsic (e.g., crystal defects) character of the solid.

Thick sections of calcite and dolomite were analyzed at an identical spatial resolution using both the acid digestion and laser technique to demonstrate how sampling protocol influences the isotopic composition of laser-generated CO<sub>2</sub>. Continuous wave and high repetition rate Q-switch mode irradiation (low peak power) promote target melting and the formation of a CO<sub>2</sub>-rich gas phase. Low repetition rate Q-switch mode irradiation (high peak power) promotes target sublimation and the production of a gas phase containing CO<sub>2</sub>, CO, and O<sub>2</sub>, which is documented for the first time in laser-generated gas. CO<sub>2</sub> concentration co-varies with repetition rate in Q-switch mode. Gas speciation can be described by a mass-balance mixing of the gaseous products from the two reactions:



which occur in cw and Q-switch mode, respectively. Minor sublimation, which occurs in cw mode, is the result of a transient energy flux which accompanies the initial release of irradiation from the laser.

The isotopic composition of CO<sub>2</sub> increases with the percentage of CO<sub>2</sub> in laser-generated gas. Since modeled equilibrium compositions predict an inverse relationship with CO<sub>2</sub> yield, exchange solely among gaseous phases cannot account for the observed trends. The δ<sup>13</sup>C of CO<sub>2</sub> can be explained by isotopic exchange between CO<sub>2</sub> and recrystallized CaCO<sub>3</sub>. Depleted δ<sup>18</sup>O values, which generally occur at low repetition rates, are probably caused by kinetic effect during short-lived devolatilization events that occur at the target surface. Secular enrichments in <sup>18</sup>O, sometimes observed during sampling in cw and high repetition rate Q-switch modes, are always associated with large volumes of melt. Perhaps secular trends reflect isotopic fractionation by adsorption/desorption reactions occurring on the surface of recrystallized solid by-product during sampling.

## EUROPLUM PUDDING: FLUID AND MELT INFILTRATION INTO THE LITHOSPHERE

ROSENBAUM, J. M., Dept. of Earth Sciences, University of Leeds, Leeds LS2 9JT UK, WILSON, M., Dept. of Earth Sciences, University of Leeds, Leeds LS2 9JT UK, and DOWNES, H., Research School of Geological & Geophysical Sciences, Birkbeck College & University College London, London WC1E 6BT UK.

Widespread Tertiary-Quaternary mafic magmatism in western and central Europe has exhumed abundant spinel lherzolite facies mantle xenoliths which have been used to study the geochemical evolution of the lower part of the lithosphere. Detailed trace element and Sr-Nd-Pb isotopic studies of xenoliths from the Massif Central of France, the Rhenish Massif of Germany and the Pannonian Basin of Hungary, suggest that at least two distinct processes have modified the lithospheric mantle. There is widespread evidence across Europe of silicate melt infiltration from an enriched mantle source region, chemically similar to the source of HIMU ocean-island basalts (OIB), into a depleted mantle protolith. Within the mantle lithosphere beneath the Pannonian Basin there is also evidence of lithospheric enrichment by aqueous fluid infiltration into a rapidly extending back-arc basin tectonic regime, which can be related to Tertiary subduction along the Carpathian arc. The geochemical signature of fluid metasomatism has been partially overprinted by silicate melt infiltration with the same geochemical characteristics to that observed beneath the Massif Central.

Lead isotopes appear to be the most sensitive indicator of the subduction-related flux which has a distinctively enriched <sup>207</sup>Pb signal, with <sup>207</sup>Pb/<sup>204</sup>Pb ratios greater than 15.74 for <sup>206</sup>Pb/<sup>204</sup>Pb ratios less than 18.5. While affecting the Pb isotopic composition of the lithosphere, the subduction fluid does not significantly alter the rare earth element (REE) content of the mantle. The plume-type component, however, affects both the radiogenic isotopic composition and the REE signature of the fluxed lithospheric mantle. Sr, Nd and <sup>206</sup>Pb/<sup>204</sup>Pb isotopic compositions change from those typical of mid-ocean ridge basalt sources to those resembling a HIMU-OIB source. Samples throughout Europe show a correlation between shift in Pb, Sr, and Nd isotopic composition and the degree of light REE enrichment.

Our data suggest that silicate melts, derived from partial melting of HIMU-type mantle plumes rising from the base of the upper mantle, are responsible for extensive modification of the mantle lithosphere across Europe during the Neogene-Quaternary. Based upon radiogenic isotope data, it is probable that the same plume activity is responsible for the mafic alkaline magmatism which exhumed the xenoliths studied. Integration of the geochemical data with geodynamic models for the evolution of the European lithosphere suggest that much of the heterogeneity seen in the mantle beneath Europe today is of recent, rather than ancient origin.

**OSMIUM ISOTOPE AND OTHER PLATINUM GROUP ELEMENT DETERMINATIONS BY LASER ABLATION ICP-MS.**

**RUIZ, J.** and **McCANDLESS, T.E.**,  
Department of Geosciences, University of  
Arizona, Tucson, Arizona 85721, and  
**TURNER, P.J.**, Finnigan MAT, Unit , Asher  
Court, Lyncastle Wa, Appleton, Warrington  
WA4 4ST, England.

Some platinum group elements and their isotopes are notoriously difficult to measure by conventional wet chemical and mass spectrometric methods. In addition by dissolving large amounts of material, important spatial information found at the mineral scale is lost. Laser ablation inductively coupled plasma mass spectrometry (LA-ICP-MS) has been used in samples from the Bushveld Complex in South Africa in order to determine the origin and distribution of the noble metal mineralization in this ultramafic/mafic intrusion. In particular, a question that can best be addressed by LA-ICP-MS is the mobility of the platinum group metals in high temperature hydrothermal fluids. The instrumentation consists of a Finnigan MAT SOLA ICP-MS and Nd:YAG Q-switched laser with frequency quadrupling hardware that allows the original infrared 1064 nm laser to operate in the UV part of the spectrum at 266  $\mu\text{m}$ . The laser was operated at a repetition rate of 5 HZ and 2 mj power per shot. The beam diameter was 25  $\mu\text{m}$ . The coupling of the laser beam with the sample when the laser operates in the UV is greatly superior to that operating at 1064 nm. The pits produced in the samples were smooth and of constant geometry and the sputtering around the crater is reduced. More importantly, matrix effects, on the laser/sample coupling seem to be minimized when the laser is operated in the UV. Thus it seems possible to use glass standards to analyze trace metals in sulfides. The analytical procedure used in this study was to analyze a major element in the sulfide sample by electron microprobe. The quantified element was then used as an internal standard. The results of this work show that Re, Pt, Ir, Rh, and Pd can be measured by La-ICP-MS to better than 7% precision in samples that are 25  $\mu\text{m}$  as long as the concentration of the platinum group element is greater than 100 ppb. Osmium isotopic ratios can be determined to better than 1% precision, based on multiple measurements of the same mineral grain, on samples that have more than 1 ppm Os.

**Sr-ISOTOPE DISEQUILIBRIUM BETWEEN FELDSPAR PHENOCRYSTS AND MELT IN LARGE-VOLUME SILICIC MAGMA SYSTEMS**

**RUIZ, JOAQUIN**, Geosciences, University of  
Arizona, Tucson, AZ 85721 USA, and Duffield,  
W.A., U.S. Geological Survey, Flagstaff, AZ  
86001 USA

Feldspar phenocrysts in many large-volume silicic volcanic deposits are in Sr-isotope disequilibrium with surrounding groundmass, which represents melt from which the crystals were growing just prior to eruption. We model such disequilibrium through contamination of phenocryst-bearing magma by melt derived from adjacent granitic (*sensu lato*) country rock. Essential features of the model are: (1) Incongruent melting of country rock introduces progressively less-radiogenic contaminant into the magma. (2) Diffusion of the country-rock derived Sr is orders of magnitude faster in magma than in feldspar phenocrysts. (3) Eruption quenches contaminated magma before Sr-isotopic equilibrium can be attained between crystals and melt.

The model embodies temporal variations and spatial differences in isotopic disequilibrium conditions for affected magma. For example, in a system with contaminant from country rock more radiogenic than uncontaminated magma, growing feldspar phenocrysts are initially less radiogenic than surrounding magma but eventually become more radiogenic. Thus, depending upon the timing of eruption, a rock may contain feldspar more radiogenic or less radiogenic than surrounding groundmass. If the contamination process continues long enough, a magma body can produce an eruptive unit that varies from one relation to the other with stratigraphic position. The model predicts the shape of isotopic profiles across individual feldspar grains.

**THE YOUNGER DRYAS EVENT: COMPARISON OF HIGH-RESOLUTION ISOTOPE RECORDS FROM GREENLAND AND CENTRAL EUROPE.**

**ROZANSKI, K.**, International Atomic Energy Agency, Vienna, Austria, **GOSLAR, T.**, Radiocarbon Laboratory, Silesian Technical University, Gliwice, Poland, **KUC, T.**, Faculty of Physics and Nuclear Techniques, University of Mining and Metallurgy, Krakow, Poland, **RALSKA-JASIEWICZOWA, M.**, Szafer Institute of Botany, Polish Academy of Sciences, Krakow, Poland, **ARNOLD, M.**, Centre des Faibles Radioactivités, CNRS-CEA, Gif-sur-Yvette, France

A high-resolution record of climate changes in central Europe during the final stages of the last deglaciation, derived from annually laminated sediments of Lake Gosciuz (central Poland), is presented and compared with the ice core data from central Greenland.

The Lake Gosciuz has accumulated in its deepest part around 18.5 meters of sediments covering the Late Glacial and Holocene. The sediment reveals a distinct lamination consisting of couplets of light and dark layers. The light layer is formed by authigenic calcite whereas the dark layer consists mainly of organic detritus and mineral fraction.

The Late Glacial/Holocene transition left a distinct record in the sediments of the lake: the onset and termination of the Younger Dryas (YD) is well marked in the isotope composition of authigenic carbonates as well as in plant and animal microfossil assemblages preserved in the lake sediments (Ralska-Jasiewiczowa et al., 1992). The  $\delta^{18}\text{O}$  variations preserved in lake carbonate reveal an analogous structure to the  $\delta^{18}\text{O}$  profiles available from the GISP 2 and GRIP ice cores drilled in central Greenland (Johnsen et al., 1992; Taylor et al., 1993), showing an abrupt decline of  $^{18}\text{O}$  content at the onset of the YD, lasting about 150 years and an even faster increase at the termination of the YD, completed within approximately 70 years. The characteristic structure of the YD/PB transition, with a very fast rise of  $^{18}\text{O}$  content at the boundary, preceded by a relatively small, but distinct minimum of  $\delta^{18}\text{O}$ , and followed by a brief, temporary drop and further gradual increase of  $\delta^{18}\text{O}$  values is well recognized in all profiles. As in the Greenland profiles, the lowest  $\delta^{18}\text{O}$  values in the Lake Gosciuz are observed in the early part of YD. The annual lamination preserved in the lake sediments allowed us to estimate the duration of the YD in central Europe to be  $1140 \pm 40$  years, in good agreement with the ice core data.

The striking similarity of the  $\delta^{18}\text{O}$  variations in sediment carbonates and that observed in Greenland ice cores confirms the prompt response of climate on the European continent to changes in the North Atlantic region during the last deglaciation.

The AMS radiocarbon dates of terrestrial plant macrofossils from the Late Glacial and the early Holocene part of the sediment fit into the plateau at ca. 10,000 radiocarbon years BP. The difference between radiocarbon and calendar time scales at the AL/YD transition (~11,000 radiocarbon years BP), derived from counting of varves and the AMS radiocarbon dates of plant macrofossils, is between 1150 and 1850 years.

Ralska-Jasiewiczowa, M., Van Geel, B., Goslar, T., and Kuc, T., 1992, The record of the Late Glacial/Holocene transition from the varved sediments of Lake Gosciuz (central Poland). in: Quaternary Stratigraphy, Glacial Morphology and Environmental Changes, Robertson, A.M., Ringberg, B., Miller, U., and Brunnberg, L., (Eds.): Svenska Geologiska Undersokning, v. C81, p. 257-268.

Johnsen et al., 1992, Irregular glacial interstadials recorded in a new Greenland ice core: Nature, v. 359, p. 311-313.

Taylor et al., 1993, The "flickering switch" of late Pleistocene climate change: Nature, v. 361, p. 432-436.

**INCORPORATION AND LOSS OF ARGON IN PHENGITES: A  $^{40}\text{Ar}/^{39}\text{Ar}$  LASER PROBE STUDY OF THE EFFECT OF THE BIELLA INTRUSION IN THE "ECLOGITIC MICASCHISTS UNIT" OF THE SESIA ZONE (WESTERN ALPS).**

**RUFFET, G.**, **FERAUD, G.**, Laboratoire de Géodynamique, URA CNRS 1279, Université de Nice-Sophia Antipolis, 06108 NICE cedex 2, France, **BALLÈVRE, M.**, Laboratoire de Tectonique, UPR CNRS 4661, Université de Rennes I, 35042 Rennes cedex, France and **AMOURIC, M.**, CRMC2 CNRS, Université Marseille, 13288 Marseille Cedex 9, France.

In an attempt to clarify the role of the temperature in the isotopic redistribution process of argon in metamorphic minerals, some peculiar results were obtained from the  $^{40}\text{Ar}/^{39}\text{Ar}$  laser probe analysis of single grains of phengites. The studied rocks were sampled in the "eclogitic micaschists unit" (EMU) of the Sesia zone (Western Alps), in the contact aureole of the Oligocene Biella syenite. Our aim was to compare the results obtained on single grains of phengites at increasing distances from the intrusion.

Strong disturbances of the isotopic distribution of argon in the phengites were observed up to more than 3km from the contact with the 8km diameter pluton. Single grains of phengites within the "contact aureole" displayed age spectra which show high apparent ages in the low temperature steps followed by a decrease down to a minimum age and an increase until reaching a flat age shape. The magnitude of the age spectra disturbances decreases regularly according to the distance to the pluton. This allow to distinguish two distinct subcontemporaneous diffusion phenomena. The first one is thermally activated and generates a total or partial radiogenic argon loss depending on the distance to the pluton. The second one could be linked to a fluid circulation process and wave of argon or argonami [1] which causes the incorporation of an excess argon component. We discuss the parameters (fluid circulation, age of the EMU, existence of several populations of phengite) as a function of the time after intrusion and the distance to the pluton to explain the observed shapes and the mechanism of excess argon incorporation.

York, D., 1993, The Discovery and Significance of a Fossilized Radiogenic Argon Wave (Argonami) in the Earth's Crust: Geophys. Res. Lett, v.20, p. 61-64..

DIRECT Pb/Pb AGE DETERMINATION OF  
PROTEROZOIC STROMATOLITES FROM THE  
ASHBURTON AND NABBERU BASINS, WESTERN  
AUSTRALIA

RUSSELL, J., Shell Research, P.O. Box 60, 2280 AB  
Rijswijk, The Netherlands, GREY, K., Geological Survey of  
Western Australia, East Perth, Western Australia 6004,  
Australia, WHITEHOUSE, M., Dept. of Earth Sciences,  
Oxford University, Oxford OX1 3PR, U.K., and  
MOORBATH, S., Dept. of Earth Sciences, Oxford  
University, Oxford OX1 3PR, U.K.

A series of Proterozoic stromatolitic carbonates has been analysed from the Ashburton and Nabberu Basins, Western Australia. Samples of *Pilbaria perplexa* (GSWA 88032) and *Asperia ashburtonia* (GSWA 46207) from the Duck Creek Dolomite of the Wyloo Group, Ashburton Basin have an inferred age of between 2.2-1.6 Ga. Nine analyses of GSWA 88032 define a Pb/Pb errorchron date of  $1717 \pm 64$  Ma and nine analyses of GSWA 46207 an isochron date of  $1741 \pm 53$  Ma. The results are in statistical agreement and indicate that the date of c.1.73 Ga is geologically significant. Petrographic evidence for carbonate recrystallisation and disruption of primary stromatolitic fabrics is interpreted as the age of diagenetic recrystallisation, possibly related to fluid activity from the greenschist facies metamorphism that can be seen to affect rocks in the vicinity.

Samples of *Yandilla meekatharrensis* (GSWA 46589) and *Pilbaria deverella* (GSWA 84767) were analysed from the Yelma Formation of the Earraheedy Group in the Nabberu Basin which has an inferred age of between 1.8-1.6 Ga. Sixteen analyses of GSWA 46589 define an errorchron date of  $2008 \pm 68$  Ma and six analyses of GSWA 84767 a concordant errorchron date of  $1946 \pm 71$  Ma. Both are significantly older than the inferred depositional age from independent data. However, evidence to support a depositional/early diagenetic age of c.2.0 Ga exists in that, (1) no similar stromatolitic taxa are found anywhere in the world in rocks younger than 1.8 Ga; (2) microfossils from the Earraheedy Group carbonates show a distinct similarity with those from the 2.0 Ga Gunflint Chert of Canada; (3) petrographic observations do not suggest extensive disruptive recrystallisation of original sedimentary fabrics; and (4) stromatolites from the underlying Glengarry Group yield an older Pb/Pb isochron date of  $2258 \pm 180$  Ma. It is concluded that sediments of the Earraheedy Group were deposited around 2.0 Ga.

Other stromatolites, however, while demonstrating excellent preservation of primary sedimentary fabrics, have failed to produce meaningful radiometric results. This may result from a failure to homogenise Pb isotopic ratios at re-crystallisation, from particularly limited variation in U/Pb ratios or subsequent disturbance of closed system conditions.

AN ATTEMPT TO DETECT POSSIBLE  
VARIATION OF ISOTOPIC COMPOSITION  
OF ZIRCONIUM IN NATURE

S. K. Sahoo and A. Masuda,  
Department of Chemistry,  
University of Electro-communications,  
Chofu, Tokyo-182, Japan

Zirconium involves five stable nuclides: These nuclides can be subject to slight variations in abundances due to a few nuclear effects. A relatively long half-life of EC decay of  $^{91}\text{Nb}$   $1.3 \times 10^8$  y or  $3.3 \times 10^7$  y leads us to an expectation of  $^{92}\text{Zr}$  variation. The variation observed by Minster and Allegre are marginal on account of empirical errors[1]. The half-life of  $^{91}\text{Nb}$  remained ambiguously "long" until recently, but a recent information indicates a "short" half-life,  $7 \times 10^2$  y. Considering N being a magic number 50, this half-life seems to be too short, being open to further examination. That is, it may be premature to rule out the potentiality of isotopic abundance variation of  $^{91}\text{Zr}$  resulting from EC of  $^{91}\text{Nb}$ . As regards  $^{96}\text{Zr}$ , there can be a possible variation related with the primordial spontaneous fission of  $^{244}\text{Pu}$  ( $T_{1/2} = 8.1 \times 10^7$  y). (Besides, it may merit a note that  $^{96}\text{Zr}$  is a rapid process nuclide.) As a special phenomenon, it does not escape our notice that  $^{92}\text{Zr}$  can be produced by double EC of  $^{92}\text{Mo}$  in molybdenite.

Except the last effect, our main purpose is to re-examine precisely the isotopic abundance ratios of Zr especially in relation with the effects of extinct nuclides. Our data are obtained for different sources of chemical reagents based on  $\text{Zr}^+$  ion generated by a triple filament ion source. These data are scrutinized in theoretical view of mass fractionation and are compared with those published by other researchers [1,2].

1. Minster, J.F., and Allegre, C.J., 1982, *Geochim. Cosmochim. Acta*, **46**, 565-573.
2. Nomura, M., Kogure, K. and Okamoto, M., 1983, *Int. J. Mass Spec. Ion Phys.*, **50**, 219-227.

K-AR AGE STUDIES ON SEVERAL  
PLUTONIC BODIES IN THE SOUTH  
FOSSA MAGNA ARC-ARC COLLISION  
ZONE, CENTRAL JAPAN

SAITO, K., SUGI, S., KATO, K.  
and OTOMO, I., Dept. Earth  
Sci., Yamagata University,  
Yamagata, Japan, 990

The South Fossa Magna region is tectonically unique of its arc-arc collisional feature. The Izu peninsula, which is located at the northern edge of the Philippine plate, is just colliding to the Honshu (the main island of Japan) arc. Many geoscientists have discussed that this area experienced multiple arc-arc collisions. The Tanzawa and Misaka blocks are candidates of such exotic terrains.

Several plutonic bodies exist in this area. The Kofu plutonic complex is the largest plutonic body in the area. Samples from the southern part of the complex (Ashigawa body) give well defined hornblende K-Ar age of 11 Ma. The southern part of the Tokuwa body, distributed to the north of the Ashigawa body, shows a systematic age decrease from south (12 Ma) to north (9 Ma). The Mizugaki-Shosenkyo body, which is located in the northwestern part of the complex, shows a similar systematic decrease in ages from north (15 Ma) to south (11 Ma). The Tanzawa tonalitic body yields hornblende K-Ar ages from 7 Ma (the northwestern part) to 5 Ma (the southeastern part). We dated both biotite and hornblende for several specimens. Some of them yielded older ages for biotite, but most of them showed insignificant age differences between these minerals.

These data suggest that the plutonic bodies in the area experienced considerably rapid cooling, but the spatial distribution of temperature in them were not uniform in the course of the cooling.

CONSTRAINTS ON THE MORB MELTING REGIME  
BASED ON THE LU-HF, SM-ND AND U-TH  
SYSTEMATICS

SALTERS, VINCENT J.M., BOURDON, B. and ELLIOTT,  
T.E. Lamont-Doherty Earth Observatory, Palisades, NY  
10964, USA..

Lu-Hf and Sm-Nd isotope systematics place the onset for MORB melting in the garnet field and are indicators for degree and depth of melting. In addition, recent results on U-Th partitioning indicates Th-disequilibria are also explained by placing the onset of melting in the garnet stability field. And, thirdly, Klein and Langmuir (1989) have shown that the normalized major element content of MORB also reveal information about the degree and the depth of melting. Especially Nag and Feg are important indicators whereby Nag is an indicator for the degree of melting and Feg is an indicator for the average depth of melting. We have taken the constraints derived from the  $^{176}\text{Hf}/^{177}\text{Hf}$ ,  $^{143}\text{Nd}/^{144}\text{Nd}$  and ( $^{230}\text{Th}/^{232}\text{Th}$ ) systematics one step further and combined the constraints derived from the isotope systematics with those derived from major elements.

Two Atlantic Ridge segments with a clear 'local' trend also show positive correlations with both Feg and Nag and the isotope melting parameters,  $\delta(\text{Sm}/\text{Nd})$  and  $\delta(\text{Lu}/\text{Hf})$ , indicating that the smaller degree of melting, the more melting takes place in the garnet stability field. This is consistent with previous explanations of incomplete mixing of the different melting columns in a triangular shaped melting regime, and the tapping of melts from different of-axis melting columns.

Klein and Langmuir (1989) interpreted the 'global' trend and its correlation with ridge depth as follows: the deep ridge segments have high Nag and low Feg indicating a low degree of relatively low pressure melting, while the shallow ridges represent a large degree of melting and a high average pressure during melting. The Mid-Cayman Rise is one of the deepest parts of the ocean, but MCR basalts have among the highest  $\delta(\text{Sm}/\text{Nd})$  and  $\delta(\text{Lu}/\text{Hf})$  indicating they represent small degrees of relatively high pressure melts. Based on the presently available data the isotopic systematics for the 'global' trend can be interpreted several ways: 1) the deeper the melting regime the less efficiently melts can be collected at the ridge and thus the lower  $\delta(\text{Sm}/\text{Nd})$  and  $\delta(\text{Lu}/\text{Hf})$ , or 2) the onset of melting for all ridges is similar, however, the depth of termination of melting varies, or 3) a significantly older isotopic reservoir for the MCR basalts compared to other MORB.

Further  $^{176}\text{Hf}/^{177}\text{Hf}$  and  $^{143}\text{Nd}/^{144}\text{Nd}$  analyses of deep ridge (American-Antarctic Discordance) and shallow ridge (Kolbeinsy) MORB combined with U-Th systematics will be presented.

PHANEROZOIC CRUSTAL GROWTH: THE IMPORTANCE OF JUVENILE TERRANES IN THE APPALACHIAN AND CORDILLERAN OROGENS

SAMSON, SCOTT D., Dept. of Earth Sciences, Syracuse University, Syracuse, NY 13244-1070

Many crustal growth models show that the last ~1 Ga of Earth history was an interval of very slow crustal generation. The concept of insignificant crustal growth during Phanerozoic time has largely been based on isotopic studies of European orogenic belts and of the Himalayas. Nd isotopic studies of the Cordillera, however, have shown that much of that orogen is composed of juvenile continental crust. The Cordillera, formed by the accretion of tectonostratigraphic terranes, is therefore a major site of new crust generated during Phanerozoic time.

The terrane concept has also been applied to the Appalachian orogen and it now appears that accretionary events within the Appalachians are similar to those that formed the Cordillera. However, because the Appalachians are often considered to be an extension of the Caledonides and the Hercynides, and the crust in those orogens is composed predominantly of recycled material, it is often assumed that the Appalachians do not represent any significant contribution of new crust. New isotopic studies in the Appalachians, however, demonstrate that this view is incorrect and that there are significant regions of juvenile crust in that orogen. For instance, the largest southern Appalachian terrane, the Carolina terrane, has felsic igneous rocks with initial  $\epsilon_{Nd}$  values ranging from +1 to +6. Positive  $\epsilon_{Nd}$  values have also been reported from the nearby Kings Mountain belt demonstrating that this crustal region is also juvenile. Granitic plutons of Pennsylvanian-Permian age, generated during the Alleghanian (Hercynian) orogeny, also document the presence of juvenile Appalachian crust. The range in initial  $\epsilon_{Nd}$  is from -8 to +3, but the vast majority of the Alleghanian plutons have values between -2 and +2 indicating that a significant amount of juvenile material must have been involved in their petrogenesis.

Mantle-derived crust also is present in the northern Appalachians. The Avalon terrane of Canada clearly contains a high percentage of juvenile crust as most  $\epsilon_{Nd}$  values are between +1 and +5. Recycled crust is also present, however, since zircons from some late Proterozoic rocks have Archean and early Proterozoic components. Volcanic and plutonic rocks of Ordovician age from the Bronson Hill Anticlinorium, central Massachusetts, are similar to those in Avalon; initial  $\epsilon_{Nd}$  values of +5 have been measured, although most samples have  $\epsilon_{Nd}$  closer to zero. Unevolved crust is therefore an important part of this Appalachian terrane as well.

Similar accretionary processes were responsible for the construction of the Appalachians and the Cordillera and both orogens are important sites of new continental crust. The formation, amalgamation and accretion of chemically evolved but isotopically juvenile terranes are thus fundamental processes of crustal growth. The isotopic results from these two major orogens show that crustal growth during Phanerozoic time is thus more important than has been previously recognized.

THE FIRST FISSION TRACK RESULTS OF THE TRANSYLVANIAN BASIN-CARPATHIAN MOUNTAIN BELT SYSTEM IN ROMANIA.

SANDERS, C.A.E and P.A.M. Andriessen.

Vrije Universiteit, Institute for Earth Sciences, Dept. of Petrology and Isotope Geology, De Boelelaan 1085, 1081 HV Amsterdam, tel 020-5483521, fax 020-6462457.

Recently an increasing amount of investigations of a variety of geological disciplines are concentrated on the Carpathian-Pannonian system in Central-Southeastern Europe.

It resulted in the understanding that discrete regional tectonic blocks in the internal part of the mountain belt have undergone different histories during the early stage of Alpine convergence.

These microplates, separated by oceanic crust during the Mesozoic, were assembled to a coherent unit in the Tertiary. Ongoing Alpine collision caused internal fragmentation and formation of various extensional basins coeval with compression in the outer Carpathians. The Tertiary event has been explained as an example of "escape tectonics" as a consequence of large scale Alpine contraction between the European plate and the African plate.

Especially this last phase is suitable to study with the Fission Track method, because the apatite FT analyses record the last low temperature stage of the thermal history.

We focus on the relation between thrusting and uplift in the outer Eastern Carpathians, subsidence in the Transylvanian Basin and tectonics in the more internal located Apuseni Mountains. FT results of volcanics, sediments and basement rock allow quantitative constraints on the amount of uplift, erosion, denudation, subsidence and sedimentation. Different thermal histories of various parts of the mountain belt are compared to each other.

These fission track data are the first data presented on this part of the Alpine orocline. Due to the quantitative character, constraints can be put on the tectonic modelling of the dynamics of this region.

## MAGMATIC CARBON FLUX FROM SUBDUCTION ZONE

SANO, Y., Department of Earth and Planetary  
Science, Hiroshima University, Higashi  
Hiroshima 724, Japan and Williams, S.N.,  
Department of Geology, Arizona State  
University, Tempe AZ 85287-1404, U.S.A.

Carbon dioxide has been discharging naturally from the Earth's mantle to the atmosphere through volcanic and hydrothermal activity for long periods of geological time. The magmatic carbon flux at mid-ocean ridge has been assessed by spreading rate of oceanic plate and carbon content or mantle  $^3\text{He}$  flux and  $\text{CO}_2/^3\text{He}$  ratio in mid-ocean ridge basalt (MORB) glasses, while degassing rate at convergent plate margins is not well documented. We present here magmatic carbon flux from subduction zone based on reported  $^3\text{He}$  flux and observed  $\text{CO}_2/^3\text{He}$  ratios of circum Pacific volcanic gases.

We have collected 14 volcanic gases from Japan, Papua New Guinea, Central and South America and measured helium and carbon isotopes and  $\text{CO}_2/^4\text{He}$  ratios. Corrected  $^3\text{He}/^4\text{He}$  ratios for atmospheric contamination vary from 4.2  $R_{\text{atm}}$  (where atmospheric  $^3\text{He}/^4\text{He}$  ratio is  $1.39 \times 10^{-6}$ ) to 8.4  $R_{\text{atm}}$ , agree well with those reported for circum Pacific volcanic gases. Observed  $\delta^{13}\text{C}$  values range from -9.5‰ to -2.6‰, are again consistent with those reported for magmatic carbon. The  $\text{CO}_2/^3\text{He}$  ratios are from  $6.6 \times 10^9$  to  $3.3 \times 10^{10}$ . Taking reported  $\text{CO}_2/^3\text{He}$  ratios for volcanic gases from New Zealand and North America, average of the ratios in circum Pacific volcanic zone is about  $2 \times 10^{10}$ .

Volcanic carbon flux of about  $3 \times 10^{12}$  mol/year is estimated for subduction zone by the  $^3\text{He}$  flux in literature and the  $\text{CO}_2/^3\text{He}$  ratio obtained in this work. This flux is larger than carbon flux of  $1.5 \times 10^{12}$  mol/year from mid-ocean ridge and may contribute significantly to natural global carbon cycle.

## THE OXYGEN AND CARBON ISOTOPIC COMPOSITIONS OF CARBONATITES

SANTOS<sup>1,2</sup>, Roberto V.; CLAYTON<sup>1</sup>, Robert N.; Univ.  
of Chicago, Dep. of Geoph. Sci<sup>1</sup>; Chicago, IL 60637, USA;  
Univ. Federal de Ouro Preto, Dep. de Geologia<sup>2</sup>, Ouro  
Preto-MG, 35400, Brazil.

We present an oxygen and carbon isotopic study of carbonatite and metasomatic rocks from South America alkaline complexes and discuss whether the observed isotopic variations are due to mantle heterogeneity or processes related to the evolution of the alkaline magma. The complexes of Jacupiranga, Araxá, Catalão, Tapira, and Mato Preto surround the Paraná Basin and were emplaced during the Wealdenian Reactivation of the South American Platform (between the Jurassic and the Eocene). Carbonatites usually comprise only a minor part of these complexes and occur as plugs, dikes, or veins intruding the alkaline silicate rocks.

Table I summarizes the results of this study and shows that except for the samples from Mato Preto, which seem to have been contaminated by limestone from the country rock, the samples from Jacupiranga, Araxá, Catalão and Tapira have similar  $\delta^{13}\text{C}$  values. The samples from Araxá, Catalão and Tapira also have a wide range in oxygen isotopic composition, which may be related to their degree of hydrothermal alteration and erosion level. For instance, while the carbonatites from Jacupiranga have a narrow range of  $\delta^{18}\text{O}$  and have not been extensively affected by fenitization, the carbonatites from Araxá, Catalão and Tapira have a wide range in  $\delta^{18}\text{O}$  and are accompanied by pervasive potash-fenitization of their host rock.

The variations of oxygen and carbon isotopes in the carbonatites may be explained by three different kind of processes: (a) magmatic processes; (b) crustal contamination; and (c) fluid-related processes. We show that most of the variations of  $\delta^{18}\text{O}$  and  $\delta^{13}\text{C}$  in carbonatites may be related to low temperature processes (i.e. below 400 °C), and may be explained by isotope exchange between  $\text{H}_2\text{O}-\text{CO}_2$  fluids and the carbonatites. We conclude that the absence of carbon isotopic differences among the complexes studied here suggests that there is no significant difference in the carbon isotopic composition of their mantle source regions. However, because carbonatites are derived from large volumes of the mantle, this conclusion does not preclude the existence small-scale heterogeneity in subcontinental mantle, such as those observed in diamonds and mantle xenoliths.

Table I: Isotopic composition of the analyzed samples.

	$\delta^{18}\text{O}$ (‰)	$\delta^{13}\text{C}$ (‰)
Mato Preto	9.1 to 13.8	-6.9 to 0
Jacupiranga	6.6 to 7.3	-6.6 to -6.2
Araxá	8.7 to 16.3	-7.2 to -4.8
Catalão	7.9 to 19.3	-7.1 to -5.3
Tapira	9.7 to 15.4	-8.6 to -4.8

## TEMPORAL VARIATIONS IN LEAD CONCENTRATIONS AND ISOTOPIC COMPOSITION IN THE SOUTHERN CALIFORNIA BIGHT

SAÑUDO-WILHELMY, S.A., Marine Sciences Research Center, State University of New York, Stony Brook, New York 11794-5000, USA, and FLEGAL, A.R., Earth Science, WIGS, University of California, Santa Cruz, California, 95064, USA.

Lead concentrations in surface waters of the Southern California Bight appear to have decreased three-fold (from  $> 170$  to  $< 60$  pM) since the 1970s. The decreased parallels a three-fold decline in anthropogenic inputs of industrial lead to the Bight over the past two decades. Moreover, mass balance calculations indicate that the primary source of lead to the Bight now is upwelling. This is evidenced by the lead isotopic compositions of surface waters in the Bight, which are most characteristics of Asian industrial lead aerosols ( $0.4793 \leq {}^{206}\text{Pb}/{}^{208}\text{Pb} \leq 0.4833$ ) deposited in oceanic waters of the North Pacific. While the decreased in surface water lead concentrations in the Bight reflects the reduction in industrial lead emissions from the United States, the isotopic compositions of surface waters in the southern reach of the Bight reflect a concurrent increase in industrial lead emissions from Mexico ( $0.4852 \leq {}^{206}\text{Pb}/{}^{208}\text{Pb} \leq 0.4877$ ). The isotopic composition ( ${}^{208}\text{Pb}/{}^{207}\text{Pb} \approx 2.427$ ) of elevated lead concentrations of surface waters in San Diego Bay indicate that lead is remobilized from contaminated sediments within that bay.

pH-ESTIMATION OF GLACIAL OCEANS BASED ON BORON ISOTOPIC COMPOSITION OF FORAMINIFERA  
SANYAL, A.<sup>1</sup>, HEMMING, N.G.<sup>2</sup>, HANSON, G.N.<sup>2</sup> and BROECKER, W.S.<sup>1</sup>

<sup>1</sup> Lamont Doherty Earth Observatory, Palisades, NY-10964, USA.

<sup>2</sup> Dept. of Earth and Space Sciences, State University of New York at Stony Brook, Stony Brook, NY 11794-2100, USA.

The boron isotopic composition of foraminifera has been suggested as a recorder of ocean pH. The relative abundances of the two dominant aqueous boron species in seawater,  $\text{B}(\text{OH})_3$  and  $\text{B}(\text{OH})_4^-$ , is dependent on pH. Isotopic fractionation between these two species enriches  $\text{B}(\text{OH})_3$  in the heavier isotope of boron. Therefore the boron isotopic composition of each species is pH dependent. Based on previous studies an assumption can be made that  $\text{B}(\text{OH})_4^-$  is the only species being incorporated into the carbonate phase with the result that carbonate shell material has the same boron isotopic composition as the aqueous  $\text{B}(\text{OH})_4^-$  species. Hence the boron isotopic composition of the shell material could be used as a pH indicator for the fluid in which it grew.

Boron isotopic compositions of planktonic foraminifera (*Globogerinoides sacculifer*) and of benthic foraminifera (mixed species) were analyzed to estimate the pH of surface and deep water respectively. Modern planktonic samples have an isotopic composition approximately 2‰ heavier than that of benthic samples. This is consistent with the difference in pH between the surface and deep waters at the sampling sites as calculated by GEOSECS. Hence the foraminifera appear to be recording the pH conditions where they grew. The uncertainty in the estimation of pH corresponding to the uncertainty in the analysis of boron isotopic ratio of foraminifera is about 0.1 pH units in the pH range of interest.

The boron isotopic compositions of glacial benthic and planktonic samples from both Atlantic and Pacific oceans have been analyzed. The boron isotopic compositions of glacial planktonics from both equatorial Atlantic and equatorial Pacific oceans are similar and consistent with an increase in pH of 0.2 - 0.3 pH units for glacial surface waters compared to modern surface waters. This pH is consistent with a decrease in  $\text{pCO}_2$  of surface water by 80-90  $\mu\text{atm}$  and an increase in alkalinity of the surface ocean by about 3%. The boron isotopic compositions of glacial benthic forams from both equatorial Atlantic and equatorial Pacific oceans are also similar and suggest that the pH of glacial deep oceans were about 0.3pH units higher than that of the respective modern deep oceans. This is in contrast to pH changes estimated from lysocline changes (between modern and last glacial periods) which suggest no change or a slight decrease in pH for the Atlantic and an increase of only about 0.05 pH units for the deep Pacific. Such an increase in pH of deep water (as suggested by boron isotopic composition of benthic foraminifera) without a significant change in lysocline depth could be explained by a decrease in the calcite to organic carbon rain rate ratio during glacial period compared to that during modern period (Archer and Maier-Reimer, 1994).

Archer, D. and Maier-Reimer, E., 1994, Nature (in press)

## RARE GAS SYSTEMATICS IN MANTLE MATERIALS

Philippe Sarda, Thomas Staudacher, and Claude J. Allègre,

Laboratoire de Géochimie, Institut de Physique du Globe, 4 place Jussieu, 75252 Paris Cedex 05, France.

We have continued to measure isotopic composition and concentrations of all the rare gases in glassy margins and olivines from oceanic basalts. We obtained high  $^{40}\text{Ar}/^{36}\text{Ar}$  of more than 28,000 in MORB basalts both by stepwise heating and crushing under vacuum. These high ratios coincide with low  $^{87}\text{Sr}/^{86}\text{Sr}$ . In contrast, the oceanic islands, including Loihi seamount, Rocard and McDonald, have  $^{40}\text{Ar}/^{36}\text{Ar}$  ratios generally (but not always) lower than 350.

The high  $^{40}\text{Ar}/^{36}\text{Ar}$  ratios in MORB coincide with high  $^{20}\text{Ne}/^{22}\text{Ne}$ ,  $^{21}\text{Ne}/^{22}\text{Ne}$ ,  $^{129}\text{Xe}/^{130}\text{Xe}$  and  $^{134}\text{Xe}/^{130}\text{Xe}$  ratios, and, in a less systematic way, with high  $^4\text{He}/^3\text{He}$  ratios of  $\approx 86,000$ . Oceanic Islands glasses have shown atmospheric  $^{129}\text{Xe}/^{130}\text{Xe}$  and  $^{134}\text{Xe}/^{130}\text{Xe}$ . Correlations for MORB in (Ar, Xe) or (Xe, Xe) diagrams indicate mixing. One end member is radiogenic, the other is close to atmospheric. The situation is less clear for Ne in this respect.  $^{20}\text{Ne}$  excesses do correlate with  $^{40}\text{Ar}$ , so that we tend to attribute them to the same radiogenic end member, the other end member of the neon mixing line being atmospheric.

We have developed several models with common structure and different assumptions. The common structure is a two layered mantle, one upper layer, strongly outgassed, and one lower mantle, less outgassed (but probably 60 to 70%). This point differs from our original model. The two different assumptions are:

1) Loihi data are representative of the lower mantle,

2) Loihi data are polluted by atmospheric gases (in situ or reinjection).

Both assumptions are discussed quantitatively, with results which are not too different qualitatively.

## EXCESS $^{129}\text{Xe}$ AND RELATIVELY LOW $^{40}\text{Ar}/^{36}\text{Ar}$ RATIOS IN CARBONATITES FROM CANADA AND BRAZIL

SASADA, T. and HIYAGON, H., Dept. of Earth and Planetary Physics, Univ. of Tokyo, Tokyo, 113, Japan, WADA, H., Inst. of Geosciences, Shizuoka Univ., Shizuoka, 422, Japan and EBIHARA, M., Dept. of Chemistry, Tokyo Metropolitan Univ., Tokyo, 192-03, Japan

Isotopic compositions of all noble gases (He, Ne, Ar, Kr, Xe) in one Brazilian carbonatite from Jacupiranga (130Ma), three Canadian carbonatites from Oka (110Ma), Prairie Lake (1030Ma) and Borden Lake (1870Ma) and one Canadian syenite from Poohbah Lake (2700Ma) were analyzed with a sector-type mass spectrometer VG5400. We separated forsterite, diopside and apatite from the samples and extracted noble gases by stepwise heating. We also measured the concentration of potassium by RNAA method.

Primordial He ( $^3\text{He}/^4\text{He}=2.74 \times 10^{-6}$ ,  $3.52 \times 10^{-6}$ ) and anomalous Ne ( $^{20}\text{Ne}/^{22}\text{Ne}=0.01-10$ ,  $^{21}\text{Ne}/^{22}\text{Ne}=0.031-0.097$ ) were observed. The  $^{40}\text{Ar}/^{36}\text{Ar}$  ratios varied from nearly the atmospheric ratio to 42420. However, apatite samples from carbonatites showed the identical  $^{40}\text{Ar}/^{36}\text{Ar}$  ratio of about 6200 at the highest temperature fractions. At the same fractions, we found the excesses in  $^{131}-^{136}\text{Xe}$  and  $^{129}\text{Xe}$ . The excess  $^{131}-^{136}\text{Xe}$  are thought to be of  $^{238}\text{U}$ -fissiogenic Xe. The  $^{129}\text{Xe}/^{130}\text{Xe}$  ratios observed in Jacupiranga and Borden Lake samples were 7.31 and 7.36, respectively, which are similar to the value observed in MORB samples. Prairie Lake sample shows a higher ratio (8.6). However, it is probably originated from  $^{238}\text{U}$ -fissiogenic  $^{129}\text{I}$  judging from very high excesses in  $^{131}-^{136}\text{Xe}$  ( $^{136}\text{Xe}/^{130}\text{Xe}=1400$ ).

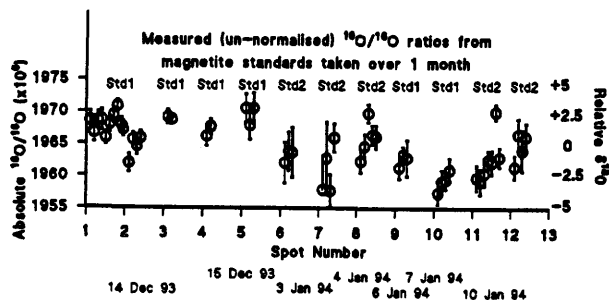
The  $^{40}\text{Ar}/^{36}\text{Ar}$  ratios of carbonatites (6200) are lower than that of MORBs (>28000). High  $^{129}\text{Xe}$  excess and relatively low  $^{40}\text{Ar}/^{36}\text{Ar}$  ratios of carbonatites suggest that the source of carbonatites is different from that of MORBs. The excess  $^{129}\text{Xe}$  also suggests that volatiles of carbonatites are juvenile.

HIGH PRECISION MEASUREMENTS OF  $^{18}\text{O}/^{16}\text{O}$  AND  $^{17}\text{O}/^{16}\text{O}$  OBTAINED FROM GEOLOGICAL AND EXTRA-TERRESTRIAL MATERIALS USING AN ISOLAB 54 ION MICROPROBE.

Saxton, J.M., Lyon I.C. and Turner, G., Department of Geology, The University of Manchester, Manchester, M13 9PL, United Kingdom.

Mass fractionation during ion probe measurements of oxygen isotope ratios at high mass resolution can arise from a mass dependent angular and energy distribution of the secondary ions. We have sought to reduce this effect by sweeping the secondary beam at high frequency (2.5kHz) across the source slit using a saw tooth wave form and integrating the total beam for each isotope. A new detector type which uses a conversion dynode in front of a channeltron (CDS detector) has also been developed. Oxygen isotopes are detected by a multicollector using a Faraday detector for  $^{16}\text{O}$ , and CDS detectors with 2000 mass resolving power for  $^{18}\text{O}$  and 6000 mass resolving power for  $^{17}\text{O}$ . The CDS detectors have proved to offer extremely high gain stability. Figure 1 shows raw  $^{18}\text{O}/^{16}\text{O}$  ratios obtained on polished sections of magnetite grains (LP204, courtesy of Dr J Valley) over a period of a month when the beam integration procedure was in operation. The ratios plotted have not been normalised relative to each other and exhibit a standard deviation (all points) of  $\sigma=1.5\text{‰}$ , the average within day reproducibility is  $\sigma=1\text{‰}$  or better. The reproducibility for  $^{17}\text{O}$  is intrinsically worse than  $^{18}\text{O}/^{16}\text{O}$  because of the low natural abundance of  $^{17}\text{O}$  and has varied between 3–4.6‰ during a day. We have performed  $^{18}\text{O}/^{16}\text{O}$  and  $^{17}\text{O}/^{16}\text{O}$  measurements on small clusters of micron sized magnetite grains from the Orgueil CI and Y82162 (CM1) meteorites. Results for Orgueil show a mean  $\delta^{18}\text{O}$  ( $-1\text{‰}$ ) and  $\delta^{17}\text{O}$  ( $+3\text{‰}$ ) which lie close to the terrestrial fractionation line but exhibit a real spread ( $\delta^{18}\text{O} = -6\text{‰}$  to  $+5\text{‰}$ ). We have also undertaken work on olivine standards from the Brenham pallesite which exhibit a similar reproducibility  $^{18}\text{O}/^{16}\text{O}$ .

Figure 1



MULTI-EPISODIC LATE OROGENIC VOLCANISM AND PLUTONISM IN THE VARISCAN FOLD BELT OF CENTRAL EUROPE

SCHALTEGGER, U. and CORFU, F., Dept. of Geology, Royal Ontario Museum, 100 Queen's Park, Toronto, Ont. M5S 2C6 Canada

The end of the Variscan orogeny in Central Europe is marked by the transition from compressive to strike-slip tectonics, causing the formation of numerous elongated pull-apart basins. They were filled with clastic sediments and volcanic rocks of upper Carboniferous age and were subsequently intruded by granitoid melts.

In the Aar massif, one of the pre-Mesozoic basement windows of the Central Alps, late Variscan magmatic rocks were emplaced during three distinct magma pulses at 334, 310 and 298 Ma, respectively. Two Carboniferous volcano-sedimentary sequences can be distinguished in the same area: (I) an older series, which was strongly deformed and metamorphosed in upper greenschist facies during a late Variscan event, is intruded by a 334±2 Ma old granite. These rocks are unconformably overlain by a younger series (II), consisting of estuarine to lacustrine sediments, conglomerates, ignimbrites and tuffs. The younger sequence only shows weak deformation. It was deposited at 299±2 Ma and was subsequently intruded by microgranites and granites, whose U-Pb age is identical within analytical uncertainty to that of the volcanic rocks.

The group I volcano-sedimentary sequence of the Aar massif may be coeval with volcanic and clastic sedimentary rocks in the southern Vosges area (Schneider, 1990). Zircon U-Pb ages of rhyolites from the bottom and the top of the Viséan stratigraphic sequence indicate that the deposition occurred within a short time-span between 345±1 Ma and ca. 342 Ma. Late volcanic activity at around 335 Ma covered the area with ignimbrites.

The zircons of volcanic rocks from both the Aar massif and the southern Vosges show abundant zircon inheritance of Late Proterozoic age indicating contamination or even derivation from crustal sources, in contrast to the coeval granites that exhibit distinct mantle affinities. The latter melts are interpreted to be derived from an enriched subcontinental mantle source and underwent various degrees of crustal contamination (Schaltegger and Corfu, 1992).

Schaltegger, U. and Corfu, F., 1992, The age and source of late Hercynian magmatism in the central Alps: evidence from precise U-Pb ages and initial Hf isotopes. *Contrib. Mineral. Petrol.* 111: 329-344

Schneider, J.L., 1990, Enregistrement de la dynamique varisque dans les bassins volcano-sédimentaires devonodiniens: exemple des Vosges du Sud (zone moldanubienne). Unpubl. PhD thesis, Univ. Louis Pasteur, Strasbourg, France, 220 pp.

THE VULKAAN ARGON LASERPROBE: INTER - CALIBRATION, PERFORMANCE, AND NEW STANDARDS.

SCHEVEERS R., WIJBRANS J.R., PRINGLE M.S., and KOPPERS A.A.P., Faculty of Earth Sciences, Vrije Universiteit, 1081 HV Amsterdam, Netherlands.

The argon laserprobe facility at the Vrije Universiteit (VULKAAN) consists of an MAP215-50 mass spectrometer fitted with a Johnston MM1 SEM, an SP 2080 18W argon-ion laser, and a low volume (ca. 100 ml) UHV inlet line. Operating the SEM at gain 10000, we measure quite reproducibly backgrounds of  $3 \cdot 10^{-16}$ ,  $1 \cdot 10^{-18}$ ,  $4 \cdot 10^{-18}$ ,  $9 \cdot 10^{-17}$ , and  $2 \cdot 10^{-17}$ A, at m/e 40, 39, 38, 37, and 36, respectively. The proportion of blank 40 from the mass spectrometer, getter cross, and sample house is 2:3:6. Virtually all 36 can be attributed to the mass spectrometer. Mass discrimination ( $1.0058 \pm 0.3\%$ ) is monitored using pneumatic pipette yielding air aliquots of ca.  $10^{-8}$  cc STP. The sensitivity of the system ( $2 \cdot 10^{-17}$  moles/mV) was determined using weighed single grains of GA1550 biotite. The laser beam can be focussed continuously between  $<20 \mu\text{m}$  and ca 5 mm. Sample temperature can be monitored with an IR microscope (Minarad MR200), fitted with a fibre optic probe, and temperature controller.

Sample irradiations were carried out at the OSU TRIGA reactor. Potassium correction factors were measured using K - glass for both the unshielded and Cd shielded CLICKIT facility ( $40/39\text{K}=0.00422 \pm 0.00049$  and  $0.00090 \pm 0.00065$ , respectively). For irradiation of older minerals we are currently assessing the HFPIF facility of the 45 MW Petten reactor, with a neutron flux of  $2.3 \cdot 10^{-18} \text{ s}^{-1}\text{m}^{-2}$  thermal neutrons, and  $0.3 \cdot 10^{-18} \text{ s}^{-1}\text{m}^{-2}$  fast neutrons. Fluxmonitor TCR Sanidine 85G003 (age 27.92 Ma) from irradiation VU1 (OSU93/30) was measured at the Amsterdam, Stanford and Menlo Park facilities, demonstrating that J-curves can be reproduced to the known reproducibility of 85G003. Using the combined J-curve, biotite GA1550 yielded ages of  $97.89 \pm 0.30$  Ma (multiple single grains), Fish Canyon biotite ages of  $28.09 \pm 0.09$  Ma (replicate analysis of multi-grain samples), and MMhb-1 ages of  $519.4 \pm 1.5$  Ma (multiple single grains).

As new in-house mineral standards we have assessed the suitability of biotite IGO-2 ( $10.68 \pm 0.04$  Ma), and sanidine DRA-1 ( $24.96 \pm 0.08$  Ma).

ANCIENT SURFACES IN THE TRANSANTARCTIC MOUNTAINS AND THE AGE OF THE SIRIUS FORMATION

SCHLÜCHTER, C., Geologisches Institut, Universität Bern, CH-3012 Bern, Switzerland, HELFER, M., Geologisches Institut, Universität Bern, CH-3012 Bern, Switzerland, BRUNO, L., Isotopengeochemie, ETH Zürich, CH-8092 Zürich, Switzerland, IVY, S., Ingenieurgeologie and Institut für Teilchenphysik, ETH Hônggerberg, CH-8093 Zürich, Switzerland,

The occurrences of Sirius Formation sediments are related to a higher elevation ancient topography of the Transantarctic Mountains (e.g. Mt. Feather, Mt. Fleming, and Table Mountain in the Dry Valleys sector). The Sirius Formation itself is an assemblage of glacial and glacial-limnic facies associations whose textural characteristics are strongly influenced by the local bedrock lithology. Detailed sediment analyses of samples from selected outcrops in the Dry Valleys now permit a more realistic interpretation of the paleoglacial parameters.

The stratigraphic position of the Sirius Formation has been under considerable debate, some scientists have recently emphasized an Upper Pliocene / Lower Pleistocene origin. Exposure age determinations have been carried out on erratic boulders from the Sirius surface and on samples from Sirius-free bedrock below and above patches of Sirius drift on Table Mountain and Mt. Fleming. The exposure ages as reported by Bruno et al. (1994) and Ivy et al. (1994) cast serious doubt on the young origin. The bearing of these age determinations on the understanding of the paleolandscape evolution is presented: the Sirius Formation was deposited at least by mid-Pliocene or, more likely, even earlier.

Bruno et al., 1994, Dating of geomorphologic surfaces in the Antarctic Dry Valleys with in situ produced cosmogenic  $^3\text{He}$  and  $^{21}\text{Ne}$  (abstract this volume).

Ivy et al., 1994,  $^{10}\text{Be}$  and  $^{26}\text{Al}$  exposure dating of the Sirius Formation, Table Mountain, Antarctica (abstract this volume).

Spectral interferences by poly-atomic or multiply charged species are major limitations to analysts currently using quadrupole based ICP-MS instruments. The recognized advantageous characteristics of atmospheric plasma ionization in respect to quantitative multi-element analysis or isotopic analysis is significantly deteriorated by the limited resolving power of these analyzers. The result is poor sensitivity for many elements and lack of selectivity. Over the last few years considerable research effort was focused by many groups on improved sample preparation and sophisticated clean up techniques to overcome these limitations. However, common interferences remain an inherent problem in elemental plasma mass spectrometry, in particular at ultra trace levels.

With respect to sensitivity and power of detection significant improvement can be achieved by using a double focusing magnetic sector based high resolution analyzers instead of quadrupole analyzers.

Unfortunately, up to now commercially available HR-ICP-MS systems have been derived from complex instruments originally designed to meet the requirements of organic mass applications. The design of such "hybrid" HR-ICP-MS compromised performance and operating convenience. For instance, significant, user accessible, parts such as torch and cone system is floating at high voltage.

To overcome those problems, a compact high performance ICP-MS was designed from first principles, exclusively tailored to the characteristics of a plasma source at atmospheric pressure.

An innovative analyzer design, combined with an expert mass control system resulted in a HR-ICP-MS which, on one hand, offers the speed, operating convenience and front-end accessibility of a quadrupole based ICP-MS and, on the other hand, provides the selectivity to resolve the most common spectral interferences.

The resolving power of this analyzer can be switched in a second from 300, 3000 and 7500 times that of a quadrupole analyzer. The trapezoid peak shape, typical for magnetic sector analyzers, is of particular benefit to analysts having to perform fast precision isotope ratio determination.

The dual-mode detector with more than 9 orders of detection dynamics, less than 0.2 counts/sec dark noise and no mass discrimination allows analyses of concentrations ranging from percent to ppq levels.

## Geochronology of the proterozoic magmatism around Kristiansand, south Norway.

By: ULRICH A.S. SCHNELL, Institute of Geology, University of Århus, DK-8000 Århus Denmark.

Kristiansand is situated in the southernmost end of the Bamble linear belt in the Proterozoic gneiss region of Southern Norway. The Kristiansand area is a complex of para- and ortho- gneisses. Some 48 samples were chosen for major element and isotopic analysis. Some 20 samples were chosen for REE and U, Th analysis on the ICP-MS. Rb/Sr whole rock age determinations were made on the four major rock units. The following geological history can be deduced: A sedimentary package is deposited on an unknown basement. The package contained among others a marl, a clay sediment and a quartz rich sandstone. A series of gabbroic or basaltic material can have been introduced. A deep burial of the sediments produced a banded gneiss, into which a highly evolved allanite bearing biotite-granite intruded (The Eeg pink-gneiss) at 1256 Ma. Large volumes of granitic to granodioritic water saturated k-feldspar megakrystic magma (augen-gneiss) intruded (1158 Ma) in a plastic regime and formed "mushroom"-shaped intrusions, followed by upper amphibolite-facies metamorphose at 15 to 20 km. Simultaneously or immediately after the intrusion of this magma the entire area was deformed under an east-west compression leading to a marked north-south striking foliation and iso-clinal folding. The marble was mobilised and transported to the hinge zones. The folding was overprinted by an east-west trending folding with a large wavelength. During the last part of the deformation (1020 Ma), granitic magma (Sødalen-Murtealdalen pink-gneisses) intruded banded gneiss and augen gneiss discordantly. The granite sended concordant apophyses into the banded-gneiss. Finally at 1009 Ma a highly evolved granitic to alkali feldspar granitic magma intruded the banded-gneiss discordantly. At 816 Ma hydro-thermal resetting effected the late pink-gneisses in fracturing zones. Indicating a postorogenic fracturing and local mobilisation of alkali-elements

As a whole the kristiansand area displays a record of sveconorwegian granitic magmatism extending from an initial formation of a granitic-granodioritic batholith thru late-kinematic intrusion of highly evolved granites to post kinematic fracturing and hydrothermal resetting.

MAGMA CHAMBER PROCESSES AND CONDUIT EVOLUTION IN THE LARAMIE ANORTHOSITES, WYOMING: Sr AND Nd ISOTOPES

SCOATES, James S., and FROST, Carol D., Dept. of Geology and Geophysics, University of Wyoming, Laramie, WY, 82071, USA.

A Sr and Nd isotopic investigation of anorthositic rocks in the 1.43 Ga Laramie anorthosite complex (LAC) of southeastern Wyoming reveals that Sr isotopes are effective monitors of magma chamber processes, while Nd isotopes constrain the influence of lower crustal structure on magma conduit evolution. The northernmost intrusion, the Poe Mountain anorthosite (PMa), contains a diapiric core of porphyroclastic and megacrystic anorthosite enveloped by a marginal layered intrusion composed of steeply-dipping leucogabbroic cumulates. Construction of the PMa involved at least three different resident magmas with distinctive initial Sr ratios: 0.7051, 0.7048, and 0.7040.

The diapiric core was emplaced as a crystal-dominated mush with initial Sr=0.7050 to 0.7051. Consolidation of the core involved extensive fractionation of liquid (Mg#=0.54 to 0.30) interstitial to suspended isothermally crystallized plagioclase ( $An_{46+/-2}$ ). Towards the margin of the diapiric core, a shift to more radiogenic initial Sr (up to 0.7055) over a stratigraphic interval of 2000m records contamination by Archean roof rocks. Within the enveloping layered intrusion, chamber-wide recharges of 0.7048 and 0.7040 magmas are recognized by abrupt shifts in initial Sr at roughly 600m intervals. Magmas in the layered intrusion were relatively crystal poor, showing coupled fractionation of plagioclase ( $An_{56}$  to  $An_{40}$ ) and interstitial melt (Mg#=0.50 to 0.27).

Cognate xenoliths of anorthosite contained within the diapiric core and the layered cumulates have a restricted range of initial Sr compositions, 0.7043 to 0.7045, indicating an earlier, isotopically distinctive period of anorthositic magmatism. A single high-Al clinopyroxene megacryst (Mg#=0.68,  $Al_2O_3=6.20$  wt %) is much more primitive than the host layered anorthosite: initial Sr=0.7041 vs. 0.7051. Crystallization at high pressures (~11 kbar) from a basaltic parent is favored for the megacryst, which was subsequently entrained in rising anorthositic magma.

There is little resolvable variation in Nd isotopic compositions within individual anorthositic intrusions in the LAC, however significant variation exists between intrusions:  $\epsilon_{Nd}=-5.0$  to  $-4.4$  in early, deformed porphyroclastic anorthosite in the centre of the complex,  $\epsilon_{Nd}=-0.7$  to  $-2.2$  in the PMa and other composite diapiric and layered intrusions, and  $\epsilon_{Nd}=-0.5$  to  $+0.9$  in late undeformed troctolitic intrusions. The trend towards more primitive  $\epsilon_{Nd}$  values with decreasing relative age is considered to reflect the effects of an evolving magma conduit which becomes increasingly insulated from crustal contamination over time.  $\epsilon_{Nd}$  values as low as  $-5.0$  also indicate contamination by Archean crust ( $\epsilon_{Nd}=-15$ ) of the Wyoming Province to the north of the LAC, rather than accreted Proterozoic island arc terranes ( $\epsilon_{Nd}=+1$  to  $-1$ ) to the south of the LAC. This corroborates seismic reflection data for a southward-dipping terrane boundary, with Archean crust at depth, in the southern Laramie Mountains.

Sr AND O ISOTOPIC RECORD OF THE EARLY - MIDDLE CAMBRIAN OCEAN

SEGEV, A.<sup>1</sup>, SASS, E.<sup>2</sup>, HALICZ, L.<sup>1</sup>, STARINSKY, A.<sup>2</sup>,

<sup>1</sup> Geological Survey of Israel, Jerusalem 95501, Israel.

<sup>2</sup> Dept. of Geology, The Hebrew University of Jerusalem, Jerusalem 91904, Israel.

The Timna Fm. in southern Israel and its stratigraphic equivalent in southwest Jordan (Burj Lst), whose age straddles the Early-Middle Cambrian boundary ( $530 \pm 10$  Ma), represent the first Phanerozoic marine sedimentation in the area.

The analysis of the strontium and oxygen isotopic data of these rocks (limestones and dolomites) has a potential bearing, therefore, to the isotopic composition of the coeval Cambrian ocean. The  $^{87}Sr/^{86}Sr$  ratios of the limestones cover a relatively narrow range, 0.7084-0.7089. The  $^{87}Sr/^{86}Sr$  ratios of the dolomites cover a wider range (0.7086 - 0.7108), whose lower value falls within the limestone field. The generally higher  $^{87}Sr/^{86}Sr$  of the dolomites seem to be related to the presence of siliciclastic minerals of granitic origin, whose contents in the dolomites are significantly higher than in the limestones. It is suggested, therefore, that the higher  $^{87}Sr/^{86}Sr$  in the dolomites reflects porewater modification during early diagenesis and dolomitization. It is quite possible that the calcite in the limestones was similarly affected, even though to a lesser degree. It is argued, accordingly, that the  $^{87}Sr/^{86}Sr$  ratio of the Early-Middle Cambrian seawater was equal to or smaller than 0.7084. This value is significantly lower than the recorded (e.g. Burke et al, 1982) Late Cambrian and Early Ordovician values ( $\geq 0.7090$ ), and may reflect a fast secular change between this value and the Late Proterozoic ratio ( $\leq 0.7070$ ; Derry et al., 1989).

The  $\delta^{18}O$  values of the studied marine carbonates are all in the range of  $-2.0$  to  $-7.5\%$  PDB. Such low values are commonly ascribed to isotopic exchange with freshwater. The present data suggest, however, that the  $\delta^{18}O$  values are not modified, as follows: (1) The  $\delta^{18}O$  values of the dolomites ( $-2.4$  to  $-5.6\%$ ) are higher by  $\sim 3\%$  on the average than that of the limestones ( $-6.2$  to  $-7.6\%$ ), which is consistent with the expected difference between co-genetic calcite and dolomite. (2) The  $^{87}Sr/^{86}Sr$  ratios of the carbonates covary positively with the  $\delta^{18}O$ . Assuming that the reason for the large variations in  $\delta^{18}O$  is due to a late exchange, it is expected that the more modified rocks would be lower in  $\delta^{18}O$  and higher in their  $^{87}Sr/^{86}Sr$  ratios (due to interaction with the admixed siliciclastic minerals). The described trend is inconsistent with the predicted one, suggesting that the observed variations in the isotopic signatures are not due to late resetting.

In summary, it seems that the  $\delta^{18}O$  values of the limestones are not modified to a large extent, and reflect the Lower - Middle Cambrian seawater. Assuming that the limestones formed from seawater at  $30^\circ C$ , the isotope composition of these waters was  $\sim -4\%$ , which is compatible with other evaluations.

Burke, W.H. et al., 1982, Variation of seawater  $^{87}Sr/^{86}Sr$  throughout Phanerozoic time. *Geology*, v. 10, p. 516-519.

Derry, L.A. et al., 1989, Sr isotopic variations in Upper Proterozoic carbonates from Svalbard and East Greenland. *Geochim. Cosmochim. Acta*, v. 53, p. 2331-2339.

## COMPARISON OF RADIONUCLIDE AND NOBLE GAS DATA SUGGESTS POSSIBLE LIMITS FOR EXPOSURE AGE DATING

**SEIDL, M.A.**, Lamont-Doherty Earth Observatory of Columbia University, Palisades, NY, 10964, USA, **HUDSON, G.B.**, **CAFFEE, M.W.**, **FINKEL, R.C.**, **HARRIS, L.**, Lawrence Livermore National Laboratory, Livermore, CA, 94550, USA, and **DIETRICH, W.E.**, Department of Geology and Geophysics, University of California, Berkeley, CA, 94720, USA.

We have calculated surface exposure ages by measuring multiple isotopic concentrations in single samples. Comparison of the data yields information on extraction techniques and nuclide retention. Cosmogenically-produced Be-10, Al-26, Cl-36, He-3, and Ne-21 were measured in rocks collected from the 5.1 m.y. Napali member flows of the Waimea Canyon Basalt on Kauai, Hawaii. All analyses were made on olivine mineral separates, with the exception of Cl-36 concentrations measured in both olivine and whole rock samples.

Several obstacles had to be overcome prior to measurement of the radionuclides. Be-10 and Al-26 are most commonly measured in quartz. Meteoric Be-10 contamination of the olivine grains proved to be a large problem, and a series of leaching experiments were performed to remove the meteoric component from the mineral surfaces. High Al concentrations (on the order of 10,000 ppm) precluded detection of the Al-26 in several samples. Cl-36 is potentially an important isotope for this study, as it can be analyzed both in mineral separates and in bulk material. However, as is the case with Be-10, there are potential meteoric Cl-36 contamination problems. Our initial Cl-36 results are systematically lower than the Be-10 and Al-26; the Cl concentrations were very low and not well determined in the analyzed olivines. We are presently repeating these experiments on bulk material.

We have also measured cosmogenic He-3 (He-3<sub>c</sub>) and Ne-21 (Ne-21<sub>c</sub>) in the olivine separates. Other investigators have observed He<sub>c</sub> loss in quartz samples and one of our goals is to determine whether He-3<sub>c</sub> is quantitatively retained in olivine. Our initial results indicate a deficit of He-3<sub>c</sub> relative to Be-10 and Al-26. It is tempting to infer that there has been diffusive loss of He-3, but until we have collected more data we are hesitant to draw a definitive conclusion. With one exception the Ne-21<sub>c</sub> concentration is low relative to the Be-10 and Al-26. In the exceptional sample, the Ne-21<sub>c</sub> was released during the low temperature heating of uncrushed 1 to 2 mm-sized grains. This suggests that over the course of 5.1 m.y. the olivine structure may alter as the result of weathering, resulting in Ne-21 migration into other sites.

These results have ramifications for analyzing cosmogenically-produced He-3 and Ne-21 in olivines from old flows, on the order of millions of years. Increased erosion may not account for discrepancies between expected and measured He-3 concentrations in weathered olivines. Of course, it is not the absolute age of the olivine that matters, but rather its "weathering age." However, absolute age may serve as a proxy for weathering age at this time.

## TIME AND CONDITIONS OF CONTINENTAL GROWTH PROCESSES IN THE GOTTHARD EXTERNAL MASSIF, CENTRAL SWISS ALPS

**SERGEEV, S.A.** and **STEIGER, R.H.**, Isotope Geochemistry ETH, Zurich, CH-8092, Switzerland.

Granitoids, wide-spread in stable segments within mobile belts, are most sensitive indicators of changes in the geodynamic regime during continental development. One of the best known External massives of the Alpine orogen, the Gotthard, exhibits three granitoid groups, different in age and mode of emplacement, allowing us to apply geochemical (REE and trace elements distribution, Sm-Nd and Rb-Sr systematics), petrographic and geochronologic (single zircon U-Pb) methods for petrogenetic and geodynamic constraints.

1. The Caledonian orthogneiss (Streifengneis, 440 Ma old) which dominates the massif as core of a pre-Variscan anticlinorium-like structure, represents Proterozoic units (>760 Ma) mobilized during the anatexis closely following the regional HPT metamorphism.

2. The older Hercynian group (Fibbia, Gamsboden and Medels gneissose stocks, 298-302 Ma old) exhibits most of the S-type, collisional granitoid diagnostic features. It was formed by metasomatic recrystallization and partial melting of acid pre-Variscan rocks (~450 and >760 Ma old) slightly different in composition from body to body with some island-arc material added. The zircons from enclaves in the granitoids are also of Proterozoic age (~760 Ma).

3. The younger Hercynian group (Rotondo/Tremola, Cristallina, Cacciola and Saedelhorn intrusives, 294-297 Ma old), surrounding the gneissose stocks, are within-plate, post-tectonic homogeneous granitoids of crustal origin, containing inherited zircon grains about 450 Ma old.

Single zircons individually separated from rock-forming minerals show presence in granitoids of oldest detrital (?) zircon grains (~1800 Ma) and allow recognition of an intensive Si-alkaline metasomatism (microcline porphyroblastesis) event 270 Ma ago which led to complete resetting of the rocks' Rb-Sr system. Alpine greenschist/chloritoid metamorphism did not affect the U-Pb zircon systems.

Our results permit to define three stages of Gotthard's geodynamic history from Late Ordovician to Carboniferous: 1) ~440 Ma: completion of the Caledonian subduction regime; 2) ~300 Ma: climax of the Hercynian plate collisional tectonics; 3) ~295 Ma: consolidation and uplift of Alpine basement. The lack of "Pan-African" (Cadomian) memory in zircon grains from the Gotthard granitoids derived from several crustal units suggest an insignificant rôle for Gondwana-incorporated material in this part of the European continental margin.

## CAN SAND DUNES BE USED AS ARCHIVES OF OLD AIR?

SEVERINGHAUS, J.P., and BROECKER, W.S., Lamont-Doherty Earth Observatory, Palisades, NY 10964 USA, and KEELING, R.F., DECK, B., MILLER, B.R., and WEISS, R.F., Scripps Institution of Oceanography, U.C. San Diego, La Jolla, CA 92093 USA

Measurement of the atmospheric  $O_2/N_2$  ratio several decades ago would reveal changes in the size of the biospheric carbon pool, after correcting for known fossil fuel burning, and show whether the "missing sink" of  $CO_2$  is the biosphere or the ocean. How then to obtain a clean sample of several-decade-old air? Sand dunes are a porous media in diffusive contact with the atmosphere, somewhat analogous to the unconsolidated layer of firn atop glaciers. Recent attempts to use firn to measure  $O_2/N_2$  in old air show promise (Todd Sowers, personal communication, 1993). Unlike firn, sand dunes are incompressible and so remain permeable to much greater depths, and may extend the firn record into the past century.

We drilled a 60 m deep test hole in the Algodones Dunes, Imperial Valley, California to see if the air in a sand dune is as old as predicted by a diffusion model, or if the dune is rapidly flushed by advective pumping during windstorms and barometric pressure changes. We dated the air with chloroflourocarbons (CFCs). Our preliminary data match the diffusion model well, suggesting that advection is negligible and the mean age of the air at 60 m depth is 11 years. Microbial metabolism is evident in elevated  $CO_2$  and subambient  $CH_4$  concentrations, suggesting that samples for  $O_2/N_2$  analysis must come from dunes in a subfreezing environment.

## NEOGENE EXTENSION IN THE WESTERN ALPS - EVIDENCE FROM FISSION TRACK DATING

SEWARD, DIANE, and MANCKTELOW, NEIL, S. Dept. Erdwissenschaften, ETH Zentrum, 8092 Zürich, Switzerland

Zircon and apatite fission track analysis has established the continuation of a zone of rapid change in mineral ages running from the Simplon Fault Zone in the Simplon Alps, through the Rhone Valley and along the south-eastern side of the Mont Blanc and Belledonne massifs. The jump in ages is interpreted to represent the position of a Neogene structure with a significant normal fault component. Apatite fission - track ages to the north-west of this zone are generally in the range 2 - 4 Ma, whereas those to the south-east range from 10 to 13 Ma. The corresponding values for zircon are 8 - 12 and 17 - 25 Ma respectively. Detailed sampling along a profile in Val de Bagnes suggests that the zircon age change may occur as a rapid gradient rather than as a single discrete discontinuity. The zone corresponds to the position of the "Frontal Pennine Thrust" in the Mont Blanc - Belledonne region. This structure, which is a prominent feature on recent deep seismic profiles in the region, may have been reactivated in Neogene times with an important normal fault component, as demonstrated by the markedly younger apatite and zircon fission - track ages in the footwall compared to the hanging wall. The normal fault component is also consistent with the observed elimination of the lower Pennine (or Simplon) nappes along this fault zone in the Rhone Valley - Mont Blanc - Belledonne region, resulting in the juxtaposition of the Valais zone and the Helvetic / Ultrahelvetic nappes at the current erosion level.

THE GUANIDINE HYDROCHLORIDE METHOD OF OXYGEN ISOTOPIC ANALYSIS AS APPLIED TO WINES.

SHADEL, C., CALDWELL, E. A., and INGRAHAM N. L., Water Resources Center, Desert Research Institute, University of Nevada System, Las Vegas, Nevada 89132.

Guanidine hydrochloride has been used for oxygen isotopic analysis of waters by the complete conversion to CO<sub>2</sub> (Dugan et al., 1985) in addition to the standard CO<sub>2</sub> equilibration method. In this method, ten μl of water are heated for 8-10 hours at 260°C with 100 mg of guanidine hydrochloride to produce ammonia and carbon dioxide. When cooled, the gases combine to produce solid ammonium carbamate. CO<sub>2</sub> is then produced by heating the ammonium carbamate with 0.5 ml of 100% H<sub>3</sub>PO<sub>4</sub> at 80°C for one hour. The CO<sub>2</sub> may then be purified and analyzed. The guanidine hydrochloride method has the distinct advantage of requiring only small amounts (10μl) of water, allowing the measurements of, for example, individual leaf or berry water.

Recently, this method has also been used for the quantitative determination of the δ<sup>18</sup>O composition of grape must and vintage wines, which is not possible with the the CO<sub>2</sub> equilibration method. The CO<sub>2</sub> equilibration method may allow some ethanol (mass 46) to be trapped in the CO<sub>2</sub> sample, yielding spuriously high δ<sup>18</sup>O values as the CO<sub>2</sub> can not be purified of ethanol by normal slushing. With the guanidine hydrochloride method, the ethanol also reacts producing ethylene (mass 28), and water which is converted to CO<sub>2</sub>. Evidence of this is not only the production of CO<sub>2</sub> but also an elevated mass 28 signal on the mass spectrum above that normally observed as N<sub>2</sub> background. Additionally, analyses of samples of varying ethanol content (0 to 100% by vol.) and water show a systematic change in total δ<sup>18</sup>O composition, and a linear relationship between δ<sup>18</sup>O and volume % (or mole %) of ethanol.

The standard process of baking water samples with guanidine hydrochloride and reducing the ethanol to CO<sub>2</sub> allows the quantitative isotopic analysis of oxygen in the closed system of the wine bottle. Such an analysis allows bottled wines to be better used as surrogate samples of precipitation for climate change studies.

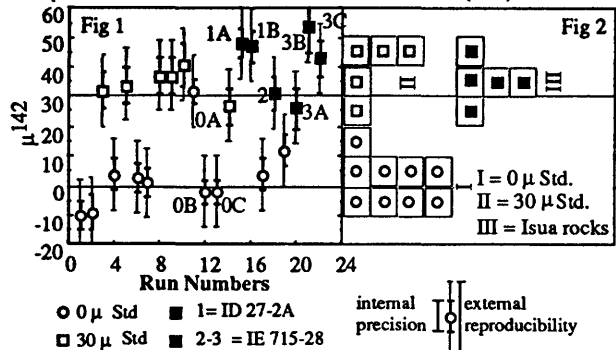
Dugan J.P. Jr., Borthwick J., Harmon R.S., Gagnier M.A., Gahn J.E., Kinsel E.P., Macleod S., Viglino J.A., and J.W. Hess, 1985. Guanidine hydrochloride method for determination of water oxygen isotope ratios and the oxygen-18 fractionation between carbon dioxide and water at 25°C. Anal. Chem., 57: 1734-1736.

POSSIBLE <sup>142</sup>Nd EXCESS IN 3.8 Æ ISUA SUPRACRUSTALS

SHARMA, M., PAPANASTASSIOU, D. A., and WASSERBURG, G. J., The Lunatic Asylum, Div. of Geol. and Planet. Sci., Caltech, Pasadena, CA 91125, and DYMEK, R.F., Dept. of Earth and Planet. Sci., Washington Univ., St. Louis, MO 63130.

Harper and Jacobsen (1992) have reported a 33 ± 4 μ (μ = ((Rock/ Standard)-1) x 10<sup>6</sup>) <sup>142</sup>Nd excess in a 3.8 Æ felsic gneiss (IE 715-28) from Isua, Greenland. If this result can be substantiated it would indicate an early (between 4.5 and 4.3 Æ) planetary differentiation and generation of reservoirs with large f<sub>Sm/Nd</sub>. Further, it would suggest the existence of mechanisms that preserved <sup>142</sup>Nd excess in a much younger 3.8 Æ old rock. These observations prompted other workers to search for <sup>142</sup>Nd excesses in other samples from early Archean terrains. So far no additional evidence for the excesses has been found. Our efforts have been directed toward addressing the central issue: high precision mass spectrometry that can resolve ~30 μ <sup>142</sup>Nd excesses. We used a F-MAT 262 multicollector mass spectrometer, similar to the instrument used by Harper and Jacobsen. The data were obtained with 2 x 10<sup>-11</sup> A <sup>142</sup>Nd<sup>+</sup> beams in static mode. Our experiments showed that position of the sample and ion source potentials can engender large (up to 60 μ) changes in <sup>142</sup>Nd/<sup>144</sup>Nd ratios. These observations led to the development of an arbitrary but strict, standard operating procedure (SOP) with fixed focusing conditions. All data obtained by SOP are considered valid.

Following the SOP a series of Nd β Standards were run for the 0 μ standard. Gravimetric standards were prepared with excesses in <sup>142</sup>Nd; analyses of the 30 μ standard were interleaved with the 0 μ standard. Results were obtained concurrently on two Isua samples, including the one analyzed by Harper and Jacobsen. Figure 1 shows samples and standards run using SOP. The data show an internal (within run) precision of 6 ppm (2σ) and an external reproducibility, following SOP of 12 ppm (2σ). Figure 2 is a histogram of the samples and standards run using SOP. It is apparent that the 0 μ and 30 μ standards are completely resolved with no overlap. Thus there is a strong indication of <sup>142</sup>Nd excess in the two Isua rocks analyzed. In order to check the robustness of our data we ran 0A and 3B by *not* following our SOP. These samples show ~30 μ increase with respect to 0B and 3A (Fig. 1) We therefore consider the results to be still ambiguous given the fact that departures from the strict but arbitrary optimization procedures can cause large shifts. Unless the running conditions are rigidly controlled and shown to yield good reproducibility, substantial artifacts can and will creep in the data. Division Contribution 5371 (845).



## OXYGEN AND HYDROGEN ISOTOPE GEOCHEMISTRY OF TALC

SHARP, Zachary D., Hunziker, Johannes C., Institut de Minéralogie, UNIL BFSH-2, CH-1015 Lausanne, Switzerland

Talc is generally formed by the metamorphism of either ultramafic rocks or siliceous dolomites, although talc is also found as a hydrothermal mineral in submarine environments, in evaporites and in high pressure metamorphosed magnesian-rich pelites. The origin of talc in some massive deposits is enigmatic. Certain chemical indicators may be used to infer a particular origin for talc. Hydrothermal talc may have high iron contents, talc derived from ultramafic rocks may contain significant nickel, and carbonate-derived talc may be recognized by a high fluorine content. Often, however, the chemical composition of talc is not diagnostic of a particular environment. Furthermore, lithological associations may indicate a particular origin, but late structural events may obscure the true origin of the deposit. Stable isotope compositions of talc may provide a less ambiguous means of determining the protolith or metasomatic fluid associated with talc formation. The  $\delta^{18}\text{O}$  and  $\delta\text{D}$  values of most magmatic fluids are approximately 6 to 10‰ and -50 to -80‰, respectively. Connate fluids from carbonates evolved during metamorphism have  $\delta\text{D}$  and  $\delta^{18}\text{O}$  values that are significantly different from those of magmatic fluids: ~20 to 25‰ and as high as 0‰, respectively. Taken together, the  $\delta^{18}\text{O}$  and  $\delta\text{D}$  values may uniquely define the origin of a given deposit.

Isotopic analysis of talc samples were made from a number of different geological environments. Talc veins in dolomites from Campolungo, Swiss Alps and the Balmat talc mines (New York, U.S.A.) have a carbonate origin. The  $\delta^{18}\text{O}$  and  $\delta\text{D}$  values are 22 to 24‰ and -25‰, respectively. Talc veins in ultramafic rocks from different locations have  $\delta^{18}\text{O}$  and  $\delta\text{D}$  values of 5 to 6‰ and -75 to -80‰. Talc from the Pamour talc mine has  $\delta^{18}\text{O}$  values of 8 to 9‰, supporting an ultramafic origin. A talc halo around a diabase intruding carbonate (Western Mine, California, U.S.A.) has an intermediate  $\delta^{18}\text{O}$  value of 11.7‰ indicating mixing between two isotopically distinct reservoirs. The  $\delta^{18}\text{O}$  and  $\delta\text{D}$  values from a talc mine and from the coesite-bearing whiteschists in the high pressure Dora Maira Massif, southern Alps (N. Italy) are 5 to 6.5 ‰ and -25 to -32 ‰, quite different from other talc deposits. Similar high-pressure rocks from the Adula nappe have the same isotopic compositions. The combined  $\delta^{18}\text{O}$  and  $\delta\text{D}$  values are similar to those of metamorphosed oceanic basalts and gabbros. These high pressure rocks may have undergone interaction with an metasomatic fluid derived from a subducting slab.

## DISTURBANCE OF RB-SR ISOTOPE SYSTEM IN CALEDONIAN GRANITES OF NORTH KAZAKHSTAN BY HERCYNIAN THERMO-TECTONIC EVENT

SHATAGIN Konstantine N., Laboratory of Isotope Geochemistry and Geochronology, IGEM RAS, Staromonetny 35, Moscow, 109017, Russia.

Rb-Sr isotope system of Caledonian granites of North Kazakhstan bears a fingerprint of a rejuvenation event, previously dated at 240-300 Ma by K-Ar method.

Results of detailed Rb-Sr isotope study of selected plutons are the following.

Zerendinsky batholith has an age of  $448 \pm 9$  Ma and  $(^{87}\text{Sr}/^{86}\text{Sr})_0 = 0.7055 \pm 5$  (isochrone on 11 whole-rock samples). Rb-Sr result on mineral separates from one isochrone sample suggest a reequilibration of strontium isotope composition between minerals some 290 Ma. Some scatter of mineral points around internal isochrone does not allow to imply that equilibrium was achieved, therefore, 290 Ma is considered to be maximum age of secondary event.

Zolotonosha leucogranitic pluton has an age of  $399 \pm 3$  Ma and  $(^{87}\text{Sr}/^{86}\text{Sr})_0 = 0.708 \pm 1$  (isochrone on 7 whole-rock samples). Three points of alaskites lie under the isochrone. One of those samples was studied on the mineral level. Points of biotite, K-feldspar and albite do not feet a common isochrone. Date for biotite measures 381 Ma, and for albite and K-feldspar (combined) -- 285 Ma. The latter is consistent with homogenization of  $^{87}\text{Sr}/^{86}\text{Sr}$  between albite and K-feldspar as a result of the same event as for Zerendinsky batholith.

Orlinogorsky alaskitic pluton presumably has the same age as Zolotonosha pluton, as they belong to the common Orlinogorsky suite. Mineral separates (each divided to the dense fractions) was studied. K-feldspar -- albite isochrone (9 points) is consistent with  $^{87}\text{Sr}/^{86}\text{Sr}$  homogenization at  $250 \pm 40$  Ma, however, biotite date (3-point isochrone) is meaningless.

Above facts confirm a presence of some Hercynian event in geological history of North Kazakhstan. A thermal nature of this event is deduced from fresh appearance of investigated samples and lack of traces of recrystallization.

BIOGEOCHEMICAL CONTROLS OF BENTHIC MICROBIAL MATS ON CH<sub>4</sub> PRODUCTION AND FLUX FROM SALINE ALKALINE LAKES

SHERWOOD LOLLAR, B., Dept. of Geology, U. of Toronto, M5S 3B1 Canada; GERITS, J., Dept. of Geography, U. of Toronto M5S 3B1; FERRIS, F.G., LANSDOWN, J. and SCHULTZE-LAM, S., Dept. of Geology, U. of Toronto, M5S 3B1.

A biogeochemical and isotopic study was carried out to investigate benthic microbial mats and organic-rich sediments in a series of saline alkaline lakes on the Cariboo Plateau of central British Columbia. The lakes present a wide spectrum of hydrochemical regimes and range from relatively deep (> 15m) perennial fresh and saline lakes to shallow hypersaline playa lakes. pH values vary significantly from 7.5 to > 10. Individual lakes support abundant microbial communities and associated authigenic mineral deposits of diverse and complex structure. Microbial mats are widely perceived to be modern analogues for the stromatolite-forming benthic microbial communities that constituted the most abundant lifeform of the Precambrian. They play a critical role in the formation of organic-rich sediments, the precipitation and diagenesis of carbonate and silicate minerals, and the biogeochemical transformation of carbon between organic, inorganic and atmospheric carbon pools. The primary objective of the research is to characterize and define the controls on these dynamic biogeochemical transformations. This presentation will focus on CH<sub>4</sub> production in these lacustrine systems, carbon gas flux to the atmosphere, and the controlling influence of microbial mats in regulating that flux.

Despite considerable geochemical diversity, 6 of the 7 lakes surveyed were supersaturated in CH<sub>4</sub> with respect to the atmosphere. Of the 3 lakes studied in detail, CH<sub>4</sub> concentrations in Goodenough Lake are 50-400 times supersaturated with respect to the atmosphere while Deer and Probe Lake concentrations are up to 5000 times supersaturated. Flux measurements made elsewhere for lakes several hundred times supersaturated are on the order of 5 mg CH<sub>4</sub>/m<sup>2</sup>/day (1). Profiles of dissolved gas and geochemical species collected within the lakes and across the sediment-water interface to depths of 30-40 cm indicate that microbial mat development plays a major role in regulating the release of CH<sub>4</sub> and other carbon gases from the sediments to the water column and the atmosphere. The degree of mat development appears to control interlake and seasonal variation in redox conditions at the sediment-water interface, and hence in the extent of CH<sub>4</sub> oxidation taking place within this zone.

(1) Oremland et al. (1987) *Geochim. Cosmo. Acta* 51:2915-2929.

NOBLE GAS SOLUBILITY IN SILICATE- AND METAL-MELTS AT HIGH PRESSURES, AND ITS APPLICATION TO THE ESTIMATION OF SURFACE TENSION

SHIBATA, T., OZIMA, M., Dept. of Earth and Space Sci., Osaka University, Toyonaka-City, 560, Japan, and TAKAHASHI, E., Faculty of Sci., Tokyo Inst. of Technology, Meguro-Ku, Tokyo 152, Japan.

We measured noble gas (He, Ne, Ar, Kr) solubility in basalt melts, olivine crystal, and metal (Au) melt at high pressures up to 2 Kbars. Basalt powder (ca. 100 μ) and olivine crystals (a few μ) were contained in a platinum capsule (2 mm φ x 5 mm) and Au chips were put in a boron-nitride capsule (5 mm φ x 5 mm.) A mixture of noble gases (volume ratio; He:Ne:Ar:Kr = 1:1:97:1) was used as a pressure medium. Samples were kept at 1250 °C, 1300 °C, and 1600 °C for 2, 5, and more than ten hours at 1, 2 Kbars.

Noble gas solubility of the gold melt at 2 Kbars was by five orders of magnitude smaller than those in the basalt melt, and there appeared little pressure effect on the solubility. Noble gas partition coefficients between silicate melt and gold melt at 2 Kbars are very small (<10<sup>-5</sup>), being consistent with the result by Matsuda et al.. Partition coefficients between basalt melt and olivine crystal are similar to those obtained by Hiyagon et al. at an atmospheric pressure.

From noble gas solubility in basalt and metals, we estimated surface tension of these materials. To a fairly good approximation, surface tension (σ) is related to noble gas solubility or to Henry's law constant (H) through the following relation,  $\ln(H) = (-4\pi\sigma R^2 + E)/KT$ , where R, K, T, and E stand for the radius of noble gas (we took a Van der Waals radius), Boltzmann constant, absolute temperature, and solvent-solute interaction energy. In the case of noble gases which do not generally interact with solvent, E may be neglected. From the noble gas solubility data, we calculated the surface tension of basalt melts, which gave 180 dyne/cm. The value agrees with those estimated by other methods. There was little pressure effect on the surface tension of basalt melt at least up to 2 Kbars.

Matsuda et al., 1993, *Science*, v. 259, p.788-790.  
Hiyagon et al., 1986, *Geochim. Cosmochim. Acta*, v.50, p.2045-2057.

GEOCHEMISTRY OF CE AND ND ISOTOPES AND REE ABUNDANCES IN PRECAMBRIAN ORTHOGNEISSES FROM THE KAMIASO CONGLOMERATE, CENTRAL JAPAN: REE EVOLUTION HISTORY OF THE PRECAMBRIAN BASEMENT IN JAPAN

SHIMIZU, H., Dept. Earth Sci., Kumamoto Univ., Kumamoto, 860, Japan, LEE, S.-G., KIGAM, Taejeon, 305-350, Korea, MASUDA, A., Univ. Electro-Communications, Chofu, 182, Japan, and ADACHI, M., Dept. Earth Planet. Sci., Nagoya Univ., Nagoya, 464-01, Japan

Cerium isotopic data, rare earth element abundances and major element compositions were determined for Precambrian orthogneisses and granites in the Jurassic Kamiaso conglomerate from central Japan; Sm-Nd age of 2.07 Ga with  $\epsilon_{Nd}(2.07 \text{ Ga}) = -1.9$  was already reported by us for these samples. Three types of REE patterns are observed for the Kamiaso samples: (1) reverse S-shaped patterns with high enrichment of LREE, (2) patterns consisting of concave La-Nd span and reverse S-shaped Nd-Lu span, and (3) patterns consisting of two or three rectilinear lines with inflection at Ho (and Nd). Major element data for the third REE pattern-type samples show low potassium content or high sodium content, implying that these samples retain the chemical features of their older protoliths. The other samples are characterized by high potassium content, which is typical of some Proterozoic potassic granites.  $\epsilon_{Ce}(0)$  values for the Kamiaso samples range from -1.1 to +2.8.

On the basis of the Ce and Nd isotopic data and REE patterns, REE evolution of Precambrian basement of the Japanese Islands was deduced. (1) Protolith of the Kamiaso orthogneisses was formed from LREE-depleted mantle in the late Archean as a part of the continental crust, and had the LREE-enriched pattern that was observed for the third type of REE pattern. (2) Granitic rocks were fractionated from the protolith in an igneous event at 2.07 Ga; in which plagioclase and REE-bearing minerals such as zircon, monazite and allanite played a significant role in REE distribution. The 2.07 Ga processes are considered to have been fractionation among granitic rocks in the continental crust. (3) The granitic rocks were metamorphosed to gneisses at 1.8-1.6 Ga, during which process REE patterns for the whole rocks were essentially unchanged.

$Xe_s$ - $Xe_n$  ISOTOPE DATING

SHUKOLYUKOV, Yuri A., MESHNIK, A. P., PRAVDIVTSEVA, O. V., Vernadsky Institute of Geochemistry and Analytical Chemistry, Russian Academy of Sciences, 117975 Moscow, Russia

$Xe_s$ - $Xe_n$  isotope dating method was suggested and intensively developed last years in Russia. The method based on the spontaneous fission of  $^{238}\text{U}$  yielded in the production of radiogenic xenon -  $Xe_s$ . During the irradiation of the mineral in nuclear reactor neutron-induced Xe of different isotopic composition -  $Xe_n$  is produced from the fission of  $^{235}\text{U}$ . If the mineral-monitor of well-known age will be irradiated together with the studied sample the age of the sample could be calculated as a function of  $Xe_s/Xe_n$  ratios measured in the sample and in the monitor, and age of the latter. So, the important advantage of  $Xe_s$ - $Xe_n$  method is that for age calculation we do not need to measure any absolute concentrations, only Xe isotopic ratios is required. The second advantage of the method is the absence of trapped radiogenic xenon in all of studied samples because of the low Xe contents in fluids in contrast to  $^{40}\text{Ar}$ . Although some part of Xe may escape from the mineral during geological time, the activation energy of Xe migration of the rest is very high (up to 100-300 kcal/mol for zircons). These values are 30 kcal/mol higher than for radiogenic Pb in the same samples. This ensures a good retention a high portion of  $Xe_s$ . By means of step wise annealing  $Xe_s$ - $Xe_n$  spectra could be obtained, with the high temperature plateau corresponding to the real age. Thus, the important advantage of the method is the ability of dating the opened isotopic systems in minerals. In contrast to the U-Pb method  $Xe_s$ - $Xe_n$  technique does not require the series of samples needed to plot isochrone, one sample is sufficient for the real age determination.

$Xe_s$ - $Xe_n$  technique have been successfully applied for dating zircons from the Baikal region, Finland, Karelia, Ukraine, Antarctic. The obtained ages turns out to be in a perfect agreement with U-Pb method.

Uranium deposits of Russia, Kazakhstan, Germany, France and South Africa, have been dated by  $Xe_s$ - $Xe_n$  method. It was found out that the hydrothermal ore deposition was a prolonged pulsate process with the definite spatial distribution.

OXYGEN AND STRONTIUM ISOTOPES IN CONTRASTING METALUMINOUS GRANITIC SUITES FROM TWO PRECAMBRIAN FOLDBELTS IN NE BRAZIL

SIAL, A.N., FERREIRA, V.P., Dept. of Geology., Stable Isotope Lab. (LABISE), UFPE, C.P. 7852, Recife, PE, 50732-970, Brazil, LONG, L.E., Dept. of Geological Sciences, U. Texas, Austin, TX, 78712, USA

Magmatic epidote (mEp)-bearing plutons in the Cachoeirinha-Salgueiro (CSF) and Seridó (SFB) foldbelts, NE Brazil, form two contrasting geochemical groups that were emplaced respectively at 7-9 and 3-4 kbar ranges, as estimated from the Al-in-hornblende geobarometer (Schmidt, 1992).

In the CSF, granodiorite/tonalite plutons which typically intrude low-grade marine metaturbidites, have abundant microgranular hbl-bi diorite to tonalite enclaves. Amphibole-rich polycrystalline clots, up to 15 cm long, are widespread and when occurring within the enclaves, they seem to be disaggregates from larger amphibolite fragments. They are composed of Ca-cpx and interstitial biotite, and zoned amphiboles (core and patchy zoning), whose grains commonly meet at ~ 120° triple junctions. They exhibit granoblastic texture in the interior of the clots, generally armored by an outer zone composed of bi + hbl. In the SFB, mEp is found in qz diorites, tonalites, qz monzodiorites, qz monzonites and granites, which intruded gneisses and schists.

Rb-Sr isochron data from CSF enclaves and host mEp-bearing granodiorite provide a highly linear regression ( $I = 0.70598$ ), indicating that enclave and host magma are cogenetic or had been isotopically equilibrated during cooling.

In SFB mEp-bearing plutons, whole-rock  $\delta^{18}\text{O}$  is +7.8 to +8.1‰<sub>SMOW</sub>, and qz diorite enclaves are ~ +7.8‰.  $\delta^{18}\text{O}$  in tonalites intruding basement rocks is about +6.4‰<sub>SMOW</sub>. CSF mEp-bearing plutons, although oxidized I-type granitoids, exhibit high  $\delta^{18}\text{O}$  (+11 to +13‰<sub>SMOW</sub>). Diopside-bearing varieties have very homogeneous O-isotope compositions (+11.6 to +12‰<sub>SMOW</sub>), consistent with their restricted variability of major and REE-chemistry. Granodiorite/tonalite host and qz diorite enclaves display the same range of whole rock  $\delta^{18}\text{O}$ , in accord with the indications of the isotope data. Values of  $\delta^{18}\text{O}$  in amphibole-rich clots in CSF plutons are +10.1 to +11.6‰<sub>SMOW</sub>, an isotope range predictable for the source of their high  $\delta^{18}\text{O}$  host magmas. Therefore, O and Sr isotopes point to the amphibole-rich clots as probable fragments from a low-T hydrothermally-altered basaltic source for these magmas. Temperature estimates for them (670-690°C, according to Nabelek & Lindsley thermometer, 1985) are < than those for granodiorite hosts (700-850°C, according to Blundy & Holland thermometer, 1990), reinforcing the contention above.

Blundy, J.D., and Holland, T.J.B., 1990, Calcic amphibole equilibria and a new amphibole-plagioclase geothermometer, *Contrib. Mineral. Petrol.*, v. 104, p. 208-224.

Nabelek, C.R., and Lindsley, T.H., 1985, Tetrahedral Al in hornblende: a potential thermometer for some mafic rocks., *Geol. Soc. Amer. Annual Meet.*, Orlando, Fla. p. 673.

Schmidt, M.W., 1992, Amphibole composition in tonalite as a function of pressure: an experimental calibration of the Al-in-hornblende barometer: *Contrib. Mineral. Petrol.*, v. 110, p. 304-310.

THE POST-VARISCAN EVOLUTION OF THE CONTINENTAL MARGINS OF THE BAY OF BISCAY: A STUDY USING APATITE FISSION TRACK ANALYSIS

SIDDALL, R., Research School of Geological and Geophysical Sciences, Dept. of Geological Sciences, University College London, Gower Street, London, WC1E 6BT, UK.

The sensitivity of apatite fission tracks to cooling and unroofing episodes in Earth history is particularly suited to the tectonic processes of rifting and the long term evolution of continental margins. Apatite fission track analyses have been made on ~70 samples of igneous, metamorphic and sedimentary rocks from coastal outcrops of Western France (the Armorican Massif) and north-western Spain (the Hesperian Massif) the aim being to unravel the potential thermal overprint associated with the opening of the North Atlantic Ocean, specifically in the Bay of Biscay.

The fission track ages range from ~70 to 270 Ma, with the youngest ages towards the Atlantic coasts, and become progressively older eastwards. The data are interpreted in terms of the thermal histories resulting from the Mesozoic post-breakup exhumation of the rift flanks in the westernmost regions of Spain and France, whilst eastwards the earliest detectable cooling episode is Early Permian, reflecting the exhumation of the Variscan mountain chain.

The data from the Armorican Massif are consistent with 2 previously unrecognised periods of burial and subsequent exhumation during the Mesozoic. The most recent (Campanian) burial episode is inferred to represent the deposition of chalk. The data from north-western Spain do not appear to reflect this second burial, probably because at this time this region was outside the chalk depocentre.

## AUSTRALIS: A MICROBEAM AMS SYSTEM FOR GEOCHRONOLOGY

S.H. Sie and G.F. Suter, Heavy Ion Analytical Facility  
CSIRO Division of Exploration and Mining  
P.O. Box 136, North Ryde, NSW 2113, Australia

The development of Accelerator Mass Spectrometry (AMS) represents significant progress in the resolution of problems of molecular and isobaric interferences, by virtue of acceleration to MeV energies and multiple charging in a tandem accelerator. The use of negative ions from the source, and availability of variety of molecular ions themselves can also be exploited to reduce or eliminate interference. The potential of AMS in isotope geology, both for geochronology and tracer applications has long been recognised.

The CSIRO Heavy Ion Analytical Facility (HIAF) was established as an analytical laboratory based on the 3 MV Tandatron, dedicated to applications in the geosciences, and research relevant to the minerals industry. A basic AMS system that enables  $^{14}\text{C}$  and  $^{10}\text{Be}$  measurements has been developed [1]. This system is now being upgraded to enable in-situ measurements of ultra-traces and isotopic-ratios in mineralogical applications. The upgraded system will include a microbeam Cs ion source which is designed to produce as low as 1  $\mu\text{m}$  diameter Cs beam to enable analyses of monomineralic grains and microscopic features. The Cs primary beam will be mass analysed in order to minimize contamination of the sample. The detection system will be upgraded to enable analyses of elements up to U, at 2.5 MV terminal voltage for charge state  $6^+$ . The system will be known as AUSTRALIS: A.M.S. for Ultra Sensitive TRAce Element and Isotopic Studies.

AUSTRALIS will enable applications of a few geochronometers or tracers previously either tedious and limited to bulk applications, or completely inaccessible. Potentially useful applications include the common Pb, U/Pb ( $^{207}\text{Pb}/^{206}\text{Pb}$ ),  $^{87}\text{Rb}/^{87}\text{Sr}$  ( $T_{1/2}=4.8\times 10^{10}\text{y}$ ),  $^{187}\text{Re}/^{187}\text{Os}$  ( $T_{1/2}=4.3\times 10^{10}\text{y}$ ) systems.

Overviews of the system and of the anticipated application will be presented.

Sie, S.H., Ryan, C.G. and Suter, G.F., 1990. An AMS facility for minerals exploration research, Nucl. Instr. Meth. B52, p.294-297

## $^{210}\text{Pb}$ - $^{226}\text{Ra}$ - $^{230}\text{Th}$ - $^{238}\text{U}$ RADIOACTIVE DISEQUILIBRIA IN VOLCANICS FROM RÉUNION ISLAND AND VESTMANNAEYJAR (ICELAND)

Sigmarrsson, O.\*, Condomines, M.\*, Bachelery, P.\*\* and Jakobsson, S.\*\*\* \*CRV and CNRS, Université Blaise Pascal, Clermont-Ferrand, France. \*\*Université de la Réunion, France. \*\*\*Museum of Natural History, Iceland.

In general oceanic island basalts have a radioactive disequilibrium pattern of  $(^{226}\text{Ra}) > (^{230}\text{Th}) > (^{238}\text{U})$  but very few data exist on  $^{210}\text{Pb}$ - $^{226}\text{Ra}$  and  $^{228}\text{Ra}$ - $^{232}\text{Th}$  systematics. Several recent basalts from Piton de la Fournaise (Réunion island) and alkali basalt, hawaiite and mugearite from Vestmannaeyjar in Iceland (Surtsey and Heimaey) have been analyzed for  $^{210}\text{Pb}$ - $^{226}\text{Ra}$ - $^{230}\text{Th}$ - $^{238}\text{U}$  radioactive disequilibria. Basalts from both localities have  $(^{238}\text{U}/^{230}\text{Th})$  around 1.2,  $(^{226}\text{Ra}/^{230}\text{Th})$  in the range of 1.3 to 1.4, and  $(^{210}\text{Pb}/^{226}\text{Ra})$  at the time of eruption in the range 0.6-0.7. If these fractionation are only due to partial melting of a mantle source in radioactive equilibrium with identical partition coefficients, these results would imply a similar degree of melting in both islands. The existence of a  $^{210}\text{Pb}$  deficit, despite of  $^{228}\text{Ra}$ - $^{232}\text{Th}$  equilibrium would imply a separation of the magma from the mantle between 30 and 100 years before eruption. However, although  $^{230}\text{Th}$ - $^{238}\text{U}$  fractionation is probably negligible during magma transfer and differentiation, it is not always the case for Ra-Th and Pb-Ra fractionations.

In Piton de la Fournaise, the Ra enrichment cannot have taken place above the magma chamber. Samples from both the 1986 summit and the contemporaneous lateral eruption display identical  $(^{226}\text{Ra}/^{230}\text{Th})$  values. On the other hand, picritic magma which has incorporated crystal mush from the magma chamber, has  $(^{226}\text{Ra}/^{230}\text{Th})$  as low as 1.18.

In Vestmannaeyjar,  $(^{226}\text{Ra}/^{230}\text{Th})$  vary from 1.4 in the 1963 alkali basalt to 1.19 in the 1973 mugearite, while Th abundances increased from 1.49 to 3.21  $\mu\text{g/g}$ . This decrease of  $(^{226}\text{Ra}/^{230}\text{Th})$  is probably due to plagioclase fractionation (with a bulk  $K_{\text{D Ra}} \sim 0.3$ ). The mugearite can be derived from an alkali basalt similar to the Surtsey magma by  $\sim 50\%$  fractional crystallization on a timescale  $\leq 10$  years.

Moreover, Pb-Ra fractionation can be due to several processes during magma differentiation or eruption: Pb loss as a volatile compound, Pb fractionation by sulfide crystallization.

The results from these volcanic islands clearly show that magma chamber processes can affect U-series disequilibria and must be taken into account before assigning them to partial melting only.

## BASALT PETROGENESIS: A COMBINED APPROACH USING U-Th DISEQUILIBRIA AND Sm-Nd ISOTOPIC SYSTEMATICS

Sims, K.W.W.<sup>1&2</sup>; DePaolo, D.J.<sup>1</sup>; Murrell, M. T.<sup>2</sup>; Baldrige, W.S.<sup>2</sup>; and Goldstein, S.J.<sup>2</sup>.

1) Berkeley Center for Isotope Geochemistry, Dept. of Geology and Geophysics, U.C. Berkeley, Berkeley CA 94720

2) LANL, Los Alamos, NM 87545

Measurements of <sup>238</sup>U/<sup>230</sup>Th disequilibria in young oceanic basalts indicate that Th is enriched in the melt relative to U, particularly in MORBs, which have (<sup>238</sup>U/<sup>230</sup>Th) as low as 0.65. While this observation demonstrates that magmatic processes are capable of fractionating even highly incompatible element ratios, large U/Th fractionations have been difficult to interpret because U and Th are thought to be too highly incompatible to allow such fractionations to occur by crystal-liquid partitioning alone, especially in MORBs where the chemistry suggests that total melt fractions are large. Although the mineral responsible for the U/Th fractionation may be identified (garnet), the magnitude of this fractionation is still difficult to reconcile without calling on other processes, e.g., volatile exsolution, fluid/melt interaction, etc.

To further investigate the controls on U-Th fractionation, we have measured Th and Nd isotopes (TIMS) and [U], [Th], [Sm] and [Nd] (ID-MS) in a series of young Hawaiian basalts and axial-MORBs which show a wide range of composition. The Hawaiian basalts range from tholeiites to basanites; the MORBs (EPR) range from N-MORB to E-MORB. We then compare inferred U/Th fractionation (<sup>238</sup>U/<sup>230</sup>Th) with inferred Sm/Nd fractionation to evaluate the relative partitioning behavior of U and Th (where the Sm/Nd source ratio is inferred by using the 1.7 Ga source model of DePaolo (1988) and the measured <sup>143</sup>Nd/<sup>144</sup>Nd of the sample).

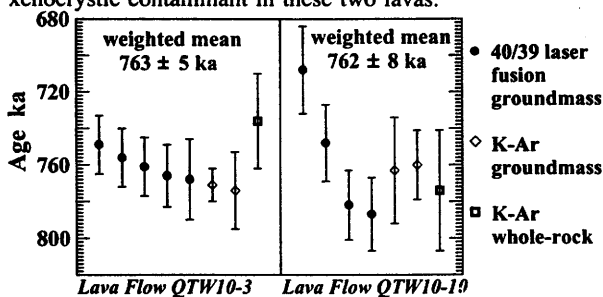
The Hawaiian lavas show a good correlation ( $r^2 = 0.93$ ) between U/Th and Sm/Nd fractionation. The tholeiites are the least fractionated, the basanites are the most fractionated. In all samples U/Th fractionation is less than Sm/Nd fractionation. Correlation of Sm/Nd fractionation with U/Th fractionation allows the Hawaiian data to be inverted in terms of batch melting models. Assuming  $D_{Nd} = 0.020$  and  $D_{Sm} = 0.050$ , this inversion yields:  $D_U = 0.00143$ ,  $D_{Th} = 0.0006$ , with melt fractions varying from 5% (tholeiites) to <1% (basanites). The coherence of Sm-Nd and U-Th behavior is strong evidence that U/Th fractionation is a result of crystal-liquid fractionation associated with partial melting. In contrast, the MORB data show a systematic but significantly different relationship between U/Th and Sm/Nd fractionation. For both U-Th and Sm-Nd, N-MORBs are less fractionated than E-MORBs. However, in all MORB samples U/Th fractionation roughly equals Sm/Nd fractionation. In fact, for most MORBs, U/Th is more fractionated than in Hawaiian basanites while Sm/Nd is less fractionated.

Our data indicate there are fundamental differences in U-Th behavior between Hawaii and MORs. While Hawaiian lavas might be expected to be more fractionated than MORBs because of smaller melt fractions and deeper origin, they are instead less fractionated. If processes other than crystal-liquid partitioning are operating, they appear to be more important at MORs than in Hawaii. Differences in the melt generation geometry exist, but it is not obvious how these can generate the relationship between U/Th and Sm/Nd fractionation observed in MORBs.

## K-Ar and <sup>40</sup>Ar/<sup>39</sup>Ar AGE OF BRUNHES-MATUYAMA BOUNDARY FROM LAVAS IN THE CHILEAN ANDES

SINGER, Bradley S., Dept. de Minéralogie, Université de Genève, 1211 Genève 4, Switzerland; EMAIL: Singer@sc2a.unige.ch. and NELSON, Stephen T., Woodward-Clyde Federal Services, 101 Convention Center Dr., Suite P110 MS 423, Las Vegas, NV 89109, USA.

In obtaining K-Ar and <sup>40</sup>Ar/<sup>39</sup>Ar ages for >30 Pleistocene samples from the frontal arc center of Volcán Tatara-San Pedro (36°S, 70.5°W), we have dated two samples from a sequence of 10 lava flows that record transitional virtual geomagnetic pole (VGP) positions corresponding to the Brunhes-Matuyama Boundary (BMB). These 10 flows have VGPs centered on northern Australia. The uppermost flow is truncated by an unconformity overlain by lavas with normal polarity <330 ka. Conventional K-Ar (USGS, Menlo Park) and laser fusion <sup>40</sup>Ar/<sup>39</sup>Ar analyses (UCLA) were collected from groundmass, whole-rock, and plagioclase aliquots from two samples with transitional VGPs. Using the laser, heating steps removed Ar with a high atmospheric component from groundmass aliquots which were subsequently fused to yield Ar from which ages were calculated. Five <sup>40</sup>Ar/<sup>39</sup>Ar fusion analyses of groundmass from the stratigraphically lower andesite flow (QW10-3) give a mean age of 760 ± 8 ka, whereas four fusions of the stratigraphically younger basaltic andesite flow (QW10-10) give 756 ± 37 ka. Eight of the nine laser fusion analyses have overlapping 1σ errors and these eight are within 1σ error of K-Ar ages from the groundmass and whole-rock aliquots. The mean age (weighted by inverse of σ<sup>2</sup>) for 8 analyses from QW10-3 is 763 ± 5 ka and the 7 analyses from QW10-10 give 762 ± 8 ka (Fig.). Four laser fusion analyses of plagioclase from QW10-3 give 786 ± 20 ka and two from QW10-10 give 754 ± 22 ka. Four other plagioclase aliquots give ages from 13 to 92 Ma, suggesting presence of a xenocrystic contaminant in these two lavas.



As most plagioclase, whole-rock, and groundmass ages overlap within error, the groundmass plus whole-rock ages (Fig.) are interpreted as the time of extrusion. The only other *direct* date of BMB lavas is from Hawaii, where the <sup>40</sup>Ar/<sup>39</sup>Ar incremental heating age of three whole rocks is 783 ± 11 ka<sup>1</sup>. Although younger than the Hawaiian age by 2.6%, our ages agree with new <sup>40</sup>Ar/<sup>39</sup>Ar laser fusion ages from sanidines that *bracket* the BMB between 790 and 760 ka<sup>2</sup>. The VGP for Hawaiian samples centers on eastern South America, thus two different "long-lived" dipolar orientations of the geomagnetic field<sup>3</sup> may have been occupied at slightly different times during this polarity transition.

<sup>1</sup>Baksi A.K., et al. (1992) *Science*. 256:356-357.

<sup>2</sup>Izett G.A., and O'Bradovich J.D., *J. Geophys. Res.* (in press).

<sup>3</sup>Hoffman A.K. (1992) *Nature*. 359:789-794.

**OBDUCTED MARGINS OF A CARIBBEAN PLATEAU: EVIDENCE FROM  $^{40}\text{Ar}$ - $^{39}\text{Ar}$  AGES AND TRACE ELEMENT CHEMISTRY FOR AN OCEANIC FLOOD BASALT PROVINCE**

**SINTON, C.W.** and **DUNCAN, R.A.**, COAS, Oregon State University, Corvallis, OR 97331; csinton@oce.orst.edu

The anomalously thick oceanic crust beneath the Caribbean Sea appears to be the remnant of an oceanic plateau wedged between the North and South American plates. Tectonically uplifted margins of this feature provide an opportunity to investigate the volcanic stratigraphy, structure, and composition of this province. Here we present evidence that mafic rock suites from the Dumisseau Formation of Haiti, Curacao, the Western Cordillera of Colombia, Gorgona Island, and the Nicoya Peninsula of Costa Rica are cogenetic, using  $^{40}\text{Ar}$ - $^{39}\text{Ar}$  ages and new and published trace element data sets.

$^{40}\text{Ar}$ - $^{39}\text{Ar}$  ages from Curacao, Haiti, Gorgona Island, and Costa Rica range from 88-90 Ma. These ages are in accord with the Coniacian to Early Campanian fossil ages of the sediments that overlie the Caribbean crust. The radiometric ages further indicate that eruption occurred simultaneously over a wide area and during a relatively short time period, similar to continental flood basalt volcanism.

Trace element patterns indicate at least three magma types within the Caribbean province. The lavas of the Western Cordillera of Colombia, the Nicoya Peninsula, and Curacao are uniform in trace element composition, having slightly enriched signatures and flat to almost flat REE patterns ( $\text{La}/\text{Yb} \sim 1.5$ ). Some tholeiitic basalts from Gorgona Island and a single sample from the Venezuela Basin are also included in this lava type. Lavas from the Nauru Basin and the Ontong Java Plateau are almost identical to this lava type in terms of trace elements. A LREE enriched lava type is typical of the upper stratigraphy of the Dumisseau Formation of Haiti and of the Beata Ridge (DSDP site 151). Komatiites and associated tholeiitic basalts from Gorgona Island have LREE-depleted patterns, similar to a single sample from the Colombian Basin. A lack of data from the Caribbean crust inhibits a more definite comparison between the submarine and the on-land portions of the plateau.

Together, the ages and the trace element data support the existence of an oceanic plateau forming the core of the Caribbean plate. The formation of the plateau was cataclysmic, occurring over a relatively short time period. Lavas bear the signatures of both an enriched and a depleted mantle source. Plate reconstructions indicate that the plateau could have formed over the present position of the Galapagos hotspot, providing a possible source for an enriched component.

**Nd-ISOTOPE SYSTEMATICS OF THE DUN MOUNTAIN OPHIOLITE: REASSESSMENT OF ITS ORIGIN AND IMPLICATIONS FOR MANTLE WEDGE PROCESSES DURING A BACK-ARC TO NASCENT ARC TRANSITION**

**SIVELL, W.J.**, Chemistry Department, University of Western Sydney, Nepean, Kingswood 2747, Australia, and **McCULLOCH, M.T.**, Research School of Earth Sciences, The Australian National University, Canberra 2601, Australia

Initial  $^{143}\text{Nd}/^{144}\text{Nd}$  ratios are reported for early Permian and latest Carboniferous igneous rocks which comprise three discrete, sequentially emplaced magmatic suites within the northern Dun Mountain Ophiolite belt (DMOB), New Zealand. Stage 1 pillow basalts ( $\epsilon_{\text{Nd}}(\text{T}) = +6.3$  to  $+7.5$ ) and Stage 2 basalt flows ( $\epsilon_{\text{Nd}}(\text{T}) = +8.4$ ) possess the chemical characteristics of incompatible element enriched and depleted back-arc basin basalts (BABB) respectively. Stage 3 basic to silicic intrusives have refractory mineralogies and high uniform initial  $^{143}\text{Nd}/^{144}\text{Nd}$  ratios ( $\epsilon_{\text{Nd}}(\text{T}) = +9.3 \pm 0.2$ ) over a wide range of  $^{147}\text{Sm}/^{144}\text{Nd}$  (0.29-0.17) including values which exceed those of MORB. They possess pronounced subduction-related geochemical signatures like island arc tholeiites from immature arcs but are isotopically more depleted than the preceding back-arc eruptives which contain a substantial enriched asthenospheric component similar to that in ocean island basalts (OIB).

Regression analysis of the Sm-Nd isotopic data only for the Stage 3 ophiolitic rocks yields a precise age of  $278 \pm 9$  Myr. (MSWD = 0.15), in agreement with the generally inferred early Permian age of the DMOB. Sm-Nd isotopic measurements for exclusively Stage 2 basalts suggest an older, albeit less precise, latest Carboniferous age of  $295 \pm 48$  Myr. (MSWD = 0.48) for the strictly oceanic-crust portion of the ophiolite. The inclusion of data for a clinopyroxene-rich ferrogabbro cumulate from the Stage 2 suite extends the range of Sm/Nd values and provides an even older but precise age of  $308 \pm 12$  Myr. (MSWD = 0.12). The back-arc seafloor and nascent arc rocks of the DMOB which we recognize should be considered as temporally discrete ophiolite components.

Island arc basalts typically have lower initial  $^{143}\text{Nd}/^{144}\text{Nd}$  ratios than either MORB or proximal BABB because slab-modification of supra-subduction zone (SSZ) mantle wedge regions often masks Nd-isotope evidence of previous significant wedge depletion, otherwise indicated by ratios between non-slab derived incompatible elements. However, subduction of young and relatively sediment-free ocean crust caused a minimal decrease in Nd-isotope values of the ophiolitic Stage 3 nascent arc magmas, enabling a more accurate assessment of intrinsic mantle wedge isotopic depletion.

The ophiolite implies a model for the general depletion of sub-arc SSZ mantle wherein preferential extraction of low-melting OIB-like mantle material at back-arc spreading centres prevents replenishment of the wedge apex in these upwelling enriched asthenospheric components, at the same time generating an increasing volume of highly depleted mantle (HDM) residual after BABB removal. In the sub-arc region continuous melting of this HDM is promoted by influx of slab-derived fluids.

**GEOCHRONOLOGY AND CRUSTAL EVOLUTION OF THE ARCHAEOAN BELOMORIAN (WHITE SEA) AND NORTH-SWEDISH HIGH-GRADE TERRAINS OF THE FENNOSCANDIAN (BALTIC) SHIELD**

SKIÖLD, T., Museum of Natural History, S-104 05 Stockholm, Sweden, BIBIKOVA, E., Vernadsky Inst. of Geochem. and Analytical Chemistry, 117334 Moscow, Russia, and BOGDANOVA, S., Lund University, S-22362 Lund, Sweden

The granite-greenstone Karelian Province of the Fennoscandian (Baltic) Shield is bordered to the northeast, north and northwest by high-grade metamorphic terrains of the Belomorian (White Sea) and North-Swedish regions. Here we combine new U-Pb zircon data with petrogenetic Nd-isotope systematics which permit us to model the crustal evolution of these terrains.

According to Nd-isotope data, both the Belomorian and the North-Swedish Archaean crust were formed no earlier than 3.0 Ga ago. This age limit is based on the calculation of maximum crustal residence ages involving a depleted mantle source.

The earliest metamorphic event recognized in these areas occurred  $2.85 \pm .05$  Ga ago (low pressure amphibolitic and granulitic conditions) and was followed by the emplacement of tonalites at 2.80-2.75 Ga.

However, the main phases of igneous and metamorphic activity took place 2.7-2.6 Ga ago. Within that time interval the intrusion of gabbros (2.69 Ga), diorites (2.67 Ga) and granites (2.58 Ga) took place. In the Belomorian, the 7-9 kbar metamorphism was accompanied by temperatures decreasing gradually from granulitic to amphibolitic conditions. The PT-regimes for the North-Swedish Archaean rocks are less well known.

The high-pressure metamorphism and its relatively short duration together with certain trace element distributions in the ortho-gneisses are taken to imply collisional conditions.

Our results indicate that the early 3.0-2.8 Ga stages of crust formation in the Belomorian and the North-Swedish areas coincide in time with those of the Karelian province. However, when it comes to the time after 2.7 Ga, the metamorphic and magmatic records are different. Thus it is inferred that the Karelian granite-greenstone province represented a stable craton during the latest Archaean. Along its northeastern, northern and northwestern margins, however, high-grade metamorphic belts were formed.

**GEOCHEMISTRY AND Sr, Nd, Ar ISOTOPE SYSTEMATICS OF HAITIAN K/T TEKTITES AND CHICXULUB IMPACT MELT.**

SMIT, J., BEETSMA, J.J., VONHOF, H.B., PRINGLE, M. J. and WIJBRANS, J.R., Dept. of Earth Sciences, Vrije Universiteit, 1081 HV, Amsterdam, the Netherlands, M. GRAJALES N., Inst.Mex.Petr.Apart. 14-805, 07730 Mexico d.f.

(Trace) elements and Sr, Nd isotope ratios were measured from Cretaceous/Tertiary (K/T) tektites from Beloc (Haiti) and impact melt from the Chicxulub crater. In addition  $^{40}\text{Ar}/^{39}\text{Ar}$  ages from black glass tektites from Beloc were determined. Some black glass tektites contain schlieren with high P content, derived from Ca-phosphate grains partially absorbed in the otherwise homogeneous tektite glass. This suggests, in combination with earlier determined high  $\text{P}_2\text{O}_5$  contents in augite from K/T microkrystites of Shatsky Rise (Pacific), the presence of phosphorite in the carbonate cap of the Chicxulub target rocks in Yucatan.

The Sr and Nd isotopic ratios of Haitian black glass tektites and a sample of hybrid impact basement melt (Y6-N17) are relatively unradiogenic. Both samples are further characterized by elevated Sr and intermediate Nd contents (~500ppm and ~20ppm respectively). The observed compositions have been modelled using binary mixing models involving estimates for the isotopic signatures of lithologies occurring in the Chicxulub area, including a 3 km thick(Late) Cretaceous carbonate platform underlain by Paleozoic siliciclastics. The unradiogenic component was thought to be represented by carbonates(phosphorites) rather than by mafic volcanics, because the latter are not described from and are not expected in the Chicxulub target rocks. The REE patterns of carbonate under- and overlying the tektites at Beloc, show a strong Ce depletion, indicative for precipitation from Pacific Ocean water. Assuming the carbonates(phosphorites) at Yucatan were also precipitated from Pacific water, we expect an unradiogenic signature in the Yucatan carbonates. The modelling suggests that in both samples (tektites and melt) a relative high proportion of unradiogenic carbonates (60-90%) have been mixed with the siliciclastics of the Yucatan basement.

	$^{87}\text{Sr}/^{86}\text{Sr}[65\text{Ma}]$	$^{143}\text{Nd}/^{144}\text{Nd}[65\text{Ma}]$
Haitian black glass	0.708446	0.512425
Y6N17 impact melt	0.708612	0.512307
Cretaceous carbonate	0.7075 (1000ppm)	0.51255 (8.8ppm)
Paleozoic schists	0.7429 (102ppm)	0.511984 (38ppm)

Replicate step heating  $^{40}\text{Ar}/^{39}\text{Ar}$  experiments (8 single tektite grains) yielded a weighted mean age of  $65.28 \pm 0.41$  Ma (1 $\sigma$ , 83 steps used out of 91). This error includes a 0.3% error in J. Taylor Creek Rhyolite sanidine 85G003(age 27.92 Ma) used as a flux monitor. Fish Canyon biotite irradiated in the same rabbit yielded an age of  $28.09 \pm 0.12$  Ma. Our results agree with previously reported ages for Beloc tektites and confirm the age of the K/T boundary.

## CONTINENTAL LITHOSPHERIC SOURCES FOR KIMBERLITE MAGMATISM

SMITH, CRAIG B., Bernard Price Institute (Geophysics), University of the Witwatersrand, WITS 2050, South Africa

The mantle reservoir(s) that serve as sources for kimberlite magmatism are unlikely to be located in plumes, the transition zone or shallow continental lithosphere, given the complex age distribution of Mesozoic kimberlites and related rocks in southern Africa, their bimodal isotopic character, petrologic constraints on melting depths, and the general restriction of kimberlites to continental areas. The Sr, Nd and Pb isotopic characteristics of kimberlite are of two main types, one being similar to slightly depleted OIB-like mantle (Group I) and a second characterized by ancient enrichment in LIL elements (Group II). Most kimberlites, however, also have a significant lithospheric (?) component incorporated during emplacement that to some degree masks the isotopic signature of the pristine source.

The subcalcic, Cr-poor discrete nodule assemblages, ubiquitous in Group I kimberlites and now known from a few Group II localities, have isotopic characteristics closely akin to host kimberlites and must either be cognate (prior to modification and evolution of the melt) or representative of discrete melts derived from the same source. Hence, Sr, Nd, and Pb isotopes in the megacrysts reflect HIMU character for Group I kimberlite sources. The occurrence of this signature in megacryst suites throughout southern Africa is not easily reconciled with hotspot origins for kimberlite, given the limited distribution of HIMU in South Atlantic plumes. The source is more likely resident in subcontinental 'tectosphere' that is substantially thicker than the circa 180-200 km currently accepted from petrologic studies of xenoliths but consistent with other lines of evidence.

Group II kimberlites represent the enriched end of a spectrum of source isotopic compositions in the African subcontinental lithosphere, with some off-craton southern African kimberlites, Brazilian kimberlites and carbonatites, and some components of east African carbonatites having intermediate isotopic character. Hart et al. (1986) originally called such a continuum of compositions defined from oceanic rocks the LoNd array, and suggested residence within subcontinental lithosphere. In southern Africa kimberlites and related rocks have tapped this reservoir in the continental setting. The occurrence of these compositions within deep subcontinental lithosphere provides support for the possibility that the DUPAL signature in some South Atlantic plumes may result from mixing of OIB sources with delaminated continental lithosphere stranded during Gondwana breakup.

Hart, S.R., Gerlach, D.C. and White, W.M., 1986, A possible new Sr-Nd Pb mantle array and consequences for mantle mixing: *Geochim. Cosmochim. Acta* 50, 1551-1557

## A COMBINED ISOTOPIC AND TRACE ELEMENT APPROACH TO DISCRIMINATING GROUNDWATER FLOW-PATHS

Smith, David K., Davisson, M.L., Volpe, A.M., Nuclear Chemistry Division, Lawrence Livermore National Laboratory, Livermore, CA 94550, Whittemore, D.O., Macfarlane, P.A., Kansas Geological Survey, Lawrence KS 66047, Niemeyer, S., Kenneally, J.M., Beiriger, J.M., Lawrence Livermore National Laboratory

Regional studies of groundwater flow at the Nevada Test Site (NTS) and in the Dakota Aquifer in western and central Kansas emphasize the validity of multiple element and isotope applications in resolving disparate waters that have mixed, discriminating water-rock and redox reactions within a complex hydrostratigraphy and establishing reliable chronometers to trace groundwater flow. Isotopic and trace element discrimination of unique end-members is required to interpret groundwater ages and the sources of recharge. Dissolved  $^{87}\text{Sr}/^{86}\text{Sr}$ ,  $^{36}\text{Cl}/\text{Cl}$ ,  $^{14}\text{C}$ , REE, transition metal, alkali and alkaline earths, halogens and actinides supplemented by analysis of major cations and anions are measured in concert from a single sample. The combined approach is important because hydrologic relations within these aquifers are complex and interpretation based exclusively on one tracer is likely to be ambiguous; as well, the independent tracers and chronometers serve as cross checks on one another.

At NTS, older (> 40,000 year apparent age) groundwaters produced from the regional Paleozoic carbonate aquifer are enriched in  $^{87}\text{Sr}/^{86}\text{Sr}$  (0.7140-0.7150), Sr (600-800  $\mu\text{g}/\text{L}$ ) and  $\text{HCO}_3^-$  (400-500  $\text{mg}/\text{L}$ ) and depleted in  $^{36}\text{Cl}/\text{Cl}$  ( $1-3 \times 10^{-13}$ ) relative to younger (<20,000 year apparent age) waters derived from overlying Tertiary volcanic and volcanoclastic alluvial aquifers. Higher bicarbonate concentrations track proportional increases in elemental and radiogenic Sr apparently derived from dissolution of Paleozoic carbonates. Lower  $^{36}\text{Cl}/\text{Cl}$  ratios for the carbonate waters confirms the presence of a "dead" chloride source in the Paleozoic rocks. The dissolution of Paleozoic carbonates has a major influence on the resulting  $^{14}\text{C}$  atom abundance in groundwater and age correction models. REE analyses of NTS spring waters are controlled both by Eh and host rock signature. Spring waters discharging from silicic Tertiary aquifers yield evolved, fractionated chondrite normalized patterns in contrast to spring waters in possible connection with the regional Paleozoic aquifer which exhibit flat chondrite normalized REE patterns and negative Ce and no Eu anomalies.

In Kansas, isotopic and elemental analysis of shallow groundwater collected along a 500km transect of the Dakota aquifer from southeastern Colorado to central Kansas indicates that a systematic modification of the groundwater chemistry is controlled by the flow system. Southwest of the Arkansas River, young (<15,000 year apparent age) oxidized water is associated with shallower depths and unconfined local flow systems where dissolved  $^{87}\text{Sr}/^{86}\text{Sr}$  (0.7094-0.7088),  $^{36}\text{Cl}/\text{Cl}$  ( $10-15 \times 10^{-13}$ ), Cr (0.01-0.3  $\mu\text{g}/\text{L}$ ) and U (7-25  $\mu\text{g}/\text{L}$ ) are relatively enriched. Northeast of the Arkansas River, older (15,000-40,000 year apparent age) and chemically reduced waters are associated with a confined, intermediate-scale flow systems within the Dakota aquifer; these waters are enriched in  $\text{HCO}_3^-$  (300-550  $\text{mg}/\text{L}$ ),  $\text{NH}_4^+$  (0.5-1.8  $\text{mg}/\text{L}$ ) and  $\text{Cl}^-$  (17-1400  $\text{mg}/\text{L}$ ) and are depleted in elemental and radiogenic Sr (Sr: 60-500  $\mu\text{g}/\text{L}$ ,  $^{87}\text{Sr}/^{86}\text{Sr}$ : 0.7080-0.7086) and  $^{36}\text{Cl}/\text{Cl}$  ( $0.01-8.0 \times 10^{-13}$ ). Ion exchange and carbonate equilibria are major controls on Sr and  $\text{HCO}_3^-$  concentrations respectively. The confined flow system is laterally recharged by water from the southwest which flows beneath the Arkansas River Valley; lower  $^{87}\text{Sr}/^{86}\text{Sr}$  and higher Cl/Br ratios (1700-8500) are indicative of deeper Permian saltwaters that migrate upwards by diffusion and discharge into the base of the Dakota aquifer. *Work performed under the auspices of the U.S. Department of Energy by the Lawrence Livermore National Laboratory under Contract W-7405-Eng-48.*

CRETACEOUS PARK:  $^{40}\text{Ar}$ - $^{39}\text{Ar}$  AGES FROM MESOZOIC LACUSTRINE BASINS, NORTHEAST CHINA

SMITH, Patrick E., EVENSEN, Norman M., YORK, Derek., Dept. of Physics, University of Toronto, Toronto, Ontario, Canada, M5S 1A7 and RUSSELL, Dale, CUMBAA, Stephen, Canadian Museum of Nature, P.O. Box 3443, Station 'D', Ottawa, Ontario, Canada, K1P 6P4

Freshwater sediments contained in small geographically restricted, fault-bound basins are often difficult to correlate globally. The middle Mesozoic Rehe Group, Liaoning, northeastern China is a notable example, being attributed to both the Jurassic and Cretaceous periods, based both on biochronology, and K-Ar and Rb-Sr geochronology. Precise dating of the Rehe sediments is particularly important because it provides a time-frame for the end of the tectonic isolation of Asia from the other continents. Thus, Mesozoic tectonics in northeast China influenced the balance between endemic and exotic taxa which represent important links for understanding the evolution of vertebrates, including dinosaurs, fish and birds, and the development of flowering plants.

To precisely constrain the age of the Rehe sediments, we have used the laser  $^{40}\text{Ar}$ - $^{39}\text{Ar}$  technique on single basaltic and andesitic whole-rock chips, complemented with analyses of minerals where possible, from volcanic horizons intercalated with lacustrine sediments, primarily from the Yixian Formation. Consecutive linear segments on plots of  $^{39}\text{Ar}/^{40}\text{Ar}$  vs.  $^{36}\text{Ar}/^{40}\text{Ar}$ , representative of gas fractions taken at intermediate temperatures, give well-defined isochron ages. A basalt from the Yixian Formation near the base of the Group gives an age of  $125.4 \pm 0.2$  Ma, whereas an andesite from the overlying Jiufotang Formation gives  $121.7 \pm 0.4$  Ma. Ages from intervening horizons are, within their uncertainties, in sequential agreement with these enclosing strata. Three dimensional plots of data from all gas fractions, where either  $^{37}\text{Ar}/^{40}\text{Ar}$  or  $^{38}\text{Ar}/^{40}\text{Ar}$  is considered in conjunction with the standard isochron plot, yield complex but often reproducible patterns.

The age control provided by the dates on the volcanic intercalations allows the significance of apparent ages measured on the intervening lacustrine sediments themselves to be tested. Some of these samples yield very good isochrons yet give apparent ages which are significantly younger than the primary ages. These ages ( $110.3 \pm 0.2$  Ma) may signify alteration events.

These results show that the lower half of the Rehe Group, with its characteristic fauna of endemic fish, dinosaurs and other taxa, was deposited within a short time interval of 3-4 Ma during the lower Cretaceous and contains no strata of Jurassic age.

LEAD ISOTOPIC COMPOSITIONS IN PARTICULATE AEROSOLS AND BLOOD OF SAN FRANCISCO AREA RESIDENTS: IMPLICATIONS FOR SOURCES OF LEAD EXPOSURE

SMITH, D.R. and OSTERLOH, J., Laboratory Medicine, University of California, San Francisco CA 94110, NIEMEYER, S., Nuclear Chemistry, LLNL, Livermore, CA 94550, and FLEGAL, A.R., Environmental Toxicology, University of California, Santa Cruz, CA 95060.

Regulation of lead alkyl additives to gasoline over the past several decades has substantially reduced air lead levels, which has had a positive impact on reducing human lead exposures. However, suspended particulate aerosols may continue to pose an important source of lead exposure to humans due to the resuspension of fine urban dusts contaminated with lead, and continued emissions from non-regulated sources. Here we measured the stable lead isotopic compositions and lead concentrations in blood from eight adults, and in suspended particulate ( $> 0.44 \mu\text{m}$ ) aerosols and tap water from several locations in the San Francisco area to evaluate whether suspended particulate aerosol lead was measurably contributing to the blood lead levels of area residents. The isotopic compositions of lead in blood of the eight individuals were similar to one another (range in  $^{207}\text{Pb}/^{206}\text{Pb} = 0.8418 - 0.8479$  and  $^{208}\text{Pb}/^{206}\text{Pb} = 2.058 - 2.070$ ,  $\pm 0.07\%$  2RSE typical measurement error) and overlapped somewhat with the range in isotopic compositions of the particulate aerosols ( $^{207}\text{Pb}/^{206}\text{Pb} = 0.8340 - 0.8454$  and  $^{208}\text{Pb}/^{206}\text{Pb} = 2.043 - 2.064$ ,  $\pm 0.07\%$  2RSE). Tap water samples were similar but more variable in isotopic compositions, and were also uniformly low in lead concentrations ( $< 1\text{ng/mL}$ ). These preliminary data suggest that particulate aerosol lead, or isotopically similar lead from additional sources (e.g., soil dusts) continues to measurably contribute to the blood lead levels of environmentally lead-exposed humans in the San Francisco area. The differences in blood isotopic compositions likely reflects varying exposures to other lead sources with different isotopic compositions.

## THE USE OF Sr ISOTOPIC STRATIGRAPHY TO DATE ABYSSAL PERIDOTITE ALTERATION

SNOW, J. E., and FRANCE-LANORD, C. CNRS /  
Centre de Recherches Pétrographiques et  
Géochimiques, 15 rue Notre Dame des Pauvres, BP  
20, 54501 Vandœuvre Cedex, FRANCE.  
jesnow@crpg.cnrs-nancy.fr

Abyssal peridotites are fragments of the oceanic mantle which have been transported to the sea floor by tectonic processes. They are typically serpentinized (60-100%) and often heavily weathered. The weathering process in abyssal peridotites commonly deposits large amounts of seawater-derived Sr in the peridotite. In the sample suite studied here, the seawater Sr reservoir accounts for up to 400 times the amount of Sr derived from the mantle. This Sr is typically hosted in aragonite (Thompson, et al., 1972) deposited late during the process of weathering of the peridotite at low temperature.

This study uses the high-precision record of the secular variation of  $^{87}\text{Sr}/^{86}\text{Sr}$  in the oceans to estimate weathering ages of abyssal peridotites from 0-20 million years of age. Age estimation at this level (about  $\pm 1$  ma) for the oceanic crust will be useful in cases where the magnetic record is difficult to interpret, or where the tectonic setting of an individual dredge haul is ambiguous.

This approach entails several potential problems. First, the contribution of mantle-derived Sr from clinopyroxenes must be assessed. In the worst case scenario, this could account for a significant deviation in the true and apparent ages. In the typical case, however, the incorporation of all mantle-derived Sr into the carbonate fraction does not result in a significant change in the apparent age. Second, the contribution of Sr from entrained detrital sediments must be considered (Snow, et al., 1993). Once again, the worst-case scenario could cause a significant shift in apparent age, but in the typical case this contribution is insignificant. Third, the bottom water from which the peridotite aragonite is precipitated must be representative of ocean waters generally. Lastly, the aragonite must have formed relatively quickly after the exposure of the peridotite. If the carbonate is deposited over a long time, then the resulting "age" will be difficult to interpret. In regions where the crustal age is well-determined, such "too young" ages would constrain the interval of formation of the aragonite, and thus the duration of alteration of the peridotite.

Thompson, G. (1970) A geochemical study of some lithified carbonate sediments from the deep sea. *Geochimica et Cosmochimica Acta* 36:1237-1253.

Snow, J, S. Hart and H. Dick (1993) Orphan  $^{87}\text{Sr}$  in Abyssal Peridotites: Daddy was a Granite, *Science* December, 1993.

## A TECHNIQUE FOR THE EXTRACTION OF O-18 FROM MICROLITER QUANTITIES OF WATER

SOCKI, R.A., Romanek, C.S., and Gibson,  
E.K., Jr., LESC and SN-4, NASA Johnson  
Space Center, Houston, TX 77058, USA.

As part of NASA's ongoing study to examine the O and H isotopes from hydrous minerals associated with Antarctic meteorites, we are currently developing a technique to extract microliter quantities of water for O-18 analysis. The need also exists for a routine O-18 extraction method of analysis for water from fluid inclusions, structural water within hydrous minerals, and for use in doubly labeled water tracer studies in the medical sciences. Furthermore, eliminating the need for potentially dangerous and costly reagents ( $\text{BrF}_5$  [1] and Guanadine-HCl [2]) associated with micro-analytical extraction techniques, is desirable. Our method is based on the traditional  $\text{CO}_2\text{-H}_2\text{O}$  equilibration technique [3]. Others have attempted  $\text{CO}_2\text{-H}_2\text{O}$  equilibration on a microliter-size sample scale [4]. The method described here involves a reaction carried out exclusively in 6mm pyrex tubes which, after  $\text{CO}_2\text{-H}_2\text{O}$  exchange is complete, are immediately attached to the inlet of the mass spectrometer for analysis.

Pyrex tubes (6mm O.D.), stored in an oven at  $80^\circ\text{C}$ , are attached to a small vacuum line consisting of both a  $\text{CO}_2$  reservoir and a sample tube septum port. After pumping to high-vacuum  $25\mu\text{l}$  of  $\text{CO}_2$  is expanded into the sample tube and septum port. 10 to  $20\mu\text{l}$  of  $\text{H}_2\text{O}$  are then injected via the septa with an air tight  $100\mu\text{l}$  syringe.  $\text{H}_2\text{O}$  and  $\text{CO}_2$  are frozen in the bottom of the tube for 3 min., sealed with a torch and placed in a furnace held at  $180^\circ\text{C} \pm 0.5^\circ\text{C}$  for 48 hrs. Sample tubes are then removed from the furnace and attached to a tube cracker on the inlet of an isotope ratio mass spectrometer (IRMS). After freezing the  $\text{H}_2\text{O}$  with a dry ice alcohol mixture,  $\text{CO}_2$  is admitted to the IRMS for O-18 analysis.

The method described here will allow for the routine measurement of microliter quantities of water without extensive extraction procedures. Routine analysis of a laboratory working water standard is reproducible to  $\pm 0.6$  per mil using this technique. International standards V-SMOW, GISP, and SLAP will be analyzed to determine the accuracy of this method.

### References:

- [1] O'Neil, J.R. and S. Epstein, *JGR* 1966,71,4955,
- [2] Wong, W.W. et al., *Anal Chem* 1987,59,690,
- [3] Epstein, S. and T. Mayeda, *GCA* 1953,4,213,
- [4] Kishima, N. and H. Sakai, *Anal Chem* 1980,52,356

**PALAEOCEANOGRAPHY WITH  $^{10}\text{Be}$**   
**B.L.K.SOMAYAJULU, Physical Research**  
**Laboratory, Navrangpura, Ahmedabad**  
**380 009, India**

Cosmic Rays interact with the earth's atmospheric constituents viz.  $\text{N}_2, \text{O}_2, \text{Ar}$  etc. producing a variety of radionuclides with varying half lives of which beryllium-10 (half life=1.5 m.y) is an important one. Its congenial sea water chemistry, and the high sensitivity of its measurement in natural samples achieved through Accelerator Mass Spectrometry makes beryllium-10 a potential tracer to decipher meltwater flooding of the oceans during interglacial times.

The basic philosophy behind this application is that the most concentrated solution of beryllium-10 on earth is rain and snow/ice and the latter accumulated for long periods during glacial times. During interglacial periods the ice/snow-meltwater containing high beryllium-10 content flooded the ocean and the beryllium-10 spike got removed by the detrital material, principally clays (that are enriched Al) transiting through the water column to form the sediment in times shorter compared to the mixing time of the ocean (ie.  $\times 10^3$  years). To be able to establish this method, one should look for oceanic areas which were subjected to intense meltwater flooding in the past and measure beryllium-10 and Al in their sediments as a function of  $\delta^{18}\text{O}$  which happens to be the prime indicator of meltwater inputs.

This is done in the Gulf of Mexico sediments and a strong negative correlation ( $r=-0.95$ ) between  $\delta^{18}\text{O}$  (range  $-1.5$  ‰ to  $0.8$  ‰) and the beryllium-10/Al is obtained. Similarly beryllium-10/Al measurements were made in cores from the Mediterranean sea and the Arctic and are compared with  $\delta^{18}\text{O}$  in nearby ones. The results are encouraging.

**SHRIMP ISOTOPE STUDIES OF GRANULITE ZIRCONS AND THEIR RELEVANCE TO EARLY PROTEROZOIC TECTONICS IN NORTHERN FENNOSCANDIA**

**SORJONEN-WARD, Peter**, Geological Survey of Finland, 02150, Espoo, Finland, **CLAOUÉ-LONG, Jon**, Research School of Earth Sciences, Australian National University, Box 4, Canberra 2601, Australia, and **HUHMA, Hannu**, Geological Survey of Finland, 02150, Espoo, Finland.

The Fennoscandian Shield of northeastern Europe can be divided into three broad tectonic domains. The Svecofennian domain in the southwest of the shield consists essentially of juvenile crust formed rapidly at 1.9-1.8 Ga, while the Kola domain in the northeast represents a mosaic of Archean and Proterozoic elements amalgamated at some time between 2.0 and 1.8 Ga. These two domains are separated from one another by the intervening 3.1-2.7 Ga Karelian craton, which formed a stable platform for terrestrial to shallow marine sedimentation and predominantly mafic to ultramafic volcanism throughout much of the early Proterozoic.

Through much of northern Finland, the boundary between the Karelian craton and the Kola domain is represented by a thick low-angle thrust system that has emplaced a highly strained, predominantly felsic granulite complex over a lower to middle greenschist facies mafic volcanic sequence. An U-Pb zircon age of 1.93 Ga for plutonic rocks intruded prior to deformation constrains the maximum age of thrusting of the granulite complex, while a nearly concordant 1.91 Ga monazite age, along with the abrupt decrease in metamorphic grade away from the thrust zone, is thought to imply that emplacement, uplift and erosion of the granulites was a relatively rapid process. Whole-rock Sm-Nd data and some conventional zircon data also suggest that the sedimentary protoliths to the granulites were formed during the early Proterozoic, instead of being derived from an Archean-dominated provenance.

In order to obtain more precise information on provenance ages, as well as metamorphic and uplift history, a sample having a monazite age of 1.91 Ga, conventional U-Pb ages based on a poorly defined chord extrapolating to an intercept between 2.02 and 2.14 Ga, and whole-rock Sm-Nd  $T_{(DM)} = 2.24$  Ga with  $\epsilon_{(1900)} = -2.4$ , was chosen for analysis using the SHRIMP in Canberra. The age spectrum for 48 zircons has a mode close to the conventional age estimate, around 2.0 Ga. In some cases these ages were recorded from cores, with distinct overgrowths having ages nearer to 1.9 Ga. Whether or not these rims are metamorphic in origin is a problem requiring careful assessment and interpretation of zircon morphology, since SEM data also suggest rounded, relict detrital surfaces. Nevertheless, the data clearly indicate that the Lapland granulite protoliths were deposited, metamorphosed and exhumed relatively rapidly, rather than representing older lower crust uplifted and exposed during a significantly younger orogenic event.

**THERMOCHRONOLOGY OF A METAMORPHIC CORE COMPLEX ASSOCIATED WITH THE BREAKUP OF GONDWANA: THE PAPAROA RANGE, SOUTH ISLAND, NEW ZEALAND**

**SPELL, T. L., MCDUGALL, I.** (Research School of Earth Sciences, The Australian National University, Canberra, ACT 0200, Australia), and **TULLOCH, A. J.** (Institute of Geological and Nuclear Sciences, PO Box 30368, Lower Hutt, New Zealand)

Continental extension during the breakup of Gondwana in the late Cretaceous produced a metamorphic core complex preserved in the Paparoa Range on South Island, New Zealand. Most features typical of Cordilleran core complexes are present including high metamorphic grade lower plate, or core, rocks (amphibolite facies gneisses), low grade upper plate rocks (lower greenschist facies metasediments), syntectonic granitic intrusions and volcanism, low angle mylonite zones (detachments) indicating extensional deformation which separate lower from upper plate rocks, and thick sequences of subaerial breccias and conglomerates.

K/Ar ages for muscovite, biotite and K-feldspar (recording cooling through the  $-400-180$  °C interval) from lower plate rocks (ortho- and paragneisses of the Charleston Metamorphic Group, Buckland and Foulwind Granites) are generally restricted to the range  $\sim 95-105$  Ma. In contrast to results from core rocks, Paleozoic granites (Barrytown and Meybillie) which intrude the upper plate metasedimentary rocks record extended cooling histories ( $>200$  Ma) beginning in the early Carboniferous to Permian and ending in the Cretaceous.  $^{40}\text{Ar}/^{39}\text{Ar}$  age spectra from hornblende, muscovite, biotite and K-feldspar from lower plate rocks (recording cooling from  $\sim 500-130$  °C) are relatively flat and nearly concordant with ages of  $\sim 90-110$  Ma.  $^{40}\text{Ar}/^{39}\text{Ar}$  spectra from upper plate granites are discordant both internally and between minerals with differing closure temperatures. Multidomain modelling of argon diffusion from K-feldspars indicates that granites from the lower plate cooled fairly rapid ( $\sim 30$  °C/Ma) from  $\sim 100$  to  $90$  Ma followed by slower cooling ( $\sim 5$  °C/Ma) to  $\sim 75$  Ma. A K-feldspar age spectrum from an upper plate granite (Barrytown Granite) indicates closure of different diffusion domains over an  $\sim 200$  Ma interval with cooling rates of  $\sim 0.1$  °C/Ma from  $\sim 350$  to  $140$  Ma followed by cooling at  $\sim 5$  °C/Ma to  $\sim 125$  Ma. All data thus indicate rapid cooling of core rocks relative to upper plate rocks.

The Pororari Group, subaerial breccias and conglomerates shed from the unroofing granites in the core complex over an  $\sim 15$  Ma interval beginning at  $\sim 113$  Ma, preserve information on the cooling history of the core complex for a substantial interval of time prior to that obtainable from presently exposed lower plate rocks. K/Ar and  $^{40}\text{Ar}/^{39}\text{Ar}$  dating of samples from the Pororari Group indicate rapid cooling rates similar to those of presently exposed lower plate rocks, thus suggesting that rapid unroofing of the core complex was continuous over at least a  $5$  Ma interval.

Combined with published U/Pb and fission-track data these results yield calculated cooling rates (over the temperature interval  $\sim 700-100$  °C) for lower plate rocks ranging from  $15$  to  $75$  °C  $\text{Ma}^{-1}$  (averaging  $\sim 35$  °C  $\text{Ma}^{-1}$ ) whereas those for upper plate rocks are  $5$  to  $0.5$  °C  $\text{Ma}^{-1}$ . Lower plate granites with intrusive ages both in the Paleozoic and Cretaceous yield identical rapid cooling curves around  $100-90$  Ma and estimated unroofing rates of  $\sim 1.5$  mm/a. The change to slower cooling rates around  $90$  Ma as seen in multidomain K-feldspar models is also seen in the combined K/Ar and fission-track data and may record cessation of continental extension and the beginning of seafloor spreading in the Tasman Sea. These data establish a temporal and spatial link between continental extensional tectonics on the Pacific margin of Gondwana, inception of seafloor spreading in the Tasman Sea (oldest crust  $\sim 85$  Ma), and subsequent rifting of New Zealand from Australia and Antarctica.

**PALEOCLIMATE INFORMATION FROM SALT (HALITE) DEPOSITS**

**SPENCER, Ron, YANG, W., ROBERTS, S.,** Dept. Geology and Geophysics, KROUSE, H.R., Dept. of Physics, The Univ. of Calgary, Calgary, Alberta T2N 1N4, Canada; **LOWENSTEIN, T., Li, J.,** Dept. Geol. Sciences, S.U.N.Y. at Binghamton, Binghamton, New York 13901

Many halite crystals contain fluid inclusions that outline primary growth textures and allow interpretations of the depositional environment of the salt to be made. Analyses of these fluid inclusions can also provide data on the temperature of formation of the salts, the major dissolved ion concentrations and stable isotope composition of the surface brines from which the salts precipitated. Some halite crystals that grow at the air brine interface also trap small amounts of air in the fluid inclusions. The gas composition of these fluid inclusions can also be analyzed to provide a record of the composition of the atmosphere in the past. Salt deposits can also be dated by a variety of radiogenic techniques, allowing temporal control of the climate record.

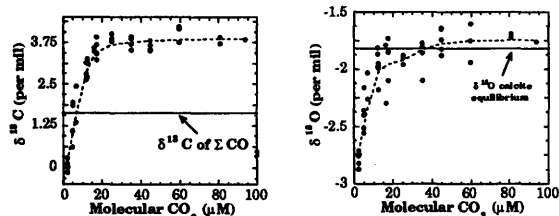
We have obtained climate data from a  $50$  metre core through the salts of the Qaidam Basin, Qinghai-Tibet Plateau, China, covering about  $50$  ka of record. These data indicate warm, but less arid conditions on the plateau from  $50$  until about  $20$  kaBP, with  $\text{CO}_2/\text{N}_2$  in the atmosphere lower than at present. The low atmospheric  $\text{CO}_2/\text{N}_2$  continues until about  $15$  kaBP, and the period from  $20$  to  $15$  kaBP is characterized by colder, but drier conditions on the plateau. The Holocene record indicates warm, dry conditions and higher  $\text{CO}_2/\text{N}_2$  in the atmosphere.

Work is now in progress on a  $180$  metre core from the Badwater Salt Pan, Death Valley, CA. It appears that this core will provide a high quality record of surface temperature, aridity, and stable isotope composition of meteoric inflow for this area.

EFFECT OF  $[CO_{2aq}]$  ON THE CARBON AND OXYGEN ISOTOPE COMPOSITION OF FORAMINIFERAL CALCITE  
 SPERO, H.J., BEMIS, B.E., Dept. of Geology, University of California, Davis CA. 95616, U.S.A., BIJMA, J., Alfred-Wegener-Institut für Polar-und Meeresforschung, P.O. Box 120161, 27515 Bremerhaven, Germany, and LEA, D.W., Department of Geological Sciences, University of California, Santa Barbara CA 93106.

The oxygen and carbon isotopic compositions of foraminiferal calcite are commonly used in paleoceanographic reconstructions of oceanic temperatures, salinities, continental ice volumes, aspects of the ocean's biological pump and shifts in terrestrial and ocean carbon reservoirs. These interpretations are based on empirically derived relationships that relate the isotopic composition of calcite to the parameters in question. A number of environmental (e.g. temperature, salinity, atmosphere-ocean equilibration times, etc.) and physiological (e.g. symbiosis, respiration, calcification rates, etc.) parameters must be considered for accurate reconstructions. Here we describe the results of laboratory experiments which show that the carbon and oxygen isotopic composition of foraminiferal calcite is also a function of the carbonate chemistry of the sea water in which it grew.

During the summer of 1993, the symbiont-bearing planktonic foraminifera, *Orbulina universa*, was grown in the laboratory under high light intensities (maximum photosynthesis) at 22°C in seawater with different  $[CO_{2aq}]$  and  $[CO_3^{2-}]$ . The experimental results show that when alkalinity is kept constant the  $\delta^{13}C$  of the tests increases linearly from approximately 0 to 3.8‰ as  $[CO_{2aq}]$  increases from 2 to 20  $\mu M$  (ambient = 11  $\mu M$ ). Above 20  $\mu M$ , shell  $\delta^{13}C$  remains constant. Across the same  $[CO_{2aq}]$  range,  $\delta^{18}O$  values increase from -2.8 to -1.9‰ and finally stabilize at -1.7‰ at a  $[CO_{2aq}]$  of 45  $\mu M$  ( $\delta^{18}O$  calcite equilibrium = -1.82‰). A clear covariance between  $\delta^{13}C$  and  $\delta^{18}O$  values is observed. In contrast, under conditions of constant pH, the  $\delta^{13}C$  of shell calcite decreases when  $[CO_{2aq}]$  increases above 20  $\mu M$ . In both sets of experiments, the  $\delta^{13}C$  of shell calcite decreases linearly as a function of increasing  $[CO_3^{2-}]$ . We hypothesize that these relationships are a function of both kinetic fractionation and physiological factors such as symbiont photosynthesis.



SULFUR ISOTOPES EVIDENCE FOR SULFATE REMOVAL PROCESSES FROM SUBSURFACE BRINES, HELETZ FORMATION (LOWER CRETACEOUS), ISRAEL

STARINSKY, A., Dept. of Geology, The Hebrew University, Jerusalem, 91904, Israel, SPIRO, B., NERC Isotope Geosciences Laboratory, Keyworth, NG12 5GG, U.K., GAVRIELI, I., Geological Survey of Israel, Jerusalem, 95501, Israel, NIELSEN, H., Dept. of Geochemistry, Gottingen University, Germany and AIZENSHTAT, Z., Department of Chemistry, The Hebrew University, 91904, Jerusalem.

Subsurface brines associated with oil ("oil brines") from four oil fields, Heletz, Brur, Kokhav and Negba, in the southern coastal plain of Israel show a deficiency in  $SO_4$  concentrations compared to brines from dry wells ("dry brines") in the same fields only a few hundred meters away. Both types of brines have  $SO_4/Cl$  ratios lower than seawater or evaporated seawater with the same salinity, the lowest ratio being  $1.9 \cdot 10^{-4}$  (wt. ratio). Previous studies suggested that the brines have evolved from evaporated Miocene seawater, which precipitated the sulfates in the Mavqim Fm. ( $\delta^{34}S = 21.7-22.7‰$ ). The present study shows that the residual brine in the Mavqim Fm. has sulfate with  $\delta^{34}S = 26.4‰$ . The  $\delta^{34}S_{SO_4}$  of the oil brines from the oil producing Heletz Fm. is 30-59‰. The  $\delta^{34}S$  of  $SO_4$  and  $H_2S$  sampled together (two pairs), were nearly identical at about 30‰. The oil has sulfur concentrations of 2-3% with relatively heavy  $\delta^{34}S$  values of +13 to +15‰.

The following overall evolutionary path for these brines was reconstructed on the basis of their sulfate concentration,  $SO_4/Cl$  ratio and  $\delta^{34}S$  in the  $SO_4$ ,  $H_2S$  and the oil.

- (1) Evaporation of a Messinian seawater which led to the precipitation of gypsum.
  - (2) Precipitation of gypsum following dolomitization.
  - (3) Bacterial sulfate reduction.
- Stages (1) through (3) removed some 50% of the initial sulfate content of the brines, changing the sulfate isotopic composition from marine ( $\delta^{34}S \approx 20‰$ ) to  $\approx 26‰$ .
- (4) Migration of the residual brines eastward into the Lower Cretaceous Heletz Fm. and mixing with oil.
  - (5) Bacterial sulfate reduction in the oil reservoir resulting in further decrease in  $SO_4/Cl$  ratio and increase of  $\delta^{34}S$  in the remaining sulfate.
  - (6) Possible secondary enrichment of the oil with sulfur through reaction with the increasingly  $^{34}S$  enriched  $H_2S$  and  $SO_4$ .

The similar sulfur isotopic composition of the coexisting sulfide and sulfate still merits a detailed study.

**ARC INPUT PARAMETERS: LARGE SCALE SR, ND AND O ISOTOPIC ANATOMY AND ABUNDANCES OF REE AND U, K, AND RB OF ALTERED OCEANIC CRUST AT DSDP/ODP SITES 417/418**

STAUDIGEL, H., DAVIES, G. R., Centrum voor Isotopen Geologisch Onderzoek, Faculteit der Aardwetenschappen, Vrije Universiteit, De Boelelaan 1085, 1081 HV Amsterdam, HART, S.R. Woods Hole Oceanographic Institution, Woods Hole MA; K. MARCHANT Scripps Institution of Oceanography, San Diego, CA.

To provide quantitative constraints on one of the major input parameters into magmatic arcs and the chemical transfer between hydrosphere and the mantle, we analysed the O, Sr, and Nd isotope ratios and the abundances of REE, U, K, Rb, and Sr for large scale compositional domains at DSDP/ODP drill Sites 417A, 417D, and 418A. The three sites combined give the large scale composition of the upper 500 m oceanic crust over a distance of about 8 kilometers. We also contrasted the bulk composition of several "average" 10-30 m depth intervals at each site and the composition of different lithologies, including submarine extrusives ("FLO") and volcanoclastics ("VCL").

The  $\delta^{18}\text{O}_{\text{SMOW}}$  and  $^{87}\text{Sr}/^{86}\text{Sr}_{\text{meas}}$  of differently altered compositional domains in the upper ocean crust correlate well with a range of 7.7 - 19.2 and from 0.70364-0.70744, and a mean of 9.96 and 0.70475, respectively. Seafloor alteration increases the Rb inventory of the upper crust by about an order of magnitude and the Sr contents only slightly. U abundances increase moderately under oxidizing alteration conditions and more dramatically during the (more common) reducing conditions. VCLs and 417A samples are the most altered and nearly double the observed range in isotope ratios. The consistency of composite analyses with individual samples from the same site and agreement between composites from two independent sites of similar alteration behavior confirm their fidelity, and the reproducibility. Even though rare earths are relatively little influenced by alteration, K correlates with  $^{143}\text{Nd}/^{144}\text{Nd}$  and La/Sm, negatively and positively respectively, suggesting consistent addition of seawater REE's with increasing alteration. The exchange of REE is minor for the budget of the oceanic crust but important for the oceans.

Even though VCLs and 417A composites are volumetrically a relatively minor component of "normal" oceanic crust, their high volatile and alkali inventory gives them a more important role during dehydration and partial melting reactions. Progressive subduction of oceanic crust is accompanied by chemical modification and dispersion of some of the seafloor-alteration imposed heterogeneity, but much of it will remain, in particular for the subduction of old oceanic crust, at high convergence velocities. Therefore, recycled oceanic crust is expected to be similar to fresh MORB with respect to  $^{143}\text{Nd}/^{144}\text{Nd}$  but with elevated and positively correlating  $\delta^{18}\text{O}_{\text{SMOW}}$  and  $^{87}\text{Sr}/^{86}\text{Sr}$  possibly resembling the EM II component. Nearly horizontal arrays in  $^{143}\text{Nd}/^{144}\text{Nd}$  -  $^{87}\text{Sr}/^{86}\text{Sr}$  correlation diagrams of island arc magmatic systems, may indicate involvement of partial melts from recycled altered volcanoclastics.

**COMPARISON OF ANALYTICAL TECHNIQUES USED IN U-Pb DATING OF ZIRCON**

STEIGER R.H., MEIER M., BICKEL R.A., Isotope geochemistry ETH, Zurich, CH-8092, Switzerland and PIDGEON R.T., School of Applied Geology, Curtin University of Technology, Perth, 6001, Western Australia

Zircon dating has developed into the most accurate and versatile method of geochronology. During the last 25 years a number of analytical improvements have contributed to a reduction of sample requirement by several orders of magnitude. This has led to progress in sample selection and sample preparation allowing the dating of small zircon populations, single grains or of single phases thereof which exhibit specific properties and which can be attributed to growth during a particular geologic event. A major advance has also been made in the recognition and interpretation of interior and exterior morphology of zircon grains. Geochemical characterization and Hf isotopic signatures help determine the environment in which the zircon grains crystallized. The combined application of these methods has resulted in making zircon investigation one of the most powerful research tools available for provenance, petrogenetic as well as time scale studies.

We are currently examining some previously analyzed zircon suites in order to determine to what degree modern analytical techniques can extract additional information from this valuable material. To this purpose we selected single grains from the original size-fractions of a reversely discordant zircon population of the pre-kinematic Caledonian Vagastie Bridge granite of NW Scotland. These fractions from sample RC662 were originally studied by PIDGEON & AFTALION (1978) and found to plot along a  $405 \pm 11$  to  $1540 \pm 42$  Ma discordia line. Among the various techniques we plan to apply are high resolution-high precision conventional isotope dilution (ID) analysis on single-fragments or abraded single-grains, the Kober evaporation technique and spot analysis with the new ion probe SHRIMP II at Perth.

Recently, the first data for single-fragment and abraded single-grain conventional ID analysis were obtained. They plot above and outside of error of the original size-fraction data points: 1) sub-microgram fragments of the zircon rim representing latest growth yield concordant ages near 430 Ma, 2) rim, zoned mantle and pop-out core from one single-grain align within limits of error on a discordia line intersecting concordia at 425 and 1540 Ma, 3) visibly core-bearing grains abraded to a fraction of their original size also fall on this line, except for one data point which plots markedly above this line and thus indicates the presence of a second inherited component. In agreement with our previous experience, the new data confirm that intrusive ages based on lower intersections extrapolated from zircon size-fractions may be too young. This is probably due to the presence of highly susceptible (and thus more discordant) U-Pb (zircon?) phases in the multi-grain fractions.

We conclude that single-fragment dating considerably increases the resolving power of conventional ID zircon dating, particularly for the late growth phases. The ion probe analyses currently under way are expected to provide better resolution for the inherited components involved and thus help in evaluating the meaning of the extrapolated upper intersections obtained by classical techniques.

Pidgeon, R.T., and Aftalion, M., 1978, Cogenetic and inherited zircon U-Pb systems in granites: Paleozoic granites of Scotland and England. Geol. Journal, Special issue No. 10, 183-220.

## MANTLE OVERTURNS AND MAJOR OROGENIES (MOMO)

**STEIN, M.** Institute of Earth Sciences, The Hebrew University, Jerusalem, Israel, and  
**HOFMANN, A.W.** Max-Planck-Institut für Chemie, Postfach 3060, 55020 Mainz, Germany.

During Earth history, periods with areally extensive crust-formation rates appear to have alternated with periods of lower rates. We propose that these fluctuations are related to alternating styles of mantle convection. High crustal growth rates occur during periods of strongly penetrative two-layer convection or whole-mantle convection, and we call these "MOMO" periods (Mantle Overturn and Major Orogenies). They alternate with "Wilsonian" periods of two-layer convection, seafloor spreading, and continental drift coupled with low crustal growth rates. During Wilsonian periods, the upper mantle is relatively isolated from the lower mantle and is progressively depleted in incompatible trace elements. During MOMO periods, the upper mantle is partly replenished in these elements.

This model is consistent with recent theoretical work on mantle convection and with several geochemical observations, the meaning of which has been controversial in the past. They all require significant but limited input of lower-mantle material into the upper mantle: (1) Initial isotopic compositions of Nd and Sr for several areally extensive major "orogenies" such as the Pan-African are relatively uniform and intermediate between primitive mantle and incompatible-element depleted, "MORB-type" mantle. (2) The trace element budget of continental crust requires extraction of trace elements from a mantle reservoir that is larger than the upper mantle but much smaller than the whole mantle. (3) The noble gas budget requires the continued presence of primordial  $^3\text{He}$  and large amounts of  $^{40}\text{Ar}$  in the lower mantle, but also significant gas transfer to the upper mantle. (4) The isotopic composition of lead is not consistent with Th/U ratios in the upper mantle, if the continental crust and upper mantle evolved as a closed system. Other critical trace element ratios in the upper mantle and continental crust also do not add up to possible primitive-mantle ratios.

## SEDIMENTARY K-AR SIGNATURES IN CLAY FRACTIONS FROM MESOZOIC MARINE SHELF ENVIRONMENTS

**STEINITZ, G., KAPUSTA, Y., SANDLER, A., KOTLARSKY, P.,** Geological Survey, Jerusalem, Israel.

K-Ar age determinations have been performed on silicate fractions (clay minerals, feldspar) separated from some 20 sedimentary rocks from Jurassic to Late Senonian formations in Israel, deposited in shallow marine carbonate shelf environments of the southern Tethys ocean. The results show that:

1. In several cases (IR,  $>10\mu$ ) the K-Ar ages are significantly higher than the stratigraphic age, reflecting the age of detrital mica and feldspar, the only K-bearing minerals in the clay fractions.
2. Some of the K-bearing clay fractions have K-Ar ages synchronous with the time of deposition. The K-Ar syn-sedimentary signal is recorded from different environments of deposition, the range of lithologies spanning rocks with IR  $<10\%$  (dolomite, chalk), through marls to shales (IR = 70-85%) and sandstones (IR  $>90\%$ ).
3. Among the clay minerals the syn-sedimentary signature was isolated in illite/smectite of the  $<2\mu$  fraction, assumed to be authigenic. The K-Ar ages have since been retained in these fractions, including in  $<0.2\mu$  fractions.
4. A prominent syn-sedimentary signature is found in Early Cenomanian K-feldspars (97 ma), from shaly and calcareous rocks, confirmed by their authigenic origin based on idiomorphic crystal morphology and a limited size (4-10 $\mu$ ) distribution.
5. Post depositional closure of the K-Ar system in mineral fractions is indicated in the ages of  $<2\mu$  fractions circa 15 ma lower than the stratigraphic age (90 ma) separated from dolomite, shale and sandstone. A distinct post-depositional event (60-65 ma) is also recorded in the formation of authigenic K-feldspar within Senonian (85 ma) chalk and shale.

The overall pattern of the results differs considerably from the K-Ar age patterns as observed in  $<2\mu$  fractions from deep sea sediments. The difference may be connected with the occurrence of brines in these shelf environments.

**CARBON ISOTOPE VALUES IN FOSSIL RATITE  
EGGSHELLS AND ASSOCIATED MATERIALS:  
FURTHER EVIDENCE FOR HABITAT EXCLUSION OF  
SOUTH ASIAN *SIVAPITHECUS* SP. DURING THE LATE  
NEOGENE**

**STERN, LIBBY A.**, Johnson, Gary D., and Chamberlain, C. Page, Department of Earth Sciences, 6105 Sherman Fairchild Science Center, Dartmouth College, Hanover, New Hampshire 03755-3571, U.S.A.

A 10+ million year sequence of ratite (e.g., ostrich and related paleognathids) eggshells from Siwalik Group sediments of northern Pakistan and India, shows a dramatic (~8‰) increase in the  $\delta^{13}\text{C}$  in biomineralogic calcite by ~4 Million years (Ma).  $\delta^{13}\text{C}$  values of pre-7 Ma ratite eggshell carbonate are about the same as those found in carbonate from fossil mammal tooth enamel and paleosols in contemporary Siwalik facies. However, after 4 Ma, the ratite eggshell carbonate  $\delta^{13}\text{C}$  values are ~5‰ less than this coexisting material.

These data provide collective evidence of the development and enhancement of a C<sub>3</sub>/C<sub>4</sub> vegetative mosaic which we interpret to mirror the sedimentologic/edaphic mosaic of the aggrading alluvial plain of an increasingly topographically differentiated Siwalik depositional system.

Although this  $\delta^{13}\text{C}$  shift has been previously recognized as coincident with a major faunal turnover occurring ~7.4 Ma in the Potwar region of Pakistan, and roughly concurrent with the local LAD of *Sivapithecus* sp. in Pakistan (recorded also in the Potwar region at ~8 Ma), the  $\delta^{13}\text{C}$  values determined from the ratite eggshell material demonstrate the persistence of a C<sub>3</sub> vegetation signature well into the upper Pliocene. This has not been recognized in previous carbon isotope studies of paleosol and fossil tooth enamel in the South Asian Neogene.

This relict C<sub>3</sub> vegetation, most likely associated with the riparian aspect of the Siwalik depositional system, is interpreted to be of insufficiency size or stability in the post-7 record of the Potwar region of Pakistan to provide suitable habitat for the South Asian sivapithecines. The exclusion of this taxa from this portion of the South Asian monsoonal belt by ~7 Ma and a subsequent eastward shift in the necessary habitat as seen from faunal indicators at Haritalyangar (India) and carbon isotope indicators Bakiya Khola (Nepal) suggests that interpretations of climate change and monsoonal development during the late Neogene in south Asia must be constrained by certain geographical and temporal qualifiers. We are currently refining this argument with additional material collected in a 500 km W-E transect originating in the Trans-Indus Ranges of northwestern Pakistan.

**PROGRESSIVE CRATONIZATION IN THE  
SUPERIOR PROVINCE**

**Stevenson, Ross K.**, GEOTOP/Dépt. des Sciences de la Terre, Université du Québec à Montréal, P.O. Box 8888, St. C.V. Montréal, Que. H3C 3P8, Canada.

Sm-Nd data are reported for several greenstone belts in the Sachigo Subprovince of the Superior Craton in NW Ontario. These greenstone belts are particularly noteworthy for their numerous granite-greenstone cycles during 300 Ma of late Archean history from 3.0-2.7 Ga. Thus, these belts offer an opportunity to monitor the evolution of the mantle and continental crust over a period of prolific crustal formation in the history of the Earth's continental crust. Recent tectonic analysis of the Sachigo Subprovince according to Phanerozoic terrane analysis concepts has subdivided the greenstone belts into different lithotectonic assemblages and grouped the belts into various tectonic terranes. When the Sm-Nd data is applied on this basis it can be used to compare the isotopic evolution of volcanic arc, platformal and oceanic tectonic settings. Isotopic data from each belt are consistent in that the earliest strata/assemblages show the smallest variation in  $\epsilon_{\text{Nd}}$  values, usually ranging from chondritic (0) to +2. Successive assemblages show progressively greater ranges of  $\epsilon_{\text{Nd}}$  values to more positive values for mafic samples and to more negative  $\epsilon_{\text{Nd}}$  values for felsic and sedimentary samples. Thus a progressive evolution in both the depletion of the mantle and the recycling of crustal material from one assemblage to the next can be traced in each of these greenstone belts. Granitoid samples from the granitoid basement enveloping the greenstone belts mimic isotopic trends within the belts, indicating that granitoid development is concomitant with greenstone belt development and that the plutonism can often be attributed to volcanic events within the associated greenstone belt. The data are consistent with the formation of the North Caribou Terrane from an embryo of amalgamated island arc and oceanic plateaus, which developed through further accretion and intracrustal differentiation over 300 Ma (progressive cratonization) into a stable micro-continental platform onto which successive terranes and subprovinces accreted.

## PALEOHYDROLOGY OF THE LATE PLIOCENE BASIN AND RANGE PROVINCE USING STRONTIUM ISOTOPES

STEWART, Brian W., HSIEH, Jean C.C., and MURRAY, Bruce C., Division of Geological and Planetary Sciences 170-25, California Institute of Technology, Pasadena, CA 91125, U.S.A.

Lake sediments exposed in the Confidence Hills of Death Valley, California, preserve a record of climate change in the western United States Basin and Range Province during the late Pliocene and early Pleistocene. Alternating cycles of lacustrine evaporites and subaerial deposits in the well-exposed Confidence Hills section record variations in shoreline facies of a large Plio-Pleistocene lake; these changes in lake level may be correlated with climate variations inferred from the marine stable isotope record [1,2]. Determining the source of waters feeding Death Valley during lake highstands can provide important information about continental glaciation, climate, and weathering patterns. The two most likely sources of water to Death Valley during the late Pliocene are the paleo-Owens River system, with water ultimately derived from the Sierra Nevada to the west, and the paleo-Amargosa River system feeding in from the east and north.

We measured  $^{87}\text{Sr}/^{86}\text{Sr}$  ratios in evaporite units (gypsum and anhydrite) spanning the length of the exposed Confidence Hills section in order to determine the source(s) of water entering Death Valley during the late Pliocene. Our samples span an age range of ~350 Ka, from the base of the Reunion Event (2.15 Ma) to just above the top of the Olduvai event (1.79 Ma). All  $^{87}\text{Sr}/^{86}\text{Sr}$  values fall within a range of  $0.7156 \pm 0.0003$ , with typical uncertainties on individual measurements of 0.00002. Although there are clear variations in  $^{87}\text{Sr}/^{86}\text{Sr}$  values outside of analytical uncertainty during this time period, the total range in values is small in comparison to possible sources of Sr to the Death Valley hydrologic system. The  $^{87}\text{Sr}/^{86}\text{Sr}$  values of Sierra Nevada granites generally fall in the range of 0.705 to 0.709, with stream waters from the Yosemite area yielding values from 0.7078 to 0.7089 [3]. In contrast, exposures of Precambrian basement to the east of the Sierra Nevada can have values in excess of 0.72. The absolute value and range of  $^{87}\text{Sr}/^{86}\text{Sr}$  ratios measured in Confidence Hills evaporites suggests that the source of waters into Death Valley during this time was relatively invariant, and that the Sr dissolved in the waters feeding the late Pliocene lake was derived primarily from Precambrian sources. Importantly, these data argue against the Owens River system as the dominant supplier of water to Death Valley during the late Pliocene. The most likely source of dissolved cations to the lake was either weathering of local Precambrian units within Death Valley itself or weathering of Proterozoic basement along the Amargosa River drainage system. Input of water from either of these sources would be enhanced if the Sierra Nevada were not sufficiently uplifted to create a strong rain shadow effect at the time of deposition of the Confidence Hills section.

- [1] Hsieh, J.C.C. and Murray, B.C. (1993) *Geol. Soc. Am. Abstr. Prog.* 25, A-456.
- [2] Beratan, K., Hsieh, J.C.C., Murray, B.C., and Gomez, S. (submitted) *J. Sed. Pet.*
- [3] Blum, J.D., Erel, Y. and Brown, K. (1993) *Geochim. Cosmochim. Acta* 58, 5019-5025.

## STRONTIUM ISOTOPE STUDY OF CATION FLUXES IN A SOIL-VEGETATION-ATMOSPHERE SYSTEM

STEWART, Brian W., Division of Geological & Planetary Sciences 170-25, California Institute of Technology, Pasadena, CA 91125, U.S.A., CHADWICK, O.A., JPL-Caltech, Pasadena, CA 91109, U.S.A., and GRAHAM, R.C., Department of Soil and Environmental Sciences, University of California, Riverside, CA 92521, U.S.A.

Quantification of changes in soil weathering and nutrient cycling on a time scale of  $10^1$ - $10^2$  years is essential in order to determine the effects of human-induced changes in atmospheric chemistry on soil-vegetation systems. As part of a U.S. Forest Service project in the San Dimas Experimental Forest in southern California, four unlined pits (5.3 x 5.3 x 2.1 m) were filled in 1937 with a locally derived, homogenized sandy loam, and were planted with monocultures of native plant species after a nine year stabilization period. These experimental soil-vegetation systems offer an unparalleled opportunity to study soil development on a decade time scale.

Studies of soil morphology [1] and C, N, and exchangeable cations [2] indicate that some changes have taken place in the lysimeter soils over their ~50 year evolution, dependant primarily on vegetation type and associated faunal activity. We carried out mass balance calculations on bulk soil samples using the equations of Chadwick et al. [3] and Brimhall et al. [4]; the total element changes are sufficiently subtle on this time scale to be undetectable with these techniques, although further work on specific fractions may yield measurable differences. Here we present isotopic measurements of Sr extracted from the soil exchange complex, and show that  $^{87}\text{Sr}/^{86}\text{Sr}$  ratios do in fact provide a sensitive method for determining patterns of cation release by weathering and input from atmospheric sources in soil-vegetation systems. Sr is an excellent proxy and serves as a tracer for divalent cations (especially Ca) in such systems, and Sr isotopic fractionation from natural processes is negligible.

The two most important fluxes of strontium to soil exchange sites are dissolved Sr from atmospheric deposition, and Sr released by weathering of soil minerals. In the San Dimas study site, the  $^{87}\text{Sr}/^{86}\text{Sr}$  ratio of Sr in rainwater is ~0.7091, and bulk soil Sr has a ratio of ~0.7099. We measured isotopic ratios of exchangeable Sr (using an  $\text{NH}_4\text{Cl}$ -MeOH leach) in soils collected in 1987 from the pine-planted lysimeter. Samples range from the A-horizon (0-1 cm) down to a depth of 100 cm, and all  $^{87}\text{Sr}/^{86}\text{Sr}$  values fall within  $0.70953 \pm 0.00014$ , nearly in the middle of the two endmembers. This suggests that neither source dominates the budget of exchangeable cations on this time scale. In detail, the data exhibit a clear trend of decreasing  $^{87}\text{Sr}/^{86}\text{Sr}$  with depth, with the upper horizons having values slightly more radiogenic than the exchangeable Sr in the original soil, and the lower horizons trending below the original value, toward the atmospheric endmember. Our preliminary interpretation is that most weathering takes place in the A-horizon, resulting in release of cations, including Sr, to local exchange sites. In contrast, Sr from the atmosphere is delivered to exchange sites throughout the profile by soil water transport.

- [1] Graham, R.C. and Wood, H.B. (1987) *Soil Sci. Soc. Am. J.* 55, 1638-1646.
- [2] Ulery, A.L., Graham, R.C., Chadwick, O.A. and Wood, H.B. (in press) *Geoderma*.
- [3] Chadwick, O.A., Brimhall, G.H. and Hendricks, D.M. (1990) *Geomorphology* 3, 369-390.
- [4] Brimhall, G.H., Chadwick, O.A. et al. (1992) *Science* 255, 695-702.

AGE ESTIMATES FROM SEMI-ARID AND ARID  
ARCHEOLOGICAL CONTEXTS: THE SUCCESSFUL  
APPLICATION OF A MULTIPLE TECHNIQUE DATING  
STRATEGY

STOKES, S., Research Laboratory for Archaeology and  
the History of Art, and School of Geography, University  
of Oxford, Oxford OX1 3QJ, UK, and VAN KLINKEN,  
G.J. Radiocarbon Accelerator Unit, University of Oxford,  
Oxford OX1 3QJ, UK.

Chronological constraints on paleoenvironmentally- or  
archeologically-significant stratified sequences from arid and  
semi-arid areas have frequently been limited by difficulties in  
the application of routine radiocarbon dating methods and a  
lack of alternative dating techniques. In this paper we describe  
the results of a combined dating strategy, incorporating AMS  
radiocarbon dating of bone protein extract and optical dating  
of quartzose sediments, as applied to a significant early  
(possibly Paleoindian) indian burial site from New Mexico.

We outline a series of bone protein separation and isolation  
techniques which we used and compare the AMS results on  
the fractions to demonstrate high degree of accordance which  
we have obtained.

Two optical dating techniques are described; comprising the  
multiple and single aliquot, additive dose dating methods.  
Close agreement between these techniques, coupled with their  
broad agreement with the AMS radiocarbon assays and  
uranium equilibrium at the site, given us confidence in the  
results which we have obtained.

Implications for the widespread application of such multiple  
dating strategies to similar arid and semi-arid region deposits  
will be discussed.

COSMOGENIC CHLORINE-36 PRODUCTION BY  
SPALLATION AND MUON-CAPTURE

STONE, J., Research School of Earth Sciences, FIFIELD,  
L.K., EVANS, J.M., ALLAN, G.L. and CRESSWELL, R.G.,  
Dept of Nuclear Physics, Research School of Physical  
Sciences and Engineering, Australian National University,  
Canberra, A.C.T., 0200, Australia

Cosmogenic isotope measurements by AMS have progressed  
so far in recent years that the accuracy of exposure dating  
methods for terrestrial surfaces is now limited by knowledge of  
isotope production rates. A case in point is  $^{36}\text{Cl}$ , which can be  
measured with exceptional sensitivity (we have made  
measurements to better than  $\pm 10\%$  at  $3 \times 10^4$  atom/g), but  
whose production is complicated by numerous nucleon- and  
muon-induced reactions with Ca, K and  $^{35}\text{Cl}$ . We have  
calibrated rates for several of these from natural surface and  
sub-surface samples, aiming to isolate the effects of specific  
reactions by choice of target minerals and sample depths.

(1) Ca spallation was calibrated using calcite ( $\text{Ca}/\text{K} > 10^3$ ,  
 $\text{Ca}/\text{Cl} > 10^4$ ) from  $\sim 10.3\text{ka}$  glacial pavements at high altitude  
in the Sierra Nevada, California. In these samples, 93-97% of  
 $^{36}\text{Cl}$  production is due to Ca spallation, 2% to negative muon  
capture by  $^{40}\text{Ca}$ , 1-5% to capture of cosmogenic secondary  
neutrons and  $< 0.1\%$  to capture of U- and Th-produced  
neutrons. Scaled to sea-level and latitudes  $> 60^\circ$  (as per Lal;  
[1]) the  $^{36}\text{Cl}$  production rate from Ca spallation derived from  
the data is  $0.733$  atom/g/yr/%Ca. We assign an uncertainty of  
 $\pm 10\%$  to this value, largely to account for uncertainty in the  
exposure history. The result is in excellent agreement with the  
estimate of Zreda et al [2], of  $0.67\text{-}0.77$  atom/g/yr/%Ca.

(2)  $^{36}\text{Cl}$  production in calcite by muon-induced reactions  
was calibrated from a 2-20m depth profile in marble. We  
estimate a surface rate of  $0.043$  atom/g/yr/%Ca for the negative  
muon capture reaction  $^{40}\text{Ca}(\mu, \alpha)^{36}\text{Cl}$ . at sea-level and high  
latitude, equivalent to  $\sim 5.5\%$  of total production from Ca. We  
calculate an overall neutron yield of  $\sim 0.75$  n/stopped muon in  
calcite, hence a production rate of  $130 \pm 40$  n/g/yr at the  
surface at sea level and high latitudes. The resulting rate for  
 $^{35}\text{Cl}(n, \gamma)^{36}\text{Cl}$  from mu-genic neutrons under these conditions  
is therefore  $\sim 0.026$  atom/g/yr/ppm Cl. Currently, uncertainties  
in the production parameters derived for muon reactions are  
 $\sim \pm 30\%$  due to simplifications in the data inversion and  
disturbance of the profile surface. Better estimates (hopefully  
 $\pm 10\%$ ) for the production parameters may be obtained with an  
improved sub-surface production model incorporating fast-  
muon-produced neutrons.

(3) We have calibrated  $^{36}\text{Cl}$  production from cosmic ray  
reactions with K using K-feldspar ( $\text{K}/\text{Ca} > 250$ ,  $\text{K}/\text{Cl} > 5 \times 10^4$ )  
in Antarctic moraine boulders. Independent age control is not  
available for these samples, necessitating calibration against  
 $^{26}\text{Al}/^{10}\text{Be}$  ages (13-17ka) on quartz from the same samples.  
The estimated rate is  $1.77$  atom/g/yr/%K, substantially higher  
than the published value [2], but in good agreement with a  
recent revision of this rate to  $1.93$  atom/g/yr/%K [3].

We hope to have further results on (4) production of  $^{10}\text{Be}$   
from C and O in calcite, (5) calibration of  $\text{K} \rightarrow ^{36}\text{Cl}$  reactions  
from independently-dated surfaces, and (6) cross-checks on  
 $^{10}\text{Be}$  and  $^{26}\text{Al}$  production in quartz, by the time of the  
meeting. Applications will be discussed if time permits.

[1] Lal, D., 1991, Earth Planet. Sci. Lett. 104, 424-439.

[2] Zreda, M.G., Phillips, F.M., Elmore, D., Kubik, P.W.,  
Sharma, P. and Dorn, R.L., 1991, Earth Planet. Sci. Lett. 105,  
94-109.

[3] Phillips, F.M., pers. comm. and presentation at GSA  
Boston meeting, 1993

ASSESSMENT OF CRUST-MANTLE CONTRIBUTIONS TO THE YOUNG (9Ma) SERIFOS AND OTHER AEGEAN GRANITES WITH MIXED S-/I-TYPE CHARACTERISTICS

STOURAITI, Christina, TARNEY, J. & NORRY, M.J., Dept. Geology, U. Leicester, UK, and BARREIRO, B.A., NERC Isotope Geoscience Laboratory, Keyworth, Nottingham, UK

The Serifos pluton is one of the youngest granite complexes in the Aegean, and lies in the back-arc region, just to the north of the active Aegean Arc. Other granites in the Aegean tend to age progressively with distance northwards from the Arc.

Serifos illustrates many of the problems of granitoid petrogenesis. The composition ranges from quartz-hornblende diorite (enclaves) through hornblende-biotite granodiorite and biotite granite to leuco-pegmatites and aplites near the margins of the complex. There are spectacular mineralised skarns and karstic Fe-Mn deposits. The fact that most rocks are generally *not* per-aluminous but are hornblende signifies an I-type granite. On the other hand having  $^{87}\text{Sr}/^{86}\text{Sr}$  ratios for the complex that range from 0.709-0.711 and  $^{143}\text{Nd}/^{144}\text{Nd}$  ratios that range from 0.51220-0.51231 is clearly a strong S-type granite characteristic. How can these features be reconciled?

A synthesis of available Sr and Nd isotopic data on Aegean and other E. Mediterranean granitoids and volcanics shows that most lie very close to a mixing curve between a Sr-enriched (relative to Nd) "Aegean mantle" component represented by Santorini basalts and a Nd-rich "Hellenic crustal" component represented by the metasedimentary basement rocks of Serifos and adjacent islands of the Cyclades. Whereas AFC (assimilation - fractional crystallisation) and similar models involving these end-members could theoretically reproduce the isotope data for Serifos, there is a problem in that Serifos occupies a very restricted field on the general isotopic mixing curve; other complexes also have a limited, but different, range. Moreover, the trace element data do not favour extensive AFC processes.

Our preferred solution relies on the fact that continental development of the Hellenic region during the Mesozoic and early Tertiary was dominated by subduction-accretion processes, as testified by the abundant blueschist and eclogitic remnants scattered amongst the metasedimentary basement rocks throughout the region. The latter represent accreted continental greywacke-shale sediments that have been deformed and dragged-down during subduction-accretion, and some must have been uplifted and exhumed from mantle depths. We suggest that such sediments heavily, but variably, contaminate the underlying lithosphere. Magmas that are generated later from the lithosphere as a result of exhumation, extension or orogenic collapse will therefore inherit a "crustal" component dependent on the extent of the earlier subduction-accretion. If subduction-accretion is important in crustal development, particularly in the Phanerozoic and late Precambrian, then this may account for some of the crustal signatures of mantle-derived magmas as much as magma-assimilation processes.

EPISODIC METASOMATISM IN PELITIC SCHISTS FROM CONTACT METAMORPHIC AUREOLES NEAR JUNEAU, ALASKA

STOWELL, H. H., and MENARD, T., Department of Geology, University of Alabama, Tuscaloosa, AL 35487

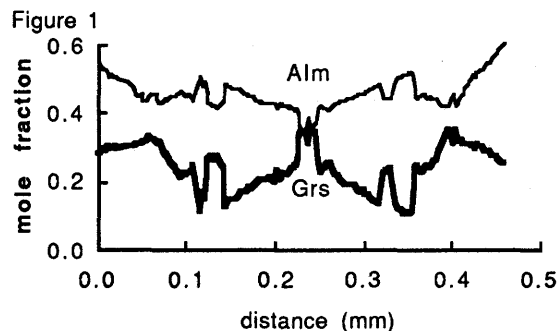
Calcic pelitic schists from contact metamorphic aureoles around the Grand Island diorite complex near Juneau, Alaska experienced multiple fluid infiltration and metasomatic events. These events are recorded in the compositional zoning of garnet and in the metamorphic reaction history.

Metamorphic aureoles around plutons of the Grand Island diorite complex range in width from 20 m to 200 m with peak metamorphism at staurolite grade. The rocks have a Ms + Bt schistosity and a weak crenulation cleavage. Calcic pelitic schists have the medium-grade assemblage Grt + Bt + Pl + Ep + Qtz + Ms + Sph.

Garnet grains are small (0.2 - 0.5 mm), contain inclusions of Qtz and Ep, and are partially resorbed to chlorite. Garnets 2 mm from a quartz vein have cyclic zoning in  $X_{\text{Grs}}$  (0.10 to 0.35) and sympathetic zoning in  $X_{\text{Alm}}$  (Fig. 1). With some exceptions,  $X_{\text{SpS}}$  decreases and Fe/(Fe+Mg) increases towards the rim. Na zoning in garnet, with concentrations in the 100's of ppm, has opposite trends as Ca. If the Na zoning in garnet reflects plagioclase compositions,  $X_{\text{Grs}}$  and  $X_{\text{An}}$  increased (and decreased) together. Ti in garnet decreases from 1800 to 100 ppm at about the same position as the first large increase of  $X_{\text{Grs}}$ . The zoning data may reflect Ca-metasomatism, which would cause growth of plagioclase and sphene, reducing the availability of Na and Ti. Garnets 2-m away from veins are similar, but do not have the initial high  $X_{\text{Grs}}$ . Zones with high  $X_{\text{Grs}}$  may reflect successive fluid infiltration and Ca-metasomatism events. Inclusion of tiny mineral grains within garnet in these zones suggests rapid growth. Garnet growth with decreasing  $X_{\text{Grs}}$  after each of these events may reflect hiatuses in fluid infiltration.

The rocks were extensively retrograded to Czo + Ab + Ms + sulfide, and in places, subsequently retrograded to minor chlorite and sericite. Epidote has subhedral cores of allanitic epidote zoned in REE's that correlate with garnet, surrounded by unzoned rims of retrograde clinozoisite. Plagioclase has equilibrium textures with the retrograde assemblage, and hence postdates the garnet. Retrograde metamorphism was associated with emplacement the foliated tonalite sill 10 km to the east, and possibly with the low-grade alteration and mineralization in the Juneau gold belt.

Thus, fluid flow varied during metamorphism. Infiltration started near veins, and then became more pervasive. Pulses of fluid flow and intervening hiatuses may be related to emplacement of multiple plutons in the complex, causing repeated changes in temperature or fluid flow. The fluid character and the resulting metasomatism changed from event to event.



## COUPLED HE-S ISOTOPE VARIATION IN M.O.R.

### HYDROTHERMAL MINERALS

STUART, Finlay, FALLICK, A.E., Isotope Geology Unit, S.U.R.R.C., East Kilbride G75 0QO, UK, and TURNER G., Dept. Geology, Manchester University, Manchester M13 9PL, UK.

Helium isotopes have been measured in fluid inclusions hosted in sulphide and sulphate minerals from active mid-ocean ridge hydrothermal systems at bare rock (21°N and 13°N, E.P.R., TAG and Snake Pit, M.A.R.) and sediment-covered sites (Middle Valley and Gorda Ridge, J.D.F.). Sulphide-hosted fluid  $^3\text{He}/^4\text{He}$  from bare rock sites (7.1-9.5  $R_A$ ) are indistinguishable from those of the venting hydrothermal fluids and are close to those of the local basalts. Fluid inclusion  $^3\text{He}/^4\text{He}$  from Middle Valley and the Gorda Ridge sulphides (4.5-6.8  $R_A$ ) contain variable amounts of radiogenic helium along with the basalt-derived helium. The radiogenic He cannot be derived by protracted hydrothermal circulation in the basaltic basement.

$\delta^{34}\text{S}$  values of EPR and MAR sulphides (0.5-7‰) are above values of basaltic sulphur (~0‰) and are consistent with the presence of reduced seawater sulphate. He isotope ratios are independent of  $\delta^{34}\text{S}$  confirming that addition of seawater to hydrothermal fluids has no effect on He isotope composition. He and S isotopes in sulphides from sediment-covered systems are coupled, displaying a broad negative  $^3\text{He}/^4\text{He}$ - $\delta^{34}\text{S}$  trend. This is consistent with a sedimentary origin for the radiogenic He and either results from a mixture of hydrothermal fluid with sediment pore fluid enriched in radiogenic He, or direct interaction between hydrothermal fluids and sediments. Combined He-S isotope studies of continental hydrothermal mineralisation is a potentially powerful tracer of fluid origins. Pb isotope measurements are being performed to provide constraints on the degree of sediment-fluid interaction.

## NEW AGE STANDARD MINERALS FOR K-Ar AND $^{40}\text{Ar}/^{39}\text{Ar}$ DATING; PRELIMINARY RESULTS OF THREE BIOTITE SEPARATES.

SUDO, M.,<sup>1</sup> UTO, K.,<sup>2</sup> TAGAMI, T.,<sup>1</sup> MATSUMOTO, A.,<sup>2</sup> HASEBE, N.,<sup>1</sup> UCHIUMI, S.,<sup>2</sup> ANNO, K.<sup>3</sup> and NISHIMURA, S.<sup>1</sup>  
<sup>1</sup>Dept. of Geology and Mineralogy, Fac. of Science, Kyoto Univ., Kyoto 606, Japan; <sup>2</sup>Dept. of Geochemistry, Geological Survey of Japan, Tsukuba 305, Japan; <sup>3</sup>Graduate School of Human and Environmental Studies, Kyoto Univ. Kyoto 606, Japan

Interlaboratory age standards are of primary importance for reliable radiometric dating. To set up new K-Ar and  $^{40}\text{Ar}/^{39}\text{Ar}$  dating systems using VG 3600 mass spectrometers, installed in Kyoto University and Geological Survey of Japan (GSJ), we prepared and analyzed three biotite standard candidates of Pliocene-Cretaceous ages separated from Japanese igneous rocks.

The biotite Sori-93 is a recollection of GSJ JG-1 biotite standard from the same locality of Sori granodiorite. The contents of argon and potassium and the argon isotopic abundances were reported previously, yielding K-Ar age ~91 Ma (e.g., Matsumoto et al., 1989). At first we measured argon and potassium at GSJ. The contents and isotope ratios of argon were determined using two systems: the VG 1200 mass spectrometer by the peak comparison method (Matsumoto et al., 1989) and the Micromass 6 by the isotope dilution. The contents of potassium were determined with the Kotaki FIP-3D flame emission spectrometer. Subsequently, the measurement of argon was repeated with the VG3600 mass spectrometer installed in Kyoto University for interlaboratory calibration.

We prepared the biotite NST from a welded tuff of the Nisatai Dacite. The K-Ar biotite and FT zircon ages are reported as ~21 Ma (Tagami et al., submitted). To evaluate whether the age of the biotite is the concordance of the different grain sizes, the biotite was sieved to several fractions of different grain size. The measurements of argon and potassium were carried out on four and six fractions, respectively. The obtained results of K<sub>2</sub>O content varied from 7.34 wt% to 8.38 wt% in the six fractions of 16 to 140 mesh sizes. However, the ages were approximately concordant (from 20.9 Ma to 21.8 Ma) among 30 to 100 mesh sizes. This may indicate that the biotite is useful as the K-Ar age standard. To investigate the cause of potassium content variation among the grain sizes, potassium distribution analysis in single biotites with EPMA is currently planned.

We also report the analysis of biotite from the Utaosa Rhyolite, which K-Ar ages are concordant at ~2.5 Ma (Uto et al., submitted). Further analytical results will be presented to assess its suitability to standard.

Matsumoto A., Uto K., and Shibata K., 1989, K-Ar dating by peak comparison method --New technique applicable to rocks younger than 0.5 Ma--: Bull. Geol. Surv. Japan, v 40, p. 565-579.

## NITROGEN ISOTOPE SYSTEMATICS OF PRIMITIVE ORDINARY CHONDRITES

SUGIURA, N., KIYOTA, K., Dept. of Earth and Planetary Physics, Univ. of Tokyo, Tokyo, Japan. HASHIZUME, K., Dept. of Earth and Space Science, Osaka Univ., Osaka, Japan.

Searching for signature of presolar grains in ordinary chondrites, we have measured nitrogen isotopic composition of about 20 primitive ordinary chondrites. The nitrogen was extracted by a stepped combustion method, and measured with a static mass spectrometer.

The primitive chondrites can be classified into 3 major groups according to the nitrogen isotopic signature. In addition, there are a couple of ungrouped chondrites.

Group-1: This is the largest group with 7 members. This group is characterized by abundant but only slightly anomalous (-60 permil) nitrogen released at 1100C.

Group-2: This group has four members and characterized by somewhat heavy (170 permil) nitrogen isotopic composition. At least three members are gas-rich chondrites as inferred from the neon isotopic composition. It is quite likely that the heavy nitrogen is of solar wind origin.

Group-3: This group has three members and characterized by isotopically light (-220 permil) nitrogen which shows bimodal release pattern (700C and 1100C) by stepped combustion. A large amount of primordial Ar is also released at these temperatures but the Ar and nitrogen are not necessarily in the same carrier according to the results of chemical treatment.

Ungrouped chondrites are Y-74191 and Mezo Madaras. The former has a very heavy (1000 permil) nitrogen, and the latter has a slightly heavy (200 permil) nitrogen.

Five chondrites with a metamorphic grade higher than 3.7 release nearly normal nitrogen although deviation of delta 15N values during stepped combustion suggests that anomalous nitrogen may be present.

## U-Pb AGES FROM THE HIGH-GRADE BARRO ALTO MAFIC-ULTRAMAFIC COMPLEX (GOIÁS, CENTRAL BRAZIL): MIDDLE PROTEROZOIC CONTINENTAL MAFIC MAGMATISM AND UPPER PROTEROZOIC CONTINENTAL COLLISION.

SUITA<sup>1,2,4</sup>, M.T.F.; KAMO<sup>3</sup>, S.L.; KROGH<sup>3</sup>, T.E.; FYFE<sup>2</sup>, W.S. & HARTMANN<sup>4</sup>, L.A. 1. Depto. Mineração, UFOP, Ouro Preto, 35400, MG, Brazil; 2. Dept. of Earth Sciences, UWO, London, Ont., Canada, N6A 5B7; 3. Dept. of Geology, Royal Ontario Museum, Toronto, Ont., Canada, M5S 2C6; 4. Instituto de Geociências/CPGq, UFRGS, Porto Alegre, 91500, RS, Brazil.

The Barro Alto Complex (BAC) is the largest mafic-ultramafic layered intrusion (156 km x 8-25 km wide x 5-6 km thick) in Goiás, Central Brazil, and among the largest in the world. The BAC, with the Niquelândia and Cana Brava Complexes, forms a 350 km-long belt of large layered mafic-ultramafic intrusions between the Archean Amazonian and São Francisco cratons. The BAC underwent granulite to amphibolite facies metamorphism with local ductile deformation and associated retrogressions to amphibolite and greenschist facies. The first U-Pb data from the BAC are presented. Zircons were analyzed from granulite and amphibolite facies noritic rocks from the basal part of the BAC (the Serra de Santa Bárbara Sequence, SSSB); a garnet-amphibolite facies quartz-diorite intrusion in the SSSB; a late-stage differentiate of pegmatitic hornblende-gabbro from the amphibolite facies BAC upper zone, the Serra da Malacacheta Sequence (SSM); and a garnet-sillimanite-gneiss from the Juscelândia Sequence (?), tectonically interleaved with SSSB rocks, from which monazite was also analyzed. The upper intercept age for the quartz-diorite is ca. 1.72-1.73 Ga and is interpreted to be a minimum primary age for the intrusion. The lower intercept age of ca. 780 Ma is suggested to be the time of syntectonic high-grade metamorphism. This metamorphic age is confirmed by those obtained for the mylonitized norites at amphibolite and granulite facies and from monazite from the garnet-sillimanite-gneiss. The SSM pegmatitic gabbro has upper and lower intercept ages of ca. 1.29-1.35 Ga and 0.77-0.82 Ga, respectively, that are interpreted as either a time of mafic magmatism related to the Uruçuano (Middle Proterozoic) Cycle or possibly local post-BAC magmatism. These U-Pb ages together with other studies provide constraints on the geotectonic setting and evolution of these large mafic-ultramafic complexes in Goiás, suggest an important event involving underplating continental mafic magmatism during the transition of Lower to Middle Proterozoic, and confirm the syntectonic high-grade metamorphism associated with the continental collision of the Amazonian and the São Francisco Cratons during the Upper Proterozoic (Brasiliano/Pan-African Cycle) in Central Brazil.

## CONSTRAINTS ON DERIVING 'UPLIFT' HISTORIES FROM THERMOCHRONOLOGIC DATA

SUMMERFIELD, M.A., Department of Geography, University of Edinburgh, Edinburgh EH8 9XP, United Kingdom, and BROWN, Roderick, W., Department of Geological Sciences, University College, London, WC1E 6BT, United Kingdom

The inability of thermochronologic data directly to identify changes in surface elevation, as opposed to the movement of rocks relative to the earth's surface, is now becoming widely recognized, although the misleading use of the term 'uplift' continues to appear in research reports. We attempt to clarify the relevant terminology by clearly distinguishing between absolute and relative frames of reference in discussing displacements of the earth's surface and of movement of rocks in the crust.

Although the consistent use of clearly defined terms is important in 'uplift' studies, our primary aim is to demonstrate that since patterns and rates of denudation are key factors in determining crustal cooling histories, an understanding of the factors controlling denudation rates is a prerequisite for the correct interpretation of thermochronologic data. In particular, we question the assumption implicit in many 'uplift' studies employing such data that denudational episodes only occur in response to specific 'uplift' events and that, consequently, thermochronologic data can be used to provide an unequivocal record of tectonic activity. The idea that an increase in elevation (arising from tectonically-driven uplift) will inevitably lead to an increase in denudation rates ignores the fact that the latter are controlled by local relief (through average slope), not elevation, and these two variables are unrelated in some morphotectonic settings. Moreover, there may be a significant time lag while tectonically-engendered base level changes propagate across the landsurface, especially in passive margin and cratonic settings. Another problem is that denudation rates can change at a regional scale in response to changes in non-topographic variables such as climate and lithology. A further difficulty arises where significant changes in drainage boundaries could potentially lead to an episode of accelerated denudation (and crustal cooling); this is most likely to be important where external systems capture the internal drainage of high, intra-orogenic plateaus.

Although thermochronologic data clearly have an important role to play in tectonic studies we argue that those interpreting such data need to consider carefully all the factors that might have contributed to the cooling history observed.

ISOTOPIC AND GEOCHEMICAL CONSTRAINTS ON THE DEVELOPMENT OF A LARGE RHYOLITIC MAGMA SYSTEM: TAUPO VOLCANO, NEW ZEALAND  
SUTTON, A.N., BLAKE S., Dept. of Earth Sciences, Open University, Milton Keynes, MK7 6AA, U.K. and WILSON C.J.N., Inst. of Geological and Nuclear Sciences, Taupo, N.Z.

Taupo, a potentially active caldera volcano in central North Island, New Zealand, is one of the most productive rhyolitic systems in the world. This study attempts to relate the isotopic and geochemical evolution of the volcano to recent work on its physical development. We aim to address important questions in the study of large silicic magma systems: Are eruptions tapping a single magma chamber, or many? Do chambers have long residence times, or are they transient phenomena? On what timescales do replenishments of magma occur?

Eruptive products from throughout Taupo's history have been 'fingerprinted' using Sr and Nd isotopes, in conjunction with major and trace element and petrographic data. The ranges of  $^{87}/^{86}\text{Sr}$  (0.70489-0.70725) and  $\epsilon\text{Nd}$  (-3.1 to +2.0), preclude a common origin for the rhyolites. Instead, analyses of rhyolites cluster on variation diagrams into compositional groups ('magma types') with distinct isotopic signatures, and limited chemical variability. Eruptions of a particular magma type are related in time and/or space, so that compositional data combined with a knowledge of the ages and vent sites, produce a picture of what magma was available, when, and where. Rather than repeated tapping of a single chamber, the evolution of Taupo has been punctuated by eruption of distinct types of magma with stepwise rather than gradual changes between them.

The caldera-forming,  $\geq 800\text{km}^3$  Oruanui eruption at 26.5ka marks a major change in the magmatic system. Prior to this event the dominant control on composition was spatial. The period 320ka to 64ka was dominated by extrusion of lava domes, often in small groups that share the same isotopic signature. These are isotopically and chemically diverse (e.g.  $^{87}/^{86}\text{Sr} = 0.70489-0.70725$ ,  $\epsilon\text{Nd} = -3.1$  to  $+2.0$ ,  $\text{SiO}_2$  69-77%), although spatially related domes often have geochemical affinities that suggest discrete magma batches. Domes and pyroclastics from ~64-27ka record the growth of an isotopically homogeneous ( $^{87}/^{86}\text{Sr} = 0.70555$ ) magma chamber prior to the climactic Oruanui eruption, though even in this period, distinct, spatially-separated magma types continued to erupt. The post-26.5ka sequence represents a new type, defined by higher  $^{87}/^{86}\text{Sr}$  (0.70598-0.70622), trace element contents, and higher temperature. There is no spatial control on chemistry, but some compositional breaks are seen with time. The first three, small volume, eruptions at 20.5-17ka were dacitic and have  $^{87}/^{86}\text{Sr}$  ratios (0.70600) similar to those of post-26.5ka rhyolites, rather than Oruanui magma. The 25 eruptions from 12ka-1800a were rhyolitic, with very similar major elements, although there appear to be two subtly distinct inputs of new magma, into the high level system beneath the same vent site region, on timescales of only a few thousand years.

Taupo shows markedly different behaviour to many other rhyolite volcanoes of comparable productivity. The unusually high frequency of eruptions at Taupo, compared to systems like Long Valley, is paralleled by rapid changes in the type of magma available for eruption, with distinct chambers erupting magma for only  $\sim 10^3-10^4$  years. It is hoped to constrain magma residence times by comparing phenocryst formation ages from U-Th disequilibria studies with known eruption ages.

STUDY ON EFFECT OF ALTERATION ON APPARENT RE-OS AGE FOR MOLYBDENITE THROUGH NEAR-INFRARED MICROSCOPY.

SUZUKI, K., Dept. Chem., Arts and Sci., Univ. Tokyo, Tokyo 153, Japan and KAGI, H., Inst. Mat. Sci., Univ. Tsukuba, Ibaraki 305, Japan

Re-Os chronometry is a promising technique to determine the ages of sulfide minerals directly. We applied this method to molybdenite ( $\text{MoS}_2$ ) and obtained Re-Os ages, which show good agreement with related wall-rock ages (an indirect indicator of the real age). (Fig. 1)

Luck and Allègre (1982) pointed out the possibility of Re loss from molybdenite through alteration. McCandless et al (1993) having investigated molybdenite through near infrared (NIR) microscopy, also reported that high NIR transparency of molybdenite would indicate alteration and Re loss. If their hypothesis were true, it means that Re-Os chronometry can give an apparent Re-Os age older than the real one.

In our study, molybdenite from Mätäsvaara, Finland, whose Re-Os age agrees with the wall-rock age (Fig. 1), was observed through NIR. After the hypothesis by McCandless, this molybdenite should give low NIR transparency because it is considered to have experienced no such alteration as causes Re loss. However, thin section (0.2mm) of Mätäsvaara molybdenite was transparent to NIR and its inner texture can be easily seen. Therefore, high NIR transparency does not seem to reflect Re loss resulting in the significant deviation of Re-Os age.

In order to clarify the effect of alteration on Re-Os age as well as NIR transparency, laboratory experiments were done. Molybdenite, in  $\text{NaCl}$ ,  $\text{AlCl}_3$ , was exposed to a heat of  $180^\circ\text{C}$  for 40 days. The result was a remarkable increase in NIR transparency and intriguing changes were found in inner structures. For further understanding of the effect, experiments were continued through microprobe, NIR, and FTIR.

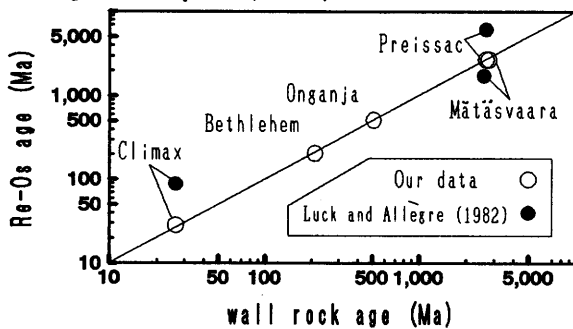


Fig. 1 Re-Os ages and related wall rock ages.

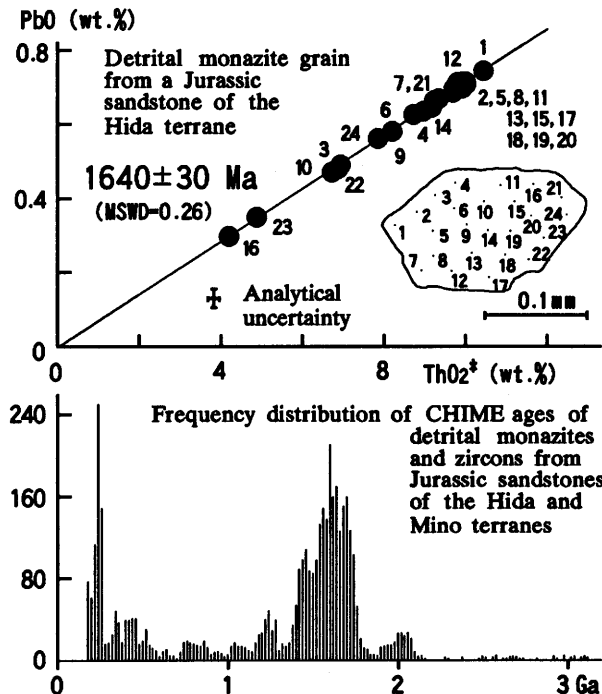
PRECAMBRIAN DETRITAL MONAZITES AND ZIRCONS FROM JURASSIC SANDSTONES IN THE JAPANESE ISLANDS, REVEALED BY "CHIME" GEOCHRONOLOGY

SUZUKI, K. and ADACHI, M., Dept. of Earth and Planetary Sciences, Nagoya University, Nagoya 464-01, Japan

A total of 3769 monazite and zircon grains from 56 Jurassic sandstones in the Mino and Hida terranes, central Japan were dated by the CHIME (CHEMICAL Th-U-total Pb Isochron METHOD; Suzuki et al., 1991; Suzuki and Adachi, 1991). Most monazite grains are chronologically unzoned and give CHIME ages of ca. 1700, 1450, 1250 or 240 Ma; several grains are zoned and show distinct core-overgrowth relations. The ca. 1700 Ma, most commonly observed, is considered to show the time of main metamorphism of the monazite-bearing gneisses that were exposed in the provenance of the Jurassic sandstone. The younger ages appear to represent some significant thermal events. Of particular interest are several Archean cores of 3000 and 2700 Ma within the ca. 1700 Ma monazites. Zircon ages range from ca. 3100 to 180 Ma, with conspicuous concentrations at ca. 2000 and 240-180 Ma. The ca. 2000 Ma age is interpreted to represent the emplacement time of original granites that provided large amounts of detritus to the protolith of the ca. 1700 Ma gneisses. The age spectra of monazites and zircons are nearly identical for sandstones from the Hida and Mino terranes. This is inconsistent with the current view that the Hida and Mino terranes were totally independent until their accretion in middle Cretaceous time.

The CHIME method, characterized by a high spatial resolution ( $2-3 \mu\text{m}$ ), is a powerful new tool for the study of clastic rocks in recycled orogens and for the terrane analysis.

Suzuki, K., Adachi, M. and Tanaka, T., 1991, *Sediment. Geol.*, 75, 141-147. Suzuki, K. and Adachi, M., 1991, *Geochem. J.*, 25, 357-376.



**NOBLE GASES IN THE SNC (MARTIAN)  
ORTHOPYROXENITE METEORITE ALH84001:  
COMPARISON WITH THE NAKHLITES**

SWINDLE, T. D., BURKLAND, M. K., and  
GRIER, J. A., Lunar and Planetary  
Laboratory, University of Arizona,  
Tucson, AZ 85721 USA

ALH84001 is an Antarctic meteorite which was recently found to be a relative of the SNC (Shergottites, Nakhrites and Chassigny) meteorites, and hence probably comes from Mars. We have measured noble gases in two samples of ALH84001: all five gases in a 18.1 mg sample, and Kr and Xe in a stepwise heating of a 142 mg sample. We find that ALH84001 bears some remarkable resemblances to the three nakhlites, but it has some intriguing differences as well.

The heavy noble gases in most shergottites can be plausibly fit as a mixture of the gas in EETA79001, ( $^{129}\text{Xe}/^{132}\text{Xe}=2.4$ ,  $^{136}\text{Xe}/^{132}\text{Xe}=0.36$ ,  $^{84}\text{Kr}/^{132}\text{Xe}=25$ ), thought to represent the martian atmosphere, and Chassigny ( $^{129}\text{Xe}/^{132}\text{Xe}=1.0$ ,  $^{136}\text{Xe}/^{132}\text{Xe}=0.30$ ,  $^{84}\text{Kr}/^{132}\text{Xe}=1$ ), perhaps representing the mantle. Nakhlites tend to have  $^{129}\text{Xe}/^{132}\text{Xe}$  ratios of 1.5 to 2.0, but  $^{84}\text{Kr}/^{132}\text{Xe}$  ratios of 5 or less, so they don't fall on the shergottite mixing line, but could represent a mixture of Chassigny-like gas and elementally fractionated atmosphere (Ott, 1988).

The  $^{129}\text{Xe}/^{132}\text{Xe}$  ratio in ALH84001 is as high as 2.05 in some extractions. Among the SNC's, only Nakhla (up to 2.2) and EETA79001 have higher values. The  $^{84}\text{Kr}/^{132}\text{Xe}$  is rather low (about 4), again similar to Nakhla. This would be consistent with a scenario in which the (isotopically) atmospheric-like noble gas in nakhlites is carried by weathering products (Drake et al., 1993), since ALH84001 contains what are probably martian weathering products, like the nakhlites. However, unlike the nakhlites, most of the temperature extractions do not fall on the Chassigny-EETA79001 mixing line in Xe three-isotope plots such as  $^{129}\text{Xe}/^{132}\text{Xe}$  vs.  $^{136}\text{Xe}/^{132}\text{Xe}$  ( $^{136}\text{Xe}/^{132}\text{Xe}$  is too low).

We calculate a preliminary cosmic-ray exposure age, based on Ne and Ar, of 15-20 Ma, considerably longer than the 10 Ma exposure age of the nakhlites and Chassigny or the  $\leq 3$  Ma of the shergottites. Thus, at least its most recent parent body was distinct from any of the previously known SNCs.

Ott, U., 1988, Noble gases in SNC meteorites: Shergotty, Nakhla, Chassigny, *GCA* 52, 1937-1948.

Drake, M.J., Owen, T., Swindle, T., and Musselwhite, D., 1993, Noble gas evidence of an aqueous reservoir near the surface of Mars more recently than 1.3 Ga. *LPSC XXIV*, 431-432.

**AGE OF FISH CANYON TUFF SANIDINE (FCTS):**

**A SINGLE CRYSTAL  $^{40}\text{Ar}/^{39}\text{Ar}$  DATING STANDARD  
SWISHER III, C.C. (1), DEPAOLO, D.J. (2), OWENS, T. (2,1):** (1) Institute of Human Origins Geochronology Center, 2453 Ridge Rd., Berkeley, CA, 94709, USA; (2) Department of Geology and Geophysics, University of California, Berkeley, CA, 94720, USA.

The Fish Canyon Tuff Sanidine (FCTS) is currently one of the most widely used  $^{40}\text{Ar}/^{39}\text{Ar}$  neutron fluence monitors (dating standard) applicable for the calibration of late Cretaceous and Cenozoic rocks. Replicate analyses of individual crystals of the FCTS yield SE's on the order of 0.1% or less, making it potentially an excellent single crystal  $^{40}\text{Ar}/^{39}\text{Ar}$  neutron fluence monitor. However, because of difficulties in assuring complete argon extraction of sanidines by K-Ar dating, the age of the FCTS is obtained largely from  $^{40}\text{Ar}/^{39}\text{Ar}$  intercalibration with first principal biotite K-Ar standards. At IHO-GC, an age of 27.84 Ma<sup>2</sup> is used based on  $^{40}\text{Ar}/^{39}\text{Ar}$  intercalibration with MMhb-I hornblende using a published age of  $520.4 \pm 1.6$  Ma<sup>1</sup>. However, the age of MMhb-I itself is disputed with younger age estimates of 513.9 Ma that result in a FCTS age of 27.55 Ma<sup>3</sup>. Consequently, despite the precision capable using the FCTS as a  $^{40}\text{Ar}/^{39}\text{Ar}$  fluence monitor, its accuracy is limited by uncertainties as to the ages of the K-Ar standards used for intercalibration.

To provide a more accurate age for the FCTS, we present age intercalibration with two K-Ar biotite standards University of California, Berkeley (UCB), GHC305 and Australian National University (ANU) GA1550. The ages of these biotite standards are based on published Ar abundances of  $1.428 \times 10^{-11}$  for GHC-305 and  $2.245 \times 10^{-11}$  for GA-1550 and potassium abundances as determined here by isotope dilution mass spectrometry. Review of potassium measurements of GHC305 by flame photometry at UCB accumulated over a 20 year period, had shown short-term reproducibility on the order of 0.5% or less while long term variation ranged over 2%. Isotope dilution mass spectrometry results of this study yielded a mean potassium value of  $7.58 \pm 0.03$  1 $\sigma$  GHC305 (7 splits) and  $7.63 \pm 0.05$  1 $\sigma$  for GA1550 (8 splits). Using these potassium values, the K-Ar age for GHC305 would be 105.49 Ma and 98.77 Ma for GA1550.

For  $^{40}\text{Ar}/^{39}\text{Ar}$  intercalibration, the FCTS was irradiated along with GHC305 and GA1550 for 14 hours in the Los Alamos Reactor. The irradiation fluence or J was calculated separately for both GHC305 and GA1550 based upon 30 analyses each (a single analysis was obtained by laser fusion of 1-3 biotite crystals). The J's were then used to calculate ages for 27 laser total fusion analyses of single crystals of the FCTS. Using the GHC305 J, we calculate a weighted mean age for FCTS of  $28.06 \pm 0.02$  Ma and using GA1550 an age of  $28.04 \pm 0.02$  Ma. Combined GHC305 and GA1550 indicate an age of  $28.05 \pm 0.02$  Ma for the FCTS.

<sup>1</sup>Samson, S.D. and E.C. Alexander, Jr. 1987. *Chem. Geol. Isot. Geosci.* 66: 27.

<sup>2</sup>Deino, A. and R. Potts. 1990. *J. Geophys. Res.* 95: 8453.

<sup>3</sup>Lanphere, M.A. 1990. *EOS* 71:1658.

**U-SERIES DATING OF SPELEOTHEMS AND TRAVERTINES FROM ESINO RIVER VALLEY (CENTRAL ITALY) AND THEIR PALEOCLIMATIC AND GEOMORPHIC SIGNIFICANCE.**

TADDEUCCI, A., Dipartimento di Scienze Geologiche, III Università di Roma, Roma, 00146, Italia, TUCCIMEI, P., Dipartimento di Scienze della Terra, Università "La Sapienza", Roma, 00185, Italia, e VOLTAGGIO M., Centro di Studio per il Quaternario e l'Evoluzione Ambientale, CNR, Roma, 00185, Italia.

U-series ages of speleothems from "Fiume-Vento" cave system and of travertines associated to the Esino River terraces have been obtained. The cave is located in the Esino River drainage basin (Central Italy) and has been developed at seven progressively deeper levels in a limestone formation due to lowering of local base level.

The cave floors can be correlated with the Esino River terraces capped with strata of travertines formed when the river started to downcut the previously deposited sediment. Dating a large number of speleothems from each cave floor and the bottom layers of travertines makes possible to estimate when the base level dropped down. This can be due to a climatic change and/or to an uplift of the Appennini mountain range.

Speleothems from the first and second level formed less than 10,000 years BP and samples from the fifth level date back to 130,000 and 200,000 years respectively. The travertine layers covering the river terraces of third order started to deposit around the end of the Last Glaciation and can be correlated to the second cave level.

Valley floor maximum downcutting rates over the last 15,000 years were calculated from the age of speleothems and travertines. They equal to about 0,20-0,21 m/1000 y.

Speleothems and travertines have also provided valuable paleoclimatic information. The periods of most abundant growth are clearly correlated to interglacials and periods of no deposition correspond to the glaciations.

Dating different portions of speleothems made possible the measurements of their radial and vertical accretion rate which show an increasing trend during the interglacial periods. Over the last glaciation the deposition rate remained stationary, whereas their decrease could be expected. Probably the lower amount of circulating water and the consequent lower concentration of dissolved carbonate were balanced by a longer residence time of seepage water through the wall-rock due to lowering of the base level.

**TOWARDS ZIRCON FISSION-TRACK THERMOCHRONOLOGY: THE NATURAL LONG-TERM ANNEALING AND FOSSIL PARTIAL ANNEALING ZONE AROUND A GRANITIC PLUTON**

TAGAMI, T., SHIMADA, C. AND NISHIMURA, S., Dept. of Geology and Mineralogy, Kyoto Univ., Kyoto, 606, Japan.

Thermal annealing characteristics of fission tracks in zircon have been better understood and precisely quantified through a series of laboratory experiments in recent years, establishing a reliable basis of zircon fission-track (ZFT) thermochronology (e.g. Tagami et al., 1990; Yamada et al., 1993, 1994; Hasebe et al., 1993). To reconstruct thermal histories of rocks using laboratory data, however, it should be elucidated that the track annealing process for geologic periods of time at low temperature is essentially the same as that for shorter laboratory heating duration at higher temperature. Here we report the analysis of ZFT annealing patterns in and around a granitic pluton to investigate the natural long-term annealing behavior.

The studied area is the Shimanto accretionary prism, Shikoku, Japan, in which several Miocene granitic bodies are exposed. Most of them show clear intrusion relationships, accompanied by the contact metamorphic aureole. We collected sandstones from two coherent units of Cretaceous age around Takatsukiyama Granite of ~15 Ma, the largest body (~5km in diameter) in the region. Sampling was carried out along an eastward traverse, with variable distances of ~1 to ~5x10<sup>4</sup> m from the contact.

ZFT ages and confined track lengths were measured on zircon separates, focusing particularly on the transient zone of track retentivity, i.e., fossil partial annealing zone (FPAZ). As approaching to the contact, original ZFT ages of ~100 Ma show a drastic, continuous reduction down to ~15 Ma at ~3 km distance. Their age spectra accordingly change from multimodal, broad distributions reflecting provenance ages to unimodal, peaky distributions characterizing the heating event. Mean track lengths and their distributions also show remarkable variations in FPAZ, as a consequence of mixing both shortened tracks to various degree by the Miocene heating and unannealed ones with original lengths formed thereafter. This track shortening pattern in nature (heating duration of ~10<sup>5</sup>y, estimated from thermal modeling) is comparable to that in laboratory. The 'gap zones' of annealed tracks are observed in the advanced stage of laboratory annealing, indicative of track segmentation process subsequent to the initial shrinking stage (Yamada et al., 1994). The same features were found in the studied samples having greater reduction in age within FPAZ, and this further supports the same annealing process. Consequently, the measured variations of those ZFT parameters within FPAZ, in conjunction with laboratory annealing data, throw lights on the proper thermochronologic interpretation of ZFT data of detrital grains in a sedimentary rock.

Hasebe et al., 1993, Chem. Geol., 110 (in press).

Tagami et al., 1990, Chem. Geol. (Isot. Geosci. Sec.), 80: 159-169.

Yamada et al., 1993, Chem. Geol. (Isot. Geosci. Sec.), 104: 251-259.

Yamada et al., 1994, this issue.

## AGE AND PALEOMAGNETIC STUDIES FOR ROCK SAMPLES FROM MAHANADI AND GODAVARI GRABEN, EAST INDIA

TAKIGAMI, Y., Kanto Gakuen University, Ohta-shi, Gumma, 373, Japan, HIROOKA, K., Toyama University, Toyama-shi, Toyama, 930, Japan, SAKAI, H., Toyama University, Toyama-shi, Toyama, 930, Japan, Funaki, M., National Institute of Polar Research, and Sakai, H., Kyushu University, Fukuoka-shi, Fukuoka, 810, Japan

Age and Paleomagnetic studies were performed on rock samples collected from Mahanadi and Godavari graben, East India, in order to reconstruct the position of Indian continent that was a part of Gondwana land before Paleozoic.

$^{40}\text{Ar}$ - $^{39}\text{Ar}$  plateau ages of about 510-520, 560 and 680 Ma were obtained for biotite samples separated from gneiss rocks. A pyroxene sample of a charnockite rock and dacite dyke rock samples had excess Ar and isochron ages were 500 - 570 Ma. There have been no  $^{40}\text{Ar}$ - $^{39}\text{Ar}$  age data in this area before and plateau ages of 500 -550 Ma are consistent with previous  $^{40}\text{Ar}$ - $^{39}\text{Ar}$  results obtained for rock samples of East Antarctica. The age of about 680 Ma has been not reported by the  $^{40}\text{Ar}$ - $^{39}\text{Ar}$  study for the Antarctic samples.

Paleomagnetic studies ( thermal demagnetization ) were performed for same samples. From one sample, good magnetic direction (  $D= 53.1^\circ$  ,  $I= 11.4^\circ$  ,  $\alpha_{95}=9.75^\circ$  ) was obtained and this data is consistent with previous data for other samples from Gondwana land at the same age.

## OXYGEN ISOTOPE STUDIES IN HUDSON BAY AND HUDSON STRAIT, CANADA

TAN, FRANCIS C., Marine Chemistry Division, Bedford Institute of Oceanography, Dartmouth, Nova Scotia, B2Y 4A2, Canada, and STRAIN, Peter M., Marine Chemistry Division, Bedford Institute of Oceanography, Dartmouth, Nova Scotia, B2Y 4A2, Canada.

The oxygen isotopic composition of surface water in arctic regions is influenced by freshwater derived from both the melting of sea ice and the input of meteoric waters (land runoff, precipitation and glacial melt). A full understanding of the chemistry and physics of such regions requires the knowledge of the spatial and temporal distributions of these low-salinity inputs. Oxygen isotope measurements can be used to distinguish between sea ice meltwater and the combined input of meteoric water from the other three sources.

The oxygen isotopic composition of water in Hudson Bay, Hudson Strait, Foxe Basin and the Labrador Shelf has been determined. The following types of oxygen isotope-salinity relationships have been observed: straight lines with different slopes and apparent freshwater components ( $\delta^{18}\text{O}_{\text{pwt}}$ ), horizontal lines, bilinear or two line segments, and single points. The oxygen isotopic composition of water in Foxe Basin (-2.0 ppt) is nearly constant over the whole salinity range (30 to 40 psu). The apparent freshwater component ( $\delta^{18}\text{O}_{\text{pwt}}$ ) for three stations has a mean value of 0 ppt indicating that sea ice meltwater is the dominant freshwater component. Similar oxygen isotope-salinity relationships are found in northwestern Hudson Bay-Strait. Surface waters in northern Hudson Bay exhibit the most negative  $\delta^{18}\text{O}$  value (-4.0 ppt) and lowest salinity (29 psu) for the entire studied area suggesting the large contribution of river runoff. The apparent freshwater component ( $\delta^{18}\text{O}_{\text{pwt}}$ ) ranges from 0 to -26 ppt from Hudson Bay to the Labrador Shelf. The significance of this variability will be discussed.

## DESERT IS A POTENTIAL SINK OF CO<sub>2</sub>: ISOTOPIC EVIDENCE

TANAKA, T., INAYAMA, E. & ASAHARA, Y.  
Dept. of Earth and Planetary Sciences,  
School of Science, Nagoya University,  
Chikusa, Nagoya 464-01, JAPAN

Carbonate carbon in desert sand was examined in respect of its abundance, <sup>87</sup>Sr/<sup>86</sup>Sr ratio and <sup>14</sup>C concentration. 18 samples of desert sand were collected from various deserts and semi-desert areas in the world. Samples were mostly collected from the edge of the deserts. More than 90% of the sand passed through an 80 mesh (160 μm) sieve and grains finer than the mesh were used for analysis.

Samples were decomposed with concentrated phosphoric acid in a vacuum system, and volume of CO<sub>2</sub> gas recovered was measured after separation of H<sub>2</sub>O. The CO<sub>2</sub> content in the sands was found to be 0.0~17.0 wt.% as carbonate. CO<sub>2</sub> tends to be concentrated more in sand of older deserts than in sand of younger ones. This indicates that the carbonate accumulated with age in desert sand because of little weathering caused by few precipitation.

<sup>87</sup>Sr/<sup>86</sup>Sr ratio was measured for the carbonate and its host sand. The ratios of the carbonate vary from 0.708 to 0.712, which are somewhat higher than those of marine carbonate in any geologic time. Low Rb/Sr ratios of the desert carbonate do not allow to accumulate the large amount of radiogenic <sup>87</sup>Sr in geologic time. Significant parts of the carbonate in desert are considered to originated in source different from limestone which was formed in ancient marine environments.

<sup>14</sup>C/<sup>13</sup>C ratios of the carbonate were measured using a tandemron accelerator mass spectrometer at Nagoya University. The obtained ratios are distributed between 0.055±0.002 and 0.024±0.002 relative to those of AD 1950. The ratios correspond to ages 24000±300 and 31000±500 yBP, respectively. This indicates that all of the carbonate is not derived from detrital limestone formed in geologic time but some parts of the carbonate have been formed during historic time in desert.

Average CO<sub>2</sub> content in the sand was 6.8 wt% as carbonate (CaCO<sub>3</sub>). When we assume that the area of desert, thickness of desert sand, density of desert sand are 8000,000km<sup>2</sup>, 10m and 2g/cm<sup>3</sup>, respectively, the total amount of CO<sub>2</sub> in desert is calculated to be 0.5×10<sup>19</sup> grams. The amount exceeds the carbon abundance in the worldwide biomass which is estimated to be 0.55×10<sup>18</sup> grams as carbon.

Desert stocks a large amount of CO<sub>2</sub>, because of its unique features such as few precipitation and quick evaporation. Desert is not a useless place as generally considered but is the potential sink of CO<sub>2</sub>.

Samples are donated by Naoyuki Ando, Takemasa Ishii and Kiyohide Mizuno of Geological Survey of Japan and Liu Peijin of Academia Sinica and Shimizu Corporation. <sup>14</sup>C/<sup>13</sup>C ratios were determined under the leading of Toshio Nakamura of Nagoya University.

## VERTICAL AND LATERAL CONTRIBUTIONS TO CRUSTAL GROWTH: GEOCHEMICAL AND TECTONIC ASPECTS

TARNEY, John and JONES, C.E., Dept. Geology,  
University of Leicester, Leicester LE1 7RH, UK

The composition of the Earth's continental crust differs from that of other planetary crusts, and is consistent both with relatively small degrees of melting and with the influence of hydrous fluids. Variations in the chemistry of crustal components with time primarily reflect differences in the thermal regime associated with subduction processes, but there are second order effects. Recent advances in modelling the thermal structure of subduction zones have helped constrain the conditions under which the slab melts, and have generally enhanced the role of the mantle wedge in magmagenesis and the importance of induced convection in replenishing the zone of magma generation. Mantle plumes may also have an important influence on crust generation, both directly and indirectly.

Extensive and continued melting of the subducted slab to produce voluminous sodic tonalites and trondhjemites is only thought possible under Archaean thermal conditions when warm hydrous crust subsides into hot mantle and melting is controlled by hornblende and garnet equilibria. Arguably, similar conditions pertain - at least for a short time - at the present day wherever there is ridge subduction. However, such melts share trace element and isotopic characteristics with wedge-derived melts initiated by pressure-controlled breakdown of hornblende where there is induced convection in the mantle wedge. Where thermal gradients are cooler, with thicker lithosphere, more mature arcs, cooler slab, etc., melting compositions will be controlled by phlogopite. A survey of the compositions of orogenic granitoids and volcanics shows that there are some consistent (but complementary) trace element differences which may reflect this mineralogical control of parental magmas at source. Extra thermal input from mantle plumes may change the thermal structure of the lithosphere and hence change the mineralogical controls on magmagenesis.

As continental growth progresses through vertical magmatic accretion, there is increasing crustal development through lateral subduction-accretion, particularly where major river systems have discharged at active margins. Here oceanic components, ocean islands, arcs, plateaus, abyssal oozes, etc., are tectonically intermixed with continent-derived upper crustal sediment, often gneissified, and suffer melting during exhumation, thermal relaxation or active extension. The sub-continental lithosphere may become heavily contaminated with subducted sediment. Such regions provide a mixture of S- and I-type granitoids with varying proportions of "mantle" and "crust" components; this type of crustal development is particularly common in the Phanerozoic and can be recognised both chemically and isotopically. However, where continental breakup produces new cordilleran margins, as in the Andes, the thermal structure of the leading edge changes to favour mantle wedge melting, mostly with hornblende control on magma chemistry and a reducing sediment/crustal involvement.

These models favour continual growth of continental crust, but with changing mechanisms of crust generation with time.

SR AND PB ISOTOPE EVIDENCE FOR THE ORIGIN OF SKARN, SULFIDES AND FLUOR MINERALIZATIONS OF THE ITAOCA GRANITOID, SOUTHEASTERN BRAZIL.

TASSINARI, C.C.G. Centro de Pesquisas Geocronológicas, Universidade de São Paulo, São Paulo, Po.Box 20899, Brazil; MELLO, I.S.C., Instituto de Pesquisas Tecnológicas do Estado de São Paulo, Brazil; GOMES, D.P., CNPq, Brazil.

Several mineralizations are associated with the post-tectonic Itaoça granitoid which is intruded into low-grade late Proterozoic metasedimentary sequences, in Ribeira region southeastern Brazil.

The granitoid comprises monzogranites, quartz-syenites and granites corresponding to a high-potassium peraluminous calc-alkaline trend. The sedimentation of the host metamorphic sequences comprising terrigenous and carbonatic sediments developed during the time period 1.8 to 1.5 Ga. ago.

The skarn type mineralizations are associated with metasedimentary roof- pendant inside the granitoid., which include schists, pelitic hornfels and marbles. They are characterized by endoskarn, garnet-pyroxene-skarn and garnet-wollastonite-skarn. Scheelite-Powellite and wollastonite are the ore minerals. Fluorite and sulfide mineralizations associated to the quartz-veins in fractures or shear zones in the granitoid also occur.

Sr and Pb isotopic analyses were carried out on ore minerals and the host rocks in order to understand the petrogenesis of the mineralizations.  $^{87}\text{Sr}/^{86}\text{Sr}$  isotopic ratios of the calcite in the skarns (0.7103 to 0.7109) display values very similar with those obtained for calcites from (host) marbles (0.7100). However these values are slightly higher in comparison with the wollastonites (0.7092 to 0.7109).

The Itaoça granitoid yielded a Rb-Sr whole rock isochron age of  $676 \pm 25$  Ma, with Sr initial ratio of  $0.7097 \pm 0.0001$  which is in close agreement with the Sr isotopic initial composition of the skarn mineralizations. This fact suggests that the Sr was derived from the granitoid intrusion responsible for the origin of the skarn. Thus we infer a magmatic origin for the mineralization.

Tardi and/or post-magmatic processes, such as albitization and greisenization probably related to the skarn genesis, took place in the central part of the granitic body, around 620 Ma ago, as supported by a Rb-Sr preliminary isochron. Therefore we assume these processes as contemporaneous with the skarn mineralization.

The Fluorite veins have  $^{87}\text{Sr}/^{86}\text{Sr}$  isotopic composition of 0.7114, so higher than that of the skarn fluids. In addition, considering that the host metasedimentary sequences include abundant fluorite mineralizations, we consider these supracrustals as the source for the Fluorite.

The galenas from the sulfide-bearing quartz veins have homogeneous Pb isotopic compositions values, and yielded Stacey-Krammers model ages of 1.4 Ga. This age and the corresponding isotopic compositions are in agreement with previous data on Pb-Ag mineralizations in the same host metasedimentary sequence. Thus the Pb of the galena inside the granitoid was leached from this sequence by exotic fluids of metamorphic origin and/or meteoric water.

ORIGIN OF HAWAIIAN BASALTS INFERRED FROM ISOTOPES

TATSUMOTO, M., U.S. Geological Survey, Box 25046, MS 963, Denver, CO 80225

Our group at USGS, Denver has undertaken studies of Nd, Sr, and Pb isotopic compositions of basalts from Emperor-Hawaiian volcanoes e.g. (1,2,3) and of xenoliths in the basalts (4) in order to obtain isotopic constraints on their origin. Hawaiian volcanoes evolve similarly and can be subdivided into three main stages: shield building tholeiitic stage, caldera-filling alkalic stage, and posterosional (PE) nephelinitic stage. Our isotopic studies lead us to propose a three component mixing model for the sources: a mantle plume (Koolau end member), the lithosphere (Kea end member), and a depleted asthenosphere (posterosional end member).

Hawaiian tholeiites can be explained by mixing of a plume with the sea water-altered lithosphere. The isotopic compositions of PE alkaline basalts are distinct from those of Koolau shield tholeiites and MORB, and are considered to have originated from the depleted asthenosphere. High trace element concentrations in PE basalts are thought to be derived from metasomatic fluids from plumes added just prior to the eruption.

Isotopic compositions of xenoliths in the Honolulu series are, however, similar to those of the host PE magma, indicating that they are genetically related and PE basalts originated from the deep lithosphere, probably the lithosphere-asthenosphere boundary. The isotopic relationships of Nd and Pb may be generated ~80 Ma which corresponds to the age of the lithosphere at Hawaii. The initial  $\epsilon_{\text{Nd}} = -8.5$  for the xenoliths, which is slightly lower than that for the East Pacific MORB, suggests a possibility that the xenoliths and the host magma originated from a body that had intermediate characteristics and intruded into the lithosphere at or near the East Pacific Rise. Such basalts with intermediate characters are observed at "off-ridge" seamounts.

We propose that the lithosphere, containing intermediate-composition bodies, moves and approaches the Hawaiian hot spot resulting in the eruption of PE basalts. If such bodies do not occur close to a volcano, then PE basalts do not erupt.

- (1) Tatsumoto, M. 1978, Isotopic composition of lead and its implication to mantle evolution: *Earth. Planet. Sci. Lett.* 38, 63-87.
- (2) Stille, P., Unruh, D. M. and Tatsumoto, M., 1986, Pb, Sr, Nd, and Hf isotopic constraints on the origin of Hawaiian basalts and evidence for a unique mantle source: *Geochim. Cosmochim. Acta* 50, 2302-2319.
- (3) Hegner, E., Tatsumoto, M., and Unruh, D. M., 1986, Sr, Nd, and Pb isotopic evidence for origin of the West Maui volcanic suit, Hawaii: *Nature* 319, 478-480.
- (4) Okano, O., Tatsumoto, M., and Leemen, W. P., 1987, Sr, Nd, and Pb isotopes in Hawaiian basalt xenoliths: inferences for the origin of Hawaiian basalts: *EOS*, 68, 1521.

## ISOTOPE GEOCHEMISTRY OF AXIAL VOLCANIC CONSTRUCTS ALONG THE REYKJANES RIDGE

TAYLOR, Rex N., Department of Geology, Royal Holloway and Bedford New College, University of London, Egham, Surrey, TW20 0EX / Department of Geology, University of Southampton, Highfield Southampton, SO9 5NH, UK., THIRLWALL, Matthew F., Department of Geology, Royal Holloway and Bedford New College, University of London, Egham, Surrey, TW20 0EX, UK., and MURTON, Bramley J. Institute of Oceanographic Sciences Deacon Laboratory, Brook Road, Wormley, Godalming, Surrey, UK.

Recent bathymetric surveys of the Reykjanes Ridge between 57°N and 63°N have shown that the spreading axis is composed of a series of en echelon axial volcanic ridges (AVR's). Using this bathymetry, a detailed sampling program was undertaken to investigate the geochemical variation within and between these constructs. Sampling was performed using dredge and rock-chipper deployed from the RRS Charles Darwin. To increase the precision of sample location, the bottom-time for each dredge was kept to a minimum (<20mins). As a result samples could be located within a  $\approx$  300m radius of the station.

Major and trace element data and Nd, Sr and Pb isotope ratios are presented from AVR's within the southern section of the Reykjanes ridge (57°N to 59°N). Data are organised relative to location within each AVR (tip, centre or flank) and with respect to the apparent age of the volcanic construct. Significant variation in La/Sm exists within each AVR at an essentially constant isotopic composition. This probably reflects a variation in melting parameters within the mantle diapir, instead of representing variable mixing proportions between MORB asthenosphere and Iceland plume. Pb isotope data do reflect such mixing, but the  $^{207}\text{Pb}/^{204}\text{Pb}$  and  $^{208}\text{Pb}/^{204}\text{Pb}$  systematics indicate that mixing is not a simple north-south increase in the magnitude of the asthenospheric component. Both the plume and the asthenospheric component are required to change in Pb isotopic composition along the ridge.

## SR AND ND-ISOTOPES OF THE DECCAN MANTLE PLUME: EVIDENCE FROM THE EARLY ALKALI IGNEOUS COMPLEXES OF MUNDWARA AND SARNU, RAJASTHAN.

TEICHMANN, F.R., AND BASU, A.R., Dept. of Earth and Environmental Sciences, University of Rochester, Rochester, New York 14627, USA.

We have recently documented (Basu et al., 1993) a high- $^3\text{He}$  plume origin for the 68.5 Ma-old alkali igneous complexes of Sarnu and Mundwara, Rajasthan, which preceded the bulk of the Deccan volcanism to the south that erupted precisely at 65 Ma, the K-T boundary. Here, we report the Sr and Nd-isotopic characteristics and the trace element geochemistry of the different lithologic units of these igneous complexes.

Alkalic ultramafic, mafic and syenitic lithologies, which comprise the major portions of the different hypabyssal intrusives, show LREE-enrichment from 20 to 1000 times chondrite in Ce. The relatively undifferentiated lithologies, such as picrites and gabbros, show also less LREE-enrichment. However, the latter group show a very restricted  $\epsilon_{\text{Nd}}$  and Sr-isotopic ratios, mostly varying between  $\epsilon_{\text{Nd}} = +1.3$  to  $+4.0$  and  $^{87}\text{Sr}/^{86}\text{Sr} = 0.70445$  to  $0.70490$ . These isotopic characteristics are remarkably similar to the Reunion mantle plume and to the least-differentiated Ambeali tholeiitic formations of the Deccan Traps. These Nd and Sr-isotopic signatures of the early alkali igneous pulses of the Deccan plume thus can be considered to represent the lower mantle source before its further modification by interactions with the Indian continental lithosphere. The high  $^3\text{He}/^4\text{He}$  ratios of  $14 R_{\text{AIR}}$  in these complexes also strongly support this Nd, Sr-isotopic characterization of the Deccan mantle plume.

Basu, A.R. et al., 1993, Early and Late Alkali Igneous Pulses and a High- $^3\text{He}$  Plume Origin for the Deccan Flood Basalts, *Science*, v. 261, p. 902-906.

40AR-39AR AND RB-SR GEOCHRONOLOGY OF THE PROTEROZOIC URUGUAYAN DIKE SWARM (URUGUAY), SOUTH AMERICA: TECTONIC SIGNIFICANCE.

TEIXEIRA, W., CPGeo - Instituto de Geociências, University of São Paulo, São Paulo, 05508-900, Brazil, RENNE, Paul, R., Institute of Human Origins, CA 94709, USA, BOSSI, J. and CAMPAL, N., Facultad de Agronomía, Universidad de La Republica, Uruguay.

The Uruguayan dike swarm in the Rio de La Plata Craton has been studied by means of 40Ar-39Ar determinations (one hornblende separate and 6 single crystals of biotite and muscovite) and Rb-Sr geochronology (7 internal isochrons on mineral concentrates and whole rocks). 40Ar-39Ar plateau ages (up to 101 steps in one case) on a coarse grained enclave (micropegmatite) in the mafic dikes, and felsic veins (located at the borders of the dikes) are concentrated in the range 1,728-1,713 Ma, although slightly younger pseudo-plateau ages (defined by a fraction of the 39Ar released in the spectrum) were also obtained (1,700 - 1,687 Ma).

Based on concordance of the hornblende and biotite plateau ages from the micropegmatite investigated (respectively 1,728 ± 2 Ma and 1,725 ± 2 Ma) it is proposed that it cooled rapidly and that its crystallization age is therefore estimated by the hornblende date. This age is considered as representing the emplacement time for the dike itself, and by extrapolation the best estimative for the age of the Uruguayan dike swarm. One Rb-Sr internal errorchron age of 1,779 ± 87 Ma ( $^{87}\text{Sr}/^{86}\text{Sr} \cong 0.705$ ) obtained for another dike is also consistent (considering the error) with the range of the 40Ar-39Ar ages obtained.

Correlation of these data with dated Precambrian mafic dike swarms, contemporaneous granitoids, and characteristic geological features of correlative crustal blocks (with similar tectonic history) in southernmost South America and South Africa, suggest that the Uruguayan diking event was coeval and genetically associated with the origin of a continental rift which took place in Western Gondwanaland, after the stability of the Transamazonian cycle (2.2 - 2.0 Ga). This igneous event is considered as anorogenic in character, which is consistent with the crustal history of the country rocks of the Craton and geological features characteristic of the dikes studied (e.g., igneous fabric, net contacts with host rocks), demonstrating the emplacement of the swarm into a previously cooled, rigid crust.

Detailed examination of the structure of the Ar spectra obtained (first steps of the plateaus; e.g. up to 4% of 39Ar released) plus interpretation of isotope correlation diagrams, when compared with most of the new Rb-Sr internal isochron ages (1.4 - 1.0 Ga and ~ 0.56 Ga) on the dikes and its felsic veins, together with the published K-Ar apparent ages on the dikes (1.6 - 1.4 Ga) indicate that the whole swarm was overprinted by differential, low temperature episodes long after its formation. This strong variation in the apparent ages obtained for both the Rb-Sr and K-Ar systems are interpreted as tectonically influenced by the tectonomagmatic activity characteristic of the Namaqualand (1.4-1.0 Ga), in South Africa, and further on by the Brasiliano events (Upper Proterozoic). Such events are well recognized in the tectonic evolution of the Gondwanaland.

THE POLYGENETIC NATURE OF THE BASEMENT ROCKS OF MALAITA AND SANTA ISABEL, SOLÓMON ISLANDS (S. MARGIN OF ONTONG-JAVA PLATEAU)

TEJADA, M.L.G., MAHONEY, J.J., SPENCER, K.J., SOEST, Honolulu, HI, 96822, USA, and HAWKINS, M.P., British Geological Survey, Vanuatu

Isotopic and chemical studies show that the igneous basements of Malaita and Santa Isabel consist of petrogenetically unrelated rocks: a) Older Series Tholeiites and Sigana Tholeiites; b) Malaita and Sigana Alkalic Suites; and c) San Jorge Volcanics. The Early Cretaceous Older Series (Malaita) and Sigana Tholeiites (Santa Isabel) define a limited range of isotopic compositions despite the wide (>200 km) spatial distribution of samples:  $\epsilon_{\text{Nd}}(\text{T}) = +3.4$  to  $+6.6$ ;  $(^{87}\text{Sr}/^{86}\text{Sr})_{\text{T}} = 0.70369$  to  $0.70423$ ;  $^{206}\text{Pb}/^{204}\text{Pb} = 18.245$  to  $18.644$ . These values are remarkably similar to those of the contemporaneous Ontong-Java Plateau (OJP) lavas at ODP and DSDP Sites 807, 803, and 289<sup>1</sup>, located 1200-1700 km to the north; the combined results indicate a rather uniform hotspot-like mantle source for the world's largest oceanic plateau. As with the ODP lavas, rare-earth-element inversion modeling supports a plume-like source and suggests that the rocks are products of high degrees of partial melting (~30%) at relatively shallow average depths.

Isotopic data also reveal that the two younger alkalic suites present on Malaita (the Younger Series and the North Malaita Alkalic Basalts) are distinct from each other, and differ from those of Santa Isabel (Sigana Alkalic Suite), indicating derivation from three different sources. The Younger Series (~45 Ma; R.A. Duncan, unpubl. data) have compositions overlapping the field for the primitive(?) mantle end-member postulated by Farley et al.<sup>2</sup> for Samoan lavas, consistent with the passage of the OJP over this hotspot during migration to its present location<sup>3</sup>. In contrast, the North Malaita Alkalic Basalts have isotopic compositions near the OJP fields (e.g.  $\epsilon_{\text{Nd}}(\text{T}) = +4.5$ - $4.7$ ,  $(^{87}\text{Sr}/^{86}\text{Sr})_{\text{T}} = 0.70367$ - $0.70370$ , and  $^{206}\text{Pb}/^{204}\text{Pb} = 18.754$ - $18.826$ ), suggesting a possible petrogenetic link. The Sigana Alkalic Suite have isotopic compositions similar to "HIMU-type" Tubuaii and Mangaia lavas<sup>4</sup>, but plate tectonic reconstructions<sup>3</sup> do not show the OJP to have passed anywhere near present "HIMU-type" hotspots at the inferred time of eruption for these basalts (~65 to 45 Ma).

The San Jorge Volcanics, which crop out to the south and west of the Sigana Tholeiites, are composed of MORB-like lavas and lavas with arc-like isotopic and chemical compositions, indicating that the San Jorge Suite is not part of the OJP. Some San Jorge Volcanics could represent abyssal sea-floor obducted onto the leading edge of the OJP during its emplacement against the old Solomons Trench, and some could represent crust formed at an arc or back-arc spreading system that was trapped during the collision.

<sup>1</sup>Mahoney et al., AGU Monogr., 77, 233, 1993.

<sup>2</sup>Farley et al. EPSL, 111, 183, 1992.

<sup>3</sup>Yan and Kroenke, Proc. ODP Sci. Res., 130, 697, 1993.

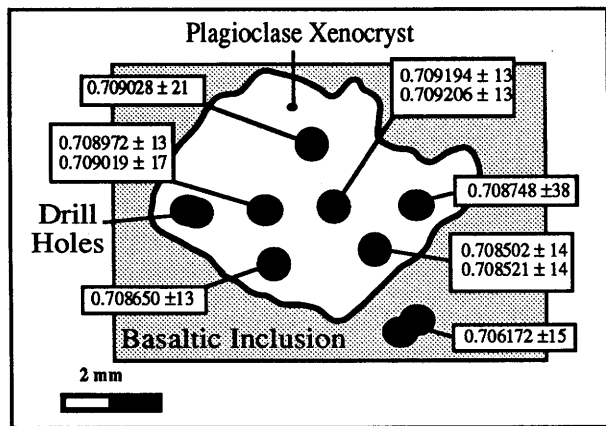
<sup>4</sup>Vidal, et al., Nature, 307, 536, 1984; Palacz and Saunders, EPSL, 79, 270, 1986.

**ISOTOPIC ZONATION IN A PLAGIOCLASE XENOCRYST: PROGRESS TOWARDS CONSTRAINING TIME SCALES OF MAGMATIC PROCESSES.**

Tepley, F.J., Davidson, J.P. and Holden, P., Dept. of Earth and Space Sciences, UCLA, Los Angeles, CA 90024, USA

Micro drilling of a plagioclase xenocryst has revealed a significant range in  $^{87}\text{Sr}/^{86}\text{Sr}$  ratios across the crystal and a large difference from its basaltic andesite. The xenocryst analyzed is believed to be derived from a local ignimbrite, and is currently hosted in a basaltic andesite magmatic inclusion from the dacite dome of Cerro Chascon, north Chile. These rocks show typical magma mingling textures.

Micro drill sampling has enabled us to examine the scale of mixing and chemical (isotopic and elemental) disequilibrium. Whereas previous results from this crystal gave a single  $^{87}\text{Sr}/^{86}\text{Sr}$  ratio of  $0.708915 \pm 37$  (Davidson, et al, 1990), the results of this study demonstrate that across-crystal variations exist and are measurable, ranging from  $0.709206 \pm 13$  near the core to  $0.708502 \pm 14$  near the rim (see figure). A chemistry Sr blank of 100 pg was measured, amounting to less than 0.5% of the Sr analyzed in the micro samples which weighed from 0.1 to 0.5 mg. Sr concentrations vary from c.500 to c.100 ppm, seemingly unsystematic with respect to location and isotope ratio. An contents are rather constant across the entire crystal ( $\text{An}_{57}$  to  $\text{An}_{64}$ ). The variations in isotope ratio are interpreted to reflect an approach to equilibrium through tracer diffusion at magmatic temperatures. The lack of  $\text{An}_x$  zonation reflects the slower diffusion rate controlling coupled CaAl-NaSi exchange. Diffusion was effectively arrested when the lava was extruded and chilled. Knowledge of appropriate isotope diffusion coefficients for Sr will enable us to estimate the time between incorporation of the xenocryst and eruption.



Davidson, J.P., de Silva, S.L., Holden, P., & Halliday, A.N. 1990, Small-scale disequilibrium in a magmatic inclusion and its more silicic host: *J. Geophys. Res.* 95, 17,661-17,674.

**WOOD IS NOT A LEAF: BIOLOGICAL CONSIDERATIONS WHEN INTERPRETING CLIMATE FROM  $\delta\text{D}$  OF CELLULOSE NITRATE**

TERWILLIGER, V. J., Depts of Geography and Botany, University of Kansas, Lawrence, KS, 66045, USA and M. J. DeNiro, Dept of Geological Sciences, University of California, Santa Barbara, CA, 93106, USA.

The  $\delta\text{D}$  of cellulose nitrate in tree rings should carry the climatic signature of water used in its synthesis. Poor understanding of hydrogen isotope effects that occur in the synthesis of cellulose prevents knowing if groundwater or leaf water produces the hydrogen isotope signature in wood cellulose. An isotopic signature from groundwater would reflect temperature whereas both temperature and humidity inferences could be derived from a leaf water signature.

To elucidate the source of the hydrogen isotopic signal in wood cellulose, we grew avocados in isotopically constant water but at different humidities. The  $\delta\text{D}$  of leaf cellulose nitrate was very significantly related to that of leaf water whereas the  $\delta\text{D}$  of wood cellulose was related to that of stem water. There was some mixing of leaf and growth waters at the site of wood formation but humidity signals were virtually absent. The quantitative natures of the relationships between the  $\delta\text{D}$  values of celluloses and waters suggested that the substrata for cellulose synthesis were partly from stored post-photosynthetic compounds. The contributions of these compounds to the  $\delta\text{D}$  of celluloses were different from the effects of the immediate products of photosynthesis. Furthermore, proportionally different contributions of immediate and recycled substrata may occur in leaves than in wood cellulose. Conditions that evoke use of stored substrata are varied for trees and would contaminate climatic inferences from stable hydrogen analyses.

**A MONAZITE U-PB AGE PROFILE THROUGH THE LOWER AND MIDDLE CRUST: A CROSS SECTION THROUGH THE IVREA ZONE, NORTHERN ITALY**

**TEUFEL, S.**, GeoForschungsZentrum Potsdam, Telegrafenberg, D-14473 Potsdam, FRG, **FRANZ, L.**, GeoForschungsZentrum Potsdam, Telegrafenberg, D-14473 Potsdam, FRG, **Ahrendt, H.**, Institut für Geologie und Dynamik der Lithosphäre, Goldschmidtstr. 3, D-37077 Göttingen, FRG and **HANSEN, B.T.**, Institut für Geologie und Dynamik der Lithosphäre, Goldschmidtstr. 3, D-37077 Göttingen, FRG

We present preliminary results of a study about the behaviour of the U-Pb system in monazite during high and medium grade metamorphism. We report geochronological and thermobarometric data of samples collected along the Val Strona across the boundary between the Ivrea and Strona Ceneri Zone. Along this profile metamorphic conditions change eastward from granulite facies (near the Insubric Line) to amphibolite facies (near Omegna). Monazites were extracted from ten metasediments and one augengneiss from both metamorphic units.

So far, only two monazite ages of 295 Ma in the upper part and 275 Ma in the transition zone between amphibolite facies and granulite facies rocks are known (Köppel 1974). Age determinations on monazite samples of about 2 mg weight have been carried out at the Zentrallabor für Geochronologie in Münster, FRG.

Within analytical error all analyses yield concordant hercynian U-Pb ages except two data points of a granulite facies sample. These points plot above the concordia, indicating a complex disturbance of the U-Pb system during post-hercynian times. U-Pb ages of the other monazites from granulite facies rocks lie in the range of 275 - 285 Ma while monazite analyses from amphibolite facies rocks give ages of 287 - 295 Ma. For one of these rocks we obtained a concordant U-Pb monazite age of 265 Ma showing a rejuvenation. Regarding the whole profile it is obvious that U-Pb ages correlate well with the degree of regional metamorphism. They decrease continuously from 295 Ma in amphibolite facies rocks near Omegna to 275 Ma in granulite facies samples near the Insubric Line. From these data no discontinuity between Ivrea and Strona Ceneri Zone can be detected. Our thermobarometric investigations revealed peak metamorphic conditions of  $8.3 \pm 1$  kb and  $810 \pm 25$  °C for granulite facies rocks continuously decreasing to amphibolite facies. All samples plot along a geothermal gradient of 26-30 °C/km. Clockwise PT-t paths mainly reveal cooling in the granulite facies whereas the prograde metamorphic history is often documented within the amphibolite facies samples.

The strong correlation between increase in metamorphic grade and decrease of the U-Pb ages leads to the following interpretation. During hercynian orogeny closing temperature of the U-Pb system in monazites were first understepped within the amphibolite facies rocks and distinctly later within the high grade series. Therefore the timing of regional metamorphism in the Ivrea Zone is best substantiated by concordant U-Pb ages of 295 Ma within medium grade rocks.

Köppel, V. , 1974, Isotopic U-Pb Ages of Monazites and Zircons from the Crust-Mantle Transition and Adjacent Units of the Ivrea and Ceneri Zones (Southern Alps, Italy): *Contr. Mineral. and Petrol.*, v.43, p.55-70.

**ND ISOTOPIC CONSTRAINTS ON THE EVOLUTION OF PALEOPROTEROZOIC SUPRACRUSTAL SEQUENCES AT THE NAIN-RAE PROVINCE BOUNDARY, EASTERN CANADA**

**THERIAULT, R.J.**, and **HAMILTON, M.A.**, Continental Geoscience Division, Geological Survey of Canada, Ottawa, Ontario, Canada, K1A 0E8.

The Nain /Rae Province boundary zone is represented by the north-trending ca. 1.85 Ga Torngat orogen of Labrador, eastern Canada. Paleoproterozoic supracrustal rocks spatially associated with the Torngat orogen consist of: 1) Mugford Group: relatively undeformed mafic continental volcanic rocks and lesser terrigenous clastic sediments unconformably overlying western Nain Province gneisses, 2) Ramah Group: siliciclastic platformal sediments at the western margin of the Nain Province, 3) Tasiuyak gneiss: migmatitic garnetiferous quartzofeldspathic paragneiss at the core of the Torngat orogen, and 4) Lac Lomier paragneisses: heterogeneous shallow- and deep-water metasediments which, with Tasiuyak metasediments, have been suggested as potential correlative continental shelf facies units on the Rae margin.

Weakly alkalic and tholeiitic basalts of the ca. 2.0 Ga Mugford Group have  $\epsilon_{Nd}(1.85 \text{ Ga})$  from +0.5 to -6.6, indicating finite contributions from Nain Province continental lithosphere. The Ramah Group shows  $\epsilon_{Nd}(1.85 \text{ Ga})$  ranging from -8.4 to -12.7. These values overlap and are slightly more positive than those of central Nain Province gneisses ( $\epsilon_{Nd}(1.85 \text{ Ga})$  ranging from -9 to -20; Hamilton, 1993) and more negative than Rae Province orthogneisses west of the Torngat orogen ( $\epsilon_{Nd}(1.85 \text{ Ga})$  from -4.6 to -9). Ramah Group data are consistent with mixing of crust similar to central Nain Province orthogneisses and more juvenile LREE-enriched crust such as Mugford Group basalts and tuffs. Lac Lomier metapelites yield  $\epsilon_{Nd}(1.85 \text{ Ga})$  values ranging from -5.1 to -7.8, overlapping with those of Rae Province crust. The Lac Lomier data display a linear trend on an  $f_{Sm/Nd}$  vs  $\epsilon_{Nd}(1.85 \text{ Ga})$  diagram, consistent with derivation from a Late Archean LREE-enriched source such as Rae crust. The Tasiuyak gneiss gives  $\epsilon_{Nd}(1.85 \text{ Ga})$  values clustering in the -2.1 to -3.1 range. These values are distinctly more positive than those of Ramah Group and Lac Lomier paragneisses, as well as those of Rae and Nain Province crust. This implies that a juvenile component not identified elsewhere in the study area is present in the Tasiuyak gneiss. The isotopic homogeneity displayed by Tasiuyak materials may echo homogeneity of source material or thorough mixing of heterogeneous detritus prior to deposition. The source terrane(s) providing the Tasiuyak gneiss with material of relatively juvenile character remains enigmatic.

Hamilton, M.A., 1993, Ph.D. thesis, University of Massachusetts.

## CHEMICALLY PRODUCED MASS INDEPENDENT ISOTOPIC FRACTIONATIONS IN THE EARLY SOLAR SYSTEM NEW OBSERVATIONS

THIEMENS, M. H., Dept. of Chemistry, University of California, San Diego, La Jolla, CA. 92093-0356, USA.

Thiemens and Heidenreich III (1983) were the first to experimentally demonstrate a chemically produced mass independent isotopic process. Perhaps the most striking feature was that the observed  $\delta^{17}\text{O}=\delta^{18}\text{O}$  fractionation pattern was essentially identical to that observed by Clayton et al (1973) in Allende inclusions. It thus is possible that the meteoritic oxygen isotopic anomalies arise from chemical rather than nuclear processes. Since oxygen is the major element in stony planetary material this must reflect a major process in the formation of the solar system.

The mechanism by which the mass independent fractionation occurs is now known to derive from molecular symmetry factors which occur during a reaction; thus the process is rather general. More recently, it has been demonstrated by this laboratory that several of the earth's most important molecules possess large mass independent isotopic compositions. In fact, as is the case for the meteorites, these anomalous isotopic compositions have provided new insights into several atmospheric processes in the stratosphere and troposphere. It has also been demonstrated that there are several types of physical chemical processes which produce mass independent isotopic fractionations, and in at least two different elements.

Most recently it has been shown that in a gas phase reaction process a solid silicon oxide condensate with a  $^{16}\text{O}$  rich mass independent isotopic composition arises. This further increases the plausibility that chemical processes may be the source of the observed meteoritic oxygen isotopic anomalies. There are several other recent advances in the study of chemically produced mass independent isotopic fractionations as they relate to the early solar system. These observations will be discussed.

Clayton, R.N. et al., 1973 *Science*, v. 182, p. 485.  
Thiemens, M.H. and Heidenreich, III, J.E. 1983, *Science*, 219, v. 1073.

CRUSTAL INTERACTION DURING CONSTRUCTION OF OCEAN ISLANDS - Pb-Sr-Nd-O ISOTOPE STRATIGRAPHY OF GRAN CANARIA SHIELD BASALTS  
M.F. THIRLWALL, C. JENKINS, P.Z. VROON & D.P. MATTEY, Geology, Royal Holloway Univ. London, Egham TW20 0EX, UK.

The largest eruption rates and greatest eruptive volumes in the oceanic island of Gran Canaria took place at the beginning of the Miocene volcanic cycle, when at least 1000m of mildly alkalic basalts were erupted, apparently over an interval as short as 1.5Ma. Five vertical sequences of basalts have been sampled, four ca. 10km apart in the NW of the island (Tazartico, San Nicolas, El Risco and Agaete from S to N), and one 30km away in the SE of the island (Angosturas). The basalts show coherent major and trace element variation trends reflecting fractional crystallisation of olivine, augite, and, in samples with <6% MgO, plagioclase. Basalts with >8% MgO are restricted to the lower parts of 3 sequences, indicating that residence time in magma chambers increased as the basaltic shield(s) grew. Zr/Nb increases upward in all sequences, probably implying that the degree of melting also increased as the shield(s) developed. Zr/Nb ranges are different in each section, suggesting that the El Risco section may be equivalent to the upper parts of the Agaete and Tazartico sections, while the San Nicolas section may be equivalent to the lower parts.

Radiogenic isotope ratios show limited variation (initial  $^{87}\text{Sr}/^{86}\text{Sr} = 0.70320-0.70390$ ,  $\epsilon_{\text{Nd}} = +6.0$  to  $+4.3$ ,  $^{206}\text{Pb}/^{204}\text{Pb} = 19.35-19.79$ ), but are strongly controlled by stratigraphy. Almost all of the variation is displayed by the lower parts of the Agaete, Tazartico and San Nicolas sections, each of which shows tight (<0.1  $\epsilon_{\text{Nd}}$ -unit vertical scatter) parallel Sr-Nd correlations. In each sequence, younger rocks show less extensive Sr-Nd arrays, parallel and offset to higher  $^{87}\text{Sr}/^{86}\text{Sr}$  and higher  $\epsilon_{\text{Nd}}$  than the older rocks. The upper part of the Agaete section is identical to the whole El Risco section, with  $^{87}\text{Sr}/^{86}\text{Sr} = 0.70333-0.70340$  and  $\epsilon_{\text{Nd}} = 6.0$  to  $5.6$ , confirming the stratigraphic correlations suggested by Zr/Nb ratios. The section in the SE of the island has similar, or slightly lower,  $^{87}\text{Sr}/^{86}\text{Sr}$ , but much lower  $\epsilon_{\text{Nd}}$  (4.9-5.2).

Pb isotopes in each section show strong negative correlations in  $^{206}\text{Pb} - ^{207}\text{Pb}$  space, with the lowest- $\epsilon_{\text{Nd}}$  samples having highest  $\Delta^{207}\text{Pb}$  (+8), and the highest- $\epsilon_{\text{Nd}}$  samples lying below the Northern Hemisphere Reference Line (NHRL). Ce/Pb is correlated with  $\Delta^{207}\text{Pb}$ , reducing from  $41 \pm 2$  in samples near the NHRL to 26 at high  $\Delta^{207}\text{Pb}$ . These data strongly suggest incorporation of a crustal component into the magmas: Pb-Pb correlations vector towards the field of local seafloor sediments, and indicate that ca. 50% sediment Pb has been incorporated into the most contaminated lava. Laser fluorination  $\delta^{18}\text{O}$  analysis of phenocryst augite confirms that sediment incorporation took place within the ocean island crust, rather than by recycling of ancient crustal material into the mantle, because  $\delta^{18}\text{O}_{\text{cpx}}$  increases from 5.56 to 6.81 with increasing  $\Delta^{207}\text{Pb}$ .

Pb isotope compositions of Miocene shield basalts in Gran Canaria are thus significantly controlled by high-level sediment assimilation. Proximity to the NHRL, or supposedly mantle-like Ce/Pb ratios, can not be used as evidence that basalt compositions reflect their mantle sources. Nor can high MgO be used, as sediment effects are observable in rocks with up to 10% MgO. The up-sequence progression to more fractionated compositions with more radiogenic Sr and Nd is not accompanied by change in  $\delta^{18}\text{O}$ , perhaps suggesting that, with greater magma input, magma chambers developed at higher crustal levels and assimilated pre-existing volcanic crust.

EVALUATION OF THE LATE OROGENIC  
EXHUMATIONAL HISTORY OF THE CALABRIAN  
ARC, SOUTHERN ITALY USING FISSION TRACK  
ANALYSIS

THOMSON, Stuart, N., Institut für Geologie,  
Ruhr-Universität Bochum, Universitätsstr. 150,  
P.O. Box 102148, Bochum 44721, GERMANY

Fission track analysis has been used to provide important new low temperature and time constraints on the late-orogenic cooling and exhumational history of the crystalline basement rocks of the Calabrian Arc, southern Italy. 65 samples yielded 57 apatite fission track ages, 54 zircon fission track ages and 25 apatite confined fission track length distributions. Interpretation of this data indicates that a phase of increased cooling rates related to exhumation occurred between approximately 35 Ma, the mid-Oligocene and 15 Ma the middle Miocene (Thomson, in press). This period of exhumation was the result of both erosional and extensional tectonic processes.

Additional chronological constraints using fission track analysis applied to localised late-orogenic extensional tectonism, recently identified within the basement rocks of the Calabrian Arc, confirms an Oligo-Miocene age for this tectonism.

In conjunction, a sedimentary provenance study, also using fission track analysis, was carried out on Oligo-Miocene conglomerates and sandstones that are known to be derived by erosion from the crystalline basement rocks of the Calabrian Arc. The fission track data confirms a local source for the sedimentary rocks, but more importantly reveals that significant erosion of the basement rocks must have occurred during the Oligo-Miocene (Thomson, 1994a).

This information is combined to produce a new model of the Oligo-Miocene tectonic evolution of the Calabrian Arc. It proposes that the crystalline basement rocks were part of a critical orogenic wedge between the mid-Oligocene and the middle Miocene.

Thomson, S. N., 1994a, Fission track analysis and provenance studies in Calabrian Arc sedimentary rocks, southern Italy: *J. Geol. Soc. Lond.*, v. 151.

Thomson, S. N., in press, Fission track analysis of the crystalline basement rocks of the Calabrian Arc, southern Italy: evidence of Oligo-Miocene late-orogenic extension and erosion: *Tectonophysics*.

RARE NOBLE GAS ISOTOPE MEASUREMENTS USING  
LASER-BASED RESONANCE IONIZATION

THONNARD, N., Institute for Rare Isotope Measurements,  
The University of Tennessee, Knoxville, TN, 37996, USA

The rare noble gases, especially  $^{81}\text{Kr}$ ,  $^{85}\text{Kr}$ , and  $^{39}\text{Ar}$ , having isotopic abundances in the  $10^{-11}$  to  $10^{-15}$  range, and  $10^{-21}$  to  $10^{-22}$  concentration in modern water, challenge present analytical capabilities. These radionuclides can contribute in many ways to a better understanding of processes in the environment, including dating of polar ice and very old ground water, deep ocean circulation, and modern water flow patterns, to name just a few. Atom Sciences, Inc. developed laser-based analytical methods for krypton, and was the only laboratory world-wide to have measured  $^{81}\text{Kr}$  from terrestrial samples, while  $^{85}\text{Kr}$  measurements were possible from samples 10 times smaller than used by the best decay counting laboratories. As the company decided to withdraw from this field, a group of researchers and non-profit organizations was organized to maintain and advance the capabilities. With funding from Oak Ridge National Laboratory, the Scripps Institution of Oceanography, and the University of Tennessee, Knoxville, the Institute for Rare Isotope Measurements (IRIM) was founded. By January 1994, laboratory space was made available to IRIM, building modifications initiated to accommodate the equipment, and a lease-purchase agreement signed for the equipment. It is anticipated that by the summer of 1994, the facility will be operational at IRIM.

For krypton, the technique presently consists of a multi-step process starting with (1) degassing of the sample, (2) separating Kr from the remainder of the gas, (3) going through a first isotopic enrichment reducing interfering isotopes by  $10^5$ , (4) proceeding with a second isotopic enrichment of  $\sim 10^3$ , and finally (5) detecting the rare krypton isotope in a time-of-flight mass spectrometer utilizing resonance ionization spectroscopy. A detection limit of  $\sim 100$   $^{85}\text{Kr}$  atoms has been demonstrated in the final mass spectrometer. Argon measurements will require charge exchange to a metastable state of a fast  $\text{Ar}^+$  beam, followed by collinear laser excitation and field ionization.

The objectives of IRIM are: (1) to define shortcomings of the present system, (2) to design and implement modifications that will increase reproducibility and accuracy, increase throughput by reducing analysis time, and reduce the minimum sample size, (3) to conduct the necessary research to implement  $^{39}\text{Ar}$  measurements, and (4) to initiate research in the geosciences utilizing the new facility both with collaborators at the University of Tennessee and from other institutions. We anticipate few-percent  $^{39}\text{Ar}$  and  $^{81}\text{Kr}$  measurements from 10 liters of water and  $^{85}\text{Kr}$  measurements from 1 liter of water, throughput reaching 500 samples per year, and IRIM becoming a user facility for the geosciences community.

We will describe the technology developed to date and the improvements planned for the next few years. Data will be presented for  $^{81}\text{Kr}$  and  $^{85}\text{Kr}$  measurements from polar ice, groundwater, and tracer studies, together with a summary of some of the unique research opportunities made possible with this technology.

**POSSIBLE IGNEOUS SOURCE FOR OLYMPIC DAM-TYPE COPPER OCCURRENCES IN PROTEROZOIC HEMATITIC BRECCIAS, YUKON, CANADA**

**THORKELSON, D.J., and WALLACE, C.A.,**  
Canada/Yukon Geoscience Office, Box 2703 (F-3),  
Whitehorse, Yukon, Y1A 2C6, Canada.

Numerous hematitic breccia zones of Middle Proterozoic age in northern Yukon host local enrichments of Copper, Cobalt, Uranium and Gold. Collectively known as Wernecke breccia, these zones are exposed in inliers of the Wernecke Supergroup, a deformed, thick miogeoclinal succession deposited in Middle Proterozoic time. Wernecke breccia crops out as individual zones up to 5 km<sup>2</sup>, distributed in curvilinear arrays over thousands of km<sup>2</sup>. The origin, timing, and significance of breccia development are being addressed by combined field and geochemical studies. Existing data implies that brecciation and mineralization resulted from explosive hydrothermal activity related to late-stage magmatic processes.

Wernecke breccia consists of rounded to angular clasts in a hydrothermally precipitated matrix. The clasts were derived mainly from the Wernecke Supergroup and to a lesser degree from mafic to intermediate dykes which intruded the Wernecke Supergroup prior to brecciation. Metasomatism affecting the breccia zones and surrounding host rocks produced ubiquitous growth of specularite and carbonate, and commonly associated magnetite, quartz, chlorite, iron and copper sulphides, and uranium minerals. The metasomatism began before and continued after brecciation. Both metasomatism and brecciation were apparently caused by voluminous upsurge of hydrothermal solutions.

Previous studies have depicted Wernecke breccia as diatremes, phreatomagmatic breccias, modified evaporite diapirs, debris flows, and mud diapirs. In these models, except for the diatreme hypothesis, brecciation is considered to have occurred prior to lithification of the Wernecke Supergroup. However, the recent discovery of kinked phyllite clasts of the Wernecke Supergroup in breccia lacking secondary petrofabrics indicates that an event of contractional deformation preceded brecciation; the models involving unlithified strata are untenable. A diatreme origin is plausible, although the breccias do not contain fragments of crustal basement, mantle, or chilled vesiculated magma.

The most likely cause of brecciation is explosive expansion of volatile-rich fluids. An igneous influence is implied by the spatial coincidence of intrusions and breccia zones, and common enrichments of Fe, Cu, and Co. The fluids may have been derived from volatile-rich residual liquids which accumulated at the top of fractionating tholeiitic magma chambers beneath the Wernecke Supergroup. In this depiction, breccia generation would represent a late- to post-magmatic stage, when the magma chambers were largely solidified; fluids enriched in Fe and volatiles escaped toward the surface and boiled explosively. The link between mineralizing fluids and tholeiitic magmatism is being tested by chemical and isotopic analysis.

**EFFECTS OF CRYSTAL STRUCTURE ON Th-U-Pb EMISSIONS FROM ZIRCONS AS DETERMINED ON THE CURTIN SHRIMP II.**

**TODT, W.A.,** Max Planck Institute for Chemistry, Mainz, 55020, Germany, **PIDGEON, R.T., KENNEDY, A.K.** and **VAN BRONSWJK, W.,** Curtin University of Technology, Kent Street, Bentley, 6012, Western Australia.

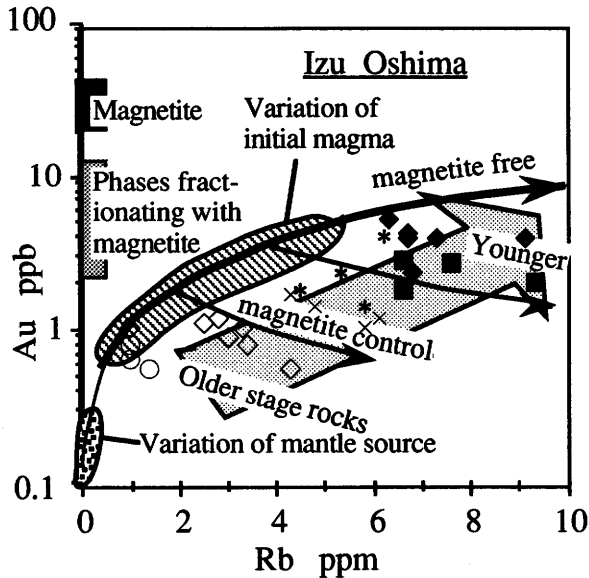
SHRIMP measurements provide a unique means for determining Th-U-Pb ages on small areas within individual zircon crystals. Such measurements are made by comparing the Th-U-Pb ion emissions of selected areas with those of a concordant, crystalline standard zircon. However, in any one zircon population the structural state of zircons can vary from completely crystallised to strongly metamict. Our aim was to examine the effects of the degree of metamictness of zircons on Th-U-Pb ion emissions during ion microprobe analysis. For this study we have investigated 5 optically homogeneous Sri Lankan zircon grains which varied in colour from translucent yellow to opaque black and had a range of uranium contents from 400 ppm to over 2100ppm and showed a corresponding range in metamict state. The state of metamictisation was determined using XRD analysis and Raman spectroscopy. Conventional ages and uranium and thorium contents of the zircons were measured by isotope dilution and filament Pb emission characteristics were determined by the Kober method. Our results at the time of preparation of this abstract suggest that the extent of radiation damage of the zircon is not a major factor in disturbing Pb/U ratios during SHRIMP analyses.

**BEHAVIOR OF GOLD DURING MAGMATIC EVOLUTION OF ISLAND ARC THOLEIITES**

**TOGASHI, S. and TERASHIMA, S.,**  
 Geol. Surv. Japan, Tsukuba, Ibaraki, 305, Japan.

High gold concentrations ( 10-25 or more ppb ) in titanomagnetite concentrates from volcanic rocks of the Izu-Oshima and Fuji volcanic areas in the East Japan arc imply that gold is strongly partitioned into titanomagnetite. The concentration of gold in volcanic rocks increases during the early stage of fractional crystallization, dominated by olivine, pyroxenes and plagioclase, but decreases with subsequent fractional crystallization involving titanomagnetite. The delay of titanomagnetite formation during fractional crystallization results in high concentrations of gold in island arc tholeiites.

A wide variation of gold concentration in rocks of primary magmas is observed across a single volcanic area (Fig.), and is positively correlated with the concentrations of incompatible elements such as Rb and Zr. These features are inherited from a mantle source, since variable degrees of partial melting do not significantly affect the gold concentrations of the primary magmas.



**U, Th, K, Li, and He and Ar ISOTOPES IN ROCKS, MINERALS, AND UNDERGROUND WATERS**

**TOLSTIKHIN** Igor, Department of Earth's Sciences, Cambridge University, Cambridge UK; **LEHMANN** Bernhard, **LOOSLI** Hugo, Physics Institute, University of Bern, 3012 Bern, and **GAUTSCHI** Andreas, Swiss National Co-operative for the Disposal of Radioactive Waste (NAGRA), Wettingen, Switzerland.

He and Ar isotope and U, Th, K, and Li concentrations were measured in sediment and metamorphic rocks from Quaternary-Carboniferous Molasses basin, Switzerland, with the aim to clear up processes controlled noble gas abundances in the minerals, rocks and related groundwaters.

Concentrations of parent elements [ppm] vary within :  $1 < U < 12$ ,  $1 < Th < 30$ ,  $1 < Li < 350$ . A comparison of calculated, assuming the water-rock system has been closed since the sedimentation age of given aquifer, and measured concentrations of  $^4He$  and  $^3He$  shows almost complete loss of the both nuclides from all but one sample. This one, Permian sandstone, contains excess trapped He with concentrations of  $^4He$  and  $^3He$  up to  $200 \times 10^{-6}$  and  $15 \times 10^{-12}$   $cm^3/g$ , respectively, which are  $\sim 10$  and  $\sim 30$  times greater than the calculated values.

[U] and [Th] in rocks and their porosity enable us to estimate [He] in the water filled pore volumes. The estimated values are a factor of 10-1000 higher than those measured in groundwaters, so a small addition of He from stagnant zones of the basin via mixing and/or diffusion into moveable waters flowing within high-permeability channels could provide its observed concentrations.

Distribution of He isotopes in rocks and, more important, in mineral separates, definitely shows that trapped He can be a principal component of He in rocks even if measured  $^3He/^4He$  ratio is similar to or lower than the production ratio. Rocks (minerals) contain negligible amount of radiogenic in situ produced He, which is almost completely lost, while He isotope inventory in the rocks is provided by trapped He as a minor component of trapped fluid.

In evaporites measured  $^3He/^4He$  ratios greatly exceed calculated values, up to  $(^3He/^4He)_{meas} = 16 \cdot 10^{-8} \sim 100 \cdot (^3He/^4He)_{calc}$ . Both mantle and atmospheric sources for the excess  $^3He$  can be eliminated. Because of  $^3H$  is a precursor of radiogenic  $^3He$ , specific H/He fractionation in the course of diagenesis and loss of He could increase  $^3He/^4He$  ratio. However other processes (e.g., spallation) can not be excluded at that stage of our knowledge. Trapped excess  $^3He$  in sandstone formed due to erosion of granites is interpreted as a result of a small contribution of mantle He.

$(^3He/^4He)$  ratios in groundwaters are similar to those in water bearing rocks or in related aquitards, also implying local sources for He isotopes in underground waters.

According to available data, i.e., the total mineralisation, [Cl], [He],  $^3He/^4He$  and  $^{40}Ar/^{36}Ar$  ratios, signatures of Permian and overlying aquifers can not be provided by advection of groundwaters from the basement.

Water-sediment interactions and redistribution of species between stagnant and moveable waters appears to be a processes responsible for observed parameters of groundwaters in the Molasses basin.

**Sr, Nd, AND Pb ISOTOPE DATA OF CRUSTAL MELTS FROM THE ISLAND OF SERAM, INDONESIA: EVIDENCE FOR DISEQUILIBRIUM MELTING DURING ANATEXIS**

**TOMMASINI, Simone** <sup>(1,2)</sup>, DAVIES, G. R., STAUDIGEL, H., HELMERS, H., (1) Faculteit der Aardwetenschappen, Vrije Universiteit, 1081 HV Amsterdam, The Netherlands, MANETTI, P., Dipartimento di Scienze della Terra, 50121 Firenze, Italy, and POLI, G., (2) Dipartimento di Scienze della Terra, 06100 Perugia, Italy

Problems associated with granitoid petrogenesis (e.g. magma mixing, AFC, source composition) have been addressed with varying degrees of success using both radiogenic isotope and trace element ratios. The assumption that crustal reservoirs attain chemical and isotopic equilibrium during high grade metamorphism and anatexis is central to these approaches. However, parameters such as the rate of elemental diffusion, the time-scale of the heating event, and the rate of melt extraction are critical in controlling the extent of chemical and isotopic equilibrium in crustal environments. Recently published experiments on the diffusion of certain trace elements in rock-forming minerals (e.g. U, Pb, REE, Sr in garnet, feldspars, micas) suggest that isotope disequilibrium may be particularly important at crustal anatexis temperatures (750-800°C) during short thermal events (1-10 Ma). Despite this possibility, little assessment has yet been made of how minerals control the trace element and isotopic composition of crustal melts by remaining closed systems during melting.

On the island of Seram, Eastern Indonesia, the Neogene obduction of hot oceanic lithosphere onto Palaeozoic metasedimentary material produced rapid crustal anatexis (< 1 Ma). Samples were obtained during the Snellius II expedition. Partial melting of metapelites produced cordierite-bearing S-type granitoids. Nd and Pb isotope ratios are the same in granitoids and metapelites ( $^{143}\text{Nd}/^{144}\text{Nd}_i = 0.51212 \pm 5$ ,  $^{206}\text{Pb}/^{204}\text{Pb}_i = 18.738 \pm 5$ ), whereas Sr isotope ratios are variable in granitoids ( $^{87}\text{Sr}/^{86}\text{Sr}_i = 0.7166-0.7268$ ) and significantly lower than in metapelites ( $^{87}\text{Sr}/^{86}\text{Sr}_i = 0.7321$ ). The less radiogenic Sr isotope signature of granitoids is consistent with feldspars not having undergone equilibration with the bulk-rock during anatexis, and contributing a large proportion of the Sr budget in the melt.

To further evaluate the nature of melting, detailed Sr isotope analyses of single minerals of both granitoids and metapelites are being carried out with microdrilling techniques. The overall data set will permit an accurate assessment of the extent of chemical and isotopic equilibrium attained by crustal reservoirs during anatexis.

**GEOCHEMICAL AND ISOTOPIC MONITORING OF MT. ETNA 1989-93 ERUPTIVE ACTIVITY: BEARING ON THE SHALLOW FEEDING SYSTEM.**

**TONARINI, S.**, Ist. Geocronologia e Geochimica Isotopica, CNR, 56127 Pisa, Italy; ARMIENTI, P.; D'ORAZIO, M. and INNOCENTI, F., Dip. Scienze della Terra, Univ. Pisa, 56126 Pisa, Italy; PETRINI, R., Ist. Min. Petr., Univ. di Trieste, 34100 Trieste, Italy.

An unusually long eruptive sequence characterized Mt Etna during 1989-1993. In this period, the persistent activity at the summit craters was accompanied by two eruptions which took place in 1989-90 and 1991-93. The former eruption produced lavas among the most primitive of this century while the latter was the largest in the last three centuries. Geochemical and isotopic data collected during this time span reveal the occurrence of complex petrogenetic processes in the feeding system of Mt Etna. The early alkali basalts emitted from Sud Est Crater during 1989 eruption displayed enrichments of Rb and K accompanied by higher levels of radiogenic-Sr and isotopic disequilibrium between host-rock and clinopyroxene (0.70364 and 0.70356 respectively). In the following K, Rb and  $^{87}\text{Sr}/^{86}\text{Sr}$  ratio decreased within one week, reaching the typical value measured in the alkali basalts outpured in the Valle del Leone (0.70355). Nd isotopic ratio did not show significant variations. These features can be explained by a selective contamination process involving essentially Rb, K and radiogenic-Sr.

During the 1991-93 eruption the largest volume of lavas was emitted between January and May 1992 and was characterized by uniform geochemical and isotopic compositions and Sr-isotopic equilibrium between whole rock and pyroxene (0.70355). On the basis of their constant composition and huge volume, these lavas are considered as a distinct magma batch supplied to the feeding system of the volcano (JML batch). In other periods (December 1991 and June 1992) we observed lower and variable Sr isotopic compositions coupled with disequilibria between lavas and their clinopyroxenes (0.70351 whole rock and 0.70345 cpx for the sample 15 Dec. 1991). Nd isotope ratios are 0.51287-0.51289. Our data do not allow to discriminate between the hypothesis of mixing or selective contamination, however lavas emitted during December 1991 evolved towards the isotope composition of JML that was never exceeded; the regular behaviour of Rb, K and radiogenic-Sr of 1989 lavas was not observed during the 1991-93 eruption. Thus we prefer to interpret these variations as mainly due to mixing processes between an end-member of JML composition and another one having the same, or lower, isotopic composition of the cpx found in the sample of December 1991.

Starting from June 1992, when the output rate significantly decreased, the products seem to reveal fractionation effects as suggested by the continuous rise in concentrations of incompatible elements.

In conclusion, several petrogenetic processes are contemporaneously active at Mt Etna; they encompass magma mixing, selective contamination and fractional crystallization. Their relative importance varies according to the original volume of each magma batch and to the status of the shallow feeding system. The complexity of these processes, acting in the short time span of a few months, claims caution about the geochemical representativity of single lava sample for each eruption.

ATMOSPHERIC  $\delta^{13}\text{C}$  VARIATIONS, 1850-1990 A.D., AS RECORDED IN C4 GRASSES.

TOOLIN, L. J., NSF Accelerator Facility, University of Arizona, Tucson, Arizona 85721, USA, and EASTOE, C.J., Department of Geosciences, University of Arizona, Tucson, Arizona 85721, USA.

We previously reported<sup>1</sup>  $\delta^{13}\text{C}$  values obtained on native species of a grass genus (*Setaria*), which utilize the four-carbon (C4) photosynthetic pathway. We were able to show that the  $\delta^{13}\text{C}$  values of the grasses tracked changes in atmospheric  $\delta^{13}\text{C}$  through time. Our mean Holocene value (-6.5 ‰) agreed with the pre-industrial value of  $\text{CO}_2$  in ice cores. Modern (1990 AD) *Setarias* from southeastern Arizona yielded a mean value of -8.2 ‰, in agreement with an atmospheric mean measured in the same region during 1983-1984 AD.

Here, we present  $\delta^{13}\text{C}$  values measured on historically-dated herbarium specimens of *Setarias*, from field collections made in the southwestern USA from 1850-1990 AD. The data show a long-term decrease in  $^{13}\text{C}$  relative to  $^{12}\text{C}$ , from the 1800's to the present. Short-term variations ("wiggles") are also revealed. For example, there appears to be a peak of more-negative values in the early 1930's, followed by a trend to heavier values until 1945, with a subsequent return to lighter values from 1946 to about 1950. Such wiggles are compared to short-term trends seen in ice-core  $\text{CO}_2$ , C3 tree rings and C4 corn.

<sup>1</sup> Toolin, L. J. and Eastoe, C. J., 1993, Late Pleistocene-Recent Atmospheric  $\delta^{13}\text{C}$  in C4 grasses: Radiocarbon, v. 35, p. 263-269.

CONTRASTING MORPHOLOGY AND U-Th-Pb-SYSTEMATICS OF ZIRCONS IN A SET OF PERALUMINOUS, METALUMINOUS AND PERALKALINE BRASILIANO-GRANITOIDS

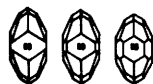
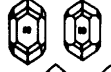
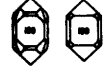
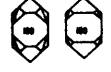
TÖPFNER, C.P., Institut für Allgemeine und Angewandte Geologie, Ludwig-Maximilians-Universität, 80333 München, Luisenstr. 37, Germany

Since in 1980, PUPIN published a petrogenetic granitoid classification scheme based on the accessory mineral zircon, there is general agreement about the fact that tectonically, genetically and petrographically comparable granitoids show morphologically comparable zircons. Nevertheless, there is only little known about the factors governing the zircons' morphology during magmatic crystallization.

In the Brazilian Federal States of Sao Paulo and southeastern Minas Gerais, acid to intermediate plutonic rocks cover more than 60% of the exposed crystalline basement belonging to the Ribeira Mobile Belt. These granitoids are directly related to the geodynamic evolution during the Brasiliano Cycle (680-450 Ma). Six different syn- to postkinematic granitoid massifs covering the genetic maintypes of PUPIN's classification were sampled:

- a synkinematic, two mica-, garnet-, sillimanite-, and tourmaline-bearing, peraluminous leucogranite with a zircon population according PUPIN's stock 1 (orogenic aluminous leucogranites of crustal origin)
- three synkinematic, metaluminous monzogranite-, granodiorite-, and quartz monzodiorite-batholiths with K-feldspar megacrysts up to several cm and zircon populations according PUPIN's stocks 4a, 4b and 4c respectively (orogenic hybrid granitoids belonging to the calc-alkaline low- (4a), medium- (4b), and high-temperature (4c) series)
- a postkinematic, pink, subalkaline rapakivi granite complex with a zircon population according PUPIN's stock 5 (orogenic hybrid granitoids of the subalkaline series)
- a peralkaline larvikite/nordmarkite complex with zircons according PUPIN's stock 6 (anorogenic alkaline series granitoids of mantle origin).

The table below summarizes selected preliminary results by isotope dilution mass spectrometry on morphologically characterized zircon fractions. Further analysis and accompanying cathodoluminescence analysis are in progress.

Prevailing zircon type	Size [µm]	U [ppm]	Pbrad [ppm]	Pbcom [ppm]	[U/Th] <sub>t0</sub> [mol]
1 	150-180	641.6	40.26	34.42	1.236
	100-125	417.8	29.63	11.25	2.105
	63-80	462.1	30.49	14.16	2.019
4a 	125-180	384.3	37.90	2.47	1.360
	100-125	347.6	34.26	2.60	1.396
	63-80	291.0	-	-	-
4b 	150-180	557.9	-	-	-
	100-125	633.1	-	-	-
	63-80	710.3	-	-	-
4c 	150-180	375.6	39.41	2.67	1.177
	100-125	384.8	40.30	1.17	1.248
	63-80	487.7	51.61	5.15	1.112
5 	150-180	227.4	22.22	1.81	0.940
	100-125	281.1	26.83	0.62	0.973
	63-80	335.3	31.46	0.46	0.903
6 	150-180	73.9	8.70	0.26	0.613
	100-125	81.2	9.48	0.17	0.579
	63-80	84.8	9.84	0.18	0.668

**U-Pb ZIRCON AGES AND Pb ISOTOPIC COMPOSITIONS OF MIDDLE PROTEROZOIC CRYSTALLINE BASEMENT IN THE CENTRAL ANDES, WESTERN BOLIVIA AND NORTHERN CHILE**

TOSDAL, R.M., U.S. Geological Survey, 345 Middlefield Road, Menlo Park, CA 94025 U.S.A.

Middle Proterozoic crystalline rocks outcrop in isolated fault-blocks in the western Andes in N. Chile and W. Bolivia, east of the Early Proterozoic (~2.0 Ga) Arequipa massif in southern Perú. Those exposures plus indirect evidence from clasts in Tertiary rocks and Pb isotopic compositions of Neogene volcanic rocks indicate that a Middle Proterozoic basement terrane extends as far south as 21°S and east to ~67°W. Near Berenguela in western Bolivia (~17.3°S), clasts in the Oligocene and Miocene Mauri Formation include boulders of sparse granites and more common gneiss characterized by amphibolite- or granulite-facies metamorphic assemblages (biotite-green amphibole-plagioclase in mafic gneiss and garnet-(up to 1 cm in diameter)-biotite-perthite-plagioclase-quartz in quartzofeldspathic gneiss). Protoliths are mostly igneous, ranging in composition from basaltic to granitic. Two augen gneisses have U-Pb crystallization ages of 1171±20 Ma and 1158±12 Ma. Other gneisses with uncertain protoliths have similar ages. A quartz-perthite-plagioclase gneiss has an U-Pb age of 1100±17 Ma. U-Pb data for a migmatitic garnetiferous quartzofeldspathic gneiss scatters about a chord with an upper intercept age of 1098±48 Ma, which may approximate the age of metamorphism. No inherited zircons are recognized. These U-Pb ages agree with published U-Pb ages and with Rb-Sr and Sm-Nd model ages for other basement occurrences north of 21°S and for inherited zircons in Mesozoic granites as far south as 26.3°S.

Present-day Pb isotopic compositions for the Middle Proterozoic rocks (19 samples:  $^{208}\text{Pb}/^{204}\text{Pb}=37.68\text{--}41.05$ ;  $^{207}\text{Pb}/^{204}\text{Pb}=15.54\text{--}15.67$ ;  $^{206}\text{Pb}/^{204}\text{Pb}=17.12\text{--}18.24$ ; five are more radiogenic) indicate time-averaged Th/U and  $\mu$  values higher than those of average crust. An orthogneiss from the Middle Proterozoic Belen Schist (18.3° S) in N. Chile has a similar Pb isotopic composition, but associated pelitic schists extend to less radiogenic values and overlap the field for the ~2.0-Ga Arequipa massif. As a group, the Middle Proterozoic rocks have higher present-day  $^{206}\text{Pb}/^{204}\text{Pb}$  than those of the Arequipa massif, which is also characterized by elevated time-averaged Th/U and  $\mu$  values. They, furthermore, have higher present-day  $^{208}\text{Pb}/^{204}\text{Pb}$  and  $^{207}\text{Pb}/^{204}\text{Pb}$  than Middle Proterozoic rocks in western Argentina, which are characterized by crustal average Th/U and distinctly lower  $\mu$  values. Age-corrected Pb isotopic compositions are also distinct for the crystalline terranes. The Pb isotopic data clearly indicate long-term involvement of old radiogenic continental crust, presumably of Archean age, in the Proterozoic rocks in S. Perú, N. Chile and W. Bolivia. This implies that these Proterozoic rocks were originally part of, or adjacent to, such an Archean craton. Furthermore, any fragment rifted away from this part of western South America in the Late Proterozoic or Early Paleozoic can be identified by these Pb isotopic and U-Pb geochronologic characteristics.

**Sm-Nd, Rb-Sr AND Pb-Pb DATING OF ARCHAEOAN SEDIMENTS: CONTRASTING RESULTS FROM WHOLE-ROCK AND CLAY MINERAL SEPARATES**

TOULKERIDIS, T.<sup>1,2,3</sup>, GOLDSTEIN, S.L.<sup>1</sup>, CLAUER, N.<sup>2</sup>, STILLE, P.<sup>2</sup>, TODT, W.<sup>1</sup> and KRÖNER, A.<sup>3</sup>

<sup>1</sup>MPI für Chemie, 55020 Mainz, Germany, <sup>2</sup>CGS-CNRS, 67084 Strasbourg, France and <sup>3</sup>Institut für Geowissenschaften, University of Mainz, 55099 Mainz, Germany

Diagenetically-formed clay minerals in sediments can often be used to determine the time elapsed since closure of the mineral isotopic systems following the last thermal event. We report preliminary results of an isotopic study of one shale and two carbonate occurrences as well as clay minerals separated from carbonates.

Samples are from the early Archean Barberton Greenstone Belt, South Africa, which underwent regional thermal events in the Kaapvaal craton at ~3.1, 2.7, 2.4, and 2.1 Ga ago. One carbonate sample comes from the ~3.4 Ga old Onverwacht Group (OG), while the other two samples are from the overlying ~3260-3227 Ma old Fig Tree Group (FTG). All sampled sedimentary sequences contain primary sedimentary structures, textures and, partly, mineralogies.

Pb-isotopic data for 45 individual chips of one OG whole-rock sample form a linear array corresponding to a Pb-Pb age of 2628±131 Ma. Sm-Nd and Rb-Sr isotopes were analyzed in WR samples of the FTG carbonates. The Sm-Nd data give an age of 2612±84 Ma with initial  $\epsilon\text{Nd}(t)=-8.1\pm 0.5$ , and the Rb-Sr data give an age of 2745±148 Ma with initial  $^{87}\text{Sr}/^{86}\text{Sr}=0.7014\pm 0.002$ . Rb-Sr and Pb isotopes were analyzed in shales, and form a Rb-Sr array of 2761±52 Ma with initial  $^{87}\text{Sr}/^{86}\text{Sr}=0.7147\pm 0.002$ , and a Pb-Pb age of 2601±29 Ma.

All three whole-rock isotopic systems of the carbonates and the shales indicate ages of ~2.7 Ga, much younger than the depositional age of the successions. This agreement indicates that a thermal event at 2.7 Ga has reset all three whole-rock isotopic systems.

Clay fractions (mainly illites) separated for isotopic analyses from the FTG carbonates were additionally treated with 1N HCl. The Sm-Nd data of leached, residual and untreated clay fractions (n=8) form a linear array corresponding to an age of 3102±64 Ma with initial  $\epsilon\text{Nd}(t)=-1.0\pm 0.6$ . This age is younger than the depositional age but older than the authigenic clays and is interpreted to reflect a thermal overprint related to widespread granitoid magmatism around the Barberton Greenstone Belt area. The highest temperature reached by the samples since the time of clay mineral formation was <300°C. The unusual feature, that the clay mineral isochron is older than the whole-rock isochron, can be explained by the fact that the primary minerals of the whole-rocks were altered, recrystallized and isotopically reset at ~2.7 Ga at a temperature of <250°C, while the newly formed clay minerals survived.

## ESR DATING OF VOLCANIC QUARTZ: APPLICATIONS TO THERMAL HISTORY

Toyoda, S. and Ikeya, M., Department of Earth and Space Science, Faculty of Science, Osaka University, Toyonaka, Osaka, 560, Japan.

Unpaired electrons created by natural ionizing radiation are accumulated in minerals. Accumulated dose ( $D_E$ ) is obtained from concentration of unpaired electrons measured by ESR (electron spin resonance) spectroscopy. ESR ages are obtained by dividing  $D_E$  by annual radiation dose ( $D$ ). This method has been successfully applied to speleothems, shells, corals, tooth enamel, gypsum in sediments, quartz in tephra and so on<sup>1)</sup>.

Dating methods using isotopes and fission tracks have been used in investigations of thermochronology. However, possibility of ESR dating method for this field has never been discussed. In this paper, results of basic research on thermal stability of paramagnetic centers (unpaired electrons) in quartz are presented as well as discussion on possibility of ESR method for applications to thermochronology. As an example, thermal history around an intrusive dike is investigated.

Quartz grains were extracted from a portion of Mannari granite in Japan and from some members of Valles Rhyolite in New Mexico, U.S.A. ESR signals were observed by ESR measurement due to Al center (an electronic hole trapped at an aluminum ion replacing silicon), Ti center (an electron trapped at a titanium ion replacing silicon), and  $E'_1$  center (an electron at an oxygen vacancy).

Thermal stabilities of the centers were investigated with isochronal (stepwise) and isothermal heating experiments. As results of isothermal heating experiments, the centers were found to decay with second order kinetics. Activation energies were obtained from an Arrhenius diagram where decay coefficients were plotted. The thermal stability of oxygen vacancies in quartz was also investigated where a method was used according to our proposal<sup>2)</sup> in order to convert oxygen vacancies to their paramagnetic states ( $E'_1$  centers).

Closure temperatures were obtained for each center and oxygen vacancy by a calculation simulating cooling of granite<sup>3)</sup> as well as dike intrusion. As for quartz in granite with a cooling rate of 10 K/Myr, the temperatures were obtained to be 91°C for  $E'_1$  center, 78°C for Al center, and 31°C for Ti center.

The concentrations of oxygen vacancies were reported to be correlated with radiometric age of host rocks in Ma-Ga range<sup>4)</sup> as well as  $E'_1$  centers<sup>5)</sup>. It is found in this study that oxygen vacancies are created by artificial  $\gamma$  ray irradiation simulating external  $\beta$  and  $\gamma$  rays. Their amount created is consistent with that in natural quartz where external  $\beta$  and  $\gamma$  rays were assumed to create oxygen vacancies. The results support our theory<sup>4)</sup> that oxygen vacancies are created by external  $\beta$  and  $\gamma$  ray in natural quartz. A thermal history around intrusive andesite will be discussed using oxygen vacancies in quartz extracted from host rocks of granite where external  $\beta$  and  $\gamma$  rays are assumed to create oxygen vacancies in quartz.

- 1) Ikeya, M., 1988, Dating and radiation dosimetry with electron spin resonance: *Magn. Reson. Rev.*, v.13, p.91-134.
- 2) Dodson, M.H., 1973, Closure temperature in cooling geochronological and petrological systems: *Contr. Mineral. Petrol.*, v.40, p.259-274.
- 3) Toyoda, S., and Ikeya, M., 1991, Thermal stabilities of paramagnetic defect and impurity centers in quartz: Basis for ESR dating of thermal history: *Geochem. J.*, v.25, p.437-445.
- 4) Toyoda, S., Ikeya, M., Morikawa, J., and Nagatomo, T., Enhancement of oxygen vacancies in quartz by natural external  $\beta$  and  $\gamma$  ray dose: a possible Geochronometer of Ma-Ga range: *Geochem. J.*, v.26, p.111-115.
- 5) Odom, A.L., and Rink, W.J., 1989, Natural accumulation of Shottky-Frenkel defects: Implication for a quartz geochronometer: *Geology*, v.17, p.55-58.

## CHARACTERIZATION OF DEFECTS INDUCED BY NEUTRON IRRADIATION : XRD RIETVELD REFINEMENT RESULTS

Hsin-Yi Tseng, Peter Heaney, and T.C. Onstott  
Dept. of Geological and Geophysical Sciences,  
Princeton University, Princeton, NJ 08544,  
USA

To investigate the relationship between the microstructures resulting from neutron irradiation and argon diffusion in vacuum, techniques capable of quantifying these structures are required. Powder X-ray diffraction (XRD) analyses followed by Rietveld refinement were applied to irradiated and unirradiated K-feldspars. Benson Mines orthoclase ( $K_{0.915}Na_{0.067}Al_{1.06}Si_{2.96}O_8$ , corresponding to Or<sub>94</sub>) was chosen because of its purity, lack of naturally formed microstructures, and because its argon diffusion behaviour is extremely well determined. XRD powder samples were irradiated by total (thermal + fast) neutron doses of  $6.3 \times 10^{18}$  n/cm<sup>2</sup> and  $1.26 \times 10^{19}$  n/cm<sup>2</sup>. We observed that clear powdered orthoclase takes on a distinct brownish coloration after irradiation. We utilized the fiber filter mounting method for sample preparation to reduce preferred orientation problems and obtained reproducible X-ray diffraction patterns. XRD analyses revealed peak broadening in irradiated orthoclase compared to the unirradiated orthoclase. Line shapes were modeled using a pseudo-Voigt profile function with the GSAS Rietveld refinement program. The anisotropic strain percentage calculated from the Lorentzian profile parameters reveals a positive correlation with the neutron dose (see table). By contrast, the calculated particle sizes are between 0.5  $\mu$ m and 5  $\mu$ m, so the contribution of particle size broadening can be approximately neglected. This strain-induced broadening probably results from vacancies created by collision cascades of recoiling atoms during neutron bombardment. Since <sup>39</sup>Ar is initially concentrated within these cascade zones compared to <sup>40</sup>Ar, enhanced diffusivity of <sup>39</sup>Ar with respect to <sup>40</sup>Ar is not surprising.

Rietveld Refinement Result			
Neutron Dose	unirradiated	$6.3 \times 10^{18}$ n/cm <sup>2</sup>	$1.26 \times 10^{19}$ n/cm <sup>2</sup>
$\chi^2$	3.111	3.026	2.906
Strain // [001]	0.2425 %	0.3153 %	0.4065 %
Strain $\perp$ [001]	0.2052 %	0.2697 %	0.3206 %
Particle // [001]	$1.822 \times 10^4$ Å	$5.076 \times 10^3$ Å	$4.108 \times 10^4$ Å
Particle $\perp$ [001]	$4.813 \times 10^3$ Å	$4.813 \times 10^3$ Å	$4.813 \times 10^3$ Å

**RELATING HYDROTHERMAL FLUID FLOW TO THERMAL MATURITY FOR A TRIASSIC BASIN: RESULTS FROM FLUID INCLUSIONS AND FISSION TRACK LENGTH DISTRIBUTIONS**

Hsin-Yi Tseng, T. C. Onstott, Dept. of Geological and Geophysical Sciences, Princeton University, Princeton, NJ 08544, USA;

R. C. Burruss, U. S. Geological Survey, Denver, CO 80225, USA; and

D. S. Miller, Dept. of Geology, Rensselaer Polytechnic Institute, Troy, NY 12180, USA.

The Late Triassic Taylorsville basin yields detrital fission track apatite and zircon dates that are younger than the age of deposition. The apatite fission track ages range from 135 to 200 Ma with the younger ages located near the center of the basin. The sparcity of intrusive igneous rocks in the basin and the spatial position of the fission track samples suggest that either the Taylorsville basin was more deeply buried than today and was exhumed prior to the Early Cretaceous.

Maximum homogenization temperatures of secondary aqueous fluid inclusions in calcite veins in shale and sandstone cuttings from a borehole near the center of the basin range from 150° to 200°C between 6650 and 10070 ft. depth, with highest temperatures in the deepest samples. A calcite vein at 8376 ft contains both two-phase aqueous and one-phase CH<sub>4</sub>-rich inclusions in healed microcracks. The CH<sub>4</sub>-rich inclusions homogenize to vapor at about -82.1°C. If both types of inclusions were trapped simultaneously, the density of the CH<sub>4</sub>-rich inclusions implies an entrapment pressure about 400 bars at the homogenization temperature (165°C) of the aqueous inclusions. This pressure falls between the hydrostatic and lithostatic pressures at the present depth of burial. If we assume that the pressure regime was hydrostatic at the time of trapping then the inclusions were trapped at 4 km in a thermal gradient of about 40°C/km. If the pressure gradient was close to lithostatic, then the thermal gradient would have been about 90°C/km.

The high temperature recorded by the secondary aqueous inclusions are consistent with the pervasive resetting of zircon and apatite fission track dates. In order to fit the fission track length distributions of the apatite data, however, a cooling rate of 1 - 2 °C/Ma following the thermal maximum is required. To match the integrated dates, the thermal maximum would have occurred at ~200 Ma. The timing of the maximum temperature is consistent with rapid burial of the Taylorsville basin to twice its present day depth and thermal reequilibration with a 40°C/km geothermal gradient, followed by slow exhumation.

**SIMS U-Pb AGE OF ZIRCONS IN ARCHEAN GRANULITES FROM THE LIMPOPO BELT, SOUTHERN AFRICA.**

TSUNOGAE, T., Fac. Education, Shimane Univ., Matsue 690, Japan, and YURIMOTO, H., Inst. Geosci., Univ. Tsukuba, Ibaraki 305, Japan.

New U-Pb age of single zircons in Archean granulites was examined by the secondary ion mass spectrometry (SIMS). A Cameca IMS-3f ion microprobe at the University of Tsukuba was employed for the present zircon analysis. Mass resolution of secondary ions for the SIMS analysis was set up to 6500 (M/ΔM, 10% valley) which is sufficient to resolve all major interferences from U, Pb, and Th isotopes. Although the Pb intensity analyzed by the 3f (about 1 to 2 cps/ppm) is lower than that by SHRIMP, it is sufficient to apply to the U-Pb method of zircon with high radiogenic Pb concentration. The relationship between <sup>206</sup>Pb<sup>+</sup>/<sup>238</sup>U<sup>+</sup> and UO<sup>+</sup>/U<sup>+</sup> ratios was used for the 3f analysis to obtain unknown <sup>206</sup>Pb/<sup>238</sup>U ratio in terms of standard zircon (SL13 provided by the ANU) as mentioned by Compston *et al.* (1984). <sup>207</sup>Pb/<sup>206</sup>Pb ratio was estimated as measured, because Pb isotopic fractionation on the SIMS analysis was negligibly small.

The analytical procedure was applied to zircons in granulites from the Limpopo Belt in southern Africa. The belt can be lithologically subdivided into the Central Zone (CZ; T=750-850°C, P>12 kbar) and the Northern and Southern Marginal Zones (NMZ and SMZ; T=700-750°C, P=7.0-7.5 kbar). Preliminary analyses of zircons in the tonalitic Sand River Gneiss (CZ) display ages of 3200-3350 Ma, which show good agreement with previous Sm-Nd age (3200-3300 Ma; Harris *et al.*, 1987) and U-Pb age (<3290 Ma; Retief *et al.*, 1990).

The CZ shows SIMS U-Pb ages of 3100-3350 Ma, while the NMZ shows younger ages of 2650-2800 Ma. Rim of the 2780 Ma zircon from the NMZ suggests a later thermal event at about 1800 Ma. There are two possible explanations for the differences in U-Pb ages between the CZ and NMZ; (1) timing of peak metamorphism of the CZ was older than that of the NMZ, which is consistent with the differences in P-T path. (2) older relict zircon from the CZ did not suffer significant reset of U-Th-Pb system during peak metamorphism, because of rapid uplifting and cooling history of the CZ.

Compston, W., Williams, I.S., and Meyer, C., 1984, *JGR*, **89**, (suppl.) B525-B534.

Harris, N.B.W., Hawkesworth, C.J., Van Calsteren, P., and McDermott, F., 1987, *EPSL*, **83**, 85-93.

Retief, E.A., Compston, W., Armstrong, A., and Williams, I.A., 1990, In J.M. Barton, Jr., Eds., *Extended Abstracts, The Limpopo Belt*. RAU, Johannesburg, 95-99.

**GAS GEOCHEMISTRY OF DEEP-SEA VENTING HYDROTHERMAL FLUIDS RELATED WITH ARC VOLCANISM: EVIDENCE FOR SUBDUCTING SLAB CONTRIBUTION IN AN ARC VOLCANISM**  
TSUNOGAI, U., ISHIBASHI, J., WAKITA, H.,  
Lab. for Earthq. Chem., Fac. of Science, Univ. of Tokyo, Hongo Bunkyo-ku, Tokyo 113, JAPAN,  
GAMO, T., ORI, Univ. of Tokyo, Minami-dai, Nakano-ku, Tokyo 164, JAPAN

Chemical and isotopic compositions of dissolved gases are analyzed for hydrothermal fluids from the Suiyo seamount (located in the southern part of the Izu-Bonin arc; depth: 1,370 m) and the Peak B seamount (located in the southern end of the Mariana arc; depth: 1,470 m). Gas geochemistry of the fluids are compared with that of MOR hydrothermal fluids and subaerial arc volcanic gases. The origin of gases is discussed in relation to arc volcanism. This is the first gas composition study of deep-sea venting hydrothermal fluids in relation to arc volcanism.

Using Japanese submersibles *SHINKAI 2000* and *SHINKAI 6500*, we collected twelve fluid samples (up to 310 °C) from the Suiyo seamount and eleven fluid samples (up to 127 °C) from the Peak B seamount. Gas compositions of these hydrothermal fluids have several common characteristic features: (1) The CO<sub>2</sub> concentration is substantially higher than that of the MOR fluids, and the CO<sub>2</sub>/<sup>3</sup>He ratio (11–12x10<sup>9</sup>) is close to that found in the subaerial arc volcanic gases. (2) The <sup>3</sup>He/<sup>4</sup>He ratio of 8.1 and 7.5 (R/R<sub>atm</sub>) are the highest value for an island-arc and are almost identical to the MOR ratio. (3) The δ<sup>13</sup>C values of dissolved gases are unusually as high as δ<sup>13</sup>C(CO<sub>2</sub>) = -1 ‰ and δ<sup>13</sup>C(CH<sub>4</sub>) = -8.5 ‰ at the Suiyo seamount and δ<sup>13</sup>C(CO<sub>2</sub>) = -1 ‰ at Peak B seamount. These are differ from those of the ordinary island-arc and MOR values.

The observed high <sup>3</sup>He/<sup>4</sup>He ratios and high δ<sup>13</sup>C values are difficult to explain by either contamination or fractionation processes during hydrothermal circulation. We conclude that they reflect the gas compositions of source magma. A modeled calculation demonstrates that a simple contribution of the subducting slab of about 3 % to the MORB mantle will produce a magma with the gas composition of these seamounts and this is the only case to generate the observed composition.

These characteristic gas compositions of the seamounts are not common to subaerial arc volcanoes, but may represent "original" features of arc magmatism. Formation of such magma may be due to its particularly different environment from subaerial volcanoes: extraordinary thin and young arc crust, lack of old sedimentary layer in crust and insignificance of biogenic materials.

**AGES OF MESOZOIC PLUTONS IN THE DAMYANG-GEOCHANG AREA, RYONGNAM MASSIF, KOREA**

TUREK, A., Dept. of Geology, University of Windsor, Windsor, ON. Canada N9B 3P4, and KIM, C.B., Dept. of Geology, Chonnam National University, Puk-ku, Kwangju, Korea 500-757.

The Damyang-Geochang area of Korea is in the southwest part of the Ryongnam massif and is made-up of Precambrian gneisses that have been intruded by Triassic to Jurassic, felsic to mafic, batholiths and stocks. All have been involved in several orogenies from Precambrian to Mesozoic. A total of eight K-Ar, Ar-Ar, and Rb-Sr ages has been reported for some of the rocks in the area and the ages range from 159-228 Ma.

This study reports the first U-Pb zircon ages for the Korean peninsula. In the Damyang-Geochang area plutonism appears to span from 219 Ma to 176 Ma. The first period of Mesozoic plutonism was the emplacement of: the foliated granite, the foliated gabbro and the Daegang foliated granite, at 219-212 Ma. A second plutonic event occurred at 187-183 Ma in which a foliated granodiorite and the Sunchang foliated granite were emplaced. The Namweon granitic batholith and an associated diorite stock, both non-foliated and post-tectonic, were emplaced at 177-176 Ma. The concordia plots for the above zircon data indicate derivation from a Precambrian protolith, 1.9-2.6 Ga in age. Pb isotopic composition measured on feldspars has an upper crustal signature. Moreover, the younger plutons are derived from a more radiogenic source than the older ones. The Jirisan gneiss complex constitutes part of the Ryongnam massif and yields a zircon age of 1940 Ma.

#### EXOTIC AND EXOGENIC OSMIUM

TUREKIAN, KARL K., Dept. of Geology and Geophysics, Yale University, P.O. Box 208109, New Haven, CT 06520-8109

The characteristic  $^{187}\text{Os}/^{186}\text{Os}$  signatures of meteoritic, mantle and crustal materials imprint the oceans and leave a record of terrestrial and cosmic events in marine deposits. The record over the past 100 million years shows the results of meteorite impacts and mountain building.

#### THE DEVELOPMENT OF IDEAS ABOUT THE GROWTH OF $^{40}\text{Ar}$ IN THE ATMOSPHERE

TUREKIAN, K.K., PORCELLI, D., SEIDEMANN, D.E., Dept. of Geology and Geophysics, Yale University, P.O. Box 208109, New Haven, CT 06520-8109

The origin of the third most abundant gas in the atmosphere, argon-40, is clearly the decay of  $^{40}\text{K}$  in the solid Earth with subsequent degassing. The crust and the mantle are the two obvious loci of production. The amounts of potassium in these two reservoirs are of the same order of magnitude. The mechanisms of escape from the two reservoirs are not obviously coupled. A simple first order degassing law has been modified to accommodate the decreasing efficiency of degassing geared to the total heat production and escape from the Earth.

Estimates of contemporary degassing rates from the mantle (at ocean spreading centers) and the crust (based on resetting of  $^{40}\text{K}$ - $^{40}\text{Ar}$  mineral chronometers) provide the entry into the problem.

## PROPOSAL FOR A QUATERNARY $^{40}\text{Ar}/^{39}\text{Ar}$ DATING STANDARD

TURRIN, B.D.<sup>1,2</sup>, DONNELLY-NOLAN, J.M.<sup>1</sup>, FLECK, R.J.<sup>1</sup>, CHAMPION, D.E.<sup>1</sup>, BECKER, T.A.<sup>2</sup>, CURTIS, G.H.<sup>2</sup>, DEINO, A.L.<sup>2</sup>, RENNE, P.R.<sup>2</sup>, SHARP, W.D.<sup>2</sup>, and SWISHER, C.C.III<sup>2</sup>: 1) U.S. Geological Survey, 345 Middlefield Rd., Menlo Park, CA, 94025, USA. 2) Institute of Human Origins, Geochronology Center, 2453 Ridge Rd., Berkeley, CA, 94709, USA.

Accuracy of the  $^{40}\text{Ar}/^{39}\text{Ar}$  dating technique, a relative dating method which compares the age of an unknown sample to the age of a known standard, is limited by the accuracy of the "known age" of the standard and by how well the interfering neutron reactions from  $^{36}\text{ArCa}$ ,  $^{39}\text{ArCa}$ , and  $^{40}\text{ArK}$  are known and corrected. The  $^{36}\text{ArCa}$  and  $^{39}\text{ArCa}$  corrections are reproducible between separate irradiations ( $\leq 1\%$ , Dalrymple et al., 1981). The  $^{40}\text{ArK}$  value varies by as much as an order of magnitude between measurements (Dalrymple et al., 1981). This correction, which becomes significant in young samples where the  $^{40}\text{Ar}_{\text{radiogenic}} (^{40}\text{Ar}^*)/K$  ratio is typically low, can be minimized in two ways: 1) reduce the amount of neutron flux, and 2) use Cd shielding. However, if the standard is significantly older than the unknowns, this correction becomes large relative to the measured  $^{40}\text{Ar}^*/^{39}\text{Ar}$  ratio of the unknowns. For example, using the youngest available standard [the Fish Canyon sanidine (FCS) 27.84 Ma], the youngest material that can be dated while maintaining optimum  $^{40}\text{Ar}^*/^{39}\text{Ar}$  ratios, and relatively small corrections for interfering neutron reactions, is 100 to 300 ka (Dalrymple et al., 1981). An ideal  $^{40}\text{Ar}/^{39}\text{Ar}$  standard for dating rocks in the range  $10^4$  to  $10^7$  yrs would be  $\sim 1$  Ma.

For this standard, we propose the sanidine from the rhyolite of Alder Creek, Ca., which is the type section of the Cobb Mountain Normal-Polarity Subchron (CMNPS) of the Matuyama Reversed-Polarity Chron of the Geomagnetic Polarity Time Scale. Because the CMNPS is a unique world-wide stratigraphic event of short duration ( $\leq 10$  ka), sanidine from the rhyolite of Alder Creek is an ideal  $^{40}\text{Ar}/^{39}\text{Ar}$  standard. Sanidine from this unit has been dated at  $1.186 \pm 0.006$  Ma using the FCS (Turrin et al., 1994). This age is concordant with the age of 1.19 Ma for the CMNPS as suggested by the Astronomical Polarity Time Scale (Shackleton et al., 1990).

The use of the CMNPS standard will optimize irradiation times of Quaternary age samples, thus providing accurate and precise age measurements relative to the age of the CMNPS for Quaternary stratigraphic and climatic dating studies.

Dalrymple, G.B., Alexander, C.E., Lanphere, M.A., and Kraker, P.G., 1981, Irradiation of Samples for  $^{40}\text{Ar}/^{39}\text{Ar}$  Dating Using the Geological Survey TRIGA Reactor: U.S. Geological Survey Professional Paper 1176, 55p.

Shackleton, N.J., Berger, A., and Peltier, W.R., 1990, An alternative astronomical calibration of the Lower Pleistocene time scale based on ODP Site 677: Royal Society of Edinburgh Trans., v. 81, p. 251-261.

Turrin, B.D., Donnelly-Nolan, J.M., and Hearn, B.C., 1994,  $^{40}\text{Ar}/^{39}\text{Ar}$  ages from the rhyolite of Alder Creek, California: Age of the Cobb Mountain Normal-Polarity Subchron revisited, *Geology*, v. 22, p. 251-254.

## PAN-AFRICAN REJUVENATION IN SUPRACRUSTALS OF KERALA KHONDALITE BELT (KKB) AND THEIR ISOTOPIC SIGNATURES

UNNIKRISHNAN-WARRIER, C., Dept. of Geosciences, Osaka City University, Sugimoto, Sumiyoshi-Ku, Osaka-558, Japan., YOSHIDA, M., Dept. of Geosciences, Osaka City University, Sugimoto, Sumiyoshi-Ku, Osaka-558, Japan and SANTOSH, M., Centre for Earth Science Studies, P.B. 7250, Akkulam, Thiruvikkal P.O, Trivandrum-695 031, India.

The southern tip of the high-grade terrain of Peninsular India is composed of a vast supracrustal sequence known as Kerala Khondalite Belt (KKB). Lithological units of this supracrustal sequence are composed of dominantly by charnockite- khondalite-leptynite group of rocks. They also host the incipient charnockites. Minor lithounits are the interlayered basic granulites, calc-silicates and quartzites.

Radio isotope investigations (Sm-Nd) on mineral separates from the garnet-biotite gneiss and the sillimanite-cordierite bearing gneiss from KKB yield  $\sim 500$  Ma similar to the age of incipient charnockites from this terrain, where as the Rb-Sr ages are slightly younger. The widespread incipient charnockite development in the KKB gneisses adjacent to Pan-African alkalic granite-syenite complex links the charnockitic alteration of the gneisses with the  $\text{CO}_2$  derived from deep crustal origin. Fluid inclusion studies as well as Carbon isotope studies of graphites from these lithologies also suggest that deep crustal fluids are instrumental for the genesis of incipient charnockites. This Pan-African tectonics can be well correlated with other parts of East Gondwana.

WIDE-AREA LINE ANALYSIS OF ISOTOPIC ABUNDANCES ON INHOMOGENEOUS INSULATORS USING AN ION MICROPROBE

UYEDA, C., TSUCHIYAMA, A. and YAMANAKA, T., Inst. Earth and Planetary Sci., Col. General Education Osaka University Toyonaka Osaka 560 Japan

In general, the isotopic analysis using an ion microprobe is accompanied by various types of instrumental mass fractionation deriving from the ionization process at the sample surface<sup>1)</sup>. The variation of the charge potential due to the inhomogeneity of the sample conductivity often interfere with the in-situ analysis for various inhomogeneous geological sample. For this reason, isotopic in-situ analysis is not popularly done for inhomogeneous insulator samples.

We have developed a new method which improves the conductivity of the sample surface, and homogenizes the surface potential<sup>2)</sup>. A metal channel is located along the line of analysis. Point to point analysis is performed along the boundary of the metal channel and the sample. Both the sample and the metal surface are bombarded with a same ion beam with the diameter of 40-80  $\mu$ m. Using this method, the line analysis of Mg isotopes is done with the spatial resolution of 4  $\mu$ m, the error of less than 3%.

A sample is attached between two laboratory standards, and the analysis line is located across the sections of the three samples. Isotopic variation of the sample is measured precisely by comparing the sample data with that of the two standards. The length of the analysis line is 6mm wide.

An isotopically enriched standard is placed between the laboratory standards from time to time to check whether the system reproduces the spatial isotopic variation correctly. In general, the amount of instrumental mass fractionation changes considerably with the position of the primary ion at the sample surface, and it is necessary to evaluate this effect day-by-day especially in the case of wide-area line analysis.

It is noted that the search of a new isotopic anomaly is done far more effectively by performing an in-situ line analysis than by separating the individual grain from the bulk samples as it is commonly done<sup>3)</sup>. Also the systematic survey of isotope data can be done for various components in the meteorite. The intrinsic mass fractionation of refractory elements, for example, would be a subject of large significance<sup>4)</sup>. Every components in the meteorites may have experienced mass fractionation by evaporation or condensation. Therefore it is desirable to carry out a systematic survey on all the components of the meteorites, in order to obtain the whole view of the process.

1) NISHIMURA, H. & OKANO, J. (1974) J. Appl. Phys. Suppl. 2 Pt. 1 339. 2) UYEDA, C., et al, Proc. SIMSIX conf. (in print) 3) e.g. McKEEGAN, J. & ZINNER, E. (1987) GCA 51 1468, 4) UYEDA, C., TSUCHIYAMA, A. & OKANO, J. (1989b) Earth Planet Sci. Lett. 107 138.

RADIOMETRIC DATING OF THE TORTONIAN/MESSINIAN BOUNDARY (N. APPENNINES, ITALY)

VAI G.B., Dip. Scienze Geologiche, I-40127, Bologna, Italy., LAURENZI, M.A., Istituto Geocronologia e Geochimica Isotopica, CNR, 56127 Pisa, Italy,

A series of new Ar/Ar datings on biotites have been made from the Monte del Casino (MdC) section in the Northern Appennines, Italy. The aim was to check the reliability of the previous radiometric datings obtained from closely related sections, which have provided mean dates of  $7.72 \pm 0.15$  close to the *Gr. suteræ* FAD,  $7.35 \pm 0.08$  Ma (biotite) and  $7.28 \pm 0.10$  Ma (plg) for the interval between *Gr. saheliana* (near M5 datum) and *Gr. conomiozea* FADs, and an interpolated age of  $7.26 \pm 0.10$  Ma for the boundary taken at the conomiozea FAD (Vai et al., 1993).

The new section sampled is continuous, biostratigraphically well subdivided, and contains a series of superposed biotite-rich volcanoclastic horizons (BRH) spanning the Tortonian/Messinian (T/M) boundary over a total thickness of about 18 m. The MgO/FeO/Ti<sub>2</sub>O and FeO/MgO/K<sub>2</sub>O tests made on biotites show an acceptable excellent degree of homogeneity suggesting that the BHR can be interpreted as original fallout deposits.

Seven out of the nine BRH have been sampled and five of them have been dated till now. The two first horizons give a mean date of  $7.30 \pm 0.02$  Ma which differs from the mean of three previous K/Ar dates from the same horizons in a different section nearby (s. above). The following two horizons have yielded dates of 7.40 Ma and 7.28 Ma, with a mean of  $7.34 \pm 0.02$  Ma, quite consistent with previous data.

The date of  $6.71 \pm 0.04$  Ma obtained from the uppermost horizon is the first one bracketing the T/M boundary (about 4 m from above). It differs from a preliminary K/Ar age of 7.15 Ma (and 7.2 Ma by Odin, pers. com.) obtained from a younger sample of the same horizon.

Considering the end members of the new dates from the last three horizons a mean sedimentation rate of  $10 \pm 0.5$  m/Ma is obtained to be compared with the figure of  $27 \pm 3$  m/ma by Vai et al. (1993). By linear interpolation between the two facing dates, the T/M is about  $7.07 \pm 0.05$  Ma old, which is fairly consistent with the previous calibration of  $7.26 \pm 0.10$  by Vai et al. (1993) and also with the astronomical calibration at 7.10 Ma (Krijgsman et al., 1993). Two further dates of about 7.1 (biotite) and 6.85 (sanidine) Ma, reported by A. Deino at the MICOP Ancona 1992, are also consistent, although more precision on their stratigraphic calibration is needed. At present, the T/M (*Conomiozea*) boundary can be assumed at  $7.1 \pm 0.2$  Ma. All ages presented here are referred to an age of 27.55 Ma for the FCT biotite (Izett et al., 1991).

Izett G.A., Dalrymple G.B. and Snee L.W., 1991, <sup>40</sup>Ar/<sup>39</sup>Ar age of Cretaceous-Tertiary boundary tektites from Haiti: Science, 252, 1539-1542.

Krijgsman W., Hilgen F.J., Langereis C.G. & Zachariasse W.J., 1993, The age of the Tortonian/Messinian boundary; Earth Planet. Sci. Letter, in press.

Vai G.B., Villa I.M. & Colalongo M.L., 1993, First direct dating of the Tortonian/Messinian boundary; C.R. Acad. Sci. Paris, 316, II, 1407-1414.

## He-Ne AND Sr-Nd-Pb ISOTOPE SYSTEMATICS IN HAWAIIAN BASALTS: EVIDENCE FOR THE MIGRATION OF GASEOUS AHEAD OF LITHOPHILE PLUME COMPONENTS?

P.J. Valbracht, Inst. de Physique du Globe, 75252 Paris, France, M. Honda, I. McDougall, The Australian National University, ACT0200 Canberra, Australia, H. Staudigel, and G.R. Davies, Vrije Universiteit, 1081HV Amsterdam, The Netherlands

Hawaiian volcanoes, the type expression of plume-related oceanic volcanism, were studied for their geochemical and chronological relationships between the isotopic ratios of gaseous (He, Ne, Ar, Kr, Xe) and lithophile (Sr, Nd, Pb) elements. An apparent decoupling of these isotopic parameters between different volcanic stages suggests that gaseous plume components migrate ahead of the lithophile components.

A wealth of scientific information is available from all four major stages of Hawaiian volcanic activity, beginning with the earliest seamount stage at Loihi Seamount (Stage I), through the massive shields (Stage II), and late alkalic (Stage III), to the rejuvenated volcanism (Stage IV). Previous studies suggest that the lithophile fraction of the volcanic products (i.e. their Sr-Nd-Pb isotopic signature) appears to be decoupled from the gaseous fraction. Stage I has a strong "Enriched Pacific MORB" lithophile component, whereas Stage II lavas, forming about 95% of these volcanoes, are dominated by a relatively "enriched" plume lithophile signature (especially on Oahu (the Koolau series), Lanai, and Kahoolawe) similar to the Bulk Silicate Earth. Stage III and IV lithophiles show more depleted compositions. With respect to  $^3\text{He}/^4\text{He}$ , Stage I appears to be dominated by a plume component, while later stages become increasingly similar to MORB. Hence the plume component appears in Stage I (Loihi Seamount), based on helium isotope systematics, but in Stage II based on Sr-Nd-Pb isotope systematics. This apparent decoupling of noble gas and lithophile tracers either requires another component in the Hawaiian basalts, or a separation of gaseous from lithophile components.

We have measured the isotopic composition of all five noble gases and Sr-Nd-Pb on a suite of young samples from the deep submarine rift zones from Loihi Seamount and Mauna Loa, and from the deep flanks of Hualalai. Our data corroborate previously published results: the combined isotopic data indicate an offset ahead in time of the helium (and neon) relative to the Sr-Nd-Pb isotopic record. This is most clearly demonstrated by Stage I, where helium is dominated by the plume component, which later becomes apparent in the Sr-Nd-Pb record during Stage II. During the latter stage, helium and neon already show a shift towards a MORB-like component, which later becomes apparent in the Sr-Nd-Pb record during Stages III and IV. Hence helium (and neon) signatures may be seen roughly one stage ahead of the equivalent Sr-Nd-Pb record. We envisage this to be caused by more rapid migration of the noble gases in a separate ( $\text{CO}_2$ -rich?) gas-phase in the melt extraction column. This is followed in time by the magmatic phase carrying the solid lithophile elements; helium and neon can be correlated with the solid lithophile elements on the scale of an evolving Hawaiian volcano, but are shifted ahead in time on the scale of individual samples. If this model is correct, a less depleted, and less degassed reservoir, relative to the upper MORB mantle, characterizes the Hawaiian plume component, and may originate in the lower mantle.

## COMPARISON OF CLIMATE DATA WITH AN AMS-DATED RECORD OF SALT MARSH ELEVATION, HAMMOCK RIVER MARSH, CONNECTICUT DURING THE LAST 1800 YEARS

VAN DE PLASSCHE, O., Institute of Earth Sciences, Vrije Universiteit, 1081 HV Amsterdam, the Netherlands, VAN DER BORG, K. and DE JONG, A.F.M., R.J. van der Graaff Laboratory, Rijks Universiteit Utrecht, 3508 TA UTRECHT, the Netherlands

The surface of mature salt marshes occurs from slightly below local mean high water (MHW) to somewhat above local mean high water spring (MHWS) tide. Salt marshes are able to keep up with high average rates of sea-level rise, provided sediment supply is sufficient and conditions for marsh plant growth are favorable. Salt marsh deposits thus contain a record of sea-level change, sediment supply and growth conditions. The deposits of New England type salt marshes are rich in organics, composed largely of the subsurface remains of plants growing at the marsh surface. Dominant peat forming plant species are *Spartina alterniflora* stunted, *Spartina patens*, and *Distichlis spicata* in the lower parts, and *Juncus gerardii*, *Scirpus robustus*, *Scirpus americanus*, and *Phragmites australis* on the higher parts.

The first step in reconstructing former local MHW(S) positions from salt marsh deposits is to establish and date paleo-marsh surface levels. We determined the level and age of 45 former marsh surfaces within the upper 1.7 m of marsh deposit in Hammock River marsh, Connecticut by means of AMS-dated subsurface stalk parts of *Scirpus robustus* and *Spartina alterniflora* and rhizomes of *Spartina patens* and *Distichlis spicata* preserved in the marsh peat. The relation of subsurface plant remains to marsh surface is based on observations of the depth of modern root systems and of the vertical length of plant remains observed in hundreds of cores. Of each sample, two targets were measured to obtain radiocarbon ages with 1 sigma values less than 50 years.

The reliability of the 45 dates is assessed by reference to stratigraphic position and internal consistency and an attempt is made to explain deviations in terms of sample contamination, sample preparation, instrument performance and statistical errors.

The paleo-marsh surface curve, which is a reasonable approximation of the local MHW curve, is compared with paleoclimate data for the past 1800 years.

RECONSTRUCTION OF PALAEOCLIMATIC  
REGIONAL VARIATIONS USING  $^{13}\text{C}$  DATA FROM  
RADIOCARBON DATABASES

VAN KLINKEN, G.J., Radiocarbon Accelerator Unit,  
University of Oxford, Oxford OX1 3QJ, UK, and VAN  
DER PLICHT, J., Centre for Isotope Research, Groningen  
University, 9747 AG Groningen, The Netherlands.

Stable isotopes of hydrogen, oxygen, and to a lesser extent carbon are used, to study palaeoclimatic change. The sensitivity of carbon to climatic influences is far less pronounced than in the other two isotopes. Carbon isotopic ratios in ecosystems are established during the photosynthetic process in plants, and are then passed on in the foodweb without much modification. In a previous study (Van Klinken et al. in press), we have analysed a very large data set derived from  $^{14}\text{C}$  databases, and have shown that  $^{13}\text{C}/^{12}\text{C}$  ratios in plant and animal tissues have close relationships with environmental factors such as temperature and relative humidity, giving an especially clear response in animal bone. These small-scale variations in  $^{13}\text{C}/^{12}\text{C}$  ratios in wood, charcoal and bone result in a regular pattern of regional variation across Europe. The close association of carbon with the biosphere makes the use of carbon isotopic ratios especially valuable.

We have extended our database with information from areas with more extreme climatic conditions, and a discussion of potential applications of this type of analysis in palaeoclimatic reconstruction will be presented.

Van Klinken, G.J., Van der Plicht, J., and Hedges, R.E.M., 1994. Bone  $^{13}\text{C}/^{12}\text{C}$  ratios reflect (palaeo-)climatic variations. *Geophysical Research Letters* in press.

DEFINITION OF CONTINENTAL HISTORY IN WEST  
GONDWANA USING SM-ND AND U-PB  
GEOCHRONOLOGY.

VAN SCHMUS, W.R., Dept. of Geol., Univ. of Kansas,  
Lawrence, KS, 66045, BRITO NEVES, B.B., and  
BABINSKI, M., Inst. Geociências, Univ. São Paulo, São  
Paulo-SP-Brasil, HACKSPACHER, P., Inst. Geociências  
et Ciências Exatas, UNESP, Rio Claro-SP-Brasil,  
TOTEU, S.F., C.R.G.M., B.P. 333, Garoua, Cameroon.

We report Sm/Nd and U/Pb results for the Borborema Province of NE Brasil and the Central African fold belt in Cameroon; we use these data to define the internal architecture of the region, with emphasis on defining the northern margin of the São Francisco-Congo craton (SF-CC), its fragmentation history, and continental domains assembled between it and the West African craton during the 600 Ma Brasiliano-Pan African orogeny associated with formation of West Gondwana.

Archean cores of the SF-CC formed about 3 Ga as juvenile crust. 2.1 Ga granulites present between these cores represent fusion of them into the SF-CC. 2.1 Ga gneisses also occur north of the craton as defineable blocks in the 600 Ma fold belt. Most 2.1 Ga rocks in this region are reworked Archean, since Sm/Nd data typically yield Archean T(DM) ages.

Several Mesoproterozoic graywacke (turbidite)-bimodal volcanic assemblages occur between older crustal blocks north of the SF-CC. U/Pb analyses from metavolcanic and granitic rocks of these domains in NE Brazil show that these supracrustal rocks formed about 1.0 Ga. Sm/Nd results for them and post-tectonic 600 Ma granites hosted by them do not indicate incorporation of large amounts of Paleoproterozoic or Archean material. We interpret these assemblages as formed in 1.0 Ga rifts or small oceans in or along a large, pre-Gondwana continent (Rodinia supercontinent?). This 1.0 Ga rifting was a major tectonic and crust-forming event north of the SF-CC; it is apparently also common in southern parts of West Gondwana. The 1.0 Ga rifting event may have created several continental fragments that were later incorporated into Brasiliano-Pan African collisional orogens at 600 Ma. There are also several other remnants of older crust in NE Brazil and central Africa that may represent exotic crustal blocks not originally part of the SF-CC; data are not sufficient as yet to answer this question. Syn- to post-tectonic granitoid plutons associated with the Brasiliano-Pan African collisional orogen all yield Nd isotopic signatures corresponding to the ages of their host rocks, typically giving T(DM) ages of ca. 1.2-1.5 Ga (rift domains) or 2.6-3.0 Ga (cratonic fragments), consistent with magmas generated by partial melting of continental crust during or immediately following assembly of West Gondwana. We have not yet found evidence for juvenile 600 Ma crust in this collisional orogen or significant juvenile 2100 Ma crust within older cratonic fragments.

In summary, combined use of U/Pb and Sm/Nd isotopic systems allows precise definition of the pre-collisional history of continental crust in this major 600 Ma continental collision belt and will allow us to define the pre-collisional history of the diverse crustal domains involved in the assembly of West Gondwana.

STABLE CHLORINE ISOTOPE MEASUREMENTS IN  
GROUNDWATER PLUMES CONTAINING  
CHLORINATED HYDROCARBONS

VAN WARMERDAM, E.M., FRAPE, S.K.,  
DRIMMIE, R.J., and CHERRY, J.A., University of  
Waterloo, Waterloo, Ontario, Canada, N2L 3G1

Chlorinated hydrocarbons such as perchloroethylene (PCE), trichloroethylene (TCE) and 1,1,1-trichloroethane (TCA), are common groundwater contaminants used in a wide variety of industries. Concentrations in these groundwater plumes vary from ppb to as high as the solubility limits of the products. For isotopic analysis of chlorine in these solvents, the chlorinated hydrocarbon is incinerated, converting the organo-chlorine to hydrochloric acid. The hydrochloric acid is then converted to methyl chloride and the Cl 37/35 value is measured using a mass spectrometer. The present known isotopic range of inorganic chloride is 3.5‰ as identified by Long *et al.* Ongoing research examining stable chlorine isotopes in PCE, TCE and TCA shows that the range of measurement in pure phase organic products using the incineration method is 6.25‰. The stable isotopes of chlorine undergo fractionation as a result of the manufacturing process. Each different manufacturing process of PCE, TCE and TCA results in a particular Cl 37/35 content. A "fingerprint" value for PCE, TCE and TCA produced by different manufacturers can be identified based on the unique chlorine ratio associated with that particular product and manufacturer. Analytical techniques are being refined for Cl 37/35 analysis of chlorinated organic solvents found in groundwater plumes. At present, plumes with dissolved concentrations as low as 10 ppm can be analyzed for the Cl ratios. Various groundwater plumes will be studied to identify whether the fingerprints vary between the plumes. If the ratios differ, this technique may improve our ability to associate plumes or portions of plumes with particular sources or source areas.

Long, A., Eastoe, C.J., Kaufmann, R.S., Martin, J.G., Wirt, L., and Finley, J.B., 1993, High-precision measurement of chlorine stable isotope ratios: *Geochimica et Cosmochimica Acta*, v. 57, p. 2907-2912.

GEOCHRONOLOGICAL CONSTRAINTS ON  
THE MECHANISMS OF EXHUMATION OF  
REGIONAL METAMORPHIC TERRAINS

VANCE, D., Dept. of Earth Sciences, The Open University, Milton Keynes, MK7 6AA, UK.  
GALLAGHER, K., School of Geological Sciences, Kingston University, Kingston-upon-Thames, KT1 2EE. KELLEY, S. and AYERS, M., Dept. Earth Sciences, The Open University, Milton Keynes, MK7 6AA, UK.

One-dimensional numerical modelling of regional metamorphism involving overthrusting and subsequent exhumation with constant erosion rates predicts cooling at increasing rates as the rock approaches the surface. This is in contrast with many regions of the Alps and the Himalaya, where thermal histories derived from a combination of garnet chronometry and Ar-Ar thermochronology require initially very fast cooling (up to 100°C Ma<sup>-1</sup>) followed by successively slower cooling. This shape of cooling path can be generated by either crustal extension or an exponentially decreasing erosion rate. In theory, the chronological data might be able to distinguish between the two mechanisms or at least yield a maximum time constant if the case of exponentially decreasing erosion rates was important.

We have modelled cooling histories for both extension (two dimensions) and a decreasing erosion rate (one dimension). The results indicate that in some cases both mechanisms can reproduce the observed thermal histories while in others the erosional time constant required to reproduce the observed cooling paths may be too small. In the case of the Tauern window, for example, the data require that the time constant for erosion is about 5 Ma with initial erosion rates of 5mm a<sup>-1</sup>. In the south-central Alps cooling is so fast early on that the time constant has to be unfeasibly small - < 1Ma. An additional result of the modelling is that the isothermal decompression often associated by metamorphic petrologists with extension can equally well be produced by the onset of rapid erosion immediately after the metamorphic peak.

The above models will be further tested using new laser Ar-Ar data from the Zanskar region of the Himalaya where a uniquely well-exposed extensional shear zone cuts through the top of the metamorphic pile.

MECHANISMS AND KINETICS OF ATMOSPHERIC, RADIOGENIC, AND NUCLEOGENIC ARGON RELEASE FROM CRYPTOMELANE DURING  $^{40}\text{Ar}/^{39}\text{Ar}$  ANALYSES

VASCONCELOS, P.M., Department of Earth Sciences, University of Queensland, Brisbane Qld 4072, Australia, RENNE, P.R., BECKER, T.A., Institute of Human Origins, Geochronology Center, 2453 Ridge Road, Berkeley, California 94709, U.S.A., and WENK, H.R., Department of Geology and Geophysics, University of California, Berkeley, California 94720, U.S.A.

Resistance furnace (RF)  $^{40}\text{Ar}/^{39}\text{Ar}$  analyses of two compositionally distinct cryptomelane samples indicate that atmospheric  $^{40}\text{Ar}$ ,  $^{38}\text{Ar}$  and  $^{36}\text{Ar}$ , radiogenic  $^{40}\text{Ar}^*$ , and nucleogenic  $^{39}\text{Ar}$  and  $^{38}\text{Ar}$  isotopes are released from the mineral structure at discrete temperature steps ranging from 300 to 900 °C. The RF analyses permit us to identify the relative contributions of Ar from different reservoirs (adsorbed gases, intercrystalline space, and intracrystalline tunnel sites) in cryptomelane. The surface sites and intercrystalline spaces host primarily modern atmospheric Ar, which is released at temperatures ranging from 300-500 °C; the tunnel sites host radiogenic, nucleogenic, and paleoatmospheric Ar, which are liberated between 650-900 °C.

Correlation between the resistance furnace results, laser-heating release spectra, and *in situ* observation of the thermal behavior of cryptomelane in the high voltage electron microscope (HVEM) suggests that degassing of specific sites in the mineral are associated with discrete temperature intervals. The lower degassing temperature (peak at ~ 400 °C) is associated with release of atmospheric Ar from intergranular spaces. Only minor  $^{40}\text{Ar}^*$  and  $^{39}\text{Ar}$  are released at this stage. Minor amounts of Ar released at intermediate steps (T = 500 °C and 600 °C) are associated with the break down of poorly crystallized phases or Ar displacement by volume diffusion from the cryptomelane tunnel sites. The most significant degassing temperature (peak at T ~ 800 °C) is associated with the phase transformations of cryptomelane into hausmannite and manganosite. Most (>94% in sample PEG-01 and >60% in F115-139.8m) of the  $^{40}\text{Ar}^*$  and  $^{39}\text{Ar}$  are released at this temperature range, which makes the gas fraction liberated in the 700-900 °C interval the most significant for cryptomelane dating by the  $^{40}\text{Ar}/^{39}\text{Ar}$  method.

The degassing behavior of cryptomelane in the RF experiment confirms that this mineral is stable during the sample preparation procedures preceding  $^{40}\text{Ar}/^{39}\text{Ar}$  analysis. The samples release no radiogenic or nucleogenic Ar at temperatures below 300 °C (Cu-cryptomelane) and 400 °C (K-cryptomelane), and the high temperature release of  $^{40}\text{Ar}^*$ ,  $^{39}\text{Ar}$ , and  $^{38}\text{Ar}$  (700-900 °C) can be directly correlated to the break down of specific crystal sites in which these isotopes are hosted. This coherent behavior is drastically different from the continuous low temperature leakage of Ar observed in poorly crystalline clays and cryptocrystalline minerals, suggesting that cryptomelane is a much more competent, stable, and Ar retentive mineral than previously studied low temperature phases. The coherent behavior of cryptomelane further suggests that this mineral is suitable for dating paleoweathering processes by the K-Ar and the  $^{40}\text{Ar}/^{39}\text{Ar}$  methods.

UNRAVELLING THE GROWTH "STRATIGRAPHY" IN GRANULITE ZIRCONS FOR SHRIMP DATING OF THE LOWER CRUST: A CASE STUDY FROM THE IVREA ZONE (SOUTHERN ALPS)

VAVRA, Gerhard, GEBAUER, D., SCHMID, R., Department of Earth Sciences, ETH Zürich, CH-8092 Zürich, Switzerland.

The timing of metamorphic and magmatic events in the lower crust is largely derived from conventional U/Pb zircon data, which do not consider in detail the processes affecting the U/Pb system in zircon. The cathodoluminescence of granulite zircons reveals a variety of growth and alteration domains which can be U/Pb-dated by ionprobe and assigned to petrogenetic processes.

In a restitic metasedimentary granulite from the Ivrea zone, zircons were separated from adjacent metapelitic and quartzitic layers. In both layers, isometric overgrowths surround Precambrian detrital cores. The first period of growth, characterized by radial growth sectors, is only observed in the metapelitic layer, whereas the second and final period of growth, characterized by rounded shells, is present in both layers. The  $^{206}\text{Pb}/^{238}\text{U}$  ages of the first period scatter between 295 and 262 Ma with a mean value of  $277 \pm 7$  Ma (95 % c. l.). Several growth pulses indicate to a long lasting growth period. In contrast, the second growth period defines a rather short event at  $262 \pm 3$  Ma. The data imply that anatectic melting started in the metapelitic layer at  $295 \pm 8$  Ma. The Zr was probably provided by reacting biotite ( $\text{Bi}+\text{Sil}+\text{Qtz} > \text{Gt}+\text{Ksp}+\text{H}_2\text{O}$ ). Several anatectic pulses may have been triggered by gabbroic intrusions. In the quartzitic layer, the detrital cores were corroded by anatectic melt. Thus, the start of anatexis in this layer cannot be dated. The final growth episode at  $262 \pm 3$  Ma is likely to be related to a phase of rapid uplift and isothermal decompression. As a result, additional anatectic melt may have formed and crystallized within a short period. The typical rounded shape of shells grown during this period may be due to rotation of grains at tectonic shearing.

In a metagranitoid from the same complex, zircon overgrowths can be correlated with those in the metasedimentary layers. In addition, the large protolithic cores of this sample allow detailed U/Pb-dating of alteration processes. Unaltered crystal domains yield an age of  $345 \pm 5$  Ma for the intrusion. Recrystallization causing strong loss of U, Th and radiogenic Pb from some domains occurred at  $275 \pm 3$  Ma. The recrystallization is related to the overstepping of a critical temperature, but does not mark the temperature maximum. A second type of alteration is present as diffusion-controlled flow structures which digested recrystallized and non-recrystallized domains. The structures indicate volume diffusion which is most likely related to the thermal peak of granulite metamorphism. Since diffusion did not efficiently expel the inherited radiogenic Pb, an U/Pb age for the thermal peak cannot be determined. However, this age is closely bracketed by the prograde recrystallization event at  $275 \pm 3$  Ma and late zircon overgrowth from a crystallizing anatectic melt at  $271 \pm 3$  Ma.

The ionprobe dating of zircon resolves the granulite facies metamorphism into a pre-climax temperature increase of long duration, with anatectic melt forming in several steps since  $295 \pm 8$  Ma, and a final event of rapid anatectic melt formation and crystallization at  $262 \pm 3$  Ma, shortly following the temperature maximum. A separate thermal pulse is recorded by partial recrystallization at  $225 \pm 5$  Ma.

## BORON ISOTOPES IN GROUNDWATER: IDENTIFICATION OF SOURCES OF CONTAMINATION

VENGOSH, A., Hydrological Service, P.O. Box 6381, Jerusalem 91063, Israel, HEUMANN, K.G, JURASKE, S Institute of Inorganic Chemistry, University of Regensburg, Universitätsstrabe 31, Regensburg D-93053, Germany, and BARTH, S. CRPG-ENSG, 15 rue Norte Dame des Pauvres, BP 20, F-54501 Vandoeuvre-les Nancy Cedex, France.

One of the main goals of environmental protection is to prevent deterioration of water quality through early recognition of contamination sources. The relatively large mass difference between the two stable isotopes of boron resulted in a wide range of  $\delta^{11}\text{B}^*$  values in natural waters, ranging from -15‰ to +60‰. The different isotopic signatures have been used for tracing the sources of dissolved boron, and in particular to distinguish marine from non-marine sources. In addition to the natural load, the application of synthetic boron compounds, especially sodium perborate as a bleaching agent in detergents, leads to an enrichment of boron in waste waters, and consequently in natural aquatic systems. The anthropogenic annual discharge flux ( $10^{11}$  g B /yr in Western Europe alone) is significant and even comparable to the natural global boron influx to the oceans ( $3 \times 10^{11}$  g B /yr).

Boron isotope composition of anthropogenic boron has been examined in raw and treated sewage effluents as well as contaminated groundwater from the the Dan Region Project and Coastal Plain aquifer in Israel. It is shown that the  $\delta^{11}\text{B}$  values of sewage effluents (5.3‰ to 12.9‰) overlap with those of natural borate minerals (-0.9‰ to 10.2‰) but are significantly different from those of regional groundwater (~30‰) and sea water (39‰). Groundwater contaminated by artificial recharge of treated sewage yields a high B/Cl ratio with a distinctive anthropogenic isotopic signature (6.8‰ to 25‰) which is different from those of natural marine-derived saline groundwater from the Coastal Plain aquifer (35‰ to 60‰). This enables utilization of the boron isotope composition of groundwater as a tracer for sources of contamination of groundwater, particularly detergents compounds in aquatic systems.

\*  $\delta^{11}\text{B} = \frac{(^{11}\text{B}/^{10}\text{B})_{\text{sample}}}{(^{11}\text{B}/^{10}\text{B})_{\text{NBS 951-1}}} \times 1000$

## Ar-Ar CHRONOLOGY OF THE LADAKH COLLISION ZONE, NORTHWEST HIMALAYA

VENKATESAN, T. R., Physical Research Laboratory, Ahmedabad 380009, India, PANDE, K, Physical Research Laboratory Ahmedabad 380009, India, SHARMA, K.K and CHAWALA, H.S, Wadia Institute of Himalayan Geology, Dehradun 248001, India.

In the Ladakh sector a more or less complete record of magmatism, sedimentation and deformation is preserved to enable a study of crustal growth and collision tectonics between the Indian and Eurasian plates. The Indus Suture zone has long been recognised as a zone of Tertiary collision between the two plates. The presence of a second Suture - the Shyok-Nubra - (Northern Megasear in Kohistan sector) - has also been recognised. However, the sequence and timing of the formation of these two Sutures are still debated. Some believe that Shyok-Nubra Suture is older than the Indus Suture while others prefer a younger age for the former.

To resolve this controversy detailed Ar-Ar chronology of the various igneous constituents of the two Sutures has been undertaken to supplement field studies. Here we report the data for volcanics from the Shyok-Nubra zone. Of the six whole rock samples analysed only one yielded a plateau age of 58 Ma. Other samples exhibit age spectra indicating a slow cooling and a loss of about 90-95% argon. From these spectra we can infer a thermal event between 14-28 Ma. Interestingly such a range of ages for Tertiary Himalayan granites (Dietrich and Gansser, 1981) and biotite Rb-Sr isochrons of 28-29 Ma from Ladakh (Trivedi et al., 1982) have been reported.

Dietrich, V and Gansser, A., 1981, The Luecogranites of the Bhutan Himalaya : Schweiz. mineral. petrogr. Mitt. v61, p177-202.

Trivedi, J.R., Gopalan, K., Sharma, K.K., Gupta, K.R, and Choubbey, V.N, 1982, Rb-Sr age of Gaik granite, Ladakh batholith, Northwest Himalaya: Proc. Indian Acad. Sci.(Earth Planet Sci), v91, p65-73.

## LOW TEMPERATURE ( $\leq 300^{\circ}\text{C}$ ) HYDROGEN ISOTOPE EXCHANGE BETWEEN HYDROUS MINERALS AND MOLECULAR HYDROGEN

VENNEMANN, Torsten, W. and O'NEIL, J.R.,  
Department of Geological Sciences, University of  
Michigan, Ann Arbor, MI 48109, USA.

In order to establish a consistent set of mineral-water D/H fractionation factors, we have used  $\text{H}_2$  as an exchange medium for hydrous minerals. Mineral-water fractionation factors may then be calculated from known water- $\text{H}_2$  fractionations. The small size of  $\text{H}_2$  as opposed to  $\text{H}_2\text{O}$  allows for good penetration to the interiors of the crystal, enhancing D/H exchange with the OH-sites at temperatures below those of previous calibrations based on mineral-water exchange. Preliminary results obtained on the basis of a method where the gas provides an "infinite" reservoir of  $\text{H}_2$  and approach to equilibrium is estimated by a change in the  $\delta\text{D}$  values of biotite, muscovite and hornblende at temperatures  $\geq 300^{\circ}\text{C}$  (Vennemann and O'Neil, 1993), together with recent ion-microprobe analyses of individual crystals (mm's to cm's in size) exposed to gases enriched in HD for short periods of time (5-7 days), confirm penetration of and exchange with  $\text{H}_2$  well below the surface of the crystals.

For temperatures below  $300^{\circ}\text{C}$  a method is chosen where the mineral provides an "infinite" reservoir of hydrogen and the approach to equilibrium is estimated by a change in the  $\delta\text{D}$  values of two isotopically distinct gases which approach an equilibrium distribution of isotopes from compositions relatively enriched and depleted in deuterium. To remove interfering gases such as  $\text{CO}_2$ ,  $\text{N}_2$ ,  $\text{H}_2\text{O}$  which remain within the crystal even after prolonged evacuation at temperatures as high as  $300^{\circ}\text{C}$ , and to avoid problems of preferential adsorption of HD, the minerals are subjected to "He-flushing" prior to exchange with  $\text{H}_2$ , and the gases used for exchange are expanded onto and removed from the minerals at temperatures of exchange. The infinite-gas method employed at temperatures above  $300^{\circ}\text{C}$  results in about 90% exchange of D/H between epidote and hydrogen after 20 days at  $300^{\circ}\text{C}$ . 100% exchange is obtained in periods of less than 2 to 3 days for epidote grains of 60 to  $125\ \mu\text{m}$  in size with the infinite-mineral method. This method also provides epidote- $\text{H}_2$  fractionation factors that are within error of the infinite-gas method ( $1000\ln\alpha = 442$  and 435, respectively).

It is concluded that laboratory calibrations of the hydrogen isotope exchange between molecular  $\text{H}_2$  and hydrous minerals provides a suitable method for the indirect evaluation of the geologically important low temperature fractionation factors between hydrous minerals and water. Minerals under investigation at present include epidote, muscovite, kaolinite, serpentine and chlorite.

Vennemann T.W., and O'Neil, J.R., 1993, *EOS*, V.74, p. 330.

## STABLE ISOTOPE AND $^{40}\text{Ar}/^{39}\text{Ar}$ CONSTRAINTS ON PREALPINE RECONSTRUCTIONS AND P-T-t PATHS WITHIN THE CENTRAL SESIA-LANZO ZONE, WESTERN ALPS, NORTHERN ITALY

VENTURINI, G., COSCA, M.A., SHARP, Z.D., and  
HUNZIKER, J.C. Institut de Minéralogie, Université  
de Lausanne, BFSH-2 1015, Switzerland,

The Sesia-Lanzo zone is composed of a belt of high pressure (HP) (granulite to eclogite) and greenschist (GS) facies units in the Western Alps of Northern Italy (Venturini et al., 1994). A new geological map of the Sesia-Lanzo zone based on detailed mapping and compilations by the authors has resulted in a new geotectonic model of this area. Stable isotope and  $^{40}\text{Ar}/^{39}\text{Ar}$  analyses have been made on mineral separates from the Sesia-Lanzo zone to determine the relationship between the Prealpine basement, the Permo-Mesozoic cover sequences, and the effects of Alpine metamorphism.

Stable isotope thermometry applied to eclogite mineral separates ( $\delta^{18}\text{O}_{\text{Qz}} = 21.5\text{‰}$ ,  $\delta^{18}\text{O}_{\text{Gt}} = 17.9\text{‰}$ ,  $\delta^{18}\text{O}_{\text{Omph}} = 17.0\text{‰}$ ,  $\delta^{18}\text{O}_{\text{Ru}} = 16.9\text{‰}$ ) yield temperatures of  $570^{\circ}\text{C}$ , consistent with cation exchange thermometers.

Over 30 whole rock oxygen isotope values have been determined from orthogneiss and paragneiss. The  $\delta^{18}\text{O}$  values of orthogneiss and I-Type metagranites are similar ( $\delta^{18}\text{O} = 8.2 - 8.8\text{‰}$ ) and distinct from S-type metagranites ( $\delta^{18}\text{O} = 11.2\text{‰}$ ), while paragneiss give values  $>10\text{‰}$  ( $\delta^{18}\text{O}_{\text{quartzites}} = 11.9 - 12.4\text{‰}$ ,  $\delta^{18}\text{O}_{\text{leucocratic gneiss}} = 11.2$ ). The consistent and distinct isotopic signature between rock types is too small to unequivocally determine protolith lithologies in strongly sheared rocks.

Incrementally heated  $^{40}\text{Ar}/^{39}\text{Ar}$  age spectra have been collected from 29 phengite both the internal HP unit and the external GS unit. Cooling ages from the well-preserved HP unit are 60-85 Ma and 45-60 Ma for the GS unit. Our field and isotopic data, combined with published data (Hurford and Hunziker, 1991), support unique cooling histories prior to 35 Ma for the HP and GS units. The two units follow a common P-T-t path subsequent to 35 Ma.

Hurford, A.J. and Hunziker J.C., 1991, Constraints on the late thermotectonic evolution of the western Alps: evidence for episodic rapid uplift: *Tectonics*, 10-4, p. 758-769.

Venturini, G., Martinotti, G., Armando, G., Barbero, M., Hunziker, J.C., 1994, The Sesia-Lanzo Zone (Western Italian Alps): new field observations and lithostratigraphic subdivisions: *Schweiz. mineral. petrogr. Mitt.*, in press.

**Sr And Nd Isotopic Constraints On The Generation Of Large-Scale Compositional Zoning In Epizonal Magma Bodies**

P.L. Verplanck and G L Farmer (Dept. of Geological Sciences and CIRES, University of Colorado, Boulder, CO 80309-0216; 303-492-1276)  
M McCurry (Dept. of Geology, Idaho State University, Pocatello, ID 83209)

A detailed isotopic and chemical study of Oligocene-age Organ Needle pluton (ONP) in south-central New Mexico and its Precambrian granitic wall-rock is underway to test models for the origin of compositional zoning in large volume silicic magma bodies. The dominant volume of the ONP is syenitic in composition, but the pluton is capped by an alkali feldspar granite (AFG), with a narrow transition between the two lithologies (1 to 10 meters). The coarse-grained syenite has  $\text{SiO}_2=60\%-70\%$ ,  $\epsilon_{\text{Nd}}=-2.3$  to  $-2.8$ , and  $^{87}\text{Sr}/^{86}\text{Sr} \sim 0.7055-0.7065$  with systematic major and trace element variations that correlate with mineralogical variations. The chemical data, combined with the narrow range in isotopic composition, suggest that the bulk of the pluton evolved by closed-system fractional crystallization. The AFG ( $\text{SiO}_2=74\%-77\%$ ) has  $\epsilon_{\text{Nd}}=-5$  to  $-5.5$  and  $^{87}\text{Sr}/^{86}\text{Sr} \sim 0.710-0.715$ , values not only distinct from the underlying syenite, but also from the wall-rock, dominantly Precambrian granite ( $\epsilon_{\text{Nd}}(36\text{Ma})=-10$  to  $-14$  and  $^{87}\text{Sr}/^{86}\text{Sr}(36\text{Ma})=0.750-0.800$ ). The isotopic constraints preclude the possibility that the AFG formed by protracted closed-system fractionation of the underlying magma body or by roof-rock melting.

Although the interior of the pluton has a relatively uniform isotopic composition and systematic chemical variations, the margins of the pluton are more chemically and texturally diverse with isotopic compositions that overlap those of the AFG. At the easternmost (and structurally deepest) exposed portions of the ONP, the margin of the pluton is coarse-grained but inequigranular with  $\text{SiO}_2=57\%$  to  $63\%$ ,  $\epsilon_{\text{Nd}}=-4$  to  $-5.5$ ,  $^{87}\text{Sr}/^{86}\text{Sr} \sim 0.708-0.711$ , and displays a wide range of trace element compositions over a geographically small region. Within 400m of the contact the border lithology grades into the more homogeneous interior portion of the pluton. Samples of the marginal portions of the pluton along other structurally higher transects also have relatively low  $\epsilon_{\text{Nd}}(-4.5$  to  $-5.5)$  but higher  $^{87}\text{Sr}/^{86}\text{Sr}$  (up to 0.719) and higher  $\text{SiO}_2$  (63%-68%). Overall the side-wall material has isotopic compositions similar to the AFG, suggesting that a genetic link may exist between these lithologies. The most likely model involves assimilation of wall-rock at the base or sides of a magma body in conjunction with side-wall differentiation and melt migration upward, culminating in the ponding of silicic magma over the main magma body at the top of the chamber.

**EVOLUTION OF THE DEPLETED MANTLE: THE HAFNIUM PERSPECTIVE**

VERVOORT, JEFFREY D. and PATCHETT, P. JONATHAN, Department of Geosciences, University of Arizona, Tucson, AZ, 85721, USA.

The Nd isotopic data set for mantle-derived rocks is characterized by two major temporal trends. First, there is a near linear increase in initial epsilon values of mantle-derived rocks from approximately 2.7 Ga to the present. This trend has been widely accepted as reflecting a widespread depleted mantle reservoir formed by the extraction of crust from the mantle. The existence of such a reservoir is easy to reconcile with the abundance of preserved Archean and younger crust. Second, the initial epsilon values of mantle-derived rocks appear to be static at approximately +1 to +3 from 3.8 to 2.7 Ga. These high, positive values require the existence of highly depleted mantle reservoirs in the early Archean which would appear to necessitate widespread differentiation of the mantle within the first few hundred million years of Earth's formation (e.g., Bennett et al., 1993). However, the Nd isotopic data for altered or metamorphosed early Archean rocks are potentially problematic in a number of ways and the validity of these data need to be evaluated. Part of the problem derives from the fact that the Sm-Nd system does not need to be disturbed very much in order to modify the apparent initial Nd isotopic compositions of these rocks. Various authors have suggested that the highly positive epsilon values of many of the earliest Archean rocks are spurious and are a product of later disturbance of the Sm-Nd system.

Because of this concern for the validity of early Archean Nd isotopic data, it is important to test models for early mantle depletion with other isotopic systems. Because zircons are robust with respect to alteration, their Lu-Hf isotopic systems are not as susceptible to later perturbations as either Sm-Nd or Lu-Hf systems in whole-rock samples. Therefore, our approach has been to obtain zircons from carefully selected suites of mantle-derived rocks throughout Earth's history, examine them for concordance, then analyze the concordant populations for Hf composition. If a zircon population is concordant, or nearly so, this should be sufficient evidence that the Lu-Hf system in the zircons has not been disturbed and their initial isotopic compositions are accurate. In order to relate the Hf and Nd isotopic data we have also analyzed the whole-rock portions of these rocks for Sm-Nd.

Preliminary results from this study will be presented for Hf isotopic compositions of previously dated, concordant, or near-concordant, zircons from Amitsoq Gneisses in the Nuuk and Isukasia regions in Greenland as well as for zircons from the early Proterozoic juvenile terranes of the Flin Flon belt of Canada.

Bennett, V.C., Nutman, A.P., and McCulloch, M.T., 1993, Nd isotopic evidence for transient, highly depleted mantle reservoirs in the early history of the Earth: Earth Planet. Sci. Letters, v. 119, p. 299-317.

VIDAL, Ph., CNRS and Univ. Blaise Pascal, Clermont-Ferrand, DUPUY, C., BARCZUS, H.G., CNRS, Montpellier, CAROFF, M., MAURY, R., CNRS and Univ. Brest, France.

Isotope (Sr, Nd, Pb) and trace element data on basalts from Marquesas archipelago can be interpreted as a mixture of EM II, HIMU and DM components. They also support the existence of three geographic groups, each of these groups having its own specificity reflecting the variable proportions of these components as well as the processes involved in the basalts generation. In addition, there is a correlation between magmatic types and isotopic compositions. For example, in one group (Ua Pou, Tahuata, Fatu Hiva), the magmatic activity started 4.5 Ma ago with tholeiites having a HIMU source, and ended up 2 Ma ago with alkali basalts having an EM II source.

These regularities in the magmatic evolutions are accompanied by two strikingly contrasting situations :

- every time a HIMU source is involved in the genesis of shield-building basalts, the post shield-building lavas exhibit a EM signature. This is the case in two Marquesas groups.

- conversely, when an EM source is involved in the genesis of the shield-building basalts, the post shield-building lavas exhibit a DM-type. This is the case in the third Marquesas group and in Society.

These observations are discussed in the frame of the current models on plume-oceanic lithosphere interactions.

## $^{85}\text{Kr}$ - $^{133}\text{Xe}$ ZIRCON DATING

IM Villa<sup>1</sup>, J Eikenberg<sup>2</sup>, E Lehmann<sup>2</sup>

<sup>1</sup>Univ Bern, Isotopengeologie, Erlachstr. 9a, 3012 Bern, CH - <sup>2</sup>Paul Scherrer Inst, 5232 Villigen, CH

$\text{Xe}_f$ - $\text{Xe}_n$  dating by neutron irradiation was established 20 years ago [1]. Our modification includes Kr and involves the following procedure:

1. Separation of  $\approx 90\%$  pure zircons. While U/Pb always requires handpicking, U-Kr-Xe only needs to avoid secondary U minerals.

2. Computer simulation, via cross-sections, of all induced activities as a function of fluence & cool-off time; of main interest: short-lived U-proxies  $^{239}\text{Np}$ ,  $^{133}\text{Xe}$ ; health hazards  $^{132}\text{Te/I}$ ,  $^{140}\text{Ba/La}$ .

3. Thermal neutron irradiation of unknown samples together with age monitors.

4. Hot-lab  $\gamma$  spectroscopy of  $^{239}\text{Np}$  to calculate U (& further trace elements from other radioisotopes).

5. Cooling period minimising health hazards but limiting  $^{133}\text{Xe}$  decay.

6. Stepwise heating analysis of Kr and Xe.

We established the feasibility on magmatic zircons from the Limpopo belt, Zimbabwe, whose concordant U/Pb age is  $2591 \pm 1$  Ma. We observed:

a. U contents via Kr, Xe agree with prel. U from Np.

b. Degassing artefacts: the ratio of artificial  $^{85}\text{Kr}$  to  $^{133}\text{Xe}$  should follow Rayleigh fractionation as T grows, as both derive from the same target, U, but it jumps irregularly, correlating with release bursts.

c. Natural loss mechanisms are complex: in 14 unirradiated overprinted U-minerals,  $^{86}\text{Kr}/^{136}\text{Xe}$  is compatible with volume diffusion in only 1 case.

**Conclusions.** What are the main advantages?

I. Complementarity to U/Pb, possible screening of most suited samples for handpicking.

II. Usual advantage of stepwise heating: constraining disturbances and/or formation ages.

III. Checking deviations from ideality of neutron-induced  $^{85}\text{Kr}/^{133}\text{Xe}$  and natural fission  $^{86}\text{Kr}/^{136}\text{Xe}$ .

IV. Assessment of kinetic processes: using two noble gases is one step further than  $^{40}\text{Ar}/^{39}\text{Ar}$ , where non-diffusive transport requires a much more elaborate proof and is therefore still denied by some.

[1] Shukolyukov et al, Dokl. Akad. Nauk 219 (1974) 952

**GEOCHRONOLOGY OF SUPRACRUSTAL SEQUENCES IN THE SLAVE PROVINCE, NWT, CANADA: IMPLICATIONS FOR AGE OF BASEMENT.**

**VILLENEUVE, M.E.**, Geological Survey of Canada, Ottawa, Ont., K1A 0E8, RELF, C., Canada-NWT Mineral Initiatives Office, Yellowknife, NWT, Canada, HRABI, B., Queen's University, Dept. of Geological Sciences, Kingston, Ont., Canada and JACKSON, V., DIAND Geology, Yellowknife, NWT, Canada.

The Slave Province of northwest Canada comprises abundant 2.7-2.65 Ga volcanic-tubidite successions (Yellowknife Supergroup) and numerous 2.7-2.55 Ga plutons. Significantly older basement is restricted to the western Slave Province, as evidenced by the reconnaissance Sm-Nd study of Davis and Hegner (1992). U-Pb geochronology has been carried out on a transect along the eastern margin of this inferred basement terrane.

At two locations along this zone, ca. 3.1 Ga rhyolite volcanic rocks have been discovered. In the central Slave Province, a massive felsic volcanic unit, dated at  $3118 \pm 11/-8$  Ma, has been mapped at the base of the Winter Lake supracrustal belt. Similar rocks are found in the north-west Slave Province. In the Napaktulik Lake map area, two samples of felsic volcanic rocks, from a sequence of interlayered mafic volcanics, felsic volcanics and meta-sediment, give ages of  $3142 \pm 1$  Ma and  $3134 \pm 1$  Ma. These rocks provide the first evidence for widespread volcanic sequences significantly older than the Yellowknife Supergroup.

Cross-bedded quartz arenites overlie the Winter Lake rhyolite. A sample of this unit yields detrital zircons that fall within a tightly restricted age range of 3.13-3.16 Ga. About 60 km north of the Napaktulik rhyolites, upper amphibolite grade quartz arenites form competent layers in gneisses, which are in fault contact the 2.7 Ga Anialik River volcanic belt. Detrital zircons from this unit range in age from 3.15-3.30 Ga. A conglomerate in the gneisses has zircons with a broader age range; from 2.88 Ga to 3.4 Ga.

Late orogenic (<2.6 Ga) polymictic conglomerates are dominated by syn-Yellowknife Supergroup (ca. 2.7 Ga) detritus, but also contain 2.96 Ga and 2.72-2.76 zircons. The latter ages are coeval with a rhyolite porphyry dated at  $2729 \pm 8/-7$  Ma and a  $2720 \pm 8/-6$  Ma deformed granite from the central Slave Province.

This data indicates at least four periods of basement crust formation in the western Slave Province. The absence of 3.6-3.96 Ga ages suggests that the Acasta gneiss block is of limited extent. The preponderance of 3.1-3.3 Ga age detritus and rhyolites suggests that western basement terrane(s) are dominantly crust of this age, although a ca. 2.85-2.96 event is also documented. Finally, a magmatic episode began at 2.75 Ga and continued through onset of Yellowknife Supergroup deposition.

Davis, W.J. and Hegner, E., 1992, Neodymium isotopic evidence for the tectonic assembly of Late Archean crust in the Slave Province, northwest Canada. *Contrib. Mineral. Petrol.*, v. 111, p. 493-504.

**MAGMATIC PROVINCES IN THE ZIMBABWE CRATON: IMPLICATIONS FOR MANTLE HETEROGENEITIES AND SOURCE REGION DEPLETION DURING THE LATE ARCHAEOAN ERA.**

**M.L. Vinyu (1)**

Dept of Geology, University of Zimbabwe, P.O. Box MP 167, Mt Pleasant, Harare, Zimbabwe.

Basement-cover relationships and new age data provide evidence that the mafic/ultramafic volcanics that are an integral part of the circa 2.7 Ga event in the Zimbabwe craton were deposited onto pre-existing crust in zones of ensialic rifting.

Geochemical data bases on these late Archean volcanics from two greenstone belts (with similar structural styles and overlapping ages) located in the southern and northern parts of the Zimbabwe craton are compared with a view to model their source composition and evolutionary histories.

The lavas from the two greenstone belts are easily distinguished, and subdivided into two distinct geochemical provinces, on the basis of their major and trace element geochemistry. Higher Al<sub>2</sub>O<sub>3</sub>, TiO<sub>2</sub>, Fe<sub>2</sub>O<sub>3</sub>, P<sub>2</sub>O<sub>5</sub>, Zr, Y, Sm<sub>n</sub> and lower Mg# contents are found in the northern segment volcanics while the lavas from the south show a distinct enrichment in SiO<sub>2</sub>, total alkalis and MnO<sub>2</sub> in addition to their higher Mg#.

Major element geotectonic discrimination diagrams favour a geodynamic eruptive environment that was transitional between an oceanic and continental marginal setting for the formation of both suites of volcanics. Trace element plots favour derivation of the lavas in both provinces from plume related activity, with the lavas from the northern part being derived from a more depleted mantle domain (Fig.1). The implications of the existence of distinct magmatic provinces in one superevent are discussed with reference to the geotectonic environment and the various processes governing mantle melt formation in the late Archean era.

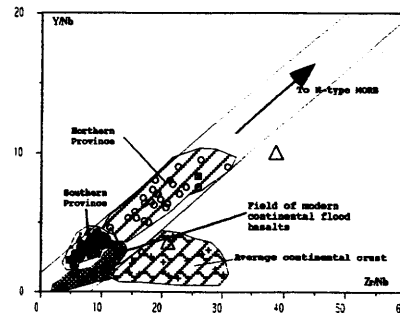


**Fig.1. Y/Nb vs Zr/Nb plot**

## CHLORINE ISOTOPIC COMPOSITION OF MARINE AEROSOLS

VOLPE, C., Scripps Inst. of Ocean., San Diego, La Jolla, CA 92093 and SPIVACK, A. J., Dept. of Earth Sciences, University of North Carolina at Wilmington, Wilmington, NC 98405

Chlorine is involved in many important atmospheric chemical reactions, in particular, the homogeneous and heterogeneous catalytic destruction of stratospheric ozone. Methyl chloride and anthropogenic halocarbons are the principle sources of reactive chlorine in the stratosphere, however, their relative contributions to the inorganic chlorine budget of the stratosphere are not well known. Chlorine may also play a role in tropospheric chemistry.

It has been suggested that chlorine liberated from synthetic halocarbons may be isotopically distinct from natural sources, yet, the isotopic composition of the various atmospheric chlorine species is still unknown. If the major chemical reservoirs and sources of atmospheric chlorine (anthropogenic halocarbons, methyl chloride, volcanic HCl, and tropospheric and stratospheric inorganic chlorine) prove to have unique chlorine isotopic compositions, it may then be possible to utilize the isotopic compositions of these species to constrain chlorine fluxes between the earth's surface, the troposphere and the stratosphere. In addition, if isotopic fractionation is associated with particular chemical reactions, it should also be possible to utilize isotopic variations to constrain atmospheric reaction mechanisms.

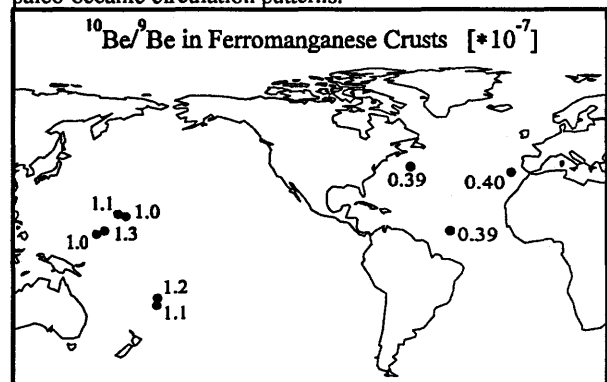
Here we report the first isotopic composition determinations of an atmospheric chlorine species, marine aerosols. These data are part of a larger project aimed at determining the isotopic systematics of atmospheric chlorine. Isotopic compositions were determined by the mass spectrometric analysis of dicesium chloride with an external reproducibility of 0.08 per mil. All of the aerosol samples analyzed so far are isotopically enriched relative to sea water, up to +2.5 per mil. The data fall on a trend that is consistent with the "fractional distillation" of chlorine with a best fit fractionation factor of 0.9969. Laboratory experiments confirm that HCl volatilized from marine sea salt particles is isotopically light relative to sea water with a fractionation factor of 0.9969.

$^{10}\text{Be}/^{9}\text{Be}$  RATIO AS A SEAWATER MASS TRACER. A WORLDWIDE STUDY OF FERROMANGANESE CRUSTS VON BLANCKENBURG, F., BELSHAW, N.S., O'NIONS, R.K. (Earth Sciences, University of Cambridge, UK), and HEIN, J.R., (U.S. Geological Survey, Menlo Park, CA 94025)

$^{10}\text{Be}/^{9}\text{Be}$  ratios for samples taken from the surface layers of oceanic ferromanganese crusts distributed worldwide have been determined using the new SIMS-based (ISOLAB) technique (Belshaw et al. 1994). Cosmogenic  $^{10}\text{Be}$  ( $T_{1/2}=1.5\text{Ma}$ ) is mainly produced by interaction of cosmic rays with the atmosphere, from where it is precipitated by rain into the oceans. Stable  $^{9}\text{Be}$  is incorporated into the deep oceans primarily by wind-blown dust. Accelerator Mass Spectrometry (AMS) results of modern sea water suggest higher  $^{10}\text{Be}/^{9}\text{Be}$  ratios for the Pacific ( $\sim 1 \times 10^{-7}$ ) than for the Atlantic ( $\sim 6 \times 10^{-8}$ , Kusakabe et al. 1990).

In an attempt to investigate whether this pattern has prevailed in the past, we have separated Beryllium from the outermost 1 millimetre of oceanic ferromanganese crusts using dissolution and a carrier-free all chromatographic technique. These crusts, sampled from seamounts, have formed authigenically; their isotope ratios should therefore have been those of sea water at time of formation. At typical growth rates of 3-10mm/Ma the measurements reflect the  $^{10}\text{Be}/^{9}\text{Be}$  ratio integrated over the ca. 100-300ka time interval represented by the samples. The results (see figure below) show a similar difference between the Pacific and Atlantic as does modern sea water. This includes both hydrogenous and hydrothermal crusts. Some scatter in the data could be due to radioactive decay of  $^{10}\text{Be}$  during growth of the layer.

The prevalence of the difference between Atlantic and Pacific  $^{10}\text{Be}/^{9}\text{Be}$  ratios over the last few ka indicates that the present oceanic circulation pattern has been maintained through this period. The isotopic composition of Be, of which the residence time in the deep oceans must be less than the mixing time of the oceans (1000a), is sufficiently sensitive to detect global patterns while averaging regional variations. It may therefore serve as a sea water mass tracer suitable to study paleo-oceanic circulation patterns.



Belshaw, N.S., O'Nions, R.K., and von Blanckenburg, F., 1993, A new SIMS technique for  $^{10}\text{Be}/^{9}\text{Be}$  ratio measurement: *J. Mass Spec. Ion Phys.*, submitted.

Kusakabe, M., Ku, T., Southon, J.R., and Measures, C.I., 1990, Beryllium isotopes in the ocean: *Geochem. J.*, v.24, p. 263-272.

**GEOCHEMICAL (REE) AND ISOTOPIC (Nd, O) INHOMOGENEITY OF THE LATE ARCHAIC UPPER MANTLE OF THE BALTIC SHIELD (EVIDENCE FROM THE PERIDOTITIC KOMATIITES)**

**VREVSKY, A.B., SVETOV, S.A.,** Inst. of Pre-cambrian Geology & Geochronology, Russian Acad. Scien., St. Petersburg, 199034, Russia)

The peridotitic komatiites (PK) from the Archaean greenstone belts of the Eastern Baltic Shield can be divided based on their REE abundances in four geochemically distinct types with: 1) flat chondrite-normalized REE patterns (0.4-1.5, 1.5-3.0, 3.0-5.0 x chondrite abundances); 2) LREE depleted and flat HREE (La/Sm)<sub>N</sub> = 0.6-0.7; 3) light LREE enrichment (La/Sm)<sub>N</sub> = 1.4-1.6; 4) strong negative Eu anomaly Eu/Eu\* = 0.04-0.1.

This geochemical types of PK can be interpreted by different petrological models: 1) single-stage 50-60% partial melting at P-35 kb of heterogenic in REE mantle source; 2) secondary 25-30% partial melting at P- 20-30 kb of residue after segregation of first stage 10-15% partial melting liquid; 3) contamination of komatiite liquid of felsic crustal material; 4) secondary melting of mantle residue after segregation of anorthositic liquid.

This geochemical and petrological data suggests the existence of lateral inhomogeneity of the upper mantle in AR<sub>2</sub>. The most depleted mantle in REE (0.4-1.5 x chondr.) is supposed for Kola peninsula and N.Karelia, chondrite type mantle (1.5-3.0) - for East and Central Karelia and slightly enriched (3.0-5.0) - for E.Finland.

Supposed lateral inhomogeneity of upper mantle can be related with isotopic age of volcanic rock of greenstone belts: Kola and N.Karelia - 2830-2790 m.y., East and Centr.Karelia - 2920-2995 m.y., E.Finland - 2790-2754 m.y.

Komatiites have a wide range of  $\delta^{18}\text{O}$  values (+4 to +7 ‰) and initial  $\epsilon_{\text{Nd}}$  values (+1.5 to +4.5). The  $\delta^{18}\text{O}$  for the less altered whole-rock samples are +4.0-5.5‰ and for carbonatized komatiites + 6.5-+7.5‰. Different initial Nd isotopic composition of the PK are in agreement with the geochemical types of PK and there pertogenesis.

**LARGE SCALE ASSIMILATION AND MIXING PROCESSES IN ETNA VOLCANO (ITALY): EVIDENCE FROM SR-ND-PB ISOTOPES AND TRACE-ELEMENTS**

**VROON, P.Z.,** Department of Geology, Royal Holloway University of London, Egham, Surrey TW20 0EX, England, DOWNES, H., Department of Geology, Birkbeck College, University of London, Malet Street, London WC1E 7HX, England, and MARRINER, G.F., Department of Geology, Royal Holloway University of London, Egham, Surrey TW20 0EX, England.

We analysed 105 samples from five stratigraphic sections at the southern wall of the Valle del Bove for major, trace elements and Sr-Nd-Pb isotopes for selected samples. All samples are quite evolved (SiO<sub>2</sub>=50.37-62.55, MgO=1.36-5.66) and sodium rich (K<sub>2</sub>O/Na<sub>2</sub>O=0.35-0.54). Isotopic ranges are fairly small for Sr and Nd isotopes: (87Sr/86Sr=0.70334-0.70360, 143Nd/144Nd= 0.51291-0.51285, but slightly larger for Pb isotopes (e.g. 206Pb/204Pb= 19.7-20.0). Different magmatic cycles exist in each stratigraphic section, which can be divided on the basis of the SiO<sub>2</sub>, Zr/Nb, La/Y and K/Nb. In general the SiO<sub>2</sub>, Zr/Nb and K/Nb decrease with stratigraphic height and scatter is found in the top part of the sampled sections.

Positive correlations exist between SiO<sub>2</sub> and 87Sr/86Sr, 206Pb/204Pb, Zr/Nb, Pb/Ce and K/Nb. These are readily explained by assimilation of up to 20% average Calabrian crust into the most mafic magma. The effects of assimilation on Nd and Sr isotopes are small due to the large concentrations of Sr (~1600 ppm) and Nd (~70 ppm), whereas Pb isotopes are easily affected (Pb=6 ppm).

However, not all within suite variations of isotopes and trace elements can be explained by assimilation and/or fractional crystallisation. The uncontaminated lavas display a mixing array between two end-members. The first end-member has low SiO<sub>2</sub> (~50%), high LILE, LREE, HFSE contents and higher 87Sr/86Sr. The second end-member has higher SiO<sub>2</sub> (~54%), lower LILE, LREE and HFSE contents and slightly lower 87Sr/86Sr. These end-members are probably a function of the complex Etna source region, which could contain subducted, lithospheric and asthenospheric components due to its peculiar tectonic position. We speculate that the low SiO<sub>2</sub> group is related to an asthenospheric source, whereas the high SiO<sub>2</sub> group is related to lithospheric mantle which has been previously modified by recent subduction processes.

# Obsidian from Japan as a 'putative' glass age standard "JAS-G1"

Kiyoshi WADATSUMI<sup>\*1</sup>, Naoko KITADA<sup>\*1</sup>,  
Gulio BIGAZZI<sup>\*2</sup>, Alan DEINO<sup>\*3</sup>, Marinella  
LAURENZI<sup>\*2</sup>, Bart KOWALLIS<sup>\*4</sup>, Keisuke  
NAGAO<sup>\*5</sup>, Harue MASUDA<sup>\*1</sup> (\*1; Osaka City  
Univ. \*2; Istituto di Geochronologia e  
Geochimica Isotopica \*3; Geochronology  
Center of the Institute of Human Origin  
<sup>\*4</sup>; Brigham Young Univ. \*5; Earth's Interior  
Inst.)

The JAS-G1 obsidian glass is produced  
as a chilled margin and no hydration  
from the analysis of index. On account  
of K-content and obtain spontaneous  
fission-tracks enough to counting easily.  
we introduce following:

- 1) Geological setting of JAS-G1 glass
- 2) result of chemical analysis
- 3) data of age determination of K-Ar,  
Ar-Ar and FT(using plateau method)  
age

At the FT dating, Moldavite glass is  
recommended as a glass age standard.  
However, Moldavite is not abundant in  
and then it difficult to keep supplying.  
This JAS-G1 sample be able to keep  
supplying well. Therefore we consider  
this sample as a 'putative' age standard  
sample of glass fission-track.

## PLIO-PLEISTOCENE VOLCANIC ROCKS AND INCISION OF THE NORTH FORK FEATHER RIVER, CALIFORNIA: TECTONIC IMPLICATIONS

WAKABAYASHI, John (1), PAGE, W. D. (2), RENNE,  
P. R. (3), Sharp, W. D. (3), and Becker, T. A. (3): (1)  
Consultant, 1329 Sheridan Ln., Hayward, CA 94544; (2)  
Geosciences Department, F22A, Pacific Gas and Electric  
Company, P.O. Box 770000, San Francisco, CA 94177;  
(3) Institute of Human Origins Geochronology Center,  
2453 Ridge Road, Berkeley CA 94709.

Three major sequences of Quaternary basalt have flowed  
from the Modoc Plateau into the Almanor basin. These flows  
have yielded Ar-Ar dates of approximately 1.1 Ma, 0.6 Ma  
and 0.4 Ma respectively. The oldest two of these flow  
sequences flowed down the North Fork Feather River canyon;  
the youngest flow ponded in the Almanor basin. Continued  
incision of the North Fork Feather River left the basalt flows  
preserved as terrace-like remnants with the highest terrace set  
being the oldest flow. Two older volcanic units were deposited  
in the ancestral canyon, but are now preserved only as limited  
remnants. These units are a 2.4 Ma basalt flow and a 2.8 Ma  
andesite related to the Yana volcanic center (Tuscan  
Formation). The various volcanic units record post-Pliocene  
deformation in the northeastern Sierra Nevada. Several faults  
have been identified and vertical separation rates range up to  
0.15 mm/yr on individual faults. The aggregate east-down  
vertical separation rate between Lake Almanor and the Sierra  
Nevada crest (Sierra Nevada Frontal fault system) is  
approximately 0.4 mm/yr. The aggregate west-down vertical  
separation northeast of Lake Almanor (east side of the Tahoe-  
Medicine Lake trough) is approximately 0.2 mm/yr.

Relative elevations of volcanic remnants above the  
bottom of the North Fork Feather River canyon place  
constraints on the long term incision rate of the North Fork  
Feather River canyon. The incision rate of the North Fork  
Feather River ranges from 0.2 to 0.4 mm/yr depending on the  
fault block and the time interval. Incision rates appear to have  
accelerated since 2.8 Ma. The apparent acceleration of  
incision rates may reflect uplift of the Sierra Nevada that  
exceeds erosion rates resulting in the geomorphic expression  
of this uplift as a mountain range. The volcanic flows are inset  
below remnants of a Tertiary erosion surface. Extrapolation of  
incision rates for different fault blocks suggest that canyon  
incision, and by inference, Sierra Nevada uplift in this region,  
began 3.5 to 4.8 million years ago (preferred value of 4.6 to  
4.8 Ma). The insight into late Quaternary faulting and the  
timing of Sierra Nevada uplift from this investigation has  
proved extremely valuable in assessing the seismic hazards for  
hydroelectric facilities in the region.

## CHRONOSTRATIGRAPHY OF THE TRANSVAAL AND GRIQUALAND WEST BASINS, SOUTH AFRICA

Walraven, F., Isotope Laboratory, Geological Survey, Private Bag X112, Pretoria 0001, South Africa.

The Transvaal Supergroup is a major Precambrian succession or chemical and clastic sediments with intercalated basic volcanics occupying two large intracratonic basins on the Kaapvaal Craton of Southern Africa, viz. the Transvaal and Griqualand West basins. In the Transvaal basin a prominent group of intermediate to acid volcanics forms the upper portion of the supergroup. Limited age data available for the Transvaal Supergroup in the past confined its chronological time span between the age of the Ventersdorp Supergroup (close to 2.71 Ga) which forms part of the basin floor and that of the Bushveld Complex (ca. 2.06 Ga) which intrudes the uppermost strata of the supergroup.

In recent years high-resolution geochronological investigations of the Transvaal Supergroup have been stimulated by chronostratigraphic studies and comparisons with other late Archean to Proterozoic successions in various parts of the world (in particular the Minas Supergroup, Quadrilatero Ferrifero and the Carajas basin of South America and the Hamersley Supergroup of Australia).

The high-resolution age data obtained so far show that basin-wide clastic sedimentation in the Transvaal Supergroup commenced at ca. 2.64 Ga (the Black Reef and Vryburg Formations). Prior to this a number of protobasins had been formed in both the eastern and western parts of the Transvaal basin had been formed. This brings the time gap separating the Ventersdorp and Transvaal Supergroups down to less than 60 Ma.

Chemical sedimentation in both the Transvaal and Griqualand West basins followed and continued up to approximately 2.43 Ga ago, after which time clastic sedimentation (mainly shale and sandstone) took over. Several episodes of non-deposition, locally coupled with erosion, occurred throughout the filling of the basins, a prominent unconformity being that separating the chemical and clastic sediments. Ages in the order of 2.24 Ga have been found for basic lava within the clastic sediments while basic volcanics at the top of the succession are less than 2.1 Ga in age. Direct ages are lacking for the intermediate to acid volcanics forming the upper part of the succession in the Transvaal basin. However, age data on related units together with geological considerations suggest that these volcanics formed part of the Bushveld Complex magmatic event. Thus their age is considered to be close to 2.06 Ga.

The Transvaal Supergroup therefore appears to have had an extremely long life span of almost 600 Ma. The new age data also show better agreement with the ages reported from the Carajas basin and Minas and Hamersley Supergroups, thereby providing additional evidence for the coeval nature of these major Precambrian successions in Southern Africa, South America and Australia.

## TEMPORAL FRAMEWORK FOR THE EVOLUTION OF *AUSTRALOPITHECUS AFARENSIS*

WALTER, Robert C., Institute of Human Origins, 2453 Ridge Rd., Berkeley, CA 94709, WOLDEGABRIEL, Giday, Los Alamos National Laboratory, Box 1633, EES-1/D462, Los Alamos, NM 87545, HART, William K., Department of Geology, Miami University, Oxford, OH 45056, and ARONSON, James L., Department of Geology, Case Western Reserve University, Cleveland, OH 44106.

From 1973 to 1981 the west-central Afar region of Ethiopia yielded important Pliocene hominid fossils from the Hadar and Middle Awash deposits. These sediments produced an array of hominid specimens that represent the presently known time range of *Australopithecus afarensis*, the oldest hominid species. Renewed investigations at these sites beginning in 1990 has produced much additional hominid material that extends our knowledge of the range of *afarensis*.

The Hadar Formation and the Middle Awash deposits are part of the Miocene to Pleistocene Awash Group. This basin developed in the Afar Rift, adjacent to the Ethiopian escarpment, and from time to time included paleolakes as well as a thoroughgoing meandering river system fed by braided streams. Numerous widespread rhyolitic tephra from volcanic sources within the Afar, the Ethiopian Highland, and Main Ethiopian Rift occur in the sedimentary sections. These tephra permit correlation and help to establish temporal relationships within and between the fossiliferous sedimentary basins.

Single-crystal  $^{40}\text{Ar}/^{39}\text{Ar}$  dates on these tephra enable us to calibrate faunal evolution with great precision, and to overcome problems of contamination and paucity of datable components that plagued earlier dating attempts using bulk methods. Roughly fifteen new  $^{40}\text{Ar}/^{39}\text{Ar}$  dates on tephra from the Hadar and Middle Awash establish a refined chronology for biostratigraphic zones, including that of *afarensis*. The presence of the Sidi Hakoma Tuff ( $3.4 \pm 0.03$  Ma; equivalent to the Tulu Bor Tuff of the Turkana Basin) links the stratigraphies of the Hadar and Middle Awash.

The oldest specimen of *A. afarensis* derives from the Middle Awash deposits between the Cindery Tuff ( $3.86 \pm 0.20$  Ma) and Vitric Tuff 1 ( $3.89 \pm 0.02$  Ma; equivalent to the Moite Tuff of the Turkana Basin). The youngest *afarensis* derives from the Hadar Formation between Bouroukie Tuff-2 ( $2.95 \pm 0.05$  Ma) and Bouroukie Tuff-1 ( $3.10 \pm 0.1$  Ma). Therefore, the currently known time range of *A. afarensis* is from about 3.9 Ma to 3.0 Ma, or roughly 900,000 years. Combined, however, these deposits date to greater than 4.2 Ma and to less than 2.3 Ma, which offers the potential for future discovery of first and last appearances of *afarensis*, and pre and post-*afarensis* specimens.

A TECHNIQUE FOR STEPWISE POTASSIUM-ARGON ANALYSIS OF ROCK SAMPLES BY LEACHING WITH HOT HYDROCHLORIC ACID

WAMPLER, J. M., School of Earth and Atmospheric Sciences, Georgia Institute of Technology, Atlanta, Georgia, 30332-0340, U. S. A.

A simple reflux reactor in which a rock sample may be continuously leached by a hot hydrochloric acid solution has been constructed with provision for stepwise analysis of the argon and potassium extracted. The reactor operates with an internal atmosphere of carbon dioxide, whose pressure determines the extraction temperature by controlling the boiling of the acid solution. At the end of each extraction step, the accumulated argon may be removed for isotopic analysis, while the water, HCl, and CO<sub>2</sub> are retained by cold trapping for use in the next extraction step. The potassium and other solids left by evaporation of the acid solution may be removed for analysis by sealing off the bottom end of a glass tube where the non-volatile products of the extraction had accumulated. The pressure of the internal gas must be a little less than one atmosphere when the glass tube is sealed off with a torch.

If the internal pressure is near one atmosphere, the reactor operates near 100°C, a temperature high enough that hornblende will dissolve at a rate sufficient for a practical schedule of steps. Biotite dissolves incongruently, and so it remains to be seen whether stepwise acid extraction will be useful for potassium-argon studies of biotite. The acid-extraction technique should be particularly useful for studies of illitic clay samples, which often contain different populations of clay particles that cannot practically be separated from one another. Owing to the smallness of the clay particles, a sufficient rate of dissolution can be obtained at 100°C.

The stepwise acid-extraction technique offers an alternative to stepwise <sup>40</sup>Ar/<sup>39</sup>Ar analysis, which should be particularly useful in cases where loss of <sup>39</sup>Ar by recoil causes problems (for example, in the study of clay samples). In other cases, age spectra obtained by acid extraction should provide information that complements <sup>40</sup>Ar/<sup>39</sup>Ar age spectra, since the pattern of susceptibility of common minerals to acid dissolution is quite different from the pattern of thermally induced argon release from these minerals. For example, a small amount of *excess argon* in a basaltic rock may be more clearly evident in an age spectrum obtained by acid extraction than in one obtained by stepwise heating, since low-potassium minerals such as olivine and pyroxene should dissolve much more rapidly than feldspar. A drawback of the technique is that it will often not be practical to obtain a complete age spectrum by acid extraction, because of the very slow dissolution of minerals such as feldspar.

OXYGEN AND HYDROGEN ISOTOPIC COMPOSITIONS IN GROUNDWATERS OF THE PENGHU ISLANDS, TAIWAN

WANG, Chung-Ho and PENG, Tsung-Ren  
Institute of Earth Sciences, Academia Sinica, P.O.  
Box 1-53, Nankang, Taipei, Taiwan 11529, ROC

Deep (>90 m) and shallow (<90 m) groundwaters together with several surface waters in the Penghu Islands were analyzed for their oxygen and hydrogen isotopic compositions. The following isotopic ranges were found for the groundwaters: δ<sup>18</sup>O, -4.5‰ to -7.6‰; δD, -31‰ to -49‰. All δ<sup>18</sup>O and δD data plot along the global meteoric-water line, and only those of surface waters shift towards more positive values during the period of high evaporation and low precipitation. Isotopic values of groundwaters from the Penghu Islands are generally heavier both in D and <sup>18</sup>O relative to those of groundwaters from the western Taiwan.

The preliminary results show that: (1) deep groundwaters of the Penghu Islands show no evidence of sea water contamination; (2) evaporation has a strong influence on the isotopic values of surface waters, but less influence on the shallow groundwaters and no effect on the deep groundwaters; (3) stable isotopic data of groundwaters suggest that the sources of deep and shallow groundwaters may have different origins. <sup>14</sup>C results confirm that deep groundwaters were formed during the last glacial period.

MODELING OF ISOTOPIC FRACTIONATION DURING THE PHASE TRANSITION OF A DIFFUSION-CONTROLLED RESERVOIR

WANG, Jianhua<sup>1</sup>, DAVIS, Andrew M.<sup>2</sup>, and CLAYTON, Robert N.<sup>1,2,3</sup>, <sup>1</sup>Department of the Geophysical Sciences, <sup>2</sup>Enrico Fermi Institute, <sup>3</sup>Department of Chemistry, University of Chicago, Chicago, IL 60637, USA

The Rayleigh fractionation law,  $R = R_0 f^{1/\alpha-1}$ , is commonly used to describe the isotopic composition of a reservoir phase transferring into another phase such as occurs during evaporation and fractional crystallization. Application of this law requires that the reservoir be completely mixed throughout the fractionation event and that the transformed phase be isolated from the reservoir. Diffusion limits mixing of the reservoir in many cases where isotopic fractionation occurs. We developed a theoretical model to study isotopic fractionation during the phase transition of a diffusion-controlled reservoir. This model quantitatively describes isotopic fractionation during evaporation of a solid reservoir and instrumental fractionation in thermal ionization mass spectrometry.

The present model uses a one-dimensional approach that assumes that the isotopic fractionation occurs only at the planar phase-transition surface of a reservoir. The coordinate of length is always perpendicular to the surface. The first step in solving this problem is to consider a semi-infinite reservoir. For this case, the origin ( $x = 0$ ) is fixed at the phase-transition surface and the reservoir occupies the positive axis ( $x \geq 0$ ). The isotopes of an element are fractionated at the surface with a factor of  $\alpha$  and diffusively transported in the reservoir with a diffusion coefficient of  $D$ . The rate of the phase transition is  $v$ . The following set of equations describes this scenario with non-dimensionalized  $X$  ( $X = \frac{vx}{D}$ ) and  $\tau$  ( $\tau = \frac{v^2 t}{D}$ ) for isotopic ratio  $R(X, \tau)$ :

$\frac{\partial R}{\partial \tau} = \frac{\partial^2 R}{\partial X^2} + \frac{\partial R}{\partial X}$ ,  $0 < X < \infty$ , with  $R = R_0$  when  $\tau=0$ ,  $\frac{\partial R}{\partial X} + \frac{\alpha-1}{\alpha} R = 0$  at  $X = 0$  and  $R = R_0$  at  $x = \infty$  for  $\tau > 0$ . Using the Laplace transform, the analytical solution can be obtained as follows:

$$\frac{R(X, \tau)}{R_0} = 1 - \frac{1}{2} \operatorname{erfc} \frac{X+\tau}{2\sqrt{\tau}} + \frac{(\alpha-1)}{2} e^{-X} \operatorname{erfc} \frac{X-\tau}{2\sqrt{\tau}} + \left(1 - \frac{\alpha}{2}\right) e^{-\frac{(1-\alpha)(\alpha X + \tau)}{\alpha^2}} \operatorname{erfc} \frac{\alpha X + (2-\alpha)\tau}{2\alpha\sqrt{\tau}}$$

The next step is to consider a reservoir with a finite thickness,  $w$ . By fixing the opposite end to the transition surface of the reservoir at  $X = 0$  and nondimensionalizing  $w$  ( $W = \frac{vw}{D}$ ), we

have the following set of equations:  $\frac{\partial R}{\partial \tau} = \frac{\partial^2 R}{\partial X^2}$ ,  $0 < X < W - \tau$ ,

with  $R = R_0$  when  $\tau = 0$ ,  $\frac{\partial R}{\partial X} = 0$  at  $X = 0$  and  $\frac{\partial R}{\partial X} - \frac{\alpha-1}{\alpha} R = 0$  at  $X = W - \tau$ . This set of equations was solved numerically by substituting  $Y$  for  $X$  ( $Y = \frac{X}{W-\tau}$ ) and using Crank-Nicolson's

implicit method. This model was used to accurately interpret instrumental isotopic fractionation in thermal ionization mass spectrometry and isotopic fractionation in residues of forsterite evaporated from the solid state.

A STABLE ISOTOPE STUDY ON DIET AND PALEOENVIRONMENT OF OLIGOCENE MAMMALS FROM BADLANDS NATIONAL PARK, S. DAKOTA

WANG, Y., Department of ESPM, University of California, Berkeley, CA 94720, CERLING, T. E. and DECOURTEN, F., Department of Geology & Geophysics, University of Utah, Salt Lake City, Utah, 84112

Stable isotopes of fossil mammal tissues from Badlands National Park, South Dakota demonstrate that diagenesis of biogenic carbonates in the tooth enamel hydroxyapatite over time is unexpectedly limited and fossil tooth enamel of Oligocene mammals preserved their paleodietary signatures. However, the stable isotopic compositions of bone carbonates have been altered completely. Bone apatite has similar isotopic values as tooth dentine, while bone carbonate displays similar isotopic ratios as carbonate in the matrix, suggesting that bone apatite is more resistant to diagenetic modification than bone carbonate. The  $\delta^{13}\text{C}$  values of tooth enamel of titanotheres of Early-Oligocene age indicate that they had a  $\text{C}_3$ -based diet. Hyracodon and oreodont specimens from early Middle-Oligocene display  $\delta^{13}\text{C}$  signatures of  $\text{C}_3$  diet which are consistent with their modern relatives. The  $\delta^{13}\text{C}$  values of tooth enamel of Meshippus specimens also indicate that these early horses are  $\text{C}_3$  eaters, implying that a graminivorous dietary specialization had not been developed during the Early and early Middle Oligocene time. The  $\delta^{13}\text{C}$  values of Perchoerus from Late Oligocene suggest a pure dietary intake of  $\text{C}_3$  plants, which might indicate that there were no  $\text{C}_4$  plants at that time in the area since peccaries are omnivorous. Our results suggest that the Oligocene herbivores studied here were browsers and lived in an environment probably composed mostly of trees and shrubs, which is in accordance with dental morphology.

ABIOTIC NATURAL GAS POOL IN PRODUCTION GASES FROM SONGLIAO BASIN, P. R. CHINA

WANG, X., Chen, J., Li, C., Yang, H., Wen, Q., Shao, B., State Key Lab. of Gas Geochemistry, LIGCAS, Lanzhou 730000, P. R. China, and Guo, Z., Daqing Institute of Petroleum Exploration & Development, Daqing 163712, P. R. China

Songliao Basin is famous for its petroleum and natural gas. This basin is an intracratonic rift basin, in which deep faults of basement, crust and super-crust are well developed and volcanic activity is very frequent from Cretaceous to Quaternary period. The  $\delta^{13}\text{C}$  value of methane in out of 13 drilled wells ranges from  $-16.7 \sim -24.2\%$ , which shows isotopic composition characteristics of abiogenic methane.

Owing to the isotopic fractionation effect during the degradation of kerogen of source rocks, the  $\delta^{13}\text{C}$  value of methane homologues ( $\text{CH}_4$ ,  $\text{C}_2\text{H}_6$ ,  $\text{C}_3\text{H}_8$ ,  $\text{C}_4\text{H}_{10}$ , etc.) from biogenic natural gas, becomes heavier with the increase of carbon number, i. e.,  $\delta^{13}\text{C}_1 < \delta^{13}\text{C}_2 < \delta^{13}\text{C}_3 < \delta^{13}\text{C}_4$  (i. e.  $-56.0\% < -37.0\% < -33.0\% < -31.0\%$ ). As for the abiogenic natural gas, the  $\delta^{13}\text{C}$  of methane homologues formed by inorganic synthetic reaction of primary methane (FTT) which shows a different feature from biogenic natural gas. Its  $\delta^{13}\text{C}$  values put in opposite order compared with the biogenic natural gas, i. e.,  $\delta^{13}\text{C}_1 > \delta^{13}\text{C}_2 > \delta^{13}\text{C}_3 > \delta^{13}\text{C}_4$ . The  $\delta^{13}\text{C}$  values of methane homologues obtained from some wells in east Songliao Basin show the aforementioned feature (i. e.  $-18.7\% > -22.4\% > -24.1\% > -28.2\%$ ).

PRELIMINARY RESULTS OF FELDSPAR  $^{40}\text{Ar}/^{39}\text{Ar}$  THERMOCHRONOMETRY FROM THE KTB DEEP CRUSTAL BOREHOLE, GERMANY

WARNOCK, A.C. and ZEITLER, P.K., Dept. of Earth and Environmental Sciences, Lehigh University, Bethlehem, Pennsylvania, 18015-3188, USA.

The KTB deep crustal borehole, located in the Oberpfalz region of Germany, will soon reach its final depth of 10 km. This great depth and the relatively steep ( $\approx 28^\circ\text{C}/\text{km}$ ) geothermal gradient measured in the hole provides the basis for our study of diffusive argon loss in feldspar during slow cooling. The temperature at 10 km is expected to be approximately  $300^\circ\text{C}$ , well into the closure interval of feldspar ( $\approx 150^\circ$  to  $350^\circ\text{C}$ ). Laboratory studies have successfully established the existence of discrete diffusion domains within single crystals of feldspar. These diffusion domains appear to be capable of recording individual segments of thermal histories. The KTB borehole offers a unique opportunity to explore the concept of diffusion domains outside of the laboratory.

Samples from the upper portion of the borehole ( $<150^\circ\text{C}$ ) record the post-orogenic thermal history of different levels in the Variscan crust. The vertical section sampled in the borehole, therefore, provides a third dimension to the geology seen at the surface. With such a cross-section, we will learn about the roles of thermal relaxation and denudation during the decay of a major metamorphic event, as well as improve our understanding of the regional tectonics.

Of the 20 core samples collected so far, the results of six pilot samples (five K-feldspar and one plagioclase) spanning depths of 0 m to 6670 m ( $\approx 200^\circ\text{C}$ ) will be presented.

## APPARENT DIFFUSIVE LOSS $^{40}\text{Ar}/^{39}\text{Ar}$ AGE PROFILES IN AMPHIBOLES.

WARTH, Jo-Anne, Department of Earth and Space Sciences, Geology Building 3806, University of California, Los Angeles, CA 90024-1567, USA.

Phone: (310) 825-5505, email: jo@argon.ess.ucla.edu

Turner et al (1966)<sup>1</sup> and Turner (1968)<sup>2</sup> presented theoretical incremental loss curves by which  $^{40}\text{Ar}/^{39}\text{Ar}$  age spectra of meteorite samples could be interpreted as revealing natural diffusion profiles, produced as a result of diffusive loss of argon from the sample. Harrison and McDougall (1980)<sup>3</sup> used Turner's theoretical curves to interpret age spectra of metamorphic hornblende samples which had been partially degassed as a result of the thermal effects of a later granite intrusion. The age spectra of three hornblende samples were interpreted as revealing argon loss by volume diffusion from uniform spheres. However, studies by Gaber et al (1988)<sup>4</sup>, Wartho et al (1991)<sup>5</sup>, and Lee et al (1991)<sup>6</sup> have shown that *in vacuo* argon release from amphiboles is controlled by phase changes and not by volume diffusion. These processes suggest that both naturally and imposed gradients of argon and inferences of kinetic parameters will be obscured.

More recently, experiments by Rex et al (1993)<sup>7</sup> showed how biotite contamination within amphibole samples could result in apparent diffusive loss  $^{40}\text{Ar}/^{39}\text{Ar}$  age gradients. However, some age spectra have been reported for amphiboles that appear to be characterised by  $^{40}\text{Ar}$  gradients that cannot be easily explained by contamination problems (e.g. Harrison and McDougall, 1980<sup>3</sup>; Berry and McDougall, 1986<sup>8</sup>, and Conrad and McKee, 1992<sup>9</sup>). In addition, Kelley and Turner (1991)<sup>10</sup> have found evidence of  $^{40}\text{Ar}$  loss profiles in  $^{40}\text{Ar}/^{39}\text{Ar}$  laser spot analysed amphibole grains.

Analysis of two amphibole samples yielding argon loss profiles (including one hornblende sample from the original Harrison and McDougall (1980<sup>3</sup>) study) has revealed the presence of complex compositional zoning within the amphiboles. Comparison of the  $^{37}\text{Ar}_{\text{Ca}}/^{39}\text{Ar}_{\text{K}}$  ratios (obtained from  $^{40}\text{Ar}/^{39}\text{Ar}$  step-heating and laser analyses) and Ca/K ratios from electron microprobe data in these zoned amphiboles indicates that the apparent diffusive loss  $^{40}\text{Ar}/^{39}\text{Ar}$  age profiles in these two samples are due to partial chemical re-equilibration within the amphibole grains (during a later thermal event) and, therefore, is not solely caused by thermally assisted volume diffusive loss of argon from the sample. The reset ages obtained from the various amphibole compositions in these samples do not correlate to any known thermal events and appear to be due to partial argon loss during major element readjustment of the amphibole grains.

- 1 - Earth Planet. Sci. Lett., 1, 155-7;
- 2 - Origin and Distribution of the Elements (L.H. Ahren, Ed.) pp 387-98;
- 3 - Geochim. Cosmochim. Acta, 44, 2005-20;
- 4 - Geochim. Cosmochim. Acta, 52, 2457-65;
- 5 - Am. Mineral., 76, 1446-8;
- 6 - Geology, 19, 872-6;
- 7 - Isot. Geosci., 103, 271-81;
- 8 - Isot. Geosci., 59, 43-58;
- 9 - Econ. Geol., 87, 185-8;
- 10 - Earth Planet. Sci. Lett., 107, 634-48.

## GEOCHRONOLOGY OF THE AREQUIPA MASSIF, PERU: CORRELATION WITH LAURENTIA

WASTENEYS, Hardolph A., Jack Satterly Geochronology Laboratory, Royal Ontario Museum, 100 Queen's Park, Toronto, M5S 2C6,

Previous Rb-Sr and U-Pb geochronology of Proterozoic granulite-facies gneisses in the enigmatic Arequipa Massif concluded that high-grade metamorphism had occurred ca. 1900 Ma and shortly after formation of the protoliths. However, new U-Pb zircon geochronology (Wasteneys et al., 1993) has demonstrated, instead, the presence of two Grenvillian granulite-facies domains implying that the Rb-Sr isochrons were not reset and that the complex Pb-loss patterns in unabraded, multi-grain zircon fractions obscured the metamorphic zircon component. More importantly, the ages for metamorphism (1198 Ma near Quilca and 970 Ma near Mollendo), orthogneiss protoliths (ca. 1950 Ma in both domains) and detrital sources (minimum ca. 1600 Ma) from the two domains suggests correlations with the Grenville Province of Canada which support the proposed Neoproterozoic continental reconstruction of Dalziel (1994) in which the conjugate margin of Laurentia was the pre-Andean margin of South America. The data also lend support to equivocally Grenvillian Rb-Sr and U-Pb ages for other Andean basement complexes in northern Chile and Bolivia. The ca. 1950 Ma ages for the Arequipa orthogneiss protolithic zircons are found in zircons of the NW zone of the Makkovik Province, Labrador while younger, ca. 1650 Ma detrital zircons may have been derived from the voluminous Trans-Labrador Batholith which cuts both Grenville and Makkovik Provinces. The 970 Ma age for granulitic metamorphism in the Mollendo domain correlates with metamorphic domains of the eastern Grenville Province which have partially overprinted the trans-Labrador Batholith. The ca. 1200 Ma Quilca domain metamorphism correlates with the main phase of high-grade metamorphism in the allochthonous Central Metasedimentary Belt of the Grenville Province in Ontario constrained by Lumbers et al. (1991) to the 1240-1160 Ma period. In the Frontenac domain of the CMB granulite-facies metamorphism commenced prior to 1180 Ma ca. based on new U-Pb ages for zircons in anatectic melts and terminated, probably by isothermal decompression, at 1166 Ma based on zircon coronas on baddeleyite from gabbros, 1160 Ma monazite and 1155 Ma sphene ages. Possibly subduction-related magmatism in the Elsevir and Adirondack terranes, which ended by 1240 Ma, heralded an imminent collision between elements of South America and Laurentia. Similar age magmatic rocks in northern Chile and Bolivia basement complexes may record the same event.

Dalziel I.W.D., 1994, Precambrian Scotland as a Laurentia-Gondwana link: The origin and significance of cratonic promontories. Geology (submitted).

Lumbers, S.B., Heaman, L.M., Vertolli, V.M., and Wu, T.W. 1991, Nature and timing of Middle Proterozoic magmatism in the Central Metasedimentary Belt, Grenville Province, Ontario. *in* GAC Special Paper 38, p.243-276.

Wasteneys, H.A., Clark, A.H., Langridge, R.J. and Farrar, E., 1993 Granulite-facies metamorphism in the Arequipa Massif, southern Peru: Grenvillian, not Early Proterozoic in age. GAC/MAC Program with Abstracts p. 108

## EVOLUTION OF THE KERGUELEN PLUME WITH TIME AND ITS ROLE IN THE GENERATION OF INDIAN OCEAN CRUST.

WEIS, D., Pétrol. Géodyn. Chimique, CP160-02, Université Libre de Bruxelles, Av. F.D. Roosevelt, 50, 1050 Brussels, Belgium and FREY, F.A., EAPS, MIT, Cambridge, MA 02139, USA.

Indian Ocean (IO) basalts are important because they are isotopically different from Atlantic and Pacific basalts. In addition the Kerguelen Plume (KP) as a main source for these differences is a definite possibility.

In order to constrain both the time evolution of the KP and its extension in space, we have undertaken a study of different IO basalts: Indian ocean crust (152 to 39 Ma), Ninetyeast Ridge basalts (90ER - 83 to 38 Ma) and different volcanic series from the Kerguelen Archipelago (KA), i.e. a 38 Ma stratigraphic sequence of transitional basalts from the Western KA, 26 Ma mildly-alkaline lavas from the eastern KA and the youngest expression of the KP on the KA, the <2 Ma highly-alkaline Ross volcano.

All the IO crust and 90ER basalts are tholeiitic and some of the basalts forming the IO crust have incompatible element contents typical of depleted MORB. However of the tholeiitic basalts of varying age from the 90ER and many from the IO crust are mildly enriched in incompatible elements (e.g., La/Yb= 2 to 5). In contrast transitional and alkalic lavas from the KA are highly enriched in LILE (e.g., La/Yb up to 15). The lava compositions erupted in the KA differ from those erupted along the 90ER and spreading ridge axes.

Isotopically, IOC basalts present Dupal signatures ( $^{207}\text{Pb}/^{204}\text{Pb} > 15.55$ ,  $^{87}\text{Sr}/^{86}\text{Sr} > 0.704$ ) starting around 115 Ma, which corresponds to the first unambiguous evidence of activity of the KP in the IO. For 90ER, the tectonic setting seems to control the geochemical signature of the basalts, tholeiitic-relatively depleted, i.e. MORB-type isotopic ratios when an active spreading ridge is involved in the process to very enriched ( $^{87}\text{Sr}/^{86}\text{Sr} > 0.705$ ,  $\epsilon_{\text{Nd}} < -3$ ), almost pure KP signature. The MORB-type source is nevertheless always entrained by the KP as reflected by ME and TE concentrations in these IO and 90ER lavas.

With age, KA lavas change from transitional to alkalic with accompanying changes in isotopic ratios, with  $^{87}\text{Sr}/^{86}\text{Sr}$  from 0.7038 to 0.7058 and correlative variations in  $\epsilon_{\text{Nd}}$  from +5 to -5. The youngest lavas have the lowest  $^{206}\text{Pb}/^{204}\text{Pb}$  ratios and have the highest Dupal signature. They are like the plume ( $^{87}\text{Sr}/^{86}\text{Sr} = 0.7052-0.7053$ ;  $\epsilon_{\text{Nd}} = -2, -3$ ;  $^{206}\text{Pb}/^{204}\text{Pb} = 18.02-18.12$ ;  $^{207}\text{Pb}/^{204}\text{Pb} = 15.53-15.56$ ;  $^{208}\text{Pb}/^{204}\text{Pb} = 38.50-38.60$ ).

In conclusion, our data show the KP to be responsible for Dupal anomalies in the IO basalts starting at 120 Ma. Although IO and 90ER lavas are compositionally different from KA lavas, there is much isotopic overlap. Both in 90ER and KA lavas, isotopes require 3-different components (sources) and aging is not a major explanation for the variations observed. The IO setting evolution (on/off ridge activity) seems to favor entrainment of surrounding mantle by the KP which may explain the existence of specific geochemical features.

## THERMOCHRONOLOGIC HISTORY OF THE MCKINLEY PLUTON, DENALI NATIONAL PARK, ALASKA

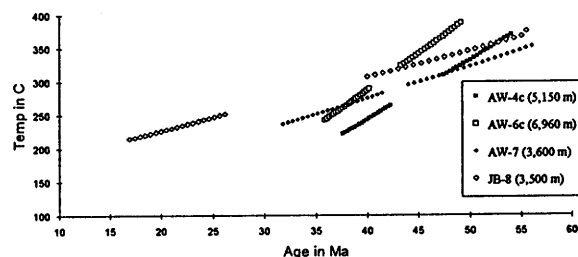
WEST, Andrew W. and LAYER, Paul W., Geophysical Institute, University of Alaska, Fairbanks, Alaska 99775, USA.

The McKinley pluton is one of the northern-most plutons of the Alaska-Aleutian Range batholith. This biotite-granite intrusion makes up most of the 6,194 m high Mt. McKinley (Denali) massif. Geochemical studies indicate that the entire pluton is homogeneous and was intruded as a single unit. Previous K-Ar and apatite fission-track studies suggest that the pluton has had a protracted cooling/uplift history since its emplacement at ~56 Ma. The great local relief available for sampling makes the McKinley pluton ideal for a thermochronometric study through  $^{40}\text{Ar}/^{39}\text{Ar}$  dating of K-feldspars and biotites. We have conducted detailed step heating experiments on samples collected from a range in elevation of 2,100 to 5,990 m.

Six biotites and one primary white mica have relatively flat age spectra with plateau ages between 55.1 and 55.8 Ma. They show a very slight age/elevation dependence with the lower biotites being younger. These consistent mica ages most likely reflect uniform cooling of the pluton at this time.

Seven K-feldspars samples exhibit saddle-shaped age spectra that vary significantly from each other. High Cl/K values are seen in the first ~5% of gas release in some samples and appear to coincide with old ages (excess argon). Cycled heating experiments carried out on the K-feldspars indicate that they contain multiple diffusion domains that we have modeled using the computer programs of Lovera (1992). From this analysis, a detailed, internally consistent, thermochronologic history spanning ~35 m.y. for the McKinley Pluton emerges. The pluton cooled slowly at rates of  $10^0$  to  $4^0$  C/m.y., with the lower samples cooling at the slower rates. The vertical variation of K-feldspar ages records an average uplift rate of 1.3 mm/Ma from 43 Ma to 25 Ma. Thus, the McKinley Pluton reached high levels in the crust by 20 Ma such that even the smallest domains of the K-feldspars do not record the rapid uplift of Mt. McKinley that began at 5 Ma indicated by apatite fission track dating.

Selected Cooling Histories for K-spars



Lovera, O. M., 1992, Computer programs to model  $^{40}\text{Ar}/^{39}\text{Ar}$  diffusion data from multidomain samples: Computers and Geosciences, v. 18, p. 789-813.

AGE AND NATURE OF CONTINENTAL CRUST IN  
YEMEN: NEW CONSTRAINTS ON PAN-AFRICAN  
CRUSTAL ACCRETION RATES

WHITEHOUSE, M.J., Dept. of Earth Sciences, University of Oxford, Oxford OX1 3PR, UK, WINDLEY, B.F., Dept. of Geology, University of Leicester, Leicester LE1 7RH, UK, and BA-B'TTAT, M.A., Dept. of Geology, University of Sana'a, Sana'a, Yemen.

The Arabian-Nubian shield is of considerable importance to our understanding of late Precambrian plate-tectonics and crust-mantle evolution. Currently there exists a major controversy regarding the crustal growth rate of the arc terranes of the shield, with estimates ranging from 20% to 100% of the present world-wide rate (reviewed in Pallister et al., 1990). The key problem revolves around the questions (1) where is the eastern boundary of the arcs of the shield; (2) does Pan African age crust continue under the cover rocks of eastern Arabia; and (3) do the Pan African island arcs continue to the Moho?

We present here isotopic data obtained on samples collected during our 1992/3 geotraverse across the previously poorly studied Precambrian of Yemen which provide additional constraints on the crustal growth-rate. In south-central Yemen we have identified two major gneiss blocks, the western Abas terrane and the eastern Al Mahfid terrane which respectively have Nd model ages (depleted mantle source) of ca. 1.9-2.2 Ga and 2.6-2.8 Ga. Our field observations suggest that Pan African reworking of these terranes was relatively minor and we conclude that the model ages probably approximate true crustal accretion ages. These terranes are separated by a major island arc terrane which is intruded by late-Pan African granitoids whose isotope systematics yield information on the deep structure of the arc.

Our data, together with earlier studies in Saudi Arabia (Stoeser et al., 1991) indicate that a much greater proportion of pre- Pan African crust exists to the east of the major arc terranes of the western Arabian peninsula than has previously been assumed. Thus, we are able to revise estimates for crustal growth rates in this major late-Precambrian orogen.

Pallister, J.S. et al., 1990, Use and abuse of crustal accretion calculations, *Geology*, v. 18, p. 35-39.

Stoeser, D.B. et al., 1991, Pan-African accretion and continental terranes of the Arabian Shield, Saudi Arabia and Yemen, *EOS*, v. 72, p. 299.

STRONTIUM ISOTOPE CHRONOSTRATIGRAPHY  
AND GEOCHEMISTRY OF THE DARAI LIMESTONE,  
PAPUA NEW GUINEA: JUHA 1X WELL

WHITFORD, D.J., ANDREW A.S., HAMILTON, P.J., Australian Petroleum Cooperative Research Centre, CSIRO Division of Petroleum Resources, North Ryde, NSW 2113, Australia, ALLAN T.L. University of Technology, Sydney, NSW 2007, Australia, VALENTI, G.L., South Pacific Chevron, Brisbane, QLD 7000, Australia.

The Miocene Darai Limestone crops out extensively in the Papuan Foldbelt, an area of high current hydrocarbon exploration activity. Dense tropical jungle, severe karst, and thick (up to 1600 m) limestone prevent the acquisition of useable seismic data. Consequently, exploration in the area is based on photogeologic and surface geologic mapping. However, neither biostratigraphy nor lithostratigraphy provide a workable subdivision of the Darai. Strontium isotope methods have been undertaken to develop a Darai chronostratigraphy in order to refine structural and stratigraphic models.

Drill cuttings have been sampled at approximately 30m intervals over a 1.5 km thick section in the Juha 1X well and analysed for Sr, C and O isotopic composition and major and trace element abundances. There is a generally consistent decrease in  $^{87}\text{Sr}/^{86}\text{Sr}$  with depth that corresponds to an increase in age from approximately 8 - 30 Ma. Comparison of  $^{87}\text{Sr}/^{86}\text{Sr}$  in whole-rock and fossil isolates from other locations in the Darai Limestone shows excellent agreement between apparent ages, consistent with petrographic evidence for very early diagenesis.

Carbon isotope values ( $\delta^{13}\text{C} = +1 \pm 1 \text{‰ PDB}$ ) for non-dolomitized samples do not vary with depth at Juha 1X. Oxygen isotope values vary more than 9 ‰ over the same depth range. From the base to the top an overall increase in  $\delta^{18}\text{O}$  of 2 ‰ corresponds with known global cooling leading to late Miocene-Pliocene glaciation. A decrease in  $\delta^{18}\text{O}$  in limestones from within the age range 22 - 12 Ma may reflect the involvement of meteoric water during deposition.

Major and trace element abundances define two zones: an upper zone above about 2000 ft ( $< \approx 17$  Ma) where dolomite is sporadically developed associated with scattered enrichment in Fe, Mn, Si, Al, Na, P and Sr. Below 2000 ft ( $> \approx 17$  Ma) the limestone is geochemically very uniform. The geochemical zonation appears to correspond to a change in depositional environment from older shallow water platform carbonates to more continuously open marine shelf conditions with a significant terrigenous input.

The internal consistency of the Sr isotopic results from Juha 1X suggests that the technique provides a robust quantitative tool by which to define local and, possibly, regional stratigraphy and structure. Combined C and O isotope studies together with major and trace element abundances can be used to resolve the effects of primary depositional variations from those due to diagenetic alteration.

## ZIRCON GEOCHRONOLOGY USING A SMALL ION MICROPROBE

Wiedenbeck, M., and Goswami, J.N., Physical Research Laboratory, Navrangpura, Ahmedabad 380009, India.

We have made the first successful use of a small geometry ion microprobe (Cameca ims 4f) for high precision  $^{207}\text{Pb}/^{206}\text{Pb}$  ages in individual Archean zircons with a spatial resolution of  $\leq 20 \mu\text{m}$ . Despite the low sensitivity provided by the ims 4f, resulting from operating at high mass resolution ( $M/\Delta M \sim 4600$  required to resolve all major isobaric molecular interferences), we can distinguish Archean components whose ages differ by as little as 50 Ma. A single measurement requires 90 minutes of data acquisition, thus a comprehensive study of a zircon population can be accomplished in a few days. With certain precautions, the ims 4f can accurately track all masses between 204 and 254; however the determination of U-Pb ratios would greatly reduce sample throughput due to the persistent need to measure calibration standards.

We have analyzed three zircon suites with previously established ages of 1.1, 2.6 and 3.8 Ga; our results are within  $\pm 2\sigma$  of the 'true' values. We conclude that no important systematic errors affect our data (e.g. no significant hydride interferences, no significant mass fractionation, accurate common Pb correction).

A limitation of our technique is the relatively low count rates which the ims 4f provides when operating at high mass resolution ( $\sim 1 \text{ cnt/sec/ppm Pb}$ ); this impediment has a particular impact on our ability to measure precisely the  $^{204}\text{Pb}/^{206}\text{Pb}$  in samples with low  $^{206}\text{Pb}$  concentrations. Nonetheless, this is not a major hindrance in dating Archean samples. Another problem encountered was how to define which analyses belong to the least disturbed sub-population within an isotopically heterogeneous population (e.g. samples containing xenocrysts only slightly older or Pb-loss components only slightly younger than the main population). In such cases the minimum age calculated for a sample can vary significantly depending on the criterion chosen for defining the least disturbed sub-population. We have identified several plausible criteria for handling this situation.

For early to mid-Precambrian samples the internal scatter of the radiogenic  $^{207}\text{Pb}/^{206}\text{Pb}$  ratio is often larger than the precision limit imposed by ion counting statistics. Our age measurements yielded  $1\sigma$  precisions ranging between  $\pm 14 \text{ Ma}$  for the mid-Proterozoic to  $\pm 3 \text{ Ma}$  for the mid-Archean.

## THERMAL EVOLUTION OF SOUTH-ALPINE CRUST: FROM VARISCAN COOLING TO ALPINE OVERPRINTING

WIJBRANS, J.R., and BERTOTTI, G., Faculty of Earth Sciences, Vrije Universiteit, 1081 HV Amsterdam Netherlands.

In the Central Alps, Lepontine metamorphism is characterised by young Miocene cooling ages. In contrast, much older Variscan to Mesozoic ages are found in the adjacent Southern Alps. The western Southern Alps (Ivrea and Strona - Ceneri zones) have been extensively studied, but in the central sector of the Southern Alps radiometric data are scarce and inconsistent. We report a detailed investigation of the crystalline basement on the eastern shore of Lake Como, applying for the first time in the central Southern Alps the  $^{40}\text{Ar}/^{39}\text{Ar}$  technique to single crystals of muscovite, biotite and hornblende.

Following the Variscan orogeny, the Southern Alps underwent Permian magmatism and graben formation, Triassic to Early Jurassic extension leading to the formation of the passive margin of the Adria Microplate, and, beginning from the Late Cretaceous/Early Tertiary, Alpine shortening. In the Lake Como area, a Pre-Alpine crustal section is exposed from the sedimentary cover to a paleo-depth of ca. 15 km. The basement section is separated into two parts by a 100 m thick mylonite band, interpreted as a normal fault related to early Mesozoic extension.

Our data allow us to quantify the poorly known thermal evolution of this crustal segment from the end of the Variscan orogeny until the onset of Alpine shortening. By comparing the radiometric signatures of clasts in the mylonite zone with the same minerals outside the fault zone, we also investigate the effects of deformation and frictional heating on the system. Our data confirm the Variscan age of the main metamorphic phase. They further reveal a strong thermal pulse in mid-crustal rocks causing muscovite plateau ages at 195 - 200 Ma, which is during Pre-Alpine rifting. The hanging wall and footwall blocks both experienced thermal overprinting, but the hanging wall block substantially less severely, resetting biotite to ca. 195 Ma, compared to 140-145 Ma biotite cooling ages in the footwall block. We also report Late Cretaceous (ca. 90 Ma) steps, which we interpret as caused by overprinting associated with the first stages of Alpine shortening.

THE EARLY SUN: PRECURSOR TO He and Ne ISOTOPES IN THE EARTH  
WITTENBERG, L.J., Fusion Technology Institute,  
University of Wisconsin, Madison WI, 53706-  
1687, USA

Mantle gases from the Earth containing high  $^3\text{He}/^4\text{He}$  ratios relative to the atmosphere but in combination with Ne isotopes of nearly atmospheric ratios have attracted much attention. This paper proposes that the formation of these gases occurred during the early Sun's pre-main-sequence phase and suggests a mechanism for their emplacement deep within the Earth.

Astrophysical models (1) propose that our solar nebula was created by a super-nova explosion. Small particles of SiC, containing nearly pure  $^{22}\text{Ne}$ , are remnants of that explosion. Dust particles and gases within the nebula, eventually, formed a solar nucleus. As in-fall continued, the deuterium-burning nuclear reaction,  $^2\text{H}(p,\gamma)^3\text{He}$ , was initiated. A wind, containing mostly H, but also the newly formed  $^3\text{He}$  and the enriched  $^{22}\text{Ne}$  isotopes, swept over the dust particles and small planetesimals which had formed a disk surrounding the Sun. Some of the planetesimals were chemically reduced forming the iron cores of the early terrestrial planets. Because the noble gases had limited solubility in the metallic core, the He and Ne dissolved mostly in the molten silicate phases

The presence of the hydrogen wind suggests the possibility of H dissolution within the metallic core. Experimental solubility measurements (2) indicate that the H/Fe ratio could have been  $\sim 3 \times 10^{-5}$ . Because of the large nuclear cross-section of  $^3\text{He}$  for neutrons, the nuclear reaction,  $^3\text{He}(n,p)^3\text{H}$ , must be considered. A high flux of neutrons can be postulated because of the abundant, neutron-rich, fissionable heavy isotopes. The  $^3\text{H}$  would have dissolved, also, in the core; however, the  $^3\text{H}$  quickly decayed to  $^3\text{He}$ , which was insoluble in the iron and could only be released by the formation of bubbles. These bubbles would migrate slowly through the core and be retained for long periods of time in the D" layer.

The  $^2\text{H}/\text{H}$  ratio was  $\sim 2.5 \times 10^{-5}$  in the early Sun. If this ratio were retained for the  $^3\text{H}/\text{H}$ , the Earth's core contained  $\sim 10^{14}$  g of  $^3\text{He}$ . A crude estimate indicates that the deep mantle plumes over the age of the Earth have released  $\sim 10^{12}$  g ( $^3\text{He}$ ). Hence, 99% of the entombed  $^3\text{He}$  still exists.

Palla, F., and Stahler, S. W., 1991, The Evolution of Intermediate-Mass Protostars: 1. Basic Results, *Astrophys. J.*, v. 375, p. 288-299.  
Fukai, Y., 1993, *The Metal-Hydrogen System: Basic Bulk Properties*, Springer-Verlag, Berlin, p. 101-119.

GRENVILLIAN PLUTONISM, DEFORMATION, AND METAMORPHISM IN THE GRENVILLE PROVINCE, ONTARIO, CANADA

WODICKA, N., PARRISH, R. R., Geological Survey of Canada, Ottawa, Ontario, K1A 0E8, Canada; and  
JAMIESON, R. A., Dept. of Earth Sciences, Dalhousie University, Halifax, Nova Scotia, B3H 3J5, Canada.

Discrimination of individual thermotectonic events in the Grenville Province requires a comprehensive understanding of the timing of plutonism, deformation, and metamorphism. We have applied a combination of U-Pb and  $^{40}\text{Ar}/^{39}\text{Ar}$  geochronology, petrology, and structural geology to reconstruct the complex Grenvillian history of the Parry Sound domain, southwest Grenville orogen, Ontario.

The Parry Sound domain is a far-travelled allochthon isolated from a proposed root zone to the southeast by parautochthonous and allochthonous rocks of the Central Gneiss Belt. Rocks of the Parry Sound domain underwent two high-grade thermotectonic events prior to their final emplacement onto the Central Gneiss Belt. U-Pb ages of syntectonic pegmatites and metamorphic zircons in mafic gneisses indicate that the earliest event, which produced widespread granulite facies assemblages, took place at  $\sim 1160$  Ma. We believe that collisional thickening and deep burial was the primary cause for this early granulite facies metamorphism; however, we emphasize that it was, at least in part, spatially and temporally associated with emplacement of the Parry Island anorthosite and mafic dykes at  $\sim 1163$  Ma. Monazite and titanite ages from schists and gneisses record a later deformation event at  $\sim 1120$  Ma, which coincided with significant exhumation and rapid cooling of Parry Sound domain rocks. Evidence for broadly contemporaneous sediment accumulation suggests that these data may be interpreted in terms of a tectonic model involving rapid exhumation in response to thrusting and concomitant erosion.

The thermochronological data provide evidence for yet another event at  $\sim 1080$ -1075 Ma. This thermal event probably resulted from major reimbrication of a structurally higher, crustal-scale shear zone at  $\sim 1080$ -1050 Ma, a consequence of continent-continent collision to the southeast of the exposed Grenville Province (McEachern and van Breemen, 1993).

Finally, the juxtaposition of hanging wall rocks with  $^{40}\text{Ar}/^{39}\text{Ar}$  hornblende ages ranging from 1070-1020 Ma against footwall units with younger cooling ages of 970-960 Ma has recorded evidence of late stage normal displacement, possibly as a result of gravitational collapse of the Grenville orogen.

McEachern, S. J. and van Breemen, O., 1993, Age of deformation within the Central Metasedimentary Belt boundary thrust zone, southwest Grenville orogen: constraints on the collision of the Mid-Proterozoic Elzevir terrane. *Can. J. Earth Sci.*, 30, p. 1155-1165.

MINERALOGY AND TEMPORAL RELATIONS OF  
AUTHIGENIC MINERALS IN ALTERED TUFFS AND THE  
UTILITY OF ALKALI ZEOLITES AS POTENTIAL LOW-  
TEMPERATURE DATEABLE MINERALS

WOLDEGABRIEL Giday, BROXTON David E., and BYERS  
Frank M., Jr., Los Alamos National Laboratory, Los Alamos, NM,  
87545

Finely-crystalline authigenic silicate mineral assemblages from altered Miocene and Plio-Pleistocene tuffs in the Barstow and Spanish Canyon Formations and the Lake Tecopa Basin and adjacent areas in south-central California provide information about the history of diagenesis. Altered tuff samples were studied petrographically and the authigenic minerals were separated and characterized by X-ray powder diffraction. The distal tuffs in the upper part of the Barstow Formation are fine-grained and contain multiple nonwelded shard morphologies with no apparent post-depositional reworking. The authigenic minerals are dominated by clinoptilolite, opal-CT, analcime, K-feldspar, quartz, illite/smectite (I/S), phillipsite, barite, and calcite that formed in a saline, alkaline lacustrine environment. The mineral assemblages are typical of a low-temperature environment and show minimal post-diagenetic alteration. The bedded tuffs in the Spanish Canyon Formation are reworked and are dominated by smectite, clinoptilolite, opal-CT, and cristobalite with minor amounts of calcite, barite, and authigenic K-feldspar. The Spanish Canyon zeolites formed in an open hydrologic system. In the Lake Tecopa basin, some of the altered tuffs are replaced by phillipsite and K-feldspar, whereas others are dominated by a mixture of clinoptilolite, erionite, phillipsite, I/S, and calcite that formed in a saline, alkaline environment. Delicate shard morphology is preserved in the clinoptilolite- and K-feldspar-rich tuffs. Clinoptilolite-rich tuffs north of the Lake Tecopa basin are Miocene in age and were probably altered during ground water percolation.

Representative authigenic mineral fractions (0.1 - 0.35, 0.35 - 1, 1 - 3, and 3 - 20  $\mu\text{m}$ ) separated from the altered tuffs were dated by the K/Ar method. Phillipsite and K-feldspar from the altered Plio-Pleistocene tuffs yielded concordant apparent ages of 0.4 and 0.5 Ma, respectively. Clinoptilolites (6.7 - 16.2 Ma), I/S (10.7 Ma), and K-feldspars (13.8 - 15 Ma) from the altered Miocene tuffs yielded similar apparent ages. Although clinoptilolite in the Miocene tuffs predated K-feldspar, the K/Ar results indicate that only one of the clinoptilolite fractions (13.5 Ma) from an undisturbed unit in the Barstow Formation is similar to the K-feldspar ages. The other two clinoptilolites are from fractured samples of the same unit close to the axis of the Barstow Syncline and yielded younger dates (6.7 - 8.7 Ma). The decrease in apparent age is due to Ar loss probably related to fracture permeability in those samples from the folded zone and to dehydration. Experimental results indicate minimal Ar loss from hydrated alkali zeolites.

In most cases, eruption and alteration ages of the tuffs are similar to each other and suggest early diagenetic alteration. The results also indicate that zeolites can retain Ar and K and may be used with other minerals to constrain the time of low-temperature diagenetic processes especially in saturated continental environments with possible application to zeolites in deep sea sediments..

NOPAL 1 NATURAL ANALOGUE: A STUDY OF  
RADIONUCLIDE MIGRATION

VIRGINA WONG, P.C. GOODELL, AND E.Y.  
ANTHONY, Univ. of Texas at El Paso, El Paso,  
Texas, 79968.

This abstract reports on activities of naturally-occurring radioisotopes for the Nopal 1 uranium deposit, located in the Peña Blanca uranium district in northern Mexico. The Nopal 1 deposit has been identified as one of the most promising site for analogue studies to the proposed nuclear waste repository site at Yucca Mountain, Nevada. Activities of 21 samples were measured using gamma-ray spectroscopy. The samples consist of an ore sample and alteration minerals of kaolinite, hematite, limonite, manganese oxide, and carbonate minerals. They were collected from the 0 m (meter), +10 m, +20 m, and +30 m levels of the mine.

In general, samples in the 0 m level have the highest activities (in Bq/g) followed by low activities in the upper levels of the mine. The ore sample from the 0 m level has the highest activity, at 78 Bq/g. The samples associated with kaolinite alteration show highest activity in the 0 m level with decreasing activity in the +10 m, +20 m, and +30 m levels (activity range = 27Bq/g to 0.9Bq/g). Hematite samples collected from 0 m and +10 m levels have an activity range from 27 Bq/g to 2 Bq/g. Limonite samples collected from 0 m, +10 m, and +20 m levels behave erratically in their activities - the sample from the 0 m level has an activity of 24 Bq/g, two limonite samples from the +10 m level have activities of 85 Bq/g and 2 Bq/g, and a sample from +20 m level has 19 Bq/g. The manganese oxide sample from the 0 m level has an activity of 40 Bq/g, and carbonate samples from +10 m level show low activities, ranging from 0.7 to 0.5 Bq/g.

The ore sample, the carbonate samples, and the manganese oxide sample are in secular equilibrium. Kaolinite samples collected from the four mine levels all show enrichment of  $^{234}\text{Th}$  relative to  $^{226}\text{Ra}$  except for the kaolinite sample from the 0 m level. This sample is deficient in  $^{226}\text{Ra}$  relative to  $^{230}\text{Th}$  implying mobility within the past 8 ka. Hematite samples show various kinds of disequilibrium. The sample from the 0 m level is enriched in  $^{234}\text{U}$  relative to  $^{234}\text{Th}$  and  $^{230}\text{Th}$ , implying that the  $^{238}\text{U}$  decay chain was broken in the past 250 ka. In addition, most hematite samples from the +10 m level show evidence of disequilibrium in the three ratios in the  $^{238}\text{U}$  decay chain ( $^{234}\text{Th}/^{234}\text{U}$ ,  $^{234}\text{U}/^{230}\text{Th}$ , and  $^{230}\text{Th}/^{226}\text{Ra}$ ), implying that the mobility for this alteration type is complex in nature. Limonite samples are observed to be in secular equilibrium in the  $^{238}\text{U}$  and  $^{235}\text{U}$  decay chains except for the sample from the 0 m level. This sample is enriched in  $^{230}\text{Th}$  relative to  $^{226}\text{Ra}$ , implying mobility of radionuclides in the past 8 ka.

## ISOTOPE AND HYDROLOGICAL FEATURES OF THE TARIM BASIN, CHINA

WUSHIKI, H., The Institute of Physical and Chemical Research (RIKEN), Saitama 351-01, Japan, TAKAHASHI, K., RIKEN, Saitama 351-01, Japan, HUANG, Z., Xinjiang Institute of Biology, Pedology, and Desert Research, Academia Sinica, Urumuqi, China, XIONG, J., Xinjiang Institute of Biology, Pedology, and Desert Research, Academia Sinica, Urumuqi, China, MASUDA, A., University of Electro-Communications, Tokyo 182, Japan, and YABUKI, S., RIKEN, Saitama 351-01, Japan.

The purpose of this study is to investigate the hydrological environment (the origin of water and the hydrologic cycle) in Tarim Basin, based on the regional characteristics of  $^{18}\text{O}$  and D contents of natural water. During the three field work seasons of 1990, 1991 and 1992, water samples, river, precipitation and ground water, were collected for the isotope analyses and chemical analyses. Analytical results were discussed as follows.

River water: Regional distribution range of the isotopic ratios was found at the highest level in southern region of Tarim basin, spanning  $-66.8\sim-46.7\text{‰}$ , in  $\delta\text{D}$ . North region fell on the second and west region on the lowest level,  $-79.1\sim-72.7\text{‰}$  and  $-88.7\sim-78.3\text{‰}$ , respectively. Rivers on the northern slope of West Kunlun Mts., which is situated at the southern edge of Tarim basin, have the isotopic ratios nearly same to the summer precipitation at West Kunlun Mts. Therefore, they were considered to be replenished mainly by the summer precipitation at West Kunlun Mts. site.

Precipitation: Precipitations, both rain and snow, were sampled in 1990/1991 and 1991/1992 at the northern slope of West Kunlun Mts. The isotope ratios varied greatly with season, ranging from  $-28.6$  to  $+46\text{‰}$  and from  $-287$  to  $+5.0\text{‰}$  in  $\delta^{18}\text{O}$  and  $\delta\text{D}$ , respectively. There is a distinct separation in isotopic value between winter and summer; transitional period can be placed between April and May with an approximate value set of  $-15\text{‰}$  and  $-100\text{‰}$ . On the  $\delta^{18}\text{O}$ - $\delta\text{D}$  plot, the summer precipitation holds larger d-index than the winter one, suggesting different origin of water vapor.

Ground water: Shallow ground water of phreatic surface depth of 1m or less are widely distributed in the peripheral zone of Taklamakan sands. Under the ground surface with poor vegetation, the isotope enrichment process in ground water may be different from that under the ground with much vegetation. Furthermore, we also performed a chemical and isotopic (Sr isotopes) studies and the results will be presented in our report.

This work was partly supported by Special Coordination Funds of Science and Technology Agency of Japanese Government.

A STUDY OF COMBINED STABLE-ISOTOPE AND TRACE-ELEMENT COMPOSITION IN LACUSTRINE OSTRACODES AS PALEOCLIMATIC INDICATORS IN THE NORTHERN GREAT PLAINS, NORTH AMERICA  
XIA, J., ITO, E. and ENGSTROM, D., all in Dept. of Geology and Geophysics, Univ. of Minnesota, 310 Pillsbury Dr., Minneapolis, MN 55455

The calcite shells of ostracodes are an important source of biogenic carbonate that can be analyzed for isotopic composition and trace element ratios to provide an account of chemistry and temperature changes in closed-basin lakes. The variations in lake chemistry and temperature can in turn provide high-resolution records of hydrologic and climatic change.

Accurate interpretation of the geochemical record from fossil ostracodes requires a solid understanding of ostracode shell formation and life-history. To explore these issues, we cultured ostracodes in the laboratory and compared the results with those obtained from monthly field collection of live ostracodes from several lakes in the northern Great Plains. The oxygen-isotope fractionation factors of the ostracode species, *Candona rawsoni*, have been calculated as 1.0305 at  $25^\circ\text{C}$  and 1.0322 at  $15^\circ\text{C}$  based on laboratory cultures. From monthly field collections in Coldwater Lake, ND and Roslyn Lake, SD, large variations in  $\delta^{18}\text{O}$ , Mg/Ca and Sr/Ca among individual adults from the same collections warn strongly that analysis of just a few individuals per sampling interval will most certainly lead to erroneous stratigraphic interpretations.

To study climatic changes in the northern Great Plains, sediment cores have been taken from several closed-basin lakes spanning an E-W moisture gradient across the region. The results from one of these sites, Coldwater Lake, North Dakota, will be discussed here. A preliminary study of the upper part of a short core covering the past 110 years shows strong coherence between instrumental records of aridity and variations in both  $\delta^{18}\text{O}$  and Mg/Ca in ostracodes. Sr/Ca in ostracodes shows a strongly negative correlation to Mg/Ca that results from aragonite precipitation and the selective removal of Sr from solution with increasing salinity. The lower part of the short core represents the last several hundred years including the so-called "Little Ice Age" event. Results thus far imply that this period was highly arid in the northern Great Plains and that climatic gradients with wetter regions to the east and south were very pronounced.

The entire Holocene record, contained within an 18m long core, shows great potential for providing high-resolution records of regional climate. Preliminary results show a number of major excursions in  $\delta^{18}\text{O}$  and Mg/Ca representing periods of wetness and aridity that are linked by abrupt transitions in hydrology and climate.

THE STUDY OF ISOTOPE GEOLOGE OF EARLY PRECAMBRIAN AND URANIUM MINERALIZATION IN THE EASTERN PART OF NORTH-CHINA PLATFORM

XIA YULIANG, ZHENG MAOGONG AND TAO QUAN

Beijing Research Institute of Uranium Geology, China  
P.O.Box 764, Beijing 100029, China

On the basis of obtained the U-Pb isotopic data from 132 samples of zircon, 32 whole-rock samples and 45 samples of uraninite (or pitchblende), we have put forward as following:

(1) The crust movement of early Precambrian

A number of isotopic ages showed that the crust movement of early Precambrian in the Eastern Part of the North-China Platform could be separated into four obvious cycles which from the older to the younger are as follows:

- 1). Qianxi Movement-----3000 ± 100 Ma
- 2). Fuping Movement-----2800 ± 100 Ma
- 3). Wutai Movement-----2500 ± 100 Ma
- 4). Luliang Movement-----1800 ± 100 Ma

(2) Time division of early Precambrian migmatitic granitoids

According to the data of obtained isotopic ages of migmatitic granitoids in North-China Platform, the migmatization in the area could be divided into four periods which corresponded to the important tectonic movement cycles of earth's crust. The migmatization at Wutai Movement spreaded to the most widespread range. This showed that the Wutai Movement at the end of Archean was the strongest period of the crust movement and could have a significance of all the world.

(3). Uranium mineralization

The mineralized types of uranium on the early Precambrian in the Eastern Part of North-China Platform are known as follows: 1) migmatitic hydrothermal type; 2) metamorphic hydrothermal type; and 3) magmatic type. No matter what the mineralized type, the time of all the uranium mineralizations was the products of Luliang Movement, the age of which is about 1800 ± 100 Ma.

HELIUM ISOTOPIC COMPOSITIONS IN NATURAL GASES IN CHINA

XU, S., NAKAI, S., WAKITA, H., Laboratory for Earthquake Chemistry, Faculty of Science, University of Tokyo, 7-3-1 Hongo, Bunkyo, Tokyo 113, Japan.

The isotopic composition of helium has been determined for more than 170 natural gases including fuel gases in 20 commercial oil/gas fields from 16 sedimentary basins, and hot spring gases in recent volcanic and geothermal areas in China. The  $^3\text{He}/^4\text{He}$  ratios range three orders of magnitude from 0.004 times the atmospheric ratio (0.004Ra) in a pre-Cambrian sedimentary reservoir in Sichuan basin up to 5.2Ra in a recent volcanic geothermal area at Tengchong, and  $^4\text{He}/^{20}\text{Ne}$  ratios vary from 0.3 to 22000.

The crust of Chinese continent thickens gradually from shallower than 30km in east to deeper than 65km in west. Several zones of steep gravity gradient divide China into four main tectonic units. The distribution of  $^3\text{He}/^4\text{He}$  ratio is consistent with the tectonic classification. The Eastern domain is typical areas undergoing continental thinning. Crustal extension linked with uplift of mantle material produces a series of basins in which R/Ra varies from 0.008 to 5.0. The extensive mantle-derived helium is introduced by melts whose generation is associated with crustal thinning. It is worthy to mention that the mantle-derived He occurs larger in geographic areas than do the distribution of surface volcanics. This may suggest that mantle-derived melts are emplaced in the deep parts of the lithosphere and that the migration of He has extensively occurred. In contrast, the tectonically stable area of the Central domain and Northwest segment, where the crust has been thickened, is characterized by typical crustal He isotopic composition and a negligible input of mantle component. In the case of Southwest segment of the Qinghai-Tibet plateau where crust has also been thickened, high values of R/Ra ranging from 0.21 to 5.2 were observed in Tengchong, a Quaternary volcanic geothermal area near the Indo-Eurasian collisional margin. Tengchong area is a fossil subduction zone where the subduction movement changed to continent-continent collision. The mantle-derived He is closely related to the volcanics caused by the collision between the Indian and Eurasian plates. The highest  $^3\text{He}/^4\text{He}$  ratio in Tengchong, 5.2Ra, is the highest value reported to date for mainland China, however, the value is lower than that of present typical subduction volcanism.

In general a good correlation is observed between the distribution of terrestrial heat flow data and  $^3\text{He}/^4\text{He}$  ratios. The heat flow values in Central domain and Northwest segment are generally as low as ~45mW/m<sup>2</sup>, while higher values from 50 up to 120 mW/m<sup>2</sup> are predominant in the Eastern domain and Qinghai-Tibet plateau. This suggests that uprising magmatic melts carry both the primordial  $^3\text{He}$  and heat in the crust of Eastern domain and Qinghai-Tibet plateau.

FISSION-TRACK ANNEALING IN ZIRCON; CONFINED TRACK LENGTH ANALYSIS AND THE ARRHENIUS PLOT

YAMADA, R., TAGAMI, T. and NISHIMURA, S., Dept. of Geology and Mineralogy, Fac. of Science, Kyoto Univ., Kyoto, 606, Japan.

To establish the basis of zircon fission-track thermochronology, we carried out a series of laboratory annealing experiments. The variation of confined fission track lengths was determined on zircon grains from the Nisatai Dacite. We primarily performed the bias estimation of track length measurement in order to achieve higher accuracy. Consequently, it was found that etching temperature, track etching criteria, measurement criteria of horizontal confined tracks (HCTs) and the orientation of HCTs significantly control observed track lengths where the samples were highly annealed (e.g.,  $\geq 600$  °C for 1 hr annealing). The first three factors may be related to the presence of gap zones in annealed zircons; whilst the fourth is caused by anisotropic etching and annealing characteristics. As a result, the experimental and analytical criteria adopted are: etching temperature, 250 °C; track etching criterion, 2  $\mu\text{m}$  width of the surface tracks perpendicular to c-axis; measurement of HCT's having  $1 \pm 0.5$   $\mu\text{m}$  width; and HCTs with the angles over 60° to c-axis.

Based on those experimental criteria, the Arrhenius-plot experiment was subsequently performed at 350 - 750 °C for  $10^{-1}$  -  $10^3$  hr (i.e., 4.5 min. - ~40 days). On the Arrhenius diagram, the fading contours of constant normalized mean track length ( $r$ ) showed as a series of straight lines. To describe the decrease in  $r$  with increasing temperature or heating time, two types of model fitting were performed, called the parallel and fanning models. We defined the lowest temperature limit of zircon partial annealing zone (ZPAZ) by  $r \sim 0.95$ , and the highest by total fading of surface tracks. The extrapolation of laboratory data to a geological time scale gives an estimate of the ZPAZ: ~210 - 280 °C by the parallel model and ~200 - 330 °C by the fanning model for the heating time of ten m.y. For an order of longer duration, the temperatures of ZPAZ decrease ~20 °C. The closure temperature ( $T_c$ ) of zircon fission-track system shows a significant discrepancy among literature: previously estimated, ~175 °C (e.g., Harrison et al., 1979) or ~240 °C (e.g., Hurford, 1986). Because  $T_c$  corresponds to the middle of ZPAZ, the present results support the higher value. The variation of etching time to satisfy the criterion revealed that the removal of alpha-radiation damage occur drastically at  $r \sim 0.93$ .

Harrison, T. M., Armstrong, R. L., Naeser, C. W. and Harakal, J. E., 1979, Geochronology and thermal history of the Coast Plutonic Complex, near Prince Rupert, British Columbia: Can. J. Earth Sci., 16, 400-410.

Hurford, A. J., 1986, Cooling and uplift patterns in the Lepontine Alps South Central Switzerland and an age of vertical movement on the Insubric fault line: Contrib. Mineral Petrol., 92, 413-427.

GENESIS OF CONTINENTAL CRUST THROUGH ARC MAGMATISM

YANAGI, T., Dept. Earth and Planetary Sci., Kyushu Univ., Fukuoka 812, Japan

Geographical configurations of island arcs indicate the alternative growth of volcanic and frontal arcs. The emplacement of granitic plutons occurs alternatively in volcanic and frontal arcs. The volcanic arc is recorded geologically as a belt of intimate association of volcanic rocks and subsequent granitic plutons, and the frontal arc as a belt of granitic plutons in metamorphic or sedimentary formations with imbricated structures (Yanagi, 1981). Geological comparison between mature and immature island arcs suggests that the arc crust evolves with time toward the crust with much continental characteristics.

The following characteristics of arc volcanic rocks are important for crustal growth: (1) intimate association of tholeiitic and calc-alkaline volcanic rocks; (2) repeated occurrence of basaltic and dacitic lavas in a volcanic succession; (3) gradational change of volcanic rocks from tholeiitic to calc-alkaline series; (4) crystallization differentiation which included the crystallization of plagioclase with other mafic minerals; (5) marked enrichment of K<sub>2</sub>O associated with slight depletion in compatible elements; (6) an evolution limit represented by, for instance, Rb/Sr ratios of 0.23-0.28 and SiO<sub>2</sub> contents of 60-66 wt.% and (7) repetitive magma mixing.

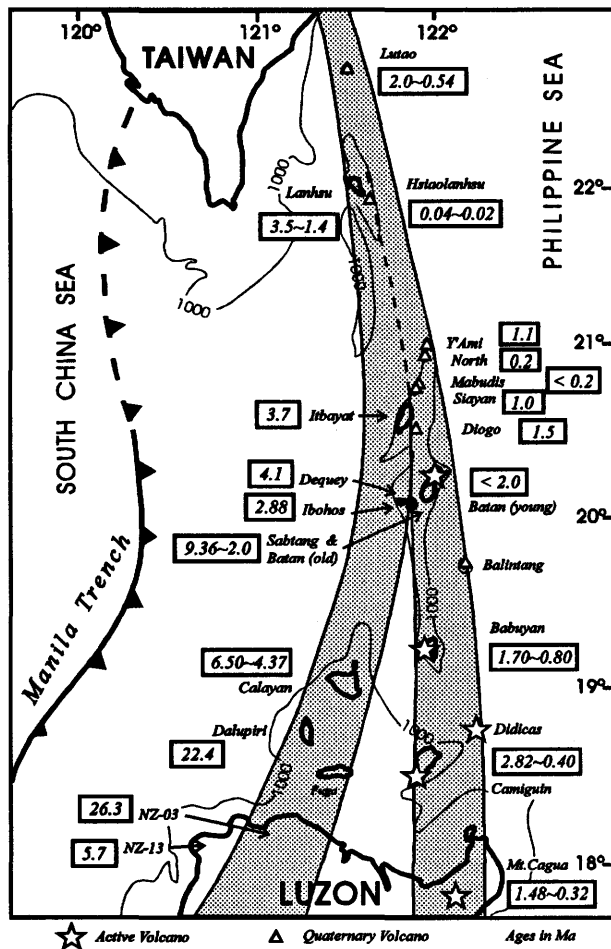
Batch fractionation in refilled magma chambers best accounts for these characteristics, transforming mantle-derived magmas through calc-alkaline magmas to magmas of composition very close to the bulk upper crust. Coupled magma chambers proposed by Yanagi et al. (1991) is a system which keeps the batch fractionation. A similar mechanism may operate in imbricated sedimentary formations to form the frontal arc immediately behind the aseismic front.

**IDENTIFICATION OF TWO VOLCANIC CHAINS IN THE NORTH TAIWAN-LUZON ARC**

YANG, Tsan-yao, F., Dept. Chemistry, WHOI, Woods Hole, MA 02543; LEE, T., Inst. Earth Sci., Acad. Sinica, Taipei, Taiwan, CHEN, C-H., Dept. Geology, Nat'l Taiwan Univ., Taipei, Taiwan, PUNONGBAYAN, R.S., RASDAS, A.S., and DAAG, A.S., PHILVOLCS, Quezon, Philippines.

Two volcanic chains of North Taiwan-Luzon Arc are recognized in this study. They are separated by 50 km in the south, however, they converge together northward intersecting ~ 20°N. The volcanic islets belonging to the West Volcanic Chain are all Miocene in age and have the characteristics of low relief, lateritic platforms, wave-cut terraces, and covered with massive recrystallized limestone. In contrast, most of the islets of the East Volcanic Chain are Quaternary in age. Some are active volcanoes with perfect cone shapes, and have well preserved eruptic records of near vent facies.

Before the eruption of East Volcanic Chain, regional uplifting occurred in this area. This might be due to the arc-continent collision in the northern part of the arc (Taiwan) and the aseismic ridge colliding with the Taiwan-Luzon Arc around 3~5 Ma ago. Subsequently, the arc magmatism shifted eastward during Quaternary. We propose that this sudden eastward shifting of the arc volcanic activities can be interpreted as caused by an abrupt change of the dip angle of the subducted slab when the aseismic ridge began to sink.



**C-, O-, AND Sr- ISOTOPE GEOCHEMISTRY OF FRANCOLITE FROM SOME SEAMOUNT PHOSPHORITE IN NORTH PACIFIC BASIN**

YEH, H.-W., Institute of Earth Sciences, Academia Sinica, P.O.Box 1-55, Nankang, Taipei, Taiwan, HEIN, J.R., U.S. Geological Survey, Menlo Park, CA. 94025, CHAN, L.-H., Department of Geology and Geophysics, Louisiana State University, Baton Rouge, LA. 70808, and WILTSHIRE, J.C., Oceanography Department, University of Hawaii, Honolulu, Hi. 96822.

The occurrence of phosphorite on seamounts in Pacific Basin was first known in late 1950. It is now apparent that phosphorite is a common rock type on seamounts in general. However, the origin of the phosphorite is still an enigma; the "upwelling, diagenetic" model is inadequate to explain it. C-, O-, and Sr-isotope methods are potential tools to gain understanding of its origin, provided we have good knowledge on the isotope geochemistry of the phosphorite. Here, we discuss the isotope geochemistry of francolite, in the light of C-, O-, and Sr-isotope data on phosphorite samples collected from eighteen seamounts of North Pacific. Francolite, a phosphate mineral, is the phosphorus carrying phase in the phosphorite. The C and O are from the structural carbonate.

The isotopic results fall into two groups against the background of prevailing Cenozoic deep-sea environment. The majority of the data have the characteristics of Cenozoic benthic foraminifera. A few of them appear to be hydrothermal in character.  $\delta^{13}C$ ,  $\delta^{18}O$  and  $^{87}Sr/^{86}Sr$  all are correlated according to the aforementioned groupings. The range of isotopic data are several ppt in  $\delta^{13}C$  and  $\delta^{18}O$  and about 1.5ppt in  $^{87}Sr/^{86}Sr$ , regardless the ages of the seamounts and the foram precursor.

The conclusions drawn from the data are:

1. The phosphorite do not suffer significant postformational modification of the isotopic composition.
2. The phosphorite appears to form in isotopic equilibrium with ambient sea water.
3. The isotopic behavior of structural carbonate in francolite appears to be practically identical to that of calcite.
4. The isotopic composition of francolite do not carry the isotopic signature of the precursor carbonate.
5. The isotopic compositions of the francolite reflects the environmental condition of the phosphogenesis.

EXHUMATION OF THE RED SEA & GULF OF ADEN  
RIFT-FLANKS: FISSION TRACK CONTRASTS  
WITHIN THE VOLCANIC & NON-VOLCANIC  
MARGINS OF THE YEMEN REPUBLIC.

YELLAND, Andrew. I. Department of Geology,  
Royal Holloway, University of London, Egham,  
Surrey, TW20 0EX, United Kingdom, MENZIES,  
M.A., Department of Geology, Royal Holloway,  
University of London, Egham, Surrey, TW20 0EX,  
United Kingdom, HURFORD, A.J., Department of  
Geological Sciences, University College, London,  
WC1E 6BT, United Kingdom.

Crustal exhumation along the proto-Red Sea margin, appears to have occurred in the early Miocene; co-eval with extension, and post-dating major Oligo-Miocene flood volcanism (33-18 Ma). The sequence of break-up (magmatism-extension-uplift & denudation) fits neither active nor passive rifting models in the traditional sense.

Regional synthesis of fission track data from Archean-Proterozoic basement and Mesozoic-Cenozoic sediments throughout the Red Sea and Gulf of Aden margins of Yemen provides important thermo-chronometric constraints on the relative stability of crustal domains both proximal and distal to active extension.

FT data from highly extended and exhumed coastal domains contrast markedly with those from more stable internal crustal domains which appear to have maintained a relatively positive structural and topographic stance since the break-up of Gondwana. Conclusions which are supported by recent sedimentological and stratigraphic observations.

Furthermore, recent reactivation of Mesozoic (Jurassic & pre-Jurassic) structural elements parallel and oblique to the Gulf of Aden is thought to have an important influence on the exhumational signature presently found along the Gulf of Aden margin, and hence to the evolution of rift margin topography.

EXPERIMENTAL AND THEORETICAL STUDIES OF  
ARGON RECOIL

YORK, Derek, EVENSEN, Norman M. and SMITH,  
Patrick E., Department of Physics, University of Toronto,  
60 St. George St., Toronto, Ontario, M5S 1A7, Canada.

The laser fusion technique has shifted the focus of  $^{40}\text{Ar}$ - $^{39}\text{Ar}$  analysis toward smaller sample and domain sizes in which fast-neutron-induced recoil of daughter nuclei ( $^{37}\text{Ar}$  and  $^{39}\text{Ar}$ ) over distances on the order of 0.1-0.2 $\mu\text{m}$  is significant. Recoil can lead to redistribution of daughter argon in the sample (affecting release patterns) or to partial loss of daughter argon from the sample (producing anomalously old ages).

We use both theoretical modelling and experimental studies to investigate recoil behaviour. In the experimental work, samples are micro-encapsulated in evacuated quartz ampoules before irradiation. Then an *in vacuo* "crusher" releases trapped recoil gas from the ampoules, followed by laser heating of the solid sample to release occluded argon. The low irradiation temperatures of the McMaster University reactor allow clean separation of the recoil and thermal release components of the sample argon, even in samples with low closure temperatures such as glauconies.

Recoil loss is a function of the geometry of the sample in relation to the distribution of parent nuclides ( $^{39}\text{K}$  and  $^{40}\text{Ca}$ ). Analytical models of Ar loss for some elementary sample geometries have appeared in the literature, but we have derived a simple approach which allows quantitative treatment of complex geometries. Examples of some basic geometries (e.g. spherical, planar, cylindrical, cubic) and some occasionally counter-intuitive consequences will be presented.

Surprisingly, vacuum irradiation, while significantly reducing recoil loss, does not result in complete re-implantation of recoil argon in adjacent sample or the container walls. This behaviour is quantitatively modelled by assuming (in accordance with experimental data) that re-implantation occurs only above a threshold energy of the recoiling argon nucleus. In glaucony grains, where recoiling nuclei pass through several thin laminae before halting, recoil losses exceed 10% even *in vacuo*. Samples with less void space, such as the hornblende standard Hb3gr, show losses much less than 1%, which may however still be significant in very precise geochronology using fine-grained standards. More extensive studies of recoil behaviour of this and other standards are in progress and will be reported.

$^{37}\text{Ar}$ , recoiling from an  $\alpha$ -particle in the reaction  $^{40}\text{Ca}(n, \alpha)^{37}\text{Ar}$ , has more recoil energy than  $^{39}\text{Ar}$ , produced by an (n, p) reaction, though rather than the  $\sim 4\times$  difference suggested by the ratio of  $\alpha$ -particle to neutron mass, the energy is only about  $2.5\times$  greater. Nevertheless, because of its greater range,  $^{37}\text{Ar}$  would be expected to be more readily lost by recoil than  $^{39}\text{Ar}$ . Experiments on glauconies show, however, that the  $^{37}\text{Ar}/^{39}\text{Ar}$  ratio of recoil gas is equal to that of the solid. This is explicable by a theory based on the threshold energy of implantation discussed above, and should be true regardless of sample geometry. Experiments are underway on a variety of materials to test this hypothesis.

**$^{231}\text{Pa}$  AND  $^{230}\text{Th}$  AS CHEMICAL TRACERS OF PARTICLE FLUX IN PALEOCEANOGRAPHY: APPLICATION IN THE SOUTH INDIAN OCEAN**

Yu, E.-F., Dept. of Marine Chemistry and Geochemistry, Woods Hole, Massachusetts, Ph. D candidate, Bacon P. M., Dept. of Marine Chemistry and Geochemistry, Woods Hole, Massachusetts, Senior Scientist, U. S. A, and Francois R., Dept. of Marine Chemistry and Geochemistry, Woods Hole, Massachusetts, Associate Scientist, U. S. A

Holocene and Last Glacial Maximum (LGM) sections of cores forming a north-south transect across the present Subtropical Convergence (STC), Subantarctic Front (SAF), and Polar Front Zone (PFZ) in the South Indian Ocean were analyzed for  $^{230}\text{Th}$ , U isotopes and  $^{231}\text{Pa}$  to reconstruct changes in the flux of sediment components. Results from the Holocene show a maximum in  $^{230}\text{Th}$ -normalized opal flux in the region of the PFZ. North of the present PF, opal flux is lower than it is immediately south of the PF. There are also remarkably higher  $^{231}\text{Pa}/^{230}\text{Th}$  ratios, reflecting enhanced scavenging, at the PFZ; the latter observation is consistent with the higher opal rain rates at the PFZ. Data from the LGM sections show similar latitudinal features. The data also suggest a higher opal flux for sediments in SAF during the LGM; an approximately constant opal flux is found for sediments in PFZ. For carbonate flux, lower values are found for LGM sections of all cores in both PFZ and SAF; whereas the terrigenous flux shows a reverse pattern for change between LGM and the Holocene. Both  $^{231}\text{Pa}/^{230}\text{Th}$  ratios and  $^{230}\text{Th}$ -normalized total flux remain approximately unchanged in the regions of both PFZ and SAF. The later feature is also confirmed by the downcore records from a core (MD88-773) in the south of the PF. However, the pronounced maximum in  $^{231}\text{Pa}/^{230}\text{Th}$  ratio and total flux are found during deglaciation in the core. We interpret these records as reflecting variations in particle rain rates associated with climate-induced latitudinal migration of the southern ocean frontal system.

**THE O, C, Sr, Pb ISOTOPE COMPOSITIONS OF REEF-FACIES CARBONATES OF CORE NY-1 IN THE SOUTH CHINA SEA AND THEIR PALAEOENVIRONMENT IMPLICATIONS**

YU JIN-SHENG, CHEN YU-WEI, GUI XUN-TANG, YU FU-JI, ZHANG DE-KE, WEI GUANG-JIAN, Guangzhou Branch, Institute of Geochemistry, Chinese Academy of Science, Wushan, Guangzhou, 510640, P. R. China.

"Core NY-1" located in the Yongshu Reef, Nansha Islands of the South China Sea, ( $09^{\circ}33'N$ ,  $112^{\circ}53.3'E$ ), was drilled by The Multidisciplinary Oceanographic Expedition Team of Chinese Academy of Sciences to the Nansha Islands, during May and June, 1990. The depth of this core is 152.07m, which consists of mainly reef-facies carbonates.

4 stages can be divided for the O, C isotope compositions of reef-facies carbonates of core NY-1. The average values of  $\delta^{18}\text{O}$  (‰) and  $\delta^{13}\text{C}$  (‰) for the 4 stages are: (I) -5.0; -0.5; (II) -7.7; -5.3; (III) -6.4; -2.8; (IV) 1.3; 2.1, respectively. The boundary age between II and III stages in depth of about 90m is 730ka, according to the palaeomagnetic dating. The characters of the II stage of  $\delta^{18}\text{O}$  fluctuating curves are the low frequencies, small amplitudes and corresponding correlation with the glacial and interglacial stages, during the Brunhes normal epoch. It has positive correlations between  $\delta^{18}\text{O}$  and  $\delta^{13}\text{C}$  values in III and IV stages, which genetically related to dolomitization.

The maximum, minimum values and all of the positive values of  $\Delta^{87}\text{Sr}$  in the core of whole hole are only occurred in the II stage. The characters of frequently changing fluctuation appeared in IV stage for both Pb and Sr isotope compositions. The leads with highly  $\mu$  values were taken in during dolomitization.

The history of palaeoclimatic and palaeoenvironmental changes in south China sea were recorded in the O, C, Sr, Pb isotope compositions of reef-facies carbonate, which is another significant information storage concerning global environmental change during Quaternary Period.

OXYGEN ISOTOPE EXCHANGE DURING  
CHONDRULE FORMATION: AN EXPERIMENTAL  
STUDY

YU, Y., HEWINS, R. H., Dept. of Geological  
Sciences, Rutgers University, Piscataway, NJ 08855  
USA, and MAYEDA, T. K., CLAYTON, R. N.,  
Enrico Fermi Institute, University of Chicago,  
Chicago, IL 60637 USA

Oxygen isotopic compositions of chondrules from primitive meteorites fall along a slope-1 trend in the three-isotope diagram. This is a mixing line which has been interpreted to be the result of isotopic exchange between chondrule material and the surrounding nebular gas, perhaps during the heating event which melted the chondrule. We have conducted laboratory experiments to determine rates and other details of this exchange process by melting chondrule-sized droplets of meteoritic material in an atmosphere consisting of a controlled mixture of water vapor, hydrogen, and helium. Experiments were done in a vertical gas-mixing furnace at 1400°C for periods of 5 minutes to 12 hours. Reaction progress was determined by measurement of  $\delta^{18}\text{O}$  and  $\delta^{17}\text{O}$  in the quenched droplets. The exchange trajectory is expected to be linear on the three-isotope graph, connecting the initial composition to the composition in equilibrium with the gas reservoir. (At equilibrium, the melt which is of ultramafic composition is about 2‰ lighter in  $\delta^{18}\text{O}$  than the water vapor.) The expected linear behavior is observed for single-phase charges in two sets of experiments, one with solid olivine, the other with a pyroxene composition above the liquidus. Two additional sets of experiments were carried out with partially molten charges, as is often the case in natural chondrules. In these experiments, the trajectory is markedly nonlinear, reflecting different exchange rates for the solid and liquid parts of the charge, which had different initial isotopic compositions.

The rate of isotopic exchange in these experiments is determined by the diffusion rate within crystals and/or melt. The slowest exchange occurred for solid olivine from the Eagle Station pallasite, which exchanged 35% in 12 hours. The fastest exchange occurred for the pyroxenic melt, which exchanged 50% in the shortest practicable experiments of 5 minutes. The experiments demonstrate that the diffusion rates within molten chondrules are sufficient for extensive isotopic exchange during the period of time during which a chondrule is hot. However, the experiments do not test the dependence of the exchange rate on the gas/melt surface processes, which are likely to be rate-determining in the case of chondrule formation due to the much lower gas pressure in the solar nebula compared to laboratory conditions.

U-Pb AND Sr ISOTOPIC STUDIES ON GRANITOIDS  
OF TAIWAN AND CHINMEN AND THEIR  
IMPLICATIONS FOR THE CRUSTAL EVOLUTION

Tzen-Fu Yui. Institute of Earth Sciences,  
Academia Sinica, R.O.C., Larry Heaman,  
Dept. of Geology, Royal Ontario Museum,  
Canada, and Ching-Ying Lan, Institute of  
Earth Sciences, Academia Sinica, R.O.C.

The time of granitoid emplacement in orogenic belts provides valuable information for deciphering the crustal evolution in complex metamorphic terrains. With these objectives in mind, several dating systems, such as Rb-Sr, K-Ar and  $^{40}\text{Ar}/^{39}\text{Ar}$ , have been employed in the past to date the granitoids in Taiwan and Chinmen. However, since the studied areas have experienced complicated metamorphic histories, the dating results can be somewhat ambiguous due to partial resetting by various kinds of subsolidus reactions. Some critical problems, therefore, remain unsolved. On the other hand, the U-Pb zircon/monazite dating can be quite successful at unraveling the timing of granitoid emplacement in high grade metamorphic terrains because the blocking temperature for Pb in these minerals is rather high (>600°C). This paper presents U-Pb zircon/monazite dates as well as Sr isotope data for granitoids from Taiwan and Chinmen. The results show that the linear correlations between  $^{87}\text{Sr}/^{86}\text{Sr}$  vs.  $^{87}\text{Rb}/^{86}\text{Sr}$  are not true isochrons, but apparent isochrons. Two end-member mixing/AFC model or late-stage alteration can account for the available data. The implications on the crustal evolution for the southeast China will be discussed.

## IN-SITU OXYGEN ISOTOPE ANALYSIS BY SIMS

YURIMOTO, H., Institute of Geoscience, University of Tsukuba, Tsukuba, Ibaraki 305, Japan

Secondary-ion mass spectrometry (SIMS) is a powerful technique used for elemental and isotopic analyses at a micro-scale surface region. Normally, positive ions, such as  $O_2^+$  and  $Cs^+$ , have been used for the primary beam in SIMS analysis. In the case of bombardment by positive ions, one of the difficulties that limits insulator analysis in SIMS is severe electrostatic charging of the sample surface. In contrast, charge compensation with negative-ion bombardment is superior to those using positive-ion bombardment. The use of an  $O^-$  primary ion beam is widespread for insulator analysis by SIMS owing to ease of generation. One of the interesting applications of SIMS is *in situ* oxygen isotope analysis of intra-mineral grains in meteorites, which are natural insulator materials. In the case of an oxygen isotope analysis by SIMS, however, the use of an  $O^-$  primary ion beam is obviously inadequate, since the primary species dilutes the oxygen in the sample.

Recently, a new type of intense negative-ion source for SIMS based on plasma sputtering was developed [1]. The ion source combined with a SIMS instrument succeeded in generating negative metal ions, such as Au and Cu, with an intense beam current and with excellent stability. Under the negative metal ion irradiation, no severe electrostatic charging occurred on the surface of polished thin section covered by gold thin film. The secondary-ion emission was stable during analysis of over several tens hours.

Oxygen isotopic measurements were made with a focused negative primary ion beam of gold. Primary beam currents were adjusted for each run to obtain a  $^{16}O^-$  count rate of  $\sim 3 \times 10^5$  counts  $s^{-1}$ . The beam size was 10-20  $\mu m$  in diameter. A mass resolution power was set to  $\sim 2,000$  (1% valley), which was sufficient to resolve all significant interferences. Measurements were made by cycling through the mass sequences 16 and 18 in a magnetic peak jumping mode. After the magnetic peak jumping, a precise peak centering of each mass was made by electrostatic peak switching scan. Secondary ion signals were detected with electron multiplier operated in a pulse counting mode. Signals measured in the electron multiplier were corrected for the counting system dead time. The isotopic composition measured by the SIMS differs from true isotopic composition of the sample by the matrix dependent instrumental mass fractionation. In order to correct the instrumental mass fractionation, a terrestrial single crystals whose composition were same to unknown samples was prepared as standards. Oxygen isotope-ratios relative to SMOW for the standards were determined by conventional mass-spectrometry method.

Under this analytical conditions,  $\delta^{18}O$  of spinel, pyroxene, plagioclase and melilite were determined with the accuracy of less than 5‰ ( $\sigma$ ) from the region of 10  $\mu m$  in diameter.

1. H. Yurimoto, Y. Mori and H. Yamamoto, 1993, Rev. Sci. Instrum. 64, 1146-1149.

## VARIATIONS ON GEOCHEMISTRY AND Nd—Sr ISOTOPE GEOLOGY OF BIMODAL VOLCANIC ROCKS FROM TWO TECTONIC SETTINGS IN SOUTH—EAST CHINA.

Gen—di ZHANG, Zhong FANG, Ying—fei XIA, Xiang—cong TAO and Hui—min LI, Department of Earth Sciences, Nanjing University, Nanjing 210008, China.

A sets of Carboniferous bimodal volcanic rocks bedded in Shi lu Group phyllites (SLG) are in a Later Palaeozoic rift, that is located at Hainan Island, where is belonged to the extensional margin of South China Plate. And a series of Permian—Triassic boundary basic—felsic subvolcanic rocks intruded in late Permian Longtan Group coal—bearing formation (LTG) are in an inner fault depression of Lower Yangtze Plate, eastern China.

The variations between the two types of bimodal volcanics are mainly from geochemistry and isotope geology of basic volcanic rocks, which are one kind of members in the bimodal volcanics. (A) SLG tholeiites:  $SiO_2$  48.82%,  $MgO$  9.21%,  $(K_2O + Na_2O)$  2.88%,  $\Sigma REE$  77.67 PPM,  $(\Sigma LREE/\Sigma HREE)$  5.9,  $(Eu/Eu^*)$  1.14,  $\epsilon_{Sr}(t)$  0~+149,  $\epsilon_{Nd}(t)$  +4.23~+7.56. (B) LTG basalts:  $SiO_2$  50.74%,  $MgO$  4.18%,  $(K_2O + Na_2O)$  4.93%,  $\Sigma REE$  166.95 PPM,  $(\Sigma LREE/\Sigma HREE)$  8.96,  $(Eu/Eu^*)$  0.84,  $\epsilon_{Sr}(t)$  +36~+188,  $\epsilon_{Nd}(t)$  -8.61~+3.57. But the geochemical and isotopic difference between the felsic volcanic ends of SLG and LTG are also obvious, such as, (A) SLG rhyolites:  $SiO_2$  77.69%,  $(Na_2O + K_2O)$  5.03%,  $(Na_2O/K_2O)$  0.029,  $\Sigma REE$  115.8 PPM,  $(\Sigma LREE/\Sigma HREE)$  5.44,  $(Eu/Eu^*)$  0.2,  $\epsilon_{Nd}(t)$  -6.84; (B) LTG rhyodacites:  $SiO_2$  65.4%,  $(Na_2O + K_2O)$  7.04%,  $(Na_2O/K_2O)$  0.931,  $\Sigma REE$  166.3 PPM,  $(\Sigma LREE/\Sigma HREE)$  19,  $(Eu/Eu^*)$  0.81,  $\epsilon_{Nd}(t)$  -15.73.

Conclusions: The Carboniferous SLG bimodal volcanic rocks were formed in continental rifting. The evolution of the rifting terminated at the stage of transition from intra—continental to inter—continental rift. The Permian—Triassic boundary LTG basic—felsic volcanic rocks are located in inner fault depression of continental plate. There are some old detrital zircons found from LTG volcanics, the U—Pb ages of the single zircons in the basic member are 2281 Ma and 746 Ma, which are determined by isotopic dilution mass spectrometer method. This is one of some important evidence about contamination between mantle and crustal rocks; Others are negative values of  $\epsilon_{Nd}(t)$ , higher (La/Yb) values, etc. The contamination is one of common features about inner fault depressions in continental plate.

### THREE TYPES OF OXYGEN ISOTOPE PROSPECTING MODELS AND APPLICATIONS

ZHANG LIGANG, CHEN ZHENSHENG and LIU JINGXIU  
Yichang Institute of geology and Mineral  
Resources, Yichang 443003, PR China

A systematic 2- or 3-dimensional mapping of oxygen isotope compositions have been carried out for the altered wall-rocks of 18 different ore deposits in China. According to the  $\delta^{18}\text{O}$  contours obtained, three types of oxygen-isotope prospecting models have been established as follows:

1. low  $\delta^{18}\text{O}$ -center system: Mineralizing centers have the lower  $\delta^{18}\text{O}$  values relative to the surrounding rocks. The mineralizations are hosted either in volcanic craters on sedimental strata or within fracture zones. Strong water-rock interactions took place on or near the surface. Cases in point are the Eren Ag deposit and the Bainaimiao Au deposit in the Inner Mongolia, the Xijiruoshan Au prospect in Heilongjiang Province. The  $\delta^{18}\text{O}$  values of the altered wall-rocks from the Xijiruoshan Au prospect are as low as -8% on the surface and decrease further downward to the position of Au-bearing ore-body. In the Eren Ag deposit, the  $\delta^{18}\text{O}$  values of vein-quartzes are lower than those of the altered wall-rocks, indicating that they are formed at 2 separate stages.

2. high  $\delta^{18}\text{O}$ -center system: Mineralizing centers have the higher  $\delta^{18}\text{O}$  values relative to the surrounding rocks. The mineralizations occur within fracture zones in subvolcanic or intrusive rocks. Cases in point are the Lengshuikeng and Yingshan Ag deposits in Jiangxi Province, the Jiaojia-type Au deposit in Shandong Province, and the Tuanjiogou Au deposit in Heilongjiang Province. The  $\delta^{18}\text{O}$  values of the altered rocks from the Tuanjiogou Au deposit are as high as +17% on the surface and gradually decrease downwards.

3. high-low-high  $\delta^{18}\text{O}$ -center system: The high  $\delta^{18}\text{O}$  zones (9-10%) are of porphyry Cu (Mo) mineralizations, outwards occur the low  $\delta^{18}\text{O}$  zones (0-8%) with Au or Pb-Zn mineralizations, further outwards occur the highest  $\delta^{18}\text{O}$  zones (>10%) without mineralization. Mineralizations are frequently related to hypabyssal rocks. Cases in point are the Tongshan Cu deposit, the Twenty-one Station Cu (Mo) deposit and Malinxi Cu deposit in Heilongjiang Province.

We have performed the prospecting experiments of oxygen isotope geochemistry based on the oxygen isotope prospecting models and the nature of water-rock interactions. As a result, a few economic ore deposits have been found.

### GRAIN SIZE CHARACTERISTICS OF A MIDDLE ORDOVICIAN ERUPTION AND ITS SOURCE AREA

ZHANG, Y-S, and HUFF, W.D., Dept. of  
Geology, University of Cincinnati, Cincinnati,  
OH 45221, USA

Grain size data from 30 K-bentonite samples representing the Middle Ordovician Millbrig K-bentonite in North America and its counterpart in northern Europe, the Kinnekulle K-bentonite, were measured to locate their source area. The source material of the Millbrig and Kinnekulle K-bentonites was silicic magma from a great eruptive event. The K-bentonite consists of clay minerals and a small portion of phenocrysts. The clay minerals were formed by the alteration of volcanic glass and no longer represent the original volcanic ash. The phenocrysts, however, are mostly unchanged. They were used as the major grain size information source of the original volcanic ash. During the measurement, fine particles  $\leq 0.074$  mm were sieved out and only the coarse phenocrysts  $> 0.074$  mm were used for grain size analysis. Log normal normalization of the phenocryst raw data was conducted to obtain the grain size characteristics of the original volcanic ash.

Based on the raw grain size data of phenocrysts, the coarse phenocryst percentage, moment mean, and the log normal normalized median were used to locate the vent and estimate the magnitude. The results are internally consistent, showing a high percentage of coarse phenocrysts in the southeastern region of North America and in the west of Baltoscandia, with the highest (59%) in Alabama. It indicates that the coarse phenocrysts accumulated in these areas and are considered proximal to the source. The coarse phenocrysts content decreases from the southeast to the northwest in North America, 59% to 1.35%, and from the west to the east in Baltoscandia, 20% to 0.58%. Moment mean and log normal normalized median calculations show the same trend. In North America, the moment mean ranges from 0.212 mm in southeast to 0.120 mm in the northwest, and the median from 0.166 mm to 0.107 mm. In Baltoscandia, moment mean varies from 0.128 mm in the west to 0.099 mm in the east, and the median from 0.075 mm to 0.053 mm accordingly. Combining the distribution patterns of coarse phenocryst percentage, moment mean, and median both in North America and in Europe, the vent position of the great eruption which produced the source materials for the Millbrig and Kinnekulle K-bentonites is on the western margin of Iapetus near the (present day) southeastern margin of Laurentia.

Through this study, it appears that the grain size analysis of the phenocrysts in K-bentonite may be an important source of information about Paleozoic volcanoes, and that the grain size characteristics of phenocrysts in K-bentonite altered from volcanic ash may serve as an approximate representative of the original ash.

REFERENCE MATERIALS FOR ISOTOPE  
GEOLOGY FROM CHINA

ZHANG ZICHAO Yichang Institute of Geology  
and Mineral Resources, CAGS, P. O. Box 502,  
Yichang, 443003, P. R. China

Following ISO Guides, a series of reference materials for geochronology and stable isotope analysis were produced in China in the last five years. These reference materials were prepared and certified by multi-laboratories and formally approved and issued by the State Bureau of Technical Supervision. The property values of these reference materials were obtained based on comparison with NBS' SRM and other reference materials which are widely used in the isotope geology community. The property values of certified reference materials issued are listed in Table 1.

Table 1 Information of isotope geological reference materials issued in China

GBW*No	material	property	values
04411	potassium feldspar	Rb $^{87}\text{Sr}/^{86}\text{Sr}$	249.47 ( $\mu\text{g/g}$ ) Sr 158.92 ( $\mu\text{g/g}$ ) $0.75999 \pm 0.00020$
04418	ho**	$^{40}\text{Ar}$	109.06 ( $10^{-6}\text{ccSTP/g}$ ) K 0.729 %, t $2060 \pm 8$ Ma
04419	rock	Sm $^{143}\text{Nd}/^{144}\text{Nd}$	3.032 ( $\mu\text{g/g}$ ) Nd 10.10 ( $\mu\text{g/g}$ ) $0.512725 \pm 0.000007$
04412	U-series dating	U $^{234}\text{U}/^{235}\text{U}$	9.31 ( $\mu\text{g/g}$ ) $^{230}\text{Th}/^{232}\text{U}$ 1.86 0.57 t $85 \pm 4$ Ma
04413	U-series dating	U $^{234}\text{U}/^{235}\text{U}$	2.20 ( $\mu\text{g/g}$ ) $^{230}\text{Th}/^{232}\text{U}$ 1.42 0.69 t $118 \pm 6$ Ma
04401	water	$\delta D_{\text{SMOW}}$	-0.4 ‰ $\delta^{18}\text{O}_{\text{SMOW}}$ 0.32‰
04402	water	$\delta D_{\text{SMOW}}$	-64.8‰ $\delta^{18}\text{O}_{\text{SMOW}}$ -8.79‰
04403	water	$\delta D_{\text{SMOW}}$	-189.1‰ $\delta^{18}\text{O}_{\text{SMOW}}$ -24.52‰
04404	water	$\delta D_{\text{SMOW}}$	-428.3‰ $\delta^{18}\text{O}_{\text{SMOW}}$ -55.16‰
04405	CaCO <sub>3</sub>	$\delta^{13}\text{C}_{\text{PDB}}$	0.57‰ $\delta^{18}\text{O}_{\text{PDB}}$ -8.49‰
04406	CaCO <sub>3</sub>	$\delta^{13}\text{C}_{\text{PDB}}$	-10.85‰ $\delta^{18}\text{O}_{\text{PDB}}$ -12.40‰
04407	cb***	$\delta^{13}\text{C}_{\text{PDB}}$	-22.43‰
04408	cb***	$\delta^{13}\text{C}_{\text{PDB}}$	-36.91‰
04409	quartz	$\delta^{18}\text{O}_{\text{SMOW}}$	11.11‰
04410	quartz	$\delta^{18}\text{O}_{\text{SMOW}}$	-1.75‰
04414	Ag <sub>2</sub> S	$\delta^{33}\text{S}_{\text{CDT}}$	-0.02‰ $\delta^{34}\text{S}_{\text{CDT}}$ -0.07‰
04415	Ag <sub>2</sub> S	$\delta^{33}\text{S}_{\text{CDT}}$	11.36‰ $\delta^{34}\text{S}_{\text{CDT}}$ 22.15‰
04416	CaCO <sub>3</sub>	$\delta^{13}\text{C}_{\text{PDB}}$	1.61‰ $\delta^{18}\text{O}_{\text{PDB}}$ -11.59‰
04417	CaCO <sub>3</sub>	$\delta^{13}\text{C}_{\text{PDB}}$	-6.06‰ $\delta^{18}\text{O}_{\text{PDB}}$ -24.12‰

\* Abbreviation of Chinese characters for National Standard Reference Material.

\*\* ho=hornblende. \*\*\* cb=carbon black.

ISOTOPE EVIDENCE OF MULTIGENESIS  
URANIUM DEPOSITS IN DALONGSHAN-  
KUNSHAN IN ANHUI PROVINCE, CHINA  
ZHENG MAOGONG, ZHU JIECHEN  
Beijing Research Institute of  
Uranium Geology, China

The uranium ore bodies occur mainly in Jurassic sandstone as tiny scattered and vein. The quartz-syenite (137Ma) intruded the sedimentary rock, and the mineralization is controlled by both stratigraphy and tectonic fractures.

Based on the isotope dating of whole rock of the ores and pitchblende, the uranium metallogenetic process can be divided into three stages:

The earliest stage, 174Ma, is the same as forming age (Rb-Sr 177Ma) of the sandstone. It means the minerals are simultaneous with the host rock; The second and the third stages are 137Ma and 112Ma respectively, which are coincident with two magma activities (Rb-Sr 130Ma, 115Ma).

The results on U-Pb system studies indicate 25-86% of uranium had lost from sandstone, and the uranium in syenite is too low to providing more materials for ore-forming.

$\delta^{18}\text{O}$  of the uranium mineralization ranges 9.16‰-14.58‰; the  $\delta^{18}\text{O}$  of syenite is 9.52‰; the  $\delta^{18}\text{O}$  of sandstone is 12.18‰. It suggests that the ore-forming solution is composed of four mixture waters which included metamorphic water enriched in heavy O from deep and precipitation with light O.

Based on the studies above mentioned, it has been ascertained that the uranium deposits are of multiple stages and polygenesis, the sandstone (J<sub>1-2</sub>) is an important uranium source and uranium pre-concentration body; the ore-forming solution is derived from four sources; the thermal events originated from the magmatic-structural activities caused multistage uranium mobilization, concentration and superimposition. So Dalongshan uranium deposits belong to complex genic deposits.

**BERYLLIUM ISOTOPIC INVESTIGATION OF  
SEDIMENTARY COLUMNS OUTBOARD OF  
SUBDUCTION ZONES**

ZHENG, S.\*, Morris, J.\*\*, Tera, F., Department of  
Terrestrial Magnetism, Carnegie Institution of  
Washington, Washington, D.C. 20015, USA  
Klein, J., and Middleton, R., Tandem Accelerator  
Laboratory, University of Pennsylvania, Philadelphia,  
PA 19104, USA

The presence of  $^{10}\text{Be}$  in island-arc volcanic lavas strongly supports the conclusion that the oceanic sediments on the subducted plate are subducted in some convergent margins. In order to evaluate the mechanism of sediment subduction, an important quantity to consider is the inventory of  $^{10}\text{Be}$  in the sediment column just outboard of the trench, i.e. the total number of atoms per unit area obtained by integrating over the thickness of the sediment column.

The  $^{10}\text{Be}$  inventories of DSDP/ODP cores 495, 183 and 777B (located just outboard of the Central American, Aleutian and Mariana trenches, respectively) are 12.9, 9.3 and  $1.2 \times 10^{12}$  atoms/cm<sup>2</sup>, respectively. The lowest value is equivalent to that predicted by globally uniform deposition of  $^{10}\text{Be}$ ; the others require preferential deposition of  $^{10}\text{Be}$  in these near-continent regions of high particle flux. Large volumes (100m, <400ka) of young, rapidly deposited arc turbidites are present at the top of DSDP 499 in the Guatemala trench and increase the  $^{10}\text{Be}$  inventory of the total sediment column by  $5.8 \times 10^{12}$  atoms/cm<sup>2</sup>. The underlying marine section at 499 shows the same lithology and  $^{10}\text{Be}$  inventory as at 495, despite dewatering and ~50% reduction in volume. Plots of  $^{10}\text{Be}$  vs depth in the three cores show scatter about the best fit regressions, where the regressions correspond to  $^{10}\text{Be}$  half-lives of 1.6-2.1 Ma. Both features indicate non-uniform  $^{10}\text{Be}$  deposition rates in these sites of continuous accumulation.

The  $^{10}\text{Be}$  concentrations in the Central America, Aleutian and Mariana arcs are 2-23, 2.5-15 and  $0.1-1 \times 10^6$  atoms/g, respectively, and represent ~40%, 40% and 0%, respectively, of the  $^{10}\text{Be}$  flux into the trench. The data require nearly complete subduction of marine sediments at central America and the Aleutians, and indicate basal accretion of young sediments in the Marianas.

\* Current address: Dept. of Geosciences, UC Irvine,  
Irvine, CA 92717

\*\* Current address: Dept. of Earth & Planetary Sciences,  
Washington University, St. Louis, MO 63130

**MANTLE DEGASSING AND DIAMOND FORMATION:  
CARBON AND SULFUR ISOTOPE PERSPECTIVE**

ZHENG, Y.-F., Department of Earth and Space  
Sciences, University of Science and Technology  
of China, Hefei 230026, P.R. China

The reservoir effects of carbon- and sulfur-bearing gaseous species degassing from the mantle on the isotope composition of diamond carbon and melt sulfur are quantitatively modeled in terms of the principles of Rayleigh distillation. The modeling is based on the observations that larger carbon and sulfur isotope fractionations can occur in the mantle during diamond formation at high temperatures.

Assuming the  $\delta^{13}\text{C}$  value of -5‰ (PDB) for the mantle,  $\text{CO}_2$  degassing can result in the large negative  $\delta^{13}\text{C}$  values of diamond (< -30‰), whereas  $\text{CH}_4$  degassing can drive the diamond  $\delta^{13}\text{C}$  values in the positive direction (> +3‰). The present results differ from the previous expectations based on a closed-system assumption and therefore can be used to explain the fall range of  $\delta^{13}\text{C}$  values from -34.4 to +5‰ in the natural diamonds. In this context, a small range of  $\delta^{13}\text{C}$  values from -9 to -2‰ for "peridotitic" diamonds can be produced by relatively weaker degassing, whereas a large range of  $\delta^{13}\text{C}$  values from -34.4 to +5‰ for "eclogitic" diamonds can be attributed to involvement of relatively stronger degassing during diamond formation.

Assuming the  $\delta^{34}\text{S}$  value of 0‰ (CDT) for the mantle, the residual sulfur in the mantle can significantly be either depleted in  $^{34}\text{S}$  ( $\delta^{34}\text{S} < -8‰$ ) due to  $\text{SO}_2$  degassing or enriched in  $^{34}\text{S}$  ( $\delta^{34}\text{S} > +8‰$ ) due to  $\text{H}_2\text{S}$  degassing. Furthermore, a large variation in the  $\delta^{34}\text{S}$  values of the mantle is accompanied diagnostically by very low sulfur contents (distinctly lower than the average content); a large variation in the sulfur contents but narrow  $\delta^{34}\text{S}$  values around 0‰ is attributable to the degassing under conditions of melt sulfide mole fraction close to the threshold value (0.90~0.93 for  $\text{H}_2\text{S}$  degassing and 0.30~0.41 for  $\text{SO}_2$  degassing, depending on the degassing temperature).

According to the present theoretical models, the large variations in the diamond  $\delta^{13}\text{C}$  values and the mantle-derived material  $\delta^{34}\text{S}$  values do not mean a mantle source with the inhomogeneous isotope compositions of carbon and sulfur. In other words, there is no need to postulate that the mantle carbon and sulfur are isotopically inhomogeneous due to the recycling of crustal sediments, given that the carbon and sulfur in diamond and its sulfide inclusion are residual ones. Diamond formation is probably related to the solid-gas reactions in the mantle and thus to the subsequent removal of gaseous species and the fractional crystallization of the melt at depth.

## KINETICS OF SULFUR ISOTOPIC EXCHANGE DURING THE REPLACEMENT OF SULFIDES

Zhiyu Jiang, P. K. Seccombe, Department of Geology, The University of Newcastle, NSW, 2308, Australia

Sulfide replacement is a common process in many important sulfide deposits. The  $\delta^{34}\text{S}$  relationships among sulfide minerals usually do not follow the sequence  $\delta^{34}\text{S}_{\text{py}} > \delta^{34}\text{S}_{\text{po}}$  or  $\delta^{34}\text{S}_{\text{sp}} > \delta^{34}\text{S}_{\text{cp}} > \delta^{34}\text{S}_{\text{gn}}$  which is established for sulfides formed under conditions of chemical and isotopic equilibrium. Such differences between observed and expected isotopic fractionation are usually attributed to chemical and isotopic disequilibrium during ore formation.

Sulfur isotopic exchange in replacement may be controlled largely by surface reactions, such as dissolution-deposition or transformation from one sulfide to another. The widespread occurrence of replacement textures among sulfides indicates that the sulfur content in ore fluids may often be too small to form new sulfide directly with metal ions even though the latter may be in high concentration in the fluid. Dissolution of the early formed sulfides would develop a high sulfur concentration in solution near these mineral surfaces. Metal ions then easily combine with the dissociated sulfur to form new sulfides so that the replacement textures and structures always appear near the surfaces. For the chemical reactions involved in this kind of replacement, it is believed that the reaction rate of deposition of the new sulfides is larger than the reaction rate of dissolution of the replaced sulfides, such that the overall rate of reaction is controlled by the rate of the dissolution reaction. This reaction process under chemical disequilibrium conditions thus may largely restrict the isotopic fractionation between the fluid and the deposited sulfides. The isotopic composition of sulfur in the replacing sulfides would be mainly controlled by the isotopic composition of sulfur in the replaced sulfide, as well as the isotopic kinetics of the dissolution process. Since the  $^{32}\text{S}$  species has a lower dissociation energy than the  $^{34}\text{S}$  species, more light sulfur would be transferred into the solution during the initial dissolution. At the same time, a surface complex would develop on the dissolving mineral, which is likely to possess a larger  $^{34}\text{S}/^{32}\text{S}$  ratio than the replaced sulfide due to the retention of residual heavy sulfur. Further, the presence of this surface complex would tend to block dissociation of light sulfur beneath and an increase in the dissociation rate of the residual heavy sulfur from the complex can be expected, due to its relatively high concentration in the complex. Ultimately, a mass balance would be reached, whereby the  $\delta^{34}\text{S}$  value of sulfur in the solution would be kept similar to, or slightly larger than the isotopic composition of the sulfur in the replaced sulfide depending on the geometric shape of the dissolving mineral.

The replacement textures and structures would tend to disappear and isotopic equilibrium would be approached due to a relatively large reaction rate of for sulfide dissolution as the reaction rate of new sulfide precipitation slowed. The presence of later sulfide overgrowths on the same sulfide phase which has undergone earlier replacement suggests that the precipitation of the new sulfide is mainly controlled by temperature. Under these conditions, isotopic equilibrium may attain among the newly formed sulfide minerals, but the isotopic compositions for the overgrowth and replaced sulfides may be different.

## POLYCYCLIC GRANULITE FACIES METAMORPHISM DETECTED BY SM-ND DATING OF GARNET: IMPLICATIONS FOR SM-ND CLOSURE TEMPERATURE

ZHOU, B and HENSEN, B. J. Department of Applied Geology, University of NSW, Kensington, 2033, Australia

The granulite facies gneisses along the Prydz Bay coastline in eastern Antarctica, have long been regarded as part of an extensive Proterozoic (c. 1000 Ma) terrane; recent work, however, has revealed that parts of the region have experienced polycyclic granulite metamorphism. On Søstrene Island in the western part of Prydz Bay, garnet grains in the mafic granulite show two stage breakdown to a coarse-grained outer (early) Opx-Plg±Hb symplectite and a fine-grained inner (late) Opx-Plg-Spl symplectite. Conditions of the early, garnet forming, metamorphic event are  $9 \pm 1$  kbar and  $850 \pm 50$  °C, and the late, isochemical, breakdown of the garnet occurred at  $6 \pm 1$  kbar and  $700 \pm 50$  °C (Thost et al 1991). Sm-Nd garnet-whole rock isotope analyses on a garnet core indicates an age of  $988 \pm 12$  Ma for the first granulite metamorphism; and the second thermal event is dated at  $498 \pm 12$  Ma from a nearby pelitic sample. This later granulite facies event is also found in other parts of Prydz Bay with ages ranging from 488 to 517 Ma. In view of these results, it is believed that the garnet cores record the earlier high P-T event and retain a memory of the timing of this event. The subsequent reheating to c. 700-750 °C at c. 500 Ma did not reset the Sm-Nd isotope system within garnet cores. Therefore it is concluded that the closure temperature of Sm-Nd system for garnet in these rocks is in excess of 700 °C.

Our investigation also demonstrates that the presence of microscopic to submicroscopic inclusions (in particular, zircon and monazite) in garnets may have significant implication in closure temperature studies of the Sm-Nd system of garnet. Most of the monazite inclusions were completely reequilibrated during garnet growth, thus the monazite-contaminated garnet analyses fall on the isochrons defined by clean garnet-whole rock/matrix. However, inherited compositions were recorded in one case where the monazite-contaminated analyses define various mixing lines with apparent older ages. Model calculations show that as little as 0.001 wt% monazite contamination would result in Sm-Nd contents of the garnet concentrates dominated by the monazite. A similar amount of zircon contamination would have little influence on the Sm-Nd system. However, it would have very significant influence on the U-Pb garnet ages.

In view of the high closure temperature at  $>700$  °C rather than 600 °C for Sm-Nd diffusion in garnet, it is worth considering that small degree of contamination of garnet with inherited zircons could be responsible for the apparent age differences, and deduced differences in diffusivity between the Sm-Nd and U-Pb systems as reported recently.

Thost, D. E., Motoyoshi, Y., & Hensen, B. J. 1991. Two-stage decompression in garnet-bearing mafic granulites from Søstrene Island, Prydz Bay, East Antarctica. *Journal of Metamorphic Geology*, v. 9, p. 245-256.

## LOMU-PM CONNECTION: A CONTINENTAL EMI DEBATE

ZHOU, Xin-Hua, and ZHANG, Jian-Bo, Both at Institute of Geology, Academia Sinica, Beijing, 100029, P.R. CHINA

Based on Sr-Nd-Pb-O isotope systematics of high-potassic volcanic rocks (dominated by leucite and basanite) erupted in northeastern China, combined with an overview of global data with typical EMI signature, such as Walvis, Leucite Hill (Wyoming) and Smoky Butte (Montana), the LOMU nature of EMI component has been emphasized. However, it was suggested naming this end-member as LOMU to bypass ambiguity (Zhou and Zhu, 1989) and has been accepted by international geochemical community (Zindler, 1993). The quantitative approaches, including major and trace elements modeling, multiple space (five to ten isotopes and trace element ratios) topographic analysis, and mixing calculations, show that the observed geochemical data can be well interpreted by an old primitive mantle component modified by multiple metasomatic episodes at different times. Furthermore, the study reveals a close connection between LOMU and PM, as well as the linear array formed by those data with a typical EMI signatures on Sr-Nd plot, as suggested here, the LOMU array. This LOMU array has distinct evolution path with respect to the normal mantle array (i.e. Normal  $\mu$  array, or called as NOMU array) and LoNd array. The LoNd array, proposed by Hart (1986), reflects the connection between EMI and HIMU, and fits most oceanic EMI data, whereas the LOMU array is the locus of connection between EMI and PM, which indicates the nature of EMI component, and fits most continental EMI data. The genesis of most EMI type rocks could be geochemically interpreted by this connection. In addition, affinity to old continental lithosphere of LOMU component is also stressed and tectonic implications are discussed.

Zhou, X.-H. and Zhu, B.-Q., 1989, Geochemical mapping of subcontinental mantle beneath eastern China, 28th International Geological Conference, Washington D.C., Abstr. Vol.3, p.III-414.

Zindler, A., 1993, V.M. Goldschmidt medal and Lester W. Strock and family honorarium, *Geochim. Coschim. Acta*, Vol. 57, p.1891-1892.

## THE STALAGMITES RECORDS OF ISOTOPIC PALEOTEMPERATURE IN BEIJING REGION

Zhu Hongshan, Dept. of Earth Sciences, Graduate School, Academia Sinica, Beijing 100039, P.R.China

This paper deals with the isotopic paleotemperature and geochronology of the stalagmites of Quaternary limestone caves in Beijing region.

The geochronology of spelean stalagmites has been studied by the U-series disequilibrium method of dating. The results show that the stalagmites were formed during the time from 440 to 78ka B.P..

The results of the oxygen isotope measurements of the stalagmites indicate that the stalagmites were formed under isotopic equilibrium condition. Isotopic paleotemperature records of the stalagmites indicate that there are three apparent periodical changes during the time

from 440 to 78 ka B.P. in Beijing region. The period of reoccurrence is about  $10^5$  years. The whole period can be divided into three spans ranging from 480 to 304 ka, 304 to 226 ka and 220 to 115 ka B.P. respectively. Their corresponding change of paleotemperature is about  $10^{\circ}\text{C}$   $3^{\circ}\text{C}$ - $12^{\circ}\text{C}$ ,  $12^{\circ}\text{C}$ - $5^{\circ}\text{C}$ - $16^{\circ}\text{C}$  and  $16^{\circ}\text{C}$ - $5^{\circ}\text{C}$ - $12^{\circ}\text{C}$  respectively. The highest mean annual temperature is  $12^{\circ}\text{C}$ - $16^{\circ}\text{C}$  and the lowest is  $3^{\circ}\text{C}$ - $5^{\circ}\text{C}$ . They may represent the temperature of interglacial and glacial respectively. The difference of temperature between glacial and interglacial is about  $7^{\circ}\text{C}$ - $9^{\circ}\text{C}$  in Beijing region. The modern mean annual temperature ( $12^{\circ}\text{C}$ ) in Beijing region is close to the highest temperature during the period from 440 to 78 ka B.P..

Compared with the paleotemperature curve and time scales of Emiliani and Shackleton (1974)\*, the curve of isotope paleotemperature in Beijing region shows a similar tendency of change.

\* Emiliani, C., and N. J. Shackleton (1974) The Brunhes epoch: Isotopic paleotemperatures and geochronology. *Science*, 183, 511-514.

## ION PROBE DATING OF MONAZITE: EXAMPLES FROM THE ISUA AND THE LEWISIAN TERRANES

ZHU, Xiangkun, O'NIONS, R.K., BELSHAW, N.S., REED, S.J.B., Dept. of Earth Sci., Univ. of Cambridge, Cambridge, CB2 3EQ, UK. and. MOORBATH, S., Dept. of Earth Sci., Univ. of Oxford, Oxford, OX1 3PR, UK

U-Pb geochronology of monazite is an established but under-utilized technique. Some studies have shown that monazite is rarely inherited in intermediate- to high-grade metamorphic rocks and usually yields concordant or near concordant age with closure temperature  $\geq 700^\circ\text{C}$  for the U-Pb system. Here we present the results of micron-scale chronology obtained by secondary ion mass spectrometry (SIMS) analysis and related EMPA studies of monazites from gneisses of the classic Archean areas: Isua, Western Greenland and the Lewisian, Northwest Scotland. Individual monazite grains were located in polished thin sections by optical microscopy and SEM study and their Pb isotope composition analysed *in situ* using the ISOLAB-120 operated at  $\sim 7000$  resolving power.

The sample studied from the Isua is a tourmaline gneiss. Three monazite grains were selected for SIMS analysis. All these grains are unzoned and have a similar chemical composition. Two larger ( $\sim 100\ \mu\text{m}$ ) grains coexisting with allanite and apatite give  $^{207}\text{Pb}/^{206}\text{Pb}$  ages of  $3568 \pm 19$  Ma and  $3580 \pm 20$  Ma. The small ( $\sim 10\ \mu\text{m}$ ) grain included in tourmaline yields a  $^{207}\text{Pb}/^{206}\text{Pb}$  age of  $3578 \pm 13$  Ma, indistinguishable from the ages obtained from two other grains in the same thin section. The consistency of the ages obtained from the different size grains of monazite suggests that these ages are concordant.

Samples studied from the Lewisian are garnetiferous felsic gneisses. Monazite occurs as discrete grains and inclusions in garnet, biotite and feldspar, and usually shows zoning with higher Th abundance at the rims, but with REE distribution patterns that are similar between both the rims and cores.  $^{207}\text{Pb}/^{206}\text{Pb}$  ages of  $2715 \pm 23$  Ma and  $2530 \pm 8$  Ma are obtained from the core and rim, respectively, of a large ( $\sim 400\ \mu\text{m}$ ) complexly zoned discrete monazite grain. Thus, this single crystal preserves a high-grade metamorphic history extending over some 200 Ma. The central regions of two smaller ( $\sim 200\ \mu\text{m}$ ) discrete monazite grains yield  $^{207}\text{Pb}/^{206}\text{Pb}$  ages of  $2745 \pm 15$  Ma and  $2741 \pm 12$  Ma, respectively. A small ( $\sim 20\ \mu\text{m}$ ) grain of monazite fully armoured by garnet gives a  $^{207}\text{Pb}/^{206}\text{Pb}$  age of  $2761 \pm 12$  Ma. This is the oldest age reported for the Lewisian high-grade metamorphism so far.

This study shows that monazite is a valuable phase for *in situ* SIMS chronology on intermediate- to high-grade metamorphic rocks. It illustrates that the host minerals, especially garnet, may play an important role in the behaviour of Pb in monazite during metamorphism. The combination of detailed petrographic study and spatially resolved chemical analysis with SIMS chronology offers a significant advance in the study of these materials.

## Pb-Sr-Nd ISOTOPIC AND GEOCHEMICAL PROFILES OF THE CRUST AND MANTLE IN EASTERN JOINT PART BETWEEN YANGTZE AND SOUTH CHINA BLOCKS

Zhu B.-Q., Wang Y.-X. and Wang H.-F.  
Institute of Geochemistry, Chinese Academy of Sciences, Wushan, Guang Zhou, 510640, P.R. China

Systematic studies on Pb-Sr-Nd isotopic and chemical compositions within crust and mantle along the geophysical sections through Yangtze (YB) and south China blocks (SCB) in Anhui and Zhejiang area, eastern China, have been done. Pb isotopic results evidently show sympathetical variation within the crust (feldspars in Mesozoic granites) and mantle (Cenozoic basalts), which the  $^{206}\text{Pb}/^{204}\text{Pb}$  and  $^{208}\text{Pb}/^{204}\text{Pb}$  in SCB are higher than 18.40 and 38.40, and those in the YB are close to 18.10 and 38.20 respectively. The boundary line between the YB and the SCB has been well established at 29.1–29.2 N through the detail Pb isotopic mapping, which is consistent with the evidence of the geophysical section. It's indicated from the Nd isotopic evidence of alkaline basalts and granitoids that the mantle beneath the boundary area was more depleted ( $\epsilon_{\text{Nd}} = +6.5$ – $+8.5$ ) and its crust possesses higher Nd model ages ( $T_{\text{DM}} = 1.8$ – $2.5$  Ga), which is consistent with zircon U-Pb age (1.8 Ga), than those in the interior of the two blocks (mantle  $\epsilon_{\text{Nd}} < +6.5$ , crust  $T_{\text{DM}} < 1.7$  Ga). The Sr isotopic ratios indicated that the YB mantle preserved primitive feature from Proterozoic to present (.7042–.7045), whereas the SCB mantle was depleted at present (.7035) and enriched during Mesozoic (.7088). The trace element data show that the crust in SCB is evidently enriched in U, Th, Rb, Sn, W and etc. and depleted in Zr, Sr, Ba and etc. It's indicated that Pb and Sr isotopic systematics possess strong terrane features in YB and SCB, but Sm-Nd systematic is mainly show vertical fractionation between crust and mantle, YB and SCB have entirely different evolution histories, and their crust and mantle have been welded since Proterozoic.

TEMPORAL ASSOCIATION OF TYRNYAUZ W-MO DEPOSIT WITH ELDJURTA GRANITE: EVIDENCE FROM Rb-Sr DATING

ZHURAVLEV Andrew Z., Institute of mineralogy, geochemistry, and crystallic chemistry of rare elements (IMGRE), Moscow 121357 Russia, and NEGREY E.V., IGEM RAS, Staromonetny 35, Moscow, 109017, Russia

Eldjurta granitic pluton is situated within Peredovoy range of North Caucasus. Tyrnyauz W-Mo deposit is spatially related to this pluton and occupies its supra-intrusive zone. On the basis of geological background and K-Ar ages of igneous rocks, it was suggested that W-Mo ores of Tyrnyauz deposit are older than granites. However, there was no any isotope data on the age of ore formation.

We determined ages of Eldjurta granite and ore-bearing metasomatite from Tyrnyauz deposit by Rb-Sr method.

It is widely accepted that precision of isochrone dating depends heavily on an amount of sample points. The granite sample contains only 3 minerals (biotite, K-feldspar and plagioclase), datable by Rb-Sr method, and the metasomatite -- only 2 (amphibole and biotite). In order to increase amount of isochrone points we separated dense fractions of the minerals using heavy liquids and hand picking under microscope.

Age of Eldjurta granite was determined by 13-point isochrone and measures  $1982 \pm 8$  Ty,  $(^{87}\text{Sr}/^{86}\text{Sr})_0 = 0.70685 \pm 3$ . Age of ore-bearing metasomatite was determined by 7-point isochrone and measures  $1963 \pm 15$  Ty,  $(^{87}\text{Sr}/^{86}\text{Sr})_0 = 0.70810 \pm 15$ .

The same age of granite and metasomatite, coupled with their spatial association, suggests a genetic relation between Eldjurta pluton and Tyrnyauz deposit. A higher  $(^{87}\text{Sr}/^{86}\text{Sr})_0$  in metasomatite may be interpreted as a result of contamination by host hornfels.

SULFUR ISOTOPIC COMPOSITION OF MASSIVE SULFIDE FROM THE MIDDLE VALLEY SEDIMENT-COVERED SEAFLOOR SPREADING CENTER

ZIERENBERG, ROBERT A., US Geological Survey, Menlo Park, CA 94025, USA; GOODFELLOW, Wayne D. and FRANKLIN, James M., Canadian Geological Survey, Ottawa, Ontario K1A 0E8.

Middle Valley is a sediment-buried part of the Juan de Fuca Ridge spreading center. Turbiditic sediment deposited during the Pleistocene fills the axial valley to depths ranging from 300 m to > 1,200 m. An active hydrothermal vent field with temperatures as high as 274°C and a fossil geothermal system that deposited a large massive sulfide deposit have been sampled by the ALVIN submersible and by drilling during Leg 139 of the Ocean Drilling Program. Turbiditic sediment away from the hydrothermal systems contains 0.1 to 0.3 wt. percent sulfur in pyrite with  $\delta^{34}\text{S}$  values of -45‰ to -20‰, typical for sulfide formed by biogenically mediated reduction of seawater sulfate. This early diagenetic pyrite is overprinted by hydrothermally-derived pyrite with  $\delta^{34}\text{S}$  values of 6‰ to 12‰. The extent of overprinting increases both with increasing depth in the sediment and with proximity to the hydrothermal upflow zones. Sediment cored below the active vent field contains disseminated anhydrite with  $\delta^{34}\text{S}$  ranging from 21‰ to 28‰, indicating partial reduction of seawater sulfate.

Massive sulfide drilled at an extinct hydrothermal center 3 km SW of the active vent field is at least 95 m thick. A primary high-temperature mineral assemblage of pyrrhotite + isocubanite + chalcopyrite + sphalerite has been partially replaced during lower temperature hydrothermal alteration by pyrite ± magnetite ± chalcopyrite ± sphalerite. Massive sulfide from both the active and fossil hydrothermal systems has a narrow range of  $\delta^{34}\text{S}$  values mostly between 5‰ to 9‰. Pyrite, pyrrhotite, sphalerite, and chalcopyrite are not in isotopic equilibrium and generally have similar values in adjacent subsamples. The isotopic data are consistent with petrographic evidence for extensive recrystallization of sulfide minerals and replacement of pyrrhotite by pyrite via sulfur-conserving reactions.

The deepest drill holes (936 m) in Middle Valley penetrated an interlayered sequence of basaltic sills and sediment altered to subgreenschist to lower greenschist assemblages. Disseminated pyrite and pyrite, pyrrhotite, sphalerite, and chalcopyrite in veins cutting the basalts have a narrow range of  $\delta^{34}\text{S}$  values generally between 7‰ to 12‰. Primary igneous sulfide (monosulfide solid solution,  $\delta^{34}\text{S}$  approx. 0‰) was leached from the basalt during hydrothermal alteration.

## DEBUNKING THE $\kappa$ CONUNDRUM

ZINDLER, A., BOURDON, B., and ELLIOTT, T., Lamont-Doherty Earth Observatory of Columbia Univ., Palisades, NY 10964, USA.

Galer and O'Nions (*Nature* 316, 778-782, 1985) noted that  $\kappa$  values measured in MORBs, or inferred from MORB U-Th systematics ( $\kappa_{Th}$ ), are substantially lower than  $\kappa_{Pb}$  values inferred from MORB Pb isotope systematics. They proposed that the solution to this " $\kappa$  conundrum" was a "steady-state" upper mantle with a  $\kappa$  of 2.5, low U, Th and Pb concentrations, and short but different residence times for these elements. In this context, MORB Pb isotope ratios are inherited from a high- $\kappa$  (~4.0) lower mantle and are not perturbed by a brief period of residence in the upper mantle. Although appealing in some respects, this model suffers from being an *ad hoc* mathematical construct that is difficult to support by direct observation.

A geologically more sound alternative solution to the  $\kappa$  conundrum lies in a reinterpretation of MORB Pb isotope systematics. Because the slope of the MORB  $^{206}Pb/^{204}Pb$  vs.  $^{208}Pb/^{204}Pb$  array is similar to that predicted for evolution over 4.5 Ga in a constant  $\kappa$  reservoir,  $\kappa_{Pb}$  values, as they are used to define the conundrum, are calculated by assuming a *single-stage* evolution for  $\kappa$ , in contrast to the *multi-stage* scenarios known to best describe Rb-Sr, Sm-Nd and U-Pb evolution in the earth. We have found, however, that the growth of Pb isotope ratios in the MORB mantle (DMM) is consistent with a marked change in  $\kappa$  evolution during the middle period of Earth history. If  $\kappa_{DMM}$  starts at ~4.0, and remains constant until ~2 to 3 Ga b.p., and then *continuously* declines to a present-day value of ~2.5, observed MORB Pb isotopic systematics are reproduced in the context of a low- $\kappa$ , present-day DMM. This change in the evolution of  $\kappa$  must occur in response to a substantial increase in the amount of U recycled from the continental crust to DMM via altered oceanic crust, and could herald the advent of oxidizing conditions at the surface and/or a change in the nature of subduction due to thermal evolution of the mantle (McCulloch, *EPSL* 115, 89-100, 1993).

In contrast to the model of Galer and O'Nions, our Post-Archean U Recycling (or PURE) model is conceptually consistent with the quasi-continuous depletion of the MORB mantle in response to the growth of the continental crust. Artificially short and different residence times for U, Th and Pb in the upper mantle are not required. A Monte Carlo exploration of the quantitative predictions and consequences of the PURE model for the mantle and crust will be presented and discussed at the meeting.

CASPIAN SEA AND GULF OF MEXICO AS CLIMATE REGISTORS FOR CONTINENTS OF THE NORTH-ATLANTIC SECTOR

ZUBAKOV V.A., Hydrological Inst., St.Petersburg, 199053, Russia.

The Caspian hydrologic-chronometric series of 48 cycles covers 7 Ma and includes 35 paleomagnetic benchmarks, tens of datings by Th/U, TL, F.t., KAr methods and many hundreds of  $^{14}C$ . It is separated into 4 independent scales compatible with the series for Russian and Siberian plains. Many boundaries of the Caspian events are properly correlated with the peaks of isotope-oxygen curves according to foraminifers from ODP 625B section in the Gulf of Mexico (Joyce, Tjalsma, Prutzman, 1990, 1993).

The boundaries of 5.1, 4.6, 3.6 and 3.3 Ma fix supercryothems 24, 22, 18 and 16 in the Ponto-Caspian which divide the Zankli / an transgression into 4 stages. At 3.0 Ma the uplift and the first glaciation of the Great Caucasus as well as the Caspian isolation occurred. At 2.5-2.4 Ma (SKT 12) the Akchgylian transgression reached its maximum (+100 m), and its water made the way through a new Manych strait. At 1.9 Ma (Termo-SKT9) Dreissena and ancestry of the Apsheon fauna penetrated into the Caspian, and at 0.9-0.8 Ma - the ancestry of the Baku fauna did.

At the Brunhes epoch the Caspian was an isolated basin but at glacial phases (Orto-KT 18, 16, 14, 12, 6; 5d, 5b) some water from the Caspian discharged to Azov-Black Sea basin together with the predominant *Didacna* species. The Khvalynian history of the Caspian is reconstructed in details, compatible with the boundaries of GRIP and Holocene (15 cycles).

Thus, the Caspian is the global recorder of Pliocene glaciation of the Antarctica and of the moistening trend of continents of the North-Atlantic sector during Pleistocene. Since continental climate-chronologic scale of Plio-Pleistocene is important for a development of climate theory and predicting future climate, the US scientists are invited to join their efforts for cooperation.

## Isotoping dating (Ar-Sr-Nd) and tracing (REE) of diagenetic and hydrothermal activities in Rotliegendes Sandstones (Central Europe)

Zwingmann, H., Clauer, N., Stille, P. and Samuel, J. (CNRS) Centre de Géochimie de la Surface, 67084 Strasbourg, France

An isotopic, geochemical and petrographic investigation on Late Permian (Rotliegendes) and Late Carboniferous rocks from gas wells permits the influence of burial and hydrothermal events on the formation of authigenic clay mineral phases to be determined. The sequences occur at a 4.5-to-5.5 km burial depth in a series of NW-SE trending graben and horst structures, where Rotliegendes and Carboniferous units are juxtaposed along distinct faults. Acidic fluids from the Late Carboniferous units which were expelled through these fault systems into the Rotliegendes units, cause feldspar dissolution and authigenic clay-mineral precipitation. The clay minerals can be quantified by REE-chemistry, chemical and petrophysical investigations. Petrographic and XRD investigations have identified several morphological types of authigenic clay minerals (illite, kaolinite, dickite, chlorite). Their REE patterns and Li concentrations are dependent on the distance from major fault systems: authigenic illites next to these faults yield REE patterns highly enriched in LREE and in Eu, as well as in Li. The decreasing positive Eu-anomaly and the Li content in fine fractions ( $<1\mu\text{m}$ ) can be used as a geochemical tracer for hydrothermal fluid pathways. Some illites show extremely high  $^{147}\text{Sm}/^{144}\text{Nd}$  ratios up to 0.48, which are related to close proximity to coal bearing Late Carboniferous units.

K-Ar dating of the authigenic illite phase from 40 samples (fractions from  $<0.2$  to  $>63\mu\text{m}$ ) yield ages between 220 and 160 Ma. K-Ar ages of 220-200 Ma predominate in the horst areas and decrease to 180-160 Ma in the graben area. With increasing distance to the major faults system the K-Ar ages become progressively younger. The dependence of age on distance from the Carboniferous units reflects the decreasing influence of hydrothermal fluid infiltration from the faults into the graben sequences. The geochemical and K-Ar data allow to reconstruct the timing and the migration-pathways of illite-forming hydrothermal fluids. The extent of hydrothermal alteration is therefore mainly controlled by tectonic position in the system.

Rb-Sr data of authigenic illite and chlorite phases support these results. The Rb-Sr isochrons defined by leachates of clay fractions (L), residues from leaching (R) and untreated aliquot (U) yield ages similar to the K-Ar ones. Sr-isotope data point to an increasing water-rock interaction from the horst area, where the hydrothermal fluids originated, into the graben area.

Sm-Nd isochrons (L-R-U) yield ages of 350 to 260 Ma which correspond approximately to the sedimentation ages of the Carboniferous and Permian units, respectively. The Sm-Nd ages seem to reflect early diagenetic processes in these stratigraphic units in contrast to the K-Ar and Rb-Sr results. The formation of the hydrothermal illite can be dated by the K-Ar and Rb-Sr systems and is correlated to a period of tectonic activity which is the opening of the central Atlantic Ocean during an early-to-mid Kimmerian event.

## $\delta\text{C}$ AND $\delta\text{O}$ SIGNALS OF PEDOGENIC CARBONATES FROM PLEISTOCENE CONTINENTAL DEPOSITS, AS PALAEO-ENVIRONMENTAL INDICATORS.

KEPPENS E., ALAM S., HAN J., NIELSEN P., VAN RIET A. and PAEPE R.: Vrije Universiteit Brussel, pleinlaan 2, 1050 Brussels, Belgium.

$\delta\text{C}$  and  $\delta\text{O}$  values of pedogenic carbonate concretions from two Pleistocene continental sequences (one in NW Bangladesh with 11 palaeosols and one in Central China with 18 palaeosols) are compared and discussed. The major objectives of this study were to test: (1) the reproducibility of the  $\delta\text{C}$  and  $\delta\text{O}$  signals within lithostratigraphic or petrological units, and (2) their variation from one unit to the other. All together more than 2000  $\delta\text{C}$  and  $\delta\text{O}$  analyses were carried out on more than 1000 samples, leading to the following observations.

(1) Lithostratigraphic units that are expected to have formed under different palaeo-environmental or palaeoclimatic conditions, provide isotopic signatures ( $\delta\text{C}$  and  $\delta\text{O}$ ) that can be clearly distinguished. In other words the differences between analytical results from a same lithostratigraphic unit are much smaller than between samples from different units. This would mean that climatic or environmental changes are recorded as significant differences in isotopic signature.

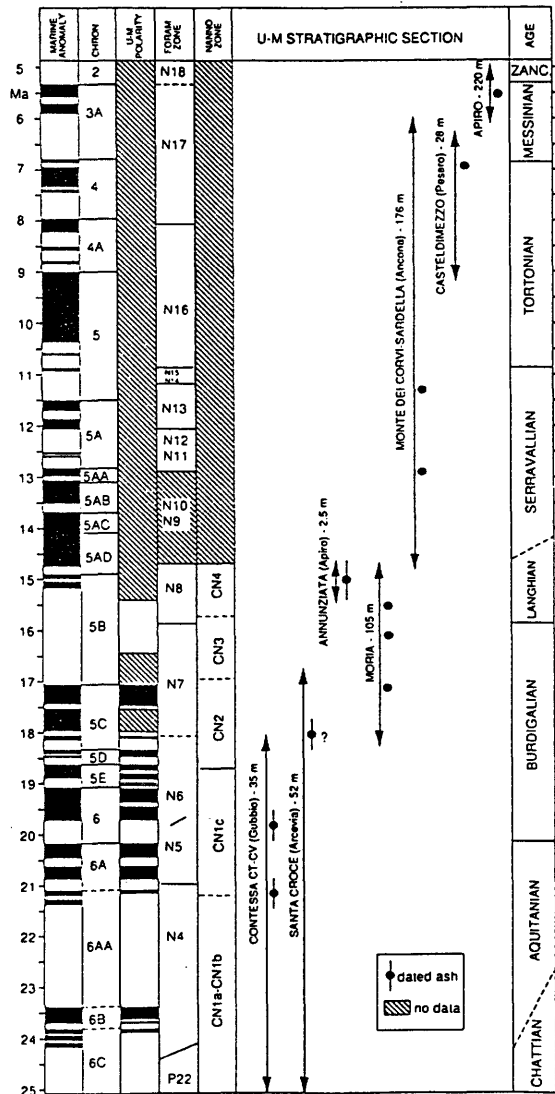
(2) Carbon isotopic compositions vary between  $-8\text{‰}$  and  $-2.5\text{‰}$  in China, and between  $-11.5\text{‰}$  and  $+1.5\text{‰}$  in Bangladesh. The relatively large  $\delta\text{C}$  variations may be explained by climatically induced changes in floral compositions in terms of C3-/C4-plants. Changes in humidity are translated into variations of C3- and C4- plant proportions, resulting in changes in soil  $\text{CO}_2$   $\delta\text{C}$  values. The extreme  $\delta\text{C}$  values found in the sequence in Bangladesh would correspond to nearly single "phase" C3 ( $\delta\text{C}$ :  $-11.5\text{‰}$ ) or C4 ( $\delta\text{C}$ :  $-11.5\text{‰}$ ) floras.

(3) Variations in the oxygen isotopic composition are much smaller: between  $-10\text{‰}$  and  $-8\text{‰}$  in China and between  $-6\text{‰}$  and  $-3.5\text{‰}$  in Bangladesh. These smaller differences can be induced by temperature changes. Contrary to the mechanism in the marine environment, here the "direct" temperature-effect, causing the change of the fractionation factor between (soil-)water and (soil-)carbonate, is opposite to the "indirect" temperature-effect, controlling the isotopic composition of the (meteoric and thus soil-) water. A temperature rise of e.g.  $+10^\circ\text{C}$  causes shifts in the  $\delta\text{O}$  of pedogenic carbonates between  $0\text{‰}$  (in the warmer climates) and  $+7.5\text{‰}$  (in the colder climates).

**$^{40}\text{Ar}/^{39}\text{Ar}$  GEOCHRONOLOGY OF AIR-FALL ASHES FROM THE MIOCENE PELAGIC SEQUENCE OF THE UMBRIA-MARCHE APENNINES (ITALY)**

DEINO, A. (Geochronology Center, Institute of Human Origins, 2453 Ridge Road, Berkeley, CA 94709), and MONTANARI, A. (Osservatorio Geologico di Coldigioco, 62020 Frontale di Apiro -MC-); COCCIONI, R. (Ist. di Geologia, 61029 Urbino), and ODIN, G.S. (Dép. Géol. Sédimentaire, Univ. P. et M. Curie, 75252 Paris, France)

We have dated with  $^{40}\text{Ar}/^{39}\text{Ar}$  laser total-fusion and incremental heating techniques several crystal separates of biotite, sanidine, and plagioclase from distal air-fall ash layers from the Miocene pelagic sequence of the northeastern Apennines (Umbria and Marche regions of Italy). The results of this work permit a detailed geochronologic calibration of biostratigraphic boundaries, magnetic polarity reversals, and chemo-stratigraphic characteristics of this pelagic sequence from the mid-upper Aquitanian to the uppermost Messinian. We have obtained the following boundary age estimates: Burdigalian/Aquitanian, 20.1 Ma; Burdigalian/Langhian, 15.8 Ma; Serravallian/Tortonian, 10.9 Ma; Tortonian/Messinian (7.2-6.8 Ma); Messinian/Zanclean (5.3 Ma).



**"EXCESS" ARGON AND HALOGENS IN GRANITE-DERIVED FLUIDS**

McCONVILLE, Paul<sup>1</sup>, STUART, F.<sup>1</sup> and TURNER, G.<sup>2</sup>  
<sup>1</sup> SURRC, East Kilbride, Glasgow, G75 0QU, UK  
<sup>2</sup> Dept. of Geology, Manchester University, M13 9PL, UK

The  $^{40}\text{Ar}$ - $^{39}\text{Ar}$  dating scheme is complicated by the release of 'excess' argon ( $^{40}\text{Ar}_E$ ) along with  $^{40}\text{Ar}_R$  from *in-situ* decay of  $^{40}\text{K}$  (i.e. radiogenic  $^{40}\text{Ar}^*$  is mixture of  $^{40}\text{Ar}_R$  and  $^{40}\text{Ar}_E$ ). Recent experiments have found that  $^{40}\text{Ar}_E$  correlates with Cl-derived  $^{38}\text{Ar}$  [1] raising the possibility of a Cl-based  $^{40}\text{Ar}_E$  correction [2]. Noble gas and chemical (K, Cl, Br, I) information obtained by  $^{40}\text{Ar}$ - $^{39}\text{Ar}$  studies show that  $^{40}\text{Ar}_E$  in granitic feldspars is trapped in fluid inclusions and that it is possible to determine the origin of these fluids [3,4].

To test this suggestion, we firstly re-examined 10 year-old unpublished  $^{40}\text{Ar}$ - $^{39}\text{Ar}$  data on the Hamlet Bjerg granite from the East Greenland Caledonides. We expected consistent Rb-Sr and K-Ar cooling histories because Rb-Sr systematics and petrographic evidence suggest that the granite cooled slowly (4-11°C/Ma) and has not been affected by later hydrothermal events.

Conventional K-Ar,  $^{40}\text{Ar}$ - $^{39}\text{Ar}$  stepped heating and laser ages of biotite grains agree well with the Rb-Sr mineral-WR isochron of  $415 \pm 23$  Ma [5]. However laser  $^{40}\text{Ar}$ - $^{39}\text{Ar}$  dates of adjacent feldspar grains lie on an isochron of  $497 \pm 7$  Ma (n = 9, MSWD = 0.9).  $^{40}\text{Ar}^*/\text{K}$  correlates with Cl/K in the feldspar. The age determined from the  $^{40}\text{Ar}^*/\text{K}$  intercept (Cl = 0) agrees with the Rb-Sr isochron age. The  $^{40}\text{Ar}^*/\text{Cl}$  ratio  $\sim 4 \times 10^{-4}$  given by the slope is somewhat higher than found in normal crustal rocks ( $10^{-6}$  to  $10^{-5}$ ). The high initial  $^{87}\text{Sr}/^{86}\text{Sr}$  ratio ( $0.7218 \pm 14$ ) is consistent with a mantle source contaminated by Late Proterozoic country rocks. About  $\sim 10^{10}$  mol  $\text{g}^{-1}$   $^{40}\text{Ar}_E$  would have to be incorporated into the feldspar (oligoclase) to elevate its age by 100 Ma. This is less than observed in other feldspars [3,4] and yet is clearly discernible in the isotope systematics.

Assuming  $^{40}\text{Ar}_E$  and halogens dissolved in circulating hydrothermal fluids are trapped in fluid inclusions, what do their concentrations and composition tell us about granite formation? Are the fluids magmatic or meteoric in origin? Is  $^{40}\text{Ar}_E$  locally derived? What is the significance of the  $^{40}\text{Ar}^*/\text{Cl}$  ratio? How reliable are corrections to K-Ar ages based on  $^{40}\text{Ar}^*/\text{Cl}$ ?

To answer these questions, we have analysed new samples from Hamlet Bjerg and the Strontian granite (Scottish Caledonides) using the  $^{40}\text{Ar}$ - $^{39}\text{Ar}$  method. We shall present results from *in vacuo* crushing and laser stepped heating of feldspar, quartz and micas and discuss the sources of fluids in the context of magma sources and fluid-rock interactions during cooling.

[1] Kelley, S. P., *et al.*, Earth Planet. Sci. Lett. 79, 303-318, 1986. [2] Turner, G. and Bannon, M. P., Geochim. Cosmochim. Acta 56, 227-243, 1992. [3] Burgess, R., *et al.*, Earth Planet. Sci. Lett. 109, 127-167, 1992. [4] Burgess, R. and Parsons, I., Contrib. Mineral. Petrol. 115, 345-355, 1994. [5] Rex, D. C. and Gledhill, A. R., Rapp. Grønlands geol. Unders. 104, 47-72, 1981.

## AUTHOR INDEX

- Abraham, J.D., 49  
 Achmedov, A.M., 257  
 Ackert, R., 184  
 Adachi, M., 290, 311  
 Adams, C., 151  
 Aeschbach-Hertig, W., 172  
 Aggarwal, J.K., 1  
 Agrinier, P., 2  
 Ahrendt, H., 320  
 Aizenshtat, Z., 301  
 Akers, W., 128  
 Alam, S., 372  
 Al-Kadasi, M., 216  
 Aleinikoff, J.N., 2  
 Alexander, C.M. O'D., 3  
 Allan, G.L., 58, 169, 306  
 Allan, J.F., 3, 69  
 Allan, T.L., 352  
 Allègre, C.J., 280  
 Alpers, C.N., 4  
 Amari, S., 4, 28  
 Amato, J.M., 5  
 Amelin, Y., 5, 68  
 Ames, L., 6  
 Amouric, M., 97, 273  
 Amundson, R.G., 6, 157  
 Anderson, R.S., 7, 265  
 Anderson, S.P., 7  
 Anderson, T.B., 44  
 Andersson, U.B., 8  
 André, L., 8  
 Andrew, A.S., 352  
 Andriessen, P.A.M., 9, 25, 270, 277  
 Anno, K., 308  
 Anthes, G., 9  
 Anthony, E.Y., 10, 355  
 Aoki, M., 90  
 Aquilina, L., 82  
 Arakawa, Y., 10  
 Archibald, D.A., 18  
 Arculus, R.J., 168  
 Arehart, G.B., 90  
 Armienti, P., 325  
 Armstrong, R.A., 11, 186  
 Armstrong, R.L., 217  
 Arnaud, N.O., 11, 166  
 Arne, D.C., 12  
 Arnold, J.R., 234, 262  
 Arnold, M., 273  
 Arnould, M., 12  
 Aronson, J.L., 13, 57, 346  
 Arth, J.G., 13  
 Asahara, Y., 14, 315  
 Ash, R.D., 14  
 Aspden, J., 234  
 Austin, P., 168  
 Awwiller, D.N., 15  
 Ayalon, A., 15  
 Ayers, M., 336  
 Ayliffe, L.K., 15, 16  
 Ayuso, R.A., 13  
 Ba-B'ttat, M.A., 352  
 Babinski, M., 16, 335  
 Bachelery, P., 292  
 Bacon, C.R., 17  
 Bacon, P.M., 361  
 Baker, J., 17  
 Baker, J.A., 18, 216  
 Bakke, A., 210  
 Baksi, A.K., 18  
 Baldridge, W.S., 293  
 Baldwin, S.L., 19, 34  
 Ball, J.D., 19  
 Ballèvre, M., 97, 273  
 Banks, D.A., 218  
 Barczus, H.G., 341  
 Barker, A.P., 20  
 Barling, J., 20, 137  
 Barovich, K.M., 219  
 Barreiro, B.A., 21, 160, 248, 307  
 Barth, S., 21, 338  
 Basei, M.A.S., 22  
 Baskakov, A.V., 114  
 Baskaran, M., 22  
 Basu, A.R., 23, 317  
 Baumgartner, P.O., 30, 226  
 Baur, H., 42, 172  
 Beaumont, V., 23  
 Bebout, G.E., 24  
 Beck, J.W., 219  
 Becker, T.A., 24, 265, 332, 337, 345  
 Beer, J., 153  
 Beets, C.J., 25  
 Beetsma, J.J., 25, 295  
 Begemann, F., 238  
 Beiriger, J.M., 296  
 Beliaty, B.V., 217  
 Bell, K., 30  
 Belshaw, N.S., 26, 343, 369  
 Belyatsky, B.V., 26  
 Bemis, B.E., 301  
 Bennett, V.C., 27  
 Benoit, P.H., 27  
 Berger, G.W., 28  
 Bernatowicz, T., 28  
 Bernius, M.T., 242  
 Bertotti, G., 353  
 Beverding, A.M., 29  
 Bhattacharya, S.K., 29  
 Bibikova, E., 60, 295  
 Bickel, R.A., 302  
 Bickford, M.E., 222  
 Bickle, M.J., 52  
 Bideau, D., 2  
 Bigazzi, G., 173, 345  
 Biino, G.G., 237  
 Bijma, J., 301  
 Bikerman, M., 30  
 Bill, M., 30  
 Bird, J.R., 58  
 Black, P.M., 196  
 Blake, S., 310  
 Blakey, S., 216  
 Blenkinsop, J., 31  
 Bloch, J.D., 272  
 Blomqvist, R., 105  
 Blum, J.D., 31, 50  
 Blusztajn, J.S., 32, 130  
 Bodvarsson, G.S., 93  
 Bogaard, P.V.D., 32  
 Bogdanova, S., 60, 295  
 Bogdanovski, O.G., 33  
 Boghossian, N.D., 33  
 Bohlke, J.K., 77  
 Bohor, B.F., 141  
 Bohrson, W.A., 34  
 Bonini, J.A., 34  
 Bonotto, D.M., 35  
 Booij, E., 35  
 Borchartt, G., 36  
 Boriani, A., 36  
 Borole, D.V., 37  
 Bossi, J., 318  
 Bottrell, S.H., 20  
 Bougault, H., 85  
 Boulegue, J., 82  
 Bourdon, B., 37, 276, 371  
 Bourles, D.L., 41  
 Boven, A., 8

Bowring, S.A., 38, 131, 138  
 Boyce, A.J., 38  
 Brack, P., 229  
 Bradshaw, J.D., 151  
 Brandon, A.D., 39, 71  
 Breaks, F.W., 67  
 Brenninkmeijer, C.A.M., 138  
 Brewer, T.S., 74  
 Bridges, J.C., 14, 104  
 Brimhall, G.H., 39  
 Briot, D., 40  
 Brito Neves, B.B., 335  
 Broecker, W.S., 40, 195, 279, 286  
 Brook, E.J., 41, 184  
 Brown, E.T., 41  
 Brown, K., 31  
 Brown, R.W., 42, 188, 310  
 Broxton, D.E., 355  
 Bruno, L.A., 42, 153, 282  
 Bryant, G., 105  
 Buchardt, B., 43, 152  
 Bukshpan, S., 190  
 Burbank, D.W., 190  
 Burgess, R., 15, 43  
 Burkland, M.K., 312  
 Burnard, P.G., 16, 44  
 Burnham, K., 44  
 Burruss, R.C., 329  
 Burton, K.W., 45, 204  
 Byers, F.M., Jr., 355  
  
 Caffee, M.A., 127  
 Caffee, M.W., 45, 93, 100, 190, 234, 285  
 Caldwell, E.A., 46, 287  
 Camargo, P.B.De, 46  
 Cameron, K.L., 47, 233  
 Campajola, L., 77  
 Campal, N., 318  
 Campbell, J.D., 171  
 Campbell, K.R., 71, 76  
 Capo, R.C., 47  
 Carignan, J., 48, 108  
 Caroff, M., 341  
 Carr, G.R., 48, 240  
 Carr, S.D., 243  
 Carroll, J., 49  
 Carroll, M.R., 166, 193  
 Carter, A., 148  
 Castaneda, C., 29  
 Castrec, M., 82  
 Cavazza, W., 31  
 Cerling, T.E., 49, 348  
  
 Chabaux, F., 50  
 Chadwick, O.A., 47, 144, 305  
 Chakravarti, A., 29  
 Chakravarty, N., 29  
 Chamberlain, C.P., 50, 304  
 Chamberlain, K.R., 51, 106  
 Champion, D.E., 51, 332  
 Chan, L.-H., 52, 359  
 Chapman, H.J., 52, 269  
 Chase, R.L., 69, 217  
 Chaudhuri, S., 61  
 Chaussidon, M., 53  
 Chawala, H.S., 338  
 Chazot, G., 216  
 Cheilletz, A., 53  
 Chen, C.-H., 54, 359  
 Chen, H.-W., 189  
 Chen, J., 54, 158, 349  
 Chen, J.C., 242  
 Chen, J.H., 25, 55  
 Chen, S.-M., 57, 120  
 Chen, Y.-G., 56  
 Chen, Y.-W., 57, 361  
 Chen, Y.D., 55, 56  
 Chen, Z.-S., 364  
 Chenery, C., 140  
 Cheng, Z., 54  
 Cheng, Z.-Y., 195  
 Chernet, T., 57  
 Cherry, J.A., 336  
 Chesley, J.T., 208  
 Childe, F.C., 58  
 Chivas, A.R., 58, 74, 107, 169, 247  
 Christensen, J.N., 122  
 Christie, D.M., 256  
 Chung, S.-L., 59  
 Churikova, T.G., 59  
 Cisar, D.J., 49  
 Civetta, L., 66  
 Claesson, S., 60  
 Claoué-Long, J., 299  
 Clark, A.H., 55  
 Class, C., 60  
 Clauer, N., 61, 327, 372  
 Clayton, R.N., 76, 247, 278, 348, 362  
 Clemens-Knott, D., 61  
 Clement, S.W.J., 62  
 Cliff, B., 149  
 Cliff, R.A., 62  
 Cliff, S.S., 63  
 Coccioni, R., 223, 373  
 Cohen, A.S., 50, 63  
  
 Cole, D.R., 143, 223  
 Coleman, D.S., 38  
 Coleman, M.L., 64, 227  
 Coler, D.G., 64  
 Colin, F., 41  
 Colley, H.C., 245  
 Colodner, D.C., 260  
 Compston, D.M., 65  
 Compston, W., 62, 65  
 Condomines, M., 292  
 Conrad, J.E., 84  
 Conrad, M.E., 66, 150, 215  
 Constantine, A., 98  
 Conticelli, S., 66  
 Copeland, P., 67  
 Cordani, U.G., 220  
 Corfu, F., 67, 281  
 Cornett, J., 83  
 Cornett, R.J., 178  
 Corriveau, L., 5, 68  
 Cosca, M.A., 68, 266, 339  
 Coulon, C., 80  
 Cousens, B.L., 69  
 Cox, S., 243  
 Cox, S.J.D., 112  
 Coyle, D.A., 69  
 Craig, H., 70  
 Cramer, J., 83  
 Creaser, R.A., 71  
 Cresswell, R.G., 169, 306  
 Criss, R.E., 71, 76  
 Crowe, B.M., 133, 248, 255  
 Crowhurst, P.V., 72  
 Crowley, S.F., 19  
 Cui, Y., 106  
 Cumbaa, S., 297  
 Curtis, C.D., 64  
 Curtis, D.B., 83  
 Curtis, G.H., 77, 265, 332  
  
 D'Antonio, M., 66  
 D'Orazio, M., 325  
 Daag, A.S., 359  
 Dahl, P.S., 72  
 Dai, T., 73  
 Dalrymple, G.B., 73, 183  
 Daly, J.S., 74, 214  
 Dammer, D., 74  
 Danhara, T., 154  
 Danti, K., 90  
 Darbyshire, D.P.F., 75  
 Darling, G., 118  
 Davidson, E.A., 46  
 Davidson, J.P., 259, 319

- Davie, R., 58  
 Davies, G.R., 75, 135, 177, 225, 302, 325, 334  
 Davis, A.M., 76, 247, 348  
 Davis, A.S., 117  
 Davis, M., 45  
 Davis, R., 262  
 Davis, S., 45  
 Davisson, M.L., 71, 76, 296  
 De Jong, A.F.M., 334  
 Deak, J., 77  
 Dean, J.A., 48  
 Deck, B., 286  
 Decourten, F., 348  
 Defant, M.J., 168  
 Deino, A.L., 77, 173, 265, 332, 345, 373  
 DeJong, K., 97  
 DeLaeter, J.R., 78, 166  
 DeLange, G.J., 25  
 Deloule, E., 78, 268  
 Demaiffe, D., 20, 79  
 Demény, A., 79  
 Deniel, C., 80  
 DeNiro, M.J., 319  
 Dep, L., 80, 91  
 DePaolo, D.J., 81, 111, 159, 293, 312  
 Derry, L.A., 81, 104  
 Descarceaux, S., 41  
 Deseo, E., 77  
 Desmons, J., 147  
 Devey, C.W., 134, 142  
 DeWit, M.J., 186  
 Dia, A.N., 82  
 Diamond, L.W., 249  
 Dick, G.S., 265  
 Dick, H., 32  
 Dickey, N., 165  
 Dickinson, W.R., 109, 112  
 Dietrich, W.E., 7, 285  
 Ding, T-P., 82, 158  
 Dingwell, D.B., 193  
 Dixon, P.R., 83  
 Doe, B.R., 83  
 Dolenc, T., 94  
 Donahue, D.J., 29  
 Dong, H., 84  
 Donnelly-Nolan, J.M., 84, 332  
 Donovan, J., 39  
 Dorn, R.I., 195  
 Dosso, L., 85  
 Downes, H., 205, 271, 344  
 Draper, D.S., 166  
 Drimmie, R.J., 85, 336  
 Drummond, M.S., 168  
 Duddy, I.R., 221  
 Duffield, W.S., 274  
 Dunai, T.J., 86  
 Duncan, R.A., 86, 91, 256, 294  
 Dunkl, I., 87  
 Dunkley, P., 21  
 Dunlap, C.E., 87  
 Dunlap, W.J., 88  
 Dunphy, J.M., 88  
 Dupuy, C., 341  
 Durakiewicz, T., 89  
 Dymek, R.F., 287  
 Eastoe, C.J., 326  
 Ebihara, M., 136, 280  
 Edwards, B.R., 106  
 Edwards, R.L., 108, 219  
 Eggenkamp, H., 64  
 Eichelberger, J.C., 209  
 Eikenberg, J., 341  
 Ekwueme, B.N., 89  
 Eldridge, C.S., 90  
 Elliot, D.H., 101  
 Elliott, C., 13  
 Elliott, T.E., 90, 202, 276, 371  
 Elmore, D., 80, 91, 176, 250, 262  
 Emslie, R.F., 124  
 Englert, P.A.J., 29, 127, 262  
 Engstrom, D., 356  
 Epstein, S., 97, 206  
 Erba, E., 91  
 Erel, Y., 31  
 Esser, B.K., 92  
 Esser, R.P., 92  
 Evans, J.A., 93  
 Evans, J.M., 306  
 Evensen, N.M., 297, 360  
 Evenson, E.B., 114  
 Ewing, R.C., 238  
 Eyal, M., 96  
 Fabryka-Martin, J., 80, 83, 93  
 Faganeli, J., 94  
 Faggart, B.E., 23  
 Fahey, A.J., 94  
 Fallick, A.E., 38, 215, 308  
 Fang, Z., 95, 363  
 Fanning, C.M., 171  
 Farmer, G.L., 340  
 Farquhar, R.M., 95  
 Farrar, E., 18, 55  
 Farrell, J.W., 121  
 Fehn, U., 96, 224  
 Feinstein, S., 96  
 Feng, X., 97  
 Feraud, G., 53, 97, 273  
 Ferguson, K.M., 98  
 Ferrara, G., 98, 201  
 Ferreira, V.P., 99, 291  
 Ferris, F.G., 289  
 Fifield, L.K., 58, 169, 306  
 Filippi, M.L., 99  
 Finkel, R.C., 45, 100, 127, 190, 234, 265, 285  
 Fitton, J.G., 188  
 Fitzgerald, J.F., 128  
 Fitzgerald, P.G., 100, 262  
 Fitzgerald, R.C., 74  
 Fleck, R.J., 101, 332  
 Flegal, A.R., 268, 279, 297  
 Fleming, T.H., 101  
 Foden, J.D., 102  
 Fogel, R.A., 149  
 Foland, K.A., 101, 102, 185  
 Forde, E.J., 103  
 Foster, D.A., 42, 72, 103, 221, 235  
 France-Lanord, C., 81, 104, 298  
 Franchi, I.A., 104  
 Francis, D., 48  
 Francois, R., 361  
 Franklin, J.M., 370  
 Franz, L., 320  
 Frape, S.K., 85, 105, 336  
 Freedman, P.A., 122  
 Frei, R., 105, 194, 230  
 Freifeld, B., 66  
 Frey, F.A., 351  
 Friedman, R.M., 106  
 Frost, C.D., 51, 106, 284  
 Fu, H-Q., 259  
 Fuck, R.A., 252  
 Funaki, M., 314  
 Furfaro, D., 251  
 Fyfe, W.S., 309  
 Gabel, M., 157  
 Gagan, M.K., 107  
 Galer, S.J.G., 263  
 Gallagher, K., 107, 336  
 Gallahan, W.E., 35  
 Gallup, C.D., 108, 219  
 Gamo, T., 330  
 Gans, C., 29

- Gans, P.B., 188, 231  
 Gärtner, M., 263  
 Gariépy, C., 108  
 Gautschi, A., 324  
 Gavrieli, I., 301  
 Gebauer, D., 109, 337  
 Gehrels, G.E., 109  
 Geissman, J., 10  
 Gelman, M.L., 110  
 Gerstenberger, H., 110  
 Gertis, J., 289  
 Getty, S.R., 111  
 Ghaleb, B., 164  
 Giacobbe, A., 116  
 Gibb, A., 26  
 Gibson, E.K., Jr., 271, 298  
 Gigenbach, W.F., 200  
 Gill, J.B., 87, 241  
 Gilmour, J.D., 14, 111  
 Giobbi Origoni, E., 36  
 Giraudeau, J., 186  
 Giret, A., 206  
 Giuliani, G., 53  
 Gleadow, A.J.W., 42, 112, 176,  
 235, 236, 261  
 Gleason, J.D., 112  
 Goldfarb, R., 210  
 Goldman, I., 127  
 Goldstein, S.J., 293  
 Goldstein, S.L., 60, 263, 327  
 Gomes, D.P., 316  
 Goodell, P.C., 355  
 Goodfellow, W.D., 370  
 Goodfriend, G.A., 113  
 Gopalan, K., 113  
 Gorokhov, I.M., 114  
 Gorokhovskiy, B.M., 191  
 Goslar, T., 273  
 Gosse, J.C., 114  
 Goswami, J.N., 115, 353  
 Gotih, R.P., 257  
 Graf, Th., 115  
 Graham, D.W., 116, 125  
 Graham, R.C., 305  
 Granger, D.E., 116  
 Graubard, C.M., 207  
 Graves, G., 50  
 Gray, L.B., 84, 117  
 Gregoire, M., 206  
 Gregory, R.T., 98, 117  
 Grey, K., 275  
 Grier, J.A., 312  
 Griesshaber, E., 118  
 Griffin, T.J., 231  
 Grimm, R.E., 262  
 Grinenko, L.N., 118  
 Grinenko, V.A., 119  
 Grove, M., 119, 128  
 Gui, X-T., 120, 361  
 Guise, P.G., 266  
 Gunn, S.H., 17, 120  
 Guo, Y., 158  
 Guo, Z., 349  
 Gust, D.A., 168  
 Haapala, I., 259  
 Hacker, B.R., 121  
 Hackspacher, P., 335  
 Haggerty, S.E., 200  
 Hajdas, I., 195  
 Halicz, L., 284  
 Hall, A.J., 38  
 Hall, C.M., 84, 121, 122, 188  
 Hall, R., 103  
 Hallett, R.B., 122  
 Halliday, A.N., 84, 122, 188  
 Hames, W.E., 123, 138  
 Hamilton, M.A., 124, 320  
 Hamilton, P.J., 352  
 Hamlin, S.N., 4  
 Han, J., 124, 372  
 Han, Y., 153  
 Hanan, B.B., 125  
 Hancock, R.G.V., 95  
 Hansen, K., 125  
 Hansen, B.T., 320  
 Hanson, G.N., 133, 279  
 Hanyu, T., 126  
 Harangi, Sz., 79  
 Harper, C.L., Jr., 126, 156  
 Harris, C., 127, 186  
 Harris, J.W., 43, 198  
 Harris, L., 285  
 Harris, L.J., 127  
 Harrison, T.M., 119, 128  
 Harrop, P.J., 129  
 Hart, C.J.R., 129  
 Hart, S.R., 32, 130, 302  
 Hart, W.K., 57, 346  
 Hartmann, J., 130  
 Hartmann, L.A., 309  
 Hasebe, N., 131, 308  
 Hashizume, K., 309  
 Hawkesworth, C.J., 22, 145,  
 211, 245  
 Hawkins, D.P., 131  
 Hawkins, M.P., 318  
 Heaman, L.M., 74, 132, 187,  
 228, 246, 258, 362  
 Heaney, P., 328  
 Hebeda, E.H., 258  
 Hedenquist, J.W., 90  
 Heijnis, H., 132  
 Heimann, A., 101  
 Heimann, M., 139  
 Hein, J.R., 45, 50, 343, 359  
 Heisinger, B., 130  
 Heithersay, P.S., 48  
 Heizler, M.T., 92, 128, 133,  
 212  
 Hékinian, R., 2  
 Helfer, M., 282  
 Helmers, H., 325  
 Hemming, N.G., 279  
 Hemming, S.R., 133  
 Hémond, C., 134  
 Henderson, C.M.B., 185  
 Henderson, G.M., 204  
 Hendricks, D.M., 47  
 Henry, C.D., 134  
 Hensen, B.J., 367  
 Hertogenk, J., 142  
 Herzog, G.F., 175  
 Hess, J.C., 135  
 Heumann, A., 135  
 Heumann, K.G., 338  
 Hewins, R.H., 362  
 Hidaka, H., 136  
 Hildebrand, A.R., 161  
 Hill, K.C., 72, 221, 261  
 Hilton, D.R., 86, 146,, 137 147  
 Hirooka, K., 314  
 Hiyagon, H., 137, 221, 280  
 Hodder, P.S., 138  
 Hodges, K.V., 138  
 Hoehndorf, A., 139  
 Hofer, M., 172  
 Hoffmann, G., 139  
 Hofmann, A.W., 249, 303  
 Hogan, L.G., 86  
 Hohmann, R., 172  
 Hoke, L., 140  
 Holden, P., 319  
 Holk, G.J., 140  
 Holliger, P., 136  
 Holm, P.M., 141, 161, 246  
 Holmes, C.W., 141  
 Holmes, R., 50  
 Honda, M., 136, 142, 211, 334  
 Hoogewerff, J.A., 142  
 Hoover, J.D., 213

- Horita, J., 143  
 Housh, T.B., 38  
 Howard, K.A., 103, 143  
 Howell, D.G., 109  
 Hrabi, B., 342  
 Hsieh, J.C.C., 144, 305  
 Hu, A., 144  
 Huang, B., 228  
 Huang, M., 145  
 Huang, Y.-M., 145  
 Huang, Z., 356  
 Hudson, G.B., 285  
 Huff, W.D., 364  
 Huhma, H., 146, 299  
 Hulston, J.R., 146, 147  
 Hunziker, J.C., 30, 68, 99, 147, 226, 288, 339  
 Hurford, A.J., 147, 148, 360  
 Huss, G.R., 94, 148  
 Hutcheon, I., 181  
 Hutcheon, I.D., 149  
 Hutchison, R., 14, 104  
  
 Ikeya, M., 328  
 Iliffe, T.M., 22  
 Imboden, D.M., 172  
 Inayama, E., 315  
 Inger, S., 149  
 Ingle, J.C., 150  
 Ingraham, N.L., 46, 287  
 Ingram, B.L., 150  
 Innocenti, F., 325  
 Ireland, T.R., 151, 196  
 Irwin, J.J., 151  
 Isachsen, C.E., 38  
 Isdale, P.J., 107  
 Ishibashi, J., 330  
 Israelson, C., 43, 152  
 Itaya, T., 152, 154  
 Ito, E., 153, 356  
 Ivanenko, V.V., 163  
 Ivanov, V., 8  
 Ivy, S.D., 42, 153, 282  
 Iwano, H., 154  
 Iwasaki, I., 154  
 Iwata, N., 155  
 Iyer, S.S., 155  
  
 Jackson, C., 127  
 Jackson, V., 342  
 Jacobsen, S.B., 126, 156  
 Jaeckel, P., 181  
 Jagoutz, E., 33, 156  
 Jahren, A.H., 157  
  
 Jakobsson, S., 292  
 Jamieson, R.A., 354  
 Javoy, M., 2, 23, 157  
 Jefferey, A., 146, 147  
 Jemielita, R., 234  
 Jenkins, C., 321  
 Jenkins, R.J.F., 65  
 Jessberger, E.K., 216  
 Jiang, S-Y., 158  
 Jiang, S., 82  
 Jiang, W., 124  
 Jiang, Z., 158  
 John, B.E., 103, 143  
 Johnson, C.M., 219  
 Johnson, G.D., 304  
 Johnson, K., 159  
 Johnson, R.G., 108  
 Johnson, T.M., 159  
 Johnston, J.C., 160  
 Jones, C., 160  
 Jones, C.E., 122, 315  
 Jones, P.W., 75  
 Jørgensen, N.O., 161  
 Joron, J-L., 85  
 Jull, A.J.T., 194, 250, 262  
 Jull, T., 29  
 Juraske, S., 338  
  
 Kagi, H., 311  
 Kamensky, I.L., 249  
 Kamioka, H., 14  
 Kamo, S.L., 161, 309  
 Kampata, M., 79  
 Kaneoka, I., 126, 155, 162  
 Kaplan, I.R., 146, 147  
 Kapusta, Y., 162, 190, 303  
 Karasaki, K., 66  
 Karhu, J.A., 163  
 Karpenko, M.I., 163  
 Karpenko, S.F., 33  
 Kashgarian, M., 164  
 Kastner, M., 245  
 Kato, K., 276  
 Kaufman, A., 164  
 Kaufmann, R.S., 165  
 Kawashima, A., 165  
 Kawashita, K., 220  
 Keeling, R.F., 286  
 Kelley, S.P., 11, 43, 166, 261, 336  
 Kelly, E.F., 144  
 Kelts, K., 153  
 Kenneally, J.M., 296  
 Kennedy, A.K., 166, 251, 323  
  
 Kennedy, M.J., 167  
 Kent, A.J.R., 167  
 Kepezhinskas, P.K., 168  
 Keppens, E., 372  
 Kersting, A.B., 168  
 Ketcham, D.H., 169  
 Keywood, M.D., 58, 169  
 Khai, N.Vu., 170  
 Kigam, T., 290  
 Kilius, L., 83  
 Kim, C.B., 330  
 Kim, J.S., 115  
 Kim, K., 29  
 Kim, S-J., 170  
 Kimbrough, D.L., 171  
 Kinny, P.D., 171  
 Kipfer, R., 172  
 Kirchner, J.W., 116  
 Kirschner, D.L., 172  
 Kiseleva, V. Yu., 254  
 Kiss, E., 58  
 Kistler, R.W., 101, 173  
 Kitada, N., 173, 345  
 Kitchen, N.E., 174  
 Kiyota, K., 174, 309  
 Klein, J., 114, 175, 234, 262, 366  
 Klötzli, U.S., 175  
 Knies, D.L., 176  
 Koehler, A.M., 29  
 Kohl, C.P., 100, 234  
 Kohn, B.P., 96, 112, 176  
 Kohn, M.J., 177  
 Kolodny, Y., 203  
 Konnerup-Madsen, J., 246  
 Koppers, A.A.P., 177, 256, 282  
 Korsch, R.J., 261  
 Korschinek, G., 130  
 Kostitsyn, Yu.A., 59  
 Kotarba, M., 178  
 Kotlarsky, P., 162, 190, 303  
 Kotov, A.B., 191  
 Kotzer, T.G., 178  
 Kowallis, B., 173, 345  
 Kramers, J.D., 179  
 Krishnamurthy, R.V., 179  
 Krogh, T.E., 56, 161, 180, 309  
 Krol, M.A., 180  
 Kröner, A., 89, 181, 327  
 Krouse, H.R., 118, 119, 155, 181, 207, 272, 300  
 Kruger, F.J., 182  
 Ku, T., 49  
 Ku, T-L., 182, 189, 199

- Kubik, P.W., 153, 262  
 Kuc, T., 273  
 Kulkarni, K.M., 183  
 Kunk, M.J., 134, 183  
 Kurz, M.D., 63, 184  
 Kusakabe, M., 182  
 Kutuyavin, E.P., 114  
 Kuzmin, D.S., 254  
 Kyle, P.R., 92, 122, 130, 184, 241  
  
 Lal, D., 262  
 Lambert, R.St.J., 39  
 Lan, C-Y, 362  
 Landoll, J.D., 185  
 Langmuir, C.H., 37  
 Lanphere, M.A., 17, 185  
 Lansdown, J., 289  
 Larimer, R.M., 127  
 Laurenzi, M.A., 173, 186, 333, 345  
 Lavelle, M., 186  
 Lawn, B.R., 114  
 Layer, P.W., 187, 210, 351  
 Lea, D.W., 301  
 LeCheminant, A.N., 187  
 Lee, D.-C., 122, 188  
 Lee, E.H., 242  
 Lee, J., 188  
 Lee, J.K.W., 189  
 Lee, K.S., 242  
 Lee, S.-G., 290  
 Lee, T., 189, 359  
 Leeman, W.P., 98  
 Lehman, T., 197  
 Lehmann, B., 324  
 Lehmann, E., 341  
 Leland, J.F., 190  
 Lempert, G.D., 190  
 Lerche, I., 49  
 Lesko, K.T., 127  
 Levchenkov, O.A., 191  
 Levkovskaya, G.M., 191  
 Levsky, L.K., 26  
 Lewis, A.J., 192  
 Lewis, R.S., 4, 28, 192, 247  
 Leybourne, M.I., 69  
 Li, C., 349  
 Li, H-m., 95, 363  
 Li, H., 193, 198  
 Li, J., 300  
 Li, X-H., 120  
 Li, Y., 82  
 Libby, W.G., 78  
  
 Libourel, G., 193  
 Liebetrau, V., 194, 253  
 Liegeois, J-P., 8  
 Lienkaemper, J.J., 36  
 Lifton, N.A., 194, 250  
 Lin, J.C., 195  
 Lin, R.-F., 195  
 Lindsay, J.M., 196  
 Lippolt, H.J., 135  
 Lipschutz, M.E., 91, 176  
 Lister, G.S., 19  
 Litherland, M., 234  
 Liu, C., 228  
 Liu, J., 193, 198, 364  
 Liu, T-K., 56  
 Liu, Y., 196  
 Lloyd, J.W., 20  
 Loague, K., 7  
 Lokhov, K.I., 191  
 Long, L.E., 99, 169, 197, 291  
 Longstaffe, F.J., 15  
 Loosli, H., 324  
 Lorand, J.-P., 264  
 Loske, W.P., 197  
 Lovera, O.M., 128  
 Lowenstein, T., 300  
 Lowry, D., 38, 198  
 Lu, H-Z., 193, 198  
 Luchitta, I., 45  
 Ludden, J.N., 48, 88  
 Ludwig, K.R., 199  
 Luo, S., 182, 199  
 Luz, B., 203  
 Lyon, G.L., 200  
 Lyon, I.C., 281  
  
 M. Grajales, N., 295  
 Ma, Z., 247  
 Maas, R., 171  
 Macdougall, J.D., 200  
 Macfarlane, P.A., 76, 296  
 Machado, N., 252  
 Machavaram, M., 179  
 MacPherson, C.G., 18, 198  
 MacRae, R.A., 229  
 Magenheim, A.J., 201  
 Maggetti, M., 253  
 Magro, G., 201  
 Mahoney, J.B., 202  
 Mahoney, J.J., 318  
 Mancktelow, N.S., 286  
 Manetti, P., 325  
 Mansfeld, J., 60  
 Marcantonio, F., 202, 239  
  
 Marchant, K., 302  
 Markel, D., 203  
 Markewich, H.W., 244  
 Marriner, G.F., 344  
 Marshall, B.D., 203  
 Marshall, J.D., 19  
 Marshintsev, V.K., 149  
 Martel, D.J., 45, 204  
 Marti, K., 115  
 Martinelli, L.A., 46  
 Masarik, J., 80, 204  
 Mason, P.R.D., 205  
 Masson, H., 172  
 Masterman, S., 210  
 Masuda, A., 145, 165, 205, 257, 275, 290, 356  
 Masuda, H., 173, 345  
 Mathez, E.A., 149  
 Matsumoto, A., 308  
 Matthey, D.P., 18, 198, 211, 321  
 Matthai, S.K., 65  
 Matthews, A., 17, 206  
 Mattielli, N., 206  
 Mattinson, J.M., 171, 207, 209  
 Matukov, D.I., 191  
 Maury, R.C., 168, 341  
 Mayeda, T.K., 362  
 Mayer, B., 207  
 Mazor, E., 208  
 McCandless, T.E., 208, 274  
 McClelland, W.C., 207, 209  
 McConnell, V.S., 209  
 McConville, P., 373  
 McCoy, D., 210  
 McCulloch, M.T., 27, 210, 294  
 McCurry, M., 340  
 McDermott, F., 211  
 McDougall, I., 74, 142, 167, 211, 300, 334  
 McDowell, F.W., 47, 212  
 McFadden, L.D., 248  
 McIntosh, W.C., 10, 92, 133, 184, 212, 241  
 McKeegan, K.D., 128  
 McKibben, M.A., 90, 213  
 McKinley, J.P., 213  
 McLelland, J., 214  
 McLennan, S.M., 133  
 McMillan, N.J., 47  
 McNaughton, N.J., 171  
 McNicoll, V.J., 258  
 McWilliams, M., 214  
 Meier, M., 21, 229, 237, 302  
 Melezhik, V.A., 215

- Mello, I.S.C., 316  
 Melnikov, N.N., 114  
 Menard, T., 307  
 Menchaca, L.B., 215  
 Menuge, J.F., 74  
 Menzies, M.A., 18, 216, 360  
 Meshik, A.P., 216, 290  
 Mezger, K., 133  
 Michael, P.J., 125, 201, 217  
 Middleton, R., 114, 175, 262, 366  
 Mikhalsky, E.V., 217  
 Millar, I.L., 218  
 Millard, H.T., 244  
 Miller, B.R., 286  
 Miller, D.S., 329  
 Miller, E.L., 188  
 Miller, M., 238  
 Miller, M.F., 218  
 Milling, M.E. Jr., 219  
 Min, G.R., 219  
 Mineev, S.D., 119  
 Mironov, A.G., 220  
 Misuzaki, A.M.P., 220  
 Mitchell, M.M., 221  
 Mitrofanov, F.P., 56  
 Miyazaki, A., 137, 221  
 Mock, T.D., 222  
 Monaghan, M.C., 176, 222  
 Moncaster, S.J., 20  
 Monger, H.C., 223  
 Montanari, A., 223, 224, 373  
 Montgomery, D.R., 7  
 Moorbath, S., 275, 369  
 Moore, W.S., 245  
 Moran, J.E., 96, 224  
 Morante, R., 225  
 Moree, M., 225  
 Morettini, E., 226  
 Morin, D., 5  
 Morishita, Y., 226  
 Morozova, I.P., 254  
 Morris, J., 366  
 Mortensen, J.K., 227  
 Mortimer, G., 210  
 Mortimer, R.J.G., 227  
 Morton, A.C., 74  
 Moser, D.E., 228  
 Moureau, J., 79  
 Mu, Z., 228  
 Muecke, G.K., 229  
 Muhs, D.R., 2  
 Muir, R., 151  
 Mukasa, S.B., 122, 184, 241  
 Mundil, R., 229  
 Murphy, W., 93  
 Murray, B.C., 305  
 Murrell, M.T., 251, 293  
 Murton, B.J., 317  
 Nagao, K., 173, 345  
 Nagasawa, H., 230  
 Nægler, Th.F., 230, 253  
 Nair, R.R., 37  
 Nakai, S., 357  
 Napier, B., 127  
 Nauert, J.L., 231  
 Nevada, S.V., 183  
 Negrey, E.V., 370  
 Nelson, D.R., 231  
 Nelson, S.T., 293  
 Nemchin, A.A., 232, 251  
 Nepstad, D.C., 46  
 Nesje, A., 41  
 Neumaier, S., 130  
 Newberry, R.J., 210  
 Neymark, L.A., 8, 232  
 Niedermann, S., 115  
 Nielsen, H., 301  
 Nielsen, P., 372  
 Niemeyer, S., 296, 297  
 Nier, A.O., 233  
 Nimz, G.J., 93, 233  
 Nishiizumi, K., 100, 234, 262  
 Nishimura, A., 14  
 Nishimura, S., 131, 308, 313, 358  
 Nishri, A., 203  
 Noack, M., 178  
 Noble, S.R., 234  
 Noble, W.P., 235  
 Nolte, E., 130  
 Norman, E.B., 127  
 Norry, M.J., 75, 307  
 Nunez-Betelu, L.K., 229  
 Nutman, A.P., 27  
 O'Brien, A., 235  
 O'Neil, J.R., 270, 339  
 O'Nions, R.K., 26, 45, 50, 63, 204, 236, 343, 369  
 O'Sullivan, A.J., 236  
 O'Sullivan, P.B., 221, 236, 237, 261  
 Oberli, F., 21, 229, 237  
 Oberthuer, T., 139  
 Odin, G.S., 223, 373  
 Okada, T., 152  
 Olinger, C.T., 234  
 Onstott, T.C., 238, 328, 329  
 Orsi, G., 77  
 Orstom, T., 53  
 Osterloh, J., 297  
 Otomo, I., 276  
 Ott, U., 238  
 Ovchinnikova, G.V., 26, 191  
 Owens, T., 312  
 Oxburgh, R., 239  
 Ozima, M., 239, 289  
 Paces, J.B., 232  
 Paepe, R., 372  
 Page, R.W., 240  
 Page, W.D., 24, 240, 345  
 Palacz, Z., 241  
 Palin, J.M., 206  
 Palmer, M.R., 1, 158, 192  
 Pande, K., 338  
 Pankhurst, R.J., 184, 241  
 Panter, K.S., 184, 241  
 Pantulu, G.V., 113  
 Papanastassiou, D.A., 242, 272, 287  
 Park, B.K., 242  
 Parkinson, D.L., 207, 243  
 Parrish, R.R., 175, 243, 354  
 Patchett, P.J., 33, 112, 244, 340  
 Patterson, D.P., 211  
 Patterson, R.T., 31  
 Pattou, L., 264  
 Paul, R.L., 127  
 Pavich, M.J., 244  
 Paytan, A., 245  
 Peacor, D.R., 84  
 Pearce, J.A., 245  
 Pearson, P.N., 152  
 Peate, D.W., 245  
 Peccerillo, A., 66  
 Pedersen, L.E., 246  
 Pedersen, S., 246  
 Pell, S.D., 247  
 Pellin, M.J., 247  
 Peng, T-H., 40  
 Peng, T-R., 347  
 Pennisi, M., 98  
 Perry, F.V., 133, 248, 255  
 Pessenda, L.C.R., 46  
 Peterman, Z.E., 203  
 Peters, M.T., 52  
 Petford, N., 248  
 Petit-Jean, C., 130  
 Petrini, R., 325

- Pettke, Th., 249  
 Petty, G., 176  
 Peucker-Ehrenbrink, B., 249  
 Péwé, T.L., 28  
 Pezdí, J., 94  
 Pezzotta, F., 252  
 Phillips, F.M., 91, 195, 250  
 Phillips, W.M., 250  
 Pickett, D.A., 251  
 Pidgeon, R.T., 232, 251, 302, 323  
 Pik, R., 80  
 Pillinger, C.T., 104, 218  
 Pimentel, M.M., 252  
 Pin, C., 99  
 Pinarelli, L., 36, 252  
 Pisotsky, B.I., 257  
 Plank, T., 90  
 Pokrovsky, B.G., 253  
 Poller, U., 194, 253  
 Ponomarchuk, V.A., 254  
 Porat, N., 254  
 Porcelli, D., 255, 331  
 Poreda, R.J., 49  
 Poths, J., 10, 234, 255  
 Poulson, S., 50  
 Praegel, N.-O., 141  
 Pravdivtseva, O.V., 256, 290  
 Prellwitz, H.S., 30  
 Pringle, M.S., 91, 177, 256, 282  
 Pringle, M.J., 295  
 Prinos, S., 165  
 Pu, Z., 73  
 Puli, G., 325  
 Punongbayan, R.S., 359  
 Pushkarev, Y.D., 257  
  
 QI-LU., 257  
 Quade, J., 250  
  
 Radhakrishna, B.P., 113  
 Rae, J.E., 227  
 Ragetti, R., 258  
 Ragnarsdottir, K.V., 1  
 Rainbird, R.H., 258  
 Raisbeck, G.M., 41  
 Ralska-Jasiewiczowa, M., 273  
 Rämö, O.T., 259  
 Ramos, F.C., 259, 263  
 Rao, S.M., 183  
 Rao, U., 96  
 Rasdas, A.S., 359  
 Rasskasov, S., 8  
  
 Ravenhurst, C.E., 260  
 Ravizza, G.E., 92, 249, 260  
 Raza, A., 261  
 Recy, J., 219  
 Reddy, S.M., 261  
 Redfield, T.F., 262  
 Reed, S.J.B., 369  
 Reedy, R.C., 29, 80, 204, 262  
 Rehkämper, M., 263  
 Reid, M.R., 34, 190, 259, 263  
 Reinfrank, R., 60  
 Reinhard, E.A., 270  
 Reinhardt, E., 31  
 Reisberg, L., 264  
 Reischmann, T., 9, 264  
 Relf, C., 342  
 Rengarajan, R., 113  
 Renne, P.R., 24, 171, 240, 265, 318, 332, 337, 345  
 Repka, J.L., 265  
 Restrepo, P., 266  
 Revesz, K., 77  
 Rex, D.C., 266  
 Reynolds, P.H., 229  
 Richardson, S.H., 267  
 Rink, W.J., 267  
 Ritson, P.R., 268  
 Robert, F., 23, 53, 78, 268  
 Roberts, S., 300  
 Robinson, A.C., 269  
 Roddick, J.C., 124, 269  
 Roden, M.K., 260  
 Roe, L.J., 270  
 Roedder, E., 151  
 Rohrman, M., 270  
 Röhrman, P., 9  
 Rokop, D.J., 83  
 Roldan-Quintana, J., 212  
 Romanek, C.S., 271, 298  
 Ronen, A., 254  
 Rosenbaum, J.M., 271  
 Ross, G.M., 33, 109, 272  
 Roy, A.B., 115  
 Roy-Barman, M., 272  
 Rozanski, K., 273  
 Rubenstone, J.L., 195  
 Ruffet, G., 53, 97, 273  
 Ruiz, J., 112, 208, 266, 274  
 Russell, D., 297  
 Russell, J., 275  
 Rye, R.O., 4  
 Ryerson, F.J., 128  
  
 Sahoo, S.K., 275  
  
 Saito, K., 276  
 Sakai, H., 314  
 Salters, V.J.M., 276  
 Saltus, R.W., 176  
 Samson, S.D., 64, 277  
 Samuel, J., 372  
 Sanders, C.A.E., 9, 277  
 Sandler, A., 303  
 Sanfo, Z., 41  
 Sano, Y., 278  
 Santos, R.V., 278  
 Santosh, M., 332  
 Sanyal, A., 279  
 Sañudo-Wilhelmy, S.A., 279  
 Sarda, P., 280  
 Sarin, M.M., 113  
 Sasada, T., 280  
 Sass, E., 284  
 Savin, S.M., 144  
 Saxton, J.M., 281  
 Schaltegger, U., 281  
 Scheveers, R., 282  
 Schirmick, C., 32  
 Schlüchter, C., 42, 153, 282  
 Schmid, R., 337  
 Schmidt, M.P., 283  
 Schmidt Mumm, A., 139  
 Schnell, U.A.L., 283  
 Schultze-Lam, S., 289  
 Schwarcz, H.P., 254, 267  
 Scoates, J.S., 51, 106, 284  
 Scrivener, R.C., 218  
 Sears, D.W.G., 27  
 Seccombe, P.K., 367  
 Segev, A., 284  
 Seghedi, I., 205  
 Seidemann, D.E., 331  
 Seidl, M.A., 285  
 Semikhatov, M.A., 114  
 Sergeev, S.A., 194, 285  
 Setsuya, N., 54  
 Severinghaus, J.P., 286  
 Seward, D., 286  
 Shadel, C., 287  
 Shao, B., 349  
 Sharma, K.K., 338  
 Sharma, M., 287  
 Sharma, P., 83, 91, 93, 176, 250  
 Sharp, W.D., 24, 265, 332, 345  
 Sharp, Z.D., 30, 68, 172, 288, 339  
 Shatagin, K.N., 288

- Shepherd, T.J., 75  
 Sherry, T., 50  
 Sherwood, L.B., 289  
 Shi, Y., 153  
 Shibata, T., 289  
 Shieh, Y.-N., 170  
 Shimada, C., 313  
 Shimizu, H., 290  
 Shimizu, N., 206  
 Shukolyukov, Yu.A., 216, 256, 290  
 Sial, A.N., 99, 169, 291  
 Siddall, R., 291  
 Sie, S.H., 292  
 Siegel, D.I., 165  
 Sigmarsson, O., 292  
 Signer, P., 42, 258  
 Silantjev, S.A., 33  
 Simonetti, A., 30  
 Sims, K.W.W., 293  
 Sinelnikova, I.M., 191  
 Singer, B.S., 293  
 Singh, B., 39  
 Sinigoi, S., 61  
 Sinton, C.W., 294  
 Sisterson, J., 29  
 Sivell, W.J., 294  
 Skiöld, T., 295  
 Smellie, J.L., 184, 241  
 Smit, J., 295  
 Smith, B.M., 215  
 Smith, C.B., 296  
 Smith, D.K., 296  
 Smith, D.R., 297  
 Smith, G.I., 195  
 Smith, I.E.M., 196  
 Smith, M., 21  
 Smith, P.E., 95, 297, 360  
 Smith, R.D., 47  
 Smithies, H., 231  
 Snee, L.W., 183  
 Snow, J.E., 298  
 Socki, R.A., 271, 298  
 Somayajulu, B.L.K., 113, 299  
 Sorjonen-Ward, P., 299  
 Southon, J.R., 45, 77, 93, 100, 127, 182, 234, 265  
 Speer, J.A., 64  
 Spell, T.L., 67, 300  
 Spencer, K.J., 318  
 Spencer, R., 300  
 Spera, F., 116  
 Spero, H.J., 301  
 Spicuzza, M.J., 209  
 Spiro, B., 140, 301  
 Spivack, A.J., 201, 343  
 Starinsky, A., 284, 301  
 Staudacher, T., 280  
 Staudigel, H., 35, 135, 177, 202, 225, 256, 302, 325, 334  
 Steckler, M.S., 96  
 Steiger, R.H., 194, 285, 302  
 Stein, M., 303  
 Steinitz, G., 162, 190, 303  
 Stephens, W.E., 38  
 Stern, L.A., 304  
 Stevenson, R.K., 304  
 Stewart, B.W., 305  
 Stewart, J.H., 109  
 Stille, P., 327  
 Stoffers, P., 134  
 Stokes, S., 306  
 Stolper, E.M., 206  
 Stone, J., 306  
 Stopforth, S., 155  
 Stott, G.M., 67  
 Stouraiti, C., 307  
 Stowell, H.H., 307  
 Strack, E., 130  
 Strain, P.M., 314  
 Stuart, F., 308, 373  
 Stuart, F.M., 44, 129  
 Stuckless, J.S., 203  
 Stump, E., 262  
 Sudo, M., 308  
 Sugi, S., 276  
 Sugiura, N., 137, 174, 221, 309  
 Suita, M.T.F., 309  
 Summerfield, M.A., 310  
 Sun, S.-s., 59, 240  
 Suppel, D.W., 48  
 Sur, B., 127  
 Suter, G.F., 292  
 Sutherland, S., 40  
 Sutton, A.N., 310  
 Suzuki, K., 311  
 Svetov, S.A., 344  
 Swabey, S.E.J., 211  
 Swager, C.P., 231  
 Swindle, T.D., 312  
 Swisher, C.C., III, 224, 265, 312, 332  
 Szakacs, A., 205  
 Taddeucci, A., 313  
 Tagami, T., 131, 308, 313, 358  
 Takahashi, E., 289  
 Takahashi, K., 136, 165, 356  
 Takigami, Y., 314  
 Tan, F.C., 314  
 Tanaka, T., 14, 315  
 Tao, Q., 357  
 Tao, X.-c., 95, 363  
 Tarney, J., 160, 307, 315  
 Tassinari, C.C.G., 316  
 Tatsumoto, M., 316  
 Taylor, F.W., 219  
 Taylor, H.P., Jr., 61, 140  
 Taylor, R.N., 317  
 Teagle, D., 122  
 Teichmann, F.R., 317  
 Teixeira, W., 318  
 Tejada, M.L.G., 318  
 Tellam, J.H., 20  
 Teng, R.T.D., 96  
 Tepley, F.J., 319  
 Tera, F., 366  
 Terashima, S., 324  
 Terrasi, F., 77  
 Terwilliger, V.J., 319  
 Teufel, S., 320  
 Theriault, R.J., 320  
 Thiemens, M.H., 63, 138, 160, 321  
 Thirlwall, M.F., 18, 103, 205, 317, 321  
 Thomas, R.L., 85  
 Thomaz-Filho, 220  
 Thompson, R.N., 247  
 Thomson, J., 260  
 Thomson, S.N., 322  
 Thonnard, N., 322  
 Thorkelson, D.J., 323  
 Tieszen, L., 157  
 Titterington, D.M., 199  
 Todt, W.A., 251, 323, 327  
 Togashi, S., 324  
 Tolstikhin, I.N., 179, 236, 249, 324  
 Tommasini, S., 325  
 Tonarini, S., 98, 325  
 Toolin, L.J., 326  
 Töpfner, C.P., 326  
 Toplis, M.J., 193  
 Torres, R., 7  
 Tosdal, R.M., 327  
 Toteu, S.F., 335  
 Toulkeridis, T., 327  
 Toyoda, S., 328  
 Travin, A.V., 254  
 Trumbore, S.E., 46

- Tseng, H-Y., 328, 329  
 Tsuchiyama, A., 333  
 Tsunogae, T., 329  
 Tsunogai, U., 330  
 Tuccimei, P., 313  
 Tulloch, A.J., 300  
 Turchenko, T.L., 114  
 Turek, A., 330  
 Turekian, K.K., 331  
 Turner, G., 14, 15, 16, 43, 44,  
 111, 129, 281, 308  
 Turner, P.J., 274  
 Turrin, B.D., 24, 84, 265, 332  
  
 Uchiumi, S., 308  
 Unnikrishnan-Warrier, C., 332  
 Uto, K., 308  
 Uyeda, C., 333  
  
 Vaasjoki, M., 259  
 Vai, G.B., 333  
 Valbracht, P.J., 334  
 Valenti, G.L., 352  
 Valley, J.W., 174, 177, 209  
 Van Bergen, M.J., 142  
 Van Bronswjk, W., 251, 323  
 Van Calsteren, P., 145  
 Van De Plassche, O., 334  
 Van Der Beek, P.A., 9, 270  
 Van Der Borg, K., 334  
 Van Der Plicht, J., 335  
 Van Donkelaar, C., 181  
 Van Klinken, G.J., 306, 335  
 Van Riet, A., 372  
 Van Schmus, W.R., 16, 335  
 Van Wagoner, N.A., 69  
 Van Warmerdam, E.M., 336  
 Vance, D., 336  
 Vasconcelos, P.M., 337  
 Vaughan, A.P.M., 218  
 Vavra, G., 337  
 Velsko, C.A., 76  
 Vengosh, A., 338  
 Venkatesan, T.R., 338  
 Vennemann, T.W., 339  
 Venturini, G., 339  
 Verplanck, P.L., 340  
 Vervoort, J.D., 340  
 Vetrin, V.R., 56  
 Vetter, U., 139  
 Viana, M.G., 252  
 Vidal, Ph., 80, 341  
 Villa, I.M., 249, 341  
 Villeneuve, M.E., 342  
  
 Vincent, J., 29  
 Vinyu, M.L., 342  
 Visona, D., 186  
 Vogt, S., 91, 176  
 Volpe, A.M., 296  
 Volpe, C., 343  
 Voltaggio, M., 313  
 von Blanckenburg, F., 26, 343  
 Vonhof, H.B., 295  
 Vrevsky, A.B., 344  
 Vroon, P.Z., 103, 142, 321, 344  
  
 Wada, H., 280  
 Wadatsumi, K., 170, 173, 345  
 Wagner, G.A., 69  
 Wakabayashi, J., 24, 345  
 Wakita, H., 330, 357  
 Walder, A.J., 122  
 Wallace, C.A., 323  
 Wallace, M.W., 167  
 Walraven, F., 346  
 Walter, M., 2  
 Walter, R.C., 265, 346  
 Wampler, J.M., 347  
 Wan, D., 82  
 Wang, C-H., 347  
 Wang, H-F., 369  
 Wang, J., 76, 348  
 Wang, L., 182  
 Wang, S., 153  
 Wang, X., 349  
 Wang, Y., 6, 348  
 Wang, Y.-X., 369  
 Warnock, A.C., 349  
 Wartho, J-A., 350  
 Wasserburg, G.J., 25, 55, 242,  
 255, 272, 287  
 Wasteneys, H.A., 350  
 Watanabe, T., 154  
 Weaver, S., 151  
 Wehmiller, J., 164  
 Wei, G-J., 361  
 Wei, K.-Q., 195  
 Weis, D., 20, 79, 206, 351  
 Weise, S., 118  
 Weiss, R.F., 286  
 Wells, S.G., 248  
 Wen, Q., 349  
 Wenk, H.R., 337  
 Wesolowski, D.J., 143  
 West, A.W., 351  
 Wheeler, J., 261  
 Wheller, G.E., 137  
  
 Whitehouse, M.J., 252, 275,  
 352  
 Whitelaw, M., 10  
 Whitford, D.J., 352  
 Whittemore, D.O., 296  
 Wickham, M., 93  
 Wickham, S.M., 52  
 Wiedenbeck, M., 115, 353  
 Wiedman, C., 164  
 Wieler, R., 42, 172, 258  
 Wieser, M., 155  
 Wightman, S., 93  
 Wijbrans, J.R., 91, 256, 282,  
 295, 353  
 Williams, A.E., 213  
 Williams, I.S., 196, 247  
 Williams, S.N., 278  
 Williams, W.J.W., 10  
 Wilson, C.J.N., 310  
 Wilson, M., 271  
 Wiltshire, J.C., 359  
 Windley, B.F., 352  
 Witt, W.K., 231  
 Wittenberg, L.J., 354  
 Wodicka, N., 354  
 WoldeGabriel, G., 346, 355  
 Wong, V., 355  
 Wooden, J.L., 17, 173  
 Woodhead, J.D., 142  
 Wright, J.E., 5  
 Wushiki, H., 356  
 Wyche, S., 231  
  
 Xia, J., 356  
 Xia, Y., 357  
 Xia, Y-f, 363  
 Xie, J., 73  
 Xiong, J., 356  
 Xu, S., 357  
 Xue, S., 175  
  
 Yabuki, S., 356  
 Yakovleva, S.Z., 191  
 Yamada, R., 358  
 Yamanaka, T., 333  
 Yamazaki, M., 154  
 Yanagi, T., 358  
 Yang, H., 349  
 Yang, J-D., 95  
 Yang, T-y. F., 359  
 Yang, W., 300  
 Yeh, H.-W., 359  
 Yelland, A.J., 216, 360  
 Yiou, F., 41

York, D., 297, 360  
Yoshida, M., 332  
Young, J., 29  
Yu, E.-F., 361  
Yu, F.-J., 361  
Yu, J.-H., 259  
Yu, J.-S., 120, 361  
Yu, Y.-W., 54  
Yu, Y., 362  
Yui, T.-F., 362  
Yurimoto, H., 329, 363

Zakariadze, G.S., 33  
Zantedeschi, C., 186  
Zartman, R.E., 232  
Zeitler, P.K., 180, 349  
Zhang, D.-K., 361  
Zhang, G.-d., 95, 363  
Zhang, J.-B., 368  
Zhang, L., 364  
Zhang, Y.-S., 364  
Zhang, Z., 365  
Zhatnuev, N.S., 220  
Zheng, M., 357, 365  
Zheng, S., 366  
Zheng, Y.-F., 366  
Zhiyu, J., 367  
Zhou, B., 367  
Zhou, T., 54  
Zhou, X.-H., 368  
Zhu, B.-Q., 369  
Zhu, H., 368  
Zhu, J., 365  
Zhu, X., 369  
Zhuravlev, A.Z., 370  
Zierenberg, R.A., 370  
Zindler, A., 37, 90, 202, 239,  
371  
Zinger, T.F., 191  
Zinner, E., 4  
Zreda, M.G., 91, 250  
Zubakov, V.A., 371  
Zuravlev, D.Z., 257  
Zwingmann, H., 372





---

# SELECTED SERIES OF U.S. GEOLOGICAL SURVEY PUBLICATIONS

---

## Periodicals

- Earthquakes & Volcanoes** (issued bimonthly).
- Preliminary Determination of Epicenters** (issued monthly).

## Technical Books and Reports

**Professional Papers** are mainly comprehensive scientific reports of wide and lasting interest and importance to professional scientists and engineers. Included are reports on the results of resource studies and of topographic, hydrologic, and geologic investigations. They also include collections of related papers addressing different aspects of a single scientific topic.

**Bulletins** contain significant data and interpretations that are of lasting scientific interest but are generally more limited in scope or geographic coverage than Professional Papers. They include the results of resource studies and of geologic and topographic investigations, as well as collections of short papers related to a specific topic.

**Water-Supply Papers** are comprehensive reports that present significant interpretive results of hydrologic investigations of wide interest to professional geologists, hydrologists, and engineers. The series covers investigations in all phases of hydrology, including hydrogeology, availability of water, quality of water, and use of water.

**Circulars** present administrative information or important scientific information of wide popular interest in a format designed for distribution at no cost to the public. Information is usually of short-term interest.

**Water-Resource Investigations Reports** are papers of an interpretive nature made available to the public outside the formal USGS publications series. Copies are reproduced on request unlike formal USGS publications, and they are also available for public inspection at depositories indicated in USGS catalogs.

**Open-File Reports** include unpublished manuscript reports, maps, and other material that are made available for public consultation at depositories. They are a nonpermanent form of publication that may be cited in other publications as sources of information.

## Maps

**Geologic Quadrangle Maps** are multicolor geologic maps on topographic bases in 7 1/2- or 15-minute quadrangle formats (scales mainly 1:24,000 or 1:62,500) showing bedrock, surficial, or engineering geology. Maps generally include brief texts; some maps include structure and columnar sections only.

**Geophysical Investigations Maps** are on topographic or planimetric bases at various scales; they show results of surveys using geophysical techniques, such as gravity, magnetic, seismic, or radioactivity, which reflect subsurface structures that are of economic or geologic significance. Many maps include correlations with the geology.

**Miscellaneous Investigations Series Maps** are on planimetric or topographic bases of regular and irregular areas at various scales; they present a wide variety of format and subject matter. The series also includes 7 1/2-minute quadrangle photogeologic maps on planimetric bases that show geology as interpreted from aerial photographs. Series also includes maps of Mars and the Moon.

**Coal Investigations Maps** are geologic maps on topographic or planimetric bases at various scales showing bedrock or surficial geology, stratigraphy, and structural relations in certain coal-resource areas.

**Oil and Gas Investigations Charts** show stratigraphic information for certain oil and gas fields and other areas having petroleum potential.

**Miscellaneous Field Studies Maps** are multicolor or black-and-white maps on topographic or planimetric bases on quadrangle or irregular areas at various scales. Pre-1971 maps show bedrock geology in relation to specific mining or mineral-deposit problems; post-1971 maps are primarily black-and-white maps on various subjects, such as environmental studies or wilderness mineral investigations.

**Hydrologic Investigations Atlases** are multicolor or black-and-white maps on topographic or planimetric bases presenting a wide range of geohydrologic data of both regular and irregular areas; principal scale is 1:24,000, and regional studies are at 1:250,000 scale or smaller.

## Catalogs

Permanent catalogs, as well as some others, giving comprehensive listings of U.S. Geological Survey publications are available under the conditions indicated below from the U.S. Geological Survey, Books and Open-File Reports Sales, Federal Center, Box 25286, Denver, CO 80225. (See latest Price and Availability List.)

"**Publications of the Geological Survey, 1879-1961**" may be purchased by mail and over the counter in paperback book form and as a set of microfiche.

"**Publications of the Geological Survey, 1962-1970**" may be purchased by mail and over the counter in paperback book form and as a set of microfiche.

"**Publications of the Geological Survey, 1971-1981**" may be purchased by mail and over the counter in paperback book form (two volumes, publications listing and index) and as a set of microfiche.

**Supplements** for 1982, 1983, 1984, 1985, 1986, and for subsequent years since the last permanent catalog may be purchased by mail and over the counter in paperback book form.

**State catalogs**, "List of U.S. Geological Survey Geologic and Water-Supply Reports and Maps For (State)," may be purchased by mail and over the counter in paperback booklet form only.

"**Price and Availability List of U.S. Geological Survey Publications**," issued annually, is available free of charge in paperback booklet form only.

**Selected copies of a monthly catalog** "New Publications of the U.S. Geological Survey" are available free of charge by mail or may be obtained over the counter in paperback booklet form only. Those wishing a free subscription to the monthly catalog "New Publications of the U.S. Geological Survey" should write to the U.S. Geological Survey, 582 National Center, Reston, VA 22092.

**Note.**--Prices of Government publications listed in older catalogs, announcements, and publications may be incorrect. Therefore, the prices charged may differ from the prices in catalogs, announcements, and publications.

